Modern Approaches in Solid Earth Sciences

Franco Pirajno
Taner Ünlü
Cahit Dönmez
M. Bahadır Şahin *Editors*

Mineral Resources of Turkey

Springer

Modern Approaches in Solid Earth Sciences

Volume 16

More information about this series at http://www.springer.com/series/7377

Franco Pirajno • Taner Ünlü • Cahit Dönmez
M. Bahadır Şahin
Editors

Mineral Resources of Turkey

Springer

Editors
Franco Pirajno
Centre for Exploration Targeting
The University of Western Australia
Crawley, WA, Australia

Cahit Dönmez
Department of Mineral Research
and Exploration
General Directorate of Mineral Research
and Exploration
Ankara, Turkey

Taner Ünlü
Department of Geological Engineering
Ankara University
Ankara, Turkey

M. Bahadır Şahin
Department of Geological Research
General Directorate of Mineral Research
and Exploration
Ankara, Turkey

Responsible Series Editor: F. Pirajno

ISSN 1876-1682 ISSN 1876-1690 (electronic)
Modern Approaches in Solid Earth Sciences
ISBN 978-3-030-02948-7 ISBN 978-3-030-02950-0 (eBook)
https://doi.org/10.1007/978-3-030-02950-0

Library of Congress Control Number: 2018966134

This Springer imprint is published by the registered company Springer Nature Switzerland AG
The registered company address is: Gewerbestrasse 11, 6330 Cham, Switzerland

We dedicate this book to Mustafa Kemal ATATÜRK, a great leader and the founder of Republic of Turkey.

A visit by Mustafa Kemal Atatürk (4th from left; grey jacket) to the Ergani Copper Mine (Elazığ-Türkiye) in 1937.

In the early years of the Turkish republic, Mustafa Kemal Atatürk, who understood the importance of mining, stated that establishment and development of a national industry strictly depended on mineral

exploration and exploitation. The development of Turkish mining in this period is related to his efforts and the following of his policies. Within these policies, in 1933 two independent institutions were established, namely: "Petroleum Exploration and Operation" and "Gold Exploration and Operations Administration", under the Ministry of Economy in order to obtain and evaluate the resources of the young Republic of Turkey. Then, for more comprehensive and systematic investigation of the mineralization and in order to reveal the geological structure of the country, on 22 June 1935, under the instruction of Atatürk, the Mineral Research and Exploration Institute (MTA) was established to work with modern scientific methods.

The MTA, has experienced many national and international research projects and plays a role in the discovery of several mineral deposits currently being operated, and is also continuing to work under the name of General Directorate of Mineral Research and Exploration as an international geological survey operating in all areas of geosciences. The mining operations in Turkey, built on a foundation laid by Atatürk in almost a century before, has made significant progress and is achieving a high economic potential.

Atatürk selected and sent five students for learning mining to Bergakademi in Freiberg (Germany) during late 1930s. These students returned to Turkey after graduation and began to work at MTA and established the Mining Department at Istanbul Technical University.

Mustafa Kemal Atatürk (1881–1938): Founder and first President of the Turkish Republic

"It is impossible to come across with leaders in every country, who change the course of history, impress a seal on it or stop grave dangers. Atatürk is a genius that the World History has rarely witnessed. After World War I, in a time that no defeated nation set up resistance, he defied the world with the civilians and the soldiers."
-Prof. Dr. İlber ORTAYLI- (Gazi Mustafa Kemal Atatürk Back cover)

Preface

Today's Turkey occupies an important geopolitical location: the junction of Europe and Asia. Geographically, Turkey is composed of Anatolia (the so-called Asia Minor) and Thrace, an eastern section of Europe. The Sea of Marmara, which is an inland sea, together with the Dardanelles and the Bosphorus separates Anatolia from Thrace and, at the same time, Asia from Europe. Being surrounded on three sides – by the Mediterranean Sea to the south, the Aegean Sea to the west and the Black Sea to the north – Turkey offers the characteristics of a peninsula.

Turkey is one of the charter members of the Organisation for Economic Co-operation and Development (OECD) and G20 (the Group of 20) where the world's leading industrialised and developing countries meet to gather and discuss international affairs. The Customs Union Agreement between Turkey and the European Union plays a significant role in the development of the foreign trade capability of the country. Construction, automotive, electronics, banking, textiles, petrochemistry, food, mining, agriculture and machinery industries are currently the leading sectors of Turkey's economy.

Turkey falls within the top five countries in the world in the production of glass, ceramic and cement industries, all of which are based on the mining sector. The most important items produced from the mining industry include metallic ores, such as chromite, copper, lead, zinc, iron, gold and industrial raw materials, such as borate, trona, feldspar, quartz sand, pumice, perlite, magnesite and marble. Nearly 60 different ore minerals are mined in Turkey today. This variety is a natural consequence of the complex geological structure of the country.

The Anatolian Peninsula is one of the areas where some of the oldest settled communities have been found. Many settlements were scattered across the Anatolian landscape dating from the Neolithic period onwards. The entity of several nations and states, so-called Anatolian civilisations, is noticeable. The early inhabitants first quarried rocks, such as limestone, flint and obsidian, for building materials and tools. Later they learned to transform ores into metals, such as lead, silver, copper and iron. They shaped simple clays into elegant pottery forms and baked them hard in hot furnaces. Gemstones also attracted the interest of the Anatolian civilisations,

and they were mined and traded far and wide. Over the long stretches of time, sophisticated material cultures emerged thanks to Turkey's earth and stones.

When we consider the antiquity of mining and quarrying in Turkey, it can be said to go back as far as 12000 Before Present (BP). The site of Göbekli Tepe (Şanlıurfa) is one of the oldest known constructions in Turkey. It is there where huge limestone blocks, weighing as much as 50 tonnes, were quarried to build impressive pillars decorated with carved reliefs. The structures at Göbekli Tepe have been described as a sanctuary of worship (Schmidt 2010) and are one of the most impressive examples of stonework from Turkey's remote past. Likewise impressive is the excavation of the Neolithic town Çatalhöyük (Konya) where archaeologists revealed one of the finest examples of settled society dating back to 8400 years BP. The stoneworkers at Çatalhöyük were very busy craftsmen. The excavations yielded a broad range of artefacts made of natural materials, such as obsidian mirrors, apatite and carnelian stone beads numbering in the thousands, grinding stones of basalt and andesite, decorative flint knives and carved limestone figurines (Birch et al. 2013). The residents of Çatalhöyük took advantage of local natural materials. Their source of obsidian came from Hasandağı, one of the most important volcanoes in central Anatolia, and they exploited the salt from Ilıcapınar, located near the Tuz Gölü (Salt Lake) Basin.

Early artisans did not restrict themselves to just stone. They explored how materials could be changed and altered. Artefacts of native copper have been found at Çatalhöyük, Çayönü Tepesi (Kaptan 1990; Mellaart 1966) and elsewhere in Turkey, bearing witness that artisans experimented with other materials. It has been suggested that early copper originated from the massive copper deposit at Ergani Maden (Kaptan 1990; Çambel and Braidwood 1970), first in native copper form and later smelted from malachite ores. These early experiments with copper and copper ore ultimately led to alloying with tin and arsenic. This technological development ushered in a period we refer to as the Bronze Age, ranging from ca. 5000 to 3200 BP.

The use of tin in Anatolia was once a mystery, as there was limited evidence where Anatolian cultures obtained this metal. However, thanks to the work of Aslihan Yener and the support from MTA, an ancient tin mine was located at Kestel near Çamardı, Niğde, along with a processing site and a village, Göltepe. Subsequently, two other ancient tin mining operations, at Hisarcik and Kıranardı, were discovered north of Çamardı (Yener 1989, 2000, 2009; Yener and Özbal 1987; Ünsal 2009; Yener et al. 2015). The discovery of these sites, together with tablets from Kültepe mentioning tin imports, set the stage for new ideas regarding the supply of tin metal in the Bronze Age.

The story of iron in Turkey is unique. Iron was first known in the Early Bronze Age (5000-4000 BP), turning up first at Alaca Hüyük. Analyses have shown that a number of iron artefacts from a tomb are meteoritic iron in origin. However, an iron dagger with a gold handle from a tomb at Alaca Hüyük was shown to be non-meteoritic (now in the Anatolian Civilizations Museum, Ankara). This provides good evidence that at least some terrestrial iron was produced in the Early Bronze Age Period (ca. 4400 BP) (Waldbaum 1978). Iron production must have been small and a carefully guarded secret known only to a select group of Anatolian metallur-

gists. In the course of time, "Hittite iron" became known throughout the ancient Near East, and many sovereigns sought to have a sword or weapon made from it.

It has been suggested that the exact transition from a bronze industry to an iron technology in Anatolia took place at ca. 3200 BP. Many cultures in Turkey may have greatly contributed to the technology of iron working, particularly the Phrygian and Urartu civilisations (Özdemir 2007), but bronze production continued well into the Classic Period.

Precious metals, such a silver and gold, have been produced in Anatolia since the beginning of ore mining. Gold was known and plentiful in the Bronze Age and continued to be produced in various parts of Turkey (Sagona and Zimansky 2009: 201). The Lydian Kingdom (900–750 BP) that reigned in western Anatolia was an important metallurgical and industrial centre where gold was produced from placers in the Pactolus River (Sart Creek) (Kaptan 1990; Sükun 1943). The Lydians are considered the first people to produce coinage (Sagona and Zimansky 2009: 364).

Thanks to the Anatolian geographer, Strabon, who lived in the first century of present era, we learn about many of the mining activities that took place during his time. His major work (Strabon 2012), *Geographica*, provides valuable information on mining yields and insights into mining techniques. Mining operations continued at many sites over long periods. In fact, many of the mining operations today were exploited in antiquity, such as the copper mine at Ergani being.

The geology of Turkey is complex involving the collision of continents, closure of oceans, widespread volcanism and plutonic activity. The Turkish landmass was subject to many types of terrains from Precambrian to more recent times, including inland seas and enormous lacustrine basins. At one point in the geological past, Turkey was located between two supercontinents, Gondwana and Laurasia, which were made up of several continental fragments. The separation of these continental fragments from the mainland by rifting or their amalgamation eventually resulted in the landmass of Turkey. The result was a landform assembled from a few continental and oceanic crust pieces with different geological features (Göncüoğlu 2010). According to Okay (2008), Turkey is divided into three tectonic units: Pontides, Anatolide-Tauride and Arabian platform (Ketin 1966). These units, which were earlier surrounded by the oceans, are presently separated by sutures that define tectonic lines or zones along the demised oceans.

The complex geotectonic setting of Turkey has given rise to the occurrence of several ore types. Of the 90 ore types listed in *Mineral Commodity Summaries* (MCS 2017) published by USGS, 68 are present in Turkey, most of which are currently exploited and traded.

Based on the Metallogeny Map of Turkey prepared by Engin et al. (2000), there are several lithological and structurally controlled metallogenic provinces in Turkey with varying ages and genetic characteristics (Engin 2002). Chromite, magnesite, olivine, asbestos and copper are found in ophiolites belts; copper, copper-lead, copper-lead-zinc and manganese occur in volcano-sedimentary basins associated with felsic volcanism; copper, copper-lead-iron, porphyry copper, skarn-type iron, hydrothermal copper-lead-zinc, wolfram, lead-zinc, gold, antimony, iron-wolfram-molybdenite, iron, fluorite, copper-lead-zinc, mercury, mercury-anti-

mony, barite and iron-phosphate are found in basins associated with felsic-intermediate magmatism; manganese, iron, red bed-type iron, copper, phosphate, strata-bound barite-lead and zinc-lead occur in sedimentary ore basins; borate, trona, salt (halite), gypsum and celestite are found in evaporitic basins and bauxitic iron, bauxite, nickel, gold deposits and occurrences are recognised in laterite and placers (Engin 2002). Pumice, perlite and zeolite deposits as the products of widespread volcanism in Turkey carry economic value. As a result of a complex formation and lithological diversity, Turkey provides a significant potential of natural stone and marble for future mining endeavours.

In the first chapter of this book, we have selected and discussed several mined or quarried materials. Chapter 2 reviews the geological evolution of Turkey that relates to the formation of ore deposits. Chapter 3 deals with ophiolites and chromitite deposits as important production and export items in Turkey's mining industry.

Precious metals such as gold and silver occurring in epithermal systems are the subject of Chap. 4 with their genetic properties, while Chap. 5 provides a general view of the iron deposits of Turkey. In Chap. 6, manganese deposits in Turkey have been categorised into four basic groups based on host rock type, geological-tectonic setting and formation processes. In Chap. 7, skarns and skarn-type deposits in Turkey take regional geological properties into account and classify them in provincial zones. Chapter 8 takes up the topic of porphyry deposits with special emphasis on geological evolution and geological setting.

Volcanogenic massive sulphide (VMS) deposits in Turkey are the subject of Chap. 9 where the mining history of Turkey is summarised. In Chap. 10, carbonate-hosted lead-zinc deposits are discussed with insights regarding their location.

Turkey's borate deposits, containing nearly two-thirds of the world's reserves, are discussed in Chap. 11. Chapter 12 explores trona deposits, another type of evaporitic mineral.

Chapter 13 summarises lateritic nickel deposits with an emphasis on their geology and economic potential. Radioactive elements, such as uranium and thorium and rare earth elements, are outlined in Chap. 14, and bauxite deposits of Turkey are the topic of Chap. 15. Finally, Chap. 16 includes olivine and magnesite mineralisation.

The purpose of the current publication is to provide a cogent overview of Turkey's mineral resources with special emphasis on geological characteristics, genetic features and economic indicators of pertinent deposits. To ensure accuracy, these studies have been written by professionals and academicians who deal intimately with mineral resources in Turkey. It is our hope that we have succeeded in our goal.

Crawley, WA, Australia
Ankara, Turkey

Franco Pirajno
Taner Ünlü
Cahit Dönmez
M. Bahadır Şahin

References

Birch T, Rehren T, Pernicka E (2013) The metallic finds from Çatalhöyük: a review and preliminary New Work. In: Hodder I (ed) Substantive technologies at Catalhöyük. British Institute of Archaeology at Ankara/Cotsen Institute of Archaeology, London/Los Angeles, pp 307–321

Çambel H, Braidwood RJ (1970) An early farming village in Turkey. Sci Am 222(3):51–56

Engin T (2002) Mineral deposits of Turkey. Mineral resource base of the southern Caucasus and systems for its management in the XXI century. Editors: Alexander G. Tvalchrelidze, Georges Morizot. ISBN:-1-4020-1124-5 (Print) 978-94-010-0084-0 (Online)

Engin T, Özkan YZ, Şener F, Toprak B (2000) Türkiye Metalojeni Haritası. Maden Tetkik ve Arama Genel Müdürlüğü, Ankara

Göncüoğlu M C (2010) Introduction to the geology of Turkey: geodynamic evolution of the pre-Alpine and Alpine terranes. General Directorate of Mineral Research and Exploration, 66 P. ISBN:6054075748, 9786054075744

Kaptan E (1990) Türkiye Madencilik Tarihine Ait Buluntular. Maden Tetkik ve Arama Dergisi 111:175–186

Ketin İ (1966) Anadolu'nun Tektonik Birlikleri. Maden Tetkik ve Arama Dergisi 66:20–34

MCS (2017) Mineral commodity summaries. Individual commodity data sheets. USGS. https://minerals.usgs.gov/minerals/pubs/mcs/

Mellaart J (1966) Excavations at Çatalhöyük 1965. Anatolian studies XVI:165–191

Okay AI (2008) Geology of Turkey: a synopsis. Anschnitt 21:19–42 Veröffentlichungen aus dem Deutschen Bergbau-Museum Bochum, Nr. 157

Özdemir HF (2007) Demir Çağı: Başlangıcı Ve Başlatanları, Anadolu'ya Etkileri Üzerine. Ç.Ü. Sosyal Bilimler Enstitüsü Dergisi 16(1):501–518

Sagona A, Zimansky P (2009) Ancient Turkey. Routledge, Abingdon/New York

Schmidt K (2010) Göbekli Tepe – the Stone Age Sanctuaries. New results of ongoing excavations with a special focus on sculptures and high reliefs. Documenta Praehistorica XXXVII:239–256

Strabon (2012) Geographika / Antik Anadolu Coğrafyası. Translation: Adnan Pekman. 4th edition. 384 P

Sükun N (1943) L'industrie Miniere Turque: P 310, Montreux

Ünsal Y (2009) Einneües Zinnvorkommen İn Kayseri-Hisarcik, Zentralanatolien: Ein Vorbericht. Tüba-Ar. Türkiye Bilimler Akademisi Arkeoloji Dergisi 12:117–122

Waldbaum J (1978) From bronze to iron. Studies in mediterranean archaeology LIV. Paul Aströms Förlag, Götenborg

Yener KA (1989) Kestel: an early bronze age source of tin ore in the taurus mountains, Turkey. Science 244:200–203

Yener KA (2000) The domestication of metals: rise of complex metal industries in Anatolia (c. 4500–2000 B.C). E.J. Brill, Leiden

Yener KA (2009) Strategic industries and tin in the Ancient Near East: Anatolia updated. TUBA-AR 12:143–154

Yener KA, Özbal H (1987) Tin in the Turkish Taurus mountains: the Bolkardağ mining district. Antiquity 61:64–71

Yener KA, Kulakoğlu F, Yazgan E, Kontani R, Hayakawa Y, Lehner J, Dardeniz G, Öztürk G, Kaptan E, Hacar A (2015) New tin mines and production sites near Kültepe in Turkey: a third-millennium BC highland production model. Antiquity 89(345):596–612

Contents

Chapter 1
Comments on the Antiquity of Mining Rocks and Minerals

Prentiss S. de Jesus

Abstract The history of mining can be written from many perspectives: mining technology, labour inputs, economic impact or materials exploitation. Hard materials were needed to advance the material culture of civilisation, and this need drove the mining and quarrying activities of antiquity. This article discusses a selected number of materials that were commonly mined or quarried in the ancient Near East. The author seeks to illustrate the value of hard rock materials, their variety and exploitation requirements. He also notes the lack of information available on human groups, communities, and the social networks involved in exploration, quarrying and mining. This article is an appeal for more research on this topic.

1.1 Introduction

As we walk along a gravel road or drive our car on a paved highway, we may not give much thought to their construction, nor the events that led up to it. The common stones and materials that make up roadways have enabled civilisation to thrive as we know it. Our association with stone, rocks and earthen materials began early in the history of humankind and has not ceased to the present day. We are still exploring the earth for useful materials, stones of all kinds for our buildings, our bridges and walkways, stones as grinding tools, vessels, beads, amulets and jewellery. When ground, pulverised, heated or fashioned in some way rocks and minerals provide us with the products that our civilisation requires. In this sense, we have never left the Stone Age.

The history of stone materials is certainly a long one and nonetheless interesting from the point of view of humanity's on-going reliance on natural materials. Here I would just like to sketch out a few cases that illustrate our binding relationship with our planet Earth and the materials it provides. Human life is, and always has been, inextricably linked to natural resources. It can be said that we have been mining the

P. S. de Jesus (✉)
American Research Institute in Turkey, Ankara, Turkey
e-mail: pdejesus@alumni.Brown.edu

F. Pirajno et al. (eds.), *Mineral Resources of Turkey*, Modern Approaches in Solid Earth Sciences 16, https://doi.org/10.1007/978-3-030-02950-0_1

Fig. 1.1 Chopper from Olduvai Gorge, dated 1.8 Myrs. (Courtesy of Smithsonian Institution)

Earth since the ancestors of our species could walk. In fact, mining is probably the earliest of *Homo sapiens*' industries.

We know little how ancient humans prospected for raw materials. However, various kinds of stones and rocks show up in excavations, thereby giving us an idea of what materials were needed or coveted. Our dependency on natural materials began long before *Homo sapiens* emerged from Africa and spread across Europe and Asia. The early hominids, Australopithecines, were the first to adapt to multi-zone primate living, which exposed them to different environments (Picq 2013).[1] Their mobility gave them the opportunity to see and explore different terrains, observe surface materials and, perhaps have the opportunity to adopt stone tools. It is not totally certain that they did. On the other hand, it is the view of many anthropologists that *Homo habilis* was the first hominid to make and use stone tools (Rudgley 1999). The rounded volcanic basalt stones found in riverbeds and strewn across the African landscape would serve aptly as pounders for food extraction or as the defense against predators. Ultimately, *Homo habilis* devised a sharp edge on a stone was intentionally designed for cutting. One such example is represented here by the Olduvai chopper in Fig. 1.1, which shows a crude retouch to form a cutting edge. This simple tool suggests two things: (1) early hominids were including a larger portion of meat in their diets, thus requiring a chopping implement to cut through tough skin and break bones (Pfeiffer 1982); and (2) they were discriminatory in selecting a material that was locally available and best suited for making such a tool. While we cannot call this crude chopper a work of art, it was the beginning of early man's use of natural materials that would improve his life and better his chances of survival. In this way, *Homo habilis* may be labelled the first manipulators of the Earth's resources.

[1] It is acknowledged that Australopithecines have now been classed in at least five different categories (Picq 2013: 70–71). I use the general term Australopithecus to represent the whole group.

Early hominids did not formally distinguish the different categories of rocks as metamorphic, sedimentary or igneous. The origins of such rocks were surely ignored, and early tool makers simply exploited stones for their convenience and immediate use. It is logical that exposed extrusive rocks would attract the attention of early toolmakers. It is not surprising, then, that basaltic rocks were selected for their weight and robust forms and were used as hammers and pounders.

Stones may even have had an aesthetic value, as early hominids collected brightly coloured silica rocks that served as decorative ornaments, amulets or talismans. As early hominids modified things to make life and survival easier, they acquired a measure of independence far above other primates. From materials that were readily available, such as animal bones, antlers and sticks, early hominids fashioned different kinds of implements to be used in food preparation or wearing apparel. Social conditions also changed which gave them an advantage over competing species. Their social structure provided superiority by virtue of numbers, both in terms of safety and communal activities. The subsequent formation of clans led to the construction of crude communal structures, such as windbreakers and walls in protection against predators, with some parts being made of stones. Along with this social organisation came an increased use of stone as a practical material and a greater need for stone tools. The type of tool, the material used, and the variations of its use represented technical choices that translate into cultural traditions (Pfeiffer 1973: 91–2). These traditions gradually became distinct from other clans. The resulting cultural repertoire of early hominids demonstrated their increased exploitation of raw materials, if not ownership of their physical environment. They may even have become protective of their territory because of the resources that it contained.

Rocks with cryptocrystalline or glass structure, like chalcedony and obsidian, break with a conchoidal fracture and can be flaked, chipped, and made into points and keen cutting edges. Gradually, tools became more distinguishable, individualised and refined, but the development of better and specialised tools at this time was still a slow process.

Even with the advent of *Homo sapiens* about 300,000 years ago (Hublin et al. 2017) the stone tools had shown only a marginal improvement (Pfeiffer 1973). Eventually, *Homo sapiens* became the dominant species and pushed its way into Europe and beyond. By 40,000 B.P humans had developed a range of craft-making skills that included many fine points and blades. Prehistorians see this period as a cultural explosion of artistic and social advances. With refined tools came the use of fire, cave art and evolved social roles. Communal life gave rise to hierarchy and ritual practices. The wonderfully expressive figurine Venus[2]of Willendorf (Fig. 1.2) reflects certain cultural elements that prehistorians have long pondered[2]. The figurine has been labelled a fertility goddess or, more personably, a self-portrait. Despite its intended use, certain details of the figurine reveal something about women of the Upper Paleolithic period. The pleated hair indicates that even at this remote time in the past women took the vain practice of presenting themselves in a beautified fashion. This may represent just one of the many hairstyles worn by women. The finding

[2] Figure 1.2, Image #326474, courtesy of the American Museum of Natural History Library.

Fig. 1.2 Venus of Willendorf. Oolitic limestone figure dating to 28,000 B.P

of beads in the Upper Paleolithic may suggest that decorative items were worn by women as well as men, which also suggests a growing self-awareness amongst humans. What is relevant to this discussion here is the use of oolitic limestone to make the Venus figurine and the dexterity required to represent the details. A *Homo sapiens* craftsman quarried this piece and carved it with great care, and importantly, the refined skill to create stonework of this quality would be passed on to succeeding generations. Stone working had become a cultural tradition.

When we look at the development of civilisation in the ancient Near East we normally use Mesopotamia (now Iraq) as our measuring stick, as that is where the first urbanized settlements developed. With that development came the exploitation of materials to sustain the economies, crafts and livelihoods of settlements. Thanks to the comprehensive work by P.R.S. Moorey on Mesopotamian materials we have a sense of where many materials came from within the borders of ancient Mesopotamia as well as from abroad. The documentation and information on materials used in ancient Turkey, on the other hand, are still scattered throughout the archaeological literature. At the moment we are only able to make sporadic references to natural materials and resources. Another problem we encounter is that rocks and minerals are not systematically and precisely identified in archaeological reports. The term marble is often loosely used and could be other substances like alabaster, even limestone. Chlorite and steatite are frequently lumped together because of their similar appearance. Some stonework is simply designated by its colour (i.e. " black stone"), and we have no idea from what kind of mineral the artefact is made. These everyday challenges should be viewed as an incentive as well as an appeal to archaeologists working in Turkey to begin compiling accurate data and information on natural materials.

Fig. 1.3 Obsidian blades from Çatal Höyük dated to ca. 6200 B.C

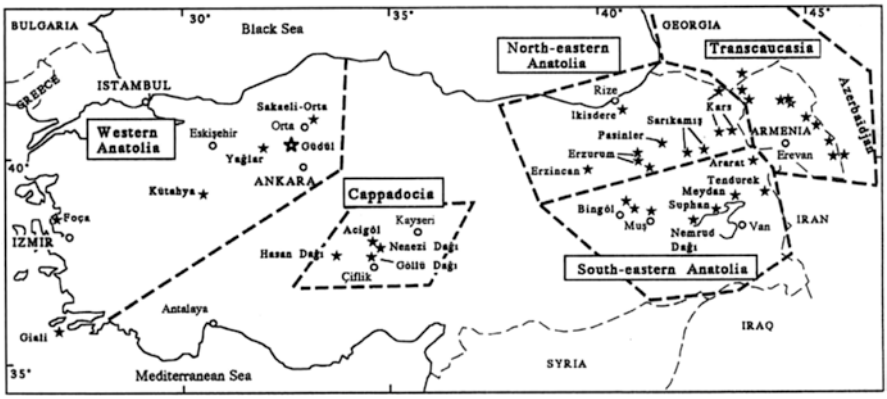

Fig. 1.4 Map showing Anatolian obsidian sources. (Courtesy C. Chataigne)

Turkey played a central role in the supply of materials, not only for its own indigenous cultures, but also for trading with neighbouring regions. Some materials traded throughout the Near East are found only in Turkey or on its borders. Take, for example, obsidian whose deposits at Hasan Dağı, and Acıgöl (Figs. 1.3 and 1.4) were exploited as early as the Neolithic (ca. 6500 B.C.). Because of its ability to be made into refined tools obsidian was traded as far away as the Arabian Peninsula, more than 1000 km to the south.

It is not my intent in this article to trace the historical use of every material found in archaeological contexts, rather raise some points for reflection and hopefully encourage subsequent research. But let us just briefly look at the extent of the rock and mineral industry in antiquity. The following materials are known to have been

found in archaeological excavations (Nazaroff et al. 2013; Moorey 1999; Lucas and Harris 1962; Nicholson and Shaw 2009; Rapp and Hill 1998; Rosenfeld 1965).

Alabaster	Granite	Pumice
Amber	Gypsum	Rhyolite
Basalt	Jasper	Salt
Chalk	Limestone	Sandstone
Chert	Marble	Schist
Chlorite	Natron	Serpentine
Diorite	Obsidian	Steatite
Flint	Onyx	Talc
Gabbro	Porphyry rock	Trachyte

Among the ornamental stones, we find

Agate	Chrysophrase	Quartz
Amethyst	Haematite	Rock crystal
Augite	Jasper	Sphalerite
Carnelian	Lapis lazuli	Turquoise
Chalcedony	Pyrites	

One of the goals of geology is to find materials that are economically viable for the support of an economy. We are indebted to hard rocks and materials, for without them we would be a struggling agricultural society. And even an agricultural economy is reliant on hard materials of some kind. Flint, and the above-mentioned obsidian were used in early agrarian societies for cutting tools in the harvest of wheat and grains. Basalt slabs and rubbing stones were used for grinding grains into flour. Soft materials were made into useful hard materials. Clays were used to make sickles, bricks, hearths, pottery, and one of the most valuable items in history: clay tablets (e.g. Moorey 1999). That said, let us now look at a few examples of how ancient societies used natural materials.

1.2 Agate

Agate is a variegated cryptocrystalline variety of chalcedony and can be found in vugs (fractures) in volcanic rocks. It is generally classed and often found with other cryptocrystalline varieties of quartz such as onyx; hence, it is not surprising then that we find both agates and onyx in archaeological excavations. There is little distinction between the two. Agate can contain patches of banding colours, varying from red, grey to brown. When the colours are in black and white flat bands, it is classed as onyx (or sardonyx if there are white and reddish brown bands).

The earliest related examples of agate from archaeological excavations come from Iraq where chalcedony is reported at Yarim Tepe I. They date to the mid-sixth

millennium B.C. and were certainly imported, as there are no known deposits in the Mesopotamian basin of chalcedony or any of its related minerals (agate, sardonyx). Agate is native to Egypt, where deposits and quarrying have been located in the eastern desert. Agate pebbles and beads have been found in Predynastic graves (i.e. before 3000 B.C.; Nicholson and Shaw 2009; Lucas 1962; Moorey 1999 for Mesopotamia), and the in Mesopotamian river basin agates turn up in graves as a popular gemstone in the third millennium B.C. Agate and chalcedony became very popular from the Neo-Assyrian period onward (ca. seventh century B.C.). They were readily available in later Classical times and used extensively in jewellery (Caley and Richards 1956). The Classical Greek botanist and philosopher Theophrastus (b. 371 B.C.) mentions agates in his treatise on stones. At that time appearance was the criteria for classifying stones, and it is possible that any attractive stone with streaks or markings against a contrasting background could be grouped under the same name (Caley and Richards 1956: 128–9). What is significant is the use of this category of stone over such a long period which entailed a fair amount of committed labour in its production and trade.

Agates have not been reported extensively in Turkey, though there is one occurrence in a burial at Kültepe Level II. In view of the Mesopotamian influence at the site at this time, it is possible that this piece was imported and not of Anatolian origin (Joukowsky 1996). Agates have one characteristic that stands out: the crafted pieces were usually small, such as amulets, beads, seals and decorative items. This may suggest something about its high intrinsic value. According to Moorey (1999) agates, along with chalcedonies, may originate from sources to the east in Iran or India. The distant source of this material should not surprise us. It has been noted by archaeologists and anthropologists that the more valuable the material, the farther it can be traded (Renfrew 1977). This is also reflected in the early trade of lapis lazuli, chlorite stone, obsidian, jade, cornelian, sea shells and processed materials such as tin (see also Moorey1999 for further examples).

1.3 Obsidian

Obsidian is a volcanic glass that has a very homogeneous structure. Being non-crystalline, its fracture is conchoidal and can be flaked into elegant forms, even bowls. It has a hardness of almost seven which means that it is harder than most organic materials. It is also harder than some rocks, such as steatite and marble, and may have been used to carve softer stones (Rosenfeld 1965). The exploitation of obsidian began very early in prehistory before established agricultural practices demanded keen-cutting harvesting tools. Obsidian has been found as early as 7500 B.C. at the site of Mureybat in Syria and continues through the Ubaid Period (ca. 5500–4000 B.C.) at many sites in Northern Mesopotamia (Wright 1969). Some of the finest Anatolian examples of worked obsidian come from Neolithic Çatal Höyük (Fig. 1.3). The spread of obsidian over a wide area of the Near East attests to its desirability as a material that could be formed into different, even elegant, shapes.

Analyses been carried out to identify the sources of obsidian artifacts found in excavations, and two general regions are considered key sources. One is in Central Turkey that comprises three volcanic areas: Göllü Dağ, Nenezi Dağ, Hasan Dağ, and Erciyes Dağ (Balkan-Atli et al. 1999; Rapp and Hill 1998; Gourgaud et al. 1998). The other is in Lake Van area and comprises a site near the lake itself, and another flow near Bayezid lies 310 km northeast of the lake. There are other flows nearer to Lake Urmia in Iran (Moorey 1999; Wright 1969). Other studies have identified outflows in northeastern and western Anatolia (see Fig. 1.4).

1.4 Albaster

This stone is a fine-grained compact form of gypsum and has been commonly found in archaeological excavations. It is often translucent and lends itself to being worked into vessels, figures, and statuary. Beads of alabaster were found at Yarim Tepe in northern Iraq dating to the mid-sixth millennium B.C. as well as at Jarmo located in northeastern Iraq in the foothills of the Zagros. For Yarim Tepe it is reported that "fragments of ten polished marble or alabaster bowls and jars and seven palettes" were recovered (Moorey 1999), here blurring the clarification between marble and alabaster. The Jarmo finds are outlined in Mellaart (1973: 80) who suggests that the source material of the latter may have come from the boulders gathered from the wadi below the site or from a ridge nearby. We can conclude from this synopsis that stonework was firmly established as a craft by the time alabaster was first used, and it was merely added to the stone craftsman's repertoire. The ease of working with this stone ensured its use over time. One has to mention here one of the most famous Mesopotamian documents of alabaster, the tall Uruk vase from a treasure hoard dated to ca. 3000 B.C. This vase is discussed in many books and documents because of its important ritual scenes carved on six registers (Parrot 1960; Oates and Oates 1976; Hansen (2003). The value of the alabaster would seem to reflect the significance of the ritual scenes of homage to the goddess Ishtar. Alabaster was frequently used for goddess figurines, such as those from Kültepe dating to Early Bronze Age II (4800–4400 B.P.; Bilgi 2014).

Moorey (1999) correctly points out that alabaster is often misreported in the archaeological literature and has been variously described as calcite, gypsum, marble and limestone. As for sources, Moorey quotes Layard who states that alabaster (called "Mosul marble") was available in northern Iraq to the east and in those parts of the Tigris and the Euphrates that emerge out of the Taurus in Turkey (Moorey 1999). Turkish studies show a major deposit at Gaziantep west of the Euphrates (MTA 1966).

1.5 Chlorite

Chlorites belong to a mineral group closely linked to micas. To the touch, they are pasty or soapy and often appear greenish. Their colour reflects their chemical composition which includes aluminium, iron magnesium, silica and magnesium. Chlorites are derived from hydrothermal alteration of silicate minerals, and their resulting chemical composition varies depending on the original mineral from which they are derived (Rosenfeld 1965). While they are similar chemically, chlorites are often confused with massive steatite because of their colour and softness. The softness of chlorites lends itself to carving, hence its use in the past for crafted items, particularly bowls.

One of the earliest attempts to sketch out the mines-to-market process of chlorite as a resource material was carried out a number of years ago in Iran by Philip Kohl (Kohl et al. 1978). He documented the extraction points, manufacture and trade in chlorite, used for luxury items, primarily carved stone bowls but also cylinder seals and other small artefacts. He initiated his study at Tepe Yahya, Iran where carving workshops were uncovered dating to 2600–2500 B.C. He identified the sources of the stone in the mountains north and west of the Soghun Valley in the southern Zagros Mountains. This research confirmed that the settlement of Tepe Yahya relied heavily on its crafted bowls and their export primarily to Mesopotamian sites in the west. Kohl (1978) tracks the export of both finished and raw cut bowls using different trade routes. Other works that have contributed to the documentation on chlorite stonework and trade can be found in Lamberg-Karlovsky (1988), Potts (1989), Aruz (2003), Potts et al. (2001) and Kohl (2001).[3] While scholars have not always identified very precisely the specific material of stonework, Kohl et al. (1978) confidently identifies the carved bowls from Tepe Yahya as chlorite.

The trade in stone bowls has aroused much attention both as an item of trade and as a material that linked different parts of the Near East. The irregular use and appearance of stone vessels over time starting in the middle of the fourth millennium B.C indicate that the supply of the basic material or finished products fluctuated for reasons we do not know (Moorey 1999). Perhaps the quarrying operations encountered difficulties involving labour availability or political control. Potts (1989) argues that the fluctuation of supply was linked not to any trade or production-related factors, but the stone bowls found in southern Mesopotamian sites were actually booty from Elam and elsewhere.

Whatever reasons governed the supply of chlorite bowls for parts of the ancient Near East, they were always highly valued. We are told that large numbers were given as offerings to gods (Potts 1989).

[3] Unfortunately I was not able to consult the latter publication for the current study.

1.6 Gypsum and Lime Plaster

Craftsmen of antiquity were more interested in what gypsum could be turned into, namely plaster, and not so much its natural form. Gypsum is a relatively common mineral and has a wide distribution in Turkey as well as elsewhere. One typical gypsum deposit is located at Sivas (Günay 2002). In its natural state, it is a hydrous calcium sulphate: $CaSO_4 \cdot 2H_2O$. Gypsum can be crystalline and monoclinic in form, but it also exists as a rock in which case it is granular, massive or fibrous (Rosenfeld 1965). When heated to a temperature of 100–200 °C gypsum undergoes a partial dehydration to form what we commonly call plaster of Paris. This is a somewhat unstable state, for if we add water back to the dehydrated substance rehydration occurs, and the material reverts back to gypsum and reacquires it original hardness (Blackman 1982; Gourdin and Kingery 1975). Because of its sensitivity to humidity, gypsum plaster does not store well in the open air.

Lime, a calcium carbonate $CaCO_3$, was also used as a source of plaster. Like gypsum, lime can be converted to plaster by dehydration of limestone, but for calcium carbonate to become lime it must reach a temperature of approximately 900 °C, and this temperature must be maintained for several hours (Blackman 1982). The resulting calcium oxide is also called *quicklime*. When quicklime is mixed with water (i.e. slaked) it becomes slaked lime. It can then be allowed to set and dry hard and become lime again due to the evaporation of the water. Lime plaster is not particularly strong and is often combined with sand, thereby converting it to a kind of mortar. Other fibrous materials can also be used in this way, such as chaff and straw (Rosenfeld 1965).

It is not a simple matter to distinguish between gypsum plaster and lime plaster. The simple test of fizzing acid with limestone that does not occur with gypsum is not conclusive proof. Gourdin and Kingery (1975) pointed out that many gypsum and limestone deposits are not pure and may be contaminated with one another. Moreover, clay inclusions may also be present that allows an acceptable cohesion between the two, resulting in an acceptable plaster. The two authors claim that the only way to determine the true composition of plaster is through precise microscopic examination as well as chemical analysis.

Indeed, both gypsum and lime plasters reveal a close relationship with clay. In the Neolithic period, liquid clay was smeared on the walls of dwellings inside and out to give them a smooth surface. Ultimately pleasing white plaster was discovered and developed into a more desirable substitute. The smooth white walls were an invitation for decoration as we find at Çatal Höyük (Figs. 1.5 and 1.6). What is important about the production of plaster in antiquity is that a heat treatment is required, resulting in the chemical transformation of material (Blackman (1982). Gourdin and Kingery (1975) cite Aşıklı Hüyük as the first occurrence of lime plaster in Anatolia in the 7000–6500 B.P. timeframe. They state that the burning of limestone at the high temperature of 750–850 °C required the use of kilns, a process that predated the introduction of fired ceramics. Based on this evidence, it can be safely argued that the development of plaster was the debut of true pyro technology. From

Fig. 1.5 A painted plaster figure of a hunter-dancer from a shrine at Çatal Höyük level III dated to ca. 5750 B.C

Fig. 1.6 Flint blade with bone handle from a Çatal Höyük burial in Level VI. Dated to ca. 5800 B.C

this point onwards, craftsmen explored other ways in which fire could transform materials. This curiosity ultimately led to the discovery of fired pottery and the smelting of metallic ores. It can hence be said that a simple pyrotechnological process gave rise to new materials and applications from which we benefit today.

1.7 First Mining and Quarrying Operations

Quarrying operations were equally demanding, and we do not know from where all the natural materials stated at the beginning of this chapter came from. There is much work to do to bring to light the natural sources of commonly used materials, such as flint, marble and steatite. Egypt is a notable exception, as we have documentation on where, for example, limestone quarries were located and insights into the time periods during which they were exploited. Lucas (1962) reports that limestone occurs in the hills bordering the Nile from south of Cairo to Esna and sporadically in other localities. The quarry at Tura may have been exploited as early as the fourth Dynasty. Nicholson and Shaw (2009: 40–42) write that limestone quarries have been identified in Wadi Zubeida, at Beni Hasan, Qau el-Kebir, and el-Sawayla. It has been well established that limestone was exploited extensively in Egypt in pre-Dynastic times (Teeter 2011), a testimony to its long stone working tradition. Storemyr et al. (2010: 39) state that there are more than 200 Egyptian quarries (not all limestone) identified as possible ancient quarrying sources.

Fig. 1.7 Archaeologist Klaus Schmidt pictured here with one of the carved limestone pillars at Göbekli Tepe

In Anatola limestone quarrying has a history of its own. The limestone quarries at the pre-Neolithic site of Gölbekli Tepe are scattered around the temple site. Schmidt (2000) states that the quarries are "located all over the limestone plateaus around Göbekli Tepe". Quarrying was not just a question of chipping away blocks of desired material, but an ambitious undertaking that harnessed a massive workforce. The late Klaus Schmidt (2012) estimated that to move a block of limestone 7 m long from its quarry emplacement, it would take close to 700 labourers. What is impressive is that such a large number of workers could be gathered from dispersed groups or clans that had not yet settled in large communities. Despite the disparity of the population at that time, there was nevertheless an underlying cultural unity that served as a basis for a common calling. While we assume that the motivation was to establish a place of worship, it is nevertheless surprising that the religious beliefs were so coherent for such a rural and dispersed population.

The location of Göbekli Tepe must have been selected for a number of strategic reasons, one being the presence of a massive limestone outcrop that would serve as the basic raw material for the shrines' pillars (Fig. 1.7). The choice also suggests that the prospective pre-Neolithic worshippers of the shrines knew the kind of stone that would best work for them. This presupposes that they already had a competent knowledge of stone working. Evidence of their previous experience with quarrying and stone carving must, therefore, exist elsewhere. The significant number of workers involved in just the quarrying operations must have required the support of a whole community that included housing, feeding and possibly tool supply. It is this aspect of the mining and quarrying activities of the past that has not yet been adequately addressed. Apart from a few disparate references to mining and quarrying activities in the Near East, the characterization of the communities that supported them is largely absent in the archaeological literature. Surveys have been carried out in many different areas of Turkey with the intent of documenting mining and smelting sites, but their nature and their available resources did not allow them to extend their research and seek out mining communities. Hence, there are many loose ends. For a sampling of past surveys, see Ryan 1960; Yalçın et al. 2008; Kaptan 1991,

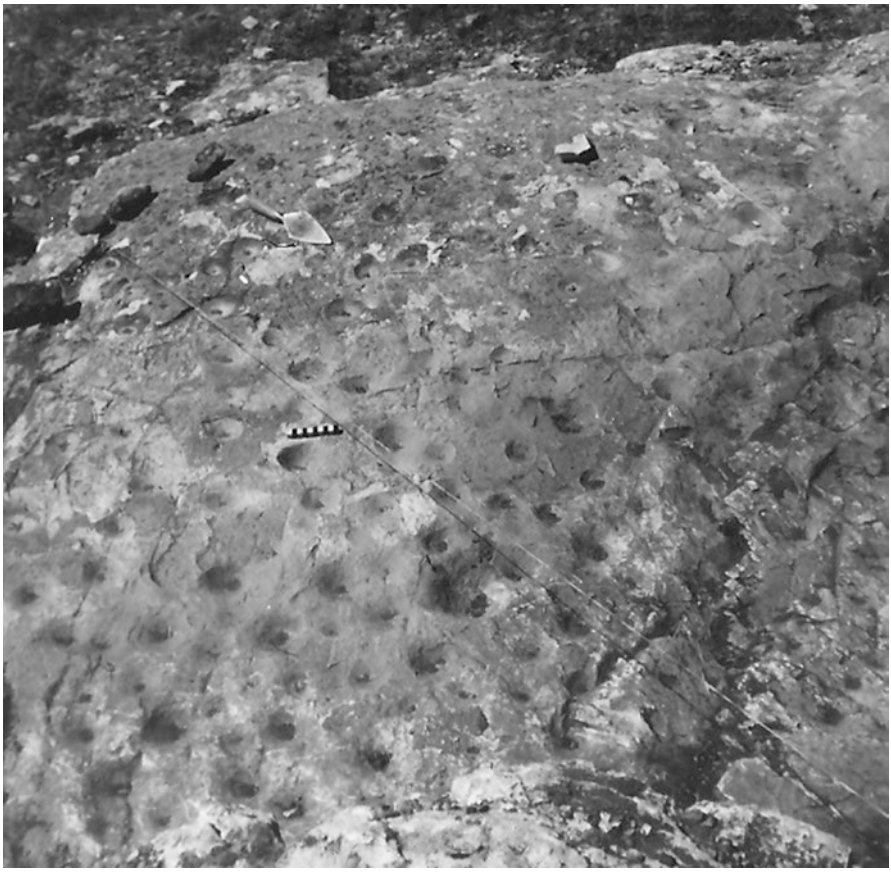

Fig. 1.8 Marble outcrop showing numerous grinding sockets at Kestel tin ore mining site. (Courtesy A. Yener)

1986, 1984, 1982; Wagner et al. 1986; Wagner 1989; Palmieri et al. 1993; de Jesus 1978, 1980, 1981.

One notable exception is the tin mining operation at Kestel that comprises an Early Bronze Age tin mine, settlement, and the ancillary work areas that processed the ore. Yener (2000) provides a cogent description of the mining operations and settlement area. Other reports complement the studies performed there (Özbal 2009; Yener and Vandiver 1993; Yener and Özbal 1987). The operation at Kestel was fully supported by the neighbouring settlement, Göltepe, whose population could have been as high as 2000 inhabitants.[4]

The grinding areas where the newly mined ore was crushed and concentrated represent the core activity of the site (Fig. 1.8) (Yener 2000). Yener (2000) reports that 50,000 ground stone tools were found "on the surface of the site". Although she

[4] This population figure is the present author's estimate, not that of the site's excavators.

classifies the operation as a "cottage industry", the scope of the production appears to have been significant. Moreover, the very existence of Kestel and its ancillary settlement are indicative of a focused industry that produced one product: tin ore. No smelting took place at the mining site or the settlement. Yener (2000) states that the ore was "transported elsewhere, presumably to a second-tier, lowland, urban workshop as yet not identified, for the next stage of processing which was alloying and casting it into a diversity of artefacts." This tells us that a single valuable product can comprise the destiny and livelihood of an entire community, just as the chlorite bowls were for Tepe Yahya. If we look at the list of natural materials above, it is not difficult to imagine that countless communities scattered across the Near East and beyond were involved in quarrying mining and processing. To a great extent only their products have been recognized in the archaeological literature. For the most part, the producing communities remain largely unidentified and unacknowledged for their contribution to the material culture of urban settlements.

1.8 Ancient Resource Exploitation and the Supernatural World

The exploitation of Earth's materials was not solely an industrial affair. Archaeology has clearly determined that there was a spiritual connection between ancient man and the earthly materials that he used. By mythological definition, the mundane world was related to the supernatural and cosmic domains, and the materials that depicted mythical beings or cosmic forces were imbued with special significance, if not power. Let us not forget the limestone pillars in the shrines at Göbekli Tepe, the stone bowls that were dedicated to Mesopotamian gods or the hundreds of goddess figurines made of marble or alabaster. The spirits were constantly honoured by human worshipers with a medium of earthy materials, worthy of the gods.

The remains of artefacts found in mines give us a sense of the level of mysticism and ritual that surrounded the act of mining. Topping and Lynott (2005) point out that stone hand axes were left behind and backfilled in the flint mines at Cissbury, England. Could this represent a symbolic effort to return material back from where it came? In one case bird remains were found in a mine, and other artefacts – pottery, offerings of different kinds and graffiti – have also been found and thought to be symbols, messages, or payment for extracting a material. In a general sense, materials brought up from deep within the Earth held a higher value than identical examples found on the surface. Topping and Lynott (2005) suggest mines may have been perceived as portals to the underworld or to an alternative dimension. Descending into a mine may have been equivalent to going through a series of transitions and accessing a spiritual world. Whatever came out from the depths of the Earth was not only highly valued but spiritually endowed, see Topping (2010), Topping and Lynott (2005), and O'Brien (2015).

The mining, and quarrying of Earth's materials required formalities or rituals before extraction could take place – a practice that was wide spread. Scott and Thiessen (2005) point out an example from the quarrying of catlinite (a native American stone) in Minnesota where it was used in the making of ceremonial pipes. North American ethnographic documents reveal that to dig in a catlinite quarry a worker had to be upstanding and beyond reproach, and he had to undergo a purification ritual before he was allowed to work in the quarry.

Not all miners saw the mines as a sanctified place. In 1556 Agricola reports that evil beings inhabited the mines: "Demons ('of ferocious aspect') are expelled and put to flight by prayer and fasting." (Agricola 1950). It is not certain that Agricola was referring to animal or insect "pests" or whether he believed, as many did in his day, that mines were inhabited by real demons or gnomes. Miners viewed their underworld in distinct ways, as not only did it contain mythical spirits, but it was deep in the hollows of the Earth where they made their livelihood. They considered mining a special opportunity and may have felt a kind of symbiosis and respect for being so close to the inner holiness of the Earth.

1.9 Conclusions

In this chapter we have reviewed a number of materials exploited in pre–Classical antiquity. Agate was used as a coveted decorative piece. Obsidian was a material worked into tools and weapons. Alabaster was shaped into vases, trinkets and goddess figurines. Chlorite was carved into bowls for export and offered as gifts to gods. Plaster was made from gypsum and lime, which introduced craftsmen to the role of fire to transform materials. In every case a hard material or mineral was mined or quarried then processed in some way.

While objects in an archaeological excavation may be viewed for their craftsmanship, they also represent a vast network of human activity. The mining and quarrying of materials often took place in remote areas, which meant that in order to exploit them workers had to travel inconvenient distances. The support system for maintaining a workforce would eventually be established, thus constituting what some refer to as "*la chaine opératoire*": a network chain that allowed support to flow in one direction and the mined product to flow in the other. For this system to be successful a number of social components had to be in place. First, a potential market had to exist, connections and agreements for trade with that market had to be firmly established, and finally, a defined and determined portion of the population had to commit to the different stages of the production-to-trade process. An excellent review of these issues is provided by O'Brien (2015) and Knapp and Piggott (1998).

Not less important is the cultural orientation that such groups had with the known mainstream populations in the market regions. Other gnawing questions arise. Were women employed in some part of the production process, or young boys who could crawl into small confined spaces of a mine? We know that there were mining opera-

tions devoted to one product, as we saw at the Kestel tin mine. To what extent were communities interwoven and interdependent? Were there many communities devoted to a selected range of economic activities that included not only the exploitation of material but complementary crafts such as charcoal making, textiles, or leather production? The availability of firewood (charcoal) may have lent itself to other industries such as pottery making or plaster production in addition to supplying charcoal to the metallurgical industry. Many configurations are possible, and hopefully, future archaeological work in the remote areas of Turkey and elsewhere in the Near East will reveal for us essential details of natural resource exploitation, and the communities involved will gain a place in the archaeological record.

References

Agricola G (1950) De Re Metallica (trans: H.C. Hoover and L.H. Hoover). Dover Publications, New York

Aruz J (2003) Art and interconnections in the third millennium B.C. In: Aruz J (ed) Art of the first cities: the third millennium B.C. from the Mediterranean to the indus. Metropolitan Museum of Art, New Haven, CT, pp 239–250

Balkan-Atli N, Binder D, Cauvin M-C, Bicakci E, Aprahamian GD, Kuzuçuoğlu C (1999) Obsidian: sources, workshops, and trade in Central Anatolia. In: Özdoğan M, Başgelen N (eds) Neolithic in Turkey: the cradle of civilization. Arkeoloji ve Sanat Yayınları, Istanbul, pp 133–145

Bilgi Ö (2014) Anthropomorphic representations in Anatolia. Aygaz, Istanbul

Blackman J (1982) The manufacture and use of burned lime plaster at Proto-Elamite Aushan (Iran). In: Wertime T, Wertime S (eds) Early pyrotechnology. The evolution of the first fire-using industries. Smithsonian Institution Press, Washington, DC, pp 107–115

Caley E, Richards JFC (1956) Theophrastus on stones. Ohio State University Press, Columbus

de Jesus PS (1978) Metal resources in ancient Anatolia. Anatol Stud 28:97–102

de Jesus PS (1980) The development of prehistoric mining and metallurgy in Anatolia. British Archaeological Reports, Oxford

de Jesus PS (1981) A survey of some ancient mines and smelting sites in Turkey. Archäol Naturwissenschaften 2:95–105

Gourdin WH, Kingery WD (1975) The beginnings of pyrotechnology: Neolithic and Egyptian lime plaster. J Field Archaeol 2(1–2):133–150

Gourgaud A, Cauvin MC, Gratuze B, Arnaud N, Poupeau G, Poidevin J-L, Chataigner C (eds) (1998) L'Obsidienne au Proche Et Moyen Orient: Du Volcan à l'Outil. British Archaeological Reports, Oxford

Günay G (2002) Gypsum Karst, Sivas, Turkey. Environ Geol 42(4):387–398

Hansen D (2003) Art of the early City states. In: Aruz J (ed) The art of the first cities. Metropolitan Museum of Art, New York, pp 21–37

Hublin JJ, Ben-Ncer A, Bailey SE, Freidline SE, Neubauer S, Skinner MM, Bergmann I, Le Cabec A, Benazzi S, Harvati K, Gunz P (2017) New fossils from Jebel Irhoud, Morocco and the pan-African origin of *Homo sapiens*. Nature 546:289–293

Joukowsky M (1996) Early Turkey: an introduction to the archaeology of Anatolia from prehistoric through the Lydian period. Kendall/Hunt Publishing Co, Dubuque

Kaptan E (1982) New findings on the mining history of Turkey around Tokat region. Bull Min Res Exp 93(94):150–162

Kaptan E (1984) New discoveries in the mining history of Turkey in the neighborhood of Gümüşkōy, Kütahya. Bull Min Res Exp 97(98):60–76

Kaptan E (1986) Ancient Mining in the Tokat Province. Anatolica XIII:19–36
Kaptan E (1991) Anadolu'da Tarihlenen Eski Yeralti Maden İsletmeleri Türkiye. *[The ancient underground mines dated in Anatolia]* Abstracts of 44th Geological congress of Turkey 1991. JMO, Ankara
Knapp BA, Piggott VC (eds) (1998) Social approaches to an industrial past: the archaeology and anthropology of mining. Routledge, London
Kohl PL (2001) Reflections on the production of chlorite at Tepe Yahya: 25 years later. In: Potts DT, Pittman H, Kohl PL (eds) Excavations at Tepe Yahya, Iran, 1967–1975: the third millennium. Peabody Museum of Archaeology & Ethnology, Cambridge, MA, pp 209–230
Kohl PL, Bäck LR, Gilman A, Hamlin CL, Hayashi K, Lamberg-Karlovsky CC, Nissen HJ (1978) The balance of trade in Southwestern Asia in the mid-third millennium B.C.. [and comments and reply. Curr Anthropol 19(3):463–492
Lamberg-Karlovsky CC (1988) The 'intercultural style' carved vessels. Iran Antiq 23:45–95
Lucas A, Harris JR (1962) Ancient Egyptian materials and industries, 4th edn. Edward Arnold Publishers Ltd., London
Mellaart J (1973) The Neolithic of the near east. Thames and Hudson, London
Moorey PRS (1999) Ancient Mesopotamian materials and industries: the archaeological evidence. Miami, Eisenbrauns
MTA (1966) Türkiye Mermer Evanteri [*Marble inventory of Turkey*] No. 134 MTA Publication Ankara
Nazaroff AJ, Baysal A, Çiftçi Y (2013) The importance of Chert in Central Anatolia: lessons from the Neolithic assemblage at Çatal Höyük, Turkey. Geoarchaeology 28(4):346–362
Nicholson PT, Shaw I (2009) Ancient Egyptian materials and technology, 2nd edn. Cambridge University Press, Cambridge, UK
Oates D, Oates J (1976) The rise of civilization. Elsevier Phaidon, New York
O'Brien W (2015) Prehistoric copper mining in Europe. Oxford University Press, Oxford
Özbal H (2009) New analytical data from Göltepe crucibles. J TUBA 12:155–163
Palmieri A, Sertok K, Chernykh E (1993) Metalwork to arsenical copper technology in Eastern Anatolia. In: Francipane M (ed) Between the Rivers and over the mountains: archaeologica anatolica et mesopotamica, Alba Palmieri dedicate. University of Rome, Rome, pp 573–599
Parrot A (1960) Sumer. Gallimard, Paris
Pfeiffer J (1973) The emergence of man. Cardinal, New York
Pfeiffer J (1982) The creative explosion: an inquiry into the origins of art and religion. Harper & Row, New York
Picq P (2013) Au commencement était l'Homme. Odile Jacob, Paris
Potts TF (1989) Foreign stone vessels of the late third millennium B.C. from Southern Mesopotamia: their origins and mechanisms of exchange. Iraq 5:123–164. https://doi.org/10.2307/4200300
Potts DT, Pittman H, Kohl PL (2001) Excavations at Tepe Yahya, Iran, 1967–1975: the third millennium. Peabody Museum of Archaeology & Ethnology, Cambridge, MA
Rapp GR, Hill CL (1998) Geoarchaeology: the earth-science approach to archaeological interpretation. Yale University Press, New Haven
Renfrew C (1977) Alternative models for exchange and spacial distribution. In: Earle T, Ericson J (eds) Exchange systems in prehistory. Academic, New York, pp 71–90
Rosenfeld A (1965) The inorganic raw materials of antiquity. Weidenfeld and Nicolson, London
Rudgley R (1999) The lost civilizations of the stone age. The Free Press, New York
Ryan CW (1960) A guide to the known minerals of Turkey. Mineral Research and Exploration Institute of Turkey, Ankara
Schmidt K (2000) Göbekli Tepe, Southeastern Turkey. A preliminary report on the 1995–1999 excavations. Paléorient 26(1):45–54
Schmidt K (2012) Göbekli Tepe. A stone age sanctuary in south-eastern Anatolia. C.H. Beck, Munich (2007)

Scott DD, Thiessen TD (2005) Catlinite extraction at pipestone national monument, Minnesota: social and technological implications. In: Topping P, Lynott M (eds) The cultural landscape of prehistoric mines. Oxbow Books, Oxford, pp 140–154

Storemyr P, Bloxam E, Heldal T, Kelany A (2010) Conservation of ancient stone quarry landscapes in Egypt. In: Brewer-LaPorta M, Burke A, Field D (eds) Ancient mines and quarries. A trans-Atlantic perspective. Oxbow Books, Oxford, pp 38–55

Teeter E (2011) Before the pyramids. The Oriental Institute, Chicago

Topping P (2010) Neolithic axe quarries and Flint mines: towards an ethnography of prehistoric extraction. In: Brewer-La Porta M, Burke A, Field D (eds) Ancient mines and quarries. A trans-Atlantic perspective. Oxbow Books, Oxford, pp 23–32

Topping P, Lynott M (eds) (2005) The cultural landscape of prehistoric mines. Oxbow Books, Oxford

Wagner GA (1989) Archäometallurgische Untersuchungen an Rohstoffquellen des Frühen Kupfers in Ostantoliens. Jahrb Römisch-Germanischen Zentralmuseums Mainz 36:637–686

Wagner GA, Pernicka E, Seeliger TC, Lorenz IB, Begemann F, Schmidt-Strecker S, Eibner C, Oztunalı Ö (1986) Geochemische Und Isotopische Charakertistika Früher Rohstoffquellen für Kupfer, Blei, Silver und Gold in der Türkei. Jahrb Römisch-Germanischen Zentralmuseums Mainz 33:723–752

Wright G (1969) Obsidian analyses and prehistoric near eastern trade: 7500 to 3500 B.C. anthropological papers. The University of Michigan, Ann Arbor, p 37

Yalçın Ü, Özbal H, Paşamehmetoğlu GA (2008) Ancient Mining in Turkey and the Eastern Mediterranean: International Conference AMITEM 2008, June 15–22. Atılım University, Ankara

Yener AK (2000) The domestication of metals: the rise of complex metal industries in Anatolia. Brill, Leiden

Yener AK, Özbal H (1987) Tin in the Turkish Taurus mountains: the Bolkardağ Mining District. Antiquity 61(232):220–226

Yener AK, Vandiver PB (1993) Tin processing at Göltepe, an early bronze age site in Anatolia. Am J Archaeol 97(2):207–238

Chapter 2
A Review of the Geology and Geodynamic Evolution of Tectonic Terranes in Turkey

M. Cemal Göncüoğlu

Abstract The geodynamic evolution of Turkey is mainly controlled by drift and collision of a number oceanic and continental plates or terranes. This can be ascribed to four orogenic episodes, namely: the Cadomian, Variscan, Cimmerian and Alpine. During these episodes, terranes were formed in a wide range of tectonic settings, including active and passive continental margins, rifts, arcs and suture complexes between the Gondwana supercontinent in the South and the Eurasian supercontinent in the North. The arrangements and re-arrangements of these terranes in the past 500 Ma gave way to a very complex mosaic of geological units with a wide variety of igneous, sedimentary and metamorphic units, as well as related mineral systems, as discussed in the chapters of this book.

In this chapter a brief review of these geological processes will be summarised within the framework of the geodynamic evolution to provide a background for the igneous activity, sedimentary rocks, metamorphic processes and formation of the mineral resources in Turkey.

2.1 Introduction

Turkey is made up of numerous fragments of continental and oceanic lithosphere (Şengör and Yılmaz 1981; Yılmaz 1990; Göncüoğlu et al. 1997; Okay and Tüysüz 1999; Stampfli 2000; Moix et al. 2008; Göncüoğlu 2010). These were rifted off from the main body of Gondwana or Eurasia, drifted by the opening of Tethyan oceanic branches and amalgamated to each other or on one of the supercontinents during the geological past. These rifting-drifting and collision events comprise distinct orogenies. In the Eastern Mediterranean area at least four orogenic events, known as the Pan-African/Cadomian, Variscan, Cimmerian and Alpine cycles have controlled the distribution of oceanic and continental plates or terranes (*sensu* Howell 1995). Each of these cycles re-distributed the terrane-configuration of the earlier ones. The Alpine orogeny, the last main orogenic event in Turkey, related to the closure of

M. C. Göncüoğlu (✉)
Department of Geological Engineering, Middle East Technical University, Ankara, Turkey
e-mail: mcgoncu@metu.edu.tr

F. Pirajno et al. (eds.), *Mineral Resources of Turkey*, Modern Approaches in Solid Earth Sciences 16, https://doi.org/10.1007/978-3-030-02950-0_2

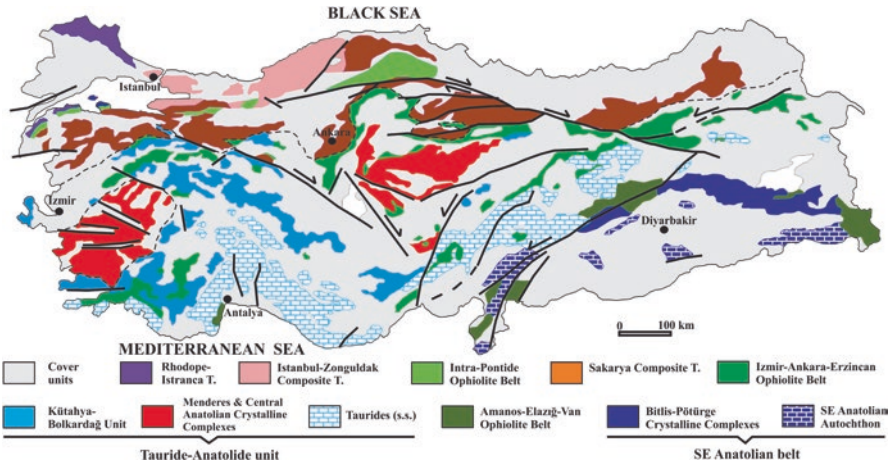

Fig. 2.1 Distribution of the main Alpine tectonic units of Turkey. (Modified after Göncüoğlu 2010)

Mesozoic-Tertiary Neotethyan oceanic branches, has roughly shaped the present distribution of these terranes. However, the final picture shown in Fig. 2.1 is controlled by a number of post-orogenic events of the"Neotectonic Period".

In this brief review, we will first describe the main terranes of the Alpine cycle with their pre-Alpine components. Secondly, we will evaluate the tectonic processes and their igneous products in relation with the main orogenic cycles within these terranes. The aim of this review is to provide a comprehensive representation for a better understanding of the distribution of the mineral resources in Turkey. It includes many over-simplifications for the sake of simplicity of the very complex geology of Turkey. For a more detailed review with a more or less complete reference list of previous studies, the reader is referred to (Göncüoğlu 2010).

2.2 Tectonic Classification of the Terranes of Turkey

The classification of the Turkish terranes is mainly based on their configuration, where a number of terranes of continental crust origin were separated by three main oceanic branches of Neotethys. From South to the North these are: the SE Anatolian Autochthon at the northern edge of the Gondwanan Arabian-Libyan Platform; the SE Anatolian Ophiolite Belt including the remnants of the southern branch of Neotethys; the Tauride-Anatolide Terrane, an Alpine unit of continental crust origin; the Izmir-Ankara-Erzincan Ophiolite Belt, representing the allochthonous oceanic assemblages and subduction-accretion complexes of the Neotethyan Ocean; the Sakarya Composite Terrane, including products of at least two orogenic events; the Intra-Pontide Ophiolite Belt, remnants of the northern branch of the Neotethys; the Istanbul-Zonguldak Terrane of continental crust origin and lastly the Istranca

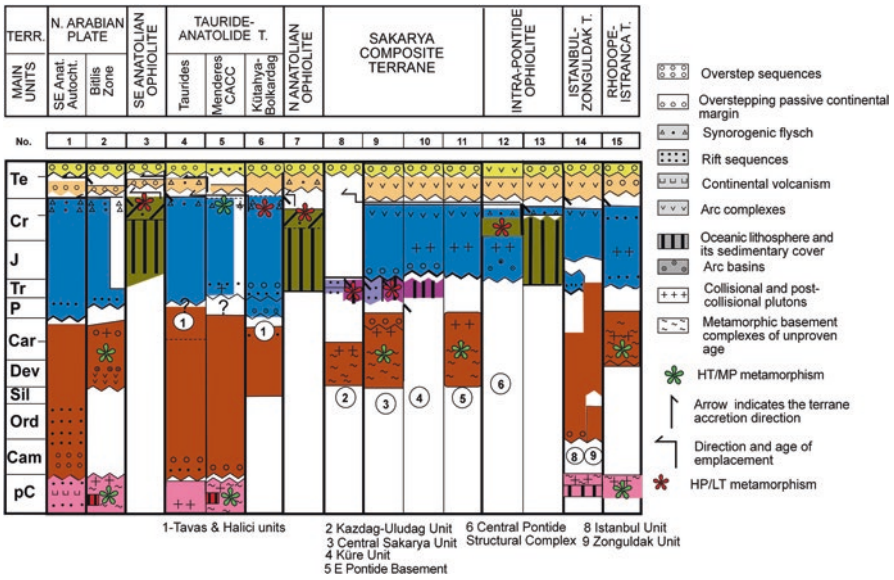

Fig. 2.2 Simplified lithostratigraphy of the Alpine terranes in Turkey. (Modified after Göncüoğlu et al. 1997; Göncüoğlu 2010)

Terrane, a suspect terrane of Laurasian affinity. A composite log with the generalized lithostratigraphies and the structural relationships of the Alpine terranes with the products of earlier orogenic events in their basement such as the Cimmerian, Variscan and Cadomian cycles, respectively, are shown in Fig. 2.2.

The log also includes information on the type of the depositional environment, general characteristics of the igneous and metamorphic processes and the age and direction of the main tectonic movements. In this way, a regional correlation of the major geological events can be accomplished across the terranes for the Alpine and pre-Alpine periods.

2.3 Description of the Alpine Turkish Terranes

2.3.1 The SE Anatolian Autochthon

This southernmost terrane in Turkey represents the northern edge of the Arabian plate and comprises a Late Neoproterozoic volcanic-volcaniclastic basement (e.g. Gürsu et al. 2015), transgressively overlain by Lower–Middle Paleozoic siliciclastic rocks (Fig. 2.3). Late Permian shelf-type limestones are unconformably overlying the older successions. This important unconformity may represent the far-field effect of a regional uplifting related to the Late Permian opening of the Southern Neotethyan branch or the Bitlis-Zagros Ocean towards N of the Arabian Plate.

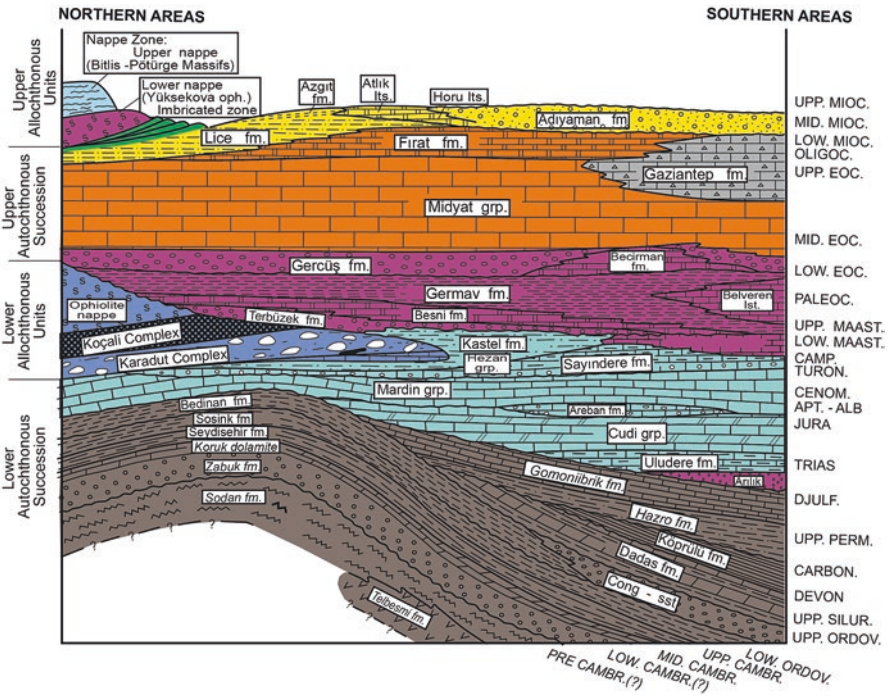

Fig. 2.3 Simplified stratigraphic section of the SE Anatolian Autochthon (After Perinçek et al. 1991)

The Late Permian platform-type carbonates are transitional to the Triassic – Early Cretaceous shallow marine sediments, indicating to stabilisation of the platform conditions (Perinçek et al. 1991). During Early to Late Cretaceous, the depositional environment changed to the slope and subsequently to basin conditions. During the Late Cretaceous, the SE Anatolian Autochthon was the site of foreland deposition where an orogenic flysch with ophiolitic detritus was laid down. Ophiolitic nappes derived from the northerly located Southern Neotethyan branch have arrived in the area at the end of Cretaceous. These Late Cretaceous allochthons are covered by Tertiary marine sediments, where a distinct and widespread bimodal volcanism (Maden Volcanics) of Middle Eocene age is recorded (e.g. Erler 1984).

The Paleogene deposits in this area are mainly shallow-marine carbonates, that grade into evaporites and finally into continental clastics. During the late Early Miocene the second set of allochthons comprising the Bitlis-Pütürge Metamorphics were emplaced onto the Southeast Anatolian Autochthon due to ongoing northward movement of the Arabian Plate.

Regarding the geological evolution, there is a consensus that the SE Anatolian Autochthon was located on the N promontory of the Arabian Plate all along its geological past.

The only pre-early Phanerozoic igneous record is the late Neoproterozoic (580–560 Ma) bimodal volcanism (Gürsu et al. 2015, typical for Andean-type active continental margins along the Cadomian continent (Fig. 2.4)).

The Mid-Miocene- Quaternary volcanism in the SE Anatolian Autochthon is the result of the regional extension, related to the mantle uplifting. The extensive

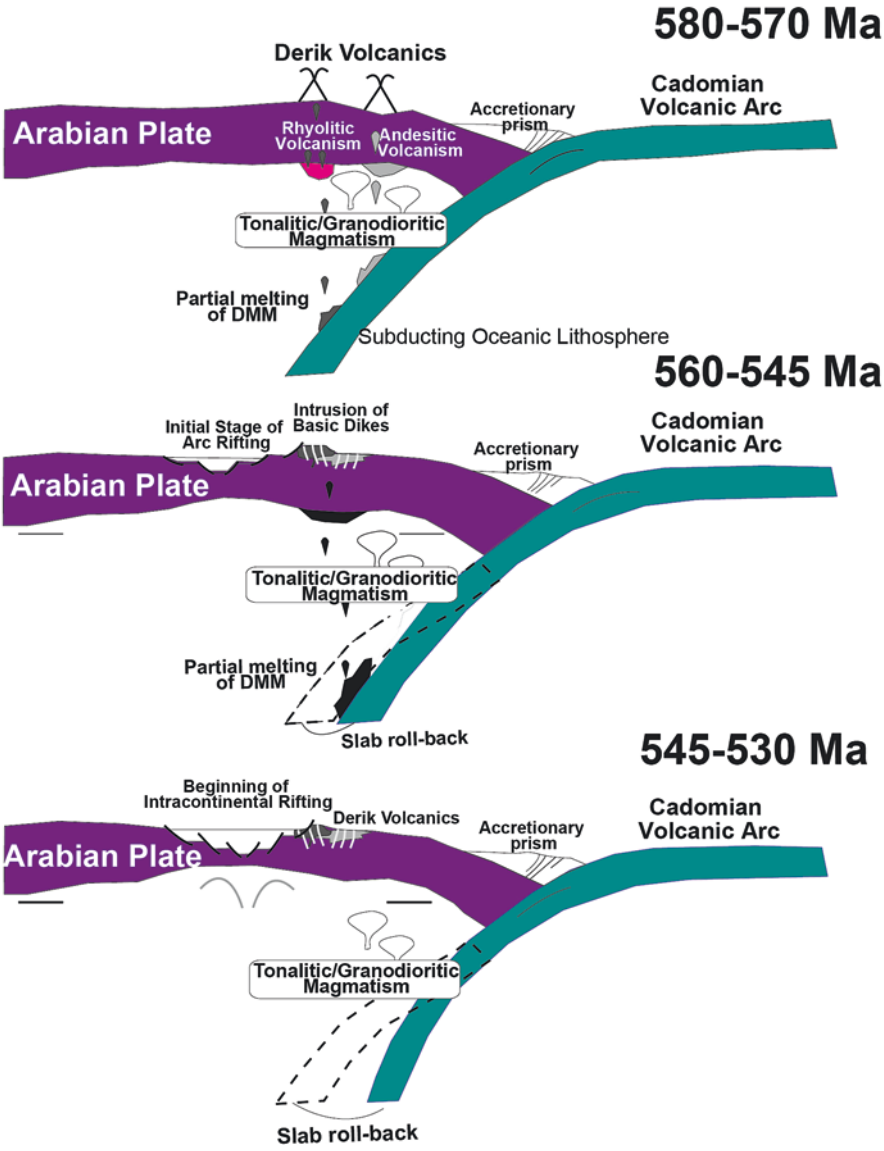

Fig. 2.4 Geodynamic evolution of the Late Neoproterozoic-Early Cambrian magmatism in SE Anatolian Autochthon. (After Gürsu et al. 2015)

volcanism on the East Anatolian-W Iranian Plateau and the formation of the East Anatolian Transform Fault Zone are also coeval with this uplifting in SE Anatolia (e.g. Perinçek et al. 1991).

2.3.2 The Bitlis-Pütürge Metamorphic Belt

The Bitlis- Pütürge Metamorphic Belt comprises S-verging slices of metamorphic rocks, ophiolitic melanges and their sedimentary covers. The overall stratigraphy of the metamorphic rocks is very similar to the SE Anatolian Autochthon (Fig. 2.5). Various para- and orthogneisses, migmatites, amphibolites and mica schists with knockers of kyanite-eclogites (e.g. Okay et al. 1985; Oberhänsli et al. 2013) make up the basement of the belt (Göncüoğlu and Turhan 1984).

The orthogneisses yielded Late Neoproterozoic-Early Cambrian radiometric ages, which are interpreted as intrusion ages (e.g. Ustaömer et al. 2009). The overlying Palaeozoic cover consists of the low-grade meta-clastic Lower Palaeozoic sequence. They are unconformably overlain by Devonian metacarbonates, Carboniferous metaclastics and felsic metavolcanic/volcanoclastic rocks, respectively. Middle Permian platform-type carbonates unconformably overlie the older successions and grade upwards into Middle Triassic metavolcanic and -volcanoclastics and finally into a condensed series with metapelites, metabasalts and metacherts of Late Triassic-Early Cretaceous age. This low-grade metamorphic succession is tectonically overlain by ophiolites and ophiolitic olistostromes of Late Cretaceous age. The metamorphic rocks and the overlying ophiolitic unit are unconformably overlain by Middle Eocene shallow marine sediments and volcanic rocks. The final emplacement of the metamorphic rocks and ophiolites together with their Eocene cover units, onto the Southeast Anatolian Autochthon, is Middle Miocene in age.

The metamorphic sequence of the Bitlis-Pütürge Metamorphic Belt is interpreted as the representative of the northern edge of the Arabian passive margin, upon which oceanic assemblages were emplaced from the northerly located Southern Branch of Neotethys. The obduction of the ophiolitic nappes onto the platform-margin and resulting crustal thickening during the Late Cretaceous have very probably gave way to the metamorphism of the belt.

2.3.3 The Southeast Neotethyan Suture Belt

The unit is also known as the Bitlis-Zagros Suture Belt or Amanos-Elazığ-Van Suture Belt (e.g. Göncüoğlu 2014). The belt comprises thrust slices representing the Southern Neotethyan oceanic lithosphere together with arc-related assemblages and a huge subduction-accretion prism (Ural et al. 2015 and the references therein). It separates the SE Anatolian Autochthon from the northerly located Tauride-Anatolide

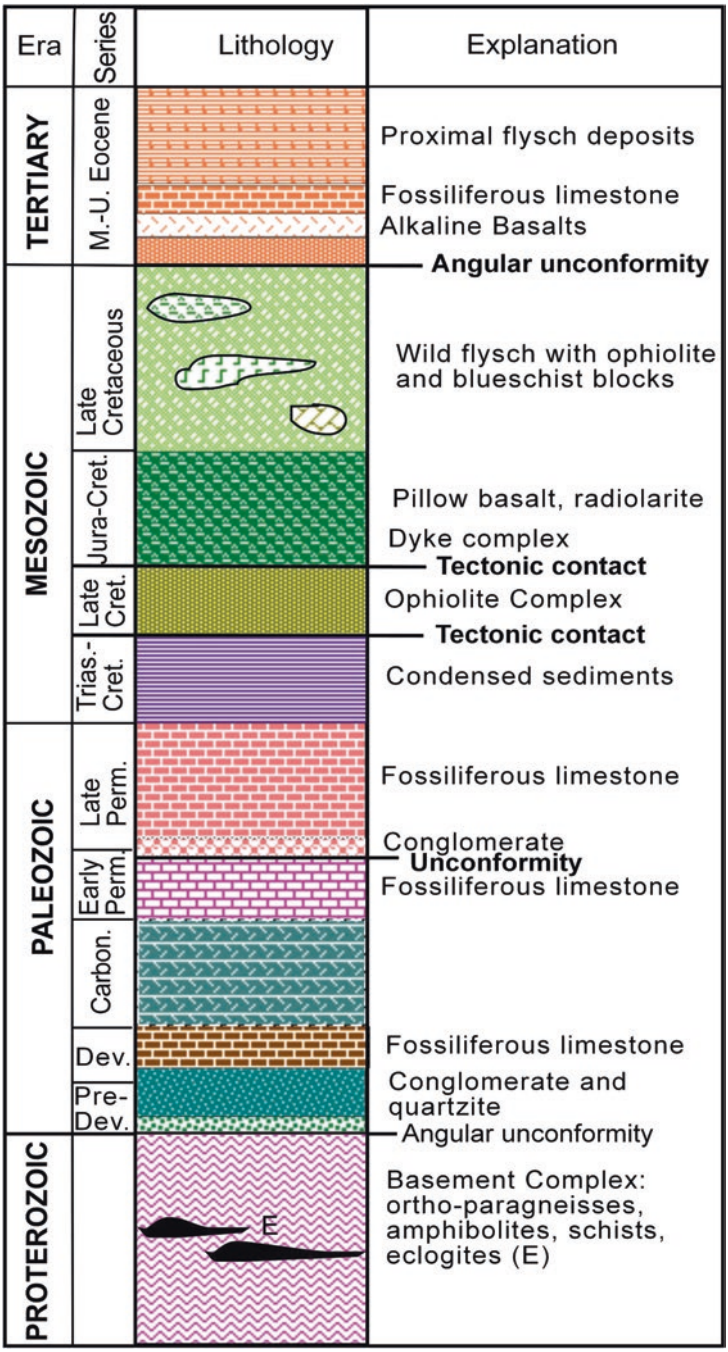

Fig. 2.5 Simplified lithostratigrahic column of the Bitlis Metamorphics. (After Göncüoğlu and Turhan 1984)

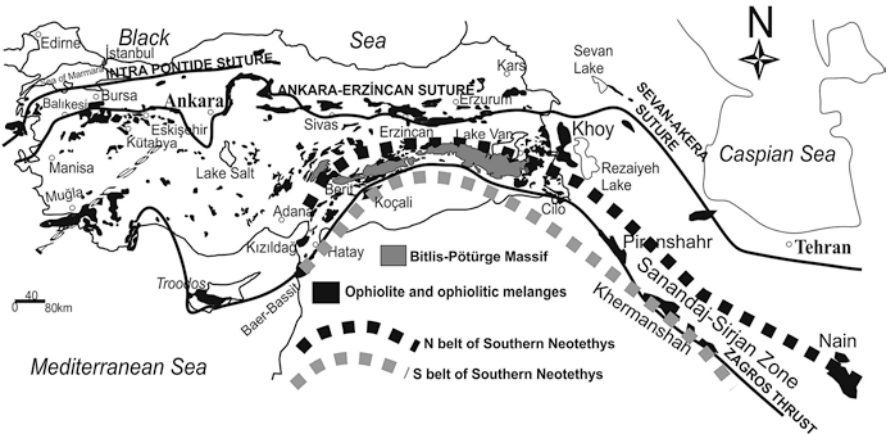

Fig. 2.6 Distribution of ophiolites and ophiolitic mélanges along the Southeast Neotethyan Suture Belt. (After Göncüoğlu 2014)

Terrane (Fig. 2.6) and its marginal arc (Yılmaz 1993; Yılmaz et al. 1993; Robertson 2002; Parlak et al. 2004; Robertson et al. 2007).

The ophiolitic bodies (e.g. Guleman, Kömürhan, Ispendere, Cilo, Kızıldağ, Troodos, Alanya ophiolites, e.g. Tekeli and Erendil 1984) within the belt include large (up to 400 km^2) tectonic units and represent an almost complete supra-subduction type oceanic lithosphere. In these bodies peridotites with podiform chromites dominate over lherzolites. Well-developed sequences of ultramafic- and mafic cumulates, gabbros, plagiogranites, variably preserved sheeted-dyke complexes and pillow lavas are common members. The oldest age yet obtained from the radiolarian chert- OIB-type pillow lava associations within the accretionary mélange is Ladinian in the W and Carnian in the E (Varol et al. 2011; Uzuncimen et al. 2011).

The youngest crustal volcanic rocks within same at the Iranian border (Yüksekova Complex of Perincek 1979) are mainly of island-arc and back-arc type and associated with Late Cretaceous (Fig. 2.7.) radiolarian cherts (e.g. Tekin et al. 2015; Çolakoğlu et al. 2014; Göncüoğlu et al. 2015).

The initial emplacement age of the ophiolites onto the Arabian margin is Late Cretaceous. The ophiolites of the SE Anatolian Suture Belt correlate with the Zagros and Oman Ophiolites in Iran (Fig. 2.6) and the Troodos Massif in Cyprus (Göncüoğlu et al. 2014). It is still a matter of debate whether the Southern Neotethys was a single or multi-armed Ocean (see Göncüoğlu et al. 2014 for the discussion). The suture belt is overlain by marine deposits of Mid-Eocene age that disconformably cover the allochthonous oceanic as well as the continental units of the suture belt and the surrounding continent margins. The roughly E-W trending Mid Eocene extensional/transtensional basins were the site of extensive volcanism known as the Maden Complex (e.g. Robertson et al. 2007).

The volcanism is represented by basalts and andesites with minor dacites and displays geochemical characteristics of within-plate basalts (e.g. Yiğitbaş and

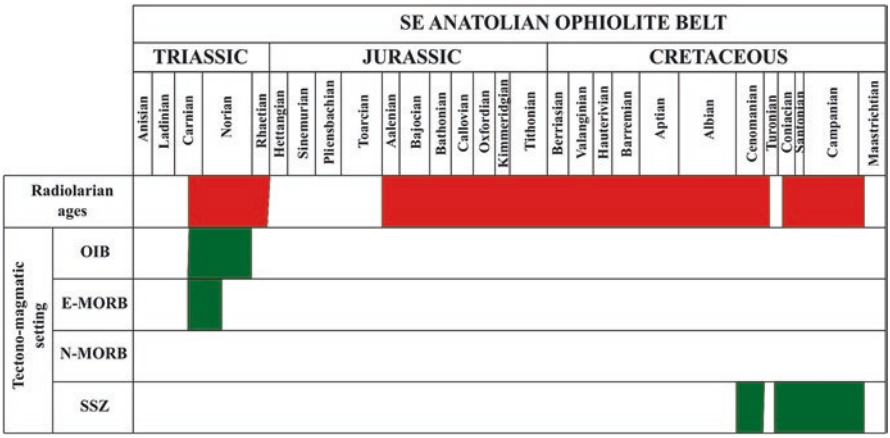

Fig. 2.7 Formation ages and tectono-magmatic classification of the oceanic lavas within the Southeast Neotethyan Suture Belt. (After Göncüoğlu et al. 2015; Abbreviations: *OIB* ocean island basalts, *MORB* mid-ocean ridge basalts, *E* enriched, *N*-; SSZ suprasubduction zone)

Yılmaz 1996). The preferred geodynamic evolutionary model of the SE Anatolian Suture Belt is given in Fig. 2.8.

2.3.4 Tauride-Anatolide Terrane

The continental microplate between the Northern and Southern Neotethyan branches is known as the Tauride-Anatolide Terrane. It is subdivided into three distinct belts: the Taurides (*sensu strictu)* the Massifs and the Kütahya-Bolkardağ Belt, that differ in their paleogeographic position and metamorphism during their alpine evolution. Of these, the Menderes and the Central Anatolian massifs together with the Kütahya-Bolkardağ Belt were included in the Anatolides in the classical nomenclature of Ketin (1966).

2.3.4.1 The Taurides

The Taurides or the Tauride Belt is characterising the main non-metamorphic body of the Paleozoic-Mesozoic succesions and was located on the Northern edge of Gondwana until its rifting during the end of Paleozoic. It remained as a platform surrounded during the Mesozoic by the Izmir-Ankara-Erzincan and Amanos-Elazığ-Van oceanic branches from North and South, respectively. The unit is represented by a Neoproterozoic basement (e.g. Gürsu and Göncüoğlu 2006) and its non-metamorphic Paleozoic-Mesozoic cover. During the closure of these branches in Late Cretaceous, a double-verging napped structure (Fig. 2.9) was formed.

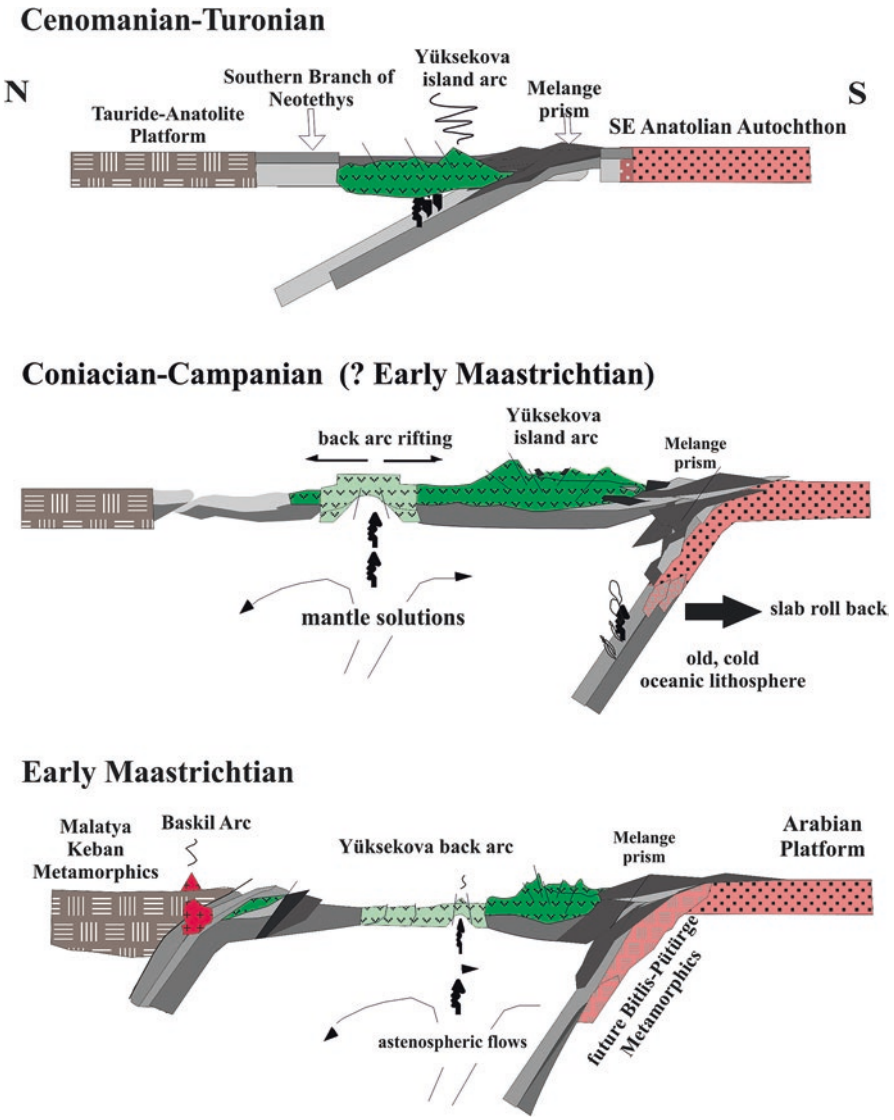

Fig. 2.8 A possible geodynamic scenario for the evolution of the Southeast Neotethyan Suture Belt. (After Göncüoğlu 2014; Ural et al. 2015)

A number of tectono-stratigraphic units (Bozkır, Bolkar, Aladag, Geyikdag) representing the N margin were sliced and thrust onto the platform. Pene-contemporaneously, others (Antalya and Alanya units) from the southern margin with distinctive stratigraphic and structural features characterising different depositional environments of the platform were thrust from S to N onto the central part of the platform (Özgül 1976) as late as the Early Eocene. The entire nappe-pile has been re-thrust

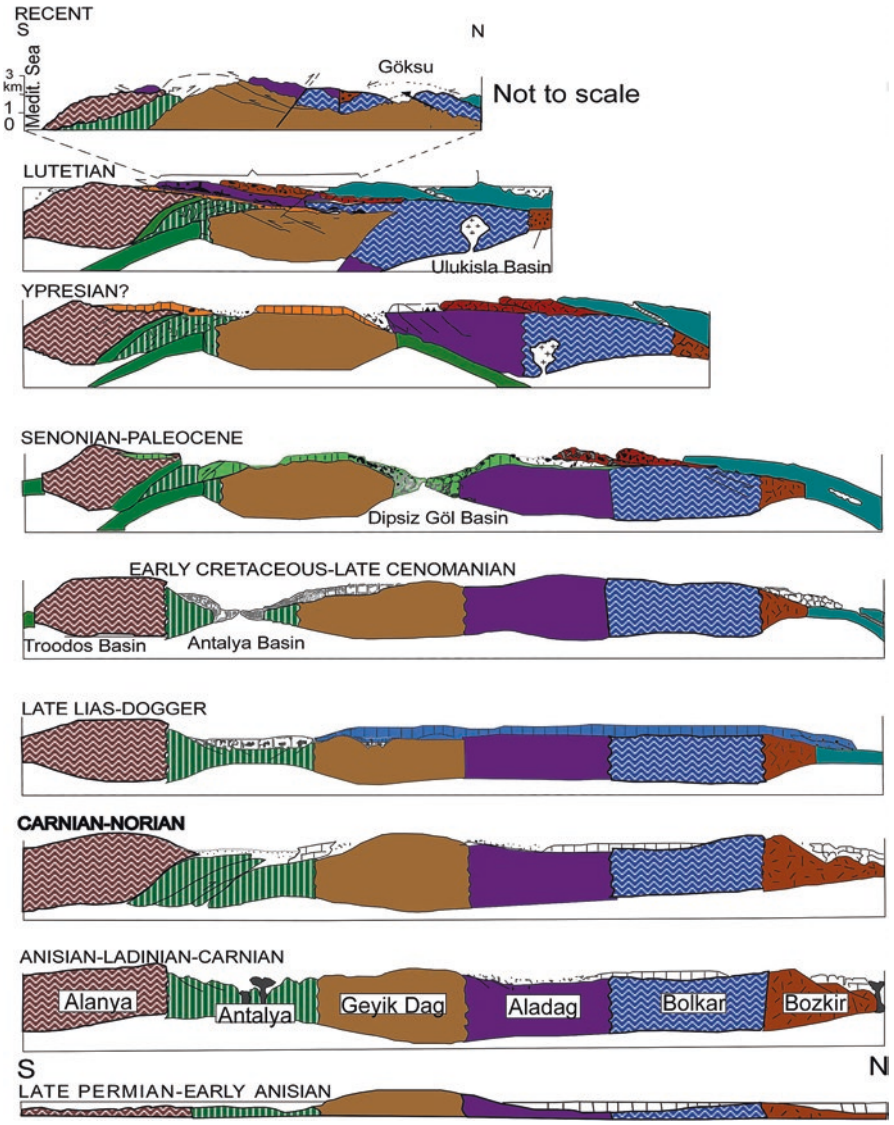

Fig. 2.9 Structural units of the Taurides and their tectonic relations. (Göncüoğlu 2010; modified after Özgül 1984)

on the Late Tertiary cover during the Mid-Miocene. Although oversimplified, the tectonic scenario of Özgül (1984) in Fig. 2.9 is beneficial for better-understanding of the Alpine geological evolution.

Regarding the generalised stratigraphy, the basement of the Taurides includes slightly metamorphosed Late Neoproterozoic metaclastic rocks (slates, conglomerates and greywackes), stromatolithic limestones and lydites, cut by rhyolites and

quartz-porphyries (Gürsu and Göncüoğlu 2006). The platform-type Palaeozoic successions show local differences in the tectono-stratigraphic units (for a detailed account see Göncüoğlu et al. 2004). The differences are controlled by the paleogeographic setting, where the external platform sequences are characterized by local unconformities compared to the continuous deposition in the axial part (Geyikdag unit) of the platform from earliest Cambrian to the Late Permian (Fig. 2.10).

A Late Carboniferous bi-modal magmatic activity and the important Early Late Permian regional unconformity in the northerly tectono-stratigraphic units (e.g. Aladag and Bolkardag units) indicates to far-distance effects of the late Variscan events to the North of the Tauride Platform (Göncüoğlu 2010). The Permian sequence represented by epicontinental carbonates is followed in the South and North of the platform by rift-related Early-Middle Triassic sediments and volcanics which indicate the opening of Neotethyan basins and thus the beginning of the Alpine cycle (Göncüoğlu et al. 2011). In the central part of the Tauride platform during the Middle Triassic-Early Cretaceous time interval neritic carbonates were mainly deposited, while in the northern as well as southern margins pelagic conditions prevailed.

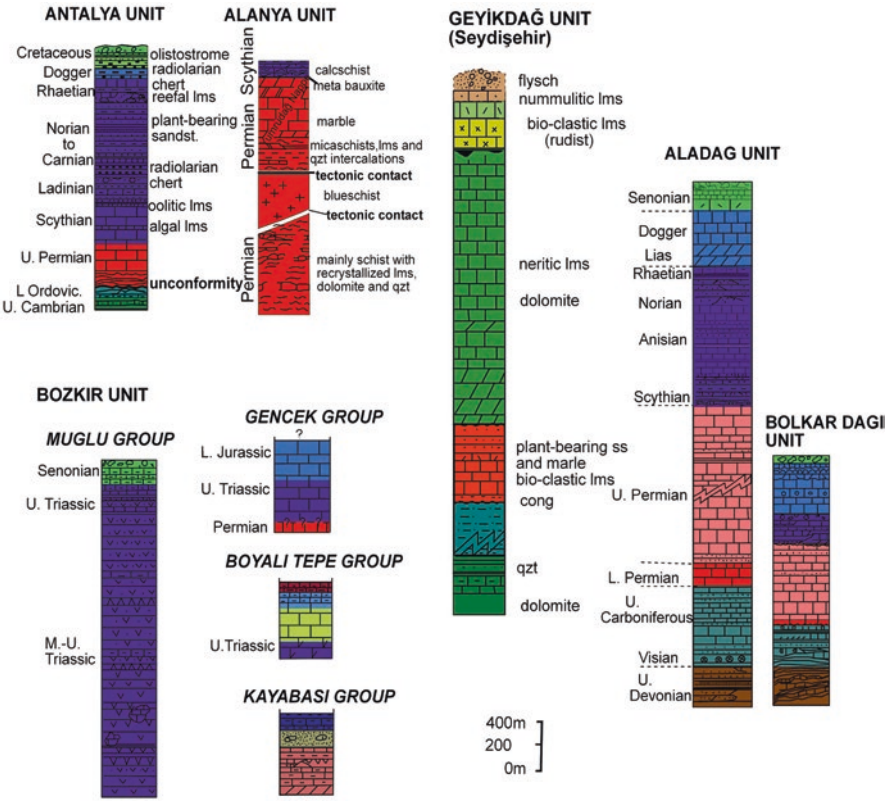

Fig. 2.10 Stratigraphy of the Tauride structural units. (After Özgül 1976, 1984)

During the Senonian ophiolitic as well as continental margin sequences were emplaced onto the more external parts of the platform by the closure the oceanic basins in the S and N of the platform. This closure resulted in subduction and high-pressure metamorphism of the margin sediments in the N (Kütahya-Bolkardağ Belt) and S (Alanya Unit). The crustal thickening in the more internal parts of the platform, on the other hand, produced the high-temperature metamorphism of the Menderes Massif and the Central Anatolian Crystalline Complex. In the southern edge of the platform, however, the northward subduction of the Amanos-Elazığ-Van oceanic lithosphere beneath the Taurides produced the Late Cretaceous arc magmatism (e.g. Baskil Magmatics, Parlak et al. 2004; Rızaoğlu et al. 2009).

Three oldest cover sediments on the imbricated units in the Central Taurides are Lutetian in age (Özgül 1984). The final re-thrusting of basement nappes onto this cover is of Middle Miocene age in Western Taurides.

2.3.4.2 The Central Anatolian Crystalline Complex and the Menderes Massif

The vast crystalline complexes in western and central Turkey are lithostratigraphically very similar to the non-metamorphic successions of the Taurides. They are assumed to represent the equivalents of the Taurides, deeply buried and metamorphosed during the Alpine crustal thickening (e.g. Özgül 1976; Göncüoğlu 1977; Bozkurt and Oberhansli 2001).

2.3.4.2.1 The Central Anatolian Crystalline Complex

The Central Anatolian Crystalline Complex (Akıman et al. 1993; Göncüoğlu and Türeli 1994) is bounded to the main body of the Taurides by the Tertiary Tuz Gölü, Ulukışla and Sivas basins. The supposed basement of the Central Anatolian Crystalline Complex is composed of sillimanite-cordierite bearing gneisses, pyroxene gneisses, micaschists, amphibolites, bands and lenses of marbles/calc-silicate marbles and migmatites (Fig. 2.11). The Late Neoproterozoic core ages of zircons from S-type granitoid (e.g. Köksal et al. 2004) suggest a Gondwanan origin.

The overlying very thick cover series begins with a thick quartzite unit, followed by an alternation of marbles, sillimanite gneisses, amphibolites, calc-silicate amphibolites and quartzites resembling the Palaeozoic successions of the Taurides. The upper unit of the cover series is the metamorphic equivalent of the Triassic-Early Cretaceous carbonate sequence of the Taurides and the Kütahya-Bolkardağ Belt. Upwards, the meta-carbonates passes into cherty marbles and finally into meta-cherts, a succession also known from the slope to basin-type sediments of the Tauride, Kütahya-Bolkardag and Menderes units (e.g. Göncüoğlu 2011). They are transitional to an ophiolite bearing meta-olistostrome and finally overthrust by disrupted supra-subduction zone-type ophiolites of early Late Cretaceous age (Yalınız et al. 1996, 2000; Floyd et al. 1998).

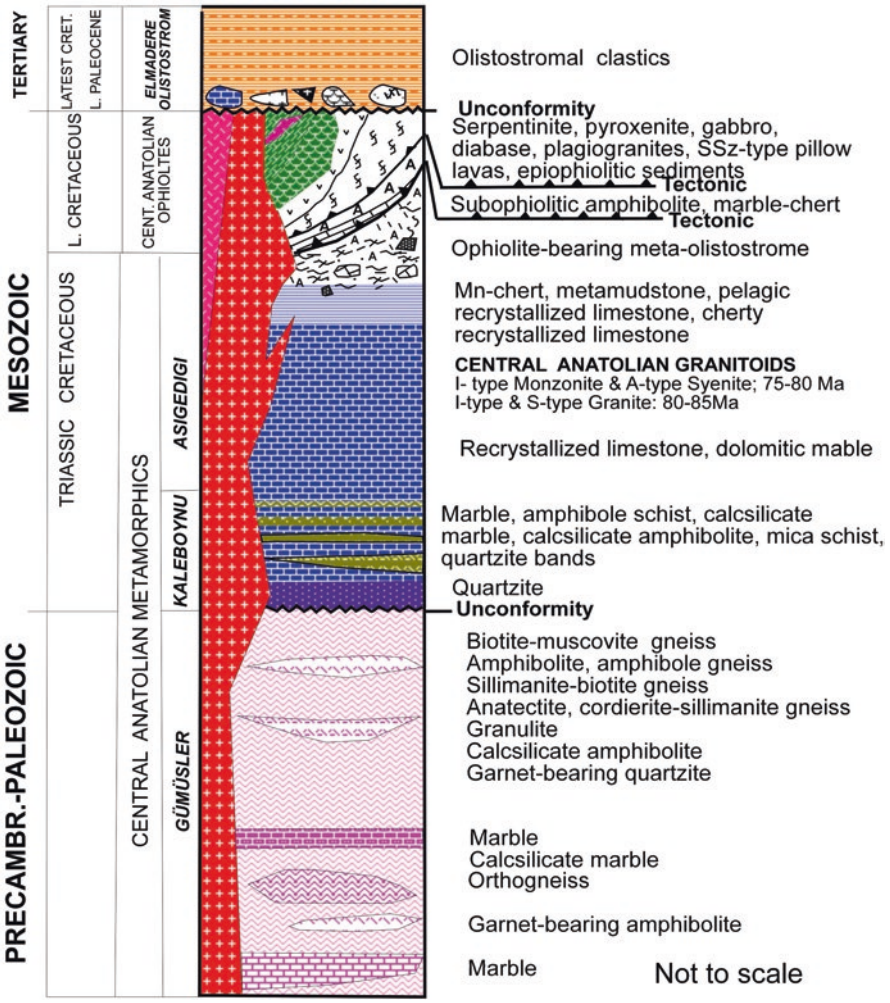

Fig. 2.11 Lithostratigraphy of the Central Anatolian Crystalline Complex. (After Göncüoğlu 2010)

The Alpine metamorphism has reached upper amphibolite facies conditions and dated by zircons as 85 Ma (Whitney and Hamilton 2004). The metamorphic successions, as well as the overthrust ophiolites, are intruded by I and S-type post metamorphic collision-type granitoid with two groups of zircon ages of 85 and 75 Ma, respectively (Köksal et al. 2004, 2013; Boztuğ et al. 2007a, b).

The Central Anatolian Crystalline Complex is disconformably overlain by Late Maastrichtian-Early Paleocene sediments. The youngest marine sediments on the complex are Middle-Upper Eocene in age. They are alternating with calc-alkaline–mildly alkaline basalts derived from subduction-modified lithospheric mantle

(Geneli et al. 2010). The Neogene-Quaternary cover is mainly fluvial and comprises in its upper part also the Cappadocian volcanic and volcanoclastics.

2.3.4.2.2 The Menderes Massif

The Menderes Massif is a classic metamorphic core complex (e.g. Bozkurt 2001) consisting of a Late Neoproterozoic "gneissic core" and a Palaeozoic -Mesozoic "schist and marble envelope" (e.g. Dora et al. 1991, Fig. 2.12). The "core" consists of para- and orthogneisses, granulitic gneisses and amphibolites with relict eclogites

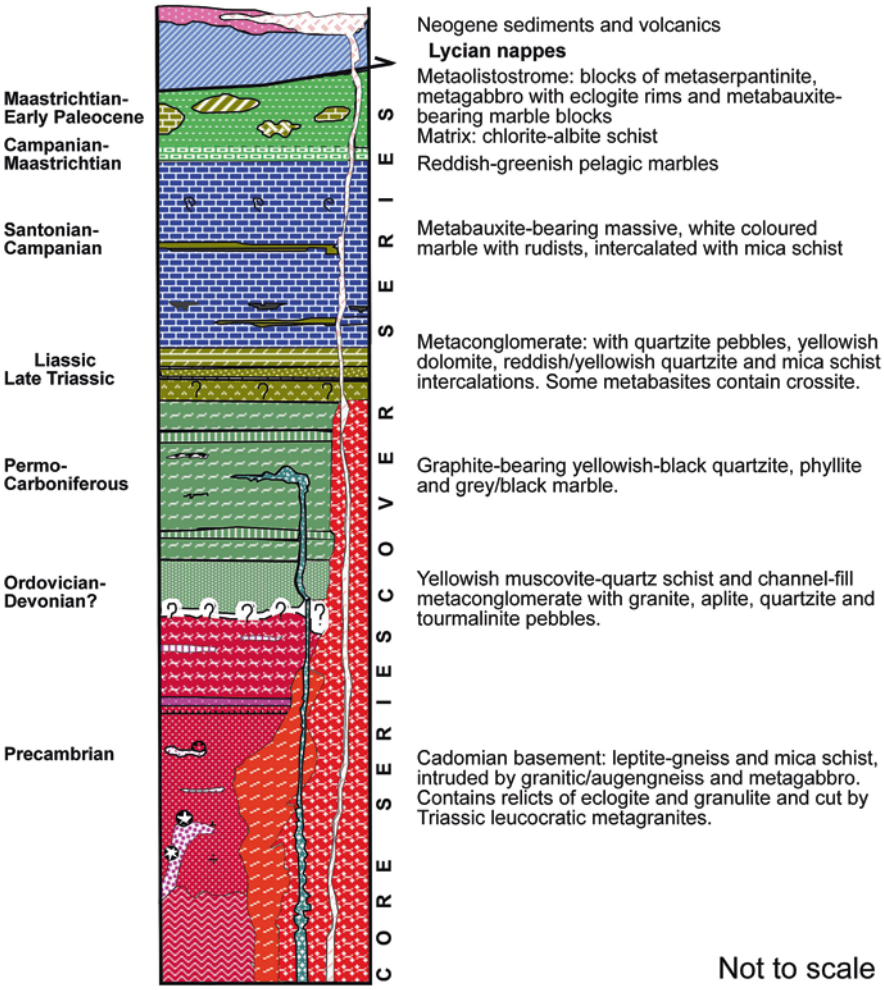

Fig. 2.12 Lithostratigraphy of the Menderes Massif. (After Candan and Dora 1998)

(Candan and Dora 1998). The youngest ages obtained from detritial zircons in paragneisses are 570–550 Ma (Zlatkin et al. 2013), whereas the protoliths of eclogitic gabbros yielded zircons with core and rim ages of 558 and 535 Ma, respectively (Candan et al. 2016). The cover succession starts with metaclastic rocks and comprises metapelites (kyanite+staurolite+garnet schists and garnet+mica schists) with minor intercalations of quartzites and garnet amphibolites with detrital zircons of Early Cambrian age. This may suggest a late Cadomian or Pan-African disconformity between the basement and the cover successions. Recently, the finding of granitoid, which were emplaced during late- to post-collisional back-arc extension at 545–560 Ma behind a Cadomian arc, in relation with the southward subduction of the Proto-Tethys Ocean along the northern margin of Gondwana (Gürsu 2016). The overlying thick meta-siliciclastic succession with alternations of quartzites, micaschists and marbles resembles the Paleozoic successions of the Taurides and yielded in its upper part some ghost macro-fossils of Carboniferous age (e.g. Erdogan and Güngör 2004; Candan et al. 2011). An interval of coarse red metaclastics, resembling the Triassic successions in the Taurides, disconformably overlies the Palaeozoic cover. Together with the finding of Middle Triassic S- type granitic gneisses of calc-alkaline affinity (e.g. Koralay et al. 2001), these red clastics may suggest a rift-related extension in the Menderes Massif. The upper part of the cover includes a very thick succession of platform type metacarbonates (marbles, calc-schists and dolomitic marbles) of Mesozoic age. The upper part of the metacarbonates is conformably overlain by thin-bedded red marbles of Paleogene age (e.g. Candan and Dora 1998; Özer et al. 2001), followed by metamorphic olistostromes with blocks of ophiolitic units. The age of the peak metamorphism of the Menderes Massif is assumed to be of Eocene age (e.g. Rimmelé et al. 2003).

Copious studies suggest that Menderes Massif has been effected by extensional tectonic and represents a Miocene "core-complex" (e.g. Bozkurt and Oberhansli 2001; Çemen et al. 2005). The age of the exhumation is Oligocene-Miocene, also supported by radiometric age data (e.g. Glodny and Hetzel 2007; Catlos et al. 2011). The E-W trending graben-structures in the massif indicate an ongoing extension in the Eastern Aegean, which is accompanied by extensive volcanism (e.g. Yilmaz et al. 2000; Seyitoğlu et al. 2004).

2.3.4.3 The Kütahya Bolkardağ Belt

The belt represents the northern margin of the Tauride-Anatolide Terrane facing the Izmir-Ankara-Erzincan branch of Neotethys. It consists of *a*- allochthonous bodies of the HP/LT metamorphic continental margin sediments (e.g. Okay 1985) of the Tauride-Anatolide Platform, ***b***- slices of the accretionary prism formed in the trench of the Izmir-Ankara-Erzincan subduction zone (Göncüoğlu et al. 2010), both of which were transported into: *c*- flysch-type deposits that were formed in foreland-basins during the closure of the Izmir-Ankara Oceanic branch (Göncüoğlu 2011). Units *a* and *b* are characterised by HP/LT metamorphism (Fig. 2.13).

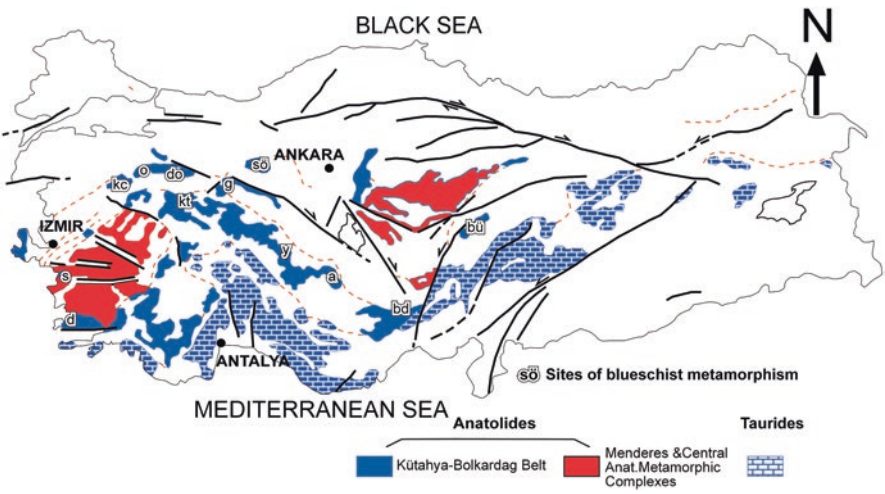

Fig. 2.13 Distribution of the HP/LT metamorphic rocks along the Kütahya-Bolkardağ Belt. (After Floyd et al. 2003)

In the least metamorphic slices of the basement, yet observed, are made up of metaclastic rocks of unknown age. They are disconformably overlain by quartz-arenites and early Late Permian carbonates (Fig. 2.14.). Lower Triassic continental red clastics with alkaline lavas unconformably cover the pre-Late Permian basement (Özcan et al. 1989). The Lower Triassic successions mainly consist of fluvial deposits with various-colored conglomerates, sandstones, mudstones and evaporitic carbonates. They are followed by a thick Middle Triassic (Anisian)-Lower Cretaceous succession made of restricted to open shelf limestones. They represent the internal part of the Tauride-Anatolide Platform. Tectonic slices or slide blocks of Ladinian-Early Cretaceous pelagic limestone-shale and radiolarian chert bodies, now found within the Late Cretaceous mélange (Tekin et al. 2002, 2012a; Tekin and Göncüoğlu 2007; Göncüoğlu 2011) suggest that the platform-margin and slope sediments are dismembered and transported into the foreland basins. These platform-margin sediments frequently display typical parageneses of HP/LT metamorphism with peak pressure and temperatures of ~24 kbar and 430–500 °C, respectively. This data clearly suggests the deep subduction of the attenuated continental-margin of the Tauride-Anatolide Platform during the Late Cretaceous (Okay and Whitney 2010). Their obduction, together with the ophiolites and the subduction-accretion mélanges onto the internal platform is pre-Middle Paleocene in age. The Middle Paleocene-Middle Eocene sediments in the Kütahya-Bolkardağ Belt represent the oldest overstep sequences and comprise shallow-marine or continental molasse-type deposits in the remnant basins on the platform.

Considering the distribution of the allochthonous bodies derived from the İzmir-Ankara-Erzincan oceanic lithosphere and the mélanges and olistostromes of the

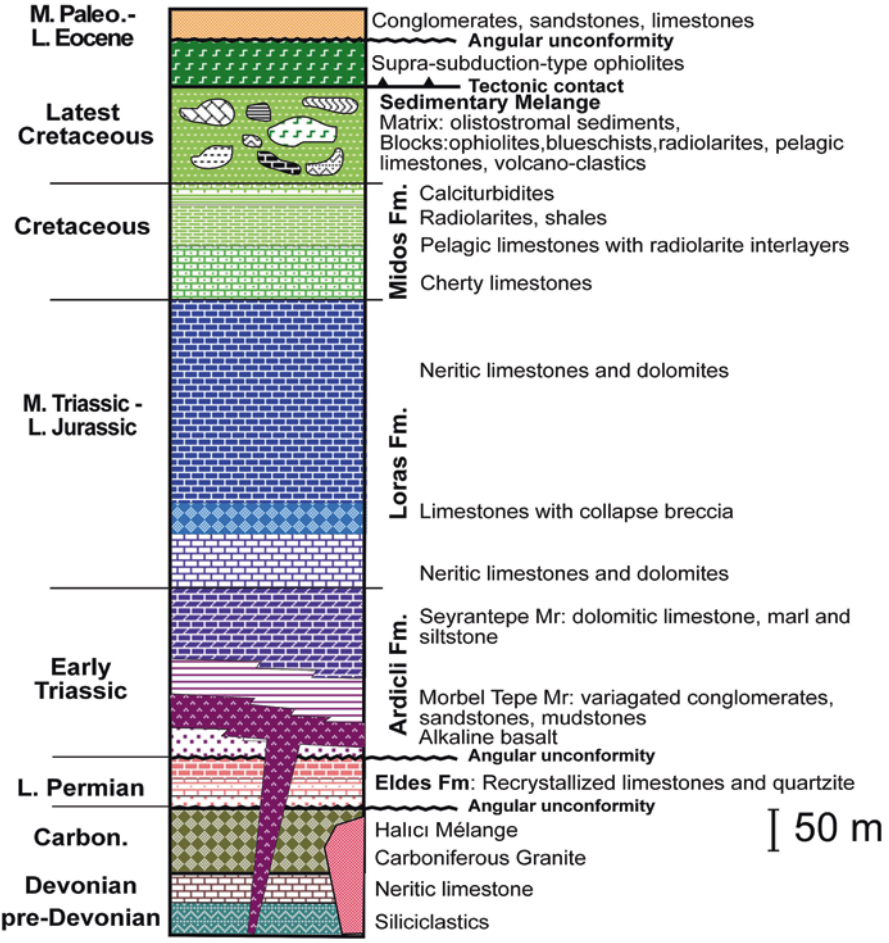

Fig. 2.14 A generalised lithostratigraphy of the Kütahya-Bolkardag Belt. (After Göncüoğlu 2011)

subduction-accretion prism in the Taurides, their transportation onto the platform as large tectonic slices was of several hundred kilometres. During their progressively southward emplacement, foreland basins were formed in front of the advancing nappes and filled with very thick flysch-type deposits (e.g. Tekeli et al. 1984). Detailed studies were performed on the tectono-magmatic characteristics and the ages of the oceanic basalts in the mélange blocks (e.g. Floyd et al. 2003; Göncüoğlu et al. 2006; Göncüoğlu et al. 2015; Gökten and Floyd 2007; Bortolotti et al. 2013) within the Kütahya-Bolkardağ Belt. The information provided on the evolution of the Izmir-Ankara-Erzincan Ocean (e.g. Robertson et al. 2009; Göncüoğlu et al. 2010) will be evaluated in the next chapter.

2.3.5 *Izmir-Ankara-Erzincan Suture Belt*

The Izmir-Ankara-Erzincan Suture Belt (Fig. 2.1) comprises the remnants of the Neotethyan İzmir-Ankara-Erzincan branch. It consists of different parts of the oceanic lithosphere, together with the subduction-accretion mélanges (Fig. 2.15) Izmir-Ankara-Erzincan that were formed along subduction zones and emplaced southward onto the Tauride-Anatolide Platform during its Late Cretaceous closure (e.g. Göncüoğlu et al. 1997, 2010; Okay and Tüysüz 1999; Robertson 2002).

The suture belt is overthrust by the Sakarya Composite Terrane, characterising the active margin of the Izmir-Ankara-Erzincan Ocean. The ophiolites include dismembered bodies of oceanic lithosphere formed in various tectono-magmatic settings such as the mid-ocean ridges, arcs and supra-subduction-type arc basins as well as intra-plate formations including ocean islands and oceanic plateaus. Variably

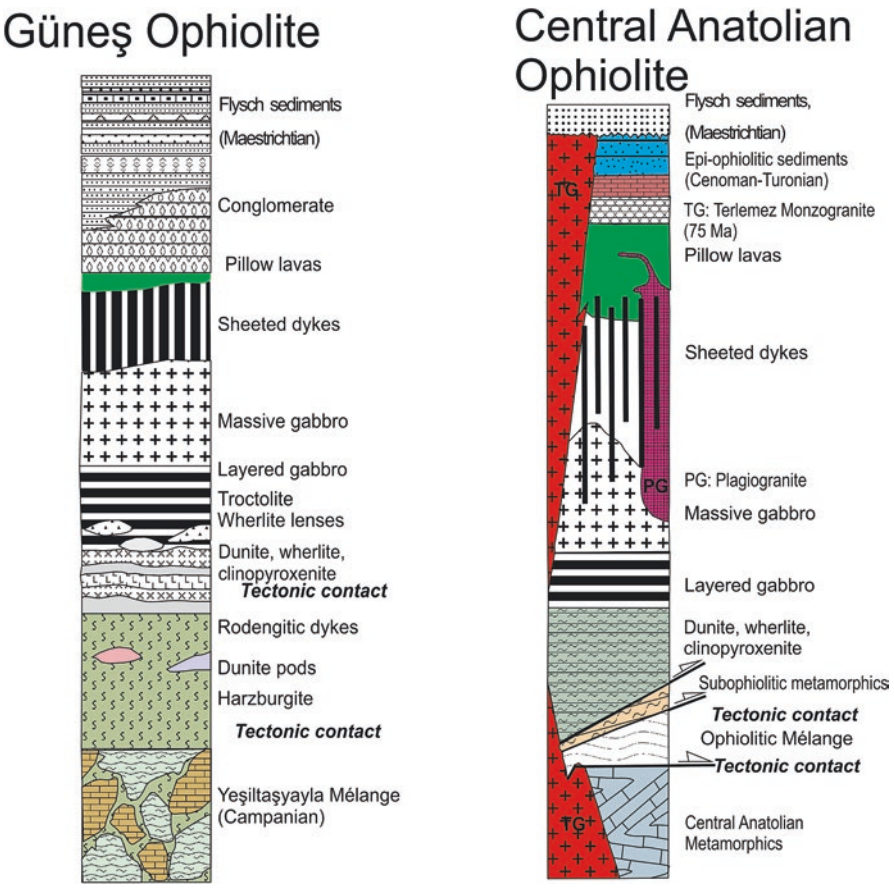

Fig. 2.15 Rock units and structural relations of the Güneş (Sivas-Divriği, Parlak et al. 2013a) and Central Anatolian (Yalınız et al. 2000) ophiolites of the Izmir-Ankara Ophiolitic belt

serpentinized peridotites, ultramafic and mafic cumulates, layered and isotropic gabbros, plagiogranites, dyke-complexes and pillowed and massive lavas with oceanic sediments occur either as several km-thick distinct bodies or as blocks of variable sizes in the mélanges. They occasionally include variably thick metamorphic soles comprising mainly amphibolites (Önen and Hall 1993). The Ar-Ar ages of these metamorphic soles varies between the late Early Jurassic (Çelik et al. 2011) to early Late Cretaceous (101–89 Ma, e.g. Parlak et al. 2013a) indicating that the intra-oceanic convergence started along different segments of the subducting ridge at different times. This would suggest an irregular northern margin of the Tauride-Anatolide continental plate as initially proposed by Yalınız et al. (2000).

Along the belt, the upper mantle rocks include depleted lherzolites and refractory harzburgites with chromites and display petrogenetic signatures of heterogeneous mantle sources (e.g. Manav et al. 2004; Uysal et al. 2007; Üner et al. 2014; Parlak et al. 2013b), very similar to their volcanic equivalents. The pillow-lavas mainly occur all along the belt as separated thrust-sheets and as blocks within the mélanges.

Geochemically, they display characteristic features of very diverse tectonic settings including E- and N- type MORB; OIB and SSZ (Aldanmaz et al. 2008; Göncüoğlu et al. 2010; Sarıfakıoğlu et al. 2010; Bortolotti et al. 2013; Topuz et al. 2013). The basalts are often interlayered with radiolarian cherts, micritic limestones and mudstones. The oldest ages obtained yet (Sayit et al. 2015) are Carnian (Fig. 2.16) whereas the youngest ones from mainly back-arc type basalts are Cenomanian. This suggests that the formation of Izmir-Ankara oceanic crust started as early as Middle Triassic (Fig. 2.17) and lasted until Late Cretaceous (Tekin et al. 2002; Göncüoğlu et al. 2015).

The Izmir-Ankara-Erzincan ophiolitic belt comprises both block-block and block-in-matrix type mélanges. The size of the blocks varies from a few m to several tens of km in size. Next to lithologies belonging to the oceanic lithosphere, high

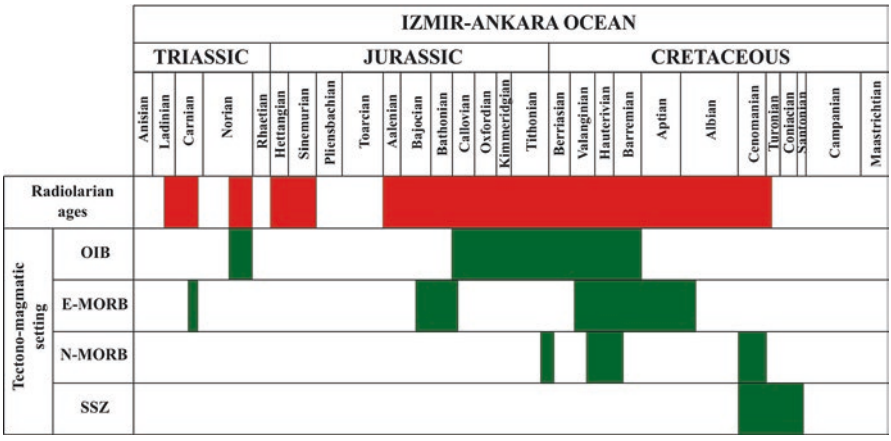

Fig. 2.16 Radiolarian ages and tectono-magmatic character of the Izmir-Ankara-Erzincan pillow lavas. (Göncüoğlu et al. 2015; for abbreviations see Fig. 2.7)

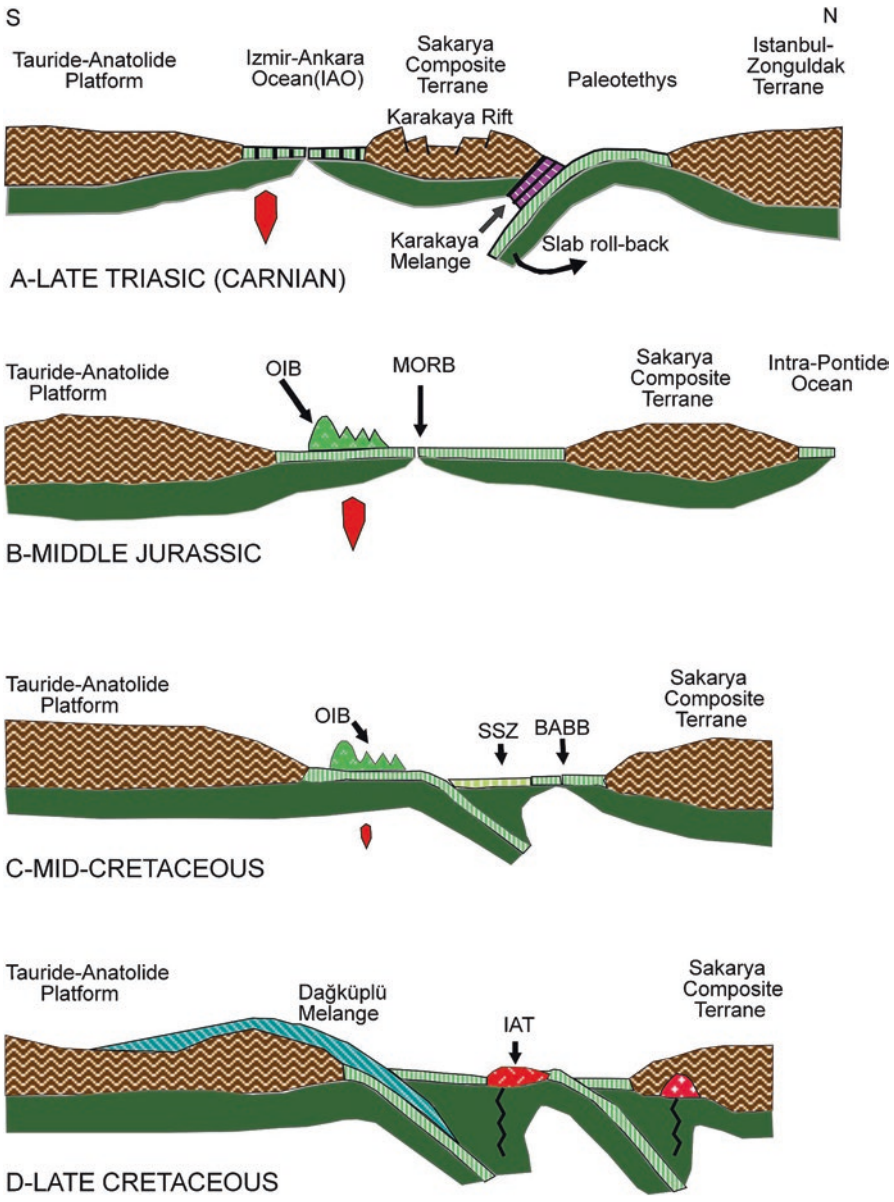

Fig. 2.17 Geodynamic scenario depicting the geological evolution of the Izmir-Ankara-Erzincan Suture Belt. (After Göncüoğlu 2010)

pressure-low temperature metamorphic assemblages such as blueschists and eclogites, variably metamorphosed carbonate and siliciclastic blocks of Mesozoic age are found within the mélanges.

Allochthonous bodies derived from the closing İzmir-Ankara-Erzincan branch of Neotethys and its subduction-accretion prism was first emplaced onto the margin of the Tauride-Anatolide platform during the Late Cretaceous. Their ongoing tectonic transportation towards S for several 100 km and subsequent imbrication resulted partly in the formation of false belts within the Tauride-Anatolide tectonic units, which were considered as remnants of separate oceanic basins within the Tauride-Anatolide Platform (e.g. Intra-Tauride Ocean, Huğlu Ocean, Bornova Mélange, etc.).

2.3.6 Sakarya Composite Terrane

Sakarya Composite Terrane is one of the main Cimmerian blocks, which was rifted from the northern Gondwana margin (e.g. Sengör 1984). In Turkey, it forms a 100–200 km wide, east-west trending belt along northern Anatolia (Fig. 2.1). Göncüoğlu et al. (1997) defined it as an Alpine "composite terrane" *sensu* Howell (1995) as it comprises several Variscan and Cimmerian continental as well as oceanic assemblages in its pre-alpine basement (Fig. 2.18).

Within the Variscan "structural basement" the oldest units defined yet are metamorphic assemblages of poorly known protolith age, intruded by arc type granitoid with radiometric ages ranging from Devonian (Aysal et al. 2012; Sunal 2012) to Carboniferous (Ustaömer et al. 2012; Topuz et al. 2010; İlbeyli et al. 2015). These metamorphic rocks are mainly ortho and para-schists/gneiss with mafic rocks and marbles (e.g. Göncüoğlu et al. 2000). Their detrital zircon content indicates a northern Gondwanan origin (e.g. Ustaömer et al. 2016). The age of the medium to high-grade metamorphism in the basement is Late Carboniferous (e.g. Ustaömer et al. 2016; Topuz et al. 2007). The oldest post-Variscan – cover in the Sakarya Composite Terrane is represented by the Lower to Middle Permian platform carbonates that grade into Late Permian olistostromes. They are unconformably covered by the Triassic clastics (Turhan et al. 2004).

The structural units related to the Cimmerian cycle in the Sakarya Composite Terrane are the remnants of the Paleotethyan (sensu Şengör et al. 1984) subduction complex (Tekeli 1981) also known as the Karakaya Complex (for a brief review see Okay and Göncüoğlu 2004).

The oceanic lithologies of the complex are mainly ocean island basalts (Fig. 2.19) and associated sediments of Middle Triassic (Anisian; Sayit and Göncüoğlu 2009) age. The Küre Complex in Central Pontides is the only larger body including supra-subduction-type ophiolites (Ustaomer and Robertson 1999) with an olistostromal cover of Late Triassic age (Kozur et al. 2000). The metamorphic assemblages within the complex include metabasic rocks and oceanic sediments affected by HP/LT metamorphism during the Late Triassic (Okay 1985; Okay et al. 2002). The matrix of the mélange is mainly made of meta-clastics rocks with Late Triassic radiolarian chert interlayers (Sayit et al. 2015) and includes slide blocks of Late Paleozoic and Triassic (e.g. Okay et al. 2015) neritic limestones.

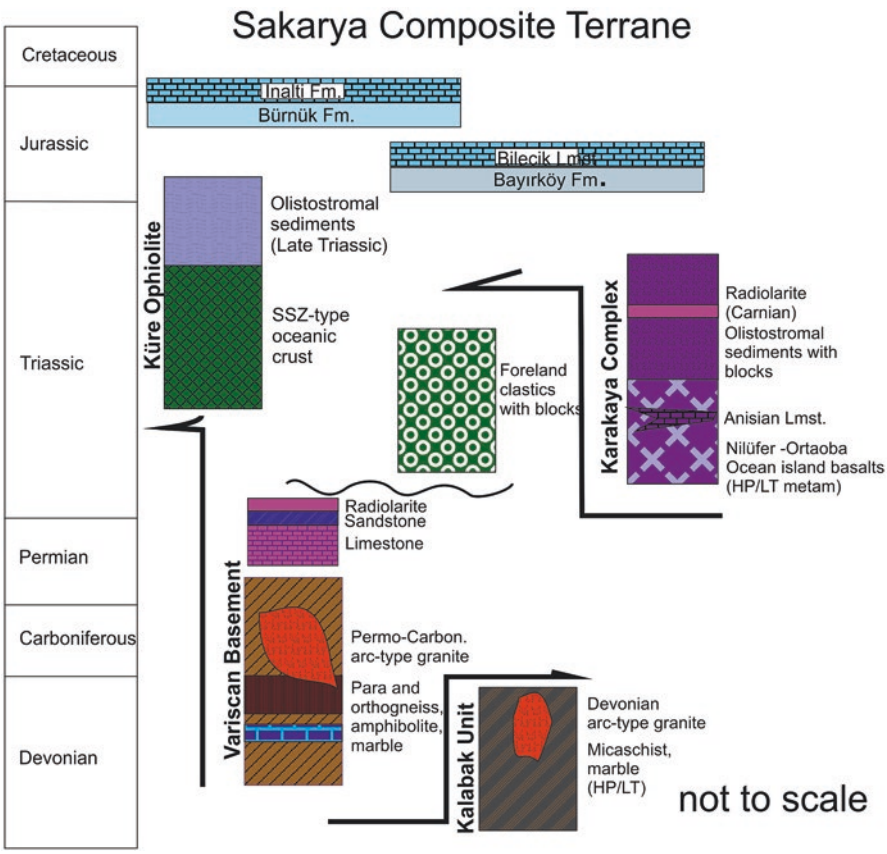

Fig. 2.18 Tectono-stratigraphy of the Sakarya Composite Terrane

The Karakaya Complex representing the oceanic lithosphere and the subduction-accretion prism of the Triassic Paleeotethys is tectonically mixed with the Variscan basement rocks, their Permian platform and the rift-related Triassic cover sediments during the end of Triassic (Koçyiğit 1991; Göncüoğlu et al. 2000; Robertson et al. 2004) by the Cimmerian event (Fig. 2.20). The post-orogenic overstep sequence is Early Jurassic in west-Anatolia and middle-Late Jurassic in the east.

The Jurassic-Early Cretaceous period in the Sakarya Composite Terrane is characterised by deposition of the platform and slope sediments (Fig. 2.21), respectively, and marks the onset of the Alpine Cycle. It is commonly accepted that it represents a ribbon-like continental microplate surrounded by the Izmir-Ankara-Erzincan Ocean in the south and the Intra-Pontide Ocean in the north until the Late Cretaceous (Şengör and Yılmaz 1981; Göncüoğlu 2010 and the references therein). In the eastern (e.g. Yılmaz and Korkmaz 1999) and the western parts of northern Anatolia, the Mesozoic stratigraphy of the cover units (Fig. 2.21) of the Sakarya Composite Terrane are considerably diverse (e.g. Altıner et al. 1991). In north-west

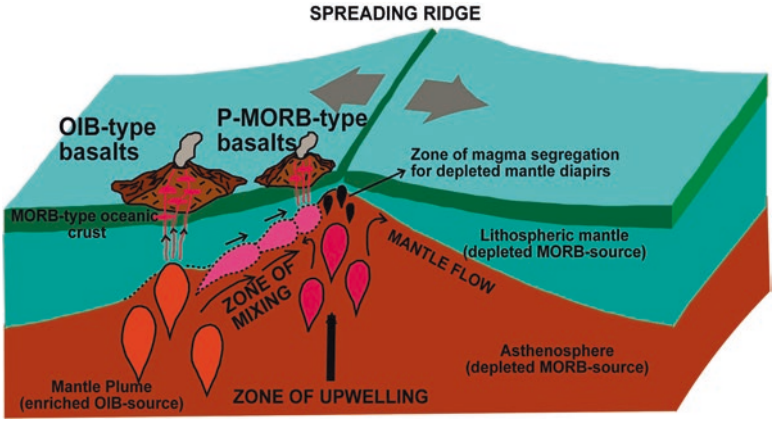

Fig. 2.19 A possible tectonic scenario for the generation of the Anisian ocean-island-type Nilüfer and Ortaoba volcanics of the Karakaya Complex within Paleotethys. (After Sayit and Göncüoğlu 2009)

Anatolia, the post-tectonic overstep sequence starts with Liassic and is represented by the platform to slope type carbonates during the Late Jurassic to the Early Cretaceous interval. The Late Cretaceous rocks are mainly flysch-type deposits. They were formed on the passive margin of the alpine Sakarya platform and slope as foreland sediments in front of the southward migrating subduction-accretion material of the subducting Intra-Pontide oceanic basin. Ophiolite-bearing oceanic assemblages were then emplacement onto these flysch-basins from north to south during the latest Cretaceous time, prior to the elimination of the Intra-Pontide basin and the oblique collision of the Sakarya and Istanbul-Zonguldak plates (e.g. Göncüoğlu et al. 2000).

In the Central Pontides, the Küre Complex representing the Paleotethyan oceanic lithosphere, the Variscan basement rocks with Late Paleozoic granitoid and the Istanbul-Zonguldak terrane are intruded by Middle Jurassic arc-type plutons (Yılmaz and Boztuğ 1986; Genç and Tüysüz 2010; Okay et al. 2014) and covered by the Late Jurassic-Early Cretaceous olistostromal deposits. The overlying Late Cretaceous sediments are again represented by flysch-type sediments. Their formation, however, is ascribed to the opening of the Black Sea basin (e.g. Okay et al. 2014). Following the ophiolite emplacement, arc-type plutons intruded the southern margin of the Sakarya Composite Terrane during the Paleocene-Eocene period due to the subduction of the southerly located Izmir-Ankara-Erzincan Ocean beneath the Sakarya Composite Terrane (e.g. Öztürk et al. 2012; Ellero et al. 2015a).

In the eastern part of the Sakarya Composite Terrane, where the Middle Jurassic to Late Cretaceous sedimentary/volcano-sedimentary successions characterises the Alpine Cycle, the very extensive igneous assemblages are collectively named as the "Pontide Magmatic Arc". The basement of the arc is mainly made of the Variscan-type units with limited outcrops of Karakaya-type mélanges (e.g. Okay and Göncüoğlu 2004). The geological features of the Eastern Pontides differ in the

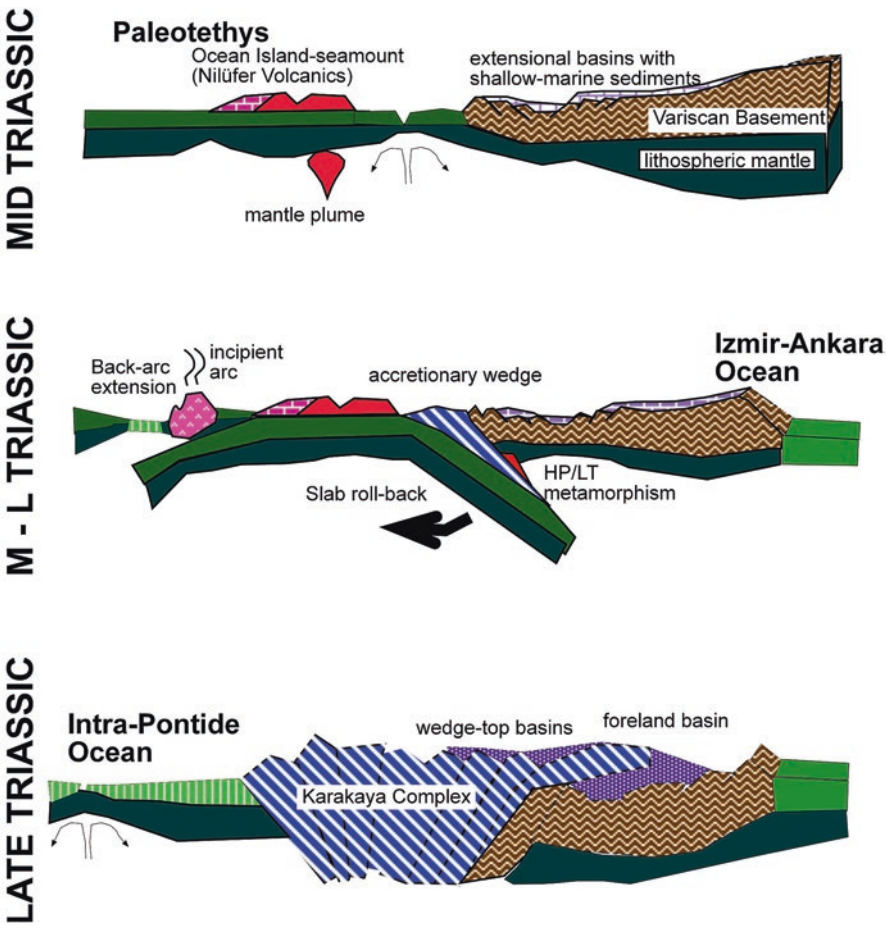

Fig. 2.20 A possible tectonic scenario for the evolution of the Sakarya Composite terrane by the closure of the Palaeotethys. (After Sayıt and Göncüoğlu 2013)

northern and southern zones definitely (e.g. Okay and Şahintürk 1998). In the Southern Zone, where sedimentary units dominate over igneous ones the post-Cimmerian deposition starts with Middle Jurassic pillow basalts, basaltic to andesitic tuffs, sandstones and shales, with local rosso ammonitico -type limestones. This succession has been interpreted as a product of back-arc rifting, formed by the southward subduction of the Paleotethyan oceanic lithosphere (e.g. Okay and Şahintürk 1998). The Upper Jurassic to Lower Cretaceous interval is characterised by platform-type carbonates (Fig. 2.21). They are interpreted as the establishment of a passive margin, facing the Izmir-Ankara-Erzincan Ocean. During the Albian–Cenomanian period the tectonic style changed to compression (e.g. Yılmaz et al. 1997) giving way to the generation of flysch-type basins in the Southern Zone.

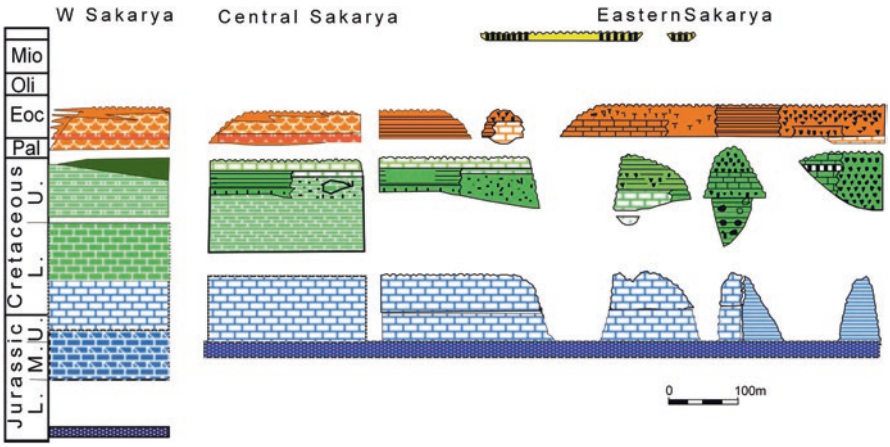

Fig. 2.21 Post-alpine cover units of the Sakarya Composite Terrane in N, Central and NE Anatolia. (Robinson et al. 1995; Göncüoğlu et al. 2000; Duru et al. 2004)

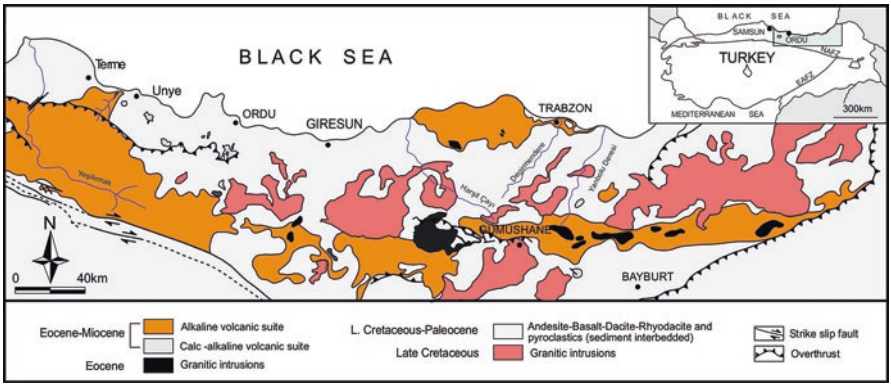

Fig. 2.22 Distribution of the Eastern Pontide Magmatic arc rocks in NE Anatolia. (From Temizel and Aslan 2008)

During the Early Tertiary, the Southern Zone was affected by the subduction of the Izmir-Ankara-Erzincan oceanic lithosphere towards N beneath the Sakarya Composite Terrane, resulting in imbrication of the continent margin successions and the subduction accretion material in the south (e.g. Dokuz and Tanyolu 2006). However, the main body of the Pontide Magmatic Arc started to form during this period in the Northern zone, where during the Cretaceous to Eocene basic and acidic volcanic rocks with Kuroko-type ore deposits and coeval granitoid were generated (e.g. Arslan et al. 1997; Şen et al. 1998; Karslı et al. 2010). The distribution of the arc magmatic and their overall geochemical characteristics are given in Fig. 2.22. An alternative interpretation is that it was the Black Sea oceanic lithosphere that

subduction towards south beneath the Sakarya Composite Terrane to produce the Pontide Magmatic Arc (e.g. Bektaş et al. 2000; Eyüboglu et al. 2011).

The collision of the Sakarya Composite Terrane and the Tauride-Anatolide Terrane in the eastern part of the belt has occurred during the Oligocene (Tokel 1977; Robinson et al. 1995).

2.3.7 The Intra-Pontide Ophiolite Belt

This northernmost and cryptic ophiolitic belt between the Sakarya Composite Terrane in the South (Fig. 2.1) and Istranca/Istanbul-Zonguldak terranes in the North (Robertson and Ustaömer 2005; Göncüoğlu et al. 2008) is the least known and frequently debated suture in NW Anatolia. This is partly because of the overlapping of the suture belt with the North Anatolian Transform Fault and the distribution of the oceanic assemblages. The detailed geology of the belt has been studied in the S of Armutlu Peninsula (e.g. Akbayram et al. 2013) and in the Central Pontides (e.g. Frassi et al. 2016). Overall, the belt includes variably metamorphosed slices of mélange complexes and an arc together with dismembered bodies of ophiolites.

The ophiolites, represented by the Aylı Dağ Ophiolite (Fig. 2.23) in the central part of the belt comprises in its lower part a mantle sequence of about 2–3 km-thick peridotites, overlain by 500–600 m-thick layered gabbros alternating with, dm- to m-thick layers of spinel-bearing dunites, mela-troctolites, troctolites, olivine-gabbros and leucogabbro (Göncüoğlu et al. 2012). It is structurally overlain by a 100–200 m-thick sheeted dyke complex, 700 m-thick massive and pillow basalts and finally by pelagic cherts with Middle Jurassic radiolarians. Geochemically, the ophiolitic basalts are akin to back-arc basin basalts.

The metamorphic bodies of the Intra-Pontide Ophiolite Belt, collectively named as the "Central Pontide Structural Complex" (Tekin et al. 2012b) are variable in size and their metamorphic evolution. The metamorphic rocks are dominated by metamafics and metaclastics with limited marble interlayers. Geochemically, the metabasic rocks are mainly products of an arc-basin (back-arc) system (Sayit et al. 2016). They display micro-textures indicating polyphase deformation and metamorphism with a distinct phase of HP-LT event overprinted by greenschist and/or amphibolite facies (Okay et al. 2006a; Aygül and Okay 2012; Marroni et al. 2014; Frassi et al. 2016). Their protolithic ages are not clearly documented yet. Detritial zircon data suggests that at least one of them (Martin Complex of Okay et al. 2013) has the post-Early Jurassic depositional age. The geochronological data suggests that they were metamorphosed during the Middle Jurassic and Early Cretaceous times, respectively (Okay et al. 2006a, b, 2013; Aygül et al. 2015).

The mélange unit of the Intra-Pontide Ophiolite Belt comprises blocks of serpentinites, gabbros, and pillow basalts, pelagic limestones and radiolarian cherts. The radiolarian chert blocks have an age –range of Middle Triassic to mid-Cretaceous (Fig. 2.24). Neritic and pelagic limestone slide-blocks are Late Jurassic to Early Cretaceous in age. The matrix consisting of shales, coarse-grained arenites, pebbly-

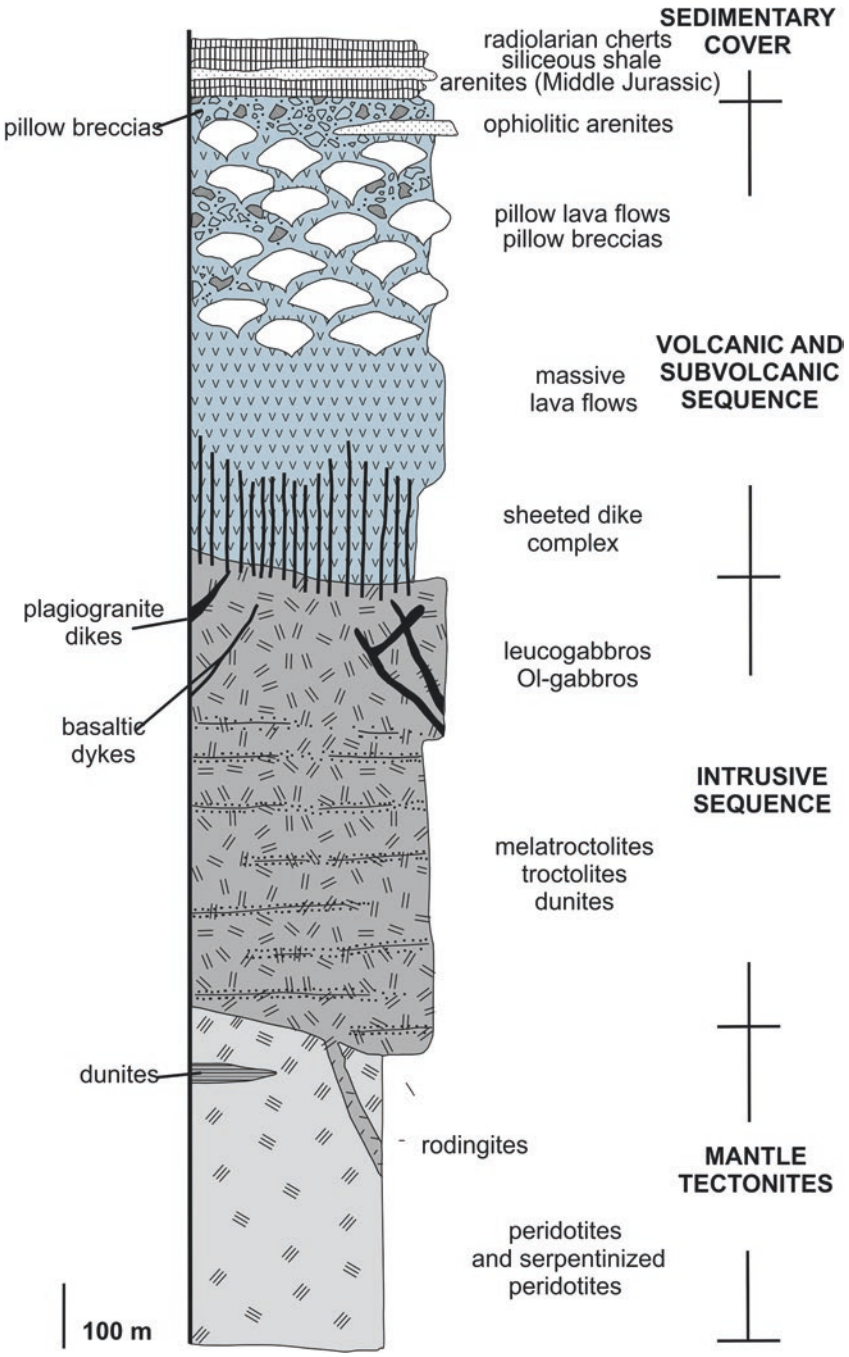

Fig. 2.23 Idealised section of the Aylı Dag Ophiolite within the Intra-Pontide Ophiolite Belt. (After Göncüoğlu et al. 2012)

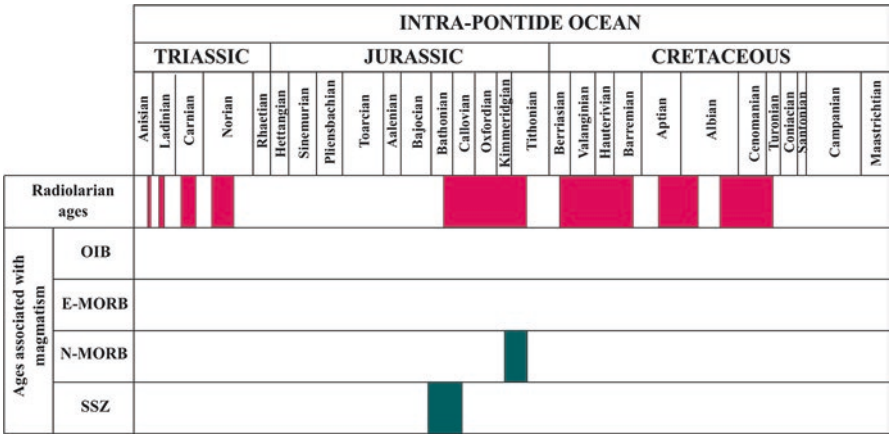

Fig. 2.24 Radiolarian ages and tectono-magmatic character of the Intra-Pontide pillow lavas. (Göncüoğlu et al. 2015; for abbreviations see Fig. 2.7

mudstones and pebbly-sandstones include late Santonian nannofossils (e.g. Göncüoğlu et al. 2014). The slide-blocks of basalts display affinities to island arc tholeiite – and back-arc basin basalt type magmas generated above subduction zones. The radiolarian ages obtained from pillow-lava – chert assemblages range between Middle Triassic to early Late Cretaceous (Göncüoğlu et al. 2008; Tekin et al. 2012b).

The arc complexes of the Intra-Pontide Ophiolitic Belt form roughly E-W trending slivers within the "Central Pontide Structural Complex" and consist of the Çangaldağ Metamorphic Complex and the Çangaldağ Pluton. The former unit comprises low-grade metamorphic rocks of intrusive, extrusive and volcaniclastic origin, displaying a wide range of felsic to mafic compositions and was formed in arc and back – arc regions above an intra-oceanic subduction within the Paleotethys (e.g. Ustaomer and Robertson 1999) or the Intra-Pontide branch of Neotethys (Çimen et al. 2016) during the Middle Jurassic (Okay et al. 2014; Çimen et al. 2016). The age of the metamorphism is Early Cretaceous (Okay et al. 2014). The Çangal Dağ Pluton, on the other hand, is characterised by diorites and leucogabbro and to a lesser extent granites, cut by dacite porphyries (Fig. 2.25). The zircon data (Çimen et al. 2016) suggests a Middle Jurassic age for the pluton.

The oldest oceanic sediments found in the Intra-Pontide Suture Belt are Middle-Late Triassic of age (Tekin et al. 2012b) indicating that this Neotethyan basin was contemporaneous with the Paleotethys. Identification of a number of back-arc to arc- type assemblages of different formation ages and types of metamorphism (e.g. Sayit et al. 2016), on the other hand, suggests episodic subduction and accretion of the crustal material of an arc-basin to the Istanbul-Zonguldak Terranere presenting a piece of the southern Eurasian continental crust (e.g. Okay et al. 2006a, b, 2013). The oldest overstep sequence on top of these accreted oceanic units is represented by Late Paleocene-Eocene (e.g. Özgen-Erdem et al. 2005) fluvial to shallow-marine

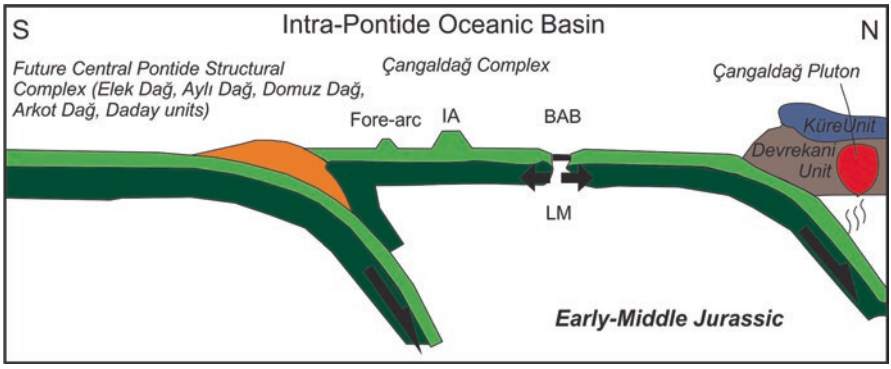

Fig. 2.25 A geodynamic model for the Early-Middle Jurassic evolution of the Intra-Pontide Suture belt. (After Çimen et al. 2016)

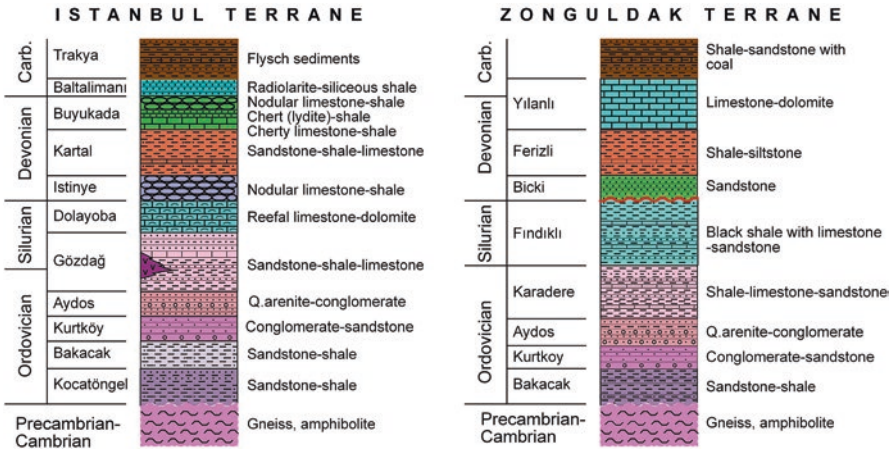

Fig. 2.26 Palaeozoic stratigraphy of the Istanbul and Zonguldak units. (After Bozkaya et al. 2012a, b)

sediments, deposited in E-W trending extensional or transtensional basins with alkaline volcanism (e.g. Keskin et al. 2008).

2.3.8 Istanbul-Zonguldak Composite Terrane

The Istanbul-Zonguldak Composite Terrane is a Gondwanan unit, including a Cadomian Late Neoproterozoic-Early Cambrian basement, a classical cycle of Variscan overstep sequences and an alpine cover (Fig. 2.26). The Cadomian basement is composed of the remnants of oceanic lithosphere and a Cambrian intra-oceanic arc that were consolidated at the end of Cambrian (e.g. Yiğitbaş et al. 2004).

The basement is unconformably covered by a well-developed Ordovician sequence, mainly made of fluvial conglomerates followed by shallow-marine clastic rocks. From Silurian onwards, the depositional characteristics of Istanbul and Zonguldak sub-terranes differ considerably. Moreover, in contrast to the typical deepening from platform to slope and finally to a flysch basin conditions in the former (e.g. Özgül 2012), a post middle Silurian-pre Middle Devonian thermal event (Bozkaya et al. 2012b) and stable platform conditions from Middle Devonian to Late Lower Carboniferous and then fluvial deposition in Middle Carboniferous is characteristic for the Zonguldak subterrane (e.g. Yanev et al. 2006). These critical differences suggest that both terranes were following different movements paths during the Variscan cycle (e.g. Göncüoğlu and Kozur 1998).

The igneous products of the Variscan-time event in the Istanbul area are represented by the Permian (e.g. Yılmaz Şahin et al. 2010) granitoids. Late Permian continental clastics are the earliest post-Variscan cover sequences on both Istanbul and Zonguldak units (e.g. Okuyucu et al. 2017). Alpine-type Triassic sediments are only formed in the Istanbul area, but the Jurassic-Early Cretaceous sequences are only represented in the NW part of the Zonguldak Unit (Fig. 2.27).

The next post-orogenic overstep sequence unconformably overlying the Istanbul-Zonguldak, and the Sakarya Composite terranes are Early Cretaceous in age,

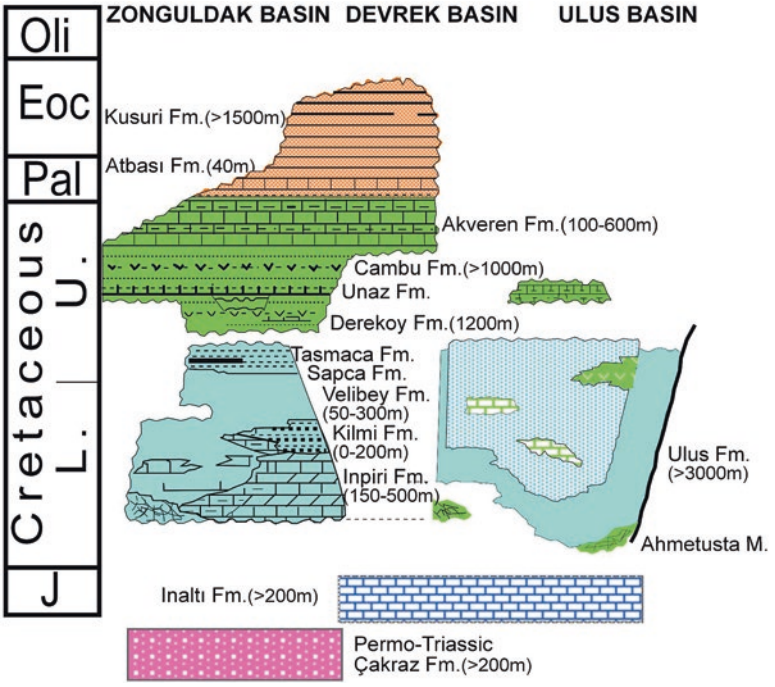

Fig. 2.27 Stratigraphic features of the Mesozoic cover units of the Istanbul-Zonguldak Terrane. (Tüysüz 1999)

indicating their initial accretion by the closure of the Intra-Pontide Ocean. This closure was very probably realised as the result of northward subduction of the Intra-Pontide oceanic lithosphere, also giving way to the opening of the Black Sea basin in back-arc setting (e.g. Görür 1988; Tüysüz et al. 1999). The Lower Cretaceous volcanoclastic flysch sequences along the Black Sea cost are considered as the result of this event. Last post-orogenic products regarding the Alpine cycle are the middle Eocene basin deposits followed by the Neogene shallow marine-fluvial deposits and lignite seams of Paratethys (Görür and Tüysüz 2001).

2.3.9 Rhodope-Istranca Terrane

In NW Anatolia two distinct geological units, the Istranca and the Ezine Terranes, are separated from each other by the Thrace Tertiary Basin. They are completely different from the surrounding terranes described above with regard to their stratigraphy, metamorphism, magmatism and succession of geological events. In some regional studies (e.g. Yanev et al. 2006; Papanikolaou 2009) they were considered as parts of the Balkan Terranes such as the Serbo-Macedonian, Rhodope, Thrace or Sredna-Gora terranes (Fig. 2.28).

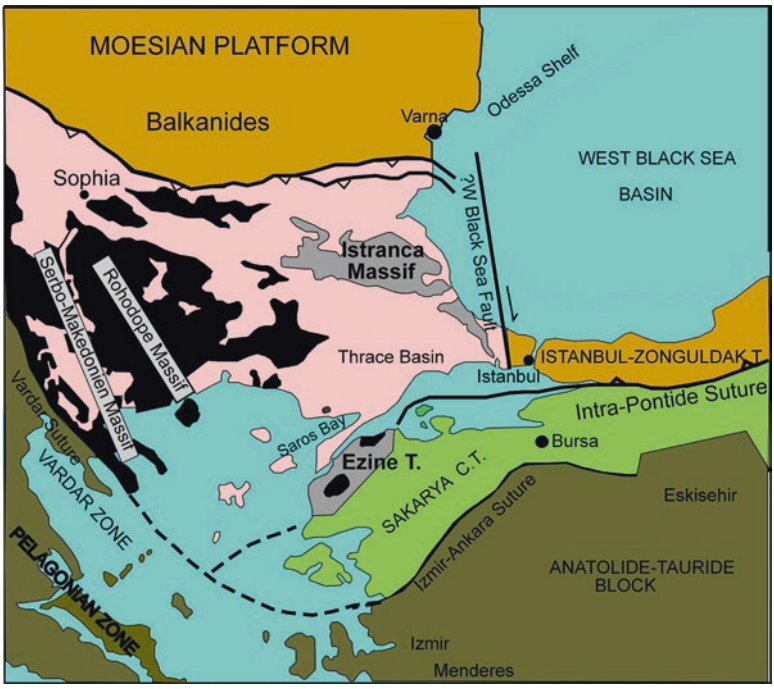

Fig. 2.28 The main tectonic units of E Balkan and W Turkey. (Modified after Göncüoğlu 2010)

2.3.9.1 Ezine Terrane

The NW part of the Kazdağ Peninsula in NW Anatolia (Fig. 2.28) is ascribed to the Ezine Zone (Beccaletto and Jenny 2004). To the south, the unit is bounded by the Intra-Pontide Suture and to the north by the North Anatolian Fault. The basement of the terrane comprises a metamorphic assemblage mainly made of metaclastics and metamafic rocks including relict eclogites with Late Neoproterozoic protolith ages (Fig. 2.29). Metamorphic overprints are reported as Variscan (Carboniferous) and Alpine (e.g. Tunç et al. 2012; Şengün and Koralay 2016).

2.3.9.2 The Istranca Terrane

The Istranca Terrane, or the Strandja (Strandhza) "Massif" in previous studies, is an almost 300 km long and 40 km wide geological unit in NW Turkey along the Black Sea coast. It can be followed across the Turkish-Bulgarian border (Chatalov 1988) into the Balkan Mountains. Recently, Bedi et al. (2013) have shown that it represents a structural complex with numerous tectonic slices that differ in lithostratigraphy, metamorphism, age and structural position.

The oldest basement within these tectonic units includes Precambrian?–Palaeozoic metasediments, intruded by Late Carboniferous-Early Permian calc alkaline granitoid (e.g. Okay et al. 2001). They are disconformably overlain by Triassic metaclastic and marbles (Hagdorn and Göncüoğlu 2007) that make up the main rock-type (Fig. 2.30).

At the end of the Triassic, these tectonic units were thrust over each other and overlain by an overstep sequence with Lower Jurassic coarse clastics. The Middle to Late Jurassic is represented by carbonates, black shales and an alternation of carbonates and siliciclastics. The N and NW parts of the Istranca Terrane are covered by Cenomanian-Santonian volcano-sedimentary successions and intruded by Santonian-Campanian granitic to dioritic rocks (e.g. Karacık and Tüysüz 2010).

The renewed post-Late Cretaceous compression in the Istranca Terrane resulted in the generation of tectonic slices and mylonitic deformation along S-verging shear-zones (e.g. Bedi et al. 2013). The Tertiary cover of the Istranca Terrane is represented by the >5000 m thick sediments of the Thrace Basin, which also overlies a probable transform fold separating the Istranca and the Istanbul-Zonguldak terranes in the west.

2.4 The Tertiary of Turkey

As is so far known, along all three oceanic branches of Neotethys oceanic lithosphere generation was vanished by the end of Cretaceous and the Early Tertiary was a period of late orogenic compression, when extensive fore-land and fore-deep-type flysch basins were generated on the passive margins of Istranca, Sakarya,

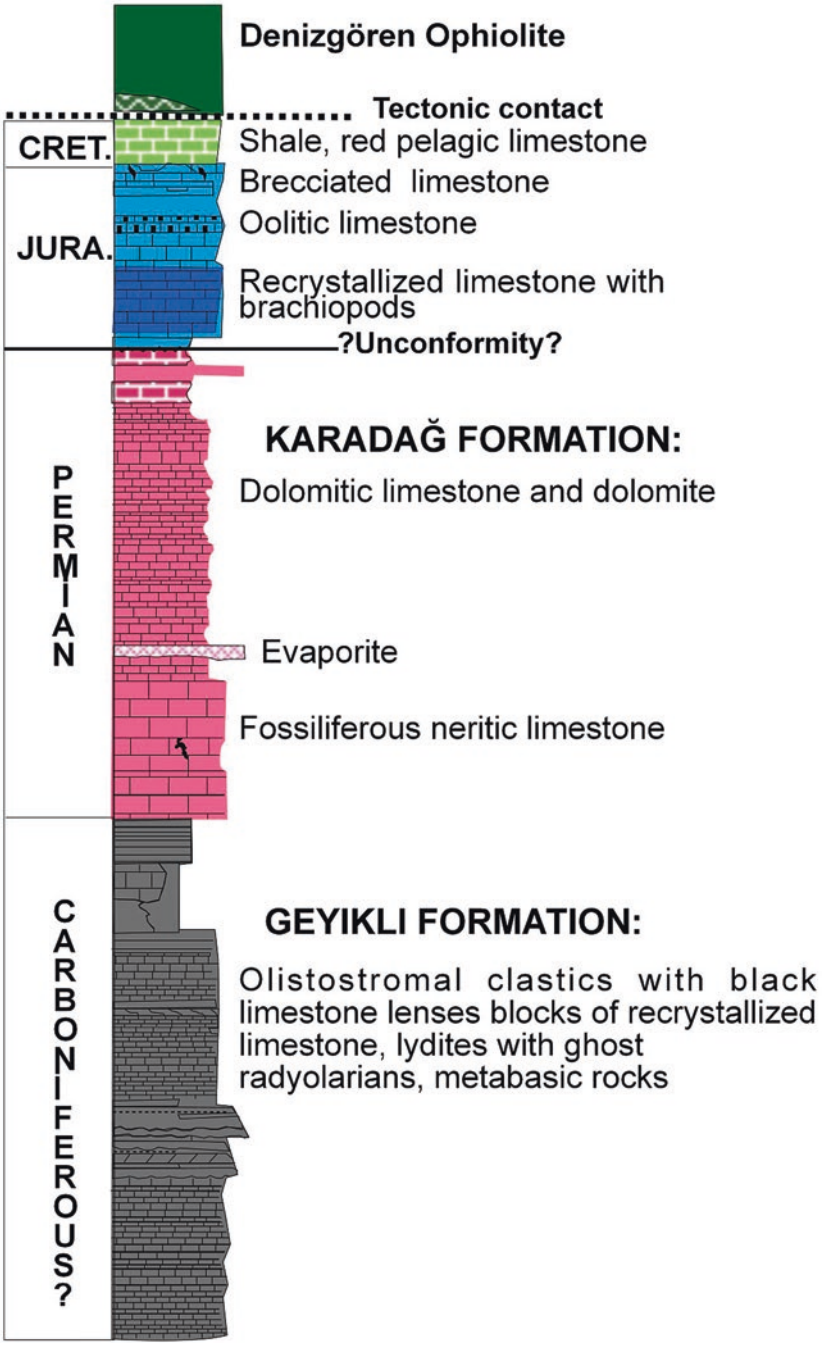

Fig. 2.29 Generalised lithostratigraphy of the Ezine Terrane. (Modified from Boccaletti and Jenny 2004)

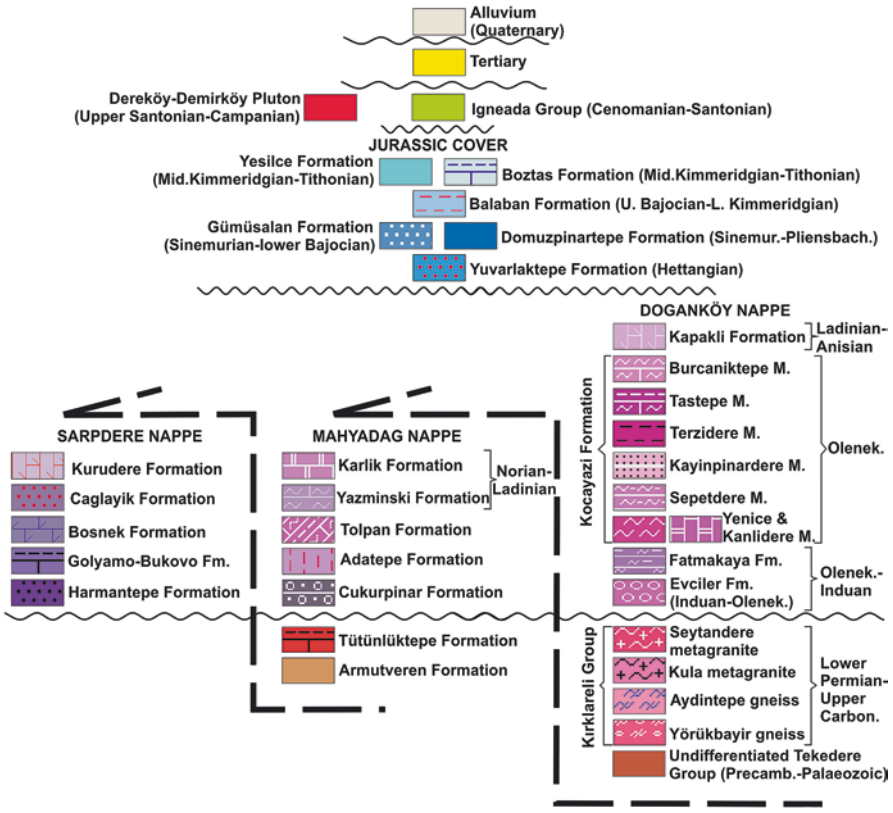

Fig. 2.30 Stratigraphy and structural relations of the rock-units of the Istranca Nappes and their covers in the Istranca Terrane. (After Bedi et al. 2013)

Tauride-Anatolide and SE Anatolian terranes. The ongoing subduction in corresponding suture zones, on the other hand, mainly produced continental arc-type magmatism in the active margins of these terranes. The collision of continental plates along the northern branch of Neotethys in NE Anatolia has resulted in a change in the geochemistry of the igneous activity from arc-related (e.g. Kaygusuz et al. 2008) towards post-collisional extension (e.g. Boztuğ et al. 2006, 2007a) due to break-off of the subducting slab or lithospheric delamination (e.g. Arslan et al. 2013). In contrast to the northward subduction of the Izmir-Ankara Ocean in these models, an alternative model (e.g. Eyüboglu et al. 2011) suggests that the Early Tertiary magmatism is the result of a slab-window of the southward subducting Neotethys which produced adakitic rocks in the Pontide Arc. In N and NW Anatolia (Fig. 2.31) the Early Tertiary magmatic rocks are also related to syn- to post-collisional extension (Keskin et al. 2008; Altunkaynak et al. 2012; Gülmez et al. 2012).

In SE Anatolia, the Early Tertiary magmatism is also ascribed to subduction-related extension (e.g Yiğitbaş and Yılmaz 1996; Robertson et al. 2007) following

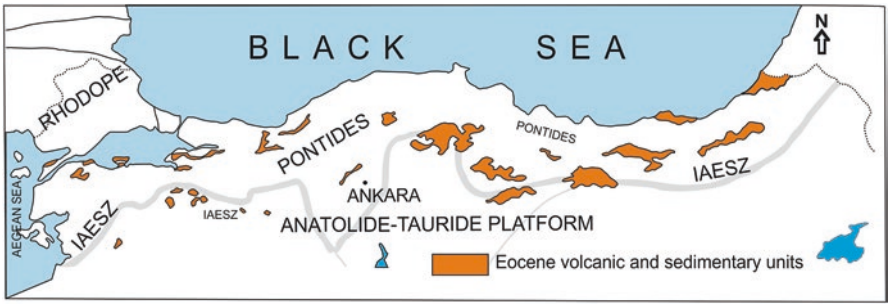

Fig. 2.31 Distribution of Eocene magmatism in N Anatolia. (After Altınkaynak et al. 2012)

the Late Cretaceous northward subduction of the Southern Neotethyan oceanic lithosphere (e.g. Ural et al. 2015). The post-collisional extension or local transtension has also resulted in the formation of numerous basins filled with fluvial and marine sediments and volcanoclastics (e.g. Görür and Tüysüz 2001) during the Early Tertiary. Some of these basins are mainly E-W trending, with long and narrow troughs. They are controlled by oblique faults and comprise volcanic rocks. Typical examples of this type are the Muş Basin in SE Anatolia, the Central Kızılırmak Basin in central Anatolia and the Eskipazar Basin in NW Anatolia. Some other extensional basins such as the Muş-Hınıs, Maden and Hakkari basins in SE Anatolia, the Sivas–Çankırı–Haymana-Tuz Gölü and Ulukışla basins in central Anatolia, the Kastamonu-Boyabat Basin in Central Pontides and the Thrace Basin in NW Anatolia are formed on top of the accretional prisms and characterized by several 1000 m-thick flysch-type sediment accumulation (e.g. Gürer and Aldanmaz 2002).

The Paleogene successions on the SE Anatolian autochthon represent the platform deposits of the eastern Tethys corridor. It was the marine connection between the Mediterranean and the Indian Ocean. The platform sediments shallow upwards and grade into evaporites and finally into continental clastic rocks (e.g. Perinçek et al. 1991) during the mid-Miocene (Tortonian). To the N of this platform, a vast wildflysch basin (Hakkari basin e.g. Elmas and Yilmaz 2003) was constructed on top of allochthonous units of the SE Anatolian suture belt.

The main Paleogene basins in Central Anatolia (e.g. Erzincan, Sivas, Çankırı, Haymana and Tuz Gölü-Ulukışla basins) are formed above the Izmir-Ankara-Erzincan suture belts (Görür et al. 1998a, b; Cater et al. 1991; Dirik et al. 1999; Yılmaz and Yılmaz 2006; Clark and Robertson 2005; Kaymakci et al. 2009). In these basins, the deposition is accompanied by within-plate-type alkaline volcanism. Paleocene and Eocene are characterised by continental red clastics, evaporites and lagoon and reef-type carbonates at the basin-margins (Fig. 2.32). In the internal parts of the basins, flysch-type deposits with olistoliths are observed. The marine deposition has ended at the end of Eocene, or probably Early Oligocene and thick fluvial-evaporitic sequences were formed during the Miocene (e.g. Çiner et al. 2002).

A transpressional period in these basins lasting until middle Miocene in the Sivas basin resulted in thrusting of basin-margin successions and basement rocks onto the

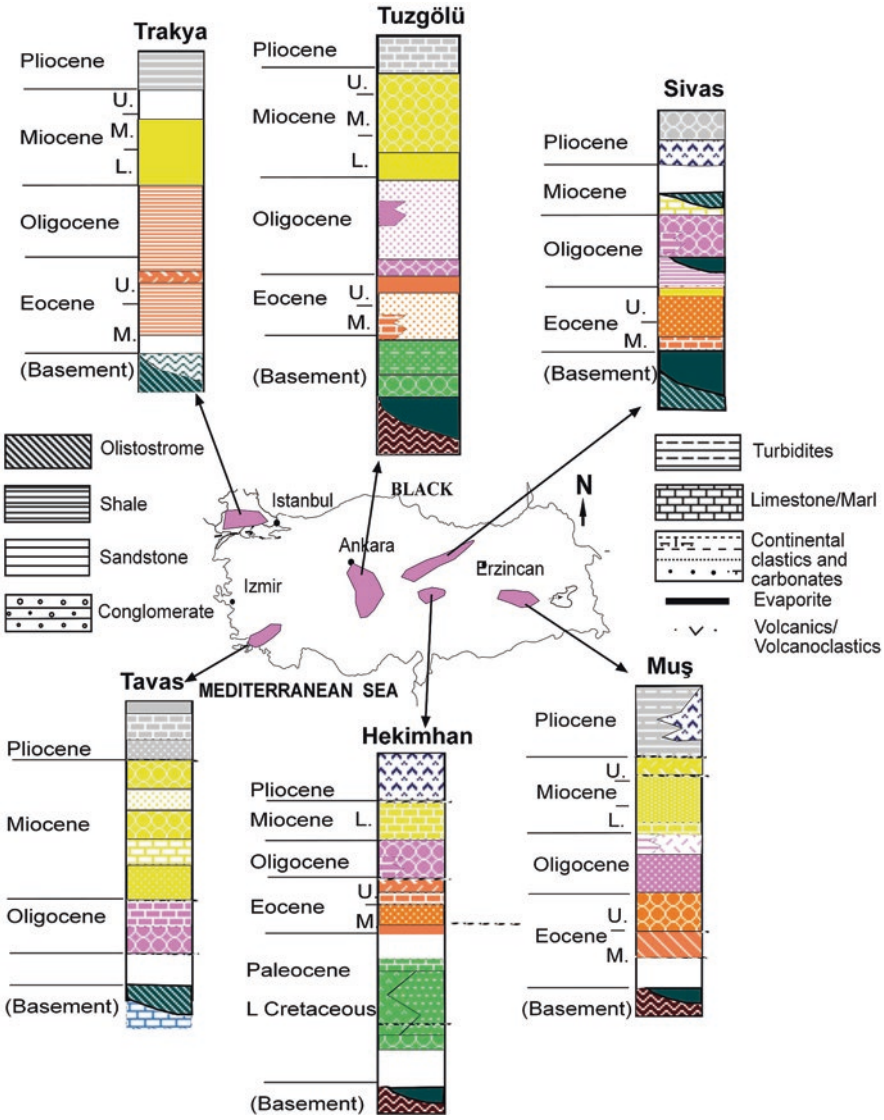

Fig. 2.32 Stratigraphy of the Tertiary Basins. (After Çemen et al. 1999; Dirik et al. 1999; Gürer and Aldanmaz 2002)

basin sediments (e.g. Dirik et al. 1999). The, Miocene-Pliocene interval is characterized by dominant continental deposition (fluvial to lake sediments associated with lavas and volcanoclastic rocks) in almost all of these basins (e.g. Helvacı et al. 2009).

In the post-collisional Thrace Basin in NW Anatolia, the Lower–Middle Eocene units were deposited in transtensional setting (Siyako and Huvaz 2007). The carbon-

ate deposition at the basin-margins during the Eocene-Oligocene is replaced by ca 9 km thick turbidites at the basin-centers and lasted until Early Miocene. During the Late Miocene, the transgression of Paratethys generated brackish-marine sediments in the eastern part of the basin (Görür et al. 2000). The Thrace Basin is interpreted as a fore-arc formation above the northward subducting Intra-Pontide oceanic lithosphere (e.g. Görür and Okay 1996).

2.5 The Neotectonic Period

The Neotectonic period, in general, is defined as the study of the post-Miocene structures and structural history of the Earth's crust (AGI 2009). In Turkey, the term covers the Late Miocene-Quaternary time-span and is mainly triggered by the collision of the Anatolian plate and the Arabian promontory. The convergence ruptured the Anatolian continental crust along the left-lateral East Anatolian Transform Fault (Koçyiğit et al. 2001) and the right-lateral North Anatolian Transform Fault that dissects north Anatolia in E-W direction (e.g. Şaroğlu et al. 1992). Along these main structures the main trunk of Anatolia escaped towards the west (Fig. 2.33).

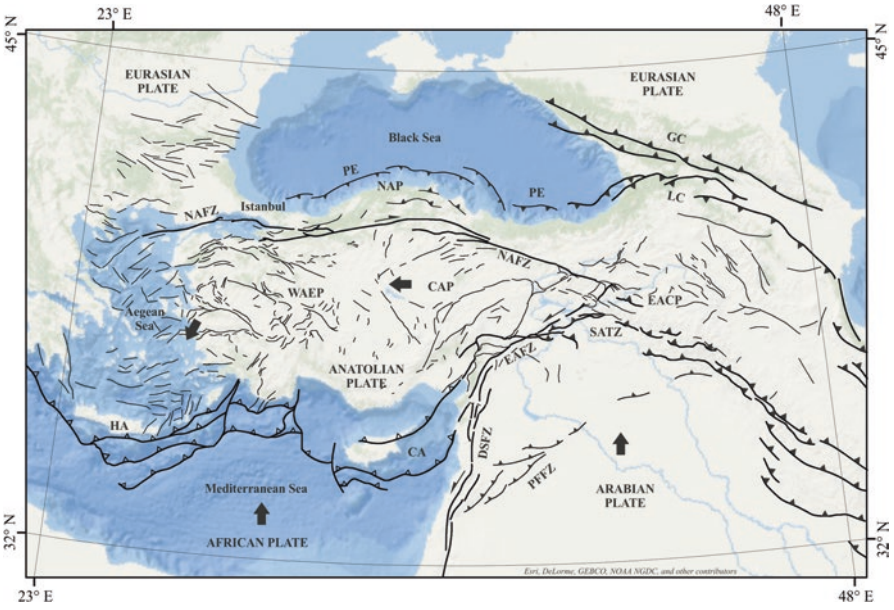

Fig. 2.33 Map showing active fault of Turkey. (After Duman et al. 2016; Abbriviations: *AA* Aegean arc, *CA* Cyprian arc, *DSFZ* Dead Sea fault zone, *EAFZ* East Anatolian fault zone, *NAFZ* North Anatolian fault zone, *SATZ* Southeast Anatolian Thrust Zone, *PE* Pontic Escarpment, *LC* Lesser Caucasus, *GC* Great Caucasus, *WEAP* West Anatolian Extensional Provence, *CAP* Central Anatolian Provence, *EACP* East Anatolian Compressional Provence, *NAP* North Anatolian Provence, *PFFZ* Palmyra Fault and Fold Zone)

Contemporaneously in southern Aegean, the remnant of the Southern Neotethyan oceanic plate was subducting towards north beneath the Aegean-Anatolian plates along the Hellenic Subduction Zone. Hence, the products of the Neotectonic period in Turkey are controlled by a collision-induced uplifting that generated large volcanic provinces and fault-controlled continental basins with transtensional and transpressional characteristics (Fig. 2.34).

On the regional scale Şengör et al. (1985) initially identified four distinct Neotectonic provinces generated by the Neotectonic regime: (i) E Anatolian contractional province with N-S shortening; (ii) N Turkish province with E-W shortening; (iii) W Anatolian extensional province with N-S extension and (iv) Central Anatolian "ova" province with NE-SW shortening and NW-SE extension. The best example for such a relationship is observed in the East Anatolian Volcanic Province (Fig. 2.35). In this area, the main Neotectonic characteristic of is a rapid uplifting of an accretionary prism (the East Anatolian Accretionary Prism, *sensu* Şengör et al. 2003) or alternatively of the attenuated Eastern Tauride continental crust, accompanied by formation of a number of mantle-derived volcanic centers (e.g. Keskin 2003). This is mainly ascribed to delamination of the lithospheric mantle in E Anatolia, which can also explain the present day uplifting of the East Anatolian Plateau as well as the widespread volcanism, low sub-crustal seismic velocities and the anomalously high surface heat flow. The East Anatolian Volcanic Province comprises geographically the northerly located Erzurum-Kars volcanic plateau (Fig. 2.35) with an almost complete record of volcanism from 11 to 1.5 Ma (Keskin et al. 2006) and the East Anatolian Province (s.s.) with a number of peculiar monogenic stratovolcanoes (e.g. Mt. Ararat or Ağrı Volcano). The volcanism in the northern sub-province shows three distinct stages: it initiated with bimodal volcanic products between 11 and 6 Ma (the early stage), turned abruptly into a unimodal intermediate volcanism dominated by andesitic lavas between 6 and 5 Ma (the middle stage), and finally reverted to

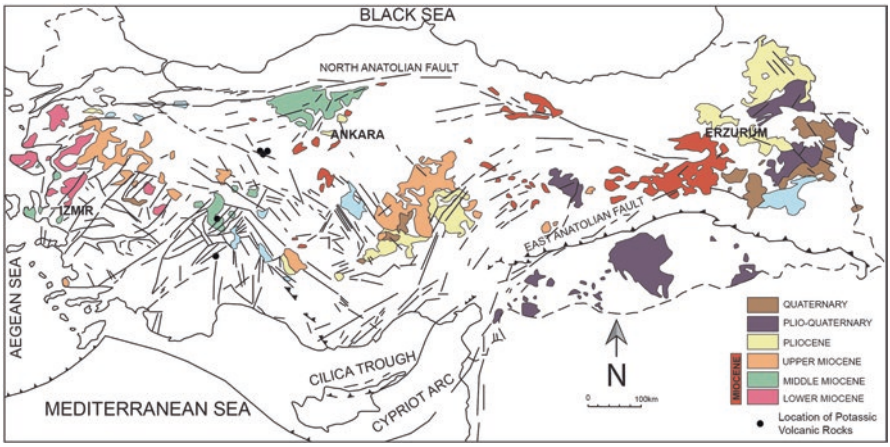

Fig. 2.34 Simplified tectonic map of Turkey showing the major Neotectonic elements and the sites of Miocene-Quaternary volcanism. (Modified after Akal 2001; Türkecan 2015)

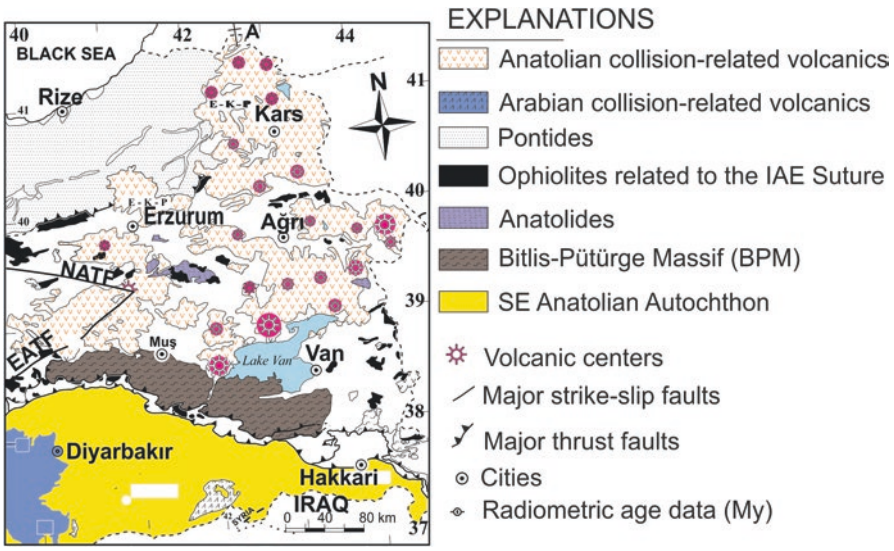

Fig. 2.35 The East Anatolian Volcanic Province and distribution of the main volcanic centres. (After Keskin 2003)

bimodal activity between 5 and 1.5 Ma (the late stage). The southern sub-province to the N of Lake Van is the locus of Pliocene-Quaternary volcanism with a series of large shield volcanoes (e.g. Tendürek) and stratovolcanoes (e.g. Ağrı, Nemrut, Süphan, Etrüsk, etc.) and vast lava plateaus, (Çaldıran and Doğubeyazıt plains). A very detailed account on the morphology, petrography and petrogenesis of the main volcanic centres is given in Türkecan (2015).

In the SE Anatolian Autochthon, the E-W extension resulted in the formation of a shield-type volcanic complex (Karacadağ Volcanic Complex) with alkaline within-plate lavas erupted along N-S trending faults during the Quaternary (e.g. Arger et al. 2000; Bridgland et al. 2007). It was sourced by a garnet bearing, deep asthenospheric mantle and covers an area of ~10,000 km^2 (Lustrino et al. 2010).

The Central Anatolian "ova" province with NE-SW shortening and NW-SE extension is another area of extensive volcanism (Central Anatolian Volcanic Province; Toprak and Göncüoğlu 1993) during the Neotectonic period. The formation of auxiliary strike-slip faults and fault-zones (e.g. Ecemiş and Tuz Gölü faults, e.g. Dirik and Göncüoğlu 1996; Özsayın et al. 2013) in Central Anatolia along which Late Neogene–Quaternary pull-apart basins were generated. Important volcanic centres such as Erciyes, Melendiz and Hasandag stratovolcanoes were formed on the intersection of the main strands of these faults (Toprak and Göncüoğlu 1993). The Neogene-Quaternary volcanism in central Anatolia is mainly characterised (e.g. Kuscu-Gençalioğlu and Geneli 2010) by calc-alkaline andesites-dacites, with subordinate tholeiitic-mildly alkaline basaltic volcanism of the monogenetic cones. Voluminous rhyolitic ignimbrite deposits (e.g. Temel et al. 1998; Aydar et al. 2012) cover the volcanic province (Fig. 2.36 CAVP). Trace ele-

ment ratio plots and REE modelling (Sen et al. 2004) indicate that the Central Anatolian volcanism was generated from a lithospheric mantle source that recorded the previous subduction events between Afro-Arabian and Eurasian plates during Eocene to Miocene times.

The Galatian Volcanic Province in NW Central Anatolia is characterised by large volumes of trachyandesitic-dacitic lava flows and pyroclastics of Miocene age. The volcanic rocks are formed in a transtensional tectonic setting associated with movement along the North Anatolian Fault zone (e.g. Wilson et al. 1997).

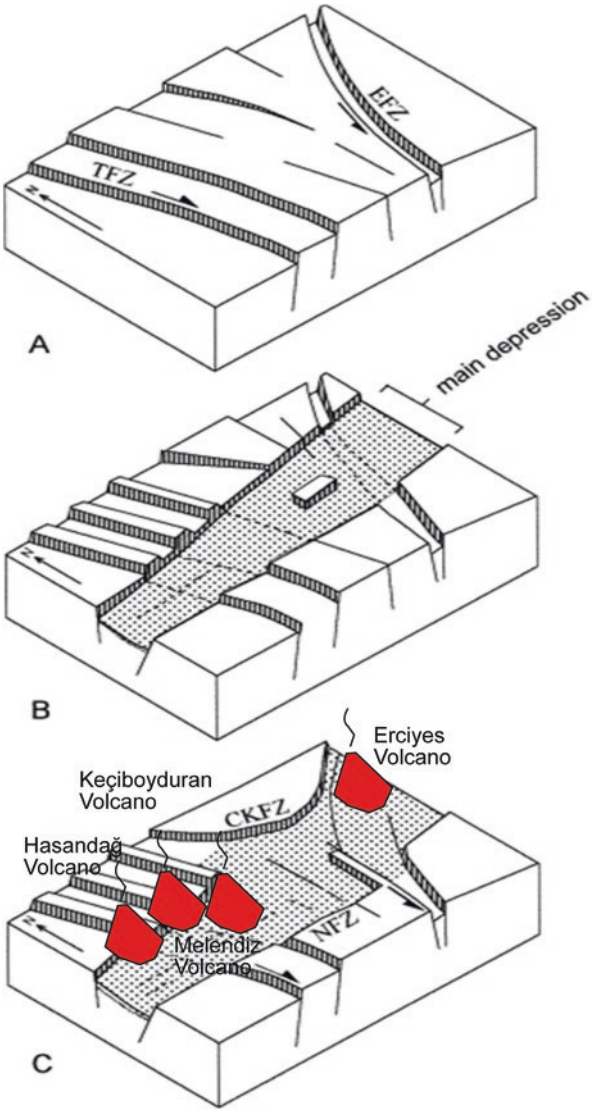

Fig. 2.36 Relationship between active tectonics and volcanism in the Central Anatolian Volcanic Province and surrounding areas (After Toprak and Göncüoğlu 1993; Toprak 1998). (**a**) Pre-Mid Miocene, (**b**) Mid Miocene-Early Pliocene, (**c**) Late Pliocene-Quaternary. Explanations: *TFZ* Tuzgölü Fault Zone, *EFZ* Ecemiş Fault Zone, *NFZ* Niğde Fault Zone, *CKFZ* Central Kızılırmak Fault Zone

The Quaternary volcanism related to the Neotectonic period in the "Isparta Angle" in SW Anatolia, is part of the post-collisional alkali-potassic to ultrapotassic magmatism, active since Miocene (Savaşçın et al. 1995). The magmatism is contemporaneous with the Aegean extensional regime initiated during the Late Miocene and active throughout the Pliocene and Quaternary. Geochemical features suggest the involvement of an asthenospheric OIB-type melt with a possible carbonatitic component, that interacted with remnants of the delaminated lithosphere during upwelling (e.g. Platevoet et al. 2014).

During the Neotectonic Period, West Anatolia was the side of ongoing extension (e.g. Alçiçek et al. 2013) where the Menderes Core Complex was the site of numerous supra-detachment (e.g. Sözbilir et al. 2011) basins. This extension was accompanied by alkaline to tholeiitic magmatism (e.g. Yılmaz 1989) ascribed to asthenospheric uplifting since Late Miocene (e.g. Seghedi et al. 2013).

The youngest products of the Neotectonic Period are the Quaternary graben-half graben system in as well as the pull-apart basins along the main transform faults in western (e.g. Bozkurt 2001, 2003; Koçyiğit 2005), northwestern (e.g. Okay et al. 2000; Aksu et al. 2000), northern (e.g. Barka et al. 2000; Ellero et al. 2015b), central (e.g. Koçyiğit and Erol 2001; Dirik 2001; Özsayın et al. 2013), southern (e.g. Rojay et al. 2001; Aksu et al. 2005) and Eastern (e.g. Collins et al. 2005; Koçyiğit et al. 2001) Anatolia.

Several alluvial planes and deltas to the Mediterranean (e.g. Çukurova alluvial plane) or the Black Sea coast (Kizilırmak delta) are sites of ongoing fluvial deposition.

The active faults of Turkey were the subject of numerous studies, and the most recent maps have been published by the General Directorate of Mineral Research and Exploration (Şaroğlu et al. 1992; Herece and Akay 2003; Emre et al. 2013).

2.6 Conclusions

During its geological past, a number of terranes that make the main body of Turkey today were located between the supercontinents Gondwana and Laurasian. During the Cadomian, Variscan, Cimmerian and Alpine orogenic cycles, pieces of these terranes were rifted off, drifted away from the supercontinents by the opening of oceanic seaways at their rear to form oceanic seaways. Their closure was followed by the amalgamation of these terranes of variable sizes in formation of distinct (especially the Neotethyan sutures) or cryptic (e.g. Cadomian suture) suture belts. By repeated reorganization of the terrane boundaries then resulted in a very complex mosaic of continental and oceanic terranes. As the formation of different mineral deposits is controlled by plate and intraplate tectonic processes, it is vital to understand the configurations of these plates and their evolution. In this brief review of the geology and geodynamic evolution of Turkey the igneous, sedimentary and metamorphic rock units of the platform, platform margin and oceanic units of the Alpine cycle were described in the previous chapters on the basis of their tectonic

setting. However, the interpretations are restricted to the quality of the state-of-art data. The author hopes that this short review provokes the reader to invalidate these interpretations by new and precise data with additional afford and a multidisciplinary approach.

Acknowledgments This review is only a brief summary of facts and speculations in an area with very complex and highly debated geological problems. The author tried to present a balanced account on the different approaches and models.

For the patient editorial handling, I am thankful to F. PIRAJNO, T. ÜNLÜ, C DÖNMEZ and M. B. ŞAHİN. Özgür ÖZERKAN, Uğur BALCI and Deniz TRINGA are acknowledged for their help in revising the figures.

References

AGI (2009) Glossary of geology. American Geological Institute, Washington, DC. online version. www.agiweb.org

Akal C (2001) Occurrence, emplacement, and origin of high-potassium volcanics in the southern part of the Afyon region. PhD thesis, Dokuz Eylül University İzmir, p 239. Unpublished

Akbayram K, Okay AI, Satır M (2013) Early Cretaceous closure of the intra-Pontide Ocean in western Pontides (northwestern Turkey). J Geodyn 65:38–55

Akıman O, Erler A, Göncüoğlu MC, Güleç N, Geven A, Türeli K, Kadıoğlu Y (1993) Geochemical characteristics of granitoids along the western margin of the Central Anatolian crystalline complex and their tectonic implications. Geol J 28:371–382

Aksu AE, Calon TJ, Hiscott RN, Yasar D (2000) Anatomy of the North Anatolian fault zone in the Marmara Sea, Western Turkey: extensional basins above a continental transform. GSA Today 10(6):3–7

Aksu AE, Calon TJ, Hall J, Yaşar D (2005) Origin and evolution of the Neogene Iskenderun basin, Northeastern Mediterranean Sea. Mar Geol 221(1):161–187

Alçiçek MC, Brogi A, Capezzuoli E, Liotta D, Meccheri M (2013) Superimposed basin formation during Neogene–quaternary extensional tectonics in SW-Anatolia (Turkey): insights from the kinematics of the Dinar fault zone. Tectonophysics 608:713–727

Aldanmaz E, Yalınız MK, Güçtekin A, Göncüoğlu MC (2008) Geochemical characteristics of mafic lavas from the Tethyan ophiolites in western Turkey: implications for heterogeneous source contribution during variable stages of ocean crust generation. Geol Mag 145:37–54

Altıner D, Koçyiğit A, Farinacci A, Nicosia U, Conti MA (1991) Jurassic-early Cretaceous stratigraphy and paleogeographic evolution of the southern part of North-Western Anatolia (Turkey). Geol Romana 27:1–68

Altunkaynak Ş, Sunal G, Aldanmaz E, Genç CŞ, Dilek Y, Furnes H, Foland KA, Jang J, Yıldız M (2012) Eocene granitic magmatism in NW Anatolia (Turkey) revisited: new implications from comparative zircon SHRIMP U–Pb and ^{40}Ar–^{39}Ar geochronology and isotope geochemistry on magma genesis and emplacement. Lithos 155:289–309

Arger J, Mitchell J, Westaway RW (2000) Neogene and quaternary volcanism of southeastern Turkey. In: Bozkurt E, Winchester JA, Piper JD (eds) Tectonics and magmatism in Turkey and the surrounding area. Geol Soc London Spec Publ 173:459–487

Arslan M, Tüysüz N, Korkmaz S, Kurt H (1997) Geochemistry and petrogenesis of the eastern Pontide volcanic rocks, Northeast Turkey. Chem Erde 57:157–187

Arslan M, Temizel I, Abdioğlu E, Kolaylı H, Yücel C, Boztuğ D, Şen C (2013) ^{40}Ar–^{39}Ar dating, whole-rock and Sr–Nd–Pb isotope geochemistry of post-collisional Eocene volcanic rocks in

the southern part of the Eastern Pontides (NE Turkey): implications for magma evolution in extension-induced origin. Contrib Mineral Petrol 166(1):113–142
Aydar E, Schmitt AK, Çubukçu HE, Akin L, Ersoy O, Sen E, Duncan RA, Atici G (2012) Correlation of ignimbrites in the central Anatolian volcanic province using zircon and plagioclase ages and zircon compositions. J Volcanol Geotherm Res 213:83–97
Aygül M, Okay AI (2012) Blueschist-facies metamorphic rocks in the Central Pontides, Northern Turkey. In: EGU General Assembly Conference Abstract, vol 14. p 157
Aygül M, Okay AI, Oberhänsli R, Schmidt A, Sudo M (2015) Late cretaceous infant intra-oceanic arc volcanism, the Central Pontides, Turkey: petrogenetic and tectonic implications. Asian J Earth Sci 111:312–327
Aysal N, Ustaömer T, Öngen S, Keskin M, Köksal S, Peytcheva I, Fanning M (2012) Origin of the early-middle Devonian magmatism in the Sakarya Zone, NW Turkey: geochronology, geochemistry and isotope systematics. Asian J Earth Sci 45:201–222
Barka A, Akyüz HS, Cohen HA, Watchorn F (2000) Tectonic evolution of the Niksar and Tasova–Erbaa pull-apart basins, North Anatolian Fault Zone: their significance for the motion of the Anatolian block. Tectonophysics 322(3):243–264
Beccaletto L, Jenny C (2004) Geology and correlation of the Ezine Zone: a Rhodope fragment in NW Turkey? Turk J Earth Sci 13(2):145–176
Bedi Y, Vasilev E, Dabovski C, Ergen A, Okuyucu C, Dogan A, Tekin UK, Ivanova D, Boncheva I, Lakova I, Sachanski V, Kuscu I, Tuncay E, Demiray DG, Soycan H, Göncüoğlu MC (2013) New age data from the tectonostratigraphic units of the Istranca "Massif" in NW Turkey: a correlation with SE Bulgaria. Geol Carpath 64:255–277
Bektaş O, Şen C, Atıcı Y, Köprübaşı N (2000) Migration of the upper Cretaceous subduction-related volcanism towards the back-arc basin of the eastern Pontide magmatic arc (NE Turkey). Geol J 34:95–106
Bortolotti V, Chiari M, Göncüoğlu MC, Marcucci M, Principi G, Tekin UK, Saccani E, Tassinari R (2013) Age and geochemistry of basalt-chert associations in the ophiolites of the Izmir-Ankara mélange east of Ankara, Turkey: preliminary data. Ofioliti 38(2):157–173
Bozkaya H, Yalcin H, Göncüoğlu MC (2012a) Diagenetic and very low-grade metamorphic characteristics of the Paleozoic series of the Istanbul terrane (NW Turkey). Swiss J Geosci 105:183–201. https://doi.org/10.1007/s00015-012-0108-2
Bozkaya O, Yalcin H, Göncüoğlu MC (2012b) Mineralogic evidences of a mid-Paleozoic tectonothermal event in the Zonguldak terrane, northwest Turkey: implications for the dynamics of some Gondwana-derived terranes during the closure of the Rheic Ocean. Can J Earth Sci 49:559–575
Bozkurt E (2001) Neotectonics of Turkey-a synthesis. Geodin Acta 14:3–30
Bozkurt E (2003) Origin of NE-trending basins in western Turkey. Geodin Acta 16(2):61–81
Bozkurt E, Oberhansli R (2001) Menderes massif (Western Turkey): structural, metamorphic and magmatic evolution – a synthesis. Int J Earth Sci 89:679–708
Boztuğ D, Erçin Aİ, Kuruçelik MK, Göç D, Kömür İ, İskenderoğlu A (2006) Geochemical characteristics of the composite Kaçkar batholith generated in a Neo-Tethyan convergence system, Eastern Pontides, Turkey. Asian J Earth Sci 27(3):286–302
Boztuğ D, Jonckheere R, Wagner GA, Ercin AI, Yegingil Z (2007a) Titanite and zircon fission-track dating resolves successive igneous episodes in the formation of the composite Kackar batholith in the Turkish eastern Pontides. Int J Earth Sci 96:875–886
Boztuğ D, Tichomirowa M, Bombach K (2007b) 207Pb– 206Pb single-zircon evaporation ages of some granitoid rocks reveal continent-oceanic island arc collision during the Cretaceous geodynamic evolution of the central Anatolian crust, Turkey. Asian J Earth Sci 31:71–86
Bridgland DR, Demir T, Seyrek A, Pringle M, Westaway R, Beck AR, Rowbotham G, Yurtmen S (2007) Dating quaternary volcanism and incision by the River Tigris at Diyarbakır, southeast Turkey. J Quat Sci 22(4):387–393
Candan O, Dora OO (1998) Granulite, eclogite and blueschist relics in the Menderes massif: an approach to Pan-African and tertiary metamorphic evolution. Geol Soc Turk Bull 41:1–35

Candan O, Koralay OE, Akal C, Kaya O, Oberhänsli R, Dora OÖ, Konak N, Chen F (2011) Supra-Pan-African unconformity between core and cover series of the Menderes Massif/Turkey and its geological implications. Precambrian Res 184(1):1–23

Candan O, Koralay OE, Topuz G, Oberhänsli R, Fritz H, Collins AS, Chen F (2016) Late Neoproterozoic gabbro emplacement followed by early Cambrian eclogite-facies metamorphism in the Menderes Massif (W. Turkey): implications on the final assembly of Gondwana. Gondwana Res 34:158–173

Cater JML, Hanna SS, Ries AC, Turner P (1991) Tertiary evolution of the Sivas Basin, central Turkey. Tectonophysics 195(1):29–46

Catlos EJ, Baker CB, Sorensen SS, Jacob L, Çemen I (2011) Linking microcracks and mineral zoning of detachment-exhumed granites to their tectonomagmatic history: evidence from the Salihli and Turgutlu plutons in western Turkey (Menderes Massif). J Struct Geol 33(5):951–969

Çelik ÖF, Marzoli A, Marschik R, Chiaradia M, Neubauer F, Öz İ (2011) Early–middle Jurassic intra-oceanic subduction in the İzmir-Ankara-Erzincan Ocean, Northern Turkey. Tectonophysics 509(1):120–134

Çemen I, Göncüoğlu MC, Dirik K (1999) Structural evolution of the Tuz Gölü (Salt Lake) basin: evidence for late Cretaceous extension and Cenozoic inversion in central Anatolia, Turkey. J Geol 107:693–706

Çemen I, Tekeli O, Seyitoglu G, Isik V (2005) Are turtleback fault surfaces common structural elements of highly extended terrains? Earth-Sci Rev 73:139–148

Chatalov GA (1988) Recent developments in the geology of the Strandzha Zone in Bulgaria. Bull Tech Univ İstanbul 41:433–465

Çimen O, Göncüoğlu MC, Sayıt K (2016) Geochemistry of the meta-volcanic rocks from the Çangaldağ Complex in Central Pontides: implications for the middle Jurassic arc – back – arc system in the Neotethyan Intra-Pontide Ocean. Turk J Earth Sci 25(6):491–512

Çiner A, Kosun E, Deynoux M (2002) Fluvial, evaporitic and shallow-marine facies architecture, depositional evolution and cyclicity in the Sivas Basin (lower to middle Miocene), Central Turkey. Asian J Earth Sci 21(2):147–165

Clark M, Robertson AHF (2005) Uppermost Cretaceous–lower tertiary Ulukışla Basin, south-central Turkey: sedimentary evolution of part of a unified basin complex within an evolving Neotethyan suture zone. Sediment Geol 173(1):15–51

Çolakoğlu AR, Günay K, Göncüoğlu MC, Oyman V, Erdogan K (2014) Geochemical evaluation of the late Maastrichtian subduction-related volcanism in the southern Neotethys in Van area, and a correlation across the Turkish-Iranian border. Ofioliti 39:51–65

Collins PE, Rust DJ, Bayraktutan MS, Turner SD (2005) Fluvial stratigraphy and palaeoenvironments in the Pasinler Basin, eastern Turkey. Quat Int 140:121–134

Dirik K (2001) Neotectonic evolution of the northwestward arched segment of the Central Anatolian fault zone, Central Anatolia, Turkey. Geodin Acta 14(1–3):147–158

Dirik K, Göncüoğlu MC (1996) Neotectonic characteristics of the Central Anatolia. Int Geol Rev 38:807–817

Dirik K, Göncüoğlu MC, Kozlu H (1999) Stratigraphy and pre-Miocene tectonic evolution of the southwestern part of the Sivas Basin, Central Anatolia. Geol J 34:303–319

Dokuz A, Tanyolu E (2006) Geochemical constraints on the provenance, mineral sorting and subaerial weathering of lower Jurassic and upper Cretaceous clastic rocks of the Eastern Pontides, Yusufeli (Artvin), NE Turkey. Turk J Earth Sci 15(2):181–209

Dora OO, Kun N, Candan O (1991) Metamorphic history and geotectonic evolution of the Menderes massif. In: IESCA proceedings. pp 102–115

Duman TY, Çan T, Emre Ö, Kadirioğlu FT, Başarır-Baştürk N, Kılıç T, Arslan S (2016) Seismotectonic database of Turkey. Earthq Eng 16 (8): 3277-3316

Duru M, Pehlivan Ş, Şentürk Y, Yavaş F, Kar H (2004) New results on the lithostratigraphy of the Kazdağ Massif in northwest Turkey. Turk J Earth Sci 13(2):177–186

Ellero A, Ottria G, Sayit K, Catanzariti R, Frassi C, Göncüoğlu MC, Marroni M, Pandolfi L (2015a) Geological and geochemical evidences for a Late Cretaceous continental arc in the Central Pontides, Northern Turkey. Ofioliti 40(2):73–90

Ellero A, Ottria G, Marroni M, Pandolfi L, Göncüoğlu MC (2015b) Analysis of the North Anatolian Shear Zone in Central Pontides (Northern Turkey): insight for geometries and kinematics of deformation structures in a transpressional zone. J Struct Geol 72:124–141

Elmas A, Yilmaz Y (2003) Development of an oblique subduction zone-tectonic evolution of the Tethys suture zone in southeast Turkey. Int Geol Rev 45(9):827–840

Emre Ö, Duman TY, Özalp S, Elmaci H, Olgun Ş, Şaroğlu F (2013) 1: 1.250.000 scaled active fault map of Turkey with explanations. General Directorate of Mineral Research and Exploration Special Publication Nr: 30, Ankara, p 89

Erdogan B, Güngör T (2004) The problem of the core-cover boundary of the Menderes Massif and an emplacement mechanism for regionally extensive gneissic granites, Western Anatolia (Turkey). Turk J Earth Sci 13(1):15–36

Erler A (1984) Tectonic setting of the massive sulfide deposits of the Southeast Anatolian Thrust Belt. In: Tekeli O, Göncüoğlu MC (eds) International symposium on the geology of the Taurus Belt. MTA Publications, Ankara, pp 237–244

Eyüboglu Y, Chung SL, Santosh M, Dudas FO, Akaryalı E (2011) Transition from shoshonitic to adakitic magmatism in the Eastern Pontides, NE Turkey: implications for slab window melting. Gondwana Res 19(2):413–429

Floyd PA, Yalınız MK, Göncüoğlu MC (1998) Geochemistry and petrogenesis of intrusive and extrusive ophiolitic plagiogranites, Central Anatolian Crystalline Complex, Turkey. Lithos 42(3/4):225–240

Floyd PA, Özgül L, Göncüoğlu MC (2003) Metabasite blocks from the Koçyaka HP-LT metamorphic rocks, Konya, central Anatolia: geochemical evidence for an arc-back-arc pair? Turk J Earth Sci 12:157–174

Frassi C, Göncüoğlu CM, Marroni M, Pandolfi L, Ruffini L, Ellero A, Ottria G, Sayit K (2016) The Intra-Pontide suture zone in the Tosya-Kastamonu area, Northern Turkey. J Maps 12 (sup1): 211–219

Genç ŞC, Tüysüz O (2010) Tectonic setting of the Jurassic bimodal magmatism in the Sakarya Zone (Central and Western Pontides), Northern Turkey: a geochemical and isotopic approach. Lithos 118(1):95–111

Geneli F, Göncüoğlu MC, Lassiter J, Toksoy-Köksal F (2010) Eocene post-collisional volcanism in the Central Anatolian Crystalline Complex, Turkey: petrology and geodynamic significance. Geol Balcan 39(1–2):127–128

Glodny J, Hetzel R (2007) Precise U–Pb ages of syn-extensional Miocene intrusions in the central Menderes Massif, western Turkey. Geol Mag 144(02):235–246

Gökten E, Floyd PA (2007) Stratigraphy and geochemistry of pillow basalts within the ophiolitic mélange of the Izmir–Ankara–Erzincan suture zone: implications for the geotectonic character of the northern branch of Neotethys. Int J Earth Sci 96:725–741

Göncüoğlu MC (1977) Geologie des westlichen Niğde Massifs. PhD thesis, Bonn F. W. Universiy, Bonn, p 176. Unpublished

Göncüoğlu MC (2010) Introduction to the geology of Turkey: geodynamic evolution of the pre-Alpine and Alpine terranes. Gen Direct Mineral Res Explor Monogr Ser 5:1–66

Göncüoğlu MC (2011) Geology of the Kütahya-Bolkardağ Belt. Bull Min Res Exp 142:223–277

Göncüoğlu MC (2014) Comments on a single versus multi-armed Southern Neotethys in SE Turkey and Iran. IGCP589 Development of the Asian Tethyan realm: Geneses, process and outcome. Abstracts and proceedings, pp 89–95

Göncüoğlu MC, Kozur H (1998) Remarks on the pre-Variscan development in Turkey. In: Linnemann U, Heuse T, Fatka O, Kraft P, Brocke R, Erdtmann BT (eds) Pre-variscan terrane analyses of "Gondwanean Europa." Proceedings, Schriften des Staatl Mus Min Geol Dresden 9:137–138

Göncüoğlu MC, Türeli TK (1994) Alpine collisional-type granitoids from the Central Anatolian Crystalline Complex. J Kocaeli Univ 1:39–46

Göncüoğlu MC, Turhan N (1984) Geology of the Bitlis Metamorphic Belt. In: Tekeli O, Göncüoğlu MC (eds) International symposium on the geology of the Taurus Belt. MTA Publications, Ankara, pp 237–244

Göncüoğlu MC, Kozlu H, Dirik K (1997) Pre-Alpine and Alpine terranes in Turkey: explanatory notes to the terrane map of Turkey. Ann Géol Pays Hellén 37:515–536

Göncüoğlu MC, Turhan N, Şentürk K, Özcan A, Uysal Ş, Yalınız K (2000) A geotraverse across NW Turkey: tectonic units of the Central Sakarya region and their tectonic evolution. In: Bozkurt E, Winchester JA, Piper JA (eds) Tectonics and magmatism in Turkey and the surrounding area. Geol Soc Lond Spec Publ 173:139–161

Göncüoğlu MC, Göncüoğlu Y, Kozlu H, Kozur H (2004) Geological evolution of the Taurides during the infra-Cambrian to Carboniferous period: a Gondwanan perspective based on new biostratigraphic findings. Geol Carpath 55:433–447

Göncüoğlu MC, Yalınız MK, Tekin UK (2006) Geochemistry, tectono-magmatic discrimination and radiolarian ages of basic extrusives within the Izmir-Ankara Suture Belt (NW Turkey): time constraints for the Neotethyan evolution. Ofioliti 31:25–38

Göncüoğlu MC, Gürsu S, Tekin UK, Köksal S (2008) New data on the evolution of the Neotethyan oceanic branches in Turkey: late Jurassic ridge spreading in the Intra-Pontide branch. Ofioliti 33:153–164

Göncüoğlu MC, Sayıt K, Tekin UK (2010) Oceanization of the northern Neotethys: geochemical evidence from ophiolitic mélange basalts within the Izmir-Ankara suture belt, NW Turkey. Lithos 116:175–187

Göncüoğlu MC, Maroni M, Sayit K, Tekin UK, Ottria G, Pandolfi L, Ellero A (2012) The Aylı Dag ophiolite sequence (central-northern Turkey): a fragment of middle Jurassic oceanic lithosphere within the Intra-Pontide suture zone. Ofioliti 37:77–91

Göncüoğlu MC, Marroni M, Pandolfi L, Ellero A, Ottria G, Catanzariti R, Tekin UK, Sayit K (2014) The Arkot Dağ Mélange in Araç area, central Turkey: evidence of its origin within the geodynamic evolution of the Intra-Pontide suture zone. Asian J Earth Sci 85:117–139

Göncüoğlu MC, Tekin UK, Sayit K, Bedi Y, Uzunçimen S (2015) Opening, evolution and closure of the Neotethyan oceanic branches in Anatolia as inferred by radiolarian research. Radiolaria 35:88–90

Görür N (1988) Timing of opening of the Black Sea basin. Tectonophysics 47:247–262

Görür N, Okay AI (1996) A fore-arc origin for the Thrace Basin, NW Turkey. Geol Rundsch 85(4):662–668

Görür N, Tüysüz O (2001) Cretaceous to Miocene palaeogeographic evolution of Turkey: implications for hydrocarbon potential. J Pet Geol 24:119–146

Görür N, Okay AI, Şengör AMC, Tüysüz O, Sakınç M, Yiğitbaş E, Yaltırak C (1998a) Triassic to Miocene palaeogeographic atlas of Turkey. In: General Directorate of Mineral Research and Exploration Publications, Ankara, p 96

Görür N, Tüysüz O, Şengör AMC (1998b) Tectonic evolution of the central Anatolian basins. Int Geol Rev 40(9):831–850

Görür N, Çağatay N, Sakinç M, Akkök R, Tchapalyga A, Natalin B (2000) Neogene Paratethyan succession in Turkey and its implications for the palaeogeography of the Eastern Paratethys. In: Bozkurt E, Winchester JA, Piper JD (eds) Tectonics and magmatism in Turkey and the surrounding area. Geol Soc London Spec Publ 173(1):251–269

Gülmez F, Genç ŞC, Keskin M, Tüysüz O (2012) A post-collision slab-breakoff model for the orgin of the middle Eocene magmatic rocks of the Armutlu–Almacık belt, NW Turkey and its regional implications. Geol Soc Lond Spec Publ 372:107–139

Gürer ÖF, Aldanmaz E (2002) Origin of the upper Cretaceous–tertiary sedimentary basins within the Tauride–Anatolide platform in Turkey. Geol Mag 139(02):191–197

Gürsu S (2016) A new petrogenetic model for meta-granitic rocks in the central and Southern Menderes Massif-W Turkey: implications for Cadomian crustal evolution within the Pan-African mega-cycle. Precambrian Res 275:450–470

Gürsu S, Göncüoğlu MC (2006) Petrogenesis and tectonic setting of Cadomian felsic igneous rocks, Sandıklı area of the western Taurides, Turkey. Int J Earth Sci 95:741–757

Gürsu S, Möller A, Göncüoğlu MC, Köksal S, Demircan H, Toksoy Köksal F, Kozlu H, Sunal G (2015) Neoproterozoic continental arc volcanism at the northern edge of the Arabian Plate, SE Turkey. Precambrian Res 258:208–233

Hagdorn H, Göncüoğlu MC (2007) Early-middle Triassic echinoderm remains from the Istranca Massif, Turkey. N Jb Geol Paleont Abh 246:235–245

Helvacı C, Ersoy EY, Sözbilir H, Erkul F, Sümer O, Uzel B (2009) Geochernistry and $^{40}Ar/^{39}Ar$ geochronology of Miocene volcanic rocks from the Karaburun Peninsula: implications for amphibole-bearing lithospheric mantle source, Western Anatolia. J Volcanol Geotherm Res 185:181–202

Herece E, Akay E (2003) Atlas of North Anatolian fault (NAF). General Directorate of Mineral Research and Exploration Special Publ No 2, Ankara

Howell DG (1995) Principles of terrane analysis: new applications for global tectonics, vol 8. Springer, Berlin

İlbeyli N, Demirbilek M, Kibici Y (2015) Geochemistry and petrogenesis of the late Paleozoic magmatism in the Sakarya Zone (NW Turkey). Neues Jb Mineral Abh 192(2):177–194

Karacık Z, Tüysüz O (2010) Petrogenesis of the late Cretaceous Demirköy igneous complex in the NW Turkey: implications for magma genesis in the Strandja Zone. Lithos 114(3):369–384

Karslı O, Dokuz A, Uysal İ, Aydin F, Kandemir R, Wijbrans J (2010) Generation of the early Cenozoic adakitic volcanism by partial melting of mafic lower crust, Eastern Turkey: implications for crustal thickening to delamination. Lithos 114:109–120

Kaygusuz A, Siebel W, Şen C, Satir M (2008) Petrochemistry and petrology of I-type granitoids in an arc setting: the composite Torul pluton, Eastern Pontides, NE Turkey. Int J Earth Sci 97(4):739–764

Kaymakci N, Özçelik Y, White SH, Van Dijk PM (2009) Tectono-stratigraphy of the Çankırı Basin: late Cretaceous to early Miocene evolution of the Neotethyan suture zone in Turkey. Geol Soc Lond Spec Publ 311:67–106

Keskin M (2003) Magma generation by slab steepening and breakoff beneath a subduction-accretion complex: an alternative model for collision-related volcanism in Eastern Anatolia, Turkey. Geophys Res Lett 30:1–4

Keskin M, Pearce JA, Kempton PD, Greenwood P (2006) Magma-crust interactions and magma plumbing in a postcollisional setting: geochemical evidence from the Erzurum-Kars volcanic plateau, eastern Turkey. Geol Soc Am Spec Pap 409:475–505

Keskin M, Genç ŞC, Tüysüz O (2008) Petrology and geochemistry of post-collisional Middle Eocene volcanic units in North-Central Turkey: evidence for magma generation by slab break-off following the closure of the Northern Neotethys Ocean. Lithos 104(1):267–305

Ketin I (1966) Tectonic units of Anatolia. Bull Min Res Exp 66:23–34

Kocyigit A (1991) First remark on the geology of Karakaya basin. Karakaya Orogen and pre-Jurassic nappes in eastern Pontides, Turkey. Geol Romana 27:2–11

Koçyiğit A (2005) The Denizli graben-horst system and the eastern limit of western Anatolian continental extension: basin fill, structure, deformational mode, throw amount and episodic evolutionary history, SW Turkey. Geodin Acta 18(3–4):167–208

Koçyiğit A, Erol O (2001) A tectonic escape structure: Erciyes pull-apart basin, Kayseri, central Anatolia, Turkey. Geodin Acta 14(1–3):133–145

Koçyiğit A, Yılmaz A, Adamia S, Kuloshvili S (2001) Neotectonics of East Anatolian Plateau (Turkey) and Lesser Caucasus: implication for transition from thrusting to strike-slip faulting. Geodin Acta 14(1–3):177–195

Köksal S, Romer RL, Göncüoğlu MC, Toksoy-Köksal F (2004) Timing of the transition from the post-collisional to A-type magmatism: titanite U/Pb ages from the alpine Central Anatolian Granitoids, Turkey. Int J Earth Sci 93:974–989

Köksal S, Toksoy-Köksal F, Göncüoğlu MC, Möller A, Gerdes A, Frei D (2013) Crustal source of the Late Cretaceous Satansarı monzonite stock (central Anatolia–Turkey) and its significance for the Alpine geodynamic evolution. J Geodyn 65:82–93

Koralay OE, Satir M, Dora OÖ (2001) Geochemical and geochronological evidence for early Triassic calc-alkaline magmatism in the Menderes Massif, western Turkey. Int J Earth Sci 89(4):822–835

Kozur H, Aydın M, Demir O, Yakar H, Göncüoğlu MC, Kuru F (2000) New stratigraphic results from the Paleozoic and early Mesozoic of the middle Pontides (Northern Turkey). Geol Croat 53:209–268

Kuscu-Gençalioğlu G, Geneli F (2010) Review of post-collisional volcanism in the Central Anatolian Volcanic Province (Turkey), with special reference to the Tepekoy Volcanic Complex. Int J Earth Sci 99(3):593–621

Lustrino M, Keskin M, Mattioli M, Lebedev VA, Chugaev A, Sharkov E, Kavak O (2010) Early activity of the largest Cenozoic shield volcano in the circum-Mediterranean area: Mt. Karacadağ, SE Turkey. Eur J Mineral 22(3):343–362

Manav H, Gültekin AH, Uz B (2004) Geochemical evidence for the tectonic setting of the Harmancik ophiolites, NW Turkey. Asian J Earth Sci 24(1):1–9

Marroni M, Frassi C, Göncüoğlu MC, Di Vincenzo G, Pandolfi L, Rebay G, Ellero A, Ottria G (2014) Late Jurassic amphibolite-facies metamorphism in the Intra-Pontide Suture Zone (Turkey): an eastward extension of the Vardar Ocean from the Balkans into Anatolia? J Geol Soc Lond 171(5):605–608

Moix P, Beccaletto L, Kozur HW, Hochard C, Rosselet F, Stampfli GM (2008) A new classification of the Turkish terranes and sutures and its implication for the paleotectonic history of the region. Tectonophysics 451:7–39

Oberhänsli R, Koralay E, Candan O, Pourteau A, Bousquet R (2013) Late Cretaceous eclogitic high-pressure relics in the Bitlis Massif. Geodin Acta 26(3–4):175–190

Okay AI (1985) Metamorphic belts in northwest Turkey. In: Ketin symposium proceedings. Geol Society Turkey Publications, pp 83–92

Okay AI, Göncüoğlu MC (2004) The Karakaya complex: a review of data and concepts. Turk J Earth Sci 13:75–95

Okay AI, Şahintürk O (1998) Geology of the Eastern Pontides. Am Assoc Petrol Geol Mem 68:291–313

Okay AI, Tüysüz O (1999) Tethyan sutures of northern Turkey. Geol Soc Lond Spec Publ 156:475–515

Okay AI, Arman MB, Göncüoğlu MC (1985) Petrology and phase relations of the kyanite-eclogites from eastern Turkey. Contrib Mineral Petrol 91:196–204

Okay AI, Kaşlılar-Özcan A, Imren C, Boztepe-Güney A, Demirbağ E, Kuşçu İ (2000) Active faults and evolving strike-slip basins in the Marmara Sea, northwest Turkey: a multichannel seismic reflection study. Tectonophysics 321(2):189–218

Okay AI, Satır M, Tüysüz O, Akyüz S, Chen F (2001) The tectonics of the Strandja Massif: late Variscan and mid Mesozoic deformation and metamorphism in the northern Aegean. Int J Earth Sci 90:217–233

Okay AI, Monod O, Monie E (2002) Triassic blueschists and eclogites from NW Turkey: vestiges of the Palaeotethyan subduction. Lithos 64:155–178

Okay AI, Satir M, Siebel W (2006a) Pre-Alpide Palaeozoic and Mesozoic orogenic events in the Eastern Mediterranean region. Geol Soc Lond Mem 32(1):389–405

Okay AI, Tüysüz O, Satır M, Özkan-Altiner S, Altiner D, Sherlock S, Eren RH (2006b) Cretaceous and Triassic subduction-accretion, high-pressure–low-temperature metamorphism, and continental growth in the Central Pontides, Turkey. Geol Soc Am Bull 118(9–10):1247–1269

Okay AI, Özcan E, Cavazza W, Okay N, Less G (2010) Basement types, Lower Eocene series, Upper Eocene olistostromes and the initiation of the southern Thrace Basin, NW Turkey. Turk J Earth Sci 19(1):1–25

Okay AI, Sunal G, Sherlock S, Altıner D, Tüysüz O, Kylander-Clark ARC, Aygül M (2013) Early Cretaceous sedimentation and orogeny on the active margin of Eurasia: Southern Central Pontides, Turkey. Tectonics 32:1247–1271

Okay AI, Sunal G, Tüysüz O, Sherlock S, Keskin M, Kylander-Clark ARC (2014) Low-pressure–high-temperature metamorphism during extension in a Jurassic magmatic arc, Central Pontides, Turkey. J Metamorph Geol 32(1):49–69

Okay AI, Altiner D, Kiliç AM (2015) Triassic limestone, turbidites and serpentinite–the Cimmeride orogeny in the Central Pontides. Geol Mag 152(03):460–479

Okuyucu C, Dimitrova TK, Göncüoğlu MC, Gedik I (2017) Late Permian (Tatarian) fluviolacustrine successions in NW Anatolia (Zonguldak Terrane, Turkey): palaeogeographic implications. Geol Mag 154(5):1073–1087

Önen AP, Hall R (1993) Ophiolites and related metamorphic rocks from the Kütahya region, northwest Turkey. Geol J 28:399–412

Özcan A, Göncüoğlu MC, Turhan N, Uysal Ş, Şentürk K (1989) Late Paleozoic evolution of the Kütahya-Bolkardağ Belt. METU J Pure Appl Sci 21:211–220

Özer S, Sözbilir H, Özkar İ, Toker V, Sari B (2001) Stratigraphy of upper Cretaceous–Palaeogene sequences in the southern and eastern Menderes Massif (western Turkey). Int J Earth Sci 89(4):852–866

Özgen-Erdem N, İnan N, Akyazı M, Tunoğlu C (2005) Benthonic foraminiferal assemblages and microfacies analysis of Paleocene–Eocene carbonate rocks in the Kastamonu region, Northern Turkey. Asian J Earth Sci 25(3):403–417

Özgül N (1976) Some geological aspects of the Taurus orogenic belt (Turkey). Geol Soc Turkey Bull 19:75–87 in Turkish with English abstract

Özgül N (1984) Stratigraphy and tectonic evolution of the Central Taurides. In: Tekeli O and Göncüoğlu MC (eds) Int. Symposium on the Geology of the Taurus Belt, pp 77–90

Özgül N (2012) Stratigraphy and some structural features of the İstanbul Paleozoic. Turk J Earth Sci 21:817–866

Özsayın E, Ciner TA, Rojay FB, Dirik RK, Melnick D, Fernandez-Blanco D (2013) Plio-quaternary extensional tectonics of the Central Anatolian Plateau: a case study from the Tuz Gölü Basin, Turkey. Turk J Earth Sci 22(5):691–714

Öztürk YY, Helvacı C, Satır M (2012) Geochemical and isotopic constraints on petrogenesis of the Beypazari Granitoid, NW Ankara, Western Central Anatolia, Turkey. Turk J Earth Sci 21(1):53–77

Papanikolaou D (2009) Timing of tectonic emplacement of the ophiolites and terrane paleogeography in the Hellenides. Lithos 108(1):262–280

Parlak O, Höck V, Kozlu H, Delaloye M (2004) Oceanic crust generation in an island arc tectonic setting, SE Anatolian orogenic belt (Turkey). Mineral Mag 141:583–603

Parlak O, Çolakoğlu A, Dönmez C, Sayak H, Yildirim N, Türkel A, Odabaşı İ (2013a) Geochemistry and tectonic significance of ophiolites along the İzmir–Ankara–Erzincan Suture Zone in northeastern Anatolia. Geol Soc Lond Spec Publ 372:75–105

Parlak O, Karaoğlan F, Rızaoğlu T, Klötzli U, Koller F, Billor Z (2013b) U–Pb and ^{40}Ar–^{39}Ar geochronology of the ophiolites and granitoids from the Tauride belt: implications for the evolution of the inner Tauride suture. J Geodyn 65:22–37

Perincek D (1979) The geology of Hazro-Korudag-Cüngüs-Maden-Ergani-Hazar-Elazığ-Malatya area. Guide Book Geological Society, Turkey, p 33

Perinçek D, Duran O, Bozdoğan N, Çoruh T (1991) Stratigraphy and paleogeographical evolution of the autochthonous sedimentary rocks in the SE Anatolia. In: Turgut S (ed) Proceedings of Ozan Sungurlu symposium. Ankara, pp 274–305

Platevoet B, Elitok Ö, Guillou H, Bardintzeff JM, Yagmurlu F, Nomade S, Poisson A, Deniel C, Özgür N (2014) Petrology of quaternary volcanic rocks and related plutonic xenoliths from Gölcük volcano, Isparta Angle, Turkey: origin and evolution of the high-K alkaline series. Asian J Earth Sci 92:53–76

Rimmelé G, Oberhänsli R, Goffé B, Jolivet L, Candan O, Çetinkaplan M (2003) First evidence of high-pressure metamorphism in the “Cover Series” of the southern Menderes Massif. Tectonic and metamorphic implications for the evolution of SW Turkey. Lithos 71(1):19–46

Rızaoğlu T, Parlak O, Höck V, Koller F, Hames WE, Billor Z (2009) Andean-type active margin formation in the eastern Taurides: geochemical and geochronogical evidence from the Baskil granitoid (Elazığ, SE Turkey). Tectonophysics 473(1):188–207

Robertson AHF (2002) Overview of the genesis and emplacement of Mesozoic ophiolites in the Eastern Mediterranean Tethyan region. Lithos 65:1–67

Robertson AHF, Ustaömer T (2005) Tectonic evolution of the Intra-Pontide suture zone in the Armutlu Peninsula, NW Turkey. Tectonophysics 381:175–209

Robertson AHF, Ustaömer T, Pickett EA, Collins AS, Andrew T, Dixon JE (2004) Testing models of late Palaeozoic–early Mesozoic orogeny in Western Turkey: support for an evolving open-Tethys model. J Geol Soc Lond 161:501–511

Robertson AHF, Parlak O, Rizaoğlu T, Ünlügenç Ü, İnan N, Tasli K, Ustaömer T (2007) Tectonic evolution of the South Tethyan ocean: evidence from the Eastern Taurus Mountains (Elaziğ region, SE Turkey). Geol Soc Lond Spec Publ 272:231–270

Robertson AH, Parlak O, Ustaömer T (2009) Melange genesis and ophiolite emplacement related to subduction of the northern margin of the Tauride–Anatolide continent, central and western Turkey. Geol Soc Lond Spec Publ 311(1):9–66

Robinson AG, Banks CJ, Rutherford MM, Hirst JPP (1995) Stratigraphic and structural development of the Eastern Pontides, Turkey. J Geol Soc Lond 152:861–872

Rojay B, Heimann A, Toprak V (2001) Neotectonic and volcanic characteristics of the Karasu fault zone (Anatolia, Turkey): the transition zone between the Dead Sea transform and the East Anatolian fault zone. Geodin Acta 14(1–3):197–212

Sarıfakıoğlu E, Özen H, Çolakoğlu A, Sayak H (2010) Petrology, mineral chemistry, and tectonomagmatic evolution of late Cretaceous suprasubduction-zone ophiolites in the İzmir–Ankara–Erzincan suture zone, Turkey. Int Geol Rev 52(2–3):187–222

Şaroğlu F, Emre Ö, Boray A (1992) Türkiye Diri Fay Haritası, Active Faults maps of Turkey. MTA Publ, Ankara

Savaşçın MY, Francalanci L, Innocenti T, Manetti P, Birsoy R, Dağ N (1995) Miocene–Pliocene potassic–ultrapotassic volcanism of the Afyon–Isparta region (centralwestern Anatolia, Turkey): petrogenesis and geodynamic implications. International Earth Sciences Colloquium on the Aegean Region (IESCA-1995) Proceedings, vol. 2:487–502

Sayit K, Göncüoğlu MC (2009) Geochemistry of mafic rocks of the Karakaya complex, Turkey: evidence for plume-involvement in the Palaeotethyan extensional regime during the middle and late Triassic. Int J Earth Sci 98:157–185

Sayit K, Göncüoğlu MC (2013) Geodynamic evolution of the Karakaya Melange Complex, Turkey: a review of geological and petrological constraints. J Geodyn 65:56–65

Sayit K, Göncüoğlu MC, Tekin UK (2015) Middle Carnian arc-type basalts from the Lycian Nappes, Southwestern Anatolia: early late Triassic subduction in the Northern Branch of Neotethys. J Geol 123(6):561–579

Sayit K, Marroni M, Göncüoğlu MC, Pandolfi L, Ellero A, Ottria G, Frassi C (2016) Geological setting and geochemical signatures of the mafic rocks from the Intra-Pontide Suture Zone: implications for the geodynamic reconstruction of the Mesozoic Neotethys. Int J Earth Sci 105(1):39–64

Seghedi I, Ersoy YE, Helvacı C (2013) Miocene–quaternary volcanism and geodynamic evolution in the Pannonian Basin and the Menderes Massif: a comparative study. Lithos 180:25–42

Şen C, Arslan M, Van A (1998) Geochemical and petrological characteristics of eastern Pontide Eocene (?) alkaline volcanic province, NE Turkey. Turk J Earth Sci 7:231–239

Sen PA, Temel A, Gourgaud A (2004) Petrogenetic modelling of quaternary post-collisional volcanism: a case study of central and eastern Anatolia. Geol Mag 141(01):81–89

Sengör AMC (1984) The Cimmeride orogenic system and the tectonics of Eurasia. GSA Spec Pap 195:1–82

Şengör AMC, Yılmaz Y (1981) Tethyan evolution of Turkey: a plate tectonic approach. Tectonophysics 75:181–241

Şengör AMC, Yılmaz Y, Sungurlu O (1984) Tectonics of the Mediterranean Cimmerides: nature and evolution of the western termination of Paleo-Tethys. In: Dixon JE, Robertson AHF (eds). The geological evolution of the Eastern Mediterranean. Geol Soc Lond Spec Publ 17:77–112

Sengör AMC, Görür N, Şaroglu F (1985) Strike-slip deformation, basin formation and sedimentation: strike-slip faulting and related basin formation in zones of tectonic escape: Turkey as a case study. Soc Econ Paleontol Mineral Spec Publ 37:227–264

Şengör AMC, Özeren S, Genç T, Zor E (2003) East Anatolian high plateau as a mantle-supported, north-south shortened domal structure. Geophys Res Lett 30:24

Şengün F, Koralay OE (2016) Early Variscan magmatism along the southern margin of Laurasia: geochemical and geochronological evidence from the Biga Peninsula, NW Turkey. Int J Earth Sci 1–16

Seyitoğlu G, Işık V, Cemen I (2004) Complete tertiary exhumation history of the Menderes massif, western Turkey: an alternative working hypothesis. Terra Nova 16(6):358–364

Siyako M, Huvaz O (2007) Eocene stratigraphic evolution of the Thrace Basin, Turkey. Sediment Geol 198(1):75–91

Sözbilir H, Sarı B, Uzel B, Sümer Ö, Akkiraz S (2011) Tectonic implications of transtensional supradetachment basin development in an extension-parallel transfer zone: the Kocaçay Basin, western Anatolia, Turkey. Basin Res 23(4):423–448

Stampfli GM (2000) Tethyan oceans. In: Bozkurt E, Winchester JA, Piper JD (eds) Tectonics and magmatism in Turkey and the surrounding area. Geol Soc London Spec Publ 173:1–23

Sunal G (2012) Devonian magmatism in the western Sakarya Zone, Karacabey region, NW Turkey. Geodin Acta 25(3–4):183–201

Tekeli O (1981) Subduction complex of pre-Jurassic age, northern Anatolia, Turkey. Geology 9:68–72

Tekeli O, Erendil M (1984) Geology and petrology of the Kızıldağ Ophiolite (Hatay). In: Tekeli O, Göncüoğlu MC (eds) Int Symposium on the Geology of the Taurus Belt. MTA Publ, Ankara, pp 127–147

Tekeli O, Aksay A, Urgün BM, Isik A (1984) Geology of the Aladag mountains. In: Tekeli O, Göncüoğlu MC (eds) Int Symposium on the Geology of the Taurus Belt. MTA Publ, Ankara, pp 143–158

Tekin UK, Göncüoğlu MC (2007) Discovery of the oldest (upper Ladinian to middle Carnian) radiolarian assemblages from the Bornova Flysch Zone in western Turkey: implications for the evolution of the Neotethyan Izmir-Ankara Ocean. Ofioliti 32:131–150

Tekin UK, Göncüoğlu MC, Turhan N (2002) First evidence of late Carnian radiolarian fauna from the Izmir-Ankara Suture Complex, Central Sakarya, Turkey: implications for the opening age of the Izmir-Ankara branch of Neotethys. Geobios 35:127–135

Tekin UK, Göncüoğlu MC, Uzuncimen S (2012a) Radiolarian assemblages of middle and late Jurassic to early late Cretaceous (Cenomanian) ages from an olistolith record pelagic deposition within the Bornova Flysch Zone in western Turkey. Bull Soc Géol Fr 183(4):307–318

Tekin UK, Göncüoğlu MC, Pandolfi L, Marroni M (2012b) Middle-late Triassic radiolarian cherts from the Arkotdağ mélange in northern Turkey: implications for the life span of the northern Neotethyan branch. Geodin Acta 25(3–4):305–319

Tekin UK, Ural M, Göncüoğlu MC, Arslan M, Kürüm S (2015) Upper Cretaceous radiolarian ages from an arc–backarc within the Yuksekova complex in the southern Neotethys melange, SE Turkey. CR Palevol 14(2):73–84

Temel A, Gündoğdu MN, Gourgaud A, Le Pennec JL (1998) Ignimbrites of Cappadocia (central Anatolia, Turkey): petrology and geochemistry. J Volcanol Geotherm Res 85(1):447–471

Temizel İ, Arslan M (2008) Petrology and geochemistry of tertiary volcanic rocks from the Ikizce (Ordu) area, NE Turkey: implications for the evolution of the eastern Pontide paleo-magmatic arc. Asian J Earth Sci 31(4):439–463

Tokel S (1977) Eocene calc-alkaline andesites and geotectonism in Black Sea Region. Geol Soc Turk Bull 20:49–54

Toprak V (1998) Vent distribution and its relation to regional tectonics, Cappadocian Volcanics, Turkey. J Volcanol Geotherm Res 85(1):55–67

Toprak V, Göncüoğlu MC (1993) Tectonic control on the development of Neogene-Quaternary Central Anatolian Volcanic Province, Turkey. Geol J 28:357–369

Topuz G, Altherr R, Schwarz WH, Dokuz A, Meyer HP (2007) Variscan amphibolite-facies rocks from the Kurtoğlu metamorphic complex (Gümüşhane area, Eastern Pontides, Turkey). Int J Earth Sci 96(5):861–873

Topuz G, Altherr R, Siebel W, Schwarz WH, Zack T, Hasözbek A, Şen C (2010) Carboniferous high-potassium I-type granitoid magmatism in the Eastern Pontides: the Gümüşhane pluton (NE Turkey). Lithos 116(1):92–110

Topuz G, Çelik ÖF, Şengör AMC, Altintaş İE, Zack T, Rolland Y, Barth M (2013) Jurassic ophiolite formation and emplacement as backstop to a subduction-accretion complex in northeast Turkey, the Refahıye ophiolite, and relation to the Balkan ophiolites. Am J Sci 313(10):1054–1087

Tunç İO, Yiğitbaş E, Şengün F, Wazeck J, Hofmann M, Linnemann U (2012) U-Pb zircon geochronology of northern metamorphic massifs in the Biga Peninsula (NW Anatolia-Turkey): new data and a new approach to understand the tectonostratigraphy of the region. Geodin Acta 25(3–4):202–225

Turhan N, Okuyucu C, Göncüoğlu MC (2004) Autochthonous upper Permian (Midian) carbonates in the Western Sakarya composite terrane, Geyve area, Turkey: preliminary data. Turk J Earth Sci 13:215–229

Türkecan A (2015) Cenozoic volcanics of Turkey. General Directorate of Mineral Research and Exploration Special Publication no 33, Ankara, p 258

Tüysüz O (1999) Geology of the Cretaceous sedimentary basins of the Western Pontides. Geol J 34:75–93

Tüysüz O, Keskin M, Sunal G (1999) The opening of Western Black Sea basin. Workshop V, Extended abstracts. General Directorate of Mineral Research and Exploration, Ankara, p 62–4

Üner T, Çakir Ü, Özdemir Y, Arat I (2014) Geochemistry and origin of plagiogranites from the Eldivan ophiolite, Çankırı (Central Anatolia, Turkey). Geol Carpath 65(3):197–207

Ural M, Arslan M, Göncüoğlu MC, Tekin UK, Kürüm S (2015) Late Cretaceous arc and back-arc formation within the southern Neotethys: whole-rock, trace element and Sr-Nd-Pb isotopic data from basaltic rocks of the Yüksekova complex (Malatya- Elazig, SE Turkey). Ofioliti 40(1):57–72

Ustaomer T, Robertson AHF (1999) Geochemical evidence used to test alternative plate tectonic models for pre-Upper Jurassic (Palaeotethyan) units in the Central Pontides, N Turkey. Geol J 34:25–53

Ustaömer PA, Ustaömer T, Collins AS, Robertson AHF (2009) Cadomian (Ediacaran–Cambrian) arc magmatism in the Bitlis Massif, SE Turkey: magmatism along the developing northern margin of Gondwana. Tectonophysics 473:99–112

Ustaömer PA, Ustaömer T, Robertson AHF (2012) Ion probe U-Pb dating of the Central Sakarya basement: a peri-Gondwana terrane intruded by late lower carboniferous subduction/collision-related granitic rocks. Turk J Earth Sci 21:905–932

Ustaömer T, Ustaömer PA, Robertson AHW, Gerdes A (2016) Implications of U–Pb and Lu–Hf isotopic analysis of detrital zircons for the depositional age, provenance and tectonic setting of the Permian–Triassic Palaeotethyan Karakaya complex, NW Turkey. Int J Earth Sci 105(1):7–38

Uysal I, Kalivoda M, Karsli O, Tarkian M, Sadiklar MB, Ottley CJ (2007) Compositional variations as a result of partial melting and melt-peridotite interaction in an upper mantle section from the Ortaca area, southwestern Turkey. Can Mineral 45:1471–1493

Uzuncimen S, Tekin UK, Bedi Y, Perincek D, Varol E, Soycan H (2011) Discovery of the late Triassic (middle Carnian–Rhaetian) radiolarians in the volcano-sedimentary sequences of the Koçali complex, SE Turkey: correlation with the other Tauride units. Asian J Earth Sci 40:180–200

Varol E, Bedi Y, Tekin UK, Uzuncimen S (2011) Geochemical and petro-logical characteristics of late Triassic basic volcanic rocks from the Kocali complex, SE Turkey: implications for the Triassic evolution of southern Tethys. Ofioliti 36:99–133

Whitney DL, Hamilton MA (2004) Timing of high-grade metamorphism in central Turkey and the assembly of Anatolia. J Geol Soc Lond 161:823–828

Wilson M, Tankut A, Guleç N (1997) Tertiary volcanism of the Galatia province, north-west Central Anatolia, Turkey. Lithos 42:105–121

Yalınız MK, Floyd PA, Göncüoğlu MC (1996) Supra-subduction zone ophiolites of Central Anatolia: geochemical evidence from the Sarıkaraman Ophiolite, Aksaray, Turkey. Mineral Mag 60:697–710

Yalınız MK, Göncüoğlu MC, Özkan-Altıner S, Parlak O (2000) Formation and emplacement ages of the SSZ-type Neotethyan ophiolites in Central Anatolia, Turkey: Paleotectonic implications. Geol J 35:53–68

Yanev S, Göncüoğlu MC, Gedik I, Lakova I, Boncheva I, Sachanski V, Okuyucu C, Özgül N, Timur E, Maliakov Y, Saydam G (2006) Stratigraphy, correlations and palaeogeography of Palaeozoic terranes in Bulgaria and NW Turkey: a review of recent data. In: Robertson AHF, Mountrakis D (eds) Tectonic development of the Eastern Meditteranean Region. Geol Soc Lond Spec Publ 260:51–67

Yiğitbaş E, Yılmaz Y (1996) New evidence and solution to the Maden complex controversy of the southeast Anatolian orogenic belt (Turkey). Geol Rundsch 85(2):250–263

Yiğitbaş E, Kerrich R, Yilmaz Y, Elmas A, Xie Q (2004) Characteristics and geochemistry of Precambrian ophiolites and related volcanics from the Istanbul–Zonguldak Unit, Northwestern Anatolia, Turkey: following the missing chain of the Precambrian South European suture zone to the east. Precambrian Res 132:179–206

Yılmaz Y (1989) An approach to the origin of young volcanic rocks of Western Turkey. In: AMC Ş (ed) Tectonic evolution of the Tethyan region. Kluwer Academic Publishers, The Hague, pp 159–189

Yılmaz Y (1990) Allochthonous terranes of Tethyan Middle East: Anatolia and the surrounding regions. Phil Trans R Soc Lond A 331:611–624

Yılmaz Y (1993) New evidence and model on the evolution of the Southeast Anatolian orogen. GSA Bull 105:251–271

Yılmaz O, Boztuğ D (1986) Kastamonu granitoid belt of northern Turkey: first arc volcanism product related to the subduction of the Paleotethys. Geology 14:179–183

Yılmaz C, Korkmaz S (1999) Basin development in the eastern Pontides, Jurassic to Cretaceous, NE Turkey. Zentralbl Geol Paläontol Teil I 10:1485–1494

Yılmaz Şahin S, Güngör Y, Aysal N (2010) Granitoids of İstanbul. Proceedings, Geology of İstanbul III, p 100–129

Yılmaz A, Yılmaz H (2006) Characteristic features and structural evolution of a post collisional basin: The Sivas Basin, Central Anatolia, Turkey. Asian J Earth Sci 27(2):164–176

Yilmaz Y, Yigitbas E, Genc ŞC (1993) Ophiolitic and metamorphic assemblages of southeast Anatolia and their significance in the geological evolution of the orogenic belt. Tectonics 12(5):1280–1297

Yılmaz Y, Tüysüz O, Yiğitbaş E, Genç ŞC, Şengör AMC (1997) Geology and tectonic evolution of the Pontides. In: Robinson AG (ed) Regional and petroleum geology of the black sea and surrounding region. Am Assoc Petrol Geol Memoir 68:183–226

Yilmaz Y, Genç ŞC, Gürer F, Bozcu M, Yilmaz K, Karacik Z, Altunkaynak Ş, Elmas A (2000) When did the western Anatolian grabens begin to develop? In: Bozkurt E, Winchester JA, Piper JD (eds) Tectonics and magmatism in Turkey and the surrounding area. Geol Soc London Spec Publ 173:353–384

Zlatkin O, Avigad D, Gerdes A (2013) Evolution and provenance of Neoproterozoic basement and Lower Paleozoic siliciclastic cover of the Menderes Massif (western Taurides): coupled U–Pb–Hf zircon isotope geochemistry. Gondwana Res 23:682–700

Chapter 3
Chromitite Deposits of Turkey in Tethyan Ophiolites

Yahya Çiftçi, Cahit Dönmez, Osman Parlak, and Kurtuluş Günay

Abstract Some parts of the Tethyan ophiolites of Alpine-Himalayan suture belt are located within Turkey. The Tethyan belt splits into two branches in Turkey. The northern branch follows the İzmir-Ankara-Erzincan Zone, while the southern branch extends along the Anatolide-Tauride and Bitlis-Zagros suture zone. The subsections of the latter reach Iran in the east and Oman ophiolites in the south east. These ophiolites are also the only environments in which chromitite deposits occur. Consequently, the ophiolites in Turkey are significantly rich in terms of Alpine type chromitite occurrences and they are the oldest metallic mine products.

There has been chromitite ore production in Turkey since the nineteenth century. With their refractory quality, chromitite produced in Turkey has always had a good standing in the market. Chromitite, which was exported as lump ore until mid-twentieth century, started to be used in the domestic market as the country's industry developed, but still, even today an important part of the production is exported. In addition, since the chromitite developments near to the surface are almost completely exhausted, the chromitite ore production in the country has evolved to concentrated ore obtained from low grade deposits, through beneficiation. Although there are many active beneficiation plants in various parts of the country, there is still a significant amount of concentrate ore production; especially in the deposits of Adana-Aladağ region.

In this chapter, the mentioned chromitite occurrences are discussed in a specific order from west to east, taking into account the ophiolite sequences to which they belong. The North Anatolian Ophiolites are introduced in the first three sections whereas the other three sections present the chromitite deposits of the South Anatolian Ophiolites. Nevertheless, considering the historical records and future production potentials, Turkey's most important chromitite production regions could be listed in order of priority as Guleman (Elazığ), Kopdağ region (Erzincan),

Y. Çiftçi (✉) · C. Dönmez · K. Günay
Department of Mineral Research and Exploration, General Directorate of Mineral Research and Exploration, Ankara, Turkey
e-mail: redaksiyon@mta.gov.tr

O. Parlak
Engineering Faculty, Geological Engineering Department, Çukurova University, Adana, Turkey

F. Pirajno et al. (eds.), *Mineral Resources of Turkey*, Modern Approaches in Solid Earth Sciences 16, https://doi.org/10.1007/978-3-030-02950-0_3

Muğla-Fethiye region, Aladağ-Pınarbaşı (Adana-Kayseri), Orhaneli-Harmancık (Bursa)-Eskişehir region and Hatay. It is clear that these should all be taken into consideration for further prospecting targeting.

3.1 Introduction

This chapter has been prepared by making use of the wide literature on Turkish chromitites. The "Turkish Chromitite Inventory" project, which is being prepared using the Chrome-Nickel Prospecting reports, has been worked on by the General Directorate of Mineral Research and Exploration for many years. Most of the presented data (tables and maps) were derived from these prospecting reports. In the first part we provide brief information about Tethyan ophiolites of the Eastern Mediterranean. The second part includes general information about chromitites and general features of chromitites in Turkey. A summary of petrogenetic studies regarding ophiolites in Turkey is also presented here. The third part is the main body of this chapter. Chromitite occurrences of Turkey presented here are based on an inventory format in accordance with County administrative requirements in Turkey. In this way, related ophiolite sequences can be described in more detail.

This Chapter aims to work through the chromite occurrences associated with the Tethys Ophiolites, thereby becoming an essential overview and a guide for new scientific studies. We also hope to have opened a new window for our colleagues and students who are studying and working on mineral systems.

3.2 Tethyan Ophiolites of the Eastern Mediterranean

The Mesozoic Tethyan ophiolites of the Alpine-Himalayan orogenic belt include the Mid-Late Jurassic ophiolites of the Dinarides, Albanides and Hellenides in the western region and the Late Cretaceous ophiolites of Turkey, Troodos, Baer-Bassit, Khoy, Kermansah, Neyriz, and Oman in the eastern region (Fig. 3.1). The Mid to Late Jurassic ophiolites in the western region formed in a transitional tectonic settings from MORB to SSZ (Bebien et al. 1998; Bortolotti et al. 2002; Robertson 2002, 2012; Robertson and Shallo 2000; Höck et al. 2002; Dilek and Flower 2003; Saccani et al. 2004; Dilek et al. 2005, 2008; Tremblay et al. 2009), whereas the late Cretaceous ophiolites in the eastern region, from Turkey to Oman, are supra-subduction zone (SSZ) type (Aktaş and Robertson 1984; Pearce et al. 1984; Hebert and Laurent 1990; Lytwyn and Casey 1993; Yalınız et al. 1996; Collins and Robertson 1998; Dilek et al. 1999; Floyd et al. 2000; Parlak et al. 1996, 2000, 2002, 2004, 2009, 2013a; Al-Riyami et al. 2002; Robertson 2002; Robertson et al. 2006, 2007; Flower and Dilek 2003; Dilek and Thy 2009; Dilek and Furnes 2009).

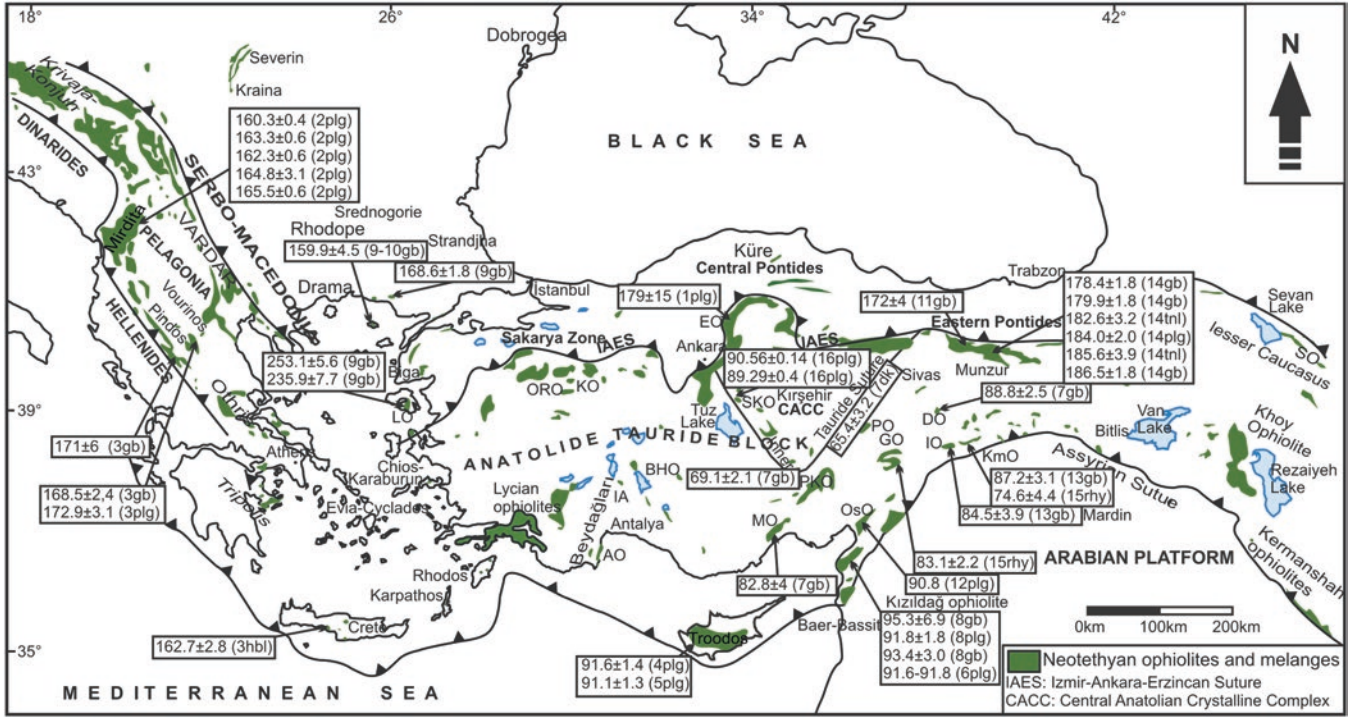

Fig. 3.1 U-Pb ages of the Tethyan ophiolites in Turkey and surrounding areas (Data are from (1) Dilek and Thy (2006), (2) Dilek et al. (2008), (3) Liati et al. (2004), (4) Mukasa and Ludden (1987), (5) Konstantinou et al. (2007), (6) Dilek and Thy (2009), (7) Parlak et al. (2013a), (8) Karaoğlan et al. (2013a), (9) Koglin (2008), (10) Koglin et al. (2009), (11) Topuz et al. (2012), (12) Sarıfakıoğlu et al. (2012), (13) Karaoğlan (2012), (14) Robertson et al. (2013b), (15) Karaoğlan et al. (2013b)). *LO* Lesvos Ophiolite, *AO* Antalya Ophiolite, *BHO* Beyşehir-Hoyran Ophiolite, *ORO* Orhaneli Ophiolite, *KO* Kınık Ophiolite, *EO* Eldivan Ophiolite, *MO* Mersin Ophiolite, *PKO* Pozantı-Karsantı Ophiolite, *OsO* Osmaniye Ophiolite, *GO* Göksun Ophiolite, *PO* Pınarbaşı Ophiolite, *IO* Ispendere Ophiolite, *DO* Divriği Ophiolite, *KmO* Kömürhan Ophiolite, *SO* Sevan Ophiolite, *plg* plagiogranite, *gb* gabbro, *dk* dyke, *tnl* tonalite, *rhy* rhyolite. (Map modified after Dilek and Flower 2003; Çelik et al. 2011)

Neotethyan ophiolites in Anatolia are located along several east-west trending suture zones separated by continental blocks, metamorphic core complexes and sedimentary basins (Şengör and Yılmaz 1981; Robertson and Dixon 1984; Robertson 2002, 2006; Okay and Tüysüz 1999; Okay 2008). These suture zones are marked by ophiolites, ophiolitic melanges and ophiolite-related metamorphic rocks (Okay 1986, 1989; Parlak et al. 1995, 2006, 2009; Önen and Hall 2000; Vergili and Parlak 2005; Robertson et al. 2009; Pourteau et al. 2010; Okay and Whitney 2010; Dilek and Furnes 2011). These tectonic units were emplaced in the Late Cretaceous as a result of series of collisions of intra-oceanic arc-trench systems with the continental margins (Robertson 2002, 2004, 2006, 2007; Flower and Dilek 2003; Dilek and Flower 2003; Dilek et al. 2007; Dilek and Thy 2009; Dilek and Furnes 2009; Okay and Şahintürk 1997; Okay et al. 2006; Okay 1989).

The ophiolites in northern Anatolia occur in the İzmir-Ankara-Erzincan suture (Fig. 3.1), cropping out in western, central and northeastern Anatolia. The ophiolites are incompletely preserved, and crustal units display a supra-subduction zone geochemical character. In western Turkey, the ophiolites were emplaced over a subducted and exhumed passive margin of the Tauride-Anatolide platform in the Campanian (Okay 1989; Yılmaz et al. 1997a, b; Göncüoğlu et al. 2000; Robertson 2002; Robertson et al. 2009). The Late Cretaceous dismembered ophiolites above the Kırşehir/Niğde metamorphic massifs, and within the Ankara Melange are interpreted mainly as remnants of SSZ-type ophiolites formed in the Late Cretaceous within a northerly Neotethyan oceanic basin. The felsic intrusives and the volcaniclastics of Middle Turonian-Early Santonian age are indicative of contemporaneous arc volcanism (Yalınız et al. 1996; Yalınız and Göncüoğlu 1998). The Late Cretaceous Central Anatolian ophiolite was emplaced southwards from the Ankara-Erzincan suture zone onto the Kırşehir/Niğde metamorphic basement before latest Maastrichtian time. However, Early-Middle Jurassic isotopic ages were reported from the Ankara melange (Dilek and Thy 2006; Çelik et al. 2011). The Ankara-Erzincan suture zone includes large bodies of ophiolites and ophiolitic melanges in northeastern Anatolia (Rice et al. 2006, 2009; Sarıfakıoğlu et al. 2009; Parlak et al. 2013b; Topuz et al. 2013). These ophiolitic units display well-preserved oceanic lithospheric sections and accretionary melanges with local blueschist assemblages. Southward-emplacement onto the Tauride passive margin and northward emplacement onto the Pontide active margin has been proposed during Late Cretaceous-Early Tertiary (Okay and Şahintürk 1997; Yılmaz et al. 1997a, b; Rice et al. 2006, 2009). These ophiolitic units are unconformably overlain by Campanian-Maastrichtian sediments that were, in turn, imbricated with the ophiolitic rocks (Okay and Şahintürk 1997; Rice et al. 2006, 2009).

The Tauride belt ophiolites start with the Lycian nappes to the west and end with the Divriği ophiolite to the east. These ophiolites (Lycian nappes, Antalya, Beyşehir-Hoyran nappes, Mersin, Pozantı-Karsantı, Pınarbaşı and Divriği) are situated either on the northern or on the southern flank of the E-W trending Tauride carbonate platform axis (Juteau 1980). They mainly consist of three tectonic units namely, in ascending order, ophiolitic mélange, sub-ophiolitic metamorphic sole and oceanic lithospheric remnants. The ophiolitic mélange in tectonic contact with the underly-

ing platform carbonates, is composed of ophiolitic rock fragments, limestone blocks ranging in age from Permian to Late Cretaceous, radiolarites, shale, and fragments of metamorphic rocks. This unit is, in turn, tectonically overlain by thin sheets of metamorphic rocks that display inverted metamorphic zonation from upper amphibolite to greenschist facies. The mantle tectonites, dominated by harzburgite, tectonically rest on the deformed metamorphic sole rocks. Well-preserved ultramafic and mafic cumulates are the most conspicuous features all over the Tauride belt ophiolites (Juteau 1980). The plutonic sections and the metamorphic soles of the Tauride ophiolites are crossed by numerous isolated diabase dykes at different structural levels. The dykes are not deformed, indicating that they were emplaced after the deformation of metamorphic soles, but they do not extend into the underlying melanges. Sheeted dyke complexes and volcanic sections are rarely present in some of the ophiolites such as Antalya, Mersin and Pozantı-Karsantı (Juteau et al. 1977; Parlak 1996; Parlak et al. 2001). The geochemistry of crustal rocks indicates SSZ origin for the Tauride ophiolites (Collins and Robertson 1998; Parlak et al. 1996, 2000, 2002, 2006; Andrew and Robertson 2002; Vergili and Parlak 2005; Çelik and Delaloye 2003; Çelik and Chiaradia 2008; Çelik 2007).

Two subparallel, NE-SW-trending belts of Upper Cretaceous ophiolitic rocks transect southern Turkey, extending through northern Syria, Cyprus and intervening offshore areas (Robertson 2002; Parlak et al. 2009). The southern belt includes the Troodos ophiolite (Cyprus), the Baer–Bassit ophiolite (northern Syria) and the Antalya (Tekirova and Gödene), Hatay, Amanos and Koçali ophiolites (southern Turkey). Geophysical evidence indicates that a submarine connection existed between the Troodos and Levant margin ophiolites (Baer-Bassit and Hatay ophiolites) via the Latakia Ridge (Ben-Avraham et al. 2006; Roberts and Pearce 2007; Bowman 2011). These ophiolites originated within the Southern Neotethys. Regional comparisons show that the Kızıldağ ophiolite has similar petrological and geochemical features to the Baer–Bassit and Troodos ophiolites. The Baer–Bassit ophiolite is the leading edge of a vast ophiolite that was emplaced southwards from the southerly Neotethyan Ocean in latest Cretaceous (Maastrichtian) time. The Kızıldag ophiolite to the north represents the undeformed, more northerly part of the same thrust sheet (Robertson 1986a, b, 2002; Al-Riyami and Robertson 2002; Al-Riyami et al. 2002). There are a number of similarities between the two ophiolites. Despite the strongly dismembered nature of the Baer-Bassit ophiolite, it can be reconstructed as a single complete ophiolite sequence from bottom to top, like the Kızıldag ophiolite (Robertson 1986a, b; Al-Riyami et al. 2002). The plutonic section of the Kızıldag ophiolite is lithologically similar to that of the Baer–Bassit ophiolite (Bağcı et al. 2005, 2008; Al-Riyami et al. 2002). Both ophiolites have well developed sheeted dyke complexes. The extrusive rocks in both ophiolites are mostly depleted and exhibit the geochemical features of island arc tholeiites (IAT) (Al-Riyami et al. 2002; Bağcı et al. 2008).

The more northerly belt includes the North Berit (Göksun) ophiolite, the İspendere ophiolite, the Kömürhan ophiolite, the Guleman ophiolite and the Killan ophiolite. These ophiolites originated from an ocean basin, here termed the Berit ocean, that was located between the Malatya-Keban platform to the north and the

Bitlis and Pütürge continental units to the south (Robertson et al. 2012a, b). The SE Anatolian ophiolites are tectonically overlain by the Malatya-Keban platform and all intruded by late Cretaceous granitoid (Parlak 2006; Rızaoğlu et al. 2009). These ophiolites were thrust over the Maden Group at the end of Middle Eocene time. They include differentiated rock units in both the plutonic (quartz diorites) and the volcanic sections (i.e. basalt to rhyolite). They are also overlain by volcanic arc units (i.e. Elazığ Unit, Yüksekova Complex), suggesting that SSZ-type crust evolved into an ensimatic island arc as subduction continued (Rızaoğlu et al. 2006; Parlak et al. 2009; Karaoğlan et al. 2013b). The Guleman ophiolite shows similar features to the Kömürhan, İspendere and Göksun ophiolites. Although it was also accreted to the base of the Malatya-Keban platform during the Late Cretaceous, it was not affected by the intrusion of the granitoid. All of the evidence suggests that the Göksun, İspendere, Kömürhan, Guleman ophiolites and the North Berit (Göksun) ophiolite were related to the northern margin of the southern Neotethys (i.e. the Malatya–Keban Platform), whereas the Kızıldağ (Hatay) ophiolite was attached to the southern margin (i.e. the Arabian Platform) of the southern Neotethys in the latest Cretaceous time (Robertson et al. 2006, 2007; Parlak et al. 2009, 2013a).

U-Pb ages of the oceanic magmatism (gabbro) reported from the Western and Central Alps range from 164 to 158 Ma (Rubatto et al. 1998; Rubatto and Scambelluri 2003; Kaczmarek et al. 2008). But the youngest oceanic magmatism was reported as 93 Ma by Liati et al. (2003) in the Central Alps. Similar Middle to Late Jurassic crystallization ages were also documented from the Mirdita (plagiogranite: 165–160 Ma), in Albania (Dilek et al. 2008); Vourinos (plagiogranite: 172.9 ± 3.1 and gabbro: 168.5 ± 2.4 Ma), Pindos (gabbro:171 ± 3 Ma), Samothraki (gabbro: 159.9 ± 4.5 Ma), Evros (gabbro: 168.6 ± 1.8 Ma), Crete (gabbro/hornblendite: 162.7 ± 2.8 Ma) ophiolites in Greece (Liati et al. 2004; Koglin 2008); and Ankara melange (plagiogranite: 179 ± 15 Ma) in northern Turkey (Dilek and Thy 2006) (Fig. 3.1). In contrast, Late Cretaceous crystallization age of the oceanic crust is well documented in the Eastern Mediterranean region, including Troodos (plagiogranite: 90–91 Ma; Mukassa and Ludden 1987; Konstantinou et al. 2007), Kızıldağ (plagiogranite and gabbro: 93–91 Ma), Divriği (88.8 ± 2.5 Ma), Mersin (gabbro: 82.8 ± 4 Ma), Pozantı-Karsantı (Gabbro: 69.1 ± 2.1 Ma), Pınarbaşı (Isolated dike: 65.4 ± 3.2 Ma) ophiolites in Turkey (Dilek and Thy 2009; Karaoğlan et al. 2013a; Parlak et al. 2013a) and the Semail ophiolite (plagiogranite: 95 Ma) in Oman (Tilton et al. 1981; Warren et al. 2005).

3.3 Chromitites: Types, Occurrences, Petrological Features

3.3.1 Types of Chromitite Deposits

Chromitite deposits are usually associated with ultramafic rocks. Generally they are divided into three main types based on their origin, geological setting, mineralogy, texture, and chemical characteristics (Thayer 1960; Jackson and Thayer 1972)

(a) Stratiform chromite deposits generally occur in mafic-ultramafic intrusions in stable continental regions: these are continuous deposits that usually have large reserves and show consistency in dip and strike, small grain size, smooth crystal shape (idiomorph), cumulate textures, high iron content, low Cr/Fe ratio. The most typical examples are deposits in the Bushveld (South Africa; Cawthorn 2015), and Stillwater (USA; McCallum 1996) complexes.
(b) Alpine (podiform) chromite deposits: these consist of lenses or irregulalry shaped chromitite masses, with limited continuity in strike and dip, widely varying Cr content, and their reserves usually do not exceed a few hundred thousand tonnes. The chromite is coarse-grained, with irregular crystallinity and Cr/Fe ratios are generally high. Such deposits are usually found in countries located on the Alpine mountain belt such as the Former Yugoslavia, Albania, Greece, Turkey, Cyprus, Iran and Pakistan. Also, Kazakhstan, India, the Philippines and New Caledonia as well as some other countries where similar types of chromitite deposits are located.
(c) Chromitite (and magnetite) deposits that have a concentric internal order, related to mafic-ultramafic rock assemblages: This type of chromite formation has no economic significance. The most typical examples exist in Alaska and are known as Alaskan-type intrusions (Johan 2002).

3.3.2 General Characteristics of the Turkish Chromitites

The chromitite deposits of Turkey are classified as "Alpine-Type" deposits. Thicknesses usually vary between 10 cm and 10 m with lengths of 100–200 m. However, in the Guleman (Elazığ) region, 1500 m long bodies were observed, boudinaged along strike, in the Uzun Damar and Ayı Damar ore deposits. Although the thicknesses of chromite masses can reach up to 50 m, it usually does not exceed a few meters.

The chromite mineralisation in Turkey can be found in the ultramafic rocks of both the cumulate and tectonite sections of the ophiolites and can be grouped according to their tectono-stratigraphic location (Engin et al. 1985). The chromite bodies of harzburgites (tectonites) are surrounded by dunite envelopes ranging in thickness from a few centimetres to a few meters (Fig. 3.2).

(a) Chromitites within the deeper part of the mantle, harzburgites could be seen as in Ayıdamar and Uzun Damar deposits in Guleman (Elazığ) region,
(b) Chromitites located below the tectonite-cumulate transition zone as in the Koca Ocak and Kıran Ocak in Harmancık (Bursa) region,
(c) Chromitites located along the tectonite-cumulate transition zone as in Batı Kef Mine in Guleman (Elazığ) region,
(d) Chromitites hosted in ultramafic zones (dunite), as in Pütyan Mine of Gölalan - Guleman (Elazığ) and Kızılyüksek (Pozantı-Karsantı) regions (Fig. 3.3).

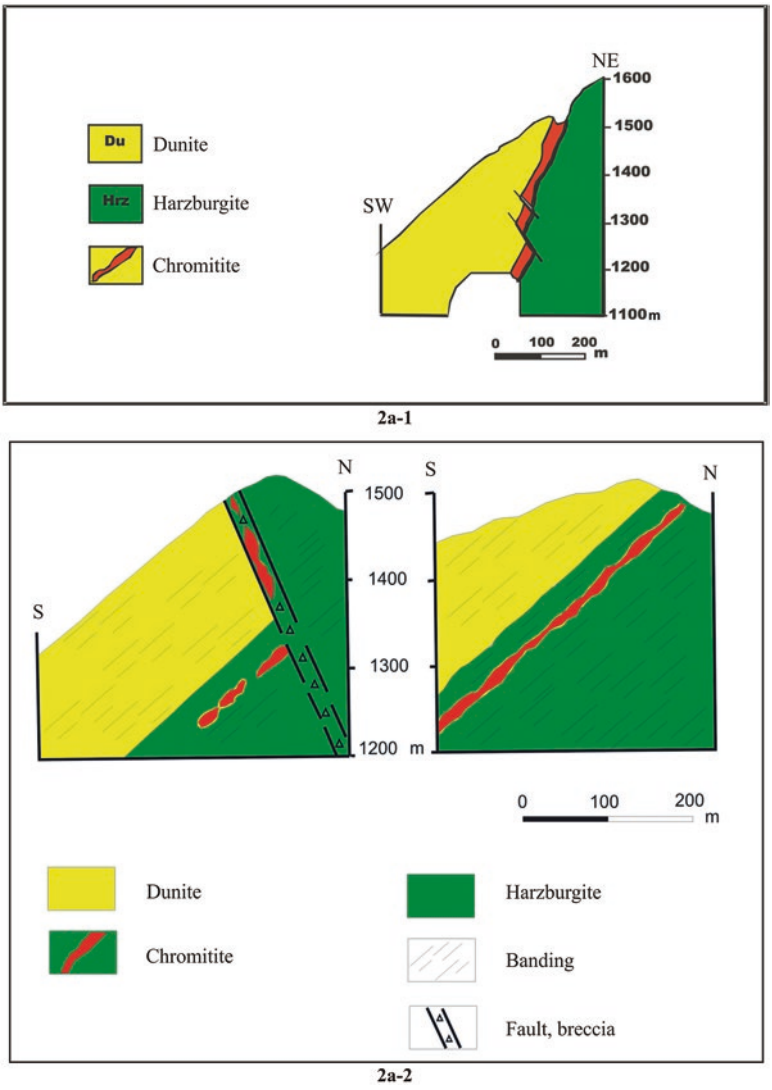

Fig. 3.2 Location of chromitites in Turkey. (After Engin et al. 1985)

The structural relationships of the chromitite bodies with the host peridotites are shown in Fig. 3.4. Chromite deposits in Turkey are mostly concordant with the foliation fabric of the peridotites (Fig. 3.4a). Although some deviations are possible due to the shape of the chromitite bodies, in general, the orientation of the chromite lenses and the foliation pattern in the peridotite are parallel to each other (Fig. 3.4a, b). However, later tectonics may have affected this primary fabric and the position of the chromitites (Fig. 3.4c–e).

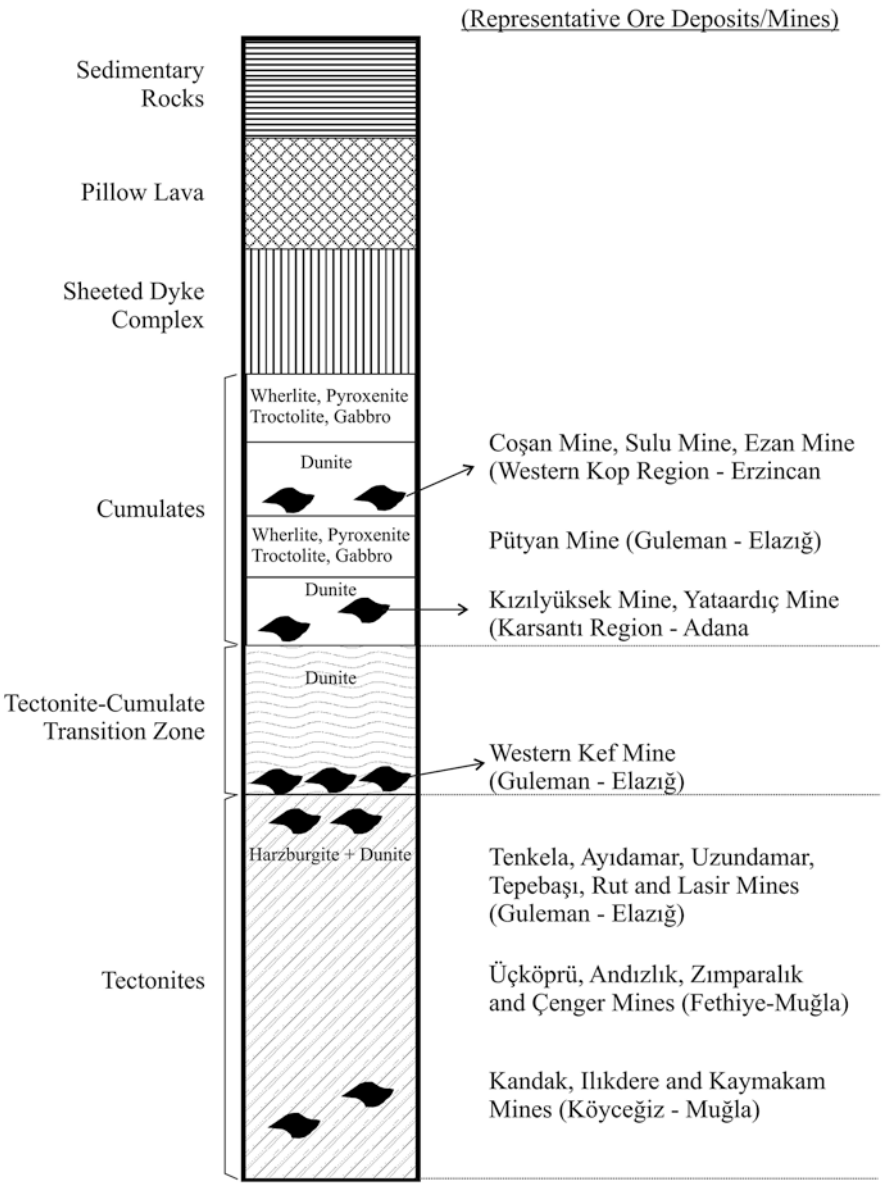

Fig. 3.3 Chromitites in Turkish ophiolites and representative ore deposits/mines. (After Engin et al. 1985)

Chromitites cutting the structural fabric of peridotites, are mainly located along fault zones (Fig. 3.4c). Some chromitite deposits although initially elongated along the foliation fabrics of peridotite, as a result of tectonic transportation and deformation, actually cut through the foliation planes (Fig. 3.4c), or are locally folded with

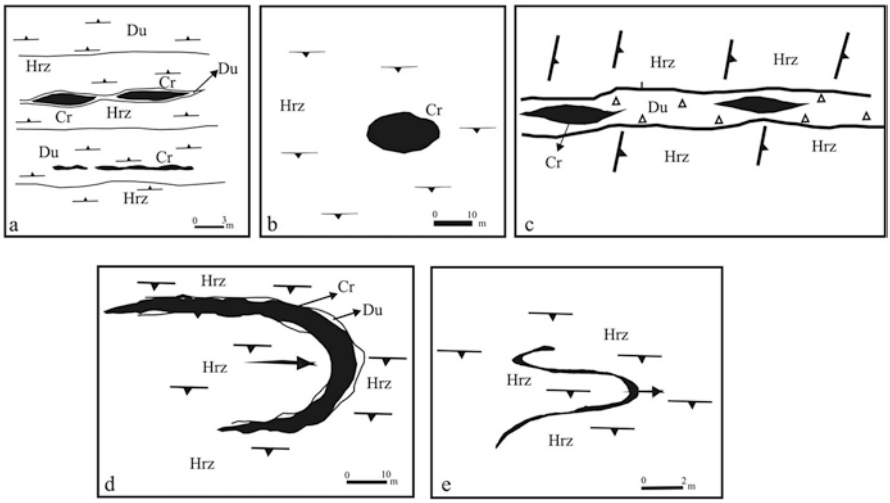

Fig. 3.4 Wallrock/chromitite ores relationship typically found in Turkey: (**a**, **b**) chromitite bodies are concordant with the internal structure of the peridotite (Uzundamar and Western Kef Mines, Guleman-Elazığ; length of the orebody in dip direction is more than ten times than strike direction (Anik Mine, Fethiye); (**c**) Structural fabric of the orebodies in the fault zone are concordant with this fault zone, but they cut the internal structure of peridotite in a diagonal direction (Eastern Kef and Kapin Mines, Guleman); (**d**, **e**) Folded chromitite bodies in peridotite; chromitite bodies are plunging, foliation of the peridotite at the fold apex diagonally intersects these fabrics of the orebody (Kandak and Biticealan Mines, Köyceğiz-Muğla). (Redrawn after Engin et al. 1985)

the wall-rock ultramafics (Fig. 3.4d, e). These types of chromitites, as shown in Fig. 3.4, have been described only in few areas, such as Kavak-Bahtiyar (Eskişehir) and Guleman (Elazığ) regions (Engin et al. 1980–1981) in Turkey, but well studied in New Caledonian ophiolites (Cassard et al. 1981).

3.3.3 Geochemical Features of Turkish Chromitites and Platinum Group Element (PGE) Contents

Apart from whole rock geochemical features available through chromite mining operations, information related to chromite mineral chemistry and PGE contents of chromites was reviewed from published articles, post-graduate theses and public reports.

As mentioned above, Turkish chromitites typically are Alpine type (podiform) deposits. These deposits are characterized by high Cr_2O_3, Al_2O_3, Cr/Fe and MgO, and low FeO and Fe_2O_3 contents. Although the Turkish chromitites are generally of economic grade, their wide range of chemistry enables their use in the refractory and chemistry industries. The average wt% Cr_2O_3 grade of deposits ranges between 5% and 45%, with a maximum of about 58 wt% Cr_2O_3. Average grades of less than

40% Cr_2O_3 are accepted as "third quality"; 40–46% is accepted as "second quality", and over 46% is accepted as "first quality" chromite ore in the market. In this regard, Turkish chromitites which are used in refractory industry should have approximately 30–40 wt% Cr_2O_3, 25–32 wt% Al_2O_3, >10 wt% SiO_2. On the other hand, the metallurgical industry needs at least 34–48 wt% Cr_2O_3, 8–15 wt% Al_2O_3, 8–12 wt% SiO_2, 16–22 wt% MgO. For the industry, average compositions should be at least 48 wt% Cr_2O_3 (base), 6–7 wt% SiO_2 and Cr/Fe rate should be 3/1 (typical) (Çiftçi et al. 2017; DPT 2001).

The chemistry of chrome spinel minerals in chromitites provides important data for genetic models of chromite formation and also for classification of chromite-bearing ophiolites. Chemistry of chrome spinels of Turkish chromitites varies significantly, and in this chapter, the average values of chrome spinel compositions are used.

Data of chrome spinel chemistry demonstrates classic features of these spinels. Turkish chromitites can generally be classified as Mg-Chromite/Chromite, according to their chromium and magnesium numbers; 0.5< Cr# (Cr/[Cr+Al], atomic ratio) and 0.4–0.8 <Mg# [100 Mg/(Mg + Fe), atomic ratio] (Fig. 3.5a) (Dönmez et al. 2014 and the references therein). Al_2O_3 wt% and Cr_2O_3 wt% contents support the podiform type generation of Turkish chromitites (Fig. 3.5b). Chrome spinels in Alpine type Turkish podiform chromitites have highly variable Cr# ranging from 0.2 to 0.9.

This compositional difference in chromitites, were reported by many researchers in the last decade and chromitites were divided into two groups according to their Cr# value intervals as high-Cr type (Cr# >0.6) and high-Al type chromitites (González-Jiménez et al. 2011; Pal 2011; Rollinson 2008; Uysal et al. 2009a, b; Zaccarini et al. 2011). Both types can exist in the same mantle source. The occurrences of high-Cr and high-Al types are still debated. Here, features that have a general consensus are addressed. In recent years, as a result of studies on Turkish chromitites, similar results were obtained about chromitites related to Muğla, Kastamonu and Van Ophiolites (Uysal et al. 2009b; Dönmez et al. 2014; Günay and Çolakoğlu 2011, 2016).

Turkish chromitites hosted in ultramafic tectonites, which dominantly consist of harzburgites and dunites. In these upper mantle rocks, chromite formations are strongly related to mantle stratigraphy. Stratigraphic levels of chromitites in an ophiolitic sequence, also appear to determine their chemistry. In this aspect, chromitites can be classified in an effective way on Rammlmair's (1986) Cr# versus Cr/Fe diagram presented in Fig. 3.5c. It is clearly seen in this figure that Turkish chromitites mainly plot within (I) and (II) areas. These areas were defined as ultramafic tectonite (mantle peridotites) and are also consistent with their geological features. However, the chromitites related to ultramafic cumulate rocks that plot within (III) and (IV) areas, are bands which are also consistent with these rocks and their occurrences are highly limited.

Turkish chromitites that mainly occur in mantle peridotites, do not contain economic quantities of PGE. Chromitites in Turkey generally have low PGE content, ranging between 200 and 350 ppb. However, it was reported that elements such as

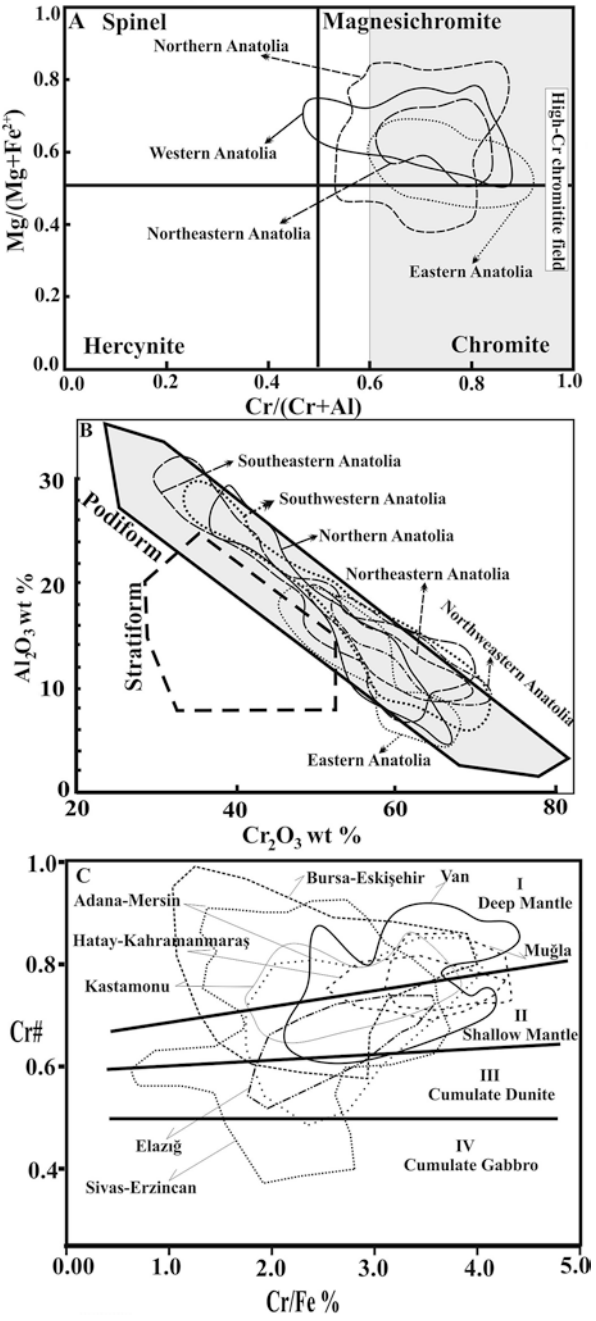

Fig. 3.5 Geochemical properties of Turkish chromitites (explanations in text)

Pt and Pd are locally enriched over 1 ppm in a few areas such as Muğla Ophiolite (Harmancık area; Uçurum and Koptagel 2006) and Kahramanmaraş Ophiolite (Berit area; Kozlu et al. 2014). There is no relation between whole-rock PGE contents of chromitites and mineral chemistry. In general, it is accepted that ophiolitic chromitites have high IPGE/PPGE (IPGE= Ru-Os-Ir; PPGE= Rh-Pt-Pd) ratios and low PGE contents (Economou-Eliopoulos 1996; Zhou et al. 1998; Proenza et al. 1998; Melcher et al. 1999; Ahmet and Arai 2002; Garuti 2004; Uysal et al. 2009a, b; González-Jiménez et al. 2011; Zaccarini et al. 2011). Turkish podiform chromite deposits exhibit enrichment in Ru-Os-Ir relative to Rh-Pt-Pd elements (Fig. 3.6a), similar to the PGE content of other ophiolitic chromitites around the World.

On the basis of their PGE contents, Turkish chromitites show similar features with geochemical behaviours of PGE's of ophiolitic chromitites in petrological processes. Total PGE contents of Turkish chromitites negatively correlating with $PPGE_N/IPGE_N$, are consistent with ophiolitic trends around the world (Fig. 3.6b; Melcher et al. 1999). In addition to this, Turkish chromitites display a trend compatible with partial melting rather than being fractionated in Pd/Ir versus $Pt/Pt^*[=Pt_N/(Rh_N{}^*Pd_N)^{1/2}]$ diagram (Fig. 3.6c; Garuti et al. 1997). It can be concluded that during the crystallization of chromites related to partial melting processes, Ir-group elements preferred chromite as the primary phase when compared to Pd-group elements.

3.4 Geological Properties of Chromitites in Turkey

Tethyan ophiolites located within the borders of Turkey are exposed mainly along the İzmir – Ankara – Erzincan, Inner Taurid and Bitlis – Zagros Suture Belt (Okay and Tüysüz 1999) (Figs. 3.1 and 3.7) and their principal features are discussed in Sect. 3.2. Chromitites, which are entirely related to these rocks, are considered in six related groups (Çiftçi et al. 2017) (Fig. 3.7). In this study, the chromite deposits of Turkey are introduced, together with the related ophiolite sequence, on the basis of this grouping, as follows:

Region 1: NW Anatolian Region: (Balıkesir, Bursa, Eskişehir and Kütahya).
Region 2: North Anatolian Region (Çankırı, Çorum, Kastamonu, Sinop, Tokat and Yozgat).
Region 3: NE Anatolian Region (Sivas, Bayburt, Erzincan, Erzurum).
Region 4: SW Anatolian Region (Antalya, Burdur, Denizli, Isparta, Konya and Muğla).
Region 5: Central Anatolian Region (İçel, Adana, Kayseri).
Region 6: SE Anatolian Region (Hatay, Osmaniye, Kahramanmaraş, Gaziantep, Elazığ, Malatya, Adıyaman, Diyarbakır, Siirt, Van, Hakkari).

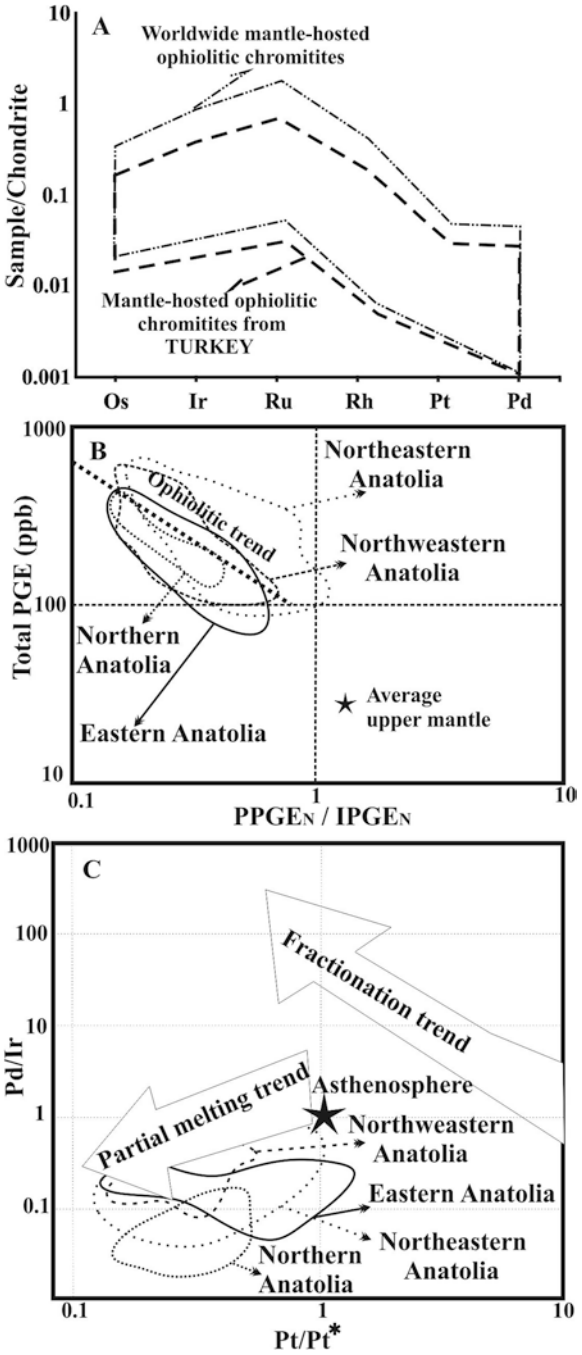

Fig. 3.6 PGE content and properties of chromitites in Turkey (explanations in the text)

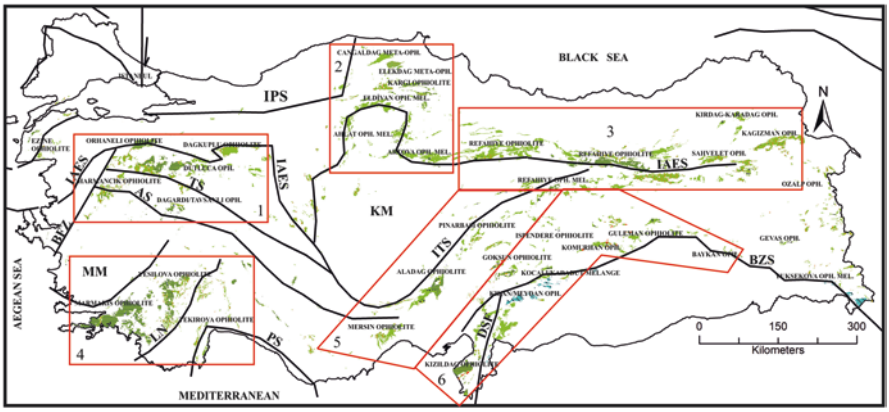

Fig. 3.7 Major structural elements of Turkey; distribution of ophiolites and related chromitites (*1*: NW Anatolian; *2*: North Anatolian; *3*: NE Anatolian; *4*: SW Anatolian; *5*: Middle Anatolian; *6*: SE Anatolian Sub-Regions). (*IAES* İzmir-Ankara-Erzincan Suture, *TS* Tavşanlı Suture, *AS* Afyon Suture, *BFZ* Bornova Flysh Zone, *MM* Menderes Massif, *KM* Kırşehir Massif, *PS* Pamphylian Suture, *ITS* Inner Tauride Suture, *IPS* Inner Pontide Suture, *BZS* Bitlis-Zagros Suture (Assyrian Suture), *DSF* Dead Sea Fault). (Modified After Okay and Tüysüz 1999) (Modified after MTA 2002)

Although the regional characteristics and the main features are discussed in the first section, it is necessary to describe them in more detail in terms of petrological and structural features because they are the primary wall-rock of chromitite ore deposits.

3.4.1 Region One: NW Anatolian (Balıkesir, Bursa, Eskişehir and Kütahya) Ophiolites and Related Chromitite Deposits

Ophiolitic rocks in this region and surrounding areas remain within İzmir-Ankara suture zone ophiolites (Fig. 3.7). The ophiolites that occur in the eastern border of Balıkesir province are part of the Yayla Melange (Ergül et al. 1980) and rocks belonging to the same section were examined under the Eydemirçay Formation towards the south (Konak and et al. 1980). In general, multi-colored units with different lithologies are in tectonic contact and form large and small blocks interpreted as ophiolitic melange (Pehlivan et al. 2007). The lithologies belonging to the Yayla Melange, which rests tectonically on the Bornova flysh, are also defined as a part of the Bornova flysch by other researchers (Ergül et al. 1980; Okay and Siyako 1993).

The chromite occurrences in the Balıkesir area are contained in harzburgites and dunites of the Harmancık Ophiolite, which is entirely composed of ultramafic tectonites. These units were cut partly by diabase dykes at different structural levels (Fig. 3.8).

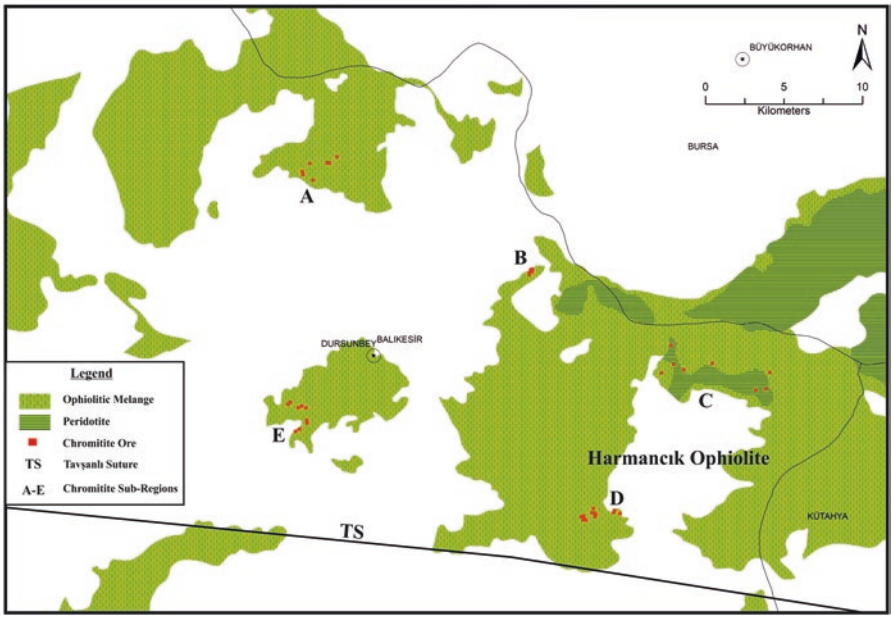

Fig. 3.8 Distribution of the chromitite occurrences in Balıkesir segment: (*a)* Karacabayır hill; (*b*) Adaören; (*c*) Akçaalan-Sağir; (*d*) Boyalıca and (*e*) Çatalçam sub-regions. (Simplified and modified after MTA 2002)

Chromitite occurrences in Bursa province are associated with approximately E–W trending Orhaneli Ophiolite or Harmancık Ophiolite (Figs. 3.9 and 3.10). While the Orhaneli ophiolites are generally represented by ultramafic to mafic cumulates, the Harmancık ophiolite is usually characterized by variably serpentinized harzburgitic to dunitic mantle tectonites (MTA 2002; Sayak et al. 2009; Ortalan et al. 1984; Bacak and Uz 2003).

The ophiolites outcropping around Kütahya, have been studied by many researchers (Arni 1942; Holzer 1954; Brinkmann 1972; Okay 1981, 2011; Konak 2002; Önen and Hall 1993; MTA 2002; Önen 2003). In the Tavşanlı Zone they display an internally coherent unit, the Tavşanlı Ophiolite, and a disordered melange, the Dağardı Melange. The Tavşanlı ophiolite is located in the north of Tavşanlı village as an E–W trending tectonic unit which is underlain by the Dağardı Melange (Fig. 3.11).

Tavşanlı zone ophiolites rest tectonically on the Ovacik Complex and Orhaneli group in the region (Okay 2011). They comprise peridotites, gabbro, pyroxenite, and diabase dykes. These ophiolitic rocks were named as “Dağardı Ophiolite” by Bacak and Uz (2003) and this ophiolite section is known as the eastern extension of the Harmancık (Bursa) Ophiolite.

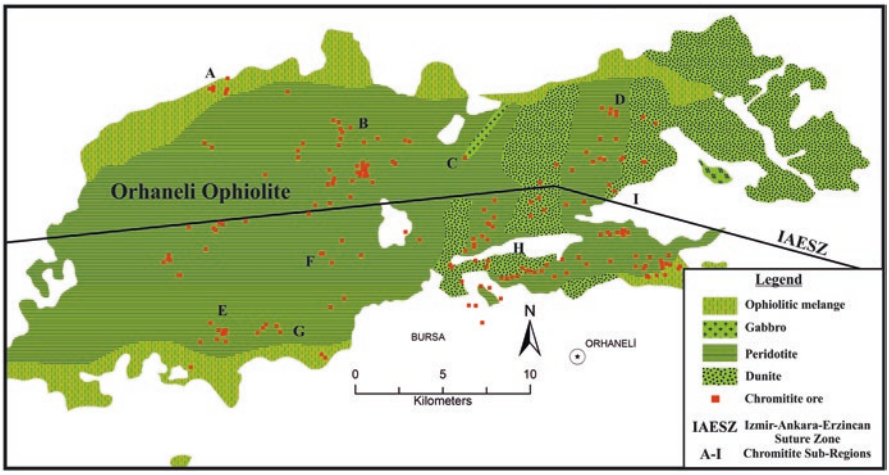

Fig. 3.9 Orhaneli sub-region and related chromitite occurrences and segments (A: Eskikızılelma; B: Çınarcık; C: Göktepe; D: Şeytanbudakköy; E: Çiviliçam; F: Ömeraltı; G: Letafet Köyü; H: Akçabük; I: Göynükbelen segments). (Simplified and modified after MTA 2002)

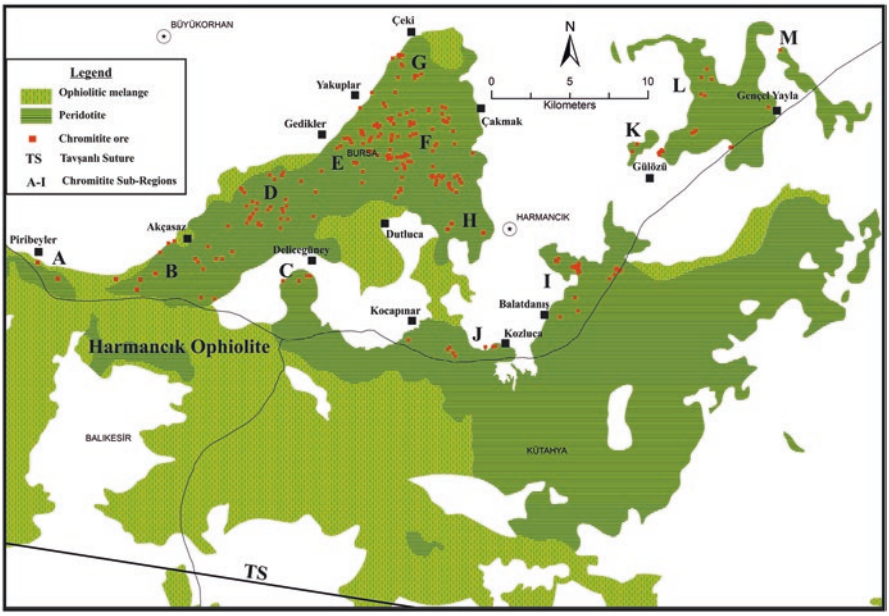

Fig. 3.10 Harmancık (Bursa) sub-region and related chromitite occurrences and segments (A: Piribeyler, B: Akçasaz, C: Delicegüney, D: Kınık, E: Yakuplar, F: Çakmak, G: Çeki Köyü, H: Harmancık, I: Balatdanış, J: Kocapınar-Kozluca, K: Eşen, L: Fındıcak, M: Gençel segments). (Simplified and modified after MTA 2002)

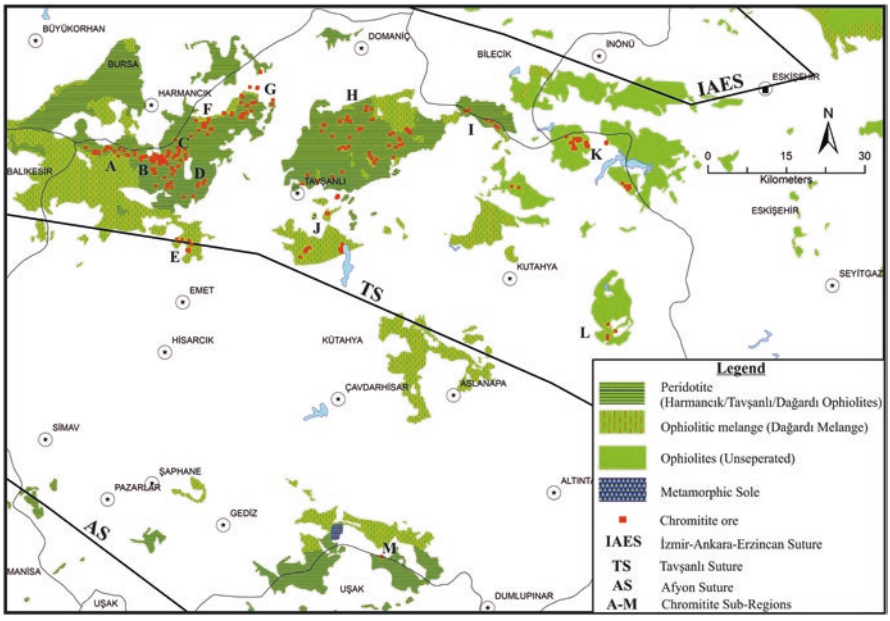

Fig. 3.11 Chromitite occurrences of Kütahya region and its segments (A: Uluçam; B: Madanlar; C: Çamalan; D: Kargılı; E: Dereli; F: Nusretler; G: Karakaya; H: Elmalı; I: Karsak; J; Tavşanlı; K: Sobran; L: Muhatboğaz; M: Çukurören segments). (Simplified after MTA 2002)

The Dağardı Melange covers a wide area between the Tavşanlı and Emet regions and consists of metamorphics, mafic to ultramafic magmatic and sedimentary rock assemblages trending NW-SE which are unconformably overlain by Tertiary sediments.

In Eskişehir province, ophiolitic units outcrop in three regions (Fig. 3.12). The first starts in the north of Eskişehir and ends in Sarıcakaya region as an E-W trending zone, and is named as Dağküplü Ophiolite. The second is Sivrihisar-Karaburhan Ophiolite Nappe outcropping in the north of Sivrihisar, and the third, the Dutluca Ophiolite, outcrops around Dutluca village. The ophiolitic rocks are made up of imbricated slices, and the assemblage from bottom to top is ophiolitic melange, mafic to ultramafic cumulates and tectonites (Özen et al. 2011).

3.4.1.1 Balıkesir Region Chromite Deposits

The chromite deposits and formations in the Balıkesir province are located within the borders of Dursunbey District (Fig. 3.8). General features of the chromitites in Balıkesir Region are given in Table 3.1. As shown in this table, chromitite ores in the region are generally limited in shape and reserve, and do not have economic importance, although chromitite ore in Turkey was first mined in this region.

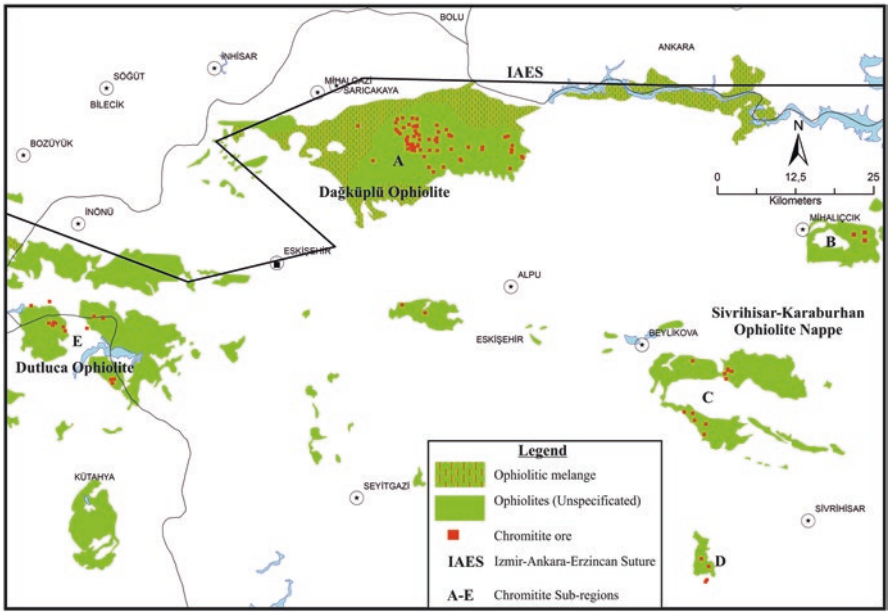

Fig. 3.12 Chromitite occurrences of Eskişehir region and its sub-regions (**A**: Dağküplü; **B**: Kavak-Bahtiyar; **C**: Sivrihisar-Karaburhan; **D**: Bahçecik; **E**: Dutluca). (Simplified and modified after MTA 2002)

3.4.1.2 Bursa Region Chromite Deposits

3.4.1.2.1 Orhaneli Sub-region

Chromitite formations in this area are largely located in Eskikızılelma, Çınarcık, Göktepe, Şeytanbudakköy, Çiviliçam, Ömeraltı, Letafet Village, Akçabük and Göynükbelen sectors. These sub-regions correspond to the zones lettered from A to I in Fig. 3.9.

The chromitite ore is generally observed in highly fractured/crushed serpentinized dunites. It can be seen in dunites, alternating with wherlite and pyroxenites as in Göktepe Sub-Region (Fig. 3.9C), but can also occurs in sheared serpentinite zones as massive, disseminated and banded zones like in the Şeytanbudakköy Sub-Region (Fig. 3.9D). There are pyroxenites and diabases around Ömeraltı Village (Fig. 3.9F). Harzburgites and dunites are partly/completely serpentinized in this region. Chromitite ores are sometimes located in cumulate dunite sections, including wherlite and clinopyroxenite layers (Fig. 3.9G–I). Also, ophiolitic rocks around the Dağgüney region display a mélange character (Fig. 3.9I).

Although Orhaneli Sub-Region is characterised mainly by disseminated ore, occurrences of several other types (massive, nodules) also exist and alternate with disseminated ore as banded layers. These ore-zones exhibit quite different

Table 3.1 General features of the chromitites in Balıkesir region

Region	Province/ophiolite	Sub-region/deposit name	Type[a]	Thickness/ length (meters)	Wall-rock	Grade ($\%Cr_2O_3$)	Map Nr. and sign
Region One (NW Anatolia)	Balıkesir/ Harmancık ophiolite	Karacabayır Tepe	Disseminated; partly massive banded	0.8–1.5/3–40	Hbj, Dn	15–25	Fig. 3.8a
		Adaören	Massive, disseminated, nodular	1–5/40–250	Hbj, Dn	30	Fig. 3.8b
		Akçaalan Sagir, Çamharmanı, Kuzköy, Çaltıcak	Brecciated, banded, disseminated	0.6–1.5/10–30	Hbj, Dn	25–40	Fig. 3.8c
		Boyalıca	Massive, lensoidal	10–90	Hbj, Dn	10–40	Fig. 3.8d
		Çatalçam	Massive banded, disseminated	1–20	Hbj, Dn	15–40	Fig. 3.8e

[a]Starts from the most abundant type; Hbj: Harzburgite; Dn: Dunite

thicknesses varying from few centimetres to tens of metres. The lengths of these deposits are usually quite short because they are cut by several faults and thrusts, but some deposits are up to 100 and 150 m in length. The average grade of the chromitite ore in Orhaneli Region is around 20 and 30 wt% Cr_2O_3, but can reach up to 50% Cr_2O_3 in massive and banded sections.

3.4.1.2.2 Harmancık Sub-Region

The chromite deposits and occurrences in the lower part of Harmancık (Bursa) are shown in Fig. 3.10 and their features are summarised in Table 3.2. All chromite deposits and occurrences in this sub-region are related to the harzburgite and dunite levels of the ophiolitic rocks, which are described as "Harmancık Peridotite Massif". These units are partly intruded by diabase dykes. According to Table 3.2, chromitite ores in this region have quite different shapes and dimensions, and include some large reserves. Since the nineteenth century it has included the most famous chromitite ore deposits in Turkey.

3.4.1.3 Kütahya Region

Kütahya province chromitite formations were mainly observed within the Tavşanlı (Dağardı) ophiolite. This ophiolite body has been described above and interpreted as the eastern extension of the Harmancık peridotite. There are no notable chromitite occurrence within Dağardı Melange (Fig. 3.11).

Chromite and magmatic bands in this section of the Dağardı Ophiolite are coherent and oriented NW – SE (Ortalan et al. 1984). The SW section of the ophiolite, east of Tavşanlı and E-SE of Çamalan Village in the north of Emet, is lateritic in character, and post-ophiolite-emplacement magmatism in the region had partly altered ophiolitic rocks through silicification and listwanitization. Chromite textures indicate a tectonic origin for this section of Tavşanlı Ophiolite (Ortalan et al. 1984).

In general, chromite mineralisation in this region has similarities with the Bursa-Harmancık region. Mineralization is usually banded and disseminated, but massive and nodular types are also present. Mineralized zones have variable thickness of between a few cm and a few meters and the Cr_2O_3 grade of ore varies between 20% and 45%. Mining activities in this region were by open pit and underground mining. General features of the chromitites in Kütahya Region are given in Table 3.3.

3.4.1.4 Eskişehir Region

Other ophiolites around the Dağküplü Ophiolite are related to the North Anatolian Ophiolite Belt. These rocks are emplaced as imbricated slices of ophiolitic mélange, mafic and ultramafic cumulates and tectonites (Fig. 3.12). Chromitite ores are

Table 3.2 General features of the chromitite deposits in Bursa region

Region	Province/ophiolite	Sub-region/ deposit name	Type[a]	Thickness/ length (meters)	Wall-rock	Grade (%Cr_2O_3)	Map Nr. and sign
Region One (NW Anatolian regions)	Bursa/Orhaneli ophiolite	Eskikızılelma	Disseminated, nodular, banded	1–4/12–40	Dn	25–40	Fig. 3.9A
		Çınarcık	Banded	1.5–2/2–12	Dn	25–48	Fig. 3.9B
		Göktepe	Banded, nodular	3–5/10–120	Wh-Px-Dn	15–30	Fig. 3.9C
		Şeytanbudakköy	Massive, banded, disseminated	1–1.5/4–110	Dn	12–46	Fig. 3.9D
		Çiviliçam	Disseminated, partly massive banded	0.8–5/1–150	Wh-Px-Dn	20–50	Fig. 3.9E
		Ömeraltı	Disseminated, banded, nodular	1–8/5–50	Hbj-Dn	20–45	Fig. 3.9F
		Letafet	Disseminated, banded	1–12/10–300	Wh-Px-Dn	20–30	Fig. 3.9G
		Akçabük	Banded, disseminated, massive	0.5–3/1–100	Wh-Px-Dn	20–35	Fig. 3.9H
		Göynükbelen	Banded	1–3/1–100	Wh-Px-Dn	20–30	Fig. 3.9I
	Bursa/Harmancık Ophiolite	Piribeyler	Disseminated, banded, massive	0.1–2.0/7–250	Hbj-Dn	5–34	Fig. 3.10
		Akçasaz	Disseminated, massive, nodular, spotted	0.2–2.0/1.0–40	Hbj-Dn	20–40	Fig. 3.10B
		Delicegüney	Banded, disseminated, nodular	0.3–2.5/1.0–20	Hbj-Dn	10–35	Fig. 3.10C
		Kınık	Banded, disseminated, spotted, massive	0.1–4.0/1.0–15	Hbj-Dn	10–35	Fig. 3.10D
		Yakuplar	Massive, disseminated, spotted	0.1–2.0/5–500	Hbj-Dn	20–30	Fig. 3.10E
		Çakmak	Massive, disseminated, nodular	0.1–1.5/5–60	Hbj-Dn	20–30	Fig. 3.10F
		Çeki Köyü	Disseminated, massive, nodular	0.2–1.5/1–5	Hbj-Dn	30–40	Fig. 3.10G
		Harmancık	Disseminated, massive, nodular	2–10/20–30	Hbj-Dn	20–40	Fig. 3.10H
		Balatdanış	Disseminated, spotted, massive	0.2–4.0/10–85	Hbj-Dn	25–40	Fig. 3.10I
		Kocapınar-Kozluca	Massive, banded, disseminated	02–4.0/10–60	Hbj-Dn	15–30	Fig. 3.10J
		Eşen	Banded, disseminated, spotted, nodular	0.2–2.0/10–30	Hbj-Dn	20–45	Fig. 3.10K
		Fındıcak	Massive, spotted, disseminated	0.1–1.5/5–35	Hbj-Dn	30–40	Fig. 3.10L
		Gençel	Massive	0.1–0.3/1–5	Hbj-Dn	20–30	Fig. 3.10M

[a]Starts from the most abundant type; Hbj: Harzburgite; Dn: Dunite; Wh: Wehrlite; Px: Pyroxenite

Table 3.3 General features of chromite deposits in Kütahya region

Region	County/ophiolite name	Sub-region/ deposit name	Type[a]	Thickness/length (meters)	Wall-rock	Grade (%Cr_2O_3)	Map Nr. and sign
Region One (NW Anatolian region)	Kütahya/Harmancık (Dağardı-Tavşanlı) ophiolite	Uluçam	Banded, disseminated	0.2–1.5/1–10	Hbj-Dn	20–30	Fig. 3.11A
		Madanlar	Banded, disseminated	0.3–3.0/1–80	Hbj-Dn	10–40	Fig. 3.11B
		Çamalan	Massive, banded, disseminated, spotted	0.1–1.5/1–70	Hbj-Dn	25–40	Fig. 3.11C
		Kargılı	Massive, disseminated, nodular	0.2–1.0/1–10	Hbj-Dn	30–45	Fig. 3.11D
		Dereli	Massive, disseminated	0.5–1.0/1–2	Hbj-Dn	20–40	Fig. 3.11E
		Nusretler	Massive, disseminated, spotted	0.1–0.7/1–10	Hbj-Dn	20–45	Fig. 3.11F
		Karakaya	Massive, nodular, disseminated	0.2–1.5/1–90	Hbj-Dn	40–50	Fig. 3.11G
		Elmalı	Banded, disseminated, nodular	0.2–2.0/1–20	Hbj-Dn	20–30	Fig. 3.11H
		Karsak	Banded, massive, disseminated, nodular	0.1–1.0/1–2	Hbj-Dn	30–35	Fig. 3.11I
		Tavşanlı	Massive, disseminated, nodular	0.2–0.8/1–12	Hbj-Dn	40–50	Fig. 3.11J
		Sobran	Massive, disseminated	0.1–1.2/1–16	Hbj-Dn	35–45	Fig. 3.11K
		Muhatboğaz	–	–	Hbj-Dn	–	Fig. 3.11L
	Dağardı Melange	Çukurören	Massive, disseminated	15 × 1 × 4	Hbj-Dn	45–50	Fig. 3.11M

[a]Starts from the most abundant type; Hbj: Harzburgite; Dn: Dunite

located within the harzburgitic and dunitic tectonites as well as within cumulate dunites. Ophiolites are strongly serpentinized and partly listwanitized in the region.

Chromite formations of Eskişehir are mostly located in Dağküplü, Sivrihisar-Karaburun, Dutluca and Kavak-Bahtiyar sub-regions (Fig. 3.12). Their general features are summarised in Table 3.4, in which it can be seen that no economically viable chromitite reserves exist in the region, except of the pipe shaped Kavak-Bahtiyar chromitite deposit. This deposit is one of the oldest chromitite mine in Turkey and operated since 1930s by Türk Maadin Company. According to the information given in the companies web-page, total production of chromitite ore (both massive and concentrated) is about 2.5 Mt and this is one of the deepest mine in the World (TMS 2017).

3.4.2 Region Two: North Anatolian (Çankırı, Çorum, Kastamonu, Sinop, Tokat and Yozgat) Ophiolites and Related Chromitite Deposits

3.4.2.1 Çankırı Region

3.4.2.1.1 Çankırı Ophiolites

Ophiolites around Çankırı and Çorum are examined under two names or labels in the literature. The first includes Eldivan Ophiolite Complex/Kargı Ophiolite Unit/Artova Ophiolite Complex (Özcan et al. 1980). The second is the Ahlat Ophiolitic Melange. The chromitite formations in the region are associated with peridotites of the Eldivan Ophiolite (Akın 1995). Akyürek et al. (1980) stated that the unit defined as Eldivan Ophiolite Complex, was emplaced as tectonic slices of oceanic crustal materials and upper mantle, separated by low angle overthrust planes (Hakyemez et al. 1986). The Complex consists of peridotite dunite, harzburgite and pyroxenite in the lower section; followed by oceanic crustal material consisting of gabbro, diabase dyke complex, pillow lava and pelagic sediment in the upper section (Akyürek 1981; Akın 1995). The internal structure of the Eldivan Ophiolite Complex is only partly known.

3.4.2.1.2 Çankırı Region Chromitites

Chromitite occurrences in Çankırı region are found in five areas: Eldivan Mountain, Çaparkayı, Sani Plateau, Yukarıöz Village and Gök Tepe sub-regions (Fig. 3.13). These occurrences are mostly in the eastern section of Eldivan County; a few are in the Northern sections of Korgun and Yapraklı Counties. General features of the chromitites in the Çankırı Region are given in Table 3.5.

Table 3.4 General features of the chromitite occurrences in Eskişehir region

Region	County/Ophiolite name	Sub-region/deposit name	Type[a]	Thickness/ Lenght (meters)	Wall-rock	Grade (%Cr_2O_3)	Map Nr. and sign
Region one (NW Anatolian regions)	Eskişehir/ Dağküplü Ophiolite	Dağküplü	Banded, disseminated, massive	0.1–3.0/0.5–5	Dn	20–30	Fig. 3.12-A
		Gündüzler-1	Massive, disseminated	0.5–4.0/2–50	Dn	20–40	Fig. 3.12-A
		Gündüzler-2	Banded, disseminated, massive	0.2–2.5/5–20	Dn	20–40	Fig. 3.12-A
		Gündüzler-3	Banded, disseminated	0.5–2.5/1–12	Dn	10–30	Fig. 3.12-A
		Sepetçi-1	Banded, disseminated, nodular, massive	0.5–2.5/10–50	Dn	30–40	Fig. 3.12-A
		Sepetçi-2	Banded, disseminated	0.2–2.5/5–60	Dn	20-40	Fig. 3.12-A
		Margı	Massive, disseminated	0.5–5.5/1–10	Dn	30-45	Fig. 3.12-A
		Taycılar-Başören	Banded, disseminated	0.2–2.0/10–50	Dn	20–35	Fig. 3.12-A
	Eskişehir/Sivrihisar-Karaburhan Ophiolite Nappe	Kavak-Bahtiyar	Massive, banded, disseminated	1.0–20/1–2.5	Dn	20–45	Fig. 3.12-B
		İmikler	Massive, banded	0.1–0.3/0.5–1.5	Hbj-Dn	30–45	Fig. 3.12-C
		Süleymaniye	Massive, banded	0.1–1.0/1–5	Hbj-Dn	30–45	Fig. 3.12-C
		Karaçam	Massive lens	0.2x0.25	Hbj-Dn	40–45	Fig. 3.12-C
		Okçu-Karaburhan	Banded, disseminated, Massive	0.1–1.0/1–40	Hbj-Dn	5–30	Fig. 3.12-C
		Bahçecik	Massive, banded	0.01–0.2/1–30	Hbj-Dn	30–40	Fig. 3.12-D
	Eskişehir/Dutluca Ophiolite	Aşağıkuzfındık	Banded, disseminated	0.3–1.5/5–15	Dn	30–45	Fig. 3.12-E
		Ballık	Massive, disseminated	0.1–0.5/1–5	Dn	30–40	Fig. 3.12-E
		Eski Sobran	Massive, disseminated	0.5–1.0/1–5	Dn	30–40	Fig. 3.12-E

[a]Starts from most abundant type; Hbj: Harzburgite; Dn: Dunite

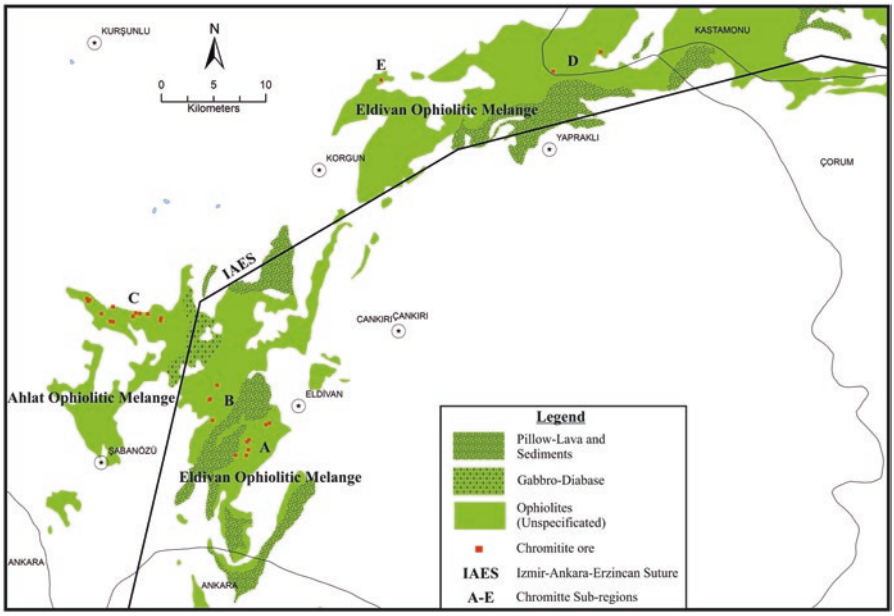

Fig. 3.13 Chromitite occurrences of Çankırı region and its sub-regions (A: Eldivan Dağı; B: Çaparkayı; C: Sani Yaylası; D: Yukarıöz Köyü; E: Göktepe). (Simplified and modified after MTA 2002)

3.4.2.2 Çorum Region

3.4.2.2.1 Çorum Region Chromitites

Chromitites of Çorum Region are observed within dunitic and harzburgitic mantle tectonites (Ortalan and Taşan 1997). These occurrences, except for the Morsümbül Stream deposit, crop out along a tectonic lineament about 25 km NW of Çorum province (Fig. 3.14, Table 3.5).

Sub-economic chromitite occurrences was exposed in open pits within serpentinized dunites and harzburgites, and included massive ore fragments, with high Cr_2O_3 grades.. Most chromite occurrences are in breccia zones along faults, and as veneers on fault walls.

3.4.2.3 Kastamonu and Sinop Regions

As chromitites in Kastamonu and Sinop regions are observed in the same ophiolite body they are both introduced in this section.

Table 3.5 General features of chromitites in Çankırı and Çorum regions

Region	County/ophiolite name	Sub-region/deposit name	Type[a]	Thickness/length (meters)	Wall-rock	Grade (%Cr_2O_3)	Map Nr. and sign
Region Two (North Anatolian region)	Çankırı/Eldivan ophiolitic melange	Eldivan Mountain	Banded, disseminated, massive	0.01–0.4/1–3	Dn	30–40	Fig. 3.13A
	Çankırı/Ahlat ophiolitic melange	Çaparkayı	Disseminated, banded, massive	0.1–1.6/1–116	Dn	33–45	Fig. 3.13B
		Sani Yaylası	Disseminated, banded, massive	0.05–0.4 (zone)	Dn	5–25	Fig. 3.13C
		Yukarıöz	Massive	–	Dn	42	Fig. 3.13D
		Gök Tepe	Massive	0.5–1.0/1–5	Dn	45–52	Fig. 3.13E
	Çorum/Artova ophiolitic complex	Uçarlık Tepe	Massive[b]	–	Dn	42–48	Fig. 3.14A
		Güllük Dere	Massive[b]	–	Dn	30–35	Fig. 3.14B
		Göl Sırtı	Massive[b]	–	Dn	30–40	Fig. 3.14C
		Yavşanlı Tepe	Disseminated, banded[b]	–	Dn	40–48	Fig. 3.14D
		Derinseki	Disseminated[b]	–	Hbj-Dn	20–30	Fig. 3.14E
		Tekçam Tepe	Massive[b]	–	Hbj-Dn	42–45	Fig. 3.14F
		Morsümbül	Massive, lens shaped	0.2–0.5/0.5–1	Hbj-Dn	38–42	Fig. 3.14G

[a]From the most abundant type; Hbj: Harzburgite; Dn: Dunite
[b]No primary occurrence observed, chromitite rubbles in excavation

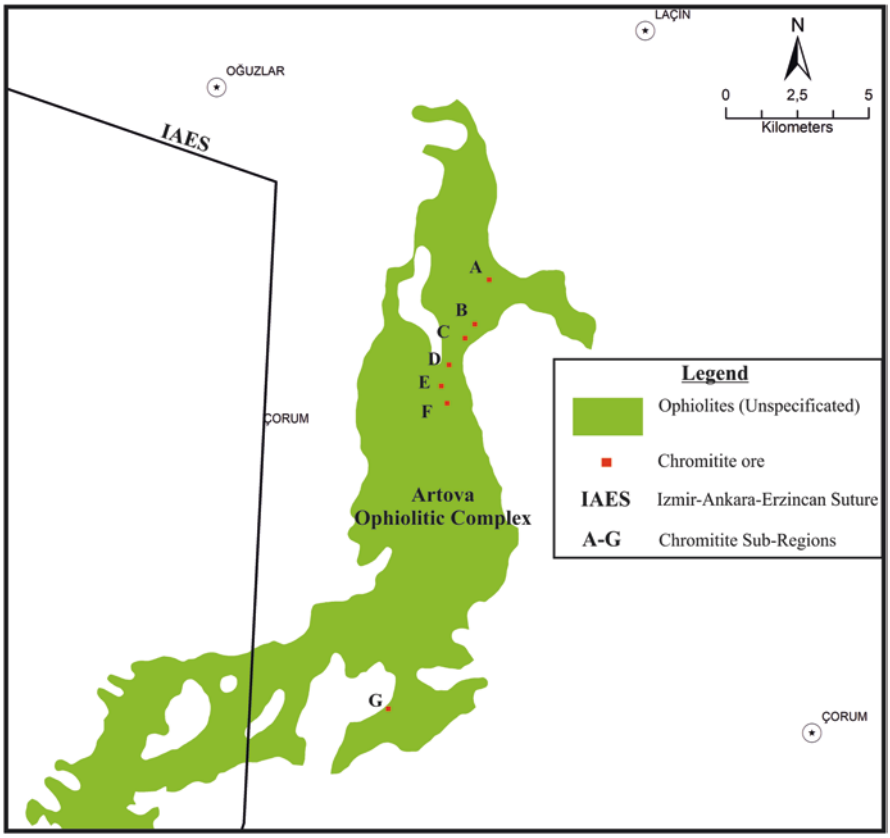

Fig. 3.14 Ophiolites and chromitite occurrences of Çorum region (A: Uçarlık Tepe; B: Güllük Dere; C: Göl Sırtı; D: Yavşanlı Tepe; E: Derinseki; F: Tekçam Tepe and G: Morsümbül Dere chromitite occurrences). (Simplified and modified after MTA 2002)

3.4.2.3.1 Kastamonu and Sinop Ophiolites

Ophiolitic rocks in the region mainly consists of eclogite-bearing ultramafics, peridotite, serpentinite, gabbro, diabase, basaltic lava, chert, radiolarite and mudstones. Although these rocks were defined under different names by several researchers, we will follow the "Elekdağ Meta-ophiolite" name used by Yılmaz and Tüysüz (1984).

According to Yılmaz and Tüysüz (1984), meta-ophiolites in Elekdağ have a "complete ophiolite section" along the long axis of the Elekdağ Mountain. Ultramafic rocks are seen in lower levels and pass upwards into layered peridotite. Serpentinite is the most common lithology and can be foliated along shear planes. Mesh texture is common in serpentinites hosting chromite mineralisation.

Peridotite and serpentinites are overlain by gabbro and diabases. Traces of high-pressure metamorphism are observed in many places within the diabases. At the highest levels, basaltic pillow lavas, mudstone and cherts are observed.

3.4.2.3.2 Kastamonu and Sinop Region Chromitites

Chromitite occurrences in this region are concentrated in meta-ophiolite that was called "Elekdağ Meta-ophiolite", and located mainly in Taşköprü territory (Fig. 3.15). The chromitite mineralisation occurs in ultramafic tectonites (harzburgite, dunite) and forms small bodies with little continuity and no economic potential. General features of the chromitites in Kastamonu and Sinop Regions are given in Table 3.6.

3.4.2.4 Tokat and Yozgat Regions

3.4.2.4.1 Tokat-Yozgat Ophiolites

Two different ophiolites were identified around Tokat and Yozgat. The first one consists of mafic and ultramafic rock slices within a Permo-Triassic metamorphic sequence. The Tokat Massif or Turhal Group, as known in the literature, can be correlated with the Kargı Ophiolite association exposed around Çorum. These rocks are named as "Artova Ophiolite Complex" (Aktimur et al. 1990). The other one is "Tekelidağ Complex" and "Refahiye Ophiolite" consisting of epi-ophiolitic sediments and oceanic crustal components that partly have a melange character, exposed in the southern part of Tokat (Yılmaz 1981, 1985; Aktimur 1986).

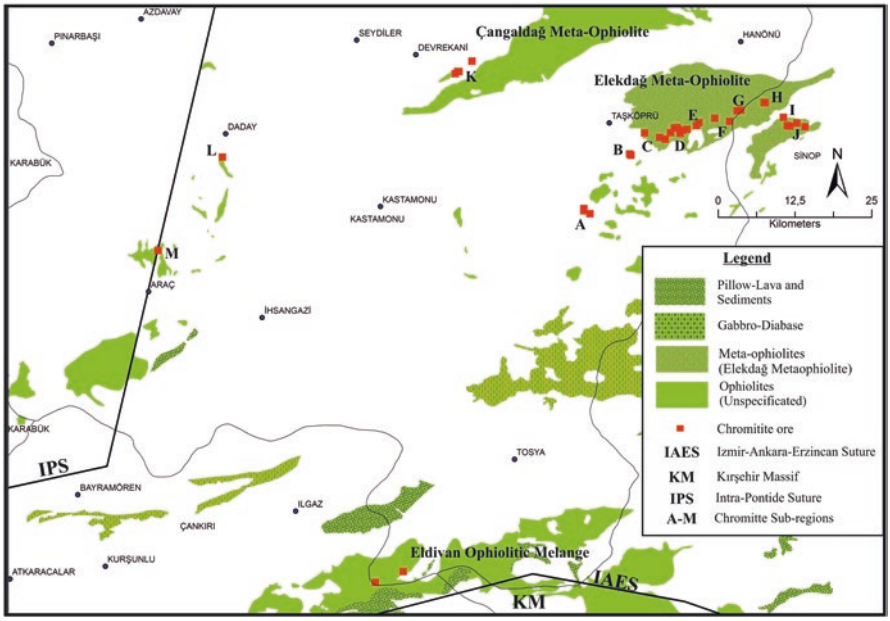

Fig. 3.15 Kastamonu (Elekdağ) chromitites and sub-regions (A: Olukbaşı; B: Belören; C: Çambaşı; D: Hacıali; E: Gündoğdu/Esentepe; F: Karapınar; G: Kovaçayır-Alıç; H: Kovaçayır-Türbe Tepe; I: Kovaçayır-Göçük Tepe; J: (Kovaçayır Alıç); K: (Örenbaşı); L: (Daday Hacıağa) ve M: (Araç Kavacık)). (Simplified and modified after MTA 2002)

Table 3.6 General features of chromitite occurences in Kastamonu-Sinop regions

Region	County/ Ophiolite name	Sub-region/deposit name	Type[a]	Thickness/length (meters)	Wall-rock	Grade (%Cr_2O_3)	Map Nr. and sign
Region two (North Anatolian Region)	Kastamonu/ Elekdağ Meta-Ophiolite	Çekiç	Massive	Small blocks	Hbj-Dn	38–48	Fig. 3.15-A
		Olukbaşı	Massive, nodular	0.2–1.5/1–20	Hbj-Dn	35–40	Fig. 3.15-B
		Belören-Bardakçı	Massive, disseminated, nodular	0.1–1.5	Hbj-Dn	35–40	Fig. 3.15-C
		Çambaşı	Massive, nodular	1.0–1.5	Hbj-Dn	40–45	Fig. 3.15-D
		Hacıali	Massive, nodular, lens shape	0.5x0.5	Hbj-Dn	40–45	Fig. 3.15-E
		Gündoğdu/ EsenHill	Nodular, massive, lens shape	0.5x0.5	Hbj-Dn	40–45	Fig. 3.15-F
		Karapınar River	Massive, nodular	0.2–0.5	Hbj-Dn	45–50	Fig. 3.15-G
	Sinop/Elekdağ Meta-Ophiolite	Kovaçayır-Göçük Hill	Massive, lens shape	0.05–0.1/10	Hbj-Dn	44–48	Fig. 3.15-H
		Kovaçayır-Türbe Hill	Massive, banded	0.05–0.1 (Massive band); 5–6 (zone)	Hbj-Dn	42–44	Fig. 3.15-I
		Kovaçayır-Alıç	Massive, banded	0.05-0.5	Hbj-Dn	40–44	Fig. 3.15-J
	Kastamonu/ Çangaldağ Meta-Ophiolite	Örenbaşı	Disseminated/massive banded	25 (zone)	Dn	38–40	Fig. 3.15-K
		Daday-Hacıağa	Massif blocks	0.1–0.2	Dn	42–44	Fig. 3.15-L
		Araç-Kavacık	Massif blocks	0.1–0.2	Dn	44–48	Fig. 3.15-M

[a]Starts from most abundant type; Hbj: Harzburgite; Dn: Dunite

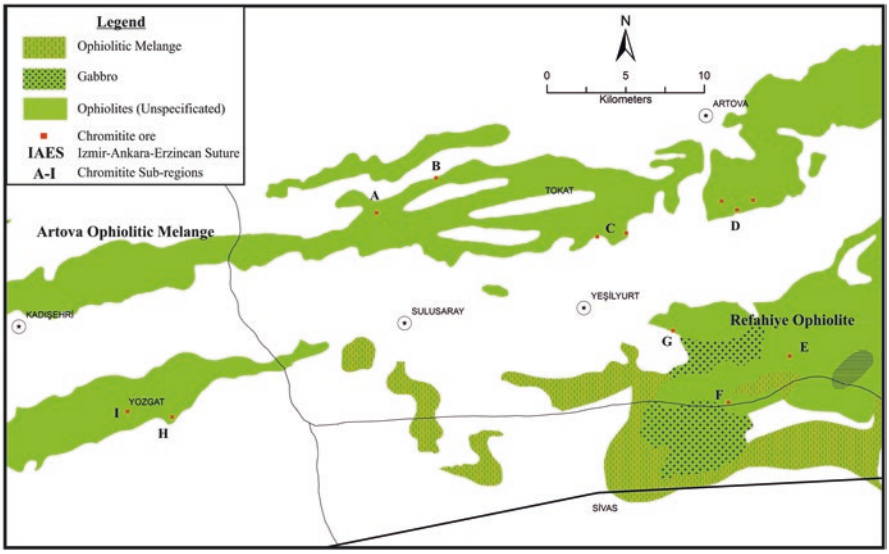

Fig. 3.16 Tokat and Yozgat chromitites (A: Arpacıkaraçay; B: Eşmebaşı; C: Doğlacık-Yağmur; D: Artova-Kazbayırdere-Demirci; E: Yamaç; F: Ağılın Tepe; G: Artova Tepe; H: Bozsırt; I: Deveçıkmazı). (Simplified and modified after MTA 2002)

3.4.2.4.2 Tokat and Yozgat Regions Chromitites

Some of the chromitite ores are located in the Artova Ophiolitic Melange, whilst others are in the Refahiye Ophiolite (Fig. 3.16). Key features of these deposits are summarised in Table 3.7. Around Arpacıkaraçay Village (A), Eşmebaşı Steam and Çukurtepe (B), and close to Doğlacık and Yağmur Village (C), occurrences of banded and disseminated chromite mineralization of no economic importance were observed.

3.4.3 Region Three: NE Anatolian (Sivas, Bayburt, Erzincan, and Erzurum) Ophiolites and Related Chromitite Deposits

3.4.3.1 Sivas Region

3.4.3.1.1 Sivas Ophiolites

Ophiolitic rocks are exposed in three different areas around the Sivas province. These ophiolite sequences include different oceanic crustal components and cover sediments, and they are partly melange in character. In the literature, they are known

Table 3.7 General features of chromitite occurrences in Tokat and Yozgat regions

Region	County/ophiolite name	Sub-region/deposit name	Type[a]	Thickness/length (meters)	Wall-rock	Grade (%Cr_2O_3)	Map Nr. and sign
Region Two (North Anatolian region)	Yozgat/Artova ophiolite	Deveçıkmazı	Massive, disseminated	0.5–1.0/2–8	Dn	40	Fig. 3.16I
		Bozsırt	Massive, disseminated	0.3–0.5/0.6–1.0	Dn	35–40	Fig. 3.16H
		Arpacıkaraçay	Banded, disseminated	–	Dn	–	Fig. 3.16A
		Eşmebaşı	Banded, disseminated	0.05–0.1/2 (zone)	Dn	45	Fig. 3.16B
		Doğlacık-Yağmur	Massive, disseminated	0.01–0.02/0.5–1.0	Dn	45	Fig. 3.16C
		Artova	Massive lenses	0.05–0.2/10–75	Dn	48	Fig. 3.16D
	Tokat/Refahiye ophiolite	Yamaç	Disseminated, spotted	0.5–1.0/1–5	Dn	30–35	Fig. 3.16E
		Ağın Tepe	Massive lenses	0.1–0.9	Dn	35–40	Fig. 3.16F
		Artova Tepe	Disseminated, massive	1–5/10–650	Dn	5–48	Fig. 3.16G

[a]Starts from the most abundant type; Dn: Dunite

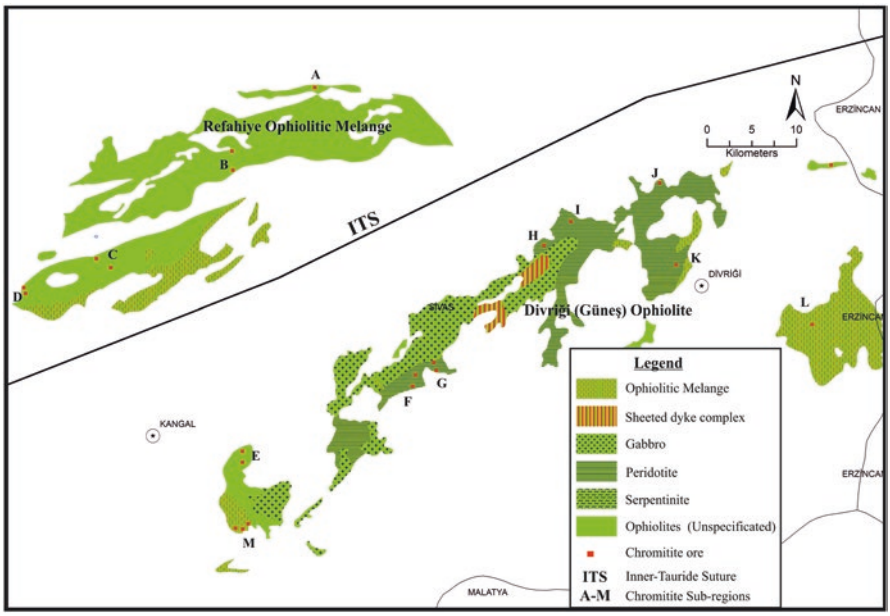

Fig. 3.17 Chromitite occurrences of Divriği and Kangal (Sivas) regions (A: Gürgen Ağılı; B:Gülkanat; C: Sivritaştepe; D: Başçayır; E: Ortadağ; F: Bostan Dere; G: Çamlıburun; H: Galin; I: Karakuz; J: Kayabaşı; K: Karatepe; L: Asmalı Dere). (Simplified and modified after MTA 2002)

as "Refahiye Ophiolite" that occur along the İzmir-Erzincan suture zone and were emplaced in the Late Cretaceous (Yılmaz 1985; Aktimur 1986, Aktimur et al. 1988) (Fig. 3.17). But the ophiolitic rocks cropping out in the north part of Kangal and west part of Divriği, are called "Divriği (Güneş) Ophiolite", and are interpreted as products of the Inner Tauride Ocean (Bayhan 1980).

3.4.3.1.2 Sivas Region Chromitites

Numerous chromite occurrences in ophiolites of Sivas province were derived from both the Ankara-Erzincan Ocean and the Inner Tauride Ocean. Chromitite occurrences in the north have a genetic link with the Erzincan region ophiolites and are explained together with occurrences in Erzincan province. Whereas the chromite occurrences observed in the south, around Kangal and Divriği regions, as shown in Fig. 3.17, occur in disseminated and massive forms hosted in dunites. These chromitites are partly hosted in Refahiye Ophiolite and partly in Divriği Ophiolite, and are summarised in Table 3.8.

Table 3.8 General features of chromitite occurrences in Sivas region

Region	County/Ophiolite name	Sub-Region/ Deposit name	Type[a]	Thickness/Lenght (meters)	Wall-rock	Grade (%Cr_2O_3)	Map Nr. and sign
Region three (NE Anatolian Region)	Sivas/ Refahiye Ophiolite	Gürgen Ağılı	Massif lensler	0.01–2.5/1–5	Hbj-Dn	40–48	Fig. 3.17-A
		Gülkanat	Banded, Massive	2–8 (zone)/40–70	Hbj-Dn	30–40	Fig. 3.17-B
		Sivritaş Tepe	Banded, disseminated	0.1–1.0/1–17	Hbj-Dn	30–40	Fig. 3.17-C
		Başçayır	Banded	0.05–0.5/20–30	Hbj-Dn	15–20	Fig. 3.17-D
	Sivas/Divriği Ophiolite	Ortadağ	banded	0.01–0.1/4–5(zone)	Dn	5–10	Fig. 3.17-E
		Bostan Dere	Disseminated, banded	2–5/60–70	Dn	20–30	Fig. 3.17-F
		Çamlıburun	Disseminated, banded	0.8–1.0/10–50	Dn	1*–30	Fig. 3.17-G
		Galin	Massive, disseminated, banded	2–10 (zone)	Dn	35–48	Fig. 3.17-H
		Karakuz	Disseminated, massive lensler	0.2–0.4/5–10	Dn	25–30	Fig. 3.17-I
		Kayabaşı	Disseminated, massive	0.5–2.5 (zone)/10–50	Dn	20–30	Fig. 3.17-J
		Kara Tepe	Massive banded	0.1–0.3 (zone)/20–100	Dn	40–45	Fig. 3.17-K
		Asmalıdere	Disseminated, massive banded	0.1–1.5/1–5	Dn	38–50	Fig. 3.17-L
		Seçenyurdu	Disseminated, massive banded	2.5–6.0/0.5–0.8	Hbj-Dn	25–30	Fig. 3.17-M

[a]Starts from most abundant type; Hbj: Harzburgite; Dn: Dunite

3.4.3.2 Erzincan Region

The Erzincan Region is located on the Eurasian plate (Pontides) and Anatolian plate suture zone, along the "İzmir-Ankara-Erzincan Suture Zone" that was defined by Brinkmann (1966, 1968). The ophiolitic rocks along this suture zone are named as Refahiye Ophiolite and the defining unit (Refahiye Ophiolitic Complex, Yılmaz 1985) is exposed in the north of Erzincan and continues toward Mercan, Tercan and Çayırlı territories (Özen et al. 2008).

From its beginning north-northeast of Erzincan, along the Keşiş Mountains that extend eastward, the ophiolitic sequence consists of mantle tectonites (harzburgite and dunite), ultramafic to mafic cumulates (wherlite, dunite, pyroxenite, gabbro), isotropic gabbro, and sheeted dyke complex (Özen et al. 2008).

3.4.3.2.1 Erzincan Region Chromitites

There are numerous chromitite mines, quarries, open pits and outcrops of various size in Erzincan region (Fig. 3.18). These and some other occurrences to the NE of Sivas, that share the same features, are summarised below.

Ores in the Erzincan region (Fig. 3.18) are banded and lens shaped, and have mineralization styles of massive, spotted, disseminated and nodular type. The contacts between ore bands and lenses and wall rock dunite are generally primary, but structural in some cases. The chromitite bands and lenses are either primary or

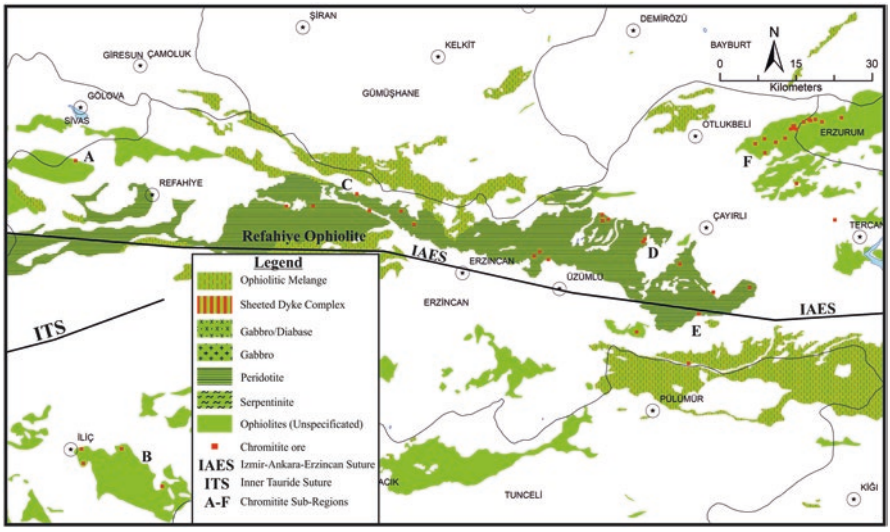

Fig. 3.18 Chromitite occurrences and sub-regions of Erzincan region (A: Refahiye; B: İliç-Kemah; C: NW of Erzincan; D: Üzümlü-Çayırlı; E: Pülümür; F: Otlukbeli-Tercan). (Simplified and modified after MTA 2002)

structural, and usually conformable with the internal structure of the peridotites. Mineralization in cumulate dunites is generally low grade (10–30% Cr_2O_3), whereas mineralization in tectonite dunites have relatively higher Cr_2O_3 grade (42–48% and above). In terms of their chemical components, they have good metallurgical characteristics (Cr/Fe ratios are high).

Chromitites in Erzincan region can be grouped in six sub-regions. These are Refahiye, İliç-Kemah, NW of Erzincan, Üzümlü-Çayırlı, Pülümür and Otlukbeli-Tercan (Fig. 3.18). The general features of these chromitites are given in Table 3.9.

3.4.3.3 Erzurum and Bayburt Regions

These are located to the east of Erzincan and its border region (Fig. 3.19). Ophiolite sequences are located in Horasan and Narman regions, north and east of Tekman and outside of the Refahiye Ophiolite Complex exposures that line up to North of Aşkale in the west of the province. Ophiolitic rocks that lie between Tekman and Pasinler were defined as "Şahvelet Ophiolite". This ophiolite sequence, from bottom to top, consists of ophiolite melange, tectonites and cumulates (Özen et al. 2008).

Ophiolite melange at the bottom is characterised by podiform chromite mineralization within harzburgites, and dunites to a lesser extent. The tectonites consist mainly of dunites and harzburgites intruded by doleritic dykes. The cumulate sequence consists mainly of gabbros, and dunite with relatively lesser amounts of wherlite and clinopyroxenite. Moreover, the ophiolitic mélange unit also contains tectonites and cumulates around Karayazı region. The cumulate rocks in the region are characterised by dunite, wherlite, clinopyroxenite and gabbro alternations. The tectonites comprise harzburgite and dunites. The chromitite quarries, open pits and outcrops in this region occur in tectonite or tectonite-cumulate transition zones, but do not have economic potential when compared to chromite mineralisations between Pasinler and Tekman regions.

There is an ophiolitic melange at the base of the ultramafic rocks in Horasan region (Çolakoğlu et al. 2014). Above this melange, spilitic basalts with cover sediments come onto the cumulate section. Two different mélange units, namely Örükyayla and Gezenek Melanges, are observed in Kırdağ (Oltu-Erzurum) region and in successions overlain by ophiolitic units from bottom to top: cumulates, isotropic gabbros and epi-ophiolitic sediments with pillow lavas in the upper part.

3.4.3.3.1 Erzurum Region Chromitites

Ophiolites of Erzurum region are exposed mainly in four regions (Fig. 3.19), and seven groups have been recognised. A small part of ophiolites to the NW of Aşkale are located in the Bayburt province border and the "Kopdağ Chromitites" is one of the most important chromitite mines of Turkey. These occurrences are interpreted as part of the Refahiye ophiolite.

Table 3.9 General Features of chromitites in Erzincan region

Region	County/ophiolite name	Sub-region/deposit name	Type[a]	Thickness/length (meters)	Wall-rock	Grade (%Cr_2O_3)	Map Nr. and sign
Region Three (NE Anatolian region)	Erzincan/Refahiye ophiolite	Refahiye-Mağara Tepe	Disseminated, banded	0.2–0.5/1–2	Dn	30 (zone)	Fig. 3.18A
		Kemah-İliç	Massive, banded, disseminated	0.3–0.5/2–5	Dn	20–45	Fig. 3.18B
		NW-Erzincan	Massive, disseminated	0.3–0.5/1–5	Dn	40–45	Fig. 3.18C
		Üzümlü-Çayırlı[b]	Massive, disseminated	5–12/90–350	Dn	45–55	Fig. 3.18D
		Pülümür	Massive (brecciated)	0.04–0.15/1–15	Dn	55–18	Fig. 3.18E
		Otlukbeli-Tercan[b]	Massive	1–10/20–60	Dn	35–45	Fig. 3.18F

[a]Starts from the most abundant type; Dn: Dunite
[b]The most important chromite deposits of Turkey

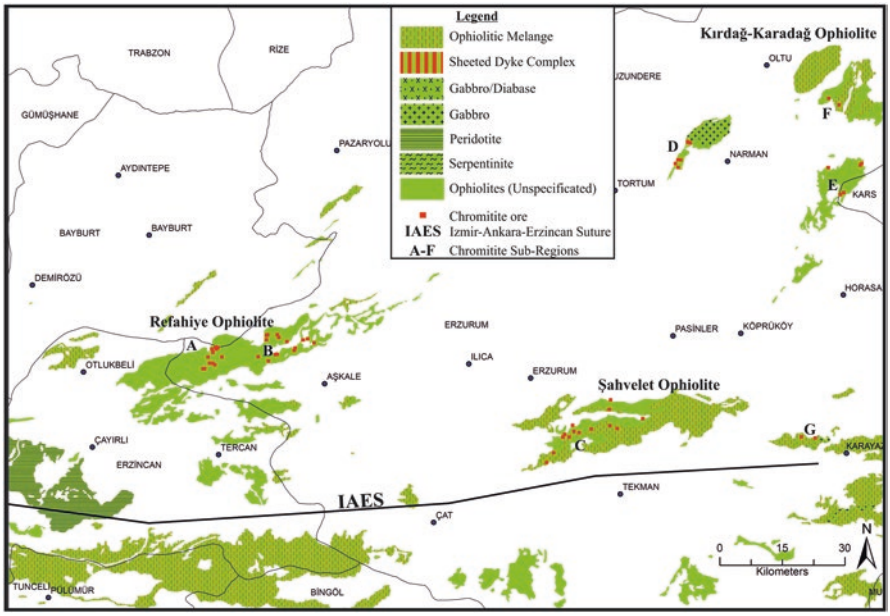

Fig. 3.19 Ophiolites, chromitite occurrences and sub-regions of Erzurum region (A: Kopdağ; B: Aşkale; C: Tekman; D: Narman; E: Horasan; F: Şenkaya; G: Karayazı). (Simplified and modified after MTA 2002)

The second group of chromitites, close to the Kopdağ Deposit, is situated in the Erzurum province borders. These are known as "*Aşkale West Chromitites"*. They outcrop in an E–W trending belt. The Şahvelet Ophiolite, between the center of Erzurum province and Tekman, are considered as the third group under the name of "Tekman Chromitites". On the other hand, the chromite occurrences hosted in dunitic-harzburgitic mantle west of Narman are the fourth sub-group: the "Narman Chromitites". The fifth group was defined as "Horasan Chromitites"; the sixth group was defined as "Şenkaya Chromitites"; the seventh group was defined under "Karayazı Chromitites" in the west of Karayazı close to SE border of province. General features of the chromitites in Erzurum and Bayburt Regions are given in Table 3.10.

3.4.4 Region Four: SW Anatolia (Muğla, Denizli, Burdur, Isparta, Konya, and Antalya) Ophiolites and Related Chromitite Deposits

3.4.4.1 Muğla, Denizli and Burdur Regions

The Muğla region is located in SW Anatolia (Figs. 3.1 and 3.7). This region is at the south of the Menderes Massif and it is widely covered by metamorphic and oceanic crustal rocks.

Table 3.10 General features of chromitites between Erzurum ve Bayburt regions

Region	County/ophiolite name	Sub-region/deposit name	Type[a]	Thickness/length (meters)	Wall-rock	Grade (%Cr_2O_3)	Map Nr. and sign
Region Three (NE Anatolian region)	Erzurum/Refahiye ophiolite	Kopdağ[b]	Disseminated, banded	1–4/1000 (zone)	Dn	20–40	Fig. 3.19A
		Aşkale-West	Disseminated, banded	1–3/10–70	Dn	30–40	Fig. 3.19B
	Erzurum/Şahvelet ophiolite	Tekman	Massive lenses	0.3 × 0.6/1–2	Hbj-Dn	40–50	Fig. 3.19C
		Narman	Massive, lenses, boulders	0.1 × 0.3/0.5–1.0	Hbj-Dn	40–50	Fig. 3.19D
		Horasan	Massive, lenses, boulders	0.2 × 0.4/0.5–1.0	Hbj-Dn	40–50	Fig. 3.19E
		Şenkaya	Massive and banded	0.2–1.0/5–50	Hbj-Dn	20–30	Fig. 3.19F
		Karayazı	Massive	0.2–0.5/3–5	Hbj-Dn	30–45	Fig. 3.19G

[a]Starts from the most abundant type; Hbj: Harzburgite; Dn: Dunite
[b]One of the important deposits of Turkey

3.4.4.1.1 Muğla-Denizli-Burdur Region Ophiolites

The distribution of ophiolitic rocks from Muğla to Burdur through Denizli, are shown on Figs. 3.1 and 3.20. Ophiolites in this area were defined as "Marmaris Ophiolite Nappe" (Şenel 1997a) and "Likya Ophiolite" (Şenel 2004). Their thicknesses are more than 2 km, and spread over a 45,000 km^2 area (Collins and Robertson 1997, 1998). Ophiolite units consist of serpentinized harzburgite, and lesser pyroxenite, podiform chromite and gabbro cutting by altered diabase dykes at different structural levels.

The Menderes Massif consists mainly of tectonite peridotites with the plutonic section completely eroded. Harzburgite is the most common rock type. Massive harzburgites exhibit foliation patterns on higher levels (Erendil 2002). Banding is defined by harzburgite-dunite or harzburgite-orthopyroxenite alternations. Banding planes are almost horizontal and it may indicate that the ophiolite nappe is close to the horizontal position.

The tectonites of Marmaris ophiolites are cut by isolated diabase and gabbroic dykes compared to the Yeşilova Ophiolite in NE areas. From the character of these isolated dykes, it was suggested that deeper sections of mantle are exposed in the massif (Reuber et al. 1984). The mantle peridotites are underlain by subophiolitic metamorphic rocks.

In the Denizli and Burdur Regions, ophiolitic rock groups are classified as Marmaris Ophiolite in the West and Yeşilova Ophiolite in the east, with the former discussed above. The general characteristics of the Yeşilova Ophiolite are as follows, the serpentinized ophiolitic rocks rich in chromite mineralization are located along the Çavdır-Tefenni-Yeşilova line. The ophiolites in this area are defined as

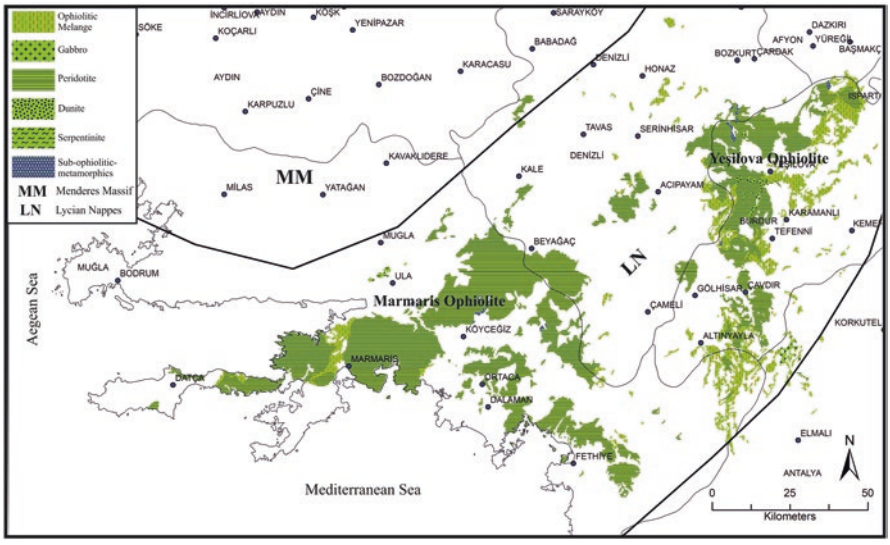

Fig. 3.20 Distribution of SW Anatolian Ophiolites (Marmaris and Yeşilova). (Simplified and modified after MTA 2002)

"Marmaris Ophiolite Nappe" (Şenel 1997a) and "Likya Ophiolite" (Şenel 2004). The ophiolites that outcrop around Çavdır-Tefenni-Yeşilova were firstly defined as "Yeşilova Ophiolite" by Sarp (1976). Rock units within the ophiolitic sequence in Yeşilova region from bottom to top consist of tectonites, cumulates, dyke rocks and volcanic rocks (Döyen 1995). The tectonites are represented mainly by harzburgites and dunites. The chromites are enveloped by dunites. In mantle tectonites, beside harzburgite, lherzolite and wherlite are also observed (Döyen 1995).

Cumulate sections of Yeşilova Ophiolite, crop out in south and western part of Yeşilova Village. Dykes are generally represented by diabase. It is suggested that these isolated dykes cutting the Yeşilova opholites, can be interpreted as big dykes in tectonites (Reuber et al. 1984). The sheeted dyke complex could not be observed, instead mafic sills and basaltic volcanics were discovered by Koralay (2000).

3.4.4.1.2 Muğla Chromitites

Chromitites in the Muğla region are found in the Marmaris Ophiolite. Although these occurrences are less common in the Marmaris sub-region, there are numerous chromite quarries in the Köyceğiz, Dalaman and Fethiye areas, where significant Cr production has been recorded (Fig. 3.21). A number of quarries and open pits contain these chromites in Nergislidüz, Kazandere, Ilıkdere-Suçıktı, Sülek, Andızlık-Meşebükü-Erengediği, Dalaman-Ortaca and east of Fethiye (Fig. 3.21). The main features of these chromitite deposits are briefly explained in Table 3.11. Although this region is one of the major chromitite mining areas in Turkey, these deposits were almost mined out at shallow depths at the beginning of the twentieth century.

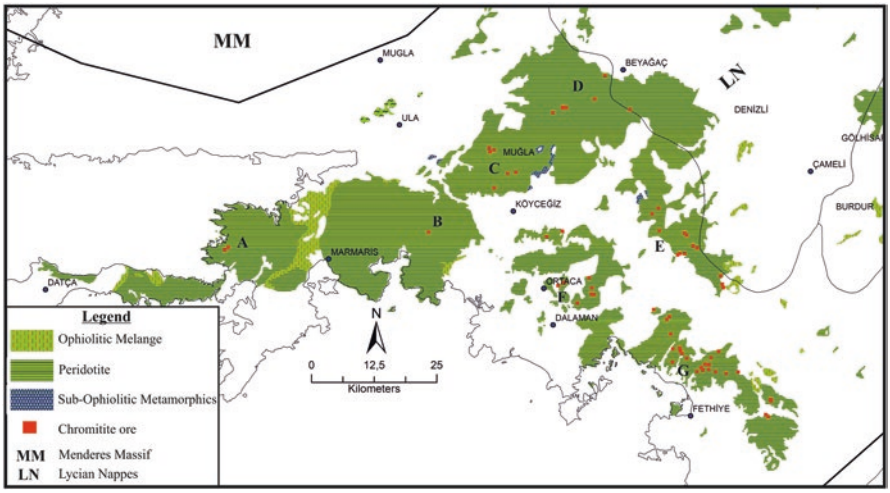

Fig. 3.21 Chromitite occurrences and sub-regions of Muğla region (A: Nergislidüz; B: Kazandere; C: Ilıkdere-Suçıktı; D: Akçaalan-Sülek; E: Andızlık-Meşebükü; F: Dalaman-Ortaca; G: Fethiye). (Simplified and modified after MTA 2002)

Table 3.11 General features of chromitite occurrences in Muğla, Denizli and Burdur regions

Region	County/ophiolite name	Sub-region/deposit name	Type[a]	Thickness/length (meters)	Wall-rock	Grade (%Cr_2O_3)	Map Nr. and sign
Region Four (SW Anatolian region)	Muğla/Marmaris ophiolite	Nergislidüz	Massive, nodular, lensoidal	1–5.5/5–25	Dn	30–45	Fig. 3.21A
		Kazandere	Massive, nodular, lensoidal	1–4/10–20	Dn	30–40	Fig. 3.21B
		Ilıkdere-Suçıktı	Banded, disseminated, massive	0.01–05/20–100	Dn	30–50	Fig. 3.21C
		Akçaalan-Sülek	Massive, lensoidal	0.1–0.3/1–5	Dn	40–50	Fig. 3.21D
		Andızlık-Meşebükü	Massive, lens/ boulder shaped	1–2/10–100	Dn	30–40	Fig. 3.21E
		Dalaman-Ortaca	Massive, lens	0.1–0.8/10–100	Dn	35–45	Fig. 3.21F
		Fethiye[b]	Massive, nodular	0.3–7.0	Dn	40–50	Fig. 3.21G
	Denizli/Marmaris ophiolite	Efekli	Massive, nodular, disseminated	0.5–1.5/5–15	Dn	35–45	Fig. 3.22A
		Topuklu	Massive banded	2 (zone)/5–25	Hbj-Dn	15–35	Fig. 3.22B
		Karanfil	Massive, disseminated, lens	1–8/10–60	Dn	30–40	Fig. 3.22C
		Çatak	Nodular, massive, disseminated	1–7/1000 (zone)	Dn	35–45	Fig. 3.22D
		Horozköy	Disseminated, massive banded	0.1–0.8/1–5	Dn	30–40	Fig. 3.22E
	Burdur/Yeşilova ophiolite	Gölhisar	Massive, banded	0.5–0.7/10–25	Dn	20–40	Fig. 3.23A
		Çavdır	Massive, nodular	0.1–0.6/1–3	Dn	30–45	Fig. 3.23B
		Tefenni	Banded, massive	0.1–0.4/1–4	Dn	30–45	Fig. 3.23C
		SW of Yeşilova	Banded, disseminated, leopar patterned	0.15–1.0/1–6	Dn	35–50	Fig. 3.23D
		West of Yeşilova	Disseminated, banded, massive, lensoidal	0.1–0.3/1–10	Dn	20–40-55	Fig. 3.23E
		NW of Yeşilova	Massive, disseminated	0.1–0.6/1–35	Dn	20–45	Fig. 3.23F
		N and NE of Yeşilova	Massive, banded	0.05–0.3/1–25	Dn	30–42	Fig. 3.23G

[a]Starts from the most abundant type; Hbj: Harzburgite; Dn: Dunite
[b]An important deposit in Turkey

This area was taken into consideration because of its economic potential and currently new exploration continues in deeper sections of the ancient ore deposits by using new methods and production technologies.

3.4.4.1.3 Denizli Chromitites

Chromitites in Denizli Region, as in the Muğla Region, are located within mantle tectonites, along the harzburgite-dunite level of Marmaris Ophiolite (Fig. 3.22). The chromite occurrences are mainly situated in the west and east sections of Beyağaç and Acıpayam. These occurrences are briefly introduced below (Fig. 3.22). The main Sub-Regions of the Denizli Region are Efekli, Topuklu, Karanfil, Çatak and Horozköy and the main features of chromitite deposits are briefly explained in Table 3.11. This region is much less active in terms of chromitite mining compared to the Muğla Region.

3.4.4.1.4 Burdur Region Chromitites

Distribution of ophiolitic rocks and chromitite deposits in Burdur region is shown in Figs. 3.21 and 3.23, respectively.

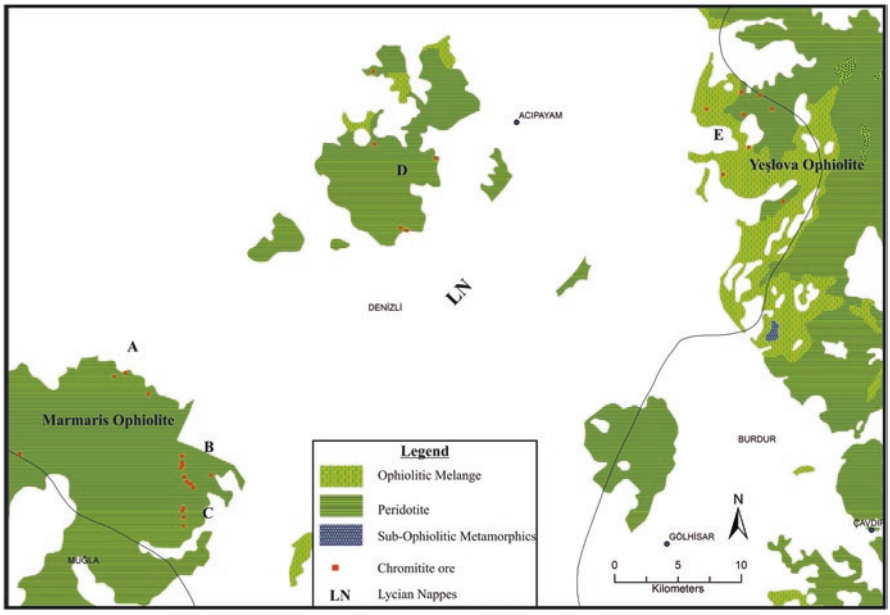

Fig. 3.22 Chromitite occurrences and sub-regions of Denizli region (A: Efekli; B: Topuklu; C: Karanfil; D: Çatak ve E: Horozköy). (Simplified and modified after MTA 2002)

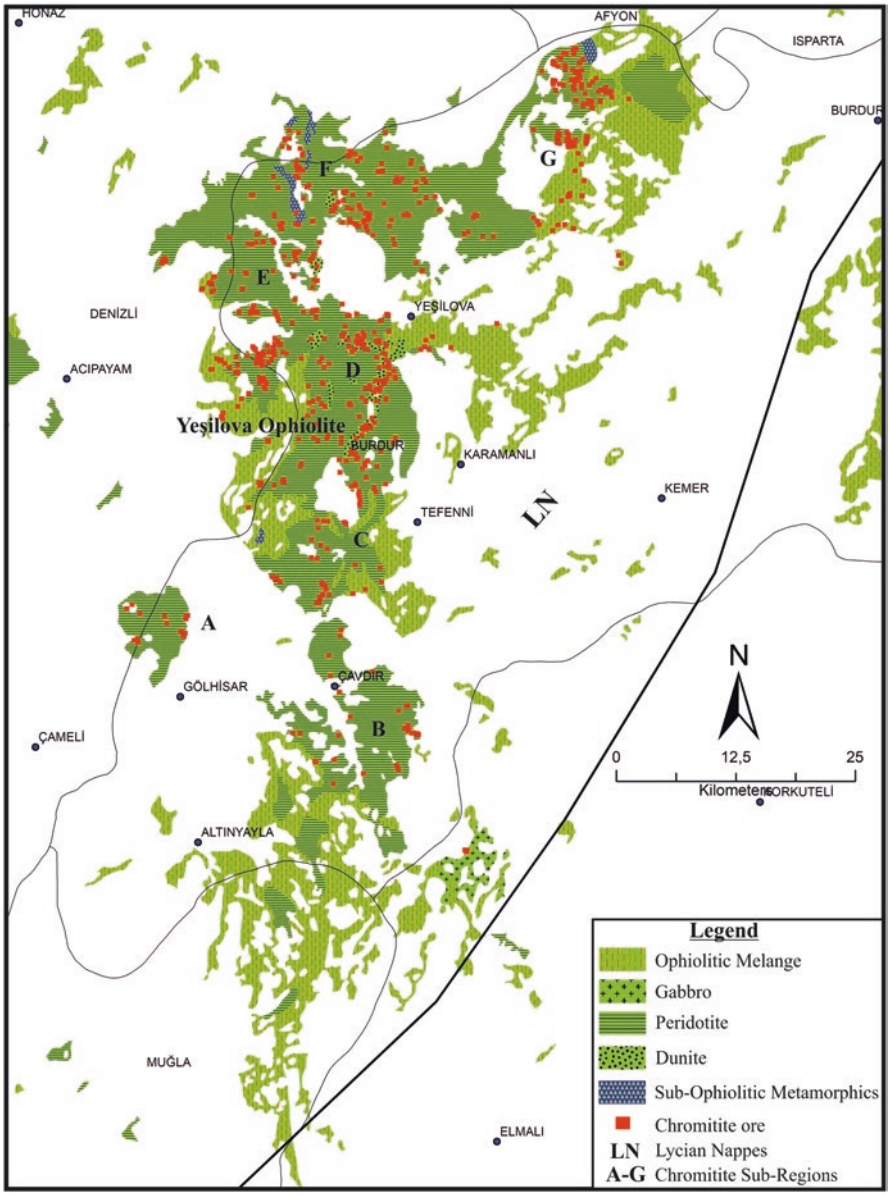

Fig. 3.23 Chromitite occurrences and sub-regions of Burdur region (A: Gölhisar; B: Çavdır; C: Tefenni; D: SW Yeşilova; E: Western of Yeşilova; F: NW of Yeşilova KB, and G: N and NE of Yeşilova). (Simplified and modified after MTA 2002)

The first chromitite prospecting in the region was done by Alpay (1951) around Salda, Horozköy, Bahtiyar and Işıklar Village of Yeşilova district. This was followed by large scale studies of Borchert (1960, 1962) and Denkel (1972). The chromite occurrences were studied in detail by Sarıkaya and Seyrek (1976) and Yıldız et al. (1976). Boyalı (1996) studied some occurrences in the north of Salda Lake, Antalya and Isparta provinces. Renewed studies were carried out by MTA (Mineral Research and Exploration Institute) in 1991, and the findings from these studies are reported here. It can be concluded that the ophiolites in the eastern section of the province are generally mélange in character and not related with chromitite occurrences (Fig. 3.23). The ophiolites which are important in terms of chromitites are serpentinized peridotites that belong to Marmaris Ophiolite along the Çavdır-Tefenni-Yeşilova line. Chromitite deposits in this region are significantly different in type and size (Fig. 3.23).

Chromite deposits in the Burdur region can be divided into six sub-regions. In each sub-region, features of a few representative and important deposits are given in Table 3.11. Chromitite mining has been stopped for a long time in the Burdur and Denizli Regions, but is still active in the Muğla Region.

3.4.4.2 Isparta-Konya-Antalya Regions

3.4.4.2.1 Isparta-Konya-Antalya Ophiolites

Isparta ophiolites generally consist of ophiolitic melange and peridotite bodies. The ophiolites from SE to NW reach the Sütçüler district, eventually ending to the S in the Serik (Antalya) district. These are parts of ophiolitic imbricates related to Antalya Nappes (Fig. 3.24).

Peridotites exposed within the Isparta province, contain chromitites in the western part of Aksu district and of Şarkikaraağaç. The peridotites are accepted as a part of Beyşehir-Hoyran nappes that outcrop around Beyşehir (Konya) towards the SE of the Province. These ophiolite piles are part of the nappe beneath the Beyşehir nappes (Mackintosh and Robertson 2009). This structural imbrication is consistent with the nappe tectonics of the Taurides (Fig. 3.24).

To the southeast of Beyşehir Lake, metamorphic sole and ophiolitic rocks were observed. The mélange unit is mostly seen in the eastern part of the Middle Taurus Mountains (Özgül 1997). Also in this region, Mesozoic Taurus platform carbonates are tectonically overlain by the Late Cretaceous mélange unit. The melange unit comprises serpentinite blocks, basalt, chert and pelagic sediments. Regionally, the Beyşehir-Hoyran ophiolite nappe was obducted towards the south over the Taurus carbonate platform in Late Cretaceous. Later on, in the Late Eocene period, the ophiolitic rocks and the Mesozoic carbonate platform thrust southward due to closing of the suture (Andres and Robertson 2002; Mackintosh and Robertson 2009).

In Antalya nappes, a number of ophiolitic melange slices of different size are present. The melange unit within the Antalya nappes generally consists of serpentinites. Within the mélange unit, large blocks derived from harzburgite, dunite,

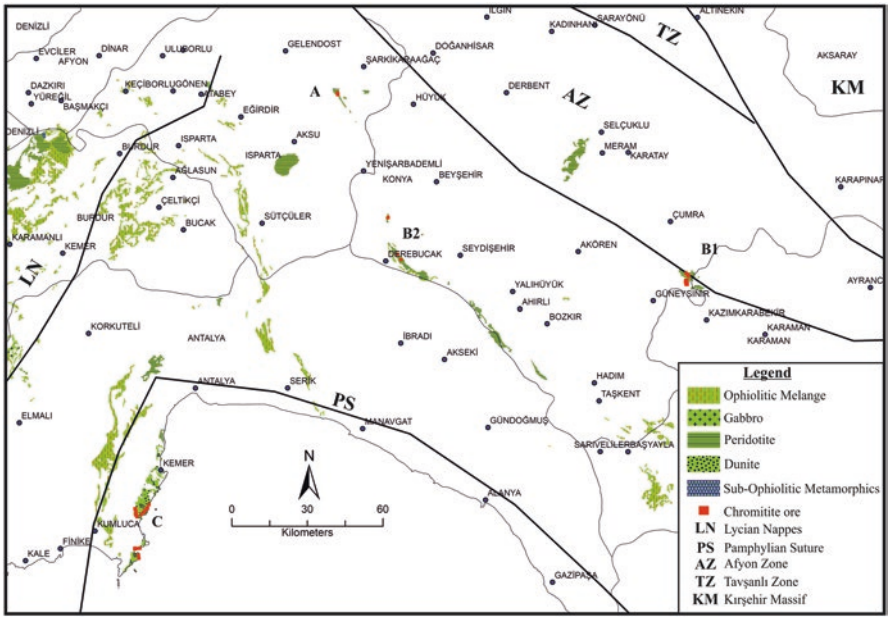

Fig. 3.24 Isparta-Konya-Antalya ophiolites and locations of chromitite occurrences. (Simplified and modified after MTA 2002)

wherlite, gabbro, amphibolite are also present (Şenel 1997b). Late Cretaceous Tekirova (Antalya) ophiolite is one of the largest nappes in Antalya of the Western Taurus and is represented by, from bottom to top, harzburgitic tectonites, ultramafic-mafic cumulates, isotropic gabbros and sheeted dyke complex (Bağcı 2004). In Tekirova (Antalya) ophiolite, volcanic complex was not preserved and rocks which belong to the metamorphic sole are seen as tectonic slices within the tectonites (harzburgite). A number of isolated dykes, and rarely pegmatitic gabbro dykes, cut the whole ophiolitic section (Fig. 3.25, Bağcı 2004).

3.4.4.2.2 Isparta Region Chromitites

Chromite deposits and occurrences in the Isparta province are shown in Fig. 3.24A. Peridotite bodies are located around Sipahiler-Yuvalı-Bağıllı-Kocular in the south; around Belceğiz-Yenicekale-Salur-Çeltek and Yaniköy areas in the east; and around Atabey-Kapıcak-Barla areas in the west. General characteristics of chromite occurrences are summarized in Table 3.12. These chromitites have no economic importance in the Turkish chromite mining sector.

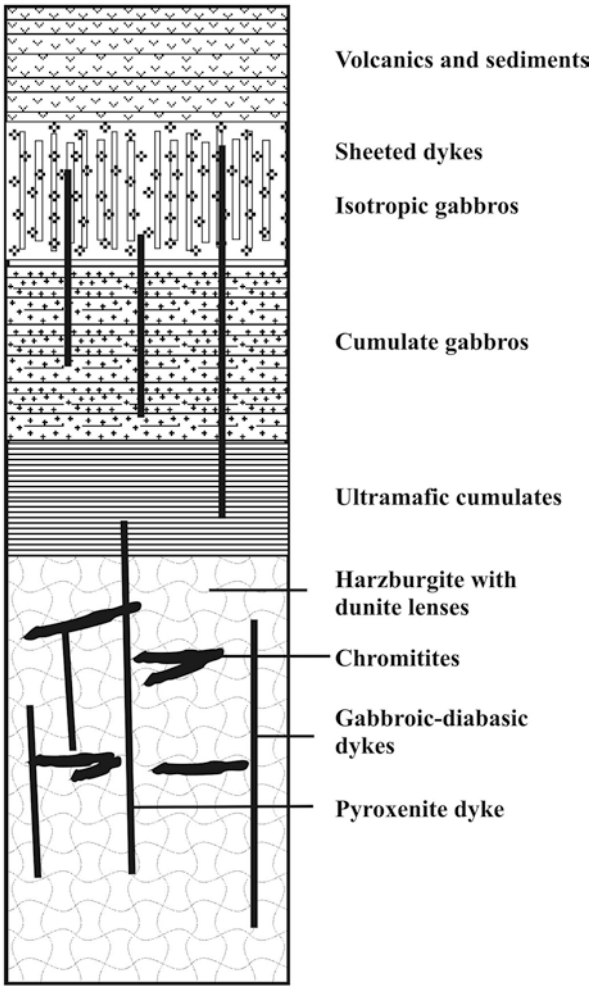

Fig. 3.25 Tectono-stratigraphic column of Antalya (Tekirova) ophiolites. (Revised after Bağcı et al. 2006)

3.4.4.2.3 Konya Region Chromitites

In the Konya region, chromite occurrences are found in two districts. The first is situated to the south of Çumra district (Fig. 3.24B1) and the second is located to the west of Seydişehir district (Fig. 3.24B2). Details of these deposits are summarized in Table 3.12. These chromitites also have no economic importance in the Turkish chromite mining sector.

Table 3.12 General features of chromitite occurrences in Isparta, Konya and Antalya regions

Region	County/ophiolite name	Sub-region/deposit name	Type[a]	Thickness/length (meters)	Wall-rock	Grade (%Cr_2O_3)	Map Nr. and sign
Region Four (SW Anatolian region)	Isparta/Antalya Nappes (Tekirova ophiolite)	Şarkikaraağaç Belceğiz-1	Spotted, massive, banded	0.4–0.6/1–5	Dn	40–50	Fig. 3.24A
		Şarkikaraağaç Belceğiz-2	Disseminated, nodular, massive banded	0.2–0.3/1–4	Dn	20–30	Fig. 3.24A
	Konya/Antalya Nappes (Tekirova ophiolite)	B1 (Eren Tepe, Tekke Tepe)	Disseminated, massive	0.05–0.5/1–10	Dn	20–48	Fig. 3.24B1
		B2 -Dedecik Tepe)	Disseminated, nodular, massive	0.1–0.7/10–70	Hbj-Dn	25–42	Fig. 3.24B2
		B2-Bayıroluk Tepe	Massive	0.1–0.7	Dn	42–48	Fig. 3.24B2
		B2-Tekke Tepe	Disseminated, massive	0.1–1.0/1–7	Dn	20–40	Fig. 3.24B2
	Antalya/Antalya Nappes (Tekirova ophiolite)	Atbükü-Tatlısu Bay	Disseminated, spotted, massive	0.2–1.0/10–30	Hbj-Dn	15–35	Fig. 3.24C
		Atbükü-Yanartaş	Massive banded	0.1–0.7	Hbj-Dn	40–48	Fig. 3.24C
		Atbükü-Atbükü Bay	Disseminated, massive banded	0.5–0.7	Hbj-Dn	30–35	Fig. 3.24C
		Kumluca-Adrasan Bay	Massive, disseminated, banded	0.2–0.5/1–5	Dn	25–44	Fig. 3.24C
		Kumluca-Kızıldağ	Disseminated, massive, spotted, banded	0.2–0.3/1–25	Dn	40–50	Fig. 3.24C

[a]Starts from the most abundant type; Hbj: Harzburgite; Dn: Dunite

3.4.4.2.4 Antalya Region Chromitites

Chromitite deposits and occurrences in Antalya are generally exposed to the SW of Antalya province center (Fig. 3.24C). One group of chromite occurrences belonging to dunite sections occur around Atbükü-Kemer and to the SE of Çavuş Village, and another group of chromite occurrences related to different sizes of dunites within harzburgites occur around Kumluca. A total of 19 chromitite occurrences occur in the Kemer and Kumluca districts. These chromitites also have no economic importance in the Turkish chromite mining sector.

All these chromitite ores and occurrences of the three Regions are summarized in Table 3.12.

3.4.5 Region Five: Central Anatolian (Mersin, Adana, Kayseri) Ophiolites and Related Chromitite Deposits

Thin slices of ophiolites from Mersin merge with the ophiolites of the IAEZ (Izmir-Ankara-Erzincan Zone) around Refahiye (Erzincan). These ophiolite slices in the eastern part of the Inner Tauride suture are discussed in the first section. Ophiolites related to this zone begin from the Mersin Ophiolite and continue to the NE as the Kızıltepe Ophiolite, Alihoca Ophiolite, Pozantı-Karsantı Ophiolite, Pınarbaşı Ophiolite and Divriği/Güneş Ophiolite (Fig. 3.26).

Although the Sivas Region ophiolites are associated with this suture zone, they are interpreted as part of the NE Anatolian Division. In this chapter, mainly chromitite deposits and related ophiolite sequences in Mersin, Adana and Kayseri provinces will be introduced.

3.4.5.1 Mersin Region

According to the map in Fig. 3.26, the ophiolites that cover the most SW part of the region are defined as the Mersin Opholite (Fig. 3.27).

3.4.5.1.1 Mersin Ophiolites

Mersin Ophiolite, exposed beneath a thick Miocene cover at the westernmost end of the Eastern Taurus Mountain, forms a large massif at the southern flank of the Bolkar Mountains. This ophiolite body rests tectonically on top of an ophiolitic mélange, named Aslanköy formation (Demirtaşlı 1984), and is covered by Eocene sediments in the north section (Ternek 1957; Demirtaşlı et al. 1975; Demirtaşlı 1984; Özgül 1976; Gedik et al. 1979) and partly by Oligocene conglomerates. Pillow lavas, volcanic breccias, hyaloclastics, radiolarites, pelagic limestones with lava intercalations (possible Triassic in age: Juteau 1979, 1980; Çapan 1980),

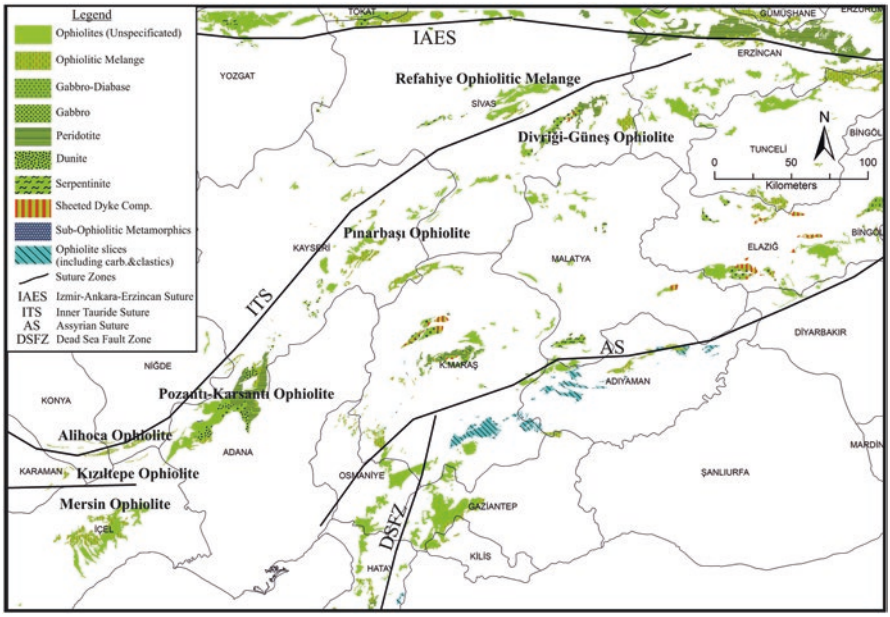

Fig. 3.26 Ophiolites and chromitite occurrences of Mersin-Adana-Kayseri and Sivas Regions (*IAESZ* Izmir-Ankara-Erzincan Suture Zone, *IPSZ* Inner Pontide Suture Zone, *BZSZ* Bitlis-Zağros Suture Zone, *DSFZ* Dead Sea Fault Zone). (Simplified and modified from MTA 2002; Suture Zones are adapted from Okay and Tüysüz 1999)

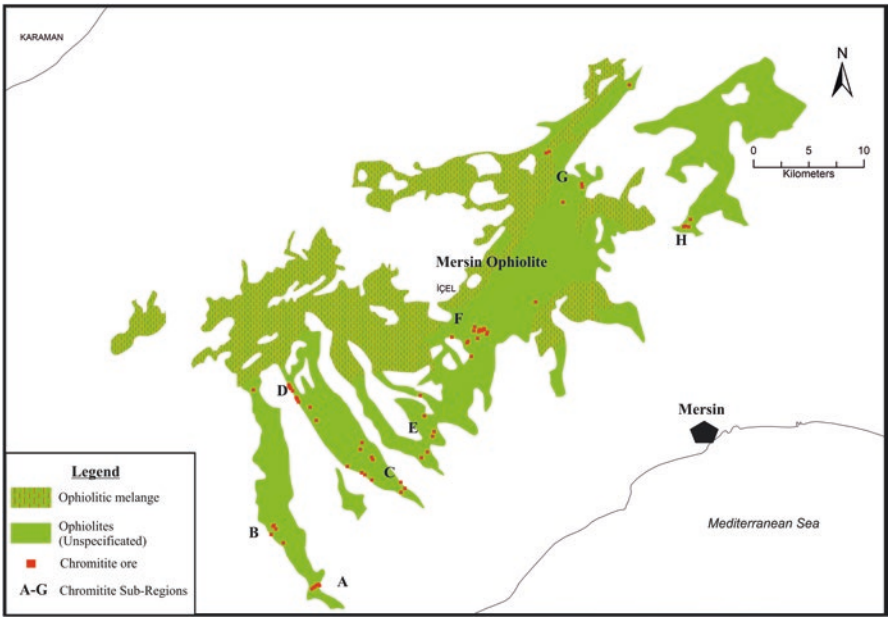

Fig. 3.27 Chromitite occurrences and sub-regions of Mersin ophiolite (A: Kösbucağı; B: Köserelli; C: Sıraç – Yassıtaş – Mühlü; D: Poyrazlı – Hacıalanı; E: Avrangedik; F: Takanlı – Akarca – Demirışık – Yeniköy; G: Horozlu – Kızılbağ; H: Musalı). (Simplified and modified after MTA 2002)

limestones (Maastrichtian; Gedik et al. 1979) and serpentinite-gabbro blocks are the typical rock association within the ophiolitic mélange that was emplaced onto the Jurassic-Cretaceous carbonate platform (Erendil 2002).

The Mersin ophiolite represents an oceanic lithospheric section, about 6 km thick, which from bottom to top consists of; a metamorphic sole, harzburgitic mantle tectonites, ultramafic to mafic cumulates, basaltic pillow lavas (Parlak et al. 1996). Metamorphic sole rocks form a thin slice, 50–70 m thick, beneath the harzburgitic tectonites. It generally consists of amphibolite, mica-schist, amphibolite-schist and marble (Parlak et al. 1995, 1996). The mantle tectonites are represented by harzburgite and dunite. The cumulate rocks start with ultramafic units, namely wherlite, pyroxenite, dunite at the bottom, passing upwards into mafic units such as olivine gabbro, gabbro norite, troctolite and anorthosite at the top (Parlak et al. 1996). The volcanics are characterized by pillow basalts and basaltic lava flows. The metamorphic sole, mantle tectonites and cumulate rocks were intruded by numerous diabase dykes (Parlak and Delaloye 1996).

3.4.5.1.2 Mersin Chromitite Occurrences

The general distribution of chromitite occurrences in ultramafic rocks of the Mersin Ophiolite was given in Fig. 3.27. These occurrences are within eight sub-regions: Kösbucağı, Köserelli, Sıraç – Yassıtaş – Mühlü, Poyrazlı – Hacıalanı, Avrangedik, Takanlı – Akarca – Demirışık – Yeniköy, Horozlu – Kızılbağ and Musalı sub-regions and summarized in Table 3.13. Although several chromitite deposits are present in the Mersin Region, they are mostly small and almost totally mined-out.

3.4.5.2 Adana Region

3.4.5.2.1 Adana Ophiolites

In Adana province, ophiolitic rocks form an important part of Aladağ Tectonic Unit that forms a belt through to the SE from Pozantı. These rocks extend to the northern borders of the province, and for about 30 km in the same strike on Kayseri province (Fig. 3.26). The most comprehensive studies about ophiolites in the region were conducted by Tekeli et al. (1984).

Pozantı-Karsantı Ophiolite or "Aladağ Ophiolite" has a nappe character sequence that includes metamorphic rocks at its base and ultramafic-mafic rocks. It is divided into two groups, based on the rock association. The first was defined as "tectonite" and is an ultramafic rock association with metamorphic texture, derived from the upper mantle. The other group is a cumulate type rock association, represented by ultramafic to mafic rocks (Fig. 3.28).

The Aladağ Ophiolite Complex consists of three units defined by rock types, structural features and location. These are, from bottom to top, ophiolite melange, metamorphic sole and oceanic lithospheric section (Tekeli et al. 1981; Çakır 1978;

Table 3.13 General features of the chromitite occurrences in Mersin, Adana and Kayseri regions

Region	County/ophiolite name	Sub-region/deposit name	Type[a]	Thickness/length (meters)	Wall-rock	Grade (%Cr_2O_3)	Map Nr. and sign
Region Five (Middle Anatolian region)	Mersin/Mersin ophiolite	Kösbucağı	Disseminated, massive, banded-lensoidal	6 (zone)/10–80	Dn	15–20	Fig. 3.27A
		Köserelli	Disseminated, massive, banded-lensoidal	1–3 (zone)/10–30	Dn	15–35	Fig. 3.27B
		Sıraç-Yassıtaş-Mühlü	Disseminated, nodular, banded	0.1–0.2/1–10	Hbj-Dn	15–20	Fig. 3.27C
		Poyrazlı-Hacıalanı	Disseminated, massive, banded-lensoidal	1–3 (zone)/10–300	Dn	10–20/30	Fig. 3.27D
		Avrangedik	Massive, disseminated	0.3–1.0/20–30	Dn	35–50	Fig. 3.27E
		Takanlı – Akarca – Demirışık – Yeniköy	Disseminated, massive, nodular, banded	0.5–4.0/10–100	Dn	10–20	Fig. 3.27F
		Horozlu – Kızılbağ	Disseminated, massive, thin banded	0.2–1.0/1–4	Dn	25–40	Fig. 3.27G
		Musalı	Disseminated, banded	0.05–0.1/10–40	Dn	25–40	Fig. 3.27H
	Adana/Aladağ ophiolite	Dereyurt Dere – Gerdağı-Beyçamı Tepe	Disseminated, nodular, massive, banded	0.6–2.5/2–20	Hbj-Dn	20–45	Fig. 3.29A
		Cehennemdere – Kırcakatran	Massive, disseminated, banded	1–2 (zone)/10–60	Hbj-Dn	30–50	Fig. 3.29B
		Gerdibi – Deveboynu-Kaklık Dere	Massive, disseminated, banded	0.5–2.0 (zone)/2–30	Dn	30–48	Fig. 3.29C
		Sivişli – Mencek Tepe – Çötlük Tepe – Badırıklı Tepe	Disseminated, banded	30–80 (zone)/100–450	Dn	2–5	Fig. 3.29D
		Kütüklü Tepe – Tozlu Tepe-Kartalkale Tepe-Gavurgeri Tepe	Disseminated, massive, banded	2–3 (zone)/80–200	Hbj-Dn	20–40	Fig. 3.29E

		Ziyaret Dağı-Kaltar Dağı-Duvarlı Tepe-Keşgöz Tepe	Disseminated, banded	0.5–8 (zone)/40–80	Dn	10–25	Fig. 3.29F
		Çanakpınarı Tepe – Kızılyüksek-Yataardıç[b]	Disseminated, nodular, massive banded	1–10 (zone)/10–220	Hbj-Dn	5–(40)[c]	Fig. 3.29G
		Darılık Köyü-Akinek Dağı-Yapraklı Tepe	Disseminated, banded	10–22 (zone)/25–250	Hbj-Dn	15–30 (40–50[c])	Fig. 3.29H
		Hova Tepe-Sulukerer Tepe-Üçsivri Tepe	Massive, banded, lensoidal	1–5/20–80	Hbj-Dn	40–50	Fig. 3.29I
	Kayseri/Pınarbaşı ophiolite	Sarıtaş Tepe	Disseminated, nodular, banded	0.2–1/2–36	Hbj-Dn	40–48	Fig. 3.30A
		Tatlar-Kanlıpınar-Zorkunlu Dere	Disseminated, massive, banded	0.7–3.5 (zone)/10–85	Hbj-Dn	10–30 (52[c])	Fig. 3.30B
		Divrikçakırı	Disseminated, massive, banded	0.1–1.0 (zone)/5–35	Hbj-Dn	25–40	Fig. 3.30C
		Ademi Mah.-Asar Tepe-Melengeçli Tepe-Delialiuşağı-Aşağı Delialiuşağı	Disseminated, massive, nodular, banded	0.4–2 (zone)/8–60	Hbj-Dn	15–20 (44[c])	Fig. 3.30D
		Kadılı-Kızılören-Artmak, Avşarsöğütlü, Toklar	Massive, disseminated;	5–20 (zone)/15–180	Hbj-Dn	10–25	Fig. 3.30E
			Lensoidal	0.7 × 17		55	
		Kaman and Dilciler	Disseminated, banded	1–3 (zone)/9–45	Hbj-Dn	5–15	Fig. 3.30F
		Kırımuşağı, Pulpınar, Demirci County, Kireçlikyayla	Disseminated, banded	1–3 (zone)/10–60	Hbj-Dn	10–20	Fig. 3.30G
		Yusuflar, Bahçecik, Emeğil, Solaklar, Büyükpotuklu	Disseminated, banded	0.1–0.3/2–200	Dn	20–30	Fig. 3.30H
		Üçsivri Tepe	Massive; banded	0.2–1.0/1–5	Hbj-Dn	40–45	Fig. 3.30I

[a]Starts from the most abundant type; Hbj: Harzburgite; Dn: Dunite
[b]One of the important deposits of Turkey
[c]Massive and banded grades

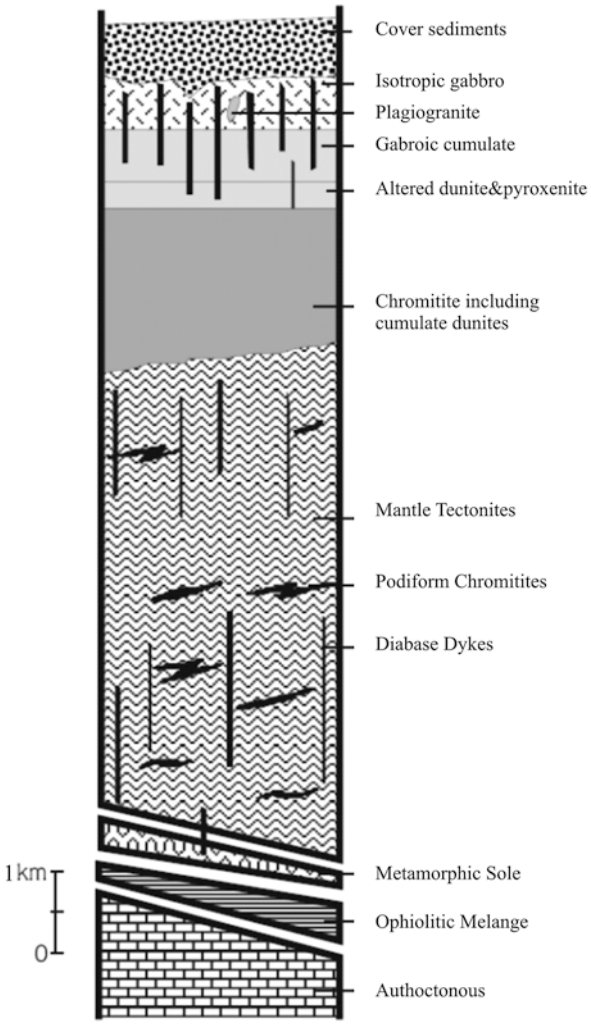

Fig. 3.28 Generalized lithostratigraphy of Aladağ ophiolite. (Re-constructed after Tekeli 1981; Çakır 1978; Bingöl 1978; Çapan 1980; Çataklı 1983)

Bingöl 1978; Çapan 1980; Çataklı 1983) (Fig. 3.28). The mantle tectonites are rich in chromitite mineralization. Even though the chromite occurrences in this area, firstly reported by MTA, are of low grade, they form one of the important chromite mineralisation regions in the world, at least in terms of mineral resources.

3.4.5.2.2 Adana Chromitites

Adana province is a region where low grade, large scale chromitite deposits occur. The Kızılyüksek-Yataardıç chromitite deposits (Table 3.13) are 200 m long with an average grade of 5.35% Cr_2O_3, according to MTA estimation. In addition, there are

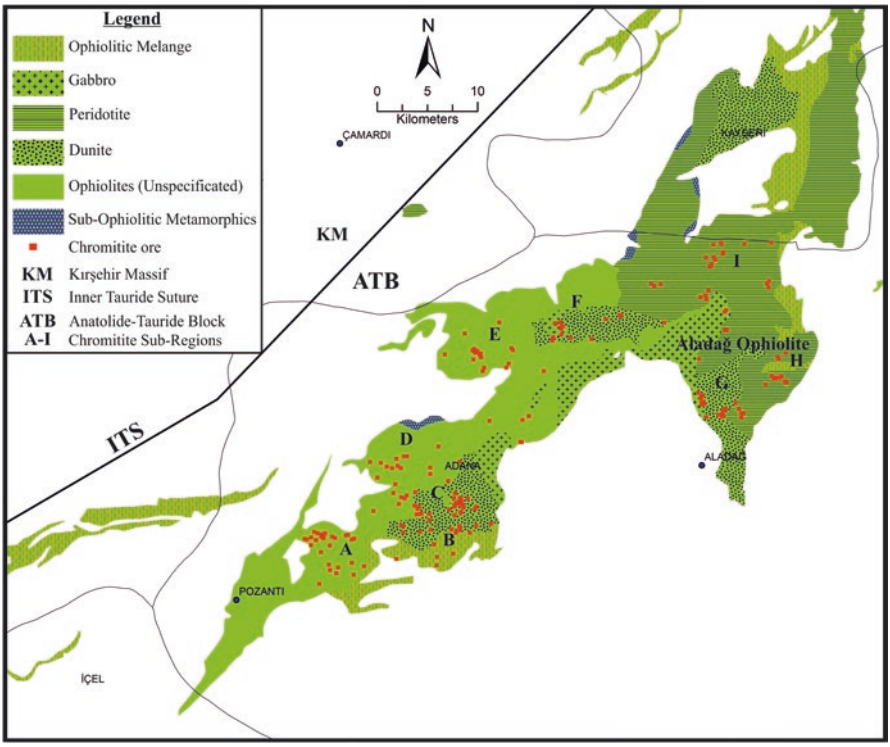

Fig. 3.29 Chromitite occurrences and sub-regions of Aladağ (Adana) region (A: Dereyurt -Gerdağı-Beyçamı; B: Cehennemdere-Kırcakatran; C: Gerdibi-Deveboynu-Kaklık Dere; D: Sivişli-Mencektepe-Çötlüktepe-Badırıklıtepe; E: Kütüklütepe-Tozlutepe-Kartalkale Tepe-Gavurgeri Tepe; F: Ziyaret Dağı-Kaltar Dağı-Duvarlı Tepe-Keşgöz Tepe; G: Çanakpınarı Tepe-Kızılyüksek-Yataardıç; H: Darılık Köyü-Akinek Dağı-Yapraklıtepe; I: Hova Tepe-Sulukerer Tepe-Üçsivri Tepe). (Simplified and modified after MTA 2002)

low grade chromitite deposits with reserves that vary between a few millions of tonnes and a few tens of millions of tonnes, embedded within cumulate dunites in this region. Rising demand for chromitite ore in the last decade has improved the economics of large, low grade deposits. Thus, Adana province is an important region in Turkey for low grade chromitite deposits, especially in terms of production capacity and potential.

The Adana chromitite deposits are shown on Fig. 3.29. The sub-regions are; Dereyurt-Gerdağı-Beyçamı, Cehennemdere-Kırcakatran, Gerdibi-Deveboynu-Kaklık Dere, Sivişli-Mencektepe-Çötlüktepe-Badırıklıtepe, Kütüklütepe-Tozlutepe-Kartalkale Tepe-Gavurgeri Tepe, Ziyaret Dağı-Kaltar Dağı-Duvarlı Tepe-Keşgöz Tepe, Çanakpınarı Tepe -Kızılyüksek-Yataardıç, Darılık Köyü-Akinek Dağı-Yapraklıtepe and Hova Tepe-Sulukerer Tepe-Üçsivri Tepe; and their characteristics are also summarized in Table 3.13.

3.4.5.3 Kayseri Region

3.4.5.3.1 Kayseri Ophiolites

Kayseri province ophiolitic sequences outcrop in two regions as shown in Fig. 3.30. One of them is located in the SW border of the province and this a NE extension of Aladağ Ophiolite.

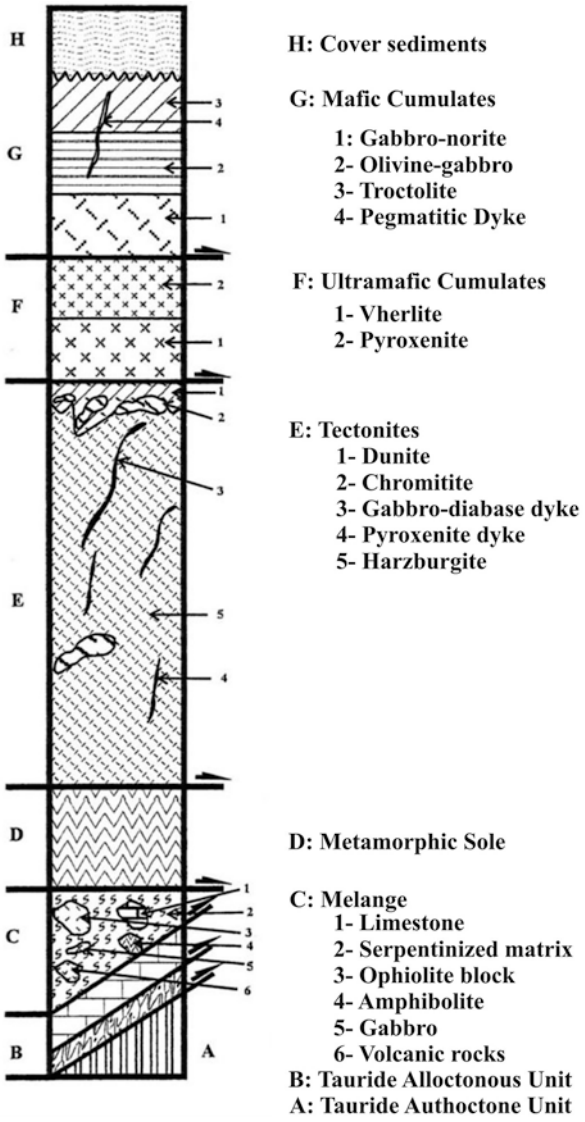

Fig. 3.30 Tectono-stratigraphic section of Pınarbaşı ophiolite. (Modifies after Vergili and Parlak 2005)

The second ophiolitic sequence in Kayseri province is the **Pınarbaşı Ophiolite** that forms a belt with a NE-SW extension around Pınarbaşı (Fig. 3.30). According to Vergili and Parlak (2005), these ophiolites are allochthonous slices emplaced onto the Eastern Taurus Autochthonous. The ophiolitic rocks mainly consist of three different rock associations, such as ophiolitic melange, metamorphic sole and a regular opholite sequence (Fig. 3.30).

3.4.5.3.2 Kayseri Chromitite Occurrences

Some of the chromitite occurrences in Kayseri province are observed in the SW, in Aladağ Ophiolite (A, B, C, D). The other important part is seen in Pınarbaşı Ophiolite (E, F, G, H and I in Fig. 3.31). Table 3.13 presents the main characteristics of the chromitite deposits in Mersin, Adana and Kayseri regions.

3.4.6 Region Six: SE Anatolian (Hatay, Osmaniye, Gaziantep, Kahramanmaraş, Adıyaman, Elazığ, Siirt, Van, Hakkari) Ophiolites and Related Chromitite Deposits

Ophiolite sections of the SE Anatolian Region extend along the Bitlis-Zağros Suture Zone (BZSZ) and are named "SE Anatolian Ophiolite Belt" (Fig. 3.32). Some of the ophiolite sections, namely the Göksun Ophiolite, Berit Metaophiolite, İspendere Ophiolite, Kömürhan Ophiolite, Guleman Ophiolite, Baykan Ophiolite, and Gevaş Ophiolite, were accreted to the metamorphic Tauride platform (Malatya-Keban platform) in the north. Other ophiolites are situated on the top of the Arabian platform in the south. These are Kızıldağ Ophiolite, Kılan/Meydan Ophiolite, Koçali-Karadut Complex and Yüksekova Complex (Sarıfakıoğlu et al. 2014) (Fig. 3.32).

Although some of these ophiolitic sequences are very fertile in terms of chromite mineralisation, like the Guleman ophiolite, they generally lackchromitite deposits.

3.4.6.1 Hatay-Osmaniye-Gaziantep-Kahramanmaraş Regions

3.4.6.1.1 Hatay Region

Kızıldağ Ophiolite

The Kızıldağ Ophiolite is exposed at the south-western end of the Amanos Mountains and consists of ultramafic and mafic rocks in a NE-SW tectonic lineament (Fig. 3.32). It displays a well-preserved oceanic lithospheric section in southern Turkey, from bottom to top: mantle tectonites, ultramafic-mafic cumulates, isotropic gabbros, sheeted dykes, volcanic rocks and cover sediments. The Kızıldağ Ophiolite is located in the Mediterranean coastline and covers a wide area.

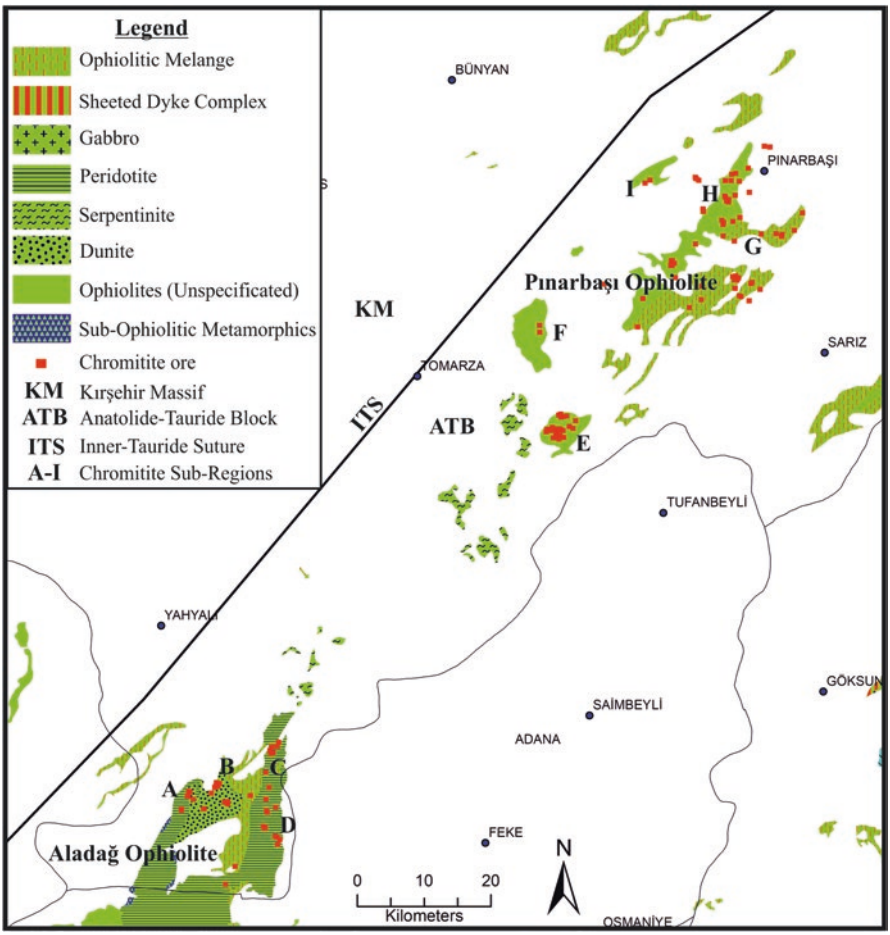

Fig. 3.31 Chromitite occurrences and sub-regions of Pınarbaşı ophiolite (Kayseri) (A: Sarıtaş Tepe; B: Tatlar-Kanlıpınar-Zorkunlu Dere; C: Divrikçakırı; D: Ademi Mah.-Asar Tepe-Melengeçli Tepe-Delialiuşağı-Aşağı Delialiuşağı; E: Kadılı-Kızılören-Artmak, Avşarsöğütlü, Toklar; F: Kaman ve Diliciler; G: Kırımuşağı, Pulpınar, Demircili-Kireçlikyayla; H: Yusuflar, Bahçecik, Emeğil, Solaklar, Büyükpotuklu; I: Üçsivri Tepe). (Simplified and modified after MTA 2002)

The mantle tectonites mainly consist of harzburgites, dunite with lesser amounts of lherzolite and wherlite. They are cut by number of dykes such as pyroxenite, pegmatite gabbro and rodingitized diabase dykes with chilled margins (Bağcı 2004). The harzburgites form 70% of the tectonites and, together with the dunites, weather to a brown colour. Both of these rocks are dark green-black in unweathered outcrops. The less common Lherzolites are mainly seen along the transition zone into the cumulate rocks.

The ultramafic and mafic cumulates form the lowest level of oceanic crust within Kızıldağ Ophiolite and are exposed along the southern flank of the Kızıldağ massif.

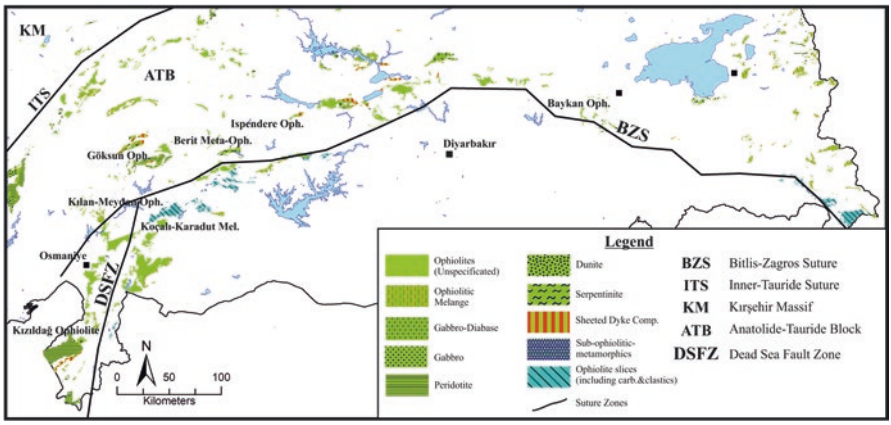

Fig. 3.32 Ophiolites in SE Anatolia along Bitlis-Zagros-Suture (BZS) Belt. (Simplified and modified after MTA 2002)

The cumulates taper from southeast to northeast, are emplaced tectonically on tectonites at the base, and exhibit a transitional contact with isotropic gabbros in their upper levels (Bağcı 2004). The cumulate rocks are cut by diabase and pegmatitic gabbro dykes, ranging in thickness from 2 to 60 cm (Bağcı et al. 2005).

Hatay Chromitites

Chromite deposits in Hatay Region are located mainly in the central part of the Kızıldağ Ophiolite, in the area at the west of Belen and in the NE section of Dörtyol district. Most of these deposits and occurrences are hosted within ultramafic tectonites. Chromitite occurrences in Kızıldağ centre are mainly located in Çerçikaya, Aşağı Zorkum, Yukarı Zorkum, Sarıgöl, Gümüşoluk and Arapgediği quarries (Fig. 3.33A1). Chromite occurrences close to the NE of Dörtyol district (Fig. 3.33A2) mainly occur in Emirali Damları and Şehmahmut Pleateu/Yanık Hill areas (see Table 3.14).

3.4.6.1.2 Osmaniye Ophiolites

Ophiolitic sequences in this region were emplaced during Late Cretaceous onto the Mesozoic Carbonate platform (Yılmaz 1984) (Fig. 3.32). They have characteristics similar to the Kızıldağ Ophiolite in the NE. Yılmaz (1984) considered these ophiolite sequences under different names based on their composition and tectonic position, with the Zorkun Ophiolitic Melange, Yarpuz Ophiolitic Melange, Tozaklı Ophiolite, Ispirler Meta-Ophiolitic Melange and Berke Ophiolite being the main sequences. The internal structures of these ophiolites are not considered in this section of Chap. 3.

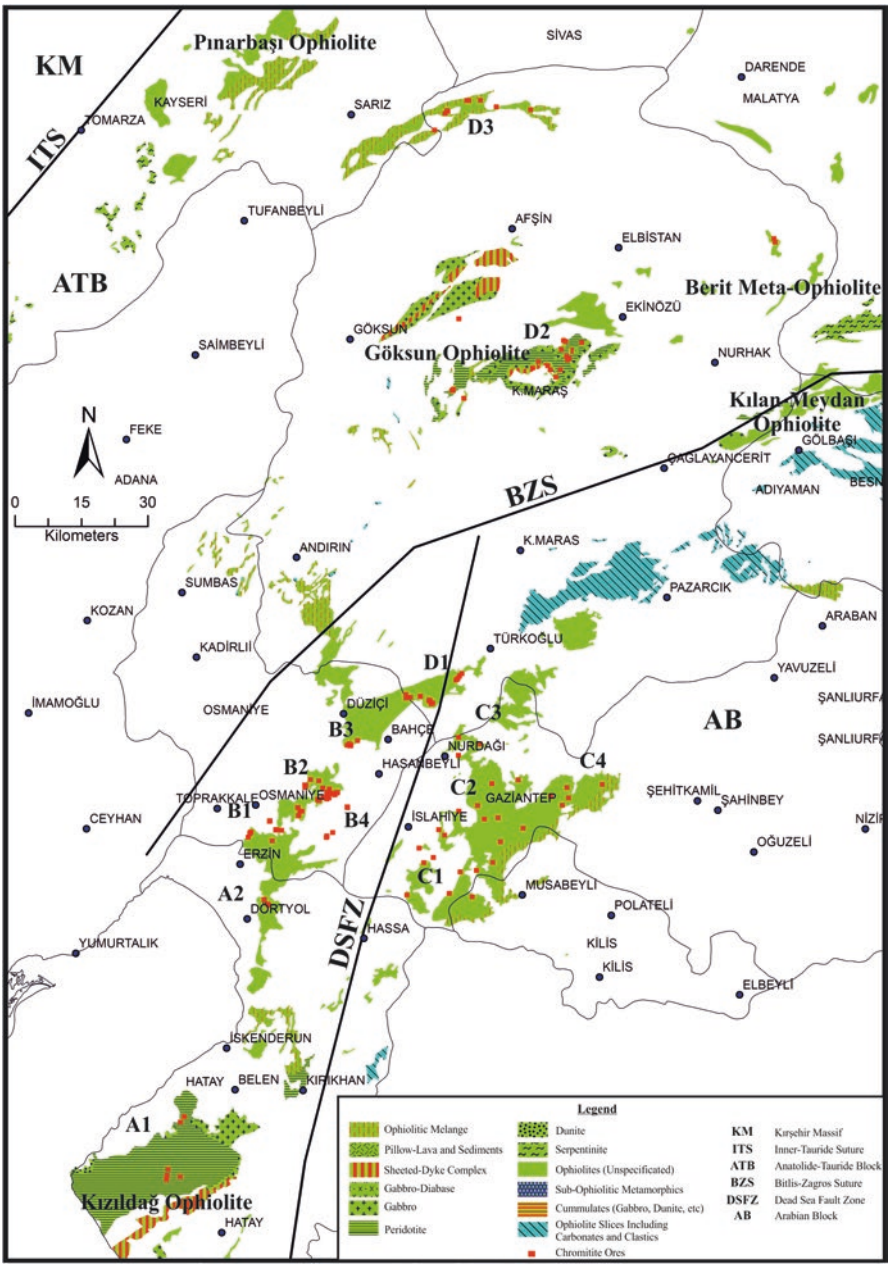

Fig. 3.33 Chromitite occurrences of Hatay, Osmaniye, Gaziantep and Kahramanmaraş (A: Hatay Region; B: Osmaniye Region; C: Gaziantep Region; D: Kahramanmaraş Region). (Simplified and modified after MTA 2002)

Table 3.14 General features of chromitite occurrences in Hatay and Osmaniye regions

Region	County/ ophiolite name	Sub-region/deposit name		Type[a]	Thickness/length (meters)	Wall-rock	Grade (%Cr_2O_3)	Map Nr. and sign
Region Six (SE Anatolian region)	Hatay/Kızıldağ ophiolite	A1	Çerçikaya	Massive, brecciated	–	Hbj-Dn	35–40	Fig. 3.33A1
			Aşağı Zorkum	Disseminated, massive, banded	1–2 (zone)/20–30	Hbj-Dn	25–40	
			Yukarı Zorkum	Disseminated, massive, banded	0.1–0.5/50	Dn	25–47	
			Sarıgöl	Massive, disseminated, banded	0.1–0.7/10–50	Hbj-Dn	37–42	
			Gümüşoluk	Disseminated, banded	0.2–0.5/1–5	Dn	15–20	
			Arapgediği	Massive, brecciated	0.5–0.6/1–5	Dn	30–40	
		A2	Emirali Damları	Massive, lens/boulder shaped	0.2 × 0.5	Hbj-Dn	40–50	Fig. 3.33A2
			Şehmahmut Yayla					
	Osmaniye/ Kızıldağ ophiolite	B1	Kanlıkoz yayla, Harak yayla, Ürün Mahallesi-Armuttarla	Disseminated, massive, banded	0.3–1.5/few meters	Dn	35–40	Fig. 3.33B1
			Konak Sırtı ve Aşağıbağ	Massive, lensoidal	Variable	Dn	48–52	
			Çamlık Sırtı – Karacaüstü	Massive, nodular, brecciated	0.2–0.4/few meters		35–42	
			Cevizlik Tepe	Massive, nodular; brecciated	0.2–0.5/few meters		35–40	
		B2	Kayalı	Massive, lens, banded	Irregular	Dn-Wh-Px	48	Fig. 3.33B2
			Issızca	Massive, nodular, lensoidal	0.4 × 3.0		30–40	
			Davutlar	Massive, lensoidal	Irregular	Hbj-Dn	45	
		B3	Burgaçlı-Arıklıtaş	Disseminated, massive, nodular, banded	0.1–0.2/few meters	Hbj-Dn	44	Fig. 3.33B3
		B4	Beşağaç Tepe, Mezar Tepe, Gördüktarla, Çamdenizi	Massive, lensoidal	Irregular	Hbj-Dn	30–40	Fig. 3.33B4

[a]Starts from the most abundant type; Hbj: Harzburgite; Dn: Dunite; Wh: Wehrlite; Px: Pyroxenite

Osmaniye Chromitites

The distribution of Osmaniye region chromitite occurrences is shown on Fig. 3.33B. They will be presented under four main groupings: Kanlıkoz Yayla – Kıvrıkoğlu Yayla, Konak Sırtı, Aşağıbağ Mevkii, Çamlık Sırtı – Karacaüstü, Ürün Mahallesi – Armuttarla Mevkii, Cevizlik Tepe (B1); Kayalı, Issızca, Davutlar, Çulhalı, Karayiğit (B2); Burgaçlı – Arıklıtaş (B3); and Beşağaç Tepe, Mezar Tepe, Gördüktarla ve Çamdenizi (B4), which are summarised in Table 3.14.

3.4.6.1.3 Gaziantep Region

Gaziantep Ophiolites

Ophiolites that were defined as "Allochthonous Series" and exposed in the west of the province, are mainly the Upper Jurassic-Early Cretaceous Koçali Complex, the Early-Middle Maastrichthian Karadut Complex, and the Middle-Late Maastrichtian Ophiolite Nappe (Fig. 3.32). These ophiolitic sequences were emplaced along the suture zone at different times and alternate with several magmatic and volcanic rocks of the Tethyan closure. Here we discuss only the chromitite deposits and not these ophiolitic sequences.

Gaziantep Chromitites

Chromite occurrences in Gaziantep province are generally centred in the Islahiye region (Fig. 3.33C1–C4). Ultramafic tectonites and cumulates of the Islahiye Ophiolite Nappe have small chromitite occurrences, reported by MTA in 1999 during chromitite-nickel prospecting surveys.

Little chromite was extracted from exploration quarries and no more than five deposits achieved a few thousand tonnes of production. The grade of chromite ores hosted in cumulate dunites, ranges from 10% to 30% Cr_2O_3 and many of these occurrences and deposits are not suitable for mining. The grade of chromitite occurrences in ultramafic tectonite basal dunite zones varies between 40% and 52% Cr_2O_3 and these higher grades have enabled a limited amount of production during periods of high demands and higher prices. The Gaziantep province chromitites and occurrences are shown as "Serial C" on Fig. 3.33. The general features of these chromitite deposits are given in Table 3.15.

3.4.6.1.4 Kahramanmaraş Region

Ophiolites

There are many lithological associations that consist of ophiolite components in the Kahramanmaraş province and these are exposed in Malatya-Bitlis ophiolites group (Erendil 2002). Ophiolites of this belt occur as tectonic slices sandwiched between

Table 3.15 General features of chromitite occurrences in Gaziantep region

Region	County/ophiolite name	Sub-region/deposit name		Type[a]	Thickness/length (meters)	Wall-rock	Grade ($\%Cr_2O_3$)	Map Nr. and sign
Region Six (SE Anatolian region)	Gaziantep/Koçali and Karadut complex islahiye ophiolite nappe	C1	Tilmenhüyük-Karapolat	Nodular, disseminated, massive banded and lenses	0.05–0.15/1–10	Hbj-Dn	35–40	Fig. 3.33C1
			Kırkpınar – Kuzoluk – Bakırcan		0.05–0.15/10–200		30–35	
			Yukarı ve Aşağı Şerikanlı, Dilan	Massive, disseminated, banded	0.2–0.5/10–40		10–20	
			Alaca – Çıbık	Massive, nodular, disseminated	Few cm/10–150		30–40	
			Yesemek	Massive, banded	0.5–1.0/5–20		20–30	
		C2	Soğucak-Fizge-Çakmak-Terken	Massive ore blocks in quarry excavations		Hbj-Dn	30–40	Fig. 3.33C2
			Toplamalar-Katrancı	Massive, banded	0.01–0.1/irregular		20–30	
			Durmuş-Kırkpınar-Ökkeşbaba Tepe-Çatal Tepe	Massive	0.5–1.0/variable		Up to 48	
			BayrakHill-Hudut Çiftliği	Disseminated, massive, nodular, banded	0.2–0.5/variable		10–20	
			Kürdikanlı – Arabuşağı	Disseminated, massive, banded	0.05–0.35/10–50		30–40	
		C3	Tepkanlı Köyü	Noduled, disseminated, banded	0.02–0.1/variable		20–25	Fig. 3.33C3
			Tandırlı-Keloso-Hamidiye	Massive, nodular, disseminated, banded	0.2–0.4/10–200		20–30	
		C4	Kartal-Terken-Sarıkaya-Şemlik	Massive banded	–		10–20	Fig. 3.33C4
			Hasancalı	Massive, disseminated	0.1–0.3/10–20		30–40	

[a]Starts from the most abundant type; Hbj: Harzburgite; Dn: Dunite

metamorphic massifs or unmetamorphosed younger deposits (Erendil 2002). Ophiolite slices of the Taurus Belt and Arabian Platform are shown in Fig. 3.32.

To the north of Afşin and Kayseri border; the Göksun Ophiolite and the Berit Ophiolite are exposed between Andırın and Türkoğlu and can be described together. They consist of slices that were emplaced in the region at different times by overthrust nappe tectonics.

Chromite mineralisation in the region, occurs mostly in small deposits (Fig. 3.33D1–D3) which have been occasionally exploited with small-scale production.

In the Dağlıca Melange exposed between Afşin and Sarız, marketable chromitites occur in small deposits. To the south of Ekinözü, in the Berit Ophiolite, low Cr_2O_3 grade occurrences were identified with the "high aluminium" content depending on dunite abundance in the ultramafic cumulate units. The general features of these chromitite deposits of the Kahramanmaraş region are given in Table 3.16.

3.4.6.2 Adıyaman and Elazığ Regions

3.4.6.2.1 Adıyaman Region

Ophiolite sequences in the Adıyaman province are defined as the Karadut Complex, the Koçali Complex and the Opholite Nappe (Fig. 3.32).

Chromitites

Chromite deposits and chromitite occurrences in this region are located in the Ophiolite Nappe, within a sequence of peridotites referred as the Koçali Complex in previous studies (Yoldemir 1987).

The early chromite exploration programs in this region were carried out by MTA in 1973. Since 1989, information about chromitite occurrences in Adıyaman region was updated by field studies, and they are located mainly in Gölbaşı, Besni, and Tut central districts (Fig. 3.34). Within the framework of the data obtained during prospecting work, it can be concluded that the chromite deposits and occurrences in the Adıyaman territory are small with a potential of between a few hundred and a few thousand tonnes. The general features of these chromitite deposits in the Adıyaman region are given in Table 3.17.

3.4.6.2.2 Elazığ Region

The Elazığ-Alacakaya (Guleman) territory has the largest chromite resources and production in Turkey and accounts for about 45% of the total chromite resources. Mining in the Elazığ-Alacakaya territory started in 1936 and still operates today. Many scientific studies were conducted in the region aimed at the understanding the mechanism of chromitite genesis in order to improve exploration studies (Kovenko

Table 3.16 General features of chromitite occurrences in Kahramanmaraş region

Region	County/ophiolite name	Sub-region/deposit name		Type[a]	Thickness/length (meters)	Wall-rock	Grade (%Cr_2O_3)	Map Nr. and sign
Region Six (SE Anatolian region)	K.Maraş/ Göksun, Berit, Tozaklı ophiolites	Türkoğlu	Küçük İmalı Köyü	Massive, lenses, nodular	Variable	Hbj-Dn	Up to 48	Fig. 3.33D1
			Kaledibi Köyü	Massive, disseminated, lensoidal	Variable		Up to 44	
		Elbistan	Süleymanlı Köyü	Disseminated, banded	0.1–0.4/1–15	Dn	20	Fig. 3.33D2
			Sarıgüzel Köyü		0.2–2.5/1–15		30	
			Kabak Tepe Köyü	Disseminated, massive, banded	Thin		40[b]	
			Kandilköy-Çıtak	Massive, banded	0.05–0.1/1–2		40	
			Demirlik Köyü	Disseminated, banded	0.5–1.0/10–35		20–25 (40[b])	
		Afşin	Sergen Mahallesi	Massive, disseminated	0.2–0.6/1–23		40	Fig. 3.33D3
			Armutalanı	Massive, lensoidal	Irregular		40	

[a]Starts from the most abundant type; Hbj: Harzburgite; Dn: Dunite
[b]Massif band grades

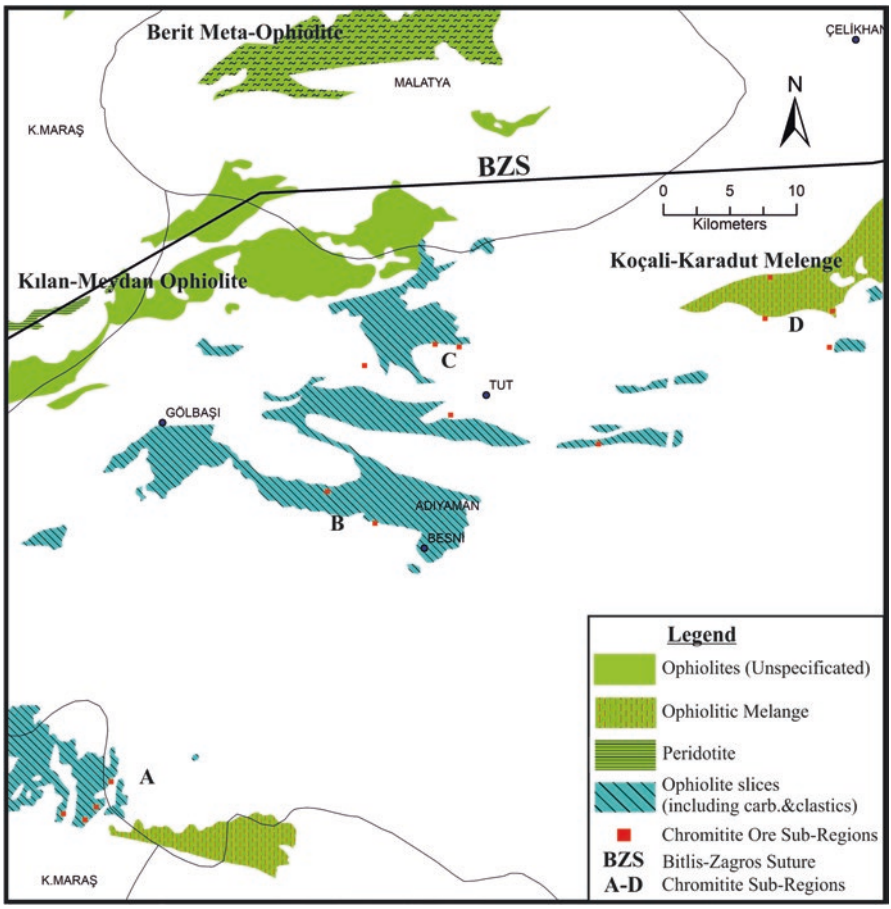

Fig. 3.34 Chromitites of Adıyaman region and sub-regions (A: Harmancık ve Çorak; B: Besni; C: Tut; D: Yazıbaşı-Akçalı-Kotur). (Simplified and modified after MTA 2002)

1940; Borchert 1952; Ercan et al. 1970; İskit 1973; İzmir and Koç 1977; Ortalan and Erdem 1977; Özkan 1977, 1982a, b; Özkan and Sümer 1986, 1987; Engin et al. 1980–1981, 1987; Balcı 1986; Engin 1986; Engin and Sümer 1987).

The Guleman ophiolite unit covers an area of 200 km^2. About 65% of the unit is represented by tectonite and the rest is cumulate rocks (Fig. 3.35). The cumulate rocks are located within the tectonites, or generally surround them. Although there are chromite deposits in both rock groups, those in tectonites are more important.

The dunite unit in Kef territory, is considered as a transition zone between tectonites and cumulates and the major Western Kef Deposit is exposed at the base of this dunite unit. Some other chromite deposits in the region occur in thin dunite envelopes within harzburgites.

Table 3.17 General features of the chromitite occurrences in Adıyaman region

Region	County/ophiolite name	Sub-region/deposit name	Type[a]	Thickness/length (meters)	Wall-rock	Grade (%Cr_2O_3)	Map Nr. and sign
Region Six (SE Anatolian region)	Adıyaman/Koçalı and Karadut complex	Harmancık and Çorak Köyleri	Massive, boulder/ lensoidal	Variable	Hbj-Dn	30–55	Fig. 3.34A
		Besni	Disseminated, banded, brecciated	0.1–0.2/1–1.5	Hbj-Dn	20–48	Fig. 3.34B
		Tut	Disseminated, massive, banded	0.1–0.15/ 1–1.5	Hbj-Dn	25–50[b]	Fig. 3.34C
		Yazıbaşı-Akçalı-Kotur	Massive, disseminated, lens, boulder	0.3 × 0.1/1–2	Dn	15–20 (48)	Fig. 3.34D

[a]From the most abundant type; Hbj: Harzburgite; Dn: Dunite
[b]Massif band grades

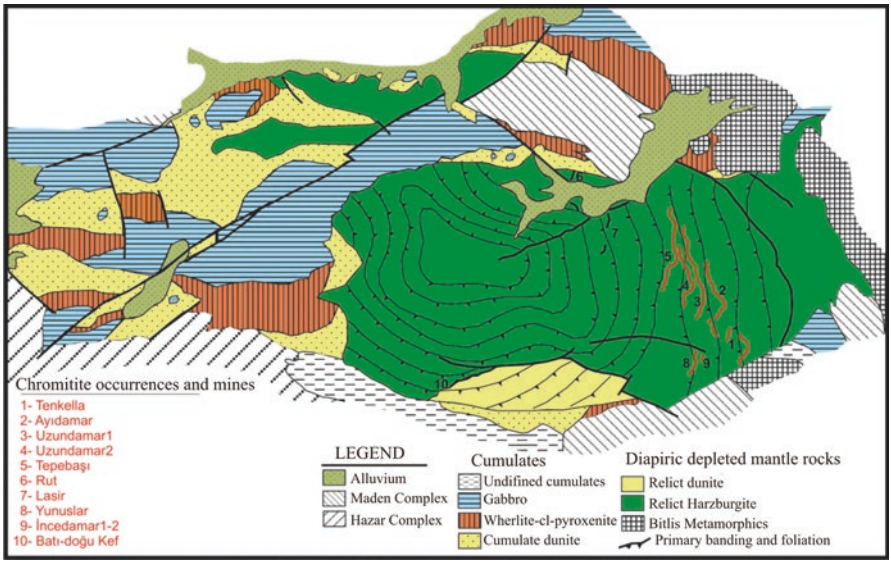

Fig. 3.35 Geology of Guleman ophiolite and major chromitite deposits. (Modified after Özkan 1982b)

Although the Guleman chromite deposits are classified as Alpine type, their continuity in terms of strike and dip directions make these deposits quite special. A large component of chromite mineralization is concordant with the internal structure of the host rocks. Figure 3.35 shows the major deposits in Guleman where mining was carried out by both open pit and underground mining operations. The principal features of these deposits are summarised in Table 3.18.

3.4.6.3 Siirt-Van-Hakkari Regions Chromite Deposits

3.4.6.3.1 Siirt Region

Ophiolites

The Siirt ophiolites are part of the Bitlis Metamorphic Massif and occur as tectonic slices within this Massif. They are generally distributed around Baykan and Şirvan and rarely NE of Pervari (Fig. 3.32). The ultramafic unit was named Guleman ultramafics by Sungurlu (1974), whereas Perinçek (1978) referred to it as the Guleman group. The best outcrop of the unit is north of the Guleman settlement area in the east of Elazığ province, Maden district (Şenel 2007). This ophiolitic sequence was examined under different names, such as Guleman Group, Şimsin Formation (Açıkbaş and Baştuğ 1975); Guleman Metamorphics (Perinçek 1978); Guleman Peridotite Unit (Engin et al. 1980–1981); Guleman Ophiolite (Özkan 1981–1982, 1983) (Fig. 3.36).

Table 3.18 General features of chromitite occurrences in Elazığ (Guleman) Region

Region	County/ophiolite name	Sub-region/deposit name	Type[a]	Thickness/length (meters)	Wall-rock	Grade (%Cr_2O_3)	Map Nr. and sign
Region Six (SE Anatolian region)	Elazığ/Guleman ophiolite	Western Kef[b]	Disseminated, banded	10–50/1000	Dn	20–44	Fig. 3.35
		Eastern Kef[b]	Disseminated, massive, banded, lensoidal, brecciated	5–8/50–100		26–46	
		Altındağ-Spotted Vein-Kapin-Şabate[b]	Disseminated, massive, banded, lensoidal, brecciated	10–25/50–110	Hbj-Dn	30–45	
		Rut-Taşlı Tepe (Sori Part)[b]	Disseminated, massive, banded, lensoidal	0.1–3.5/100–1600	Hbj-Dn	30–50	
		Gölalan, Tosinler, Sitealtı, Aşağı ve Yukarı Kündikan[b]	Disseminated, massive; banded, lensoidal	Many podiform lenses/boulder	Hbj-Dn	40–53	

[a]From the most abundant type; Hbj: Harzburgite; Dn: Dunite
[b]One of the important deposits of Turkey

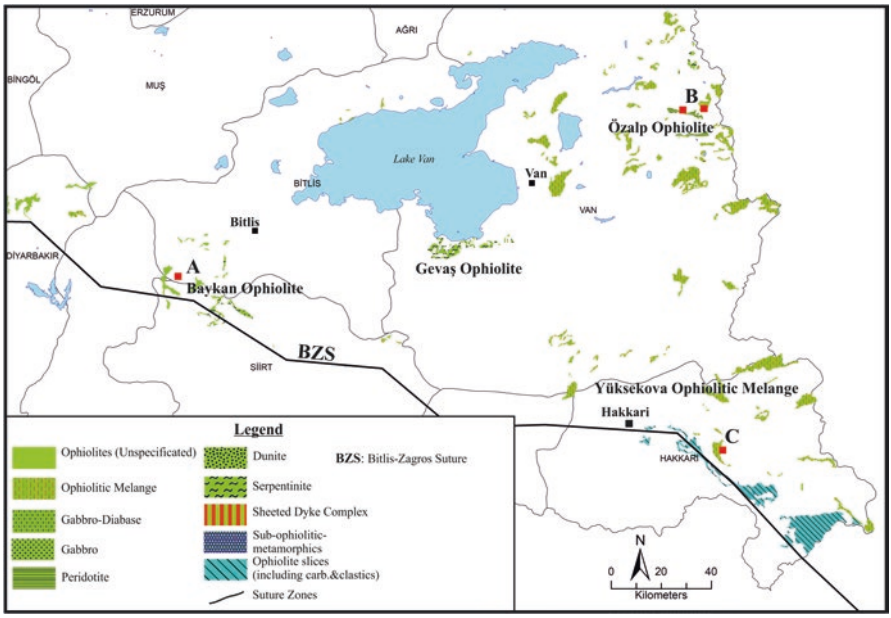

Fig. 3.36 Ophiolites of SE Anatolia and major chromitite deposits (A: Siirt Region; B: Van-Özalp Region; C: Hakkari Region). (Simplified and modified after MTA 2002)

Chromitites

In the Siirt province, at Büzügan section, 41 chromitite outcrops have been identified. They occur mostly in serpentinized harzburgites in a melange environment, And exhibit limited continuity in both strike and dip (Fig. 3.36A).

Information for this region, is largely based on prospecting work conducted by MTA in 1974. Private companies subsequently carried out both exploration and production however, considering the geological structure of the region, the potential for substantial chromite production is considered limited.le.

3.4.6.3.2 Van Region

The Gevaş Ophiolite around Gevaş and the Özalp Ophiolite around Özalp and Saray areas, are the main ophiolitic sequences in the Van region. All chromitite occurrences in the region are located in the Özalp Ophiolite.

Özalp Ophiolite

This ophiolite outcrops in a wide region from Van in the centre to the east, near the Iran border (Fig. 3.36). Ophiolitic complex (melange) forms a layered structure around Özalp and Saray districts, consisting of basic components like deep-sea

lavas (mostly spilitic), serpentinites and diabases, radiolarites-limestones-multicolored shales and marls (Ketin 1977). The Özalp Ophiolite is overlain by Neogene age sediments, suggesting that it was emplaced in Late Cretaceous-Paleocene time. The ophiolitic sequence is represented mostly by upper mantle harzburgites and minor amounts of gabbros. The tectonite peridotites are cut partly, or completely, by rodingitised diabase dykes (Günay et al. 2012).

Van Region Chromitites

Chromitite occurrences in Van Region are located in Özalp and Saray Villages, along the Land Border of Iran and Turkey (Fig. 3.36B). The main features of these chromitite deposits are summarized in Table 3.19. According to this table, chromitites in Özalp region are mainly in massive character, lens shaped, and banded in lesser amount. In contrast, the character of chromitites in eastern and SE part of Özalp Village are disseminated and they are mostly brecciated, partly lens shaped. Dimensions are also quite limited in both section, means that no significant chromite reserve has expected in the region.

3.4.6.3.3 Hakkari Region

The ophiolites that are common in the Hakkari region (Fig. 3.36) are known as Yüksekova Complex and outcrop around Cilo Mountain of Hakkari and Yüksekova along the Bitlis –Zagros Suture Zone (Perinçek 1989). The Yüksekova Complex is mainly represented by spilitic basalt, agglomerate, volcanic sandstone, conglomerate, limestone, chert, granite, granodiorite, quartz diorite, tonalite and flysch facies rocks and in lesser amounts serpentinite, gabbro and diabase units (Sungurlu et al. 1985).

Hakkari Chromitites

Ophiolite occurrences in the Hakkari region are generally of melange character and they exhibit an orderly internal structure, belonging to a cumulate group, they show alternation of serpentinized dunite, wherlite and gabbro. In the ophiolitic melange extending for about 15 km SW of Yüksekova district in an approximate N-S direction, these bodies contain localised with chromitite occurrences. Due to lack of prospecting activity of the ophiolitic melange units to the east and NE sections of Yüksekova district, there is no detailed information about the structure of these sections (Boyalı and Sayın 1974; Sümer and Artan 1983).

Some prospecting and mineral exploration was conducted by MTA in 1983 in the Hakkari-Yüksekova Complex, with the specific aim of assessing the potential of the chromitites. This work showed that the chromitite mineralization is mainly associated with dunites in ultramafic cumulate units. Chromitites in peridotites are highly cataclastic and occur as discontinuous lens-shaped masses. The general features and potential for chromititite occurrences in the territory are presented below.

Table 3.19 General features of chromitite occurrences in Van region

Region	County/ophiolite name	Sub-region/ deposit name	Type[a]	Thickness/length (meters)	Wall-rock	Grade (%Cr_2O_3)	Map Nr. and sign
Region Six (SE Anatolian region)	Van/Gevaş ve Özalp ophiolite; Yüksekova complex	Aşağı Dikme	Massive, lens	0.5 × 3.5	Hbj-Dn	30–45	Fig. 3.36B
		Yukarı Balıkçı	Massive, lens, boulder	0.4–0.6 × 0.8–4.0			
		Çavuşlar	Massive, banded, lens, boulder	0.5–1.5 × 1–7.5			
		Savatlı	Massive, lens, boulder	0.8–1.6 × 0.9–2.8			
		Karaharabe Tepe	Disseminated, brecciated, lens	1.2 × 6.4			
		Bot Tepe	Disseminated, brecciated, lens	0.1–0.5/30 (zone)			
		Söylemez Tepe	Disseminated, brecciated, lens	0.9–1.5 × 3.2–10			
		Öküzyolu Tepe	Disseminated, brecciated, lens	0.5–1.1 × 2–5			
		Saray-1	Disseminated, banded	1–2/20–25			
		Saray-2	Disseminated, brecciated, lens	0.5-1 × 1–2			

[a]From the most abundant type; Hbj: Harzburgite; Dn: Dunite

Ophiolite rocks in the Kışlacık village section in the Cilo Mountains are located in an area with a NW-SE trend in a 600–1000 m wide belt of cumulates alternating with dunite, wherlite and gabbro.

They are generally melange in character, but retain much of their internal structures. Chromitite lenses in serpentinized dunites, generally show a parallel sequence to ophiolite-limestone. Here, chromitites can be grouped as those between Kışlacık Village and Görhele Hill (2.718 m) and the ones between Alakan Village and Öküzölen Hill (2200 m).

Between Kışlacık Village and Görhele Hill, the serpentinized cumulate dunites, host about 24 chromitite lenses in 8 groups that have a general N-S trend. These lenses are generally in structural contact with serpentinized dunites, and are between 1 and 13 m long, with thicknesses varying between 0.5 and 7 m. The strike of these chromitite lenses is generally N60–65°E or 50–55°SE, but they have limited continuity along strike and down dip. Chromitites also occur in the form of large tectonic blocks. Chemical analysis of samples from chromitite lenses, indicate Cr_2O_3 grades of between 17.86% and 47.45% Cr_2O_3; SiO_2 content is between 1.66% and 17.74%. The dominant Cr_2O_3 content is around 30–35% (Sümer and Artan 1983).

Lens shaped chromitite bodies located mostly on the SW side of Öküzölen Hill (2.200 m, a.s.l.), SW of the Alakan Village, consist of two sequences, with a stratigraphic separation of 30 m, that continue in parallel, but with similar interruptions, for 400 m.

The chromitite lenses are between 0.5 and 30 m long and between 0.2 and 4 m thick. Strikes and dips are N25E, 40° SE; N55E, 46°SE and N50W, 42°SW. Chemical analysis of samples taken from chromitites in Öküzölen Hill, where disseminated chromitites are dominant, indicate that the Cr_2O_3 grade varies between 5.30% and 20.55%; SiO_2 content varies between 13.65% and 20.45% (Sümer and Artan 1983).

3.5 Conclusions

The demand from metallurgy and chemistry industries in Turkey are not sufficient to influence the chromitite market prices. As this sector is highly dependent in exploration, the fluctuations in the global market tend to affect Turkey's chromitite production as well. Nevertheless, as the chromitite occurrences near the surface began to run out, junior mining companies in the country started to close down with the market scene being left to the larger companies with greater investment capabilities. In this circumstances, unless there is a global economic crisis, Turkey's chromitite production may be stabilised. But, this would have a negative effect on a high number of employees who work for the junior mining companies, as they would be forced to find another sources of income.

In terms of high quality steel production, chrome is still an unmatched resource today. Therefore, chromitite as a metallic ore will always have a global demand in the short and medium term. All the same, it is evident that producing chromitite from shallow depths using traditional methods will soon no longer be desirable in

Turkey. Aiming for deeper targets makes it necessary to invest more for research and exploration. Necessary operations have started in Turkey by using more sophisticated software technologies and modelling, more geological and geophysical data which can be helpful in reaching deeper levels of these ore deposits,. Historical mining activities and their records serve as a guiding source for these operations. In addition to this some important deposits which were abandoned without being processed before, are today being considered for producing concentrated ore. This can be taken as a hopeful development, paving the way for new opportunities in the chromitite mining sector in Turkey.

Acknowledgements This chapter includes valuable data from prospecting reports of MTA, accrued during many years, resulting from long-lived studies. Dr. Tandoğan Engin, Dr. Yusuf Ziya Özkan, Bayazıt Erdem, Ali Kemal Akın and İlhan Odabaşı should be mentioned first. A. Olcay Çolakoğlu, Aytekin Türkel and Serdar Keskin were also active prospectors for these Projects. We have to present our gratitude to all prospectors in the past and the present, for their enormous efforts and contribution to the mining sector.

References

Açıkbaş D, Baştuğ C (1975) V. Bölge Cacas-Hani yöresi kuzey sahalarının jeoloji raporu ve petrol olanakları [Geology report and petroleum resources of 5th Region, Cacas-Hani Region]. Report No: 917. TPAO, Ankara (in Turkish, unpublished)

Ahmet AH, Arai S (2002) Unexpectedly high-PGE chromitite from the deeper mantle section of the northern Oman ophiolite and its tectonic implications. Contrib Mineral Petrol 143:263–278

Akın AK (1995) Kurşunlu-Ilgaz-Çankırı-Araç-Tosya-Kastamonu-Kargı-Çorum ve çevresinin krom prospeksiyon raporu [Chromite prospecting report of Kurşunlu-Ilgaz-Çankırı-Araç-Tosya-Kastamonu-Kargı-Çorum and related area]. Report No: 9886. MTA, Ankara (in Turkish, unpublished)

Aktaş G, Robertson AHF (1984) The Maden Complex, SE Turkey: evolution of a Neotethyan continental margin. In: Dixon JE, Robertson, AHF (eds) The geological evolution of the Eastern Mediterranean, Geological Society special publications, vol 17. Geological Society, London, pp 375–402

Aktimur HT (1986) Erzincan, Refahiye ve Kemah dolayının jeolojisi [Geology of Erzincan-Kemah region]. Report No: 7932. MTA, Ankara (in Turkish, unpublished)

Aktimur HT, Atalay Z, Ateş Ş, Tekirli ME, Yurdakul ME (1988). Munzur Dağları ile Çavuşdağ arasının jeolojisi [Geology between Munzur and Çavuş Mountains]. Report No: 8320. MTA, Ankara (in Turkish, unpublished)

Aktimur HT, Tekirli ME, Yurdakul ME (1990) 1:100.000 ölçekli, açınsama nitelikli Türkiye Jeoloji Haritaları Serisi, Tokat D22 (UTM: G 36) Paftası [Geology of Turkey, 1:100.000 scale exploration map series, G36 sheet]. MTA, Ankara (in Turkish, with English abstract)

Akyürek (1981) Ankara-Elmadağ-Kalecik dolayının jeolojisi [Geology of Ankara-Elmadağ-Kalecik region]. Report No: 7298. MTA (in Turkish, unpublished)

Akyürek B, Bilginer E, Çatal E, Dağer Z, Soysal Y, Sunu O (1980) Eldivan-Şabanözü (Çankırı) Hasayaz-Çandır (Kalecik-Ankara) dolayının jeolojisi [Geology of Eldivan-Şabanözü (Çankırı) Hasayaz-Çandır (Kalecik-Ankara) region]. Report No: 6741. MTA (in Turkish, Unpublished)

Alpay B (1951) Burdur İli'nin Yeşilova ilçesine bağlı Salda, Horozköy, Bahyar ve Işıklar köyleri hudutları içinde bulunup Rıfat Kasanoğlu ve Mehmet Erkazancı ortaklığına ait ruhsatname sahalarında yapılan taharriyat hakkında fen raporu [Prospecting report of Burdur-Yeşilova-

Salda–Horozköy-Bahtiyar and Işıklar Villages, licensed to Rıfat Kasanoğlu and Mehmet Erkazancı corporation]. Report No: 3809. MTA Ankara (in Turkish, unpublished)

Alriyami K, Robertson AHF (2002) Mesozoic sedimentary and magmatic evolution of the Arabian continental margin, northern Syria: evidence from the Baer-Bassit Melange. Geol Mag 139:395–420

Alriyami K, Robertson AHF, Dixon J, Xenophontos C (2002) Origin and emplacement of the Late Cretaceous Baer-Bassit ophiolite and its metamorphic sole in NW Syria. Lithos 65:225–260

Andrew T, Robertson AHF (2002) The Beyşehir–Hoyran–Hadim Nappes: genesis and emplacement of Mesozoic marginal and oceanic units of the northern Neotethys in southern Turkey. J Geol Soc Lond 159:529–543

Arni P (1942) Tavşanlı (Kütahya) Linyit Yatakları Raporu [Tavşanlı (Kütahya) lignite report]. Report No:1373. MTA Ankara (in Turkish, unpublished)

Bacak G, Uz B (2003) Dağardı güneyi (Kütahya) ofiyolitinin jeolojisi ve jeokimyasal Özellikleri [Geology and geochemical properties of Dağardı South (Kütahya) ophiolite]. J Istanbul Tech Univ 2(4):86–98

Bağcı U (2004) Kızıldağ (Hatay) ve Tekirova (Antalya) Ofiyolitlerinin Jeokimyası ve Petrolojisi [Geochemistry and petrology of Kızıldağ (Hayat) and Tekirova (Antalya) ophiolites]. PhD thesis, Çukurova Univ Institute of Science, 383 p (in Turkish with English abstract, unpublished)

Bağcı U, Parlak O, Höck V (2005) Whole rock and mineral chemistry of cumulates from the Kızıldağ (Hatay) ophiolite (Turkey): clues for multiple magma generation during crustal accretion in the Southern Neotethyan Ocean. Min Mag 69:53–76

Bağcı U, Parlak O, Höck V (2006) Geochemical character and tectonic environment of ultramafic to mafic cumulate rocks from the Tekirova (Antalya) ophiolite (southern Turkey). Geol J 41(2):193–219

Bağcı U, Parlak O, Höck V (2008) Geochemistry and tectonic environment of diverse magma generations forming the crustal units of the Kızıldağ (Hatay) ophiolite southern Turkey. Turk J Earth Sci 17:43–71

Balcı M (1986) Rut-Taşlıtepe (Guleman-Elazığ) yöresi krom yataklarının jeolojisi [Geology of chromite deposits in Rut-Taşlıtepe (Elazığ) region]. Report no: 7909. MTA, Ankara (in Turkish, unpublished)

Bébien J, Shallo M, Manika K, Gega D (1998) The Shebenik Massif (Albania): a link between MOR- and SSZ-type ophiolites. Ofioliti 23:7–15

Ben-avraham Z, Woodside J, Lodolo E, Gardosh M, Grasso M, Camerlenghi A, Vai GB (2006) Eastern Mediterranean basin systems. In: Gee DE, Stephenson RA (eds) European lithosphere dynamics, Memories, vol 32. Geol Society, London, pp 263–276

Bingöl AF (1978) Pétrologie du massif ophiolitique de Pozantı-Karsantı (Taurus Cilicien, Turquie); étude de la partie orientale: thèse de spécialité (3 ème cycle). Univ. Louis Pasteur, Strasbourg (unpublished)

Borchert H (1952) Etibank Şark kromları mıntıkasında krom cevheri yataklarında yapılan jeolojik tetkik hakkında rapor [Report of the geological prospectivity on chromite deposits in Etibank eastern chromite region]. Report No: 2082. MTA, Ankara (in Turkish, unpublished)

Borchert H (1960) Yeşilova – Burdur havalisindeki kromit yatakları [Chromite ores around Yeşilova-Burdur region]. Report No: 3245. MTA, Ankara (in Turkish, unpublished)

Borchert H (1962) Tefenni (Vilayeti Burdur) peridotit massifindeki kromit zuhurları [Chromite occurrences of the Tefenni (Burdur) peridotite massif]. Report No: 260. MTA, Ankara (in Turkish, unpublished)

Bortolotti V, Marroni M, Pandolfi L, Principi G, Saccani E (2002) Interaction between mid-ocean ridge and subduction magmatism in Albanian ophiolites. J Geol 110:561–576

Boyalı İ (1996) Salda Gölü Kuzeyi (Yeşilova-Burdur), Eğridir-Sütçüler (Isparta), Serik (Antalya) Çevresi Krom Prospeksiyon Raporu [Chromite prospectivity report of northern of Salda Lake (Yeşilova-Burdur), Eğridir-Sütçüler (Isparta) and Serik (Antalya) region]. Report No: 6336. MTA, Ankara (in Turkish, unpublished)

Boyalı İ, Sayın A (1974) Van-Özalp civarındaki peridotitlerde krom prospeksiyon raporu [Chromite prospectivity report of peridotites around Özalp-Van region]. Report No: 5457. MTA, Ankara (in Turkish, unpublished)

Brinkmann R (1966) Geotektonische Gliederung von Westanatolien. N Jb Geol Paleo, Stuttgart, pp 603–618

Brinkmann R (1968) Einige geologische Leitlinien von Anatolien. Geol Paleontol 2:111–119

Çakır Ü (1978) Petrologie du massif de Pozantı – Karsantı (Taurus Cilicien, Turquie): Etude de la partie centrals, These 3 eme cyl, 251. Strasbourg

Çapan UZ (1980) Toros kuşağı ofiyolit Massiflerinin (Marmaris, Mersin, Pozantı, Pınarbaşı ve Divriği) iç yapıları, petroloji ve petrokimyalarına yaklaşımlar [Approaches to the internal structures, petrology and petrochemistry of the Tauride belt ophiolite massifs (Marmaris, Mersin, Pozantı, Pınarbaşı and Divriği)]. PhD thesis, HU Institute of Science (in Turkish, unpublished)

Çataklı AS (1983) Assemblage ophiolitique et roches associees de la partie occidentale du Massif de Pozantı-Karsantı (Taurus Cilicien, Turquie). These d'Etat, Universite de Nancy I

Cawthorn RG (2015) The Bushveld complex, South Africa. In: Charlier B, Namur O, Latypov R, Tegner C (eds) Layered intrusions. Springer, Dordrecht, pp 517–588

Çelik ÖF (2007) Metamorphic sole rocks and their mafic dykes in the eastern Tauride belt ophiolites (southern Turkey): Implications for OIB-type magma generation following slab break-off. Geol Mag 144:849–866

Çelik ÖF, Chiaradia M (2008) Geochemical and petrological aspects of dike intrusions in the Lycian ophiolites (SW Turkey): a case study for the dike emplacement along the Tauride Belt Ophiolites. Int J Earth Sci 97:1151–1164

Çelik ÖF, Delaloye M (2003) Origin of metamorphic soles and their post-kinematic mafic dykes swarms in the Antalya and Lycian ophiolites, SW Turkey. Geol J 38:235–256

Çelik ÖF, Marzoli A, Marschik R, Chiaradia M, Neubauer F, Öz I (2011) Early–Middle Jurassic intra-oceanic subduction in the İzmir-Ankara-Erzincan Ocean, Northern Turkey. Tectonophysics 509(1–2):120–134

Çiftçi Y, Dönmez C, Çolakoğlu AO, Odabaşı İ (2017). Türkiye Krom Envanteri 1. ve 2. Bölüm [Chrome inventory of Turkey: part 1 and 2]. MTA Inventory Series: 205. Ankara

Çolakoğlu AO, Dönmez C, Çiftçi Y, Sayak H, Türkel A (2014) Oltu-Narman-Horasan (Erzurum) Yöreleri Krom-Nikel Prospeksiyon Raporu [Cr-Ni Prospectivity report of Oltu-Narman-Horasan (Erzurum) region]. Report No: 11730. MTA, Ankara (in Turkish, unpublished)

Collins AS, Robertson AHF (1997) Lycian melange, southwestern Turkey: an emplaced Late Cretaceous accretionary complex. Geology 25:255–258

Collins AS, Robertson AHF (1998) Processes of Late Cretaceous to Late Miocene episodic thrust sheet translation in the Lycian Taurides, SW Turkey. J Geol Soc Lond 155:759–772

Demirtaşlı E (1984) Stratigraphy and tectonics of the area between Silifke and Anamur, Central Taurus Mountains. In: Tekeli O, Göncüoğlu MC (eds) Proceeding of the int symp on the geology of the Taurus Belt, 26–29 September, MTA, Ankara, pp 101–118

Demirtaşlı E, Bilgin AZ, Erenler W, Işıklar S, Sanlı DY, Selim M, Turhan N (1975) Geology of the Bolkar mountains. In: Alpan S (ed) Congress of earth sciences, 50th year of the republic. MTA Special Publ, Ankara, pp 42–57

Denkel U (1972) GB Anadolu kromit yatakları hakkında bazı ekonomik mülahazalar [Some economic aspects of SW Anatolian chromite ores]. Report No: 3550. MTA (in Turkish, unpublished)

Dilek Y, Flower MFJ (2003) Arc-trench rollback and forearc accretion: 2. A model template for ophiolites in Albania, Cyprus, and Oman. Geol Soc Lond Spec Publ 218:43–68

Dilek Y, Furnes H (2009) Structure and geochemistry of Tethyan ophiolites and their petrogenesis in subduction rollback systems. Lithos 113(1–2):1–20

Dilek Y, Furnes H (2011) Ophiolite genesis and global tectonics: geochemical and tectonic fingerprinting of ancient oceanic lithosphere. GSA Bull 123(3–4):387–411

Dilek Y, Thy P (2006) Age and petrogenesis of plagiogranite intrusions in the Ankara melange, central Turkey. Island Arc 15(1):44–57

Dilek Y, Thy P (2009) Island arc tholeiite to boninitic melt evolution of the Cretaceous Kizildag (Turkey) ophiolite: model for multi-stage early arc-forearc magmatism in Tethyan subduction factories. Lithos 113(1–2):68–87

Dilek Y, Thy P, Hacker B, Grundvig S (1999) Structure and petrology of Tauride ophiolites and mafic dyke intrusions (Turkey): implications for the Neotethyan ocean. GSA Bull 111:1192–1216

Dilek Y, Shallo M, Furnes H (2005) Rift-drift, seafloor spreading and subduction tectonics of Albanian ophiolites. Int Geol Rev 46:147–176

Dilek Y, Furnes H, Shallo M (2007) Suprasubduction zone ophiolite formation along the periphery of Mesozoic Gondwana. Gondwana Res 11:453–475

Dilek Y, Furnes H, Shallo M (2008) Geochemistry of the Jurassic Mirdita Ophiolite (Albania) and the MORB to SSZ evolution of a marginal basin oceanic crust. Lithos 100:174–209

Dönmez C, Keskin S, Günay K, Çolakoğlu AO, Çiftçi Y, Uysal İ, Türkel A, Yıldırım N (2014) Chromite and PGE geochemistry of the Elekdağ Ophiolite (Kastamonu, Northern Turkey): implications for deep magmatic processes in a supra-subduction zone setting. Ore Geol Rev 57:216–228

Döyen A (1995) Yeşilova (Burdur) civarı kromit yataklarının mineralojik, petrografik ve jeokimyasal incelemesi [Mineralogical, petrographical and geochemical prospection of chromite deposits around Yeşilova (Burdur) region]. PhD thesis, SU Institute of Science, (in Turkish, unpublished)

DPT (2001) Sekizinci Beş Yıllık Kalkınma Planı, Madencilik Özel İhtisas Komisyonu, Metal Madenler Alt Komisyonu, Krom Çalışma Grubu Raporu [8th five years development plan, commission of mines, chrome sub-commission report]. DPT: 2626-ÖİK: 637, 66p

Economou-Eliopoulos M (1996) Platinum-group elements distribution in chromite ores from ophiolite complexes: implications for their exploration. Ore Geol Rev 11:363–381

Engin T (1986) Petrology of the peridotite and structural setting of the Batı Kef-Doğu Kef chromite deposits, Guleman-Elazığ, eastern Turkey. In: Gallagher JM, Ischer RA, Neary CR, Prichard HM (eds) Metallogeny of basic and ultrabasic rocks. British IMM, London, pp 229–240

Engin T, Sümer Y (1987) Kefdağ-Kapin (Guleman-Elazığ) yöresinin jeolojisi, Batı Kef-Doğu Kef krom yataklarının maden jeolojisi [Geology of Kefdağ-Kapin (Guleman-Elazığ) and mining geology of West and East Kef chromite deposits]. Report No: 8123. MTA (in Turkish, unpublished)

Engin T, Balcı M, Sümer Y, Özkan YZ (1980–1981) General geological setting and the structural features the Guleman Peridotite unit and the chromite deposits (Elazığ, Eastern Turkey). Bull Min Res Exp 95(96):34–56

Engin T, Özkan YZ, Balcı M (1985) Türkiye Krom Yatakları ve MTA'nın Krom Aramacılığındaki Yeri [Chromite ore deposits of Turkey and the role of the MTA in chromite exploration]. 50th Year Symposium Abstracts Ankara, MTA

Engin T, Özkoçak O, Artan Ü (1987) General geological setting and character of chromite deposits in Turkey: in evolution of chromium ore fields. In: Stowe CXW (ed) Evolution of chromium fields. Von Nostrand Reinhold Company, New York, pp 195–219

Ercan T, Soykal T, Pehlivanoğlu H (1970) Elazığ-Diyarbakır (Maden-Ergani-Guleman) bölgesi jeolojisi [Geologyof Elazığ-Diyarbakır (Maden-Ergani-Guleman) region]. Report No: 5038. MTA, (in Turkish, unpublished)

Erendil M (2002) Türkiye Ofiyolitleri [Ophiolites of Turkey]. Seminar Notes, MTA publ. (in Turkish, unpublished)

Ergül E, Öztürk Z, Akçaören F, Gözler MZ (1980) Balıkesir İli-Marmara Denizi arasının jeolojisi [Geology between Balıkesir and Marmara Sea] Report No: 6760. MTA, (in Turkish, unpublished)

Flower MFJ, Dilek Y (2003) Arc-trench rollback and forearc accretion: 1.A collosion-induced mantle flow model for Tethyan ophiolites. In: Dilek Y, Robinson PT (eds) Ophiolites in earth history, vol 218. Geol Soc, London Sp Public. pp 21–41

Floyd PA, Winchester JA, Seston R, Kryza R, Crowley QG (2000) Review of geochemical variation in Lower Palaeozoic metabasites from the NE Bohemian Massif: intracratonic rifting and

plume-ridge interaction. In: Franke W, Haak V, Oncken O, Tanner D (eds) Orogenic processes: quantification and modelling in the Variscan Belt, vol 179. Geological Society special publication, Geological Society, London, pp 155–174

Garuti G (2004) Chromite-platinum group element magmatic deposits. In: De Vivo B, Stüwe K (eds) Geology, encyclopedia of life support systems (EOLSS). UNESCO, EOLSS Publisher, Oxford. http://www.eolss.net

Garuti G, Fershtater G, Bea F, Montero PG, Pushkarev EV, Zaccarini F (1997) Platinum-group element distribution in mafic-ultramafic complexes of central and southern Urals: preliminary results. Tectonophysics 276:181–194

Gedik A, Birgili Ş, Yılmaz H, Yoldaş R (1979) Mut – Ermenek – Silifke yöresinin jeolojisi ve petrol olanakları [Geology and petroleum resources of Mut-Ermenek-Silifke region]. Bull Geol Soc Turk 22:7–26 (in Turkish with English abstract)

Göncüoğlu MC, Turhan N, Şentürk K, Özcan A, Uysal S, Yalınız MK (2000). A geotraverse across northwestern Turkey: tectonic units of the Sakarya region and their tectonic evolution. In: Bozkurt E, Winchester JA, Piper JDA (eds) Tectonics and magmatism in Turkey and the surrounding area, vol 173. Geol Soc of London, Sp Public. pp 139–161

González-Jiménez JM, Proenza JA, Gervilla F, Melgarejo JC, Blanco-Moreno JA, Ruiz-Sánchez R, Griffin WL (2011) High-Cr and High-Al chromitites from the Sagua de Tánamo district, Mayarí-Cristal ophiolitic massif (eastern Cuba): constraints on their origin from mineralogy and geochemistry of chromian spinel and platinum-group elements. Lithos 125(1):101–121

Günay K, Çolakoğlu AR (2011) Geochemical properties and platinum group element (PGE) contents of Eastern Turkey (Van Area) chromitite. Geol Bull Turk 54(1–2):1–24

Günay K, Çolakoğlu AR (2016) Spinel compositions of mantle-hosted chromitite from the Eastern Anatolian ophiolite body, Turkey: implications for deep and shallow magmatic processes. Ore Geol Rev 73(1):29–41

Günay K, Çolakoğlu AR, Çakır Ü (2012) Geochemical properties and rodingitization of diabase dykes cutting peridotites in Yüksekova complex (Özalp, Van – Turkey). Bull Min Res Exp 144:1–22

Hakyemez Y, Barkut MY, Bilginer E, Pehlivan Ş, Can B, Dağer Z, Sözeri B (1986) Yapraklı-Ilgaz-Çankırı-Çandır dolayının jeolojisi [Geology of Yapraklı-Ilgaz-Çankırı-Çandır region]. Report No: 7966. MTA (in Turkish, unpublished)

Hébert R, Laurent R (1990) Mineral chemistry of the plutonic section of the Troodos ophiolite: new constraints for genesis of arc-related ophiolites. In: Malpas J, Moores E, Panayiotou A, Xenophontos C (eds) Proceedings of Troodos ophiolite symposium, geological survey, Cyprus, pp 149–163

Höck V, Koller F, Meisel T, Onuzi K, Kneringer E (2002) The Jurassic South Albanian ophiolites: MOR- vs SSZ-type ophiolites. Lithos 65:143–164

Holzer H (1954) Beyce 54-1 ve Simav 71-2 Paftalarının Jeoloji Raporu [Geology report of the Beyce 54-1 and Simav 71-2 sheets]. Report No: 2366. MTA (in Turkish, unpublished)

İskit M (1973) Etibank Şark kromları Kef Dağı krom yatakları arama raporu [Prospectivity report of the Kef Dağı chromite deposits in eastern chromites of Etibank]. Etibank Report

İzmir M, Koç İ (1977) Pütyan-Bişeran (Guleman-Elazığ) yöresi, Pütyan krom ocakları çevresinin jeolojisi raporu [Geology report of Pütyan-Bişeran (Guleman-Elazığ), Pütyan chromite deposit and adjacent areas]. Report No: 6603. MTA, Ankara (in Turkish, unpublished)

Jackson ED, Thayer TP (1972) Some criteria for distinguishing between stratiform, concentric and alpine type peridotite-gabbro complexes. In: Proceeding of international geological Congress 24th, Montreal, vol 2, pp 280–296

Juteau T (1979) Ophiolites des Taurides: Essai sur leurhistorie oceanique. Rev Geol Dyn Geogr Phys 21(3):191–214 Paris

Juteau T (1980) Ophiolites of Turkey. Ofioliti 2:199–237

Juteau T, Nicolas A, Dubessy J, Fruchard JC, Bouchez JL (1977) Structural relationships in the Antalya ophiolite complex, Turkey: possible model for an oceanic ridge. GSA Bull 88:1740–1748

Kaczmarek MA, Müntener O, Rubatto D (2008) Trace element chemistry and U-Pb dating of zircons from oceanic gabbros and their relationship with whole rock composition (Lanzo, Italian Alps). Contrib Mineral Petrol 155:295–312

Karaoğlan F (2012) Geochronology of the ophiolitic and granitic rocks along the SE Anatolian orogen. PhD thesis. Çukurova University, Adana, (in Turkish with English abstract)

Karaoğlan F, Parlak O, Klötzli U, Thönim, Koller F (2013a) U–Pb and Sm–Nd geochronology of the Kızıldağ (Hatay, Turkey) ophiolite: implications for the timing and duration of suprasubduction zone type oceanic crust formation in the southern Neotethys. Geol Mag 150(2):283–299

Karaoğlan F, Parlak O, Klötzli U, Koller F, Rizaoğlu T (2013b) Age and duration of intra-oceanic arc volcanism built on a suprasubduction zone type oceanic crust in Southern Neotethys, SE Anatolia. Geosci Front 4(4):399–408

Ketin İ (1977) Van Gölü ile Iran sınırı arasındaki bölgede yapılan jeoloji gözlemlerinin sonuçları hakkında kısa bir açıklama [Short explanatory notes about the results of the survey between Van Lake and Iran–Turkey state border]. Bull Geol Soc Turk 20:79–85 (in Turkish with English abstract)

Koglin N (2008) Geochemistry, petrogenesis and tectonic setting of ophiolites and mafic-ultramafic complexes in the Northeastern Aegean region: new trace-element, isotopic and age constraints. PhD thesis, Department of Chemistry, Pharmacy and Geosciences of the Johannes Gutenberg University

Koglin N, Kostopoulos D, Reichmann T (2009) Geochemistry, petrogenesis and tectonic setting of the Samothraki mafic suite, NE Greece: trace-element, isotopic and zircon age constraints. Tectonophysics 473:53–68

Konak N (2002) Türkiye Jeoloji Haritası, İzmir Paftası 1/500.000 [Geological Map of Turkey, Izmir sheet in 1:500.000 scale] MTA (in Turkish with English abstract)

Konak N, Akdeniz N, Armağan F (1980) Akhisar-Gölmarmara-Gördes-Sındırgı dolaylarının jeolojisi [Geology of Akhisar-Gölmarmara-Gördes-Sındırgı region]. Report No: 6916. MTA, Ankara (in Turkish, unpublished)

Konstantinou A, Wirth KR, Vervoort J (2007) U-Pb isotopic dating of Troodos plagiogranite, Cyprus by LA-ICP-MS. In: 2007 GSA Denver Annual Meeting (28-31 October 2007) Paper No. 143–16

Koralay T (2000) Niyazlar Köyü (Yesilova–Burdur) ile Tefenni Yaylası (Tefenni–Burdur) Ofiyolitlerinin Jeolojik, Petrografik ve Petrokimyasal incelenmesi [Geological, petrographical and petrochemical investigation of Niyazlar Village (Yeşilova-Burdur) and Tefenni Highland (Tefenni-Burdur) ophiolites]. MSc thesis, PU Institute of Science (in Turkish with English abstract, unpublished)

Kovenko V (1940) Soridağ mıntıkası krom yataklarına yapılan ziyaret hakkında rapor [Report about the visit of Soridağ chromite deposits]. Report No: 1024. MTA (in Turkish, unpublished)

Kozlu H, Prichard H, Melcher F, Fisher P, Brough, Stueben D (2014) Platinum group element (PGE) mineralisation and chromite geochemistry in the Berit ophiolite (Elbistan/Kahramanmaraş), SE Turkey. Ore Geol Rev 60:97–111

Liati A, Gebauer D, Fanning CM (2003) The youngest basic oceanic magmatism in the Alps (Late Cretaceous; Chiavenna unit, Central Alps): geochronological constraints and geodynamic significance. Contrib Mineral Petrol 146:144–158

Liati A, Gebauer D, Fanning CM (2004) The age of ophiolitic rocks of the Hellenides (Vourinos, Pindos, Crete): first U-Pb ion microprobe (SHRIMP) zircon ages. Chem Geol 207:171–188

Lytwyn JN, Casey JF (1993) The geochemistry and petrogenesis of volcanics and sheeted dikes from the Hatay (Kızıldağ) ophiolite, southern Turkey: possible formation with the Troodos ophiolite, Cyprus, along fore-arc spreading centers. Tectonophysics 232:237–272

Mackintosh PW, Robertson AHF (2009) Structural and sedimentary evidence from the northern margin of the Tauride platform in south central Turkey used to test alternative models of Tethys during Early Mesozoic time. Tectonophysics 473:149–172

McCallum IS (1996) The stillwater complex. In: Cawthorn RG (ed) Layered intrusions, developments in petrology. Elsevier, Amsterdam, pp 441–484

Melcher F, Grum W, Thalhammer TV, Thalhammer OAR (1999) The giant chromite deposits at Kempirsai, Urals: constraints from trace element (PGE, REE) and isotope data. Mineral Depos 34:250–272

MTA (2002) 1:500,000 scale geology map of Turkey. General Directorate of Mineral Research and Exploration, Ankara

Mukasa SB, Ludden JN (1987) Uranium–lead ages of plagiogranites from the Troodos ophiolite, Cyprus, and their tectonic significance. Geology 1:825–828

Okay AI (1981) The geology and blueschist metamorphism of the ophiolites in Northwest Turkey (Tavşanlı – Kütahya). Bull Geol Soc Turk 24:85–95 (in Turkish with English abstract)

Okay AI (1986) High pressure/low temperature metamorphic rocks of Turkey. In: Evans BW, Brown EH (eds) Blueschists and eclogites, vol 164. GSA Memoir, pp 333–348

Okay AI (1989) Alpine-Himalayan blueschists. Annu Rev Earth Planet Sci 17:55–87

Okay AI (2008) Geology of Turkey: a synopsis. Anschnitt 21:19–42

Okay AI (2011) Tavşanli zone: the northern subducted margin of the Anatolide Tauride block. Bull Min Res Exp 142:191–211

Okay AI, Şahintürk Ö (1997) Geology of the Eastern Pontides. In: Robinson AG (ed) Regional and petroleum geology of the Black sea and surrounding region, vol 68. AAPG, pp 291–311

Okay AI, Siyako M (1993) İzmir-Balıkesir arasında İzmir-Ankara Neo-Tetis kenedinin yeni konumu. Türkiye ve çevresinin tektoniği-petrol potansiyeli [The new position of Izmir-Ankara Neo-Tethyan suture between Izmir and Ankara. Tectonics and petroleum potential of Turkey and surroundings)]. In: Turgur S (eds) Ozan Sungurlu Semposium, Abstract Book. pp 333–355

Okay AI, Tüysüz O (1999) Tethyan sutures of northern Turkey. In: Durand B et al (eds) The Mediterranean Basins: tertiary extension within the Alpine Orogen, vol 156. Geol Soc of London. pp 475–515

Okay AI, Whitney DL (2010) Blueschists, ophiolites and suture zones in northwest Turkey. In: Field trip guide book of Pre-Congress Excursion 1-3.10.2010, Tectonic Crossroads: evolving Orogens of Eurasia-Africa-Arabia, Geological Society of America, Ankara, 4–8 October 2010

Okay AI, Tüysüz O, Satır M, Özkan-Altıner S, Altıner D, Sherlock S, Eren RH (2006) Cretaceous and Triassic subduction-accretion, HP/LT metamorphism and continental growth in the central Pontides, Turkey. GSA Bull 118:1247–1269

Önen AP (2003) Neotethyan ophiolitic rocks of the Anatolides of NW Turkey and comparison with Tauride ophiolites. J Geol Soc Lond 160:947–962

Önen AP, Hall R (1993) Ophiolites and related metamorphic rocks from the Kütahya region, northwest Turkey. Geol J 28:399–412

Önen AP, Hall R (2000) Sub-ophiolite metamorphic rocks from NW Anatolia, Turkey. J Metamorph Geol 18:483–495

Ortalan F, Erdem B (1977) Kelhasi-Beyazkaya (Guleman-Elazığ) Gölalan, Tasinler, Sitealtı, Kündikan krom ocaklarının jeolojisi raporu [Geology report of the Kelhasi-Beyazkaya-Gölalan-Tasinler-Sitealtı and Kündikan (Guleman-Elazığ) chromite ore deposits]. Report No: 6579. MTA, Ankara (in Turkish, unpublished)

Ortalan F, Taşan N (1997) Çorum, Laçin, Sungurlu, Alaca, Ortaköy, Mecitözü (Çorum) arasında yüzeyleyen ofiyolitlerin krom prospeksiyon raporu [Cr-prospection report of Laçin-Sungurlu-Alaca-Ortaköy-Mecitözü (Çorum) ophiolites]. Report No: 10011. MTA, (in Turkish, unpublished)

Ortalan F, Seçer Y, Özen H (1984) Harmancık-Orhaneli (Bursa), Tavşanlı-Emet (Kütahya), Dursunbey (Balıkesir) yöresinde krom prospeksiyonu [Cr-prospectivity report of Harmancık–Orhaneli (Bursa), Tavşanlı-Emet (Kütahya) and Dursunbey (Balıkesir) region]. Report No: 7640. MTA (in Turkish, unpublished)

Özcan A, Akın E, Keskin E, Oral A, Sümengen M, Tekeli O (1980) Kuzey Anadolu Fayı-Kırşehir Massifi Arasının Temel Jeolojisi [Basic geology of North Anatolian Fault and Kırşehir Massif]. Report No: 6722. MTA (in Turkish, unpublished)

Özen H, Çolakoğlu A, Sayak H, Dönmez C, Türkel A, Odabaşı İ (2008). Erzincan-Tercan-Çayırlı Yöresi Ofiyolit Jeolojisi ve Krom-Nikel Prospeksiyon Raporu [Cr-Ni prospection report and

geology of ophiolites around Erzincan-Tercan-Çayırlı region]. Rep.No: 11050. MTA (in Turkish, unpublished)
Özen H, Gültaşlı ÖF, Çolakoğlu A (2011) Sivrihisar-Beylikova-Mihaliççik-Sarıcakaya (Eskişehir) yörelerindeki ofiyolitlerin jeolojisi ve metalojenezi [Geology and metallogenesis of the ophiolites in Sivrihisar-Beylikova-Mihaliçikik-Sarıcakaya (Eskişehir) regions]. Report No: (11458). MTA (In Turkish, unpublished)
Özgül N (1976) Toroslar'ın bazı temel jeolojik özellikleri [Some geological aspects of the Taurus Orogenic Belt (Turkey)]. Bull Geol Soc Turk 19(l):65–78 (in Turkish with English abstract)
Özgül N (1997) Bozkır-Hadim-Taşkent (Orta Toroslar'ın kuzey kesimi) dolayında yer alan tektonostratigrafik birliklerin stratigrafisi [Stratigraphy of the tectonostratigraphic units around Hadim-Bozkır-Taşkent Region (northern part of the Central Taurides, Turkey)]. Bull Min Res Exp 119:113–174 (in Turkish with English abstract)
Özkan YZ (1977) Kunt-Cordik-Genepi köyleri (Elazığ-Maden) arasında görülen krom oluşumları hakkında jeoloji raporu [Geology report about chromite occurrences around Kunt-Cordik-Genepi villages (Maden-Elazığ)]. Report No: 6955. MTA (in Turkish, unpublished)
Özkan YZ (1981–1982) Structural investigation of Guleman (Elazığ) ophiolite. Bull Min Res Exp 97(98):32–39
Özkan YZ (1982a) Guleman (Elazığ) Ofiyolitlerinin jeolojisi ve petrolojisi [Geology and petrology of Guleman (Elazığ) ophiolites]. PhD thesis, IU Earth Science Faculty, (in Turkish, unpublished)
Özkan YZ (1982b) Guleman-Elazığ Ofiyolitlerinin Jeoloji ve Petrolojisi [Geology and petrology of Guleman (Elazığ) ophiolites]. Ist J Earth Sci 3–4(6):33–39 (in Turkish with English abstract)
Özkan YZ (1983) Effects of metamorphism in the Guleman ophiolite. In: Tekeli O, Göncüoğlu MC (eds) Proceeding of the int symp on the geology of the Taurus belt, MTA, Ankara. p 87
Özkan YZ, Sümer Y (1986) Rut, Orta Lasir ve Yeni Lasir ocakları maden jeolojisi raporu [Mining geology report of Rut, Middle Lasir and New Lasir mines]. Report No: 8030. MTA (in Turkish, unpublished)
Özkan YZ, Sümer Y (1987) Uzundamar-2 ve Uzundamar-1 Ocakları (Guleman-Elazığ) jeolojisi raporu [Geology report of Uzundamar 1 and Uzundamar-2 mines (Guleman-Elazığ)]. Report No: 8278 MTA, Ankara (unpublished)
Pal T (2011) Petrology and geochemistry of the Andaman ophiolite: melt–rock interaction in a suprasubduction-zone setting. J Geol Soc 168(4):1031–1045
Parlak O (1996) Geochemistry and geochronology of the Mersin ophiolite within the eastern Mediterranean tectonic frame. PhD thesis, Terre and Environnement 6, University of Geneva, Switzerland
Parlak O (2006) Geodynamic significance of granitoid magmatism in the Southeast Anatolian Orogen: geochemical and geochronogical evidence from Göksun-Afşin (Kahramanmaraş, Turkey) region. Int J Earth Sci 95:609–627
Parlak O, Delaloye M (1996) Geochemistry and timing of postmetamorphic dike emplacement in the Mersin ophiolite (southern Turkey): new age constraints from $^{40}Ar/^{39}Ar$ geochronology. Terra Nova 8:585–592
Parlak O, Delaloye M, Bingöl E (1995) Origin of subophiolitic metamorphic rocks beneath the Mersin ophiolite, southern Turkey. Ofioliti 20(2):97–110
Parlak O, Delaloye M, Bingöl E (1996) Mineral chemistry of ultramafic and mafic cumulates as an indicator of the arc–related origin of the Mersín ophiolite (southern Turkey). Geol Rundsch 85:647–661
Parlak O, Höck V, Delaloye M (2000) Supra-subduction zone origin of the Pozantı-Karsantı ophiolite (Southern Turkey) deduced from whole rock and mineral chemistry of the gabbroic cumulates. In: Bozkurt E, Winchester JA, Piper J (eds) Tectonics and magmatism in Turkey and its surroundings, Geological Society special publications, vol 173. Geological Society, London, pp 219–234
Parlak O, Delaloye M, Demirkol C, Ünlügenç UC (2001) Geochemistry of Pliocene/Pleistocene basalts along the central Anatolian fault zone (CAFZ), Turkey. Geodin Acta 14:159–167

Parlak O, Höck V, Delaloye M (2002) The suprasubduction zone Pozantı-Karsantı ophiolite, southern Turkey: evidence for high-pressure crystal fractionation of ultramafic cumulates. Lithos 65:205–224

Parlak O, Höck V, Kozlu H, Delaloye M (2004) Oceanic crust generation in an island arc tectonic setting, SE Anatolian Orogenic Belt (Turkey). Geol Mag 141:583–603

Parlak O, Delaloye M, Kozlu H, Rizaoğlu T, Bağci U (2006) The petrography and the geochemistry of the tectono-magmatic units outcropped around the Baskil and Sivrice (Elazığ) regions. Project Report No: YDABÇAG-102Y041 Scientific & Technological Research Council of Turkey (TÜBITAK), Ankara

Parlak O, Rizaoğlu T, Bağci U, Karaoğlan F, Höck V (2009) Tectonic significance of the geochemistry and petrology of ophiolites in southeast Anatolia, Turkey. Tectonophysics 473(1–2):173–187

Parlak O, Karaoğlan F, Rızaoğlu T, Klötzli U, Koller F, Billor Z (2013a) U-Pb and $^{40}Ar/^{39}Ar$ geochronology of the Ophiolites and Granitoids from the Tauride Belt: implications for the evolution of the inner Tauride suture. J Geodyn 65:22–37

Parlak O, Çolakoğlu A, Dönmez C, Sayak H, Yildirim N, Türkel A, Odabaşı İ (2013b) Geochemistry and tectonic significance of ophiolites along the İzmir–Ankara–Erzincan Suture Zone in northeastern Anatolia. Geol Soc Lond Spec Publ 372:75–105

Pearce JA, Harris NBW, Tindle AG (1984) Trace element discrimination diagram for the tectonic interpretation of Granitic rocks. J Petrol 25:956–983

Pehlivan Ş, Duru M, Dönmez M, Ilgar A, Akçay AE, Erdoğan K, Özer D (2007) 1:100.000 Ölçekli Türkiye Jeoloji Haritaları, Balıkesir İ-19 Paftası [Geology maps of Turkey in 1:100.000 scale: I–19 sheet]. No: 96. MTA Publ (in Turkish with English abstract)

Perinçek D (1978) Çelikhan-Sincik-Koçali (Adıyaman) alanının jeolojik incelemesi ve petrol olanaklarının araştırılması [Geology and petroleum resources of Çelikhan-Sincik-Koçali (Adıyaman) region] PhD thesis, IU Science Faculty, Applied Geology Chair, İstanbul (in Turkish, unpublished)

Perinçek D (1989) Hakkari İli ve Dolayının Stratigrafisi, Yapısal Özellikleri, Petrol İmkanları [Stratigraphy, structural elements and petroleum resources of Hakkari region]. Report No: 2545. TPAO, Ankara (in Turkish, unpublished)

Pourteau A, Candan O, Oberhanslı R (2010) High-pressure metasediments in central Turkey: constraints on the Neotethyan closure history. Tectonics 29:TC5004

Proenza JA, Gervilla F, Melgarejo JC, Reve D, Rodríguez YG (1998) Ophiolitic chromitites from the Mercedita deposit (Cuba). Example of Al-rich chromites at the mantle-crust transition zone. Acta Geol Hisp 33:179–212

Rammlmair D (1986) Chromite in the Philippines and the tectonic setting of the host ophiolites: case examples Zambales and Palawan. In: Monography on chromite deposits. IGCP project 197, Theophrastus publications. pp 285–309

Reuber I, Juteau T, Whitechurch H (1984) Genese en cotexte transformant des ophiolites d'Antalya (Turquie). Bull Soc Geol Fr 26:945–954

Rice SP, Robertson AHF, Ustaomer T (2006) Late-Cretaceous-Early Cenozoic tectonic evolution of the Eurasian active margin in the central and eastern Pontides, northern Turkey. In: Robertson AHF, Mountrakis D (eds) Tectonic development of the Eastern mediterranean region, vol 260. Geol Soc, London, pp 413–445

Rice SP, Robertson AHF, Ustaomer T, İnan T, Tasli K (2009) Late Cretaceous–Early Eocene tectonic development of the Tethyan suture zone in the Erzincan area, eastern Pontides, Turkey. Geol Mag 146(4):567–590

Rızaoğlu T, Parlak O, Höck V, İşler F (2006) Nature and significance of Late Cretaceous ophiolitic rocks and its relation to the Baskil granitoid in Elazığ region, SE Turkey. In: Robertson AHF, Mountrakis D (eds) Tectonic development of the Eastern Mediterranean region, vol 260. Geol Soc, London, pp 327–350

Rızaoğlu T, Parlak O, Höck V, Koller F, Hames WE, Billor Z (2009) Andean-type active margin formation in the eastern Taurides: Geochemical and geochronogical evidence from the Baskil granitoid (Elaziğ, SE Turkey). Tectonophysics 473:188–207

Roberts G, Pearce D (2007) Hydrocarbon plays and prospectivity of the Levantine Basin, offshore Lebanon and Syria from modern seismic data. Geo Arab 12:99–124

Robertson AHF (1986a) Geochemistry and tectonic implications of metalliferous and volcaniclastic sedimentary rocks associated with late ophiolitic extrusives in the Hatay area, southern Turkey. Ofioliti 11:121–140

Robertson AHF (1986b) The Hatay ophiolite (southern Turkey) in its Eastern Mediterranean tectonic context: a report on some aspects of the field excursion. Ofioliti 11(2):105–119

Robertson AHF (2002) Overview of the genesis and emplacement of Mesozoic ophiolites in the Eastern Mediterranean Tethyan region. Lithos 65:1–67

Robertson AHF (2004) Development of concepts concerning the genesis and emplacement of Tethyan ophiolites in the Eastern Mediterranean and Oman regions. Earth Sci Rev 66:331–387

Robertson AHF (2006) Contrasting modes of ophiolite emplacement in the Eastern Mediterranean region. Geol Soc Lond Mem 32:235–261

Robertson AHF (2007) Overview of tectonic settings related to the rifting and opening of Mesozoic ocean basins in the Eastern Tethys: Oman, Himalayas and Eastern Mediterranean regions. In: Karner G, Manatschal G, Pinheiro LM (eds) Imaging, mapping and modelling continental lithosphere extension and breakup, Geological Society special publications, vol 282. Geological Society London, pp 325–389

Robertson AHF, Dixon JE (1984) Introduction: aspects of the geological evolution of the Eastern Mediterranean. In: Robertson AHF, Dixon JE (eds) The geological evolution of the Eastern Mediterranean, vol 17. Geol Soc London, Sp Public. pp 1–74

Robertson AHF, Shallo M (2000) Mesozoic-Tertiary tectonic evolution of Albania in its regional Eastern Mediterranean context. Tectonophysics 316(2–4):197–254

Robertson AHF, Ustaömer T, Parlak O, Ünlügenç UC, Tasli K, İnan N (2006) The Berit transect of the Tauride thrust belt, Turkey: Late Cretaceous-Early Cenozoic accretionary/collisional processes related to closure of the Southern Neotethys. Asian J Earth Sci 27(1):108–145

Robertson AHF, Parlak O, Rizaoğlu T, Ünlügenç UC, İnan N, Tasli K, Ustaömer T (2007) Tectonic evolution of the South Tethyan Ocean: evidence from the Eastern Taurus Mountains (Elazığ region, SE Turkey). In: Ries AC, Butler RWH, Graham RH (eds) Deformation of the continental crust, vol 272. The Legacy of Mike Coward, Geological Society special publications. Geol Society, London, pp 231–270

Robertson AHF, Parlak O, Ustaomer T (2009) Melange genesis and ophiolite emplacement related to subduction of the northern margin of the Tauride–Anatolide continent, central and western Turkey. In: Van Hinsbergen DJJ, Edwards MA, Govers R (eds) Collision and collapse at the Africa–Arabia–Eurasia subduction zone, Geological Society special publications, vol 311. Geological Society, London, pp 9–66

Robertson AHF, Parlak O, Ustaömer T (2012a) Overview of the Palaeozoic–Neogene evolution of Neotethys in the Eastern Mediterranean region (southern Turkey, Cyprus, Syria). Pet Geosci 18:381–404

Robertson AHF, Parlak O, Ustaömer T (2012b) Interrelation of microcontinents and carbonate platforms in the Late Mesozoic-Early Cenozoic assembly of the Anatolian continent. In: Robertson AHF, Parlak O, Ünlügenç UC (eds) Geological development of the Anatolian continent, Geological Society special publications, vol 372. Geological Society, London

Rollinson P (2008) The geochemistry of mantle chromitites from the northern part of the Oman ophiolite: inferred parental melt compositions. Contrib Mineral Petrol 156:273–288

Rubatto D, Scambelluri M (2003) U-Pb dating of magmatic zircon and metamorphic baddeleyite in the Ligurian eclogites (Voltri Massif, Western Alps). Contrib Mineral Petrol 146:341–355

Rubatto D, Gebauer D, Fanning M (1998) Jurassic formation and Eocene subduction of the Zermatt-Saas-Fee ophiolites: implications for the geodynamic evolution of the Central and Western Alps. Contrib Mineral Petrol 132:269–287

Saccani E, Seghedi N, Nicolae İ (2004) Evidence of rift magmatism from preliminary petrological data on lower Triassic Mafic Rocks from the north Dobrogea Orogen (Romania). Ofioliti 29(2):231–241

Sarifakioğlu E, Özen H, Winchester JA (2009) Whole rock and mineral chemistry of ultramafic-mafic cumulates from the Orhaneli (Bursa) ophiolite, NW Anatolia. Turk J Earth Sci 18:55–83

Sarıfakıoğlu E, Sevin M, Dilek Y (2014) Türkiye Ofiyolit Envanteri [Ophiolite inventory of Turkey]. MTA Publ, Ankara (in Turkish)

Sarıkaya AR, Seyrek T (1976) Yeşilova – Tefenni peridotit Massifindeki krom ve nikel zenginleşmeleri prospeksiyon raporu [Report of the Cr-Ni enrichments in Yeşilova-Tefenni (Burdur) peridotite massif]. Report No: 5764. MTA (in Turkish, unpublished)

Sarp H (1976) Etude geologique et petrographique du cortege ophiolitique de la region situee au nord-quest de Yeşilova (Burdur-Turquie). These, Univ Geneve, 377p

Sayak H, Özen H, Çolakoğlu AO, Gültaşlı ÖF, Başta Ö (2009) Orhaneli (Bursa) Ofiyoliti ve Metalojenezi [Metallogeny of Orhaneli (Bursa) ophiolite]. Report No: 11121. MTA (in Turkish, unpublished)

Şenel M (1997a) 1/100.000 ölçekli Türkiye Jeoloji Haritaları, Isparta-K11 paftası [Geology of Turkey in 1:100.000 scale: Isparta K-11 sheet]. No: 11. MTA (in Turkish with English abstract)

Şenel M (1997b) 1:250.0000 Ölçekli Türkiye Jeoloji Haritaları No: 3 Antalya Paftası [Geology of Turkey in 1:250.000 scale: antalya sheet] (in Turkish with English abstract)

Şenel M (2004) Stratigraphic and structural features of Yeşilyaprak Nappe in Western Taurus Range and its comparision with the similar units in SE Anatolia and Northern Cyprus. Bull Min Res Explor 128:1–26

Şenel M (2007) 1:100.000 Ölçekli Türkiye Jeoloji Haritaları, Cizre M48 Paftası [Geology of Turkey in 1:00.000 scale: Cizre M-48 sheet]. No: 58 MTA (in Turkish with English abstract)

Şengör AMC, Yılmaz Y (1981) Tethyan evolution of Turkey: a plate tectonic approach. Tectonophysics 75:181–241

Sümer Y, Artan Ü (1983) Kışlacık mahallesi ve Alakan Köyü (Yüksekova/Hakkari) yöresinin krom etüdü [Cr-Prospection report of Kışlacık district and Alakan village (Yüksekova-Hakkari)]. Rep No: 7309. MTA (in Turkish, unpublished)

Sungurlu O (1974) VI. Region kuzey sahalarının jeolojisi [6th region: geology of North of the]. Report No: 871. TPAO. (in Turkish, unpublished)

Sungurlu O, Perinçek D, Kurt G, Tuna E, Dülger S, Çelikdemir E, Naz H (1985) Elazığ–Hazar–Palu alanının jeolojisi [Geology of Elazığ-Hazar-Palu region]. Bull Gen Direct Pet Aff 29:83–189 (in Turkish)

Tekeli O, Aksay A, Ertan İE, Işık A, Örgün BM (1981) Toros Ofiyolit Projeleri, Aladağ Projesi [Tauride ophiolite projects: Aladağ project]. Report No: 6976. MTA, (in Turkish, unpublished), Ankara

Tekeli O, Örgün BM, Işık A (1984) Geology of the Aladağ Mountains. In: Tekeli O, Göncüoğlu CM (eds) International symposium on the geology of the Taurus Belt, 1983. MTA, Ankara, pp 143–158

Ternek Z (1957) Adana Havzasının Alt Miyosen (Burdigaliyen) formasyonları; bunların diğer formasyonlarla olan münasebetleri ve petrol imkanları [Lower Miocene (Burdigalian) formations of Adana Basin and its relation with other formations and petroleum resources]. Bull Min Res Exp 49:48–66 Ankara (in Turkish)

Thayer TP (1960) Some critical differences between alpine – type and stratiform peridotite gabbro complexes. 21st International geological Congress, Copenhagen, Reports, vol 13, pp 247–259

Tilton GR, Hopson CA, Wright JE (1981) Uranium-lead isotopic ages of the Semail ophiolite Oman, with applications to Tethyan ocean ridge tectonics. J Geophys Res B 86:2763–2776

Topuz G, Göçmengil G, Rolland Y, Çelik ÖF, Zack T, Schmitt AK (2013) Jurassic accretionary complex and ophiolite from northeast Turkey: no evidence for the Cimmerian continental ribbon. Geology 41(2):255–258

Tremblay A, Meshi A, Bédard JH (2009) Oceanic core complexes and ancient oceanic lithosphere: insights from Iapetan and Tethyan ophiolites (Canada and Albania). Tectonophysics 473(1–2):36–52

Uçurum A, Koptagel O (2006) Main-component geochemistry and platinum-group element potential of Turkish chromite deposits, with emphasis on the Mugla area. Int Geol Rev 48:241–254

Uysal I, Zaccarini F, Sadıklar B, Bernhardt HJ, Bigi S, Garuti G (2009a) Occurrence of rare Ru–Fe–Os–Ir-oxide and associated platinum-group minerals (PGM) in the chromitite of Muğla ophiolite, SW-Turkey. N Jb Mineral (Abh) 185:323–333

Uysal I, Tarkian M, Sadıklar B, Zaccarini F, Meisel T, Garuti G, Heidrich S (2009b) Petrology of Al- and Cr-rich ophiolitic chromitites from the Muğla, SW Turkey: implications from composition of chromite, solid inclusions of platinum-group mineral, silicate, and base-metal mineral, and Os-isotope geochemistry. Contrib Mineral Petrol 158(5):659–674

Vergili Ö, Parlak O (2005) Geochemistry and tectonic setting of metamorphic sole rocks and mafic dikes from the Pınarbaşı (Kayseri) ophiolite, Central Anatolia (Turkey). Ofioliti 30:37–52

Warren CJ, Parrish RR, Waters DJ, Searl MP (2005) Dating the geologic history of Oman's Semail ophiolite: insights from U–Pb geochronology. Contrib Mineral Petrol 150:403–422

Yaliniz MK, Göncüoğlu MC (1998) General geological characteristics and the distribution of the Central Anatolian ophiolites. HU Earth Sci Bull 20:19–30

Yaliniz KM, Floyd P, Göncüoğlu MC (1996) Supra-subduction zone ophiolites of Central Anatolia: geochemical evidence from the Sarikaraman ophiolite, Aksaray, Turkey. Min Mag 60:697–710

Yıldız M, Balcı M, Sarıkaya A (1976) Burdur (Yeşilova-Tefenni) ve Denizli (Acıpayam) peridotit Massiflerinde krom – nikel prospeksiyonu [Cr-Ni prospecting report of Burdur (Yeşilova-Tefenni) and Denizli (Acıpayam) peridotite massifs]. Report No: 6336. MTA, (in Turkish, unpublished)

Yılmaz A (1981) Tokat ile Sivas arasındaki ofiyolitli karışığın içyapısı ve yerleşme yaşı [Inner structure of the ophiolitic melange and age of its emplacament]. Bull Geol Soc Turk 24(1):31–38 (in Turkish with English abstract)

Yılmaz Y (1984) Amanos Dağlarının Jeolojisi [Geology of Amanos Mountains]. Report No: 1920. TPAO, (in Turkish with English abstract)

Yılmaz A (1985) Yukarı Kelkit Çayı ile Munzur Dağları Arasının Temel Jeoloji Özellikleri ve Yapısal Evrimi [Basic geological characteristics and structural evolution of the region between the Upper Kelkit Creek and the Munzur Mountains]. Bull Geol Soc Turk 28(2):79–92 (in Turkish with English abstract)

Yılmaz Y, Tüysüz O (1984) Kastamonu-Boyabat-Vezirköprü-Tosya arasındaki Bölgenin jeolojisi [Geology of the Kastamonu-Boyabat-Vezirköprü-Tosya region]. Report No: 7838. MTA (in Turkish, unpublished)

Yılmaz A, Bedi Y, Uysal Ş, Aydın N (1997a) 1:100.000 ölçekli, açınsama nitelikli Türkiye Jeoloji Haritaları, Elbistan İ 23 paftası [Geology Maps of Turkey in 1:100.000 scale: İ-23 sheet] No: 50. MTA, (in Turkish with English abstract)

Yılmaz Y, Tüysüz O, Yiğitbaş E, Genç SC, Şengör AMC (1997b) Geology and tectonic evolution of the Pontides. In: Robinson AG (ed) Regional and petroleum geology of the Black sea and surrounding region, vol 68. AAPG, pp 183–226

Zaccarini F, Garuti G, Proenza JA, Campos L, Thalhammer OAR, Aiglsperger T, Lewis J (2011) Chromite and platinum-group elements mineralization in the Santa Elena ophiolitic ultramafic nappe (Costa Rica): geodynamic implications. Geol Acta 9(34):407–423

Zhou MF, Sun M, Keays RR, Kerrich RW (1998) Controls on platinum group elemental distributions of podiform chromitites: a case study of High-Cr and High-Al chromitites from Chinese orogenic belts. Geochim Cosmochim Acta 62(4):677–688

Chapter 4
Epithermal Deposits of Turkey

Tolga Oyman

Abstract In Europe and Middle East, Turkey is currently positioned as the largest producer of gold with a 2015 production of 27.5 t from predominantly porphyry and epithermal deposits. Although exploration for gold by advanced geochemical methods started in 1980s, Turkey entered into hard-rock mining based on cyanide process for extracting gold from low-grade ore in 2001. Before that, apart from placer mining, gold was sold in concentrate ore as by product in some deposits chiefly mined for base metals. Epithermal deposits are high-grade deposits dominated by open-space textures generally formed at depths of ~2 km with temperatures of < 400 °C. Due to their shallow-depth location, it is regarded that they represent easily mineable source of gold. This chapter is designed to focus attention on the geology of important epithermal gold mineralisation in Turkey with the aim to understand the basic regional and local geological setting and mineralogical and geochemical properties setting for the mineralisation. In the chapter the brief summary of selected epithermal deposits is emphasized the principal characteristics of important epithermal mineralisation all over Turkey including low, intermediate and high sulphidation types without taken into account their major economic element content on the base of reports from government and private companies and published or unpublished studies. Up to date, although literature on epithermal mineralisation in Turkey has been increasing with significant exploration and published data, still numerous questions remain unanswered and provide a source for future research.

4.1 Introduction

Mining in Anatolia dates back to nearly 3200 BC with the archaeological evidence showing that many of the epithermal deposits in western Anatolia and surroundings were exploited. The gold mining industry has a long history with its roots reaching ancient times in Anatolia, called also as Asia Minor. Around 550 BC, the first gold

T. Oyman (✉)
Department of Geological Engineering, Dokuz Eylül University, İzmir, Turkey
e-mail: tolga.oyman@deu.edu.tr

F. Pirajno et al. (eds.), *Mineral Resources of Turkey*, Modern Approaches in Solid Earth Sciences 16, https://doi.org/10.1007/978-3-030-02950-0_4

coin was minted in Salihli (West Anatolia) which had been known in antiquity as Sardis capital of Lydian Kingdom. Alacahöyük located at the junction of three trade routes: to Mesopotamia, to the Black Sea, and to the Aegean Sea was the most important civilisation in the production of gold artefacts in the Bronze age. Alacahöyük near the modern Turkish city Çorum (Central Anatolia), is regarded as the wealtiest city of pre-Hittite times. Due to its coarser gold grain size ranging up to visible gold and shallow emplacement, epithermal vein systems were the main targets for the Romans who had experienced mining methods from the different nations they had conquered and accumulated considerable experience which had been acquired in the course of centuries by many different ethnic groups. The Romans and their descendants mined on a large scale throughout Europe and Africa.

Gold is one of the most important items in Turkish economy both as investment instrument and raw material for the jewellery sector. As the world's fourth largest consumer of gold Turkey is in second place behind India in the production of gold jewellery. The Turkish gold mining industry is small when compared with giant gold producing countries but it is growing rapidly. Gold mining and extraction with cyanide-leach methods started in 2001 with the Ovacık gold mine by Newmont. Increasing gold production almost every year since 2001, growing from 2 tonnes to almost 35 tonnes in 2015 promotes Turkey as Europe's largest gold producer. More than 200 tonnes of gold were being produced between 2001 and 2014 and the Turkish Gold Miners Association estimates c.US$ 700 million has been spent on exploration by foreign companies in the past 25 years. Since a peak was reached in 2012–2013, the number of foreign companies with active exploration projects has decreased somewhat and this is partly due to the reduction of exploration budgets globally. Gold was produced as a by products or coproduct from base-metal and silver mines. Aegean, Black Sea and Central-East Anatolia are the leading gold-producing regions of Turkey. The scientific study on ore deposits in Turkey using modern methods of mineralogy and geochemistry started in the early 2000s. Most of these studies were focused on the deposits of Western Anatolia. In this chapter, on the basis of our studies and the cited published literature, we summarize and describe the principal geological, mineralogical and geochemical characteristics of selected epithermal deposits in Turkey.

The term "epithermal" was first defined by Lindgren (1933) according to the mineralogy, textures, alteration, and temperature and depth of ore formation. In the beginning of 1980s paragenesis based nomenclature has been started to identify the certain type epithermal deposit owing to its high sulphidation state sulphides and characteristic acid-sulphate alteration mineral assemblages (Ashley 1982; Bethke 1984; Bonham 1984, 1986; Berger 1986; Heald et al. 1987; Berger and Henley 1989). Between 1987 and 2003 epithermal deposits have been divided into two groups as high-sulphidation (acid-sulphate, quartz-alunite) and low-sulphidation (adularia-sericite) types, by different workers on the base of their position relative to the magmatic hydrothermal system which is responsible for the associated metal contents and hydrothermal alteration (Henley 1985; Heald et al. 1987; White and Hedenquist 1990; Cooke and Simmons 2000; Hedenquist et al. 1996, 2000). More recently on the base of tectonic setting and volcanic associations, the nature of fluids

involved and the mineral assemblages of epithermal deposits are subdivided into low (LSEM: Low Sulphidation Epithermal Mineralisation), intermediate (ISEM: Intermediate Sulphidation Epithermal Mineralisation), and high (HSEM: High Sulphidation Epithermal Mineralisation) sulphidation subtypes (Sillitoe and Hedenquist 2003). Intermediate sulphidation deposits correspond to "carbonate base metal deposits" of Corbett and Leach (1998). For this review, we use the widely accepted classification scheme of high-sulphidation low-sulphidation type deposits and intermediate sulphidation and the term "intermediate sulphidation" will be used to describe both sulphidation state and a separate sub-type for "carbonate base metal deposits" of Corbett and Leach (1998).

4.2 Tectonic Settings and Ages of Mineralisation

The Tethyan Orogenic Belt is one of the most complex tectonically active regions of the Earth's crust. Turkey encompasses several continental fragments of the super-continents, Gondwana and Laurasia which were sutured during the closing of the Tethyan oceanic basins during the late Paleozoic to Cenozoic period (Şengör and Yılmaz 1981; Şengör et al. 1984). The Izmir-Ankara-Erzincan suture (IAES) (Brinkmann 1966), representing by the closure of the northern branch of the Neo-Tethys along a northern-dipping subduction and the following continental collision between Laurasia and Gondwana during in the Late Cretaceous-Eocene is accepted as the main structure in the tectonic framework of Turkey (Ketin 1966; Okay and Tüysüz 1999). The IAES zone extending nearly 1500 km between Rhodope-Stranca in the west and Caucasus in the east separates the Sakarya Zone of Pontides (Laurasia) from the Anatolide-Tauride Platform (Gondwana) (Şengör and Yılmaz 1981; Okay et al. 1996).

In the West of Anatolia IAES separates the Sakarya Zone of Pontides from the Bornova Flysch and Afyon and Tavşanlı Zones which were derived from deeply buried northern edge of the Anatolide-Tauride Platform. In the east however, IAES zone represents northward subduction of the northern branch of the Neotethys beneath the southern margin of the Laurasia and continental collision between Eastern Taurides and Pontides. This subduction generated well-developed Cretaceous arc magmatism which is known as the Pontide arc. The Intra-Pontide Suture which is accepted as a small oceanic branch within the Neotethyan system separates the Istanbul and Sakarya fragments in northwest Turkey. Furthermore, the existence of another suture zone, Inner Tauride Suture, is still controversial. In many studies, this suture zone is placed between Central Anatolian Crystalline complex (CACC) which is accepted as an isolated microcontinent rifted from northern margin of Gondwana during the Triassic time and eastward continuation of the Afyon zone (Okay and Tüysüz 1999). This oceanic branch is assumed to have closed along northward subduction beneath the CACC during the Late Cretaceous (Pourteau et al. 2010).

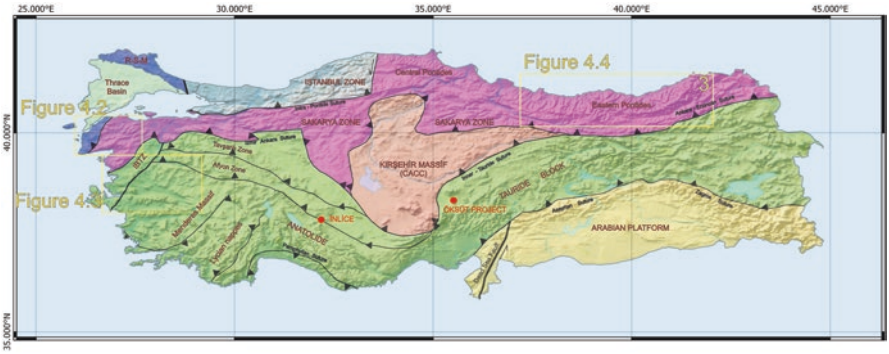

Fig. 4.1 Tectonic framework of Turkey showing the major sutures and continental blocks. (Modified after, Okay and Tüysüz 1999)

Within this tectonic framework epithermal gold deposits occur mainly in three regions: Western Anatolia, Central Anatolia and Eastern Black Sea. These regions are separated from each other with distinct geodynamic evolution and associated magma generations with different geochemical character reflecting spatial and temporal variations (Fig. 4.1).

4.3 Distribution and Geological Features of Epithermal Deposits of Turkey

4.3.1 Western Anatolia Volcanic and Extensional Province (WAVEP) in Western Turkey

The province consists of several NE-trending structural domes composed of metamorphosed Palaeozoic and Mesozoic rocks, volcanic piles and intrusive complexes, and intervening east to northeast trending extensional basins filled with Paleogene and younger volcanoclastic sequences (Fig. 4.2). WAVEP hosts metallogenic province in the Biga Peninsula (NW Anatolia-Turkey) covering an area both in the Sakarya block and a slice of Rhodope Massif. Pre-Jurassic basement rocks, including the Kazdağ metamorphic core complex and numerous exhumed igneous bodies with coeval volcanic rocks (e.g. Okay et al. 1991; Bonev and Beccaletto 2007; Cavazza et al. 2009) can be found throughout the Sakarya block. Northward subduction of northern branch of Neo-Tethyan Ocean initiated the magmatism in the Biga Peninsula during the Late Cretaceous to Eocene. The Late Eocene-Early Oligocene ages (e.g. Kozak and Eybek plutons) may record the subduction related magmatism and the initiation of continental collision. Magma generation during Late Oligocene and Early Miocene is strongly associated with astenospheric uplift in an extended continental crust due to the slab roll-back and/or break-off the

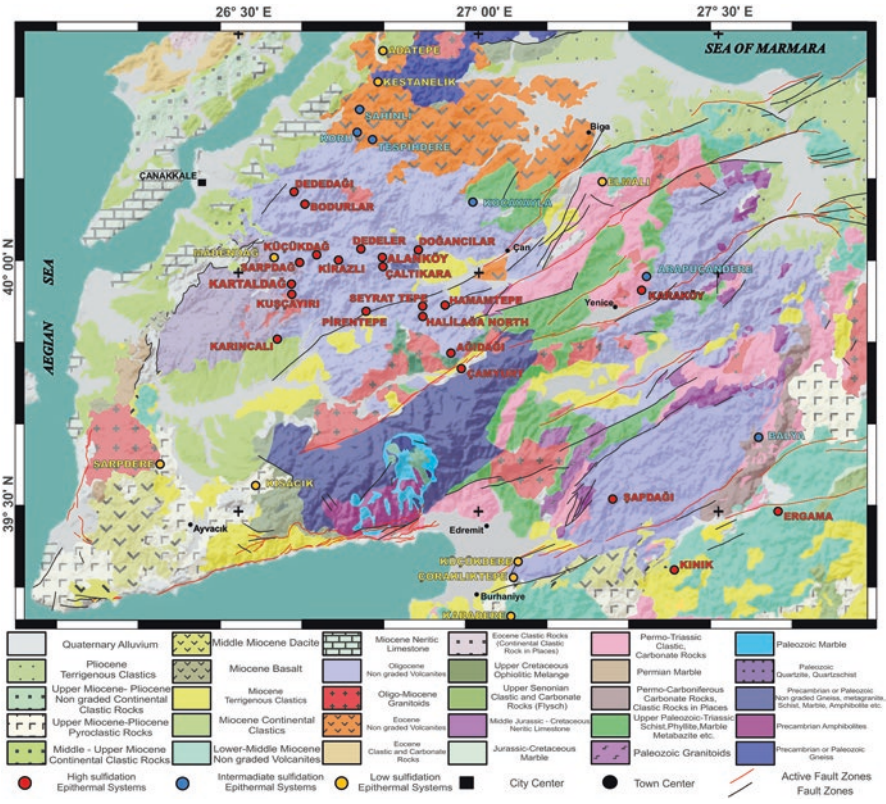

Fig. 4.2 Regional geological map of Biga Peninsula and spatial distribution of significant epithermal mineralisation. (Geology modified from MTA Emre et al. 2013; Akbaş et al. 2017)

subducted slabs (Altunkaynak et al. 2012, Black et al. 2013; Aysal 2015). Recent Sr and Nd isotope results from plutons North of Yenice (Çanakkale) indicate that intrusions were generated by magmatic assimilation and fractional crystallization and formed during large-scale lithospheric thinning during the Late Oligocene (Çiçek et al. 2017).

In Biga Peninsula, world class epithermal gold deposits and prospects are mainly hosted and spatially associated with Cenozoic volcanic rocks (Pirajno 2009). The Cenozoic volcanic rock associations in Biga Peninsula can be divided into three main groups based on their geochemical features and ages. The Eocene volcanic rocks, known as Balıklıçeşme volcanics in the Biga Peninsula, include andesitic and basaltic lavas with medium- to high-K in character which are interlayered with shallow marine sedimentary rocks towards the upper part of the volcanic sequence (Ercan et al. 1995; Altunkaynak et al. 2012; Gülmez et al. 2013). The K-Ar dating of these volcanic rocks yields 52–34 Ma (Dönmez et al. 2005; Kürkçüoğlu et al. 2008; Gülmez et al. 2013). Widespread high-K calc-alkaline volcanism took place during the Late Oligocene to Early Miocene and comprise andesite, dacite and

trachyandesite with large amounts of dacitic-rhyolitic ignimbrite, pyroclastic and tuffaceous rocks (Ercan et al. 1995; Chakrabarti et al. 2012). The Oligocene-Miocene volcanic associations comprise the Oligocene Çan volcanics (34.3 ± 1.2 and 29.2 ± 0.6 Ma), Kirazlı volcanics (31.1 ± 0.7 and 27.6 ± 0.6 Ma) and Early-Middle Miocene Behram volcanics (21.5–6.8 Ma) in the Biga Peninsula (Ercan et al. 1995). Continuation of Cenozoic volcanic activity to the late Miocene is represented by Na-alkaline volcanism including basaltic-trachyandesitic lavas and dykes. They are known as Ezine volcanics in northern Anatolia and yield an Upper Miocene age ranging from 11.68 ± 0.25 to 6.47 ± 0.47 Ma (Ercan et al. 1995; Aldanmaz 2002). In the North and around Kozak Pluton the volcanic association comprises lavas and pyroclastic rocks of nearly equal proportions. The compositions range from dacite-rhyolite to basaltic andesites (Altunkaynak and Yılmaz 1998). In the south Dikili group is Early-Middle Miocene in age and consists mainly of pyroclastic rocks, andesitic-dacitic lavas, lava breccia, lahar flows and associated sedimentary rocks. The Çandarlı group consists of Upper Miocene-Pliocene lavas and sediments. The volcanic rocks consist mainly of rhyolitic domes and basaltic trachyandesite-basaltic andesite lavas erupted along the NW–SE and NE–SW trending fault systems; the faults controlled the development of the Çandarlı depression (Karacık et al. 2007).

4.3.2 Epithermal Systems In Biga Peninsula

The Biga Peninsula located in northwestern Anatolia, represents one of the important Turkish metallogenic province, which has been divided into several tectonic zones separated by suture zones. This area is one of the most widely recognised metallogenic provinces in terms of precious and base metal potential in the world due to the diversity in metallogeny and abundance of mineral occurrences with >50 hydrothermal Pb-Zn-Cu ± Ag ± Au and Au-Ag deposits (e.g., Koru, Tesbihdere, Balya, Arapuçandere, Kalkım-Handeresi, Küçükdere) and ongoing projects (e.g., Şahinli, Kartaldağ, Kestanelik, Çataltepe, Kirazlı, Ağı Dağı, TV Tower), (Fig. 4.2). Until the early 2000s the importance of this metallogenic province had not been fully understood, but has since emerged in the spotlight of geological studies with modern analytical techniques (Bozkaya and Gökçe 2001, 2009; Bozkaya 2009; Yılmaz et al. 2010; Yalçınkaya 2010; Çiçek et al. 2012; Yiğit 2012; Çiçek 2013; Bozkaya et al. 2014; Çiçek and Oyman 2016). Among the most essential and debatable problems regarding the genesis of the base metal ± silver ± gold and gold ± silver deposits in Biga Peninsula can be given as the origin of the fluids, spatial and temporal relationship between volcanism and ore-forming hydrothermal activity.

4.3.2.1 TV Tower

The TV Tower prospect is located in the central part of Biga Peninsula. The basement rocks of the TV Tower property is composed of metamorphic basement rocks of Paleozoic and Early Mesozoic mainly including various schists and phyllite. The basement is intruded by the Eocene (~43 Ma) calc-alkali Kuşçayırı pluton composed of feldspar-hornblende-biotite porphyritic monzonite (Yiğit 2012) at the southern end of the property. Both basement and intrusive rocks are overlain by a thick pile of volcanic rocks including rhyodacitic to basaltic-andesite lavas. The volcanic rocks are overlain by crystal lapilli tuffs and sedimentary rocks with a wide grain size spectrum from mud to conglomerates. The property covers an area of 67 km^2 and contains nine targets including Küçükdağ, Kayalı/Nacak, Karaayı/K2, Sarp/Columbaz, Valley, Kestanecik, Gümüşlük, Tesbihçukuru and Kartaldağ West. Küçükdağ target that is hosting the third largest silver resources in Turkey, is characterized characterised by a high sulphidation gold-pyrite-enargite assemblage and associated silicification and advanced argillic alteration. Many of the targets, except Gümüşlük and Kestanecik which are low-sulphidation epithermal gold targets, are characterised by high-sulphidation ore assemblages in TV Tower property. These targets are in association with lithocaps which are spatially, temporarily and genetically linked to shallow seated mineralised porphyritic intrusions.

The Küçükdağ target is one of the most important project among nine target areas in TV Tower property (Fig. 4.2). Tuff and volcaniclastic rocks are ideal hosts for structure controlled mineralisation due to their high permeability in Küçükdağ. Gold is predominantly found in the permeable lithic lapilli tuffs and epiclastic rocks with lesser amounts in andesitic breccias and welded lithic lapilli tuff. Copper is mainly associated with Au in the sedimentary sequence and volcaniclastic rocks respectively. In the upper oxide zone gold mineralisation is associated with massive to weakly vuggy quartz alteration with hematitic breccias, WNW- and NS-striking shears, and fracture infills in rhyodacitic crystal and lapilli tuff (Smith et al. 2014). The lower gold zone is largely hosted in dacitic tuff with different subtypes of ore formation styles that can be divided into three subzones including (a) Stratiform gold in zones of dark grey to black vuggy quartz (b) ESE-WNW trending gold-sulphide veins with varying amounts of quartz, (c) Au-Ag breccia (Smith et al. 2014). The silver-rich zone is primarily hosted in the fluvial-lacustrine sequence and overlying andesitic breccia and gold-copper mineralisation. Characteristic sulphide minerals and sulphosalts of high-sulphidation systems represented by enargite which is precipitated in veins and breccia zones. Tetrahedrite-tennantite, famatinite, bournonite, seligmannite, pyrite, marcasite, chalcopyrite, covellite are the main sulphide and sulphosalt minerals (Ross 2013a, b). While principal sulphide minerals associated with pyrite-marcasite which are banded and very fine grained along main silver mineralisation. Alunite, barite, dickite and kaolinite are widespread clay minerals associated with ore in veins and breccia zones.

4.3.2.2 Ağı Dağı

Similar to worldwide HSEM hosted volcanic sequences, the Ağı Dağı deposit formed in the Oligo-Miocene volcanic suite composed of andesitic, dacitic and rhyolitic rocks. Igneous rocks of intermediate composition formed either as porphyritic intrusions or porphyritic andesite lavas at the bottom of the sequence, whereas the dacite-rhyolite facies are located at the top. The entire volcanic sequence is cut by mushroom shape pipes of phreatic and phreatomagmatic breccias. Although gold mineralisation is present in five zones including the Baba, Ayı Tepe, Fire Tower, Ihlamur and Deli Zones, resources will only be exploited at Baba, Deli and Fire Tower zones. The Ağı Dağ north-east trending silica cap and associated alteration occupies a discontinuous zone of 4 × 2 km extent characterised by a massive vuggy silica core. The Baba, Fire Tower and Deli zones occur along the east side of the NE-SW trending mountain ridge, characterised by silicified dacite and phreatic breccia that fills a paleo-basin in dacite and feldspar porphyritic andesite. Alteration assemblages including massive silica, vuggy silica, advanced-argillic, argillic, propylitic, and sericitic facies indicate the role of hot acidic fluid and vapour phases associated with a deeper intrusion related hydrothermal system. As a result of leaching by the hot acidic fluid and vapour phases both vuggy and massive silica formed in the core of the high sulphidation system. The gold is associated mainly with pyrite in the intense silicic alteration comprising both massive and vuggy silica.

Çamyurt is located about 3.5 km southeast of Ağı Dağı. It is a silica ridge lying along 1.5 km at NE-SW direction. Main lithological unit at Çamyurt is andesite which is locally cut by phreatic breccia. Dacite is shown only at northern area. Gold mineralisation is mostly in andesite which is covering the largest part of the area and less in phreatic breccia. The main alteration trend is NE to SW along the main structure trend. Silica alteration, advanced argillic, argillic and propylitic alterations are the main alteration types at Çamyurt. Gold mineralisation is associated with silica alteration which has NE-SW trend along the main structure. Çamyurt has a higher contained Au grade than both Kirazlı and the Ağı Dağı deposits.

4.3.2.3 Kirazlı

Kirazlı is situated 25 km to the northwest of Ağı Dağı mineralisation and 10 km east of TV Tower property (Fig. 4.2). Çamlıca Metamorphics of Lower-Middle Triassic Karakaya Complex are exposed as basement rocks. Various schists and ultramafic rocks of Çamlıca Metamorphics are overlain by andesitic tuffs of Oligocene Çan Volcanics. Mineralisation consists of gold-silver-copper bearing veins and veinlets, hydrothermal breccia, phreatic and phreatomagmatic breccias hosted in dacitic-andesitic volcanic rocks. The sequence is cut by gold-hosted heterolithic, phreatic and phreatomagmatic breccias that were emplaced as mushroom-shaped pipes. The root zones of mushroom-shaped breccia pipes were intersected at a vertical depth of 400 m. Multistage generation of silicification is represented by grey massive and vuggy silica, chalcedonic to opaline silica, grey quartz with a high pyrite content

and fracture-filling crystalline silica is the most prominent alteration type with advanced argillic alteration. Silica ledges and their sub-vertical roots are surrounded by advanced argillic alteration. Degassing of hot acidic magmatic vapour prompted intense leaching of volcanic rocks to form vuggy quartz texture of the silica ledges and the associated advanced argillic alteration around it. Vuggy silica derived as a residual product of acid leaching which is characteristic texture of silicification with massive and sugary silica. Hydrothermal breccia with vuggy silica, advanced argillic and silicic alterations are the prominent alteration facies in association with high grades of gold and silver. In advanced argillic alteration the main minerals in association with silica are alunite, dickite and pyrophyllite. Well developed, multiphase silicification is the most common and widespread alteration in association with phreatic and hydrothermal breccias. Earlier argillic and later advanced argillic alterations formed around the margins of phreatic breccia pipes due to induced secondary porosity and permeability. Propylitic alteration which has been intersected in deeper levels seems earlier than the argillic alteration. Based on spatial and temporal relationship with breccia pipes, sulphide and gangue paragenesis, alteration assemblages this mineralisation is classified as high-sulphidation epithermal gold deposit (Alamosgold company report 2012).

4.3.2.4 Kartaldağ

The Kartaldağ gold mine is located 55 km southwest of Çanakkale. The Kartaldağ gold mine as similar to many epithermal deposits, the gold in Kartaldağ has been exploited since ancient times. Kartaldağ property was subjected to an exploration program including trenching, tunnelling and drilling by MTA during 1960–1962. The mine was reopened by Çanakkale Mining Co. in the late 1980s. The Kartaldağ epithermal vein system is hosted by Middle Miocene dacite porphyry which is the volcanic equivalent of granodioritic intrusions in the area. Kartaldağ fault is the most prominent structure in the area which acts as a conduit for the ore-forming hydrothermal fluids. In the early phase of silicification, vuggy quartz is accompanied by massive silicification. Vuggy texture formed due to leaching of the phenocrysts (e.g., plagioclase and hornblende) of the host dacitic volcanic rocks by acidic hydrothermal fluids. The Au mineralisation is in association with intensive pinkish coloured hypogene quartz-alunite and vuggy quartz assemblages. The late phase of silicification is represented by coarse to medium grained, banded, comb, sometimes colloform, and generally zoned quartz crystals truncating early phase massive silicification. Leaching of the host volcanic rocks was followed by the development of argillic alteration dominated by quartz-alunite-pyrophyllite and quartz-kaolinite from core to rim. Quartz-kaolinite alteration is the most widespread type of alteration, enveloping the quartz-alunite-pyrophyllite±kaolinite assemblage extending to the NW. Chlorite/smectite–illite±kaolinite form the propylitic alteration zone.

The spatial association of the alteration and ore minerals, dominated by pyrophyllite, kaolinite, and alunite, vuggy quartz texture, enargite, and covellite, pyrite, and light coloured sphalerite (indicating high Fe^{3+}/Fe^{2+}) support the formation of the

Kartaldağ epithermal gold mineralisation under the control of low pH-oxidising fluid typical of high sulphidation type epithermal deposits (Ünal-İmer et al. 2013; Einaudi et al. 2003; Sillitoe and Hedenquist 2003). Although homogenisation temperatures from vein quartz are distributed in a wide range, they are scattered mainly between two intervals; 190–290 °C and 300–370 °C (Vural 2006). Vural (2006) ascertained that the quartz crystallisation in association with gold precipitation started to occur at 370 °C and it lasts till about 190 °C. Based on fluid inclusion studies of quartz samples, primary fluid inclusions from late quartz exhibit with relatively low homogenisation temperatures (245–285 °C) and low salinities (<1.7 wt.% NaCl eq.) indicating that a significant amount of meteoric water interacted with the hydrothermal system. The formation of pyrophyllite, kaolinite, alunite-bearing alterations and pyrite alteration and vuggy quartz were generated by leaching under oxidising conditions. Enargite also formed in relatively oxidising conditions. Combined petrographic and geochemical studies suggest that, gold mineralisation at/below the boiling level might have occurred at temperatures greater than 285 °C. The Kartaldağ epithermal gold mineralisation was formed under low pH-oxidising fluids typical of high-sulphidation type epithermal deposits (Ünal-İmer et al. 2013).

4.3.2.5 Madendağ

The Madendağ gold deposit is located nearly 20 km northwest of the Kartaldağ mine and 50 km southwest of Çanakkale (Fig. 4.2). Mining in this deposit was first recorded in the beginning of the last century. An exploration program including trenching, tunnelling and drilling was conducted by MTA during 1960–1962. The deposit is hosted by quartz-mica schists of Paleozoic Çamlıca formation, (Okay et al. 1991) which is overlain and intruded by Middle Miocene to Late Oligocene volcanic rocks including andesite and dacite flows and domes. The Çamlıca formation comprises mainly of quartz-mica schists and calc-mica schists. Both mica schists and dacitic, andesitic volcanic rocks display widespread argillic alteration. The main mineralisation is hosted in the two main silicified structures trending E-W to WNW-ESE and almost parallel to each other with southward dip. In the vein zone multi-stages of ore deposition including network of quartz veins, brecciation and intensive alteration are observed.

Detailed studies by Ünal (2010) and Ünal-İmer et al. (2013) reveal that mineralogy of argillic alteration around mineralisation in Madendağ is controlled both by host rock composition and the distance from the quartz veins. Although the main mineralisation is sulphide poor, in places pyrite disseminations are associated with low grade gold. The gold quartz-cemented breccias have values ranging from 0.27 to 20.60 ppm Au. The low homogenisation temperatures mostly in the range between 235 and 255 °C and low salinities (0.0–0.7 wt.% NaCl eq.) combined with paragenetic and stable isotope characteristics indicate that Madendağ could be regarded as “Low Sulphidation” epithermal deposit (Ünal-İmer et al. 2013).

4.3.2.6 Kestanelik (Şahinli)

The Kestanelik gold deposit is located 35 km NE of the regional centre of Çanakkale, 4 km west of Şahinli village on the Biga Peninsula. Traces of small-scale historical mining activities are observed around the epithermal quartz veins. Low sulphidation epithermal veins hosted within Paleozoic metamorphic rocks and Lutetian quartz-feldspar-hornblende porphyry stock (Ünal-İmer et al. 2013). Kestanelik property consists of a series of low sulphidation style epithermal quartz vein zones namely Karatepe, Karakovan (KK1, KK2 KK3), K (K1, K2, K3, KS and KW) and Meydan zone from north to south respectively. NE-SW and E-W trending vein systems exposed over a strike length up to 400 m and vary in width from 1 to 13.6 m. Veins are dipping as moderately to shallow towards southeast and south respectively. The Meydan Zone, which lies in the southern part of the porphyry intrusion, is characterised as a zone of silicification rather than representing discrete quartz vein zone. However, the gold tenor is generally much less then major quartz veins. The majority of gold-silver mineralisation is in association with multiple episodes of fluid flow. At Kestanelik epithermal system, the degree of erosion can be inferred from near surface high-grade zones in combination with variety of textures including cockade, hydrothermal brecciated, colloform-crustiform banding. At Kestanelik recent studies show that, structural locations along pathways such as vein bends are more favourable than replacement processes for gold precipitation (Gülyüz et al. 2017). Pyrite is the only sulphide mineral associated with the gold mineralisation. It is not particularly widespread and is usually finely disseminated in the breccia matrix and some of the quartz veins. The dominant alteration that appears to be associated with the mineralisation is clay in the form of illite-smectite. An alteration halo of clays is common around the veins.

The Scoping Study Update assumes processing of approximately 844,000 tonnes of ore per year, at an average grade of approximately 2.53 g/t gold and 1.9 g/t silver for life of mine production averaging 63,000 oz of gold and 38,000 oz of silver per year. The Scoping Study Update has a proposed mine life of 8 years (Chesser Resources, news release 2013). It is planned that first gold production will commence at the end of 2017.

4.3.2.7 Koru and Tesbihdere

The Koru and Tesbihdere mining districts in the Biga Peninsula, consist of twelve deposits covering approximately 12 km^2. Early-Oligocene basaltic andesite lavas and dacitic lava and tuffs in the south and Late-Oligocene rhyolitic tuff-lava domes and late stage andesite dykes of Çan Volcanics are the main volcanic units around the Koru and Tesbihdere mining districts (Siyako et al. 1989; Ercan et al. 1995, 1998). Mineralisation in the Koru and Tesbihdere mining districts are mainly hosted by rhyolitic lava-domes and tuffs. While the NW-trending fault system between domes and tuffs hosts the Au-Ag enriched base metal epithermal veins, hanging wall rocks of the vein system host brecciated, stockworks and disseminated ore

(Beşir 2003; Yalçınkaya 2010; Çiçek et al. 2012; Çiçek 2013; Çiçek and Oyman 2016). Çiçek and Oyman (2016), focused on seven mineral systems in the Koru and Tesbihdere districts, which show a complex paragenetic sequences and mineral zonations. On the basis of the paragenetic sequence, hydrothermal alteration assemblages, and the nature of the ore-forming fluids, the Au-Ag enriched base metal epithermal deposits in the Koru and Tesbihdere districts are classified as volcanic-hosted intermediate-sulphidation epithermal deposit (Çiçek and Oyman 2016). In the Koru district, galena is the dominant ore mineral in barite-quartz veins containing sphalerite, chalcopyrite, pyrite, bornite, enargite and tennantite can be subdivided into sphalerite-galena dominated Tesbihdere mineralisation and chalcopyrite-pyrite dominated Bakır and Kuyu mineralisation. The Ag/Au ratio is high in Ag showing assays of up to few hundreds of ppm associated with small quantities of gold with maximum 3.14 g/t Au values either as free grains in quartz or as micro inclusions in pyrite and galena. The most widespread silver minerals are polybasite, pearceite, argentite and native silver, which commonly occur as replacements of galena, sphalerite and pyrite, and other sulphides, or as fillings of microfractures in sulphides and quartz. Isotopic composition indicates a progressive dilution of ore forming fluids as a result of increasing input of meteoric water during transportation along fluid flow path from the Koru to Tesbihdere mining district. The intensity of boiling in the area may also show a decrease with distance away from the Koru mining district and an increase in δ^{18} O in the residual liquid, which probably resulted by steam separation during boiling (Çiçek and Oyman 2016).

4.3.2.8 Arapuçandere

Arapuçandere Pb-Zn-Cu (Au-Ag) ISEM is located in the northeastern part of Yenice (Çanakkale-Biga Peninsula), and is hosted by Triassic metasandstones and metadiabase dykes of the Hodul unit of the Karakaya Complex (Fig. 4.2). The first studies at Arapuçandere were conducted by MTA (i.e. Mineral Research and Exploration Institute of Turkey) as part of a research project in the 1970s. The deposit contains a total reserve of 4 Mt at 16.4% Pb, 12.1% Zn and 2.2% Cu averaging of 4 g/t Au and 260 g/t Ag (MTA 1993a, b). The highest gold grade is obtained from upper part of the deposit (308 m asl) which reaches up to 20 g/t Au, while low-grade gold is observed in deeper levels where Au assayed up to 4 g/t in massive ore. The Arapuçandere mining area contains five sets of mineralised veins parallel to each other in the east-west trending structural zones and these veins were numbered I to V, from NW to SE (Bozkaya et al. 2008; Bozkaya 2011; Yiğit 2012). After intermittent mining operations in the early 1980s, I, II and III veins have been closed because of the uneconomic ore contents. At present, Nesco mining company is actively operating the ore production from IV and V veins. These two veins systems show a close genetic relationship as suggested by their temporal and spatial relationships. Both veins show an E-W strike with steep dips 70–80°S at the surface, however the dips of these veins tend to decrease (approximately 40–50°S) downward and the

veins crosscut at an elevation of 120 m above sea level (asl). The IV and V veins extending to lower level are vary from 0.6 to 17 m in width and mining by conventional underground techniques from 6 different production levels show that they are about 200 m length and extend to a depth of 120 m (asl). The veins (IV and V) and associated stockworks at Arapuçandere show various textures including crustiform, colloform, bladed and brecciated. Ore paragenesis within the veins display a similar assemblage, in order of abundance, comprising mainly galena, sphalerite, chalcopyrite, pyrite, Ag-sulphosalts and minor amount of tennantite-tetrahedrite, magnetite, hematite and chalcosite-covelline. Gangue minerals in both veins exhibit a zonation pattern represented by decrease in quartz and increase in calcite with locally minor barite towards deeper levels of the deposit. Silver mainly occurs as Ag-sulphosalts which fills fractures and cavities within the earliest sulphides.

4.3.2.9 Kısacık

The Kısacık gold deposit is a characteristic multi-stage gold mineralisation within the Ayvacık-Karabiga tectonic zone of the Biga Peninsula (Fig. 4.2). The property was discovered by MTA during 2008 exploration program by defining two old adits and at least four small pits which are suspected to represent gold mining operations (Özpinar et al. 2012). Deposit area is underlain by basement rocks of the Paleozoic Kazdağ Metamorphic Group, which is unconformably overlie younger Upper Cretaceous Çetmi Ophiolitic Melange. Mid-Miocene volcanic rocks including ignimbrites, rhyolite, rhyolitic tuffs and lapilli tuffs mainly host the gold mineralization and has angular disconformity over pre-Tertiary rocks. The Pliocene conglomerates, sandstones and siltstones unconformably overlie older rock units.

Gold mineralisation at Kısacık property is controlled by structure and lithology. Gold occurs as two different type of mineralisation. The first one is relatively high grade gold ore associated with quartz-sulphide veins within pumice and low grade disseminated gold mineralisation within thick layers of pyroclastic rocks. NE-SW trending quartz-sulphide veins at the centre are surrounded by illite-sericite and chlorite-carbonate clay alterations from inner to outer respectively. Based on the MTA's resource estimations, property comprises 56.5 Mt (proven+probable+possible) grading 0.5 g/t Au mineralisation (Özpinar et al. 2012).

4.3.3 Epithermal Systems in the South of Biga Peninsula

4.3.3.1 Küçükdere and Çoraklık Tepe

The Küçükdere deposit is a fracture-filling vein-type formed in extensional tectonic settings (Fig. 4.2). Well developed tension fracture systems and normal faults are the major components of the extensional tectonic settings. The vein zone

is associated with the main fault which extends in a SW to NE direction. The vein system consists of two main segments with different inclinations. The main vein extends east to northeast and dip towards the south with an inclination varying between 60 and 90°. The vein system is traced over approximately 5000 m strike length and few tens of metres down plunge from surface with a different thickness varies between 1 and 50 m. A subhorizontal vein formed as a branch of the main vein and outcrops in the east and south east of Germe vein. It strikes east to northeast and dips 0–30° to the northwest. Ore and gangue minerals precipitated as episodic open-space filling with various internal textures including colloform-crustiform, cockade, brecciated, drusy, comb and bladed textures. Intense brecciation and stockworking occur in the hanging wall and are closely associated with the main fault zone. Among the four mineralisation centres namely Germe, Karayanık, Çoraklık, Çengel in the Küçükdere, the abundance and variations of sulphide minerals are significant in Germe pit. While higher gold grades are controlled by sulphide-rich assemblages (>5% Py) in Germe, textural control plays a far greater role in Karayanık and Çoraklık, such as bladed and brecciated-cockade without the significant sulphide assemblage. The total amount of sulphide minerals in Germe, did not exceed 10% of the total vein minerals. The ore minerals include: pyrite, sphalerite, galena, chalcopyrite as the major phases with minor amounts of tetrahedrite, bornite, hessite, argentite, electrum and native gold with supergene phases. Combined fluid inclusion and stable isotope analysis in Germe and Karayanık suggests that precious metal mineralisation most likely occurs in a wide range of vertical depth.

In Çoraklık pit, from NE to SW the vein curves to E-W and slightly to WNW along its strike while the dip ranges between 47 and 50° to N. Textural variation along the open pit walls indicates that the vein cross cut and are displaced vertically by normal faults. The Çoraklık vein and associated silicified zone are enveloped by a mushroom-shaped argillic alteration and both hosted by propylitic altered andesitic rock. Along the contact between the vein and the hanging-wall disseminated and stockwork ore is hosted extensively by an argillic alteration zone in the hanging wall. The propylitic assemblage consists of chlorite, calcite with lesser amounts of epidote and pyrite. In addition, amorphous silica, crustiform-colloform, cockade and breccia, bladed, comb and carbonate replacement textures were identified macroscopically in Çoraklık. Jigsaw, plumose and spherulitic textures were identified in thin section. In the boiling zone gold mineralisation is strongly related to sulphides including chalcopyrite, pyrite, sphalerite and galena. According to our preliminary fluid inclusion measurements, fluids responsible for Çoraklık Tepe mineralisation showed that the fluid was a low T, low salinity, H_2O-NaCI-$CaCI_2$-$MgCI_2$ brine. Inclusions from the Çoraklık open pit are two-phase, liquid-rich inclusions and occur in coarse quartz crystal with a cockade texture. The final melting of the ice occurred with a final temperature range of −0.4 to −0.9 °C which yielded salinities between 0.7 and 1.6% wt. NaCl equivalent.

4.3.3.2 Kubaşlar

The Kubaşlar property is located on the northwest margin of Kozak Caldera of the Kozak Plutonic Complex (Fig. 4.3). The district also contains the Ovacık and Küçükdere mines and a number of other exploration prospects including Karadere and Gömeç. A low sulphidation quartz vein and associated multi-stage breccia structures 200 m in width and 1400 m in length extends NW-SE between Cenozoic volcanic-plutonic rocks and meta-sedimentary rocks of the Kınık Formation.

Good examples of flamboyant, feathery, plumose, colloform banded plumose textures have been identified in the vein system. This texture is regarded as a typical recrystallisation texture related to boiling and thought to develop after the amorphous silica phase and before the later crystalline quartz phase. Clast supported breccia composed mainly of quartz and rock fragments supported by microcryptocrystalline quartz and opaque minerals (Tezer 2006). Fragments with well-developed colloform banded, colloform-crustiform, plumose jigsaw textures with amorphous and crystalline quartz phases indicate repeated episodes of sealing and fracturing during the lifetime of the shallow hydrothermal system. Opaque minerals are pyrite and marcasite in outcrop samples. Since the acquisition in 2008 by Koza Gold, exploration included drilling programs in 2011 and 2012 as well as surface

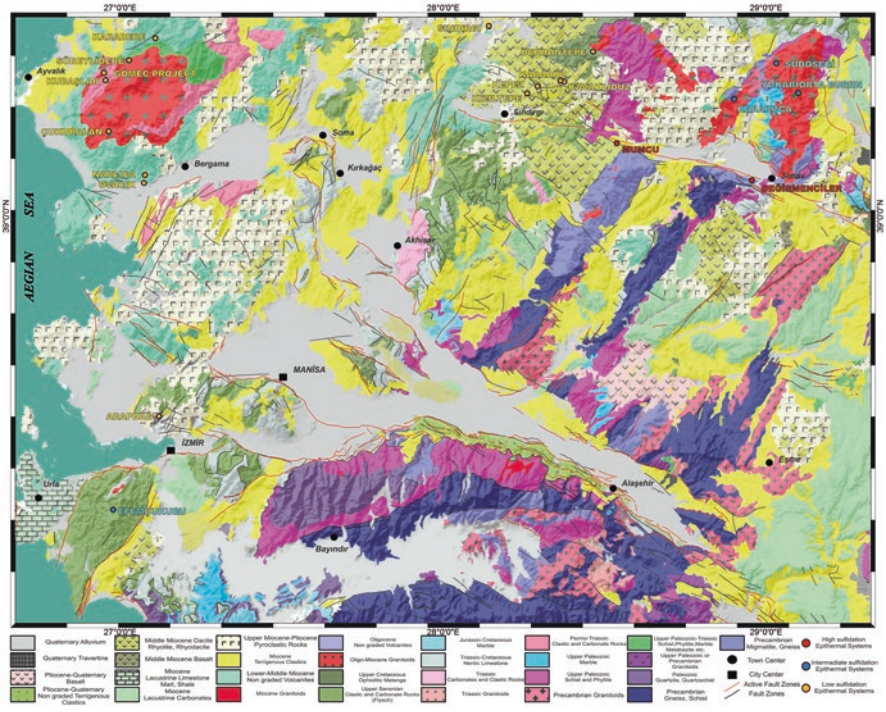

Fig. 4.3 Regional geological map of Inner-west Anatolia and spatial distribution of significant epithermal mineralisation. (Geology modified from MTA Emre et al. 2013; Akbaş et al. 2017)

sampling, geophysics, geochemistry and resource modelling. Kubaşlar deposit has 70.000 oz grading 2.31 g/t Au and 14.53 g/t Ag.

4.3.3.3 Gömeç

The Gömeç Project comprises five contiguous exploration licenses and is an early-stage gold exploration project located 35 km northwest of Ovacık and 20 km southwest of the Havran-Küçükdere gold deposit and 1 km south of Koza Gold's Kubaşlar low-sulphidation gold Project (Fig. 4.3). The Gömeç project was acquired through government tender by Royal Road's JV-Partner, Oremine Madencilik Sanayi ve Ticaret Inc. ("Oremine") in 2008. Soil geochemistry within the Samantaşı and Oremine's Kubaşlar (Kubaşlar East) licences indicated anomalous gold values in excess of 0.5 ppm up to 6 ppm Au which are interpreted to reflect gold-bearing zones. Soil anomalies are fault-controlled and extending E-W in Kubaşlar. At Gömeç 4494 m of combined reverse circulation and diamond drilling was conducted in two separate drilling campaigns during 2014 and 2015. In 2016, a new drilling program was started. The Kocakıran prospect is represented by both outcrop and sub-crop of low-sulphidation epithermal veining and silicified fault systems which extend north-west along strike for approximately 1 km. Mineralisation in Kocakıran consists of silica veins and associated quartz breccia bodies within silicified and altered volcanic rocks in an area of 100–200 m in width. The silica veins with a low sulphide content, display characteristic epithermal textures such as colloform and crustiform silica with banding of quartz-pseudomorphs with bladed calcite and multiphase episodic hydrothermal breccias.

The fragments of the hydrothermal breccia are angular to sub-angular in shape ranging up to few centimetres down to micron scale. The fragments mainly comprise micro-crystalline quartz crystals with irregular and interpenetrating grain boundaries. The clasts of the breccia are supported by dark-coloured, sulphide dominated cryptocrystalline quartz matrix. Disseminated pyrite and marcasite are the most widespread sulphide minerals in the hydrothermal breccia with lesser chalcopyrite, galena and sphalerite. Gold and silver sulphosalts including pyrargyrite were identified either as disseminated individual crystals or adjacent crystals.

4.3.3.4 Karadere

At the Karadere low-sulphidation prospect, five different rock units are recognised; from oldest to youngest these are metamorphic rocks, intrusive rocks, and volcanic-volcanoclastic sequences consisting of agglomerate, volcanic breccia, andesitic flow-dome complexes and basaltic andesite. Gold and silver mineralisation are hosted by quartz veins confined to high to moderate angle normal faults traversing the andesitic domes, and overlying agglomerate-volcanic breccia. The veins are confined to a structural corridor bounded on the south by a NE-trending low-angle

normal fault, and on the north by a high angle normal fault. The structures within this corridor appear to be sub-parallel faults trending in N45–50E direction. The mineralised veins are enclosed within quartz-clay-sericite alteration, sericite being closer to the veins (Aluç et al. 2014). PIMA (Portable Infrared Mineral Analyzer) analyses show three alteration zones: Chlorite-epidote, illite-sericite, and quartz stockworks. The low-sulphidation mineralised veins are composed predominantly of sugary quartz with occasional bladed to brecciated textures. No significant vertical zoning with respect to ore-vein texture association is observed throughout the veins. Based on the geographical distribution, five different main ore zones are recognised in Karadere: South Ore zone, Ballık Ore zone, Kabak Ore zone, Kartaldere Ore zone and Göktepe Ore zone.

4.3.3.5 Ovacık

The Ovacık gold-silver mine is located in West Anatolia about 100 km north of İzmir near the historical city of Pergamon (Fig. 4.3). The cyanide leaching method was first used in the Ovacık mine in Turkey and the mine has been operating since early June, 2001. The Ovacık gold–silver deposit consists of six epithermal quartz veins. Among them production is still ongoing on M and Z veins by underground operation. Both mineralised and unmineralised epithermal quartz veins are controlled by sinistral faults generally oriented E-W and NW-SE. The high-grade, low-sulphidation quartz veins are dominantly northwest-southeast-trending, with dips ranging from 65 to 85° to N. The veins at Ovacık have six main textural types of ores: (a) crustiform/colloform banded ore, which occurs in both the veins and as breccia clasts; (b) coarse, bladed carbonate, occurring as distinct bands or infilling vugs; (c) clast-supported crackle (shattered) breccia with angular monomictic fragments; (d) matrix-supported fluidised (milled) breccia with angular to subrounded polymictic fragments, in which the clasts consist mainly of quartz and adularia with common crustiform banding and quartz-cemented breccia; (e) cockade texture; formed from clasts of silicified wall rock overgrown by crustiform/colloform bands and cockades of chalcedonic quartz and adularia; and (f) a hanging wall zone of silicified porphyritic andesite and sheeted quartz veinlets. High grade gold values up to 100 ppm occur in crustiform/colloform banded quartz-adularia veins and late stage crackle breccia and silicified wall-rock hydrobreccia. Sulphide content is low (<2%) and is dominated by pyrite with traces of chalcopyrite arsenopyrite, acanthite, argentite, pyrargyrite, stibnite, galena and bornite. Alteration minerals are smectite, mixed layer illite/smectite, quartz, adularia and calcite. Fluid inclusion data from the Ovacık Au deposit suggest that the ore-forming fluids were low salinity (<2 wt.% NaCl equiv.) and low temperature ranging from 150 to 250 °C, with most below 200 °C. $^{40}Ar/^{39}Ar$ dating of adularia from gold-bearing quartz veins indicates an age of mineralisation of about 18.2 ± 0.2 Ma. $\delta^{18}O$, $\delta^{18}O_{H2O}$ and δD values suggest that mineralising solutions were a mixture of meteoric and magmatic waters. The $\delta^{34}S_{\Sigma sulphide}$ data at Ovacık and Narlıca range from −2.1 to 5.3‰

(average: +1.7) and from −4.6 to +2.7‰ (average: −0.36), respectively. These $\delta^{34}S_{\Sigma sulphide}$ values are consistent with a magmatic source for S (Yılmaz et al. 2007).

4.3.3.6 Efemçukuru

Efemçukuru is an outstanding example among the epithermal deposits in western Anatolia with its gold and /or silver rich assemblages with diverse gangue minerals, and structural control on vein formation. Efemçukuru shows characteristics of both low and intermediate sulphidation epithermal deposits. Physical and mineralogical properties of the wall rock, erosion level of the different segments of the vein, direction of the hydrothermal fluid path and the distance from the heat source are the main controls on three dimensional zonations of the veins. Along the strike of the veins, there is also a zonation characterised by both ore and gangue mineral distribution and base and precious metal geochemistry in Kestanebeleni vein from South (South Ore Shoot) through middle part (Middle Ore Shoot) to North (North Ore Shoot) respectively. There are several lines of evidence for multiple stages (or pulses) of ore formation. In different levels and in different sectors of the Kestanebeleni vein, more than one generation of sulphide crystallisation (e.g., galena, sphalerite and pyrite) is present. The hydrothermal gangue minerals (mainly quartz and rhodonite, but also axinite, rhodochrosite ± adularia) are crosscut by sulphide assemblage in some core samples (e.g., in North Ore Shoot). Extensive crosscutting relationship among the different hydrothermal gangue phases also indicates distinct pulses of gangue mineral generation. Change in either strike and dip of the vein system reflects the changing volume of the space for the precipitation of gold from boiling hydrothermal fluid. On the base of this approach it has been stated that, most NW-oriented and steepest segments correlate to areas of elevated gold mineralisation. The spaces formed at the joints of two different fracture system are the site of gold rich zones. The Kestanebeleni hydrothermal system produced a sequence of vein textures and breccias in different stages during its evolution. On the basis of a recent study by Boucher et al. (2016) veins in different stages have different mineral assemblages and internal textures such as;

Stage I. Calc-Silicate (qtz-chl-act-ep-py veinlets), Stage II. Quartz-Rhodochrosite Breccia (qtz-rdn-rds), Stage III. Quartz-Rhodochrosite (colloformbanded qtz-rds-rdn±py), Stage IV. Quartz-Sulphide (colloform-crustiform, cockade qtz-rds-py-gn-sp), Stage V. Base Metal Sulphide (massive to colloformbanded gn-sp-py-qtz-cpy), Stage VI. Late Quartz-Carbonate (stringers of qtz-cal±rds). Gold occurs as inclusions in galena and pyrite of Stage IV and V, and as electrum in Stage III and IV. The fluid inclusions clearly indicate that a complex geothermal system existed.

4.3.3.7 Ergama (Gokceyazi)

Ergama Property is situated 35 km West of Balıkesir city centre. The property involves a HSEM gold deposit within a large area of propylitic and argillic alteration. The project area consists of a complex Late Oligocene volcanic structure developed on a slightly metamorphosed basement of Permian age. High grade gold mineralisation is mostly associated with tectonic controlled brecciation and silicification. Silicified zones at higher elevations are represented by fine sugary and drusy cavities and thin breccia zones composed by vein quartz fragments in gossanous matrix. Alunite, pyrophyllite, dickite, kaolinite, diaspore are the main clay minerals along advanced argillic alterations while illite-sericite, smectite are common along argillic alterations. Chlorite dominant propylitic alteration surround all clay minerals at the outer part of the system. Property also comprises high-level porphyry mineralisation zone represented by sheeted or stockwork type dark greyish quartz veinlets and quartz-sericite alterations towards the northern margins of the HSEM.

Recent drilling by Sandstorm Gold Co. (formerly Mariana Resources) intersected long intervals of gold-bearing, porphyry-style quartz (pyrite-chalcopyrite) stockwork mineralisation. Best intersections up to date, 141 m @ 0.23 g/t Au and 156.4 m @ 0.25 g/t Au including 56.4 m @ 0.33 g/t Au and 0.12% Cu (Mariana Resources, News Release, 2017).

4.3.4 Kütahya-Afyon-Uşak Region

The Menderes Massif is a well-studied metamorphic complex, which is made up of a polymetamorphic Precambrian basement which is dominated by orthogneisses and unconformably overlying Paleozoic to Early Tertiary cover series consisting of metaclastic and platform-type metacarbonates (Başarır 1970; Şengör et al. 1984; Dora et al. 2001; Candan et al. 2011). E–W trending active graben systems, dividing the Menderes Massif into submassifs and associated detachment faults are the main structures that give to the Menderes Massif its present structure. In the northernmost area the prominent structure in the Simav region is the Simav detachment fault that is characterised by mylonites in core rocks. They consist of migmatitic-banded gneiss, orthogneiss, biotite gneiss, high-grade schist, amphibolite, and marble and separates so-called mylonitic core rocks of the northern Menderes Massif in the footwall from the Akdere Basin in the hanging-wall (Işık and Tekeli 2001; Bozkurt et al. 2011).

The Eğrigöz pluton is one of the largest (approximately 550 km^2) exhumed granitoid body coexisting with the Koyunoba and Alaçam plutons in Western Anatolia (Fig. 4.3). The pluton is assumed to be a syn-extension following the subduction of African/Arabian Plate beneath Anatolide-Tauride block (Catlos et al. 2012). These syn-extensional granitoid plutons intrude pre-existing regionally metamorphosed basement in the footwall (e.g., Akay et al. 2011; Ring and Collins 2005; Thomson and Ring 2006; Özgenç and İlbeyli 2008; Erkül 2010; Hasözbek et al. 2010; Catlos

et al. 2012). The plutons are surrounded by contact-metamorphic aureoles of pyroxene hornfels and hornblende hornfels facies that grade from the pluton to greenschist facies rocks. Zircon crystals from southern, central and northern portions of the Eğrigöz pluton yield $^{238}U/^{206}$ Pb ages of 20.4 ± 0.5 Ma, 20.8 ± 0.4 Ma and 20.8 ± 0.4 Ma (weighted mean) respectively. Similar to Eğrigöz pluton, zircon crystals from the southern, centre and northern flanks of the Karakoca pluton yield $^{238}U/^{206}$ Pb ages of 26.0 ± 0.6 Ma, 20.6 ± 0.8 Ma and 24.1 ± 0.5 Ma respectively (Catlos et al. 2012). These ages are in agreement with U-Pb zircon ages reported from Hasözbek et al. (2010) and SIMS U–Th–Pb zircon ages by Ring and Collins (2005), which are 19.4 ± 4.4 and 20.7 ± 0.6 Ma, respectively.

The Kalkan Formation is the lowermost unit that is crosscut by the Eğrigöz Pluton and mainly consists of banded migmatites, gneiss, and marble lenses of the Menderes Massif. It is assumed that these high-grade rocks are unconformably overlain by low-grade Simav Metamorphics representing the cover series of the Menderes Massif (Akdeniz and Konak 1979). The Simav metamorphic rocks are made up biotite-muscovite schist, muscovite-quartz schist, biotite-muscovite-chlorite schist, garnet schist, quartzite, chlorite-bearing calc schist (Akdeniz and Konak 1979). The Balıkbaşı Formation conformably overlies the Simav Metamorphic rocks and consists of locally dolomitized marbles derived from neritic limestones. The Balıkbaşı formation is unconformably overlain by Upper Paleozoic-Lower Triassic Sarıcasu Formation consisting of low-grade schist, phyllite, quartzite and marble intercalations. The Sarıcasu Formation is overlain by the Arıkaya Formation. The age of the Arıkaya Formation is thought to be Permian, based either on lithological similarities with the fossiliferous Permian limestone or boundary with overlying fossiliferous Middle-Upper Triassic rocks. The Arıkaya Formation is composed mainly of crystalline limestone, which is obscured by dolomitization in places (Akdeniz and Konak 1979).

The Karakoca and Sudöşeği Pb-Zn-(Cu-Ag) mineralisation are good examples of intra-plutonic epithermal vein type base-metal deposits in the Inner Western Anatolia. They are hosted by Koyunoba and Eğrigöz Plutonic Complex (EPG) respectively (Fig. 4.3). Although there are a number of iron skarns occur in the contact zone between the plutons and carbonate rocks of the Afyon Zone and Menderes Massif, vein type Pb-Zn (Cu-Ag) mineralisation similar to the Karakoca and Sudöşeği have been rarely recognised.

4.3.4.1 Karakoca

The intra-plutonic Karakoca vein, hosted by Karakoca pluton, strikes NW discontinuously for 1400 m and dips 60° to SW. The true thickness of the vein is variable, in a range between a few cm to 2–3 m. Mining operations in Karakoca were only carried out for 1 year in 1960 with the production of ore containing 11% Pb, 3–4% Zn and 2–3% Cu. High grade massive ore with colloform-crustiform texture passes gradually to brecciated and stockwork ore in the hangingwall of the vein zone. The ore paragenesis is represented by pyrite, galena, sphalerite and chalcopyrite with

lesser tetrahedrite-tennantite, bornite and hematite. In the oxidation stage, chalcocite, covellite, goethite, malachite and cerussite replace the hypogene ore minerals. Primary two phases (liquid-rich) inclusions from quartz samples have yielded homogenisation temperatures (T_h), ranging between 250.2 and 322.7 °C (avg. 283 °C with 51 measurements) (unpublished data). Corresponding salinity based on final ice melting (T_{mice}) temperatures are clustered in a wide range of area in between 0.4 and 15.3 wt.% NaCl equivalent (avg. 4.72 wt.% NaCl eq.) The first ice melting (T_{mf}) measurements are 29–63 °C, indicating NaCl, $CaCl_2$, $MgCl_2$ and KCl (Li and Br free) dominated fluids are responsible for the quartz crystallisation in association with mineralisation. Sulphur isotope results close to zero ($\delta^{34}S$ ‰) from sphalerite, pyrite and galena indicate a major contribution of magmatic fluids (unpublished data). The characteristics of Karakoca vein in terms of its texture, composition, ore mineralogy and ore-forming fluid correspond to intermediate sulphidation epithermal veins.

4.3.4.2 Su Döşeği

Similar to Karakoca, Su Döşeği is another example of intra-plutonic vein system which crops out along a NE-SW fracture-fault system in the Eğrigöz Plutonic Complex. High-grade ore is found in the hanging wall of the vein system, showing clear colloform-crustiform texture, while some stockwork and brecciated ore are found in the footwall. Although, there is no recorded mining activity in Sudöşeği, small excavations and some dumped floats were found during our field study, suggesting that short-lived operations took place.

Ore mineralisation consists of a sulphide mineral assemblage containing galena, sphalerite and chalcopyrite in colloform-crustiform and stockwork zones. Galena and sphalerite with subordinate chalcopyrite are more common in colloform-crustiform banded zones, while pyrite, quartz and carbonate gangue are more abundant in stockworks and brecciated zones. The oxidation stage is characterised by goethite, limonite, siderite, cerussite, azurite, malachite and chalcocite-covellite. Fluid inclusion assemblages in quartz yielded T_h between 211 and 349 °C (avg. 269 °C with 32 measurements) with salinities between 0.7 and 9 wt.% NaCl equivalent (mean 4.5 wt.% NaCl eq.). The first ice melting (Tmf) measurements are 29–63 °C, indicating NaCl, $CaCl_2$, $MgCl_2$ and KCl (Li and Br free) dominated fluids are responsible for quartz crystallisation. Similar to Karakoca, sulphur isotope results ($\delta^{34}S$ ‰) close to zero from sphalerite, pyrite and galena indicate magmatic origin for the fluids are responsible in ore generation (unpublished data).

4.3.4.3 Yukarı Ortaburun (Katrandağ)

Katrandağ Pb-Ag (Au) is a complex epithermal and associated skarn type mineralisation, hosted by a roof pendant of dolomitic limestone of Balıkbaşı formation, Simav Metamorphics and Eğrigöz pluton. Epithermal veins extend along N-NE/SW

striking faults. Although there has been some manganese mining in vicinity of Katrandağ, no mining activity has occurred in the area.

The upper part of the system is thought to occur at the interface between the water table and the overlying surficial zone, based on the occurrences of silica cap, oxidation and supergene alteration. The hydrothermal mineralisation occurs in silica cap including silica-rich veins and silicified dolomitic limestone (Balıkbaşı formation), which hosts a Ag-Au rich zone for approximately 6–6.5 m at the uppermost section. Below the Ag-Au rich ore, massive galena, barite with lesser amounts of sphalerite and pyrite are observed. At further depths, the contact zone of Eğrigöz pluton with Balıkbaşı formation and Simav Metamorphics show distal and proximal skarn zone with about 1–1.5 m thickness in average. Based on core samples, the copper-rich distal skarn zone is thinner and characterised by chalcopyrite, bornite and pyrite association, while the iron dominated proximal skarn zone is represented by abundant magnetite, sphalerite, pyrite, chalcopyrite and galena with a thickness up to 4.5 m. Additionally, veinlets of 50–55 mm width in stockworks and stringer zones are observed in the interior of the pluton, which shows roughly % 1–2 sulphide mineralisation including chalcopyrite, galena and pyrite.

4.3.4.4 Mumcu

Mumcu is a poorly studied epithermal system, cropping out along N-S transfer faults linked with the Simav Graben. It is situated within Paleozoic Metamorphics and Miocene andesitic volcanics. The mineral system is associated with silicified, brecciated and opal bearing zones and surrounding argillic alteration mineral assemblages including kaolinite, montmorillonite and cristobalite. The ore minerals including cinnabar, arsenopyrite, electrum and low grade gold (500 and 340 ppb from Hg bearing opal and pyrite samples) are found in opal-rich zones (Oygür 1997). Since there are no core samples, the data from Mumcu epithermal system is only limited to surface observations. However, the presence of arsenopyrite, wall rock alteration and gold anomalies point to the outlying section corresponding to an upper parts of an epithermal system, which also means that higher ore grades might be found at depth.

4.3.4.5 Değirmenciler

The Değirmenciler is an antimony bearing epithermal deposit, hosted in silica replaced limestone lenses of Paleozoic metamorphic rocks. The silicified host rocks show colloform-crustiform texture and jasperoid alteration as a result of calcite-silica replacement. Argillic and advanced argillic alteration represented by montmorillonite, smectite, quartz, opal, cristobalite and dickite surround this epithermal system. Hydrothermal breccia with dark grey silica and abundant pyrite is associated with high grade ore. Lesser amount of galena, chalcopyrite, molybdenite, bismuth, gold and silver accompany to the main ore.

4.3.4.6 Kaymaz

Kaymaz Gold Mine situated at the Kaymaz village near Sivrihisar town of Eskişehir city. Kaymaz is located in the Tavşanlı Zone of the Anatolide-Tauride Block, that was subjected to high pressure-low temperature metamorphism during the Cretaceous. Paleozoic and Mesozoic metamorphic rocks of the Tavşanlı Zone were intruded by the Eocene dykes. Under the influence of these granite dykes, three styles of mineralisation are evident; manto-type mineralisation, quartz stockworks and veinlets and episodic brecciation adjacent to the granite dyke. Mineralisation is hosted mainly in the serpentinites and quartz schists at Damdamca, Karakaya, Küçük Mermerlik and Kızılağıl districts (Yavuz 2013).

Among these, the Damdamca and Main Zone are the two most important districts because of their reserves and exploration activities. The vein in Damdamca has been traced along its N-S strike for over 220 m and dips 45–60° to the east. Similar to Damdamca the vein in the Main Zone has been traced for a length of 1100 m along a N-S strike dipping 45–60° S. Early hydrothermal ore assemblage is composed mainly of magnetite, millerite, pentlandite, nickeline, arsenopyrite, marcasite, pyrite-I, bravoite, gold and silver. Late hydrothermal ore assemblage is composed of pyrite-II and supergene hematite, pyrolusite, goethite, limonite, lepidocrocite and rarely chalcocite-covellite (Yavuz 2013). Quartz, serpentine, ankerite, and dolomite are the main gangue minerals. Homogenisation temperatures for liquid-rich inclusions in quartz, range from 240 to 390 ° C with salinities between 0.3 and 14 NaCl wt.% (Yavuz 2013). On the basis of field relations, petrography and fluid inclusion studies, the Kaymaz gold mineralisation can be considered as listwanite type deposit which formed under epithermal conditions.

4.3.4.7 Red Rabbit (Kızıltepe)

The epithermal mineralisation at Kızıltepe is hosted within the Sındırgı Volcanic Complex, which comprises a sequence of dacitic and rhyolitic intrusions, lava flows and pyroclastic rocks. The Sındırgı Volcanic Complex is considered to be of Miocene age on the basis of K-Ar ages of 19.0 ± 0.4 and 20.2 ± 0.5 (Erkül et al. 2005). Dating of the lower ignimbrite host-rocks also yielded a comparable 40Ar/39Ar plateau age of 19.82 ± 0.14 Ma. There are four main epithermal quartz (-adularia) vein swarms located across the region, namely: Kızıltepe, Kepez, Karakavak, and Kızılçukur (listed from SW to NE). Epithermal gold was discovered in the region during a regional bulk leach extractable gold (BLEG) and 180-μm stream-sediment sampling program, carried out by EuroGold (Yılmaz 1992) and TUPRAG in 1990 and 1992 respectively (Yılmaz 1992). At Kızıltepe, low-sulphidation type epithermal veins, including four economically viable veins referred to as Arzu South, Arzu North, Banu and Derya, are controlled by NW and NNW trending structures in the lower ignimbrite sequence. The subparallel and curvilinear Arzu and Banu vein systems dip steeply 75–85° to the NE and 75–80° to the SW respectively. Along their strikes, the total length of the veins reach up to

19.5 km (Şener et al. 2006a, b). The Kızıltepe deposit exhibits characteristics of an adularia-bearing low sulphidation paragenesis with a low total sulphide content and with a simple ore mineralogy. Disseminated pyrite and associated supergene oxides with traces of electrum and acanthite are the main ore minerals.

Crustiform, carbonate replacement and associated bladed, breccia and associated cockade textures are the prominent textures, which yield the highest gold grades ranging from 12 to 32.5 ppm in the Kızıltepe vein system (Yılmaz et al. 2013). The Kızıltepe low sulphidation epithermal system possesses characteristic textures that are directly or indirectly related to boiling hydrothermal fluids. Silver mineralisation is represented by native silver and acanthite and associated with gold in both the mineralised quartz veins and the stockwork envelope around the veins. Overall, a wide range of Ag:Au ratios has been recorded, commonly between 5:1 and 30:1. Detailed fluid inclusion studies were conducted by Yılmaz et al. (2013), on medium-grained quartz from crustiform banding, carbonate replacement and hydrothermal breccia textures of Phase II, which is regarded as the main phase of Au-Ag deposition. These yielded an average homogenisation temperature of 231 °C (number of samples, n = 85) and salinity of 1.1 wt.% NaCl equivalent (n = 85), suggesting that relatively low temperature diluted fluids of mixed origin were responsible for the Phase II mineralisation.

4.3.4.8 İnkaya

The İnkaya Cu–Pb–Zn–(Ag) is an epithermal vein-type ore mineralisation, hosted by Simav Metamorphics and Arıkaya formation. The epithermal veins extend E-W along strike with a thickness of up to 2 m. Galena, sphalerite, chalcopyrite, pyrite and fahlore with lesser amounts of cerussite, anglesite, digenite, enargite, chalcocite-covellite, bornite are the ore minerals within an iron oxide dominated quartz gangue. Grades of Cu, Pb, Zn and Ag are 77,400 ppm, 102,600 ppm, 6843 ppm and 203 ppm, in average respectively. Microthermometry results from quartz range from 235 to 340 °C with salinities, between 0.7 and 4.49 wt.% NaCl equivalent. Based on wide range of homogenisation temperatures and lower salinities, multiple fluid generations from same source is thought to have occurred as a result of meteoric water mixing with magmatic fluids (Özen and Arık 2015).

4.4 The Central Anatolian Province

Tectono-magmatic evolution of Central Anatolia is closely related to multiphase compressional and extensional events following the continental collision of Gondwana and Eurasian plates. As a consequence of this convergence processes, NE to SW trending volcanic arc extended from Konya to Nevşehir developed during Neogene to Quaternary times. Central Anatolian Crystalline Complex (CACC),

which is also known as Kırşehir Block is bounded on the North by the İzmir Ankara Erzincan Suture that separates the Pontides from both CACC and from Anatolide–Tauride (Fig. 4.1).

In the southwest, CACC is separated from Anatolide–Tauride block by the Inner Tauride suture (Görür et al. 1984, 1998; Dilek et al. 1999; Okay and Tüysüz 1999; Andrew and Robertson 2002; Robertson et al. 2009; Pourteau et al. 2010). The Inner Tauride suture is assumed to have been formed by the closure of an oceanic branch located between the Tauride-Anatolide Block and the CACC. On the basis of geochronological data obtained from ophiolites of the metamorphic soles (Parlak et al. 2013) this oceanic basin is suggested to have been consumed as a result of northward subduction which initiated between 95 and 90 Ma. The latest Cretaceous to Early Cenozoic age is envisaged for the complete consumption and following continental collision of this (Parlak et al. 2013).

The Central Anatolian Crystalline Complex experienced high-temperature, medium-pressure (HT-MP) Barrovian metamorphism at 5–6 kbar/>700 °C, dated about 91–84 Ma. The metamorphic rocks of the Kırşehir Block were subjected to regional high-temperature, medium-pressure (HT-MP) conditions and are subdivided into three massifs namely Akdağ, Kırşehir, and Niğde-Ağaçören-Hırkadağ (Lefebvre 2011; Van Hinsbergen et al. 2016) (Fig. 4.1). The ophiolites and the underlying high-grade metamorphic rocks of the metamorphic basements are intruded by granitoids suites range in age from Late Cretaceous to Eocene with a large compositional diversity from calc-alkaline through subalkaline to alkaline as a result of closure of the Inner Tauride Ocean (Akıman et al. 1993; Aydın et al. 1998; Whitney and Dilek 1998; Fayon et al. 2001; Whitney et al. 2001, 2003; Whitney and Hamilton 2004; İlbeyli et al. 2004; İlbeyli 2005; Kadıoğlu et al. 2003, 2006; Köksal et al. 2004; Önal et al. 2005; Boztuğ 1998, 2000; Boztuğ et al. 2007; Kuşçu et al. 2010). The North-west segment is known as "Kırıkkale granitoid belt" and composed of several calc-alkaline granitoid stocks including Sulakyurt, Keskin, Behrekdağ, Çelebi granitoid and alkaline stocks including Buzlukdağ and Baranadağ granitoids. Ağaçören calc-alkaline intrusive suite which can be divided into two bodies as Ağaçören and Ekecikdağ granitoids lie along the arc which is parallel NW–SE trending Tuz Gölü Fault (Kadıoğlu and Güleç 1996; Türeli 1991). Baranadağ and Buzlukdağ stocks are the well-known examples of alkali plutonism in the Kaman-Kırşehir region.

Development of the intensive Neogene-Quaternary volcanism in the Central Anatolian Volcanic Complex is related to subduction and the following continental collision between the Afro-Arabian and Eurasian plates. The main transcurrent faults such as the North Anatolian, the East Anatolian, the Tuz Gölü and the Ecemiş faults were formed in association with compressional and extensional forces during the closure of the Northern branch of Neo-Tethys (McKenzie 1972; Şengör 1979; Şengör and Yılmaz 1981; Pasquare et al. 1988; Toprak and Göncüoğlu 1993). As the largest volcanic province of the central Anatolia, it includes Upper Miocene-Holocene ignimbrites, volcanic ash deposits and lava flows intercalated with fluvio-lacustrine sediments (Çiner et al. 2015). Central Anatolian Volcanic Province hosts

numerous monogenetic volcanoes including Erciyes, Hasandağ and Melendiz main stratovolcanoes which are responsible for the volcanic activities between Miocene to recent. The Melendizdağ Volcanic Complex hosts several high sulphidation mineralisation and comprises Miocene-age coalescing lava domes, flows, vent breccias, and pyroclastic deposits. The Miocene Develidağ volcanic complex is situated at the southeastern end of the Sultansazlığı pull-apart basin and the southern part of the eastern Ecemis fault. Ecemiş and Tuz Gölü Faults create an area of crustal extension resulting in tectonic depressions such as pull apart basins exemplified by Sultansazlığı and Tuz Gölü basins. Tuz gölü and Sultansazlığı basins along with the Ecemiş Fault Zone are active pull apart basin since the Early Quaternary (Dirik and Göncüoğlu 1996). Previous structural studies suggest that Develidağ volcanism was generated prior to and during the extension of the Sultansazlığı pullapart basin (Koçyiğit and Beyhan 1998; Toprak 1998). The common features of the central Anatolian volcanic rocks are abundant tholeiitic and calc-alkaline rocks, followed by alkaline activities at the final stage of the volcanic events. Develidağ eroded stratovolcano is represented mainly by tholeiitic basalts associated with minor calc-alkaline products (Kürkçüoğlu 2010). The CAFZ transform microplate boundary separates Sultansazlığı basin from the Develidağ volcanic system.

Within the Anatolian block, some sedimentary basins are related to these faults (Şengör 1979; Şengör and Yılmaz 1981), such as the Sultansazlığı and Tuz Gölü basins (pull-apart basins, according to Pasquaré et al. 1988). The common features of the central Anatolian volcanic rocks are abundant tholeiitic and calc-alkaline associations, followed by alkaline activities at the final stage of this volcanism. The Develidağ volcanic system is represented mainly by tholeiitic basalts associated with minor calc-alkaline rocks. Melting modelling suggests that basaltic rocks can be derived by partial melting (3–4%) of a spinel peridotite source component, whereas calc-alkaline rocks show minor amount of crustal contribution during differentiation as indicated by LIL/HFS element ratios and supported by AFC modelling. Development of the tholeiitic calc-alkaline associations for Develidağ volcanic system could be related to the activities of the eastern segment of the Ecemiş fault. Tholeiitic and calc-alkaline associations can be explained either by combined development of partial melting of a mantle source and following crustal involvement or by the change in the rate of the melting degree. The lack of alkaline rocks seems to be attributed to either the lack of extensional development or to the poor extension in Central Anatolia before the late Miocene.

Another important volcanic centre Konya Volcanics outcrop along a 60 km, northwest trending zone which is up to 40 km in width, between the cities of Konya and Beyşehir. Permo-Mesozoic autocthon-para autocthon Gökçeyurt Group and allocthonous Ladic Metamorphics are the main components of the metamorphic basement. The basement is overlain unconformably by subduction related calc-alkaline volcanic and volcano-sedimentary rocks of the Late Miocene-Pliocene Konya Volcanics. The Konya Volcanics comprise dykes, lava flows, tuffs, ignimbrites, volcanic breccias and agglomerates in composition vary from rhyolite to andesite. The Konya belt is a recently discovered metallogenic unit defined by at

least 15 alteration zones of gold and/or silver mineralisation including İnlice, Doğanbey and Karacaören in the Central Anatolia of Turkey. Mineralisation is related to a belt of Miocene volcanic rocks, most of which constitute a series of large compound stratovolcanoes of calc-alkaline composition.

4.4.1 Öksüt

Öksüt is a high-sulphidation epithermal gold deposit located in Develidağ Volcanic Complex (DVC) in Central Anatolia (Fig. 4.1). The deposit was discovered by Stratex in early 2007. Develidağ is an eroded stratovolcano represented by tholeiitic basalts and minor calc-alkaline rocks composed mainly of andesites (Kürkçüoğlu 2010). The deposit covers two reasonably well-defined targets, known as Kel Tepe and Güney Tepe, which are characterised by intense silicic alteration and advanced argillic alteration. Keltepe and Güneytepe deposit are both considered to be controlled by NW-SE and NE-SW trending faults.

Intense silicic alteration formed as massive silica and massive silica breccia with lesser vuggy silica. Advanced argillic alteration is characterised by the presence of the mineral assemblage comprising alunite, kaolinite, dickite, pyrophyllite, diaspore, aluminium-phosphate-sulphate minerals (woodhouseite-svanbergite series), zunyite, minamyite, pyrite and enargite.

In Kel Tepe four different types of breccia have been identified on the basis of their clasts, matrix and alteration features. These are massive silica breccia, silica-hematite-limonite breccia, alunite breccia and the quartz-kaolinite ± alunite breccia. Texturally a variety of polymictic breccias and a texturally uniform porphyritic andesite are the main host rock for gold mineralisation (Sillitoe 2012).

Massive to vuggy residual quartz commonly occurred at increasing elevations with a vertical limit of up to 100 m. (Massive to vuggy residual quartz with associated silicification were formed at the higher levels of the system with a vertical extent of up to 100 m. However, quartz-alunite and quartz-kaolinite alteration is encountered at lower levels of the system. These two alteration controlled by NW-SE and NE-SW trending faults are the most prominent alteration types associated with gold mineralisation. The property contains probable reserves of 26.1 Mt at 1.4 g/t gold, containing 1.16 million ounces of gold. The Öksüt feasibility study evaluates a mine plan of two open pits operated over an 8 year mine life (http://sandstormgold.com/news/2016/index.php?&content_id=475).

Mineralisation at Öksüt is believed to be related to the contemporaneous emplacement of a subvolcanic breccia and a porphyritic andesite. A 2012 site visit by Dr. Richard Sillitoe described gold mineralisation as being *"preferentially precipitated in the siliceous ledge and its immediate quartz-alunite halo,"* and having been *"fed by at least one, and probably several steep structures represented by massive silicification."*

4.4.2 İnlice

This prospect was the first of more than twenty hydrothermal alteration zones discovered by Stratex in the Konya Volcanic Belt. The İnlice epithermal gold project is located in the Konya (Erenlerdağ) Volcanic Belt, approximately 40 km northeast of Konya (Fig. 4.1). In the area, Miocene-Pliocene volcanism with calk-alkaline and high-K calk-alkaline affinity is composed mainly of andesitic and dacitic lavas and tuffs. The widespread alteration of the andesitic and dacitic lavas consists mainly of kaolinite, and associated halloysite, alunite, cristobalite, quartz, illite, montmorillonite, and zeolite group minerals (Karakaya et al. 2001).

The İnlice epithermal gold project comprises WNW to NW trending subvertical silica ledges referred to as Ana Zone, Batı Zone and Keşif Zone which are hosted within intensely altered dome-like andesitic body. Silica veins which crosscut the dome-like andesitic body are controlled by oblique-slip normal faults. Ana zone is the widest and longest silica ledge which striking N 50–80° W and dipping 60–70° SW. Alteration typically changes outwards from silica to quartz-alunite and quartz-kaolinite, illite-chlorite and smectite-chlorite respectively, which reflects the decreasing temperature and the increasing pH of the hydrothermal fluid. The vuggy and sugary quartz host the gold mineralisation in the main zone, and show outward transition to advanced-argillic and argillic alteration zones, typical of the outflow path of a high sulphidation epithermal system in which alteration and gold precipitation is controlled by mainly pH and temperature changes. Chalcedony after opal is also present in the eastwards of Ana East section.

Doğanbey alteration zone is located near the side of the eroded stratovolcanoapproximately 15 km NE of İnlice deposit. Doğanbey prospect is believed to have similar potential to İnlice and is in the focus of continuing exploration. The silica alteration is largely represented by opalisation of andesitic and dacitic volcanic rocks that are covered by unaltered rhyodacitic lavas. Beneath the opalised horizon the pyroclastic volcanic rocks in andesitic to dacitic composition were crosscut by structurally controlled quartz-alunite ledges. Kaolinite dominated illite-bearing alteration widespreadly outcrops between the quartz-alunite ledges. Advanced argillic alteration is represented by vuggy quartz with infilling alunite, kaolinite and hematite.

The anomalous gold grades up to 0.6 gr/t encountered at Doğanbey, occur with the network of quartz veinlets with a thickness varies between 1 and 3 mm. Gold is positively corellated with Mo, Sb, Pb, S, As, and S in soil samples and with Mo, Pb, Ag, Hg, Sb, Bi, Cu in rock samples. Further exploration activities including shallow drill programme to test the porphyry and or gold enriched zone are necessary.

4.5 Eastern Black Sea, Pontide Metallogenic Province: Northeastern Turkey

Due to its complex geological dynamics, the Pontide Belt hosts numerous kuroko, porphyry, skarn and epithermal prospects and deposits associated with Late Cretaceous-Mid-Eocene magmatism. The Pontide Belt extends east–west along the Black Sea coast and was formed in the eastern part of Alpine-Himalayan belt between the Rhodopes in the west and the Caucasus in the east. The subduction of the northern branch of the Neo-Tethyan oceanic crust beneath the Eurasian (Laurasian) plate (Okay and Şahintürk 1997; Şengör and Yılmaz 1981; Yılmaz et al. 1997) caused an arc-type magmatism during the Late Mesozoic-Early Cenozoic (e.g., Şengör and Yılmaz 1981; Okay and Şahintürk 1997; Boztuğ et al. 2004, 2006; Rice et al. 2006, 2009; Yılmaz and Boztuğ 1996; Altherr et al. 2008; Çinku et al. 2010; Karslı et al. 2010, 2011, 2012; Meijers et al. 2010; Ustaömer and Robertson 2010; Topuz et al. 2011). This subduction, was followed by collision of the Tauride–Anatolide block with the Pontide and Kırşehir blocks in the Late Paleocene and Early Eocene closing the Ankara–Erzincan branch of the northern Neotethys (Richards 2015). It is also suggested that northward subduction of Paleotethys formed the eastern Pontides orogenic belt during the Paleozoic–Mesozoic (e.g., Adamia et al. 1977, 1981; Dilek et al. 2010; Rice et al. 2009; Ustaömer and Robertson 1997). The Pre-Jurasic basement units are composed mainly of Carboniferous metamorphic rocks, and associated Permocarboniferous granitoids and sedimentary rocks (Topuz et al. 2004, 2007). In this crystalline basement cross-cutting granitoids of the Late Carboniferous age were also recognised previously (e.g., Çoğulu 1975; Dokuz 2011; Kaygusuz et al. 2012; Okay and Şahintürk 1997; Topuz et al. 2010).

Plutonic rocks in Eastern Pontide Belt are dominantly I-type metaluminous, calc-alkaline to high-K and shoshonitic with lesser A-type constituting more than 50% of the present erosion surface of the Eastern Pontides. The emplacement age of these intrusive rocks ranges a time interval from Cretaceous to Paleocene (Delaloye et al. 1972; Giles 1974; Taner 1977; Gedikoğlu 1978; Moore et al. 1980; Jica 1986; Okay and Şahintürk 1997; Yılmaz et al. 2000; Köprübaşı et al. 2000; Yılmaz-Şahin 2005; Boztuğ et al. 2006; Kaygusuz et al. 2008, 2009; Boztuğ 2008; İlbeyli 2008; Kaygusuz and Aydinçakir 2009) and the *Eocene* (Boztuğ et al. 2004; Arslan et al. 2004; Yılmaz-Şahin 2005; Topuz et al. 2005; Karslı et al. 2007).

The Pontide Belt is divided into three zones by Bektaş et al. (1995) and Bektaş et al. (1999) as the northern, southern and axial zones, based on their characteristic tectonic and lithological features. Konak et al. (2009) proposed to divide Eastern Pontides into two zones as northern/outer and southern/inner zones on the basis of geochemical, geochronological and tectono-magmatic features. The Northern zone is characterised dominantly by arc-related igneous rocks of Late Mesozoic and Cenozoic volcanic and volcanoclastic rocks. The occurrences of VMS deposits and some porphyry type mineralisation are usually attributed to the formation of the Late Cretaceous arc related igneous activity in the region. Post-collisional Early to

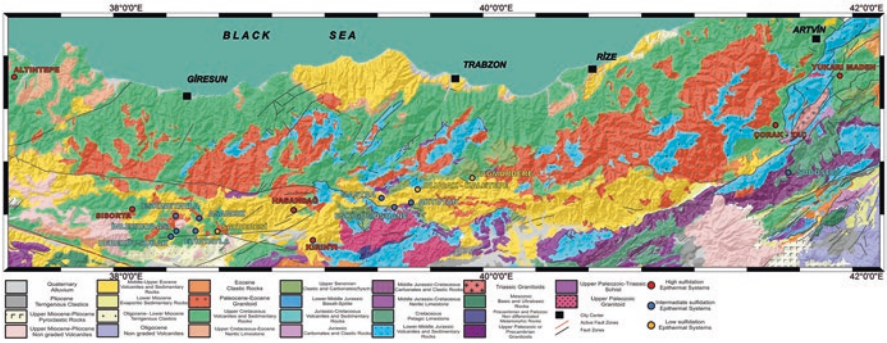

Fig. 4.4 Regional geological map of Eastern Pontides and spatial distribution of significant epithermal mineralisation. (Geology modified from MTA Emre et al. 2013; Akbaş et al. 2017)

Late Eocene volcanic and plutonic rocks are very important in terms of hosting porphyry and epithermal mineralisation and prospects in the Southern Zone of the eastern Pontides orogenic belt (Fig. 4.4) (Akçay and Gündüz 2004; Yiğit 2009; Eyüboğlu et al. 2014; Richards 2015).

The Pontide Belt is considered to be the most important lead-zinc-copper metallogenic province of the Turkey. Porphyry and epithermal deposits are also common, however, just few of them are of economic interest. Below, brief geological data are given on selected epithermal systems (e.g., Mastra, Hasandağ, Sisorta, Arzular, Olucak, Eskine, Etir, Asarcık, İnler) scattered mainly on Southern Zone of the eastern Pontides orogenic belt. The Altıntepe, Bahçecik, Midi, Kırıntı, Aktutan, Taç and Çorak are the other important mineralisation in this belt (Fig. 4.4).

4.5.1 Mastra

The Mastra Gold Mine is located approximately 5 km northwest of Gümüşhane, in the southern zone of East Pontides (Fig. 4.4). Although it has been known since the 1980s, the mine commenced open pit production in May 2007 and underground mining in 2008. The ore production is carried out by open pit and underground mining until the open pit production was terminated at the end of 2013. Porphyritic andesitic lavas and volcanoclastic rocks of Eocene age are the most widespread rocks in the area. Andesitic lavas gradually change to pyroclastic rocks towards the north and to agglomerates towards the south. Andesitic lavas are unconformably overlain by Eocene sedimentary rocks. The ore vein is envelopped by the intense argillic alteration which overprint porphyritic andesites. Outwards from argillic alteration zone, a propylitic alteration zone is present changing gradually to unaltered andesitic volcanics. Mineralisation and associated argillic alteration at Mastra are controlled by NW-SE striking and NE dipping structures. Occurences of barite

and alunite confirm that higher oxidition and sulphidation states are present in the evolutionary history of the deposit (Bilir 2015; Bilir and Kuşçu 2016). In addition to barite and alunite, characteristic minerals of acid-sulphate alteration (e.g., kaolinite, jarosite and gypsum) were found in the alteration assemblage (Tüysüz et al. 1995). However, adularia-sericite were identified as main gangue minerals in the boiling zone with bladed calcite. Mineralisation at the Mastra deposit is divided into two stages. The first stage is represented by galena and sphalerite with lesser chalcopyrite, pyrite, argentite and tetrahedrite-tennantite. The second phase is dominated by native gold, pyite and chalcopyrite. Detailed fluid inclusion studies from two stages of quartz related to gold mineralisation have been realized by Tüysüz et al. 1995. In this study the homogenisation temperatures ranging from 160 to 340 °C with salinities ranging from 4.1 to 10.9 wt.% NaCl equivalent. Similarly more recent fluid inclusion study shows that the ore forming solution varies in temperature between 113 and 390 °C (Aslan and Akçay 2011). Free gold in Mastra was formed in association with quartz predominantly in the native state with lesser amounts as electrum. The ore and alteration mineral assemblages in association with ore textures and fluid inclusion data are consistent with a low-sulphidation epithermal environment.

4.5.2 Hasandağ

The Hasandağ epithermal gold mineralisation located 20 km northeast of Alucra (Giresun) (Fig. 4.4). The Hasandağ mineralisation is hosted in Eocene volcanic rocks including andesite, dacite andesitic tuff, brecciated andesite and andesitic dykes in the southern zone of East Pontides. The volcanic succession is crosscut by intrusions varying in composition from quartz-monzodiorite to syenogranite. The volcanic and intrusive rocks of the area have experienced several stages of intense hydrothermal alteration. It seems like that the intrusions of felsic magma along the fracture zones prompted advanced argillic alteration due to high temperature, acidic fluids and associated diatreme formation. Silicification and argillisation are widespread as the main types of hydrothermal alteration (Acarlıoğlu et al. 2013). Field and paragenetic studies demonstrate that centres of acid-sulphate-altered rock are internally zoned and transition outward from argillic (smectite ± illite) into propylitic zones (chlorite ± epidote ± sericite ± calcite). Vuggy quartz dominated silicification with advanced argillic to argillic alteration which formed due to the leaching of host rocks by hot acidic hydrothermal fluids are indicators of high-sulphidation type mineralisation (Acarlıoğlu et al. 2013). The ore minerals are pyrite, native gold, hematite, goethite-lepidochrosite (Acarlıoğlu et al. 2013; Bilir 2015). Iron oxide alteration dominated by hematite and goethite is associated with higher gold assays indicating gold enrichment via supergene alteration.

4.5.3 Sisorta

The Sisorta epithermal mineralisation is located in 120 km northeast of Sivas and 60 km southwest of Giresun city (Fig. 4.4). Igneous rocks of Eastern Pontide arc varying ages between Late Jurassic to Pliocene with different composition and facies unconformably overlie the metamorphic basement and cover large areas in the region. The calc-alkaline volcanics of Late Cretaceous are characterised by andesitic dacitic lava, agglomerate and tuffs. Andesite and andesitic tuffs are the main volcanic rocks, which host the HSEM and the associated alteration. The volcanic successions are intruded by stock-like intrusions ranging from quartz-monzonitic to monzo-gabbroic in composition.

Sisorta alteration system covers a large area of more than 5 × 5 km and displays typical features of the HSEM systems, including vuggy silica lithocap, underlain by advanced argillic style alteration, high level multi-stage phreatic and hydrothermal breccias and associated intrusions. Gold is enriched at the top of the HSEM system, and is localised within silica cap which is surrounded by the advanced argillic alteration assemblage dominated by alunite, dickite, kaolinite, pyrophyllite and diaspore.

Post-mineral faults are responsible for secondary enrichment of gold and oxide and sulphide assemblages (Bilir 2015). In hydrothermal breccia zone, the silica cap with the significant gold assays comprises pyrite, chalcopyrite, barite and hematite. The lithocap represents the largely oxidised, gold enriched top of the system, and is underlain by less oxidised mineralisation enriched at depth. Petrographic studies indicate that Sisorta deposit includes fine to medium grained pyrite with some chalcopyrite, and tetrahedrite-tennantite group minerals with minor enargite.

$^{40}Ar/^{39}Ar$ age dating is ranging from 78.85 ± 0.94 to 76.59 ± 2.19 Ma as a plateau age and 78.25 ± 0.42 and 75.30 ± 0.90 Ma as an isochron age in K-alunite, 80.44 ± 0.84 in hornblende minerals from unaltered andesitic volcanic rocks. This shows that hydrothermal gold mineralisation was deposited 3 Ma later than the volcanic host rock eruption (Şahin Demir and Uçurum 2016).

4.5.4 Arzular

Arzular is hosted in the Eocene volcanic rocks in the southern part of the Eastern Pontides Orogenic Belt (Fig. 4.3). The Eocene volcanic sequences around the project area are subduction related basaltic-andesitic volcanic and associated pyroclastic rocks. These volcanic sequences are the final products of Early Cenozoic adakitic magmatism and cut by non-adakitic granitoid intrusions. The alteration and associated mineralisation are formed under the control of NE-SW and NW-SE striking fault zones (Akaryalı and Tüysüz 2013; Bilir 2015). The E-W trending fracture zone where the LSEM emplaced in, extends over 400 km along its strike and dips about 70 to the north. The thickness of quartz veins varies from 10 cm or less up to 50 cm. In the early stage of silicification, the quartz-chlorite assemblage is not associated

with significant mineralisation. However, in the later stage of silicification, quartz is formed in association with sulphides dominated by pyrite and gold (Bilir 2015).

Fluid inclusion petrography and vein mineral textures are the indicatives of boiling conditions in an open system (Akaryalı and Tüysüz 2013). The homogenisation temperatures for fluid inclusions from quartz vary from 130 to 295 °C, with an average of 214 °C. Ice melting temperatures ranges from −2.6 to −8.6 °C, and the corresponding salinities of the inclusions are 4.3–12.4 wt.% NaCl eq. Sphalerite crystallisation was achieved at a temperature between 90 and 133 °C from hydrothermal fluids with a salinity in a narrow range between 0.7 and 2.7 wt.% NaCl with a mean of 1.7 wt.% NaCl eq. (Akaryalı and Tüysüz 2013). The O and H isotope compositions of sericite and quartz suggest derivation of hydrothermal fluids from mixed sources including magmatic, metamorphic and meteoric waters.

The main ore minerals are native gold, silver, galena, sphalerite, chalcopyrite, fahlore minerals, pyrite and covelline, and associated gangue minerals are calcite, quartz, clay and gypsum. Gold commonly occurs as native Au intimately associated with chalcopyrite or as isolated grains, and ranges in size from 1 to 15 mm. The Fe content of analysed sphalerite ranges between 0.54 and 1.76 wt.%, corresponding to FeS contents of 0.85–2.77 mol%. The range of FeS content between 0.85 and 2.77 is comparable with those of the lower limit of the ISEM systems ranging from 1 to 20 mol% FeS.

4.5.5 Olucak

This property is situated within the central part of the Eastern Pontides. The property is located approximately 100 km South-southwest of Trabzon and 13 km northeast of Gümüşhane (Fig. 4.4). Silicified zones hosting anomalous gold-silver and associated base metals were originally identified by MTA in 1990 by stream sediment sampling surveys.

The Early to Middle Lutetian basaltic–andesitic lavas and their pyroclastic equivalents widely crop out in the area. The Early to Middle Lutetian volcanic sequence was cut by Late Lutetian non-adakitic granitic intrusions. The vein and veinlet zones are hosted by altered andesitic and dacitic volcanic rocks. Silicified zone extends for 600 m along strike with a thickness up to 50 m until it is covered with overburden. Intermediate argillic alteration is widespread in the andesitic lavas and represented by illite and smectite with lesser kaolinite. Phenocrysts of plagioclase, hornblende and biotite are replaced by clay minerals. The argillic alteration grades outwardly propylitic alteration. Epidotisation is the most prominent alteration with chloritisation in basaltic lavas.

Mineralisation and associated alteration are mainly controlled by sets of NW-SE trending strike slip and oblique faults typically dipping at high-angles between 70 and 90°. Pyrite, chalcopyrite, sphalerite, fahlore group, galena are the major sulphides in gold-bearing veins. Hematite, limonite, bornite, covellite, chalcosite and digenite are observed as supergene enrichment. Quartz, barite, sericite, calcite,

adularia, illite and kaolinite are the main gangue and clay minerals of the veins. Epithermal textures including crustiform banding, comb textures, alteration mineralogy and patterns and geothermometres of fluid inclusion studies are indicative of low sulphidation epithermal system (Bilir 2015).

4.5.6 Eskine Yayla

Granitoid rocks in the Eskine Yayla area (Şebinkarahisar), host polymetallic (Pb, Zn, Cu, U) vein-type mineral deposits (Fig. 4.4). The host granitic rocks belong to the Upper Cretaceous–Middle Eocene metaluminous, subduction-related plutonic rocks composed of quartz syenite, syenite, granite, monzonite and quartz monzonite. The veins are dispersed in an area of about 1 km^2. The strikes of the veins are N 75–85° E with dips of 70–80° SE. The veins extend for about 10–200 m with thicknesses of 10 cm and 3 m. Sphalerite, galena, pyrite and chalcopyrite are the most common ore minerals in the vein paragenesis of Eskine Yayla. Fahlore group minerals, Bi-sulphides and sulphosalts, green and purple fluorites are present in minor amounts. Quartz is the major gangue mineral with fluorite in some veins and with barite in the rest. Some carbonate minerals are also present. Three successive crystallisation stages of quartz are identified during the formation of vein system. Native gold is recorded in between the crystals of stage II quartz. The homogenisation temperatures are in the range of 200–260 °C concentrating between 220 and 240 °C for quartz I and in the range of 100–200 °C concentrating between 120 and 160 °C for quartz II. The homogenisation temperatures on fluid inclusions in green fluorites range from 160 to 330 °C concentrating between 270 and 300 °C for green fluorite I and between 160 and 190 °C for the green fluorite II. The inclusions from purple fluorites homogenise to liquid in the range between 120 and 220 °C concentrating between 140 and 170 °C. Salinities were 9.5–15 wt.% NaCl equivalent for inclusions trapped within quartz II, 5.0–11 wt.% NaCl equivalent for green fluorites and 7–13 wt.% NaCl equivalent for purple fluorites (Ayan 1991).

4.5.7 Etir Yayla

Etir Yayla veins are hosted in andesite and andesitic breccia of the Upper Cretaceous volcanic succession of the region (Fig. 4.4). Three subparallel vein systems strike mainly N 10–40° W and dip about 80–85° to SW. The longest vein has been traced for more than 300 m. Sphalerite is the most common sulphide in the ore paragenesis which also includes pyrite, arsenopyrite, chalcopyrite, Bi-minerals, fahlore group minerals, and galena. Fluorite is the dominant gangue mineral and most of the fluorite veins have thickness of 1–15 cm with some of them exceeding 50 cm. Both green and purple fluorites are common gangue minerals of the Etir Yayla veins formed under a wide range of temperatures between 110 and 290 °C (Ayan 1991).

4.5.8 Asarcık

The Asarcık intermediate sulphidation type vein system is hosted by granitoids composed mainly of syenite, monzonite (Fig. 4.4). Tourmaline is the most prominent gangue phase with lesser quartz in Asarcık vein system, which is controlled by a steeply-dipping, NW–SE strike-slip fault zone. The vein system has lengths of up to 3050 m with thicknesses varying from a few cm up to 4 m. The strike of the vein is N45–50°W, dipping nearly vertically southwest. Three phases of mineral deposition are recorded: early pyrite-pyrrhotite, and arsenopyrite, intermediate arsenopyrite, chalcopyrite, Bi-minerals and base metals. The highest ore-forming temperatures are with the sulphide minerals including pyrrhotite, pyrite and arsenopyrite associated with quartz I which has higher homogenisation temperature interval mainly scattered in between 320 and 360 °C. On the basis of homogenisation temperatures from sphalerite and quartz III, the main base metal mineralisation is formed in the range of between 130 and 160 °C with salinities between 6.5 and 14 wt.% NaCl equivalent (Ayan 1991).

4.5.9 İnler Yaylası

The İnler Yaylası system is hosted in a series of volcanic rocks of rhyolitic, rhyodacitic, andesitic composition, and consists mainly of veins with strike lengths of between 80 and 450 m. Their thickness vary from 0.5 to 2 m and their vertical extension vary between 100 and 300 me. Sphalerite, galena, chalcopyrite and pyrite are the most common ore minerals. Fahlore group minerals, enargite-luzonite are present as accessory minerals. Quartz and minor carbonates and barite are the main gangue minerals. Inclusions in quartz I are primary, two-phase (L+V), liquid-rich, and irregular to negative crystal shaped, and have homogenisation temperatures ranging from 180 to 330 °C (mainly between 240 and 270 °C). Inclusions from sphalerite have yielded homogenisation temperatures of 160–270 °C, and ranging between 190 and 230 °C (Ayan 1991).

4.6 Ore Mineralogy

Well developed mineralised veins of low-sulphidation epithermal systems provide convenient material for advancing our knowledge of the nature of the vein formation systematics. In a typical low and intermediate epithermal system, ore bodies include veins, veinlets, stockwork, stringer, brecciated and disseminated ore. Precipitation of precious minerals and associated sulphide and sulphosalts is a function of diverse factors including temperature, pressure and redox state of the solution oxygen and sulphur fugacity. Although the elemental association is represented by ore elements such as Au, Ag, As, Sb, Hg, Tl, Te, Pb, Zn and Cu, the mineralogy

of sulphide, sulphosalt and associated gangue minerals are rather complex. Characterisation of gold-bearing ore including the distribution of gold in different mineral phases, grain size, and, if present, the distribution and nature of invisible gold is important for the best method of metallurgical recovery. A rather complex system of fluid circulation seems to have been involved in the genesis of the both intermediate and high sulphidation subtypes, which have a more complex mineralogy and metal suite that includes gold, silver, copper, zinc, lead, bismuth sulphides and sulphosalts that tend to be associated with porphyry systems. Correlations between gold, silver and Te-Se sulphosalts in epithermal deposits has not been studied yet in Turkey.

The total sulphide content is negligible or lower than 5 wt% of the whole vein in LSEM. The gold in some LSEM in western Anatolia is associated mainly with pyrite and subsequently with other sulphides such as galena, sphalerite and chalcopyrite. Although sulphide and sulphosalt contents are in trace amounts in the paragenesis of LSEM their composition and paragenetic relationship with gold and silver minerals furnish important data both in exploration and mine development processes. The ISEM sub-type is characterised by the highest content of base-metals among all the sub-types of epithermal deposits. The Ag/Au ratio is also higher than those of LSEM and HSEM. The most common sulphide minerals in both Au-Ag ISEM and base metal ISEM are galena, sphalerite, pyrite and chalcopyrite. Bornite, arsenopyrite, cubanite, chalcocite, marcasite, hessite, native gold, electrum, tellurides occur in different quantities.

4.6.1 Pyrite

Without a depth limit, pyrite is the most common and widespread sulphide in most of the epithermal systems in Turkey. Different grain size, crystal shape and textures of pyrite in epithermal deposits have been documented in Turkey. It occurs in more than one generation and in general one is formed in the early stages of sulphide precipitation. Crystal morphology of the pyrite may be a useful indicator during exploration. Changes in the crystal morphology of the pyrite from cubes through octahedra to gelpyrite, generally coincides with the changes from barren to mineralised systems (e.g., Mauk et al. 1998).

Porous pyrite of early stages in Efemçukuru is an important host for gold mineralisation. Pyrite, particularly arsenian pyrite and arsenopyrite, are the major sulphides that carry significant quantities of invisible gold. The term “invisible” arises from the fact that one cannot distinguish, by conventional microscopy, between gold chemically bound in the mineral and submicroscopic inclusions (Cabri et al. 2000). The laser ablation inductively coupled plasma mass spectrometry (LA-ICP-MS) has been successfully used for in situ determination of gold and trace elements in minerals and their inclusions in last two decades (Cook et al. 2009; Maslennikov et al. 2009; Large et al. 2009; Sung et al. 2009; Thomas et al. 2011; Ye et al. 2011; Zhao et al. 2011; Winderbaum et al. 2012; Zheng et al. 2013). It has

been inferred that the solubility of Au in nonarsenian pyrite does not exceed few ppm, however Au content increases with As-rich compositions in pyrite growth zones (Cook and Chryssoulis 1990; Wells and Mullens 1973; Sha 1993; Arehart et al. 1993; Fleet and Mumin 1997; Simon et al. 1999; Cline 2001; Pals et al. 2003). The quasi-steady arsenian pyrite in Carlin-type and epithermal deposits has abundant Au contents, because those pyrites are formed at low-temperatures (<250° C) in which disequilibrium conditions and surface defects are pervasively developed (Zhu et al. 2011).

Pyrite is abundant in Efemçukuru with variable morphology and grain size from sub-mm, idiomorphic single and clustered grains, making this deposit worthwhile to study the distribution of invisible gold in pyrite. In Küçükdere, pyrite is common however less abundant than Efemçukuru. The pyrite content is increased with the total sulphide content in certain parts of the deposit. Pyrite is the most common sulphide throughout the deposit, with its subhedral to euhedral cubic and pyritohedron crystals. Laser Ablation studies were performed on pyrites of Efemçukuru and Küçükdere to provide analytical data on precious and trace element composition. Laser Ablation data in Efemçukuru show a positive correlation between Au content and As-rich zones (Oyman et al. 2010). Gold concentration in pyrite and arsenopyrite ranges from below one ppm to several hundred ppm. In HSEM of Turkey, pyrite is the most widespread sulphide in association with gold mineralisation.

4.6.2 Sphalerite

In epithermal deposits the common occurrence of sphalerite provides an additional useful measure of sulphidation state. The mol% FeS in sphalerite coexisting with pyrite or pyrrhotite is continuously variable as a function of sulphidation state (Scott and Barnes 1971; Czamanske 1974); 40–20mol % FeS at low sulphidation states, 20–1 at intermediate sulphidation states, 1.0–0.05 at high, and <0.05 at very high. Unfortunately, there are few studies that document sphalerite compositions in any detail and address the question of equilibrium with iron sulphides (Einaudi et al. 2003).

Sphalerite from both Şahinli and Tesbihdere is very poor in iron. The iron content of sphalerite vary between 0.4 and 1 wt.% Fe which corresponds 0.6–1.4 mol% FeS (Yılmaz et al. 2010). Çiçek and Oyman 2016, reported that the Fe content of sphalerite from Tespihdere is 0.89 wt.%, corresponding to FeS content of 1.41 mol% which is consistent with the data of Yılmaz et al. (2010). The highest Fe concentration of sphalerite in the Koru and Tesbihdere mining districts is in the Kuyutaşı mineralisation where it reaches up to 3.09 wt.% Fe content, corresponding to 4.86 mol% FeS. In general, the Fe content of sphalerite from both mining districts is compatible with the values of intermediate sulphidation epithermal base metal-rich deposits ranging from 1 to 20 mol% FeS, while high sulphidation epithermal deposits usually contain <1 mol% FeS (Shikazono 1974, 2003; Watanabe and Soeda 1981; Einaudi et al. 2003; Yılmaz et al. 2010). Early-stage sphalerite in V. Viraj

(Koru Mining district, Çanakkale), which surrounds and postdates early-stage pyrite, commonly occurs as euhedral to subhedral crystals without distinct exsolutions. Contrary, late-stage sphalerite contains exsolutions of chalcopyrite as tiny blebs and replaces other abundant sulphide minerals such as galena, chalcopyrite and pyrite. The Fe content of late-stage sphalerite vary from 0.71 to 1.12 wt.%, corresponding to FeS contents of 1.12–1.76 mol%.

In Efemçukuru, grains of sphalerite with overgrowths were analysed from North Ore Shoot (N2, 9 spots). The data show that the cores have mean concentrations of 13.5 wt.% Fe, with very high Ag (mean 1880 ppm) and are also rich in Cd (mean 8400 ppm), Sn (mean 180 ppm) and Ga (mean 62 ppm) (Oyman et al. 2010).

In Arapuçandere deposit, the ore assemblages and moderate iron content up to 11 mol% of FeS in sphalerite typically refer to the properties of base metal-rich Ag±Au ISEM. The FeS content of sphalerite ($Zn_{0.85–0.98}Fe_{0–0.11}Cu_{0–0.06}Cd_{0–0.02}S_{0.97–1.03}$) displays an increase towards the deeper levels of the mineralisation (Çiçek et al. 2017). In sphalerite of ISEM, it seems like high Cd contents positively correlated with gold assays.

4.6.3 Fahlore Group

The composition and substitution mechanisms of "Fahlore" group minerals have been used as a petrogenetic indicator of ore forming processes in epithermal environments. The composition of fahlores and its evolution could be used as an important guide to follow up the flow pattern and fluid evolution with respect to time and space. Chemical evolution of fahlores from porphyry to epithermal systems is determined in mining districts all over the world.

Such sulphides, including the relatively high-sulphidation state minerals tennantite-tetrahedrite (Barton and Skinner 1979), are typically rare or absent in low-sulphidation deposits. In Turkish LSEM fahlore group minerals are rare and tetrahedrite is the dominant fahlore mineral. Up till now, mineral chemistry on sulphide and sulphosalts including fahlore group minerals are based on SEM and EDS analysis. In Ovacık and Küçükdere LSEM fahlore group minerals are represented by tetrahedrite. Tetrahedrite at Ovacık is associated with chalcopyrite, bornite and gold with lesser galena and sphalerite. At the Ovacık gold deposit, tetrahedrite–tennantite is represented by Sb–Ag-rich tetrahedrite (26.7–29.6 wt.% Sb, 1.3–2.5 wt.% Ag, 29.5–33.9 wt.% Cu, 1.5–2.7 wt.% As), with minor As-rich tennantite (14.6–19.6 wt.% As, 0.4–0.9 wt.% Ag, 33.9–34.8 wt.% Cu, 2.3–3.9 wt.% Sb). It is clear that some paragenetic overlap occurs between bornite and tetrahedrite, since these minerals enclose one another (Yılmaz et al. 2007). In Küçükdere, tetrahedrite (20 wt.% Sb; <5 wt.% As) replaced chalcopyrite both of which are replaced by the late stage sphalerite.

Minerals of tetrahedrite-tennantite solid solution series are more abundant in intermediate sulphidation assemblages in western Turkey. ISEM with fahlore group minerals are more common in accordance with their higher base metal content and

sulphidation state. Fahlore group minerals in ISEM are closely associated with precious metal tellurides and/or gold-silver alloy (e.g., electrum). Fahlore group minerals in Koru, Tesbihdere and Şahinli ISES were studied using SEM in the beginning of 2010s.

It has been inferred that the fahlore group minerals such as goldfieldite, tellurian tennantite and extreme "Cu-excess" tennantite and tetrahedrite are indicative of high-sulphidation, enargite/luzonite-bearing assemblages and a very close association with native gold (Repstock et al. 2015).

4.6.4 Gold and Silver

Native gold and electrum either as free grains within gangue or associated with sulphides, sulphosalts, tellurides and selenides are the main gold phases which have been identified in the epithermal deposits of Turkey. Efemçukuru has a more complex paragenesis due to multiple pulses of fluid in a short period of time with different geochemical character even in the same zone (SOS, MOS or NOS) of the vein system. Although native gold occurs associated with all sulphides, pyrite is the most common gold-host followed by galena, sphalerite, chalcopyrite and arsenopyrite in descending order. In SOS, we observe that gold is tied to galena (notably where relictic galena is present in sphalerite), as droplet-shaped inclusions up to 50 μm in size. In MOS, gold in association with silver minerals is present in pyrite, especially in the porous bands, as sub-rounded to elongate grains, up to 10–20 μm in size (Fig. 4.5a, b). In NOS, native gold is present in arsenopyrite as sub-5 μm-sized grains.

As documented in most of the epithermal systems free gold is present chiefly in pyrite as is the case for the Küçükdere deposit. Pyrite is the main sulphide in Küçükdere including gold and some tellurides dominated by hessite (Fig. 4.5c, d). In Çoraklık, our preliminary petrographic studies show that in high-grade samples, gold is intimately associated with silver minerals and sulphosalts in sulphides including pyrite, chalcopyrite, galena and sphalerite (Fig. 4.5e). Gold distribution and associated fluid flow is well documented in the Ovacık deposit. Both electrum and native gold are associated with sulphides at certain depths below the current topographic level. It seems like that the base metal zone is related to the boiling zone at least along 300 m vertically. Detailed mineralogical studies combined with geochemistry showed that gold is associated with chalcopyrite more than other copper minerals including bornite and tetrahedrite and tennantite in Ovacık (Fig. 4.5f). In the Red Rabbit Project a relatively simple ore mineralogy has been documented by Yılmaz et al. (2013). Pyrite is the essential sulphide where the sulphides are in trace amounts in the vein paragenesis. Gold is commonly found as individual crystals or in association with acanthite.

ISEM are characterised by high Ag:Au ratios and base metal content. Silver mineral assemblage is well documented in the Koru and Tesbihdere mining districts by Çiçek (2013) and Çiçek and Oyman (2016). In Koru, the Kuyutaşı mineralisation

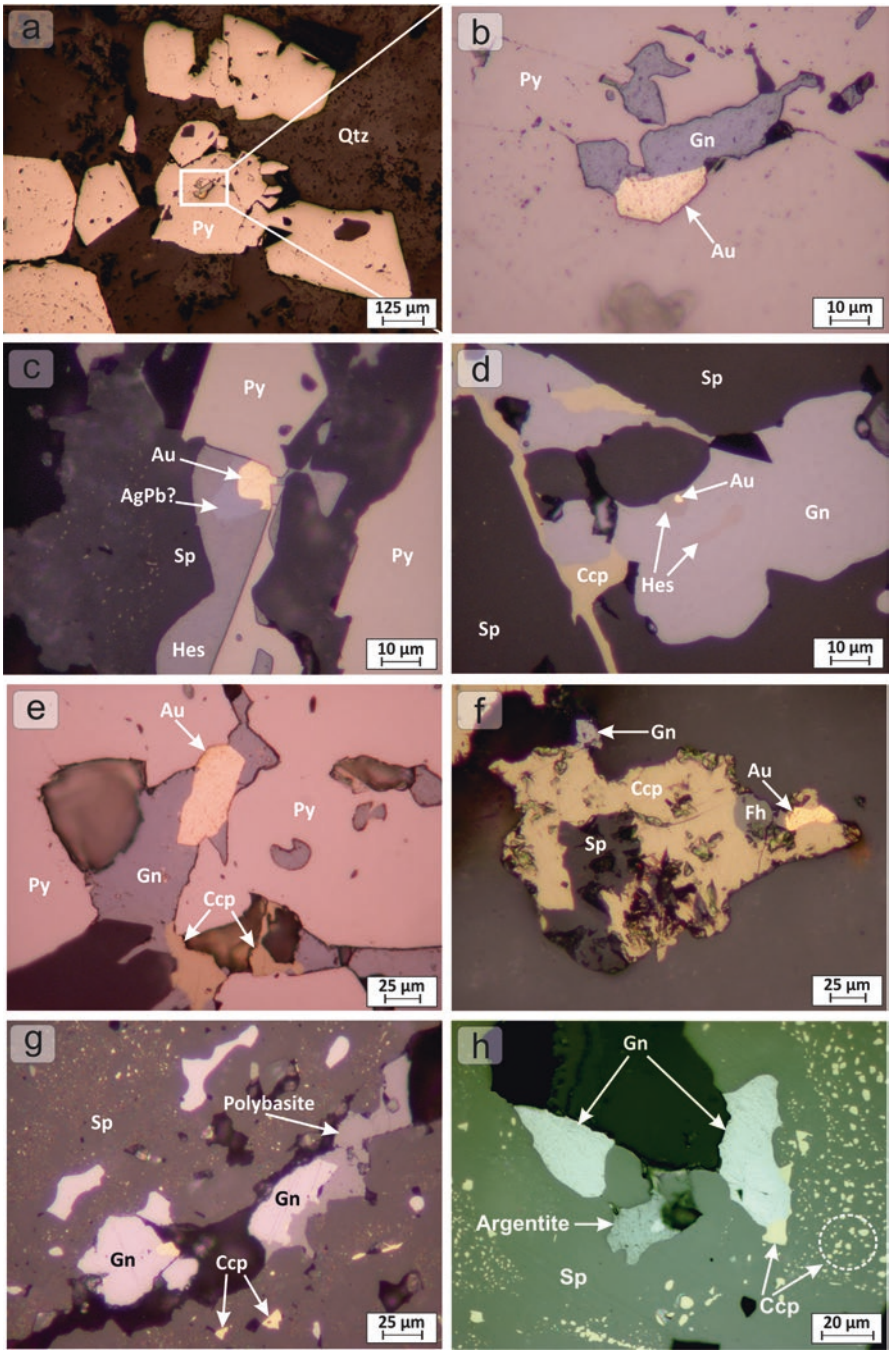

Fig. 4.5 Photomicrographs under reflected light (//N), showing textural relationships between Au-Ag minerals and associated sulphide minerals at the selected epithermal deposits. (**a**, **b**) Gold in association with silver minerals in pyrite (Py) in Middle Ore Shoot of Efemçukuru gold deposit.

commonly contains Ag-sulphosalt, up to 80 μm in size, which occurred as cavity-filling in pyrite in the later stages of the mineralisation. The Kuyutaşı mineralisation comprises pearceite type Ag-sulphosalt, which has lower Sb (0.29 wt.%) and As (4.16 wt.%) contents. Furthermore, fine-grained gold ranging between 1 and 6.5 μm in size is usually found as free grains in association with euhedral quartz. The abundance of gold and silver tends to increase with the increase in copper ore at depth (Çiçek 2013). At Şahinli, economic concentrations of Au occur mainly within quartz-rich veins whereas higher Ag concentrations are associated with base metal-rich quartz veins, particularly those rich in Pb.

Argentite, acanthite, jalpaite, polybasite-pearceite, freibergite and Ag-rich tetrahedrite-tennantite are the most widespread Ag-bearing sulphosalt minerals in the overall Arapuçan vein zone. They are associated with late stage mineralisation, and mainly occur either as fracture-fillings, or as haloes surrounding the early sulphides. Gold occurs as rounded-shaped inclusions within chalcopyrite and galena, and present variable Au and Ag contents. Electron microprobe measurements also have shown that most gold grains are compositionally zoned. Gold grains present a marked variation in their contents in Cu, Fe and S, as a function of their host sulphide and sulphosalt phases (Çiçek et al. 2017).

4.7 Epithermal Textures and Associated Minerals

The recognition and interpretation of textural features of epithermal systems and to be able to determine the physical and chemical environments where the hydrothermal fluids circulate is one of the important approaches in exploration. In epithermal systems, varieties of silica with carbonates are the main gangue minerals. The carbonates mainly consist of calcite with rhodonite, ankerite and siderite. Multiphase calcite generations are found in most of LSEM and ISEM systems in Turkey. While barite is found in some ISEM in Koru Mining district of the Biga Peninsula, fluorite is abundant in epithermal deposits in the Şebinkarahisar area in the Black Sea Region.

Boiling is often temporally and spatially associated with gold and silver mineralisation in epithermal systems and the boiling horizon also outlines a possible precious metal zone in an epithermal system where rising magmatic fluids mix with oxidising near surficial groundwater. Occurrence of hydrothermal breccias is

Fig. 4.5 (continued) (**c**, **d**) Euhedral gold and some tellurides dominated by hessite (Hes) is present chiefly in pyrite as the main sulphide with galena (Gn) and sphalerite (Sp) in Küçükdere. (**e**) Gold and sulphide association after pyrite represented by enclosed gold (Au) in galena in Çoraklık. (**f**) Positive correlation between gold and copper is emphasized by the close relationship between chalcopyrite (Ccp) fahlore (Fh) and native gold (Au) in Ovacık. Galena and sphalerite are the common accompanying sulphides. (**g**) Silver minerals are represented by native silver, acanthite, polybasite and pearceite in Tesbihdere. (**h**) In Arapuçandere argentite is one of the dominated silver minerals in association with galena and sphalerite.

regarded as an evidence of boiling. Hydrothermal breccias are formed when hydrothermal fluid exceeds the lithostatic pressure, resulting in the fracturing of the rock showing typical jig-saw structures. Beside brecciation, quartz veins in the epithermal environment are characterised by multiple generations of chalcedonic, microcrystalline, and comb-textured quartz exhibiting crustiform and colloform bands and cockade overgrowths.

The style of carbonate occurrences in epithermal deposits is discussed broadly in some papers and examples mentioned in economic geology literature. In epithermal systems, carbonates assemblages are composed mainly of calcite with rhodochrosite, ankerite with lesser amounts of siderite. Multistage calcite generations are found in both LSEM and ISEM systems. Either as barren or as boiling-related calcite is a widespread mineral in epithermal systems in western Anatolia. As long as boiling continues, volatiles such as CO_2, H_2S, CH_4, SO_2, SO_4 are lost to the steam phase along the open system up to the paleosurface. Partitioning of CO_2 in the steam phase causes precipitation of calcite and a rise of pH in the remaining solution. Thus the occurrence of bladed calcite is accepted as evidence of boiling in epithermal systems. Microthermometric studies on bladed calcite would guide us to approach the true trapping temperatures. Although calcite is a widespread gangue in LSEM and ISEM bladed-like texture is more likely developed in classic LS epithermal vein deposits. In some epithermal deposits including Küçükdere, Çoraklık, Ovacık, Efemçukuru, Çukuralan and Kepez (Red Rabbit) carbonates are the most common gangue minerals in association with quartz. Küçükdere is one of the best examples of LSEM with its carbonate content and carbonate paragenesis. Calcite, ankerite, rhodochrosite are the most common carbonates in and around the veins. Most of the rhodochrosites are at and near the surface, well developed examples of bladed calcite were found in the Karayanık vein in Küçükdere. Replacements of bladed calcites pseudomorphly by silica were not observed. This observation suggests that bladed calcite formation is the latest hydrothermal event in the mineralisation. Parallel type bladed calcites vary in thickness from 0.3 to 2 mm. Lattice type bladed calcites were formed as thin and discontinuous lamellas. There are at least four stages of calcite precipitation in Karayanık Tepe. Early calcites (Cal I) tend to be thicker, reaching a maximum thickness of 2 mm and range in length from 0.3 to 2 cm (Fig. 4.4a). The early calcites (Cal I and Cal II) show bright blue or yellow colours of the fourth and fifth orders in thin section. The later calcites which form as lattice type bladed crystals range in thickness from 20 μm to about 800 μm. Under the microscope, calcites from the third and fourth generations (Cal III and Cal IV) are pale brown or grey colours. Although not widespread as in Küçükdere and Çoraklık, in Ovacık calcite, ankerite and siderite are the most common carbonates associated with mineralisation. Networks of intersecting blades of calcite were replaced by quartz. Lattice-bladed carbonate replacement texture is well developed in Karadüz area in Kızıltepe vein system (Sındırgı-Balıkesir).

The crustiform texture is usually interpreted to represent episodic rapid nucleation that occurs as a result of intermittent boiling and changes in pressure (Taylor 2009). The crustiform textures in the veins system are represented by rhythmic alternation of bands different mineral proportions dominated by cryptocrystalline

quartz, calcite, manganese-bearing calcite, sulphides, rhodochrosite and rhodonite with lesser amounts of adularia. Crustiform texture is the most widespread texture in Germe Tepe vein. Calcite is the major constituent of some veins (e.g., Germe Tepe and Karayanık Tepe) where it precipitates in different stages of vein formation either as bladed, crustiform or infilling forms. The mineralogy of crustiform textures gives important clues about the formation of precious mineral deposition in epithermal deposits. In the Efemçukuru, complex crustiform texture shows successive bands with different orientations and defined by differences in mineralogy or colour. Calcite is an abundant carbonate with rhodochrosite in concentric and banded vein formations. Calcite bands of the concentric structures are replaced by euhedral crystals of manganaxinite and tinzenite (Oyman et al. 2003). Cockade structures are widespreadly occurred. Drusy quartz is commonly occurring in the cavities, vugs either in breccia or in crustiform bands.

The study of textural features of hydrothermal breccia is one of the requirement to be able to ascertain the chronology, mechanism and classification of ore deposition. Hydrothermal breccias are commonly observed in veins that were formed close to the surface where it is favourable for brittle deformation (Genna et al. 1996). As mentioned a boiling occurs when pressure drops due to fracturing when fluid pressure exceeds lithostatic pressure.

Critical fracturing is related to the destruction of the equilibrium between the pressure of the fluid and the regional stress within a vein (Hobbs 1985). High fluid pressures and the local structural context combine to maintain open the hydrothermal channelways, enabling hydraulic fracturing within the vein (Phillips 1972). Fluid pressure decreases in response to a sudden opening of space generated by rapid slip or by the intersection between different veins. Within the vein system, repeated episodes of brecciation due to cyclic self-sealing and overpressuring could result in the multi-phase enrichment of gold. One of the most diagnostic feature of epithermal breccias is the widespread occurrence of fine grained chalcedonic quartz both as replacement of fragments and a cement between fragments (Sillitoe 1985). Rock-flour is silicified in most of epithermal system-related breccia. The lithology of fragments, rock flour and intensity of silicification of both matrix and fragments are controlled by various factors (e.g., depth of the system, duration of the hydrothermal activity, permeability of surrounding rocks, and inclination of the vein).

The clast-supported breccia is composed mainly of wall-rock fragments in some LSEM and ISEM such as Küçükdere and Efemçukuru. As observed in most LSEM systems (e.g., Ovacık, Red Rabbit, Küçükdere) clasts of vein material, cemented by silica or other materials including sulphides are commonly due to hydraulic fracturing or to multiple generations of quartz. The Ovacık examples of clast-supported crackle (shattered) breccia with monomictic fragments and matrix-supported fluidised (milled) breccia with angular to subrounded polymictic fragments have been well documented in Yılmaz et al. (2007). Examples of cockade breccias are also well documented in Efemçukuru, Red Rabbit, and Küçükdere deposits. The Efemçukuru deposit provides an exceptional example of mineralised breccias, and in particular cockade breccias. The cockade breccias varying in size from few centimetres up to decimetres were observed in various depths in Kestanebeleni vein

system in Efemçukuru. In Efemçukuru, the fragments which formed the nuclei of the breccias are composed mainly of hornfels which formed by the contact metamorphism of pelitic rocks of the Bornova Flysch Formation. Low permeability of the hornfels is diminished in time as a result of repeated silicification during the active period of the Efemçukuru hydrothermal system. The fragments of hornfels are coated by alternating manganaxinite–tinzenite, rhodonite, rhodochrosite, quartz and calcite bands to form cockade textures (Oyman et al. 2003). Significant rotation of clasts was observed.

In Germe Tepe (Küçükdere), cockade textures composed mainly of concentric layers of quartz were formed around the nucleus of the propylitically altered andesite breccia fragments. Gangue minerals are mainly quartz, calcite and Mn-oxides with lesser barite. In Çengel Tepe (Küçükdere), relatively coarse (up to cm in length) crystal aggregates of quartz have a comb-like radial disposition around the nucleus of the phyllic altered andesite breccia fragments. The cockades are interpreted as reflecting the occurrence of hydraulic fracturing within open-space domains (Genna et al. 1996). Matrix or clast-supported hydrothermal breccia with angular-subround monomictic to polymictic fragments is also common. Best examples of hydrothermal breccias were observed in Çoraklık Tepe vein system. In between 50 and 150 m of depth in drillholes well developed matrix-supported breccias are thought to have formed during repeated brecciation. Angular to sub-angular clasts of the breccia composed mainly of calcite and bladed-calcite indicate boiling and related self-sealing.

4.8 Fluid Inclusions

Due the limited space in most of the recent papers on epithermal deposits in Turkey, fluid inclusion studies are not fully considered or represented. The fluid inclusion data from epithermal mineralisation in Turkey are summarized in Table 4.1. Fluid inclusion studies were performed mainly on LS and IS type epithermal systems in Turkey. One of the most crucial features related to boiling hydrothermal fluids are the fluid inclusion assemblages trapped from the boiling horizon to the surface. Coexisting liquid-rich and vapour-rich inclusions of a same paragenetic stage is accepted as one of the most reliable evidence of boiling. It should be taken into account that boiling causes higher homogenisation temperatures than the true trapping temperatures. These coexisting inclusions indicate trapping also in an immiscible fluid environment. As mentioned earlier, the occurrence of platy or bladed calcite is a good indicator of boiling conditions (Browne 1978; Simmons and Christenson 1994), consistent with the occurrences of some coexisting liquid-rich and vapour-rich inclusions (Bodnar et al. 1985). Therefore, it is believed that homogenisation temperatures obtained from calcite represent true trapping temperatures, excluding the need for pressure corrections. The lattice-bladed calcite could

Table 4.1 Selected fluid inclusion data for the epithermal mineralisation in Turkey

Deposits	Type of inclusions	$T_{H\ (°C)}$		$T_{H\ (°C)}$ ort	Salinity (wt.% NaCl)		Salinity ort	Tm_{first}	Minerals	References
Şahinli	Primary	180	321	–	0.5	7.7	–	–	Quartz	Yılmaz et al. (2010)
		229	321	–	2.6	7.6	–	−24.5 to −19.0	Sphalerite	
Alakeçi-Kısacık	Primary	148	389	241.3	0.1	6.5	2.6		Quartz	Vural (2006)
Kuşçayırı	Primary	192	370	294	0	31.2[a]	2.7		Quartz	Vural (2006)
Sındırgı	Primary	150	395	250	0.2	4.8	1.8	−20 to −33	Quartz	Yılmaz et al. (2013)
Ovacık	Primary	147.6	298.3	187.3	0.7	2.1	1.4	–	Quartz	Yılmaz et al. (2007)
Narlıca	Primary	205	303	236	0.1	0.8	–	–	Quartz	Dag (1993) and Ebert (2004)
Kaymaz	Primary	238	389	319.7	0.3	14	–	−72.1 to −49.6	Quartz	Yavuz (2013)
Arzular	Primary	130	295	214	4.3	12.4	8.5	−30.2 to −36.4	Quartz	Akaryalı and Tüysüz (2013)
		90	133	109	0.7	2.7	1.7	−32.4 to −37.2	Sphalerite	
Arapuçandere	Primary	150.2	438	–	0	34.0	–	−37.5 to −10.1	Quartz	Orgun et al. (2005), Bozkaya et al. (2008) and Bozkaya and Banks (2015)
		186	384	–	1.7	29.2	–	−30.8 to −12.4	Sphalerite	
		206.1	321.9	263.6	22.5	29.6	27.1	−31.4 to −20.1	Calcite	
	Secondary	193.7	354.4	278.2	13.6	27.5	22.7	−28.1 to −9.7	Quartz	
		139.8	345.2	279.2	14.3	32.0	22.7	−34.9 to −10.3	Calcite	
Kartaldağ	Primary	135	285	–	0	1.7	–	–	Quartz	Ünal-İmer et al. (2013)
	Secondary-pseudosecondary	93	279	–	0	1.4	–	–	Quartz	
Madendağ	Primary	235	255	–	0	0.4	–	–	Quartz	Ünal-İmer et al. (2013)
	Secondary-pseudosecondary	90	285	–	0	0.7	–	–	Quartz	
İnkaya	Primary	235	340	299.8	0.7	4.5	3.0	−32.9 to −49.6	Quartz	Özen and Arık (2015)
Altınpınar	Primary	170	380	–	2.4	7.3	4.7	–-	Quartz	Akaryalı (2016)

(continued)

Table 4.1 (continued)

Deposits	Type of inclusions	$T_{H\ (°C)}$		$T_{H\ (°C)}$ ort	Salinity (wt.% NaCl)		Salinity ort	Tm_{first}	Minerals	References
Mastra	Primary	113	331	213.5	0.4	10.2	4.7	−31 to −17	Quartz	Aslan (2011)
		150	390	280.3	0.7	10.1	3.7	−19.5 to 28.3	Barite	
	Secondary	110	240	159.4	2.4	6.6	4.4	–	Quartz	
		218	267	249.0	–	–	–	–	Barite	
Tesbihdere/ Sarıoluk	Primary	152.0	387.0	–	0.2	10.6	–	−58.0 to −25.0	Quartz	Yılmaz et al. (2010), Bozkaya et al. (2014), and Çiçek and Oyman (2016)
		220.0	342.0	266.5	0.7	6.0	4.3	−46.2 to −19.0	Sphalerite	
	Secondary	177.0	333.0	–	–	–	–	–	Quartz	
Koru	Primary	146.0	358.0	254.5	0.2	6.3	2.1	−51.0 to −32.3	Quartz	Çiçek and Oyman (2016)
		191.2	371.5	277.0	2.1	12.5	6.7	−52.2 to −29.5	Sphalerite	
		160.6	407.0	314.6	0.7	11.6	4.2	−54.0 to −34.0	Barite	
	Primary	129.7	159.3	145.0	2.1	9.9	6.8	−55.0 to −49.5	Sphalerite	Bozkaya and Gökçe (2001)
		54.3	79.8	71.3	6.0	11.1	8.6		Barite	
	Secondary	92.8	224.9	129.0	0.9	9.5	4.3		Barite	
Efemçukuru	Primary	174	328	243.1	0.2	9.9	–	–	Quartz	Oyman et al. (2003)
		185	224	211	2.1	4.0	–	–	Sphalerite	
Balcılar	Primary	70	135	102.3	0.0	1.4	0.7	–	Barite	Özdemir (2011)
		142	187	161.8	0.0	2.1	0.8	–	Sphalerite	
		203	286	250.0	6.3	7.2	6.7	–	Quartz	
		135	198.1	167.6	18.1	20.0	19.2	–	Barite	Bozkaya and Gökçe (2007)
		114.7	277.1	200.7	15.8	26.9	21.9	–	Sphalerite	
		71.2	246.8	–	14.0	22.6	18.6	–	Quartz	

[a]Salt value

be observed as being indicator of boiling throughout a wide range of vertical depth in Germe and Karayanık in Küçükdere deposit. The best examples of lattice-bladed calcite bearing samples, were proved of having higher gold values, thus indicating their relationship with the boiling zone. In Karayanık the fluid inclusion studies on the bladed calcites, indicates similar homogenisation temperatures with the adjacent quartz.

Fluid inclusion data indicate that the low-sulphidation deposits (e.g., Ovacık, Red Rabbit) have very low salinity ore-forming fluids. Low salinity (<2 wt%) fluids are responsible for the gold precipitation of quartz and calcite gangue (Albinson et al. 2001). Such low-salinity fluids were incapable of transporting significant quantities of silver and base metals (Henley 1990), explaining their generally low contents in these ores.

In ISEM systems such as Tesbihdere and Koru, Ag sulphosalt minerals (e.g., polybasite, pearceite) are precipitated by saline fluids with about >10 wt% NaCl equiv (Bozkaya et al. 2014; Çiçek and Oyman 2016). In Arapuçandere there are at least two episodes of quartz precipitation. Petrographical studies indicate that euhedral quartz crystals of an early generation were surrounded by sulphide dominant ore minerals representing the main ore phase. Fluid inclusion assemblages in these quartz crystals are good examples of primary fluid inclusions which form when fluid is trapped on the active growth surfaces of a crystal (Bozkaya and Banks 2015). Fluid inclusion data of Orgun et al. (2005) indicate that these veins were deposited at temperatures ranging from 242 to 438 °C with an average of 303 °C in quartz and from 229 to 384 °C with an average of 295 °C in sphalerite. Although salinity of the fluid inclusions had not been measured because of the low salinity and small size of the inclusions, the salinity was estimated between 1.7 and 18.5 wt.% NaCI equivalent by using the temperature-depth diagram. The fluid inclusion measurements of Bozkaya et al. (2008) were performed on primary and secondary inclusions within sphalerite, quartz and calcite, which represent the early and late stage deposition at Arapuçandere. The homogenisation temperatures in sphalerite range from 276.3 to 319.7 °C with an average of 301.4 °C and salinity varying from 16.3 to 29.2 wt.% NaCI equivalent with an average of 18.3 wt.% NaCI equivalent (Bozkaya et al. 2008). These high homogenisation temperature and intermediate salinity were interpreted to indicate sulphide precipitation during the early stage of mineralisation. The later stages are represented by a slightly decreasing homogenisation temperature with increasing salinity which reflects multiple precipitation of quartz (an average of: Th = 240.2 °C and salinity = 25.3 wt.% NaCI equiv.) and calcite (an average of: Th = 263.6 °C and salinity = 27.1 wt.% NaCI equiv.) (Bozkaya et al. 2008). Recent fluid inclusion data of Bozkaya and Banks (2015) shows that fluid inclusions in quartz have very low salinity values varying from 1.7 to 0 wt.% NaCI equivalent and wide ranges of homogenisation temperatures from 360 to 160 °C.

In Efemçukuru the fluid inclusion data indicate a broad range in T_h from about 200 to 300 °C and range in salinity from near zero to about 9 eq. wt.% NaCl. The higher salinities are more common at depth with no apparent difference in T_h with depth (Oyman et al. 2003). Fluid inclusion assemblages in high grade plunges from Kestanebeleni and Kokarpınar contain coexisting liquid-rich and vapour-rich

inclusions with a high varying liquid/vapour ratios indicating the boiling of fluids. Higher homogenisation temperatures (over 300 °C) and moderate salinities (>10 eq. wt.% NaCl) in coexisting liquid-rich and vapour-rich inclusions in Kokarpınar indicating relatively higher temperatures for the boiling and associated gold precipitation in Kokarpınar vein (unpublished data).

Up till now, there no published data are available on fluid inclusions from HSEM in Turkey. Fine grain size of the quartz in such systems is one of the main reasons for the Kartaldağ HSEM homogenisation temperatures associated with mineralisation being in the range of 245–285 °C. The salinities calculated from these fluid inclusions are low.

4.9 Stable Isotopes

In Turkey sulphur isotopes have been widely applied for the study of ore deposits to determine the formation temperatures of sulphide assemblages and the origin of the sulphur in the epithermal deposits. Characteristic intervals of sulphur isotope compositions of some geological environments are given in Fig. 4.6. The $\delta^{34}S$ values of sulphide minerals from various epithermal deposits in Turkey are distributed in the interval of $\delta^{34}S$ values of granitic rocks (Fig. 4.6). Caution should be taken in the use of sulphur isotopes to distinguish between ore deposits originating in sedimentary (e.g., sea water) and igneous environments due to the extensive overlap of $\delta^{34}S$ values (Fig. 4.6). ISEM and HSEM tend to have greater variation in the sulphur isotope composition of ore minerals because of the precipitation of significant quantities of both sulphide and sulphate from the hydrothermal fluids at the time of mineralisation. Low-Fe sphalerite is a characteristic mineral of intermediate sulphidation state with sulphide-rich Ag-Au bearing base-metal veins containing chalcopyrite, pyrite, galena and fahlore group minerals. In most base metal rich ISEM, galena is a common sulphide mineral together with sphalerite. They precipitate contemporaneously in similar conditions in at least one of the ore deposition stage of an individual deposit, implying that the galena-sphalerite pair is a reliable geothermometer. In epithermal systems, pyrite is the most common sulphide which tends to precipitate at different stages and at different temperatures of ore deposition. Similar to pyrite, more than one generation of sphalerite and/or galena precipitation could be responsible for the widely scattered $\delta^{34}S$ values in epithermal deposits. Additionally, in most ISEM systems the broad distribution of sulphide $^{\delta 34}S$ values suggests either a mixture of several sulphur sources or disequilibrium mineralisation in an open system.

Oxygen isotopes have been widely used since the 1970s to determine the nature and source of the fluids associated with oxygen-bearing gangue minerals, alteration and ore minerals in ore deposits. In Turkey since the 2000s some papers including contributions to O and D isotope compositions of ore forming hydrothermal fluids have been published (e.g., Yılmaz et al. 2007, 2010; Çiçek and Oyman 2016). In the final analysis, O and D isotope systematics of hydrothermal fluids can only be

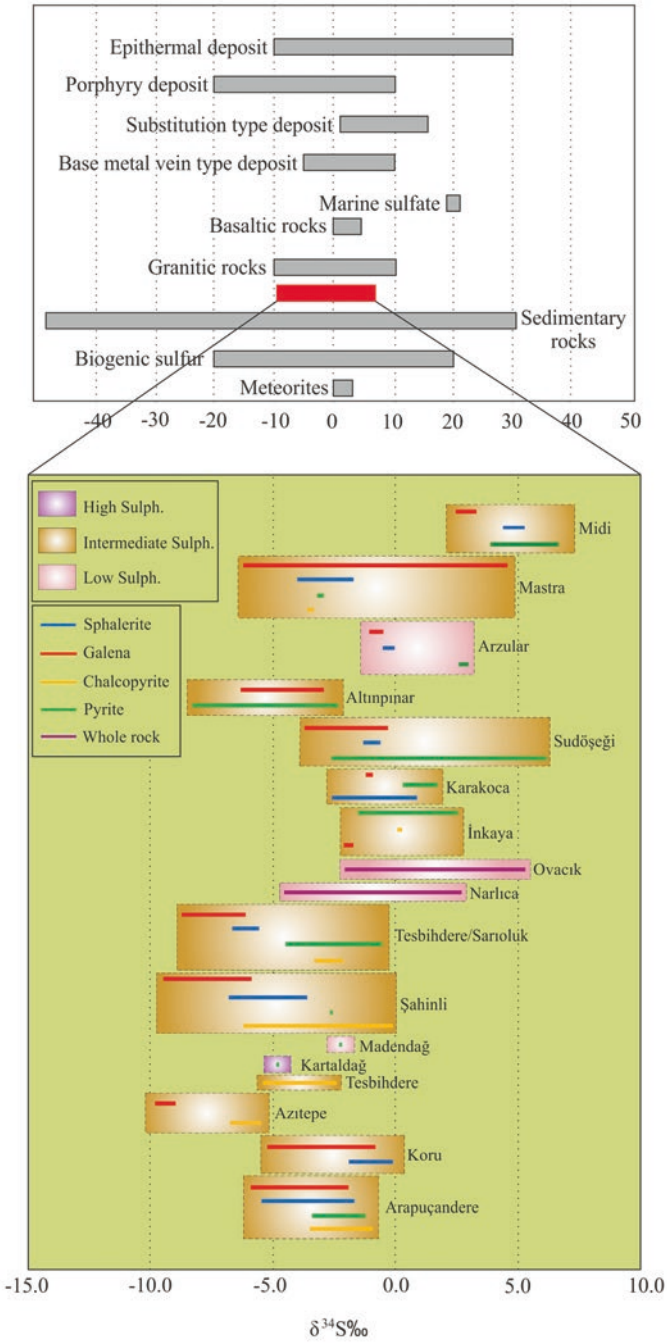

Fig. 4.6 Sulphur isotope composition diagram for different environments and some epithermal deposits in Turkey

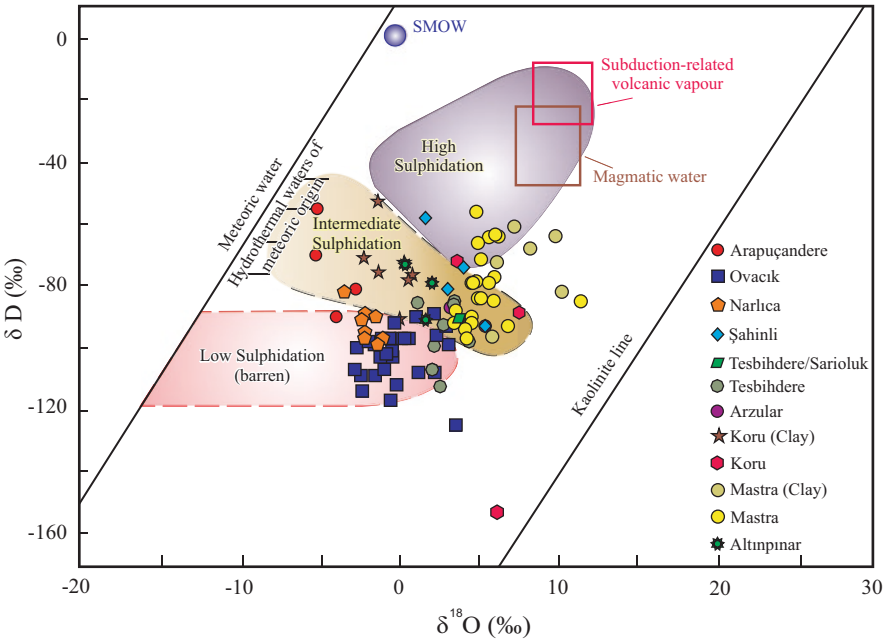

Fig. 4.7 Summary diagram showing the variation in $\delta^{18}O_{H2O}$ and δD isotopic compositions of hydrothermal fluids in the selected epithermal deposits in Turkey

realistically evaluated in conjunction with other data, including fluid inclusion measurements, petrography and, importantly, field relations (Pirajno 2009).

The D and O isotopic data for the ore fluids obtained from quartz and clay samples indicates varying degrees of $\delta^{18}O_{water}$ enrichment relative to the meteoric water line (Fig. 4.7). The wide range in the ^{18}O values of the LSEM systems can be interpreted by different degrees of mixing and/or boiling in an individual hydrothermal system. Most of the quartz samples plot in the low sulphidation area through the O-shift (black arrow), which represents the effect of isotope exchange between meteoric water, magmatic water, wall-rock and the formation waters. This trend can also be explained by isotopic exchange as a result of the interaction between deep circulating meteoric fluid and the wall-rock (Taylor 1979). However, clay samples from varying depths associated with mineralisation plot on the mixing field which exhibits an involvement of magmatic fluid. In most of the epithermal systems the early hydrothermal fluids, associated with the main Au mineralisation, have oxygen and hydrogen isotope compositions that plot in a field close to waters which are associated with magmatic ore deposits and felsic magmas, but they are displaced slightly towards values of present-day meteoric water. One of the effects of boiling on fluid chemistry might be relative enrichment and depletion in isotope compositions. In most of LSEM in western Anatolia the D and O data for the ore fluids obtained from the quartz samples exhibit a trend emphasized by the relative

enrichment of the $\delta^{18}O_{water}$ combined with a relative depletion in D. This trend could have occurred due to vapour separation due to boiling.

There can be some problems with the quartz from epithermal systems regarding the source of fluid. It should be considered that the O and D isotopic composition of water from fluid inclusions reflects the possible mixture of late stage meteoric dominated water mixing, depending on the amount of secondary fluid inclusion in the analysed quartz. The D and O data for ore fluids obtained from quartz identified by their low salinity and temperature, indicates varying degrees of $\delta^{18}O_{water}$ enrichment relative to the local meteoric water. This is the result produced by the exchange of igneous or metamorphic rocks at relatively shallow levels of formation (b1.0 kbar): the classic ^{18}O-shift (Criss and Taylor 1983; Larson and Taylor 1986; Larson and Zimmerman 1991).

Although it is not suitable quantitative comparison of O and D isotope values yielded with different techniques, we have plotted some data from epithermal deposits on a O versus D diagram. Conventional fluorination techniques involve sample heating between 500 and 700 °C (Clayton and Mayeda 1963) using an external furnace whereas the new generation laser-fluorination technique use IR or UV laser for localised heating of the samples (Mattey and Macpherson 1993; Young et al. 1998; Sharp 1990; Elsenheimer and Valley 1992). Recently, the fluorination based IRMS is a preferred technique producing data with high precision better than 0.1%.

4.10 Conclusions

Anatolia (Turkey) is part of the Tethyan orogenic belt, which formed by the amalgamation of microcontinental blocks as a result of evolution through complex tectonic periods from the Late Paleozoic to the late Cenozoic. The epithermal gold provinces of Turkey occupy three main tectonic domains including Western Anatolian Extensional Province, Pontides and Central Anatolian Volcanic Complex. Epithermal deposits of Turkey are hosted essentially in poorly eroded volcanic terrains which are genetically linked with relatively younger or active subduction zones.

In the Late Paleocene–Early Eocene, the Anatolide-Tauride block began to subduct northwards beneath the Pontides of Eurasian Plate, resulting widespread igneous activity, strike-slip faulting and the following extensional tectonic regime in Oligo-Miocene. The porphyry and epithermal deposits of the Black Sea Region are genetically linked with back arc extension which follows the collision between Pontide and Anatolide-Tauride blocks. The ore deposits in Black Sea Region are related to Late Cretaceous arc-magmatism in association with subduction and post collisional extension related Eocene magmatism. Late Cretaceous volcanic, volcano-sedimentary rocks in Eastern Pontide metallogenic belt has been known as the host lithological assemblage mainly for the Kuroko type VMS (e.g., Murgul, Çayeli and Lahanos). Early Cretaceous epithermal systems were preserved in the

Jurassic-Late Cretaceous Banatitic Metallogenic Belt in the western extension and Lesser Causcasus in the eastern extension of Pontide belt. Due to the intimate linkage between the Eastern Pontides with these two belts, Eastern Pontide should be tested for the buried epithermal systems in association with Late Cretaceous arc type volcanism.

Currently active dextral North Anatolian Fault zone becomes wider from east to west and splits in to dextral strike-slip fault branches covering almost whole of the Biga Peninsula. The pull-apart–originated basins of various sizes along North Anatolian Fault System have been recorded. In Biga Peninsula, the epithermal systems are associated spatially and temporally with the NE-SE trending pull-apart basins and volcano-tectonic depressions or calderas (e.g., TV Tower, Kirazlı, Arapuçan). In the Aegean Region NNE-SSW directed continental extension and associated graben development resulted from the combination of Anatolian extrusion and Hellenic subduction roll-back. The graben systems (e.g., Bergama, Edremit, Simav grabens) and associated extensional structures are the conduits for both the calcalkaline igneous activity and the circulation of the hydrothermal fluids between Late Miocene and Late Pliocene.

Epithermal systems are closely related to extensional deformation and magmatism during the Oligocene-Miocene interval in Biga, Eocene in Black Sea, Miocene in South Central Turkey. Epithermal deposits in Black sea region are hosted by Eocene volcanic suits associated with lavas and pyroclastic rocks of volcanic complexes that show mainly andesitic compositions with dacite in lesser amounts. There is only few epithermal mineralisation has been recognised in Late Cretaceous-Paleocene volcanic rocks, which developed due to the arc-type magmatism during the Late Mesozoic-Early Cenozoic.

In Biga Peninsula, epithermal deposits are hosted by Paleogene to Neogene (Oligo-Miocene) volcanic association that records bimodal, calc–alkaline, high-K calc-alkaline shoshonitic and midly alkaline volcanism at several discrete volcanic centres. The epithermal mineralisation and prospects in the Kütahya region are hosted by the Eğrigöz and Koyunoba plutons and their sedimentary roof pendants.

The epithermal deposits in South-central Anatolia are hosted in volcanic rocks with ages ranging from Miocene to Pliocene, of which the Messinian volcanic sequences are the most important. Formation of HSEM systems is associated with the subvolcanic-volcanic systems including stratovolcanos, calderas, phreatomagmatic breccia pipes and fracture systems. In the central Anatolia, HSEM are hosted in stratovolcanos comprising the lava flows and pyroclastic units in andesitic to rhyolitic compositions (e.g., Öksüt, İnlice, Doğanbey). Spatial and temporal distribution of ore in some HSEM were controlled by caldera structures and geometry of related faults systems (e.g., Kirazlı and Kartaldağ). Large scale phreatomagmatic brecciation which caused by the contact of the magma with groundwater is the one of most characteristic indicator for HSEM systems in Biga Peninsula (e.g. Kirazlı, Ağıdağı). Flow dome complexes are important volcanic edifices for vein type and associated stockwork, disseminated and replacement type epithermal mineralisation. In western Anatolia, post-dome vein type epithermal mineralisation is hosted

in rhyolitic to dacitic flow-dome complexes (e.g., Koru, Tesbihdere, Ağı Dağı, Kirazlı, Kuşçayırı, TV Tower prospects).

Host-rock rheology as a function of mineralogical compositions of the host rocks is one of the key issues on the control of the permeability and open spaces for the circulating hydrothermal fluids and volatiles. Andesite like intermediate volcanic rocks is reactive lithologies permitting to develop different hydrothermal alteration types. Fractures that are path for the ascending ore-bearing fluids are better developed in silicified host rocks than shales or phyllites. Unlike HSEM, the vein zones of LSEM and ISEM systems are mostly associated with narrow alteration haloes dominated by clay alteration giving illite, smectite, illite-smectite mixed layers and kaolinite (e.g., Red Rabbit, Ovacık, Küçükdere, Efemçukuru, Tesbihdere and Koru). Both LSEM and ISEM systems have appreciable carbonate contents, however the amount and the minerals of carbonates are different.

Well-developed hypogene advanced argillic alteration related to the low pH and oxidised volatiles and fluids are characteristic for HSEM systems. In this context, it seems like oxidised zones characterised by hematite-rich iron-oxides after sulphides are one of the exploration keys for HSEM. Whereas lath-like and/or fibrous hypogene hematite crystals in subordinate amounts are characteristic for ISEM systems. However, it should be taken in to consideration there are also post mineralisation barren porphyritic intrusions particularly in Biga region.

References

Acarlioğlu S, Kadir S, Abdioğlu E, Arslan M (2013) Epithermal-alteration geology, mineralogy and geochemistry of Eocene volcanic rocks in the Hasandağ (Giresun) area, eastern Pontides, NE Turkey. N Jb Mineral Abh 190(1):79–99

Adamia SA, Lordkipanidze MB, Zakariadze GS (1977) Evolution of an active continental margin as exemplified by the Alpine history of the Caucasus. Tectonophysics 40:183–199

Adamia SA, Chkhotua T, Kekelia M, Lordkipanidze MB, Shavishvili I, Zakariadze G (1981) Tectonics of the Caucasus and adjoining regions – implications for the evolution of the Tethys Ocean. J Struct Geol 3(4):437–447

Akaryalı E (2016) Geochemical, fluid inclusion and isotopic (O, H and S) constraints on the origin of Pb–Zn ± au vein-type mineralizations in the Eastern Pontides Orogenic Belt (NE Turkey). Ore Geol Rev 74:1–14

Akaryalı E, Tüysüz N (2013) The genesis of the slab window-related Arzular low-sulphidation epithermal gold mineralisation (eastern Pontides, NE Turkey). Geosci Front 4–4:409–421

Akay E, Işintek İ, Erdoğan B, Hasözbek A (2011) Stratigraphy of the Afyon Zone around Emet (Kütahya, NW Anatolia) and geochemical characteristics of the Triassic volcanism along the northern Menderes Massif. Neu Jb Mineral Abh 188(3):297–316

Akbaş B, Akdeniz N, Aksay A, Altun İ, Balcı V, Bilginer E, Bilgiç T, Duru M, Ercan T, Gedik İ, Günay Y, Güven İH, Hakyemez HY, Konak N, Papak İ, Pehlivan Ş, Sevin M, Şenel M, Tarhan N, Turhan N, Türkecan A, Ulu Ü, Uğuz MF, Yurtsever A (2017) Geological map of Turkey, General Directorate of Mineral Research and Exploration Publication. Ankara Türkiye

Akçay M, Gündüz O (2004) Porphyry Cu–Au mineralisation associated with a multiphase intrusion, and related replacement fronts in limestones in an island arc setting near the Gümüşhane village (Artvin) in the Eastern Black Sea Province (Turkey). Chem Erde 64:359–383

Akdeniz N, Konak N (1979) The rock units of the Simav region of Menderes Massif and the situation of metabasic and metaultramafic rocks. Bull Geol Soc Turk 22(2):175–183 (in Turkish with English abstract)

Akıman O, Erler A, Göncüoğlu MC, Güleç N, Geven A, Türeli TK, Kadioğlu YK (1993) Geochemical characteristics of granitoids along the western margin of the central Anatolian Crystalline Complex and their tectonic implications. Geol J 28:371–382

Albinson T, Norman DI, Cole D, Chomiak B (2001) Controls on formation of low sulphidation epithermal deposits in Mexico: constraints from fluid inclusion and stable isotope data. In: Albinson FT, Nelson CE (eds) New mines and discoveries in Mexico and Central America. Soc Econ Geol Spec Publ 8:1–32

Aldanmaz E (2002) Mantle source characteristics of alkali basalts and basanites in an extensional intracontinental plate setting, western Anatolia, Turkey: implications for multi-stage melting. Int Geol Rev 44:440–457

Altherr R, Topuz G, Siebel W, Şen C, Meyer H-P, Satır M (2008) Geochemical and Sr–Nd–Pb isotopic characteristics of Paleocene plagioleucitites from the Eastern Pontides (NE Turkey). Lithos 105:149–161

Altunkaynak Ş, Yılmaz Y (1998) The Mount Kozak magmatic complex, Western Anatolia. J Volcanol Geotherm Res 85(1–4):211–231

Altunkaynak Ş, Dilek Y, Genç CS, Sunal G, Gertisser R, Furnes H, Foland K, Yang J (2012) Spatial, temporal and geochemical evolution of Oligo-Miocene granitoid magmatism in western Anatolia, Turkey. Gondwana Res 21:961–986

Aluç A, Gürler Z, Kuşcu İ, Aydoğan S (2014) A new low sulphidation epithermal Au – Ag mineralisation within Biga Peninsula: Karadere (Burhaniye, Balıkesir, Turkey). 8th International Symposium on Eastern Mediterranean Geology, Muğla-Turkey, p 32

Andrew T, Robertson AHF (2002) The Beyşehir-Hoyran-Hadim Nappes: genesis and emplacement of Mesozoic marginal and oceanic units of the northern Neotethys in southern Turkey. J Geol Soc 159:529–543

Arehart GB, Chryssoulis SL, Kesler SE (1993) Gold and arsenic in iron sulphides from sediment-hosted disseminated gold deposits; implications for depositional processes. Econ Geol 88:171–185

Arslan M, Kolaylı H, Temizel İ (2004) Petrographical, geochemical and petrological characteristics of the Güre (Giresun, NE Turkey) Granitoid. Bull Earth Scis Appl Res Cent Hacet Univ 30:1–21

Ashley RP (1982) Occurrence model for enargite-gold deposits. In: Erickson RL (ed) Characteristics of mineral deposit occurrences. United States Geological Survey, Open-File Report 82–795:144–147

Aslan N (2011) Mastra (Gümüşhane) Yatağı'nın jeolojik, mineralojik ve jeokimyasal özellikleri. Master's Thesis, Karadeniz Technical University, Trabzon, pp 190 (unpublished)

Aslan N, Akçay M (2011) Mastra (Gümüşhane) Au-Ag yatağının jeolojik, minerolojik ve jeokimyasal özellikleri [Geologic, minerologic and geochemical characteristics of Au-Ag deposits in Mastra (Gümüşhane)]. 64th Geological Congress of Turkey, Proceedings book, 25–29 April 2011, Ankara, p 181–182

Ayan Z (1991) Şebinkarahisar (Giresun) Kuzeybatısındaki Pb-Zn-Cu Cevherleşmelerinin Mineralojik-Jeokimyasal İncelenmesi ve Kökensel Yorumu [Petrogeologic and Mineralogical-geochemical investigation and genetic interpretation of Pb-Zn-Cu mineralizations in northwest of Şebinkarahisarın (Giresun)]. PhD Thesis Dokuz Eylul Universty, Izmir (In Turkish, unpublished)

Aydın NS, Göncüoğlu MC, Erler A (1998) Latest Cretaceous magmatism in the central Anatolian crystalline complex: review of field, petrographic and geochemical features. Turk J Earth Sci 7:259–268

Aysal N (2015) Mineral chemistry, crystallization conditions and geodynamic implications of the Oligo–Miocene granitoids in the Biga Peninsula, Northwest Turkey. Asian J Earth Sci 105:68–84

Barton PB, Jr Skinner BJ (1979) Sulphide mineral stabilities. In: Barnes HL (ed) Geochemistry of hydrothermal ore deposits, 2nd edn. Wiley, New York, pp 278–403

Başarır E (1970) Bafa gölü doğusunda kalan Menderes masifi güney kanadının jeolojisi ve petrografisi. [The petrology and geology of the southern flank of the Menderes Massif east of the Bafa Lake]. Scientific Reports of the Faculty of Science, Ege University No. 102 (in Turkish with English abstract)

Bektaş O, Yılmaz C, Taslı K, Akdağ K, Özgür S (1995) Cretaceous rifting of the eastern Pontide carbonate platform (NE Turkey): the formation of carbonates breccias and turbidites as evidences of a drowned platform. Giorn Geol 57:233–244

Bektaş O, Şen C, Atıcı Y, Köprübaşı N (1999) Migration of the upper cretaceous subduction-related volcanism towards the back-arc basin of the Eastern Pontide magmatic arc (NE Turkey). Geol J 34:95–106

Berger BR (1986) Descriptive model of epithermal quartz-alunite Au. In: Cox DP, Singer DA (eds) Mineral deposit models. USGS Bull 1693:158

Berger BR, Henley RW (1989) Advances in understanding of epithermal gold-silver deposits, with special reference to the western United States. Econ Geol Monogr 6:405–423

Beşir D (2003) Koru Köyü (Lapseki-Çanakkale) Pb-Zn-Ag Yatağının Jenetik İncelenmesi. [Genetic Investigation of the Koru Village (Lapseki-Çanakkale) Pb-Zn-Ag Deposit]. Master's thesis, Dokuz Eylul University (In Turkish, unpublished)

Bethke PM (1984) Controls on base and precious metal mineralisation in deeper epithermal environments. United States Geological Survey, Open-File Report 84890:40

Bilir ME (2015) Geochemical and geochronological characterization of the early-middle Eocene magmatism and related epithermal systems of the Eastern Pontides, Turkey. Master's thesis, Muğla Sıtkı Koçman University, pp 138 (unpublished)

Bilir E, Kuşcu, İ (2016) Geochemical and geochronological characterization of the early-middle Eocene magmatism and related epithermal systems of the Eastern Pontides, Turkey. SEG 2016 Conference

Black KN, Catlos EJ, Oyman T, Demirbilek M (2013) Timing Aegean extension: evidence from in situ U–Pb geochronology and cathodoluminescence imaging of granitoids from NW Turkey. Lithos 180–181:92–108

Bodnar RJ, Reynolds TJ, Kuehn CA (1985) Fluid inclusion systematics in epithermal systems. In: Berger BR, Bethke PM (eds) Geology and geochemistry of epithermal systems. Rev Econ Geol 2:73–98

Bonev N, Beccaletto L (2007) From syn-to post-orogenic Tertiary extension in the north Aegean region: constraints on the kinematics in the eastern Rhodope Thrace, Bulgaria Greece and the Biga Peninsula, NW Turkey. In: Taymaz T, Yılmaz Y, Dilek Y (eds) The Geodynamics of the Aegean and Anatolia. Geol Soci Lond Spec Publ 291:113–142

Bonham HF Jr (1984) Three major types of epithermal precious metal deposits. Geol Soc Am Abstr Programs 16:449

Bonham HF Jr (1986) Models for volcanic-hosted epithermal precious metal deposits; a review. Int Volcanol Congr N Z Proc Symp 5:13–17

Boucher K, Misković A, Sánchez M, Baker T, Hart CRJ (2016) Structural and hydrothermal fluid evolution at the Efemçukuru epithermal Au deposit, Western Turkey. Mineral exploration roundup 2016. Association for Mineral Exploration British Columbia, p 9

Bozkaya G (2009) Fluid inclusion and stable isotope (O, H and S) evidence for the origin of the Balcılar vein type barite-galena mineralisation in Çanakkale, Biga Peninsula, NW Turkey. J Geochem Explor 101:1–8

Bozkaya G (2011) Sulphur- and lead-isotope geochemistry of the Arapuçandere (Karaköy-Yenice, Çanakkale) Pb-Zn-Cu deposit, Biga Peninsula, NW Turkey. Int Geol Rev 53:116–129

Bozkaya G, Banks DA (2015) Physico-chemical controls on ore deposition in the Arapuçandere Pb–Zn–Cu-precious metal deposit, Biga Peninsula, NW Turkey. Ore Geol Rev 66:65–81

Bozkaya G, Gökçe A (2001) Geology, ore petrography and fluid inclusion characteristics of the Koru (Çanakkale) Pb-Zn deposits. Eng Fac Bull Cumhuriyet Univ Earth Sci 18–1:55–70 (in Turkish with English abstract)

Bozkaya G, Gökce A (2007) Fluid inclusion and isotope geochemistry studies of the galena-barite veins in Balcılar (Lapseki-Çanakkale) area. Abstract of 60th Geological Congress of Turkey, 188–190

Bozkaya G, Gökçe A (2009) Lead and sulphur isotope studies of the Koru (Çanakkale, Turkey) lead–zinc deposits. Turk J Earth Sci 18:127–137

Bozkaya G, Gökçe A, Grassineau NV (2008) Fluid-inclusion and stable-isotope characteristics of the Arapuçandere Pb-Zn-Cu deposits, NW Turkey. Int Geol Rev 50:848–862

Bozkaya G, Banks DA, Özbaş F, Wallington J (2014) Fluid processes in the Tesbihdere base metal-Au deposit: implications for epithermal mineralisation in the Biga Peninsula, NW Turkey. Cent Eur J Geosci 6:148–169

Bozkurt E, Satır M, Buğdaycıoğlu C (2011) Surprisingly young Rb/Sr ages from the Simav extensional detachment fault zone, northern Menderes Massif, Turkey. J Geodyn 52(5):406–431

Boztuğ D (1998) Post-collisional Central Anatolian alkaline plutonism, Turkey. Turk J Earth Sci 7:145–165

Boztuğ D (2000) S-I-A type intrusive associations: geodynamic significance of synchronism between metamorphism and magmatism in Central Anatolia, Turkey. In: Bozkurt E, Winchester JA, Piper JAD (eds) Tectonics and magmatism in Turkey and the surrounding area. Geol Soc Lond Spec Publ 173:441–458

Boztuğ D (2008) Petrogenesis of the Kösedağ Pluton, Suşehri-NE Sivas, east-central Pontides, Turkey. Turk J Earth Sci 17:241–262

Boztuğ D, Jonckheere R, Wagner GA, Yeğingil Z (2004) Slow Senonian and fast Palaeocene-Early Eocene uplift of the granitoids in the Central Eastern Pontides, Turkey: apatite fission-track results. Tectonophysics 382:213–228

Boztuğ D, Erçin I, Kuruçelik MK, Göç D, Kömür I, İskenderoğlu A (2006) Geochemical characteristics of the composite Kaçkar batholith generated in a Neo-Tethyan convergence system, Eastern Pontides, Turkey. Asian J Earth Sci 27:286–302

Boztuğ D, Harlavan Y, Arehart GB, Satır M, Avci N (2007) K–Ar age, whole-rock and isotope geochemistry of A-type granitoids in the Divrigi-Sivas region, eastern-central Anatolia, Turkey. Lithos 97:193–218

Brinkmann R (1966) Geotektonische gliederung von West-Anatolien. N Jb Geol Paläont 10:603–618

Browne PRL (1978) Hydrothermal alteration in active geothermal fields. Annu Rev Earth Planet Sci 6:229–250

Cabri LJ, Newville M, Gordon RA, Crozier ED, Sutton SR, Mcmahon G, Jiang DT (2000) Chemical speciation of gold in arsenopyrite. Can Miner 38:1265–1281

Candan O, Koralay OE, Akal C, Kaya O, Oberhänsli R, Dora OÖ, Konak N, Chen F (2011) Supra-Pan-African unconformity between core and cover series of the Menderes Massif/Turkey and its geological implications. Precambrian Res 184:1–23

Catlos E, Jacob L, Oyman T, Sorensen S (2012) Long-term exhumation of an Aegean metamorphic core complex granitoids in the northern Menderes Massif, Western Turkey. Am J Sci 312:534–571

Cavazza W, Okay AI, Zattin M (2009) Rapid early-middle Miocene exhumation of the Kazdağ Massif (Western Anatolia). Int J Earth Sci 98:1935–1947

Chakrabarti R, Basu AR, Ghatak A (2012) Chemical geodynamics of Western Anatolia. Int Geol Rev 54:227–248

Çiçek M (2013) Koru ve Tesbihdere (Lapseki-Çanakkale) epitermal Pb-Zn-Cu+-Au+-Ag yataklarına ait hidrotermal akışkanların kökeni ve evrimi [Origin and Evolution of Hydrothermal Fluids in Koru and Tesbihdere (Lapseki-Çanakkale) Epithermal Pb-Zn-Cu ± Ag ± Au Deposits] MSc thesis, Dokuz Eylul University (In Turkish, unpublished)

Çiçek M, Oyman T (2016) Origin and evolution of hydrothermal fluids in epithermal Pb-Zn-Cu ± Au ± Ag deposits at Koru and Tesbihdere mining districts, Çanakkale, Biga Peninsula, NW Turkey. Ore Geol Rev 78:176–195

Çiçek M, Oyman T, Özgenc I, Akbulut M (2012) Fluid evolution of the Koru Pb-Zn deposit, Çanakkale (NW-Turkey). International Earth Science Colloquium on the Aegean Region, IESCA-2012 Abstract Book, 1–5 Oct, p. 158

Çiçek M, Oyman T, Kaliwoda M, Hochleitner R (2017) Mineralogy and mineral chemistry of the Arapuçandere Pb-Zn-Cu (Ag-Au) mineralization in the Northeast of Yenice (Çanakkale), Biga Peninsula, NW Turkey. In: International Workshop on Subduction Related Ore Deposit, 23–23 Sept 2017, Karadeniz Technical University, Trabzon-Turkey, p 18

Çiner A, Doğan U, Yıldırım C, Akçar N, Ivy-Ochs S, Alfimov V, Kubik PW, Schlüchter C (2015) Quaternary uplift rates of the Central Anatolian Plateau, Turkey: insights from cosmogenic isochron-burial nuclide dating of the Kızılırmak River terraces. Quat Sci Rev 107:81–97

Çinku MC, Ustaömer T, Hirt AM, Hisarli ZM, Heler F, Orbay N (2010) Southward migration of arc magmatism during latest Cretaceous associated with slab steepening, East Pontides, N Turkey: new paleomagnetic data from the Amasya region. Phys Earth Planet Inter 182:8–29

Clayton RN, Mayeda TK (1963) The use of bromine pentafluoride in the extraction of oxygen from oxides and silicates for isotopic analysis. Geochim Cosmochim Acta 27:43–52

Cline JS (2001) Timing of gold and arsenic sulphide mineral deposition at the Getchell Carlin-type gold deposit, north-central Nevada. Econ Geol 96:75–89

Çoğulu E (1975) Gümüşhane ve Rize Granitik Plutonlarının Mukayeseli Petrojeolojik ve Jeokronolojik Etüdü. [Petrogeologic and Geochronologic Investigation of Gümüşhane and Rize Granitic Plutons and Their Comparison]. Dissertation thesis, İstanbul Technical University (in Turkish with English abstract, unpublished)

Cook NJ, Chryssoulis SL (1990) Concentrations of invisible gold in the common sulphides. Can Mineral 28:1–16

Cook NJ, Ciobanu CL, Pring A, Skinner W, Shimizu M, Danyushevsky L, Saini-Eidukat B, Melcher F (2009) Trace and minor elements in sphalerite: a LA-ICPMS study. Geochim Cosmochim Acta 73(16):4761–4791

Cooke DR, Simmons SF (2000) Characteristics and genesis of epithermal gold deposits. Rev Econ Geol 13:221–244

Corbett GJ, Leach TM (1998) Southwest Pacific Rim gold-copper systems: structure, alteration and mineralisation. Soc Econ Geol Spec Publ 6:236

Criss RE, Taylor HP (1983) An $^{18}O/^{16}O$ and D/H study of tertiary hydrothermal systems in the southern half of the Idaho batholith. GSA Bull 94:640–663

Czamanske GK (1974) The FeS content of sphalerite along the chalcopyrite-pyrite-bornite sulphur fugacity buffer. Econ Geol 69:1328–1334

Dag N (1993) Fluid inclusion study on Narlica prospect. Eurogold, Unpublished company report, p 1–11

Delaloye M, Çoğulu E, Chessex R (1972) Etude géochronometrique des massifs cristallins de Rize et de Gümüşhane, Pontides Orientales (Turquie). Arch Sci Phys Nat 25(Supplement 7): 43–52

Dilek Y, Thy P, Hacker B, Grundvig S (1999) Structure and petrology of Tauride ophiolites and mafic dike intrusions (Turkey): implications for the Neo-Tethyan ocean. GSA Bull 111:1192–1216

Dilek Y, Imamverdiyev N, Altunkaynak S (2010) Geochemistry and tectonics of Cenozoic volcanism in the Lesser Caucasus (Azerbaijan) and the peri-Arabian region: collision-induced mantle dynamics and its magmatic fingerprint. Int Geol Rev 52(4–6):536–578

Dirik K, Göncüoğlu MC (1996) Neotectonic characteristics of Central Anatolia. Int Geol Rev 38:807–817

Dokuz A (2011) A slab detachment and delamination model for the generation of Carboniferous high-potassium I-type magmatism in the Eastern Pontides, NE Turkey: the Köse composite pluton. Gondwana Res 19:926–944

Dönmez M, Akçay AE, Genç SC, Acar S (2005) Middle-Upper Eocene volcanism and marine ignimbrites in Biga Peninsula. Bull Mineral Res Exp 131:49–61 (in Turkish)
Dora OÖ, Candan O, Kaya O, Koralay E, Dürr S (2001) Revision of the so-called "leptite-gneisses" in the Menderes Massif: a supracrustal metasedimentary origin. Int J Earth Sci 89(4):836–851
Ebert S (2004) Ovacik Normandy gold mine, Turkey. Unpublished company report, Normandy, pp 1–18
Einaudi MT, Hedenquist JW, İnan EE (2003) Sulfidation state of fluids in active and extinct hydrothermal systems: transitions from porphyry to epithermal precious metal deposits. In: Simmons SF (ed) Sulfidation state of hydrothermal fluids. Soc Econ Geol Spec Publ 10:285–314
Elsenheimer D, Valley JW (1992) In situ oxygen isotope analysis of feldspar and quartz by Nd:YAG laser microprobe. Chem Geol 101:21–42
Emre Ö, Duman TY, Özalp S, Elmacı H, Olgun Ş, Şaroğlu F (2013) 1/1.125.000 scaled active faults map of Turkey. General Directorate of Mineral Research and Exploration, Sp Publ Series-30, Ankara-Turkey
Ercan T, Satır M, Steinitz G, Dora A, Sarıfakioğlu E, Adis C, Walter HJ, Yıldırım T (1995) Features of tertiary volcanism observed at Biga Peninsula and Gökçeada, Tavsan Islands. Bull Mineral Res Exp 117:55–86 (in Turkish with English abstract)
Ercan T, Türkecan A, Guillou H, Satır M, Sevin D, Saroğlu F (1998) Features of the tertiary volcanism around the Sea of Marmara. Bull Mineral Res Exp 120:97–118
Erkül F (2010) Tectonic significance of synextensional ductile shear zones within the early Miocene Alaçamdağ granites, northwestern Turkey. Geol Mag 147(4):611–637
Erkül F, Helvacı C, Sözbilir H (2005) Stratigraphy and geochronology of the Early Miocene volcanic units in the Bigadiç Borate Basin, Western Turkey. Turk J Earth Sci 14:227–253
Eyüboğlu Y, Santosh M, Yi K, Tüysüz N, Korkmaz S, Dudas FO, Akaryalı E, Bektaş O (2014) The Eastern Black Sea-type volcanogenic massive sulphide deposits: geochemistry, zircon U-Pb geochronology and an overview of the geodynamics of ore genesis. Ore Geol Rev 59:29–54
Fayon AK, Whitney DL, Tessier C, Carver JI, Dilek Y (2001) Effects of plate convergence obliquity on timing and mechanisms of exhumation of a mid-crustal terrain, the Central Anatolian Crystalline Complex. Earth Planet Sci Lett 192:191–205
Fleet ME, Mumin AH (1997) Gold-bearing arsenian pyrite and marcasite and arsenopyrite from Carlin Trend gold deposits and laboratory synthesis. Am Mineral 82:182–193
Gedikoğlu A (1978) Harşit Granit Karmaşığı ve Çevre Kayaçları [Harşit Granite Complex and its Country Rocks (Giresun-Doğankent)]. PhD thesis, Karadeniz Technical University, Trabzon (in Turkish with English abstract, unpublished)
Genna A, Jébrak M, Marcoux E, Milési JP (1996) Genesis of cockade breccias in the tectonic evolution of the Cirotan epithermal gold system, West Java. Can J Earth Sci 33:93–102
Giles DL (1974) Geology and mineralisation of the ulutaş copper–molybdenum prospect, mineral exploration in two areas. UNDP Technical Report, 6, MTA, Ankara (unpublished)
Görür N, Oktay FY, Seymen I, Şengör AMC (1984) Paleotectonic evolution of Tuz Gölü Basin complex, central Turkey. In: Dixon JE, Robertson AHF (eds) The geological evolution of the Eastern Mediterranean. Geol Soc Lond Spec Publ 17:81–96
Görür N, Tüysüz O, Şengör AMC (1998) Tectonic evolution of the central Anatolian basins. Int Geol Rev 40:831–850
Gülmez F, Genç SC, Keskin M, Tüysüz O (2013) A post-collision slab-breakoff model for the origin of the Middle Eocene magmatic rocks of the Armutlu-Almacık belt, NW Turkey and its regional implications. In: Robertson AHF, Parlak O, Ünlügenç UC (eds) Geological development of Anatolia and the Easternmost Mediterranean Region. Geol Soci Lond Spec Publ 372:107–139
Gulyuz N, Shipton Z, Gulyuz E, Lord R, Kaymakci N, Kuscu İ (2017) Gold grade distribution within an epithermal quartz vein system, Kestanelik, NW Turkey: implications for gold exploration. In: 19th EGU General Assembly, EGU2017, 23–28 April 2017, Vienna, Austria, p 1210
Hasözbek A, Satır M, Erdoğan B, Akay E, Siebel W (2010) Early Miocene post-collisional magmatism in NW Turkey: geochemical and geochronological constraints. Int Geol Rev 53(9):1098–1119

Heald P, Foley NK, Hayba DO (1987) Comparative anatomy of volcanic-hosted epithermal deposits: acid-sulphate and adularia-sericite types. Econ Geol 82:1–26
Hedenquist JW, Izawa E, Arribas A Jr, White NC (1996) Epithermal gold deposits: styles, characteristics, and exploration. Poster Booklet Resour Geol Spec Publ 1:17 (with translations to Spanish, French, Japanese, and Chinese)
Hedenquist JW, Arribas A Jr, Gonzalez-Urien E (2000) Exploration for epithermal gold deposits. Rev Econ Geol 13:245–277
Henley RW (1985) The geothermal framework of epithermal deposits. Rev Econ Geol 2(l):–24
Henley RW (1990) Ore transport and deposition in epithermal environments. Univ West Aust Geol Dept Publ 23:51–69
Hobbs BE (1985) The geological significance of microfabric analysis. In: Wenk HR (ed) Preferred orientation in deformed metals and rocks: an introduction to modern texture analysis. Academic, Orlando, pp 463–479
İlbeyli N (2005) Mineralogical–geochemical constraints on intrusives in central Anatolia, Turkey: tectono-magmatic evolution and characteristics of mantle source. Geol Mag 142:187–207
İlbeyli N (2008) Geochemical characteristics of the Şebinkarahisar granitoids in the Eastern Pontides, northeast Turkey: petrogenesis and tectonic implications. Int Geol Rev 50:563–582
İlbeyli N, Pearce JA, Thirwall MF, Mitchell JG (2004) Petrogenesis of collision-related plutonics in Central Anatolia, Turkey. Lithos 72:163–182
Işık V, Tekeli O (2001) Late orogenic crustal extension in the northern Menderes massif (western Turkey): evidence for metamorphic core complex formation. Int J Earth Sci 89(4):757–765
JICA (1986) The Republic of Turkey report on the cooperative mineral exploration of Gümüşhane area, consolidated report. Japanese International Cooperation Agency, Metal Mining Agency of Japan
Kadıoğlu YK, Güleç N (1996) Mafic microgranular enclaves and interaction between felsic and mafic magmas in the Ağaçören Intrusive Suite: evidence from petrographic features and mineral chemistry. Int Geol Rev 3(8):854–867
Kadıoğlu YK, Dilek Y, Güleç N, Foland KA (2003) Tectonomagmatic evolution of bimodal plutons in the central Anatolian crystalline complex, Turkey. J Geol 111:671–690
Kadıoğlu YK, Dilek Y, Foland KA (2006) Slab breakoff and syncollisional origin of the Late Cretaceous magmatism in the Central Anatolian Crystalline Complex, Turkey. In: Dilek Y, Pavlides S (eds) Postcollisional tectonics and magmatism in the Mediterranean Region and Asia. GSA Spec Pap 409:381–415
Karacık Z, Yılmaz Y, Pearce JA (2007) The Dikili-Çandarlı volcanics, Western Turkey: magmatic interactions as recorded by petrographic and geochemical features. Turk J Earth Sci 16:493–522
Karakaya MÇ, Karakaya N, Temel A (2001) Kaolin occurrences in Erenler Dağı volcanics, southwest Konya Province, Turkey. Int Geol Rev 43/8:711–722
Karslı O, Chen B, Aydın F, Şen C (2007) Geochemical and Sr-Nd-Pb isotopic compositions of the Eocene Dölek and Sarıçiçek Plutons, Eastern Turkey: implications for magma interaction in the genesis of high-K calc-alkaline granitoids in a post-collision extensional setting. Lithos 98:67–96
Karslı O, Dokuz A, Uysal I, Aydin F, Kandemir R, Wijbrans J (2010) Generation of the Early Cenozoic adakitic volcanism by partial melting of mafic lower crust, Eastern Turkey: implications for crustal thickening to delamination. Lithos 114:109–120
Karslı O, Ketenci M, Uysal İ, Dokuz A, Aydın F, Chen B, Kandemir R, Wijbrans J (2011) Adakite-like granitoid porphyries in the Eastern Pontides, NE Turkey: potential parental melts and geodynamic implications. Lithos 127:354–372
Karslı O, Caran Ş, Dokuz A, Çoban H, Chen B, Kandemir R (2012) A-type granitoids from the Eastern Pontides, NE Turkey: records for generation of hybrid A-type rocks in a subduction-related environment. Tectonophysics 530–531:208–224
Kaygusuz A, Aydinçakır E (2009) Mineralogy, whole-rock and Sr–Nd isotope geochemistry of mafic microgranular enclaves in Cretaceous Dagbasi granitoids, Eastern Pontides, NE Turkey: evidence of magma mixing, mingling and chemical equilibration. Chem Erde 69:247–277

Kaygusuz A, Siebel W, Şen C, Satir M (2008) Petrochemistry and petrology of I-type granitoids in an arc setting: the composite Torul pluton, Eastern Pontides, NE Turkey. Int J Earth Sci 97:739–764

Kaygusuz A, Chen B, Aslan Z, Siebel W, Şen C (2009) U-Pb zircon SHRIMP ages, geochemical and Sr-Nd isotopic compositions of the early cretaceous I-type Sarıosman Pluton, Eastern Pontides, NE Turkey. Turk J Earth Sci 18:549–581

Kaygusuz A, Arslan M, Siebel W, Sipahi F, İlbeyli N (2012) Geochronological evidence and tectonic significance of Carboniferous magmatism in the southwest Trabzon area, eastern Pontides, Turkey. Int Geol Rev 54(15):1776–1800

Ketin İ (1966) Tectonic units of Anatolia (Asia Minor). Bull Mineral Res Exp 66:23–34

Koçyiğit A, Beyhan A (1998) New intracontinental transcurrent structure: the Central Anatolian fault zone, Turkey. Tectonophysics 284(3–4):317–336

Köksal S, Romer RL, Göncüoğlu M, Toksoy-Köksal F (2004) Timing of postcollisional H-type to A-type granitic magmatism: U–Pb titanite ages from the Alpine central Anatolian granitoids (Turkey). Int J Earth Sci 93:974–989

Konak N, Okay AI, Hakyemez HY (2009) Tectonics and stratigraphy of the eastern Pontides: field Trip guide Book. 2nd International Symposium on the Geology of the Black Sea Region, Ankara, p 120

Köprübaşı N, Şen C, Kaygusuz A (2000) Doğu Pontid adayayı granitoyidlerin karşılaştırılmalı petrografik ve kimyasal özellikleri [Comparative petrographical and chemical features of the eastern Pontide arc granitoid]. Uygulamalı Yerbilimleri 1:111–120 (in Turkish with English abstract)

Kürkçüoğlu B (2010) Geochemistry and petrogenesis of basaltic rocks from the Develidağ volcanic complex, Central Anatolia, Turkey. Asian J Earth Sci 37:42–51

Kürkçüoğlu B, Furman T, Hanan B (2008) Geochemistry of postcollisional mafic lavas from the North Anatolian Fault zone, Northwestern Turkey. Lithos 101:416–434

Kuşcu İ, Gençalioğlu-Kuşcu G, Tosdal RM, Ullrich T, Friedman R (2010) Magmatism in the southeastern Anatolian orogenic belt: transition from arc to post-collisional setting in an evolving orogen. In: Sosson M, Kaymakçı N, Stephenson RA, Bergerat F, Starostenko V (eds) Sedimentary basin tectonics from the Black Sea and Caucasus to the Arabian Platform. Geol Soc Lond Spec Publ 340:437–460

Large R, Danyushevsky L, Hollit C, Maslennikov V, Meffre S, Gilbert S, Bull S, Scott R, Emsbo P, Thomas H, Singh B, Foster J (2009) Gold and trace element zonation in pyrite using a laser imaging technique: implications for the timing of gold in orogenic and Carlin-style sediment-hosted deposits. Econ Geol 104:635–668

Larson PB, Taylor HP (1986) $^{18}O/^{16}O$ relationships in hydrothermally altered rocks from the Lake City caldera, San Juan Mountains, Colorado. J Volcanol Geothermal Res 30:47–82

Larson PB, Zimmerman BS (1991) Variations in δ18O values, water/rock ratios, and water flux in the Rico paleothermal anomaly, southwest Colorado. Geochem Soc Spec Publ 3:463–469

Lefebvre C (2011) The tectonics of the Central Anatolian Crystalline Complex: a structural, metamorphic and paleomagnetic study. Utrecht Univ Utrecht Stud Earth Sci 3:1–147

Lindgren W (1933) Mineral deposits, 4th edn. McGraw-Hill, New York, p 930

Maslennikov VV, Maslennikova SP, Large RR, Danyushevskiy LV (2009) Study of trace element zonation in vent chimneys from the Silurian Yaman-Kasy volcanic-hosted massive sulphide deposit (Southern Urals, Russia) using laser ablation-inductively coupled plasma mass spectrometry (LA-ICPMS). Econ Geol 104:1111–1141

Mattey D, Macpherson C (1993) High-precision oxygen isotope microanalysis of ferromagnesian minerals by laser-fluorination. Chem Geol 105:305–318

Mauk JL, Hoskin PWO, Seal II RR (1998) Morphology of pyrite and marcasite at the Golden Cross mine, New Zealand. In: Arehart GB, Hulston JR (eds) Water–rock interaction, Balkema, Rotterdam 9:557–560

McKenzie DP (1972) Active tectonics of the Mediterranean region. Geophys J R Astron Soc 30(2):109–185

Meijers MJM, Kaymakci N, Van Hinsbergen DJJ, Langereis CG, Stephenson RA, Hippolyte J-C (2010) Late Cretaceous to Paleocene oroclinal bending in the central Pontides (Turkey). Tectonics 29:TC4016

Moore WJ, Mckee EH, Akıncı Ö (1980) Chemistry and chronology of plutonic rocks in the Pontide mountains, northern Turkey. Symposium of European Copper Deposits, Belgrade, pp 209–216

MTA (1993a) Türkiye Altın ve Gümüş Envanteri [Gold and silver inventory of Turkey]. MTA Publication no.198 (in Turkish)

MTA (1993b) Türkiye Kurşun-Çinko envanteri [Lead-zinc inventory of Turkey]. MTA Publication no. 199, p 94 (in Turkish)

Okay AI, Şahintürk Ö (1997) Geology of the Eastern Pontides. In: Robinson AG (ed) Regional and petroleum geology of the Black Sea and surrounding Region. Am Assoc Pet Geol Mem 68:291–310

Okay AI, Tüysüz O (1999) Tethyan sutures of northern Turkey. In: Durand B, Jolivet L, Horvath L, Serranne M (eds) The Mediterranean Basins: tertiary extension within the Alpine orogeny. Geol Soci Lond Spec Publ 156:475–515

Okay AI, Siyako M, Burkan KA (1991) Geology and tectonic evolution of the Biga Peninsula. Bull Tech Univ İstanbul 44:191–255

Okay AI, Satır M, Maluski H, Siyako M, Monie P, Metzger R, Akyüz S, Yin A (1996) Paleo- and Neo-Tethyan events in Northwestern Turkey: geologic and geochronologic constraints. In: Harrison M (ed) Tectonics of Asia. Cambridge University Press, Cambridge, MA, pp 420–441

Önal A, Boztuğ D, Kürüm S, Harlavan Y, Arehart GB, Arslan M (2005) K–Ar age determination, whole-rock and oxygen isotope geochemistry of the postcollisional Bizmişen and Çaltı plutons, SW Erzincan, Eastern Central Anatolia, Turkey. Geol J 40:457–476

Orgun Y, Gultekin AH, Onal A (2005) Geology, mineralogy and fluid inclusion data from the Arapucan Pb-Zn-cu-ag deposit, Canakkale, Turkey. J Asian Earth Sci 25:629–642

Oygür V (1997) Anatomy of an epithermal mineralisation: Mumcu (Balıkesir-Sındırgı), inner-Western Anatolia, Turkey. Bull Mineral Res Exp 119:29–39

Oyman T, Minareci F, Piskin O (2003) Efemcukuru B-rich epithermal gold deposit (İzmir, Turkey). Ore Geol Rev 23:35–53

Oyman T, Ciabonu CL, Cook NJ, Danyushevsky L (2010) The Efemçukuru gold deposit, western Turkey: petrography and invisible gold in arsenian pyrite. IAGOD Symposium 2010, Giant Ore Deposits Down-Under, Adelaide- Australia

Özdemir S (2011) Çanakkale-Balcılar polimetal Cevherleşmesi Oluşumunun incelenmesi. Master's Thesis, Ankara University, pp 110 (unpublished)

Özen Y, Arık F (2015) S, O and Pb isotopic evidence on the origin of the İnkaya (Simav-Kütahya) Cu–Pb–Zn–(Ag) Prospect, NW Turkey. Ore Geol Rev 70:262–280

Özgenç İ, İlbeyli N (2008) Petrogenesis of the Late Cenozoic Eğrigöz pluton in western Anatolia, Turkey: implications for magma genesis and crustal processes. Int Geol Rev 50(4):375–391

Özpınar Y, Kılıç M, Avşar M, Sarı R, Küçükefe Ş, Agnerian H, Doygun Z, Yenigün K (2012) Anew assessment of the Kısacık gold mineralisation (Ayvacık-Çanakkale NW Anatolia). Rom J Earth Sci 86(2):111–116

Pals DW, Spry PG, Chryssoulis SL (2003) Invisible gold and tellurium in arsenic-rich pyrite from the Emperor gold deposit, Fiji; implications for gold distribution and deposition. Econ Geol 98:479–493

Parlak O, Karaoğlan F, Rızaoğlu T, Klötzli U, Koller F, Billor Z (2013) U–Pb and ^{40}Ar–^{39}Ar geochronology of the ophiolites and granitoids from the Tauride belt: implications for the evolution of the Inner Tauride suture. J Geodyn 65:22–37

Pasquarè G, Poli S, Vezzoli L, Zanchi A (1988) Continental arc volcanism and tectonic setting in Central Anatolia, Turkey. Tectonophysics 146:217–230

Phillips WJ (1972) Hydraulic fracturing and mineralisation. J Geol Soc Lond 128:337–359

Pirajno F (2009) Hydrothermal processes and mineral systems. Springer, Berlin, p 1250

Pourteau A, Candan O, Oberhänsli R (2010) High-pressure metasediments in central Turkey: constraints on the Neotethyan closure history. Tectonics 29:TC5004

Repstock A, Voudouris P, Kolitsch U (2015) New occurrences of watanabeite, colusite, "arsenosulvanite" and Cu-excess tetrahedrite-tennantite at the Pefka high-sulphidation epithermal deposit, northeastern Greece. Neu Jb Mineral Abh 192:135–149

Rice SP, Robertson AHF, Ustaömer T (2006) Late Cretaceous–Early Cenozoic tectonic evolution of the Eurasian active margin in the Central and Eastern Pontides, northern Turkey. Geol Soc Lond Spec Publ 260:413–445

Rice SP, Robertson AHF, Ustaömer T, İnan N, Tasli K (2009) Late Cretaceous–Early Eocene tectonic development of the Tethyan suture zone in the Erzincan area, Eastern Pontides, Turkey. Geol Mag 146:567–590

Richards JP (2015) Tectonic, magmatic, and metallogenic evolution of the Tethyan orogen: from subduction to collision. Ore Geol Rev 70:323–345

Ring U, Collins AS (2005) U-Pb SIMS dating of synkinematic granites; timing of core-complex formation in the northern Anatolide Belt of western Turkey. J Geol Soc 162(2):289–298

Robertson AHF, Parlak O, Ustaömer T (2009) Melange genesis and ophiolite emplacement related to subduction of the northern margin of the Tauride-Anatolide continent, central and western Turkey. In: Van Hinsbergen DJJ, Edwards MA, Govers R (eds) Collision and collapse at the Africa-Arabia-Eurasia subduction zone. Geol Soc Lond Spec Publ 311:9–66

Ross K (2013a) Petrographic report on the TV tower project, Turkey Pilot Gold 87 (unpublished)

Ross K (2013b) Petrographic report on samples from the TV tower project, Biga Peninsula, Turkey. Pilot Gold, Inc, p 84 (unpublished)

Şahin Demir Ç, Uçurum A (2016) Geology-mineralogy and isotope (O-D, S, Cu and Ar/Ar) geochemistry of Sisorta high sulphidation epithermal gold deposit (Koyulhisar-Sivas). Geol Bull Turk 59(1):87–114 (In Turkish with English abstract)

Scott S, Barnes H (1971) Sphalerite geothermometry and geobarometry. Econ Geol 66:653–669

Şener AK, Menteş B, Sarı R, Saygılı A, Tufan V (2006a) Geological synthesis of epithermal gold deposits in the Sındırgı district, Balıkesir Province, Western Turkey. In: Cook NJ, Özgenç İ, Oyman T (eds) Au-Ag-Te-Se deposits. Proceedings of 2006 Workshop of IGCP-486, İzmir, Turkey, pp 148–153

Şener AK, Tufan V, Sarı R, Kaplan EH (2006b) Sındırgı Gold Project. Galata Madencilik, Turkey Company Unpublished Report, pp 1–20

Şengör AMC (1979) The North Anatolian transform fault: its age, offset and tectonic significance. J Geol Soc Am 136:269–282

Şengör AMC, Yılmaz Y (1981) Tethyan evolution of Turkey: a plate tectonic approach. Tectonophysics 75:181–241

Şengör AMC, Satır M, Akkok R (1984) Timing of tectonic events in the Menderes Massif, western Turkey: implications for tectonic evolution and evidence for pan-African basement in Turkey. Tectonics 3:693–707

Sha P (1993) Geochemistry and genesis of sediment-hosted disseminated gold mineralisation at the Gold Quarry mine, Nevada. PhD thesis, University of Alabama, Tuscaloosa

Sharp ZD (1990) A laser-based microanalytical method for the in situ determination of oxygen isotope ratios of silicates and oxides. Geochim Cosmochim Acta 54:1353–1357

Shikazono W (1974) Physicochemical environment and mechanism of volcanic hydrothermal ore deposition in Japan, with special reference to oxygen fugacity. Univ Tokyo Fac Sci J 19:27–56

Shikazono W (2003) Geochemical and tectonic evolution of arc-backarc hydrothermal systems: implication for the origin of Kuroko and epithermal vein-type mineralisations and the global geochemical cycle, Developments in Geochemistry, 8. Elsevier, London

Sillitoe RH (1985) Ore-related breccias in volcanoplutonic arcs. Econ Geol 80:1467–1514

Sillitoe RH (2012) Copper provinces. Soc Econ Geol Spec Publ 16:1–18

Sillitoe RH, Hedenquist JW (2003) Linkages between volcanotectonic settings, ore-fluid compositions, and epithermal precious-metal deposits. In: Simmons SF, Graham IJ (eds) Volcanic, geothermal, and ore-forming fluids: rulers and witnesses of processes within the earth. Soc Econ Geol Spec Publ 10:315–343

Simmons SF, Christenson BW (1994) Origins of calcite in a boiling geothermal system. Am J Sci 294:361–400

Simon G, Kesler SE, Chryssoulis SL (1999) Geochemistry and textures of gold-bearing arsenian pyrite, Twin Creeks, Nevada; implications for deposition of gold in Carlin-type deposits. Econ Geol 94:405–421

Siyako M, Burkan KA, Okay AI (1989) Tertiary geology and hydrocarbon potential of the Biga and Gelibolu Peninsula. TAPG Bull 1–3:183–199

Smith MT, Lepore WA, İncekaraoğlu T, Shabestari P, Boran H, Raabe K (2014) Küçükdağ: a new, high sulphidation epithermal Au-Ag-Cu deposit at the TV Tower property in Western Turkey. Econ Geol 109:1501–1511

Sung YH, Brugger J, Ciobanu CL, Pring A, Skinner W, Nugus M (2009) Invisible gold in arsenian pyrite and arsenopyrite from a multistage Archaean gold deposit: Sunrise Dam, Eastern Goldfields Province, Western Australia. Mineral Depos 44:765–791

Taner MF (1977) Etude géologique et pétrographique de la région de Güneyce-İkizdere, située au sud de Rize (Pontides orientales, Turquie). PhD thesis, Université de Geneve (unpublished)

Taylor HP (1979) Oxygen and hydrogen isotope relationships in hydrothermal mineral deposits. In: Barnes HL (ed) Geochemistry of hydrothermal ore deposits, 2nd edn. Wiley, New York, pp 236–277

Taylor R (2009) Ore textures: recognition and interpretation. Springer-Verlag, Berlin, p 287

Tezer EB (2006) Balıkesir–Ayvalık İlçesi Kubaşlar Altın Oluşumunun Maden Jeolojisi. [Ore geology of the Kubaşlar (Balıkesir-Ayvalık) gold formation]. Master's thesis, Ankara University (In Turkish, unpublished), p 70

Thomas H, Large R, Bull SW, Maslennikov V, Berry RF, Fraser R, Froud S, Moye R (2011) Pyrite and pyrrhotite texture and composition in sediments, laminated quartz veins, and reefs at Bendigo Gold Mine, Australia: insight for ore genesis. Econ Geol 106:1–31

Thomson SN, Ring U (2006) Thermochronologic evaluation of postcollision extension in the Anatolide Orogen, western Turkey. Tectonics 25:TC3005

Toprak V (1998) Vent distribution and its relation to regional tectonics, Capadocian Volcanics, Turkey. J Volcanol Geotherm Res 85:67–77

Toprak V, Göncüoğlu MC (1993) Keçiboyduran-Melendiz Fayı ve bölgesel anlamı (Orta Anadolu). [Keçiboyduran-Melendiz Fault (Central Anatolia) and its regional geological significance]. Haçet Univ Yerbilimleri 16:55–65 (in Turkish)

Topuz G, Altherr R, Kalt A, Satır M, Werner O, Schwarz WH (2004) Aluminous granulites from the Pulur complex, NE Turkey: a case of partial melting, efficient melt extraction and crystallisation. Lithos 72:183–207

Topuz G, Altherr R, Schwarz WH, Siebel W, Satır M, Dokuz A (2005) Post-collisional plutonizm with adakite-like signatures: the Eocene Saraycık granodiorite (Eastern Pontides, Turkey). Contrib Mineral Petrol 150:441–455

Topuz G, Altherr R, Schwarz WH, Dokuz A, Meyer HP (2007) Variscan amphibolite-facies rocks from the Kurtog˘lu metamorphic complex. Gümüşhane area, Eastern Pontides, Turkey. Int J Earth Sci 96:861–873

Topuz G, Altherr R, Siebel W, Schwarz WH, Zack T, Hasözbek A, Barth M, Satır M, Şen C (2010) Carboniferous high-potassium I-type granitoid magmatism in the Eastern Pontides: the Gümüşhane pluton (NE Turkey). Lithos 116:92–110

Topuz G, Okay AI, Altherr R, Schwarz WH, Siebel W, Zack T, Satır M, Şen C (2011) Post-collisional adakite-like magmatism in the Ağvanis Massif and implications for the evolution of the Eocene magmatism in the Eastern Pontides (NE Turkey). Lithos 125:131–150

Türeli TK (1991) Geology, petrography and geochemistry of Ekecikdağ plutonic rocks (Aksaray region – Central Anatolia). PhD thesis, (Unpublished) Middle Eastern Technical University (METU), Ankara, p 194

Tüysüz O, Dellaloğlu AA, Terzioğlu N (1995) A magmatic belt within the Neo-Tethyan suture zone and its role in the tectonic evolution of northern Turkey. Tectonophysics 243(1–2):173–191

Ünal E (2010) Genetic investigation and comparison of Kartaldağ and Madendağ epithermal gold mineralisation in Çanakkale-region. Master's thesis, Middle East Technical University (Unpublished), p 181

Ünal-İmer E, Güleç N, Kuşcu İ, Fallick AE (2013) Genetic investigation and comparison of Kartaldağ and Madendağ epithermal gold deposits in Çanakkale, NW Turkey. Ore Geol Rev 53:204–222

Ustaömer T, Robertson AFH (1997) Tectonic-sedimentary evolution of the north Tethyan margin in the Central Pontides of northern Turkey. In: Robinson AG (ed) Regional and petroleum geology of the Black Sea and surrounding Region. Mem Am Assoc Pet Geol 68:255–290

Ustaömer T, Robertson AFH (2010) Late Palaeozoic–early Cenozoic tectonic development of the Eastern Pontides (Artvin area), Turkey: stages of closure of Tethys along the southern margin of Eurasia. Geol Soc Lond Spec Publ 340:281–327

Van Hinsbergen DJJ, Maffione M, Plunder A, Kaymakcı N, Ganerød M, Hendriks BWH, Corfu F, Gürer D, de Gelder GINO, Peter K, PcPhee PJ, Brouwer FM, Advokaat El Vissers RLM (2016) Tectonic evolution and paleogeography of the Kırşehir Block and the Central Anatolian Ophiolites, Turkey. Tectonics 35:983–1014

Vural A (2006) Bayramiç (Çanakkale) ve çevresinin altın zenginleşmelerinin araştırılması. [Investigation of gold enrichments in Bayramiç (Çanakkale) and its surroundings]. PhD thesis, Ankara University, p 267 (In Turkish, unpublished)

Watanabe M, Soeda A (1981) Distribution of polytype contents of molybdenite from Japan and possible controlling factor in polytypism. Neues Jb Mineral Abh 141:258–279

Wells JD, Mullens TE (1973) Gold-bearing arsenian pyrite determined by microprobe analysis, Cortez and Carlin Gold mines, Nevada. Econ Geol 68:187–201

White NC, Hedenquist JW (1990) Epithermal environments and styles of mineralisation: variations and their causes, and guidelines for exploration. In: Hedenquist JW, White NC, Siddeley G (eds) Epithermal gold mineralisation of the circum-pacific: geology, geochemistry, origin and exploration. J Geochem Explor 36:445–474

Whitney DL, Dilek Y (1998) Metamorphism during Alpine crustal thickening and extension of Central Anatolia, Turkey: the Niğde Massif core complex. J Petrol 39:1385–1403

Whitney DL, Hamilton MA (2004) Timing of high-grade metamorphism in central Turkey and the assembly of Anatolia. J Geol Soc 161:823–828

Whitney DL, Teyssier C, Dilek Y, Fayon AK (2001) Metamorphism of the Central Anatolian Crystalline Complex, Turkey: influence of orogen-normal collision vs. wrench dominated tectonics on P–T–t paths. J Met Geol 19:411–432

Whitney DL, Teyssier C, Fayon AK, Hamilton MA, Heizler M (2003) Tectonic controls on metamorphism, partial melting, and intrusion: timing and duration of regional metamorphism and magmatism in the Niğde Massif, Turkey. Tectonophysics 376:37–60

Winderbaum L, Ciobanu CL, Cook NJ, Paul M, Metcalfe A, Gilbert S (2012) Multivariate analysis of an LA-ICP-MS trace element dataset for pyrite. Math Geosci 44:823–842

Yalçınkaya N (2010) Koru Köyü (Lapseki-Çanakkale) Pb-Zn-Ag Yatağının, Jeolojik, Mineralojik ve Jeokimyasal İncelenmesi. [Geological, Mineralogical and Geochemical Investigation of the Koru (Lapseki-Çanakkale) Pb-Zn-Ag Deposit]. Master's thesis, Çanakkale Onsekiz Mart University, p 181 (In Turkish, unpublished)

Yavuz H (2013) Kaymaz (Eskişehir) Listvenitik Altın Yatağı'nın Özellikleri ve Kökenine Bir Yaklaşım [Properties of Kaymaz listvenitic gold deposit and an approach to genesis of Kaymaz (Eskişehir) gold deposit genesis]. MSc thesis, Dokuz Eylül University, İzmir, Turkey, p 110 (In Turkish, unpublished)

Ye L, Cook NJ, Ciobanu CL, Liu YP, Zhang Q, Liu TG, Gao W, Yang YL, Danyushevskiy L (2011) Trace and minor elements in sphalerite from base metal deposits in South China: a LA-ICPMS study. Ore Geol Rev 39:188–217

Yiğit O (2009) Mineral deposits of Turkey in relation to Tethyan metallogeny: implications for future mineral exploration. Econ Geol 104:19–51

Yiğit O (2012) A prospective sector in the Tethyan Metallogenic Belt: geology and geochronology of mineral deposits in the Biga Peninsula, NW Turkey. Ore Geol Rev 46:118–148

Yılmaz H (1992) Turkey Regional Project. EuroGold, Unpublished company report, p 1–20

Yılmaz S, Boztuğ D (1996) Space and time relations of three plutonic phases in the Eastern Pontides, Turkey. Int Geol Rev 38:935–956

Yılmaz Y, Tüysüz O, Yiğitbaş E, Genç SC, Şengör AMC (1997) Geology and tectonics of the Pontides. In: Robinson AG (eds) Regional and petroleum geology of the Black Sea and surrounding region. Am Assoc Pet Geol Memoir 68:183–226

Yılmaz A, Adamia S, Chabukiani A, Chkhotua T, Erdoğan K, Tuzcu S, Karabıyıkoğlu M (2000) Structural correlation of the southern Transcaucasus (Georgia) –eastern Pontides (Turkey). In: Bozkurt E, Winchester JA, Piper JDA (eds) Tectonics and magmatism in Turkey and surrounding area. Geol Soc Lond Spec Publ 173:171–182

Yılmaz H, Oyman T, Arehart GB, Çolakoğlu AR, Billor Z (2007) Low-sulphidation type Au-Ag mineralisation at Bergama, İzmir, Turkey. Ore Geol Rev 32:81–124

Yılmaz H, Oyman T, Sönmez FN, Arehart GB, Billor Z (2010) Intermediate sulphidation epithermal gold-base metal deposits in tertiary subaerial volcanic rocks, Şahinli/Tespih Dere (Lapseki/Western Turkey). Ore Geol Rev 37:236–258

Yılmaz H, Sönmez FN, Akay E, Şener AK, Tufan ST (2013) Low-sulphidation epithermal Au-Ag mineralisation in the Sındırgı District, Balıkesir Province, Turkey. Turk J Earth Sci 22:485–522

Yılmaz-Şahin S (2005) Transition from arc- to post-collision extensional setting revealed by K-Ar dating and petrology: an example from the granitoids of the Eastern Pontide Igneous Terrane, Araklı-Trabzon, NE Turkey. Geol J 40:425–440

Young ED, Coutts DW, Kapitan D (1998) UV laser ablation and irm-GCMS microanalysis of $^{18}O/^{16}O$ and $^{17}O/^{16}O$ with application to calcium-alluminium-rich inclusion from Allende meteorite. Geochim Cosmochim Acta 62:3161–3168

Zhao HX, Frimmel HE, Jiang SY, Dai BZ (2011) LA-ICP-MS trace element analysis of pyrite from the Xiaoqinling gold district, China: implications for ore genesis. Ore Geol Rev 43:142–153

Zheng Y, Zhang L, Chen Y, Hollings P, Chen H (2013) Metamorphosed Pb–Zn–(Ag) ores of the Keketale VMS deposit, NW China: evidence from ore textures, fluid inclusions, geochronology and pyrite compositions. Ore Geol Rev 54:167–180

Zhu Y, An F, Tan J (2011) Geochemistry of hydrothermal gold deposits: a review. Geosci Front 2(3):367–374

Chapter 5
Turkish Iron Deposits

Taner Ünlü, Özcan Dumanlılar, Levent Tosun, Sinan Akıska, and Deniz Tiringa

Abstract Iron ore, which plays an important role in the development of civilisation, is one of the most familiar of ancient Anatolian people. It is known that iron had a long journey from Asia through Mesopotamia, Egypt, Cyprus, Rome and eventually through Europe. The oldest information about iron mining in Anatolia is based on the fact that the iron deposits of Firnis and Kartal in Maraş were operated around 3600 BC by Hittites in Southeastern Turkey.
In 1937, the first recorded study of iron mines in Turkey was carried out by General Directory of Mineral Research & Exploration of Turkey (MTA) in Sivas Divriği, Central Anatolia. This chapter, on Iron Deposits in Turkey, is a compilation of works that are unique to iron deposit studies ranging from exploration of the Divriği iron mine to today's operations.

Different iron occurrences belong to different geological environments in Turkey, located in the Tethyan-Eurasian Metallogenic Belt. These occurrences are usually very small or small with only a few being of medium size.

Geographically, the occurrences exhibit different spatial distributions and are clustered around four regions, i.e., Kayseri-Adana, Balıkesir-Kütahya, Sivas-Malatya and Kırşehir-Yozgat.

The iron deposits of Turkey are generally located along the contacts with granitic rocks. However, some studies show that iron deposits may also be associated with ophiolitic rocks within the same region.

T. Ünlü (✉) · S. Akıska
Faculty of Engineering, Department of Geological Engineering, Ankara University, Gölbaşı, Ankara, Turkey
e-mail: tunlu@eng.ankara.edu.tr; akiska@eng.ankara.edu.tr

Ö. Dumanlılar · L. Tosun
Demir Export A.Ş., Exploration Department, Kızılay, Ankara

D. Tiringa
General Directorate of Mineral Research and Exploration, Department of Mineral Research and Exploration, Çankaya, Ankara

F. Pirajno et al. (eds.), *Mineral Resources of Turkey*, Modern Approaches in Solid Earth Sciences 16, https://doi.org/10.1007/978-3-030-02950-0_5

5.1 Introduction

A total of about 900 iron occurrences are known in Turkey and of these 496 were investigated in detail.

Investigated iron occurrences and deposits are found to be densely distributed in some regions while in some others they are sparsely scattered. These occurrences are mostly located Kayseri-Adana, Balıkesir-Kütahya, Sivas-Malatya and Kırşehir-Yozgat regions (Fig. 5.1).

Distribution of iron occurrences and deposits based on total metal iron contents is given in Table 5.1 and their cumulative distributions are shown in Fig. 5.2. Eighty-eight percent of the deposits are categorized as very small-scale deposits (total 100% metal Fe <500,000 tonnes), 11% as small-scale deposits (total 100% metal Fe 500,000–25,000 tonnes) and 1% as middle-scale deposits. In Turkey only four deposits are of middle-scale. They are: Çamdağ, Deveci, Divriği A+B Kafa and Hasançelebi deposits.

Nearly 88% of deposits have a total metal content less than 10 Mt while the remaining 12% (a total of 10 deposits) have a total metal content greater than 10 Mt Iron ore reserves were estimated to be about 500 Mt containing 100% iron. In the iron distribution map of Turkey, the Hekimhan basin (36.8%) and Divriği basin (21.6%) seem to include the major deposits (Fig. 5.3). Divriği, Hekimhan, Saimbeyli-Feke, İçel, Elbistan and Antakya-Gaziantep regions comprising 74.3% of the total iron metal content of Turkey are strategically important regarding iron exploration (Fig. 5.4). Important iron ore regions in Turkey are summarised below.

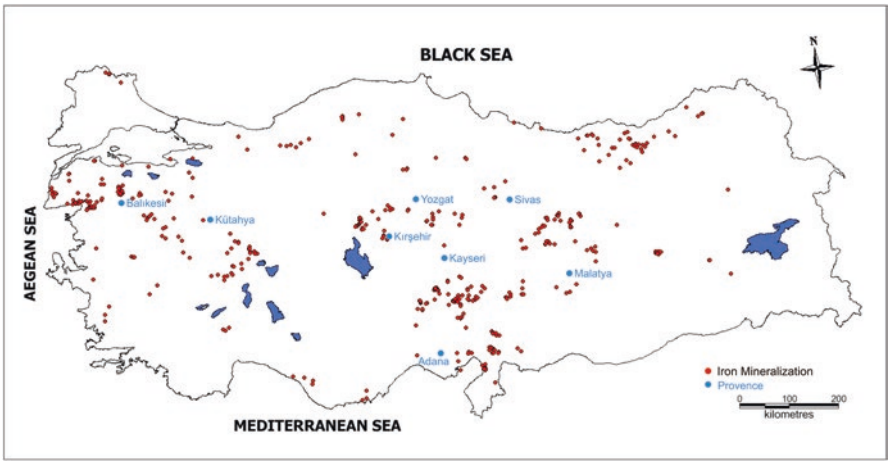

Fig. 5.1 Geographic distribution of 496 iron ore occurrences and deposits in Turkey. (Compiled from MTA data)

Table 5.1 Distribution of iron ore occurrences and deposits in Turkey on the basis of metal iron contents

100% metal Fe (thousand tons)	Number of occurrence and deposits	Occurrence and deposit percent	Deposit size
0–20	344	70	Very small
20–50	21	4	
50–100	21	4	
100–250	32	7	
250–500	15	3	
500–750	6	1	Small
750–1000	7	1	
1000–5000	29	6	
5000–10,000	10	2	
10,000–25,000	7	1	
25,000–35,000	2	0.4	Middle
35,000–50,000	1	0.2	
>50,000	1	0.2	

Ünlü (1989)

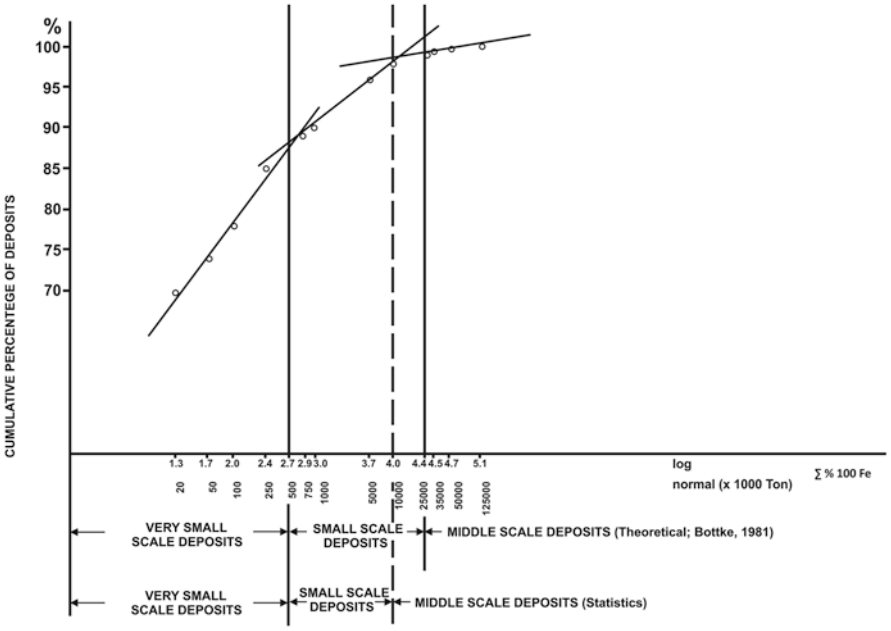

Fig. 5.2 Cumulative distribution of Turkish iron ore occurrences and deposits based on metal iron contents (number of deposits is 496). (Ünlü 1989)

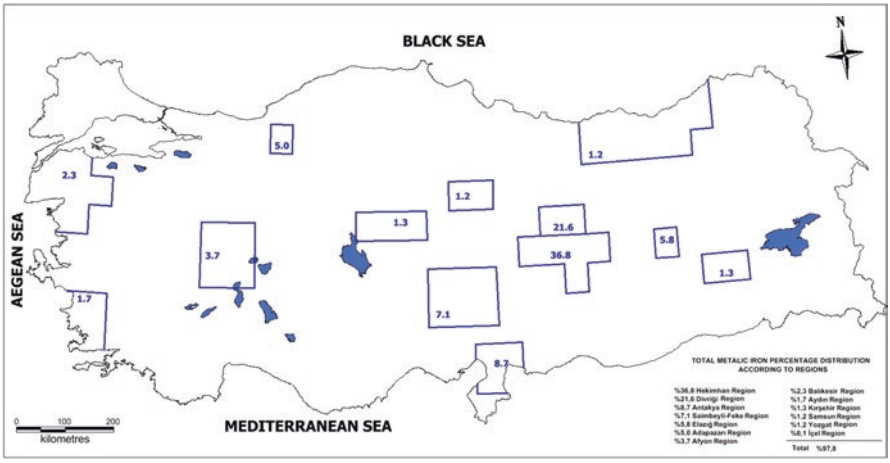

Fig. 5.3 Density distribution map of metal iron contents for iron ore occurrences and deposits (based on 496 deposits with total metal iron content of 499.5 Mt). (Ünlü 1989)

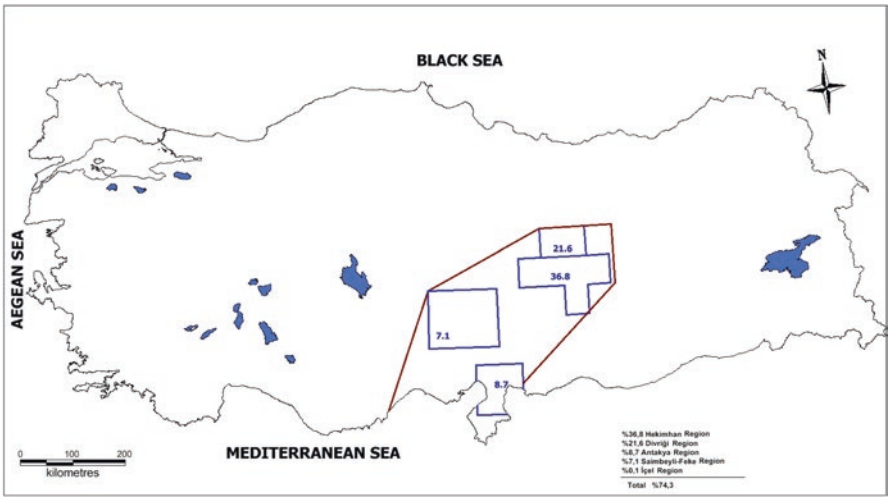

Fig. 5.4 The first-degree target region which needs to be considered in the studies of Turkish iron deposits. (Ünlü 1989)

5.2 Sivas-Malatya-Erzincan Region

This region is the largest iron ore district in Turkey since it comprises most the currently operated deposits with low-grade and high tonnage reserves that could be used in the future. It is also the centre of high-grade ore production that is direct reduced iron ores in their bodies for blast furnaces.

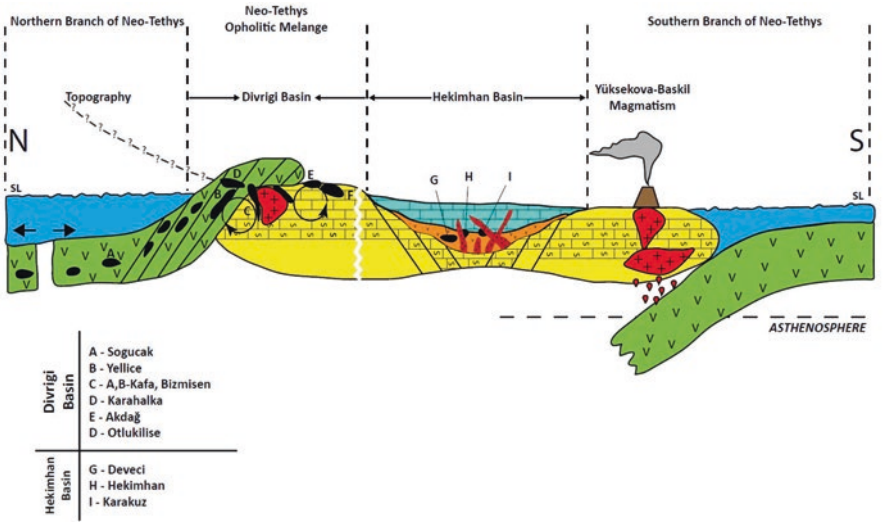

Fig. 5.5 A schematic model for the genesis of iron deposits in Divriği and Hekimhan basins. (Modified from Ünlü 1991)

The Divriği Concentrate and Pellet Facility which started operation in 1985 is a mining centre in Turkey that has operated for many years, and some additional facilities to be established are also situated in the same region – the calcination facilities to process low-grade Hekimhan-Deveci siderites and the concentrate and pellet facility to process low-grade Hekimhan-Hasançelebi magnetite deposits. Studies conducted in this region during 1989–1993 years resulted in significant improvement of the reserve.

The major iron ore deposits of this region (Fig. 5.5) are: Divriği A and B Kafa (Sivas), Dumluca-Divriği (Sivas), Pınargözü-Çetinkaya (Sivas), Otlukilise- Gürün (Sivas), Hasançelebi-Hekimhan (Malatya), Karakuz-Hekimhan (Malatya), Deveci-Hekimhan (Malatya), Bizmişen-Kemaliye (Erzincan) and Sarıkaya-Sorgun (Yozgat).

5.2.1 Divriği A and B Kafa Iron Deposits

Divriği A and B Kafa deposits are located about 100 km south-east of Sivas city.

The main geological units in and around the Divriği A and B Kafa iron deposits are serpentinized ultramafic rocks which are associated with Jurassic-lower Cretaceous limestones and the Upper Cretaceous-Paleocene granites that cut all the younger rocks. Ore and skarn occurrences are common along contacts between granitic rocks and wall rocks (Cihnioğlu et al. 1994).

Wall rocks are composed mostly of granitic rocks, serpentinites and locally silicified and carbonatized rocks.

Ore and wall rock make up an intricate structure resembling a shell like appearance. The mineralisation occurs in serpentinized ultramafic rocks or along the contact between granitic rocks and serpentinites (Koşal 1971, 1973; Ünlü and Stendal 1986, 1989; Zeck and Ünlü 1987, 1988, Ünlü et al. 1995, Yıldızeli 1998; Işık 2002).

Magnetite is the main ore mineral accompanied by pyrite and chalcopyrite veins (Koşal 1971).

The Divriği A and B Kafa iron deposits are contact metasomatic-pneumatolytic and pneumatolytic- hydrothermal type that are associated with Upper Cretaceous-Paleocene syenitic-monzonitic intrusions. The A-Kafa ore and several skarn minerals are emplaced along the contact between these intrusions and Mesozoic limestones and Pre-upper Cretaceous serpentinites. The B Kafa ore which is distal with respect to the intrusions was formed in pneumatolytic-hydrothermal phase in the limestone-serpentinite thrust zone (Koşal 1973).

Results of chemical analysis conducted on samples from Divriği iron deposits indicate two different types mineralisation. The first type mineralisation has high Cr, Co and Ni and MgO contents representing an ultramafic geochemical trend (Stendal and Ünlü 1991) while the second type shows a sedimentary character (e.g. high Ba content). It is suggested that mafic and ultramafic sections of the ophiolites hosting tectonically emplaced ores are formed by tectonic processes (Ünlü and Stendal 1986) (Fig. 5.6).

Alkali metasomatism in and around the Divriği deposit, mineralogy of deposit, tectonic setting of plutonic rocks and structural control in mineralisation led Yılmazer et al. (2003) and Kuşçu et al. (2002, 2010) to suggest that the Divriği deposit resembles an Fe-oxide-Cu-Au (IOCG) mineral system.

Öztürk et al. (2016), showed that iron ores concentrate at triple junctions of limestones, serpentinized ultramafic rocks and granitic rocks in the region. Magmatic activity was associated with post- collisional rifting and gave rise to the skarn type or vein type and volcano sedimentary type iron ore deposits in the Late Cretaceous.

The Divriği A Kafa mineralisation occurs within widespread skarn zones of the Murmano pluton. The mineralisation occurs as phlogopite-magnetite veins along NE-SW trending fracture-cracks and faults or as lenses and pockets within the plutonic rock. The largest ore body is developed along the contact between serpentinized ultramafic rocks and pluton confined to an ENE-WSW trending fault (Yılmazer et al. 2003).

As a result of drilling works and geological surveys, a total of 120 Mt reserve was determined most of which has been mined out (Kara et al. 2005).

In the vicinity of Divriği A and B Kafa deposits, there is a placer occurrence (referred to as the C placer) which is thought to be derived from these deposits. In areas surrounding the deposits, serpentinites and limestones of the ophiolitic complex of pre-Cretaceous age and Upper Cretaceous-Paleocene granites are exposed. Neogene fluvial sediments and colluvial deposits comprise the youngest units.

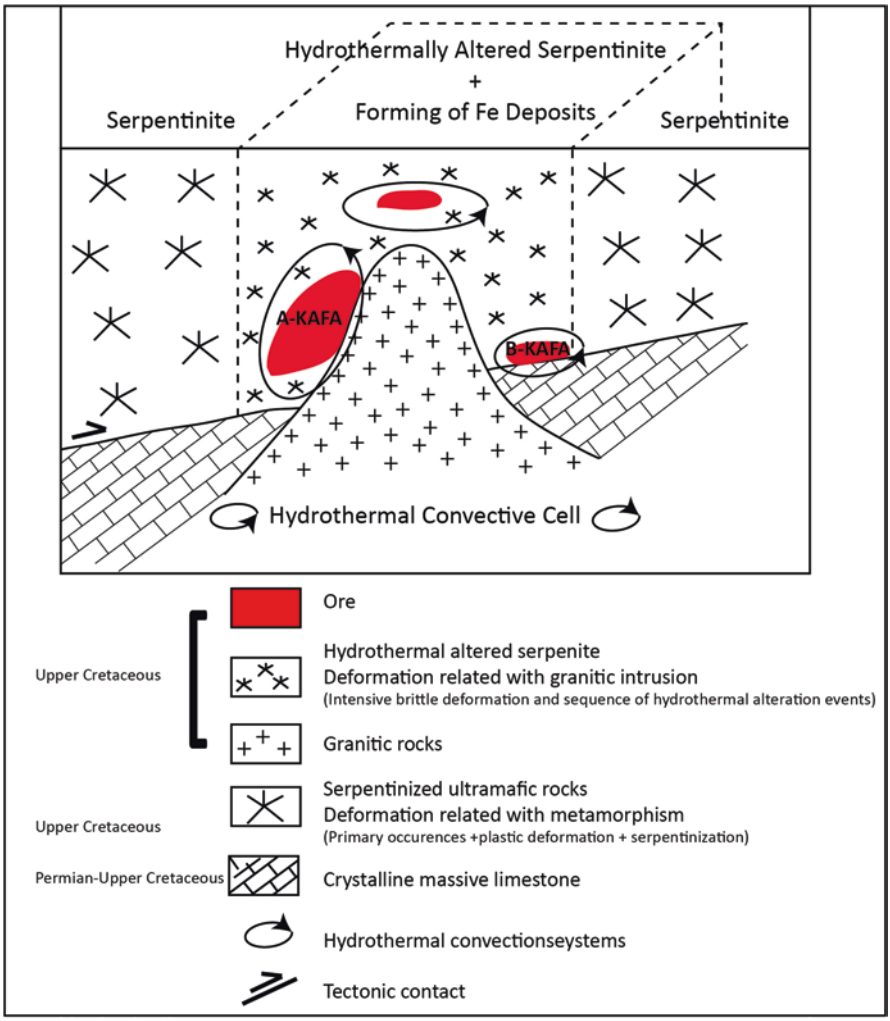

Fig. 5.6 Schematic model for the Divriği A and B Kafa iron deposits. (Ünlü et al. 1995)

The C placer is a secondary iron ore. Transportation distance is not much, and aggregation took place in areas where ore blocks of various type and size were accreted with no significant gangue material. The C placer is believed to have resulted from a landslide originated from a 500 to 600 m high ore exposure about 1 km from the Divriği and A and B Kafa iron deposits as a result of graben formation during middle Pliocene (Koşal 1973).

5.2.2 Dumluca-Divriği Iron Deposit

The Dumluca iron deposit is located 10 km southwest of Divriği A-Kafa iron deposit about 100 km south-east of the city of Sivas.

Serpentinized ultramafic rocks and tectonically related Jurassic-lower Cretaceous limestones and Upper Cretaceous-Paleocene (syenite and diorite) are exposed around the Dumluca iron deposit. Most part of deposit is covered by Pliocene conglomerates and basalts. The ultramafic rocks are altered to serpentine, chlorite, carbonate, quartz and uralite (a variety of amphibole). Limestones are mostly dolomitized and silicified. Skarn minerals occur at the contacts between syenites and wall rock (Ünlü et al. 1989).

The Dumluca iron deposit is genetically similar to A Kafa iron deposit. The ore occurs as an irregular lens shape and extends in the N-S direction. The ore is chiefly composed of pyrite-bearing magnetite, which is altered to martite in the upper levels.

The deposit has a reserve of 8 Mt of iron with Fe grade of 54–58% (Yıldızeli 1977).

5.2.3 Pınargözü-Çetinkaya Iron Deposit

The Pınargözü iron deposit is located 80 km south-west of the city of Sivas.

Rocks exposed around the deposit from bottom to top comprise Jurassic-lower Cretaceous recrystallized and silicified limestones, ophiolitic rocks of pre-upper Cretaceous age and volcano- sedimentary units of Upper Cretaceous age. These units have tectonic contacts. All these rocks are cut by microdiorite-microsyenite dykes of middle-upper Eocene age (Gümüş 1963; Yıldızeli 1983).

The Pınargözü iron deposit includes two open pits: the Main pit and Elkondu pit. These two pits are located on a N70E tectonic line. The deposit shows two different mineralisation types. The first type is concordant to the bedding of the volcano-sedimentary units and exposed in a limited area. The second type occurs in association with middle-upper Eocene intrusive rocks along the N70E trending fractures in serpentinites and limestones or along their contact. The deposit has a volcano-sedimentary origin and is either reworked by micro diorites or a hydrothermal type associated with microdiorites.

The ore is accompanied by albite, feldspar, epidote, scapolite, quartz, chalcedony, apatite, tourmaline, chlorite, hydrogarnet and sericite. Hematite is the main ore mineral that is formed by martitization of magnetite although pyrite and magnetite are also detected at depths. Chalcopyrite is locally observed in the deposit and biotite, calcite, dolomite, chalcedony, apatite, tourmaline and zircon accompany the ore (Karakaya 2011).

The deposit contains 15 Mt of hematite ore with an Fe grade of 51% (Yıldızeli 1983).

5.2.4 *Otlukilise-Gürün Iron Deposit*

The Otlukilise iron deposit is located 95 km southwest of the city of Sivas.

Recrystallized limestones of Upper Cretaceous age, Tertiary andesitic tuffs, breccias and hornblende andesites are exposed around the deposit (Cihnioğlu et al. 1994).

The deposit hosts two different ore types. The first type is massive that occurs within Upper Cretaceous recrystallized limestones. The ore is thought to be a product of siderite that replaced limestones by hydrothermal solutions or a product of alteration siderites within the volcano- sedimentary units. The second type was formed by aggregation of in-situ weathered massive ore and Neogene units within large depressions (Çiftçi et al. 1996).

Hematite is the main ore mineral accompanied by lesser amount of goethite. Ore pebbles of hematite composition are dominated in the aggregate type mineralisation (Çiftçi et al. 1996) (Fig. 5.7).

According to Gülibrahimoğlu (1979) the Otlukilise iron deposit is an epigenetic deposit occurring in fractures of limestones in the basement. However Çiftçi et al. (1996) suggest that it is a Lahn–Dill type syn-sedimentary volcanogenic or exhalative deposit.

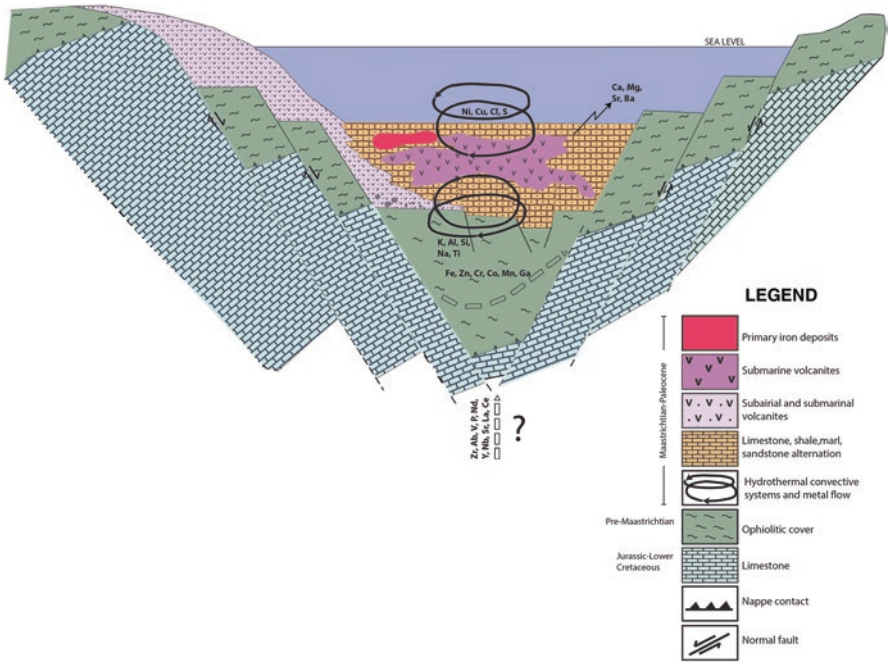

Fig. 5.7 Schematic ore genesis model of Otlukilise iron deposits. (Çiftçi et al. 1996)

The main massive ore contains 53% Fe and 7.5% SiO2 while aggregate type ore contains 31.7% Fe and 30.1% SiO2 and the whole massive ore and aggregate ore reserves are 12.6 and 35 Mt, respectively (Gülibrahimoğlu 1979).

5.2.5 Hasançelebi-Hekimhan Iron Deposit

The Hasançelebi-Hekimhan iron deposit is located 94 km north-west of the city of Malatya.

The basement around the deposit is represented by serpentinized ultramafic rocks of pre-upper Cretaceous emplacement age and they are overlain by Upper Cretaceous volcano-sedimentary sequence of mafic composition. The whole sequence is cut by Upper Cretaceous-Paleocene syenite porphyries (Gürer 1992).

The mineralisation occurs within scapolite-bearing rocks along the contact between syenite porphyries and volcano-sedimentary sequence. It is suggested that in the Hasançelebi deposit iron originated from mafic volcanics and ophiolite during scapolite alteration which formed magnetite as replacements, disseminations and veins (Stendal et al. 1995) (Fig. 5.8). In the study of Fe-oxide-Cu-Au deposits in Turkey, Kuşçu et al. (2005a, b) set forth the same findings for the formation of Hasançelebi- Hekimhan iron deposit.

The ore zone has an EW trend and has a length of 12 km and a width of 2 km.

The main ore mineral is magnetite which is accompanied by hematite. The secondary minerals are scapolite, biotite, diopside, amphibole, garnet, tourmaline, pyrite, titanite, calcite, zircon, lepidolite, apatite, rutile and quartz.

The total reserve of Hasançelebi iron deposit is found 1.9 Bt with an average Fe3O4 grade of 15.7%. The deposit also contains 250 Mt iron with a Fe3O4 grade of 27.5% and 130 Mt iron with a Fe3O4 grade of 32.3%.

The deposit also contains 30.6% SiO2, 1.35% S and 0.06% P. TiO_2 content varies and locally is up to 7% (Akçakoca and Kurt 1974).

5.2.6 Karakuz-Hekimhan Iron Deposit

The Karakuz-Hekimhan iron deposit is located 60 km north-west of the city of Malatya.

Syenite porphyries, scapolite-rich rocks and Miocene-Pliocene volcanic rocks of trachytic composition are exposed in the vicinity of Karakuz-Hekimhan iron deposit (Gürer 1992).

The deposit shows two different ore types. The iron ore within trachyte constitutes the main Karakuz- Hekimhan iron deposit. It is suggested that Karakuz-Hekimhan iron deposit was formed by the emplacement of an intrusion of trachytic composition in a within-plate tectonic environment (Gürer 1992). The other type of ore is Hasançelebi iron occurrences as magnetite vein and lenses within scapolite-rich rocks.

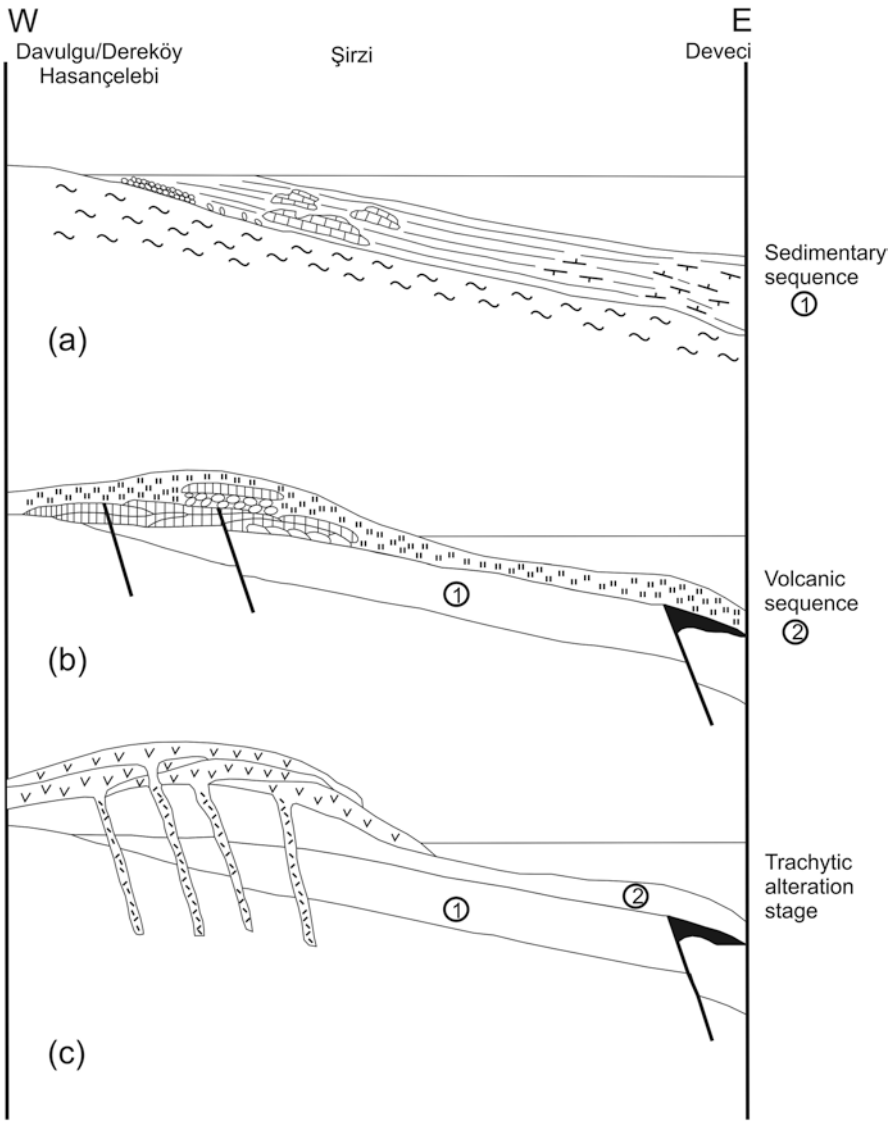

Fig. 5.8 Schematic model for the Hasançelebi iron deposit. (Stendal et al. 1995)

The mineralisation styles are veins and stockwork veinlets within altered trachytes and martitized hematite is the main ore mineral, while limonite is a secondary phase. Pyrite and chalcocite are rare and quartz, calcite and barite are the main gangue minerals (Uçurum et al. 1996).

In the Karakuz-Hekimhan iron deposit reserve is 5.7 Mt with an Fe grade of 41–54%.

5.2.7 *Deveci-Hekimhan Iron Deposit*

The Deveci-Hekimhan iron deposit is located about 60 km north-west of the city of Malatya.

Flysch rocks of the Upper Cretaceous Hekimhan formation consisting of conglomerate, sandstone, marl and limestone and spilite-keratophyre units that are vertically and laterally intercalated with the sedimentary rocks are exposed around the Deveci-Hekimhan iron deposit (Yılmaz and Türkyılmaz 1998).

The Deveci-Hekimhan mineralisation was deposited within these volcanic and flysch rocks. At depth the ore body consists of siderite while it occurs as limonite and goethite in the upper sectors. The volcanic rocks in the deposit are composed of tuffs of mafic composition and those around the deposit there are keratophiric rock fragments. In most cases, there is a continuous change from siderites to volcanic ashes (Ünlü 1983, 1987).

The mineralisation is composed of Mn-bearing siderite, clay and dolomite/ankerite. The abundances of kaolinite, illite and quartz that accompany the ore are variable. It is believed that siderite and clays were deposited concurrently. The deposit is regarded as a volcano-sedimentary occurrence associated with mafic-type volcanism or an exhalative mineral system (Lahn-Dill type deposit) (Ünlü 1987; Stendal et al. 1995) (Fig. 5.9).

The Deveci-Hekimhan iron deposit contains 59 Mt of siderite with a grade of 36.5% Fe and 3.7% Mn and 14 Mt of limonite-goethite with a grade of 50% Fe (Özer and Kuşçu 1982; Ünlü 1983).

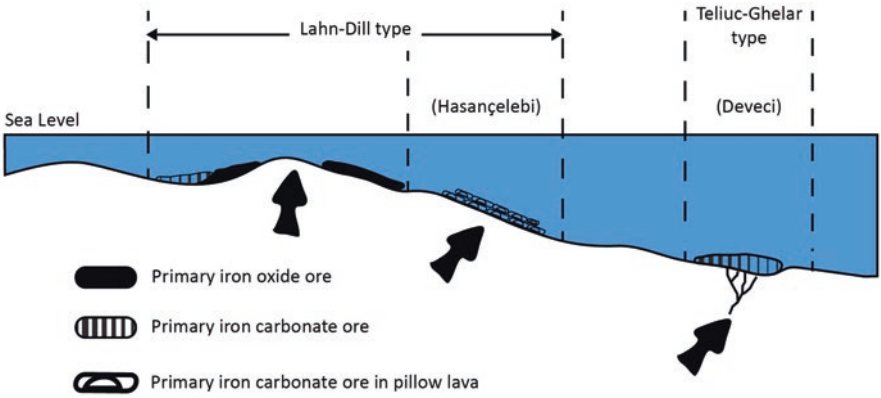

Fig. 5.9 Volcanic-exhalative model for the deposition of iron mineralisation at Hasançelebi and Deveci compared to stratiform Lahn-Dill and Teliuc-Ghelar. (Stendal et al. 1995)

5.2.8 *Bizmişen-Kemaliye Iron Deposit*

The Bizmişen-Kemaliye iron deposit is located 100 km southwest of Erzincan city and consists of four different sectors.

Upper Triassic-Upper Cretaceous limestones, ophiolitic rocks of pre-upper Cretaceous emplacement age and Upper Cretaceous-Paleocene granites are exposed around the Bizmişen-Kemaliye iron deposit (Yıldırım and Hamarat 1984).

Mineralisation occurs at the contact of limestone-serpentine-diorite or diorite-limestone. At these triple or binary contacts, various contact metasomatic (skarn type) and hydrothermal type mineral systems are recorded. Diopside, grossular and andradite are common alteration products in the skarn at the diorite-limestone contact while phlogopite, grossular and andradite occur in the skarn at the serpentine-diorite contact (Yıldırım and Hamarat 1984).

Magnetite and hematite are the main ore minerals and as a result of further mineralogical studies at the deposit sulphide minerals of retrograde hydrothermal stage (pyrrhotite, pyrite, chalcopyrite, sphalerite and marcasite) and chromites that are replaced by to magnetite are present. Barite, rutile and apatite are also found in the paragenesis.

The Bizmişen-Kemaliye iron deposit has 23 Mt reserve with a grade of 53% Fe (Yıldırım and Hamarat 1984).

5.2.9 *Sarıkaya-Sorgun Iron Deposit*

The Sarıkaya-Sorgun iron deposit is located 30 km east of Yozgat city.

Paleozoic (?) metamorphic rocks consisting of gneiss, marble, amphibolite, schist, muscovite schist and biotite-amphibolite schist are oldest rocks around the deposit. This rock sequence which is unconformably overlain by Eocene nummulitic limestones is cut by Upper Eocene aged intrusions of felsic composition. All units in the region are covered with a Neogene sequence (Durgun 1977).

Considering mineral paragenesis and field data, the Sarıkaya-Sorgun iron deposit (manganese-bearing) is regarded as a metamorphic deposit of sedimentary origin (Çağatay and Arda 1976).

Hematite and magnetite are the main ore minerals which are accompanied by manganese, chalcopyrite, pyrite and fluorite.

5.3 Kayseri-Adana Region

The region is the second important iron ore district in Turkey. It supplies high-grade ore that is suitable direct reduced iron ores in their bodies for blast furnaces and has provided significant amount of ore to the domestic iron-steel industry for years. As

a result of surveys and drilling works conducted by the General Directorate of MTA, important reserves were discovered at the Mansurlu-Attepe area and this reserve potential could be increased by further exploration works.

During late Neoproterozoic as a result of southeastward subduction of proto-Tethys oceanic crust into the Tauride-Anatolide platform, arc magmatism was developed on the continental margin and in this area of regional tectonic activity the Emirgazi formation was deposited which is composed of volcanics and pyroclastics of both felsic and mafic composition some of which are represented by arc-related volcanics. As a result of continuing collision and decrease in subduction angle the volcanic arc widened and a rift structure was formed in a back-arc basin in the early Cambrian. Thinning of continental crust at the beginning of rifting resulted in the formation of anatexic granites. Meanwhile, submarine volcanics of mafic or intermediate composition were erupted in the basin through fractures and deposited contemporaneously with sediments (flysch) resulting in a volcano-sedimentary series called the Koçyazı formation. In this tectonic environment, depending on bottom topography the basin waters may have different pH and Eh values in which stratiform and stratabound mineral systems occur. Metals in these mineral systems originated from metal–rich solutions derived from seawater which penetrated through fractures and was heated and then ascended to the sea floor. Fe^{+2}–rich solutions originated by weathering of ultramafic rocks in continental areas to the basin are another source. Metal–rich solutions discharged to the sea floor may be deposited as magnetite, siderite and/or hematite and pyrite depending on pH and Eh of the environment (Gürsu and Göncüoğlu 2005; Rajabi et al. 2015; Tiringa 2016; Tiringa et al. 2016) (Fig. 5.10). Continuing subduction of oceanic crust and increase in the subduction angle or tearing/breaking off of the subducted slab in later stages resulted in a variation of the mineralisation. Mineral systems that are affected by intense post- depositional deformation and metamorphism processes are uplifted to the surface by faults where they obtained their current shape. These fault zones paved the way for karstification processes and caused the formation of the primary ore minerals siderite and/or hematite replaced by limonite and goethite (Tiringa 2016; Tiringa et al. 2016).

Karamadazı (Kayseri), Karaçat-Kızıl (Kayseri), Mağarabeli (Kayseri) and Attepe-Mansurlu (Adana) iron deposits are located in this region.

5.3.1 Karamadazı Iron Deposit

The Karamadazı iron deposit is located 65 km southwest of Kayseri city.

Around the deposit, the Yahyalı pluton intrudes the quartzite-interbedded metacarbonates of late Permian age. Skarn minerals formed by metasomatism along this contact (Oygür et al. 1978).

The Karamadazı deposit is a skarn type and is classified as calcic by Oygür et al. (1978) and calcic or magnesian skarn by Kuşçu et al. (2001). Skarn minerals are garnet, epidote, scapolite and diopside. Ore is composed of magnetite that is partly

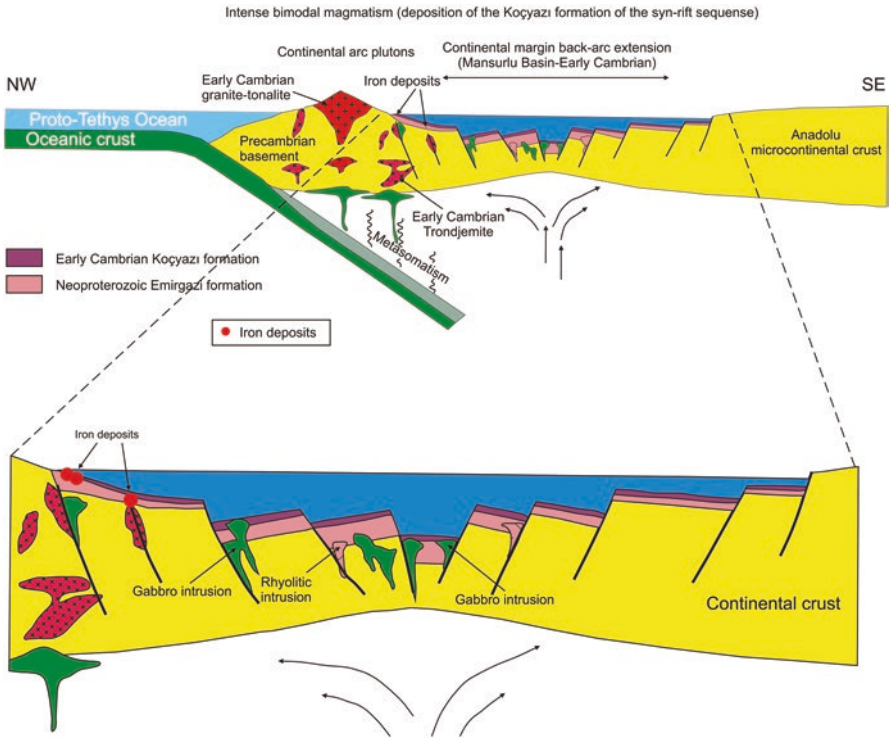

Fig. 5.10 A tectonic model for the geodynamic evolution of the Mansurlu rift basin and formation of iron mineralisation. (From Tiringa 2016; Tiringa et al. 2016 compiled from Gürsu and Göncüoğlu 2005; Rajabi et al. 2015)

overprinted by maghemite and hematite. Magnetite is associated with pyrite and less chalcopyrite and pyrrhotite. Gangue minerals are diopside, feldspar (plagioclase, orthoclase), epidote, clinozoisite, quartz, biotite, chlorite, calcite, garnet and sericite. The ore body is E-W trending and has a length of 400 m and dipping to the south-east.

The reserve of deposit is 6.5 Mt with grades of 54% Fe, 1.7% S and 11% SiO2 (Oygür 1986).

5.3.2 Karaçat-Kızıl Iron Deposit

The Karaçat-Kızıl iron deposit is located 78 km south of Kayseri city.

Cambrian quartzites, limestones and Ordovician schists outcrop around the deposit. Cambrian units are in tectonic contact with the Ordovician units (Özgül and Kozlu 2002).

The Karaçat-Kızıl iron deposit is formed on a NE-SW trending fault where schist and phyllite in the hanging wall and quartzite in the footwall, are present. The ore has a vein geometry with a length of 600 m and thickness of 80–100 m.

It was established that karstification and surface weathering conditions on the post-mineralisation fault zones have given rise to alteration of siderite and most of other iron minerals to limonite and goethite. The ore is accompanied by gangue minerals quartz and lesser amounts of barite. These iron-rich zones are the main raw material of the deposit (Tiringa et al. 2009).

The deposit has 40 Mt of reserves with a grade of 79.7% Fe2O3.

5.3.3 Mağarabeli Iron Deposit

The Mağarabeli iron deposit is located 85 km south of Kayseri city.

Middle Cambrian limestones and Ordovician schists are in tectonic contact around the deposit (Özgül and Kozlu 2002).

In the Mağarabeli deposit, the iron ore body has a length of 350–400 m and an average thickness of 35 m and occurs on a NE-SW trending tectonic line dipping 30° SE. In this vein-type deposit, hematite, siderite, goethite and limonite are the main ore minerals, while barite, calcite and quartz are the gangue minerals. Ore microscopy studies on the hematites show the presence of carbonate pseudomorphs which indicate that the hematite is a product of alteration from siderite (Tiringa et al. 2009).

Detailed studies on the Mağarabeli deposit revealed 5.7 Mt of iron reserves with a grade of 53.7% Fe (Dağlıoğlu and Arda 2000). Today, all the reserve is exhausted and the mining activity has stopped.

5.3.4 Karahalka Iron Deposit

The Karahalka iron deposit is located 120 km northeast of Kayseri city.

Jurassic-lower Cretaceous limestones, ophiolitic units of pre-upper Cretaceous age (emplacement age) and Neogene cover units are exposed around the deposit (Yılmaz et al. 1997). The Karahalka iron mineralisation is seen in karstic cavities within the limestones, as a lateritic occurrence along the contact between limestones and ophiolites and as listwaenite occurrences.

The lateritic occurrences partly show a massive appearance, whereas the conglomeratic ore is represented by hematite±magnetite, limestone and serpentinite pebbles and a hematite-limonite matrix (Keskinler et al. 2010). The vein type secondary mineralisation occurs within the limestone or along the limestone-ophiolite contact associated with N30°-45°E trending faults. The vein-type mineralisation is represented by hematite-magnetite and lesser amounts of chalcopyrite-pyrite, quartz and barite.

The reserve of Karahalka deposit is 1.1 Mt with grade of 49% Fe.

5.3.5 *Attepe Iron Deposit*

The Attepe iron deposit is located 110 km northeast of Adana city.

Precambrian graphite-schist, early Cambrian quartzite, middle Cambrian limestone and Ordovician shale and calc-schist are exposed around the deposit (Özgül and Kozlu 2002).

Goethite, pyrite, siderite, and hematite are the main ore minerals in the deposit; limonite is seen near the surface. The source of the ore is graphite schist including pyrite, primary siderite and hematite (Dayan 2007; Dayan et al. 2008; Arda et al. 2008; Tiringa et al. 2011). The main ore zone, a linear zone which has a length of 800–900 m, runs in a NNW-SSE direction.

The reserve of the Attepe iron deposit is 36 Mt at 58.4% Fe; and almost all the reserve has now been extracted.

5.4 Ankara-Kesikköprü Region

The region covers the area between Bala (Ankara) and Keskin (Kırıkkale). Ore has been transported from this region to the Karabük iron-steel plant for many years.

As a result of surveys and exploration works conducted by General Directorate of Mineral Research and Exploration (MTA), the calculated reserves in the region have significantly increased.

The Kesikköprü-Bala (Ankara) deposit is the most important deposit of the region.

5.4.1 *Kesikköprü-Bala Iron Deposit*

The Kesikköprü-Bala deposit is located 80 km northwest of the city of Ankara.

Re-crystallized limestone and ultramafic-mafic rocks of the ophiolite complex of pre-Upper Cretaceous emplacement age are exposed around the deposit. The complex is covered with Upper Cretaceous sedimentary and volcanic-volcanoclastic rocks. All this sequence is intruded by Upper Cretaceous- Paleocene granitoids. Skarn occurrences are also common at the contact between the granitic rocks and crystallized limestone blocks of the complex (Doğan et al. 1998) (Fig. 5.11).

The deposit is regarded as a granite-associated skarn-type by Kraeff (1962), Boroviczeny (1964a, b, c, d), Sözen (1970), and Öztürk and Öztürk (1983). Alternatively, Doğan et al. (1998) have suggested that the deposit should be classified as being related to “magmatic- metamorphic” processes.

The main ore minerals are magnetite, hematite, goethite, mushketoffite, maghemite with lesser amounts of ankerite and siderite. The sulphide minerals present are chalcopyrite, bornite, chalcocite, covellite and pyrite while the gangue min-

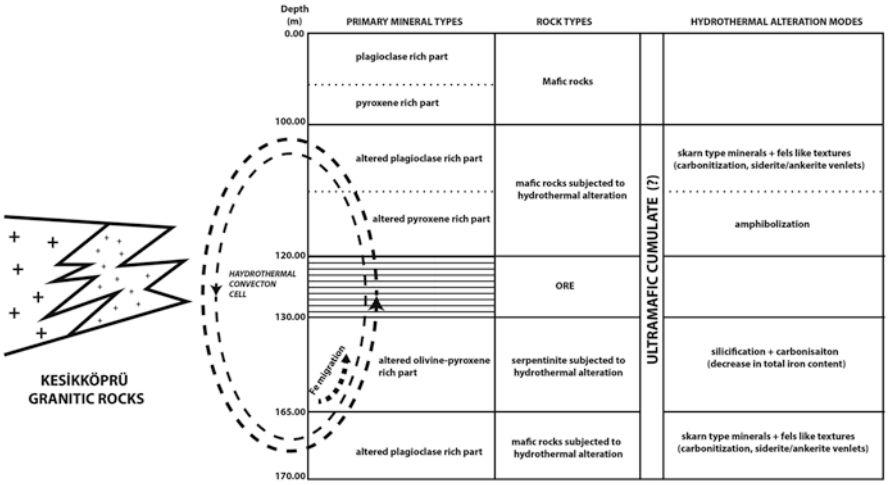

Fig. 5.11 A model for the origin of Kesikköprü iron deposits. (Doğan et al. 1998)

erals are garnet, diopside, epidote, tremolite, chlorite, quartz, tourmaline, titanite and apatite (Doğan et al. 1998).

The reserve of Kesikköprü-Bala deposit is rated at 3.8 Mt with a grade of 44–60% Fe (Sözen 1970).

5.5 Western Anatolian Region

Although iron ore deposits in western Anatolia are generally of high grade, they contain some impurities. Ore produced from these deposits are blended with those from higher-grade ores to reduce their impurity to tolerable levels and thus become suitable for directly- reduced iron ores for use in blast furnaces. Some of the deposits with impurities in the region are the Şamlı deposit (which has a Cu impurity), the Eymir deposit (which has an As impurity) and the Ayazmant deposit, which has Cu and S impurities.

The Yazıbaşı-Hortuna (İzmir), Çavdar-Söke (Aydın), Ayazmant (Balıkesir), Şamlı (Balıkesir) and Büyük Eymir (Balıkesir) iron deposits are located in this region.

5.5.1 Yazıbaşı-Hortuna Iron Deposit

The Yazıbaşı-Hortuna deposit is located 25 km south-east of İzmir city.

Muscovite schist, chlorite schist and recrystallized limestone of Permian age, diabase of Upper Cretaceous age and granodiorite intrusions of Eocene-Miocene age are exposed around the deposit (Durgun 1980).

The iron mineralisation is of the metasomatic type related to limestones and of vein-type within the faults in schists. In addition, disseminated sulphide mineralisation centres are also found within diabase. Iron mineralisation is composed of limonite, hematite and less amounts of magnetite and pyrite and secondary pyrrhotite. Quartz, calcite and amorphous silica are the gangue minerals. The presence of As, Pb, Zn and Cu suggests that the system was developed at a low temperature in the hydrothermal system (Durgun 1980).

The Yazıbaşı-Hortuna iron mineralisation has a 2.2 Mt reserve with 45% Fe, 17.6% Si and 1.7% As (Durgun 1980).

5.5.2 Çavdar-Söke Iron Deposit

The Çavdar-Söke deposit located 31 km south-west of Aydın city. It is the most important iron deposit on the Menderes Massif.

Augen gneiss, quartzite, almandine-muscovite schist, quartz dykes; iron oxide-bearing opal breccia and iron mineralisation are exposed around the Çavdar-Söke deposit (Cihnioğlu et al. 1994).

Mineralisation within the schists and gneisses of the Menderes massif core is Fe- and U-rich and mainly hosted in muscovite schists. Considering the position and structure of mineralisation centres that are concordant with the schistosity fabrics, this deposit is classified as a sedimentary-type deposit (Durgun 1981; Nuhoğlu 1983) and is suggested to be a itabiritic type deposit that is a subgroup of the Taberg type (Nuhoğlu 1983).

Faults postdating mineralisation and metamorphism are mostly NE-SW trending dip-slip reverse faults. As a result of these faults, which caused fracturing and folding of ore levels, secondary ores were emplaced within fractures and cavities (Gümüş 1998).

The ore minerals are magnetite, hematite, maghemite, martite, pyrite and specularite, with secondary limonite and hematite. Gangue minerals are feldspar, muscovite, biotite, chlorite, quartz, garnet, tourmaline and zircon. The quartz content of the ore zone is especially high (Cihnioğlu et al. 1994; Gümüş 1998).

The reserve of Çavdar-Söke deposit is 13.5 Mt with a grade of 42.6–67.6% Fe, 22.1% SiO2 and 3% S (Durgun 1981).

5.5.3 Ayazmant Iron Deposit

The Ayazmant iron deposit is located 85 km southwest of Balıkesir city.

Permo-Carboniferous re-crystallized limestones are the oldest rocks exposed around the Ayazmant iron deposit. They are unconformably overlain by Triassic schists. Spilite and diabase of Upper Cretaceous age also outcrop in the region, and Eocene granitoids cut all these units (Kara 1984).

Skarnization and mineralisation are common at the contacts of the granitoids and Permo-Carboniferous and Triassic rocks. Ore lenses and veins within the skarn zone are NE-SW extending and dip to the NW. These lenses have the length of 10–50 m and thickness of 3–5 m (Kara 1984).

The mineralogical compositions of the skarn zone are garnet, epidote, actinolite, tremolite, amphibole, wollastonite, diopside, scheelite, titanite, apatite, chlorite, feldspar, biotite, sericite, quartz and calcite. Magnetite is the main ore mineral of the deposit, which is partly altered to hematite. Magnetite is formed in the first stage of skarn alteration and in the following stages of retrograde hydrothermal process, sulphide- bearing ore minerals were re-crystallized. Chalcopyrite, pyrrhotite, pyrite, digenite, marcasite, bornite, mackinawite, molybdenite, linneite, bismuthinite, bismuth sulphide, sphalerite, galena, altaite, cubanite and valleriite are the main sulphide minerals. In addition, native gold was also rarely detected (Kara 1984).

The Ayazmant deposits hosts a 5.8 Mt reserve with 46% Fe, 16.8% SiO2, 1.1% S and 0.6% Cu (Kara 1984).

5.5.4 Şamlı Iron Deposit

The Şamlı iron deposit is located 25 km north of Balıkesir city.

Metamafic rocks of spilitic composition, crystallized limestones, metasandstones of Triassic Karakaya formation with ore and skarn occurrences associated with the lower Miocene-aged (Leo and Genç 1970) Şamlı granitoid are exposed around the Şamlı iron deposit. All these units are unconformably overlain by volcano-sedimentary Miocene-Pliocene deposits and Upper Pliocene basalt.

The mineralisation occurs in the skarn zone at the contact between the Şamlı granitoid with metaclastic and metamafic rocks of the Karakaya formation. The skarn zone and iron mineralisation are east-west trending.

Magnetite and less abundant hematite are the principal iron ore minerals, with pyrite and chalcopyrite as the sulphide minerals. In the skarn-type mineralisation, garnet and pyroxene as the products of prograde stage are found in the vicinity of iron mineralisation. Epidote, calcite, quartz, chlorite, albite, actinolite and tremolite of the retrograde stage overprint garnets and pyroxenes (Çolakoğlu and Murakami 2004).

According to Yılmazer et al. (2014), mineralisation is a skarn and IOCG type deposit associated with hydrothermal fluids derived from the Şamlı pluton, which includes the phases of both felsic and mafic composition.

The Şamlı deposit hosts 1.6 Mt reserve with 47.66% Fe (Leo and Genç 1970).

5.5.5 Büyük Eymir Iron Deposit

The Büyük Eymir iron deposit is located 55 km west of Balıkesir city.

Neogene volcanic rocks (porphyritic andesite, altered andesite, tuff and agglomerate and silicified andesite) unconformably overlying sedimentary units including mineralisation are exposed around the deposit (Kara 1995).

The sedimentary units belong to a lacustrine environment and contain levels of brecciated and massive hematite. The presence of leaves of the 'Aulnes' tree in this unit might indicate that both the ore and wall rocks (volcanics) are of Neogene age. The SW-NE trending ore zone has a width of 60–300 m, length of 1300 m and thickness of 6–23 m (Kara 1995).

The massive ore is concentric–crusted, reniform and botryoidal textured. The ore is composed of fine- grained hematite and lesser amount of goethite with a mostly porous, spongy appearance. The ore contains partly martitized magnetite and ilmenite that has been altered to rutile and anatase. The Büyük Eymir iron deposit also includes intensely argillized and silicified volcanic rock fragments of various size. Dacite and liparite are the main components of these rock breccias. These breccias that are filled by hematite form a brecciated-type ore.

The reserve of Büyük Eymir iron deposit is 6 Mt with a grade of 32–57% Fe (Kara 1995).

5.6 Other Regions

The Çataktepe, Domuzbayırı-Dereköy (Kırklareli), Çamdağ-Ferizli (Sakarya), Çambaşı (Ordu), Kotana-Dereli (Giresun), Kartiba-Fındıklı (Rize), Avnik-Genç (Bingöl) and Çelikhan (Adıyaman) deposits can be included with the other deposits except for the regions mentioned above. Iron deposits in Osmaniye-İskenderun region may also be included with this group.

The Bingöl-Genç-Avnik deposit is the most important. Although this deposit has a significant reserve, it needs advanced technological processing due to its high phosphate impurity. In addition to this deposit, the Sakarya-Çamdağ carbonaceous-silicified iron ore deposit also requires specialized industrial processing.

5.6.1 Çataktepe-Domuzbayırı and Göltepe-Balaban Iron Deposits

The Çataktape-Domuzbayırı and the Göltepe-Balaban deposits are 20 km and 40 km northeast, respectively, of Kırklareli city.

Triassic-Jurassic metasandstone-limestone and late Cretaceous diorite-granodiorite-granite intrusions are present in the vicinity of the mineralisation centres. Skarn occurrences and mineralisation are found at the contact between these intrusions and the limestones. Volcano-sedimentary type ore systems also occurred in metasandstone-limestone units (Fig. 5.12).

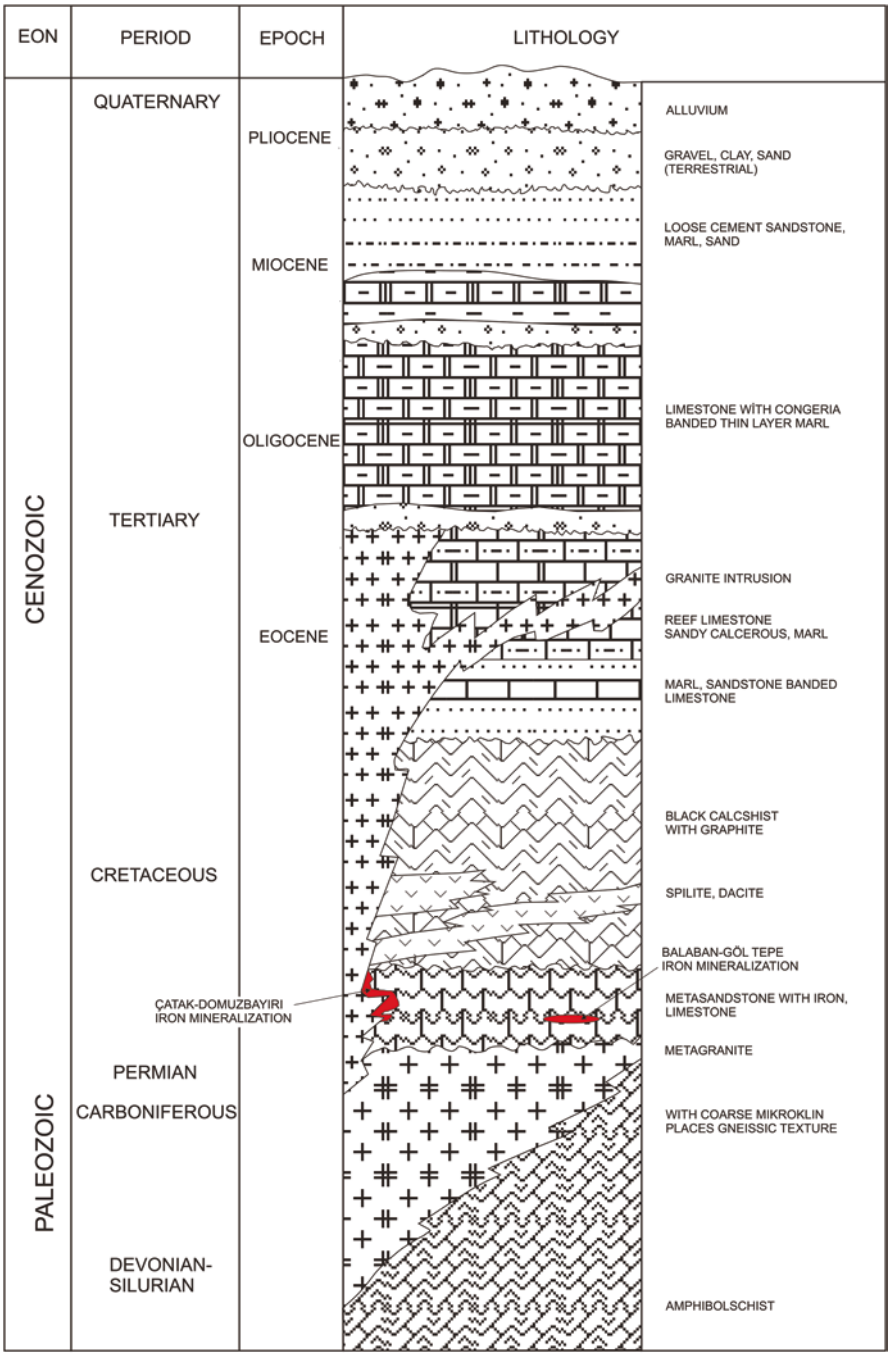

Fig. 5.12 Stratigraphic column showing the position of Istranca massif iron deposits. (Modified from Atılgan and Bakanyıldız 1977)

The Çataktepe-Domuzbayırı mineralisation is represented by skarns at the contact between the Demirköy granitoid and limestone-calcschists. These skarn zones, which are composed of garnet- epidote hornfels and silicified zones, are accompanied by an intensely silicified, pyrite-chalcopyrite- pyrrhotite-rich dykes. In the Çataktape-Domuzbayırı mineralisation, magnetite is the principal ore mineral and the alteration to hematite is also recorded as a result of martitization.

The Göltepe-Balaban mineralisation is composed of low-grade hematites that are disseminated within NW-SE extending metasandstones of Early Jurassic age. Post-depositional faults gave rise to an increase in grade and resulted in the formation of hematite-cemented brecciated mineralisation. According to Atılgan and Bakanyıldız (1977), the Balaban deposit is a volcano-sedimentary type.

The Çataktepe-Domuzbayırı deposit contains 420,000 tonnes of iron with an average grade of 34–55%. However, the reserve of the Göltepe-Balaban ore is 12.6 Mt with an average grade of 30%.

5.6.2 Çamdağ-Ferizli Iron Deposit

The Çamdağ-Ferizli iron mineralisation is located 30 km north-east of Sakarya city.

Arkose, greywacke, oolitic hematite, limestone and dolomitic limestone of Palaeozoic age, and unconformably overlying Triassic conglomeratic sandstones, oucrop around the Çamdağ iron ores. Upper Cretaceous and Cenozoic sedimentary rocks unconformably overlie all these units (Kipman 1974).

The ore occurs within lower-middle Devonian sandstones and limestones (Fig. 5.13). Oolitic mineralisation is carbonaceous at lower levels and silicified in the upper section. The nature of mineralisation, which is thought to be of marine origin, is characterized by physicochemical conditions of environment, wave movements, and morphologic structure of the seafloor. It is suggested that carbonaceous ore is deposited initially as siderite and hematite oolites in narrow straits and barriers on the seafloor topography whereas the overlying silicified ore is formed as a result of alteration of the carbonaceous ore (Kipman 1974; Kurt et al. 1976).

The carbonaceous ore contains a significant amount of hematite and some hydroxyl. The ore is composed of oolites with grain size of 0.01–1.5 mm of which core is made up by quartz, iron oxide, limestone or fossil fragments.

Hematite, followed by altered iron oxides, is predominant in the silicified ore. Clay and iron-chlorite provide the matrix for the hematite and iron oxide. Most of the iron minerals are in the oolitic structure. The centre of grains with length of 0.15–0.9 mm is represented by quartz, iron oxide and fossil fragments.

In the deposit, which covers an area of 281 km^2, the Fe content of carbonaceous ore is 13–23% and that of silicified ore is 35–40%. The reserve is estimated as 1.5 Bt.

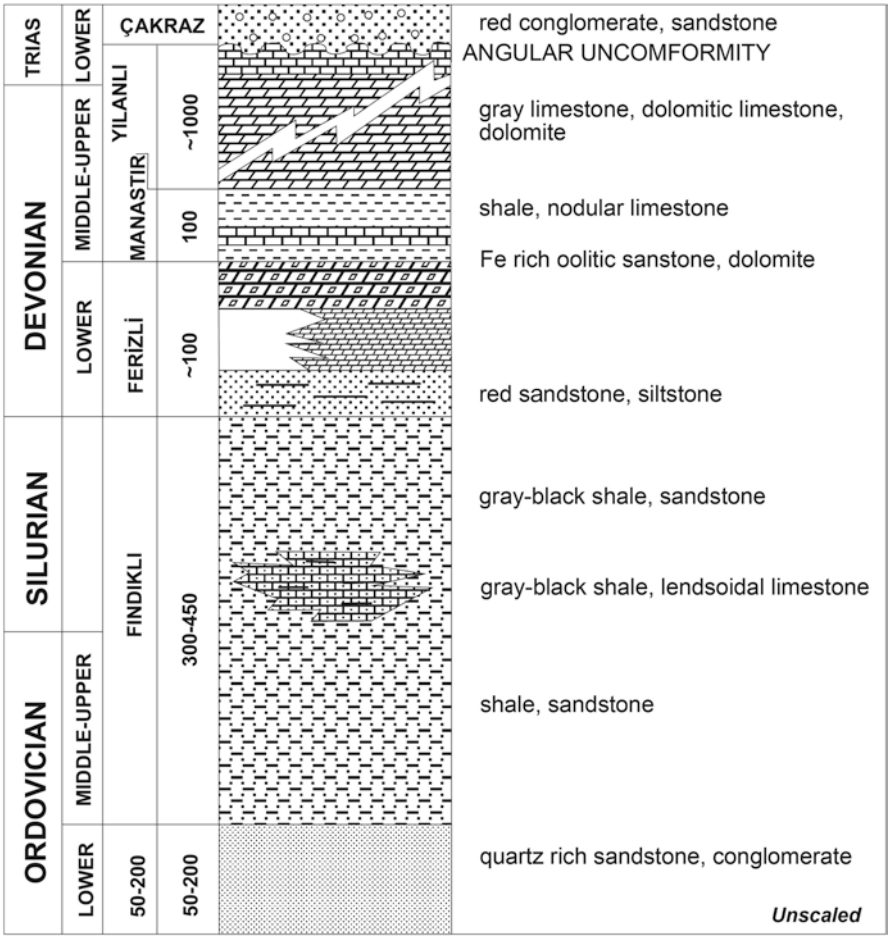

Fig. 5.13 Generalised stratigraphic section of Paleozoic units in the Çamdağ region. (Modified from Gedik and Önalan 2001)

5.6.3 Çambaşı Iron Deposit

The Çambaşı iron deposit is located 40 km south-east of Ordu city.

Upper Cretaceous andesite, recrystallized limestone, lavas and pyroclastics of mafic composition comprise the volcano-sedimentary sequence which crops out in the area. Monzonitic intrusions of Upper Cretaceous-Paleocene or younger age intrude these volcano-sedimentary unit around the Çambaşı iron deposit.

The mineralisation in the region occurs within marbles and trachyandesite in association with skarns, which are described as exoskarn. These zones are composed of two basic parts; garnet and pyroxene skarns. Mineral composition of skarns is composed mostly of garnet, pyroxene, epidote, actinolite, chlorite, plagio-

clase, sericite, quartz and calcite. Titanite and opaque minerals are the accessory minerals (Cihnioğlu et al. 1994; Saraç and Van 2005).

The principal ore minerals of the deposit are magnetite and lesser hematite (Cihnioğlu et al. 1994; Saraç and Van 2005).

The mineralisation has a length of 120 m and thickness of 5 m (Cihnioğlu et al. 1994).

The Çambaşı iron deposit hosts a reserve of 750,000 tonnes with 31–43% Fe and 8–43% SiO2.

5.6.4 Kotana-Dereli Iron Deposit

The Kotana-Dereli iron deposit is located 28 km south of Giresun city.

Pre-Liassic metamorphic rocks comprise marble interlayered schists, Jurassic-Lower Cretaceous volcano-sedimentary units; and aLate Cretaceous-Eocene Aksu granitoid complex, consisting of granite, granodiorite and quartz-diorite (Moore et al. 1980; Yılmaz and Boztuğ 1996; Saraç 2003), occur around the Kotana-Dereli iron deposit.

The ore generally occurs at skarn zones that are developed between the metamorphic rocks and the granitoid complex. The hornfelsic rocks are mostly green coloured and contain clinopyroxene, garnet and calcite. Skarn minerals in the exoskarn zone are garnet, clinopyroxene, calcite, epidote, actinolite, quartz and chlorite.

Magnetite, hematite, ilmenite, chalcopyrite, pyrrhotite and trace pyrite are the ore minerals (Cihnioğlu et al. 1994; Saraç and Van 2005; Çiftçi 2011).

The reserve of Kotana-Dereli iron deposit is 360,000 tonnes with 48% Fe and 10% SiO2 (Topaloğlu 1978).

5.6.5 Kartiba-Fındıklı Iron Deposit

The Kartiba-Fındıklı Fe deposit is located 65 km northeast of Rize city.

Around the deposit, Upper Cretaceous sandstone, red limestone and a volcano-sedimentary unit consisting of pyroclastic rocks of felsic-mafic composition are cut by Paleocene-aged granitoids with different textural characteristics. The mineralisation is developed at the contacts between these rocks.

The iron ore occurs within skarn zones at the contact between the granitoid and andesite. The skarn zone includes actinolite, epidote, quartz and garnet. Magnetite is the main ore mineral. Hematite and trace amounts of maghemite, due to alteration of magnetite, are also observed. Limonite and pyrite are also recorded (Türk 1980).

The iron ore is exposed at two different locations; Kartiba ridge and Fidanlık creek. The mineralisation on the Kartiba ridge has a length of 500 m and that in the

Fidanlık creek has a length of 400 m. The skarn zone, with a thickness of 1–5 m, is represented by massive and banded ore units of 1–5 m in thickness.

The Kartiba-Fındıklı deposit has a total of 3.6 Mt of iron with Fe content of 42.8–47.9% and SiO2 content of 22.9–26.7%.

5.6.6 Avnik-Genç Iron Deposit

The Avnik-Genç iron mineralisation is located 30 km south-east of Bingöl city.

Metavolcanics, gneiss, micaschist and marbles are exposed around the deposit. Metavolcanics with an age of 454 ± 13 Ma are the oldest rocks in the region (Helvacı and Griffin 1983; Yılmaz et al. 1981). Metavolcanics and metatuffites are thought to play an important role in the formation of these mineral deposits.

Mineralisation is observed in transition zones of gneisses and felsic metavolcanics-metatuffites and in alternations with these rocks. Structural characteristics of all the mineral occurrences are similar and consistent with the internal structure of the wall rocks. Due to the folded structure, the thickness of lenses is between 5 and 10 m and their depth is up to 300 m (Çelebi 1985). Ore lenses are massive, banded, disseminated and of stockwork type.

In the Avnik-Genç iron deposit, the principal ore minerals are magnetite and fluoroapatite, which are accompanied by rare martite and hematite. Titanite, rutile, spinel and ilmenite are also observed in trace amounts and quartz, actinolite, epidote and apatite are the gangue minerals.

The Avnik-Genç apatite-bearing magnetite deposit is classified as a metamorphosed magmatic type (Helvacı 1984a, b; Çelebi 1985). It is believed that the mineralisation is a product of the magmatic activity of 454 ± 13 Ma old (Helvacı 1984a) (Fig. 5.14). However, it also suggested that the deposit is a volcano-sedimentary occurrence (Erdoğan and Dora 1983) (Fig. 5.15). Considering the ore composition and trace element patterns, the Avnik iron deposit resembles the Kiruna-type (Sweden) apatite-bearing magnetite deposit (Helvacı 1984b; Çelebi 1985).

The Avnik-Genç iron deposit contains a 45 Mt reserve with Fe3O4 content of 41.2–82.7% and P2O5 content of 0.95–1.11%.

5.6.7 Çelikhan Iron Deposit

The Çelikhan iron deposit is located 30 km north-west of Adıyaman city.

Palaeozoic metamorphic rocks and unconformably overlying middle Eocene volcano-sedimentary units crop out in the vicinity of Çelikhan iron deposit. Permo-Carboniferous metamorphic rocks consisting of limestone and schists and the volcano-sedimentary units are in tectonic contact (Yazgan et al. 1987; Yazgan and Chessex 1991).

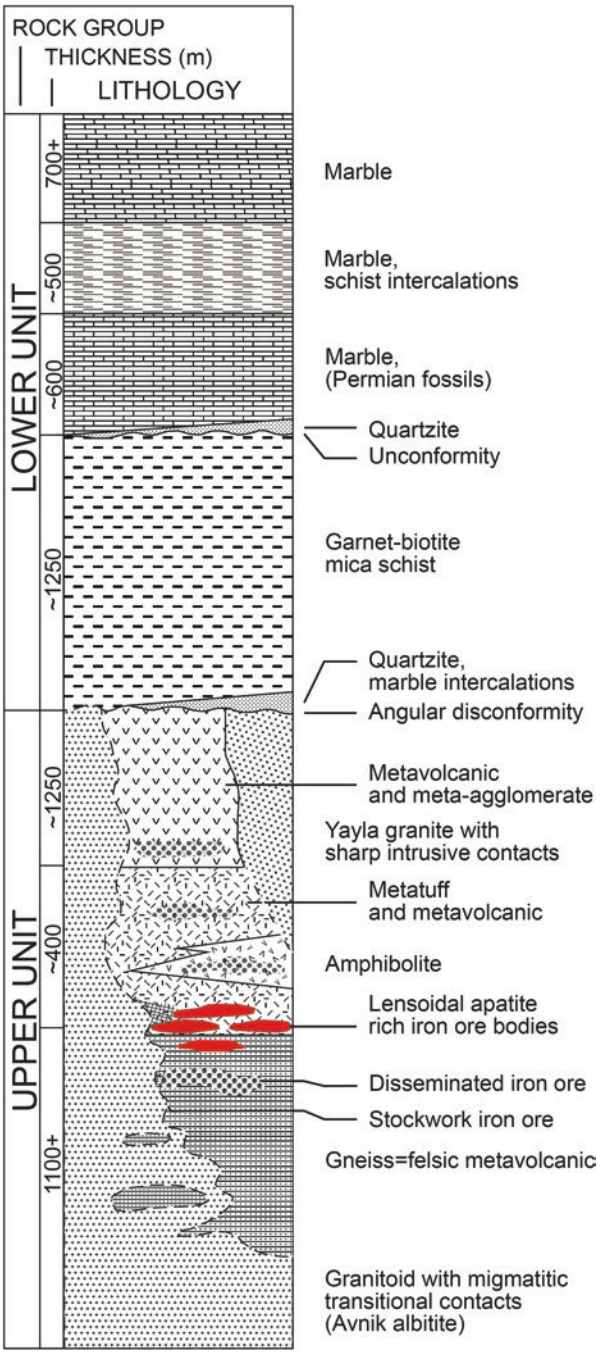

Fig. 5.14 Generalized stratigraphic section of the Avnik region. (Helvacı and Griffin 1983 modified from Erdoğan and Dora 1983)

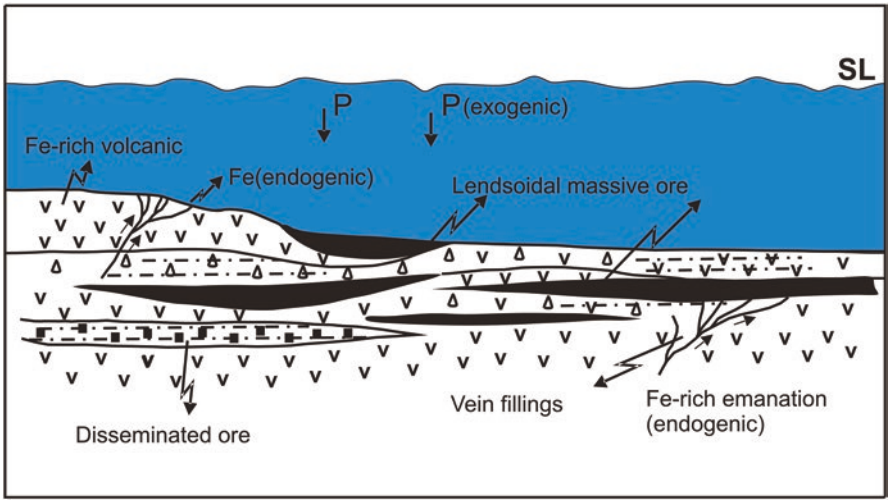

Fig. 5.15 Genetic model for apatite-bearing magnetite deposits in the Bitlis massif (Avnik). (Erdoğan and Dora 1983)

The iron ore occurs at the contact between Permo-Carboniferous marble and schist. The mineralisation is NS-trending, dipping to 25–35° W and displays 2.5 km length and 30–80 m width. The ore forms massive, banded and disseminated types along the marble-schist contact and alternating within the schists. The main ore minerals of the deposit are goethite, specularite, magnetite and hematite. Towards the bottom of the sequence, siderite joins this paragenesis. Ore minerals commonly contain interlocking apatite crystals (Tüfekçi et al. 1982).

The Çelikhan iron deposit hosts 70 Mt of iron with 28.56% Fe and 2.01% P2O5 (Büyükkıdık and Aras 1984; Çelebi et al. 2010).

5.6.8 Osmaniye-İskenderun Region

Several iron deposits in southern part of Turkey are lateritic or sedimentary deposits, which were formed by transportation and deposition of lateritic material. These occurrences observed between Osmaniye-İskenderun are clustered into three different areas; namely Fe-Ni laterites to the east of Osmaniye city, transported laterite-type sedimentary Fe occurrences to the northeast of Osmaniye city and lateritic Al-Fe occurrences between Iskenderun and Osmaniye.

In the region within the Amanos mountain chain, autochthonous Arabian platform rocks, ophiolite nappes and overlying post-tectonic deposits of neo-autochthonous character are exposed (Tekeli and Erendil 1984).

There are hematite-limonite and silica-carbonate zones just above the serpentinites in the vicinity of lateritic Fe-Ni occurrences to the east of Osmaniye. Fractures and cracks of serpentinites contain Ni- bearing clay and silicates. To the northeast

Table 5.2 Iron occurrences of the Osmaniye-İskenderun region

Occurrence	District	Wall rock	Ore mineral	Type	Grade	Reserve	References
Ağoluk	Osmaniye	Serpantinite	Hematite-limonite asbolan-garniyerit	Laterite	53,64% Fe	41,000 tons	Bahçeci and Güven (1978)
Yunt Mağarası	Osmaniye	Serpantinite	Hematite-limonite-asbolan	Laterite	34,74%	?	Bahçeci and Güven (1978)
Hızır Yaylası	Osmaniye	Claystone (?)	Chamosite-limonite	Sedimentary (transported laterite)	45,90%	?	Bahçeci et al. (1977)
Kızılyüce	Osmaniye	Serpantinite	Hematite-limonite	Sedimentary (transported laterite)	54,5–30% Fe	~62,000 tons	Bahçeci and Güven (1978)
Haruniye-Çatlu	Osmaniye	Limestone – Shale	Hematite-chamosite	Sedimentary (transported laterite)	%15–50	1 million tons	Bahçeci (1978)
Kastal	Hatay	Dolomitic limestone – sandstone	Limonite-hematite	Sedimentary	%15–35 Fe – % 9–12 Al_2O_3	2.9 million tons	Bahçeci (1978)

of Osmaniye, Fe mineralisation with the main ore minerals being hematite and chamosite is of sedimentary origin (clastic-chemical) and is found within Upper Cretaceous chloritic shales (Bahçeci 1978). Mineralisation between Iskenderun and Osmaniye is of iron-sandstone and iron-clayey sandstone. These sandstones were deposited in a detrital environment on the Upper Cretaceous limestones. Limonite and hematite are the main ore minerals (Bahçeci 1978). The worked and investigated iron occurrences of the region are summarized in Table 5.2.

5.7 Conclusions

In Turkey, when the distribution of iron mineral deposits are examined in terms of their iron content and metal production, the Divriği, Hekimhan and Saimbeyli-Feke basins attract most of the attention. The Divriği basin, hosts a large number of iron ore centres, located within the inner Taurides suture zone. The iron deposits in the basin are mainly found in serpentinite, limestone and along granite contacts. Ünlü (1989) suggests that the Fe mineral systems developed within the basin occurred as a result of the serpentinization of ultramafic and mafic rocks and subsequent changes caused by multiple hydrothermal phases. The Hekimhan Basin, located within the Tauride Mountains, consists of sedimentary and igneous rocks. Mesozoic dolomitic limestones and the ophiolitic rocks, which were emplaced during Late Cretaceous,

constitute the basement rocks (İzdar and Ünlü 1977). This basement is overlain by Upper Cretaceous volcano-sedimentary units and is cut by syenite intrusions. The iron mineralisation in the Hekimhan Basin is related to these volcano-sedimentary units and igneous intrusions. In this context, the iron mineral systems in the basin can be classified into two main groups, (I) iron mineralisation hosted in volcano-sedimentary units and (II) the iron mineralisation resulting from remobilization of ore in the first group by syenite intrusions. The iron ores in the Divriği and Hekimhan basins show genetic, spatial and temporal association. For this reason, the iron deposits in these basins should be considered together in future studies. Moreover, it should not be overlooked that the relationship between ophiolitic rocks and granitic rocks has great importance for exploration studies in the region. The Saimbeyli-Feke basin located in the western part of the Eastern Taurides differs from the Divriği and Hekimhan basins in terms of its geotectonic setting. The iron occurrences in the basin are mainly of three different types:

(I). The iron deposits are conformable with Lower Cambrian to Upper Devonian sedimentary units,

(II). The iron ores are within the tectonic structures developed during the Late Cretaceous to Eocene period (including the remobilization of the type I ores) and,

(III). The iron ores are related to karstification process developed during the Early Paleogene period. With the help of detailed stratigraphy, sedimentology and tectonic studies and a study of the origin of the Fe ore systems, will help to identify why we have different ores in the region. Other than the Taurides, another important iron province of Turkey is in western Anatolia. Despite the existence of different types of iron occurrences in the region, skarn type mineral systems are prevalent in terms of their metal content. These skarns are generally associated with the Paleogene magmatic rocks intruded into Triassic Karakaya Formation. Detailed studies of igneous intrusions during and after emplacement of the Karakaya formation will facilitate the discovery of new iron occurrences in the region. To sum up, although there are many different types of iron occurrences in Turkey, it is clear that high potential regions are clustered around ophiolitic and granitic rocks. Therefore, during the exploration for new iron deposits in Turkey, the geodynamic evolution and petrogenesis of ophiolitic belts and magmatic rocks should be examined thoroughly.

References

Akçakoca A, Kurt M (1974) Malatya-Hekimhan-Hasançelebi demir yatağının jeoloji raporu. [Geology report of Malatya-Hekimhan-Hasançelebi iron deposit]. General Directorate of Mineral Research and Exploration Report No: 6349. (in Turkish, unpublished)

Arda N, Tiringa D, Ateşçi B, Akça A, Tufan E (2008) Yahyalı (Kayseri)-Mansurlu (Feke-Adana) yöresi demir sahaları maden jeolojisi ara raporu. [Mining geology interim report of Yahyalı (Kayseri)-Mansurlu (Feke-Adana) region iron deposits]. General Directorate of Mineral Research and Exploration Report No: 44437. (in Turkish, unpublished)

Atılgan A, Bakanyıldız M (1977) Kırklareli Demirköy Dereköy demir zuhurları ön raporu. [Preliminary report of Kırklareli Demirköy Dereköy iron occurrences]. General Directorate of Mineral Research and Exploration Report No: 3838. (in Turkish, unpublished)

Bahçeci A (1978) Hatay-Kırıkhan-Kastal Demir Madeni Jeoloji Ön Raporu. [Preliminary geology report of Hatay-Kırıkhan-Kastal iron mine]. General Directorate of Mineral Research and Exploration Report No: 6693. (in Turkish, unpublished)

Bahçeci A, Güven E (1978) Adana-Osmaniye-Yarpuz Yuntmağara ve Kızılyüce demir zuhurları jeoloji raporu. [Geology report of Adana-Osmaniye-Yarpuz Yuntmağara and Kızılyüce iron occurrences]. General Directorate of Mineral Research and Exploration Report No: 6146. (in Turkish, unpublished)

Bahçeci A, Türkoğlu E, Güven E (1977) Adana-Osmaniye-Yarpuz-Ağoluk demir zuhuru rezerv safhası jeoloji raporu. [Reserve phase geology report of Adana-Osmaniye-Yarpuz-Ağoluk iron ocurrences]. General Directorate of Mineral Research and Exploration Report No: 5984. (in Turkish, unpublished)

Boroviczeny F (1964a) 200/240 no.lu ruhsat sahasının Kesikköprü yakınındaki demir yatağı hakkındaki rapor. [Report on the iron deposit near Kesikköprü on 200/240 License]. General Directorate of Mineral Research and Exploration Report No: 3481. (in Turkish, unpublished)

Boroviczeny F (1964b) 200/212 no.lu ruhsat sahasında yapılan jeolojik etütler hakkında sunulan rapor. [Report on the geological study on 200/212 License]. General Directorate of Mineral Research and Exploration Report No: 3570. (in Turkish, unpublished)

Boroviczeny F (1964c) Kesikköprü yakınındaki 200/240 no.lu ruhsat sahasında yapılan jeolojik etütler hakkında rapor. [Report on the iron deposit near Kesikköprü on 200/240 License]. General Directorate of Mineral Research and Exploration Report No: 3591. (in Turkish, unpublished)

Boroviczeny F (1964d) 200/248 no.lu ruhsat sahasında yapılan jeolojik etütler hakkında sunulan rapor. [Report on the geological study on 200/248 License]. General Directorate of Mineral Research and Exploration Report No: 3584. (in Turkish, unpublished)

Büyükkıdık H, Aras A (1984) Adıyaman-Çelikhan-Pınarbaşı apatitli demir madeni jeoloji raporu. [Adiyaman-Çelikhan Pınarbaşı apatite iron mine geology report]. General Directorate of Mineral Research and Exploration Report No: 1803. (in Turkish, unpublished)

Çağatay A, Arda O (1976) Yozgat-Sarıkaya manganezli demir yatağının mineralojik etüdü. [Mineralogical study of Yozgat-Sarıkaya manganese iron deposit]. Bull Min Res Exp 86:113–126 (in Turkish)

Çelebi H (1985) Die Genese der Magnetit-Apatit Lagerstätte Avnik, Provinz Bingöl/Türkei und ihre wirt schafts geologische Bewertung. PhD Thesis, p 214 Berlin (unpublished)

Çelebi H, Helvacı C, Uçurum A (2010) Pınarbaşı (Adıyaman) apatitli manyetit yatağının jeolojisi, jeokimyasal özellikleri ve ekonomik potansiyeli. [Geology, geochemical features and economic potential of apatite- magnetite deposit on Pınarbaşı (Adıyaman)]. Bull Min Res Exp 141:29–53 (in Turkish with English abstract)

Çiftçi E (2011) Sphalerite associated with pyrrhotite-chalcopyrite ore occurring in the Kotana Fe-skarn deposit (Giresun, NE Turkey): exsolution or replacement. Turk J Earth Sci 20:307–320

Çiftçi D, Ünlü T, Sönmez İ (1996) Discussion on the origin of Otlukilise iron deposit (Gürün-Sivas). Bull Min Res Exp 118:25–50

Cihnioğlu M, Isbasarir O, Ceyhan U, Adigüzel O (1994) Demir Envanteri. [Iron inventory of Turkey]. General Directorate of Mineral Research and Exploration 367 p. (in Turkish, unpublished)

Çolakoğlu AR, Murakami H (2004) Karakaya kompleks zonu içinde gözlenen şamlı ve ayazmant (Balıkesir) Fe skarn yataklarının jeolojisi, parajenezi ve oluşumu, Batı Anadolu. [Geology, paragenesis and genesis of Şamlı and Ayazmant iron skarn deposits on Karakaya coplex zone, Western Anatolia]. 57th Geological Congress of Turkey Abstract Book

Dağlıoğlu C, Arda N (2000) Koruyeri (Mağarabeli) ile Kovalı ve Mustafabeyli (TDÇİ Gen. Müdürlüğüne ait) demir sahalarının jeoloji raporu. [Geology Report of Koruyeri (Mağarabeli) and Kovalı and Mustafabeyli iron deposits]. Mineral Research and Exploration Report No: 2891. (in Turkish, unpublished)

Dayan S (2007) Adana-Mansurlu Attepe civarındaki demir yataklarının jeolojik, petrografik ve yapısal özelliklerinin incelenmesi. [Geological, petrographic and structural investigation of iron deposits in the region of Mansurlu, Attepe-Adana]. Master Thesis, Ankara University 125 p, Ankara (In Turkish, unpublished)

Dayan S, Ünlü T, Sayılı İS (2008) Adana-Mansurlu Attepe Demir Yatağı'nın maden jeolojisi. [Mining geology of Attepe Iron Deposit, Mansurlu-Adana]. J Geol Eng 32(2):1–44 (in Turkish with English abstract)

Doğan B, Ünlü T, Sayılı İS (1998) Kesikköprü (Bala–Ankara) demir yatağının kökenine bir yaklaşım. [An approach to the origin of iron deposits of Kesikköprü (Bala-Ankara)]. Bull Min Res Exp 120:1–33 (in Turkish with English abstract)

Durgun H (1977) Yozgat-Sarıkaya demir zuhurları istikşaf sahası raporu. [Report on preliminary study of Yozgat-Sarikaya iron occurrences]. Mineral Research and Exploration Report No: 6348. (in Turkish, unpublished)

Durgun H (1980) İzmir-Torbalı-Yazıbaşı köyü demir zuhurları raporu. [Report on iron occurrences of İzmir-Torbalı-Yazıbaşı village]. Mineral Research and Exploration Report No: 7157. (in Turkish, unpublished)

Durgun H (1981) Aydın-Söke-Çavdar demir madeni jeoloji raporu. [Geology report of Aydın-Söke-Çavdar iron deposit]. Mineral Research and Exploration Report No: 6983. (in Turkish, unpublished)

Erdoğan B, Dora OÖ (1983) Geology and genesis of the apatite-bearing iron deposits of the Bitlis Massif. Bull Geol Soc Turk 26:133–144 (in Turkish with English abstract)

Gedik I, Önalan M (2001) Çamdağ (Sakarya İli) Paleozoyik Stratigrafisine Ait Yeni Gözlemler. [New observations on the Paleozoic stratigraphy of Çamdağ (Sakarya Province)]. Istanbul Univ Earth Sci 14:61–76 (in Turkish with English abstract)

Gülibrahimoğlu İ (1979) Sivas-Gürün–Otlukilise demir yatağının jeolojisi ve sondajları. [Geology and drilling of Sivas-Gürün-Otlukilise iron deposit]. Mineral Research and Exploration Report No: 6613. (in Turkish, unpublished)

Gümüş A (1963) Iron ore deposits of Turkey. Symposium On Iron Ore in Esphahan, Iran, Cento Publication, 61–80

Gümüş A (1998) İç olaylara bağlı maden yatakları. [Mineral deposits formed by internal processes]. Bilim Ofset Press, İzmir, p 481

Gürer ÖF (1992) Hekimhan-Hasançelebi (Malatya) dolayının jeolojik incelemesi. [Geological review around Hekimhan-Hasançelebi (Malatya)]. PhD Thesis, Istanbul University. p 323. (in Turkish, unpublished)

Gürsu S, Göncüoğlu MC (2005) Early Cambrian back-arc volcanism in the western Taurides, Turkey: implications for rifting along the northern Gondwanan margin. Geol Mag 142(05):617–631

Helvacı C (1984a) Apatite-rich iron deposits of the Avnik (Bingöl) Region, Southeastern Turkey. Econ Geol 79(2):354–371

Helvacı C (1984b) Bitlis Masifi Avnik (Bingöl) yöresindeki zengin demir yataklarının oluşumu. [Genesis of the apatite-rich iron ore deposits, Avnik (Bingöl) region, Bitlis Massif, Turkey]. J Geol Eng 19:33–51 (in Turkish with English abstract)

Helvacı C, Griffin WL (1983) Metamorphic feldspathization of metavolcanics and granitoids, Avnik area, Turkey. Contrib Mineral Petrol 83(3–4):309–319

İzdar KE, Ünlü T (1977) Hekimhan – Hasançelebi – Kuluncak bölgesinin jeolojisi [The geology of Hekimhan –Hasançelebi – Kuluncak Region]. VI. Colloquim of Geology of the Aegean Region, 303–330

Işık MA (2002) Divriği kontakt metazomatik demir cevherleşmelerindeki ilmenit manyetit eksolusyon dokularının cevher oluşum koşullarının belirleme açısından önemleri. [The exsolution textures of ilmenite and magnetite in the contact metasomatic iron ores of the Divriği and their importance for aspect of identification of mineralization conditions]. 55th Geological Congress of Turkey Abstract Book. pp 124–125. (unpublished)

Kara A (1995) Çanakkale, Ezine manyetit ön etüt raporu. [Preliminary study report of magnetite on Çanakkale, Ezine]. Mineral Research and Exploration Report No: 1068. (in Turkish, unpublished)

Kara A (1984) Balıkesir-Ayvalık-Ayazmant demir madeni jeolojisi ve rezerv tahmini. [Geology and reserve estimation of Balıkesir–Ayvalık–Ayazmant iron mine]. General Directorate of Mineral Research and Exploration Report No: 7618 (in Turkish, unpublished)

Kara AS, Seyhan Z, Öztürk K, Yılmaz K, Altındaş N, Dağabak Y, Sönmez B, Dinç Y, Kartal Y, Açıkgöz T (2005) Türkiye ve Erdemir Maden'in sahip olduğu demir yataklarının değerlendirilmesi. [The evaluation of iron deposits owned by Turkey and Erdemir Mines]. Study Report No: p 193. (in Turkish, unpublished)

Karakaya AO (2011) Sivas-Kangal-Çetinkaya-Pınargözü Demir Yatağının Jeolojisi ve Jeokimyası. [Geology and geochemistry of Sivas-Kangal-Çetinkaya-Pınargözü iron deposits]. Master Thesis, Hacettepe University. p 69. Ankara (unpublished)

Keskinler SY, Avgan M, Dumanlılar Ö, Karakaya AO, Turunç O (2010) Karahalka (Pınarbaşı-Kayseri) Fe yatağının jeolojisi. [Geology of Karahalka (Pınarbaşı- Kayseri) iron deposit]. 63th Geological Congress of Turkey Abstract Book. pp 358–359. (in Turkish with English abstract)

Kipman E (1974) Sakarya Çamdağ (Kestanepınar-Yassıgeçit köyleri arası) deniz çökeltisi demir cevherinin jeolojisi. [Geology of sedimentary iron ore on Sakarya Çamdağ (between Kestanepınar-Yassıgeçit villages)]. İstanbul Univ Sci Fac Monogr 25:1–72 (in Turkish with English abstract)

Koşal C (1971) Divriği A-B-kafa demir yataklarının sondajlı aramalar jeolojik raporu. [Mineral prospection geological report of Divriği A-B-kafa iron deposit]. General Directorate of Mineral Research and Exploration Report No: 4304. (in Turkish, unpublished)

Koşal C (1973) Divriği ABC demir yataklarının jeolojisi ve oluşumu üzerine çalışmalar. [Studies on geology and formation of Divriği ABC iron deposits]. Bull Min Res Exp 81:1–22 (in Turkish with English abstract)

Kraeff A (1962) Kesikköprü konsesyonu. [Kesikköprü consultation]. Mineral Research and Exploration Report No: 3349. Turkish (unpublished)

Kurt M, Akkoca A, Başarı N, Maviş M, Sezen E, Yıldızeli N (1976) Sakarya-Karasu-Çamdağ çökel demir zuhurları istikşaf safhası jeoloji ön raporu. [Preliminary geology report of reconnaissance phase Sakarya-Karasu-Çamdağ sedimentary iron occurrences]. Mineral Research and Exploration Report No: 1598. Turkish (unpublished)

Kuşçu İ, Gençalioğlu Kuşçu G, Göncüoğlu MC (2001) Karamadazı demir zonlarında skarn zonlanması ve mineralojisi. [Skarn mineralogy and zoning patterns of Karamadazi (Yahyali-Kayseri) iron deposit]. Geol Bull Turkey 44(3):1–14 (in Turkish with English abstract)

Kuşçu İ, Yılmazer E, Demirela G (2002) Sivas-Divriği Bölgesi skarn tipi demir oksit yataklarına fe-oksit-cu-au (Olympic Dam tipi) perspektifinden yeni bir bakış. [A new Fe-Oxide-Cu-Au (Olympic Dam type) perspective to skarn type iron oxide in Sivas-Divriği Region]. Geol Bull Turkey 45(2):33–47 (in Turkish with English abstract)

Kuşçu İ, Marschik R, Kaymakçı N, Yılmazer E, Demirela G, Gökçe H, Güleç N (2005a) Hasançelebi ve Karakuz (Malatya) demiroksit yataklarındaki alterasyonların kökeni: tuzlu evaporitik sularla yıkanma modeline karşı magmatik-hidrotermal model. [Genesis of the alterations zones in iron oxide deposits of Hasançelebi and Karakuz (Malatya): leaching by brines versus magmatic-hydrothermal models]. 58th Geological Congress of Turkey Abstract Book. pp 75–77. (in Turkish with English abstract)

Kuşçu İ, Yılmazer E, Demirela G, Gökçe H (2005b) Orta ve Batı Anadolu'daki bazı skarn tipi Fe oksit yataklarının Fe-oksit-cu-au (doba) potansiyeli. [Fe-oxide-Cu-Au (IOCG) potential of some skarn type iron-oxide deposits in Central and Western Anatolia] In: Öztürk H, Kahriman A, Hanilçi N (eds) Symposium on Turkey's iron deposits geology, mining and existing problems Abstract Book 181–206 (in Turkish with English abstract)

Kuşçu İ, Gençalioğlu Kusçu G, Tosdal RM, Ulrich TD, Friedman R (2010) Magmatism in the southeastern Anatolian orogenic belt: transition from arc to post-collisional setting in an evolving orogen. Geol Soc Sp Publ Lond 340(1):437–460

Leo G, Genç VM (1970) Balıkesir, Şamlı sahasının jeolojisi ve demir yatakları. [Geology and iron deposits of Balikesir, Şamlı site]. Mineral Research and Exploration Report No: 2891. (in Turkish, unpublished)

Moore WJ, Mc Kee EH, Akıncı ÖT (1980) Chemistry and chronology of plutonic rocks in the Pontide Mountains, Northern, Turkey. European Copper Deposits. pp 209–215

Nuhoğlu İ (1983) Çavdar-Demirtepe (Söke-Aydın) demir yatağının jenetik incelenmesi. [Genetic investigation of Çavdar-Demirtepe (Söke-Aydın) iron deposits]. PhD Thesis, Dokuz Eylül University. p 214. İzmir (unpublished)

Oygür V (1986) Karamadazı (Yahyalı-Kayseri) Kontak Metazomatik Manyetit Yatağının Jeolojisi ve Oluşumu. [Geology and formation of the Karamadazı (Yahyalı-Kayseri) contact metasomatic magnetite deposit]. J Geol Eng 27:1–9

Oygür V, Yurt MZ, Yurt F, Sarı U (1978) Kayseri-Yahyalı-Karamadazı ve Kovalı Demir Yataklarının Jeoloji Raporu. [Geological report on the Kayseri-Yahyalı-Karamadazı and Kovalı iron-ore deposits]. Mineral Research and Exploration Report No: 6609. (in Turkish, unpublished)

Özer T, Kuşçu AE (1982) Malatya–Hekimhan-Deveci Demir Madeni Jeoloji Raporu. [Geology report of Malatya-Hekimhan-Deveci iron deposit]. Mineral Research and Exploration Report. (in Turkish, unpublished)

Özgül N, Kozlu H (2002) Data on the stratigraphy and tectonics of the Kozan–Feke region (Eastern Taurides). TAPG Bull 14:1–36

Öztürk K, Öztürk M (1983) Ankara-Bâlâ-Yukarıtepeköy-Kartalkaya Demir Cevherleşmesi Jeoloji Etüt ve Arama Raporu. [Report geological research and exploration on Ankara-Bâlâ-Yukarıtepeköy-Kartalkaya iron mineralization]. Mineral Research and Exploration Report No: 7357. (in Turkish, unpublished)

Öztürk H, Kasapçı C, Cansu Z, Hanilçi N (2016) Geochemical characteristics of iron ore deposits in central eastern Turkey: an approach to their genesis. Int Geol Rev 58:1673–1690

Rajabi A, Canet C, Rastad E, Alfonso P (2015) Basin evolution and stratigraphic correlation of sedimentary-exhalative Zn-Pb deposits of the Early Cambrian Zarigan-Chahmir Basin, Central Iran. Ore Geol Rev 64:328–353

Saraç S (2003) Doğu Karadeniz Bölgesi demirli skarn yataklarının karşılaştırılmalı mineralojik ve jeokimyasal özellikleri [Comparative mineralogical and geochemical characteristics of Eastern Black Sea Region Scarn deposits]. PhD Thesis, Karadeniz Technical University. p 259. (in Turkish, unpublished)

Saraç S, Van A (2005) Çambaşı (Ordu) ve Dereli (Giresun) yörelerindeki skarn yataklarının karşılaştırılmalı kimyasal ve mineralojik özellikleri: Doğu Pontid Kuzey zonu (KD Türkiye). [Comparative mineralogical and chemical of Çambaşı (Ordu) and Dereli (Giresun) areas skarn deposits: Northern Zones of Eastern Black Sea (NE Turkey)]. J Geol Eng 29(2):27–44 (in Turkish with English abstract)

Sözen A (1970) Kesikköprü, Madentepe manyetit zuhuru hakkında rapor. [Report of Kesikköprü, Madentepe magnetite occurrences]. Mineral Research and Exploration Report No: 4212. (in Turkish, unpublished)

Stendal H, Ünlü T (1991) Rock geochemistry of an iron ore field in the Divriği region, Central Anatolia, Turkey. A new exploration model for iron ores in Turkey. J Geochem Explor 40:281–289

Stendal H, Ünlü T, Konnerup-Madsen J (1995) Geological setting of iron deposits of Hekimhan Province, Malatya, Central Anatolia, Turkey. Trans Inst Min Metall (Sect B Appl Earth Sci) 104:46–54 London

Tekeli O, Erendil M (1984) Kızıldağ ofiyolitinin jeolojisi ve petrolojisi. [Geology and petrology of Kızıldağ ophiolite]. Mineral Research and Exploration Report No: 7778. (in Turkish, unpublished)

Tiringa D (2016) Karaçat Demir Yatağı (Mansurlu Havzası, Adana) ve doğusunda yer alan demir yatakları ve zuhurlarının jeolojisi [Geology of the Karaçat iron deposit (Mansurlu Basin, Adana) and iron deposits and occurrences in its Eastern part]. PhD Thesis, Ankara University. p 283. (in Turkish, unpublished)

Tiringa D, Ünlü T, Sayılı İS (2009) Kayseri-Yahyalı-Karaköy, Karaçat Demir Yatağının Maden Jeolojisi. [Mining geology of Karaçat iron deposit in Kayseri-Yahyalı-Karaköy]. Master Thesis, Ankara University. p 139. Ankara (in Turkish, unpublished)

Tiringa D, Çelik Y, Ateşçi B, Akça İ, Keskin S (2011) Kayseri-Adana Havzası demir aramaları ve Menteş Dere (Yahyalı-Kayseri) ruhsat sahasının maden jeolojisi raporu. [Mining geology report of iron explorations in Kayseri-Adana Basin and Menteş Dere (Yahyalı-Kayseri) license area]. Mineral Research and Exploration Report No: 11435. (in Turkish, unpublished)

Tiringa D, Ünlü T, Gürsu S (2016) An approach to the origin of the Early Cambrian Karaçat iron deposit (Mansurlu Basin, Adana) and the iron deposits outcrops at its Eastern part. Bull Min Res Exp 152:121–141

Topaloğlu H (1978) Giresun-Dereli-Kurtulmuş köyü demir zuhuru jeoloji raporu. [Geology report of iron occurrence on Giresun-Dereli-Kurtulmuş villages]. Mineral Research and Exploration Report No: 6706. Turkish (unpublished)

Tüfekçi MŞ, Kadıoğlu H, Cengiz R (1982) Adıyaman Çelikhan Pınarbaşı Demir Madeni Jeoloji Raporu. [Geology report of Adıyaman Çelikhan Pınarbaşı iron deposit]. Mineral Research and Exploration Report No: 314. (in Turkish, unpublished)

Türk O (1980) Rize-Fındıklı-Kartiba yöresi demir zuhuruna ilişkin jeoloji raporu. [Geology report of iron occurrences on Rize-Fındıklı-Kartiba areas]. Mineral Research and Exploration Report No: 7008. (in Turkish, unpublished)

Uçurum A, Larson LT, Boztuğ D (1996) Geology, geochemistry, and petrology of the alkaline subvolcanic trachyte-hosted iron deposit in the Karakuz area, northwestern Hekimhan- Malatya, Turkey. Int Geol Rev 38(11):995–1005

Ünlü T (1983) Die Genese der Siderit – Lagerstätte Deveci in der Hekimhan – Provinz Malatya/Turkei und ihre wirthschaftliche Bewertung. PhD Thesis Berlin Technical University, (in German. unpublished) (The same work was originally published by the General Directorate of Turkish Iron and Steel Works at 1987 p 84 Ankara)

Ünlü T (1987) Maden yataklarının değerlendirilmesi yöntemine bir örnek: Deveci Siderit Yatağı [An example to the mineral deposits evaluation method: Deveci siderit deposit]. Süleyman Demirel Univ J Nat Appl Sci 2(2)

Ünlü T (1989) Türkiye demir yatakları arama çalışmalarında 1. Derecede ağırlıklı hedef saha seçimi ve maden jeolojisi araştırmaları ile ilgili proje teklifi. [Project proposal related to Turkey iron deposits exploration studies in the first degree target selection and mining geology research]. Mineral Research and Exploration Report No: 8593. (in Turkish, unpublished)

Ünlü T (1991) TDÇİ-Ankara Üniversitesi, Divriği çevresi Demir Aramalar Projesi. [Iron research project in Divriği surroundings, TDÇİ-Ankara University]. Mineral Research and Exploration Report No: 10139. Turkish (in Turkish, unpublished)

Ünlü T, Stendal H (1986) Divriği Bölgesi demir yataklarının element korelasyonu ve jeokimyası (Orta Anadolu–Türkiye) [Geochemistry and element correlation of iron deposits in the Divriği Region, Central Anatolia, Turkey]. J Geol Eng 28:5–19 (in Turkish with English abstract)

Ünlü T, Stendal H (1989) Divriği bölgesi demir cevheri yataklarının nadir toprak element (REE) jeokimyası; Orta Anadolu, Türkiye. [Rare Earth Element (REE) geochemistry from the iron ores of the Divriği Region, Central Anatolia, Turkey]. Geol Bull Turkey 32:21–37 (in Turkish)

Ünlü T, Yıldızeli N, Yıldırım A, Yurt Z, Adıgüzel O, Özcan H, Avcı N, Çubuk Y (1989) Divriği (Sivas) yöresi granitik kayaç-yan kayaç ilişkilerine yönelik jeoloji raporu. [Geological report on the relations between granitic rocks and wall rocks in Divriği (Sivas) Region]. Mineral Research and Exploration Report No: 8914. Turkish (in Turkish, unpublished)

Ünlü T, Stendal H, Makovicky E, Sayılı S (1995) Genesis of the Divriği iron ore deposit, Sivas, central Anatolia, Turkey: an ore microscopy study. Bull Min Res Exp 117:17–28

Yazgan E, Chessex R (1991) Geology and tectonic evolution of the southeastern Taurides in the region of Malatya. TAPG Bull 3(1):1–42

Yazgan E, Gültekin MC, Poyraz N, Sirel E, Yıldırım H (1987) Malatya güneydoğusunun jeolojisi ve Doğu Toroslar'ın jeodinamik evrimi. [Geology of South east of Malatya and geodynamic evolution of East Taurus]. Mineral Research and Exploration Report No: 2268. (in Turkish, unpublished)

Yıldırım A, Hamarat O (1984) Erzincan-Kemaliye-Bizmişen Demir Yatağı Jeoloji ve Rezerv Ön Raporu. [Geology and reserve preliminary report of Erzincan-Kemaliye-Bizmişen iron deposit]. Mineral Research and Exploration Report No: 223. (in Turkish, unpublished)

Yıldızeli N (1977) Divriği-Dumluca Sondajlı Etüd Raporu. [Drilling study report on Divriği-Dumluca]. Mineral Research and Exploration Report No: 5986. (in Turkish, unpublished)

Yıldızeli N (1983) Sivas Kangal Çetinkaya-Pınargözü Jeoloji ve Rezerv Raporu. [Geology and reserves report on Sivas Kangal Çetinkaya-Pınargözü] Mineral Research and Exploration Report No: 7452. (in Turkish, unpublished)

Yıldızeli N (1998) Divriği (GD Sivas) yöresinde ofiyolit-granitoyid ilişkisiyle gelişen fels tipi demir yatakları. [Fels type iron deposits formed by ophiolite-granitoid interaction in the Divriği Region, (SE Sivas), Turkey]. In: Proceedings Book Boztuğ D, Özer T and Otlu N (eds). pp 130–138. (in Turkish with English abstract)

Yilmaz S, Boztuğ D (1996) Space and time relations of three plutonic phases in the Eastern Pontides, Turkey. Int Geol Rev 38(10):935–956

Yılmaz H, Türkyılmaz B (1998) Malatya-Hekimhan-Karakuz Demir Yatağı Maden Jeolojisi Raporu. [Mining geology report on Malatya-Hekimhan-Karakuz iron deposits]. Mineral Research and Exploration Report No: 10242. Turkish (in Turkish, unpublished)

Yılmaz O, Michel R, Vialette Y, Bonhomme M (1981) Réinterprétation des Donner Isotopiques Rb-Sr Obtenues Sur les Métamorphites de la Partie Méridionale du Masif de Bitlis (Turquie). Bull Sci Géol Strasbourg 34:59–73

Yılmaz A, Bedi Y, Yusufoğlu H, Atabey E, Aydın N (1997) 1/100000 ölçekli açınsama nitelikli Türkiye Jeoloji Haritaları. [Geological Map of Turkey explanatory notes, 1/100000 scale]. MTA Publications, Elbistan (in Turkish, unpublished)

Yılmazer E, Kuşçu I, Demirela G (2003) Divriği AB Kafa Cevherlesmeleri: Alterasyon zonlanması ve zonlanma süreçleri. [A-B Kafa Mineralizations in Divriği: alteration zoning]. Geol Bull Turkey 46(1):17–34 (in Turkish with English abstract)

Yılmazer E, Güleç N, Kuşçu İ, Lentz DR (2014) Geology, geochemistry, and geochronology of Fe-oxide Cu (±Au) mineralization associated with Şamlı pluton, western Turkey. Ore Geol Rev 57:191–215

Zeck HP, Ünlü T (1987) Parallel whole rock isochrons from a composite monzonitic pluton, Alpine Belt, Central Anatolia, Turkey. N Jb Miner Mh H 5:193–204

Zeck HP, Ünlü T (1988) Alpine ophiolite obduction before 110 ± 5 Ma ago, Taurus Belt, Eastern Central Turkey. Tectonophysics 145(1):55–62

Chapter 6
Manganese Deposits of Turkey

Hüseyin Öztürk, Cem Kasapçı, and Fatih Özbaş

Abstract Turkey comprises different types of manganese deposits which were identified by the Mineral Research and Exploration Institute of Turkey (MTA) in 1965 (MTA. Manganese ore deposits of Turkey. General Directorate of Mineral Research and Exploration. Pub. No: 120, 38 p. (In Turkish), 1972). After many research works conducted on the formation and genesis of marine pollymetalic oxides that occur in the modern oceanic sediments, a new genetic classification of the marine ferromanganese manganese deposits was made by several workers (Frakes LA, Bolton BR. Geology 12:83–86, 1984; Rona 1992). Based on newly acquired knowledge, the manganese deposits of Turkey were divided into four main types according to host rocks, geological-tectonic settings and formation processes by Öztürk (Geol Eng 43:24–33. (In Turkish with English abstract), 1993a; Öztürk H. Ore Geol Rev 12:187–203, 1997; Öztürk H, Hein JR. Econ Geol 92:733–744, 1997). These types are (1) Black shale – hosted deposits, (2) Radiolarian chert – hosted deposits, (3) Oligocene – hosted deposits, (4) Volcanic arc – hosted and/or vein -type deposits. Although radiolarian chert – hosted type Mn oxides mineralization is widely distributed, they generally are small occurrences associated with ophiolitic mélanges but some of them may be of economic value. Economically important Mn deposits are in the black shale rocks in southwestern Turkey and in the Oligocene sediments in the Thrace Basin. The Oligocene deposits are connected to the Black Sea region deposits, including Varna (Bulgaria), Nikopol (Ukraine) and Chiatura (Georgia). Exploration studies by drilling programs have been made by MTA for the Oligocene – hosted Binkılıç deposit of the Thrace Basin (Bora E. Binkılıç ve Sefaalan Bölgesinin jeolojisi ve manganez yatakları. [The geology and Mn deposits of the Binkılıc¸ and Sefaalan area]. M.Sc. Thesis, Istanbul University, 47 p. (In Turkish, unpublished), 1969) and black shale – hosted Ulukent Mn deposit in Tavas region (Doğan H, Turkmen H. Ulukent – Tavas çevresindeki manganez yataklarının jeoloji Raporu. [Geological report of the manganese deposits of the

H. Öztürk (✉) · C. Kasapçı · F. Özbaş
Department of Geological Engineering, Avcilar Campus, İstanbul University-Cerrahpaşa, İstanbul, Turkey
e-mail: ozturkh@istanbul.edu.tr

F. Pirajno et al. (eds.), *Mineral Resources of Turkey*, Modern Approaches in Solid Earth Sciences 16, https://doi.org/10.1007/978-3-030-02950-0_6

Ulukent-Tavas and surrounding area]. General Directorate of Mineral Research and Exploration Report No: 345, 87 p. (In Turkish, Unpublished), 1983).

The representative manganese deposits or occurrences of each type are identified in this chapter on the basis of their age, host rocks, mineralogy, geochemistry and reserve – grade relationships. The distribution of the manganese mineral systems and the location of the important deposits in Turkey are shown in Fig. 6.1. The Mn ores of the main deposits were sampled and analyzed by ICP- MS at Acme laboratories in Canada, in 2015 exclusive for this chapter.

6.1 Introduction

Turkey is located in the Alpine – Himalayan orogenic belt and includes E-W trending manganese deposits that formed related to the evolution of Tethyan ocean. Most of deposits occur in a radiolarite-shale alternating deep sea sediments which have been subjected to broad mining activities. However, these occurrences or deposits occur as tectonic sheets or blocks in the accretionary complex of Cretaceous age and very rarely reach an economic grade. Only six deposits have been defined as economically viable among the more than 200 surveyed occurrences. Black shale – hosted manganese carbonate – silicate deposits also occur in passive margin sediments on the Taurus belt. A few hundred thousand tonnes of ore were extracted from these deposits, however, mining has stopped in these ore beds due to the

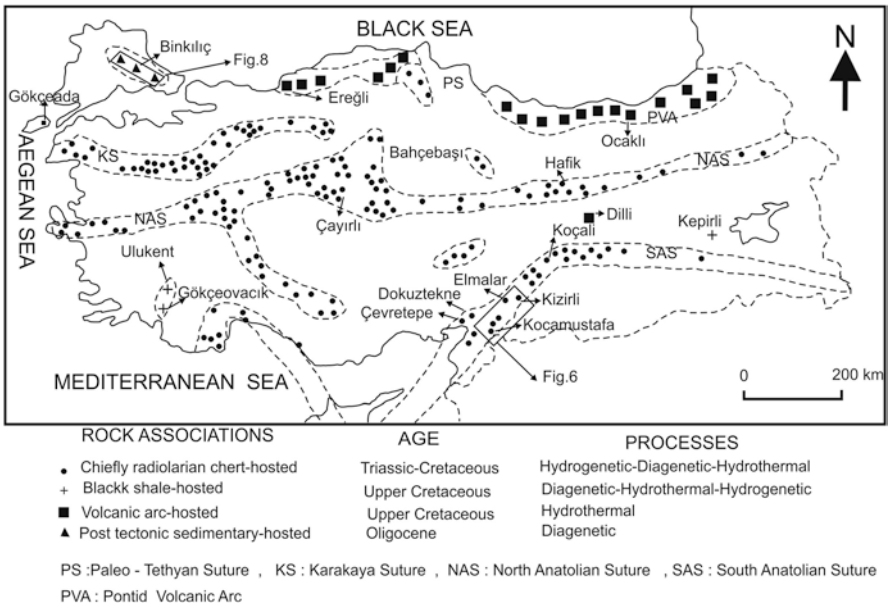

Fig. 6.1 Distribution and types of the manganese deposits in Turkey according to rock associations, ages and processes of formation. The map also shows the location of Figs. 6.6 and 6.8

increase in the stripping ratio. The licenses of these deposits belong to iron and steel factories of Turkey (Oyak Group) and the deposits have not been sufficiently investigated. In the Pontides, manganese ore deposits related to arc magmatism are seen along the Black Sea margin. A limited ore production was obtained from these hydrothermal veins and exported. Sedimentary manganese oxide beds of Oligocene age are located in the Thrace basin, NW Turkey where mining still continues. The geology, mineralogy and geochemistry of four types of manganese deposits are presented in this study.

6.2 Black Shale: Hosted Type Mn Deposits

Black shale-hosted Mn deposits are the most important in Turkey and annually 20,000 tonnes of ore are produced from the Ulukent deposit from 1980s to 2000s and a few hundred thousand tonnes of ore were obtained from the Gökçeovacık deposit from 1930 to 1950s.

6.2.1 Ulukent and Gökçeovacık Deposits

Black shale – hosted manganese deposits of Turkey are located in the western part of Tauride Mountains. The largest one of this type is the Ulukent deposit licensed to the Erdemir Mining Industry & Trade Inc.. Exploration studies of the Ulukent deposit have been carried out by MTA with a total of 54 drill holes (Doğan and Türkmen 1983). Kirmanlı and Nasuf (1998) made a reserve calculation for the Ulukent deposit using 42 drill hole data. According to the authors the Ulukent deposit includes a total of 6,922,714 tonnes of ore of which 3,428,303 tonnes are above the cut- off grade (32% Mn) whereas 3,494,411 tonnes of below this cut-off. Approximately 240,000 tonnes of ore with 25% grade has been mined form the Ulukent deposit with open pit method and sold to the Erdemir Iron and Steel factory. Owing to increased stripping ratio, mining was abandoned in 2001. The other important deposit of this type is Gökçeovacık deposit that occurs the south of the Ulukent deposit (Fig. 6.2).

The black shale – hosted manganese province of the western Anatolia has a large ore potential because of good outcrops of the both shale – carbonate rocks and associated mineralization which extend from the Ulukent to the Fethiye region (Kuşçu and Gedikoğlu 1989; Öztürk and Hein 1997). Despite large outcrops of the host carbonates, post mineralization tectonism has highly deformed and metamorphosed the ore zone associated with nappe emplacements in the Paleocene (Graciansky 1968) and also related to the extensional tectonism in the Miocene. Exploration and mining of these deposits reveal some difficulties owing to these multi stage tectonic deformations which resulted in modification of the original stratigraphic position and chemical mineralogical composition of the ore body.

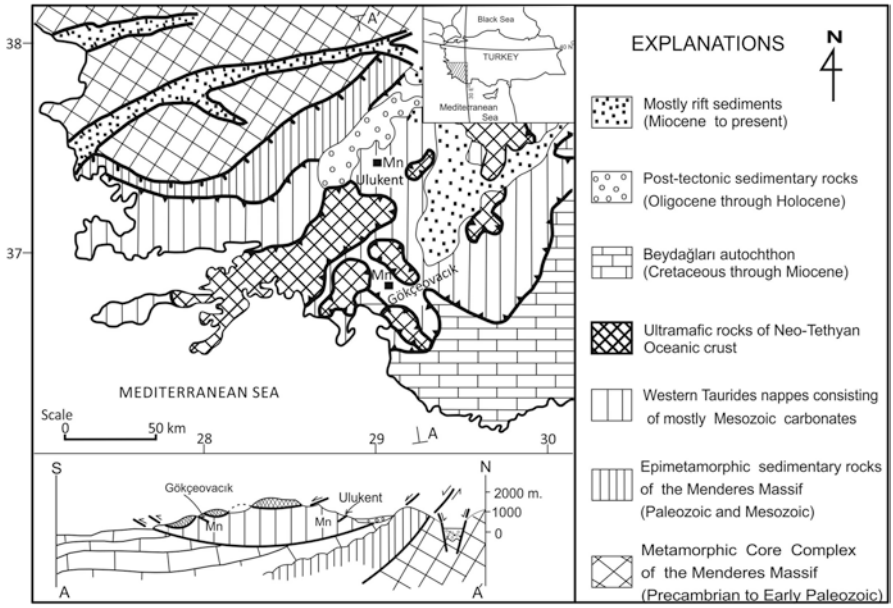

Fig. 6.2 Regional geologic map showing major tectonostratigraphic units of the western Taurides and locations of the Ulukent and Gökçeovacık Mn deposits. (Modified from Öztürk and Hein 1997)

The ore zone is situated between two shale units in the thick bedded passive margin carbonates (Fig. 6.3). Black bituminous shale at the base, includes coarse and cataclastic pyrites up to 15 mm in size. This black shale horizon also includes chalcedony – quartz veinlets. Gray colored shale does not include and large pyrites and silicification. The ore section begins with pisolitic – bauxitic low grade ore (detrital phase) at the bottom gradually passing to the carbonate – silicate ore and lastly oxidized ore. The brownish – pinkish bauxitic ore represents a sudden terrigenous input from the land into the sea associated with tectonic activity. This ore horizon mainly consists of anatase, diaspore, hausmannite, kutnohorite and hematite.

Silicate-oxide-carbonate is the most common ore type of the Ulukent Mn deposit and is composed of bustamite, tephroite, braunite, and hausmannite, the lesser amounts of jacobsite, kutnohorite, rhodocrosite, and Mn calcite. Gangue minerals include epidote, calcite, dolomite, quartz and stilpnomelane. Primary bedding planes within the ore can be seen in the both hand specimens and in polished sections. Silicate – oxide – carbonate ore shows very strong magnetism and XRD analyses indicated that the main magnetic mineral is hausmannite.

High-grade oxidized ore represents the supergene oxidation product of the silicate-oxide-carbonate ore, which locally caps the ore horizon with a thickness of up to 5 m. This high grade and porous ore shows a weak magnetism. This ore zone

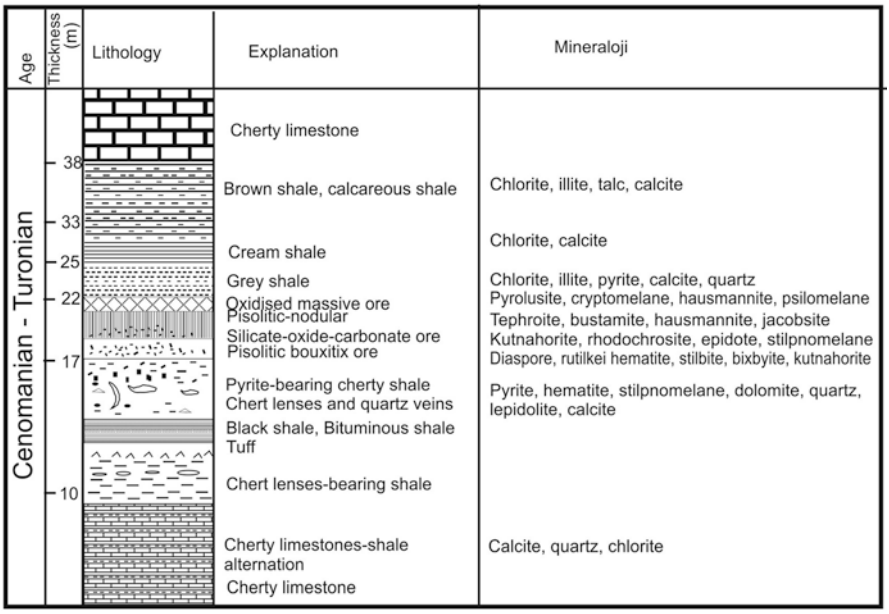

Fig. 6.3 Measured stratigraphic section of the Ulukent manganese deposit showing the main ore types, ore and gangue minerals

especially well developed along the fracture – fault zone that crosscuts the ore body and gained porosity due to alteration processes. This high quality ore zone consists of pyrolusite, psilomlane, limonite and lesser amounts of hausmannite and ranciete.

The Ulukent deposit displays some similarities and differences to well-known black shale – hosted Mn deposits, for example the Jurassic Urkut deposit in Hungary (Polgari et al. 1991), Molango deposit in Mexico (Okita 1992; Okita et al. 1988), and Taojiang deposit in China (Fan et al. 1992). The mean $\delta^{13}C$ and $\delta^{18}O$ values of eight ore samples which consisted of rhodoscrosite and kutnohorite are −12.2 and −4.5 per mil (PDB), respectively (Öztürk and Hein 1997). These values are so close to the Molango deposit of Mexico a world class black shale – hosted Mn deposits. $\delta^{13}C$ values of the Ulukent manganese deposit is lower than the Oligocene – hosted the Binkılıç manganese deposit whereas $\delta^{18}O$ values is higher. The C and O isotope systematics suggest a role of fresh water during the formation of the Binkılıç manganese deposit, whereas marine and more reducing conditions would have been more important during the formation of Ulukent manganese deposit (Fig. 6.4).

The black shale – hosted type Mn ore deposits are associated with anoxic basins with precipitation of primary mineral Mn carbonate silicate ore. Submarine volcanic activity may have been introduced the Mn into the sea water. A thin tuff unit at the bottom of the Ulukent manganese ore suggests such an activity. The primary

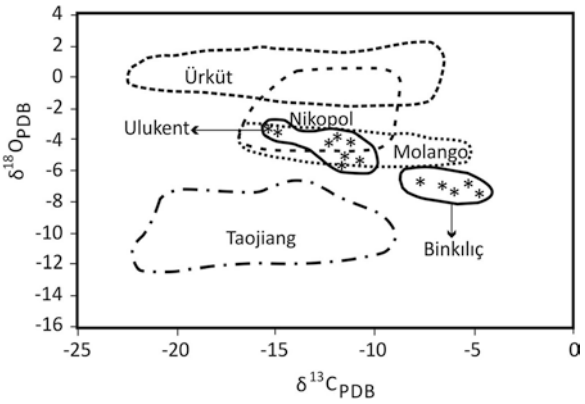

Fig. 6.4 Diagram of carbon vs oxygen isotopes of important Mn carbonate deposits of the world compared with the Ulukent and Binkılıç Mn deposit. (Data are from Oligocene Binkılıç (Öztürk and Frakes 1995); Cretaceous Ulukent (Öztürk and Hein 1997), Oligocene Nikopol, Ukraine (Hein and Bolton 1992), Jurassic Molango, Mexico (Okita 1992), Jurassic Urkut, Hungary (Polgari et al. 1991), Ordovician Taojiang, China (Fan et al. 1992))

carbonate silicate ore was buried and was subjected to greenschist facies metamorphism. The outcropping metamorphosed silicate and carbonate ore was then oxidized to the trivalent and tetravalent Mn oxides. The Ulukent manganese deposit is located close to the suture zone of nappe tectonism, Gökceovacık Mn deposit at the southern margin of the region was not significantly affected by metamorphism because of its lesser involvement in nappe tectonism (Öztürk and Hein 1997). Geological and mineralogical features of the Ulukent deposit indicate that the ore can be explored such as geophysical exploration by magnetic (magnetic hausmannite), gravity (due to gravity contrast with limestone) and electric methods (due to the bottom pyrites).

The Gökçeovacık manganese deposit represents the southward continuity of the Ulukent deposit because of the presence in a similar shale units of thick carbonates section (Fig. 6.2). This deposit is located the 70 km south of the Ulukent deposits. The ore body continues for 600 m on the surface with 1 m in thickness and was underground mined during the World War I. The ore was transported to the Göcek port by a wire line system 4 km long. Today the Gökçeovacık Mn ore zone is in a special protected area. The ore of the Gökçeovacık consists of two ore seams each about 0.4 m in thickness and the main ore mineral is braunite. Manganite, pyrolusite, hematite and chalcedony are minor. The bottom limestone is cherty, whereas limestone is at the top calciturbiditic, including fragmented algea fossils and lime clasts associated with oxygenation of the basin.

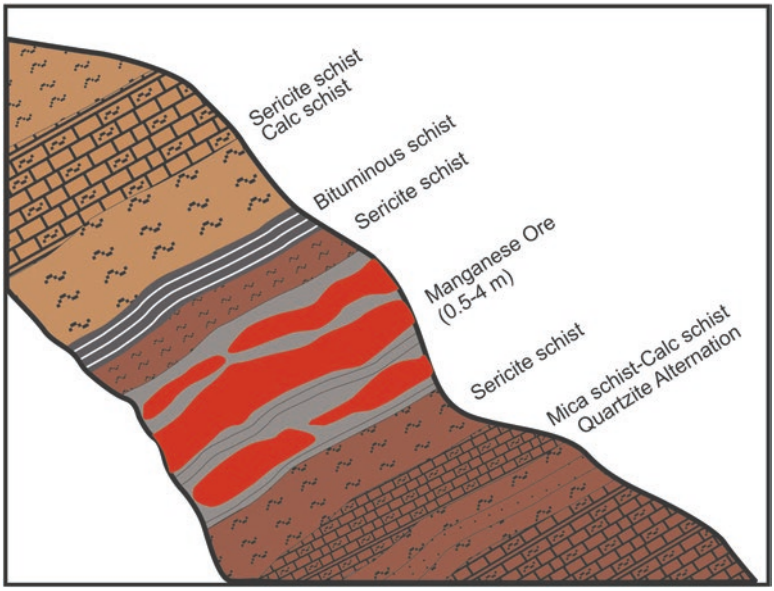

Fig. 6.5 Cross section (not-to-scale) showing the host rock relationships of the Kepirli manganese mineralization in the Bitlis metamorphic massif

6.2.2 The Kepirli Mn Mineralization

This mineralization is defined as a black shale – hosted deposit that occurs west of Kepirli Village (ancient name is Nurs) of the Hizan town of Bitlis city (Fig. 6.1). The ore body is hosted in the metapelitic rocks of the Bitlis Metamorphic Massifs in Eastern Anatolia (Fig. 6.5). The thickness of ore body varies between 0.5 and 4 m and extends for 350 m on the surface. A few thousand tonnes of ore has been mined with 30% average grade. Chemical composition of the ore body is characterized by high silica (7–25%) and iron (9–7, %). The chemical compositions of the Kepirli ore is shown in Table 6.1.

Rock associations of the ore consists of calc-schist, chlorite schist and bituminous schist that indicate a black shale associations deposited in semi closed or closed basins like the modern Black Sea and the Baltic Sea.

6.3 Radiolarian Chert: Hosted Manganese Deposits

Radiolarian chert-hosted manganese deposits and occurrences of Turkey are in four belts that represent deep sea sedimentary rocks. These four belts from north to south are known as Paleo Tethyan, Karakaya and two branches of the Neotethyan ocean, respectively. The most important Mn deposits occur in the pelagic sediments of the

Table 6.1 Major oxides (%) of the selected Mn deposits of Turkey

Deposits	SiO2	Al2O3	Fe2O3	MgO	CaO	Na2O	K2O	TiO2	P2O5	MnO	Cr2O3	TOT/C	TOT/S
Çayırlı	16.66	1.06	1.77	0.06	0.34	0.03	0.06	0.07	0.05	58.12	0.004	<0.02	<0.02
Binkılıç	6,45	2,2	1,65	0,82	8,29	0,36	0,79	0,11	0,26	48,56	<0.002	1,84	0,03
Dilli	2,33	1,01	1,68	0,17	0,42	0,06	0,13	0,06	0,06	64,71	<0.002	0,05	<0.02
Elmalar	25,59	1,38	0,6	0,09	0,27	0,04	0,24	0,06	0,05	52,99	<0.002	0,02	<0.02
Gökçeada	6,03	0,7	12,7	0,64	4,42	<0.01	0,1	0,03	0,02	42,67	<0.002	7,76	0,77
Kepirli	14,65	3,49	10,88	5,02	8,29	0,21	0,74	0,19	0,38	25,81	<0.002	9,8	0,05
Uluk. -o	3,85	1,61	4,31	0.16	2,16	0,09	0,19	0,07	0,31	59,53	<0.002	0,5	0,05
Uluk.-os	15,15	1,63	4,32	2,18	2,65	0,01	0,01	0,06	0,16	53,83	<0.002	3,33	0,03
Çay. nod	7,72	1,64	0,63	0,27	0,39	0,07	2,22	0,06	0,05	61,97	<0.002	<0.02	<0.02

Cayırlı nod Çayırlı Mn nodule, *Ulukento* Ulukent oxidised ore, *Ulukent os* Ulukent oxide and silicate ore

Northern Branch of the Neotethyan Ocean (Izmir–Ankara–Erzincan Suture zone). These deposits are represented by the Çayırlı, the Çorum and the Hafik region deposits. Mn deposits of the Southern branch of Neotethyan Ocean (Bitlis – Zagros suture zone) consist of Koçali, Kilis, Çevretepe and the Dokuztekne region deposits (Erdemoğlu and Yaman 1992; Van and Yalçınalp 2010). These deposits are generally small being 5000–30,000 tonnes of ore reserve with a 20% Mn and high Si (30%) content. These deposits are mined by open pit methods.

Chert – hosted Mn deposits are widely scattered within the reddish- brownish colored radiolarian chert series, displaying tectonically imbricated structure. The most common exploration practice is by using excavators for digging some of the Mn oxide olistoliths or tectonic slices of Mn oxides. Oceanic sediments of the Paleo Tethyan and the Karakaya sutures do not include economically important manganese deposits. The general characteristics of the radiolarian chert – hosted ore deposits are, as follows: (1) limited by faults, (2) enriched by silica associated with hydrothermal quartz or opal – cristobalite tridimite formation or radiolarian fossils, (3) showing well stratified structure or laminations, (4) alternated with thin radiolarian chert and siliceous shale beds (5) include reddish and soft iron oxides – okr levels at the bottom of the manganese oxides, (6) rarely include Mn nodules (Öztürk 1993b), (7) include trace amount of Ni, Co and Cu, (8) ore mineralogy consists of pyrolusite, psilomelane and manganite, (9) reflect a strong post sedimentary deformation, (10) have generally high Mn/Fe ratio.

The most representative chert-hosted deposit of the Izmir–Ankara–Erzincan suture zone is the Cayırlı Mn deposit studied by Oygür (1990). The Çayırlı manganese deposit is one of the largest hosted by the radiolarian chert – radiolarites of a tectonic mélange of Cretaceous Age (Öztürk 1997). Approximately 250,000 tonnes of ore has been mined up till now and still under production with an ore processing plant consisting of jigging separation process. The ore body continues for 200 m and is concordant with thick-bedded reddish brown radiolarian chert and siliceous shale. Reddish and earthy iron oxides occur at the bottom of the manganese oxide zone indicating a gradual increase in redox potential and/or oxygenation of the deep oceanic water. The ore minerals consists of pyrolusite and psilomelane as disseminated and microscopic–submicroscopic grains. Stockworks of secondary ores are also common and these consist of relatively coarse pyrolusites and minor psilomelane minerals. Ore chemistry with moderate Ni, Co and Cu indicate that mineralization was formed by circulating hydrothermal solutions with minor hydrogenetic input according to Oygür (1990).

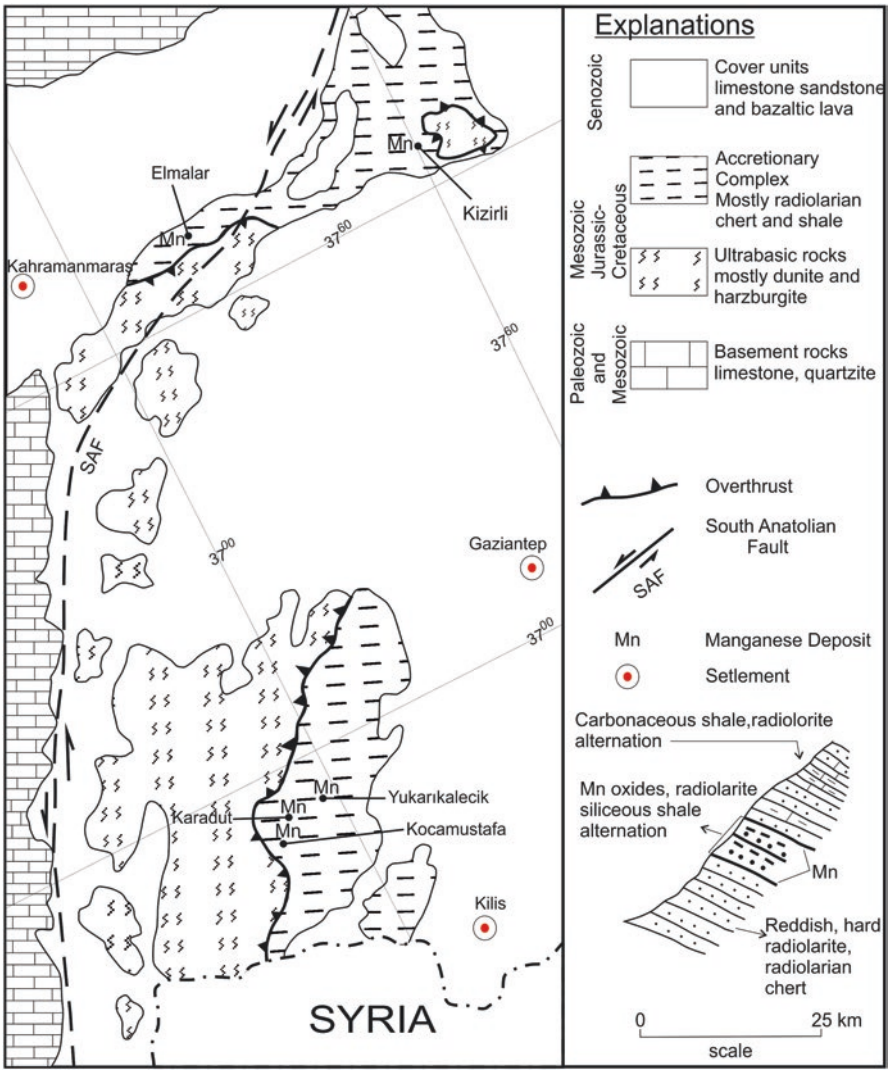

Fig. 6.6 Geological map showing of the Kilis region manganese deposits, and cross section of the Karadut Mn deposit

6.3.1 The Kilis Region Deposits

The Kilis – Maraş region includes three low grade manganese deposits, known as Elmalar, Karadut, and Kocamustafa which belong to the Demeka Mining Co. These deposits are similar to each other in terms of mineralogy, host rocks, chemical composition, and ore grades (Fig. 6.6). The Elmalar manganese ore occurs as concordant seams within the pinkish radiolarian chert and brownish siliceous shale rocks.

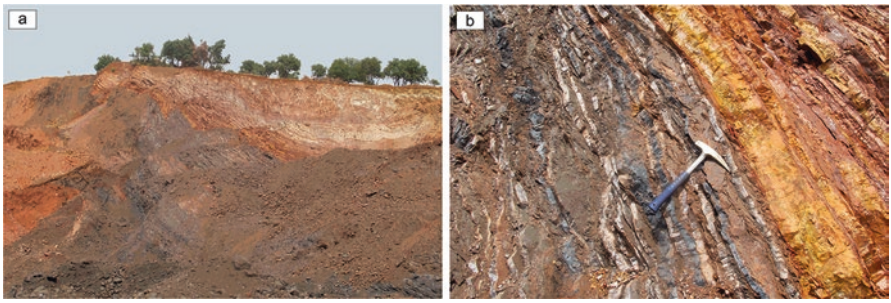

Fig. 6.7 (**a**) Outcrop of chert – hosted the Karadut manganese deposit showing highly deformed deep sea pelagic sediments with thin bedded manganese oxide layers. (**b**) Details of the alternations of the syn sedimentary Mn oxide bandings (3–10 cm in thickness) with radiolarian cherts (reddish brown) and with brownish siliceous shales in the Karadut mine. The upper yellowish red layer consists of Fe oxide- rich clay and siliceous shale

The Mn ore minerals are pyrolusite and minor psilomelane. The ore zone extends for 200 m with 6 m average thickness and dips to NW with 45°. A few tens of thousand tonnes of ore with 12% Mn average grade has been mined from this deposit. The ore is carried to the Türkoğlu processing plant by a 45 km road. The ore material is first crushed to 3 cm then concentrated by the jigging method. Concentrated ore with 57% Mn which is gained by an average 60% recovery. Approximately 1 tonne of concentrated ore is obtained from 9 tonense of bulk ore. The ore is characterized by high Mn and low iron content as shown in Table 6.1. The mining being carried out at Elmalar by open pit method with a stripping ratio of about three. The ore reserve as provided by the company is 120,000 tonnes. However, owing to tectonic structural repetition, some additional new reserve can be found by drilling in or around the license area.

The Kocamustafa deposit is located 3 km north of the Karadut deposit. This deposit was investigated by MTA which defined a few hundred thousand tonnes of ore with low grade. The ore zones extends N 30 W and dips 75° to NE. The general features are similar to the Karadut deposit. A few thousand tonnes of ore was produced by open pit mining. The Karadut deposit exhibits all characteristic features of a chert – hosted ore (Fig. 6.7). The deposits extends for more than 400 m on the surface with an average thickness of 8 m and probable reserves of 620,000 tonnes of ore with 11% Mn. The ore consists of manganese oxide and SiO_2 trace amounts of Al and Fe.

Owing to its wide distribution, some researchers recently studied the chert-hosted manganese deposits (Türkyılmaz 2004; Özküz 2011). These authors defined a similar geochemistry in their studied deposits in North and South Anatolian suture zone.

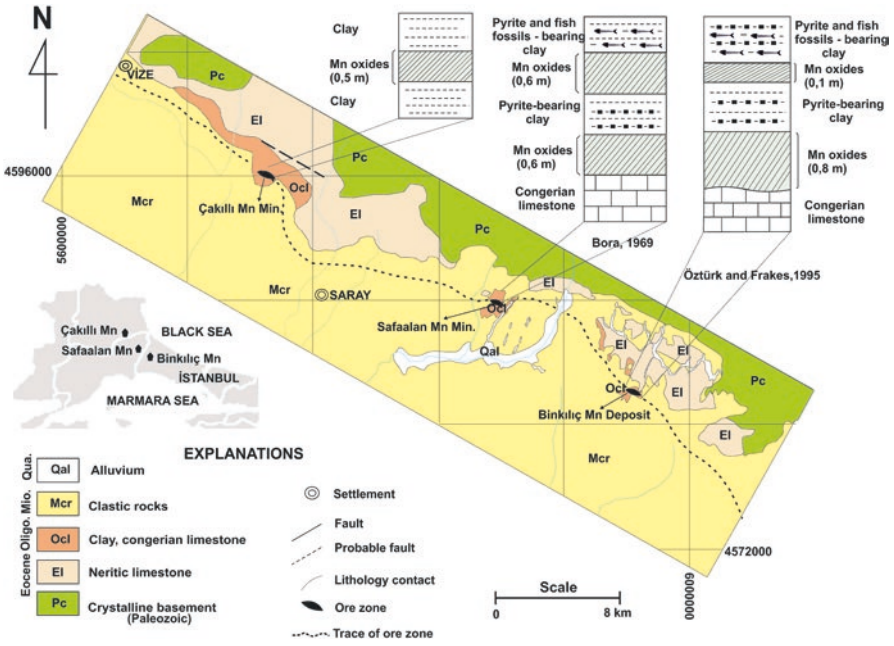

Fig. 6.8 General trends of the Oligocene – hosted manganese mineralizations along the northern rim of the Thrace Basin and the ore – host rock relationships at some locations

6.4 Oligocene: Hosted Manganese Deposits

The Oligocene-hosted manganese deposits form a northwest southeast trend in the Thrace Basin in the northwestern part of Turkey. The ore zone generally occurs between the congeria fossils-bearing limestone and pyrite and fish fossils – bearing clays. Manganese oxide formation begins in Çatalca region and extends to Saray along the 150 km the basin margin (Fig. 6.8). Mn oxides and host lithologies gently dip to southwest, whereas in the Bulgaria these rocks dip to the northeast. This situation suggests more than one isolated basinal conditions during the Oligocene and a stratigraphic control of the mineralization.

6.4.1 The Binkılıç Mn Deposit

Investigation of the Binkılıç and Sefaalan, the latter being the westward continuity of Binlılıç was begun 1966 by MTA for the Tuna Mining company. According to 18 drill hole data a 1.118.293 tonnes of measured ore reserve with 29.4% Mn grade has been defined in Binkılıç (Bora 1969). Beside this, 3.5 Mt and 2.5 Mt of possible ore reserve are also reported in this study for the Binkılıç and Sefaalan deposits, respectively.

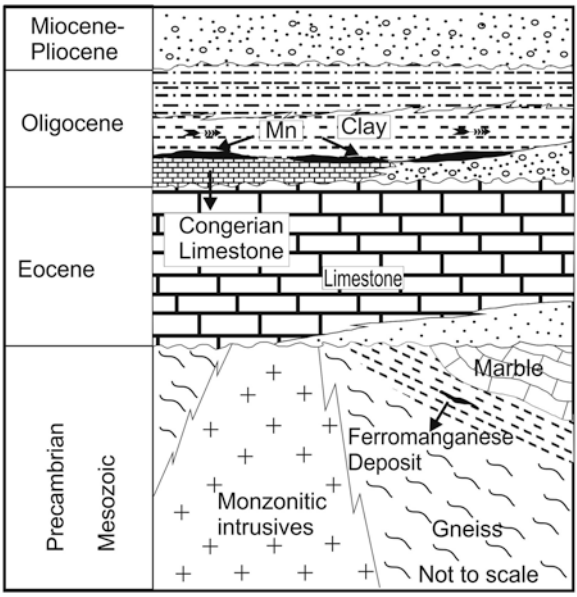

Fig. 6.9 Simplified cross section showing the stratigraphic positions of the Mn deposits of the Thrace basin. (Öztürk 1997)

According to Uzkut (1971) 120,000 tonnes of ore was produced from the Binkılıç deposit from 1952 till to 1970. The deposits has been the focus of studies based on mineral processing (Ateşok 1979) and the ore geochemistry (Gültekin 1998).

At Binkilic, the basement is represented by metamorphic rocks overlain by the Eocene micritic limestone and the Oligocene Congerian limestone rocks (Fig. 6.9). The Miocene is represented by clastic rocks including Mn oxides penetration.

Thickness of the manganese ore seams varies from 0.2 to 1 m. The ore zone includes soft and low quality ore and hard and high quality ore levels or patches, pisolitic, oolitic and concretionary ore types. The ore mineralogy consists of pyrolusite, psilomelane, manganite, rhodochrosite, kutnohorite, limonite and goethite, and gangue consists of Mn calcite, quartz, calcite, montmorillonite and illite.

Average major oxide composition of the ore is 45% MnO, 1.5% Fe_2O_3, 8% SiO_2, 2% Al_2O_3, 5%CaO, 1.3% MgO, 0.4%K_2O, 0.6% Na_2O, 0.06%$Ti O_2$, and 0.3% P_2O_5. Major oxides of the ore show a low terrestrial input and/or chemical depositional process or diagenetic replacement of carbonatic parental rocks. The phosphorus content of the ore is not high for the iron and steel industries. High Ba and Sr are remarkable whereas low amounts of Ti, Cr, Zr and Al indicate a limited terrigenous input. Heavy metals such as Co, Ni, Cu, V and Zn are relatively enriched in the ore possibly associated with absorbing mechanism on to the manganese oxides. Rare earth element contents of the ore is lower than the NASC and the Chondrite values. Chondrite normalized REE pattern of the ore is characterized by negative Ce and positive Eu anomalies. $\delta\ ^{13}C$ values from the rhodocrosite and kutnohorite in the ore zone vary between −7%0 and −5%0, PDB which indicates fresh water environment.

Formation of the Oligocene rocks hosted manganese deposits around the Black Sea is explained as due to sea level change by Bolton and Frakes (1985) and then

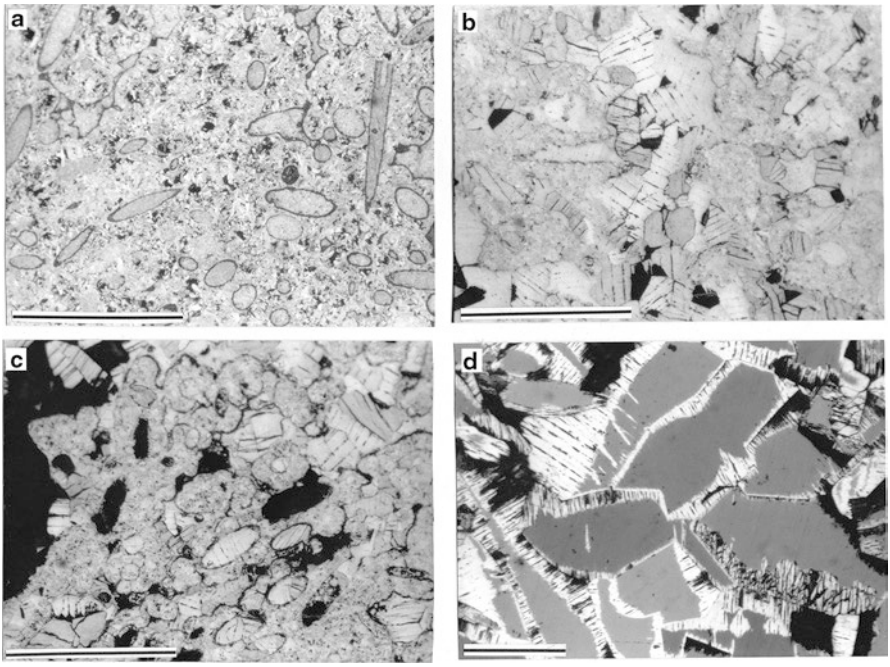

Fig. 6.10 Polished section photomicrographs from the high grade and hard ore of the Binkılıç manganese deposit showing very well preserved diagenetic replacement features of the mono axon sponge spicules by manganese ions. Sponge spicule structures reveal needle or circular shape in relation to the section planes (**a**–**c**): Oxidation of open space forming manganites (dark gray) to pyrolusite (white) and formation of dehydration fissures in pyrolusites. All scale bars indicate 1 mm (**d**). Black area is quartz. Unbroken spicules indicate a quite water conditions like a lagoon for carbonate deposition

diagenetic replacement process by Öztürk and Frakes (1995). Monaxon sponge spicule relics in the high grade ore clearly indicates the replacement of spiculite or spicule – bearing limestone by manganese (Fig. 6.10). Manganese is possibly concentrated in an isolated lagoon lake or marsh environment under both anoxic and acidic conditions was possibly created by volcanic ash and/or acid rain in a shallow water body after a volcanic eruption in the northwestern Anatolia. Manganese carbonate and oxides may have been deposited associated with supergene replacement process as a reactions of downward diffusing or lateral flowing Mn – bearing water. Mn deposition is associated with Eh and pH increase after the reaction between the anoxic Mn – rich surface waters with the host Congerian limestone.

6.5 Vein: Type Manganese Deposits

These Mn deposits mostly occur within the volcano-sedimentary rocks of the Upper Cretaceous age along the Black Sea coast and rarely in eastern central Anatolia and the Gökçeada Island. A volcano-sedimentary rock sequence was formed by the subduction of the Neo-Tethyan oceanic crust beneath the Pontide plate. Volcanic arc rifting during that time with bimodal volcanism and the related Mn deposits formed as metasomatic, hydrothermal and stratabound types in the Pontides. Rock associations of the Mn deposits in this region include dacitic tuff, reddish limestone and hemipelagic-claystone, marl and shale. Similar small – sized Mn mineralization is related to Tertiary magmatism and hydrothermal activity around the Çanakkale city and the central Anatolia.

Manganese minerals of the Black Sea region deposits generally consist of braunite, bixbyite, pyrolusite, psilomelane, hausmannite, asbolane, rhodochrosite, Mn-calcite. Gangue minerals of the deposits are barite, quartz, chalcedony, montmorillonite, illite and kaolinite. Distinctive deposits of the province are the Ereğli and Topkirazlar deposits in the west and the Ocaklı deposit in the east. The Topkirazlar and Ereğli ore deposits are the largest deposits in the area which occur in a volcano-sedimentary succession of Upper Cretaceous age. The ore reserve is estimated to be 200,000 tonnes, but near-surface sections of the deposits are generally exhausted (Öztürk 1997).

Volcanic arc hosted deposits are characterized by relatively K, Na, Ba, As, Sb and P enrichment however these elements do not affect the quality of ore (MTA 1972). The hydrothermal origin of the deposits is characterized by its high As, Sb and Pb contents The Ocaklı manganese deposit, and similar deposits of the region, studied by Gedikoglu et al. (1985), are believed to have been formed by hydrothermal replacement and infilling processes.

6.5.1 The Dilli Manganese Deposit

A distinctive vein – type hydrothermal Mn deposit occurs along the tectonic contact between the crystallised limestone and serpentinised ultramafic rocks 2 km SE of Dilli Village of Erzincan city (Fig. 6.11). The serpentinised ultramafic rocks are highly deformed and display brownish green to yellowish green color. The crystalised limestone represents the basement autochthon of the region which is highly brecciated and karstified. The grade of manganese ore is high and shows lenticular geometry with a 4 m average thickness. The ore was mined from the surface to 40 m depth by open pit at the beginning and then by underground methods. The deposit belongs to a private company and approximately 5000 tonnes of high grade (45% Mn) ore mined form the deposit without any exploration study by drilling. The ore

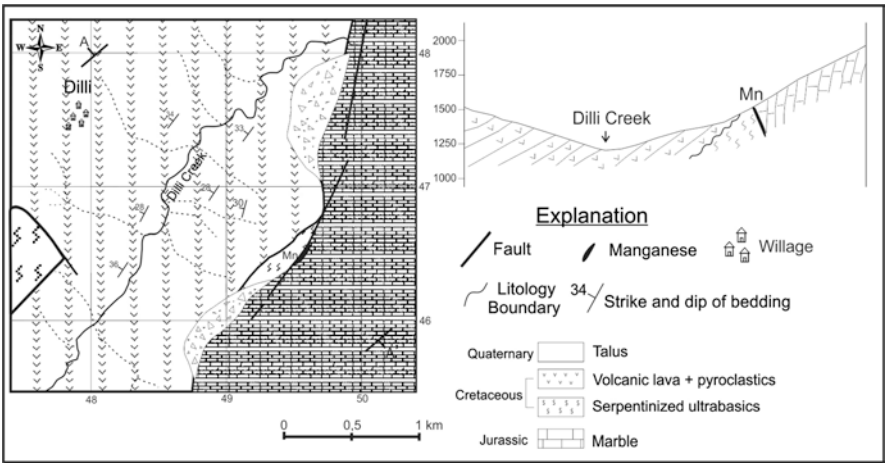

Fig. 6.11 Geological map and cross section of the Dilli manganese deposit

is sold to a zinc metallurgy factory in Turkey which is known as Çinkur Co. The ore minerals of the deposits are pyrolusite and psilomelane. The ore reveals both soft and hard ore which are characterized by Ni enrichments up to 0.5% Ni (Table 6.3). This indicates that the Mn and Ni were scavenged from the serpentinised ultramafics and pelagic sediments of Cretaceous and deposited along the tectonic fabrics related to increase in Eh and pH.

6.5.2 The Gökçeada Manganese Mineralization

This mineralization occurs as a vein up to 1.5 m in thickness and 200 m length in the south of the Gökçeada island in the Aegean Sea. The mineralization occurs in the Oligocene volcanoclastics as a vein with dips of 70–80° to NE. The volcanoclastic rocks around the ore vein display argillic alteration. The geometry of the ore body can be seen in the open pit. Owing to low grade of Mn the mining stopped. The ore minerals are pyrolusite and psilomelene, limonite and goethite. The gangues are calcite, quartz, dolomite and barite. The ore includes high amount of Pb, Zn, Sb and Au (Table 6.3) that clearly indicate an epithermal vein origin.

6.6 Geochemistry

As a major oxides, The Ulukent and Binkılıç deposit reveal high P contents relative to the other deposits (Table 6.1). The highest P_2O_5 contents of the Ulukent deposit could be related to storage of phosphates in the anoxic water column. The Çayırlı manganese nodule includes 2.2% K_2O which is possibly related to cryptomelane or

psilomelane. The Ulukent deposit is relatively enriched in iron and silica which is possibly associated with Mn silicate mineral, braunite, and some quartz.

The Kepirli manganese deposit reveals Mg enrichment which is related to dolomite. The chert hosted ores of the Elmalar and Çayırlı reveal high silica associated with radiolaria fossils and chalcedony.

Trace elements are enriched in vein – type hydrothermal deposits such as Dilli, Gökçeada and Kepirli. The Dilli Mn deposit includes 0.4% Ni, 1.3% Ba, 0.1% Sr, 0.104% Co and 0.1% V which suggest that the manganese was possibly extracted from the ultramafic-mafic rocks and pelagic sediments of the ophiolitic mélange (Table 6.2). Contrary to the vein – type hydrothermal deposits, the black shale – hosted type Ulukent manganese deposit includes the lowest amount of trace elements. Ba and Sr elements are enriched in the Binkılıç and Dilli and Mn nodules of the Çayırlı despite their formation conditions is different. Ba and Sr enrichment in the syn sedimentary deposits may be associated with alteration of the feldspars. Uptake of the Ba and Sr from the deep sea sediments may explain the enrichment of these elements in the hydrothermal Dilli deposit. Ba discharges into the sea water from hydrothermal vents is reported by several workers (Rona 1984 and references therein), in this context, the Ba of the Mn nodule could be formed close to sea floor hydrothermal discharge sites. Ba especially enriched in psilomelane, (Ba (Mn^{2+}) $(Mn^{4+})_8$ $O_{16}(OH)_4$, rich soft ore because of Ba enters into the crystal lattice of psilomelane.

The total rare earth elements (REEs) contents of the studied deposits ranges between 342 ppm (Ulukent deposit) and 36 ppm (Çayırlı). REEs are relatively enriched in the Ulukent manganese deposit and show a positive correlation with phosphorous. Both oxide and the oxide – silicate ore of the Ulukent deposit show a typical positive Ce anomaly (Table 6.2). This enrichment may have been related to concentration of Ce^{3+} in the sea water during the anoxia and then oxidation to Ce^{4+} and absorbsion on to the Mn oxides as CeO_2 in oxic conditions.

6.7 Conclusions

Although there are many different types of manganese deposits in Turkey, they do not exceed reserves of a few million tonnes. Potentially and economically two important manganese deposits are black shale – hosted and the deposits of Oligocene age.

The black shale – hosted Ulukent manganese ores of Turkey were formed in an anoxic basin comparable to today's Black Sea, and similar to the Urkut manganese deposit of Hungry. The primary carbonate ore, consisting of rhodocrocite and kutnohorite, has been undergone regional metamorphism and changed to silicate – oxide ore and gained a magnetic signature. Magnetic hausmanite – rich ore body in the shales and recrystallised limestone offers the best opportunity for geophysical (magnetic) survey.

The Congerian limestone – hosted manganese deposits of Oligocene age and black shale – hosted manganese deposits of Cretaceous age occur as concordant with host shales or limestone and sandy clays. The Oligocene-aged manganese

Table 6.2 REEs values (ppm) of the studied Mn deposits of Turkey

Deposits	La	Ce	Pr	Nd	Sm	Eu	Gd	Tb	Dy	Ho	Er	Tm	Yb	Lu
Çayırlı	6,1	14,5	1,35	5,7	1,44	0,39	1,8	0,29	1,59	0,34	1,24	0,14	0,85	0.16
Binkılıç	10,7	15,6	2,28	10,1	1,82	0,23	1,94	0,29	1,65	0,33	0,86	0,15	0,85	0.14
Dilli	10	22,1	1,58	7,3	1,53	0,17	2,1	0,35	2,24	0,5	1,67	0,27	1,97	0.32
Elmalar	11,1	37,4	4,23	18,2	3,91	0,9	4,74	0,65	3,26	0,54	1,48	0,18	1,23	0.17
Gökçeada	8,4	16	2,05	9,6	2,53	1,81	3,86	0,64	3,94	0,93	2,76	0,37	2,32	0.36
Kepirli	57,9	137,1	11,12	44,1	9,5	2,12	10,04	1,47	7,82	1,48	3,94	0,56	3,24	0.45
Ulukent-o	28,4	196,2	7,41	32,9	5,95	1,37	6,33	0,95	5,69	0,96	2,58	0,35	2,03	0.29
Uluk.-os	33,2	234,3	8,82	35,4	6,77	1,49	7,82	1,11	6,04	1,14	3,04	0,4	2,11	0.32
Çay. nod	15,4	16,2	3,02	11,6	2,29	0,42	2,64	0,36	2,2	0,42	1,35	0,21	1,35	0.23

Cayırlı nod Çayırlı Mn nodule, *Ulukento* Ulukent oxidised ore, *Ulukent os* Ulukent Mn oxide and silicate ore

Table 6.3 Trace element compositions of the studied Mn deposits, Hg, Au and Ag are as ppb and the others are as ppm

Deposits	Mo	Cu	Pb	Zn	Ni	As	Cd	Sb	Bi	Ag	Au	Hg	Tl	Se	Y
Çayırlı	122,6	111,2	1,9	102	162,6	48,5	0,1	1,9	<0.1	<0.1	2,4	0,01	2,2	<0.5	14,8
Binkılıç	36,1	16,3	4,5	72	181,3	86,9	0,4	4,6	<0.1	<0.1	1,4	0,4	8,5	<0.5	9,5
Dilli	107,9	633,4	2912	865	4107	198,3	0,2	10,4	<0.1	<0.1	3,3	0,05	61,4	<0.5	11,7
Elmalar	57,1	793,8	15,3	50	30,9	49,3	<0.1	1	<0.1	<0.1	0,6	0,02	2,1	<0.5	13,8
Gökçeada	5,8	47,7	1493	3639	249,5	27,6	4,9	49,6	0,3	4,5	33,2	0,12	2,4	0,9	36
Kepirli	3	38,1	281,4	329	71,1	17,8	3,2	1,3	0,4	0,4	<0.5	0,18	0,1	<0.5	43,1
Ulukent-o	3,4	8,9	151,6	314	60	30,3	0,5	4,5	<0.1	0,3	1,8	0,29	0,5	<0.5	25,4
Ulukent-os	2,2	1,7	3,6	15	15,3	16,7	<0.1	0,8	<0.1	<0.1	<0.5	0,01	<0.1	0,7	25,4
Çayırlı nod	97,6	34,4	2,3	208	175,5	27,1	0,2	1	<0.1	<0.1	2,8	<0.01	23,1	<0.5	13,8
Deposits	**Ba**	**Be**	**Co**	**Cs**	**Ga**	**Hf**	**Nb**	**Rb**	**Sr**	**Ta**	**Th**	**U**	**V**	**W**	**Zr**
Çayırlı	1432	<1	51,8	0,2	58,3	0,2	0,5	1,3	747,6	<0.1	0,3	7,5	281	<0.5	8,6
Binkılıç	13,106	<1	51,2	0,7	47,1	0,5	1,3	9,9	4181	0,1	0,9	9,9	111	1,7	22,1
Dilli	20,310	2	1442	0,2	64,4	0,3	0,2	1,2	1229	<0.1	0,3	9,5	990	1	21,9
Elmalar	3717	<1	192,6	0,2	60,6	0,4	0,7	2,5	352,3	<0.1	0,7	3	48	0,6	17
Gökçeada	839	5	85,5	1,1	35,3	0,2	0,7	5,6	68,9	<0.1	0,8	2,5	33	0,9	8,8
Kepirli	377	3	15,2	1,1	29,5	1,6	9,9	28,3	251,1	0,5	3,3	1	<8	2,4	76,6
Uluk.-o	1471	<1	33,7	1,9	55,1	0,5	1,6	5,5	630,7	0,1	1,3	1,5	22	3,3	26,5
Uluk.-os	830	<1	54,1	0,2	48,4	0,6	1,4	0,8	96,6	<0.1	1,1	0,5	<8	2,2	31,6
Çay. nod	10,619	<1	37,8	0,2	57	0,4	0,8	5,4	3259	<0.1	0,7	2,4	248	0,7	15,3

deposit consists of a horizontal tabular ore body, averaging 1 m in thickness, and annually 60,000 tonnes of ore with 36% Mn are still being open pit mined. These deposit include small amounts of phosphorus, which is an unwanted elements for iron and steel sector (0.35% P_2O_5). The ore deposit was formed by diagenetic replacement processes, in Mn – rich water. Pyrite- rich clays layer (hanging wall rock) indicates a strong reducing conditions during the primary Mn carbonate deposition which was oxidized to tetravalent Mn oxides by supergene alteration. Pyrite-rich bluish gray clay layer, which is so electrically conductive, can be use a guide during geophysical exploration. The Turkish manganese deposits that occurs in the congerian limestone of Oligocene age are genetically and temporally linked to the Ukrainian (Nikopol) and Georgian (Chiaturi) manganese deposits.

Despite the wide distribution of the radiolarian chert-hosted ferromanganese deposits in Turkey, they are small-sized and therefore economically unimportant. Relatively small-sized radiolarian chert hosted -manganese mineralization of Turkey can be economic if mining and ore processing plants are properly planned at a whole regional scale. The same situation is also true for the magmatic arc -hosted hydrothermal manganese deposits.

Acknowledgements I thank to J. R. Hein, L. A. Frakes and G. Glasby for valuable discussions during the field study in Turkey, to N. Hanilci for sharing data of the Kepirli Mn mineralization, and research assistant Zeynep Cansu (İstanbul University) for contribution in drafting the figures. Thanks to Demeka mining company for their permission and kindly helps during the field study. Thanks go to the editorial group of this book for inviting me the preparation of the manganese chapter.

References

Ateşok G (1979) Trakya-Binkılıç yöresi düşük tenörlü manganez cevherlerinin zenginleştirilmesi. [Mineral processing of the low grade Mn ores of the Thrace-Binkılıç Region] Ph. D. Thesis, Istanbul Technical University, 134 p. (in Turkish with English abstract)

Bora E (1969) Binkılıç ve Sefaalan Bölgesinin jeolojisi ve manganez yatakları. [The geology and Mn deposits of the Binkılıc¸ and Sefaalan area]. M.Sc. Thesis, Istanbul University, 47 p. (In Turkish, unpublished)

Doğan H, Turkmen H (1983) Ulukent – Tavas çevresindeki manganez yataklarının jeoloji Raporu. [Geological report of the manganese deposits of the Ulukent-Tavas and surrounding area]. General Directorate of Mineral Research and Exploration Report No: 345, 87p. (In Turkish, Unpublished)

Erdemoğlu M, Yaman S (1992) Çevretepe-Ceyhan-Adana manganez yatağının metalojenik incelenmesi [Metallogenical investigation on manganese deposits of the Çevretepe -Ceyhan-Adana]. J Fac Eng Çukurova Univ 7:25–42 (in Turkish with English abstract)

Fan D, Lui T, Ye J (1992) The process of formation of manganese carbonate deposits hosted in black shale series. Econ Geol 87:1419–1429

Frakes LA, Bolton BR (1984) Origin of manganese giants: sea level change and anoxic– oxic history. Geology 12:83–86

Gedikoğlu A, Van A, Eyupoğlu I, Yalçınalp B (1985) Doğu Karadeniz manganez cevherleşmelerine bir örnek: Ocaklı (Maçka, Trabzon) manganez zuhuru. [An example of manganese mineralization in the eastern Pontide: The Ocaklı (Maçka, Trabzon) manganese prospect]. Geol Eng 25:23–37 (in Turkish with English abstract)

Graciansky P (1968) Teke yarımadası (Likya) Torosları'nın üst üste gelmiş ünitelerinin Stratigrafisi ve Dinaro-Toroslar'daki yeri. [The stratigraphy of the imbricated tectonic units around Teke Peninsula Liciyen and their position at the Taurides]. Bull Min Res Exp 71:73–93 (In Turkish and French)

Gultekin AH (1998) Geochemistry and origin of the Oligocene binkılıç manganese deposit; Thrace Basin. Turk J Earth Sci 7:11–23

Hein JR, Bolton BR (1992) Stable isotope composition of Nikopol and Chiatura manganese ores, USSR: implications for genesis of large sedimentary manganese deposits [abs.]. International Geological Congress, 29th, Kyoto Japan, Abstracts, 1, 209

Kirmanlı C, Nasuf E (1998) Denizli-Tavas-Ulukent manganez açık işletmesinin jeoistatistik yöntemle rezerv-tenör ilişkisinin belirlenmesi. [Determination of reserve-grade relation of Denizli-Tavas-Ulukent manganese open pit mine using geostatistics]. Madencilik 37:19–27 (In Turkish)

Kuşçu M, Gedikoğlu A (1989) Ulukent (Tavas-Denizli) güneyi manganez yataklarının jeokimyasal özellikleri. [The geochemical properties of the manganese deposits at the south of Ulukent Tavas–Denizli]. Geosound 17:29–48 (in Turkish with English abstract)

MTA (1972) Türkiye manganez yatakları. [Manganese ore deposits of Turkey]. General Directorate of Mineral Research and Exploration. Pub. No: 120, 38 p. (In Turkish)

Okita PM, Maynard JB, Spiker EC, Force ER (1988) Isotopic evidence for organic matter oxidation by manganese reduction in the formation of stratiform manganese carbonate ore. Geochim Cosmochim Acta 52:2679–2685

Okita PM (1992) Mnganese carbonate mineralization in the Molango District. Econ Geol 87(5):1345–1366

Oygür V (1990) Çayırlı (Ankara-Haymana) manganez yatağının jeolojisi, oluşumu ve kökeni üzerine görüşler. [Implications on geology, genesis and origin of Çayırlı manganese deposit, Ankara, central Anatolia]. Bull Min Res Exp 110:114–122 (In Turkish with English abstract)

Özküz N (2011) Derbent (Yozgat) manganez yatağının jeokimyası ve oluşumu. [Geochemistry and the origin of manganese mineralizations in Derbent (Yozgat) Region]. Bull Earth Sci Applic Res Cent Hacet Univ 3:213–234 (In Turkish with English abstract)

Öztürk H (1993a) Manganese mineralizations in Turkey: processes of formation and types. Geol Eng 43:24–33 (In Turkish with English abstract)

Öztürk H (1993b) Characteristics and formations of fossil manganese nodules in the Koçali Komplex, Adıyaman, Turkey. Geol Bull Turk 36:159–169 (In Turkish with English abstract)

Öztürk H (1997) Manganese deposits in Turkey: distribution, types and tectonic setting. Ore Geol Rev 12:187–203

Öztürk H, Frakes LA (1995) Sedimentation and diagenesis of an Oligocene manganese deposit in a shallow subbasin of the Paratethys, Thrace Basin, Turkey. Ore Geol Rev 10:117–132

Öztürk H, Hein JR (1997) Mineralogy and stable isotopes of black shale – hosted manganese ores, Southwestern Taurides. Econ Geol 92:733–744

Polgari M, Okita PM, Hein JR (1991) Stable isotope evidence for the origin of the Urkut manganese ore deposit, Hungary. J Sediment Petrol 61:384–393

Rona PA (1984) Hydrothermal mineralization at seafloor spreading centers. Earth Sci Rev 20:1–104

Rona PA (1992) Deepsea geysers of the Atlantic. Natl Geogr Mag 182(4):104–109

Roy S (1992) Environments and processes of manganese deposition. Econ Geol 87:1218–1237

Türkyılmaz B (2004) Güneydoğu Anadolu bindirme kuşağındaki mangan yataklarının mineralojik, jeokimyasal ve kökensel olarak incelenmesi. [Mineralogical, geochemical and genetic investigation of the manganese deposits of the Southeast Anatolian thrust belt]. Ph.D. Thesis. Fırat University. Elazıg, 160 p. (in Turkish with English abstract)

Uzkut I (1971) Türkiye manganez madenciliği, ekonomisi ve geleceği. [Economy of manganese mining in Turkey and its feature]. Bull Min Res Exp 77:98–112 (in Turkish with English abstract)

Van A, Yalçınalp B (2010) Geological setting and geochemical characteristics of Kuşkayası Manganese deposit, Otlukbeli, Erzincan, Türkiye. Geol Eng 34:41–55 (in Turkish with English abstract)

Chapter 7
Skarns and Skarn Deposits of Turkey

İlkay Kuşcu

Abstract The skarns and skarn deposits, an important class of mineral deposits in Turkey, are formed during major periods of subduction, continental collision, and post-collisional evenst in response to the convergence between Eurasia and Afro-Arabia between Late Cretaceous and Oligo-Miocene period. The skarns in Turkey are generally classified as calcic exoskarns and occasionally as magnesian exoskarns. The economic mineralization are largely confined to calcic exoskarns with exception of some Fe-skarns hosted by endoskarns. They are widely distributed over the calcitic meta-carbonates and recrystalllized limestones within metamorphic sequences or intercalations within sedimentary and/or volcanic sequences. The skarns are classified as Fe-, Fe-Cu, Cu-, W-, Fe-W, Mo and Pb-Zn-skarns according to dominant metal they contain. No gold or gold-only skarn is present while gold occurs as sub-economic to anomalous enrichment associated with Fe-Cu skarns. The Fe and Pb-Zn skarns have been the prime target for companies for centuries. The Fe and Fe-Cu skarns are commonly associated with oxidized I-type intermediate to mafic intrusives or sub-volcanic domes Late Cretaceous to Eocene in age that also formed economic porphyry Cu deposits. However, Fe and W skarns are co-genetic to porphyry Cu depoists associated with oxidized to mildly oxidized intrusives of Middle Eocene to Oligocene in age. The skarns that coexist as proximal calc-silicate assemlages within major high-level porphyry Cu systems are largely controlled by regional, large-scale structures such as strike-slip faults or core-complex systems. Where both Fe, Fe-Cu and Pb-Zn-skarns are observed in the same region, the Fe- and Fe-Cu skarns are classified as proximal, and Pb-Zn skarns as distal skarns.

The vast majority of Fe-, and Fe-W skarns are associated with endoskarn assemblages whereas some Fe-, and Pb-Zn-skarns are associated both with calcic and magnesian exoskarns. The wall rocks span age range rom Cambrian to Permian, and to Upper Cretaceous. The most common era for skarn generations are likely to be Late Cretaceous, Middle Eocene and Oligocene. No or a few skarn associated with intrusions younger than Miocene period is present.

İ. Kuşcu (✉)
Department of Geological Engineering, Muğla Sıtkı Koçman University, Muğla, Turkey
e-mail: ikuscu@mu.edu.tr

F. Pirajno et al. (eds.), *Mineral Resources of Turkey*, Modern Approaches in Solid Earth Sciences 16, https://doi.org/10.1007/978-3-030-02950-0_7

The main skarn-producing events in Turkey are related to the Late Cretaceous obduction of oceanic crust at the collision sutures resulted in the formation of a series of magmatic arcs, that also resulted in porphyry systems at the Pontides, but not at the Bitlis-Zagros suture. The second major skarn-producing events took place during Late Cretaceous post-dating the collision between the Anatolide-Tauride Block collided and the Eurasian plate.

This era is characterized by the generation of post-collisional (late-orogenic) I- to H-type calc-alkaline granitoids. These granitoids are the products of mixing/mingling of two coexisting magmas derived from the mantle and continental crust. This is the major period during which the most economic skarn deposits in central Anatolia have been resulted in. The third skarn-producing events took place at the Mesozoic-Tertiary boundary (Uppermost Cretaceous to Lower-Mid Paleocene during which a major crustal extension is predominant throughout Turkey.

7.1 Introduction

Turkey contains various mineral resource base formed formed by subsequent events in response to convergence between Afro-Arabian and Eurasian plates and closure of NeoTethys ocean during Late Cretaceous to Late Miocene. The convergence resulted in subsequent subductional, collisional and post-collisional events that formed in a geologically active environment, making it possible for magma and hot fluids to rise up from the mantle that have created innumerable mineral deposits. Mineral deposits in Turkey almost cover the spectrum in age (the Late Cretaceous to the Late Miocene even to MioPliocen) and type (porphyry Cu, epithermal, skarn, ironoxide-Cu-Au (IOCG), volcanogenic massive sulfide and orogenic gold). Therefore, Turkey has been an ancient center of mining for several civilizations as metal mining goes back at least to 9000 years. For example, the first bronze (an alloy of copper and tin) was compounded in Turkey (ca. 2900 B.C.), and that the first iron was refined here by the Hittites (ca. 1500 B.C.). Besides, the first gold coin was compounded during ancient Lydians.

The skarns and skarn deposits, an important class of mineral deposits in Turkey, manifest themselves as a unique class that have been mined and explored since the ancient civilizations. Old smelters, slugs and dumpsites are still found at the majority of the Pb-Zn and Fe-skarns in central and western Turkey. In this review, the term "skarn" refers to a simple rock type defined by its mineralogy dominated by coarse-grained calc-silicate minerals such as garnet and pyroxene (Meinert et al. 2005). In addition, the term skarn that may also refer to a rock or an alteration of previously existing rocks, is free of any geologic and/or genetic meaning. Therefore, the deposits and/or prospects included in this review share a common characteristic in that they are identified and mapped in the field based on their available calc-silicate mineralogy. These deposits are the prime sources of iron, tungsten, lead and zinc commodities of Turkey. Kuşcu (2005) reviewed and documented major types, tectonic setting, available mineralogy, host rocks and timing of some selected skarn deposits in Turkey. The present work is an update to his compilation of individual

skarn deposits based on major tectonic terranes in Turkey. In addition, the spatial distribution, summaries and important geologic features for skarns at each terrain are presented for ease of comparison between each terrane and skarns.

7.2 Geological Framework

Turkey is part of the great Tethyan belt that extends from the Atlantic Ocean to the Himalayas. This belt was formed by the complex convergence between Eurasian, Arabian and African plates; and the closure of the Tethys ocean. The Tethys ocean is a westward narrowing embayments between Laurasia and Gondwana at least since the Carboniferous (Şengör and Yılmaz 1981; Şengör 1987). In the Tethys terminology, two oceans, namely the PaleoTethys and NeoTethys, are recognized (Şengör and Yılmaz 1981). The economic magmatic-hydrothermal deposits including porphyry and skarn deposits are mostly due to the closure and subsequent collisional events related to NeoTethys Ocean. The closure of the NeoTethys ocean resulted in complex convergent plate boundaries and generation of several synchronous subduction zones at the Pontides, Bitlis-Zagros, and Aegean subduction zones. The Aegean subduction is still going on beneath the southern margin of Eurasian plate (Anatolides) along Helenic-Cyprean arc to the south of Turkey. The closure of NeoTethys Ocean between Middle and Late Cretaceous and collision during Tertiary times accreted and amalgamated multiple volcanic-arc segments and microcontinental fragments as well as ophiolites and mélanges to the Eurasian and Arabian plates (Fig. 7.1) (Şengör and Yılmaz 1981; Göncüoğlu et al. 1997; Okay and Tüysüz 1999). Each microcontinental fragments are bounded by

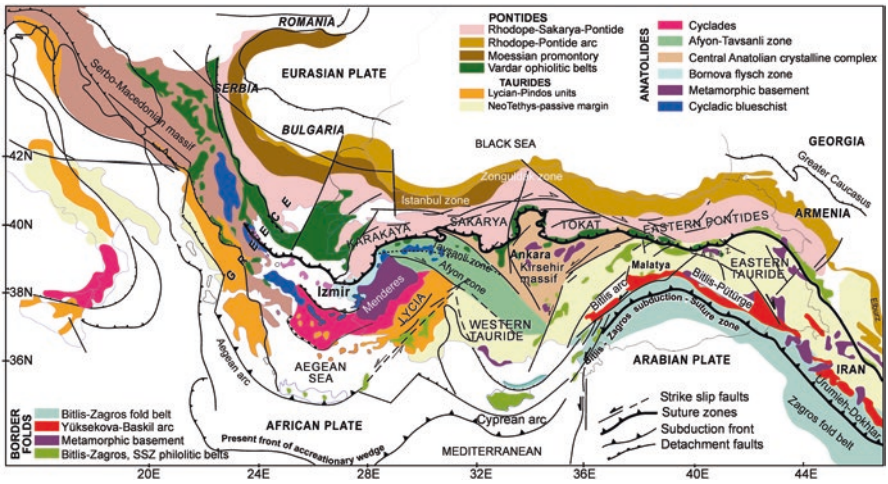

Fig. 7.1 Simplified map showing the main continental fragments, suture zones and major tectonic units of Turkey

several tectonic structures and sutures (Okay and Tüysüz 1999) that has complex tectonic and geological history. From north to south, these fragments are known as the Pontides that includes Strandja, İstanbul and Zonguldak terranes, the Karakaya complex, Sakarya terrane and eastern Pontides; Bornova flysch zone, Tavşanlı and Afyon zones, Menderes massif, Kirsehir massif (or Central Anatolian Crystalline Complex, CACC) are included in larger Tauride-Anatolide Block (TAP). The southeastern Anatolian orogenic belt (SEAOB) and the Arabian Platform form the southernmost terranes to the northern promontory of Arabian plate (Fig. 7.1). In this review, western Karakaya complex, Bornova flysch zone, Tavşanlı and Afyon zones, Menderes massif are included in a larger western Anatolian province (WAP). These fragments have been repeatedly affected by ongoing continental collision, subduction and sedimentation. The final amalgamation of these fragments took place during Late Tertiary when the Arabian plate collided with Anatolian plate.

7.2.1 Continental Fragments

7.2.1.1 Pontides

The Pontides comprises the northern coastal ranges of Turkey and the thrace peninsula (Fig. 7.1). It is composed of three tectonostratigraphic terranes. From west to east, these terranes in the Pontides are, Strandja terrane (western Pontides, Fig. 7.2a) in the west, Istanbul-Zonguldak in the center and Sakarya containing eastern Pontides (Fig. 7.2b) in the east. The magmatic rocks are widely exposed in the eastern Pontides, Strandja massif (western Pontides) and Sakarya terrane (Fig. 7.1). In the Pontides, the magmatic rocks form two distinct age groups, Late Cretaceous and Eocene. The eastern Pontides contain both groups roughly in in three subparallel east-trending belts (Fig. 7.2b), whereas Eocene magmatic rocks are restricted only in the eastern Pontides. The Late Cretaceous rocks belong to the Pontide arc and consist of volcanic, volcaniclastic rocks and intrusive rocks. Whereas, the Middle Eocene rocks consisting of volcanic, volcaniclastic and plutonic rocks, are considered to be related to post-collisional events after the final suturing of Anatolide-Tauride Block with Pontides. A slab roll back or break-off is invoked for the generation and emplacement of the Middle Eocene rocks (Kuşcu et al. 2018 and references therein). The Late Cretaceous volcanic and volcaniclastic rocks represent an earlier magmatic arc phase whereas the plutonic rocks a later phase. Eruption and deposition of Late Cretaceous arc volcanic and volcaniclastic rocks were accompanied locally by formation of volcanogenic massive sulfide deposits in marine environments (Eyüboğlu et al. 2011, 2013 and references therein). The Late Cretaceous volcanic and volcaniclastic rocks are intruded both by Late Cretaceous plutonic rocks and a later by Eocene intrusive rocks, and both resulted in skarns. The intrusive rocks are mostly monzonite, granodiorite, quartz diorite to diorite within the western and eastern Pontides (Fig. 7.2b), and form

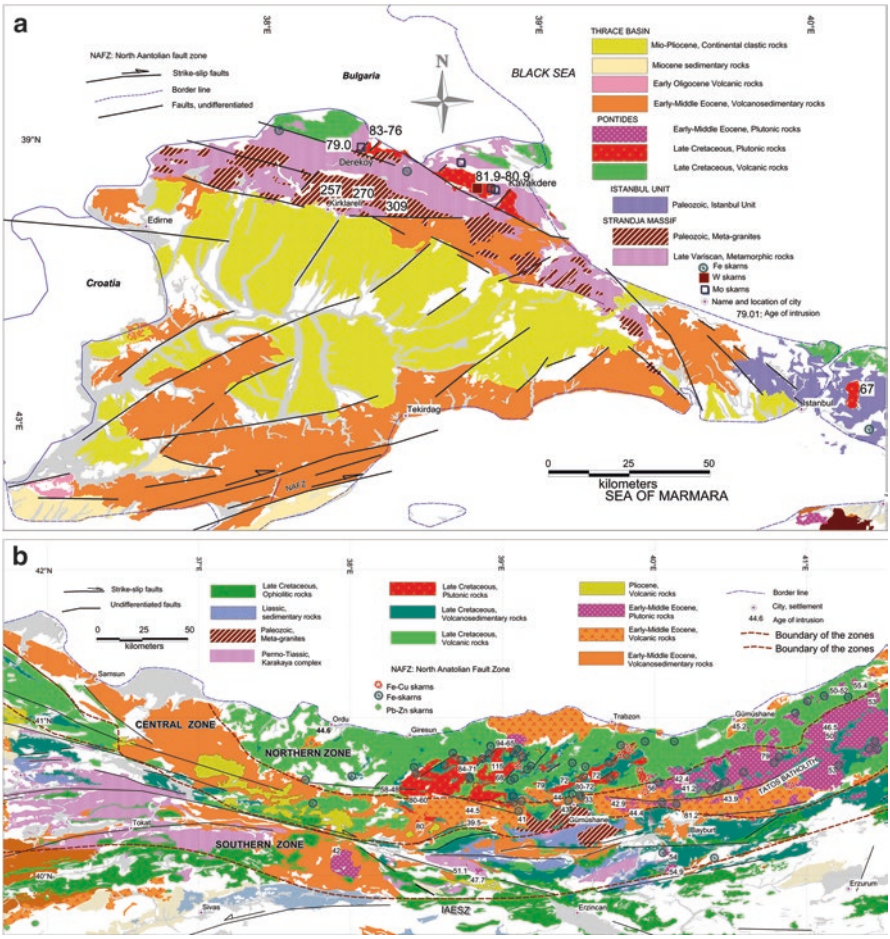

Fig. 7.2 Simplified geological map of (**a**) western (Strandja Massif) and (**b**) eastern Pontides, showing the major magmatic phases and associated skarns. (Modified from Kuşcu et al. 2018) (*NAFZ* North Anatolian fault zone, *IAESZ* Izmir-Ankara-Erzincan suture zone)

northeast-elongated intrusions (Moore et al. 1986; Aslan 2005; Yılmaz-Şahin 2005; Boztuğ et al. 2006) emplaced into the lower parts of the volcanic sequences in the eastern Pontides and the metamorphic basement rocks in the Strandja terrane (Figs. 8.2A and 8.2B).

Eocene volcanic and plutonic rocks are widely exposed in the eastern Pontides (Figs. 8.2A and 8.2B). Eocene volcanic rocks are mostly andesite to dacite in composition and occur as domes and lavas and associated pyroclastic and volcaniclastic rocks (Aslan 2010; Kaygusuz et al. 2011; Temizel and Arslan 2009). These rocks erupted synchronously with deposition of Eocene sedimentary sequences unconformably overlying Late Cretaceous intrusive rocks (Okay et al. 1997; Rice et al.

2009; Temizel and Arslan, 2009; Aslan, 2010; Kaygusuz et al. 2011). Numerous small to large ellipsoidal Eocene plutons (Akıncı, 1984) are elongated in NE direction parallel to major faults (Fig. 7.2b). The skarns in the eastern Pontides are commonly associated with Eocene intrusive rocks particularly they are emplaced into sedimentary sequences and/or older metamorphic sequences.

7.2.1.2 Central Anatolian Crystalline Complex/Kirsehir Massif

The Central Anatolian Crystalline Complex (CACC; Göncüoglu et al. 1991) is part of Tauride-Anatolide Block. It is separated from the main trunk of the Anatolides by the Tertiary Tuzgolü and Ulukisla Basins. The CACC is bounded to the north by ophiolitic slivers of the IAESZ (Fig. 7.3). Its southern boundary is covered by

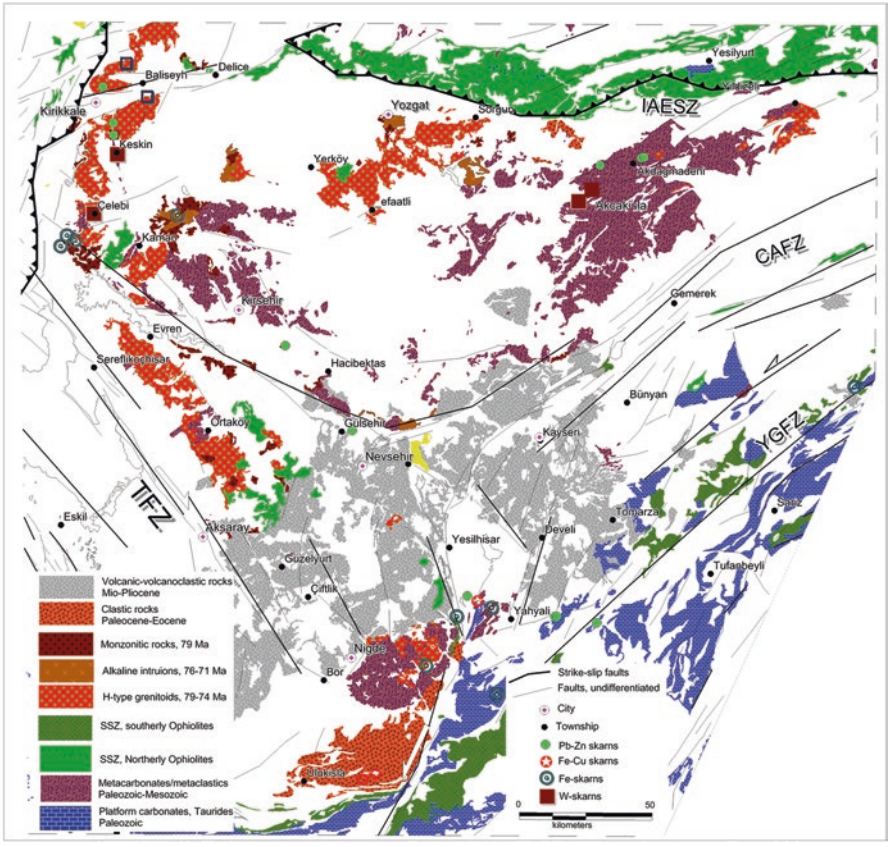

Fig. 7.3 Simplified geological map of central Anatolian crystalline Complex (CACC) showing major magmatic phases, metamorphic rocks and associated skarns. (Modified from Kuşcu et al. 2018) (*TFZ* Tuzgolu fault zone, *YGFZ* Yakapinar-Goksu-Sariz fault zone, *CAFZ* central Anatolian fault zone)

Tertiary sedimentary rocks of Tuzgolü, Ulukisla and Sivas Basins (Fig. 7.3). It consists of Kırşehir and Niğde metamorphic massifs, ophiolitic nappe piles, and felsic granitoids. The rocks at both massifs are medium- to high-grade metamorphic rocks (mainly metacarbonates and metapelites) of Pre-cambrian to Late Mesozoic age (Göncüoğlu et al. 1991) (Fig. 7.3). It is suggested that the pre-metamorphic stratigraphy of CACC is comparable to Tauride-Anatolide Platform (Göncüoglu et al. 1991). The metamorphic rocks consisting of migmatite, paragneisses with minor marbles and amphibolites are included in the Gümüşler metamorphics; thinly bedded package of marbles, quartzites, micaschists and amphibolites are included in Kaleboynu metamorphics overlain by a thicker layer of marble/dolomitic marble with thin amphibolite and quartzite interbeds included in Aşıgediği metamorphicss. These metamorphic sequences are overlain by metaophiolites, ophilitic rocks of Late Cretaceous age and both are intruded by S-to I-type granitoids. These ophiolites are slivers or packages of supra subduction zone ophiolites once developed and emplaced southward during the closure of the Vardara or Izmir-Ankara-Erzincan ocean to the north. The southward emplacement of the ophiolitic nappes after final suturing of Tauride-Anatolide Block with Pontides, resulted in crustal thickening and high grade metamorphism of protoliths of CACC. The metamorphism varies from greenschist to granulite facies and is of high-temperature-medium/low-pressure type. Whitney and Dilek (1998) estimated near-peak P-T conditions at around 5–6 kbar and >700 °C in garnet-sillimanite paragneisses of the Gümüşler metamorphics, the results of garnet-biotite thermometry suggesting temperatures in the range of 680–780 °C. The age of regional metamorphism, although widely accepted as Late Cretaceous, is constrained mostly by U-Pb geochronology on zircon and monazite. The U-Pb geochronology yielded an age range between 91 and 84 Ma (Göncüoğlu 1986; Whitney et al. 2003; Whitney and Hamilton 2004).

The magmatic rocks in the CACC are mainly of I-S- (H-) and A-type type granitoids formed during the early collisional and metamorphic, and post-collisional periods. The early magmatic phase is the represented by S-type two mica granites, Uckapili granitoid in the Nigde massif and some granitoids in the Yozgat batholith. This type is mainly granite to granodiorite in composition. I- and H-type granitods are relatively younger and have textural, geochemical and mineralogical features suggesting varying degrees of mixing/mingling of mafic and felsic magmas. These graniotoids are largely monzonite, monzodiorite, quartz monzonite to granodiorite in compostion. The A-type granitods are the youngest phase in the CACC, and are syenite, syenite porphyry and aplitic syenite in composition.

7.2.1.3 Western Anatolian Province

The western Anatolian province (WAP) in west-northwest Turkey is bounded in the north by the Sea of Marmara, in the west by the Aegean Sea and in the south by the Menderes massif (Fig. 7.4). It represents the western end of the Sakarya terrane and Tauride–Anatolia Block (Fig. 7.4). The WAP is characterized mainly by Tertiary magmatic-sedimentary rocks and metamorphic core complexes underlain by

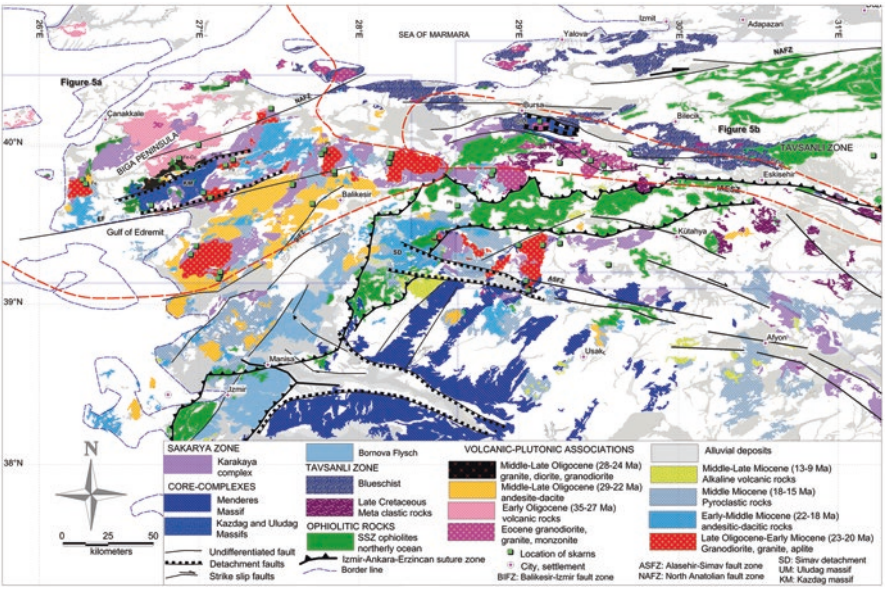

Fig. 7.4 Simplified geological map of western Anatolia province showing major magmatic phases and associated skarns. (Modified from Kuşcu et al. 2018) (*EF* Edremit fault)

Paleozoic and Mesozoic metamorphic rocks. The metamorphic rocks as basement rocks to the Tertiary sequences include parts of the Karakaya complex, Tavşanlı zone, and İzmir-Ankara Erzincan Suture Zone (IAESZ), amalgamated during early Tertiary collisions across the NeoTethys. The metamorphic rocks are intruded by Tertiary plutons and overlain by easterly to northeasterly trending structural basins filled with Tertiary sedimentary and volcanic rocks (Fig. 4). Normal and low-angle detachment faults striking in E-W to NE directions traverse the whole province. These faults form northward tilted fault-bounded horst-graben or half-grabens that accommodated the sedimentary sequences and volcanic successions. The province is currently undergoing a north–south directed extensional strain above the Hellenic-Aegean subduction zone (McKenzie 1972; Le Pichon and Angelier 1979).

The Karakaya complex (Fig. 7.1) is a composite continental block included in the Sakarya terrane. It consists of a Pre-Cambrian-Triassic metamorphic basement, Permo-Carboniferous sedimentary rocks (Fig. 7.4) and Permo-Triassic ophiolitic and accretionary-type mélange units (Okay et al. 1996; Göncüoğlu et al. 2004; Okay and Göncüoğlu 2004). The metamorphic core complexes include the Kazdağ massif in the north, Uludağ massif in the east and Menderes massif in the south (Fig. 7.4). The northeast-trending Kazdağ massif (Schuiling 1959; Okay et al. 1996; Pickett and Robertson 1996; Okay and Satır 2000) is correlated with the Rhodope crystalline complex in northern Greece and Bulgaria (Papanikolaou and Demirtaşlı 1987). The metamorphic rocks in the Kazdağ and Uludag massifs are intruded by undeformed Late Oligocene to Oligo-Miocene granitoids from which W and Fe-Cu skarns (Table 7.1) and porphyry intrusions around Halilağa and Ağıdağ were

Table 7.1 Host rocks, causative plutons, mineralogy, characteristic features and ages of skarn in Turkey

Skarn type	Location N	Name	Host rock	Associated igneous rock	Composition	Age of magmatism	Prograde minerals	Retrograde minerals	Ore minerals	Grade	Accompanying metal	X coordinate	Y coordinate
Skarns in Tavsanli zone and Menderes Massif													
Mo	Bursa	Saricayir	Marble and schist intercalations	Topuk pluton	Granodiorite	43–45 Ma	ad, gr, sc, wo	ep, chl, qt	Mg, hm, ccp, Mo	n.s.	Mo, Au	719270	4424404
Mo	Bursa	Yelekkkaya	Triassic Taşrası Marble	Topuk pluton	Granite, granodiorite		ad, gr, hd, hb, wo	ep, cc, qt	Mo, sch, mg	0.1-02%Mo	Cu	694562	4418680
Mo	Bursa	Muratdere	Paleozoic meta-carbonate	Muratdere pluton	Q-diorite, granodiorite	43–45 Ma	ad, hd, sc, wo	ep, ch	ccp, mo	0.36% Cu, 0.0125% Mo	Au	752664	4420549
Mo	Bursa	Demirtepe	Silurian schist, Permain marble	Demirtepe pluton	Granodiorite, diorite, monzodiorite	Middle Eocene	ad, gr, wo, hd, di, sc	ep, ch, cc, qt		n.s	Au, Fe, Wo	723565	4423044
Fe-Cu	Bursa	Kozbudaklar	Mesozoic İnönü marble,	Topuk pluton	Monzodiorite, granodiorite	45 Ma	ad, di, hd, wo	ep, ch, cc, qt	mg, ccp, sch	0.3% WO3	Mo	681124	4428415
W	Bursa	Uludag	Metacarbonates in Uludag masssif	Uludağ pluton	Granite, granodiorite	28–32 Ma	wo, ad, gr, cpx	ep, ch, cc, qt	sch	0.437 % WO3	Fe, Cu	685683	4440037
W	Balıkesir	Susurluk	Mesozoic carbonates	Çataldağ granite	Granite, granodiorite, syenogranite	20–25 Ma	hd, pl, tt in endoskarns, gr, py, wo, sc	ch, ep, qt, cc	sch, ccp, mo	n.s	n.s	612568	4410148
Fe	Kutahya	Kureci	Pelitic schist and carbonates of Sarıcasu formation	Eğrigöz pluton	Granodiorite, monzonite	20 Ma	ad (95–99), gr, di, hd, sc	ep, cc, tr,	mg, hm, py, cp, asp, po	50%	Cu	685212	4359833
Fe	Kutahya	Catak	Pelitic schist and carbonates of Sarıcasu formation	Eğrigöz pluton	Granodiorite	20 Ma	ad (97–99), gr, di, hd, wo	ep, cc, qt, ch	mg, spc, ccp, py	50%	Cu	672289	4359536
Fe	Kutahya	Kalkan	Metasedimenats and marble lenses in Simav metamorhics	Eğrigöz pluton	Granodiorite, monzonite	20 Ma	ad, gr, di, hd	ep, cc, tre	mg, hm, ccp	50%	Cu	678300	4328100

(continued)

Table 7.1 (continued)

Skarn type	Location N	Name	Host rock	Associated igneous rock	Composition	Age of magmatism	Prograde minerals	Retrograde minerals	Ore minerals	Grade	Accompanying metal	X coordinate	Y coordinate
Fe	Kutahya	Karaağıl	Metasedimenats and marble lenses in Simav metamorhics	Eğrigöz pluton	Granodiorite, monzogranite	20 Ma	di, hd	n.s	mg, hm, py, pyr	49%	n.s	683710	4344044
Pb-Zn	Uşak	Baklan	Metasedimenats and marble lenses in Simav metamorhics	Baklan granite	Granodiorite, monzogranite	19 Ma	ad, wo, act, pyx	ep, cc, qt	sp, ga, py, ccp	n.s	Cu	736500	4309390
Skarns in biga Peninsula													
Fe,Cu	Balikesir	Ayazmant	Metapelitic rock, metacarbonates, Karakaya	Kozak pluton	Granodiorite, monzonite	18–20 Ma	Di, sc, ab, ad,	ep, act, ch, cc, qt, ph	mg, hm, ccp, py	51.02%	Cu, Au	511624	4338770
Pb-Zn	Balıkesir	Sağırlar	Paleozoic schist-marble in Simav metamorphics	Alaçam granite	Granite, granodiorite	Paleosen-Eosen	wo, gn, pyx	ep, cc, qt	sp, ga	16.95–1.69 %	Cu	631270	4371310
Fe	Balikesir	Yasyeri	Meta pelitic rocks, carbonate lenses	Eybek pluton	Granite, granodiorite	23–26 Ma	di, hd	ep, cc	mg, hm, ccp, py, sp, ga	30–50%	Cu	506000	4390600
Pb-Zn	Balikesir	Bağırkaç	schist with metacarbonate lenses in Karakaya complex	Eybek pluton	Granite, granodiorite	23–24 Ma	Wo, ad, gr, di, h sc	cc, tr	sp, ga, hm, py	10% Pb+Zn	Cu	519986	4398456
Pb,Zn	Balikesir	Kulatçiftliği	Kayacıklar limestone	Çataldağ granite	Granite, granite porphyry	Oligocene	Jo, hd, gr	ep, cc, ch	ga, sp	1–2%	Cu	644858	4357146
Fe	Balikesir	Şamlı	Karakaya complex	Şamlı pluton	Granodiorite, diorite, granite porphyry	23 Ma	ab, sc, ph, ad, hd	act,ep, cc, tr	mg, hm	58.5%	Au, Cu	572500	4407500
Fe,Cu	Canakkale	Evciler	Metamorphics of Kazdag massif	Evciler pluton	Granodiorite, qtz diorite	26 Ma	ad, di	ep, cc, tre, ch, qt	mg, hm, ccp, pyr	52%	Au, Cu	485000	4401000

Pb,Zn	Canakkale	Bergaz	Permian limestones in Bozalan formation	Kestanbol pluton	Monzodiorite, granodiorite	19 Ma	ad, jo, di, hd	ep, cc, ch	mg, hm,	49.98%	Fe	437486	4403385
Fe,Cu,Pb	Canakkale	Uskufcu (Aladag)	Permian, Bozalan carbonates	Kestanbol pluton	Monzonite, qtz monzonite	19 Ma	di, gro, fo	ep, tr, act	gal, sph, mg, ccp	n.s	Pb-Zn	438349	4407302
Fe,Cu	Canakkale	Bakırlık	Oligocene sedimentary rocks	Halilaga subvolcanic domes	Diorite porphyry	26 Ma	gn, hd	ep, ch, act	ccp, mg	n.s	Fe	482380	4419266
Pb,Zn	Canakkale	Handere	Metacarbonates in Kazdag massif	subvolcanic andesitic rocks	Andesite porphyry	Oligocene	gn, jo	ep, cc, qt	sp, ga,	3.25% Pb, 1.75% Zn	Cu	518553	4401550
Pb,Zn	Canakkale	Karaaydın	Metacarbonates in Kazdag massif	Eybek pluton, subvolcanic andesitic rocks		Oligocene	wo, di, hd, ad, gr	ep, ch, cc, qt	ga, sp, py, pyr	8.48% Pb+Zn	n.s	518300	4404200
Fe	Istanbul	Soganlik	Paleozoic meta-carbonate	Soganlik pluton	Granite, granodiorite	Late Cretaceous	gr, an, hd	ep, ch	mt, hm	63.4% Fe	n.s	686915	4533148
Skarns in Western Pontides													
Cu,Mo	Kirklareli	Demirkoy	Jurassic Dolapdere formation, dolomitik limestone	Demirköy pluton	Diorite, granodiorite	Ar-Ar, 80.94±0.57	di, sc, gro, ad, wo, vs	ep, act, ch, qt, cc	mg, ccp, W, Mo	% 0.3–0.4Cu, %56 Fe Cu	Mo	568934	4629911
Fe, Cu, Mo	Kirklareli	Dereköy	Meta dolomitik limestone, calc-schist	Dereköy pluton	Diorite, qtz diorite	Ar-Ar, 79.01	di, sc, gn, en	ph, ep, act	mg, ccp, sph, ga, en, mo, sch, Au,bo,hm, tt, Ag	0.25–	Mo	543147	4636370
Cu, Mo, Fe	Kirklareli	Şükrüpaşa	Jurassic dolomite, calc-schist	Şükrüpaşa pluton	Qtz diorite, granodiorite	Ar-Ar, 77.64±0.51	di, sc, gro, ad, wo, vs	ep, act, ch, act, qt, cc	mg, ccp,Mo, en, bi, sph	0.4	Mo	542163	4643523
Cu-Mo-W	Kirklareli	Ikiztepe	Dolomitik	Demirköy pluton	Diorite, granodiorite	Ar-Ar, 80.94±0.57	di, hd, ad, gro,bt	ep, act, ch, qt, cc	ccp, bo, Mo, sch	0.5 %	Mo	575228	4637631
Cu-Mo	Kirklareli	Kavakdere	Calc-schist, sichst	Demirköy pluton	Diorite, granodiorite	Ar-Ar, 80.94±0.58	di, hd, ad, gro,bt	ep, act, ch, qt, cc	py, pyr, ccp, mo, tt	none	Mo		

(continued)

Table 7.1 (continued)

Skarn type	Location N	Name	Host rock	Associated igneous rock	Composition	Age of magmatism	Prograde minerals	Retrograde minerals	Ore minerals	Grade	Accompanying metal	X coordinate	Y coordinate
Skarns in Eastern Pontides													
Pb,Ag,Au	Çorum	Gumushacikoy	Late Cretaceous volcanoclastic rocks	Eocene subvolcanics	Dacite porphyry	Middle Eocene	gn, pyx	ep, cc, qt	gal, sph	5.34%Pb	n.s	683712	4526402
Fe	Bolu	Fulusulvi (Yukari Camli Koyu), Yukari Holoz			Dacite porphyry	Late Cretaceous	n.s	n.s	mg, sp	56%	Cu	399200	4517800
Fe	Ordu	Kertilyayla	Middle Eocene volcanosedimentary rocks	Middle Eocene plutons	Diorite, granodiorite	Middle Eocene	gn, pyx	ch, ep, qt		mg	n.s	390392	4498040
Fe	Ordu	Cambasi Yayla	Dacite, volcanoclastics intercalated with limestone	Çambaşı granitoid	Monzonite, monzodiorite	Middle Eocene	gn (Gr92), di	ep,cc, qt, act		45%	SiO2	416131	4500313
Fe	Rize	Aslandere	Volcanoclastics intercalated with limestone	Dacitic intrusions	Dacite porphyry	Late Cretaceous	gn, gro, di	ep, cc, qt	mg, hm	45.8%	n.s	690598	4560095
Cu,Fe	Gumushane	Egrikar	Late Cretaceous carbonates	Eğrikar granitoid	Granodiorite, granite	Eocene?	di, gn, hd	act, ep, tr, qt	ccp, mg	2.45%	Fe	485105	4492665
Fe,Cu	Trabzon		Late Cretaceous dolomite	Camibogazi pluton	Diorite, monzodiorite, monzogranite	Late Cretaceous	ad, vs, ph	act, tr, ep, qt	mt, ccp, py	43.86%	n.s	559065	4494033
Fe	Gumushane	Camibogazi	Late Cretaceous dolomitic limestone	Zigana granitoid	Diorite, monzodiorite, monzogranite	76–74Ma	di96, ad, ph	act, ep, tr, qt	mt, hm	n.s	n.s	513726	4504783
Zn,Cu	Gumushane	Kiran Maden	Late Cretaceous carbonates	Zigana granitoid	Granite, granodiorite, syenogranite	Late Cretaceous	cpx, gn	ep, cc, qt	ccp, ga	n.s	Pb	508446	4507102

Cu,Pb,Zn	Gumushane	Deremaden & Kurumaden	Late Cretaceous volcanoclastic sequence with limestone intercalations	Late phase Pontide intrusives	Diorite, qtz diorite	Late Cretaceous	cpx, gn	ch, ep, cc, qt	ccp, hm, py, sp	7.18%	Zn	506788	4511448
Fe	Giresun	Kurtulmuş	Pre-Liassic Kotana metamorphics	Dereli granitoid	Granite, granodiorite	Middle Eocene?	gn (Ad47), di	act, cc, qt	mg	53–57%	n.s	450869	4506434
Fe,S	Giresun	Kiran Maden	Jurassic clastics and limestone	Late phase Pontide intrusives	Granite, q-diorite	Late Cretaceous	gn (gro), pyx	act, ep, tr, qt	mg, hm	3%	Fe	467906	4507533
Fe	Giresun	Olucaktepe	Volcanoclastics intercalated with limestone	Late phase Pontide intrusives	Granite, granodiorite	Late Cretaceous	gn, pyx	ep, ch	mg, hm	n.s	n.s	477041	4511436
Fe,Cu	Giresun	Hukala Maden	Volcanoclastics intercalated with limestone	Late phase Pontide intrusives	Granite, granodiorite	Late Cretaceous	act,wo, gn	ep, qt, cc	mg, hm, ccp	n.s.	Cu	501200	4511593
Fe,Cu	Giresun	Keltas guney	Jurassic clastics and limestone	Late phase Pontide intrusives	Granite, granodiorite	Late Cretaceous	gn, pyx	ep, ch	mg, hm, ccp	n.s.	Zn, Cu	503216	4513003
Cu	Giresun	Armutlu	Jurassic clastics and limestone	Late phase Pontide intrusives	Granite, granodiorite	Late Cretaceous	gn, pyx	ep, ch	mg, hm, ccp	n.s.	Zn, Cu	509575	4514612
Fe,Cu	Giresun	Eskimaden	Volcanoclastics intercalated with limestone	Late phase Pontide intrusives	Grantic dikes and plugs	Late Cretaceous	act,wo, gn	ep, qt, cc	mg, hm, ccp	n.s.	Cu	491611	4518972
Fe	Giresun	Dereiçi	Volcanoclastics with recrystallized limestones		Dacite porphyry	Late Cretaceous	gn, pyx	ch, cc, qt	mg, hm	40%	Cu	508030	4519350
Fe,Cu,Pb	Giresun	Atmacik	Volcanoclastics intercalated with limestone	Late phase Pontide intrusives	Granite, granodiorite	Late Cretaceous	gn, pyx	ep, cc, ch	mg, hm	n.s	Cu	494585	4519707

(continued)

Table 7.1 (continued)

Skarn type	Location N	Name	Host rock	Associated igneous rock	Composition	Age of magmatism	Prograde minerals	Retrograde minerals	Ore minerals	Grade	Accompanying metal	X coordinate	Y coordinate
Fe,Cu,Zn	Giresun	Dongüldere	Volcanoclastics intercalated with limestone	Late phase Pontide intrusives	Granite, granodiorite	Late Cretaceous	di, ad, fo	cc, qt	mg, ccp	n.s	Cu	493620	4520215
Cu, Fe	Giresun	Seku	Volcanoclastics intercalated with limestone	Late phase Pontide intrusives	Granite, granodiorite	Late Cretaceous	ad, act	tr, cc, cc, qt	sp, ccp,	n.s	Cu	493373	4521648
	Giresun	Kelete										507903	4522934
Fe	Trabzon	Asokoy	Volcanoclastics intercalated with limestone	Eocene volcanics	Andesite	Middle Eocene	cpx	ep, ch	mg	n.s	Cu	595210	4525839
Cu	Trabzon	Ayman	Volcanoclastics intercalated with limestone	Eocene volcanics	Andesite	Middle Eocene	cpx	ep, ch	ccp	upto 1.1%	Au	579487	4488379
Fe,Cu,Zn	Trabzon	Bogali	Limestone intercalated with volcanic rocks	Eocene subvolcanic rocks	Dacite porphyry	Middle Eocene	gn, cpx	ch, tr, ep	mg, ccp, hm	22.6%	Cu	584924	4491354
Fe,Cu	Trabzon	Gunbuldu	Volcanoclastics intercalated with limestone	Late phase Pontide intrusives	Granite, granodiorite	Late Cretaceous	gn, pyx	ep, cc, ch, qt	mg, gt	n.s	Cu	598199	4492042
Fe,Cu	Trabzon	Gebe Yayla	Volcanoclastics intercalated with limestone	Late phase Pontide intrusives	Granite, granodiorite	Late Cretaceous	cpx, gn	ep, cc, qt	mg, gt	39.58%	Cu	580659	4492401
Fe,Cu,Zn	Trabzon	Asot Yayla	Volcanoclastics intercalated with limestone	Late phase Pontide intrusives	Granite, granodiorite	Late Cretaceous	di, gn, hd	ep,tr, ch, qt	mg, hm, ccp, mlc	20%	Cu	587280	4493032
Fe	Trabzon	Arpaozu	Volcanoclastics intercalated with limestone	Late phase Pontide intrusives	Granite, granodiorite	Late Cretaceous	gn, cpx	ep, ch		n.s.	n.s	620080	4493629

Cu	Trabzon	Bahcecik	Volcanoclastics intercalated with limestone	Late phase Pontide intrusives	Granite, granodiorite	Late Cretaceous	cpx, gn	ep, cc, qt	ml, gt	n.s.	n.s	584155	4493427
Cu,Pb,Zn,Mo	Trabzon	Atalar (Zimera)	Volcanoclastics intercalated with limestone	Late phase Pontide intrusives	Granite, granodiorite	Late Cretaceous	gn, pyx	ch, cc, qt	mg, hm	130–200 ppm	Pb	536100	4493700
	Trabzon	Tapanoz Yayla	Volcanoclastics intercalated with limestone	Kaçkarbatolith	Monzosyenite, monzodiorite	Middle Eocene	gn, pyx	ep, cc, ch	mg	n.s	n.s	615789	4490134
Fe	Trabzon	Arpali	Volcanoclastics intercalated with limestone	Late phase Pontide intrusives	Granite, granodiorite	Late Cretaceous	gn, pyx	ch, cc, qt	mg,hm	33.5%	n.s.	587080	4495866
Cu,Fe	Trabzon	Derebasi	Volcanoclastics intercalated with limestone	Late phase Pontide intrusives	Granite, granodiorite	Late Cretaceous	gn, pyx	ep, cc, ch	mg, gt, ml	n.s.	Cu	599702	4496210
Fe	Trabzon		Volcanoclastics intercalated with limestone	Late phase Pontide intrusives	Granite, granodiorite	Late Cretaceous	cpx, gn	ep, cc, qt		54.75%	SiO2	559891	4498105
Cu,Zn,Fe	Trabzon	Koprubasi, B. Ayven	Volcanoclastics intercalated with limestone	Late phase Pontide intrusives	Granite, granodiorite	Late Cretaceous	gn, pyx	ep, ch		1.5%	Zn	580149	4498669
Fe	Trabzon		Jurassic volcanics	Late phase Pontide intrusives	Qtz diorite, granodiorite	Late Cretaceous	cpx, gn	ep, cc, qt	mg, spc, ml	39.65%	Cu	545054	4499286
Cu,Fe	Trabzon	Ciftepinar	Jurassic volcanics	Late phase Pontide intrusives	Diorite, granodiorite	Late Cretaceous	cpx	ep, cc, qt	hm, ml, ccp, mg	47.28%	Fe	576879	4500752
Cu,Fe	Trabzon		Limestone intercalated with volcanic rocks	Eocene subvolcanic rocks	Dacite porphyry	Middle Eocene	gn, cpx, act	ep, cc, qt, chl	mg, ccp, hm	47%	Cu	556420	4501890
Fe	Trabzon		limestone in volcanics	Late phase Pontide intrusives	Granodiorite, diorite	Late Cretaceous	gn	ep	mg, hm	n.s	n.s	546032	4506851

(continued)

Table 7.1 (continued)

Skarn type	Location N	Name	Host rock	Associated igneous rock	Composition	Age of magmatism	Prograde minerals	Retrograde minerals	Ore minerals	Grade	Accompanying metal	X coordinate	Y coordinate
Fe	Trabzon	Kuruyayla	Volcanoclastics intercalated with limestone	Late phase Pontide intrusives	Diorite, granite	Late Cretaceous	cpx, gn	ep, cc	mg, hm	n.s	n.s	538797	4509655
Fe	Trabzon	Camii	Volcanoclastics intercalated with limestone	Late phase Pontide intrusives	Granite, granodiorite	Late Cretaceous	gn,hd	ep, cc, qt	mg, hm	n.s	n.s	565573	4522621
Fe	Trabzon		Volcanoclastics intercalated with limestone	Late phase Pontide intrusives	Granodiorite, diorite	Late Cretaceous	gn, cpx	ch, ep, tr	mg, hm	n.s	n.s	559131	4509868
Cu,Fe	Trabzon	Ocak	limestone in volcanics	Late phase Pontide intrusives	Granite, granodiorite	Late Cretaceous	cpx	ep	ccp, mg	0.81%	n.s	568790	4514727
Cu	Trabzon	Gavran Mah.	Volcanoclastics intercalated with limestone	Late phase Pontide intrusives	Granite, granodiorite	Late Cretaceous	gn, cpx	ep	ccp, mg	n.s	n.s	568880	4521098
Fe	Rize	Gabahor	Volcanoclastics intercalated with limestone	Late phase Pontide intrusives	Granite, granodiorite	Late Cretaceous	cpx	ch, ep	mg	n.s.	n.s.	633940	4503861
Fe	Rize	Kirechactepe	Volcanoclastics intercalated with limestone	Late phase Pontide intrusives	Granite, granodiorite	Late Cretaceous	cpx, gn	ep, cc, qt	mg, sp, hm	55%	SiO2	653647	4515663
Fe	Rize	Akkaya	Volcanoclastics intercalated with limestone	Late phase Pontide intrusives	Granite, granodiorite	Late Cretaceous	gn, cpx	ch, ep, tr	mg, hm	42.15%	SiO2	668265	4556394
Fe	Rize	Ortaalan	Volcanoclastics intercalated with limestone		Granodiorite	Late Cretaceous	cpx	ep, ch, qt	mg, hm, sp pyr, ccp	n.s	n.s	668265	4556394

Fe	Rize	Avupdağ	Volcanoclastics intercalated with limestone		Granodiorite	Middle Eocene	gn, hd	ep, ch	mg, hm	31.63%	n.s	647500	4547691
Fe	Rize	Kartiba	Jurassic volcanics	Late phase Pontide intrusives	Diorite, granodiorite	Late Cretaceous	cpx, gn, hd	ep, cc, qt	hm, ml, ccp, mg	45.8%	n.s	690598	4560095
Fe	Bayburt	Suryayla	Limestone	Sorkunlu pluton	Granite, granodiorite	Middle Eocene	gn, hd	ep, ch,	mg, hm	n.s	n.s	597906	4479991
Fe	Bayburt	Suryayla	Limestone in volcanics	Sorkunlu pluton	Granodiorite, diorite	Middle Eocene	cpx, gn, hd	ep, ch,	mg, hm	n.s	n.s	588819	4481383
Fe	Bayburt	Saraycık	Pulur metacarbonate	Saraycık granite	Granodiorite, diorite	Ar-Ar bt, 52	gn, cpx, ab	ep, ch, act	n.s	n.s	nome	590171	4445651
Fe	Artvin	Cucebag	Volcanoclastics intercalated with limestone	Yusufeli pluton	Monzonite, monzodiorite	Middle Eocene	cpx, gn	ep, ch, cc	mg	n.s	n.s	686698	4509899
Fe	Artvin	Peterek	Volcanoclastics intercalated with limestone	Yusufeli pluton	Monzonite, monzodiorite	Middle Eocene	gn,hd	ep, cc, qt	mg, hm	n.s	n.s	707993	4522415
Fe	Artvin	Mindor	Limestone in volcanics	Yusufeli pluton	Monzonite, monzodiorite	Middle Eocene	gn, cpx, ab	ep,ch	mg	54%	n.s	703263	4522381
Fe	Artvin	Sogukpinar	Limestone in volcanics	Yusufeli pluton	Monzonite, monzodiorite	Middle Eocene	gn, hd	ep,tr, ch, qt	mg, hm	44.8%	n.s	706383	4527913
Skarns in CACC													
Fe	Ankara	Madentepe	Limestone blocks within ophiolitic melange	Kesikköprü pluton	Granodiorite	79 Ma	di, hd, an, ph	ep, tr, ch	mg, hm, ccp	40.9–54.8%	Cu	532750	4355750
Fe	Ankara	N of Bayindir	Metacarbonates in Asigedigi metamorphics	Bayındır pluton	Senite porphyhry	69–71 Ma	hd, cpx	ep, ch, cc, qt	mg, hm	52%	n.s	576251	4369233

(continued)

Table 7.1 (continued)

Skarn type	Location N	Name	Host rock	Associated igneous rock	Composition	Age of magmatism	Prograde minerals	Retrograde minerals	Ore minerals	Grade	Accompanying metal	X coordinate	Y coordinate
Fe	Ankara	East of Kesikkopru	Metacarbonates in Asigedigi metamorphics	Kesikköprü pluton	Quartz diorite, granite	Late Cretaceous	hd, ad, act	ep, ch, tr, ccc	mg, hm	50%	n.s	538820	4358440
W	Kirikkale	Denek	Metacarbonates in Asigedigi metamorphics	Keskin pluton	Granite	Late Cretaceous	Jo, hd, gro	ep, tr, cc	ga, sph, wt, ccp	%37.3 Pb, %0.91 Zn%	Zn	545000	4368500
Fe	Kirsehir	Celebi	Metacarbonates in Asigedigi metamorphics	Çelebi pluton	Granodiorite, diorite	75–79 Ma	hd, ad	ep, ch, qt	mg, hm, sp, ccp	54%	Cu	541005	4368284
Fe	Kirsehir	Buguz	Metacarbonates in Asigedigi metamorphics			Late Cretaceous	hd, ad, act	ep, ch, tr, ccc	mg, hm	20–55%	n.s	537813	4358317
Pb	Nevsehir	Acioz	Metacarbonates in Asigedigi metamorphics	İdişdağ pluton	Syenite porphyry	Late Cretaceous	gn, cpx	ep, cc, qt	sp, ga	5–12%	n.s	618586	4320791
Pb,Zn,W	Yozgat	Akcakisla	Schist-marble in Kaleboynu metamorphics	Akçakışla granite	Granite	Late Cretaceous	di-hd-ad>gro	ep-tr-cc-qt	sp, ga, ccp, ml	7.5%	Zn	730281	4381035
Pb,Zn,Ag	Yozgat	Akdagmadeni	Schist-marble in Kaleboynu metamorphics	Yozgat batholith	Granite, granodiorite	Late Cretaceous	jo, hd, gro, ad	ep-tr	sp, ga	6.2%	An, Ag	750437	4396109
Pb,Zn	Yozgat	Karapir Koyu	Schist-marble in Kaleboynu metamorphics	Yozgat batholith	Granite, granodiorite	Late Cretaceous	jo, hd, gro, ad	ep-tr		22.3%	Zn	751450	4396400
Fe	Kayseri	Kovali	Permian carbonates in Aladag formation	Karamadazı pluton	Granite, q-diorite	48–52 Ma	gro, hd	tr, ep, qt	sp, ga	n.s	Zn	686718	4221066

Fe,Py	Kayseri	Karamadazi	Permian carbonates in Aladag formation	Karamadazı pluton	Granodiorite, qtz diorite	48–52 Ma	ad, gro, hd	act, tr, ep, qt	mg, hm, ccp, mlc	54.46%	Cu, au	699787	4224708
Fe, Cu	Nigde	Elmali	Reefal limestone in Ulukisla volcanics	Çiftehan syenite	Syenite, monzonite	Eocene?	gn, pyx	ep,cc, qt, act	mg, hm	50%	Cu, Au, Co	652493	4156044
Skarns in SEAOB													
Fe	Sivas	Dumluca	Recrystallized limestone blocks in ophiolitic melange			75 Ma	ad, gro, sc, hd, ol, tt	ep, cc, qt, cc	mg, hm, sph, pyr, ccp	54–55%		414600	4356900
Fe	Sivas	Calti	Munzur limestones in Keban metamorphics	Çaltı pluton	Diorite, qtz diorite	48 Ma	ad, sc, bt, ol, tt	ep, act, cc, ch	mg, hm, sph, pyr, ccp	52–55%	Cu	444008	4357830
Fe	Erzincan	Bizmisen	Munzur limestones in Keban metamorphics			48 Ma	ph, di, ad, gro	ep, act, cc, ch	Mg, hm	53%	Cu, Mn	453601	4354290
Fe	Erzincan	Kurudere	Munzur limestones in Keban metamorphics			48 Ma	ph, di, ad, gro	ep, act, cc, ch	Mg, hm	62–52%	Cu, Mn	444033	4357322
Fe	Elazig	Asvan	Recrystallized limestones in Keban metamorphics	Baskil arc	Diorite, granite	79 Ma	ad, gro, sc, hd, ol, tt	ep, cc, qt	mg, hm, il	54.49%	Mo	498476	4202499
Fe	Malatya	Dedeyazi	Recrystallized limestones in Keban metamorphics	Polat granitoid	Granodiorite, qtz diorite	48 Ma	ad, gro, di, hd, ab, sc	ep, cc, qt, ch		55%	n.s	399850	4230920
Cu,Mn	Erzincan	Çöpler	Recrystallized limestones in Pütürge metamorphics			47–51 Ma	gn, cpx	ep, cc, qt	hematite, pyrolusite	46%	n.s	459200	4364200
Fe	K. Maraş	Çakçak	Recrystallized limestones in Keban metamorphics	Baskil arc	Qtz diorite, granodiorite	82–79 Ma	gn, cpx, act	cc, ch, ep, qt	mg, hm, gt	39–42%	n.s	406053	4206149

(continued)

Table 7.1 (continued)

Skarn type	Location N	Name	Host rock	Associated igneous rock	Composition	Age of magmatism	Prograde minerals	Retrograde minerals	Ore minerals	Grade	Accompanying metal	X coordinate	Y coordinate
Fe-Ti	Tunceli	Tuzbaşı	Recrystallized limestones in Keban metamorphics	Baskil arc	Qtz diorite, gabro, diorite	Middle Eocene?	ad, gro, sc, hd	ep, ch, act	mg, hm, il	n.s	TiO3	506370	4307773
Fe	Tunceli	Demurek	Recrystallized limestones in Keban metamorphics	Baskil arc	Diorite	Middle Eocene?	ad, gro, sc, fo, tt	ep, ch, act, cc	mg, hm, spc, bo,ml, az	60%	Cu	516100	4305052
Fe-Cu	Tunceli	Mamlis-Sin	Recrystallized limestones in Keban metamorphics	Baskil arc	Qtz diorite, gabro, diorite	Middle Eocene?	ad, cpx, di,gro, act	ch, ep, act	ccp, mg, hm	4.52%	Fe	520152	4335046
Pb-Zn	Elazığ	Sarımağara	Munzur limestones in Keban metamorphics	Keban pluton	Syenite, monzonite	70–75 Ma	ad,gro, cpx, di, hd, wo	ep, ch, cc, qt	sph, gal, Ag, sch	4.51 Pb, 5.28% Zn	Mo-W	476782	4294540

Coordinates are in UTM ED 50

bt biotite, *gn* garnet, *il* ilmenite, *go* grossular, *ol* olivine, *ad* andradite, *tt* titanite, *bo* bournite, *vs* vesuvianitbi, bismuth, *sch* scheelite, *cpx* clinopyroxene, *ab* albite, *ep* epidote, *ch* chlorite, *act* actinolite, *ph* phlogopite, *sc* scapolite, *mg* magnetite, *ccp* chacopyrite, *ml* malachie, *az* azurite, *Mo* molybdenite, *W* tungsten, *pnt* pentlandit, *asp* arsenopyrite, *hm* hematite, *gt* goethite, *ga* galena, *sph* sphalerite, *tt* titanite, *en* enargite, *po* pyrrrhotit, *spc* specularite

n.s not specified

sourced. The Uludağ massif, another northeast-trending core complex in Turkey is exhumed along a ductile strike-slip shear zone (Okay et al. 2008). The Uludağ massif contains Oligocene metagranites (Okay et al. 2008), was intruded by the post-kinematic ~33 Ma-age Uludağ granite that also resulted in W-skarns within wollastonite-rich skarns.

The Menderes massif is a polymetamorphosed metamorphic core complex located between Kütahya, Muğla, and Manisa. It was exhumed to the surface in Miocene, and has been overprinted by retrograde metamorphism associated with early Miocene exhumation (Bozkurt and Oberhänsli 2001; Whitney and Bozkurt 2002; Régnier et al. 2003; Rimmelé et al. 2003).

The Tavşanlı zone is a blueschist belt lying south of the ophiolitic rocks, ophiolitic mélanges and SSZ ophiolites within the İzmir-Ankara-Erzincan Suture Zone (Figs. 1 and 4). The blueschist sequence is overlain by ophiolites and ophiolitic mélange. These refer largely to subducted and subsequently exhumed passive continental margin of the Tauride–Anatolide Block (Okay 1984; Okay and Satır 2006).

The İzmir-Ankara-Erzincan suture zone is an east-trending belt of dismembered allocthonous assemblages of ophiolitic nappes and mélanges emplaced onto the Tauride-Anatolia Block and Tavşanlı zone (Figs. 8.1 and 8.4). The ophiolitic rocks, representing fragments of the northerly Vardar ocean, separate the Sakarya terrane to the north from the Tauride-Anatolia Block to the south. It forms the northern boundary between Tauride Anatolide block and Pontides whereas Lycian nappes mark the southern boundary between Tauride Anatolide block and Taurides.

Magmatism in the western Anatolian province shares geochemical and geochronological characteristics similar to that of Rhodope Massif and Thracian area of northern Greece. Overall, the magmatism gets younger from NW to SE or roughly from N to S (Fytikas et al. 1984; Kuşcu et al. 2018), and this is attributed to arc migration from N to south between Late Cretaceous to Tertiary (Fytikas et al.1984). The volcanic rocks are interbedded with or grade into marine and lacustrine-fluvial sedimentary rock sequences within the listric to low angle normal fault-bounded sedimentary basins. The plutonic rocks are exposed as isolated stocks or large batholithic masses commonly on the hanging-wall block of the detachment faults in response to exhumation during superposed extensional strain as the arcs migrated progressively southward (Kuşcu et al. 2018). The plutonic rocks vary in age from Early-Middle Eocene to Oligocene (Kuşcu et al. 2018). The Eocene plutonic rocks are mostly exposed within the Karakaya complex and Tavşanlı zone as elongate to isolated small plutons that form a NE-striking belt with variable diameters ranging between up to 30 km. Whereas Oligocene plutonic rocks are exposed mostly within the Karakaya complex and Menderes massif as large batholithic masses intruding the Oligocene volcanic rock sequences. Both types are associated with Fe- and Fe-Cu skarns, and have genetic connections to porphyry Cu, Cu-Mo systems as well. The volcanic sequences are exposed as NE-trending linear belts that are more or less parallel to the splays of dextral North Anatolian Fault Zone in the Biga peninsula (Fig. 7.4). Younger Oligocene and Miocene volcanic rocks are mostly aligned parallel to İzmir-Balıkesir fault zone, or form northeast-trending belts of that parallel normal and detachments faults in the Biga Peninsula (Fig. 7.4). The youngest

plutonic rock suite is represented by middle to late Miocene alkaline rocks consisting mainly of subvolcanic intrusions of latite porphyry and monzonite porphyry. The monzonitic rocks occur as northerly to northwest-trending dikes or plugs emplaced into the alkaline lava flows and pyroclastic rocks. These intrusions are associated with porphyry and high sulfidation mineralization at Afyon-Sandıklı (AS) and Kışladağ.

7.2.1.4 Southeastern Anatolian Orogenic Belt

The southeastern Anatolian orogenic belt is located to the north of the Bitlis-Zagros suture zone (Figs. 8.1 and 8.5). In this belt, the Arabian Platform is a basement to Late Cretaceous and younger magmatic and sedimentary rocks. It includes early Cambrian to middle Miocene autochthonous and parautochthonous marine rocks deposited on a Pan-African crystalline basement (Perinçek and Kozlu 1984; Yılmaz 1993). This platform is overlain by Bitlis-Pütürge massif, ophiolitic rocks (imbrication zone), and olistostromal and mélange-type rocks along southern-verging thrust sheets (nappe zone). Malatya-Keban metamorphics representing low grade metamorphic carbonate sequences overly the Bitlis-Puturge massif. The Late Cretaceous subduction-related magmatic rocks of Baskil arc are emplaced into the Arabian platform and overlying ophiolitic nappe piles. The Eocene volcanic, plutonic, and sedimentary rocks, and post-Eocene sedimentary rocks represent younger post-collisional, extension related rock units of the belt (Kuşcu et al. 2010). Supra-subduction zone-type ophiolitic rocks and mélange occur as large structurally bounded packages, and thrust southward in the Divriği and Keban areas over platform-type sedimentary rocks and Malatya-Keban metamorphic rocks before the end of Cretaceous (~77 Ma) (Kuşcu et al. 2010, 2013) (Figs. 8.1 and 8.5). Late Cretaceous to Tertiary sedimentary and volcaniclastic rocks bury the northern ophiolites (Kuşcu et al. 2011).

Magmatic rocks are divided into four main groups depending on their geochronology and location. These are (1) Late Cretaceous rocks of the Baskil arc in the south at Baskil, Malatya and Göksun, (2) Late Cretaceous volcanic and plutonic rocks mainly at Hasançelebi and Keban towards the northern part of the province, (3) Eocene post- orogenic intrusions at Çöpler, Kabataş, Doğanşehir-Polat, Bizmişen-Çaltı, Karamadazı, and Horoz regions, and Oligocene volcanic and plutonic rocks to the west and NW of Tunceli as Cevizlidere pluton, Mamlis and Demürek plutons. Except for late Cretaceous arc-related rocks, each plutonic rock is associated with Fe and Fe-Cu skarns most which are considered to be proximal skarns to porphyry Cu and IOCG systems (Kuşcu et al. 2013).

7.2.2 NeoTethyan Evolution

A review of skarns and skarn deposits of Turkey requires an understanding of NeoTethyan evolution and major magmatic episodes of Turkey. The following is a brief summary of evolutionary stages and major magmatic episodes defined by Kuşcu et al. 2018. Three major subduction and collisional events that played a role in the formation of Turkish magmatic-hydrothermal mineral deposits are; (1) closure of the northerly ocean, also known as the Vardar, and Pontide arc on the north between *ca.* 110–39 Ma (2) closure of the southerly ocean, NeoTethys, Bitlis arc to the south between *ca.* 83–44 Ma, and (3) northeastward subduction of the Ionian partof the eastern Mediterranean Sea, a remnant of the NeoTethys ocean, to form the Aegean arc in the western Anatolia since 42 Ma to present (Kuşcu et al. 2018).

In the Late Cretaceous, the oceanic lithosphere of northerly and southerly NeoTethsy oceans were consumed by northward subduction beneath the Eurasian plate, forming the laterally continuous Pontide arc on the north (Şengör and Yılmaz 1981) between ca. 110 and 85 Ma, and short-lived subduction-related Baskil arc on the southern margin of the Tauride-Anatolide Block in what is now known as the southeastern Anatolian orogenic belt (Yazgan and Chessex 1991; Beyarslan and Bingöl 2000; Agard et al. 2005; Robertson et al. 2005; Kuşcu et al. 2010; Rolland et al. 2011). The final closure of the northerly NeoTethys ocean gave rise to collision of the Tauride-Anatolide Block with the Pontide arc in the Campanian formed the metamorphosed ophiolitic mélange and blueschist facies metamorphic rocks of the Tavşanlı zone (Fig. 7.1) along the İzmir-Ankara-Erzincan Suture Zone (Şengör and Yılmaz 1981; Okay and Tüysüz 1999; Taymaz et al. 2007; Stampfli and Borel 2004; Moix et al. 2008; Rolland et al. 2011). After the final suturing of the Pontides and Tauride–Anatolia Block, the closure of the NeoTethys ocean was re-established to the south of the Tauride–Anatolia Block to form short-lived (83–79 Ma, Kuşcu et al. 2018) Baskil arc. The Baskil arc was terminated when the Tauride–Anatolide Block collided with the northward advancing Arabian plate (Kuşcu et al. 2011, 2017), and the subduction jumped to eastern Mediterranean (Rolland et al. 2011) during Early to Middle Eocene.

The collision and suturing of the Pontides with Tauride–Anatolia Block and Arabian plate, resulted in crustal thickening in the colliding plates. A subsequent decrease in the convergence rate between Eurasian and Arabian plates following the collision enabled the exhumation of metamorphic masifs and post-collisional extensional tectonics at least at thickened crust of Kırşehir massif or CACC and eastern Pontides (Savostin et al. 1986; Rosenbaum et al. 2002; Kaymakçı et al. 2006). The post-collisional extension was accompanied by voluminuous magmatic complexes across the accreted terranes (Fig. 7.5). At least in the CACC, eastern Pontides and southeastern Anatolian orogenic belt, broadly contemporaneous late Paleocene to Eocene sedimentary basins (Kuşcu et al. 2010). These basins are bounded by faults with normal and strike-slip components, and are characterized by coarse-grained continental clastic sedimentation followed by shallow marine carbonate and fine grained clastic sedimentation. The sedimentation and extensional or transtensional

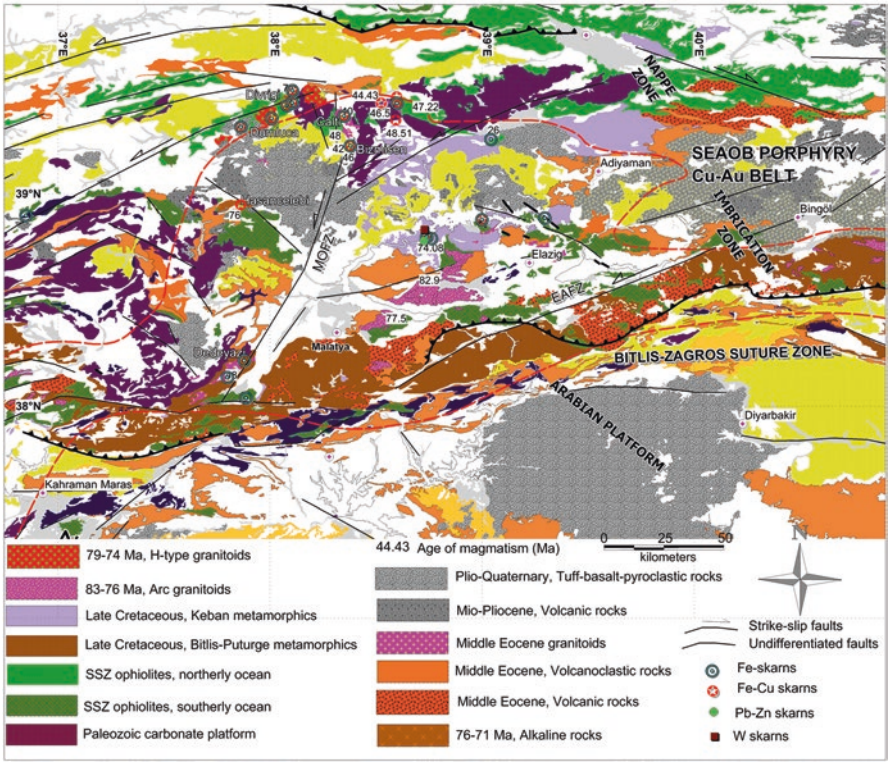

Fig. 7.5 Simplified geological map showing main intrusive phases and associated skarns in SEAOB. (Modified from Kuşcu et al. 2018) (*MOFZ* Malatya-Ovacik fault zone, *EAFZ* East Anatolian fault zone)

tectonism accompanied by Paleocene to Eocene magmatism (Kaymakçı et al. 2006; Kaymakçı and Kuşcu, 2007; Kuşcu et al. 2010, 2017; Black et al. 2013). The magmatic complexes outcrop along faults that are parallel or transverse to the magmatic arc axis.

The northward advancing Arabian plate collided with the amalgamated Tauride–Anatolide Block along the Bitlis-Zagros subduction zone between late Eocene to Oligocene (Keskin, 2003; Şengör et al. 2003). This collision resulted in extrusion of Tauride–Anatolide Block toward Greece, and a southward subduction jump (Rolland et al. 2011) to Aegean subduction zone. The remaining NeoTethys ocean, Mediterranean sea, is still being consumed along north-northwest dipping shallow subduction under Anatolide-Tauride block. This subduction zone is characterized by continental arc magmatism, that was also accompanied by a complex lithospheric extension (Collins and Robertson 1997; Gautier et al. 1999; Aldanmaz et al. 2000; Jolivet 2001; Bozkurt and Oberhänsli 2001; Doglioni et al. 2002; Ring et al. 2010; van Hinsbergen et al. 2010).

7.3 Skarns in Turkey

The skarns and skarn deposits in Turkey manifest themselves as a unique class that have been mined and explored since the ancient civilizations. To date, 112 skarn deposits/prospects are known to occur in Turkey (Table 7.1). These deposits are distributed mainly along the intrusive boundaries between lare batholitic masses to small plugs (Fig. 8.6). Old smelters, slugs and dumpsites are still found at the majority of the Pb-Zn and Fe-skarns in central and western Turkey. They appear to form distinct clusters at the eastern and western Pontides; WAP and CACC where large intrusive masses are emplaced into carbonate and metacarbonate rocks (Fig. 7.6). This section summarizes the main points related to the host rocks, skarn types and dominant mineral assemblages of the skarns within different tectonic units inTurkey.

7.3.1 Skarns in Pontides

The skarns in the pontides are classified mainly as Fe and Cu-Mo or W skarns based on the dominant metal they contain. The Cu-Mo and W skarns are largely found at the Strandja massif, and are formed by the emplacement of late arc magmatic phase into the crystalline rocks of the Strandja massif (Figs. 8.6 and 8.7). Whereas, Fe and Fe-Cu skarns are largely exposed at the eastern Pontides where early arc magmatic phase is traversed by late Cretaceous and middle Eocene plutonic associations (Figs. 8.6 and 8.7).

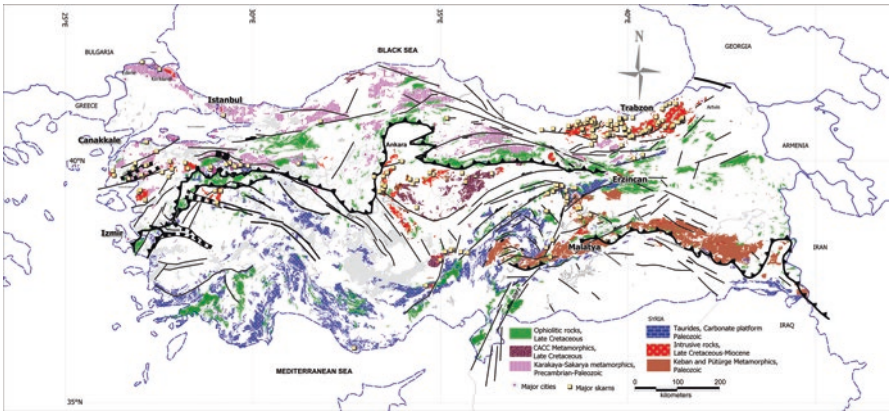

Fig. 7.6 Major host rocks, causative plutons and spatial distribution of associated skarns. (Modified from Kuşcu et al. 2018)

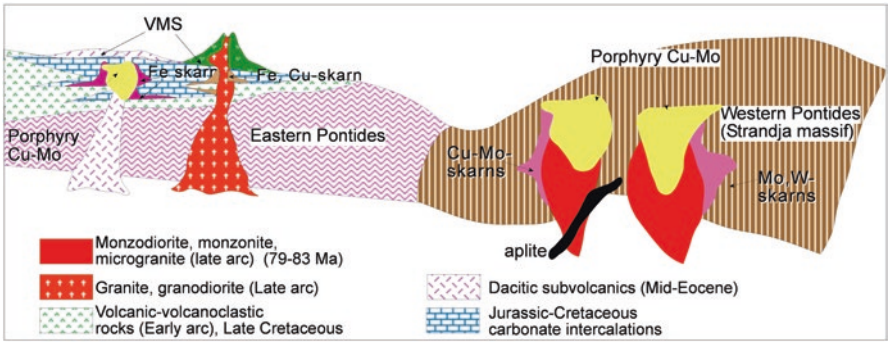

Fig. 7.7 A schematic diagram illustrating the spatial and temporal associations between skarns, host rocks and causative plutons in the Pontides

7.3.1.1 Skarns in Western Pontides (Strandja Massif)

In general, Fe-skarns with subordinate Cu skarns are prominent skarn types in the western Pontides (Table 7.1; Fig. 7.2a). Mo and W is either sub-economic or occur as accessory elements with Fe-skarns. Occasionally, scheelite-wolframite is accompanied by chalcopyrite-bournite and molybdenite in Demirkoy, Sukrupasa, Derekoy, Armutveren and Ikiztepe in western Pontides (Fig. 7.8). The skarns are formed by intrusion of either Demirköy or Dereköy plutons (83–76 Ma in age, Kuşcu et al. 2018) into metamorphosed cover sequences of crystalline basement in the Strandja massif (Fig. 7.2a). The wall rocks are commonly metasandstone, recrystallized limestone Triassic to Jurassic in age that has undergone metamorphism at greenschist facies. The plutonic rocks are largely monzodiorite, quartz diorite, monzonite, microgranite porphyry in composition and are traversed by lamprophyre and aplite dikes (Fig. 7.7). The skarns in the western Pontides are of of both endo and exoskarn type (Fig. 7.8), and exoskarns are more common and mineralized. These skarns are considered as proximal skarns for porphyry Cu-Mo prospects such as those at Derekoy, Ikiztepe, and Sukrupasa and Demirkoy porphyry Cu-Mo deposits (Fig. 7.8). They are composed of diopside, garnet (both andradite and grossular), hedenbergite, with occasional wollastonite and scapolite (Şükrüpaşa skarn) as prograde assemblage; tremolite, epidote, actinolite, calcite, quartz, monticellite, and vesuvianite as retrograde assemblage. The economic Cu and Mo with subordinate W is hosted by retrograde assemblages (Taner 1981). The ore minerals are magnetite, hematite, chalcopyrite, molybdenite, scheelite, wolframite, galena, bournite, pentlandite, wittichenite, covellite, azurite, malachite and goethite (Taner 1981). The average Fe and Cu grade of the ore bodies are 51.02% with 1.08% Cu, respectively (Taner 1981). The W-skarns are not of economic importance, and there is no operating deposit at present. The W mineralization is commonly considered to be accessory phase associated with Mo and Cu mineralization. The aplite dikes and porphyrytic intrusions near to the granitic rocks are also associated with the W mineralization.

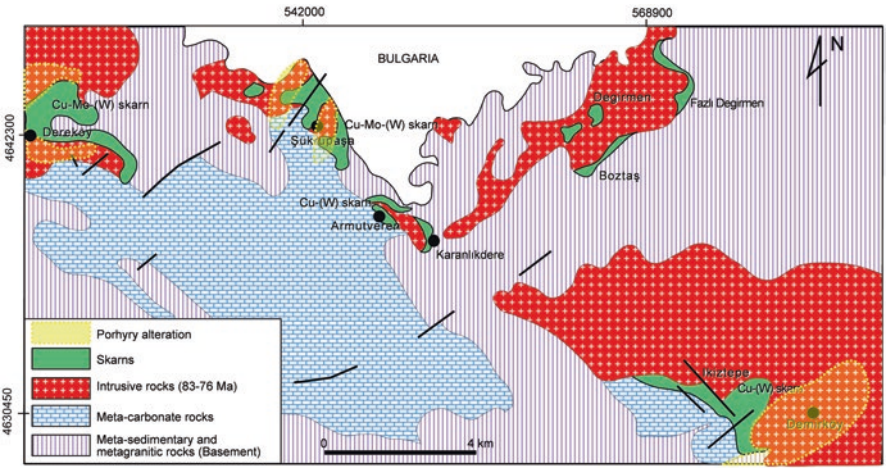

Fig. 7.8 Simplified geological maps showing spatial association between skarns, causative plutons and carbonate rocks, and associated porphyry systems

7.3.1.2 Eastern Pontides

The skarns within eastern Pontides cluster mainly on or associated with the Late Cretaceous or Middle Eocene intrusions that are largely emplaced into relatively older Jurassic-Cretaceous clastic-carbonate rocks or Late Cretaceous volcanic-volcanoclastic rocks (Figs. 8.2a and 8.7). These skarns form clusters either along the long axis of the major Late Cretaceous intrusions (Fig. 7.2b) or parallel to NE-trending faults. The principal skarn types in the eastern Pontides are Fe-skarns with occasional Fe-Cu or Cu skarns. In general, Fe and Fe-Cu skarns are commonly classified as calcic exoskarns with subordinate magnesian skarns. The spatial distribution of calc-silicate mineral assemblages within the ore bodies would indicate that the skarns are of proximal skarns that were later replaced by low temperature assemblages. The predominant calc-silicate assemblages include garnet (mainly andradite with occasional grossular if garnet is zoned), hedenbergite and diopside along with wollastonite as prograde minerals; tremolite, epidote, chlorite, calcite and quartz as retrograde minerals. The mineralization occurs as magnetite lenses with minor pyrite and chalcopyrite hosted by retrograde assemblages in calcic exoskarns. The predominant ore minerals are magnetite and hematite as massive lenses within retrograde skarns. Chalcopyrite and native gold is also associated with the magnetite skarns. The Fe and Cu grade ranges between 32% and 46% ad 0.1% and 7.18%, respectively (Table 7.1).

The Fe-skarns are formed either along the contacts between the Late Cretaceous granitoids of the Pontides arc and carbonate rocks intercalated with Late Cretaceous volcanoclastic rocks or limestones within Jurassic-Cretaceous sedimantry rocks (Fig. 7.6); or scarcely formed by the intrusion of Middle Eocene plutonic to

sub-volcanic rocks into either Late Cretaceous or Tertiary sedimentary-volcanosedimanetary sequences interlayered with carbonate rocks at Gumushane and Trabzon districts (See Fig 7.2b for spatial association of the skarns with intrusions of different ages). In general these skarns form sub-economic low-tonnage deposits, and are considered to be marginal ones compared to those at the western Anatolian province and southeastern Anatolian orogenic belt. These form several small ore bodies such as Kartiba (Rize), Akkaya (Rize), Kotana, Catak (Giresun), Kurtulmus (Giresun), Karabork, Arnastal, Camibogazi, (Gumushane), and Cambasi-Fundacik (Ordu), (Fig. 7.2b; Table 7.1). In these deposits, magnetite and hematite along with goethite are the main ore minerals with subordinate specularite. These skarns are characterized by andradite-grossular, diopside and epidote (Table 7.1).

The Cu-skarns are mostly sub-economic to uneconomic occurrences or occur as byproducts associated with Fe-skarns. They are commonly formed along the contacts between Jurassic-Cretaceous clastic-carbonate rocks and Late Cretaceous intrusions. A few are formed along the contacts between Late Cretaceous carbonate rocks and Middle Eocene intrusions (Fig 7.2b). The Fe-Cu-skarns include Armutlu, Deregözü (Görele, Giresun), Özdil, Tuzlak mezra (Araklı, Trabzon), Dağbaşı, Köprübaşı, Gezge, Ayman (Araklı, Trabzon), Kıranmaden (Kürtün), Egrikar (Torul) and Ispir (Ulutas, Erzurum). In addition to the main Fe-skarn deposits, the Pontides also host many small skarn occurrences and showings subordinate magnetite-hematite and goethite. Some of these include Cimildag and Camii, Asakoy, Arpalı (Rize), Kartal (Istanbul, exploited at present), Kele, Ayidere, Madentepe, Olucaktepe, Çatak, Deregözü, Ambarlıyayla, Cardaklı, and Basmahalle occurrences (Fig. 7.2b; Table 7.1). No or very limited Zn-Pb skarn is formed in Pontides. The examples of this type are associated with Jurassic-Cretaceous carbonate rocks mainly limestones intercalated with volcanic-volcanosedimentary rocks, (Fig. 7.2b).

7.3.2 Skarn Deposits of SEAOB

The skarns within the SEAOB are formed by the emplacement of post-collisional (late orogenic) Late Cretaceous post-collisional and Early-Middle Eocene granitoids or Oligocene subvolcanic intrusions into the Permian to Cretaceous recystallized limestones, and/or marbles of Tauride platform and Keban metamorphics (Figs. 8.5 and 8.9). The skarns and skarn deposits in SEAOB, are mainly of Fe-, Pb-Zn, Mo-W-CaF_2 type (Fig. 7.5). Both endoskarns and exoskarns are present. However, the Fe-mineralization is mainly hosted by the endoskarns. The Fe-skarns are the largest deposits to meet the domestic iron demand of Turkey. Late supergene alteration characterized by extensive manganese oxides or iron hydroxides are common surface indicators of these skarns particularly if they are accompanied by mineralized porphyry Cu deposits.

The skarns associate with Late Cretaceous intrusions also have temporal and spatial association with ironoxide-Cu-Au deposits (IOCG) (Fig. 7.9). They occur either as barren calc-silicate rocks or as sub-economic Fe occurrences proximal to

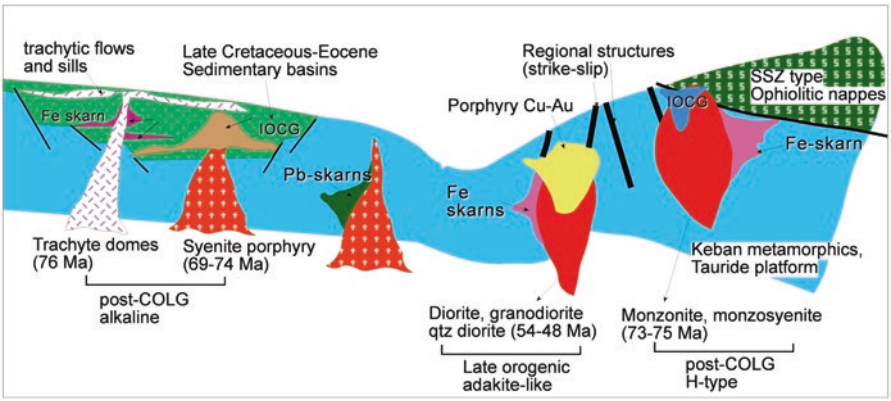

Fig. 7.9 Schematic diagram illustrating, tectonic setting, geologic environment, host rocks and causative plutons associated with skarns within the SEAOB. (*SSZ* supra-subduction zone, *post-COLG* post collisional)

or overprinted by IOCG deposits. The origin of these skarns are still debatable, and some belive that they are not skarns but of calcic end members of a regional sodic-calcic alterations hosting IOCG deposits (Kuşcu 2005; Kuşcu et al. 2013). The skarns formed by the Early-Middle Eocene intrusions are classified as proximal skarns cogenetic with porphyry Cu, Cu-Au deposits such as those at Copler, and Kabatas porphyry deposits at Tunceli, and both are hosted by Permian to Late Cretaceous Keban metamorphics (Fig. 7.9). The Middle Eocene ones are genetically associated with adakite-like subvolcanic and plutonic rocks strictly emplaced along regional transform or strike-slip faults (Fig. 7.5) like the porphyry Cu-Au deposits. The Cevizlidere, Mamlis-Sin, Tumurek Fe skarns are fomed by the explacement of Oligocene plutons into the metacarbonates at Tunceli.

7.3.2.1 Fe-Skarns

The Fe-skarns are the most common and the predominant skarn type in the SEAOB. The skarn zones developed particularly at the limestone–granodiorite and/or diorite porphyry contacts where the intrusions cut through the metacarbonate rocks (Fig. 7.9). They are mostly classified as calcic skarn characterized by garnet, diopside, epidote, pyrite, and calcite. Both endo and exoskarns are present, and exoskarns contain pods and irregular lenses of massive magnetite ore bodies. The endoskarns are restricted to Late Cretaceous intrusions at Divriği, Hasancelebi and Aşvan, and Middle Eocene diorite and quartz diorite in Çöpler. Of these, only Divriği and Dumluca endoskarns are mineralized. The ore boides form small and marginal occurrences to large deposits with millions of tones of reserves. Except for those in the east-central Anatolia at Sivas they are commonly accompanied by an early pervasive sodium metasomatism that resulted in scapolite and albite

alteration. The main Fe-skarns of SEAOB namely are; Karamadazi (Yahyali, Kayseri), Horoz, Esendemirtepe (Çiftehan, Niğde) deposits in central Taurides, Divrigi (Sivas), Dumluca (Divriği), Kuluncak-Hasancelebi (Malatya), Aşvan-Birvan (Keban, Elazığ), Copler (Ilic, Erzincan), and Dedeyazi-Cavuslu, Bizmisen, Calti, Mamlis, Sin, Tuzbaşı, Temurek (Tunceli) deposits (Table 7.1). In general, the Fe-skarns in SEAOB are larger in size and grade compared to Fe-skarns in other terranes; also they have economic copper and gold mineralization (Kuşcu et al. 2013).

The granitoids associated with the Fe-skarns are (1) arc related diorites and granitic rocks of Late Cretaceous age (83–79 Ma) from Baskil pluton, (2) I-to H-type Late Cretaceous post collisional monzonites, syenite (Kuşcu et al. 2010, 2017), (3) Early-Middle Eocene adakitic to adakite-like (Kuşcu et al. 2010, 2013) diorite, granodiorite, and (4) quartz diorite and Oliocene (ca. 25 Ma) diorite to grandiorite porphyries particularly in Tunceli district (Tuzbaşı, Cevizlidere skarns). They all show chemical and petrographic and field evidence of mixing/mingling.

The skarn zones consist of garnet (mainly of andraditic), diopside, ferrosalite, hedenbergite, phlogopite, scapolite, forsterite albite and wollastonite as prograde assemblages, and actinolite, epidote, chlorite, croscite, calcite, quartz, tourmaline, sericite, barite and dolomite as retrograde assemblages. Scapolite, albite and K-feldspar are characteristic minerals of skarns only in Aşvan-Birvan (Keban) Divrigi and Kuluncak-Hasancelebi, and occasionally at Dedeyazi-Cavuslu (Malatya) deposits. These are also accompanied by titanite. All Fe-skarns are accompanied by chalcopyrite and to some extent gold (Kuşcu et al. 2013) mineralization. The ore minerals are predominantly magnetite, hematite and chalcopyrite, specularite ± scheelite and ilmenite that were later altered to goethite, malachite, chalcocite and limonite during late stage alteration events. The chalcopyrite and pyrite mineralization is associated with calcite and quartz veins replacing both the magnetite and skarn assemblages in Karamadazi, Aşvan-Birvan, Esendemirtepe, Cevizlidere, Mamlis-Sin and Divrigi deposits, however, a disseminated low-grade magnetite mineralization is found within the Kuluncak-Hasancelebi deposit. The ilmenite mineralization is very limited and observed in Tuzbaşı (Pertek, Tunceli) Fe-skarn. In this deposit, the ilmenite is largely hosted by The ore bodies occur as lenses and pockets of several meters within the skarns garnet–pyroxene calcic exoskarns along (gabbro–diorite)–marble contacts as lensoid bodies upto 15.83 wt% (Altunbey and Sağıroğlu 2003). The Divrigi and Hasancelebi deposits contain anomalous Th, F, P, Cr, Ni, REE abundance. In these, considerable amounts of apatite, ilmenite and titanite minerals are also present. The skarns and associated magnetite-hematite mineralization are largely controlled by NE-SW trending regional strike-slip faults that also control the loci of the associated granitoids.

The total reserves of the large individual deposits within the SEAOB are about 10,400,000 tones at 54.46–58 Fe% with a maximum of 58.47% at the Karamadazi. The total reserve of Hasancelebi deposit is about 855 million tons at 15.04 Fe%

(average), Low Fe grade and high Ti content as impurity (reaches up to 7.51%) basically precludes mining in the deposit. The Divrigi deposit has the total reserve of about 100 million tons at 53.94–63% Fe (average).

7.3.2.2 Pb-Zn Skarns

The SEAOB are scarce in terms of lead and zinc skarns, and only a few deposit and prospects/showings are known. The economic deposits are mainly located in the Keban, Harput (Elazığ) districts, whereas they also occur as peripheral to distal skarns associated with porphyry Cu-Au deposits at Cevizlidere (Ovacık, Tunceli). The economic Pb-Zn skarns in Keban and Harput known as the "Keban madeni", Alayaprak (Harput) and Harput Pb-Zn deposits, respectively (Table 7.1). Small occurrences are also found in Avlarkoy (Hekimhan, Malatya) and in Develi (Yahyali, Kayseri) deposits. The skarns are developed along the boundary between Late Cretaceous syenite porphyry and Paleozoic recrystallized limestones (Keban, Harput), and Middle Eocene and Permian limestones (Cevizlidere and Yahyalı). Exoskarns consisting mainly of hedenbergitic pyroxene and zoned garnets are the predominant skarns at every skarns in this belt. Some exoskarns contain unusual mineral assemblages including vesuvian garnet and wollastonite (e.g. Keban skarn). The endoskarn is present only in the syenite porphyritic rocks of Keban pluton and contains coarse-grained ganets only (Çalık and Öngen 2000). The economic Pb-Zn mineralization is hosted mainly by exoskarns and is accompanied by occasional magnetite. The ore minerals are sphalerite, galena, silver-tetrahedrite, and minor chalcopyrite; gangue minerals are pyrite and calcite.

7.3.2.3 Mo-W-CaF2-Skarns

The Mo-skarns rich in Mo accompanied by fluorite is termed as the Mo-W-CaF_2 skarns. This type is known only from the SEAOB in the Elazig (Keban district). The skarns are either developed along the contacts between the late Cretaceous syenite porphyry or Middle Eocene to Oligocene dioritic intrusions and recrystallized limestones (Munzur limestones) of Keban metamorphics. The skarns associated with Middle Eocene and Oligocene intrusions are considered to be proximal skarns cogenetic with porphyry Cu-Mo mineralization (e.g. Çöpler and Cevizlidere porphyry Cu deposits). The skarn zones are a few meters thick, and structurally controlled. The molyndenite mineralization is hosted by exoskarns extensively developed marbles and calc-schist of Keban metamorphics and Permian Aladag formation. The fluorite mineralization is typically formed along the recrystallized limestone and mica-schist contacts close to the syenite porphyry stocks. The W is accompanied partly by Mo and chalcopyrite as well. The ore minerals are scheelite, fluorite and chalcopyrite with occasional magnetite, sphalerite and galena. The gangue minerals are garnet, epidote, pyrite and pyrrhotite (Aydoganli 1978).

7.3.3 *Skarns in Western Anatolian Province*

The skarns in the WAP are associated with Middle-Late Eocene to Miocene plutonic and volcano-plutonic associations exposed within NE and NW trending structural corridors (Fig. 7.4). Each skarn within these corridors exhibit compositional zoning. For example, the Middle Eocene plutonic associations are largely exposed along NW-striking strike-slip faults such as Eskisehir fault zone or Alasehir-Simav fault zones, are commonly Cu-Mo and/or Mo-W skarns (Fig. 7.4) in the Tavşanlı zone. Whereas, the skarns associated with Late Eocene to Miocene volcano-plutonic rocks are exposed within NE-trending corridors that also define core-complex to detachment related normal and strike-slip faults, are largely Fe, Fe-Cu skarns and Pb-Zn skarns (Fig. 7.10) in the Biga peninsula. The latter group also exhibit zoning in vertical and horizontal directions such that Fe skarns occur deeper levels or close to causative plutons whereas the Pb-Zn skarns occur as distal to or at shallow levels (Fig. 7.11). This is a common feature where both Fe and Pb-Zn skarns occur within the same district such as Dursunbey, Soma, Banaz, Evciler, and Balya.

The skarns within WAP are located in Biga peninsula, Tavsanli zone and Menderes massif (Fig. 7.4). They are commonly Fe, Fe-Cu, Mo, Mo-W and Pb-Zn skarns. Among these, Fe-skarns and Pb-Zn skarns are the most common ones, and are operated at present. It is author's opinion that the numerous low temperature

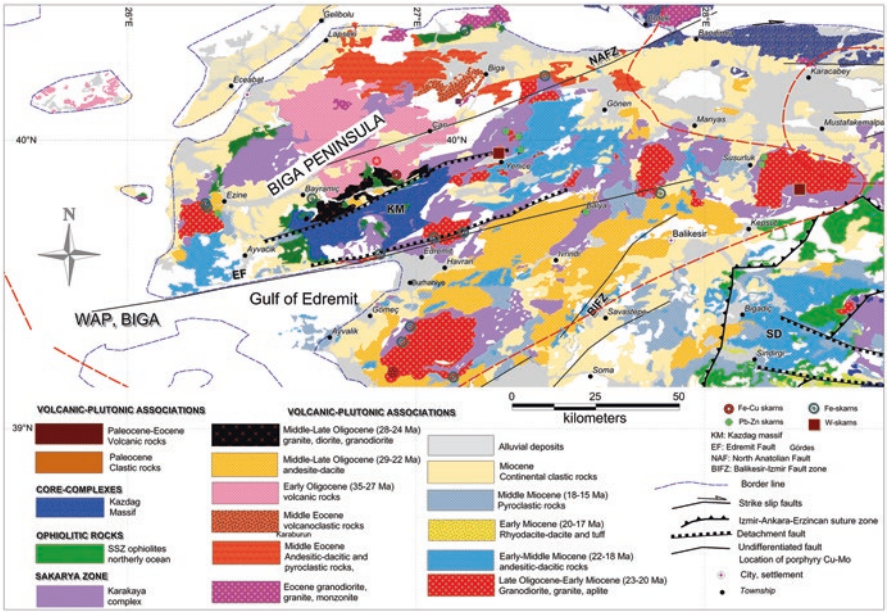

Fig. 7.10 Geologic map showing the spatial distribution, magmatic association and structural position of various skarns in the Biga Peninsula

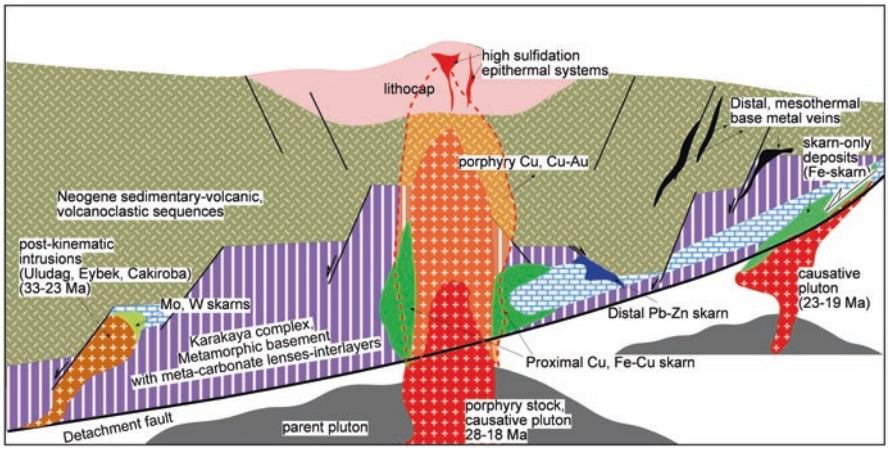

Fig. 7.11 Cartoon illustrating the spatial and temporal associations between skarns and other precious metal mineralization in the Biga peninsula (not to scale)

garnet and epidote-rich veins, associated with or hosting the Pb-Zn mineralization are not skarn, but of distal mesothermal veins enveloping blind porphyry systems (Fig. 7.11).

7.3.3.1 Skarns in the Biga Peninsula

Fe-Skarns The Fe-skarns and skarn deposits are the most common type in the western Anatolia. They are formed by the emplacement of plutonic rocks into metamorphosed sedimentary to volcanosedimentary rocks (phyllite, meta-carbonates, marble, metabasalt) such as Karakaya complex (Fig. 7.10). The exoskarns with coarse-grained calc-silicate minerals are the common assemblage within the meta-carbonates and marbles. Whereas, calc-silicate hornfels are quite common if the intrusion is emplaced into fine-grained rocks consisting of metasiltsone, phyllitic rocks or schist (E.g. Evciler and Ayazmant skarn deposits). These skarn deposits are genetically and temporarily associated with the porphyry Cu-Au deposits or shares many components of skarns cogenetic with porphyry Cu deposits or epithermal Au deposits (e.g. Halilaga porphyry Cu and Bakırlıktepe skarn, Ayazmant Fe-Cu skarn and Soğancı, Kubaşlar epithermal gold deposits), In this respect, the Fe-skarns are regarded as part of larger magmatic-hydrothermal systems formed in high-level porphyry environments (Fig. 7.11). Skarns not associated to porphyry (skarn-only) deposits are also available in the regions where subvolcanic intrusions or felsic-evolved granitoids are emplaced into Tertiary sedimentary to volcanosedimentary basins (Fig. 7.11). All skarns appear to be formed by emplacement of porphyritic I-type, oxidized Late Eocene-Oligocene to Miocene age intrusions. They are mostly granodiorite, monzodiorite, quartz diorite to diorite in composition (Kuşcu et al.

2018). The timing of formation and emplacement of these plutons are almost coeval with nearby or associated porphyry Cu-Au deposits. The Fe-skarns are commonly accompanied by Cu mineralization as well. The Cu mineralization in these skarns are found as veins or irregular pockests traversing magnetite ore bodies. Some of the Fe-skarns containing economic Cu mineralization also host economic Au mineralization in trace amounts or Au may localy reach economic grades in Cu concentrates. Typical examples to this type include Ayazmant, Evciler, Bağırkaç, Çatak, Dursunbey, Demirlitepe, Aladağ, Üsküfçü, Karadoru, and Yaşyer skarns (Table 7.1). In these skarn deposits, Au is associated with pyrrhotite-marcasite-pyrite-rich sulfide-bearing skarns. Although, endo and exoskarns are both developed, the exoskarns are more common, and both are mineralized. The endoskarns locally contain hydrothermal albite and scapolite veins which were later replaced by actinolite and phlogopite minerals indicating limited sodic alteration. In these skarns, magnetite is the predominant ore mineral, and is synchronous with phlogopite and actinolite. Alteration of magnetite to hematite is quite common process that also resulted in supergene copper enrichment. Garnet is the most common mineral, the composition ranges from andradite to grossular, andraditic garnets being more predominant.

The mineralization in these skarns occurs as magnetite, chalcopyrite lenses or pockets in the epidote-chlorite altered prograde skarns. Apart from magnetite, abundant sulfide mineralization is also observed particularly in Fe-Cu skarns (Ayazmant, Evciler, Dursunbey, Demirlitepe, Table 7.1), and scheelite mineralization is also observed but very limited. Unlike the sulfides, scheelite mineralization is not economic. The sulfide assemblage includes chalcopyrite with subordinate molybdenite, bornite, pyrrhotite, galena and sphalerite. The galena and sphalerite exist in the exoskarns quite distal to precursor intrusion within the same skarn zone containing magnetite. Dursunbey, Aladag and Üsküfçü skarns exemplify this association.

Cu-Skarns The Cu-skarns are associated with Oligocene to Lower Miocene granitoids diorite and monzodiorite in composition. They are developed either along the roof pendants of graphitic recrystallized limestone diorite-monzodiorite dike contact. The Cu-skarns are very limited and include Uskufcu (Ezine, Canakkale), Demirtepe deposit (Tahtakopru, Bursa), Evciler (Canakkale) and Bakirlik (Halilaga, Canakkale). The skarns are associated with Oligocene to Lower Miocene granitoids diorite and monzodiorite in composition. They are developed either as roof pendants of graphitic recrystallized limestone and along the contact of diorite-monzodiorite dikes or along the monzonite, monzodiorite, monzonite porphyry-marble interfaces. Some of these skarns are associated with high-level porphyry systems such as those at the Uskufcu and Bakirlik skarns. The skarns consist of mainly of garnet-pyroxene and wollastonite-garnet skarns along the granitoids-marble interface. The wollastonite dominant assemblage is mainly hosted by exoskarn whereas garnet dominant assemblage is hosted by endoskarn zones. In wollastonite-garnet rich skarns, the wollastonite is earlier in the sequence and was replaced/overprinted almost by garnet. The garnets are commonly dark brown to red in color suggesting they are of high temperature types or close to the causative intrusions. A pervasive scapolite

develops extensively on the plagioclases in the endoskarns with anorthite and garnet (Demange et al. 1998). Ferrohastingsite and late phlogopite also appear in association with sulfides in the endoskarns (Demange et al. 1998). The garnets are either andraditic or grossular in composition. The andraditic garnets are more predominant at skarns not associated with high level porphyry systems. The grandite-series (grossular-andadite) garnets are largely found at skarns associated with high-level porphyry systems, 26–28 Ma in age (Kuşcu et al. 2018).

The known mineralization in these skarns is associated with the epidote-chlorite-rich retrograde assemblage that overprinted the wollastonite-garnet exoskarns. Bornite and minor chalcopyrite, and pyrite fill the in terstitial spaces between the garnet-rich endoskarn assemblages. Although no Cu skarn is operated to data, slugs are still visible at dump sites at ancient operations (e.g. Uskufcu, Demirtepe, Bakirlik). As these skarns are known to be proximal skarns for high-level porphyry Cu systems, they have been the prime target for many mid-tier to junior companies.

Mo-Skarns The Mo skarns are very scarce compared to Fe, and are found mainly as uneconomic occurrences or small deposits within the WAP. These include Sogucak, Sofularkoy, Ayvalik and Cakiroba (Yenice, Canakkale) (Table 7.1). Unlike the world Mo-skarns, the Mo-skarns in the WAP are accompanied by W and Cu mineralization as well. For example, those in the Yenice (Canakkale) and Ayvalik (Balikesir) are commonly associated with the scheelite and chalcopyrite mineralization that occur as irregular concentrations within axinite, garnet and pyoxene-rich skarn zones. The plutons associated with Mo, W and Cu skarns are product of magmatism characteristically older than the other skarns in WAP. They are either hosted by quartz veins within the granitoids or occur as quartz lenses within the marbles in contact with the granites. The grade of the deposits ranges from 0.1% to 0.6% Mo. (Table 7.1). The ore minerals include molybdenite, pyrite and chalcopyrite.

7.3.3.2 Skarns in Menderes Massif

The skarns in the Menderes Massif are very scarce, and are called the "post-metamorphic" deposits which were formed by the intrusion of felsic syn-tectonic stocks and plutons into the metacarbonate rocks of the Menderes massif. The skarns in this region are largely Fe-skarns. These include Çatak, Karaagil, Küreci, Güldüren, Sopali deposits in Emet (Kutahya) district, and Dagardi and Kalkan deposits in Simav (Kutahya) district (Table 7.1). The mineralization in these skarns is very limited, and occurs as sporadic, discontinuous magnetite and hematite lenses. The ore minerals are magnetite and hematite replacing the garnet-diopside-rich skarn zones. The Retrograde minerals include epidote, calcite, actinolite, pyrite and pyrrhotite (Kuşcu 2005). The total reserves of the deposits in Emet district are about 7 million tones with Fe grade ranging from 45% to 59%, and are about 1.2 million tones with 45–65% Fe in Simav district.

7.3.4 Skarns in Tavsanli Zone

The skarns in the Tavsanli zone are mainly of two-types; Mo and W skarns formed by the intrusion of Early-Middle Eocene to Early Oligocene plutons into the metamorphic rocks exposed within Tavsanli zone (Fig. 7.12). The Mo-skarns formed by the emplacement of Early-Middle Eocene plutons are the most common types, and considered to be proximal skarns cogenetic with porphyry Cu-Mo prospects/deposits. The W-skarns, on the other hand, are formed by the emplacement of Early-Oligocene to Miocene post-kinematic, syn-tectonic intrusions along the core-complex boundaries or a along the low-angle normal faults (Fig. 7.13). Both endoskarns and exoskarns occur in the zone that range from several tens or meters

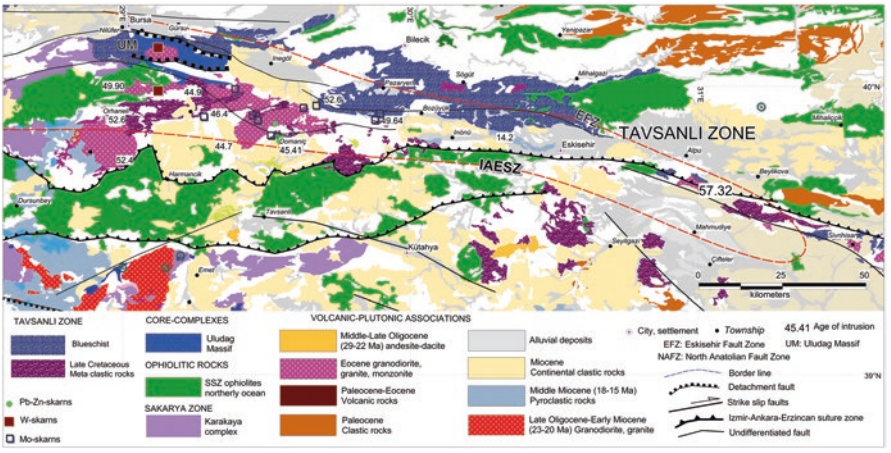

Fig. 7.12 Simplified geologic map showing, major magmatic phases, distribution of various skarn types, age of associated/causative plutons, regional structures and host rocks within the Tavsanli zone

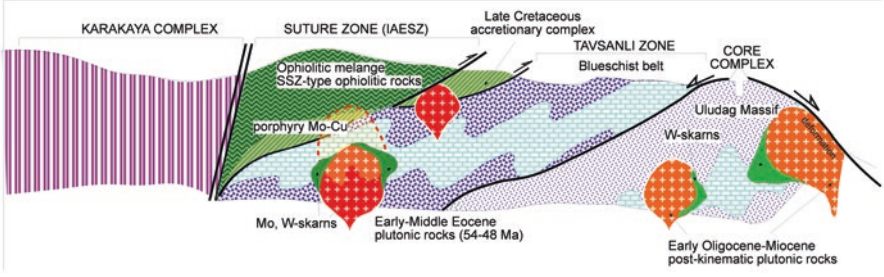

Fig. 7.13 Cartoon illustrating the spatial and temporal association of W-skarns and Mo-W skarns, porphyry Cu-Mo systems and regional structures within Tavsanli zone

to upto 200 m. The endoskarns appear to preserve igneous textures and minerals partly overprinted by skarn minerals. The endoskarns consists dominantly of hedenbergitic pyroxene and garnet.

7.3.4.1 Mo-Skarns

The Mo skarns are the most significant skarns in the Tavsanli zone, that are also considered to be proximal skarns cogenetic with porphyry Mo-Cu systems (Fig. 7.13). They are formed by emplacement of Early-Middle Eocene intrusive rocks into the metamorphic rocks consisting of schist and marble intercalations (Fig. 7.13). The intrusive rocks are commonly granodiorite, quartz diorite-to-diorite porphyry in compostion. Both endo and exoskarns are well developed along marble and quartz diorite contacts, whereas calc-silicate hornfels are the most common rock type along schist and granodiorite to quartz diorite contacts. The endoskarns consists mostly of andraditic garnets overprinted by epidote and calcite. The exoskarns, the most widely exposed type in these skarns consists mostly of diopside, andraditic to grossular garnet, and wollastonite. Wollastonite largely occurs distal to the causative pluton however; it is the most common skarn mineral hosting majority of the Mo and Cu mineralization when they are overprinted by epidote, chlorite and quartz during retrograde skarn stage. These skarns were operated mostly for Cu and Fe, and ancient slugs are still preserved in historical mining sites such as Gurculer, Gelemic and Saricayiryayla.

7.3.4.2 W-Skarns

The W-skarns are generally developed along the contacts between the Oligocene granitoids and Paleozoic gneiss-schist or core-complex related metamorphics within the Tavsanli zone (Fig. 8.13). Uludag and Kozbudaklar skarns are well known examples of this type in the Tavsanli zone. Uludag, the largest W-deposit in Turkey is abandoned, and sporadic exploration is still continuing at Kozbudaklar skarn. The causative plutons are granodiorite to granite in composition. They are cut by several aplite and pegmatite dikes. The skarns show a spatial and temporal zoning with respect to causative plutons as garnet, garnet-pyroxene (as endoskarns), pyroxene-wollastonite-calcite (as exoskarns). The W mineralization is generally characterized by scheelite replacing the early wolfromite (Inan 1979, Orhan 2008). The W mineralization is also accompanied by chalcopyrite and molybdenite infilling the microfractures within the magnetite, and fractures within the retrograde skarn minerals. Mineralized aplites and porphyrys close to the granitic rocks are also associated with the W-mineralization. Apart from scheelite, pyrite, chalcopyrite, magnetite, hematite, sphalerite, cozzalite, bursait, wolframite, bismuthinite, pyrrothite, bornite, tetrahedrite, molibdenite are also present (Inan 1979; Orhan 2008). The Uludag, Susurluk and Kozbudaklar skarns, the most well known W-skarns have the resource of 16.587.177 and 238,000 tons, respectively. In Uludağ

skarn, the ore grade is 0.44–0.41%WO_3. The average WO_3 grade in Kozbudaklar is 0.31% (Inan 1979). The W mineralization at Kozbudaklar is considered as byproduct in Fe-Cu skarns hosted by prograde andraditic garnet-rich skarns (Orhan 2008). These deposits have not been operating at present. Apart from W-only skarns, W mineralization is commonly considered to be accessory phase associated with Mo and Cu skarns, particularly within NW-trending blueschist belt of Tavsanlı zone.

7.3.5 Skarn Deposits of the Central Anatolian Crystalline Complex (CACC)

The skarns in the CACC are mostly Pb-Zn and Fe skarns, and are largely localized at the western, northwestern and northern tip of the batholithic masses. Kuşcu and Erler (1998) have classified the skarns in CACC as Fe, Fe-W and Pb-Zn skarns, and documented that they are developed at the dual contacts consisting of granitoid-marble and granitoid-ophiolite. The skarns exhibit a zonal distribution from granitoid (proximal) to marble (distal) as Fe-W, Fe, and Pb-Zn skarns, respectively (Kuşcu and Erler 1998). Fe-and Fe-W skarns are restricted to both ophiolite-granitoid (Kesikköprü-Kirikkale) and marble-granitoid contacts (Çelebi-Kirikkale, Karamadazı-Kayseri, and Yıldızeli-Sivas), respectively. Pb-Zn skarns tend to localize at metacarbonate-granitoid contacts only (Akdagmadeni, Akcakisla, Lökköy (Yozgat), Keskin (Kirikkale) or within the meta-carbonates as distal veins. Kuşcu et al. (2003, 2005) documented that there is a correlation between the composition of plutons and type of skarns in the CACC in that the Pb-Zn skarns are largely formed by the emplacement of felsic, evolved and high Rb/Sr ratio plutons whereas Fe and Fe-W skarns are formed are formed by mafic, primitive high MgO and Sc-bearing plutons. Besides, the multivariate statistical evaluation of the data related to several skarn-related plutons showed that sodic alteration appear to be the principal component for plutons associated with Fe-skarns. Whereas, Rb/Sr ratio and SiO2 appear to be principal component for plutons associated with Pb-Zn skarns (Kuşcu 2005). Kuşcu et al. (2002) documented that the overall composition of causative pluons for Fe and Pb-Zn skarns in the CACC share characteristics akin to Au and Cu, and Mo-skarns worldwide, respectively. Kuşcu et al. (2003) also showed that the magma-mixing between felsic-crustal originated magmas with mafic-mantle originated magmas and mantle-underplating played and important role for the generation of H-type (hybrid) magmas and Fe-skarns.

7.3.5.1 Fe- and Fe-W- Skarns

Fe-and Fe-W-skarns being the most widely distributed type among the others (Kuşcu and Erler 1998; Kuşcu 2005) are still mined. They form along the boundaries of the batholiths and marbles, as opposed to small isolated granitoid outcrops, and are regarded as proximal skarns that occur adjacent to marble-granitoid contacts. The

deposits are found around Kesikköprü, Hirfanli, Buguz, Durmuslu and Celebi (Fe-W), Akcakisla and Akdagmadeni (Pb-Zn with Fe-W) and Yildizeli deposits (Fig. 7.3) (Table 7.1). Based on their pyroxene compositions, and sub-economic copper and gold occurrences within the retrograde skarns, Kuşcu et al. (2001, 2002) suggested that the Fe-skarns in Çelebi, Kesikkopru districts have Cu-Au potential. Kuşcu et al. (2001, 2002) also compared the major and trace element compositions of the plutonic rocks associated with Fe-W, and Fe-skarns with world-class Cu-Au skarns, and suggested that these skarns have Cu-Au potential that should be investigated in detail. The W-mineralization accompanied by Fe skarns such as Celebi and Huseyinbeyobasi are genetically related to more felsic members (granitic) of the same hybrid pluton (Kuşcu et al. 2002). The Fe skarns are mostly classified as calcic skarn-type, rich in garnet-pyroxene-epidote (Kuşcu 2001); whereas olivine and phlogopite skarns are also observed at contacts with dolomitic rocks. Exoskarns either appear as narrow zones with limited distributions, commonly along the fracture zones in the meta-carbonates of the CACC or are sandwiched between endoskarn zones and smaller marble outcrops. Extensive endoskarns form along margins of the granitoid represented by epidote-pyroxene skarn with some garnet, and pyroxene-garnet skarns are the main skarn zones from granitoid to marble in the district. The skarnification within the endoskarns begins with incipient metasomatism producing the epidote that replaces the plagioclase. The exoskarns are mainly characterized by pyroxene and greenish-brown garnet which was later replaced by tremolite, actinolite, epidote and chlorite. The exoskarns are cut by a prominent calcite-quartz veining system at the distal parts close to meta-carbonate fronts. These veins are infilled by disseminated to massive sulfide mineralization. Garnet is present as sporadic crystals in endoskarns. They are generally andraditic with Gro_5And_{95} to $Gro_{60}And_{40}$ (Bayhan 1984). The latter is confined mainly to vein-type skarns close to exoskarn zones. They become more andraditic as the granitoids are approached.

Among the Fe-skarn districts, The Hirfanli, Buguz, Celebi and Kesikkopru districts are known as the best-exposed Fe-skarn districts in CACC. Production has come from a series of small isolated skarns, with 250,000 tons @ 50–62% Fe and variable WO_3 (0.93%) and about 3 million tones @ 54% Fe at Kesikkopru, developed along offshoots of the granitoids into marble. Mining occurred from ancient times until the late 1960s and renewed exploration studies have been initiated by the Mineral Research and Exploration Directorate of Turkey.

7.3.5.2 Pb-Zn Skarns

Unlike the Fe- and Fe-W skarns in CACC, the Pb-Zn skarns tend to occur in relation to thick meta-carbonate sequences at variable distances from the granitoids, and are called as distal skarns. Their occurrence is partly controlled by tectonic features, and in part by their distance to intrusions. The most prominent lead-zinc skarns of CACC are located around Akcakisla, Akdagmadeni (Vache 1963; Tulumen 1980; Sagiroglu 1982, 1984; Kuşcu and Erler 1998); Lokkoy and Keskin (Kovenko 1947; Çagatay and Tesrekli 1979) (Fig. 3) (Table 7.1). The Pb-Zn deposits are hosted by

the exoskarns, and rarely along the fault zones within meta-carbonates. They are observed mainly as patches in association with the granitoids, and are classified as the magnesian and calcic exoskarns (Sagiroglu 1982; Kuşcu and Erler 1998; Kuşcu et al. 1998, 2001). The magnesian skarns have limited exposures since the dolomitic marbles are subordinate compared to calcitic marbles. The calcic skarns in the district are of two types as garnet-pyroxene and epidote skarns. The garnet-pyroxene skarns are composed of garnet as predominant mineral associated with pyroxene, and magnetite, hematite, pyrrhotite, and some pyrite. They occur within the skarn zones next to or close to the granitoid contacts, and their thickness decreases away from the granitoids. The epidote skarns include epidote, pyroxene, wollastonite, tremolite, calcite, chlorite, quartz, and sulfide minerals (sphalerite, galena, chalcopyrite, and pyrite). The skarn zones and lead-zinc mineralizations in the districts are associated with faults as the main agents that control the skarnification and ore deposition. They generally trend NE-SW, and occur along the peripheries of the granitoids displacing both the granitoids and meta-carbonates. The garnets are generally grossular. The pyroxenes are characteristically johansenitic, however, some diopsidic pyroxenes are also found (Kuşcu 2005). The principle ore minerals of the Pb-Zn skarns are sphalerite, galena, chalcopyrite, and wittichenite (Çagatay and Tesrekli 1979). The presence of silver and copper as well as lead-zinc ore is a common feature for these deposits. Grade of silver is higher in Keskin district than it is in Akcakisla and Akdagmadeni districts.

The causative granitoids of the Pb-Zn-skarn are member of post-COLG H-type granitoids of CACC formed due to the post-collisional extension. However, they differ in composition from the Fe-skarns granitoids in that they represent more evolved counterparts of the H-type granitoids represented by granite to tonalite (Kuşcu et al. 2001), hornblende granite, monzonite to adamellite (Sağıroglu 1982). The geochemical studies showed that they are of subalkaline type with metaluminous character, and are of cafemic-calcalkaline trend. The recent studies have shown that the granitoids associated with the Pb-Zn skarns in CACC share similarities to granitoids associated with W-Zn skarns, Zn skarns, and Mo+Sn skarns based on their MgO, K_2O and SiO_2 values and comparison with world averages of W-Sn –Mo and Zn skarn granitoids. Also Kuşcu et al. (2003) have shown that the granitoids associated with the Pb-Zn granitıoids have distinctive (Al_2O_3+Sr)/SiO_2 ratio, and K_2O+Rb total, representing a late alteration effect and crustal component (or a more differentiated granitoids family), respectively.

7.4 Discussions

7.4.1 Major Variables in Skarn Deposits

The skarns in Turkey are classified mainly as calcic exoskarns and occasionally as magnesian exoskarns. The economic mineralization are largely confined to calcic exoskarns with exception of Fe- and Fe-W skarns. They are widely distributed over

the calcitic meta-carbonates and recrystalllized limestones within metamorphic sequences or intercalations within sedimentary and/or volcanic sequences. The skarns are classified as Fe-, Fe-Cu, Cu-, W-, Fe-W, Mo and Pb-Zn-skarns according to dominant metal they contain. The vast majority of Fe-, and Fe-W skarns are associated with endoskarn assemblages whereas some Fe-, and Pb-Zn-skarns are associated both with calcic and magnesian exoskarns. The wall rocks span an age range rom Cambrian to Permian, and to Upper Cretaceous. The most common periods for skarn generations are Late Cretaceous, Middle Eocene and Oligocene. No or a few skarn formation is associated with intrusions younger than Miocene period. The skarns that coexist as proximal calc-silicate assemlages within major high-level porphyry Cu systems are largely controlled by regional, large-scale structures such as strike-slip faults or core-complex systems. Where both Fe, Fe-Cu and Pb-Zn-skarns are observed in the same region, the Fe- and Fe-Cu skarns are classified as proximal, and Pb-Zn skarns as distal skarns. The chemistry of the associated skarns is different for each class. The I-type and mafic characteristics are predominant in Fe-skarns while more felsic and crustal signature is diagnostic for Pb-Zn skarns. In general, the Fe-skarns are associated with less evolved magmas that formed granitoids monzonite, monzodiorite, and occasionally granodiorite in composition. However, the Pb-Zn skarns are associated with strongly evolved magmas that formed granite to granodiorite in composition. In general, a weak sodic alteration is significantly developed in Fe skarns.

7.4.2 Temporal and Spatial Relations Between Skarns and Associated Intrusive Rocks

7.4.2.1 Pontides

The skarns in eastern Pontides are related to Late Cretaceous and Eocene intrusions, mostly restricted to the region between Artvin and Giresun, and Kırklareli-Edirne at the western Pontides (Fig. 8.2A and 8.2B). Late Cretaceous plutonic rocks are the common rock types that formed skarns, and are mostly arc-related, late phase intrusions (Fig. 8.2A and 8.2B). Several Fe-, Fe-Cu skarns, prospects and showings are hosted by or associated with Late Cretaceous porphyry intrusions in the central and northern zones of the eastern Pontides whereas fewer skarns are hosted by or associated with Middle Eocene plutonic rocks (Fig. 7.2B).

The Dereköy, Demirköy and İkiztepe are the best-known Fe-Cu-Mo-W Cu-Mo skarns related to Late Cretaceous plutonic rocks (Demirköy, Dereköy, Armutveren plutons) in the western Pontides and metacarbonates in the Strandja massif (Table 7.1).

Published U-Pb, K-Ar, and $^{40}Ar/^{39}Ar$ geochronological data for the Pontides volcanic and plutonic rocks are limited (Table 7.1). Available geochronological data show that the magmatism in the Pontides clusters in three intervals between 80–76, 65–66 and 50–40 Ma (Kuşcu et al. 2018; Table 7.1). This shows that magmatism in

the Pontides spans much of the Cretaceous, with volcanic rocks ranging in age from 110 to 81 Ma (Okay et al. 2006; Eyüboğlu et al. 2014) and plutonic rocks having cooled between ~81 and 66.5 Ma locally reported on silica-undersaturated alkalic volcanic rocks with younger K-Ar and $^{40}Ar/^{39}Ar$ ages between ~81 and 79 (Table 7.1). The Latest Paleocene to Eocene rocks have predominantly K-Ar and lesser U-Pb ages that cluster between 39.9 and 44.4 Ma (Table 7.1). Eocene volcanic and plutonic rocks in the eastern Pontides span a similar time range (Table 7.1). Dated intrusions in the eastern Pontides have ages of *ca.* 75.7–91.1 Ma, but are mainly 83.6–76.9 Ma in the Strandja massif on the west (Kuşcu et al. 2018; Table 7.1). Plutonic rocks associated with the older metamorphic rocks are also present, but occur as metamorphosed bodies not associated with skarns. Based on the spatial association of skarns and age of causative plutons, the skarns in the Pontides are considered to be formed by granodioritic, dioritic to monzodioritic plutons ca. 80 Ma in age and granodiorite, syenite and monzodioritic plutons ca. 52–39.9 Ma.

7.4.2.2 SEAOB

The Fe- and Mo-F skarns and Pb-Zn skarns along with IOCG-related skarns associated Divrigi and Murmano pluton at Divriği yield biotite $^{40}Ar/^{39}Ar$ ages between 75.63 ± 0.44 and 75.7 ± 0.5 Ma (Kuşcu et al. 2011, 2013), whereas the syenitic rocks and syenite porphyry in the Hasançelebi yielded zircon U-Pb and $^{40}Ar/^{39}Ar$ ages between 74.8 ± 0.5 and 74.08 ± 0.39 Ma (Kuşcu et al. 2011, 2013). At Keban, the syenitic rocks and syenite porphyry were dated at 74.8 ± 0.5 and 74.1 ± 0.4 Ma by U-Pb on zircon and at 74.08 ± 0.39 Ma by $^{40}Ar/^{39}Ar$ on biotite (Kuşcu et al. 2011, 2013).

The Eocene Karamadazı granitoids, Horozköy pluton, Çöpler and Kabataş plutons, Bizmişen-Çaltı pluton, and Dedeyazı-Polat granitoids have broadly similar ages that range from 50.44 ± 0.28 to 44.43 ± 0.61 Ma, whereas published K-Ar ages of hornblende from the Bizmişen and Çaltı plutons range from 46.3 ± 0.4 to 42.1 ± 0.9 Ma and 48.8 ± 0.9 to 40.5 ± 0.9 Ma, respectively (Önal et al. 2005; Kuşcu et al. 2013; İmer et al. 2013). Collectively the data suggest a narrow period of magmatism between 43 and 50 Ma, with limited evidence for slightly younger magmatic activity. The skarns at Cevizlidere was formed by intrusion of a Cevizidere granitoid at ca. 25 Ma (İmer et al. 2015). The causative plutons at Demurek, and Mamlis-Sin share the same magmatic belt, and located along the same intrusive phase. Therefore, these skarns are also interpreted to be related to Oligocene intrusions.

7.4.2.3 Western Anatolian Province (WAP)

Published $^{40}Ar/^{39}Ar$, and U-Pb geochronology for the mineralized magmatic rocks in the WAP constrains magmatism between *ca.* 57 and 9 Ma (Kuşcu et al. 2017 and references therein). Based on the published ages for the igneous rocks, three

broad magmatic pulses between Eocene and the Pliocene are responsible for skarn generations within the WAP. The volcanic and plutonic rocks Early to middle Eocene in age form the oldest pulse (*ca.* 52–48 Ma). The intrusions of this pulse have not resulted in skarns and skarn deposits. The volcanic and plutonic associations Middle Eocene (*ca*. 42–35 Ma) in age form the second pulse. These are temporarily associated mostly with Mo skarns associated with post-kinematic intrusions. The Oligocene to early Miocene rocks (29–18 Ma) form the third pulse (Kuşcu et al. 2017). This magmatic pulse is associated mostly with proximal Fe-, Fe-Cu and distal Pb-Zn skarns. The youngest magmatic pulse between *ca*. 16 and 9 Ma, is related to alkaline magmatism and associayed volcano-plutonic rocks in the southern part of the province. This pulse appears to be barren in terms of skarns in WAP.

7.4.2.4 Tavsanli Zone

The Tavsanli zone consists of Elongate Eocene to Oligocene plutons with variable diameters intruded the Karakaya complex and Tavşanlı zone at shallow crustal levels from Marmara island to Sivrihisar pluton (Figs. 8.12 and 8.13). These plutons are largely associated with Cu-Mo skarns and high-level porphyry Cu-Mo deposits. Diorite, quartz diorite, granodiorite, granite, and syenite plutons include the Şevketiye, Armutlu (48.2–34.3 Ma), Karabiga (45.3 Ma), Avşa (44.0 Ma), Fıstıklı (35.4 Ma), and Kapıdağ (42.2–36.1 Ma) plutons. In the Tavşanlı zone, farther to the east, slightly older plutons are represented by the Tepelidağ (44.9 Ma), Orhaneli (53–51 Ma), Topuk (49–48 Ma), Gürgenyayla (49.9 Ma), and Göynükbelen, Tüfekcikonak (49.2 Ma) granitoids (Kuşcu et al. 2018). Apart from these, the W-skarns are formed by relatively younger plutonic phase of Oligocene in age, and are related to post-kinematic to syn-tectonic intrusions coeval to core-complexing within the WAP and Tavsanli zone.

7.4.2.5 CACC

The Late Cretaceous post-collisional S-, H- and A-type calc-alkaline to alkaline rocks ranging in age from 82 to 67 Ma (Kuşcu 2005) are the causative plutons for most of the skarns within the CACC. Zircon cores in granite and metapelitic gneiss record Proterozoic through Mesozoic ages, but rims consistently yield Late Cretaceous (78–91 Ma) U/Pb (SHRIMP) ages (Whitney and Hamilton 2004). The H- and I-type rocks are both associated with or host to Fe, Fe-W, and Pb-Zn skarns majority of which are still operating. The age of intruding granitoids was constrained by Ar-Ar geochronology. Whitney et al. (2003) obtained $^{40}Ar/^{39}Ar$ ages between 85 and 75 Ma on zircons from the Üçkapılı granitoid. The $^{40}Ar/^{39}Ar$ geochronology on several granitoids in the CACC gives ages between 82 and 67 Ma (Kuşcu et al. 2003). The Ar-Ar geochronology of the H-type granitoids associated with Fe-skarns yielded a slightly older age of ca 79 Ma, compared to Pb-Zn skarns

which yielded an age of ca. 75 Ma. The H-type granitoids, the prime source for Fe-skarns in Celebi, Kesikkopru, Buguz and Hirfanli deposits (Kuşcu et al. 2003), and are not only associated with skarns but also considered to be related to porphyry Mo systems.

7.4.3 Petrogenesis of Skarns and Compositional Characteristics of Intrusive Rocks

7.4.3.1 Pontides

Major and trace element compositions of Late Cretaceous causative granitoids are characterized by depletion in Nb, Y and enrichment in K, Rb, Ba and Th along with Rb/Sr and Nb/Y ratios that are typical for subduction-related granites (Karacık and Tüysüz 2010). This suggests that the Late Cretaceous skarns in the Pontides are considered to be resulted from arc-related intrusions (Arslan and Aslan 2006; Boztuğ and Harlavan 2008; Karslı et al. 2010; Topuz et al. 2011). They have higher Th/Yb with increasing Ta/Yb compared to Eocene rocks (Arslan and Aslan 2006; Boztuğ and Harlavan 2008; Eyüboğlu et al. 2010; Karslı et al. 2010; Topuz et al. 2011). The Fe-Cu-Mo skarns in Demirkoy, Derekoy, Sukrupasa, Ikiztepe and Armutveren are caused by the Late Cretaceous granitoids in the Strandja massif; and Akgoz, Karabork, Kartiba, Canakci, Akkaya, Cimildag and Akkaya are caused by arc-related intrusions in eastern Pontides. The granitoids associated with Fe-skarns in the eastern Pontides represent more mesocratic character compared to W-skarn granitoids in western Pontides which are more leucocratic in composition. The Eocene plutonic rocks in the eastern Pontides are composed of plutonic rocks granodiorite, quartz diorite and diorite in composition. They are are enriched in LIL elements with respect to HFS elements with negative Nb, Ta, Zr, Hf, Ti, and positive Pb, and Sr anomalies (Arslan and Aslan 2006; Eyüboğlu et al. 2010; Karslı et al. 2010). These suggest that the Eocene plutonic rocks have geochemical characteristics consistent with a subduction-related setting. However, Kuşcu et al. (2017) suggested that these characteristics could also be ascribed to partial melting of metasomatized mantle. The Eocene Plutonic rocks have low Ni, Co, Y, Yb and HFS element concentrations, but high Sr, Ba, and La concentrations (Arslan and Aslan 2006; Boztuğ and Harlavan 2008; Eyüboğlu et al. 2010; Karslı et al. 2010; Topuz et al. 2011). Overall, the geochemical characteristics of Eocene plutonic rocks suggest adakitic compositions in the eastern Pontides, although Late Cretaceous normal arc-type plutonic rocks are present (Eyüboğlu et al. 2011, 2013) in western and eastern Pontides. The Sivritas-Sivrikaya, Cimildag, Ulutas, Kurtulmus and Yaglidere skarns are associated with mostly plutonic rocks Eocene in age.

7.4.3.2 WAP and Tavsanli Zone

The subduction-related and post-collisional Eocene to Miocene magmatic rocks in the WAP and Tavsanli zone commonly have medium to high-K compositions. They are evolved from low-K to high-K to shoshonitic series and calc-alkaline to alkaline with decreasing age (Kuşcu et al. 2018). In general, the magmatic rocks range from diorite-gabbro to granite or quartz diorite to granite in composition (Kuşcu et al. 2018). Eocene rocks appear to be more mafic compared to Oligocene and Miocene rocks. The causative magmatic rocks are characterized by trace element characteristics suggesting a ametasomatized mantle or a source modified by subduction (Kuşcu et al. 2018). There is no significant difference in multi-element patterns between magmatic rocks regardless of age (Kuşcu et al. 2018). Overall, LIL elements and LREE are enriched compared to HFSE and HREE. The REE and trace element concentrations of the rocks tend to increase from the Eocene to Miocene; except for Oligocene plutons that have overall lower concentrations and negative Eu anomalies. The youngest volcanic rocks have the highest REE and trace element abundances. The Sr/Y and La/Yb ratios of the magmatic rocks tend to increase from Middle Eocene to Late Miocene that could be ascribed either to melting at deeper sources with time or melting at source regions at more hydrous conditions (Kuşcu et al. 2018). The La/Sm, La/Yb, Sm/Yb, Th/Nb and ratios indicate a geochemical shift from normal arc andesites to an affinity with adakite-like rocks with decreasing age from Middle Eocene to Miocene (Kuşcu et al. 2018).

7.4.3.3 Southeastern Anatolian Orogenic Belt

The following is a summary of geochemical, petrogenetic characteristics extensively described in Kuşcu et al. (2010, 2013) of magmatic rocks in southeastern Anatolian orogenic belt (SEAOB). The Late Cretaceous plutonic rocks in Baskil arc are not related to or host to skarns. The Late Cretaceous intrusions exposed at Divriği, Hasançelebi and Keban are gabbro, monzodiorite, syenite and syenite porphyry in composition. These intrusions are also associated with IOCG mineralization. The Late Cretaceous alkaline rocks contain trace and REE compositions higher than slightly older Baskil arc rocks. They are characterized by Ba and Th enrichment and depletion in Nb and Ti. In general, Late Cretaceous magmatic rocks exhibit three distinct chemical groups, principally based on LREE compositions. In these groups, LREE enrichment becomes more pronounced in the Late Cretaceous rocks with decreasing age (Kuşcu et al. 2013).

The Eocene calc-alkaline magmatic rocks at Karamadazı and Dedeyazı are low-K, whereas those at Kabataş, Bizmişen, Çaltı and Horoz are medium-K with more calc-alkalic to calcic affinities (Kuşcu et al. 2013; İmer et al. 2013). They are granodiorite, diorite, and monzodiorite to gabbro in composition at Bizmişen, Çöpler, Kabataş, and Dedeyazı, whereas monzodiorite to gabbro in composition at Çaltı, Karamadazı and Horoz. The whole-rock geochemical composition of these rocks

intrusions suggest a derivation from partial melting of the metasomatized mantle and appears to be related to a major kinematic reorganization that took place during the switch from subduction to collisional tectonics in eastern Anatolia (Imer et al. 2015). This is interpreted to be due to break-off of the Southern Neo-Tethys oceanic slab prior to the Arabia–Eurasia continent-continent collision (~12 to 10 Ma) following widespread middle Eocene extensional magmatism (Imer et al. 2015). The rocks are characterized by LIL element enrichment with respect to HFS elements, and weak Nb negative anomalies with HFS elements concentrations similar to MORB.

7.4.3.4 Central Anatolian Crystalline Complex

The geological evidence indicates two phases of magmatism associated with two-successive obductions. An early but post-metamorphic group is of S-type syn-collisional (ca. 91 Ma, Rb/Sr whole rock age; Goncuoglu 1986) type, and formed by partial melting of thickened crust due to a northward subduction of northern margin of TAP beneath Pontide unit during Early to Late Cretaceous (Kuşcu and Erler 1998). The later group are of H- and A-types post-collisional (67–82 Ma) type, and was formed due to obduction of a supra-subduction zone ophiolitic sequence onto the metamorphics during the Campanian. These are also named as monzonitic to quartz monzonitic-monzodioritic rock associations. The post-collisional granitoids were formed by melting of two different sources; continental crust and mantle materials, and that a mixing/mingling process (Gencalioglu-Kuşcu et al. 2001; İlbeyli and Pearce 2001; Kuşcu et al. 2013) is suggested for the formation of the granitoid magmas in CACC (Kuşcu et al. 2002). They all show enrichment in LILE and LREE relative to HFS and high Sr and Nd isotope ratios (Ilbeyli et al. 2001) that may indicate an enriched mantle source region(s) carrying a subduction component inherited from pre-collision-subduction events.

The Fe-skarns in Central Anatolian Crystalline Complex (CACC) (Turkey) are associated with magmas formed after the major period of subduction and collision between Pontides and Tauride-Anatolide Platform during Late Cretaceous (collision between Eurasian and African-Arabian plates sensu lato). They are known as H-type monzonitic associations formed by the mixing and mingling of mantle-derived and crustal originated magmas at different levels. Therefore, one of the most significant feature assigned to the skarn-related granitoids in Central Anatolia is that they all show various textures and geochemical signatures of magma mixing indicating that they are more or less the products of homogeneous to heterogeneous mixing of two different magmas formed at two different tectonic setting, these granitoids have two distinct end members as mesocratic and leucocratic granitoids. Kuşcu et al. (2002, 2003) showed that the granitoids associated with the Fe-skarns are more mafic with a characteristic sodic alteration represented by their (Fe2O3(T)+CaO+MgO/Na2O) ratio. Also, these granitoids have a characteristic high Sr/(K2O+Rb) ratios indicating a less magmatic evolution compared to Pb-Zn and W-associated granitoids.

The recent studies dealing with the skarn deposits related to post-collisional I-type granitoids showed that the W-skarns are associated with leucocratic subtype of the H-type intrusive associations such as Çelebi, Kesikköprü and Akdagmadeni (Kuşcu et al. 2001, 2002). Kuşcu et al. (2001, 2002) showed that the Çelebi Fe-skarn deposit is associated with mesocratic counterparts of the H-type intrusives such as monzodiorite, granoidiorite and diorite. However, W mineralization is observed within the quartz veins and aplite dikes in the granite intrusion itself, and a considerable gold is associated with W mineralization. W mineralization with sporadic Cu association in Akdagmadeni is also hosted by more evolved counterparts of the H-type intrusive association.

7.5 Metallogeny of Skarns

As a part of the Tethyan-Eurasian belt, Turkey has many characteristics similar to surrounding countries and host many skarn deposits. The magmatic and metallogenic processes were dominant in the Jurassic-Miocene time interval (Aral and Erler 1981), the principal skarn deposits have been formed during Late Cretaceous-Oligocene times.

The main skarn-producing events in Turkey associated with the geological evolution of the Neotethys. The earliest significant mineralization events of the Neotethys in Turkey occurred during the Cretaceous. Late Cretaceous subduction of oceanic crust at the colliding plate boundaries resulted in the formation of a series of magmatic arcs in northern and southern Turkey, and consequently formation of economically significant skarn and porphyry systems at the Pontides, but not at the Bitlis-Zagros suture. The skarns are also accompanied by a series of porphyry systems that intruded the older VMS terrains in Turkey and in other locations along TEMB. Examples include Demirkoy in the Thrace region (western Pontides) of Turkey and numerous Cu-skarn centers in southern Bulgaria. The second major metallogenic event occurred in the Late Cretaceous post-dating the collision between the Anatolide-Tauride Block collided and the Eurasian plate. This era is characterized by the generation of post-collisional (late-orogenic) I- to H-type calc-alkaline granitoids. The granitoids are the products of mixing/mingling of two coexisting magmas derived from the mantle and continental crust. This is the major metallogenic epoch that created the most economic skarn deposits in central Anatolia and southeastern Anatolian orogenic belt. The third metallogenic event took place at the Mesozoic-Tertiary boundary (Uppermost Cretaceous to Lower-Mid Paleocene during which a major crustal extension is predominant throughout Turkey. This tectonic regime is attributed to either thermal perturbation of metasomatized lithosphere by delamination of the thermal boundary layer or removal of a subducted plate (Ilbeyli et al. 2001) during Uppermost Cretaceous times. This era is dominated mainly by alkaline magmatism that produced syenitoids that intruded the earlier calc-alkaline granitoids. These are occasionally associated with skarns the examples of which are best exposed in eastern Turkey (Eastern Taurides). A series

of mineralizing events in the Eocene-Oligocene epochs resulted in the formation of numerous porphyry copper/molybdenum/gold systems in the eastern Pontides and the WAP along with centers of epithermal mineralization. The last major mineralizing event occurred in the Late Oligocene-Miocene epochs that gave rise to porphyry and skarn deposits in the WAP and sporadically in the SEAOB. Epithermal gold deposits were also formed at this time, particularly in west Anatolia (Menderes massif) within zones of regional extension.

7.6 Conclusions

The main skarn-producing events in Turkey are associated with the geological evolution of the Neotethys. As part of the Tethyan-Eurasian belt, Turkey has many characteristics similar to surrounding countries and host many skarn deposits. The magmatic and metallogenic processes were dominant in the Jurassic-Miocene time interval, the principal skarn deposits have been formed during Late Cretaceous-Oligocene times. The skarns and skarn deposits are formed during major periods of subduction, continental collision, and post-collisional evenst in response to the convergence between Eurasia and Afro-Arabia between Late Cretaceous and Oligo-Miocene period. The main skarn-producing events in Turkey are related to the Late Cretaceous subduction of oceanic crust at the collision sutures resulted in the formation of a series of magmatic arcs, that also resulted in porphyry systems at the Pontides, but not at the Bitlis-Zagros suture. The second major skarn-producing event took place during Late Cretaceous post-dating the collision between the Anatolide-Tauride Block collided and the Eurasian plate. This era is characterised by the generation of post-collisional (late-orogenic) I- to H-type calc-alkaline granitoids. These granitoids are the products of mixing/mingling of two coexisting magmas derived from the mantle and continental crust. This is the major period during which the most economic skarn deposits in central Anatolia have been resulted in. The third skarn-producing events took place at the Mesozoic-Tertiary boundary (Uppermost Cretaceous to Lower-Mid Paleocene during which a major crustal extension is predominant throughout Turkey.

The skarns in Turkey are classified mainly as calcic exoskarns and occasionally as magnesian exoskarns. The economic mineralization are largely confined to calcic exoskarns with exception of Fe- and Fe-W skarns. They are widely distributed over the calcitic meta-carbonates and recrystalllized limestones within metamorphic sequences or intercalations within sedimentary and/or volcanic sequences. The skarns are classified as Fe-, Fe-Cu, Cu-, W-, Fe-W, Mo and Pb-Zn-skarns according to dominant metal they contain. The wall rocks span an age range from Cambrian to Permian, and to Upper Cretaceous. The most common periods for skarn generations are Late Cretaceous, Middle Eocene and Oligocene. No or a few skarn formation is associated with intrusions younger than Miocene period. The skarns that coexist as proximal calc-silicate assemlages within major high-level porphyry Cu systems are largely controlled by regional, large-scale structures such as strike-slip faults or core-complex systems. Where both Fe, Fe-Cu and Pb-Zn-skarns are observed in the

same region, the Fe- and Fe-Cu skarns are classified as proximal, and Pb-Zn skarns as distal skarns. The Fe and Fe-Cu skarns are commonly associated with oxidized I-type intermediate to mafic intrusives or sub-volcanic domes Late Cretaceous to Eocene in age that also formed economic porphyry Cu deposits. However, Fe and W skarns are co-genetic to porphyry Cu depoists associated with oxidized to mildly oxidized intrusives of Middle Eocene to Oligocene in age.

The chemistry of the associated skarns is different for each class. The I-type and mafic characteristics are predominant in Fe-skarns while more felsic and crustal signature is diagnostic for Pb-Zn skarns. In general, the Fe-skarns are associated with less evolved magmas that formed granitoids monzonite, monzodiorite, and occasionally granodiorite in composition. However, the Pb-Zn skarns are associated with strongly evolved magmas that formed granite to granodiorite in composition.

References

Agard P, Omrani J, Jolive L, Mouthereau F (2005) Convergence history across Zagros (Iran): constraints from collisional and earlier deformation. Int J Earth Sci 94:401–419

Akıncı Ö (1984) The Eastern Pontide volcano-sedimentary belt and associated massive sulphide deposits. Geol Soc Lond Sp Publ 7:415–428

Aldanmaz E, Pearce JA, Thirlwall MF, Mitchell JG (2000) Petrogenetic evolution of late Cenozoic, post-collision volcanism in western Anatolia. Turkey J Vol Geo Res 102:67–95

Altunbey M, Sagıroglu A (2003) Skarn-type ilmenite mineralization of the Tuzbasi-Tunceli region, Eastern Turkey. J Asian Earth Sci 21:481–488

Aral H, Erler A (1981) Porfiri bakır yatakları [Porphyry copper deposits] ODTU Müh Fak Publ 67, 100p (in Turkish with English abstract)

Arslan M, Aslan Z (2006) Mineralogy, petrography and whole-rock geochemistry of the Tertiary granitic intrusions in the Eastern Pontides, Turkey. J Asia Earth Sci 27:177–193

Aslan Z (2005) Petrography and petrology of the calc-alkaline Sarihan granodiorite (NE Turkey): an example of magma mingling and mixing. Turk J Earth Sci 14:185–207

Aslan Z (2010) U-Pb zircon SHRIMP age, geochemical and petrographical characteristics of tuffs within calc-alkaline Eocene volcanics around Gümüşhane (NE Turkey), Eastern Pontides. Neues Jahrbuch Mineral 187:329–346

Aydoganlı E (1978) Turkiye volfram envanteri [Turkish wolframite inventory]. MTA publ. 170, 40p (in Turkish)

Bayhan H (1984) Kesikköprü skarn kuşağının (Bala-Ankara) mineralojisi ve petrojenezi [Petrogenesis and mineralogy of the Kesikköprü skarn zone (Bala, Ankara)], Hacettepe Üniv. Yerbilimleri Bull 11:45–58 (in Turkish with English Abstract)

Beyarslan M, Bingöl AF (2000) Petrology of a supra-subduction zone ophiolite (Elazığ, Turkey). Can J Earth Sci 37:1411–1424

Black KN, Catlos EJ, Oyman T, Demirbilek M (2013) Timing Aegean extension: evidence from in situ U–Pb geochronology and cathodoluminescence imaging of granitoids from NW Turkey. Lithos 180–181:92–108

Bozkurt E, Oberhänsli R (2001) Menderes massif (Western Turkey): structural, metamorphic and magmatic evolution-a synthesis. Int J Earth Sci 89:679–708

Boztuğ D, Harlavan Y (2008) K-Ar ages of granitoids unravel the stages of NeoTethyan convergence in the eastern Pontides and central Anatolia, Turkey. Int J Earth Sci 97:585–599

Boztuğ D, Erçin AI, Kuruçelik MK, Göç D, Kömür I, İskenderoğlu A (2006) Geochemical characteristics of the composite Kaçkar batholith generated in a NeoTethyan convergence system, eastern Pontides. Turk: J Asian Earth Sci 27:286–302

Çağatay A, Teşrekli R (1979) Vitişenit minerali içeren Keskin-Karamağara kurşun-çinko zuhurunun mineralojisi ve kökeni. (Mineralogy and genesis of vittichenite-bearing lead-zinc skarn at Keskin-Karamağara). Türk Jeol Kur Bull 22:203–208 (in Turkish with English abstract)

Çalık A, Öngen S (2000) Keban Skarn Oluşumu, Kd Elazığ Bölgesi (Formatin of skarns at Keban, NE Elazığ). İstanbul Univ Mühendislik Fakültesi Yerbilimleri Bull 13:1–14 (in Turkish with English abstract)

Collins AS, Robertson AHF (1997) Lycian melange, southwestern Turkey: an emplaced Late Cretaceous accretionary complex. Geology 25:255–258

Demange M, Berson F, Fontelles M, Pascal M, Öngen S, Forette MC (1998) Wollastonite-garnet skarns of Demirtepe, Tahtakopru (province of Bursa, Turkey). Acad des Sci/Elsevier, Paris 326:771–778

Doglioni C, Agostini S, Crespi M, Innocenti F, Manetti P, Riguzzi F, Savasçın Y (2002) On the extension in western Anatolia and the Aegean sea. In: Rosenbaum G, Lister GS (eds) Reconstruction of the evolution of the Alpine-Himalayan Orogen. J Vir Expl 8:161–176

Eyüboğlu Y, Dilek Y, Bozkurt E, Bektaş O, Rojay B, Şen C (2010) Structure and geochemistry of an Alaskan-type ultramafic-mafic complex in the eastern Pontides, NE Turkey. In: Santosh M, Maruyama S (eds) A tribute to Akiho Miyashiro. Gondwana Res 18: 230–252

Eyüboğlu Y, Chung SL, Santosh M, Dudas FO, Akaryalı E (2011) Transition from shoshonitic to adakitic magmatism in the eastern Pontides, NE Turkey: implications for slab window melting. Gondwana Res 19:413–429

Eyüboğlu Y, Santosh M, Dudas FO, Akaryalı E, Chung SL, Akdağ K, Bektaş O (2013) The nature of transition from adakitic to non-adakitic magmatism in a slab-window setting: a synthesis from the Eastern Pontides, NE Turkey. Geosci Front. https://doi.org/10.1016/j.gsf.2012.10.001

Eyüboğlu Y, Santosh M, Yi K, Tüysüz N, Korkmaz S, Akaryali E, Dudas FO, Bektaş O (2014) The Eastern Black Sea-type volcanogenic massive sulfide deposits: geochemistry, zircon U–Pb geochronology and an overview of the geodynamics of ore genesis. Ore Geol Rev 59:29–54

Fytikas M, Innocenti F, Manetti P, Mazzuoli R, Peccerillo A, Villari L (1984) Tertiary to Quaternary evolution of volcanism in the Aegean region. In: Dixon JE, Robertson AHF (eds) The geological evolution of the eastern Mediterranean. Geol Soc, Lond Sp Publ 17: 687–700

Gautier P, Brun JP, Moriceau R, Sokoutis D, Martinod J, Jolivet L (1999) Timing, kinematics and cause of Aegean extension: a scenario based on a comparison with simple analogue experiments. Tectonophysics 315:31–72

Gençalioğlu-Kuşcu G, Göncüoğlu MC, Kuşcu İ (2001) Post-collisional magmatism on the Northern Margin of the Taurides and its geological implications: geology and petrology of the Karamadazı-Yahyalı granitoid. Turk J Earth Sci 10(3):103–120

Göncüoglu MC (1986) Geochronologic age data from the southern part of the Central Anatolian Massif. M.T.A. Bull 105(106):111–124 (in Turkish with English abstract)

Göncüoğlu MC, Toprak V, Kuşcu İ, Erler A, Olgun E (1991) Orta Anadolu Masifi'nin batı bölümünün jeolojisi, Bölüm 1: Güney Kesim [The geology of the western part of central Anatolian massif; Part 1: Southern part] TPAO Report Rep No. 2909, 140p (in Turkish with English abstract)

Göncüoglu MC, Dirik K, Kozlu H (1997) Pre-Alpine and Alpine terranes in Turkey: explanatory, notes to the terrane map of Turkey. Ann Geol Pays Hellén 37:515–536

Göncüoğlu MC, Boncheva I, Göncüoğlu Y (2004) First finding of Middle Tournasian conodonts in the Griotte-type limestones of the "Palaeozoic of Istanbul": implications for the Variscan evolution. Rev Ital Pal Strati 110:431–439

van Hinsbergen D, Kaymakçı N, Spakman W, Torsvik TH (2010) Reconciling the geological history of western Turkey with plate circuits and mantle tomography. Earth Planet Sci Lett 297:674–686

Ilbeyli N, Pearce JA (2001) Genesis of enclaves in the Central Anatolian plutonics. Fourth international Turkish geology symposium Adana-Turkey, Abstracts vol, pp 205

Ilbeyli N, Pearce JA, Thirwall MF, Mitchell JG (2001) Genesis of collision related plutonic rocks in the Central Anatolian massif (Turkey). Fourth international Turkish geology symposium Adana-Turkey, Abstracts vol, pp 201

İmer A, Richards JP, Creaser RA (2013) Age and tectonomagmatic setting of the Eocene Çöpler–Kabataş magmatic complex and porphyry-epithermal Au deposit, East Central Anatolia, Turkey. Mineral Deposita 48:557–583

İmer A, Richards JP, Creaser RA, Spell TL (2015) The late Oligocene Cevizlidere Cu-Au-Mo deposit, Tunceli Province, eastern Turkey. Mineral Deposita 50:245–263

Inan K (1979) Uludag skarn kusagının petrojenezi ve jeokimyası [Petrogenesis and geochemistry of Uludağ skarn]. Dissertation Thesis, Istanbul Tech. University, 133p (in Turkish with English abstract)

Jolivet L (2001) A comparison of geodetic and finite strain pattern in the Aegean, geodynamic implications. Earth Planet Sci Lett 187:95–104

Karacık Z, Tüysüz O (2010) Petrogenesis of the Late Cretaceous Demirköy Igneous Complex in the NW Turkey: implications for magma genesis in the Strandja Zone. Lithos 114:369–384

Karslı O, Dokuz A, Uysal İ, Aydın F, Kandemir R, Wijbrans J (2010) Generation of the Early Cenozoic adakitic volcanism by partial melting of mafic lower crust, Eastern Turkey: implications for crustal thickening to delamination. Lithos 114:109–120

Kaygusuz A, Arslan M, Siebel W, Şen C (2011) Geochemical and Sr-Nd isotopic characteristics of post-collisional Calc-alkaline volcanics in the Eastern Pontides (NE Turkey). Turk J Earth Sci 20:137–159

Kaymakçı N, Kuşcu İ (2007) Late Cretaceous to recent kinematic evolution of Turkey, European Geosciences Union 2007. Geophysical Research Abstracts 9, 05426, SRef-ID: 1607–7962/gra/EGU2007-A-05426

Kaymakçı N, İnceöz M, Ertepınar P (2006) 3D-architecture and neogene evolution of the Malatya Basin: inferences for the kinematics of the Malatya and Ovacık fault zones. Turk J Earth Sci 15:123–154

Keskin M (2003) Magma generation by slab steepening and break off beneath a subduction-accretion complex: an alternative model for collision-related volcanism in eastern Anatolia, Turkey. Geophys Res Lett 30:8046. https://doi.org/10.1029/2003GL018019

Kovenko V (1947) Kuzey Anadolu bölgesinin bazı kurşun-çinko ve antimuan madenleri (Denek, Akdağ, Turhal) [Lead-zinc and antimony ore deposits of northern Anatolia region (Denek, Akdağ, Turhal)]. M.T.A. Bull 37:61–96 (in Turkish with English abstract)

Kuşcu İ (2001) Geochemistry and mineralogy of the skarns in the Çelebi district, Kırıkkale, Turkey. Turk J Earth Sci 10:121–132

Kuşcu İ (2005) World skarn deposits: skarns of Turkey. Econ Geol 100th Anniv Vol. Soc Econ Geol, Littleton, pp 299–336

Kuşcu İ, Erler A (1998) Mineralization events in a collision related setting: the central Anatolian crystalline complex. Int Geol Rev 40(6):552–565

Kuşcu İ, Kuşcu G, Göncüoğlu MC, Meinert LD (1998) Orta Anadolu Kristalen Karmaşığı'nda yer alan granitoyidler ve skarn yataklarının kökensel birlikteliklerinin magmatik petrojenez ile ilişkilendirilmesi [The genetic association between skarns and granitoids of the central Anatolian crystalline massif]. TUBITAK Project rep. No. YDABCAG-198Y098, 142 p (in Turkish with English abstract)

Kuşcu İ, Erler A, Gencalioglu-Kuşcu G (2001) Geochemical signatures of granitoids associated with skarns in Central Anatolia. Int Geol Rev 43(8):722–735

Kuşcu İ, Gencalioğlu-Kuşcu G, Meinert LD (2002) The tectonic setting and petrogenesis of the Celebi Granitoid, (Kırıkkale-Turkey) and geochemical comparison with world-class skarn granitoids. J Geochem Explor 76(3):175–194

Kuşcu İ, Gençalioğlu-Kuşcu G, Soylu M (2003) Post-collisional H-type granitoid magmatism in Central Anatolia and time-space relation with Fe-oxide mineralization, mineral exploration and sustainable development, vol 1. In: Eliopoulos et al (eds) Proceedings of the 7th biennial SGA meeting, Rotterdam, pp 307–311

Kuşcu İ, Yılmazer E, Demirela G, Gökçe H (2005) Orta ve Batı Anadolu'daki Bazı "Skarn-Tipi" Fe-Oksit Yataklarının Fe-Oksit-Cu-Au (Doba) Potansiyeli [The ironoxide-Cu-Au potential of the central Anataolian Fe-skarns]. In Öztürk H, Kariman A, Hanilçi N (eds). In: Öztürk H, Kariman A, Hanilçi N (eds) Türkiye Demir Yatakları Jeolojisi, Madenciliği ve Mevcut Sorunları Sempozyumu Bildiriler Kitabı, pp 179–204 (in Turkish with English abstract)

Kuşcu İ, Gençalioğlu-Kuşcu G, Tosdal RM, Ullrich T, Friedman R (2010) Magmatism in the southeastern Anatolian orogenic belt: transition from arc to post-collisional setting in an evolving orogeny. In: Stephenson RA, Kaymakçı N, Sosson M, Starostenko V, Bergerat F (eds) Sedimentary Basin Tectonics from the Black Sea and Caucasus to the Arabian Platform. Geol Soc, Lond Sp Publ 340: 437–460

Kuşcu İ, Yılmazer E, Bayır S, Sezerer-Kuru G, Güleç N, Demirela G, Gençalioğlu-Kuşcu G, Kaymakçı N (2011) U-Pb and Ar-Ar age dating and fluid inclusion constraints on the genesis of Hasançelebi iron oxide-copper-(gold) mineralizations, Malatya (Turkey). Econ Geol 106:261–288

Kuşcu İ, Tosdal RM, Gençalioğlu-Kuşcu G, Friedman R, Ullrich TD (2013) Late Cretaceous to middle Eocene magmatism and metallogeny of a portion of the Southeastern Anatolian Orogenic Belt, east central Turkey. Econ Geol 108:641–666

Kuşcu İ, Tosdal RM, Gençalioğlu-Kuşcu G (2018) Episodic Porphyry Cu (-Mo-Au) formation and associated magmatic evolution in Turkish Tethyan collage. Ore Geol Rev (in review)

Le Pichon XN, Angelier J (1979) The Hellenic arc and trench system: a key to the neotectonic evolution of the eastern Mediterranean area. Tectonophysics 60:1–42

McKenzie D (1972) Active tectonic of the Mediterranean region. Geophys J R Astrol Soc 30:109–185

Meinert L, Dipple G, Nicolescu S (2005) World skarn deposits. In: Hedenquist JW et al (eds) Economic geology 100th anniversary volume. Society of Economic Geologists, Littleton, pp 299–336

Moix P, Beccaletto L, Kozur HW, Hochard C, Rosselet F, Stampfli GM (2008) A new classification of the Turkish terranes and sutures and its implication for the paleotectonic history of the region. Tectonophysics 451:7–39

Moore WJ, McKee EH, Akıncı Ö (1986) Chemistry and chronology of plutonic rocks in the Pontide mountains, northern Turkey. In: Jankovic S, Sillitoe RHS (eds) European copper deposits. Faculty of Geology and Mining, Belgrade University, Belgrade, pp 209–215

Okay Aİ (1984) Distribution and characteristics of the Northwest Turkish blueschists, in The geological evolution of the Eastern Mediterranean. In: Dixon JE, Robertson AHF (eds) Geol Soc, Lond Sp Publ17: 455–466

Okay Aİ, Göncüoğlu MC (2004) The Karakaya Complex: a review of data and concepts. Turk J Earth Sci 13:77–95

Okay Aİ, Satır M (2000) Coeval plutonism and metamorphism in a latest Oligocene metamorphic core complex in northwest Turkey. Geol Mag 137:495–516

Okay Aİ, Satır M (2006) Geochronology of Eocene plutonism and metamorphism in northwest. Geodin Acta 19:251–266

Okay AI, Tüysüz O (1999) Tethyan sutures of northern Turkey. In: Durand B, Jolivet L, Horvath F, Seranne M (eds) The Mediterranean Basins: tertiary extensions within the Alpine Orogen. Geol Soc, Lond Sp Publ 156: 475–515

Okay Aİ, Satır M, Maluski H, Siyako M, Monié P, Metzger R, Akyüz S (1996) Paleo- and Neo-Tethyan events in northwestern Turkey: geologic and geochronologic constraints. In: Yin A, Harrison TM (eds) The tectonic evolution of Asia. Cambridge University Press, Cambridge, pp 420–441

Okay Aİ, Şahintürk Ö, Yakar H (1997) Stratigraphy and tectonics of the Pulur (Bayburt) region in the Eastern Pontides. M.T.A Bull 119:1–24

Okay A, Satır M, Siebel W (2006) Pre-Alpide orogenic events in the Eastern Mediterranean region. In: Gee DG, Stephenson RA (eds) European Lithosphere Dynamics. Geol Soc, Lond, Mem 32: 389–405

Okay Aİ, Satır M, Zattin M, Cavazz W, Topuz G (2008) An Oligocene ductile strike-slip shear zone: the Uludağ Massif, northwest Turkey-implications for the westward translation of Anatolia. Geol Soc Am Bull 120:893–911

Önal A, Boztuğ D, Kürüm S, Harlavan Y, Arehart GB, Arslan M (2005) K-Ar age determination, whole-rock and oxygen isotope geochemistry of the postcollisional Bizmişen and Çaltı plutons, SW Erzincan, Eastern Central Anatolia, Turkey. Geol J 40:457–476

Orhan A (2008) Susurluk (Balıkesir) skarn yatağının jeokimyasal karakteristikleri [Mineralogical and geochemical characteristics of the Susurluk (Balıkesir) skarn deposit]. Ph.D. Thesis, Eskisehir Osmangazi University, Eskisehir, 258p (unpublished; in Turkish with English abstract)

Papanikolaou DJ, Demirtaşlı E (1987) Geological correlations between the Alpine segments of the Hellenides-Balkanides and Taurides-Pontides. In: Flügel HW, Sassi FP, Grecula P (eds) Pre-variscan and variscan events in the Alpine-mediterranean mountain belts. Alfa Publishers, Bratislava, pp 387–396

Perinçek D, Kozlu H (1984) Stratigraphical and structural relations of the units in the Afşin-Elbistan-Doğanşehir region (Eastern Taurus). In: Tekeli O, Göncüoğlu MC (eds) Proceedings of international symposium on the geology of the Taurus Belt, pp 181–198

Pickett EA, Robertson AHF (1996) Formation of the Late Paleozoic–Early Mesozoic Karakaya Complex and related ophiolites in NW Turkey by Paleotethyan subduction-accretion. J Geol Soc Lond 153:995–1009

Régnier J, Ring U, Passchier CW, Gessner K, Güngör T (2003) Contrasting metamorphic evolution of metasedimentary rocks from the Çine and Selimiye nappes in the Anatolide belt, western Turkey. J Metamorph Geol 21:699–721

Rice SP, Roberson AHF, Ustaömer T, İnan T, Taşlı K (2009) Late Cretaceous-early Eocene tectonic development of the Tethyan suture zone in the Erzincan area, eastern Pontides, Turkey. Geol Mag 146:567–590

Rimmelé G, Oberhänsli R, Goffé B, Jolivet L, Candan O, Çetinkaplan M (2003) First evidence of high-pressure metamorphism in the "Cover Series" of the southern Menderes massif. Tectonic and metamorphic implications for the evolution of SW Turkey. Lithos 71:19–46

Ring U, Glodny J, Will T, Thomson SN (2010) The Hellenic subduction system: highpressure metamorphism, exhumation, normal faulting, and large-scale extension. Annu Rev Earth Planet Sci 38:45–76

Robertson AHF, Ustaömer T, Parlak O, Ünlügenç UC, Taşlı K, İnan N (2005) Late Cretaceous–Early Tertiary tectonic evolution of south-Neotethys in SE Turkey: evidence from the Tauride thrust belt in SE Turkey (Binboğa-Engizek segment). J Asian Earth Sci https://doi.org/10.1016/j.jseaes.2005.02.004

Rolland Y, Perinçek D, Kaymakçı N, Sosson M, Barrier E, Avagyan A (2011) Evidence for 80–75 Ma subduction jump during Anatolide–Tauride–Armenian block accretion and 48 Ma Arabia–Eurasia collision in Lesser Caucasus–East Anatolia. J Geodynamics https://doi.org/10.1016/j.jog.2011.08.006

Rosenbaum G, Lister GS, Duboz C (2002) Reconstruction of the tectonic evolution of the western Mediterranean since the Oligocene. In: Rosenbaum G, Lister GS (eds) Reconstruction of the evolution of the Alpine-Himalayan Orogen. J Virtual Expl 8:107–130

Sağıroğlu A (1982) Contact metasomatism and ore deposition of the lead-zinc deposits of Akdağmadeni, Yozgat, Turkey, Ph.D. Thesis, University of London, London, 314p

Savostin LA, Sibuet JC, Zonenshain LP, Le Pichon X, Rolet J (1986) Kinematic evolution of the Tethys belt, from the Atlantic to the Pamirs since the Triassic. Tectonophysics 123:1–35

Schuiling RD (1959) Uber eine Pre-Herzynische Faltungs-phase im Kazdag Kristaalin. MTA Bull 53:89–93

Şengör AMC (1987) Tectonics of the Tethysides: orogenic collage development in a collisional setting. An Rev Earth Planet Sci 15:213–244

Şengör AMC, Yılmaz Y (1981) Tethyan evolution of Turkey: a plate tectonic approach. Tectonophysics 75:181–241

Şengör AMC, Özeren S, Genç T, Zor E (2003) East Anatolian high plateau as a mantle-supported, North–south shortened domal structure. Geo Res Lett 30 https://doi.org/10.1029/2003GL017858

Stampfli GM, Borel GD (2004) The TRANSMED transects in space and time: constraints on the paleotectonic evolution of the Mediterranean domain. In: Cavazza W, Roure F, Spakman W, Stampfli GM, Ziegler P (eds) The TRANSMED Atlas: the Mediterranean Region from crust to mantle. Springer Verlag, Berlin, pp 53–76

Taner MF (1981) Şükrüpaşa (Demirköy-Kırklareli) çevresinde jeolojik, petrografik inceleme ve Cevherleşme üzerine görüşler [On the geological, petographical and mineralization of Şükrüpaşa (Demirköy, Kırklaeeli)], M.T.A Report No 1777 (in Turkish with English abstract)

Taymaz T, Yılmaz Y, Dilek Y (2007) The geodynamics of the Aegean and Anatolia: introduction. In: Taymaz T, Yılmaz Y, Dilek Y (eds) The geodynamics of the Aegean and Anatolia. J Geol Soc Lond Sp Publ 29: 1–16

Temizel İ, Arslan M (2009) Mineral chemistry and petrochemistry of post-collisional tertiary mafic to gelsic cogenetic volcanics in the Ulubey (Ordu) Area, Eastern Pontides, NE Turkey. Turk J Earth Sci 18:29–53

Topuz G, Okay AI, Altherr R, Schwarz WH, Siebel W, Zack T, Satır M, Şen C (2011) Post-collisional adakite-like magmatism in the Ağvanis Massif and implications for the evolution of the Eocene magmatism in the Eastern Pontides (NE Turkey). Lithos 125:131–150

Tülümen E (1980) Akdağmadeni (Yozgat) yöresinde petrografik ve metalojenik incelemeler [Metallogenic and petrographical investigations on Akdağmadeni (Yozgat)]. Ph.D. Thesis, Karadeniz Tek. Üniv Trabzon, 157p (in Turkish with English abstract)

Vache R (1963) Akdağmadeni kontak yatakları ve bunların Orta Anadolu Kristalinine karşı olan jeolojik çerçevesi [Contact metasomatic deposits of the Akdağmadeni and their geologic association with the central Anataolian crystalline massif]. MTA Bull 60:22–36) (in Turkish with English abstract)

Whitney DL, Bozkurt E (2002) Metamorphic history of the Southern Menderes massif, Western Turkey. Geol Soc Am Bull 114:829–838

Whitney DL, Dilek Y (1998) Metamorphism during crustal thickening and extension in central Anatolia: the Nigde metamorphic core complex. J Petrol 39:1385–1403

Whitney DL, Hamilton M (2004) Timing of high-grade metamorphism in central Turkey and the assembly of Anatolia. J Geol Soc Lond Sp Publ 161(5):823–828

Whitney DL, Teyssier C, Fayon AK, Hamilton MA, Heizler M (2003) Tectonic controls on metamorphism, patial melting, and intrusion; timing and duration of regional metamorphism and magmatism in the Niğde massif, Turkey. Tectonophsics 376:37–60

Yazgan E, Chessex R (1991) Geology and tectonic evolution of southeastern Taurus in the region of Malatya. Turkish Ass Petr Geol Bull 3:1–42

Yılmaz Y (1993) New evidence and model on the evolution of the southeast Anatolian orogeny. Geol Soc Am Bull 105:251–271

Yılmaz-Şahin S (2005) Transition from arc- to post-collision extensional setting revealed by K–Ar dating and petrology: an example from the granitoids of the eastern Pontide igneous terrane, Araklı-Trabzon, NE Turkey. Geol J 40:425–440

Chapter 8
Porphyry-Cu Deposits of Turkey

İlkay Kuşcu, Richard M. Tosdal, and Gonca Gençalioğlu-Kuşcu

Abstract Turkey, located within the western Tethyan-Eurasian Belt contains numerous porphyry copper deposits formed by the subduction, collision and post-collisional events during the closure of NeoTethys Ocean between the latest Cretaceous and late Miocene. These porphyry systems and associated epithermal and skarn deposits are associated with the subduction and post-subduction magmatic rocks emplaced along arc-parallel belts as in eastern Pontides and arc transverse extensional terranes as in the western Anatolian province (WAP) and Southeastern Anatolian Orogenic Belt (SEAOB).

The porphyry deposits are formed in magmatic-arc (Pontides, Aegean and Bitlis-Zagros subduction), post-collisional settings (Pontides, WAP, SEAOB) after continental collision (Central Anatolian Crystalline Complex), and extensional arc setting (WAP). The porphyry Cu systems begin in the Late Cretaceous at the north, and generally young southward, where paired Late Cretaceous and Eocene metallogenic episodes are present in the eastern Pontides, WAP and SEAOB. The dominance of ages between ca. 83 and 70 Ma broadly coincides with the final stages of Late Cretaceous magmatism at the Pontides and SEAOB. The available ages are indicative of epidocity and a limited period of formation for porphyry Cu systems in these belts, and comparable to the metallogenic evolution of Turkey. The Eocene porphyry systems in discontinuous belts across Turkey reflect collisional to post-collisional processes.

The number of known porphyry deposits in porphyry belts is related to the level of erosion. Therefore, the magmatic belts with fewer known porphyry may indicate too shallow or too deep crustal levels for their exposure. The estimates of numbers of undiscovered deposits combined with grade and tonnage models in Monte Carlo simulation revealed a lower density of known porphyry deposits in the Pontides,

İ. Kuşcu (✉) · G. Gençalioğlu-Kuşcu
Department of Geological Engineering, Muğla Sıtkı Koçman University, Muğla, Turkey
e-mail: ikuscu@mu.edu.tr

R. M. Tosdal
Mineral Deposit Research Unit, Department of Earth and Ocean Sciences, University of British Columbia, Vancouver, BC, Canada

PicachoEx LLC, North Potomac, MD, USA

F. Pirajno et al. (eds.), *Mineral Resources of Turkey*, Modern Approaches in Solid Earth Sciences 16, https://doi.org/10.1007/978-3-030-02950-0_8

WAP and SEAOB relative to well-explored provinces around the world. This suggests that undiscovered deposits are likely present in Pontides, WAP and SEAOB.

8.1 Introduction

Turkey, at the boundary between the African and Eurasian plates in the Eastern Mediterranean, is in continental collision with Eurasia and Afro-Arabia along the Pontides, Bitlis-Zagros suture, and active Aegean subduction (Fig. 8.1). Turkey is located within the western Tethyan-Eurasian Metallogenic Belt (TEMB), which is about 7000 km long, stretching from the eastern Pontides, the Lesser Caucasus, Iran, southeast Afghanistan reaching to the area of Himalayas to Endonesia. This belt is an extremely complex geological terrane caught between colliding continents (Fig. 8.1).

The common association of porphyry Cu deposits worldwide with subduction-related calc-alkaline magmas in continental arcs are quite clear, and are well documented; Andes, North American Cordillera, Papua New Guinea, and China (e.g., Sillitoe 1972, 2010; Mitchell 1973; Titley and Beane 1981; Lang and Titley 1998; Richards et al. 2001; Richards 2003; Cooke et al. 2005; Hollings et al. 2005; Zhang et al. 2006). The porphyry Cu deposits in continental arc in central Andes are related to flattening of the subducting oceanic slab, associated crustal thickening and block uplift (Richards et al. 2001; Bissig and Tosdal 2009; Perello et al. 2003; Cooke et al. 2005). The recent works, however, showed the existence of a suite of porphyry Cu deposits in collisional zones (Hou et al. 2003; Hou and Cook 2009) and intracontinental settings (Hou et al. 2004, 2011). Turkey as an integral part of the Tethyan orogen forms a belt where subduction-related and post-collision related porphyry deposits are

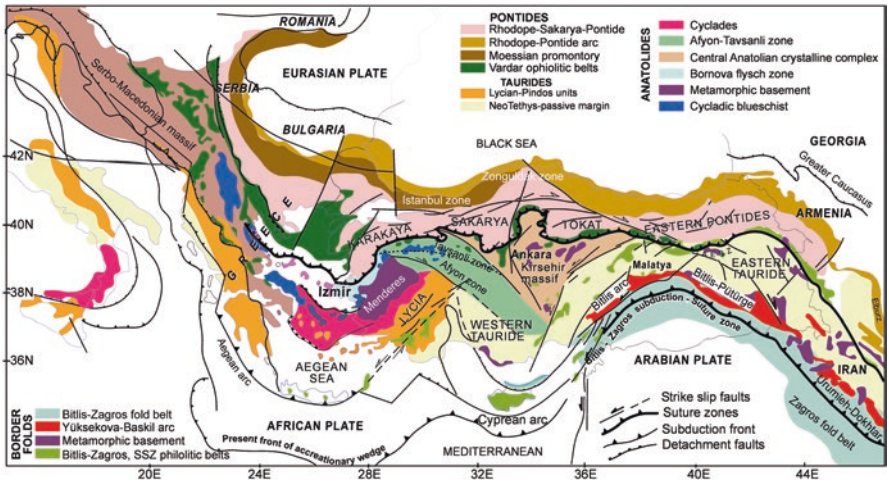

Fig. 8.1 Simplified geologic map showing major sutures, microcontinental terranes, regional structures in Turkey. (From Kuşcu et al. 2018 and references therein)

present at the expense of colliding Eurasian, Arabian and African plates during the opening, final closure and terminal suturing of the Tethys Ocean (Şengör and Yılmaz 1981; Görür et al. 1984, 1997; Robertson and Dixon 1984; Şengör et al. 1984), between Late Cretaceous to Quaternary period. This collisional assemblage generated a highly fertile metallogenic environment with abundant porphyry Cu deposits in the entire TEMB and Turkey, clustering in narrow arc segments, and post to late orogenic extensional settings (Kuşcu et al. 2011, 2018). A deep-seated source, visible by mantle tomography, has been postulated as the cause of the magmatism during the Tertiary (Angus et al. 2006; Özacar et al. 2008, 2010; Biryol et al. 2011) and associated mineralization that is superimposed on an earlier Late Cretaceous calc-alkaline magmatic and metallogenic event (Kuşcu 2009; Kuşcu et al. 2011, 2012, 2018).

The geochronological framework, spatial-temporal associations between magmatism and porphyry deposits, tectono-magmatic evolution of porphyry deposits in subduction, collisional and post-collisional zones, and the tectonic setting of porphyry Cu deposits have been recently documented by Kuşcu et al. (2018). This chapter is the descriptive summary of their recent work, and aims at describing the major characteristics of the significant porphyry Cu deposits and newly discovered prospects/occurrences, and summarizes the geology, geodynamic setting, geochronology and geochemistry-petrogenesis of porphyry deposits/prospects and associated magmatism in relation to Tethyan evolution of Turkey. Therefore, the existing literature on the mineral deposits/prospects in Turkey was synthesized, and geochronological, geochemical, and field geological data were summarized in order to provide a petrochemical, geochronological and tectonic framework to diverse magmatic events and various porphyry-style deposits for the entire Turkey. In this chapter, the database on the field characteristics and geochemical characteristics of the magmatic and mineralized rocks either hosting or associated with porphyry copper deposits/prospects are based on the recent work by Kuşcu et al. (2018). Similarly, the timing of magmatic and hydrothermal events based on $^{40}Ar/^{39}Ar$ and U-Pb geochronology of mineral separates from igneous and mineralized rocks was provided by Kuşcu et al. (2018).

8.2 Geologic Setting and Nomenclature: Oceanic Domains, Continental Fragments-Terranes and Suture Zones in Turkey

8.2.1 Definition of Oceanic Domains

As the porphyry Cu deposits manifest themselves in the active margins or collisional zones, a synthesis on the oceanic domains is necessary to explain the subduction, collision and post-collisional settings in relation to porphyry Cu formation in Turkey. Turkey is a complex geodynamic area formed as a response to the episodic closure of Mesozoic oceanic domain called Tethys, a westward narrowing embayment between Laurasia and Gondwana since the Carboniferous (Şengör and Yılmaz

1981; Şengör 1987). Two significant oceans in the Tethys evolution have been defined, i.e., the PaleoTethys and NeoTethys (Şengör and Yılmaz 1981; Şengör 1987). The PaleoTethys, the older ocean is a Paleozoic ocean north of the Cimmerian continent opened in Devonian–Carboniferous, and NeoTethys is a relatively younger Late Paleozoic-Mesozoic ocean that separated the Cimmerian blocks from Gondwana (Şengör 1979; Stampfli and Borel 2002). Northward subduction of PaleoTethys also triggered the opening of other short-lived back-arc spreading along the Eurasian margin during Permo-Triassic. The spreading of some of these back-arc oceans like the Maliac, Pindos, and Karakaya oceans terminated before the end of the Triassic; others like Meliata stayed open and their delayed subduction resulted in the opening of younger marginal oceans and/or oceanic basins or back-arc oceans. In the geologic context of Turkey, the NeoTethys was originally recognized as (a) northern (northerly ocean) and southern (southerly ocean) branches of NeoTethys located to the north and south of the Tauride-Anatolide block. However, this classification was recently revised in recent works claiming that the northern branch (northerly ocean) was a marginal basin called Vardar or İzmir-Ankara-Erzincan (İAE) ocean (Stampfli 2001; Handy et al. 2010 and references therein), and the southern branch (southerly Ocean), part of which still exists in the Aegean part of the Eastern Mediterranean Sea, is referred to simply as the Neotethys ocean (Stampfli 2001). The Vardar, İAE Ocean existed between the Sakarya microcontinent and the Tauride-Anatolide block (or Tauride-Anatolide Platform (TAP) during Liassic and Late Cretaceous (Şengör and Yılmaz 1981; Görür et al. 1984; Yılmaz et al. 1997 and the references therein). The main part of İAE Ocean is preserved as E-W trending ophiolitic rocks and mélanges widely exposed along the İzmir-Ankara-Erzincan Suture Zone (İAESZ) in Anatolides as shown in Fig. 8.1. The southerly ocean, on the other hand, is marked by ophiolitic rocks or mélanges lying parallel to the main Bitlis-Zagros Suture Zone (Fig. 8.1).

8.2.2 Microcontinental Fragments-Terranes in Turkey

The closure of NeoTethys Ocean and collision with Eurasian, Afro-Arabian plates during Tertiary times resulted in accretion and amalgamation of multiple volcanic-arc segments, microcontinental fragments and sub-arcs to the Eurasian and Afro-Arabian plates (Fig. 8.1) (Şengör and Yılmaz 1981; Göncüoğlu et al. 1997; Okay and Tüysüz 1999). Each of these fragments once rifted-off from the Gondwanaland, are bounded by several tectonic structures and sutures (Okay and Tüysüz 1999). From north to south, these fragments are known as the Pontides, Tauride-Anatolide Block (TAB), and Border Folds (Arabian Platform) since Ketin (1966). This subdivision was partly modified by Okay and Tüysüz (1999) namely as; the Strandja terrane, İstanbul and Zonguldak zones, the Sakarya terrane (SM), Karakaya complex in Pontides; Afyon zone, Bornova flysch zone, Tavşanlı zone, Menderes Massif (MM), Kırşehir massif (or Central Anatolian Crystalline Complex, CACC) in Anatolides; western and Central Taurides and Southeastern Anatolian Orogenic

Belt (SEAOB) in Taurides; and the Arabian Platform (Okay and Tüysüz 1999; Stampfli 2001; Guest et al. 2006; Moix et al. 2008; Hassanzadeh et al. 2008) (Fig. 8.1). The classification scheme by Kuşcu et al. (2018) was partly adopted in this chapter, and Karakaya complex, Bornova flysch zone, Tavşanlı and Afyon zones, and Menderes Massif (MM) are included in western Anatolian province (WAP). The Strandja, the İstanbul and Zonguldak zones, the Sakarya microcontinent (SM), and Karakaya complex were collectively termed as the Pontides.

8.2.3 Suture Zones

The suture zones in the context of porphyry-producing collisional zones within the Turkish Tethyan collage include the İzmir-Ankara-Erzincan suture zone (İAESZ; Fig. 8.1), separating the Tauride-Anatolide block from the Pontides. The İAESZ marks the boundary between Eurasian plate and TAB, and was formed by the closure of the İAE ocean. It consists of remnants of the marginal İAE oceanic basins, and suture-parallel supra-subduction zone ophiolites and ophiolitic mélanges. The Bitlis Suture Zone (Fig. 8.1) within the southeastern Anatolian orogenic belt, marks the boundary between the TAB and the Arabian plate, and was resulted from the closure of the southerly NeoTethys ocean between Late Cretaceous and Eocene. The Zagros suture is the eastern continuation of the Bitlis suture zone, marking the boundary between the Arabian platform and the earlier accreted fragments in the Middle East. Collectively, these are known as Bitlis-Zagros suture (Fig. 8.1) in the NeoTethys terminology.

8.3 NeoTethyan Geologic Evolution of Turkey

The porphyry Cu deposits and prospects in Turkey are hosted by and/or associated with volcano-plutonic rocks formed at active, convergent margins and subductional settings or transtensional to post-collisional settings accompanying the subductional events. Therefore, this section summarizes the geologic evolution of Turkey in terms of major magma-producing events through several subduction and collision events since the Early-Late Cretaceous. The magmatism in Turkey is largely related to convergent plate margin evolution by the closure PaleoTethys and NeoTethys oceans. The traces and products of PaleoTethyan magmatism have almost been erased by subsequent metamorphism, uplift, erosion and obductional events since the Precambrian. During the closure of the NeoTethyan Ocean, three subductional-collisional events have been recognized (Okay and Tüysüz 1999; Göncüoğlu et al. 2000; Stampfli 2001; Bozkurt and Mitwede 2001; Taymaz et al. 2007; Stampfli and Borel 2004; Moix et al. 2008). These events are; (1) closure of the northerly ocean, İAE ocean (collision between TAB and SM (Eurasian plate, sensu lato)) in the north between *ca.* 110–39 Ma (2) closure of the southerly ocean,

NeoTethys (collision between Arabian plate and TAB) to the south between 83–44 Ma (Kuşcu et al. 2018), and (3) closure of the Mediterranean Sea, the remaining NeoTethys ocean (collision between TAB and African plate) to the west between 42 Ma to recent. These events resulted in the generation of active margin magmatism, accretion of continents, amalgamation of microcontinental fragments and ophiolitic thrust slices. The first event formed the Pontide magmatic arc and also resulted in generation of a supra-subduction zone ophiolites (northerly ophiolites) that were later emplaced over the TAB and that resulted in regional metamorphism (Fig. 8.1). The second event formed Baskil arc, and Bitlis-Zagros subduction in the SEAOB, and resulted in generation of a supra-subduction zone ophiolites (southerly ophiolites). The third event formed Helenic-Aegean subduction in the western Anatolia, and resulted in Aegean and Cyprean arc magmatism.

During the first subduction event, most of the oceanic lithosphere of marginal Vardar-İAE ocean was consumed firstly by intra-oceanic subduction that formed intra-oceanic OIB-type seamounts with (supra-subduction zone ophiolites, northerly ophiolites, SSZ) at *ca.* 117 Ma and active margin along the Pontide subduction (Şengör and Yılmaz 1981; Kaymakçı et al. 2009), and secondly by an Andean-type northward subduction. This subduction resulted in generation of Pontide magmatic arc, and arc-parallel or transverse regional structures that formed extensional basins on the overriding plate and at the back arc settings. The available geochronology suggests that Pontide arc magmatism took place in two successive pulses; the volcanic and volcaniclastic rocks as the first pulse (*ca.* 110–81 Ma, Okay et al. 2006; Eyüboğlu et al. 2010), and the intrusive rocks as the second pulse (*ca.* 79–76 Ma; Table 8.1, and references therein). The volcanic-volcaniclastic rocks cover large areas in the eastern Pontides, and form the major rock types in the northern zone (Fig. 8.2). The intrusive rocks as the second pulse are found within the Strandja massif and eastern Pontides (Fig. 8.2). They mostly occur as NE-SW trending elongated intrusion in the eastern Pontides parallel to the exposures of Early-middle Eocene intrusive rocks.

When the oceanic lithosphere of the İAE was completely consumed by northward subduction beneath Eurasian plate, the Pontides collided with TAB, and SSZ ophiolites were obducted onto the TAB (Şengör and Yılmaz 1981; Okay and Tüysüz 1999; Göncüoğlu et al. 2000; Stampfli 2001; Bozkurt and Mitwede 2001; Taymaz et al. 2007; Stampfli and Borel 2004; Moix et al. 2008; Rolland et al. 2009, 2011; Kuşcu et al. 2011, 2012). Also during the Late Cretaceous, a separate but short-lived Baskil arc formed on the southern margin of the Tauride-Anatolide Block, known as the Southeastern Anatolian orogenic belt (Agard et al. 2005; Robertson et al. 2007; Kuşcu et al. 2010, 2012; Rolland et al. 2011). The emplacement of ophiolitic nappes marked the final suturing of the Pontides and TAB along the İAESZ (Figs. 8.1 and 8.2). This emplacement also resulted in regional HP metamorphism of TAB and the metamorphic soles below ophiolites, and generation of metamorphic massifs. The Strandja Massif, Menderes Massif and Central Anatolian Crystalline Complex (Şengör et al. 1984; Göncüoğlu et al. 1997; Okay et al. 2001; Gautier et al. 2002; Whitney et al. 2003; Bozkurt 2007, and references therein) are examples of such metamorphic massifs (Fig. 8.2). Rolland et al. (2009) suggested that the continental

Table 8.1 Summary of geochronological data for Pontides

Geographic setting	Tectonic unit/ setting[a]	Magmatic suite[a]	Rock composition[a]	Method[a]	Age (Ma)[a]
Western Pontides					
Kırklareli	Strandja Massif	Demirköy pluton	Diorite	K-Ar	83.10 ± 2.0
Kırklareli	Strandja Massif	Demirköy pluton	Diorite	K-Ar	83.50 ± 2.5
Kırklareli	Strandja Massif	Şükrüpaşa pluton	Monzodiorite/ granodiorite	K-Ar	81.70 ± 1.6
Kırklareli	Strandja Massif	Dereköy pluton	Q-diorite	Ar-Ar	79.01 ± 0.5
Kırklareli	Strandja Massif	Demirköy pluton	Granodiorite	K-Ar	78.30 ± 1.3
Kırklareli	Strandja Massif	Demirköy pluton	Granodiorite	K-Ar	79.10 ± 2.3
Kırklareli	Strandja Massif	Dereköy pluton	Tonalite porphyry	K-Ar	76.70 ± 3.8
Kırklareli	Strandja Massif	Dereköy pluton	Monzonite porphyry	K-Ar	70.90 ± 3.5
Kırklareli	Strandja Massif	Dereköy pluton	Tonalite porphyry	K-Ar	76.70 ± 3.8
Kırklareli	Strandja Massif	Demirköy pluton	Q-monzonite	Ar-Ar	80.94 ± 0.5
Eastern pontides					
Amasya	Eastern Pontides	Bakırçay pluton	Granodiorite, granite	K-Ar	42.30 ± 2.6
Giresun	Eastern Pontides	Çayırbağ formation	Dacite	U-Pb	82.60 ± 1.0
Giresun	Eastern Pontides	Dereli pluton	Granitte	K-Ar	71.40 ± 1.0
Giresun	Eastern Pontides	Kurtulmuş pluton	Granite	U-Pb	70
Giresun	Eastern Pontides	Konak pluton	Granite porphyry	U-Pb	80.79 ± 0.8
Gümüşhane	Eastern Pontides	Dölek pluton	Tonalite	K-Ar	43.50 ± 1.8
Gümüşhane	Eastern Pontides	Gümüşhane pluton	Granite	K-Ar	162
Gümüşhane	Eastern Pontides	Gümüşhane pluton	Granodiorite	K-Ar	107
Gümüşhane	Eastern Pontides	Tertiary volcanics	Basalt to dacite	Ar-Ar	37.70 ± 0.2
Gümüşhane	Eastern Pontides	Tertiary volcanics	Basalt to dacite	Ar-Ar	44.50 ± 0.2
Gümüşhane	Eastern Pontides	Harşit pluton	Granodiorite-Q-diorite	K-Ar	65.30
Gümüşhane	Eastern Pontides	Torul pluton	Monzonite-syenite	Rb-Sr	77.90 ± 0.3

(continued)

Table 8.1 (continued)

Geographic setting	Tectonic unit/ setting[a]	Magmatic suite[a]	Rock composition[a]	Method[a]	Age (Ma)[a]
Gümüşhane	Eastern Pontides	Dölek pluton	Granite	K-Ar	42.90 ± 1.8
Gümüşhane	Eastern Pontides	Sarıçiçek pluton	Monzonite	K-Ar	44.10 ± 2.2
Gümüşhane	Eastern Pontides	Sarıçiçek pluton	Monzonite	K-Ar	42.70 ± 2.2
Gümüşhane	Eastern Pontides	Saraycık granodiorite	Granodiorite	Ar-Ar	52.80 ± 0.7
Gümüşhane	Eastern Pontides	Güvemli granitoid	Andesite porphyry	U-Pb	47.03 ± 0.4
Gümüşhane	Eastern Pontides	Saraycık granodiorite	Granodiorite	Ar-Ar	52.2 ± 0.4
Artvin	Eastern Pontides	Ardala volcanics	Dacite prophyry	U-Pb	50.83 ± 0.6
Artvin	Eastern Pontides	Ayder pluton	Granite poprhyry	U-Pb	82.81 ± 1.2
Artvin	Eastern Pontides	Esendal syenite	Syenite porphyry	U-Pb	80.79 ± 1.3
Artvin	Eastern Pontides	Barhal pluton	Monzosyenite	U-Pb	79.77 ± 0.7
Artvin	Eastern Pontides	Kızılkaya formation	Dacite	U-Pb	91.10 ± 1.3
Rize	Eastern Pontides	Kaçkar batholith	Granodiorite	K-Ar	79.30 ± 1.0
Rize	Eastern Pontides	Kaçkar batholith	Granodiorite	K-Ar	47
Rize	Eastern Pontides	Kaçkar batholith	Granodiorite	K-Ar	41
Rize	Eastern Pontides	Kaçkar batholith	Granodiorite	K-Ar	39.90 ± 0.3
Rize	Eastern Pontides	Kaçkar batholith	Granodiorite	K-Ar	80.70 ± 0.6
Rize	Eastern Pontides	Kaçkar batholith	Granodiorite	K-Ar	63.30 ± 0.4
Trabzon	Eastern Pontides	Çamlıkaya pluton	Granodiorite-granite	K-Ar	57.60 ± 3.0
Trabzon	Eastern Pontides	Boğalı pluton	Monzogranite	K-Ar	66.50 ± 1.5
Trabzon	Eastern Pontides	Boğalı pluton	Monzogranite	K-Ar	75.70 ± 0.0
Trabzon	Eastern Pontides	Uzuntarla pluton	Granodiorite	K-Ar	43.70 ± 1.8
Trabzon	Eastern Pontides	Uzuntarla pluton	Granodiorite	K-Ar	40.20 ± 1.4
Sivas	Eastern Pontides	Kösedağ pluton	Syenite	Rb-Sr	37 ± 2.6
Sivas	Eastern Pontides	Kösedağ pluton	Syenite	Rb-Sr	42 ± 4
Sivas	Eastern Pontides	Kösedağ pluton	Syenite porphyry	Ar-Ar	42.27 ± 0.2
Sivas	Eastern Pontides	Kösedağ pluton	Syenite porphyry	Ar-Ar	42.39 ± 0.2
Erzurum	Eastern Pontides	İspir pluton	Granodiorite	U-Pb	42.39 ± 0.7

[a]From Kuşcu et al (2018)

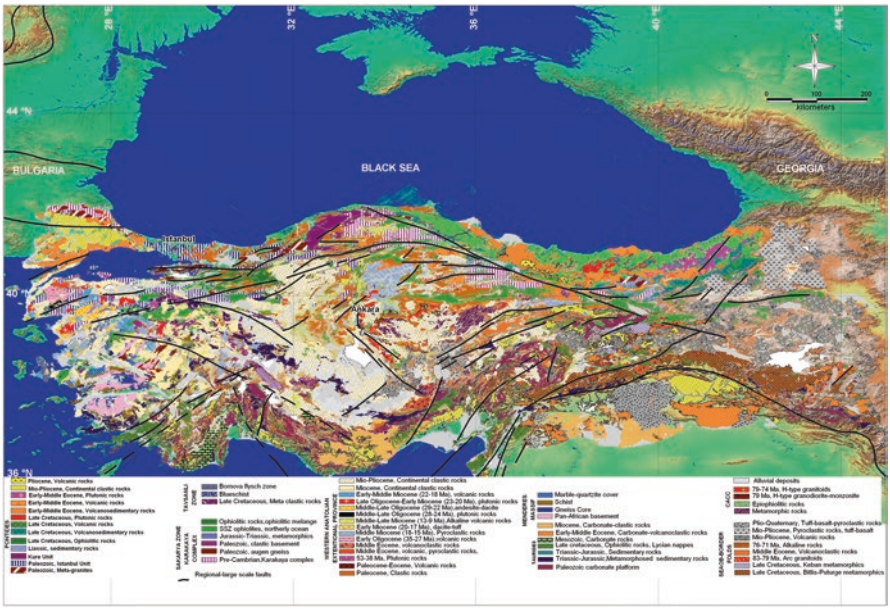

Fig. 8.2 Simplified geological map of Turkey showing the predominant rock types and regional structures. (Modified from Kuşcu et al. 2018 and references therein)

collision between SM and TAB and southward emplacement of the ophiolites and OIB sequence onto the TAB took place at *ca.* 85–80 Ma. The blueschist metamorphics exposed in the Tavşanlı zone (Figs. 8.1 and 8.2) marks the timing and location of subduction-collision. Phengite Rb–Sr and Ar–Ar data from the blueschists indicate a Late Cretaceous (80 ± 5 Ma) age for the HP/LT metamorphism (Sherlock et al. 1999). Besides, the age of blueschists and geochronological data obtained in other works suggest a collision at the latest Cretaceous at least after the 79 Ma (Şengör and Yılmaz 1981; Okay and Tüysüz 1999; Okay et al. 2001; van Hinsbergen et al. 2010; Kuşcu et al. 2011, 2018). This is also supported by the recent geochronological data on the H-type intrusive suites cutting through metamorphic rocks and obducted ophiolites that yielded an age between 79 and 69 Ma (Kuşcu et al. 2018 and references therein). The final suturing of the Pontides and TAB was followed by subsequent post-collision related extensional tectonics at the Pontides. This gave rise to generation of (1) bimodal, shallow-seated and extensional NE-SW trending volcano-plutonic complexes emplaced into the central and eastern Pontides during *ca.* 48–42 Ma (Arslan and Aslan 2006; Boztuğ et al. 2005, 2007; Karslı et al. 2008, 2010; Dilek et al. 2010; Eyüboğlu et al. 2011a, b), (2) E-W to NW-SE trending plutonic complexes emplaced into the SM and TAB along the İzmir-Ankara-Erzincan suture zone (İAESZ) during *ca.* 55 to 38 Ma (Yılmaz et al. 2001; Altunkaynak and Dilek 2006; Karacık et al. 2007; Altunkaynak and Genç 2008). The available data are in favor of a slab break-off or slab-roll back process in the generation of these magmatic rocks in the Pontides (Genç and Yılmaz 1997; Yılmaz

et al. 2001; Altunkaynak and Dilek 2006; Karacık et al. 2007; Arslan and Aslan 2006; Boztuğ et al. 2006; Altunkaynak and Genç 2008; Keskin et al. 2008; Kaygusuz et al. 2011). However, some argues that the break-off or roll back process are unlikely, and they propose that these magmatic rocks were formed in a post-collisional environment due to delamination (Eyüboğlu et al. 2011a, b, 2013).

Kuşcu et al. (2018) considered that the final suturing of the Pontides-TAB, and ophiolite obduction onto the TAB are contemporaneous. They also suggest that this obduction temporally coincides with generation of Bitlis-Zagros active margin at *ca.*83–79Ma, and HT metamorphism in the southern (Malatya) margin within the Southeastern Anatolian Orogenic Belt (SEAOB). This showed that when the northern margin of TAB docks into the Sakarya terrane, and the second subduction initiated at the southern part of the TAB along Bitlis-Zagros subduction (Kuşcu et al. 2018 and references therein). This temporal relationship is interpreted to be a subduction jump from the north to the south of the TAB at *ca.* 85–80 Ma (Rolland et al. 2011). At the south, the TAB was in collision with Afro-Arabian plates between *ca.* 83 and 79 Ma along northward subduction of Neotethys (the second subduction event) forming the Bitlis-Zagros active margin (e.g., Agard et al. 2005; Robertson et al. 2007; Rolland et al. 2011; Kuşcu et al. 2010, 2012 and references therein). During the second subduction event, most of the oceanic lithosphere belonging to southerly ocean, between Arabian plate and TAB was consumed firstly by intra-oceanic subduction that also resulted in supra-subduction zone (southerly ophiolites, SSZ) ophiolites at *ca.* 90–95 Ma (Parlak 2005). The termination of intra-oceanic subduction was followed by emplacement of southerly SSZ ophiolites over the southern margin of the TAB (Fig. 8.1). The ophiolite obduction gave rise to formation of Malatya-Keban metamorphics (Robertson et al. 2007; Kuşcu et al. 2010, 2012). This was followed by the active margin along the Bitlis-Zagros subduction between 83 and 79 Ma (Kuşcu et al. 2010, 2012). The subduction resulted in voluminous calc-alkaline intrusive magmatism emplaced into Malatya-Keban metamorphics (Fig. 8.2) (Yazgan and Chessex 1991; Beyarslan and Bingöl 2000; Robertson et al. 2007; Kuşcu et al. 2010). This short-lived subduction was terminated due to collision between Arabian plate and TAB, and is marked by the emplacement of the ophiolitic nappes over the Bitlis-Pötürge metamorphic massifs within the SEAOB. The final consumption of the NeoTethys oceanic basin was followed by continental lithospheric subduction (underthrusting) underneath the TAB that gave way to HT metamorphism, and generation of Bitlis-Pötürge metamorphics (*ca.* 74–71 Ma, Hempton 1985; Oberhänsli et al. 2010; Rolland et al. 2011) at the SEAOB (Rolland et al. 2011). The short-lived subduction that formed the Baskil arc terminated when the Tauride-Anatolide Block collided with the northward advancing Arabian plate closing this part of the NeoTethys between the late Eocene and Oligocene along the Bitlis-Zagros suture zone (Keskin 2003; Şengör et al. 2003; Kuşcu et al. 2011, 2013). Collision led to thickened continental lithosphere, and decrease in the convergence rate following collision. This is considered to have permitted extensional tectonics to at least dominate the upper crust (Rosenbaum et al. 2002; Kaymakçı et al. 2006; Kuşcu et al. 2010, 2013, 2018), and generation of NNE-SSW trending shallow-seated plutonic complexes in the SEAOB at 55–44 Ma

(Kuşcu et al. 2012). This also resulted in the delamination of the thickened crust or roll-back of the subducted slab between *ca.* 77 to 54 Ma (Harris et al. 1994; Genc and Yılmaz 1997; Yılmaz et al. 2001; Köprübaşı and Aldanmaz 2004; Kaymakçı et al. 2009; Kuşcu et al. 2010, 2013; Rolland et al. 2011). These features described above suggest mechanisms that unroofed previously obducted ophiolites, exhumed the metamorphic basement, and filled basins with Maastrichtian to Paleocene subaerial and submarine sedimentary rocks (Kuşcu et al. 2018 and references therein) throughout Turkey. The unroofing and exhumation of metamorphic rocks are accompanied by generation of S- to H-type post-collisional magmatism between 77 and 74 Ma, peaking at *ca.* 75 Ma (Kuşcu et al. 2010, 2013) throughout the metamorphic massifs and obducted ophiolites at Anatolides (Fig. 8.2). Initial extension coincided with emplacement of calc-alkaline to alkaline magmatism ranging from *ca.* 77 to 73 Ma in central and southeastern Anatolia (Kuşcu et al. 2010, 2011), then by alkaline magmatism peaking at 74–71 Ma (Kuşcu et al. 2010, 2013) mostly at eastern and southeastern Anatolia. The geological works suggested that the decrease in convergence rate between Arabian and Eurasian plates was accompanied by subsequent magmatism related to Bitlis-Zagros subduction took place between early to Middle Eocene (~50 and 44 Ma, peaking at 48 Ma; Kuşcu et al. 2010, 2013).

Şengör et al. (2003) argued that TAB and its metamorphosed counterparts at the eastern Taurides collided with the Arabian plate, and NeoTethys oceanic realm in the Bitlis-Zagros subduction was closed in a period between Late Eocene to Oligocene (Keskin 2003; Şengör et al. 2003), and a regional compression dominated the whole Turkey during this period. Subsequent to final continental collision and suturing of Arabia with the TAB and metamorphosed counterparts of eastern Taurides in the middle Miocene was followed by a slab-steepening and break-off beneath the ATB (Şengöret al. 2003; Keskin 2003; Angus et al. 2006; Kaymakçı et al. 2010). This was followed by a major episode of widespread volcanism with varied and complex composition affected most of the eastern Anatolian region starting at about 11 Ma (e.g. Keskin 2003).

The final continental collision and suturing of Arabia with the TAB also gave rise to extrusion of the TAB into Greece, and a resumation of subduction (Rolland et al. 2011) at the Helenic-Aegean active margin (third subduction event). As the African plate continue to collide with the Eurasian plate by the closure of the remaining NeoTethys ocean, and Anatolia is extruded towards Greece, Kuşcu et al. (2018) stated that the Eurasia and Africa convergence was accommodated to the south along the Helenic-Aegean subduction zone. The Aegean subduction produced isolated continental arc magmatism at about 42–38 Ma (Kuşcu 2009; Kuşcu et al. 2018) mainly in the western, northwestern Turkey. In their recent woks Kuşcu et al. (2018) suggested that the Aegean subduction is accompanied by a lithospheric extension, exhumation, core-complex development, subduction and extension-related magmatism and large-scale, probably gravitational gliding of the Lycian Nappes system approximately between 38 and 23 Ma to Plio-Quaternary (Collins and Robertson 1997; Gautier et al. 1999; Aldanmaz et al. 2000; Jolivet 2001;

Bozkurt and Oberhänsli 2001; Doglioni et al. 2002; Ring et al. 2003; Kuşcu 2009; Tirel et al. 2009; Ring et al. 2010; van Hinsbergen et al. 2010; Kuşcu et al. 2012).

8.4 Geology of Microcontinental Terranes

8.4.1 Geology of the Pontides and Geochemistry, Tectonic Setting, Petrogenesis and Geochronology Characteristics of Magmatic Rocks

The Pontides extend from Rhodope (Bulgaria) to northern Turkey and to Lesser Caucasus (Figs. 8.1 and 8.2). It comprises three tectonostratigraphic terranes, bordered to the south by Late Cretaceous SSZ-type ophiolitic belts, ophiolitic mélanges, TAB and east Anatolian accretionary complex. From west to east, these terranes are; Strandja terrane (western Pontides), İstanbul-Zonguldak zones (central Pontides) and Sakarya terrane (Karakaya complex and eastern Pontides) (Fig. 8.1) (Moix et al. 2008). The known porphyry deposits are prospects are largely hosted by or associated with Late Cretaceous to Oligo-Miocene magmatism in Strandja terrane, Karakaya complex and eastern Pontides. The Strandja massif, is a part of crystalline massifs in the southern Balkans, and is the eastern continuation of the Rhodope and Serbo-Macedonian massifs. This terrane was formed by rifting of Gondwana that also resulted in generation of Cimmerian continent. It consists of highly deformed and regionally metamorphosed rocks (high-amphibolite facies with granitoid intrusions) and metamorphic-magmatic crystalline basement (Fig. 8.3) formed during the Late Variscan and Late Jurassic-Early Cretaceous (greenschist facies) orogens (Bozkurt and Mittwede 2001). This basement is nonconformably overlain by metasedimentary succession of Triassic-Middle Jurassic transgressive sequence (Okay et al. 2001; Sunal et al. 2006). These are covered by a sequence thick pile of shallow marine sandstones, and all are intruded by a late Cretaceous magmatic arc (western Pontide magmatic arc) that consists of volcanic, volcanogenic and plutonic rocks (Figs. 8.2 and 8.3) developed above the northward subduction of marginal Vardar-İAE ocean beneath the Sakarya and İstanbul terranes.

The Sakarya terrane, a metamorphic belt stretching from the Aegean Sea (Biga peninsula) to the Lesser Caucasus (Figs. 8.1 and 8.2) consists of four major tectonic units; (1) A high-grade Variscan metamorphic sequence of gneiss, amphibolite, marble and scarce metaperidotite formed in the Carboniferous (330–310 Ma; zircon and monazite ages; (Okay et al. 2001), (2) Permo-Triassic sequence called Karakaya complex at the west (3) Küre unit at the center, and (4) late Cretaceous magmatic arc at the east (eastern Pontide magmatic arc) (Fig. 8.4) (Okay and Göncüoglu 2004) at the east and west. The Karakaya complex is considered as a fore-arc/foreland basin formed during the northward subduction of the PaleoTethys along the southern margin of Eurasia (Stampfli and Kozur 2006), and accreted to the margin of Laurasia during the Late Permian to Triassic. It is overlain by a Liassic continental to shallow

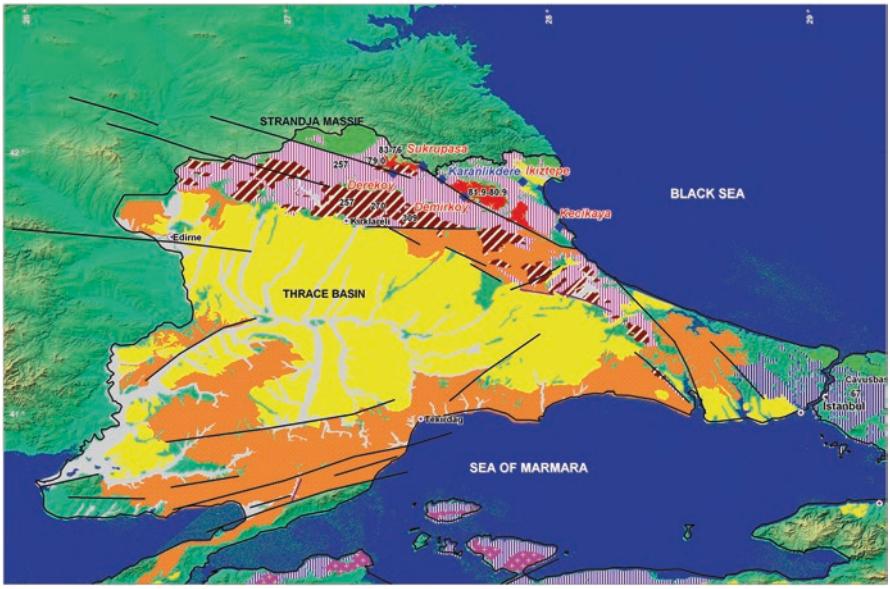

Fig. 8.3 Simplified geological map of Strandja massif and Thrace basin showing the major rock types, porphyry Cu-Mo-W deposits/prospects, and their spatial association with Late Cretaceous arc-related intrusive rocks; the prospects are shown in red, occurrences in blue color; the numbers on metamorphic and intrusive rocks refers to Ar-Ar ages shown in Table 8.1. (From Kuşcu et al. 2018; the explanations and legend as in Fig. 8.2)

marine sedimentary rocks (Altıner et al. 1991). The Karakaya complex is intruded by Tertiary volcano-plutonic complexes and plutonic rocks, now classified as the magmatic rocks in the western Anatolian province (WAP) in Biga peninsula. The eastern Pontides is a well-preserved Late Cretaceous and Middle Eocene magmatic and volcano sedimentary belt emplaced into a Sakarya metamorphic basement. This belt is traced along the Srednogoria in Bulgaria and eastern Pontides along the Black Sea coast towards Georgia (Fig. 8.4). Based on their characteristic features, tectonic setting and facies characteristics the eastern Pontides are divided into three geographic zones; northern, central and southern zones.

The magmatic rocks in the Pontides are well preserved in the eastern Pontides and Strandja massif, and are formed in two tectonic environments; magmatic arc and post-collisional extensional environments. Based on the field characteristics and available geochronological data Kuşcu et al. (2018) suggested that the arc magmatism has been formed in two successive pulses; the volcanic-volcaniclastic rocks that cover large areas in the eastern Pontides (Fig. 8.4) form the first magmatic arc pulse. These rocks are the major rock types in the northern zone (Fig. 8.4), and are characterized by a sequence of submarine lavas, pyroclastic rocks and intercalated sediments, and consists of basalt, andesite, dacite, rhyodacite, trachy-andesite, subaerial to submarine dacitic lapilli tuff, and agglomerate. The intrusive rocks as the second pulse are found within the Strandja massif and eastern Pontides. They mostly

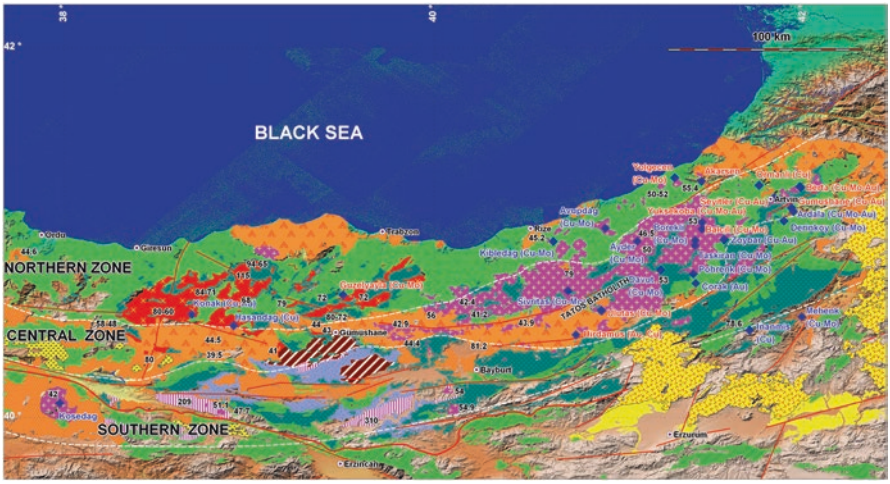

Fig. 8.4 Simplified geological map of eastern Pontides showing major rock types, age (Ar-Ar, U-Pb) of magmatism, porphyry deposits/prospects and occurrences (Modified from Kuşcu et al. 2018; the explanations and legend as in Fig. 8.2, the prospects are shown in red, occurrences in blue; the numbers refer to Ar-Ar ages in Table 8.1; solid red lines show strike-slip and undifferentiated faults; dashed white lines show the zones in Pontides)

occur as NE-SW trending elongated intrusions in the eastern Pontides parallel to the exposures of Early-middle Eocene intrusive rocks. They are monzonite, granodiorite, quartz diorite to diorite in composition, and contain volcanic and metamorphic xenoliths and dioritic mafic microgranular enclaves (Aslan 2005; Yılmaz-Şahin 2005; Boztuğ et al. 2006). The Early-middle Eocene magmatic rock associations, the most widely exposed magmatic rocks in the Pontides are exposed in the eastern Pontides forming isolated volcanic and plutonic bodies (Fig. 8.4). They represent the post-collisional extension related magmatic rock associations that consist of volcanic, pyroclastic and plutonic end-members (Topuz et al. 2011). The volcanic rocks occur as domes and lava flows, and are mostly andesite to dacite in composition (Aslan 2010; Kaygusuz et al. 2011; Temizel and Arslan 2009), and are located mostly in the central and eastern parts of the central and northern zones (Fig. 8.4) of the eastern Pontides. They are synchronous with Early-Late Eocene sedimentary (Okay et al. 1997; Rice et al. 2009) and a Middle Eocene (Lutetian) volcano sedimentary sequence, and unconformably overlie the Late Cretaceous intrusives (Temizel and Arslan 2009; Aslan 2010; Kaygusuz et al. 2011). The geochronology, mineral assemblage, field and textural characteristics of the late Cretaceous and Early-Late Eocene magmatic belt in the entire Pontides are presented in Kuşcu et al. (2018). In general, the major and trace element geochemistry and REE compositions of late Cretaceous volcanic rocks suggest a subductional setting with variation from hydrous arc to anhydrous back-arc melting conditions (Kaygusuz et al. 2009, 2011; Kuşcu et al. 2018 and references therein). These characteristics were interpreted to reflect an ensimatic arc signature due to an intra-oceanic subduction

(supra-subduction) *ca.* 117 in age, which existed in the İAE ocean during the period between the Turonian and Campanian (Çapan and Floyd 1985; Tüysüz et al. 1995; Gökten and Floyd 2006).

The overall geochemical features such as enrichment in LIL elements and LREE, depletion in HFS elements relative to MORB, with positive Sr, K_2O, Ba, and Rb, and negative Zr, Nb, TiO_2, and Y anomalies (Karslı et al. 2010), Ba is enriched relative to Rb and Th, of the Early-middle Eocene volcanic and volcano-plutonic rocks are consistent with a subduction-related setting and suggestive of melting of a metasomatized mantle inherited from an earlier subduction (Arslan and Aslan 2006; Boztuğ and Harlavan 2008; Eyüboğlu et al. 2010, 2011a, b; Karslı et al. 2010; Topuz et al. 2011).

Kuşcu et al. (2018) presented a detailed review of geochronology and documented the geochronologic data for the Pontides (Table 8.1). The probability density plot of all the available ages of rocks in the Pontides prepared by Kuşcu et al. (2018) emphasizes the two prominent peaks of magmatic activity and cooling of the terrane after magmatic activity. Based on the available data, the peak of thermal activity associated with the older magmatic activity event appears to have been between 76 and 83 Ma, whereas the younger event thermally peaked between 40 and 50 Ma. There is a suggestion of a third event of enhanced magmatism or cooling around 70–74 Ma, although with only a few ages reported to date the significance of these ages is not known. Based on the available geochronological data, they also suggested that the arc magmatism took place during two different episodes of magmatic pulses; the volcanic and volcaniclastic sequences as the early magmatic pulse appears to be formed in a time interval between late Turonian and the latest Campanian (Okay et al. 2001) or 88–80.9 ± 0.9 Ma (Eyüboğlu et al. 2010), while the plutonic complexes were formed at the interval of 83.5–62.4 Ma (Table 8.1) as the later pulse.

8.4.2 Geology of Western Anatolian Province and Geochemistry, Tectonic Setting, Petrogenesis and Geochronology Characteristics of Magmatic Rocks

The western Anatolian province (WAP) represents the western end of the Sakaryaterrane and TAB (Figs. 8.2 and 8.5). The WAP is the amalgamation of several tectonostratigraphic units, structural and metamorphic features during the Early Tertiary continent-continent collision across the NeoTethys. It consists of several northeasterly trending structural domes of Paleozoic and Mesozoic metamorphic rocks, east-west to northeast trending extensional basins filled with Paleogene sedimentary sequences, and Tertiary plutonic and volcanic-volcaniclastic, pyroclastic rocks emplaced into Paleozoic crystalline basements and sedimentary sequences (Fig. 8.5). These rocks are said to be result of the present-day north–south extension, and characterized by S–SW migration of the subduction zone above the

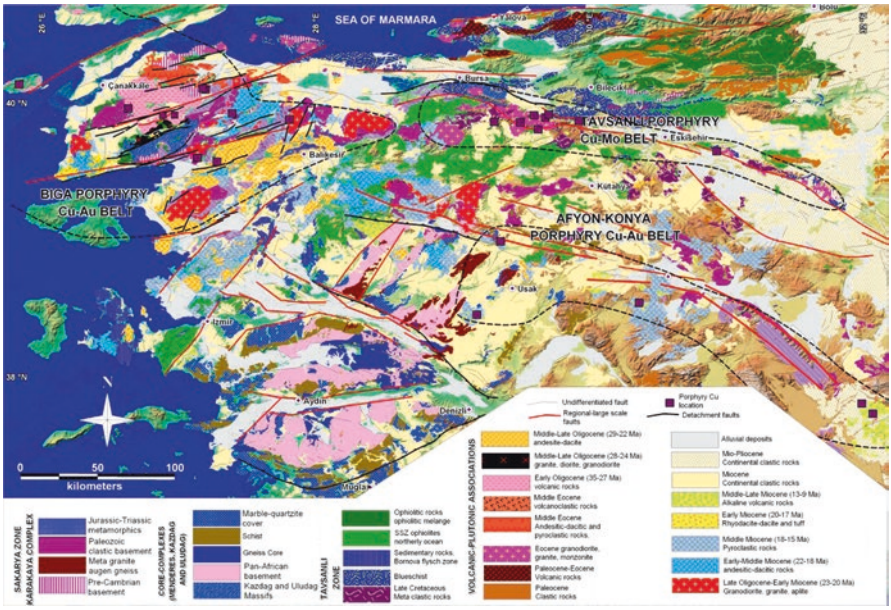

Fig. 8.5 Simplified geological map of WAP showing the major rock types, and tectonostratigraphical units along with major porphyry belts. (From Kuşcu et al. 2018)

Aegean-Hellenic subduction zone (McKenzie 1972; Le Pichon and Angelier 1979) since at least the Early-Middle Eocene.

The tectonostratigraphical units in the WAP are Karakaya complex, metamorphic core-complexes, volcano-plutonic associations, Tavşanlı zone, and İzmir-Ankara Erzincan-suture zone (İAESZ) (Fig. 8.5). These units are bounded by suture zones, and are truncated by numerous high to low-angle normal, dextral strike-slip and detachment faults. The Karakaya complex, also forming the western end of Pontides, is the basement for extensive Tertiary magmatism and sedimentation in the WAP. Two tectonostratigraphic units are defined in the Karakaya Complex: the first one consisting of greenschist facies metamorphosed mafic rocks (spilitic basalt and gabbro) and metasedimentary rocks (metachert, phyllite and marble) is called lower Karakaya complex (Okay and Göncüoğlu 2004), also known as Nilüfer unit of 203–208 Ma (Okay and Monie 1997). The second unit is called upper Karakaya complex (Okay and Göncüoğlu 2004), and contains highly deformed epiclastic and volcaniclastic rocks.

The metamorphic core complexes in the WAP are Kazdağ massif at the north, Uludag massif at the east and Menderes Massif at the south (Fig. 8.5). The Kazdağ Massif (Schuiling 1959; Okay et al. 1991; Pickett and Robertson 1996; Okay and Satır 2000) bordering the northern margin of the Edremit Gulf, is a NE-trending extensional metamorphic core complex. The Kazdağ massif contains gneiss, marble, amphibolite, migmatite, meta-ultramafic rocks, an accretionary mélange with

exotic Upper Cretaceous eclogite blocks (Pickett and Robertson 1996). It is correlated with the Rhodope crystalline complex in northern Greece and Bulgaria (Papanikolaou and Demirtaşlı 1987). The metamorphic assemblage at the amphibolite facies, is latest Oligocene in age (24 Ma), with Carboniferous inherited zircon ages (Okay et al. 1997; Okay and Satır 2000). Extensional deformation was synchronous with the regional metamorphism and magmatism, and resulted in the exhumation of the metamorphic rocks from ~14 to ~7 km along a northward dipping ductile shear zone (Okay and Satır 2000) and emplacement of granitoids along the shear zones.

The Uludağ massif, another metamorphic core-complex exhumed along ductile strike-slip shear zone (Okay et al. 2008), is located along the boundary between TAB and Sakarya terrane. The Uludag massif is exposed as NW-SE trending elongate body that consists of orthogneiss, metagranites and marble (Okay et al. 2008). The zircon ages of gneisses cluster between 300 and 200 Ma (Okay et al. 2008). The exhumation and syn-tectonic metamorphism was dated to be 48.7 and 30.5 (Okay et al. 2008) based on Rb/Sr biotite geochronology from the gneisses. The Uludağmassif is intruded by syn-tectonic Uludağ granite, *ca.* 33 Ma in age, and was exhumed during Early Miocene (Okay et al. 2011).

The Menderes Massif (MM), a dome-like structure between Kütahya (Simav), Muğla (Yatağan), Denizli (Gördes) and Manisa (Turgutlu) another core complex, is exhumed to the surface in Miocene times in WAP. It is bounded by the İzmir-Ankara-Erzincan suture zone at north and Lycian nappes at the south (Fig. 8.5). It is separated from the lower Miocene Simav extensional detachment (Işık and Tekeli 2001) by the Afyon zone (Fig. 8.5). The Menderes Massif consists of Precambrian gneissic basement and the structurally overlying Paleozoic−Paleocene greenschist- to amphibolitic metasedimentary rocks. The classic terminology in the MM refers to “core” and “cover” (Schuiling 1962) series referring to Precambrian gneissic basement and overlying metasedimentary rocks, respectively (Şengör et al. 1984; Candan 1995, 1996; Candan et al. 2001; Dora et al. 1990). The deformed tonalitic-granitic intrusions at the core series yielded a Rb/Sr whole rock age of 470 ± 9 Ma (Satır and Friedrichsen 1986). This was taken as a piece of evidence marking the end of Pan-African collision and associated post-collisional convergence (Şengör et al. 1984). The cover units include Ordovician to Devonian schists with sporadic metaconglomerate levels consisting mainly of quartzite and granite pebbles. They also comprise Permo-Carboniferous metaquartzites with metacarbonates with graphite veins. The Menderes Massif has undergone a complex metamorphism with six distinguished phases (Bozkurt and Oberhänsli 2001 and references therein; Whitney and Bozkurt 2002; Régnier et al. 2003; Rimmelé et al. 2003; Ring et al. 2003). Only the ‘core’ rocks were affected by the first two pre-Alpine phases that took place between *ca.* 550 and 230Ma (Bozkurt and Oberhänsli 2001), and are related to collision and crustal thickening and post-collisional events, respectively during Pan-African orogeny. As the traces of earlier phases have been superimposed by the last four metamorphic phases during Alpine events between *ca.* 40 and 19.5 Ma, evidence for pre-Alpine metamorphism is limited and rare. Following the major

Alpine compressional period, the MM was exhumed along shear zones and low-angle normal faults that accompanied early-middle Miocene extensional tectonics (Bozkurt and Oberhansli 2001).

The Tavşanlı zone, the easternmost tectonostratigraphical unit in the WAP, is a HP/LT metamorphic belt with blueschist rocks exposed to the south of the İASEZ (Figs. 8.2 and 8.5). The metamorphic sequence consists of metapelitic schist, blueschist at the base, marbles in the middle and a series of metabasite, metachert and phyllite at the top (Okay 1984). These metamorphic rocks are considered to be the subducted and subsequently exhumed passive northern continental margin of the TAB (Okay 1984; Okay and Satır 2006). The age of metamorphism is 80 ± 5 Ma (Late Cretaceous) based on phengite Rb-Sr and Ar-Ar geochronology from the blueschists (Sherlock et al. 1999). Large tectonic slabs of ophiolite, predominantly peridotite derived from the İAESZ, lie over the coherent blueschists or over the accretionary complex. The blueschists and overlying ophiolitic rocks are intruded by Early-Late Eocene (*ca.* 55–50 Ma, Kuşcu et al. 2018 and references therein) plutonic rocks exposed in a belt extending from the Sivrihisar (west of Ankara) to the Marmara Sea. They refer to older plutonic associations within the WAP, and are commonly diorite to granodiorite in composition. An extensional setting due to slab break-off is commonly accepted (Altunkaynak 2007; Kuşcu 2009).

The İzmir-Ankara-Erzincan suture zone is an E-W trending belt of disrupted ophiolitic nappes and mélanges derived the northerly ocean (Vardar-İAE ocean) (Figs. 8.2 and 8.5) that occurs as allocthonous assemblages emplaced onto the TAB and Tavşanlı zone. They separate the Sakarya terrane from the north and TAB including Menderes Massif, Afyon and Tavşanlı zones, and CACC, at the south. It consists of dismembered ophiolitic sequences, tectonic and ophiolitic mélanges and epi-ophiolitic sequences. These are found as ophiolitic nappes exposed at Orhaneli (Bursa), Harmancık (Bursa), Tavşanlı (Kütahya), Dağküplü (Eskişehir) and Sivrihisar-Mihalıççık (Eskişehir) in the western part of the İAESZ. The mélanges are overthrust by unmetamorphosed peridotites cut by diabase dikes, and are underlain by metamorphic soles. The geochemical data from the basaltic blocks in the mélanges indicate that the ophiolitic rocks were formed in the earliest stages of island arc development in a supra-subductional (SSZ), forearc tectonic setting in the İAE (northerly) ocean. The geochronology of the metamorphic soles for the obducted ophiolites is based on hornblende, plagioclase, phengite, biotite separates by K-Ar and Ar-Ar method that yielded an age range between 93 and 125 Ma (Önen and Hall 1993; Harris et al. 1994; Okay et al. 1996; Dilek and Whitney 1997; Önen 2003; Çelik et al. 2006).

The WAP is characterized by widespread magmatism since Early-Late Eocene to recent. This magmatism was developed on the overriding along the Aegean-Helenic subduction. This magmatism extends southward from the Rhodope Massif-Thrace through the central Aegean Sea and western Anatolia to the south Aegean active Volcanic arc, with an age varying from Early-Late Eocene to present (Fytikas et al.

1984). The magmatism produced volcanic, volcanoclastic, volcano sedimentary and plutonic rocks with variable age and geochemical characteristics. The plutonic rocks in WAP are exposed throughout Biga peninsula and Afyon-Tavşanlı zones forming Biga, Afyon and Tavşanlı porphyry belts (Fig. 8.5). The available geochronologic database including Rb/Sr whole rock and recent works using conventional $^{40}Ar/^{39}Ar$ incremental-heating, U-Pb zircon and Re-Os molybdenite ages for the magmatism in the WAP is presented in Kuşcu et al. (2018) and summarized here in Table 8.2. These ages range from *ca.* 57 to 9 Ma, peaking at *ca.* 52–48 Ma, 35–42 Ma and 29–18 Ma (Kuşcu et al. 2018; Table 8.2). According to Kuşcu et al. (2018 and references therein) this database is suggestive of four broad magmatic pulses between Eocene and the Miocene. Early to middle Eocene volcanic and plutonic rock form the oldest pulse (*ca.* 52–48 Ma, phase (1); Middle Eocene (*ca*. 42–35 Ma, phase, (2) volcanic and plutonic associations form the second pulse, and Oligocene to early Miocene rocks (29–18 Ma, pulse, (3) form the third pulse. The available geochronologic data quoted the final magmatic pulse between *ca*. 16 and 9 Ma (pulse 4), and is largely concentrated in the southern part of the province (Kuşcu et al. 2018). Based on the spatial distribution of the magmatic rocks in WAP, Kuşcu et al. (2018) indicated that magmas erupted or intruded from the first and last pulses get younger from north to south, suggesting significant syn-magmatic migration of the volcanic axis in response to an extensional strain. They also emphasized that this southward migration during a single magmatic phase is in stark contrast to any of the other magmatic episodes.

The geochemical characteristics of magmatic rocks in the WAP are presented in detail by Kuşcu et al. (2018), and the reader is referred to their recent work for a better understanding of the petrogenesis and geochemical features of the magmatic rocks in WAP. In this chapter, a brief summary of their work will be presented. Kuşcu et al. (2018) showed that the magmatic rocks evolve from low-K to high-K to shoshonitic series and mafic to more felsic through time. The chondrite-normalized plots of rare earth elements (REE) indicate a continuum in the mantle mantle enrichment in LREE spreads southeastward from Karakaya complex towards Afyon zone (Kuşcu et al. 2018). Besides, all rocks are characterized by negative anomalies in Rb, Nb, Ta, Sm and Y, and positive anomalies in Th and Hf suggesting a subduction origin for their genesis. The ratios of La/Yb, Sm/Yb and Sr/Y display distinct compositional characteristics for the magmatic rocks formed in time from earliest to last pulse. Overall, La/Yb, Sm/Yb and Sr/Y ratios to increase in time from pulse 1 to pulse 4 (Kuşcu et al. 2018). Kuşcu et al. (2018) concluded that this increase is likely to correspond to melting in different source regions characterized by amphibole-pyroxene-bearing phases while the last two in amphibole and garnet-bearing phases.

Table 8.2 Geochronology of western Anatolian province

Geographic setting	Tectonic unit/ setting[a]	Magmatic suite[a]	Rock composition[a]	Method[a]	Age (Ma)[a]
Afyon	Afyon zone	Alaşehir volcanics	Granite-granodiorite	K-Ar	19.5 ± 1.4
Afyon	Afyon zone	Kırka volcanics	Alkaline rhyolite to trachyte	ns	18
Afyon	Afyon zone	Sandıklı volcanics	Trachyte-Basalt	K-Ar	11.6 ± 0.25
Balıkesir	Karakaya complex	Karabiga pluton	Granite	K-Ar	45.3 ± 0.9
Balıkesir	Karakaya complex	Northern kapıdağ	Granite	Rb-Sr	35.0 ± 0.3
Balıkesir	Biga Peninsula	İvrindi volcanics	Tuff	K-Ar	19.5 ± 0.1
Balıkesir	Biga Peninsula	Işıklı volcanics	Rhyolite	K-Ar	27.3 ± 0.8
Balıkesir	Biga Peninsula	Kızıldam granitoid	Granite	K-Ar	22.3 ± 0.8
Balıkesir	Biga Peninsula	Yenice volcanics	Granite	K-Ar	20.2 ± 1.2
Balıkesir	Sakarya zone	Şevketiye pluton	Granite	K-Ar	71.9 ± 1.8
Balıkesir	Sakarya zone	Çataltepe granitoid	Granite	K-Ar	21.7 ± 0.1-25.9 ± 0.5
Balıkesir	Sakarya zone	Oligocene volcanics	CA High-K	K-Ar	24.8 ± 1.0
Balıkesir	Sakarya zone	Eybek granite	Granite	K-Ar	23.8 ± 1.4
Balıkesir	Sakarya zone	Havran volcanics	Andesite porph.	Ar-Ar	24.18 ± 0.2
Balıkesir	Sakarya zone	Evciler granitoid	Granodiorite	Rb-Sr	20.7 ± 0.2
Balıkesir	Sakarya zone	Şamlı pluton (west)	Granite	K-Ar	19.5 ± 1.2
Balıkesir	Sakarya zone	Gökçeyazı volcanics	Tuff	Ar-Ar	29.36 ± 0.56
Balıkesir	Sakarya zone	Şamlı pluton	Granite	K-Ar	20.3 ± 1.1
Balıkesir	Sakarya zone	Kozak granitoid	Granite	K-Ar	14.6 ± 1.0-23.0 ± 3.8
Balıkesir	Afyon zone	Alaçam pluton	Granite-granodiorite	K-Ar	20.6 ± 0.8
Balıkesir	Afyon zone	Baklan/ Muratdağı pluton	Granite-granodiorite	K-Ar	19.4 ± 0.9
Balıkesir	Afyon zone	Koyunoba pluton	Granite-granodiorite	U-(Th-Pb)	21.0 ± 0.2
Balıkesir	Afyon zone	Emet volcanics	ns	K-Ar	19
Balıkesir	Afyon zone	Eğrigöz pluton	Granite-granodiorite	K-Ar	24.6 ± 1.4
Balıkesir	Afyon zone	Uşak volcanics	Basalt	K-Ar	15.8 ± 0.3
Balıkesir	Izmir-Ankara Suture	Kepsut volcanics	Andesitic lava	K-Ar	21.71 ± 0.2

(continued)

Table 8.2 (continued)

Geographic setting	Tectonic unit/ setting[a]	Magmatic suite[a]	Rock composition[a]	Method[a]	Age (Ma)[a]
Bursa	Tavşanlı zone	Tepeldağ granodiorite	Granodiorite	U-Pb	44.99 ± 0.23
Bursa	Tavşanlı zone	Orhaneli granodiorite	Granite	Ar-Ar	52.6 ± 0.4
Bursa	Tavşanlı zone	Çataltepe granitoid	Granite-granodiorite	K-Ar	21.7 ± 0.1-25.9 ± 0.5
Bursa	Tavşanlı zone	Topuk pluton	Granite	Ar-Ar	49.64 ± 0.2
Bursa	Tavşanlı zone	Topuk pluton	Aplite dike	Ar-Ar	49.90 ± 0.30
Bursa	Tavşanlı zone	Kınık ophiolites	Amphibolite	K-Ar	95.0 ± 3.3
Kütahya	Tavşanlı zone	Kırka volcanics	Tuff	K-Ar	21 ± 0.4
Kütahya	Tavşanlı zone	Alaçamdağ pluton	Granite	K-Ar	19.9-27.9
Eskişehir	Tavşanlı zone	Sivrihisar granite	Granite	Ar-Ar	57.32 ± 0.3
Eskişehir	Tavşanlı zone	Domaniç granitoid	Granodiorite	Ar-Ar	52.6 ± 1.1
Çanakkale	Karakaya complex	Karabiga pluton	Granite-granodiorite	K-Ar	45.3 ± 0.9
Çanakkale	Karakaya complex	Avşa pluton	Granite	Rb-Sr	44.0 ± 0.4
Çanakkale	Karakaya complex	Fıstıklı pluton	Granite	K-Ar	35.4 ± 0.8
Çanakkale	Karakaya complex	Kapıdağ pluton	Granodiorite	K-Ar	38.3 ± 0.8
Çanakkale	Biga Peninsula	Sarısu volcanics	Andesitic lava	K-Ar	42.0 ± 0,8
Çanakkale	Biga Peninsula	Balıklıçeşme volcanics	Dacite	K-Ar	37.3 ± 0.9
Çanakkale	Biga Peninsula	Çan volcanics	Andesitic lava	K-Ar	28.0 ± 0.9
Çanakkale	Biga Peninsula	Kirazlı volcanics	Andesite	Ar-Ar	27.20 ± 0.1
Çanakkale	Biga Peninsula	Ezine basalt	Basalt	K-Ar	11.0 ± 0.4
Çanakkale	Biga Peninsula	Evciler granitoid	Granodiorite	Ar-Ar	28.44-25.2 ± 4.3
Çanakkale	Sakarya zone	Dedetepe formation	Andesite	K-Ar	22.3 ± 1.3
Çanakkale	Sakarya zone	Hallaçlar formation	Andesite	K-Ar	22.4 ± 0.8
Çanakkale	Sakarya zone	Serçeler granite	Granodiorite	Ar-Ar	40.80 ± 0.36
Çanakkale	Sakarya zone	Kartaldağ volcanics	dacite porphyry	Ar-Ar	42.19 ± 0.4
Çanakkale	Sakarya zone	Lapseki volcanics	Andesite	Ar-Ar	32.58 ± 0.27
Çanakkale	Tavşanlı zone	Bigadiç volcanics	Andesitic lava	K-Ar	23.6 ± 0.9

(continued)

Table 8.2 (continued)

Geographic setting	Tectonic unit/ setting[a]	Magmatic suite[a]	Rock composition[a]	Method[a]	Age (Ma)[a]
Isparta	Isparta angle	Gölcük basalt	Olivine basalt	Ar-Ar	19.7 ± 0.4
İzmir	Menderes Massif	Ödemiş volcanics	Andesite	Rb-Sr	18 ± 0.2
İzmir	Izmir-Ankara Suture	Kozak pluton	Granite	K-Ar	22.1 ± 0.7
İzmir	Izmir-Ankara Suture	Dumanlı volcanics	Basalt	Rb-Sr	17 ± 0.3
İzmir	Izmir-Ankara Suture	Yamanlar volcanics	Dacite and andesite	K-Ar	14.7 ± 0.5
İzmir	Izmir-Ankara Suture	Altıntepe volcanics	Andesitic dike	K-Ar	18.9 ± 0.4
Kütahya	Izmir-Ankara Suture	Bigadiç volcanics	Andesite	Ar-Ar	19.6 ± 0.6
Manisa	Menderes Massif	Gördes metagranite	Andalusite pegmatoid	FT	37 ± 7
Manisa	Menderes Massif	Gördes metasediments	Pelite	Th-Pb	41.4 ± 1.3
Manisa	Menderes Massif	Beşparmak metamorphics	Mica-quartz vein	Rb-Sr	53.2 ± 0.5
Manisa	Menderes Massif	Kiraz volcanics	Basalt	K-Ar	17.9 ± 2.4
Manisa	Menderes Massif	Turgutlu granodiorite	Granodiorite	U-Pb	16.1 ± 0.2
Manisa	Menderes Massif	Salihli granodiorite	Granodiorite	U-Pb	15.0 ± 0.3
Manisa	Menderes Massif	Gördes volcanics	Basalt	K-Ar	16.9 ± 0.3
Muğla	Lycian nappes	Kadıkalesi monzonite	Monzodiorite	K-Ar	11.2 ± 1.6
Muğla	Lycian nappes	Kadıkalesi volcanics	Trachyandesite	K-Ar	11.9 ± 0.3
Muğla	Lycian nappes	Yatağan volcanics	Basaltic tuff	K-Ar	10.2 ± 0.1
Muğla	Lycian nappes	Yatağan volcanics	Basaltic tuff	K-Ar	11.1 ± 0.2
Uşak	Menderes Massif	Selendi volcanics	Basalt	Rb-Sr	18 ± 0.2
Uşak	Menderes Massif	Selendi volcanics	Basalt	K-Ar	8.5 ± 0.2
Uşak	Menderes Massif	Selendi volcanics	Lava dome	Ar-Ar	12.15 ± 0.1

[a]From Kuscu et al (2018)

8.4.3 Geology of Southeastern Anatolian Orogenic Belt, Geochemistry, Petrogenesis and Geochronology of the Magmatic Rocks

Kuşcu et al. (2010, 2013) described the geology, geodynamic evolution, geochronology and geochemistry of the Southeastern Anatolian orogenic belt (SEAOB). This chapter will summarize the main points obtained in these works. The SEAOB is an easterly trending belt that lies subparallel to the Bitlis-Zagros suture zone (Figs. 8.2 and 8.6). It includes three distinct tectonostratigraphic units separated by major N-dipping thrust faults. From south to north, these units are; the Arabian platform, imbrication zone, and nappe zone (Yılmaz 1993). The tectonostratigraphical units are unconformably overlain by Late Cretaceous to Tertiary sedimentary and volcaniclastic rocks. In most areas in the SEAOB, only the Cretaceous and younger rock units are exposed. The Late Cretaceous subduction-related magmatic rocks (Baskil arc), extension-related Early-middle-Eocene volcanic, plutonic and sedimentary rocks, and post-Eocene sedimentary rocks in the region are included in the imbrication zone. The present day configuration of these tectonostratigraphic units is the result of southerly transported nappes during three major periods, the Late Cretaceous, Late Eocene, and Early to Middle Miocene (Kuşcu et al. 2012). The first two periods are related to the convergent plate margin evolution when Arabian and Eurasian plates coverage through a north-dipping subduction beneath TAB, and is also accompanied by obduction of southerly SSZ ophiolites over the Malatya-Keban platform (Yiğitbaş and Yılmaz 1996). Granitoid intrusions (83–70 Ma) into the metamorphic massifs and overlying ophiolites in eastern-southeastern Turkey were broadly contemporaneous with metamorphism (Beyarslan and Bingöl 2000; Robertson et al. 2007; Kuşcu et al. 2010). During the Miocene, a nappe package composed of the amalgamated ophiolitic rocks and the metamorphic massifs was accreted to the Arabian platform, possibly accompanied by transtensional deformation (Robertson 1998; Stampfli 2001).

The magmatic rocks in the SEAOB are divided in four main groups depending on their ages and spatial distribution (Kuşcu et al. 2010, 2013). The geochemical, field geological and geochemical characteristics of these groups are given in Kuşcu et al. (2010, 2013, 2018). Therefore, in this contribution we adopted their data and summarized the main points raised by their works. These groups are (1) Late Cretaceous, subduction-related rocks, dominantly in the south at Baskil (Elazığ), Malatya and Göksun (K. Maraş), (2) Late Cretaceous, post-collisional (Divriği, Sivas) to late-orogenic, within-plate magmatic rocks mainly at Hasançelebi (Malatya) and Keban (Elazığ) towards the northern part of the belt, (3) early to middle Eocene, post-collisional, intrusions at Çöpler, Kabataş (Erzincan), Doğanşehir-Polat (Malatya), Bizmişen-Çaltı (Sivas), Karamadazı (Kayseri), and Horoz (Niğde) regions, and (4) Late Oliocene magmatic rocks at Ovacık, Cevizlidere (Tunceli).

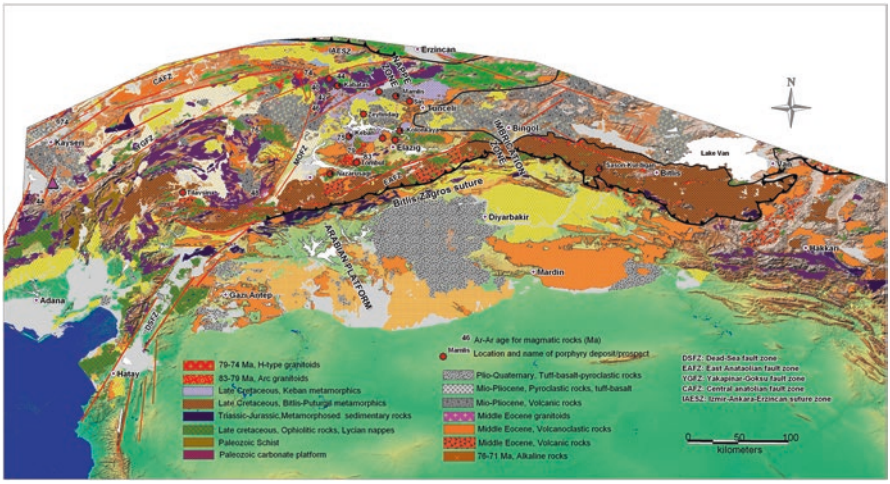

Fig. 8.6 Simplified geological map of SEAOB. (Modified from Kuşcu et al. 2018)

Late Cretaceous magmatic rocks in the SEAOB include (1) subduction-related Baskil arc to the immediate north and west-northwest of the Bitlis-Zagros suture zone that extend southeastward into Iran (Fig. 8.6), and (2) two main clusters of widespread post-collisional magmatism at Divriği, (Sivas) and (3) late-orogenic, within-plate volcano-plutonic associations (Hasancelebi, Malatya) to the north and close to the İzmir-Ankara-Erzincan suture zone (İAESZ), and the Keban pluton (Elazığ) at the center of the SEAOB (Kuşcu et al. 2018; Fig. 8.6). Early-Middle Eocene magmatic rocks in SEAOB are located to the north and northwest of the Late Cretaceous subduction-related rocks, and are unrelated to the Maden complex and Helete volcanics defined by Şengör and Yılmaz (1981) and Yiğitbaş and Yılmaz (1996). Late Oligocene magmatic rocks include volcanic and subvolcanic rocks widely exposed to the north, northwest of the Pertek and around Ovacık-Cevizlidere (Tunceli) as E-W trending belts.

All Late Cretaceous rocks are generally enriched in LREE, characterized by significant flattening of the HREE, and contain a negative Eu anomaly. Enrichment in Ba and Th and depletion in Nb and Ti compared to the slightly older Baskil arc rocks are reported. The Baskil arc rocks have the lowest LREE and moderate HREE content as well as La/Sm ratios where compared to younger Late Cretaceous rocks (Kuşcu et al. 2018). Except for younger ones, these are considered to be geochemical affinities akin to arc magmas (Kuşcu et al. 2012, 2018); and compositions commonly associated with porphyry Cu deposits on a global basis (Lang and Titley 1998; Richards and Kerrich 2007). The younger rocks exhibit almost identical LREE pattern, but distinct HREE pattern with a flatter HREE patterns (Kuşcu et al. 2018). The fact that the younger rocks are emplaced into obducted ophiolites, and they volcanic counterparts of the younger rocks are synchronous with the continen-

tal to marine sedimentation, field observations, the younger rocks are suggested to have formed in post-collisional environments.

Early-Middle Eocene granitoids in Horoz, Karamadazı, Çöpler, Kabataş, Bizmişen-Çaltı, and Dedeyazı-Polat regions are characterized by LILE enrichment with respect to HFSE, and strong K and weak Nb negative anomalies with HFS elements concentrations similar to MORB. The light rare earth elements (LREE) are generally enriched relative to chondrite. The La/Yb increases in time starting from arc-related Late Cretaceous magmatic rocks to late orogenic Early-Middle Eocene magmatic rocks (Kuşcu et al. 2012, 2018 and references therein). The La/Ta ratios, however, decrease from late Cretaceous to Early-middle Eocene magmatic rocks. These ratios were used to infer the crustal thickening or a shift from arc to continental margin (Kuşcu et al. 2010, 2013).

Kuşcu et al. (2010, 2013) reported igneous hornblende and biotite $^{40}Ar/^{39}Ar$ and hydrothermal phlogopite, sericite, K-feldspar plateau ages in the SEAOB (Table 8.3). The following is a brief summary of the geochronological data from their works. The hornblende and biotite on the magmatic rocks from Baskil arc yield $^{40}Ar/^{39}Ar$ plateau ages between 82.90 ± 0.43 and 79.43 ± 0.58 Ma (Table 8.3), similar to published K-Ar ages between about 85 and 77 Ma (Table 8.3) (Yazgan and Chessex 1991; Parlak 2005; Robertson et al. 2007). These indicate that Baskil magmatism probably was short lived, between about 83 and 79 Ma. Baskil arc magmatism was followed by post-collisional H-type to late orogenic-within plate magmatism. Kuşcu et al. (2011, 2012) also showed that the Early-Middle Eoceneis another era for extensive magmatism at SEAOB during which skarn and porphyry Cu forming plutons have been emplaced (Table 8.3). Interpreted $^{40}Ar/^{39}Ar$ and model Re-Os ages reported by Kuşcu et al. (2018 and references therein) collectively suggest a narrow time of magmatism between 44 and 50 Ma, with most of the ages being approximately 48 Ma. The probability density plot based on the available ages of rocks in the SEAOB emphasizes the three prominent peaks of magmatic activity between Late Cretaceous and Early-Middle Eocene (Kuşcu et al. 2018). The peak of thermal activity associated with the Late Cretaceous magmatic activity event appears to have been between 80 and 83 Ma, whereas the younger event thermally peaked at about 74–75 Ma refers to post-collisional magmatism. An age peak between 44 and 50 Ma records a third event of enhanced magmatism that in the SEAOB is associated with economic porphyry Cu-Au deposits. Although recent studies (Imer et al. 2015) confirmed that late Oligocene magmatism is a major host to porphyry Cu-Au mineralization at Ovacık (Tunceli), this has not been supported by extra data. However, this era may also be accepted as the fourth period for magmatism in the SEAOB.

Table 8.3 Geochronology of SEAOB

Geographic setting	Tectonic unit/setting[a]	Magmatic suite[a]	Rock composition[a]	Method[a]	Age (Ma)[a]
Elazığ	Baskil arc	Baskil magmatics	Granodiorite	K-Ar	86.5 ± 2.5
Elazığ	Baskil arc	Baskil magmatics	Q-Monzodiorite	K-Ar	83.5 ± 2.5
Elazığ	Baskil arc	Baskil magmatics	Q-Monzodiorite	K-Ar	86.0 ± 2.5
Elazığ	Baskil arc	Baskil magmatics	Q-Monzodiorite	K-Ar	84.0 ± 2.5
Elazığ	Baskil arc	Baskil magmatics	Q-Monzodiorite	K-Ar	84.0 ± 2.5
Elazığ	Baskil arc	Baskil magmatics	Diorite	K-Ar	75.5 ± 2.5
Elazığ	Baskil arc	İspendere pluton	Monzodiorite	Ar-Ar	81.1 ± 1.0
Elazığ	Baskil arc	İspendere pluton	Granite pophyry	Ar-Ar	80.15 ± 0.5
Elazığ	Baskil arc	Baskil magmatics	Granodiorite pophyry	Ar-Ar	79.43 ± 0.5
Elazığ	Baskil arc	Baskil magmatics	Q-Monzodiorite	Ar-Ar	82.90 ± 0.4
Elazığ	Eastern taurides	Keban pluton	Syenite	K-Ar	78.5 ± 2.5
Elazığ	Eastern taurides	Keban pluton	Syenite	K-Ar	76.0 ± 2.5
Elazığ	Eastern taurides	Keban pluton	Syenite poprhyry	Ar-Ar	74.08 ± 0.4
Elazığ	Eastern taurides	Keban pluton	Syenite poprhyry	U-Pb	74.8 ± 0.5
Elazığ	Eastern taurides	Keban pluton	Gabbro	K-Ar	77.5 ± 4.5
Elazığ	Eastern taurides	Keban pluton	Granitoid	K-Ar	76 ± 2.45 to 78 ± 2.5
Erzincan	Eastern taurides	Çöpler granitoid	Diorite porphyry	Ar-Ar	44.43 ± 0.6
Erzincan	Eastern taurides	Kabataş granitoid	Diorite	Ar-Ar	48.51 ± 0.3
Erzincan	Eastern taurides	Kabataş granitoid	Sericitic alteration	Ar-Ar	47.22 ± 0.5
Erzincan	Eastern taurides	Kabataş porphyry	Molybdenite	Re-Os	43.0 ± 0.2
Erzincan	Eastern taurides	Kabataş porphyry	Molybdenite	Re-Os	44.6 ± 0.2
Erzincan	Eastern taurides	Çöpler granitoid	Microdiorite porphyry	Ar-Ar	48.51 ± 0.34

(continued)

Table 8.3 (continued)

Geographic setting	Tectonic unit/setting[a]	Magmatic suite[a]	Rock composition[a]	Method[a]	Age (Ma)[a]
Kahramanmaraş	Baskil arc	Esence granite	Granodiorite	K-Ar	72.90 ± 1.7
Kahramanmaraş	Baskil arc	Esence granite	Granodiorite	K-Ar	73.30 ± 1.7
Kahramanmaraş	Baskil arc	Esence granite	Granodiorite	K-Ar	73.90 ± 1.7
Kahramanmaraş	Baskil arc	Esence granite	Granodiorite	K-Ar	72.30 ± 1.6
Kahramanmaraş	Baskil arc	Esence granite	Granodiorite	K-Ar	74.40 ± 1.5
Kahramanmaraş	Baskil arc	Esence granite	Granodiorite	K-Ar	71.53 ± 1.7
Kahramanmaraş	Baskil arc	Esence granite	Granodiorite	K-Ar	70.05 ± 1.7
Kahramanmaraş	Baskil arc	Esence granite	Granodiorite	K-Ar	85.76 ± 3.1
Kahramanmaraş	Baskil arc	Esence granite	Granodiorite	K-Ar	79.19 ± 1.9
Kahramanmaraş	Baskil arc	Esence granite	Granodiorite	K-Ar	79.38 ± 1.9
Kahramanmaraş	Baskil arc	Esence granite	Granodiorite	K-Ar	78.48 ± 1.9
Kahramanmaraş	Baskil arc	Esence granite	Granodiorite	K-Ar	80.42 ± 2.0
Kahramanmaraş	Baskil arc	Esence granite	Aplitic dike	K-Ar	77.49 ± 1.9
Kayseri	CACC	Karamadazı granitoid	Granodiorite	Ar-Ar	48.74 ± 0.7
Malatya	Eastern taurides	Hasançelebi volcanics	Trachyte	Ar-Ar	76.84 ± 0.6
Malatya	Eastern taurides	Hasançelebi volcanics	Diabase dike	Ar-Ar	74.32 ± 0.4
Malatya	Eastern taurides	Yüceşafak syenite	Syenite porphyry	U-Pb	75.7 ± 0.5
Malatya	Eastern taurides	Yüceşafak syenite	Syenite porphyry	U-Pb	75.3 ± 0.4
Malatya	Eastern taurides	Polat granitoid	Diorite, Q-diorite	Ar-Ar	48
Niğde	Eastern taurides	Horoz granite	Q-Monzodiorite	Ar-Ar	50.44 ± 0.3
Sivas	Eastern taurides	Murmano pluton	Monzonite	Ar-Ar	75.63 ± 0.4
Sivas	Eastern taurides	Murmano pluton	Monzodiorite	Ar-Ar	73.48 ± 0.4

(continued)

Table 8.3 (continued)

Geographic setting	Tectonic unit/setting[a]	Magmatic suite[a]	Rock composition[a]	Method[a]	Age (Ma)[a]
Sivas	Eastern taurides	Murmano pluton	Granite	Ar-Ar	73.40 ± 0.4
Sivas	Eastern taurides	Bizmişen granite	Q-Diorite	K-Ar	42.1 ± 0.9
Sivas	Eastern taurides	Bizmişen granite	Q-Diorite	K-Ar	42.0 ± 0.5
Sivas	Eastern taurides	Bizmişen granite	Q-Diorite	K-Ar	43.8 ± 0.9
Sivas	Eastern taurides	Bizmişen granite	Q-Diorite	K-Ar	46.3 ± 0.4
Sivas	Eastern taurides	Çaltı granite	Q-Diorite	K-Ar	43.7 ± 0.9
Sivas	Eastern taurides	Çaltı granite	Granodiorite-tonalite	K-Ar	44.7 ± 0.9
Sivas	Eastern taurides	Çaltı granite	Granodiorite-tonalite	K-Ar	48.8 ± 0.9
Sivas	Eastern taurides	Çaltı granite	Granodiorite-tonalite	K-Ar	40.5 ± 0.9

[a]From Kuscu et al (2013, 2018)

8.5 Types and General Characteristics of Porphyry Deposits/Prospects in Turkey

Turkey contains numerous historical and newly discovered porphyry copper deposits/prospects. These include porphyry Cu, porphyry Cu-Mo, porphyry Cu-Au and porphyry Au sub-types, and widely occur within four tectono-magmatic settings; Pontides, western Anatolian province (WAP) including Karakaya complex, Tavşanlı and Afyon zones, central Anatolian crystalline complex (CACC), Central Anatolian volcanic province (CAVP), and southeastern Anatolian orogenic belt (SEAOB). These deposits are hosted by or associated with volcanic, plutonic and volcano-plutonic complexes formed as a result of a long subduction, collision and post-collision events at the expense of closure of NeoTethys Ocean between the latest Cretaceous and late Miocene. The available information and the database for a total of 66 porphyry deposits/prospects and occurrences are listed in Table 8.4. The spatial distribution of these deposits is shown on Fig. 8.7. The porphyry systems are more abundant in the Pontides although there is no operating deposit. Pontides appears to be a regional porphyry belt, and is called Pontide porphyry belt (PPB) with 30 prospects, abandoned mines and occurrences. The WAP, including the Afyon and Tavşanlı zones, Karakaya complex and Biga Peninsula hosts three significant porphyry belts; Biga, Tavşanlı and Afyon-Konya porphyry belts (Fig. 8.7). In these belts 19 prospects/deposits are found. The Kışladağ porphyry Au deposit, the Europe's largest deposit lies in the Biga porphyry belt along with some others

Table 8.4 Porphyry Cu-Mo deposits-prospects in the Pontides

Name of the deposit/ prospect	Location[a]	Metal/Ore[a]	Host rocks[a]	Alteration[a]	Ore-related Minerals[a]	Average grade[a]	Resource (Mt)[a]	Age of host rock[a]	Age of mineralization[a]
Eastern Pontides Cu-Mo belt									
Elbeyli	Ordu	Cu-Mo	Monzonite, monzodiorite	Advanced argillic	Mp, cpy, en	n.a	n.a	77 ± 1 Ma	Late Cretaceous
Güvemli	Gümüşhane	Cu-Au-Mo	Andesite, basaltic andesite	Argillic overprinting potassic	mag, cpy	10.2 g/t from soil surveys	n.a	Middle Eocene	Middle Eocene
Emeksen	Giresun	Mo	Granodiorite, granite	Potassic, phyllic,	M0, ga, sph	0.08–2.87% Mo	n.a	78. ± 0.5 Ma 79 ± 0.5	Late Cretaceous
Konak	Konak, Giresun	Cu-Mo, Au	Granodiorite, dacite	Phyllic alteration with qtz-Mo stockwork	cpy, mlc, mo, py	5.18 Mt 0.23% Cu 0.07 g/t Au	n.a	Late Cretaceous	Late Cretaceous
Bakırçay	Merzifon, Amasya	Cu-Mo	Granodiorite, tonalite	Quartz-sericite	qtz cpy, mo	0.2% Cu	200 Mt @0.2% Cu	42.3 ± 2.61.6 Ma	38.0 ± 1.28 Ma
Hasandağı	Trabzon	Cu	Granodiorite porphyry	Advanced argillic	qtz-py	n.a	n.a	Late Cretaceous	Late Cretaceous
Güzelyayla	Maçka, Trabzon	Cu-Mo	Dacite porphyry, granodiorite porphyry	Pb-Zn skarn Potassic, phyllic	cpy	0.18–0.3% Cu 0.012% Mo	186.2 Mt @ 0.3 % Cu equiv	81.5 ± 1 Ma	Late Cretaceous
Seyitler	Artvin	Cu-Mo (Au?)	Quartz monzonite, granite	n.a	cpy, mo, mag	n.a	n.a	Early-Middle Eocene	Eocene(?)

(continued)

Table 8.4 (continued)

Name of the deposit/ prospect	Location[a]	Metal/Ore[a]	Host rocks[a]	Alteration[a]	Ore-related Minerals[a]	Average grade[a]	Resource (Mt)[a]	Age of host rock[a]	Age of mineralization[a]
Corak	Yusufeli, Artvin	Ag, Au	Andesitic volcaniclastics and flows	Supergene argillic overprinting advanced argillic	n.a	n.a	0.760 Moz Ag (indicated resource)	Eocene	Eocene
Yolgeçen	Arhavi, Artvin	Cu-Mo	Quartz diorite, granodiorite and mafic dikes	Quartz-sericite	qtz py, mlc	8 g/t Au (rock samples)	n.a	Middle Eocene	Middle Eocene
Ardala	Artvin	Cu-Mo-Au	Granodiorite porphyry, andesite, dacite	Pervasive clay alteration overprinting potassic alt.	cpy, mo	2.03 g/t Au, 0.3% Cu	1.09 Moz Au equiv.	Late Cretaceous?	Late Post Paleocene, Middle-Upper Eocene
Balcılı	Yusufeli, Artvin	Cu-Mo	Tonalite, granite	Subtle sericitic	py, mo, cpy, cct	0.1–0.2 % Cu	145 Mt @ 0.25% Cu equiv (Cu+Mo)	Paleocene	62.3 ± 4.2 Ma
Börekli	Yusufeli, Artvin	Cu-Mo	Granodiorite	Subtle sericitic	py, mo, cpy, cct	n.a	n.a	Post Paleocene, Middle-Upper Eocene	Middle Eocene
Pöhrenk	Yusufeli, Artvin	Cu-Mo	Granodiorite, andesite	n.a	cpy	0.2 % Cu	n.a	Post Paleocene	Middle Eocene
Taşkıran	Yusufeli, Artvin	Cu-Mo	Granodiorite, andesite	Propylitic	cpy	n.a	n.a	Late Cretaceous	Middle Eocene
Gümüşhane (Derinköy)	Artvin	Au, Cu-Mo	Granodiorite porphyry	Argillic	cpy, mo	0.30–0.50% Cu	30 Mt @ 0.3 g/t Au	Late Cretaceous	52.5 Ma
Yüksekoba	Yusufeli, Artvin	Cu-Mo-Au	Granodiorite	Argillic, phyllic	cpy, mo, mlc	n.a	n.a	Eocene	Eocene

Berta	Artvin	Cu-Mo-Au	Feldspar porphyry	Argillic, phyllic	py	5.07–0.28% Cu 0.17–0.31g/t Au	n.a	Late Cretaceous	Late Cretaceous
Ovit	Artvin	Cu-Mo	Granodiorite porphyry	Quartz-sericite	mo, cpy		n.a	Middle Eocene	Middle Eocene
Durusu	Artvin	Cu-Au	Granodiorite porphyry, andesite, pyroclastics	n.a	py, mag	0.3%Cu, 0.4g/t Au	140 Mt	Middle Eocene(?)	Eocene(?)
Sivritaş	İkizdere, Rize	Cu-Mo	Granite	Propylitic	cpy, mo	n.a	n.a	Eocene	Eocene
Avupdağ	Pazar, Rize	Cu-Mo	Granite, quartz diorite	n.a	cpy, py	n.a	n.a	Late Cretaceous	Late Cretaceous
İspir-Ulutaş	Erzurum	Cu-Mo	Quartz monzonite, granodiorite and andesite	Phyllic alteration with qtz Mo veins, proximal Cu-, Pb-Zn skarn	cpy, mo, sph.	1.5 % Cu, 0.02 %Mo 3 % Zn	200 Mt @ 0.3% Cu	Early Eocene	59 Ma
Oltu-Mehenk	Erzurum	Cu-Mop ??	Andesite	n.a	py, cpy, bn, mag	n.a	n.a	Late Cretaceous	Late Cretaceous (?)
Hirdamus	Hirdamus, Erzurum	Au, Cu	Andesite basalt lava, pyroclastics	n.a	py, cpy, mag, gal	0.3 g/t Au	n.a	Eocene	Eocene
Inanmış	Erzurum	Cu-Mo	Dacite	n.a	py, cpy	n.a	n.a	Late Cretaceous	Eocene(?)

(continued)

Table 8.4 (continued)

Name of the deposit/ prospect	Location[a]	Metal/Ore[a]	Host rocks[a]	Alteration[a]	Ore-related Minerals[a]	Average grade[a]	Resource (Mt)[a]	Age of host rock[a]	Age of mineralization[a]
Western Pontides (Strandja) Cu-Mo-W Belt									
Keçikaya	Kıyıköy, Kırklareli	Cu-Mo	Granite	skarn	cpy, mo, mlc	0.015 % Cu	n.a.	Late Cretaceous	Late Cretaceous
Dereköy	Kırklareli	Cu-Mo	Quartz diorite	Fe-Cu skarn	sch, mag	0.24% Cu 0.023% Mo	221	79.01 ± 0.54	76.96 ± 0.42 Ma
Karanlıkdere	Kırklareli	Cu-Mo	Granodiorite	Fe-Cu skarn	cpy-py, minor mo, sch	n.a.	n.a	Late Cretaceous	Late Cretaceous
Şükrüpaşa	Kırklareli	Cu-Mo-W (Au?)		Potassic, phyllic	cpy, wlf, gold	0.02% Mo	Mt@ 0.01 WO_3, 0.3% Cu	Late Cretaceous	77.64 ± 0.51 Ma
Demirköy	Kırklareli	Cu-Mo-(W?)	Quartz monzonite	Potassic, phyllic	en, cpy, gal	0.39% Cu, 0.05% Mo	n.a	80.94 ± 0.57 Ma	Late Cretaceous
İkiztepe	İğneada, Kırklareli	Cu-Mo-(W-Au)	Quartz monzonite, granodiorite	Fe-Cu skarn	cpy-en, mo, sch, gold	0.5 %Cu eqv. Mo	13	Late Cretaceous	Late Cretaceous

Abbreviations: *n.a* not available, *n.d* not detected, *n.i* no information, *qtz* quartz, *mag* magnetite, *gal* galena, *hem* hematite, *sp* sphalerite, *cpy* chalcopyrite, *py* pyrite, *fl* fluorite, *bn* bornite, *mo* molybdenite, *goe* goethite, *tou* tourmaline, *mlc* malachite, *co* covellite, *bar* barite, *sch* scheelite, *al* alunite, *ser* sericite, *cct* chalcocite, *pyt* pyrite

[a]From Kuşcu et al (2018)

[a]From Kuscu et al (2013, 2018)

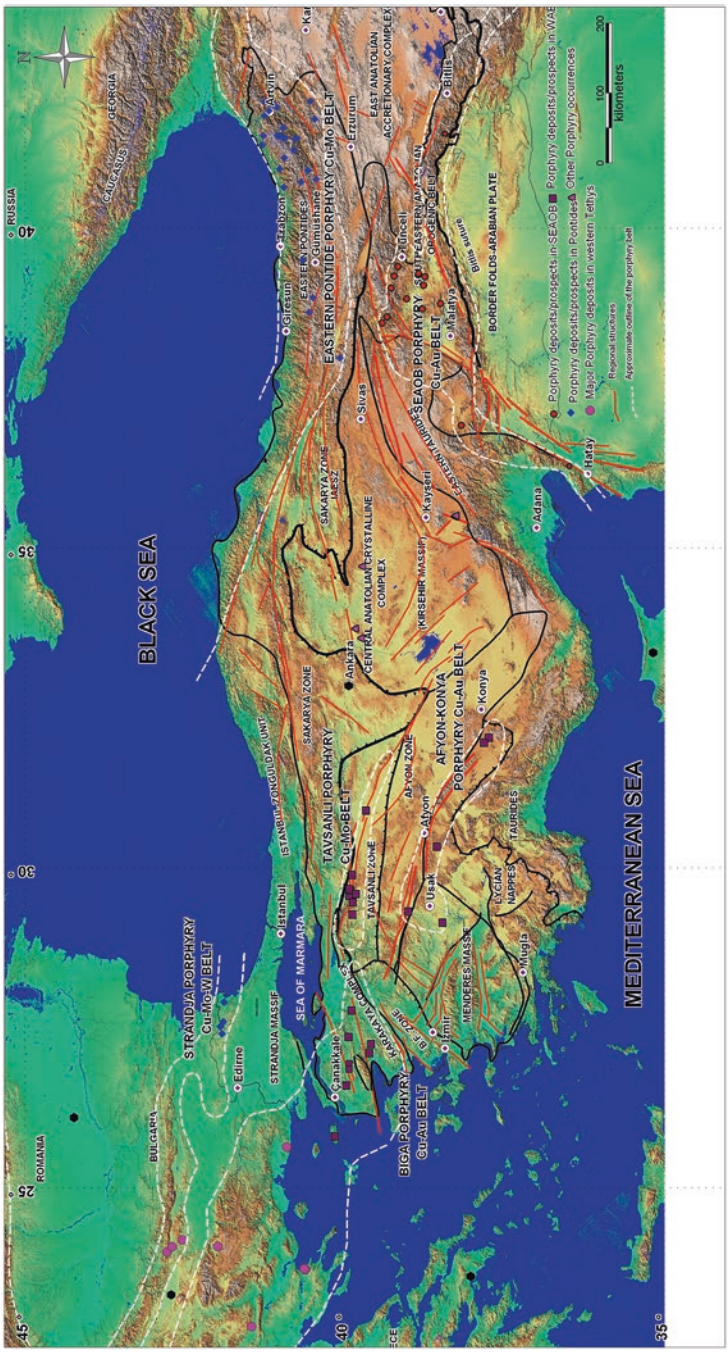

Fig. 8.7 The spatial distribution of porphyry deposits/prospects and porphyry belts in Turkey (From Kuşcu et al. 2018; white dashed lines showing the approximate boundaries of porphyry belts; red solid lines showing the regional strike-slip and normal faults)

(Ağıdağ and Halilağa). SEAOB is another terrane hosting several economically viable porphyry deposits/prospects. The SEAOB contains several economic porphyry deposits and prospects including Çöpler, Karakaya, Kabataş, Keban, Tilavşun (Höyük) and a newly discovered one, Cevizlidere. Central Anatolian volcanic province with Neogene magmatism is also a host to several epithermal prospects with a potential porphyry mineralization, but none have yet been discovered. Öksüt is one of important new discoveries in this province. There are some intrusion-related systems having porphyry potential at the central Anatolia. Kuşcu et al. (2018) presented resource/reserve data for the porphyries in Turkey, and adopted in this chapter. Only operating deposits have modern resource-reserve database. Inferred resource database for the prospect, mostly compiled from the news release, is given in separately for each province in Tables 8.4, 8.5, and 8.6. No porphyry copper deposit contains sufficient metal to achieve the status of a "giant" one (Singer et al. 2005), although the Europe's largest porphyry Au deposit (Kışladağ) is in Turkey. Reported Cu grade and intersections range from 0.1 to 2.02 wt.%. Reported Mo grade ranges from 0.01 to 1 wt.%. Reported Au grade ranges from 0.1 to 10.8 g/t (Tables 8.4, 8.5, and 8.6). The operating porphyry Mo deposits are found only within the Biga porphyry belt. Subvolcanic environments with preserved extrusive rocks are the preferred setting for porphyry Cu-Au and Au systems in the Biga porphyry belt while plutonic and volcano-plutonic environments are more common in Pontides porphyry belt. Epithermal system of high-sulfidation affinity is associated with some porphyry deposits in the Biga, as seen in the Halilağa, Kışladağ and Ağıdağ deposits.

8.5.1 Porphyry Copper Deposits/Prospects in the Pontides

Beginning at the frontier with Bulgaria, the porphyry Cu systems in the Pontides form a belt extending across northern Turkey parallel to the Banatitic-Pontide subduction front. The porphyry copper systems in Pontides include a great number of porphyry Cu-Mo deposits/prospects with Au and W association (Table 8.4). Au association is confined mostly to eastern Pontides whereas W association is more common in the Strandja massif (Table 8.4). No or a few porphyry deposits are recorded in the central Pontides (Zonguldak unit), the only known deposit in central Pontides is the Bakırçay Cu-Mo deposit at Merzifon (Amasya). The Pontides include (1) Late Cretaceous Strandja porphyry Cu-Mo-Wbelt at the NW close to Bulgarian border and (2) Late Cretaceous to Middle Eocene eastern Pontide porphyry Cu-Mo beltin the eastern Pontides (Fig. 8.7). The porphyry Cu-Mo deposits/prospects in the eastern Pontides are mostly parallel to the axial trend of arc-magmatism. No porphyry deposit has been operating in the eastern Pontides, although there were some porphyry Cu-Mo deposits in production several decades ago. The companies have begun an aggressive multi-phase exploration program on these prospects to discover an economic deposit or to bring some of them into production.

Table 8.5 Porphyry Cu deposits-prospects of western Anatolian province

Name of the deposit/ prospect	Location	Commodity	Host rocks[a]	Alteration[a]	Ore-related minerals[a]	Average grade[a]	Resource (Mt)[a]	Age of host rock[a]	Age of mineralization[a]
Tavşanli Porphyry Cu-Mo Belt									
Demirtepe	Bursa	Cu-Au, Ag	Granodiorite, marble	Phyllic, argillic	bn, > cpy	0.7–2.02% Cu, 0.26–0.96 g/t Au	n.a	Tertiary	Middle Eocene?
Muratdere	Muratdere, Bursa	Cu-Au-(Mo-Re?)	Quartz diorite	Phyllic, argillic	cpy, mo	0.36 % Cu, 0.12 g/t Au	51M@ 0.36% Cu	49.64 ± 0.28 Ma	46.4 ± 0.3 Ma
Gelemiç	Yaylaçal, Bursa	Mo, Cu-Mo	Granodiorite, tonalite	Phyllic	cpy, mo	4 % Mo	0.23	n.a	n.a
Tüfekçikonak	İnegöl, Bursa	Cu-Mo	Monzonite, rhyolite, tonalite, granodiorite	Potassic phyllic, argillic	mag, pyt, cpy, bn and mo	Up to 0.37%	n.a	52.6 ± 1.1 Ma	49.16 ± 0.7 Ma
Karapınar	Karapına, Bursa	Cu-o-Au	Granite, granodiorite, diorite porphyry	Weak potassic, argillic	cpy, sp	0.5–1 % Cu 0.02% Mo, 0.2g/t Au	0.4 Moz Au (inferred)	Eocene?	44.7
Sarıçayır	Tahtaköprü, Bursa	Cu	Quartz diorite porphyry, quartz diorite	Weak potassic	Cpy, mo	0.17% Cu	0.12Mt @ 0.17% Cu	50 Ma	Early Eocene(?)
Gürcüler	İnegöl, Bursa	Cu-Mo-Au (?)	Granite, granodiorite, diorite porphyry	Potassic	disseminated cpy	Up to 1% Cu, 47–92 ppm Mo	n.a	Eocene?	Eocene(?)

(continued)

Table 8.5 (continued)

Name of the deposit/ prospect	Location	Commodity	Host rocks[a]	Alteration[a]	Ore-related minerals[a]	Average grade[a]	Resource (Mt)[a]	Age of host rock[a]	Age of mineralization[a]
Topukdere	Domaniç, Kütahya	Cu-Mo	Granodiorite, diorite	Potassic,	disseminated cpy	0.17% Cu	120 @0.17 %Cu	49.64 ± 0.28 Ma	46.74 ± 0.37 Ma
Gürgenyayla	Bursa	Cu-Mo	Granite, granodiorite, diorite porphyry	Weak potassic, argillic	cpy veinlets, disseminated mo	n.d	n.d	49.90 ± 0.28 Ma	47.49 ± 0.27 Ma
Biga Porphyry Cu-Au Belt									
Halilağa	Halilağa village, Etili Çanakkale	Cu-Au	Quartz monzonite, andesite porphyry, andesite	Potassic	mag, cpy	0.31 g/t Au, 0.30 %Cu	198 Mt Mt @ 0.23% Cu,0.31 g/t	26 Ma	26.27 ± 0.19 Ma
Ağıdağ	Terzialan, Çanakkale	Au-Cu	Andesite porphyry, granodiorite	Advanced argillic, phyllic,	cpy, cct, mag, mo	1 g/t Au	1.9 Moz @ 0.53 g/t Au	27.20 ± 0.18 Ma	26.36 ± 0.16 Ma
Kuşçayır-Karaayı	Bayramiç, Çanakkale	Cu-Au	Ignimbrite, andesite porphyry	Advanced argillic,	mag, cpy, al, py	0.52 g/t Au	n.a	42.68 ± 0.25 Ma	39.99 ± 0.27 Ma
Tepeoba	Havran, Balıkesir	Cu-Mo	Granodiorite, granite	Potassic	cpy, mo, mlc	%0.33 Cu; % 0.041 Mo	4.8 Mt@ 0.32 Cu	24.70 ± 0.15 Ma	24.56 ± 0.16 Ma
Bakırlık	Balıkesir	Cu-Mo	Granodiorite	Phyllic, argillic	cpy, mlc, mag, cct		n.a	23 Ma	Oligo-Miocene
Kocatarla	Çanakkale		Granodiorite granite	Phyllic, advanced argillic	mag, cpy		n.a	n.a	Mid-Eocene
Dikmen	Dikmenköy, Çanakkale	Au-Cu-Mo	Granite			4.6 gr/t	n.a	n.a	Mid-Eocene

Gökçeada	Gökçeada, Çanakkale	Cu-Au	Dacite, granodiorite	Argillic silicified ledges	Cpy, py	0.1–0.6 ppm Au, 0.6 %Cu	750Mt @ 0.1–0.6 ppm Au and 1000–0.6% Cu	n.a	38 Ma (?)
Afyon-Konya Porphyry Au Belt									
Kışladağ	Ahmetli, Uşak	Au	Trachyte porphyry, latite porphyry, pyroclastic rocks	Advanced argillic, phyllic	tou-qtz	1.16 g/t Au	135.02 @ 1.16 g/t	14.81 ± 0.15 Ma	13.81 ± 0.26 Ma
Inlice	Inlice, Konya	Au	Trachyte-latite porphyry	Advanced argillic		6.22–10.8 g/t	0.327 Mt @ 2.90 g/t Au (epithermal)	8.98	Late Miocene
Doğanbey	Konya	Au-Mo	Trachyte, tuff, ignimbrite	Advanced argillic		Mo up to 327 ppm	n.a	Late Miocene	Late Miocene
AS (Sandıklı)	Karacahisar, Afyon	Cu	Latite porphyry, monzonite	Advanced argillic, phyllic, potassic	tou, py, cpy		n.a	12.19 ± 0.75 Ma	12.36 ± 0.20 Ma
Öksüt	Develi, Kayseri	Cu-Au	Rhyolite, andesite flows	Advanced argillic	cpy, mlc	n.a	n.a	Mio-Pliocene (?)	Mio-Pliocene (?)

[a]From Kuşcu et al. (2018)

Table 8.6 Porphyry Cu deposits-prospects in the SEAOB

Name of the deposit/ prospect	Location	Metal/ore	Host rocks[a]	Alteration[a]	Ore-related minerals[a]	Average grade[a]	Resource (Mt)	Age of host rock[a]	Age of mineralization[a]
Kabataş	İliç, Erzincan	Cu-Au	Diorite porphyry, microdiorite, hornblende qtz monzonite porphyry	Phyllic, argillic	Oxidized	n.a	n.a.	48.51 ± 0.3 Ma	47.22 ± 0.5 Ma
Çöpler	İliç, Çöpler	Au-Cu	Diorite porphyry, microdiorite, hornblende qtz monzonite porphyry	Phyllic, argillic	cpy, co, cct	4.74 g/t Au, 0.15 % Cu	4.4 Moz	44.43 ± 0.6 Ma	40.2 ± 6.8 Ma 43.0 ± 0.2 Ma 44.6 ± 0.2 Ma
Karakartal	İliç	Cu-Au	Diorite	Phyllic, argillic	cpy, co, cc	0.3 g/t Au, and 0.22% Cu	13.8 Mt@0.5 g/t Au and 0.29% Cu	Eocene (?)	Eocene (?)
Tilavsun (Höyüklü)	Afşin, K. Maraş	Cu-Au	Dacite, dacite porphyry	Argillic	cpy, gt, hem, sp	0.2 % Cu, 0.001% Mo	250 Mt	Late Cretaceous?	Eocene (?)
Kızılviran	Tunceli	Cu-Au-Mo	Qtz diorite	Potassic, phyllic, argillic	bn, cpy, py, mag, hem	1.03 % Cu, 0.17 g/t Au	n.a	Eocene	Eocene (?)
Kolonkaya	Pertek, Tunceli	Cu-Au	Hornblende porphry	Phyllic	cpy	up to 37.8 g/t from surface samples	n.a	Late Cretaceous	Late Cretaceous
Cevizlidere	Ovacık, Tunceli	Cu-Au-Mo	Andesite, dacite porphyry	Fe-Cu skarn	cpy, mo	0.38 % Cu, 0.11g/t Au	445	Middle Eocene	26.0 ± 0.2Ma
Mamlis-Sin	Ovacık, Tunceli	Cu	Dacite, diorite porphyry stock	Potassic, phyllic	cpy, mag	0.1–0.2% Cu	n.a	Middle Eocene	Eocene (?)

Nazaruşağı	Baskil, Elazığ	Cu-Au	Granodiorite, granite porphry	Propylitic, potassic	cpy, mag	n.a	n.a	82.90 ± 0.4Ma	79.43 ± 2.7Ma
İspendere	Kale, Elazığ	Cu-Au	Tonalite, qtzdiorite	Propylitic, argillic	cpy	n.a	n.a	Late Cretaceous	77.5 ± 2.7Ma
Kızıldağ	Harput, Elazığ	Cu	Granodiorite, granite porphry	Phyllic	cpy, mag	n.a	n.a	Late Cretaceous	Eocene (?)
Keban	Keban, Elazığ	Mo-Cu	Syenite porphyry, trachyte	Pb-Zn skarn	Pb, Zn, Mo	0.8% Mo	100	74.08 ± 0.0Ma	71.85 ± 0.5Ma

Abbreviations: *n.a* not available, *n.d* not detected, *n.i* no information, *qtz* quartz, *mag* magnetite, *gal* galena, *hem* hematite, *sp* sphalerite, *cpy* chalcopyrite, *py* pyrite, *fl* fluorite, *bn* bornite, *mo* molybdenite, *goe* goethite, *tou* tourmaline, *mlc* malachite, *co* covellite, *bar* barite, *sch* scheelite, *al* alunite, *ser* sericite, *cct* chalcocite, *pyt* pyrite

[a]From Kuşcu et al (2013, 2018)

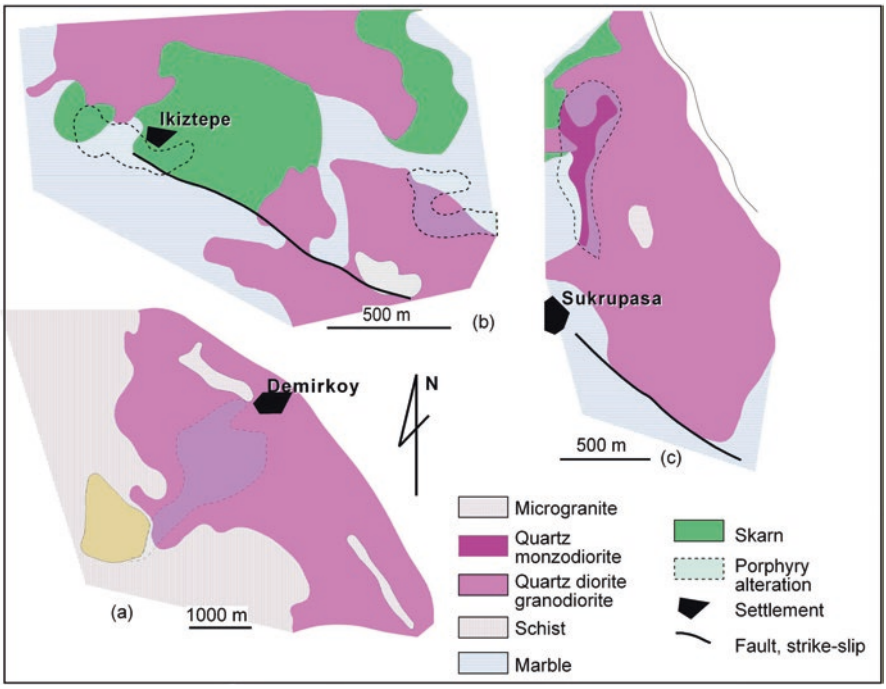

Fig. 8.8 Simplified geological maps showing the limits of porphyry alterations in (**a**) Demirköy, (**b**) İkiztepe (Armutveren) and (**c**) Şükrüpaşa porphyry deposits

8.5.2 The Strandja Porphyry Cu-Mo-W Belt

The Strandja porphyry Cu-Mo-W belt (Figs. 8.3 and 8.7) is the eastward continuation of the Late Cretaceous Srednogorie–Timok magmatic belt in Serbia and Bulgaria (Ciobanu et al. 2002; Lips et al. 2004; von Quadt et al. 2005). The porphyry systems form a northwest-trending belt, about 70 km length and about 15 km wide. In this belt, six porphyry deposits/prospects (Fig. 8.3) and numerous medium to small-sized skarns are known, and are associated with numerous medium-to small-sized Fe-Cu skarns (Ohta et al. 1988; Kuşcu 2009). These are from east to west Keçikaya, İkiztepe, Karanlıkdere, Demirköy, Şükrüpaşa and Dereköy (Figs. 8.3, 8.8, and 8.9). The skarns are classified as proximal Fe-Cu skarns at the margins (Kuşcu 2009). These deposits/prospects are not operating to date while the private companies have been sporadically exploring the region since the early 1960s, and some have been recently explored but little modern work has been completed. The outcrops in these prospects are generally poor due to dense vegetation and thick soil cover. The porphyry Cu prospects in Strandja massif are hosted by and/or associated multi-phase Late Cretaceous intrusive rocks, quartz diorite, monzodiorite, monzonite and granite in composition, that are emplaced into limestone, mica schist, quartzite and gneissose rocks in the basement. The

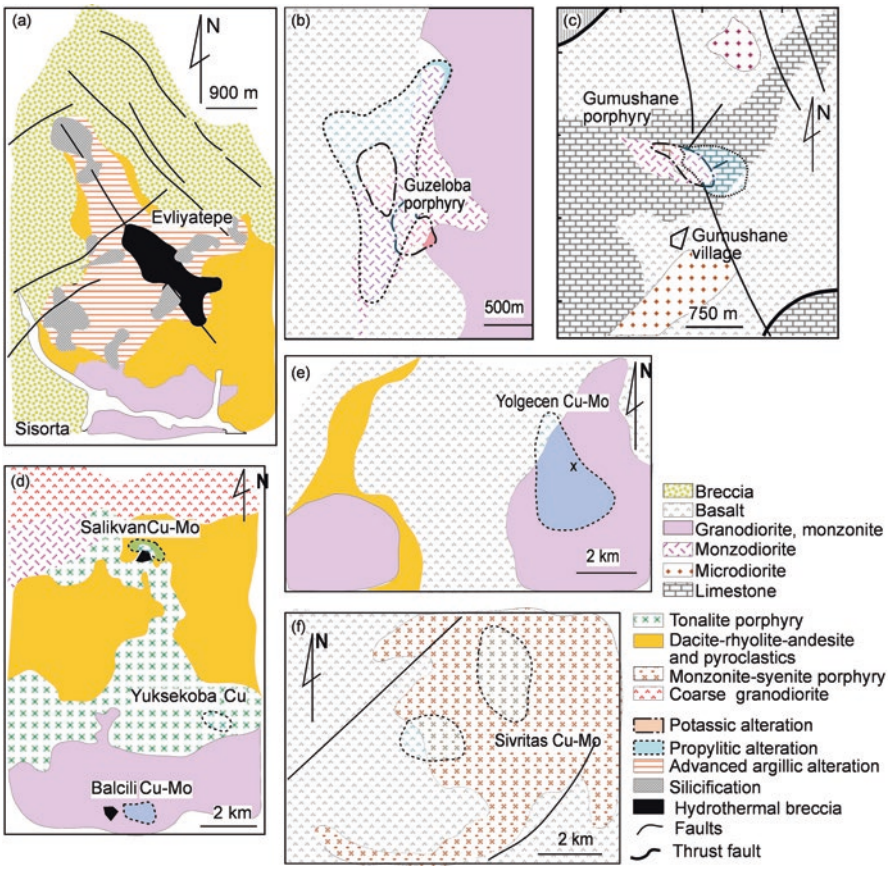

Fig. 8.9 Simplified geological maps showing the major rocks types and alteration zones within the eastern Pontides; (**a**) Sisorta, (**b**) Güzeloba, (**c**) Ardala, (**d**) Yüksekoba, Balcılı, Salıkvan, (**e**) Yolgeçen and (**f**) Sivritaş

intrusives are cut by steeply-dipping NW-SE to E-W trending microgranite porphyry dikes (Figs. 8.8 and 8.9). Quartz diorite generally forms dikes and stocks, whereas monzonitic to monzodioritic rocks are the main host rocks for the hydrothermal systems (Kuşcu 2009). They have elongated exposures with a NW axial trend (Fig. 8.3), and are locally weathered down to at least 40 m below surface (Kuşcu 2009). They are commonly bounded by NW-SE trending normal to strike slip faults juxtaposing metamorphic basement and intrusive rocks (Fig. 8.8). The porphyry Cu and Cu-Mo-W prospects hosted by or associated with quartzdioritic rocks are co-genetic with proximal skarns where they cross-cut metacarbonates (Fig. 8.8). The porphyry intrusions hosting mineralized quartz veins are altered to potassic assemblages overprinted by phyllic assemblages with peripheral propyllitic assemblages (Kuşcu 2009). This suggests collapse of hydrothermal system during hydrothermal alteration (Kuşcu 2009). The primary hypogene

mineralization mainly comprises chalcopyrite and pyrite with accessory molybdenite. Despite weathering to depths approaching 40 m, only minor supergene Cu-minerals are reported (Kuşcu 2009). Miocene to Pliocene sedimentary rocks of the Thrace basin unconformably overlie the western Pontide porphyry belt, suggesting the potential for undiscovered resources.

The Dereköy, Demirköy and İkiztepe are the three best-known porphyry Cu-Mo systems (Fig. 8.8). These have been mined sporadically for centuries. Tungsten is present in the Şükrüpaşa and İkiztepe systems. Gold is sporadic, and occurs as native crystals associated with enargite. Dereköy is the largest deposit with a reported resource of 221 Mt @ 0.24% Cu and 0.023% Mo (Singer et al. 2008). The İkiztepe system has reported past production resource data of 13 Mt @ 0.5% Cu-0.05% Mo equivalent of Mo (Table 8.4). The Demirköy deposit has the highest copper and molybdenum grades, but only an indicated reserve of 12.7 Mt (Table 8.4). Cu mineralization is common for all prospects, and is hosted by phyllic alteration. The ore bodies trend in E-W, and are characterized by oxidized quartz-biotite and stockwork veins. The thickness of the veins is variable, ranging from a few mm to 2 cm. The ore minerals are commonly chalcopyrite, pyrite, with minor molybdenite, found as stockwork to disseminated ore bodies.

8.5.2.1 Geochronology of Strandja Porphyry Cu-Mo-W Belt

The geochronology of the Strandja porphyry Cu-Mo belt was compiled from Kuşcu et al. (2018), and are based on publically available data and biotite separates from oxidized quartz-biotite veins in the phyllic alteration within Demirköy, Dereköy and Şükrüpaşa Cu-Mo deposits (Table 8.1, Kuşcu et al. 2018). Hydrothermal biotite from Dereköy and sericite from Şükrüpaşa Cu-Mo deposits gives $^{40}Ar/^{39}Ar$ ages of 76.96 ± 0.42 and 77.64 ± 0.51 Ma, respectively (Table 8.1). Demirköy deposit did not yield reliable plateau and isochron age, therefore was excluded in this evaluation. As the published K-Ar ages for these systems either are in general agreement, or are significantly younger (e.g. Ohta et al. 1988) than the ages, Kuşcu et al. (2018) noted that these ages need to be used with caution until more reliable ages are obtained for these deposits. These age intervals (within error limits) coincides with or slightly younger than the age of host intrusives (Table 8.1).

8.5.3 Eastern Pontide Porphyry Cu-Mo Belt

The eastern Pontide porphyry Cu-Mo belt (EPPB) is located on the eastern margin of the Pontide terrane (Figs. 8.4 and 8.7), and associated with late Cretaceous magmatic-arc to Middle Eocene post-collisional magmatic belt also known as eastern Pontide magmatic arc (EPMA). The EPPB is the eastern continuation of the Rhodope-Pontide, and western continuation of the lesser Caucasus. It extends eastwards towards Georgia, then to Iran. In this belt 25 prospect/deposits, that are

mostly restricted to the easternmost part of the belt between Artvin and Giresun, are known (Table 8.4). In this chapter, the occurrences that have preliminary assessment only are excluded. The porphyries in this belt are mostly Cu-Mo with rare Au and W (Table 8.4). There are also minor amounts of Cu-Au, Cu-only and Au-only subtypes. The porphyry Cu deposits in this belt are hosted either by Late Cretaceous arc magmatics or by Early-Middle Eocene post-collisional (Table 8.4) magmatic rocks within E-W trending belts mostly parallel to the geologic boundaries between Eocene and Late Cretaceous rocks (Figs. 8.4 and 8.9). These belts have been defined based on the relative timing and tectonic setting of magmatism, and spatial association of porphyries in the EPPB from north to south. Eocene rocks host most of the porphyry systems, whereas fewer prospects are hosted by or associated with Late Cretaceous volcanic and plutonic rocks. Late Cretaceous (?) porphyry Cu-Mo systems are concentrated in the northern magmatic zone whereas Eocene Cu-Mo systems are concentrated in the central to southern zones (Fig. 8.4).

8.5.3.1 Late Cretaceous Porphyry Cu-Mo Deposits/Prospects in Eastern Pontides

The late Cretaceous porphyry Cu-Mo belt lies in NE-SW trending elongated area between Giresun, Trabzon and Gümüşhane (Fig. 8.4). Ten Late Cretaceous (?) prospects are known (Table 8.4; Fig. 8.4). Selected prospects are Konak Cu-Au, Hasandağı Cu, Güzelyayla Cu-Mo, Avupdağ, Ardala, Berta, Zoybar (Esendal) and Güvemli Cu-Mo-Au. They are hosted by or associated with NE-SW-trending volcanic domes, stocks and small intrusions in the area between Tamdere, Beytarla, Yaylalı and Maçka villages in Giresun and Trabzon. The host intrusive rocks are multi-phase, and mostly quartz microdiorite, granite porphyry, and granodiorite in composition. A maximum of 12 intrusion phases has been identified (Akçay and Gündüz 2004). These intrusions are emplaced into the metamorphic basement, and intruded by Eocene andesitic and dacitic dikes. The porphyry mineralization appears to be confined the contacts between late Cretaceous volcanic-volcaniclastic rocks and Late Cretaceous intrusions. They have the characteristics of magnetite series granitoids with commonly medium to high-K calc-alkaline in nature. They show poikilitic, anti-rapakivi and myrmekitic textures (Table 8.4). Cu/S ratios of some granitoids are as high as those of the granitoids in the Chilean Cu-Au province (Terashima et al. 1988). The field and geochemical characteristics are favor of collision and arc-subduction environment for the generation of the host Late Cretaceous magmatic rocks (Terashima et al. 1988; Yalçınalp 1995; Soylu 1999; Soylu et al. 2003). For example, the high field strength (HFS) large ion lithophile element characteristics such as depletion in Nb, Y and enrichment in K, Rb, Ba and Th along with Rb/Sr and Nb/Y ratios of the plutonic rocks resemble to that of I-type volcanic-arc granitoids (Aslan 2005; Yılmaz-Şahin 2005; Boztuğ et al. 2006). The subduction is due to the closure of the İAE ocean in response to collision between Sakaryaterrane and TAB during Late Cretaceous to Early Paleocene (Robinson

et al. 1995; Okay et al. 1997) or *ca.* 110–105 (Okay et al. 2006) to 88–71 Ma (Table 8.1).

The alterations in host intrusives are mainly phyllic, propylitic and argillic with rare potassic alteration being present. The potassic alteration is locally exposed in Ardala, Güzelyayla and Güvemli prospects, but commonly is overprinted by epidote-chlorite-bearing alteration assemblages. The potassic alteration consists of dark grey quartz veins with rims of magnetite. Hydrothermal biotite occurs as fine-grained aggregates replacing the primary magmatic biotite (Soylu et al. 2003). The propylitic alteration is more intense along the contacts with volcanic rocks. Telescoping epithermal systems associated with the late Cretaceous Cu-Mo prospects are rare. Locally, epithermal-like quartz-barite and vuggy quartz veins overprinted quartz-magnetite stockwork veins at the Güvemli prospect, suggesting the potential for telescoped hydrothermal systems. The porphyry prospects at Hasandağ, and Sisortaco exist with advanced argillic lithocaps with epithermal Au mineralization Konak, Hasandağı, Esendal and Güvemli are occurrences have been discovered by regional soil-rock geochemical surveys, later tested by a few drill holes. Cu-Mo porphyries are characterized by low grade Cu-Mo, and have poorly developed secondary copper enrichment zone.

No reliable grade and resource data is available for these occurrences. The Güzelyayla is regarded as potential ore deposit tested by several drill holes with the resource of 186.2 Mt @0.3% Cu (Table 8.4, Singer et al. 2008). Ardala is at the development stage with the resource of 1.09 Moz Au @ 2.03 g/t Au and 0.3% Cu. Konak Cu-Mo prospect has the reported resources of 5.18 Mt @ 0.23% Cu (Table 8.4). İspir-Ulutaş porphyry has the reported resource of 200 Mt @ 0.3% Cu, 0.02% Mo. These deposits contain chalcopyrite and molybdenite accompanied by pyrite as the hypogene sulfide assemblage. No or little supergene-oxidized mineral is reported. The available sulfide minerals occur as dissemination and quartz-pyrite veins in argillitized rocks.

No geochronological data for the porphyry copper deposits is publicly available for this belt. Some companies have Re-Os ages for some of the porphyry Mo prospects. As these are classified data and not released yet, no geochronological data for the porphyry Cu systems are available. Thus, the timing of hydrothermal alteration in the porphyry Cu-Mo systems associated with Late Cretaceous rocks can only be assumed to be of Late Cretaceous (?) age.

8.5.3.2 Early-Late Eocene Porphyry Cu-Mo Deposits/Prospects in the Eastern Pontides

The Early-Late Eocene porphyry Cu-Mo-(Au) deposits/prospects are located at the NE part of the eastern Pontides mainly following main axial trend of Early-Late Eocene stocks, plugs and subvolcanic domes (Figs. 8.5 and 8.7). They are scattered in an elongated-ellipsoidal are between Gümüşhane at the west, Rize at the north, Artvin at the east and Erzurum-Bayburt at the south. In this belt 26 small-sized deposits, prospects, and numerous mineralized stocks are found. A spectrum of

Cu-Mo-Au and skarn and epithermal (intermediate sulfidation, high sulfidation and low sulfidation types) mineralization is present. Sivritaş, İspir-Ulutaş, Gümüşhane (Ardala), Yüksekoba, Balcılı, Yolgeçen, Dikmen and Berta (Table 8.4) are the significant porphyry Cu-Mo-Au prospects explored by the private and state companies.

The porphyry Cu-Mo mineralization in these prospects is spatially clustered along the southern margin of the intrusive rocks that follow a structural NE trend, and are hosted by stock, plug, breccia and dike complexes. Porphyry Cu-Mo bearing intrusives are typically calc-alkaline in composition with magnetite-series diorite porphyry, quartz diorite, granodiorite, quartz monzonite, quartz microdiorite as the dominant rock types. Those stocks are predominantly centered to multiphase porphyritic intrusions that have steeply dipping, dike-like geometries. Quartz monzonitic intrusions contain pebble dikes and breccia complexes localized commonly along the NE trending shear planes. The contacts of the intrusions with the volcanic rocks are sharp, epidotized and include volcanic xenoliths. The intrusions show variations in both color and mineralogy with fine to medium granular, monzonitic, poikilitic, rapakivi, anti-rapakivi and graphic textures (Arslan and Aslan 2006). The major mineral assemblage in the host intrusives includes quartz, orthoclase, plagioclase, hornblende, biotite and augite. The accessory phases consist of apatite, allanite, titanite, zircon and opaque minerals. The host intrusive and volcanic rocks have calc-alkaline and high-K calc-alkaline characteristics, and are peraluminous. They are characterized by low Ni, Co, Y, Yb and HFSE, and high Sr, Ba, and La abundance (Arslan and Aslan 2006; Boztuğ and Harlavan 2008; Eyüboğlu et al. 2010, 2011a; Karslı et al. 2010; Topuz et al. 2011). These rocks exhibit enrichments in large ion lithophile elements including the light rare earth elements, depletions in Nb, Ta and Ti and have high La/Yb and Sr/Y ratios (Karslı et al. 2010; Arslan and Aslan 2006; Boztuğ and Harlavan 2008). The previous works on the intrusive and volcanic rocks in the Early-Late Eocene porphyry Cu-Mo belts are favor an adakite-like signature (Arslan and Aslan 2006; Boztuğ and Harlavan 2008; Eyüboğlu et al. 2010, 2011a, b; Karslı et al. 2010; Topuz et al. 2011).

These deposits/prospects consist commonly of pyrite, chalcopyrite and molybdenite, magnetite, galena, sphalerite, secondary chalcocite, malachite, FeOx, azurite, cuprite and rare fluorite with barite, and these occur as veins, dissemination and stockworks (Table 8.4). The veins are generally steeply dipping, and trend in NW-SE direction. The sulfide mineralization in the drill holes from the prospects occurs as stockworks, fracture fillings and disseminations within the host rocks. The sulfides mostly occur as fracture fillings, and may locally exceed 20%. The Cu and Mo grade ranges between 5.07% (in Berta) and 0.1%, and Mo grade ranges between 0.02% and 0.012%, respectively. The gold is not always associated, and ranges between 8 and 0.3 g/t (Table 8.4). The highest Cu and Au grade are associated with early, magnetite-bearing high-temperature quartz veins.

Hydrothermal alteration in these deposits/projects consists of hypogene phyllic, peripheral propylitic and supergene argillic assemblages in surface outcrops. These are developed along the structural lineaments within the host stocks as well as in the wall rocks such as dacitic lava flows, pyroclastic rocks of Tertiary in age. Potassic

alteration is rarely observed, but is recorded in the exploration drill holes, and contains secondary biotite, quartz, K-feldspar and magnetite (Taylor 1981; Yalçınalp 1995). Secondary biotite is locally observed as vein swarms, rims and pseudomorph after hornblende, and flooding in the groundmass. The main sulfide mineralization dominated by chalcopyrite and molybdenite is hosted by potassic alteration. The percentage of molybdenite tend to increase in the deeper parts of the potassic zone (Kuşcu et al. 2018). The molybdenite occurs mostly as wormy quartz veins. The phyllic and propylitic alteration have limited exposures due to soil cover and dense vegetation or steep slopes and very active drainage systems aided by surface oxidation. The phyllic alteration is traced only along the main N-S flowing streams. They occur as patchy outcrops proximal to faults and fault-intersections over the dioritic, monzodioritic to granodioritic stocks with intense quartz and pyrite veins and sheeted stockwork, locally with molybdenite. The propylitic alterations in these prospects are largely irregular in shape, and are developed around the margins of granodioritic-dioritic stocks. The argillic alterations are largely composed of patchy kaolinite with abundant pyrite. In some prospects, the argillic alterations are confined to structural corridors (e.g. Konak and Berta). Several prospects (Sisorta, Bakırçay, Hasandağı and Güzelyayla) are overlain and flanked by quartz-alunite-rich lithocaps at higher elevations. The Sisorta and Hasandağı lithocaps host quartz-alunite epithermal gold mineralization. Preservation of lithocaps and the dominance of phyllic alteration assemblages suggest that the depth of erosion in the Early-Late Eocene porphyry Cu-Mo deposits/prospects is generally moderate or relatively shallow.

The quartz-Mo-Cu veins are exposed at the surface at Bakırçay, Balcılı, Sivritaş, Ulutaş and Ardala porphyry prospects. The Ardala, Balcılı, Bakırçay and Ulutaş prospects have outcrops of Cu-Mo veins within phyllic altered dacite porphyry and granodiorite to monzonite at Bakırçay, Balcılı, Ardala and granodiorite-quartz diorite at Ulutaş. At Ulutaş, a mineralized Cu-, Pb-Zn skarn is present where the porphyry intrusions cut the metamorphic basement rocks. The skarn is at the development stage, and going to be in operation by Mid 2017.

The timing of the host magmatism was obtained from publicly available Ar-Ar and U-Pb geochronology of the stocks and domes associated with the porphyry Cu-Mo mineralization. Although there are abundant geochronological data for the host magmatic rocks in the entire belt, fewer or no geochronological data from hydrothermal minerals are available. Most of the stocks associated with porphyry systems have been dated as Eocene in age. The age of host intrusives at the NE edge of the Early-Late Eocene porphyry Cu-Mo belt ranges from *ca.* 53 to 50, mostly around 46–45 Ma (Table 8.1). The age of intrusives are mostly around 43–41 Ma at the central and SW part of the belt. This suggests that the magmatism gets relatively younger from NE to SW in this belt. Except for the Bakırçay, no geochronological work is available to constrain the timing of hydrothermal event. The hydrothermal biotite separates from the potassic and propylitic alterations in the Bakırçay yielded a K-Ar age of 38.0 ± 1.28 Ma and 37.9 ± 1.21 Ma (Taylor 1981; Table 8.1). This age coincides coincides within the limits of the analytical uncertainties with the age (within error limits) of the unaltered host intrusive rock 42.3 ± 1.2.61 Ma in age. The age of mineralization in other deposits and prospects are missing. Therefore, Kuşcu

et al. (2018) assumed that the age of hydrothermal activity in other prospects are of Eocene age based on their association with dated stocks.

8.5.4 *Porphyry Copper Deposits/Prospects in Western Anatolian Province*

The western Anatolian province has long been known as metallogenic province for Au porphyry mineralization since the discovery of Kışladağ Au porphyry deposit. Although a number of prospects and several new occurrences are known to occur in the WAP, only three are operating (as of 2016); Kışladağ Au, Tepeoba Mo and Muratdere Cu-Mo deposits. Ağıdağ is at the development stage and will be brought to production soon. Kışladağ contains 6.05 million ounces of gold based on proven and probable reserves of 431 Mt @ 0.69 g/t Au (*www.eldoradogold.com/assets/resources-and-reserves*). The important prospects and at the advanced development stages are Halilağa (Etili, Çanakkale), Ağıdağı (Etili, Çanakkale), Karaayı (Kuşçayır, Çanakkale) (Table 8.5) contains several porphyry deposits/prospects and newly discovered occurrences (Table 8.5). The other occurrences include Gürcüler, Alaçam, Dikmen, Sarıçayıryayla, Karapınar, Gelemiç, Topuk (Bursa), Tüfekçikonak (Kütahya),Tepeköy (Gökçeada), (Table 8.5), Doğanbey, İnlice (Konya), Öksüt (Ortacam, Kayseri), and Kocatarla (Çanakkale), Eğmir (Edremit). These prospects have been explored largely by surface soil and geophysical surveys, and drilled by private companies, but no publically reported information is available.

These porphyries are classified as porphyry Cu-Mo, porphyry Cu-Au, porphyry Au and porphyry Mo based on their predominant metal content. Porphyry Cu-Mo, porphyry Cu-Au, porphyry Au and porphyry Mo present in the WAP form distinct belts that are, from oldest to youngest and northernmost to southernmost, Tavşanlı, Biga, and Afyon-Konya porphyry belts (Figs. 8.5 and 8.7). Porphyry Cu-Mo systems are the most common within the Tavşanlı porphyry belt where the oldest (pulse 1) plutonic rocks are exposed, while porphyry Cu-Au and porphyry Mo systems characterize the Biga porphyry belt where the second and third pulses are recorded. Porphyry Au systems hosted by alkaline rocks of pulse 4, are restricted to Afyon-Konya porphyry belt. Several porphyry (e.g. Halilağa and Ağıdağı) related to late Oligocene (28–25 Ma) volcano-plutonic rocks are associated with shallow-level intermediate porphyry systems telescoped by high-sulfidation volcanic-hosted epithermal deposits of economic importance. Both alkalic and calc-alkalic varieties of porphyries occur within the WAP. The alkalic type (Kışladağ and AS; 14–9 Ma) is more like Au to Cu-Au porphyry type, and refer to a younger phase of the mineralization and economically more significant compared to calc-alkalic (Ağıdağ, Halilağa, İnlice) counterparts associated with latite to trachytic rocks. The calc-alkalic types are volcanic and plutonic hosted. The compositions of plutonic rocks are quartz diorite, granodiorite, and granite and quartz monzonite in composition. The volcanic rock associations are mainly andesite-andesite porphyry and dacite in

compositions for the calc-alkalic; whereas latite porphyry to trachyte in compositions for the alkali porphyry Cu deposits/prospects. The plutonic rocks are commonly exposed within the Biga and Tavşanlı porphyry Cu-Mo belt.

8.5.4.1 Geochronology of Porphyry Deposits/Prospects in the WAP

In the Biga porphyry belt, the available geochronological data (Table 8.2) indicate that the known and outcropping porphyry Cu-Au deposits formed during the late Eocene and late Oligocene. Kuşcu et al. (2018) presented new $^{40}Ar/^{39}Ar$ geochronology (Table 8.2) together with the published data for a better understanding of the timing of hydrothermal activity, and confirmed that the hydrothermal activity in the western Anatolian province lasted between the Paleocene and Miocene (*ca.* ~53 to ~9 Ma). The ages they reported on hydrothermal minerals generally agree within analytical uncertainty with the $^{40}Ar/^{39}Ar$ ages of host igneous rocks (see previous sections, Table 8.2).

Kuşcu et al. (2018) showed that porphyry Cu systems in the Biga Peninsula are Eocene and Oligocene in age (Table 8.2) with the Dikmen system (51.9 ± 2.6–46.6 ± 2.3 Ma; Yiğit 2012 and references therein), Alanköy (28.3 ± 2.6 Ma; Yiğit 2009) and Tepeoba systems (22.8 ± 1.4–25.11 ± 0.14 Ma; Murakami et al. 2005; Kuşcu 2009) being the only dated systems prior to their study. Serçeler, Karaayı-Kuşçayır and Gökçeada are examples of Eocene deposits with ages between 42 and 39 Ma; $^{40}Ar/^{39}Ar$ ages on sericite of 40.11 ± 0.28 Ma and 39.99 ± 0.27 Ma from Kuşçayır (Kuşcu et al. 2018). Halilağa, Ağıdağı, Eğmir and Tepeoba are examples of late Oligocene porphyry systems formed between 28 and 22 Ma. Reported $^{40}Ar/^{39}Ar$ ages on sericite are 27.48 ± 0.34 Ma and 26.36 ± 0.16 Ma from Ağıdağı quartz-alunite epithermal systems and a nearly identical age on sericite of 26.27 ± 0.19 Ma from the nearby Halilağa porphyry Cu-Au deposits (Kuşcu et al. 2018). A slightly younger $^{40}Ar/^{39}Ar$ age of 22.77 ± 0.16 Ma on sericite is reported from Eğmir (Havran) system (Kuşcu et al. 2018). Recently, Kuşcu et al. (2018) suggested that their geochronological data is consistent with four major hydrothermal episodes, spatially and temporally associated with four magmatic episodes in the western Anatolia. They suggested that porphyry Cu-Au deposits have been formed at two periods; (1) 42–39 Ma (Serçeler, Karaayı-Kuşcayır and Gökçeada) and (2) 26–24 (Ağıdağı, Halilağa, Eğmir and Tepeoba). They also concluded that the second period refers to a period during which the most economic porphyry gold deposits have been formed. According to them, the host magmatic rocks; plutonic rocks range from *ca.* 43 to 20 Ma, but with a tight cluster between 26 and 20 Ma. The volcanic rocks appear to be associated with plutonic rocks both in space and time, and Ar-Ar ages of the volcanic rocks range from 45 to 36 Ma, 33–25 Ma and 21–17 Ma (Table 8.2; Kuşcu et al. 2018). Reported ages of alteration in the Tavşanlı porphyry-Cu-Mo belt obtained on sericite and K-feldspar from the Tüfekçikonak, Topuk and Gürgenyayla porphyry prospects are between 52.6 ± 1.1, 46.74 ± 0.37 and 47.49 ± 0.27 Ma, respectively (Kuşcu et al. 2018; Table 8.2). The hydrothermal activity in the Afyon-Konya porphyry Au belt is younger with two poor quality sericite $^{40}Ar/^{39}Ar$ ages of 14.81 ± 0.16 Ma and 14.18 ± 0.44 Ma for Kışladağ (Kuşcu et al. 2018). Sericite from the Afyon-Sandıklı (AS) system

yielded a younger age of 12.50 ± 0.10 Ma, whereas the İnlice system with a biotite $^{40}Ar/^{39}Ar$ age of 8.98 ± 0.11 Ma appears to be one of the younger hydrothermal systems in the belt (Kuşcu et al. 2018). The age of host volcanic rocks in these porphyries overlap with the ages of volcanic rocks within the Afyon-Konya porphyry belt formed at pulse 4. However, the age of plutonic rocks hosting or associated with the porphyry deposits/prospects within the Biga porphyry belt overlaps with the age of plutonic rocks formed at pulses 1 and 3 in the WAP (Kuşcu et al. 2018).

In the WAP, abundant epithermal deposits presumably are related to deeper unexposed porphyry systems. These appear to have formed between 42 and 29 Ma (Keditaşı, Koru, Pirentepe, Kirazlı, TV-tower and Kartaldağ; Smith et al. 2014), 29 and 26 Ma (Küçükdere, Balya and Culfaçukur), and 17 and 14 Ma (Arapdağ, Kubaşlar-Yataktaş, Doğancılar and Kısacık) (Kuşcu et al. 2018). Intrusion related Cu-Fe skarn deposits formed at three periods; (1) 26–23 Ma (Evciler Cu skarn, Bakırlık Cu-Fe skarn, Şamlı Cu-Fe skarn), (2) 23–20 Ma (Ilıca Cu-Fe skarn and Ayazmant Fe-Cu skarn), and (3) 20–18 Ma (Ezine-Üsküfcü Pb-Cu skarn and Baklan Pb-Zn skarn) (Kuşcu 2009).

8.5.4.2 Biga Porphyry Cu-Au Belt

The Biga porphyry Cu-Au belt is located to the south of Sea of Marmara (NW Turkey). It is wedge-shaped region bounded by Bornova flysch zone to the south, Strandja massif to the north and Tavşanlı zone between Çanakkale, Lapseki (Çanakkale), Gönen (Balıkesir), Balıkesir, Bergama and Dikili (İzmir) (Figs. 8.7 and 8.10). This belt contains metamorphic rocks of Paleozoic clastic rocks, Çamlıca metamorphics, Karakaya complex and Kazdağ massif, intruded by various magmatic rocks formed in three different phases at *ca.* 42–35 Ma, 29–18 Ma (Figs. 8.7 and 8.10). The porphyry Cu-Au deposits/prospects in the Biga belt are hosted by plutonic and volcanic rocks accompanied by thick tuffaceous layers and basaltic andesite flows. These host magmatics are formed at the second and third pulses of WAP magmatism. The field relations and geochemical data suggest that magmatic activity began with an earlier phase of volcanic activity, and continued with a later phase of plutonic activity followed by a later phase of volcanism. Apart from large plutonic bodies, there are several small-scale granitoid rocks in the belt. They were emplaced mostly into the basement metamorphic rocks and associated volcanics and generated well-developed high temperature metamorphic aureoles (e.g. Halilağa, Evciler, Üsküfçü and Aladağ). The volcanic-pyroclastic rocks in Gökçeada, Kuşçayır, Halilağa, Ağıdağı, Kocatarla and Eğmir porphyry deposits/prospects are common hosts, and are calc-alkaline in nature. These volcanic rocks are largely ash-lapilli tuff, enveloped and intruded by more coherent feldspar porphyritic unit. They are variably altered, brecciated, mineralized and display a range of intensities of brittle deformation. The plutonic hosts are exposed in Halilağa (Bakırlıktepe), Ağıdağ, Tepeoba partly to Gökçeada and Dikmenköy. The plutonic-hosted porphyries are also associated with Cu-skarns (e.g. Halilağa, Ağıdağ, Aladağ, Üsküfcü and Bakırlıktepe). The plutonic rocks range in composition from quartz diorite to quartz

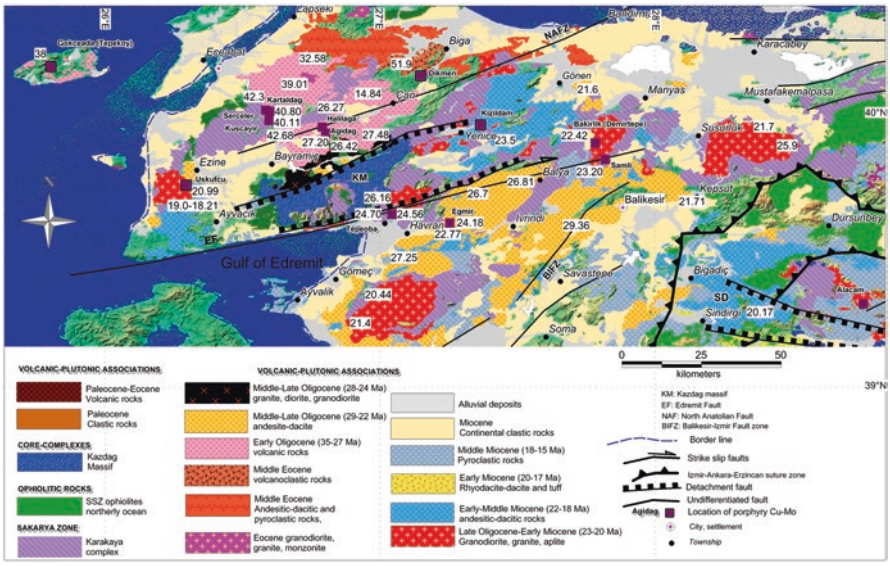

Fig. 8.10 Simplified geological map of Biga porphyry Cu-Au belt showing the major rock types, porphyry deposits and prospects, Ar-Ar ages for host magmatic rocks. (From Kuşcu et al. 2018)

monzonite-granite. The volcanic rocks range in composition from andesite, andesite porphyry to dacite porphyry, andesite porphyry being the most common type. The pyroclastic rocks are cut by these volcanics, and they are overlain by basaltic andesite, rhyolite, latite flows and associated pyroclastic rocks intercalated with coal-bearing lacustrine sedimentary rocks. The Gökçeada and Kuşçayır porphyry Cu-Au deposits are hosted by and/or associated with volcanic flow-dome complexes andesite-to-andesite porphyry in composition (*ca.* 42–35 Ma). Ağıdağı, Halilağa, Kocatarla, Tepeoba, Dikmenköy and Bakırlıktepe porphyry deposits/prospects are associated with andesitic to dacitic rocks or plutonic rocks granodiorite to granite in composition 28–23 Ma in age.

In this belt, nine small to medium sized deposits and Cu deposits and prospects are known; Starting from the western margin, the porphyries included in the Biga porphyry belt are Ağıdağ (Etili, Çanakkale), Halilağa (Etili, Çanakkale), Kuşçayır (Karaayı-Kuşçayır, Çanakkale), Tepeoba (Havran, Balıkesir), Dikmenköy (Çanakkale), Tepeköy (Gökçeada, Çanakkale) (Fig. 8.11a–f), Kocatarla (Balıkesir), Bakırlıktepe (Şamlı, Balıkesir), and Eğmir (Havran, Balıkesir). This belt also hosts a wide spectrum of intrusion-related deposit types including skarn, high, low and intermediate sulfidation, iron oxide-Cu-Au (IOCG) and distal vein Pb-Zn. Of these, low and high sulfidation, Skarn Cu, distal vein Pb-Zn types are being operated. The ore minerals in these porphyry deposits are dominantly chalcopyrite, gold, enargite, magnetite, chalcocite, pyrite, and molybdenite. The average grade of Cu and Au ranges from 0.1% to 0.33% and 0.31–4.6 g/t, respectively (Table 8.5). The highest Cu grade is in the Halilağa and Tepeoba. The highest Au grade is in the Dikmenköy

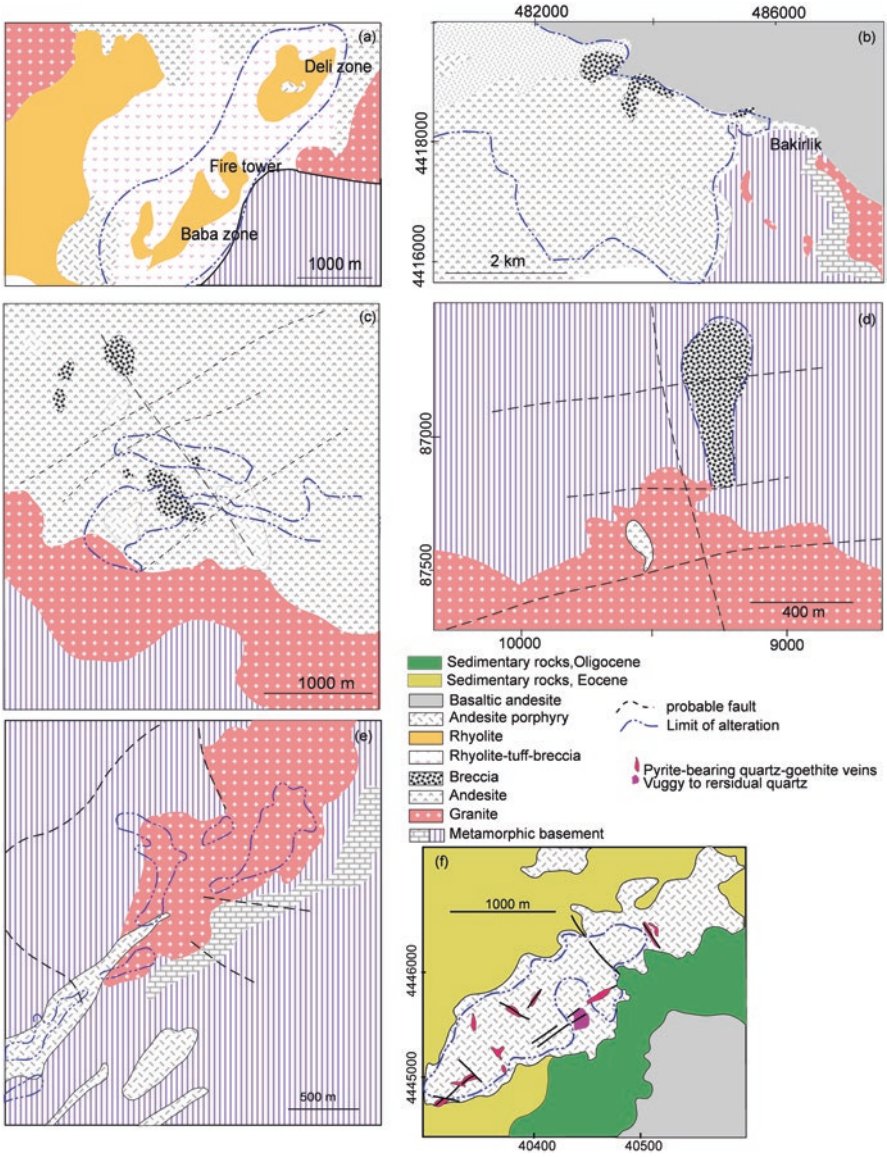

Fig. 8.11 Simplified geological maps of some porphyry deposits/prospects showing main rock types, limits of argillic-phyllic alterations at (**a**) Ağıdağ, (**b**) Halilağa (Simplified from Pilot Gold web sites), (**c**) Kuşçayır-Karaayı (Simplified from Chesser Resources web site, (**d**) Tepeoba (From Murakami et al. 2005), (**e**) Dikmenköy, (**f**) Gökçeada (From Sarı et al. 2014)

and Ağıdağ deposits. Except for Halilağa and Ağıdağ the resource and reserve data remain to be examined.

Halilağa porphyry Cu-Au systems has an indicated sulfide resource in the porphyry system of 166.2 Mt @ 0.30% Cu, 0.31 g/t Au, and 0.006% Mo (http://www.pilotgold.com/Halilağa-resource-estimate), whereas the nearby and potentially related Ağıdağı epithermal system has measured and indicated resources of 93.9 Mt @0.53 g/t Au and 3.56 g/t Ag (*http://www.alamosgold.com/mines-and-projects/development-projects/agi-dagi- turkey/default.aspx*). A resource of 17.5 Mt @ 0.96 Cu equiv. Mo% has been reported for Tepeoba (Table 8.5) (http://www.ozdogu.net/main.asp?sayfa=8).

The porphyry deposits/prospects in the Biga porphyry belt are commonly bounded by major ENE-WSW, E-W trending normal faults and transtensional NE-SW structures exposed in the region between Yenice, Gönen and Etili (Çanakkale). These structures are also regarded as splays of NAFZ (Grieve 2009). The ENE-WSW and E-W trending faults commonly occur along the northern margin of the gulf of Edremit and southern margin of Bergama graben (Fig. 8.10). The transtensional regime with local restraining and releasing bends and oblique extensional relay ramps have been interpreted to be key elements, which increase structural permeability controlling the emplacement of porphyry, meso-, and epithermal mineral deposits in the Biga porphyry belt (Grieve 2009; Sanchez 2012). These structures appear to control the sedimentation and volcanic activity during Middle Eocene to Oligocene to Early Miocene period. These faults appear to be loci for the emplacement of magmatic rocks into the metamorphic basement and sedimentary basins during Middle-Late Eocene to Oligocene times. Local transpression resulted in restraining bends and consequent uplift- exhumation of older stratigraphy and some prospects (Ağıdağı and TV-Tower). The post-mineral slip on the faults appears to be displaced and to some extent tilted some porphyry deposits (e.g. Halilağa).

The porphyry Cu-Au deposits/prospects in this belt consist of propylitic, phyllic and potassic alterations overprinted by advanced argillic lithocaps. The advanced argillic lithocaps are considered as pyritic, silicified argillic alterations containing quartz-alunite veins (e.g. Halilağa, Ağıdağ, Kuşçayır and Eğmir), and that overprinted by late supergene clay alteration (kaolinite, goethite, hematite, quartz, halloysite). The lithocaps are largely hosted by felsic to intermediate tuffs and andesite-dacite flows, and occasionally by phreatic breccia bodies that are underlain by medium to high level granodiorite plugs and dacite domes (Kuşcu 2009). These lithocaps are reported to contain million ounces of gold resource and numerous other high grade intercepts (e.g. Eğmir, Kuşçayır-Karaayı, Gökçeada and Ağıdağı porphyry Cu-Au deposits; Kuşcu 2009). The gold mineralization in these lithocaps is characterized by disseminated or fracture-controlled pyrite, variable amounts of residual to vuggy quartz veins, hematite/pyrite matrix breccias and moderate to weak sacchoroidal to crystalline quartz stringer stockwork veins. Hydrothermal breccias (crackle, jigsaw, hydrothermal) and ferricrete formation is common feature of the silicified rocks (Kuşcu et al. 2012). Pyrite is by far the most abundant primary sulfide mineral associated with gold. Trace to minor amounts of enargite, covellite

and molybdenite are present locally (e.g. Ağıdağı). The potassic alteration zones are either exposed to the surface, as is the case in Halilağa or intercepted at depth by drilling (e.g. Kuşçayır and Ağıdağı). In the potassic alterations, most quartz veins are "B-type" and "A-type" veinlets locally up to 20% of the rock by volume. The potassic alteration at Kuşçayır-Karaayı prospect contains A-veins with locally M-veins at deeper holes. In some deposits, biotite flooding or biotite clots or aggregates within the host rock or breccia pipes characterize the potassic alteration. The Tepeoba porphyry Mo deposit is the only deposit with biotite flooding accompanied by molybdenite, chalcopyrite and pyrite within the hydrothermal breccia. The A and B vein types do not always co-exist in the same deposit. Halilağa, for example, contains mostly B-veins and very rare A veins whereas Ağıdağı contains both types. B-veins observed on the outcrops occur as oxidized veins with predominant shreddy biotite-hematite-goethite (jarosite)-quartz veins. The A-veins are typical in the Kuşçayır-Karaayı deposit, and are intercepted after an oxide zone developed over a phyllic alteration containing pyrite-quartz, quartz-chalcopyrite and "D-veins". The phyllic alteration is the most common alteration type in all these deposits. Halilağa and Ağıdağı are two examples with porphyry Cu-Au deposits containing partly exposed phyllic outcrops at the surface. Stockwork veins, oxidized to form quartz-hematite or quartz-goethite veins characterize the phyllic zones in these deposits. In some deposits such as Ağıdağı and Kuşçayır, as the oxidation and weathering so intense that the phyllic alteration is almost obscured or erased. In the zone of oxidation, disseminated pyrite or iron-oxide minerals (dependent on the rock's position relative to the redox horizon) are also ubiquitous. Argillic and advanced-argillic alteration is largely preserved, and forms different mappable zones that range from quartz-alunite altered andesites (Halilağa, and Ağıdağı) to near complete silica replacement of tuffs and volcanics (Ağıdağı, Kuşçayır, Kocatarla and Alaçam) or residual to vuggy quartz (Kuşçayır, Halilağa), and is characterized by fine-grained, soft, grey illite/montmorillonite/dickite/kaolinite, and varying amounts of pyrophyllite, halloysite and quartz. Halloysite is resulted from supergene events, or occur occasionally as hypogene mineral in advanced argillic alterations. The quartz-alunite bearing zones are interpreted to be distal outflow of acidic fluids from the porphyry source.

8.5.4.3 The Tavşanlı Porphyry Cu-Mo Belt

The Tavşanlı porphyry belt forms a NW-SE trending belt of Cu-Mo porphyry deposits/prospects at the northeastern and eastern margin of the WAP (Figs. 8.12 and 8.13). This belt is bounded on the north by a major structure, NW-SE trending Eskişehir Fault. The ophiolitic rocks bound the belt on the north along the major İAESZ. Younger sedimentary and volcanic rocks cover the metamorphic and plutonic rocks. Subsequent core-complex and exhumation resulted in the removal of much of the volcanic edifices, and exposed the plutonic rocks and associated porphyries to the surface. In this belt, nine porphyry prospects are found, although only one, Muratdere Cu-Mo porphyry, is in the operation yet (Table 8.5). They are;

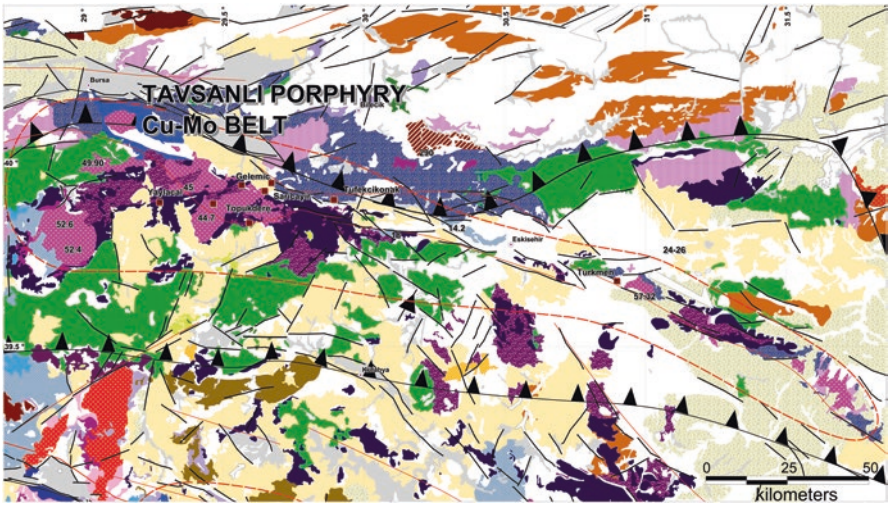

Fig. 8.12 Simplified geological map showing the main rock units, major structures, porphyry prospects, associated intrusive rocks and Ar-Ar ages (From Kuşcu et al. 2018; filled squares show the name and location of the porphyry Cu deposit/prospect in the Tavşanlı belt; explanations and legend as in Fig. 8.5)

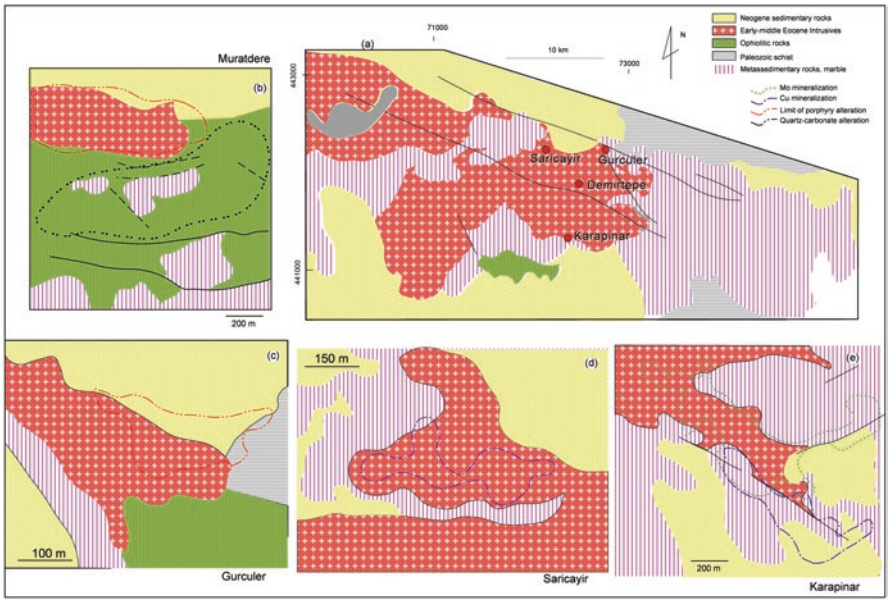

Fig. 8.13 Simplified geological maps of (**a**) Tavşanlı porphyry Cu-Mo belt, (**b**) Muratdere, (**c**) Gürcüler, (**d**) Sarıçayır and (**e**) Karapınar porphyry prospects. (Modified from Alacer Gold company website, and Yıldırım et al. 2001)

namely Muratdere, Gürcüler, Sarıçayır, Karapınar, Gelemiç, Demirtepe, Tüfekçikonak, and Türkmen (Figs. 8.12 and 8.13a–e). The porphyry mineralization is predominantly Cu with subordinate Mo type with distinct calc-silicate alteration along the mutual contacts between intrusives and metamorphic rocks. Demirtepe is one of the best-exposed wollastonite-Cu skarn in the belt. Demirtepe was originally explored by MTA as a wollastonite skarn deposit, but it contains disseminated chalcopyrite and occasional semi-massive bornite mineralization. The technical reports by private companies recognize the Muratdere as Cu-Au porphyry system with strong Mo and Re anomalies.

The porphyries within the Tavşanlı belt are hosted by or associated with plutonic rocks 52.6–44.9 Ma in age (Table 8.2). The intrusions are mainly granodiorite-diorite in composition. The intrusions are commonly elongated parallel to the major structures, and are likely to be exposed to the surface by these faults. The field, compositional, element abundance and textural characteristics of the porphyry hosted or associated plutonic rocks are similar to those of Early-Middle Eocene plutonic rocks elsewhere in the WAP. The plutonic rocks associated with or hosting the porphyry mineralization include (2) Tepeldağ (44.9 Ma), Topuk (50–48 Ma) plutons and Domaniç granitoid (52 Ma) (Table 8.2). The granodioritic intrusives are exposed at surface as arcuate window emplaced into metacarbonates with schists. They have equigranular and porphyritic texture containing K-feldspar and hornblende phenocrysts up to 1 cm in diameter. The porphyritic types are commonly diorite porphyry, granodiorite porphyry and granite porphyry in composition. They are cut across by aplitic granite and aplite dikes.

Hydrothermal alterations reported in these prospects are argillic at the surface with potassic alteration assemblages reported at from the drill holes or in outcrops at depth along valleys. Apart from the Tüfekçikonak and Gürcüler, potassic alteration is not exposed to the surface. The potassic alteration is composed of hydrothermal biotite either as quartz-biotite vein or as biotite-flooding in the groundmass or pervasive replacement of host rocks. The hydrothermal biotite forms irregular clots within the groundmass, and these locally contain disseminated hydrothermal albite crystals. Sheeted quartz-hematite, quartz-goethite veins, stockwork veins and disseminated mineralization types are developed within the intrusives. The porphyry prospects/deposits at the Tavşanlı belt are proactively being explored by surface geochemical surveys, and some are drill-tested (Gelemiç and Sarıçayır, Karapınar). No or limited epithermal is associated with the porphyries. Disseminated sulfide minerals are more common in Muratdere and Gürcüler, whereas stockwork veins dominate the Karapınar porphyry. Hypogene sulfide minerals include pyrite, chalcopyrite and molybdenite. As no advanced argillic alteration assemblages or epithermal style alteration have been reported, the porphyry Cu systems in the Tavşanlı porphyry belt presumably have relatively deeper levels of erosion.

Most of the resources are not compliant with international reporting codes or not clearly outlined to date. Only Muratdere has resource database, and other prospects/occurrences remain to be examined and explored based on geochemical and mineral occurrence information. The available resource data was obtained from the press releases by companies. The Muratdere porphyry Cu-Au system contains anomalous

Mo and Re (51 Mt @ 0.36% Cu, 0.12 g/t Au, 2.40 g/t Ag, 0.0125% Mo and 0.34 ppm Re (http://www.stratexinternational.com/project/muratdere). The Gelemiç and Sarıçayır, and Karapınar have been explored, but no resources reported. Drill hole intersections with reported Cu grades range between 0.17% and 2.02% (Table 8.5), with the highest grades reported from Demirtepe and lowest grades reported from Topukdere. Molybdenum grades in drill hole intersections range between 0.02% and 4%. Although, gold is not economically viable in the porphyry deposits, Au grades ranges between 0.12 and 0.96 ppm, with the highest intersection being reported from Demirtepe.

8.5.4.4 Afyon-Konya Porphyry Au Belt

The Afyon-Konya porphyry Au belt is at the western and southwestern margin of the WAP, and forms a belt combining the Afyon zone and central Anatolian volcanic province including Konya volcanic complex (Figs. 8.5 and 8.14). It is a NW-SE trending belt between Taurides and Tavşanlı zone. This belt consists mainly of Miocene to Pliocene (*ca.* 14–9 Ma) volcanic and pyroclastic rocks deposited in lacustrine basins intruded by alkaline intrusive rocks (Figs. 8.5 and 8.14). The Miocene rocks unconformably overlie the Paleozoic carbonate platform and clastic sedimentary rocks of the Tauride-Anatolide Block. The Kışladağ porphyry Au deposit is the only operating mine in this belt. Other prospects include Pınarbaşı, Afyon-Sandıklı (AS), Doğanbey and İnlice prospects. Although both Au and Cu-Au subtypes occur, this belt is known to be a porphyry Au-only type belt.

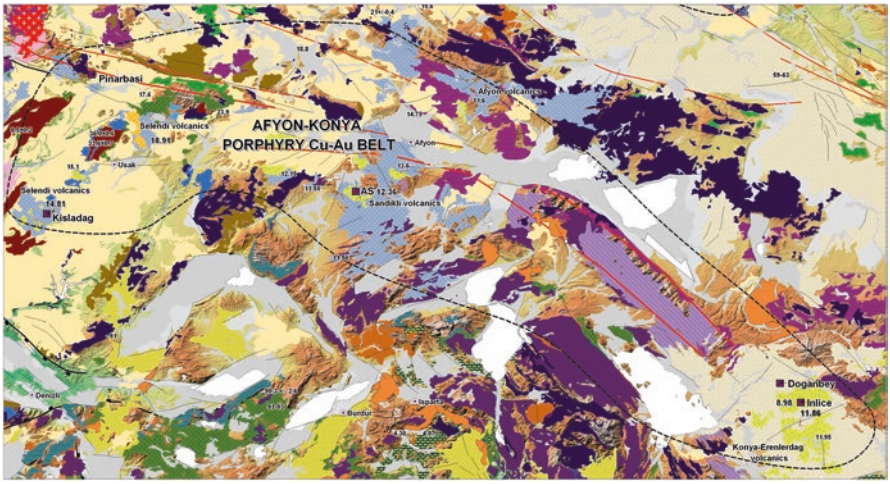

Fig. 8.14 Simplified geological map showing the main rock types, major structures, porphyry deposits/prospects, magmatic rocks and their Ar-Ar ages within the Afyon-Konya porphyry Au belt. (From Kuşcu et al. 2018, explanations as in Fig. 8.5)

Alkaline porphyritic latite-trachyte domes and andesites cutting pyroclastic sequences host the hydrothermal systems in the belt. These systems are now bounded by or at least exposed along NW-SE trending strike-slip faults (Akşehir fault) with normal component (Fig. 8.14). Apart from these faults, the porphyry deposits/prospects in this belt are also controlled by NE-SW trending low-angle normal faults oblique to NW-SE trending ones. The latter is relatively younger than the first one. The porphyry deposits in this belt all have well developed advanced argillic lithocaps and telescoping high sulfidation (HS) epithermal systems. Although, they all have telescoping HS systems, only those in the İnlice and Doğanbey are gold-bearing. Kışladağ and AS porphyry deposits have barren advanced argillic lithocaps with well-developed quartz-alunite alterations. The Kışladağ was discovered in mid 1990s and was brought into production in early 2000s. Doğanbey and İnlice are relatively recent discoveries at 2005 and are at the pre-development stage. Pınarbaşı is a new discovery after a regional geochemical and ground geophysical survey. The Kışladağ and AS are two important porphyry Cu-Au and porphyry Au deposits hosted by alkaline porphyritic latite-trachytes within volcanic complexes bounded by NE-SW trending faults. Sandıklı volcanics and Selendi volcanics are observed in graben-like depressions (Sandıklı graben and Selendi graben) within the lacustrine-fluvial sedimentary basins unconformably overlying augen gneiss and schist from the Menderes massif. The porphyry deposits/prospects in these rocks are associated with the nested-calderas, and are genetically related to re-surgent domes cutting through the pyroclastic sequences (e.g. Kışladağ and AS, and to some extent İnlice).

Kışladağ and AS exemplify two deposits with typical concentric alteration halos centered to a host intrusive rock. The potassic alteration in these porphyry deposits is not exposed to the surface, but is intercepted at depth in Kışladağ and AS (Fig. 8.15). In İnlice and Doğanbey, the halos are not reported to intercept potassic alteration assemblages, which suggests these prospects represent only minimal exhumation of a porphyry-related hydrothermal system. The phyllic alteration is widespread and consists of quartz-tourmaline-pyrite salvages throughout the groundmass of the volcanic and pyroclastic rocks or quartz-tourmaline-pyrite-molybdenite stockworks and quartz-tourmaline-breccia veins cutting through the groundmass and volcanic stratification. Gold, where present, is confined mainly to quartz-tourmaline-pyrite stockwork veins hosted by latite-trachyte porphyry and pyroclastic rocks. Advanced argillic alteration assemblages including alunite-barite associated with vuggy and residual quartz-dickite form lithocaps. Prominent quartz-alunite residual to vuggy quartz veins cut the host pyroclastic sequences at İnlice and Doğanbey epithermal gold deposits. Weak to moderate phyllic alteration assemblages underlie the mineralized advanced argillic assemblages. Gold at İnlice and Doğanbey occurs in steeply dipping residual to vuggy quartz, veins and quartz-alunite ledges. These veins are characterized by pseudomorphed feldspar, biotite and hornblende phenocrysts, and lithic clasts. A propylitic alteration assemblage dominated by epidote-chlorite overprinted the metamorphic country rocks on the periphery of the hydrothermal systems.

The porphyry deposits/prospects in this belt are hosted by alkaline plutonic rocks, lava-dome complexes and pyroclastic rocks (Konya-Erenlerdağ volcanics, Konya volcanic province, Selendi volcanics and Sandıklı volcanics) of Late Miocene

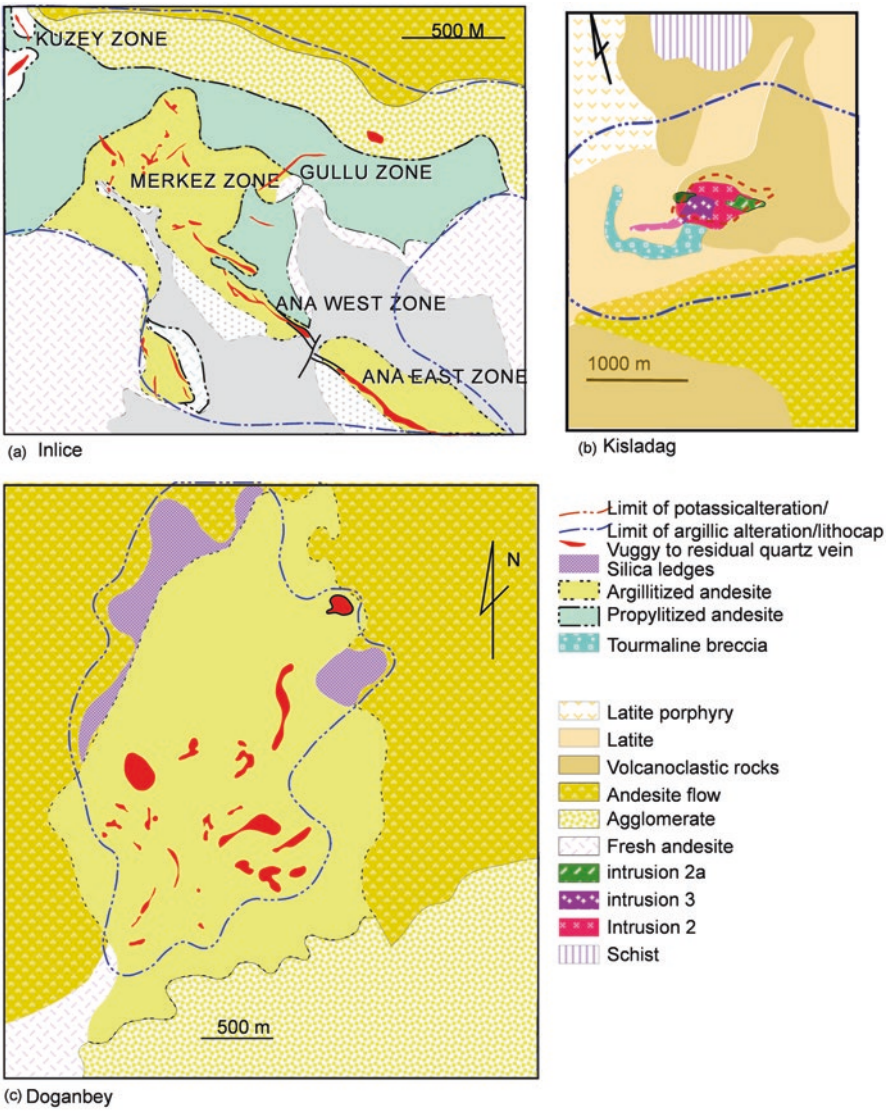

Fig. 8.15 Simplified geologic maps of (**a**) İnlice (Hall et al. 2007), (**b**) Kışladağ (Juras et al. 2010) and (**c**) Doğanbey porphyry Au, Cu-Au and epithermal Au prospects

to Pliocene (*ca.* 14–9 Ma). The rocks comprise monzonite, monzonite porphyry, trachyte, latite, dacite and andesite overlain by ignimbrites, lava domes, and tuffs and breccias associated with domes. The monzonitic rocks are exposed only at Pınarbaşı and AS, and occur as truncating the mineralized volcanic rocks. The monzonitic rocks in AS, for example display sub-vertical dike-like emplacements trending in N-S. The volcanic-pyroclastic sequences are interbedded with sedimentary rocks, predominantly of fluvial-lacustrine limestone, marl and shales. The volcanic

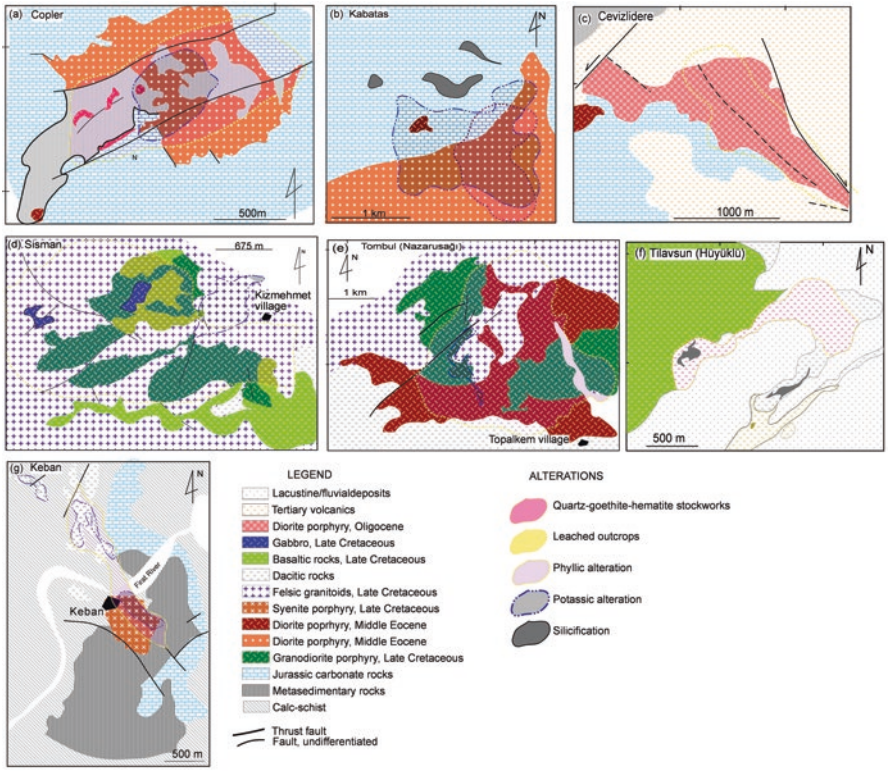

Fig. 8.16 Simplified geological maps of (**a**) Çöpler Au (Simplified from İmer et al. 2013), (**b**) Kabataş Au-Cu (Simplified from Alacer Gold, www.alacergold.com), (**c**) Cevizlidere (Kocuimbas and Page 2009); Keban Cu-Mo (Simplified from Kuşcu 2009); (**d**) Şişman Cu-Au porphyry, (**e**) Nazaruşağı Cu-Au porphyry (Simplified from Dumanlılar et al. 1999), (**f**) Tilavşun (Höyüklü) Cu-Au porphyry (Vergili et al. 2013), (**g**) Keban Cu-Mo porphyry (Çelebi 1997) deposits/prospects

rocks are classified as high-K calc-alkaline series rocks. These rocks represent the latest magmatic pulse (phase 4) in the WAP. The latite and trachytic to dacitic rocks are said to be typical host multi-phase intrusives in Kışladağ and AS emplaced at least two pulses.

8.5.5 Porphyry Deposits in the Southeastern Anatolian Orogenic Belt

The porphyry Au, Cu and Cu-Au deposits cluster as three spatially distinct groups (Figs. 8.6 and 8.16); (1) To the north, Çöpler porphyry Cu-Au deposit (Fig. 8.16a), Kabataş porphyry Cu-Au prospect (Fig. 8.16b), and Kızılviran porphyry Cu-Au

prospect, Karakartal porphyry Cu-Au at İliç (Tunceli) are associated with Eocene calc-alkaline rocks (Kuşcu et al. 2013, 2018; İmer et al. 2013); Çöplerporphyry-skarn Au, Cu-Au deposit, Kabataş porphyry Cu-Au prospect at İliç (Erzincan). İmer et al. (2015) newly found that Cevizlidere Cu-Au-Mo (Fig. 8.16c) is the youngest porphyry phase in the southeastern Anatolian orogenic belt; (2) To the south, İspendere-Şişmanköy (Şişman) Cu-Au prospect (Fig. 8.16d) at Kale, Nazaruşağı-Topalkem (Tombul) porphyry Cu prospect (Fig. 8.16e) at Baskil, Kızıldağ (Zeytindağ) Cu-Au prospect at Pertek and the Tilavşun (Höyüklü) porphyry Cu-Au prospect (Fig. 8.16f) at Elbistan are associated with Late Cretaceous calc-alkaline arc-related complexes (Kuşcu et al. 2012, 2013, 2018, (3) Kolonkaya Cu and Keban Cu-Mo porphyry prospect (Fig. 8.16g) and distal Pb-Zn veins are related to a Late Cretaceous alkaline magmatic complex in a central group (Kuşcu et al. 2013, 2018). Associated with other Eocene intrusive complexes are Fe±Cu skarns with porphyry potential such as Mamlis-Sin (İmer et al. 2015; Kuşcu et al. 2018) based on their similar tectono-magmatic setting and ages. Kuşcu et al. (2018) suggest that there are important elements of both E-W and WNW-ESE faulting and some NE-SW faulting as predominant controls of alteration and mineralization. The faults are mostly normal faults, except for a thrust observed in the Sin and Kızılviran prospects where a dextral transpressive structure was recognized.

Resource or reserve data are available for few systems. The largest deposit is Çöpler, recently has been put into production, having combined sulfide and oxide measured and indicated reserves of 194.2 Mt @ 1.4 g/t Au, 3.8 g/t Ag, and 0.1% Cu and an additional inferred resources of 49.6 Mt @ 0.9 g/t Au, 3.0 g/t Ag, and 0.1% Cu (*www.alacergold.com/operations/resources-and-reserves*). In addition and based upon exploration to date, the Cevizlidere system has an inferred resource of 445.7 Mt @ 0.38% Cu and 0.11 g/t Au, whereas the Karakartal system has a smaller inferred resource of 13.8 Mt @ 0.29% Cu and 0.46 g/t/Au (www.alacergold.com/operations/resources-and-reserves).

The alterations at the porphyry deposits and prospects differ in mineralogy and alteration zoning with respect to the age, location and structural controls of mineralization (Fig. 8.16a–g). The alterations in the southern group are mostly argillic to propylitic on the surface exposures, and potassic to phyllic in drill holes. However, the porphyries in northern group are characterized dominantly by potassic alterations exposed to the surface overprinted by argillic alterations. The early stage alteration and mineralization is represented by rare "wormy" indistinct "A veins", late magmatic quartz-magnetite-chalcopyrite veins, but are largely straight "B-veins" hosted by monzonitic to dioritic rocks with disseminated magnetite. The magnetite shows a close paragenetic association with chalcopyrite and subordinate bornite, and composite bornite-chalcopyrite grains are observed frequently within magnetite as rounded inclusions. The late stage alterations mostly refer totelescoping epithermal systems characterized by clay-carbonate alteration overprinting early feldspar-subtle quartz-magnetite-chalcopyrite. Locally, the original porphyritic texture is almost completely destroyed by the flooding of the matrix and phenocrysts by carbonate and clay minerals.

Kuşcu et al. (2013, 2018) reported Late Cretaceous minimum ages of 74.2 ± 0.4 Ma for K-feldspar and a poor, but a slightly older age of 77.5 ± 2.7 Ma at

the Nazaruşağı-Topalkem porphyry Cu prospect. No direct ages on hydrothermal minerals are available for the Keban alkaline porphyry systems, but they are generally assumed to be of similar age as the host Late Cretaceous intrusive rocks (Kuşcu et al. 2013, 2018). The Kabataş system has an age of 47.22 ± 0.49 Ma (Table 8.3). Hydrothermal biotite and sericite as well as Re-Os ages of molybdenite indicate that mineralization at Çöpler system formed between 43.0 and 44.6 Ma (İmer et al. 2013) (Table 8.3). The late Oligocene (~25 Ma) Cevizlidere Cu-Au-Mo (İmer et al. 2015) is the youngest porphyry system in region, and suggests that the porphyry Cu metallogeny of this part of Turkey may be more complex than currently considered (Kuşcu et al. 2018).

8.5.5.1 Southern Group; Late Cretaceous Porphyry Cu±Au±Mo Deposits/Prospects

The southern group porphyry Cu±Au±Mo deposits/prospects are exposed in the area between Pertek (Tunceli), Elbistan (Kahramanmaraş), Kale and Baskil (Elazığ). The Nazaruşağı-Topalkem porphyry Cu-Au prospect is hosted by granodiorite, granodiorite porphyry, hornblende porphyry, dacite porphyry (Figs. 8.6 and 8.16), and diorite intruded by granitic and post-ore diabase. The host rocks are affected by potassic and propylitic alterations. Potassic altered rocks are overprinted by sheeted quartz-sericite-pyrite veins. In outcrop, weak potassic alteration is composed of biotite-quartz±green amphibole in veins (Dumanlılar et al. 1999, 2006), and chloritized igneous biotite, actinolite-quartz assemblages. Propylitic alteration (epidote-chlorite±carbonate-magnetite) envelops the potassic alteration. The small İspendere-Şişmanköy porphyry Cu-Au prospect, located 20 km east of Malatya, (Dumanlılar et al. 1999, 2006), is hosted by dacite porphyry, granodiorite porphyry and tonalite late Cretaceous in age. The latter host most of the hydrothermal alteration whereas the others are only weakly altered. Weak potassic alteration is composed of biotite-quartz±green amphibole veins. Superposed, limited phyllic alteration is restricted to NE-trending fracture zones. Propylitic alteration is widespread on the surface where it is commonly obscured by argillic alteration, consisting of kaolinite, pyrophyllite and montmorillonite superimposed on propylitic alteration (epidote and chlorite) (Dumanlılar et al. 1999). Disseminated chalcopyrite and veins of quartz-chalcopyrite±bornite and quartz-magnetite compose the mineralized zones. Quartz magnetite-hematite±chlorite veins are localized along the intrusive contacts between tonalitic and dacitic rocks. Phyllic alteration may locally contain up to 1.07% Cu (Tüfekçi and Dumanlılar 1994).

The Tilavşun (Höyük) porphyry Cu-Au prospect, hosted by dacite quartz porphyry, is characterized by pervasive advanced argillic alteration assemblages and oxidized phyllic-altered rocks in east-trending faults. The phyllic alteration, largely exposed along major NE-SW trending strike-slip faults, is characterized by quartz-goethite stockworks (after pyrite-chalcopyrite). The patches of propylitic alterations are exposed along the NW-SE trending strike-slip faults (Kuşcu 2009).

8.5.5.2 Central Group; Late Cretaceous Porphyry Cu±Au±Mo Deposits/Prospects

Central Group includes porphyry porphyry Cu±Au±Modeposits/prospects, and several distal base-metal veins and skarns at Keban (Elazığ) and porphyry Cu occurrence at Kolonkaya (Pertek) districts (Figs. 8.6 and 8.16). The Keban porphyry Cu prospect is centered on a syenite and trachyte porphyry intrusive complex. This district contains Mo-W and Pb-Zn veins peripheral to the porphyry Cu-Mo prospect, which also contains fluorite (MTA 1980), and Pb-Zn and magnetite skarns. The syenite porphyry and trachyte complex intruded into limestone and calc-schist (Malatya-Keban metamorphics) host the porphyry Cu-Mo prospect. Coarse-grained syenite porphyry is strongly altered to K-feldspar, sericite, biotite and garnet along easterly trending veinlets. Sparse veins and more common sheeted veinlets of quartz-magnetite-chalcopyrite±bornite are hosted by monzonitic to dioritic rocks. Barite-calcite-fluorite and molybdenite with minor chalcopyrite-sphalerite veins are hosted by syenite porphyry, and are cut by microsyenite and trachyte porphyry dikes.

8.5.5.3 Northern Group; Early-Middle Eocene Porphyry Cu-Au ± Mo Deposits/Prospects

The northern porphyry Cu-Au±Mo deposits/prospects include Çöpler, Kabataş, Karakartal (İliç, Erzincan) and Ovacık, Cevizlidere (Ovacık, Tunceli; Fig. 8.6). Çöpler is a porphyry Cu, epithermal gold and skarn complex with 6.3 M oz Au (including 2.8 M oz in proven and probable reserves, Marek et al. 2008), with proven and probable reserves in the epithermal deposits current at 91.3 Mt at an average grade of 1.5 g/t for a total of 4.4 M oz (Table 8.6). The recent findings suggest that epithermal deposit at Çöpler overprinted the porphyry Cu-Au deposit (İmer et al. 2013). The magmatic-hydrothermal system is centered on a composite diorite to monzonite porphyry stock that has intruded into the surrounding metasediments and marbles (Keban metamorphics). Skarn type mineralization, where remnants and slugs of ancient mining operations are widely exposed, lies adjacent to the intrusions within the calcareous country rocks.

The Kabataş Cu-Au porphyry prospect (İliç-Erzincan), located about 15 km southeast of Çöpler, is hosted by a complex sequence of monzonite to monzodioritic sills, dikes and stocks that intruded the Munzur limestone of eastern Taurides. In the prospect, deeply weathered and leached quartz vein stockwork, sheeted veinlets and skarnified metasedimentary rocks are present. Potassic alteration zone contains sparse to locally intense veinlets of biotite with chalcopyrite, magnetite, pyrite and bornite. Veinlets with chalcopyrite, lesser magnetite, minor bornite and no quartz are present in both the stockworks and country rocks. Phyllic alteration overprinted the potassic-altered zone (Kuşcu et al. 2018).

The Cevizlidere (Ovacık, Tunceli) deposit is spatially related to a NW–SE-elongated, composite, porphyritic, medium-K calc-alkaline diorite and granodiorite stocks emplaced into Paleozoic limestones of Keban metamorphics and Paleogene

andesitic rocks. A plug of diorite crops out near the central part of the prospect and post-dates all of the other igneous phases (Kociumbas and Page 2009; İmer et al. 2015). The host porphyry phases have been subjected to potassic and phyllic alteration. Potassic alteration is characterized by abundant secondary K-feldspar and also by fine-grained hydrothermal biotite either as pseudomorphs after hornblende or along hairline veinlets (Kociumbas and Page 2009). Potassic alteration is surrounded and partly overprinted by intense quartz-sericite alteration, also exposed to the surface, and are recognized in drillcore (Kociumbas and Page 2009). Both potassic and phyllic alterations are enveloped by a propylitic alteration halo characterized by chlorite, epidote, carbonate, and pyrite (Kociumbas and Page 2009).

B-type quartz – magnetite – chalcopyrite – pyrite ± molybdenite ± bornite veinlets and disseminations of chalcopyrite and bornite are commonly observed in close association with the potassic alteration. Copper grades within the potassic alteration zone range between 0.2% and 0.5% Cu, whereas Au and Mo grades in this zone range between 0.09–0.15 and 30–110 g/t, respectively (Kociumbas and Page 2009). Sheeted to stockwork D-type quartz-pyrite-sericite veinlets in the phyllic alteration contain subtle chalcopyrite, and hypogene Cu grades are considerably lower than in the potassic alteration zone (typically <0.2% Cu) (Kociumbas and Page 2009). Late supergene oxidation, extending to depths of 100–150 m below surface, resulted in significant redistribution of copper mineralization into a relatively high-grade (~0.8 to 1% Cu) chalcocite blanket and a near-surface oxide zone consisting of water-soluble Cu minerals (Kociumbas and Page 2009). Early drilling at Cevizlidere has confirmed an inferred resource of 445 million metric tonnes of ore grading 0.38% Cu (cutoff grade at 0.20%), 0.11 g/t Au, and 48 ppm Mo (Kociumbas and Page 2009), and it seems that Cevizlidere is going to be the largest porphyry Cu deposit in Turkey when it is brought to operation.

$^{40}Ar/^{39}Ar$ geochronology of two igneous biotite separates from syn-mineral diorite porphyry yielded late Oligocene cooling ages of 25.49 ± 0.10 and 25.10 ± 0.14 Ma, whereas hydrothermal biotite yielded an age of 24.73 ± 0.08 Ma (İmer et al. 2015). Re-Os ages from two molybdenite separates (24.90 ± 0.10 and 24.78 ± 0.10 Ma) indicate that porphyry-style alteration and mineralization developed shortly after magma emplacement (İmer et al. 2015).

8.6 Porphyry Cu Metallogeny of Turkey

Better understanding of the porphyry Cu metallogeny and causes and formation mechanisms of the porphyry deposits/prospects in Turkey requires evaluation of the magma producing environments, geodynamic setting, compositional and spatial changes on the host magmatics, and temporal and spatial association between the host magmatic rocks and known porphyry Cu deposits/prospects. This section is the summary of discussions by Kuşcu et al. (2018); therefore, the reader is referred to their recent work for a detailed overview.

8.6.1 Tectonomagmatic Settings of Host Magmatic Rocks in Turkey

The available data on the host magmatics and associated porphyry deposits show that the porphyry deposits in Turkey occur in three tectonic settings; magmatic-arc (Pontides, Aegean and Bitlis-Zagros subduction), post-collisional settings (Pontides, WAP and SEAOB) after continental collision, and extensional settings within overriding plate in a subduction zone (Biga peninsula, WAP). In these settings, the porphyry deposits are mainly controlled by large-scale structures including; (1) arc-parallel strike-slip faults, (2) crustal-scale or transverse faults related to tearing or break-off of the subducted slab, and (3) block and detachment faults. In the arc settings, the porphyry deposits were formed from the hydrothermal fluids exsolved from the Late Cretaceous, and late Eocene-Oligocene arc magmas that undergone a complex processes of melting, crystallization, mixing and assimilation processes at the crust-mantle boundary, and exsolution of hydrothermal fluids. Late Cretaceous arc-related igneous rocks consisting mostly of plutonic suites are widely exposed in Pontides and SEAOB while late Eocene-Oligocene arc-related host magmatic rocks consisting of volcano-plutonic association are exposed within WAP. The fact that the Anatolides began to collide with African plate after the final suturing of Arabian plate and Anatolides, the subduction was resumed along the Aegean-Cyprean subduction zone. Therefore, the remaining Neothethyan Ocean began to subduct underneath Anatolides and resulted in arc magmatism throughout the Balkans, Greece and WAP during late Eocene-early Oligocene times (*ca.* 43–39 Ma; Kuşcu et al. 2018). Kuşçayır-Karaayı (Çanakkale), Gökçeada (Çanakkale) porphyry Cu and some high sulfidation epithermal deposits in WAP have been formed during this arc magmatism.

In the post-collisional settings, the porphyry deposits were formed by the fluids exsolved from the shallow-seated early-middle Eocene magmas (*ca.* between 52 and 40 Ma; Kuşcu et al. 2018) that produced plutonic and volcanic rocks. The plutonic rocks of this type are typically exposed within the eastern Pontides and Tavşanlı porphyry belts (Kuşcu et al. 2018). The volcano-plutonic and volcanic rocks are exposed within the eastern Pontides, and share geochemical features akin to adakitic or adakite-like rocks (see previous sections). In the extension-driven post-collisional settings, the magmatism is triggered by a prolonged extension due to roll-back or slab break-off or slab tear/rupture immediately after final suturing of the Afro-Arabian and Eurasian plates. The products of post-collisional magmatism are widely exposed in Pontides, SEAOB and WAP. Ages of host magmatic rocks in eastern Pontides suggest a time span between 52 and 40 Ma, but there is a lack of ages on hydrothermal minerals and thus the true ages of formation can only be inferred to be Eocene. The porphyry Cu deposits/prospects were formed between 48 and 43 Ma in the southeastern Anatolian orogenic belt, between 53 and 46 Ma in Tavşanlı porphyry belt, and between 43 and 39 Ma in the Biga porphyry belt (Kuşcu

et al. 2018). The latter two areas are located in the western Anatolian province. The post-collisional magmatism in Pontides (Genç and Yılmaz 1997; Arslan and Aslan 2006; Boztuğ et al. 2006; Keskin et al. 2008; Kaygusuz et al. 2011; Eyüboğlu et al. 2013), SEAOB (Önal et al. 2005; Boztuğ et al. 2005; Parlak 2007; Kuşcu et al. 2010, 2011) and WAP (Yılmaz et al. 2001; Altunkaynak and Dilek 2006; Karacık et al. 2007; Altunkaynak and Genç 2008) took place during Early-Late Eocene (*ca.* 55–40 Ma). The works on the geochronology, petrogenesis and tectonic setting of the post-collisional host magmatic rocks in Pontides, WAP and SEAOB culminated during last decade showed that the extension is due to (1) decrease in the convergence rate between Eurasian and Arabian plates (Savostin et al. 1996; Rosenbaum et al. 2002; Kaymakçı et al. 2006; Kuşcu et al. 2011); (2) breaking-off (Yılmaz et al. 2001; Önal et al. 2005; Boztuğ et al. 2005; Keskin et al. 2008; Temizel and Arslan 2009; Altunkaynak and Genç 2008; Kaygusuz et al. 2011; Altunkaynak et al. 2012) or (3) initial slab rupture (Kuşcu et al. 2010, 2011) of the subducting slab (oceanic lithosphere of İAE ocean) after final amalgamation of Anatolides with Pontides along the İAESZ. The porphyry deposits hosted by or associated with these host magmatic rocks are mainly of Cu-Mo, Cu-Mo-Au and Cu-type in Pontides and WAP; and Cu-only or Cu-Au type in the SEAOB. The porphyry Cu-Mo, and porphyry Cu deposits in western Pontides and Tavşanlı porphyry belt contain proximal Mo-W skarns. The porphyry Cu-Mo, Cu deposits at WAP and SEAOB, respectively contain proximal Fe-Cu skarns and telescoping high sulfidation epithermal gold deposits, Fe-Cu skarns are being predominant at the SEAOB.

In the extensional settings within overriding plate within subduction environment at the Aegean subduction (Helenic arc), the porphyry deposits were formed from hydrothermal solutions exsolved from magmas generated by partial melting due to time-progressive extension during Early Oligocene to late Miocene (*ca.* 29–9 Ma; Kuşcu et al. 2018). The porphyry deposits in these settings are best exposed within the Biga peninsula, Biga porphyry Cu-Au belt. The porphyry deposits in this setting are also accompanied by proximal Fe-Cu and Cu skarn deposits.

8.6.2 Major Episodes of Porphyry Cu Deposits

The geologic and geochronologic data presented in Kuşcu et al. (2018) on igneous and hydrothermal rocks associated with or hosting the porphyry Cu±Mo±Au deposits and prospects demonstrate distinct magmatic and metallogenic episodes between the Late Cretaceous and the Miocene. Available geochronology suggests that porphyry Cu and intrusion-related hydrothermal systems begin in the Late Cretaceous to the north, and generally young southward with the exception of the eastern Turkey, where paired Late Cretaceous and Eocene metallogenic episodes are present in the eastern Pontides, western Anatolia and southeastern Anatolian orogenic

belt (Kuşcu et al. 2018). The available ages are also indicative of episodocity and a limited time frame of formation for porphyry Cu and related hydrothermal systems in the porphyry Cu belts, and comparable to the metallogenic evolution of Turkey (Kuşcu et al. 2018), as it does on a global basis (e.g. Sillitoe and Perelló 2005).

Late Cretaceous magmatic and porphyry systems in the Pontides, geographically most continuous porphyry Cu belt, represent the oldest event (83–76 Ma). In the southeastern Anatolian orogenic belt, uneconomic porphyry Cu and intrusion-related hydrothermal systems related to calc-alkaline rocks are similar in age to those in the Pontides, but are followed by post-collisional rocks associated in time with the formation of iron-oxide Cu-Au (IOCG) deposits in Turkey (76–74 Ma; Kuşcu et al. 2011) and still younger (74–70 Ma) alkaline rocks with associated porphyry-type systems (Kuşcu et al. 2018).

Eocene marked a second time of a really widespread magmatism and associated porphyry and intrusion-related hydrothermal activity across Turkey. Ages of rocks hosting porphyry deposits in eastern Pontides suggest a potential time span between 52 and 40 Ma, but there is a lack of ages on hydrothermal minerals and thus the true ages of formation can only be inferred to be Eocene. In the southeastern Anatolian orogenic belt, porphyry Cu systems formed between 48 and 43 Ma, between 53 and 46 Ma in Tavşanlı porphyry belt, and between 43 and 39 Ma in the Biga porphyry belt, the latter two areas located in the western Anatolia province (Kuşcu et al. 2018).

Kuşcu et al. (2018) demonstrated that the Oligocene and Miocene are two major episodes during which porphyry and intrusion-related hydrothermal systems such as epithermal, skarn, and intrusion-hosted veins dominate the western Anatolian province. They also noted that no porphyry deposits or intrusion-related hydrothermal systems of this age are known in the Pontides, but only one porphyry Cu deposit is reported in the SEAOB. The magmatic and associated hydrothermal activity, accompanying a southward migration of activity, formed between 29 and 18 Ma within the Biga porphyry belt. Within the western Anatolian province, Oligocene and early Miocene centers are located largely in the center and southern parts of the region, south of the Eocene porphyry centers. Within the Afyon-Konya porphyry belt, known magmatic and hydrothermal centers formed between 16 and 9 Ma (Kuşcu et al. 2018).

8.6.3 Geochemical Characteristics of Host Magmatic Rocks

In the Pontides, the magnetite series granitoids related to the porphyry systems are characterized by typical arc compositions as shown by the high field strength and large-ion lithophile elements. In the southeast Anatolia orogenic belt, the Late Cretaceous magmatic rocks show a shift from subalkaline, arc type compositions to alkaline compositions. Based on the available data, LILE enrichment with respect to HFSE is greater in the younger Late Cretaceous rocks compared to Baskil arc. All the Late Cretaceous rocks are generally enriched in LREE relative to chondrite with steep slopes of LREE, significant flattening of HREE, and a negative Eu anomaly.

The Baskil arc rocks have lower LREE and La/Sm ratios, and moderate HREE content compared to younger Late Cretaceous rocks Geochemical features of host magmatic rocks show that collision and final amalgamation of continental blocks beginning in the late Paleocene (Moix et al. 2008) fundamentally changed the magmatic characteristics from older rocks characterized by typical arc-type compositions to those referred to as collisional or post-collisional compositions from the Late Cretaceous to Miocene. The Late Cretaceous host magmatic rocks are of arc-related, and have been formed during subduction beneath the Eurasian plate in the Pontides (Şengör and Yılmaz 1981; Ustaömer and Robertson 1996; Adamia et al. 2011) and beneath Anatolides and an inter-oceanic continental fragment in the Southeastern Anatolia Orogenic Belt and WAP (Kuşcu et al. 2013). Therefore, the compositions of Late Cretaceous porphyry systems in the Pontides and SEAOB, and Late Eocene-Oligocene porphyry systems are related to active margin and arc magmatism, respectively.

Magmatic compositions in the Eocene are somewhat more complex across Turkey. The Eocene host magmatics in the eastern Pontides are low- to medium-K calc-alkaline to alkaline, and their trace-element characteristics are consistent with a subduction-related setting (Eyüboğlu et al. 2011b). Eocene magmatism in this terrane has been ascribed to an extensional regime immediately after collision of the Tauride-Anatolia Block with Eurasia (e.g., Karslı et al. 2007). In contrast, Eyüboğlu et al. (2014) interprets the Eocene magmatism in the eastern Pontides to represent a back-arc environment formed by southward subduction beneath the Pontide arc.

In the Southeastern Anatolia Orogenic Belt, subalkaline, metaluminous Eocene granitoids have trace element characteristics of arc magmas that also trend toward adakitic compositions. These rocks are interpreted to reflect collisional or back arc environments (İmer et al. 2013; Kuşcu et al. 2013), and not to represent the main magmatic arc in the Eocene.

In the western Anatolian province, post-collisional Eocene to Miocene rocks are subalkaline, and medium to high-K calc-alkaline series rocks, with the exception of several early Miocene plutonic rocks, which are characterized by low-K compositions (Kuşcu et al. 2018). Despite the major element compositional diversity, the trace element characteristics in the magmatic rocks exhibit patterns slightly different from typical arc and within-plate (OIB) settings (Kuşcu et al. 2018), which might be explained by a post-collisional setting as proposed by Chen et al. (2012) for Miocene porphyry Cu–related magmas in Tibet. Nonetheless, the Eocene to Miocene magmatic rocks in the WAP do have trace element compositions parallel to the mantle array and subduction zone enrichment, but at higher values. Kuşcu et al. (2018) proposed that low to medium-K calc-alkaline compositions characterize the Eocene rocks in the northern parts of Biga porphyry belt and Tavşanlı porphyry belt, whereas high-K to shoshonitic compositions characterize the Oligocene and Early Miocene rocks in southern part of Biga porphyry belt and the Miocene rocks of the Afyon-Konya porphyry belt.

8.6.4 *Temporal Changes in Composition of the Host Magmatic Rocks*

The Late Cretaceous porphyry deposits formed from normal arc magmas that had presumably undergone complex processes of melting, crystallization, mixing and assimilation processes in the MASH zone at the crust-mantle boundary (Kuşcu et al. 2018). The collision of the Tauride-Anatolide Block with the Pontide arc was accompanied by a fundamental change in magmatic compositions towards post-collision type compositions (Kuşcu et al. 2018). Systematic changes in trace elements such as La/Yb and Sr/Y in time illustrate how compositions shifted from Late Cretaceous to Miocene (Kuşcu et al. 2018). In the Late Cretaceous, the trace elements are typical for arc volcanic rocks with low overall ratios. Based on the geochronology of the magmatic rocks, the youngest arc-related magmatic rocks marking the final stage of subduction in the region were formed at *ca.* 79 Ma. After collision and final suturing along the İAES, Paleocene-Eocene rocks in the eastern Pontides, Tavşanlı belt and Miocene rocks in the Afyon-Konya porphyry belt have some compositional characteristics of adakitic rocks as defined by Defant and Drummond (1990). The changing magmatic compositions with time are best demonstrated by the progressive increase in the Sr/Y, La/Sm, La/Yb (Fig. 8.17), Th/Nb and Sm/Yb ratios. Beginning in the Late Cretaceous the compositions typical of arc magmas changed with time toward higher ratios in the Miocene alkaline rocks associated with porphyry and quartz-alunite epithermal systems in the Afyon-Konya porphyry belt (Kuşcu et al. 2018). The Sr/Y ratio tends to stay relatively low, and scatter between normal arc rocks and the adakite field for the Tertiary rocks (Fig. 8.17). Kuşcu et al. (2018) also presented time-integrated compositional shifts

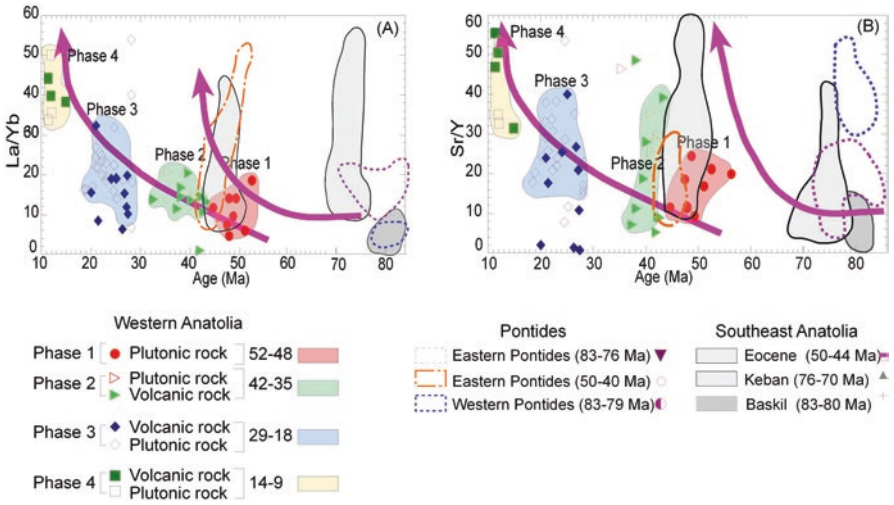

Fig. 8.17 Change in Sr/Y and La/Yb ratios vs age of host magmatic rocks. (Simplified from Kuşcu et al. 2018)

in trace elements with increasing Sr/Y, Sm/Yb, La/Sm and La/Yb ratios in the WAP from Eocene through the Oligocene to the Miocene time (Fig. 8.17). Although they have Yb concentrations higher than normal arc magmas, these trace element characteristics suggest the rocks evolve towards to adakitic compositions with decreasing age from north to south in the western Anatolia region (Kuşcu et al. 2018).

The compositional changes in the magmas between the Late Cretaceous and Eocene in Turkey was interpreted to reflect the effects of collision and onset of crustal thickening, which led to a transition from arc type magmas to post-collisional magmas with tendencies toward adakitic compositions (Kuşcu et al. 2018). Partial melting in such environments is a likely process marking the thinning of continental crust (e.g. Zhai et al. 2007; Liu et al. 2007; Wang et al. 2014). The extensional tectonics is likely to trigger the partial melting and emplacement of early-late Eocene host magmatism in the Pontides, WAP and SEAOB. This indicates that compositional characteristics of host magmatics for the early-Late Eocene porphyry Cu, Cu-Mo, Cu-Au(?) deposits/prospects in Turkey are largely influenced by the partial melting and assimilation of rocks through time. Kuşcu et al. (2018) showed, at least in the western Anatolian province, that starting from the Oligocene and into the Miocene, there is evidence that western Anatolia was beginning to undergo extensional strain and collapse (Fig. 8.18). Therefore, the gradual thinning of the crust that accompanied extensional collapse may have transferred garnet-bearing rocks from deeper crustal levels into the zone of magma generation and assimilation, thus imparting the trace element patterns to the magmas. The WAP is one of the most rapidly extending areas of continental crust in the world, with the southern Aegean

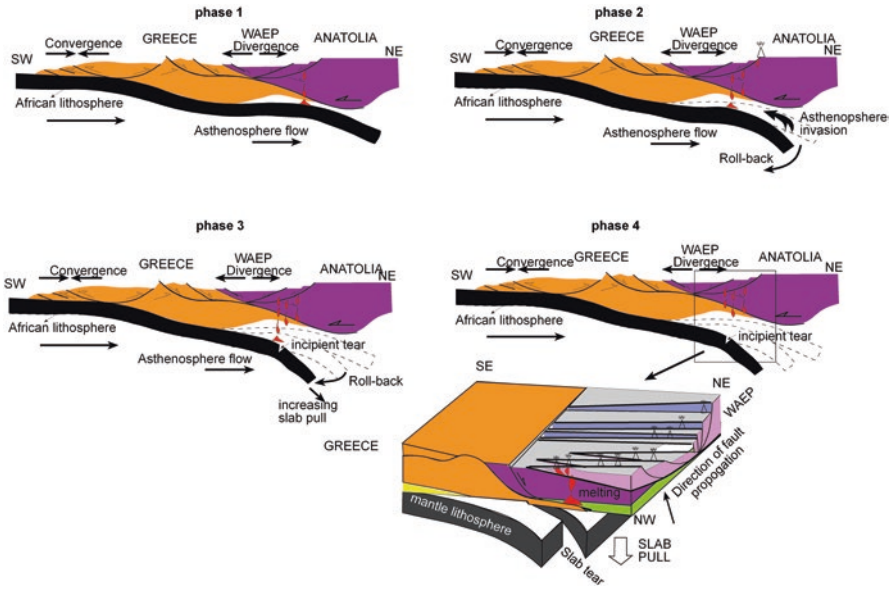

Fig. 8.18 Schematic diagrams illustrating tectono-magmatic evolution and mechanism of extension in WAP

moving at about 35 mm/year relative to Eurasia (Jackson 1994; Reilinger et al. 1997). Several lines of evidence provided by basic mantle tomography (Meulenkamp et al. 1988; Bijwaard et al. 1998; Wortel and Spakman 2000), slab roll-back (Royden 1993; Okay and Satır 2000); plate convergence and paleogeographic plate constructions are in favor of a alternating episodes of extensional and compressional regime since Middle Eocene to Late Miocene in the region. According to the geodynamic model (Doglioni et al. 2002; Innocenti et al. 2005), the extension in the WAP, Aegean sea, Greece and Bulgaria is the result of differential convergence rates between the NE-directed subduction of Africa relative to the hanging wall Eurasian lithosphere. The north-eastward subduction of Africa along the Hellenic margin shows faster convergence rates (about 37 mm year^{-1}, as computed via GPS measurements) than along the Cyprus trench (8 mm year^{-1}), generating a differential velocity in the overriding plate of about 29 mm year^{-1} (Doglioni et al. 2002). The differential velocities between the hanging wall plates, enabling a faster southwestward convergence of Greece over the Ionia compared to the convergence rate of Turkey and Cyprus over the eastern Mediterranean is defined as the most probable mechanism creating extension in WAP and in the area between the two regions (Doglioni et al. 2002; Innocenti et al. 2005). Since, the magmatic rocks in the WAP display a temporal and spatial shift from *ca.* 37 to 9 Ma, and are exposed more or less in NE-SW trending linear belts parallel to the main splays of dextral NAFZ. The geochronological database on the extension related magmatic rocks, and geochemical characteristics indicating deeper magma source in time from NW to SE indicate that this rupture is inferred to have started at least at 37 Ma (Kuşcu et al. 2018), and should proceed to increase southeastward in time producing magmas at phase 2 to phase 4 (Fig. 8.18).

The metasomatism of upper mantle or lower crustal regions through time by subduction processes must have occurred throughout Turkey, as the subduction zone progressively moved southward due to collision or simple trench retreat and slab break-off at the convergent plate margin (Kuşcu et al. 2018). Changes in trace elements such as Sm/Yb, La/Sm, Sr/Y (Fig. 8.17), La/Yb and Ta/Yb can be explained by subduction process and by crustal contamination as the magma rose towards the surface. Ultimately, magma related to a porphyry-type hydrothermal system must have been generated by melting an enriched mantle coupled with crustal interaction, assimilation, and fractionation processes, as the magma rose to an upper crustal location. The moderately elevated Sr/Y ratio, listric shaped REE patterns, and weak to negligible Eu anomalies furthermore suggest that magmas are somewhat oxidized (Richards 2013; Loucks 2014), conditions required to form porphyry Cu systems.

8.6.5 Metallogenic Belts of Porphyry Cu Deposits

The spatial association of porphyry deposits and associated magmatic rocks in Pontides, WAP and SEAOB defined herein indicates that there are seven distinct porphyry belts in Turkey (Fig. 8.19). Each belt tends to occupy a reasonably

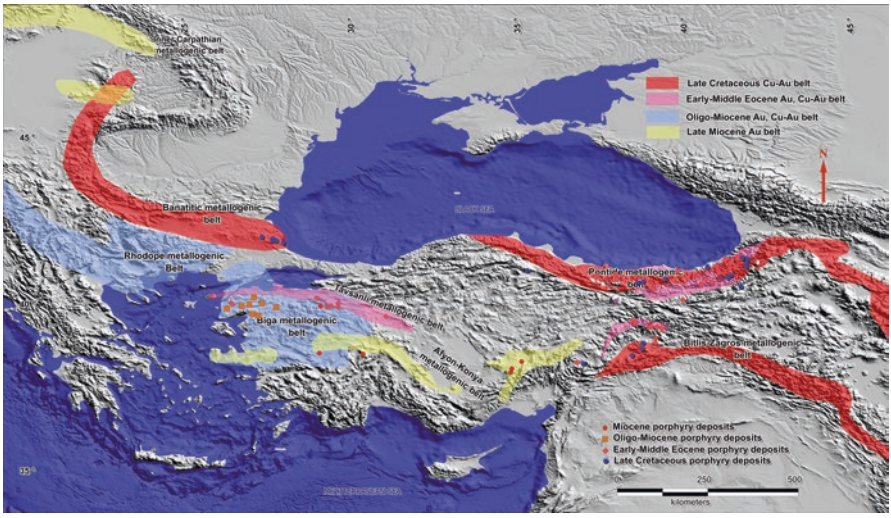

Fig. 8.19 Major metallogenic Cu-Au belts in Turkey in correlation with Tethyan Eurasian metallogenic belts. (Modified from Kuşcu et al. 2018)

well-defined tectonomagmatic niche rather than occurring randomly. The belts span a spectrum of tectonic settings and magma compositions ranging from subduction, post-collision and extensional settings. These belts are not only porphyry belts but also refer to belts in which variety of deposit types including epithermal (HS, LS and intermediate sulfidation types), mesothermal vein type base metal and skarn deposits coexist. These occupy only a small proportion of Turkish Tethyan collage limited mainly to Pontides, SEAOB and WAP. Each porphyry belt was typically generated in less than 2–12 m.y (see previous sections), with individual large deposits (Kışladağ and Ağıdağı) having lifespan of <0.5 m.y. (Table 8.4). The major porphyry deposits and largest gold concentrations were formed either immediately after major contractional episodes or during prolonged extensional in association with calc-alkaline and alkaline magmatism. These belts are localized along arc-parallel as in eastern Pontides, and arc-transverse faults as in the WAP and SEAOB. Although the spatial and temporal restriction of the major belts can be ascribed to specific tectonomagmatic events, the overall distribution of porphyry deposits in Turkey suggest that the subduction and post-subduction magmatic rocks and associated porphyry systems are commonly related to kilometer-scale continental arc-parallel and arc transverse extensional terranes.

The Late Cretaceous porphyry Cu systems of the Pontides are accepted to be the continuation of the Timok-Srednogorie porphyry and quartz-alunite epithermal systems (Fig. 8.19; Kuşcu et al. 2018) that range in age from 92 to 75 Ma (Kouzmanov et al. 2009; von Quadt et al. 2005; Kolb et al. 2013; van der Toorn et al. 2013) in east central Serbia and Bulgaria. The Oligocene systems of the Biga porphyry belt are

represented in Macedonia and Serbia (Fig. 8.19), where the Buchim porphyry Cu deposit (Macedonia), Kiseljak (Serbia) and many undeveloped porphyry Cu-Au prospects (Márton et al. 2010; Lehmann et al. 2013) as well as the porphyry Mo system at Surdilica (Corley et al. 2010; Kouzmanov and Pokrovski 2012) are known. The early Miocene alkalic porphyry Cu-Au deposit at Skouries as well as uneconomic systems on various Greek islands in the Aegean Sea, (Heinrich and Neubauer 2002; Neubauer and Heinrich 2003; Mao et al. 2014; Vouduoris et al. 2013), seemingly represent a continuation of the alkaline porphyry Au-Cu systems of the Afyon-Konya porphyry belt (Kuşcu et al. 2018).

The porphyry belts of eastern Turkey continue into the Lesser Caucasus of Georgia and Armenia, and southeastward into Iran (Fig. 8.19) (e.g. Richards 2003, 2015; Zarasvandi et al. 2005; Singer et al. 2005 and references therein; Richards et al. 2012 and references therein; Aghazadeh et al. 2015). Cretaceous porphyry systems are known in Armenia, but are older than those in the Pontides, being of Early Cretaceous age (Sosson et al. 2010; Adamia et al. 2011; Hässig et al. 2013 and references therein). Eocene porphyry systems are less common with poorly explored systems at Shadan and Maher Abad in the Lut Block of Iran (Richards et al. 2012; Aghazadeh et al. 2015). The Lut Block represents a continental fragment, much like the Tauride-Anatolide Block in central Turkey that collided with Eurasia as the NeoTethys Ocean closed, and is now embedded in the Tethyan collage. The Eocene porphyry systems of Iran thus reflect a similar post-collisional environment, similar to that considered for the Eocene deposits in the eastern Pontides.

East of Turkey, the Miocene represents the major metallogenic event. The Early Miocene porphyry Mo-Cu deposit at Kadjaran in Armenia and the world-class Miocene deposits at Sarcheshmeh and Songon in Iran are notable deposits formed at this time (McInnes et al. 2005; Singer et al. 2005 and references therein; Richards et al. 2006, 2012 and references therein; Shafiei et al. 2009; Aghazadeh et al. 2015). A continuous Miocene porphyry Cu belt is not represented in central and eastern Turkey, presumably because of the on-going collision of the Arabian continent with Eurasia. However, alkaline systems such as Kışladağ porphyry Au in western Anatolia and the Skouries shoshonitic porphyry Cu-Au system in Greece are of a similar age, and formed as subduction and collision continued east and west of the Arabia-Eurasia collisional zone in the Bitlis-Zagros suture zone in eastern Turkey (Kuşcu et al. 2018).

8.6.6 Porphyry-Related Metallogenic Evolution of Turkey

Porphyry systems on a worldwide basis are generally associated with convergent or collisional plate margins (Seedorff et al. 2005; Richards 2009; Tosdal et al. 2009; Sillitoe 2010). The collisional margins have largely been undergoing contractile strain with the site of porphyry formation being an area of limited deformation that may have accompanied broad scale uplift and consequent exhumation (Houston and Dilles 2013; Tosdal et al. 2015). Formation of porphyry Cu systems is facilitated by

limited deformation, much of which can be accommodated by an interplay of regional far field and local magmatic induced deformation, to account for the multiplicity of vein orientations (Tosdal and Richards 2001; Tosdal 2012; Gruen et al. 2010; Harris and Holcombe 2014). Low magnitude contraction to extension that accompanied tectonic transitions has been proposed to be important to porphyry formation (Tosdal and Richards 2001; Richards 2003, 2009; Cooke et al. 2005). Porphyry Cu systems have been formed during the latter stages of a prolonged magmatic event, as magmatism and deformation waned (Richards 2003, 2009, 2011; Chiaradia et al. 2009; Haschke et al. 2010; Sillitoe 2010; Jun Lu et al. 2013).

In the context of Turkey, the Late Cretaceous porphyry systems in the Pontides and Southeastern Anatolian Orogenic Belt are clearly the result of simple subduction related magmatism, with emplacement facilitated by upper crustal faults. The dominance of ages between *ca.* 83 and 70 Ma (Kuşcu et al. 2018) broadly coincides with the final stages of Late Cretaceous magmatism. The Late Cretaceous systems also broadly formed prior to the onset of collision and cessation of subduction.

In contrast, the Eocene porphyry systems found across Turkey in discontinuous belts presumably reflect collisional to post-collisional processes as they postdate the onset of the accretion of continental blocks to the Eurasian continental margin. The geochemical compositions of the magmas are all characterized by a gradual increase in La/Yb ratios, and are thus akin to the post-collisional Miocene porphyry systems in the Himalayas (Kuşcu et al. 2018) and some of the Pliocene and younger porphyry systems in Papua New Guinea (Kay et al. 2005; Cloos et al. 2005; Hou et al. 2009, 2011; Sillitoe 2010; Richards 2011, 2015; Holm et al. 2013; Wang et al. 2014). In Turkey, the magmatic locus shifts southward with time, a geographic progression that is most evident in the western Anatolian province. Southward shifts of the magmatic locus may be related to successive collision and underthusting of the Tauride-Anatolide Block beneath the Eurasian plate, and the attending progressive thickening of the crust, and to breaks in the subducting slab (Kuşcu et al. 2018).

The western Anatolia is one of the best-studied and complex regions in the world (e.g. van Hinsbergen and Schmid 2012). This region has been dominated by extensional and strike-slip deformation as the Hellenic-Aegean subduction zone stepped southward and the back-arc region in western Turkey bounded by the Anatolia fault systems collapsed toward the Aegean Sea. Eocene to Miocene porphyry Cu system formed in the region that over time has undergone collision followed by extensional collapse. However on a global scale, the association of porphyry Cu systems with extensional deformation is not widely documented, although the association of epithermal deposits with extensional terranes is well known as syn-mineral extension enhances the ability of the metalliferous hydrothermal fluids to rise buoyantly through the porphyry environment into the shallow crustal epithermal environment (Fournier 1999; Tosdal 2012). Thus, constraining the timing of whole-crustal extension with respect to the formation of porphyry system is a critical question to address, but will require for western Anatolia a better understanding of the rapidly changing sequence of events. On a broader scale, Bertrand et al. (2014) suggest that the Eocene to Miocene porphyry systems in western Anatolia reflect crustal relaxation that accompanied a decrease in convergence rate between Africa, Arabia, and Eurasia during this time (Rosenbaum et al. 2002; Kaymakçı et al. 2006; Kuşcu et al. 2011).

8.6.7 Exploration Opportunities for Undiscovered Deposits

This section is largely adopted from recent work of Zurcher et al. (2015) based on their porphyry Cu assessment of Tethyan belt. They emphasized that the spatial distribution of known porphyry deposits and prospects are related to the level of erosion in the Tethyan belt. They concluded that magmatic belts with fewer known porphyry sites display either high or low volcanic-to-plutonic ratios and (or) greater cover, indicating crustal levels that are too shallow or too deep for exposure of porphyry deposits. They used probabilistic estimates of numbers of undiscovered deposits combined with grade and tonnage models in a Monte Carlo simulation to estimate probable amounts of contained metal. According to them, the density of known porphyry deposits in the Pontides is low when compared to densities in well-explored provinces of this size around the world. This suggests that undiscovered deposits are likely present in Pontides. Estimates for undiscovered porphyry copper deposits in the Pontide yielded in a mean of 4.13 undiscovered deposits with a standard deviation of 3.02 ($Cv\% = 73$). In the Biga, Tavşanlı and Afyon-Konya porphyry belts, geologic factors favorable for the occurrence of undiscovered porphyry deposits include (1) tectonically transported (?) continental-arc segment; (2) fertile calc-alkaline compositions; (3) known Cu-Mo, Au porphyry deposits; and (4) favorable conditions for supergene enrichment (likely enhanced by postmineral extensional tectonics) (Zurcher et al. 2015). Unfavorable factors for the occurrence of undiscovered porphyry deposits include (1) small arc segment (as exposed), (2) known porphyry deposits that exhibit smaller tonnages and copper grades than the median porphyry deposit around the world, (3) deeper levels of exposure for porphyry systems, and (4) extensive cover (Zurcher et al. 2015). In spite of lower density of known porphyry deposits in WAP relative to worldwide densities for the porphyry belts, Zurcher et al. (2015) suggested that undiscovered deposits are likely present within WAP. Besides, the relatively high number of known porphyry occurrences within this province, is considered to support moderate levels of uncertainty expected in the estimation of numbers of undiscovered deposits (Zurcher et al. 2015). The Monte Carlo simulation model for this province shows estimates of 0 and 1 undiscovered deposits for the 90-, 50-, and 10-percent probability levels, which resulted in a mean of 0.78 undiscovered deposits with a standard deviation of 0.60 ($Cv\% = 78$) (Zurcher et al. 2015). They concluded that this result reflects the level of favorability and moderate uncertainty assessed for this tract. In the SEAOB, the geologic factors favorable for the occurrence of undiscovered porphyry deposits include (1) magmatic arc(s) and late-orogenic magmatic centers emplaced in a large extensional intraoceanic basin, (2) fertile (permissive) alkaline to calc-alkaline magmas, (3) known Au-(Cu) porphyry-skarn (for example Çöpler, Karakartal, Kabataş, Cevizlidere) and Cu-Mo-Au porphyry (for example, Keban, Agarak) deposits, and (4) appropriate levels of exposure along uplifted accretionary prisms (Zurcher et al. 2015). Unfavorable factors for the occurrence of undiscovered porphyry deposits include (1) relatively extensive cover and (2) tonnages in known deposits that are lower than the median in the global porphyry copper tonnage

model (Zurcher et al. 2015). They noted that the density of known porphyry copper deposits is lower than that of well-explored provinces of equivalent aerial extent elsewhere. This suggests that undiscovered deposits are likely present. The estimates for undiscovered porphyry copper deposits in the Anatolide-Tauride–Eastern Turkey-Caucasus sub-tract at the 90-, 50-, and 10-percent probability levels yielded a mean of 2.23 undiscovered deposits with a standard deviation of 2.04 ($Cv\% = 92$) (Zurcher et al. 2015). This result reflects the level of favorability and moderate to high uncertainty assessed for the SEAOB. Simulation results for estimated for copper, molybdenum, gold, silver, and the total volume of mineralized rock suggested that the mean estimate of undiscovered copper resources in the SEAOB is 8.2 Mt (Zurcher et al. 2015).

8.7 Conclusions

Porphyry systems on a worldwide basis are generally associated with convergent or collisional plate margins. In Turkey, porphyry deposits occur in three tectonic settings; magmatic-arc (Pontides, Aegean and Bitlis-Zagros subduction), post-collisional settings (Pontides, WAP and SEAOB), following continental collision, and extensional settings within overriding plate in NeoTethyan subduction zone (Biga peninsula, WAP). The geological and geochronological data on igneous and hydrothermally altered rocks, associated with or hosting the porphyry Cu±Mo±Au deposits and prospects demonstrate distinct magmatic and metallogenic episodes between the Late Cretaceous and the Miocene. Late Cretaceous arc-related igneous rocks consisting mostly of plutonic suites are widely exposed in the Pontides and SEAOB, while late Eocene-Oligocene arc-related host magmatic rocks, consisting of volcano-plutonic association, are exposed within WAP. The Late Cretaceous systems are broadly formed prior to the onset of collision and cessation of subduction. Late Cretaceous post-collisional magmatism and associated porphyry Cu-Mo deposits are best exposed within the CACC. The Eocene to Miocene porphyry systems found across Turkey are in discontinuous belts, presumably reflect collisional to post-collisional processes as they postdate the onset of the accretion of continental blocks to the Eurasian continental margin. In these settings, the porphyry deposits are mainly controlled by large-scale structures including; (1) arc-parallel strike-slip faults, (2) crustal-scale or transverse faults related to tearing or break-off of the subducted slab, and (3) block and detachment faults. In the arc settings, the porphyry deposits were formed from hydrothermal fluids exsolved from the Late Cretaceous, and late Eocene-Oligocene arc magmas, which had undergone a complex processes of melting, crystallization, mixing and assimilation processes at the crust-mantle boundary.

Available geochronological data suggest that porphyry Cu and intrusion-related hydrothermal systems begun in the Late Cretaceous to the north, and generally younging southward, with the exception of eastern Turkey, where paired Late Cretaceous and Eocene metallogenic episodes are present in the eastern Pontides,

western Anatolia and southeastern Anatolian orogenic belts. The available ages are also indicative of episodicity and a limited time frame of formation for porphyry Cu and related hydrothermal systems in the porphyry Cu belts. In the Pontides, the magnetite series granitoids related to the porphyry systems are characterized by typical arc compositions. In the southeast Anatolia orogenic belt, the Late Cretaceous magmatic rocks show a shift from subalkaline, arc-type compositions to alkaline compositions. Magmatic compositions in the Eocene are somewhat more complex across Turkey. The Eocene in the eastern Pontides is characterised by low- to medium-K calc-alkaline to alkaline, with their trace-element characteristics being consistent with a subduction-related setting. In the Southeastern Anatolia Orogenic Belt, subalkaline, metaluminous Eocene granitoids have trace element characteristics of arc magmas that also trend toward adakitic compositions. These rocks are interpreted to reflect collisional or back arc environments. In the western Anatolian province, post-collisional Eocene to Miocene rocks are subalkaline, and medium to high-K calc-alkaline series rocks, with the exception of several early Miocene plutonic rocks, which are characterized by low-K compositions.

The host magmatic rocks exhibit systematic changes in trace element composition in time from Late Cretaceous to Miocene. These changes are best demonstrated by the progressive increase in the Sr/Y, La/Sm, La/Yb, Th/Nb and Sm/Yb ratios from late Cretaceous to Miocene for Pontides, WAP and SEAOB. Beginning in the Late Cretaceous the compositions typical of arc magmas changed with time toward higher ratios in the Miocene alkaline rocks associated with porphyry and quartz-alunite HS epithermal systems in the Afyon-Konya porphyry belt. The Sr/Y ratio tends to stay relatively low, and scatter between normal arc rocks and the adakite field for the Tertiary rocks. The compositional changes in the magmas between the Late Cretaceous and Eocene in Turkey was interpreted to reflect the effects of collision and onset of crustal thickening, which led to a transition from arc type magmas to post-collisional magmas with tendencies toward adakitic compositions.

The spatial association of porphyry deposits and magmatic rocks in Turkey indicates that there are seven distinct porphyry belts. Each belt tends to occupy a reasonably well-defined tectono-magmatic niche rather than occurring randomly; (1) These belts are localized along arc-parallel as in eastern Pontides, (2) and arc-transverse faults as in the WAP and SEAOB. These belts span a spectrum of tectonic settings and magma compositions ranging from subduction, post-collision and extensional settings since the Late Cretaceous. These belts are not only porphyry belts but also belts in which variety of deposit types including epithermal (HS, LS and intermediate sulphidation types), mesothermal vein type base metal and skarn deposits coexist. Each porphyry belt was typically generated in less than 2–12 myrs, with individual large deposits having lifespan of <0.5 myrs. (e.g. Kışladağ). The major porphyry deposits and largest gold concentrations were formed either immediately after major contractional episodes or during prolonged extensional in association with calc-alkaline and alkaline magmatism.

Acknowledgements The work is part of a collaborative research project generously sponsored by Barrick Gold Corp, Teck Cominco Ltd., and Eldorado Gold-Tüprag Metal-Mining Ltd. The financial and logistical support from these companies are greatly appreciated. Part of the work is also supported by TÜBİTAK via a research project (ÇAYDAG-103Y098) by the first author. MDRU contribution no.256.

References

Adamia S, Zakariadze G, Chkhotua T, Sadardze N, Tseretelli N, Chabukiani A, Gventsadze A (2011) Geology of the Caucasus: a review. Turk J Earth Sci 20:489–544

Agard P, Omrani J, Jolivet L, Mouthereau F (2005) Convergence history across Zagros (Iran): constraints from collisional and earlier deformation. Int J Earth Sci 94:401–419

Aghazadeh M, Hou Z, Badrzadeh Z, Zhou L (2015) Temporal-spatial distribution and tectonic setting of porphyry copper deposits in Iran: constraints from zircon U-Pb and molybdenite Re-Os geochronology. Ore Geol Rev 70:385–406

Akçay M, Gündüz O (2004) Porphyry Cu–Au mineralisation associated with a multi-phase intrusion, and related replacement fronts in limestones in an island arc setting near the Gümüşhane village (Artvin) in the Eastern Black Sea Province (Turkey). Chem Erde 64:359–383

Aldanmaz E, Pearce JA, Thirlwall MF, Mitchell JG (2000) Petrogenetic evolution of late Cenozoic, post-collision volcanism in western Anatolia, Turkey. J Volcanol Geotherm Res 102:67–95

Altıner D, Koçyiğit A, Farinacci A, Nicosia U, Conti MA (1991) Jurassic, Lower Cretaceous stratigraphy and paleogeographic evolution of the southern part of northwestern Anatolia. Geol Rom 18:13–80

Altunkaynak S (2007) Collision-driven slab break-off magmatism in northwestern Anatolia, Turkey. J Geol 115:63–82

Altunkaynak S, Dilek Y (2006) Timing and nature of postcollisional volcanism in western Anatolia and geodynamic implications. In: Dilek Y, Pavlides S (eds) Postcollisional tectonics and magmatism in the Mediterranean region and Asia. Geol Soc Am Sp Pap 409:321–351

Altunkaynak Ş, Genç ŞC (2008) Petrogenesis and time-progressive evolution of the Cenozoic continental volcanism in the Biga peninsula, NW Anatolia (Turkey). Lithos 102:316–340

Altunkaynak S, Sunal G, Aldanmaz E, Genç S, Dilek Y, Furnes H, Foland KA, Yang J, Yıldız M (2012) Eocene granitic magmatism in NW Anatolia (Turkey) revisited: New implications from comparative zircon SHRIMP U–Pb and ^{40}Ar-^{39}Ar geochronology and isotope geochemistry on magma genesis and emplacement. Lithos 155:289–309

Angus DA, Wilson DC, Sandvol E, Ni JF (2006) Lithospheric structure of the Arabian and Eurasian collision zone in Eastern Turkey from S-wave receiver functions. Geophys J Int 166(3):1335–1346

Arslan M, Aslan Z (2006) Mineralogy, petrography and whole-rock geochemistry of the Tertiary granitic intrusions in the Eastern Pontides, Turkey. Asian J Earth Sci 27:177–193

Aslan Z (2005) Petrography and petrology of the calc-alkaline Sarıhan granodiorite (NE Turkey): an example of magma mingling and mixing. Turk J Earth Sci 14:185–207

Aslan Z (2010) U-Pb zircon SHRIMP age, geochemical and petrographical characteristics of tuffs within calc-alkaline Eocene volcanics around Gümüşhane (NE Turkey), Eastern Pontides. Neu Jb Miner Abh 187:329–346

Bertrand G, Guillou-Frottier L, Loiselet C (2014) Distribution of porphyry copper deposits along the western Tethyan and Andean subduction zones: insights from a paleotectonic approach. Ore Geol Rev 60:174–190

Beyarslan M, Bingöl AF (2000) Petrology of a supra-subduction zone ophiolite (Elazığ, Turkey). Can J Earth Sci 37:1411–1424

Bijwaard H, Spakman W, Engdahl ER (1998) Closing the gap between regional and global travel time tomography. J Geophys Res 103:30–55

Biryol CB, Beck SL, Zandt G, Özacar AA (2011) Segmented African lithosphere beneath the Anatolian region inferred from teleseismic P-wave tomography. Geophys J Int 184:1037–1057
Bissig T, Tosdal RM (2009) Petrogenetic and metallogenetic relationships in the Eastern Cordillera Occidental of Central Peru. J Geol 117:499–518
Bozkurt E (2007) Extensional and contractional orogen for the southern Menderes massif, southwest Turkey: tectonic and metamorphic implications. Geol Mag 144:191–210
Bozkurt E, Mitwede SK (2001) Introduction to the geology of Turkey-a synthesis. Int Geol Rev 43:578–594
Bozkurt E, Oberhänsli R (2001) Menderes Massif (Western Turkey): structural, metamorphic and magmatic evolution-a synthesis. Int J Earth Sci 89:679–708
Boztuğ D, Harlavan Y (2008) K-Ar ages of granitoids unravel the stages of Neo Tethyan convergence in the eastern Pontides and central Anatolia, Turkey. Int J Earth Sci 97:585–599
Boztuğ D, Jonckheere RC, Arslan M, Şen C, Karslı O, Erçin Aİ (2005) Eocene slab break-off revealed by the E-W distribution of the multi-sourced granitoids and tectonic denudation in the eastern Pontides, Turkey. Geophys Res Abs 7:02129 2005. S Ref-ID: 1607-7962/gra/EGU05-A-02129
Boztuğ D, Erçin AI, Kuruçelik MK, Göç D, Kömür I, İskenderoğlu A (2006) Geochemical characteristics of the composite Kaçkar batholith generated in a NeoTethyan convergence system, eastern Pontides, Turkey. J Asian Earth Sci 27:286–302
Boztuğ D, Jonckheere RC, Wagner GA, Yeğingil Z (2007) Titanite and zircon fission-track dating resolves successive igneous episodes in the formation of the composite Kaçkar batholith in the Turkish eastern Pontides. Int J Earth Sci 96:875–886
Candan O (1995) Relict granulite-facies metamorphism in the Menderes Massif. Turk J Earth Sci 4:35–55
Candan O (1996) Petrography and metamorphism of the gabbros around Kiraz-Birgi region, Ödemiş-Kiraz submassif of the Menderes Massif. Yerbilimleri 18:1–25
Candan O, Dora Ö, Oberhanslı O, Çetinkaplan R, Partzsch M, Warkus FC, Dürr S (2001) Pan-African high-pressure metamorphism in the Precambrian basement of the Menderes Massif, western Anatolia, Turkey. Int J Earth Sci 89:793–811
Çapan UZ, Floyd A (1985) Geochemical and petrographic features of metabasalts within units of the Ankara mélange, Turkey. Ofioliti 10:3–18
Çelebi H (1997) Geochemistry of silver bearing manganese ores of west-Euphrates sector of lead-silver deposit Keban (Elazığ). Geol Bull Turk 40:19–36
Çelik ÖF, Delaloye M, Feraud G (2006) Precise 40Ar-39Ar ages from the metamorphic sole rocks of the Tauride Belt Ophiolites, Southern Turkey: implications for the rapid cooling history. Geol Mag 143:213–227
Chen JL, Zhao WX, Xu JF, Wang BD, Kang ZQ (2012) Geochemistry of Miocene trachytes in Bugasi, Lhasa Block, Tibetan Plateau: mixing products between mantle-and crust-derived melts? Gondwana Res 21:112–122
Chiaradia M, Merino D, Spikings R (2009) Rapid transition to long-lived deep crustal magmatic maturation and the formation of giant porphyry-related mineralization (Yanacocha, Peru). Earth Planet Sci Lett 288:505–515
Ciobanu CL, Cook NJ, Stein H (2002) Regional setting and geochronology of the late cretaceous banatitic magmatic and metallogenic belt. Miner Depos 37:541–567
Cloos M, Sapiie B, Quarles van Ufford A, Weiland RJ, Warren PQ, McMahon TP (2005) Collision delamination in New Guinea: the geotectonics of subducting slab breakoff. Geol Soc Am Spec Pap 400:51pp
Collins AS, Robertson AHF (1997) Lycian melange, southwestern Turkey: an emplaced Late Cretaceous accretionary complex. Geology 25:255–258
Cooke DR, Hollings P, Walshe JL (2005) Giant porphyry deposits: characteristics, distribution, and tectonic controls. Econ Geol 100:801–818
Corley D, Mazzoni P, Smith R (2010) Surdulica project. Serbia: National Instrument 43–101 Technical report. p 111

Defant MJ, Drummond MS (1990) Derivation of some modern arc magmas by melting of young subducted lithosphere. Nature 347:662–665

Dilek Y, Whitney DL (1997) Counterclockwise *P-T-t*rajectory from the metamorphic sole of a Neo-Tethyan ophiolite (Turkey). Tectonophysics 280(3-4):295–310

Dilek Y, Altunkaynak S, Öner Z (2010) Syn-extensional granitoids in the Menderes core complex and the late Cenozoic extensional tectonics of the Aegean province. In: Ring U, Wernicke B Extending a continent: architecture. Rheology and heat budget, Geological Society special publicaitons. Geological Society, London, pp 197–223

Doglioni C, Agostini S, Crespi M, Innocenti F, Manetti P, Riguzzi F, Savasçın Y (2002) On the extension in western Anatolia and the Aegean Sea. In: Rosenbaum G, Lister GS (eds) Reconstruction of the evolution of the Alpine-Himalayan Orogen. J Virtual Explor 8:161–176

Dora OÖ, Kun N, Candan O (1990) Metamorphic history and geotectonic evolution of the Menderes masif. IESCA Proc 2:102–115

Dumanlılar HD, Aydal D, Dumanlılar Ö (1999) İspendere (Malatya) bölgesindeki sülfid cevherleşmelerinin jeolojidi, mineralojisi ve jeokimyası. [*Geology, mineralogy and geochemistry of sulfide mineralization in the İspendere region (Malatya)*]. Bull MTA 121:225–250 (in Turkish with English abstract)

Dumanlılar Ö, Aydal D, Dumanlılar H, Alıcı-Şen P (2006) Geological and geochemical characteristics of Granitoids in the Eastern Tauride Belt, Southeastern Turkey. Int Geol Rev 48:443–465

Eyüboğlu Y, Dilek Y, Bozkurt E, Bektaş O, Rojay B, Şen C (2010) Structure and geochemistry of an Alaskan-type ultramafic-mafic complex in the eastern Pontides, NE Turkey. In: Santosh M, Maruyama S (eds) A tribute to Akiho Miyashiro. Gondwana Res 18:230–252

Eyüboğlu Y, Santosh M, Chung S (2011a) Crystal fractionation of adakitic magmas in the crust–mantle transition zone: petrology, geochemistry and U-Pb zircon chronology of the Seme adakites, eastern Pontides, NE Turkey. Lithos 121:151–166

Eyüboğlu Y, Santosh M, Chung SL (2011b) Petrochemistry and U-Pb Zircon ages of adakitic intrusions from the Pulur Massif (Eastern Pontides, NE Turkey): implications for slab rollback and ridge subduction associated with Cenozoic convergent tectonics in the Eastern Mediterranean. J Geol 119:394–417

Eyüboğlu Y, Santosh M, Dudas FO, Akaryalı E, Chung SL, Akdağ K, Bektaş O (2013) The nature of transition from adakitic to non-adakitic magmatism in a slab-window setting: a synthesis from the Eastern Pontides, NE Turkey. Geosci Front 4:353–375

Eyüboğlu Y, Santosh M, Yi K, Tüysüz N, Korkmaz S, Akaryalı E, Dudas FO, Bektaş O (2014) The Eastern Black Sea-type volcanogenic massive sulfide deposits: geochemistry, zircon U-Pb geochronology and an overview of the geodynamics of ore genesis. Ore Geol Rev 59:29–54

Fournier RO (1999) Hydrothermal processes related to movement of fluid from plastic into brittle rock in the magmatic-epithermal environment. Econ Geol 94:1193–1212

Fytikas M, Innocenti F, Manetti P, Mazzuoli R, Peccerillo A, Villari L (1984) Tertiary to quaternary evolution of volcanism in the Aegean region. In: Dixon JE, Robertson AHF (eds) The geological evolution of the Eastern Mediterranean, Geol Soc Sp Publ, vol 17, pp 687–699

Gautier P, Brun J-P, Moriceau R, Sokoutis D, Martinod J, Jolivet L (1999) Timing, kinematics and cause of Aegean extension: a scenario based on a comparison with simple analogue experiments. Tectonophysics 315:31–72

Gautier P, Bozkurt E, Hallot E, Dirik K (2002) Dating the exhumation of a metamorphic dome: geological evidence for pre-Eocene unroofing of the Nigde Massif (Central Anatolia, Turkey). Geol Mag 139:559–576

Genç ŞC, Yılmaz Y (1997) An example of post-collisional magmatism in northwestern Anatolia: the Kızderbent Volcanics (Armutlu Peninsula, Turkey). Turk J Earth Sci 6:33–42

Gökten E, Floyd PA (2006) Stratigraphy and geochemistry of pillow basalts within the ophiolitic melange of the İzmir-Ankara-Erzincan Suture Zone: implications for the geotectonic character of the Northern Branch of Neotethys. Int J Earth Sci 96:725–741

Göncüoğlu MC, Dirik K, Kozlu H (1997) General characteristics of pre-Alpine and Alpine terranes in Turkey: explanatory notes to the terrane map of Turkey. Ann Geol Pays Hell 37:515–536

Göncüoğlu MC, Turhan N, Şentürk K, Özcan A, Uysal SA (2000) Geotraverse across NW Turkey: Tectonic units of the Central Sakarya Region and their tectonic evolution, in: Bozkurt E, Winchester JA and Piper JDA (eds) Tectonics and magmatism in Turkey and the surrounding area. Geol Soc Lond Sp Publ 173:139-161

Görür N, Oktay PY, Seymen İ, Şengör AMC (1984) Paleotectonic evolution of the Tuzgölü basin complex, central Turkey: sedimentary record of a Neotethyan closure, in: Dixon JE and Robertson AHF (eds) The geological evolution of the Eastern Mediterranean: Geol Soc Lond Sp Publ 17: 467-482

Görür N, Monod O, Okay Aİ, Şengör AMC, Tüysüz O, Yiğitbaş E, Sakınç M, Akkök R (1997) Paleogeographic and tectonic position of the Carboniferous rocks of the western Pontides (Turkey) in the frame of the Variscan belt. Bull Soc Géol Fr 168:197–205

Grieve PL (2009) NI43-101 Technical report on the Halilağa Exploration Property, Çanakkale, Western Turkey, March 2009

Gruen G, Heinrich C, Schroeder K (2010) The Bingham Canyon porphyry Cu-Mo-Au deposits. II. Vein geometry and ore shell formation by pressure-driven rock extension. Econ Geol 105:69–90

Guest B, Stockli DF, Grove M, Axen GJ, Lam PS, Hassanzadeh J (2006) Thermal histories from the central Alborz Mountains, northern Iran: implications for the spatial and temporal distribution of deformation in northern Iran. GSA Bull 118:1507–1521

Hall DJ, Foster RP, Yıldız B, Redwood SD (2007) The İnlice high-sulphidation epithermal gold discovery: defining a potential new gold belt in Turkey. In: Andrew CJ et al (eds) Proceedings of the 9th SGA Meeting. Dublin, Digging Deeper, pp 113–116

Handy MS, Schmid M, Bousquet R, Kissling E, Bernoulli D (2010) Reconciling plate-tectonic reconstructions of Alpine Tethys with the geological-geophysical record of spreading and subduction in the Alps. Earth Sci Rev 102:121–158

Harris AC, Holcombe RJ (2014) Quartz vein emplacement mechanisms at the E26 porphyry Cu-Au deposit, New South Wales. Econ Geol 109:1035–1050

Harris NB, Kelley S, Okay Aİ (1994) Post-collision magmatism and tectonics in northwest Anatolia. Contrib Mineral Petrol 11:241–252

Haschke MR, Ahmadian J, Murata M, McDonald I (2010) Copper mineralization prevented by arc-root delamination during Alpine-Himalayan collision in central Iran. Econ Geol 105:855–865

Hassanzadeh J, Stockli DF, Horton BK, Axen GJ, Stockli LD, Grove M, Schmitt AK, Walker JD (2008) U–Pb zircon geochronology of late Neoproterozoic-Early Cambrian granitoids in Iran: implications for paleogeography, magmatism, and exhumation history of Iranian basement. Tectonophysics 451:71–96

Hässig M, Rollanda Y, Sossona M, Galoyanb G, Sahakyan L, Topuz G, Çelik ÖF, Avagyan A, Müller C (2013) Linking the NE Anatolian and Lesser Caucasus ophiolites: evidence for large-scale obduction of oceanic crust and implications for the formation of the Lesser Caucasus-Pontides Arc. Geodin Acta 26:311–330

Heinrich C, Neubauer F (2002) Cu-Au-Pb-Zn-Ag metallogeny of the Alpine-Balkan-Carpathian-Dinaride geo-dynamic province. Miner Deposita 37:533–540

Hempton MR (1985) Structure and deformation history of the Bitlis Suture near Lake Hazar, SE Turkey. GSA Bull 96:223–243

Hollings P, Cooke D, Clark A (2005) Regional geochemistry of Tertiary igneous rocks in central Chile: implications for the geodynamic environment of giant porphyry copper and epithermal gold mineralization. Econ Geol 100:887–904

Holm RJ, Spandler C, Richards SW (2013) Melanesian arc far-field response to collision of the Ontong Java Plateau: geochronology and petrogenesis of the Simuku Igneous Complex, New Britain, Papua New Guinea. Tectonophysics 603:189–212

Hou ZQ, Cook NJ (2009) Metallogenesis of the Tibetan Collisional Orogen: a review and introduction to the special issue. Ore Geol Rev 36:2–24

Hou ZQ, Ma HW, Zaw K, Zhang YQ, Wang MJ, Wang Z, Pan GT, Tang RL (2003) The Himalayan Yulong porphyry copper belt: product of large-scale strike-slip faulting in eastern Tibet. Econ Geol 98:125–145

Hou ZQ, Gao YF, Qu XM, Rui ZY, Mo XX (2004) Origin of adakitic intrusives generated during mid-Miocene east–west extension in southern Tibet. Earth Planet Sci Lett 220:139–155

Hou Z, Yang Z, Qu X, Meng X, Li Z, Beaudoin G, Rui Z, Gao Y, Zaw K (2009) The Miocene Gangdese porphyry copper belt generated during post-collisional extension in the Tibetan Orogen. Ore Geol Rev 36:25–51

Hou Z, Zhang H, Pan X, Yang Z (2011) Porphyry Cu (-Mo-Au) deposits related to melting of thickened mafic lower crust: examples from the eastern Tethyan metallogenic domain. Ore Geol Rev 39:21–45

Houston RA, Dilles JH (2013) Structural geologic evolution of the Butte district, Montana. Econ Geol 108:1397–1424

İmer A, Richards JP, Creaser RA (2013) Age and tectonomagmatic setting of the Eocene Çöpler-Kabataş magmatic complex and porphyry-epithermal Au deposit, East Central Anatolia, Turkey. Miner Depos 48:557–583

İmer A, Richards JP, Creaser RA, Spell TL (2015) The late Oligocene Cevizlidere Cu-Au-Mo deposit, Tunceli Province, eastern Turkey. Miner Depos 50:245–263

Innocenti F, Agostini S, Di Vincenzo G, Doglioni C, Manetti P, Savaşçın MY, Tonarini S (2005) Neogene and quaternary volcanism in western Anatolia: magma sources and geodynamic evolution. Mar Geol 221:397–421

Işık V, Tekeli O (2001) Late orogenic crustal extension in the northern Menderes Massif (western Turkey): evidence for metamorphic core complex formation. Int J Earth Sci 89:757–765

Jackson J (1994) Active tectonics of the Aegean region. Annu Rev Earth Planet Sci 22:239–271

Jolivet L (2001) A comparison of geodetic and finite strain pattern in the Aegean, geodynamic implications. Earth Planet Sci Lett 187:95–104

Jun Lu Y, Loucks RR, Fiorentini ML (2013) Genesis of fertile hydrous adakite-like melts in post-subduction porphyry Cu systems of Tibet: metallogenesis of collisional orogens in the Tethyside domain, 12th SGA Biennial Meeting Proceedings 3: 1443-1446

Juras S, Miller R, Skyman P (2010) Technical Report for the Kışladağ Gold Mine. Prepared for Eldorado Gold, 120p

Karacık Z, Yılmaz Y, Pearce JA, Ece ÖI (2007) Petrochemistry of the south Marmara granitoids, northwest Anatolia, Turkey. Int J Earth Sci 97:1181–1200

Karslı O, Chen B, Aydın F, Şen C (2007) Geochemical and Sr–Nd–Pb isotopic compositions of the Eocene Dölek and Sarıçiçek Plutons, Eastern Turkey: implications for magma interaction in the genesis of high-K calc-alkaline granitoids in a post-collision extensional setting. Lithos 98:67–96

Karslı O, Dokuz A, Uysal İ, Aydın F, Kandemir R, Wijbrans J (2010) Generation of the Early Cenozoic adakitic volcanism by partial melting of mafic lower crust, Eastern Turkey: implications for crustal thickening to delamination. Lithos 114:109–120

Kay SM, Godoy E, Kurtz A (2005) Episodic arc migration, crustal thickening, subduction erosion, and magmatism in the south-central Andes. GSA Bull 117:67–88

Kaygusuz A, Chen B, Aslan Z, Siebel W, Şen C (2009) U-Pb SHRIMP zircon ages, geochemical and Sr-Nd isotopic compositions of the late cretaceous I-type Sarıosman Pluton, eastern Pontides, NE Turkey. Turk J Earth Sci 18:549–581

Kaygusuz A, Arslan M, Siebel W, Şen C (2011) Geochemical and Sr-Nd Isotopic characteristics of post-collisional calc-alkaline volcanics in the eastern Pontides (NE Turkey). Turk J Earth Sci 20:137–159

Kaymakçı N, İnceöz M, Ertepınar P (2006) 3D-architecture and neogene evolution of the Malatya Basin: inferences for the kinematics of the Malatya and Ovacık fault zones. Turk J Earth Sci 15:123–154

Kaymakçı N, Özçelik Y, White SH, van Dijk PM (2009) Tectono-stratigraphy of the Çankırı Basin: late Cretaceous to early Miocene evolution of the Neotethyan suture zone in Turkey. In: van Hinsbergen DJJ, Edwards MA, Govers R (eds) Collision and collapse at the Africa-Arabia-Eurasia subduction zone, Geol Soc Lond Sp Publ, vol 313, pp 67–106

Kaymakçı N, İnceöz M, Ertepınar P, Koç A (2010) Late Cretaceous to recent kinematics of SE Anatolia (Turkey). Geol Soc Lond Spl Publ 340:409–435

Keskin M (2003) Magma generation by slab steepening and break off beneath a subduction-accretion complex: an alternative model for collision-related volcanism in eastern Anatolia, Turkey. Geophys Res Lett 30:8046. https://doi.org/10.1029/2003GL018019

Keskin M, Genç SC, Tüysüz O (2008) Petrology and geochemistry of post-collisional Middle Eocene volcanic units in North-Central Turkey: evidence for magma generation by slab break-off following the closure of the Northern Neotethys Ocean. Lithos 104:267–305

Ketin İ (1966) Anadolu'nun (Küçük Asya) tektonik birlikleri. [*Tectonic units of Anatolia (Asia Minor)*]. Bull Mineral Res Explor (MTA) Turk 66:20–34 (in Turkish with English abstract)

Kociumbas M, Page RH (2009) The Cevizlidere porphyry deposit, Tunceli Province, Turkey. Technical report by Watts, Griffis and McQuat Limited for Anatolia Minerals Development Limited, 94p.

Kolb M, von Quadt A, Peytcheva I, Heinrich CA, Fowler SJ, Cvetkovic V (2013) Adakite-like and normal arc magmas: distinct fractionation paths in the eastern Eastern Serbian segment of the Balkan-Carpathian arc. J Petrol 54:167–170

Köprübaşı N, Aldanmaz E (2004) Geochemical constraints on the petrogenesis of Cenozoic I-type granitoids in northwest Anatolia, Turkey: evidence for magma generation by lithospheric delamination in a post-collisional setting. Int Geol Rev 46:705–729

Kouzmanov K, Pokrovski G (2012) Hydrothermal controls on metal distribution in porphyry Cu (-Mo-Au) systems. Sp Publ Soc Econ Geol 16:573–618

Kouzmanov K, Moritz R, von Quadt A, Chiradia M, Peytcheva I, Fontignie D, Ramboz C, Bogdanov K (2009) Late Cretaceous porphyry Cu and epithermal Cu-Au association in the Southern Panagyurishte district, Bulgaria: the paired Vlaykov Vruh and Elshitsa deposits. Miner Depos 44:611–646

Kuşcu İ (2009) Metallogenesis of the Tethyan Collage: Magmatic association and age of ore deposition in Turkey, MDRU-Industry collaborative initiative, Project report: Update to sponsor companies, MDRU contribution No. 269, 38p

Kuşcu İ, Gençalioğlu-Kuşcu G, Tosdal RM, Ullrich T, Friedman R (2010) Magmatism in the southeastern Anatolian orogenic belt: transition from arc to post-collisional setting in an evolving orogen. In: Stephenson RA, Kaymakçı N, Sosson M, Starostenko V, Bergerat F (eds) Sedimentary basin tectonics from the Black Sea and Caucasus to the Arabian Platform, Geol Soc Lond Sp Publ, vol 340, pp 437–460

Kuşcu İ, Yılmazer E, Bayır S, Sezerer-Kuru G, Güleç N, Demirela G, Gençalioğlu-Kuşcu G, Kaymakçı N (2011) U-Pb and Ar-Ar age dating and fluid inclusion constraints on the genesis of Hasançelebi iron oxide-copper-(gold) mineralization, Malatya (Turkey). Econ Geol 106:261–288

Kuşcu İ, Gençalioğlu-Kuşcu G, Tosdal RM, Friedman R (2012) The geochronology of gold-copper deposition, temporal association with magmatic rocks and petrochemical controls in Western Anatolia, Turkey, IESCA-2012 International Earth Science Colloquium on the Aegean Region, İzmir, Turkey, 2012, Abstracts, 151

Kuşcu İ, Tosdal RM, Gençalioğlu-Kuşcu G, Friedman R, Ullrich TD (2013) Late Cretaceous to Middle Eocene magmatism and metallogeny of a portion of the Southeastern Anatolian Orogenic Belt, east central Turkey. Econ Geol 108:641–666

Kuşcu İ, Tosdal RM, Gençalioğlu-Kuşcu G (2018) Episodic Porphyry Cu (-Mo-Au) Formation and Associated Magmatic Evolution in Turkish Tethyan collage. Ore Geol Rev (in review)

Lang JR, Titley SR (1998) Isotopic and geochemical characteristics of Laramide magmatic systems in Arizona and implications for the genesis of the genesis of porphyry copper deposits. Econ Geol 93:138–170

Le Pichon XN, Angelier J (1979) The Hellenic arc and trench system: a key to the neotectonic evolution of the eastern Mediterranean area. Tectonophysics 60:1–42

Lehmann B, Zhao X, Zhou M, Du A, Mao J, Zeng P, Henjes-Kunst F, Heppepage K (2013) Mid Silurian back-arc spreading at the northeastern margin of Gondwana: The Dapingzhang dacite-

hosted massive sulfide deposit, Lancangjiang zone, southwestern Yunnan, China. Gondwana Res 24:648–663
Lips ALW, Herrington JR, Stein G, Kozelj D, Popov K, Wijbrans RJ (2004) Refined timing of porphyry copper formation in the Serbian and Bulgarian portions of the Cretaceous Carpatho-Balkan Belt. Econ Geol 99:601–609
Liu L, Zhang JF, Green HW II, Jin ZM, Bozhilov KN (2007) Evidence of former stishovite in metamorphosed sediments, implying subduction to ~350 km. Earth Planet Sci Lett 263:180–191
Loucks RR (2014) Distinctive composition of copper-ore-forming arc magmas. Aust J Earth Sci 61:5–16
Mao J, Pirajno F, Lehmann B, Luo M, Berzina A (2014) Distribution of porphyry deposits in the Eurasian continent and their corresponding tectonic settings. Asian J Earth Sci 79:576–584
Marek JM, Moores RC, Pennstrom WJ, Reynolds T (2008) Technical report, Çöpler gold project: independent mining Consultants report to Anatolia minerals. Development, 132 p
Márton I, Moritz R, Spikings R (2010) Application of low-temperature thermochronology to hydrothermal ore deposits: formation, preservation and exhumation of epithermal gold systems from the Eastern Rhodopes, Bulgaria. Tectonophysics 483:240–254
McInnes IA, Evans NJ, Fu FQ, Garwin S, Belousova E, Griffin WL, Bertens A, Sukarna D, Permanadewi S, Andrew RL, Deckart K (2005) Thermal history analysis of selected Chilean, Indonesian and Iranian porphyry Cu-Au-Mo deposits, In: Porter TM (ed) Super porphyry copper and gold deposits: a global perspective: Adelaide, PGC Publishing, 1: 27-42
McKenzie D (1972) Active tectonic of the Mediterranean region. Geophys J Int 30:109–185
Meulenkamp JE, Wortel MJR, Van Wamel WA, Spakman W, Hoogerduyn-Starting E (1988) On the Hellenic subduction zone and the geodynamic evolution of Crete since the late Middle Miocene. Tectonophysics 146:203–216
Mitchell AHG (1973) Metallogenic belts and angle of dip of Benioff zones. Nature 245:49–52
Moix P, Beccaletto L, Kozur HW, Hochard C, Rosselet F, Stampfli GM (2008) A new classification of the Turkish terranes and sutures and its implication for the paleotectonic history of the region. Tectonophysics 451:7–39
MTA (1980) Türkiye Maden Envanteri. [*Mineral deposit inventory of Turkey*] MTA Publ, No. 179, 571 p (in Turkish with English abstract)
Murakami H, Watanabe Y, Stein H (2005) Re–Os ages for molybdenite from the Tepeoba breccia-centered Cu-Mo-Au deposit, western Turkey: Brecciation triggered mineralization, in: Mao J and Bierlein FP (eds) Mineral deposit research: Meeting the global challenge, Proceedings of the Eighth Biennial SGA Meeting, Beijing, China, 2005 1: 805-808
Neubauer F, Heinrich C (2003) Late Cretaceous and Tertiary geodynamics and ore deposit evolution of the Alpine-Balkan-Carpathian-Dinaride orogeny. In: Eliopoulos et al (eds) Proceedings mineral exploration and sustainable development, vol 1133–1136
Oberhänsli R, Candan O, Wilke FDH (2010) Geochronological evidence of Pan-African eclogites from the Central Menderes massif. Turk J Earth Sci 19:431–447
Ohta E, Doğan R, Batik H, Abe M (1988) Geology and mineralization of Dereköy porphyry copper deposit, Northern Thrace, Turkey. Bull Geol Soc Jpn 39:115–134
Okay Aİ (1984) Distribution and characteristics of the northwest Turkish blueschists. In: Dixon JE, AHF R (eds) The geological evolution of the eastern Mediterranean, Geol Soc Sp Publ, vol 17, pp 455–466
Okay Aİ, Göncüoğlu MC (2004) The Karakaya Complex: a review of data and concepts. Turk J Earth Sci 13:77–95
Okay A, Monie P (1997) Early Mesozoic subduction in the eastern Mediterranean: evidence from Triassic eclogite in northwest Turkey. Geology 25:595–598
Okay Aİ, Satır M (2000) Coeval plutonism and metamorphism in a latest Oligocene metamorphic core complex in northwest Turkey. Geol Mag 137:495–516
Okay Aİ, Satır M (2006) Geochronology of Eocene plutonism and metamorphism in northwest. Geodin Acta 19:251–266

Okay Aİ, Tüysüz O (1999) Tethyan sutures of northern Turkey. In: Durans B, Jolivet L, Horvarth F, Seranne M (eds) The Mediterranean basins: tertiary extension within the Alpine Orogen, Geological Society special publications, vol 156. Geological Society, London, pp 475–515

Okay Aİ, Siyako M, Bürkan KA (1991) Geology and tectonic evolution of the Biga Peninsula, northwest Turkey. Bull Tech Univ İstanbul 44:191–256

Okay Aİ, Satır M, Maluski H, Siyako M, Monié P, Metzger R, Akyüz S (1996) Paleo- and Neo-Tethyan events in northwestern Turkey: geologic and geochronologic constraints. In: Yin A, Harrison TM (eds) The tectonic evolution of Asia. Cambridge University Press, Cambridge, pp 420–441

Okay Aİ, Şahintürk Ö, Yakar H (1997) Stratigraphy and tectonics of the Pulur (Bayburt) region in the Eastern Pontides. Bull Min Res Exp 119:1–24

Okay AI, Satır M, Tüysüz O, Akyüz S, Chen F (2001) The tectonics of the strandja massif: late-variscan and mid-mesozoic deformation and metamorphism in the northern aegean. Int J Earth Sci 90:217–233

Okay Aİ, Satır M, Siebel W (2006) Pre-Alpide orogenic events in the Eastern Mediterranean region: European lithosphere dynamics. Geol Soc Lond Mem 32:389–405

Okay Aİ, Satır M, Zattin M, Cavazza W, Topuz G (2008) An Oligocene ductile strike-slip shear zone: the Uludağ Massif, northwest Turkey-Implications for the westward translation of Anatolia. GSA Bull 120:893–911

Okay Aİ, Satır M, Zattin M, Cavazza W, Topuz G (2011) Oligocene dextral strike-slip faulting in Anatolia: an early escape. American Geophysical Union, Fall Meeting 2011, abstract vol. no. T31F-06

Önal A, Boztuğ D, Kürüm S, Harlavan Y, Arehart G, Arslan M (2005) K-Ar age determination, whole-rock and oxygen isotope geochemistry of the post-collisional Bizmişen and Çaltı plutons, SW Erzincan, eastern Central Anatolia, Turkey. Geol J 40:457–476

Önen AP (2003) Neotethyan ophiolitic rocks of the Anatolides of NW Turkey and comparison with Tauride ophiolites. J Geol Soc Lond 160:947–962

Önen AP, Hall R (1993) Ophiolites and related metamorphic rocks from the Kütahya region, northwest Turkey. Geol J 28:399–412

Özacar A, Gilbert H, Zandt G (2008) Upper mantle discontinuity structure beneath East Anatolian Plateau (Turkey) from receiver functions. Earth Planet Sci Lett 269:426–434

Özacar AA, Zandt G, Gilbert H, Beck SL (2010) Seismic images of crustal variations beneath the East Anatolian Plateau (Turkey) from teleseismic receiver functions. In: Stephenson RA, Kaymakçı N, Sosson M, Starostenko V, Bergerat F (eds) Sedimentary basin tectonics from the Black Sea and Caucasus to the Arabian Platform, Geol Soc Lond Sp Publ, vol 340, pp 485–496

Papanikolaou DJ, Demirtaşlı E (1987) Geological correlations between the Alpine segments of the Hellenides-Balkanides and Taurides-Pontides. In: Flügel HW, Sassi FP, Grecula P (eds) Pre-Variscan and Variscan events in the Alpine-Mediterranean mountain belts. Alfa Publishers, Bratislava, pp 387–396

Parlak O (2005) Geodynamic significance of granitoid magmatism in the southeast Anatolian orogen: geochemical and geochronological evidence from Göksun-Afşin (Kahramanmaraş, Turkey) region. Int J Earth Sci 95:609–627

Parlak O (2007, April) Petrology of NeoTethyan ophiolites in Turkey: Diverse magma types and their tectonic significance: European Geosciences Union General Assembly, Vienna-Austria. Geophys Res Abstr 9: 00407.

Perello J, Carlotto V, Zarate A, Ramos P, Posso H, Neyra C, Caballero A, Fuster N, Muhr R (2003) Porphyry-style alteration and mineralization of the Middle Eocene to early Oligocene Andahualas-Yauri belt, Cuzco region, Peru. Econ Geol 98:1575–1606

Pickett EA, Robertson AHF (1996) Formation of the Late Paleozoic–Early Mesozoic Karakaya Complex and related ophiolites in NW Turkey by Paleotethyan subduction-accretion. J Geol Soc Lond 153:995–1009

Régnier JL, Ring U, Passchier CW, Gessner K, Güngör T (2003) Contrasting metamorphic evolution of metasedimentary rocks from the Çine and Selimiye nappes in the Anatolide belt, western Turkey. J Metamorph Geol 21:699–721

Reilinger RE, McClusky SC, Oral MB, King W, Toksöz MN (1997) Global Positioning System measurements of present-day crustal movements in the Arabia-Africa-Eurasia plate collision zone. J Geophys Res 102:9983–9999

Rice SP, Roberson AHF, Ustaömer T, İnan T, Taşlı K (2009) Late Cretaceous-early Eocene tectonic development of the Tethyan suture zone in the Erzincan area, eastern Pontides, Turkey. Geol Mag 146:567–590

Richards JP (2003) Tectono-magmatic precursors for porphyry Cu–(Mo–Au) deposit formation. Econ Geol 98:1515–1533

Richards JP (2009) Post-subduction porphyry Cu-Au and epithermal Au deposits: products of remelting of subduction-modified lithosphere. Geol Soc Am 37:247–250

Richards JP (2011) Magmatic to hydrothermal metal fluxes in convergent and collided margins. Ore Geol Rev 40:1–26

Richards JP (2013) Tectonic controls on the formation of major ore deposit types, with focus on convergent and collisional margins: GSA Annual Meeting in Denver. Geol Soc Am Abstr Programs 45:297

Richards JP (2015) Tectonic, magmatic, and metallogenic evolution of the Tethyan orogen: from subduction to collision. Ore Geol Rev 70:323–345

Richards JP, Kerrich R (2007) Adakite-like rocks: their diverse origins and questionable role in metallogenesis. Econ Geol 102:537–576

Richards JP, Boyce AJ, Pringle MS (2001) Geological evolution of the Escondida area, northern Chile: a model for spatial and temporal localization of porphyry Cu mineralization. Econ Geol 96:271–305

Richards JP, Wilkinson D, Ullrich T (2006) Geology of the Sarı Günay epithermal gold deposit, northwest Iran. Econ Geol 101:1455–1496

Richards JP, Spell T, Rameh E, Razique A, Fletcher T (2012) High Sr/Y magmas reflect arc maturity, high magmatic water content, and porphyry Cu±Mo±Au potential: examples from the Tethyan arcs of central and eastern Iran and western Pakistan. Econ Geol 107:295–332

Rimmelé G, Oberhänsli R, Goffé B, Jolivet L, Candan O, Çetinkaplan M (2003) First evidence of high-pressure metamorphism in the "Cover Series" of the southern Menderes massif. Tectonic and metamorphic implications for the evolution of SW Turkey. Lithos 71:19–46

Ring U, Johnson C, Hetzel R, Gessner K (2003) Tectonic denudation of a Late Cretaceous–Tertiary collisional belt: regionally symmetric cooling patterns and their relation to extensional faults in the Anatolide belt of western Turkey. Geol Mag 140:421–441

Ring U, Glodny J, Will T, Thomson SN (2010) The Hellenic subduction system: highpressure metamorphism, exhumation, normal faulting, and large-scale extension. Annu Rev Earth Planet Sci 38:45–76

Robertson AHF (1998) Mesozoic-Cenozoic tectonic evolution of the easternmost Mediterranean area: integration of marine and land evidence In: Robertson AHF, Emeis KC, Camerlenghi A (eds) Proceedings of the Ocean Drilling Program, Scientific Results, College Station, Texas, vol 160. pp 723–782

Robertson AHF, Dixon DE (1984) Introduction: aspects of the geological evolution of the eastern Mediterranean. In: Dixon JE, Robertson AHF (eds) The geological evolution of the eastern Mediterranean, Geol Soc Lond Sp Publ, vol 17, pp 1–74

Robertson AHF, Parlak O, Rızaoğlu T, Ünlügenç UC, İnan N, Taşlı K, Ustaömer T (2007) Tectonic evolution of the south Tethyan ocean: evidence from the eastern Taurus Mountains (Elazığ region, SE Turkey). Geol Soc Lond Sp Publ 272:231–270

Robinson AG, Banks CJ, Rutherford MM, Hirst JPP (1995) Stratigraphic and structural development of the Eastern Pontides, Turkey. J Geol Soc Lond 152:861–872

Rolland Y, Billo S, Corsini M, Sosson M, Galoyan G (2009) Blueschists of the Amassia–Stepanavan Suture Zone (Armenia): linking Tethys subduction history from E-Turkey to W-Iran. Int J Earth Sci 98:533–550

Rolland Y, Perinçek D, Kaymakçı N, Sosson M, Barrier E, Avagyan A (2011) Evidence for 80–75 Ma subduction jump during Anatolide–Tauride–Armenian block accretion and 48 Ma Arabia-Eurasia collision in Lesser Caucasus–East Anatolia. J Geodyn 56–57:76–85

Rosenbaum G, Lister GS, Duboz C (2002) Reconstruction of the tectonic evolution of the western Mediterranean since the Oligocene. In: Rosenbaum G, Lister GS (eds) Reconstruction of the evolution of the Alpine-Himalayan Orogen. J Virtual Exp 8:107–130

Royden LH (1993) Evolution of retreating subduction boundaries formed during continental collision. Tectonics 12:629–638

Sanchez SMG (2012) Tectonics of the Biga peninsula and implications on Cu-Au porphyry and epithermal Au deposits, northwestern Anatolia, Turkey: Unpublished PhD Thesis, London, UK, University of London

Sarı R, Küçükefe S, Avşar M, Eyüpoğlu M, Metin S (2014) Gökçeada'nın (Çanakkale) Au, As, Cu, Pb, Zn ve Mo Jeokimyası. [Au, As, Cu Pb, zn and Mo geochemistry of Gökçeada (Çanakkale)] MTA Doğal Kaynaklar ve Ekonomi Bull no, 17 175p (in Turkish)

Satır M, Friedrichsen H (1986) The origin and evolution of the Menderes Massif, West Turkey; A Rb/Sr and oxygen isotope study. Geol Rundsch 75(3):703–714

Savostin LA, Sibuet JC, Zonenshain LP, Le Pichon X, Rolet J (1996) Kinematic evolution of the Tethys belt, from the Atlantic to the Pamirs since the Triassic. Tectonophysics 123:1–35

Schuiling RD (1959) Uber eine Pre-Herzynische Faltungs-phase im Kazdag Kristaalin. Bull Min Res Exp 53:89–93

Schuiling RD (1962) On petrology, age and evolution of the Menderes Massif, West Turkey: a rubidium/strontium and oxygen isotope study. Bull Min Res Exp 58:703–714

Seedorff E, Dilles JH, Proffett JM Jr, Einaudi MT, Zurcher L, Stavast WJA, Johnson DA, Barton MD (2005) Porphyry deposits: characteristics and origin of hypogene features. Econ Geol 100th Anniversary Volume:251–298

Şengör AMC (1979) Geometry and kinematics of continental deformation in zones of collision: examples from central Europe and eastern Mediterranean: unpublished MSc Thesis, State University of New York at Albany

Şengör AMC (1987) Tectonics of the Tethysides: orogenic collage development in a collisional setting. Annu Rev Earth Planet Sci 15:213–244

Şengör AMC, Yılmaz Y (1981) Tethyan evolution of Turkey: a plate tectonic approach. Tectonophysics 75:181–241

Şengör AMC, Satır M, Akkök R (1984) Timing of tectonic events in the Menderes massif, western Turkey: implications for tectonic evolution and evidence for Pan-African basement in Turkey. Tectonics 3:693–707

Şengör AMC, Özeren S, Genç T, Zor E (2003) East Anatolian high plateau as a mantle-supported, North–south shortened domal structure. Geophys Res Lett 30:8045

Shafiei B, Haschke M, Shahabpour J (2009) Recycling of orogenic arc crust triggers porphyry Cu mineralization in Kerman Cenozoic arc rocks, southeastern Iran. Miner Depos 44:265–283

Sherlock S, Kelley SP, Inger S, Harris N, Okay Aİ (1999) ^{40}Ar-^{39}Ar and Rb-Sr geochronology of high-pressure metamorphism and exhumation history of the Tavşanlı Zone, NW Turkey. Contrib Mineral Petrol 137:46–58

Sillitoe RH (1972) A plate tectonic model for the origin of porphyry copper deposits. Econ Geol 67:184–197

Sillitoe R (2010) Porphyry copper systems. Econ Geol 105:3–41

Sillitoe RH, Perelló J (2005) Andean copper province: tectonomagmatic settings, deposit types, metallogeny, exploration, and discovery. Econ Geol 100:845–890

Singer DA, Berger VI, Menzie WD, Berger BR (2005) Porphyry copper deposit density. Econ Geol 100:491–514

Singer DA, Berger VI, Moring C (2008) Porphyry copper deposits of the world: database and 928 grade and tonnage models, 2008. U.S. Geological Survey Open-File Report 2008-1155, 45 p

Smith MT, Lepore WA, İncekaraoğlu T, Shabestari P, Boran H, Raabe K (2014) Küçükdağ: a new, high sulfidation epithermal Au-Ag-Cu deposit at the Tv tower property in western Turkey. Econ Geol 109:1501–1511

Sosson M, Rolland Y, Müller C, Danelian T, Melkonyan R, Kekelia S, Adamia S, Babazadeh V, Kangarli T, Avagyan A, Galoyan G, Mosar J (2010) Subductions, obduction and collision in the Lesser Caucasus (Armenia, Azerbaijan, Georgia), new insights. Geol Soc Lond Spec Publ 340:329–352

Soylu M (1999). Modelling of porphyry copper mineralization of the eastern Pontides. Ph. D. Dissertation Thesis (unpublished), Middle East Technical University, Ankara, Turkey, 127p

Soylu M, Kuşcu İ, Gençalioğlu-Kuşcu G (2003) Post-collisional H-type granitoid magmatism in central Anatolia and time-space relation with Fe-oxide mineralization. Mineral Exploration and Sustainable Development, 7th Biennial SGA Meeting, Athens, Greece, p 307

Stampfli GM (2001) Tethyan oceans, in: Bozkurt E, Winchester JA and Piper JDA (eds) Tectonics and magmatism in Turkey and the surrounding area. Geol Soc Lond Sp Publ 173: 1-23

Stampfli GM, Borel GD (2002) A plate tectonic model for the Paleozoic and Mesozoic constrained by dynamic plate boundaries and restored synthetic oceanic isochrones. Earth Planet Sci Lett 1096:17–33

Stampfli GM, Borel GD (2004) The TRANSMED transects in space and time: Constraints on the paleotectonic evolution of the Mediterranean domain. In: Cavazza W, Roure F, Spakman W, Stampfli GM, Ziegler P (eds) The TRANSMED Atlas: the Mediterranean Region from Crust to Mantle. Springer Verlag, Berlin, pp 53–80

Stampfli GM, Kozur HW (2006) Europe from the Variscan to the Alpine cycles. In: Gee DG, Stephenson RA (eds) European lithosphere dynamics, Mem Geol Soc Lond, pp 57–82

Sunal G, Natalin BA, Satır M, Toraman E (2006) Paleozoic magmatic events in the Strandja massif, NW Turkey. Geodin Acta 19:283–300

Taylor RP (1981) Isotope geology of the Bakırçay porphyry copper prospect, Northern Turkey. Miner Depos 16:375–390

Taymaz T, Yılmaz Y, Dilek Y (2007) The geodynamics of the Aegean and Anatolia: Introduction, in: Taymaz T, Yılmaz Y and Dilek Y (eds) The Geodynamics of the Aegean and Anatolia. J Geol Soc Lond Sp Publ 29: 1-16

Temizel İ, Arslan M (2009) Mineral chemistry and petrochemistry of post-collisional Tertiary mafic to felsic cogenetic volcanics in the Ulubey (Ordu) area, eastern Pontides, NE Turkey. Turk J Earth Sci 18:29–53

Terashima S, Taner MF, Yjima J, Ishihara S (1988) Geochemistry of the Pontides granotoids in Turkey. Bull Geol Surv Jpn 39:251–268

Tirel C, Gautier P, van Hinsbergen DJJ, Wortel MJR (2009) Sequential development of metamorphic core complexes: numerical simulations and comparison to the Cyclades, Greece, in: van Hinsbergen DJJ, Edwards MA and Govers R (eds) Collision and collapse at the Africa-Arabia-Eurasia subduction zone. Geol Soc Lond Sp Publ 311: 257–292

Titley SR, Beane RE (1981) Porphyry copper deposits, part 1: geologic setting, petrology and tectogenesis. Econ Geol 75:214–269

Topuz G, Okay Aİ, Altherr R, Schwarz WH, Siebel W, Zack T, Satır M, Şen C (2011) Post-collisional adakite-like magmatism in the Ağvanis Massif and implications for the evolution of the Eocene magmatism in the Eastern Pontides (NE Turkey). Lithos 125:131–150

Tosdal RM (2012) Structural controls on and exploration for porphyry Cu deposits: AIG conference, Structural Geology and Resources 2012, Kalgoolie 164-166

Tosdal RM, Richards JP (2001) Magmatic and structural controls on the development of porphyry Cu±Mo±Au deposits. Rev Econ Geol 14:157–181

Tosdal RM, Dilles JH, Cooke DR (2009) From source to sinks in auriferous magmatic-hydrothermal porphyry and epithermal deposits. Elements 5:289–295

Tosdal RM, Márton I, Strmbanović I, van der Toorn J, Davidović D, Knaak M, Hasson (2015) Two suites of plutonic rocks associated with hydrothermal ore deposits in the north-western Timok Magmatic. Complex: 13th SGA Biennieal Meeting 2015, Mineral Resources in a Sustainable World, 1: 369-372

Tüfekçi MŞ, Dumanlılar Ö (1994) Malatya-İspendere ve Elazığ-Baskil-Nazaruşağı arasında görülen cevherleşmelerin genel görünümü ve maden jeolojisi çalışma raporu. [General characteristics and geology of the ore deposits located between Malatya-İsoendere-Nazaruşağı] MTA Report no. 9739, Ankara (unpublished, in Turkish)

Tüysüz O, Dellaloğlu AA, Terzioğlu N (1995) A magmatic belt within the Neo-Tethyan suture zone and its role in the tectonic evolution of northern Turkey. Tectonophysics 243:173–191

Ustaömer T, Robertson AHF (1996) Paleotethyan tectonic evolution of the North Tethyan margin in the central Pontides, N Turkey. In: Erler A, Ercan T, Bingöl E, Örçen S (eds) International symposium on the geology of the Black Sea Region, Proceedings-I, 24-3

van der Toorn J, Davidovic D, Hadjieva N, Strbanovic I, Marton I, Knaak M, Tosdal RM, Davis B, Hasson S (2013) A new sedimentary rock-hosted gold belt in eastern Serbia.12th Biennial SGA Meeting: mineral deposit research for a high-tech world. Proceedings 2: 691-694

van Hinsbergen D, Schmid SM (2012) Map view restoration of Aegean-west Anatolian accreation and extension since the Eocene. Tectonics.31: TC5005.

van Hinsbergen D, Kaymakçı N, Spakman W, Torsvik TH (2010) Reconciling the geological history of western Turkey with plate circuits and mantle tomography. Earth Planet Sci Lett 297:674–686

Vergili Ö, Taptık MA, Çakır C, Öcal H (2013) Ülkemizde bir ilk; Okyanusal yayda keşfedilen Hüyüklü porfiri Cu Mo yatağı, Afşin, Kahramanmaraş, Türkiye. [Firt of its kind in the country: discovery of an island-arc related porphyry Cu-Mo deposit, Afşin, Kahramanmaraş] MTA Doğal Kaynaklar ve Ekonomi Bull 16: 270 p [in Turkish]

von Quadt A, Moritz R, Peytcheva I, Heinrich CA (2005) Geochronology and geodynamics of Late Cretaceous magmatism and Cu–Au mineralization in the Panagyurishte region of the Apuseni-Banat-Timok-Srednogorie belt, Bulgaria. Ore Geol Rev 27:95–126

Voudouris P, Melfos V, Spry PG, Bindi L, Moritz R, Ortelli M, Kartals T (2013) Extremely Re-rich molybdenite from porphyry Cu-Mo-Au prospects in northeastern Greece: mode of occurrence, causes of enrichment, and implications for gold exploration. Fortschr Mineral 3:165–191

Wang R, Richards JP, Hou Z, Yang Z (2014) Extent of underthrusting of the Indian plate beneath Tibet controlled the distribution of Miocene porphyry Cu–Mo±Au deposits. Miner Depos 49:165–173

Whitney DL, Bozkurt E (2002) Metamorphic history of the southern Menderes massif, western Turkey. GSA Bull 114:829–838

Whitney DL, Teyssier C, Fayon AK, Hamilton MA, Heizler M (2003) Tectonic controls on metamorphism, partial melting, and intrusion; timing and duration of regional metamorphism and magmatism in the Niğde massif, Turkey. Tectonophysics 376:37–60

Wortel MJR, Spakman W (2000) Subduction and slab detachment in the Mediterranean-Carpathian region. Science 290:1910–1917

Yalçınalp B (1995) Güzelyayla (Maçka-Trabzon) Porfiri Cu-Mo cevherleşmesinin jeolojik yerleşimi ve jeokimyası. [Geology and geochemistry of the Güzelyayla (Maçka-Trabzon) porphyry Cu-Mo mineralization]. PhD Dissertation Thesis, Karadeniz Technical University, Turkey. 177 p (in Turkish with English abstract)

Yazgan E, Chessex R (1991) Geology and tectonic evolution of southeastern Taurus in the region of Malatya. Turk Assoc Petrol Geol Bull 3:1–42

Yiğit Ö (2009) Mineral deposits of Turkey in relation to Tetyhan metallogeny: implications for future mineral exploration. Econ Geol 104:19–51

Yiğit Ö (2012) A prospective sector in the Tethyan Metallogenic Belt: geology and geochronology of mineral deposits in the Biga Peninsula. Ore Geol Rev 46:118–148

Yiğitbaş E, Yılmaz Y (1996) New evidence and solution to the Maden complex controversy of the southeast Anatolian orogenic belt (Turkey). Int J Earth Sci 85:250–263

Yıldırım S, Ersoy H, Adıgüzel O, Katipoğlu B, Yıldız H (2001) Muratdere (Bozüyük-Bilecik) Porfiri Cu-Mo-(Au) sahasının jeoloji ve jeokimya raporu. [Geological and geochemical report on the Muratdere (Bozüyük-Bilecik) porphyry Cu-Mo-(Au) project]. MTA Report No: 10550 (in Turkish)

Yılmaz Y (1993) New evidence and model on the evolution of the southeast Anatolian orogen. GSA Bull 105:251–271

Yılmaz Y, Tüysüz O, Yiğitbaş E, Genç SC, Şengör AMC (1997) Geology and tectonic evolution of the Pontides**.** In: Robinson AG (ed) Regional and petroleum geology of the Black Sea and surrounding region. Chapter 11: geology and tectonic evolution of the Pontides. AAPG Mem 68:183–226

Yılmaz Y, Genç SC, Karacık Z, Altunkaynak Ş (2001) Two contrasting magmatic associations of NW Anatolia and their tectonic significance. J Geodyn 31:243–271

Yılmaz-Şahin S (2005) Transition from arc- to post-collision extensional setting revealed by K-Ar dating and petrology: an example from the granitoids of the eastern Pontide igneous terrane, Araklı-Trabzon, NE Turkey. Geol J 40:425–440

Zarasvandi A, Liaghat S, Zentilli M (2005) Geology of the Darreh-Zerreshk and Ali-Abad porphyry copper deposits, Central Iran. Int Geol Rev 47:620–646

Zhai M, Fan Q, Zhang H, Sui J, Shao J (2007) Lower crustal processes leading to Mesozoic lithospheric thinning beneath eastern North China: underplating, replacement and delamination. Lithos 96:36–54

Zhang LC, Xiao WJ, Qin KZ, Ji JS, Zhang Q (2006) The adakite connection of the Tuwa–Yandong copper porphyry belt, eastern Tianshan, NW China: trace element and Sr–Nd–Pb isotope geochemistry. Miner Depos 41:188–200

Zürcher L, Bookstrom AA, Hammarstrom JM, Mars JC, Ludington S, Zientek ML, Dunlap P, Wallis JC, with contributions from Drew LJ, Sutphin DM, Berger BR, Herrington RJ, Billa M, Kuşcu I, Moon CJ, Richards JP (2015) Porphyry copper assessment of the Tethys region of western and southern Asia: U.S. Geological Survey Scientific Investigations Report 2010-5090-V 232 p., and spatial data. doi:https://doi.org/10.3133/sir20105090V

Chapter 9
Volcanogenic Massive Sulfide (VMS) Deposits of Turkey

Emin Çiftçi

Abstract Volcanogenic massive sulfide (VMS) deposits of Turkey occur in three tectonically distinct regions: (I) Kuroko-type deposits in the eastern Pontides Tectonic belt (EPTB); (II) Cyprus-type VMS deposits occur both in Küre area (Kastamonu) and along the Bitlis-Zagros Suture Zone (BZSZ), and (III) Besshi-type VMS deposits in the Hanönü–Taşköprü area (Kastamonu).

The Kuroko type VMS deposits are all associated with Late Cretaceous felsic volcanics consisting mainly of dacitic and rhyolitic lavas and pyroclastics that outcrop within a narrow zone running parallel to eastern Black Sea coast and represent the axial zone of a paleo-magmatic arc. Subtypes of the deposits include Cu-, Zn-Cu-, Cu-Zn-, Zn-Pb-Cu metal associations. These deposits are typically mined for Cu, Zn, and Pb. Some of them may also contain significant gold (e.g. Cerattepe and Hod deposits - Artvin) and silver (e.g. Köprübaşı deposit - Giresun).

The Cyprus type deposits occuring along the BZSZ are all allochthonous and associated with mafic volcanics of supra-subduction ophiolites: (I) Middle Eocene Maden Complex – a pile of mafic volcanics, pelagic sediments with limestone blocks and (II) Late Triassic-Late Cretaceous Koçali Complex – a sequence of tectonically imbricated slices of pelagic rock suites, platform carbonates, clastic sediments, serpentinites, and mafic volcanics. Major occurences include Madenköy (Şirvan-Siirt) - currently the largest known VMS deposit in Turkey with about 40 Mt reserve and Maden (aka Ergani) (Maden-Elazığ) area deposits, both hosted by the Maden Complex and Ortaklar (Gaziantep) hosted by the Koçali Complex. The VMS deposits occurring in the Küre area are also allochthonous and are all hosted within mafic volcanics-black shales of Late Triassic Küre Complex, a fairly thick pile of thrust-imbricated deep-sea sediments, intercalated with a dismembered supra-subduction ophiolite. Major past and current producers include Aşıköy, Toykondu, Kızılsu, and Bakibaba deposits.

E. Çiftçi (✉)
Faculty of Mines, Department of Geological Engineering, Istanbul Technical University, Istanbul, Turkey
e-mail: eciftci@itu.edu.tr

F. Pirajno et al. (eds.), *Mineral Resources of Turkey*, Modern Approaches in Solid Earth Sciences 16, https://doi.org/10.1007/978-3-030-02950-0_9

The Besshi-type VMS deposits are fairly recent discoveries. They only occur in Hanönü-Taşköprü area and hosted by Akgöl Formation, which consists of low-grade metamorphic siliciclastic sedimentary rocks within the Middle Jurassic Çangaldağ Complex comprising ensimatic island arc volcanics and front-arc basin sediments, remnants of oceanic crust, and volcano-clastics. Major examples include Zeybek, Hanönü, Gökırmak, and past producer Cozoğlu deposits, which are typically low grade but may reach up to 25 Mt.

9.1 Introduction

Turkey lies on an orogenic belt, which is a cohesive part of one of the world's major orogenic belts, the Alpine-Himalayan belt. The Alpine-Himalayan belt that was formed during the Alpine orogeny, extends from the Alps in Europe, through the Carpathians, Anatolia, Caucasus, Zagros, and Alborz to the Himalayan ranges of northern India and southern China. The geological structure is the consequence of long-lived subduction, accretion and collision events associated with the closure of the Tethyan Ocean. During these events many favorable sites for ore deposition developed. Thus Anatolia is not only tectonically active but also has great potential for the formation of diverse ore deposits of various sizes and grades.

Viewed from scientific perspective, volcanogenic massive sulfide deposits (VMS) occupy a special position among the ore deposits. VMS deposits have a unique mineralogy, structure, and origin that distinguish them from other mineral systems. VMS deposits are strata-bound accumulations of sulfide minerals deposited at or near the seafloor in spatial, temporal, and genetic association with a contemporaneous volcanism. Thus the VMS deposits are partly or wholly syngenetic mineralizations. The VMS deposits generally consist of syngenetic concordant lenticular massive sulfide bodies in which sulfide minerals account for >60% and a discordant near vertical, vein-type stockwork (aka stringer) zones in the footwall rocks.

During the 1960s and 1970s, VMS deposits attracted enormous attention. After intense research during those two decades, it was found that they range in age from Archean to the present, are hosted by volcanic rocks, and usually revealed some evidence of submarine volcanic activity. The VMS deposits are a thoroughly studied deposit class. By the late 1980s, more than a thousand VMS deposits had been recognized. From the economic point of view, they are still major suppliers of Cu, Pb, Zn, Ag, and Au and rank second only to porphyry Cu-Mo-type deposits in economic importance among nonferrous metallic mineral deposits. The VMS deposits are significant sources for Co, Sn, Se, Mn, Cd, In, Bi, Te, Ga, and Ge. Some also contain significant amounts of As, Sb, and Hg. Although they have relatively modest reserves (generally less than 50 Mt), due to the high grades and diverse metal contents, they have always been highly favored by mining operations. Because of their polymetallic content, VMS deposits continue to be one of the most desirable deposit types for security against fluctuating metal prices.

The VMS deposits have been a major source of copper, to a lesser extent of zinc and lead and made important contributions to the economic development of Turkey over more than half a century. Examples include important past producers (e.g. Köprübaşı (Tirebolu-Giresun), Damar, Bognari, Çarkbaşı (Murgul-Artvin), Karaerik, Ağalık, Karılar deposits (Espiye-Giresun), Küre deposits (Kastamonu) and Maden deposits (Elazığ) (aka Ergani) and developing producers (e.g. Cerattepe and Hod deposits (Artvin) and Madenköy (Şirvan-Siirt). New discoveries with future production potential include Hanönü-Taşköprü area deposits (Kastamonu) and Ortaklar (Gaziantep).

The VMS deposits of Turkey are distributed in three distinct tectonic environments (Fig. 9.1). These deposits located in the Eastern Pontides, the Central Pontides and along the Bitlis-Zagros suture zone, have also made a substantial contribution to the understanding of regional and local controls on the formation of VMS mineral systems considering that the formation of some ore deposits require specific geochemical environments. For example, while the Eastern Pontide VMS deposits are associated with the felsic volcanics of the late Cretaceous age without exception and are formed within the axial zone of a paleo-arc, ophiolite-hosted VMS deposits of the Bitlis-Zagros suture zone, the boundary between Anatolian and Arabian plates in SE Turkey, are associated with mafic volcanics of the ophiolite sequence of Late Cretaceous age (66–100 Ma).

This chapter provides an overview for the regional-scale attributes including their tectonic settings, regional and local stratigraphic environments, mineralogical, geochemical characteristics, host-rock associations, and alteration patterns. It will review the potentials, past and current status and future potentials of the VMS deposits of Turkey, and will place these deposits in the context of modern classifications and their tectonic environments.

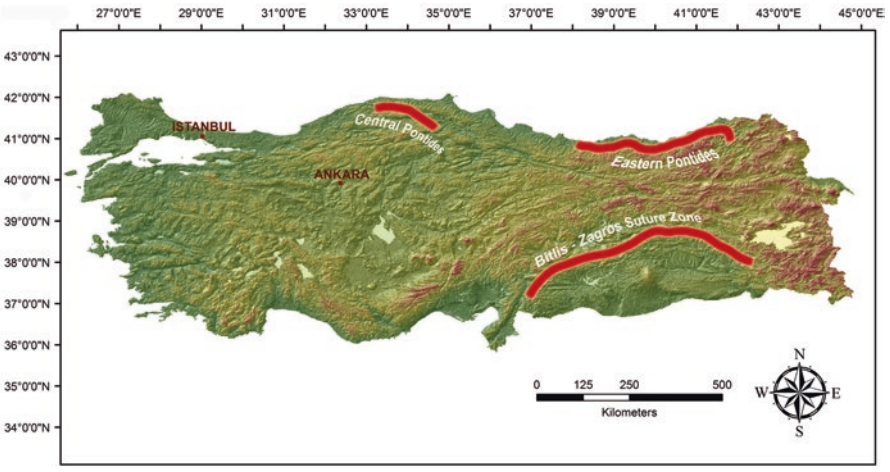

Fig. 9.1 Major districts hosting past and current VMS deposits of various types in Turkey

Although there is a long history of mining, and to a lesser extent of exploration of the VMS deposits in Turkey, extensive research on these deposits has been relatively limited since 2000. In recent years, interest in the Kastamonu area and Bitlis-Zagros suture zone has grown in the wake of interesting new discoveries (e.g. Hanönü-Kastamonu; Ormanbaşı Hill and Koçali-Adiyaman, Ortaklar-Gaziantep). There has also been sustained interest in the old and abandoned mines of the eastern Pontides, although no significant discoveries have been made since the Cerattepe Cu-Au VMS deposit in early 1990s, which is currently under development. Table 9.3 summarizes major attributes for the VMS occurrence in Turkey.

9.2 Mining History

Anatolia has one of the oldest civilizations in the world and also has some of the oldest usage of metals by humans in the world. Archeological records indicate that the earliest metal mining activities were practiced in Anatolia. For instance, artifacts including fishing lines, hooks and beads made out of native copper are found in Çayönü (Diyarbakır) and Aşıklı Höyük (Mound) (Aksaray) both dating around the mid-9th millennium BC (Maddin et al. 1999; Schoop 1995; Yalçın 2000; Esin and Harmankaya 1999). Copper mining in Ergani (Elazığ) dates back to 6000 BC, in Bayat (Çorum) to about 6500 BC, and in Gümüşköy (Kütahya – Western Anatolia) to about 2000 BC (Kaptan 1982).

Moreover, first recorded mining license in the world was granted during the Neo-Hittite Period (circa 800 BC) was carved on a stone in Alihoca village (Ulukışla-Niğde) (Bossert 1954; Hawkins 1969) and the first gold coin was issued at 560 BC by the King Croesus of Lydia in Sardis, the capital of an ancient kingdom at the location of modern Sart in Manisa province (western Anatolia).

Within the chronological framework, copper was very important for the Anatolian civilization during the chalcolithic age (3500–1700 BC). Miners were not just collecting ore from surface; they were also able to practice underground mining for polymetallic ores. Towards the end of 4000 BC, first silver, then lead and finally gold was utilized. Accidental discovery of bronze initiated the contiguous Bronze Age (3000–1200 BC) followed by the Iron Age (1200–550 BC). Many miner tools and remains such as kindling woods, ceramics or grinding stones related with ancient mining activities have been found in ancient galleries and settlements have been dated as early as the third millennium BC (Yalçın and İpek 2016; Yener 2000).

During the Hittite (1650–1250 BC), Urartian (850–585 BC), Phrygian (750–650 BC), and Lydia (650–550 BC) civilizations, many parts of Anatolia were mined for lead and copper. Mining became even more important for the Romans, Byzantines, and Seljuks. During the Ottoman Period, mining also was supported by the empire. Mining activities were regulated for the first time in 1861 through which the empire was entitled to have a 25% share. It was not implemented due to insufficient supervision. However, three more mining laws in 1869, 1886 and 1906 were made to improve the situation. The first mining law (legislation 6309) of the Turkish Republic

was enacted in 1954, it was revised later in 1972 (legislation 2172), and then in 1985 (legislation 3213; updated in 2015).

Following the tragic war years, in 1935 the General Directorate of Mineral Research and Exploration (MTA) was founded by the Turkish Republic in order to lead the mining sector and to explore the state's natural resources using more rational methods of the time. Another government agency, Etibank, was concurrently founded to exploit the mines. In 1940, Ereğli Coal Operation (EKI) and in 1954 Turkish Petroleum (TPAO) were established. In 1968, Etibank took the initiative to found Karadeniz Copper Operations (KBI) to exploit copper mines of the eastern Pontides, which was privatized later in 2006. Other copper mines, Küre (Kastamonu), Ergani (aka Elaziğ-Maden), and Madenköy (Siirt) deposits were also mined by Etibank until their privatization. Within this framework, deposit specific information on past mining activities is given under relevant sections.

9.3 Classification of Turkish VMS Deposits and Terminology

Volcanogenic massive sulfide (VMS) deposits are also known as volcanic-associated (VAMS), volcanic-hosted (VHMS), and volcano-sedimentary-hosted massive sulfide (VSHMS) deposits. However, the term *"VMS"* has genetic connotation. Whereas all the others refer to their host rocks or indicate their associated host-rock lithologies. They typically occur as concordant lenses of polymetallic massive sulfides that form at or near the seafloor in submarine volcanic environments through the focused discharge of hot, metal-rich hydrothermal fluids. Thus, the VMS deposits can also be classified under the general heading of "concordant massive sulfide" deposits (Fig. 9.2).

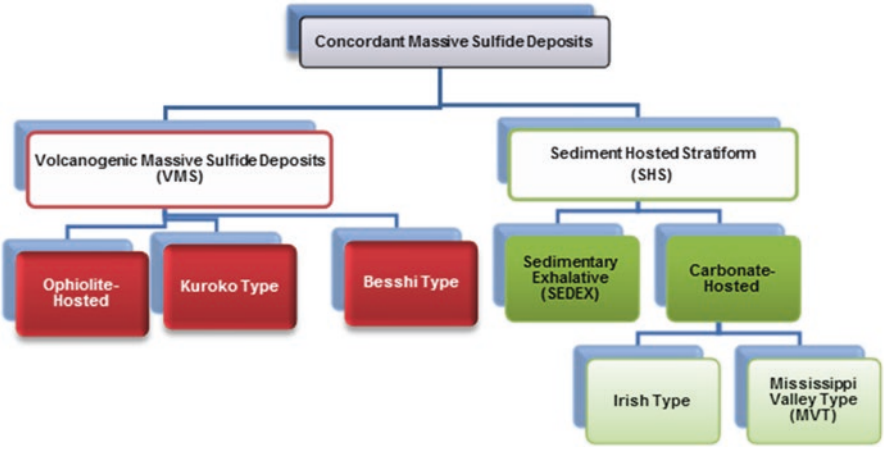

Fig. 9.2 General classification of concordant massive sulfide deposits

The sediment-hosted stratiform (SHS) deposits are out of scope of this chapter and will not be discussed here. The VMS deposits are further classified based on a number of criteria that includes the geotectonic setting, the host rock lithology, ore composition, metal ratios, relative abundances of the ore minerals, and principal concurrent lithologies rather than on the characteristics of individual deposits. However, each classification has certain practical advantages for definite purposes over the others.

The base metal classification proposed by Franklin et al. (1981) and later refined by Large (1992) and Franklin et al. (2005) is probably the most preferred. In general, VMS deposits are divided into Cu-Zn, Zn-Cu, and Zn-Pb-Cu metal associations.

Poulsen and Hannington (1995) preferred a simple bimodal definition of "normal" versus "Au-rich" VMS deposits. A third classification system that is gaining acceptance is a fivefold grouping initially suggested by Barrie and Hannington (1999), then later modified by Franklin et al. (2005). This system classifies VMS deposits by their host lithologies, which includes all rocks within a host succession defining a distinctive time-stratigraphic event. These five different groups include (I) bimodal-mafic (e.g. Prieska belt, Canada), (II) mafic-back arc (e.g. Caledonides, Norway), (III) pelitic-mafic (e.g. Besshi district, Japan), (IV) bimodal-felsic (e.g. Kuroko-type deposits, Japan), and (V) siliciclastic-felsic (e.g. Iberian pyrite belt, Portugal-Spain). These lithologic groupings largely compare with different submarine tectonic settings varying from the most primitive VMS environments (i.e. ophiolite settings), through oceanic rifted arc, evolved rifted arcs, continental back-arc to sediment-filled back-arc environments.

For the sake of simplicity, particularly considering metal contents, host-rock association and tectonic settings, the VMS deposits of Turkey can be classified into three major subgroups: Kuroko-type, Besshi-type, and Ophiolite-hosted-type. The Kuroko-type and the ophiolite-hosted VMS deposits can be further classified based on their metal contents, host rock associations, and their tectonic environments (Fig. 9.3).

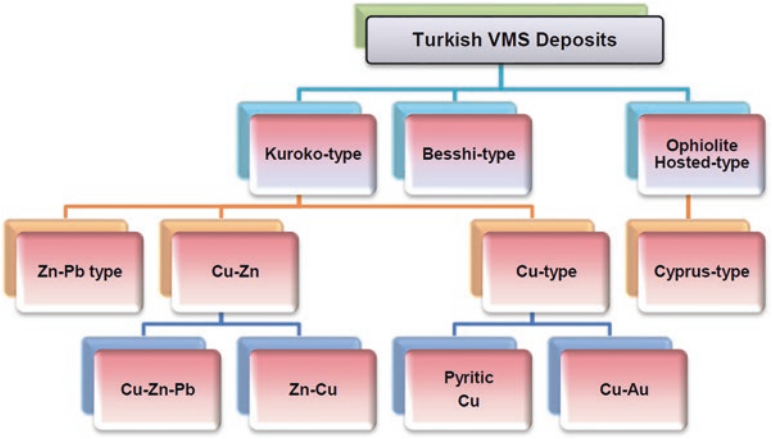

Fig. 9.3 Classification of VMS deposits occurring in Turkey

Kuroko, a Japanese term strictly for black ore (sphalerite and galena dominating massive ore), is however used in a looser and broader sense for Miocene-age deposits that contain not only black ore but also one or more additional ore types: (I) Oko-type, yellow colored, chalcopyrite dominating ore, and (II) Keiko-type, siliceous, quartz and pyrite rich ore in the stockwork type ore formations. In this chapter, to emphasize the ore types for each massive sulfide deposit, the original Japanese terms will be used as the author's choice. Occurrence of the Kuroko-type deposits is strictly limited to the Eastern Pontide Tectonic Belt (EPTB) in Turkey.

Besshi, also a Japanese term, has originally been used to define the volcanogenic massive sulfide (VMS) deposits resembling the type deposits occurring in the southern Japanese island of Shikoku. These deposits typically are comprised of thin sheets of massive to well layered sulfides including pyrrhotite, chalcopyrite, sphalerite, pyrite and minor galena within interlayered, terrigenous clastic rocks and calc-alkaline basaltic to andesitic tuffs and flows and/or their metamorphosed equivalents. In this chapter, the term is loosely used to emphasize their host-rock lithology and ore mineralogy. The Besshi-type deposits of Turkey occur only in the Central Pontides.

Cyprus-type has been used to define the volcanogenic massive sulfide (VMS) deposits represented by the well-documented type deposits strictly occurring in Cyprus. However, the term is loosely used to encompass all kinds of ophiolite-hosted VMS-type deposits occurring in a number of tectonic settings including mid-ocean ridges (MIR) and supra-subduction zones (SSZ) and is considered to be an ancient analog of modern sea-floor sulfide deposition as sulfide chimneys in spreading centers. Irrespective of their tectonic settings, these deposits are hosted within the mafic volcanics of the ophiolitic sequences. In this chapter, the term "Cyprus-type" is used strictly for the VMS deposits occurring in SSZ and associated with mafic host-rocks. The Cyprus-type deposits of Turkey occur in the Central Pontides in the Kure area and along the Bitlis-Zagros Suture Zone in southeastern Turkey, all associated with the ophiolites of Late Cretaceous age.

9.4 Kuroko-Type Deposits

9.4.1 Introduction

A significant number of the Kuroko-type VMS deposits are hosted in the Eastern Pontides Tectonic Belt (EPTB) (aka Eastern Pontides Orogenic Belt; EPOB) in northeastern Turkey (Çağatay 1993; Ciftci 2000; Yiğit 2009; Eyüboğlu et al. 2012, 2014; Revan et al. 2013, 2014) (Fig. 9.4). The EPTB is one of the four major tectonic units forming Anatolia. It is a complex assembly of island arc terrains, which have evolved during the subduction of the Afro-Arabian plate beneath the Euro-Asian plate and the resulting closure of the northern branch of Tethys Ocean (Robinson et al. 1995; Okay and Şahintürk 1997). The EPTB lies within a larger metal rich tectonic corridor stretching from southern Georgia and northern Armenia to Bulgaria and Romania.

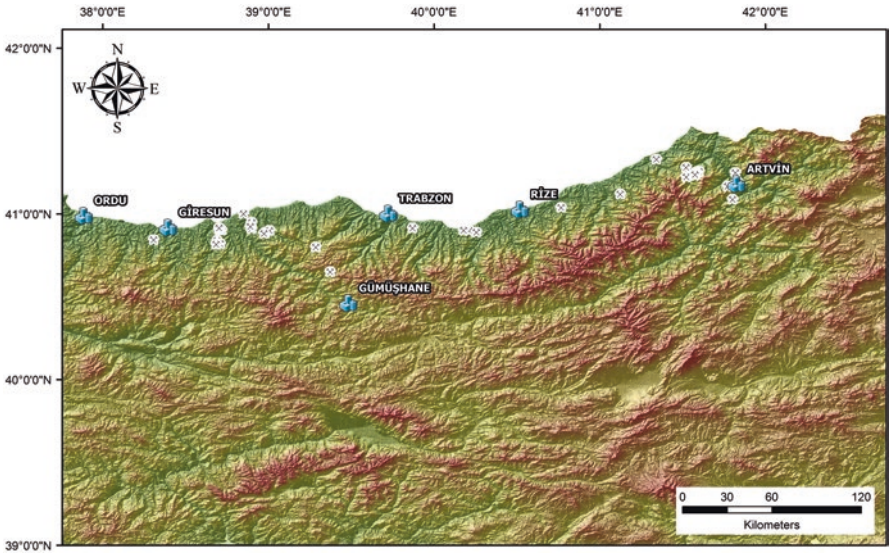

Fig. 9.4 Distribution of Kuroko-type VMS deposits throughout the EPTB

Various investigators proposed a number of genetic models and classifications from 1938 to the present both for long known individual deposits and all deposits occurring along the EPTB: (1) Zimmer (1938) suggested that deposits occurring in Murgul could be pluton-related based on his field-work; (II) Kovenko (1944) postulated the same genetic idea and related the Murgul deposit to the Tertiary granites; (III) Egeran (1946) interpreted the Murgul mineralization to be epithermal in character; (IV) Schneirderhöhn (1955) identified the deposit as a specific Murgul-type of silicate sub-volcanic deposit; (V) Petraschek (1955) considered the entire Pontide district to be a subdistrict of the metallogenic zoning of the Anatolian-Balkan region, in which he identified two types of subvolcanic deposits, the Murgul-type and the Gümüşhane-type; (VI) Kraeff (1963) proposed that the deposits of the Murgul district were dacite-related and associated with the Late Cretaceous-Eocene volcanism; (VII) Ovalioglu (1969) distinguished 26 massive sulfide deposits in the region as exhalative-sedimentary and disseminated hydrothermal-type mineralizations; (VIII) Hutchinson and Hodder (1972) proposed that the deposits of the Murgul district are a transitional-type between true massive sulfide and true porphyry-type deposits; (IX) Aslaner (1977) considered the Pontide region as a massive-stratiform sulfide belt; (X) Pejatovic (1979) was the first to use the term "Pontide-type" for the region's massive sulfide deposit and proposed that these deposits are highly analogous to the Miocene Kuroko-type deposits of Japan. These deposits are now considered to be the Kuroko-type because of their fairly similar geological and geotectonic settings, host-rock associations, element contents and isotope systematics (Aslaner and Gedikoğlu 1984; Kolaylı 1989; Van 1990; Çiftçi 1993; Ciftci 2000; Çağatay 1993; Aslaner et al. 1995; Tüysüz 1995;

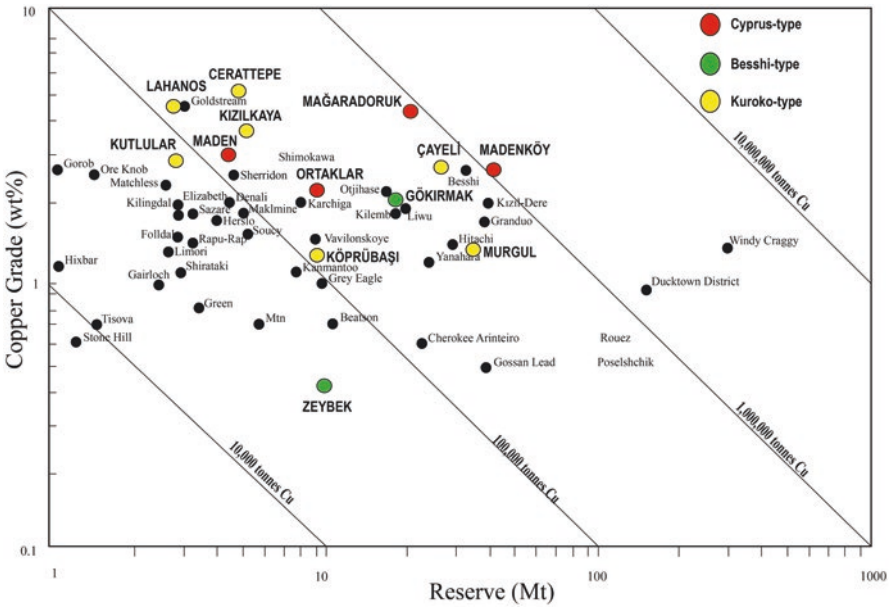

Fig. 9.5 Distribution of the major VMS deposits in Turkey on the Cu-grade vs reserve diagram as compared with the other worldwide VMS deposits. (Modified after Lobanov et al. 2014)

Yiğit 2009; Eyüboğlu et al. 2012, 2014; Revan et al. 2014). The large number of VMS occurrences with varying sizes and grades, in an approximately 500 km-long and 75 km-wide belt, makes this region a world class VMS province (Figs. 9.4 and 9.5; Tables 9.1 and 9.2). The VMS deposits in the EPTB are hosted by intensely altered, Late Cretaceous felsic volcanics reaching up to 150–300 m in thickness, and they occur in a fairly narrow zone running parallel to the Black Sea coast (Fig. 9.4). About 40 of more than 400 known sulfide mineralizations in the region are of mineable size. The VMS deposits are located in the intra-arc rift zone of the Pontide island arc. The belt can be subdivided into three parts where the VMS occurrences show clustering: (I) western part (from Batlama valley being the western most boundary of the belt to Vakfıkebir Fol creek), (II) central part (from Vakfıkebir to Ardeşen), and (III) eastern part (Artvin area). From east to west, ore mineralogy and related characteristics show noticeable changes as zinc and particularly lead contents increase. Yellow ore, in the form of either pyritic copper or stockwork copper prevails in the eastern deposits thus they have Cu >> Zn + Pb. Subsequently the deposits show changes westward first to Cu-Zn (Cu = Zn + Pb) and then to Pb-Zn-Cu (Zn + Pb >> Cu) metal associations in the form of massive semi-black and black ore bodies. Although gold and silver contents of the deposits are within the typical range for the VMS deposits, some deposits contain unusually high gold (e.g. Cerattepe deposit).

Table 9.1 Average grade and tonnage data for VMS deposits of selected worldwide districts

	Type	# of deposits	Cu (%)	Zn (%)	Pb (%)	Ag (ppm)	Au (ppm)	Reserve (Mt)
Abitibi Belt, Canada	Cu-Zn	52	1.47	3.43	0.07	31.9	0.8	9.2
Norwegian Caledonides	Cu-Zn	38	1.41	1.53	0.05	N/a	N/a	3.5
Bathurst N.B., Canada	Zn-Pb-Cu	29	0.56	5.43	2.17	62.0	0.5	8.7
Green Tuff Belt, Japan	Zn-Pb-Cu	25	1.63	3.86	0.92	95.1	0.9	5.8
EPTB, Turkey	Cu-Zn-Pb	34	5.51	3.42	1.33	71.03	0.76	4.5

Modified from Lydon (1988)

9.4.2 Geological Framework

The eastern Pontides tectonic belt is located in the northeastern part of Anatolia and is an integral segment of the Alpine-Himalayan belt. The geological structure of the EPTB is the consequence of long-lived subduction, accretion and collision events associated with the closure of the Tethyan Ocean (Ketin 1966; Akıncı 1984; Robinson et al. 1995; Okay and Şahintürk 1997). The geodynamic evolution of this region is still controversial due to lack of systematic geological, geochemical, geochronological and paleontological data. Some believe that the eastern Pontides orogenic belt formed as a result of the northward subduction of Paleotethys during the Paleozoic-Mesozoic time (e.g. Adamia et al. 1977, 1981; Ustaömer and Robertson 1996; Rice et al. 2009; Dilek et al. 2010). However, other researchers suggest that the eastern Pontides orogenic belt was produced by southward subduction of Tethys oceanic lithosphere that was located in the northern part of the orogenic belt during the Paleozoic-Mesozoic-Cenozoic time and that the Black Sea is a remnant of the Tethys ocean (e.g. Dewey et al. 1973; Bektaş et al. 1999; Eyüboğlu et al. 2007, 2012; Eyüboğlu 2010). Alternatively, Şengör and Yılmaz (1981) suggested that Paleotethys was located north of the Pontides, and hence southward subduction operated from the Paleozoic until the early Mesozoic, followed by northward subduction from the late Mesozoic until the early Cenozoic (Eyüboğlu et al. 2014).

The EPTB sit largely on pre-Liassic composite basement rocks consisting of (i) high-temperature low-pressure metamorphic units intruded by high-K I-type granitoids of Early Carboniferous age (Okay 1996; Topuz and Altherr 2004; Topuz et al. 2004, 2007, 2010), (ii) low temperature high pressure metamorphic units of Permo–Triassic age (e.g. Okay and Göncüoğlu 2004; Topuz et al. 2004), and (iii) molassic sedimentary rocks of Permo-Carboniferous age (Okay and Leven 1996; Çapkınoğlu 2003). The basement is overlain transgressively by a sequence of Liassic volcanics and volcaniclastics, which were deposited in an extensional arc environment. The volcanic members of this sequence are represented by calc-alkaline to tholeiitic basaltic to andesitic rocks (Şen 2007; Kandemir and Yılmaz 2009). The Liassic

Table 9.2 Summary of major geological, geochemical and mineralogical characteristics of the VMS deposit of Turkey

Parameter	Besshi-type deposits	Cyprus-type deposits	Kuroko-type deposits
Tectonic setting	Intra-oceanic island arc	Intra-oceanic island arc	Magmatic arc
Ore-controlling structures	Obscured	Poorly preserved within ocean ridge basalts associated with SSZ ophiolites	Rhyolitic domes and subvolcanic acidic intrusives
Host-rocks	Meta-siliciclastic sediments	Imbricated basic volcanics, serpentinites, sedimentary cover of ophiolitic sequence	Felsic volcanics
Age	Middle Jurassic	(I) Norian-Toarcian for Küre area; (II) Late Triassic-Early Cretaceous for Koçali Complex; (III) Early-Middle Eocene for Maden Complex	Late Cretaceous
Metamorphism of host-rocks	Greenschist facies	None	None
Morphology of orebody	Alternating concordant thin layers	Lenticular, irregular, stockwork	Concordant/semi-concordant lenticular, stockwork
Main ore minerals	Ccp, Sp, Py	Ccp, Sp, Mt, Hem, Py	Ccp, Sp, Gn, Tt-Tn, Bo, Py
Main gangue minerals	Qtz, Cal	Qtz, Cal	Qtz, Cal, Ba, Gyp
Main alteration minerals	Chl, Ser, Qtz	Chl, Qtz, Cal	Qtz, Kao, Ser
Main ore structures	Massive, dissemination	Massive, clastic, stock-work	Massive, stock-work, clastic
Principal ore textures	Replacement, dissemination, vein/veinlet	Dissemination, replacement, vein/veinlet	Colloform, replacement, dissemination, vein/veinlet
Principal commodity	Cu	Cu, Zn, Fe	Cu, Zn, Pb
Cu/Cu+Zn ratio	>0.8	>0.8	0.1–0.95
By-products	Nr[a]	Au, Ag, Co	Au, Ag, Cd
Average Au (g/t)	<0.2	1.5	1.2
Average Ag (g/t)	1–18	15	40
$\delta^{34}S$	+3 – +7	+3 – 10	−2.5 – +7
Th (°C)	Nr	161.5–317	235–310
Average salinity (eq. NaCl %)	Nr	0.9–5	3–9

[a]*Nr* not reported

volcanics and volcaniclastics pass into Late Jurassic (Malm) – Early Cretaceous carbonates (Korkmaz et al. 1995; Okay and Şahintürk 1997). Late Cretaceous is represented by a >2 km thick volcano-sedimentary rock succession in the north and by flyschoid sedimentary rocks with limestone olistoliths in the south. Late Cretaceous volcanics compositionally range from basalt to rhyolite (Eğin et al. 1979; Manetti et al. 1983; Çamur et al. 1996; Arslan et al. 1997; Okay and Şahintürk 1997; Boztuğ and Harlavan 2008).

9.4.3 Ore Geology

The VMS deposits are associated with the Late Cretaceous felsic volcanics – mostly by the Kızılkaya Formation and to much lesser extent by the Tirebolu (aka Çayırbağ) Formation (Schneider et al. 1988; Çağatay 1993; Özgür 1993; Çiftçi et al. 2005; Yiğit 2009; Karakaya et al. 2012; Eyüboğlu et al. 2014; Revan et al. 2014). There have been various lithologic descriptions by previous investigators, e.g. albite dacite I (Kraeff 1963), quartz porphyry (Buser 1970), quartz albite porphyry (Vıcıl 1975) and mineralized dacite (Alpan 1971; Aslaner 1977; Pelin et al. 1982). Due to abrupt lithological changes within short distances in most pyroclastic sequences and their being not mappable in most of the places, and to avoid local names, they were later termed as "felsic volcanic complex – FVC" by Ciftci (2000). The terms "pyritic/pyritized, pyrite-bearing, ore-bearing, mineralized" have been attributed to the common presence of disseminated pyrite within the dacitic rocks.

The Late Cretaceous magmatism occurred as a result of the northward subduction of the Izmir-Ankara-Erzincan Neotethyan ocean (Şengör and Yılmaz 1981; Okay and Şahintürk 1997; Yılmaz 1997). The collision between the Eastern Pontides and the southern Tauride-Anatolide block is constrained to have occurred during the Paleocene to Early Eocene (Okay and Şahintürk 1997; Okay and Tüysüz 1999). Post-collisional Eocene volcanics and volcaniclastics unconformably overlie the older units, and locally seal the Izmir-Ankara-Erzincan suture (Altherr et al. 2008).

The eastern Pontides straddle the North Anatolian transform fault and display three major volcanic cycles of Liassic, Late Cretaceous and Tertiary age. Volcanic rocks of Liassic age are transitional, those of Late Cretaceous ages are subalkaline, and Eocene volcanic rocks are alkaline and subalkaline in character (Arslan et al. 1997, 2007; Arslan and Aslan 2006). The volcanism that began during the Liassic time with the formation of mafic rocks in a rift environment (Tokel 1972; Schneider et al. 1988; Arslan et al. 1997), developed on a Precambrian to Paleozoic basement (Yılmaz 1972; Okay and Şahintürk 1997; Topuz et al. 2001; Topuz 2002). The Liassic volcanism is comprised of calc-alkaline volcanics and volcanoclastics with locally deposited sedimentary rocks (Arslan et al. 1997). These units are overlain by Dogger to Early Cretaceous platform carbonates. Following the deposition of the carbonate rocks, island arc volcanic activity began (Eğin et al. 1979). In the Late Cretaceous, early mafic rocks were followed by a felsic rock series, and then by

overlying mafic rocks that consist extensive andesitic volcanism inland and basaltic lavas and agglomerates along the coast.

The late Cretaceous rocks that host the volcanogenic massive sulfide (VMS) deposits in the region consist mainly of dacitic and rhyolitic lavas and pyroclastics alternating with mudstone, marly limestone and pelitic tuff. Most of the deposits including Murgul, Akarşen, Hod, Tunca, Çayeli, Kotarakdere, Kutlular, Kanköy, Fol, Eseli, Sadegöre, İsraildere, İsrail, Harköy, Killik, Kızılkaya, Lahanos, and Akköy are hosted by "Kızılkaya Formation", which consists mainly of dacite-rhyodacite and associated pyroclastics rocks, with locally interbedded marl and limestone beds, suggesting submarine volcanism during its evolution. The dacitic and rhyodacitic rocks, which constitute the dominant lithology of the formation, generally occur as lava flows, small dome-shaped bodies and also lava flows displaying columnar jointing that are formed as a result of contraction during cooling (Eyüboğlu et al. 2014). They are generally massive and well-jointed, and characterized by abundant euhedral to subhedral quartz, plagioclase and disseminated pyrite crystals in hand specimen. The pyroclastic members of the Kızılkaya Formation are represented mainly by intensely altered tuffs and subordinate volcanic breccia. All lithological units of Kızılkaya Formation are cut by purple dacites, which are unaltered and pyrite-free. They are easily distinguished due to their characteristic purple color in the field. They occur as both dome-shaped bodies and well-developed prismatic columns.

The Kızılkaya formation is covered by the Çağlayan Formation consisting of basaltic-andesitic volcanics and associated pyroclastic rocks, with intercalated limestone beds and/or laterally discontinuous, lens-shaped limestone bodies (Güven 1993; Eyüboğlu 2000). The Çağlayan Formation grades upward into the Çayırbağ Formation including biotite-bearing rhyolites – rhyodacites and associated pyroclastic rocks that are the latest products of the late Cretaceous volcanism in the Tirebolu area. The Köprübaşı (Tirebolu) deposit is hosted in the pyroclastic equivalents of felsic rocks of the late Cretaceous Çayırbağ Formation, suggesting that the VMS deposits occur in two different stratigraphic horizons in the northern part of the eastern Pontides orogenic belt – the Kızılkaya and the Çayırbağ formations (Eyüboğlu 2000, 2010). The tuffs occurring in both stratigraphic horizons have been considered to be lapilli tuffs due to their particle size that is generally >2 mm (Çiftçi 1993). They show localized layering that commonly strikes NE-SW and NW-SE with 50–60° dips. Pyroclastics are very significant due to their porous nature and their role as footwall-rocks for most of the VMS deposits.

Microscopically, they generally show microlitic porphyritic and microgranular microtextures. They consist mainly of quartz that occurs mostly as subhedral and rare euhedral crystals commonly eroded by the groundmass and of andesine euhedral plagioclase crystals. The plagioclases in the tuffs and pyroclastics are completely altered to sericite, kaolinite, and calcite. Due to the intense alteration, except for local biotite, no other mafic phases were observed. The groundmass consists mainly of cryptocrystalline quartz – both primary and secondary and alteration products of the microlites. Presence of apatite and zircon has been reported (Gedikoğlu 1978). Secondary minerals are sericite, chlorite, calcite, clay minerals

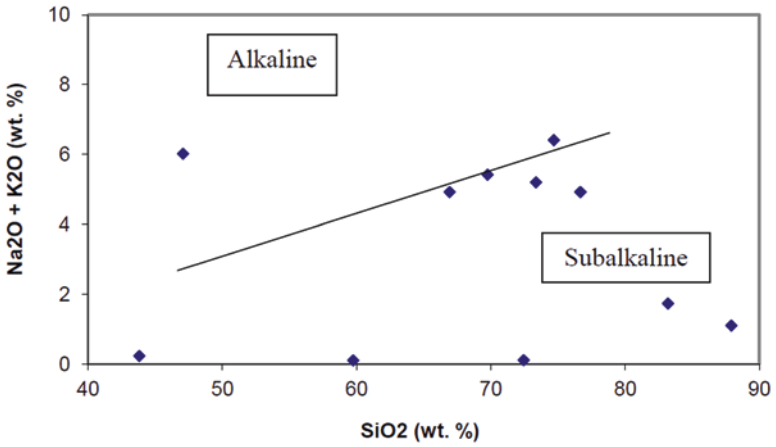

Fig. 9.6 Distribution of samples from the VMS host-rocks on the $Na_2O+ K_2O- SiO_2$ diagram. (Gorshkov 1969)

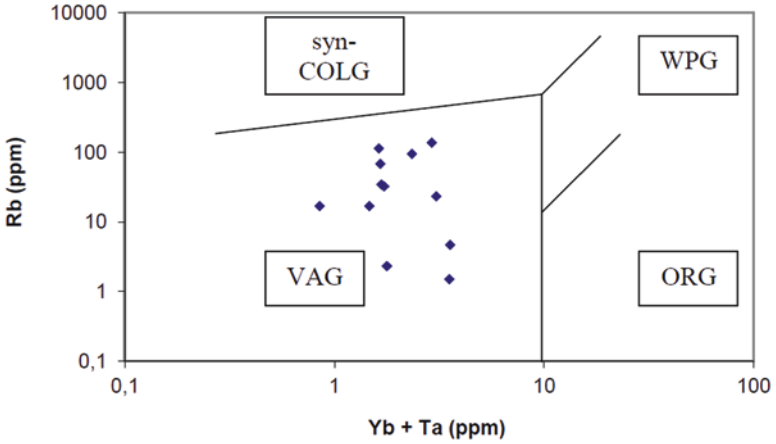

Fig. 9.7 Distribution of samples from the felsic volcanic complex on the Rb-Yb+Ta diagram. (Pearce et al. 1984)

(mainly kaolinite and montmorillonite), and very sporadic ankerite and epidote. Euhedral to subhedral visible pyrite along with iron-oxide-hydroxides accounts for the opaque content (Ciftci 2000).

The total alkali versus silica diagram indicates that the felsic rocks are mainly subalkali in character (Fig. 9.6). Samples representing the VMS host-rocks throughout the region fall in the VAG field inferring a volcanic arc environment (Fig. 9.7). The felsic volcanics show great geochemical similarity with the granitoids indicating a potential genetic relationship (Figs. 9.8 and 9.9) (Ciftci 2000; Eyüboğlu et al. 2014 and references therein).

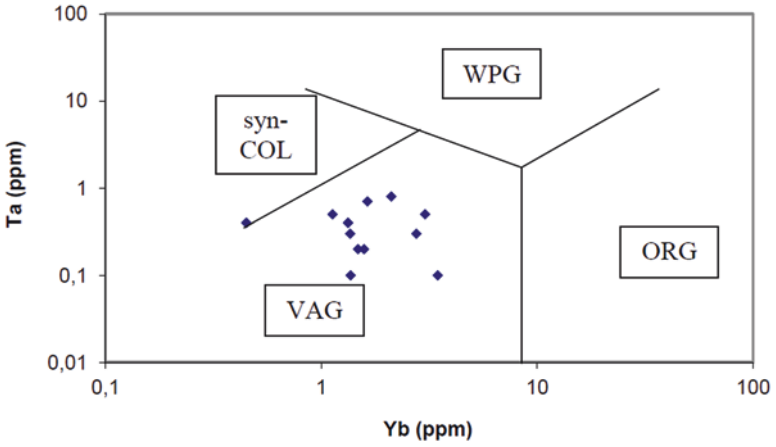

Fig. 9.8 Plot of the host-rock samples on the Yb-Ta diagram. (Pearce et al. 1984)

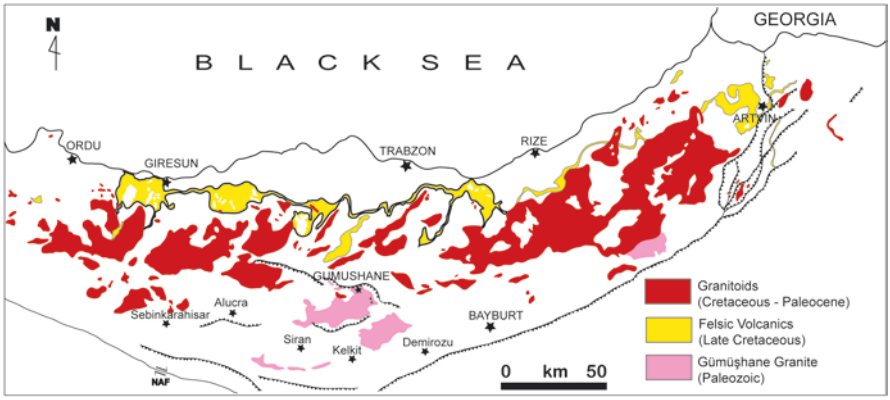

Fig. 9.9 Areal distributions of the VMS-hosting felsic volcanics and granitoids in the EPTB

The granitoids in the Eastern Pontides range from Early Carboniferous to Late Eocene in age (Boztuğ et al. 2004, 2006; Topuz et al. 2007, 2010; Arslan and Aslan 2006; Karslı et al. 2007; Kaygusuz et al. 2008; Kaygusuz and Aydınçakır 2009). These granitoids are mostly shallow intrusions, and have well-developed contact aureoles. The Cretaceous granitoids are of particular significance for the VMS deposits in Turkey due mainly to their being large heat sources for the hydrothermal convection systems and for being roots of felsic volcanics hosting the VMS deposits.

Figure 9.9 shows areal distribution of the VMS-hosting felsic volcanics with the granitoids in the region. Although these do not extend over a very large area, their spatial relationship with the deposits makes it a target formation for geochemical

exploration programs in the region, which is going to be cover in later part of this chapter. They also form dome-like structures that are similar to the rhyolite plugs occurring in the Green Tuff tectonic belt of Japan.

9.4.4 Mineralogy and Geochemistry

The VMS deposits in the eastern Pontides often show mineralogical zoning consisting of an upper black ore or semi-black ore zone with major galena, sphalerite, and pyrite with minor to trace chalcopyrite and bornite, which is often overlain by either barite or gypsum, a yellow ore zone consisting of major pyrite and chalcopyrite with minor to trace sphalerite, which overlies a massive pyritic zone. The massive stratiform and strata-bound ore bodies are underlain by epigenetic stringer or stockwork ore zone in highly altered felsic volcanic rocks (Çiftçi and Hagni 2005).

Sulfide minerals in the deposits mainly include pyrite, chalcopyrite, sphalerite, galena, tetrahedrite (in black/semi black ore dominating deposits) – tennantite (in yellow ore dominating deposits), bornite with minor to trace covellite, marcasite, chalcocite and digenite. Common gangue minerals are quartz, calcite, and barite with minor to trace anhydrite, gypsum, and dolomite (Table 9.3).

The presence of gold and silver within the Turkish VMS deposits show substantial variations from deposit to deposit. Gold becomes significant in some of the deposits although it ranges from 0.2 (e.g. Köprübaşı black ore) to 8 ppm (e.g. Lahanos yellow ore) and 1–220 ppm, respectively. Gold occurs mainly within the yellow-ore dominated deposits, generally as electrum and petzite associated with chalcopyrite, pyrite, and quartz, especially in some deposits such as Cerattepe (Artvin). Here, the Au rich zones occur as an oxidized pod and as a siliceous zone containing about 5 ppm Au due to an epithermal overprinting (Çiftehan and O'Brien 1998). In some of the deposits, gold occurs in association with semi-black ore (e.g. Çayeli Madenköy deposit). Silver, ranges from 1 to 221 ppm, in Murgul stockwork ore and Köprübaşı black ore, respectively. Silver however, rarely forms discrete minerals. When it does occur, acanthite associated with chalcopyrite is the most common silver mineral (e.g. Murgul deposits). However, major silver presence is with tetrahedrite and to lesser extent with bornite. Silver association with galena appears to be insignificant.

The deposits show very similar textural and mineralogical characteristics. Figure 9.10 shows generalized paragenetic sequence for the major ore minerals throughout the region. The major differences between Cu-rich and Cu-poor deposits are that the former does not contain the Stage-II mineral association, whereas the latter lacks the Stage-IV mineral association. Some of the Cu-poor deposits exhibit some indications of this stage, whereas others completely lack it. This could be attributed to the availability of certain metal ions (i.e., Cu ions) within the ore-forming system. The fact that all of the deposits have common host-rocks can be explained through localized convection cells that were enriched in certain metal ions and deposited a variety of VMS deposits within a single district.

Table 9.3 Common minerals reported from the major examples of the Kuroko-type deposits occurring in Turkey

Ore minerals	Gangue minerals
Pyrite	Quartz
Chalcopyrite	Calcite
Sphalerite	Barite
Galena	Siderite
Fahlerz	Sericite
Bornite	Chlorite
Enargite	Gypsum
Pyrrhotite	Anhydrite
Carrollite	Dolomite
Electrum	Apatite
Petzite	Ankerite
Chalcocite	Zircon
Marcasite	Zeolites
Covellite	Clay minerals
Native gold	Rutile
Native silver	Graphite
Acanthite	Anatase
Limonite	Rhodochrosite
Malachite	
Azurite	
Neodigenite	
Bismuth	
Copper	
Siderite	
Tetradymite	
Tellurobismuthite	
Hessite	
Proustite	
Pyrargyrite	
Polybasite/pearceite	
Boulangerite	
Ilmenite	
Pyrolusite	
Brounite	
Hausmannite	
Seligmannite	
Gratonite	
Geochronite	
Aikinite	
Luzonite	
Idaite	
Bournonite	
Argentite	
Goethite	
Lepidocrocite	
Hematite	
Magnetite	
Manganite	
Bixybite	

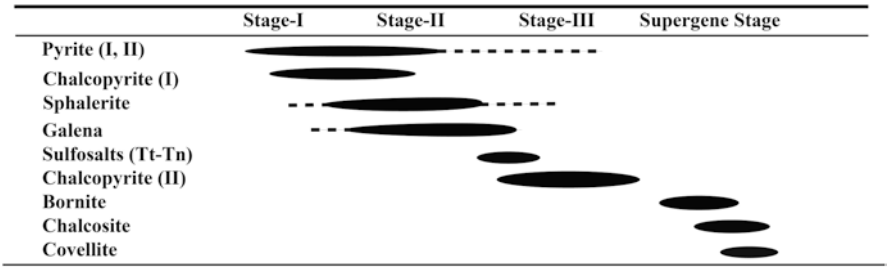

Fig. 9.10 Generalized regional paragenetic sequence for the major ore minerals in the Kuroko-type VMS deposits of Turkey

Well-preserved micro-ore textures that are commonly observed include dissemination and veins/veinlets in epigenetic stockwork ore zones and dissemination, colloform, massive, concentric banding, clastic (due to local slumpings) and replacement textures in syngenetic massive ore zones. Representative ore textures and prevailing ore minerals are shown in Fig. 9.11.

The base metal contents of the VMS deposits show great variations from 0.56% (e.g. Köprübaşı black ore) to 20% (e.g. Murgul yellow ore) for copper, 0.01% (e.g. Murgul yellow ore) to 12.10% (e.g. Lahanos semi black ore) for zinc, and 0.01% (e.g. Lahanos pyritic ore) to 8.96% (e.g. Köprübaşı black ore) for lead. Based on the ratios of Cu:Zn:Pb, the deposits are further classified as Cu-type (e.g. Murgul deposits – Damar, Kızılkaya, Çakmakkaya), Cu-Zn-type (e.g. Akarşen, Kuvarshan and Çayeli), Cu-Zn-Pb-type (e.g. Lahanos, Killik, Kızılkaya deposits), and Zn-Pb-Cu-type (e.g. Köprübaşı) (Fig. 9.3). Table 9.4 lists major deposits of the region with known reserve, grade and sub-type.

The average metal contents of the host-rocks are 119, 239, and 357 ppm for Cu, Zn, and Pb, respectively. The average metal contents of unaltered felsic volcanic rocks for the same elements are 12, 51, and 18 ppm, respectively (Rose et al. 1979). The Cu-Zn-Pb ternary diagrams based on the base metal contents of representative samples from both the host rocks and the ore deposits appear to be significantly scattered, but they are somewhat enriched towards the zinc corner. The ternary plots suggest that the felsic complex could have been a potential source, especially for Cu-Zn-Pb-type mineralizations (Figs. 9.12 and 9.13). Figure 9.13 confirms the further classification of the Kuroko-type deposits of Turkey. Copper content of the region's deposits is one of the major differences as compared with the Japanese Kuroko deposits. This is because the basement rocks (up to 800 m thick), which are mainly mafic volcanics and metamorphic rocks contain copper.

All the deposits investigated were deposited at temperatures ranging from 235ºC to 310ºC based on the homogenization temperatures (Th). Higher temperatures account for the stockwork ore zones. The salinities of the fluid inclusions range between 3 to 9 wt. % NaCl eq. The fact that fluid inclusions are generally liquid-rich (LV-type with vapor ration is less than 20%) and have consistent liquid-to-vapor ratios, indicate a lack of boiling, probably due to relatively deep formation depths

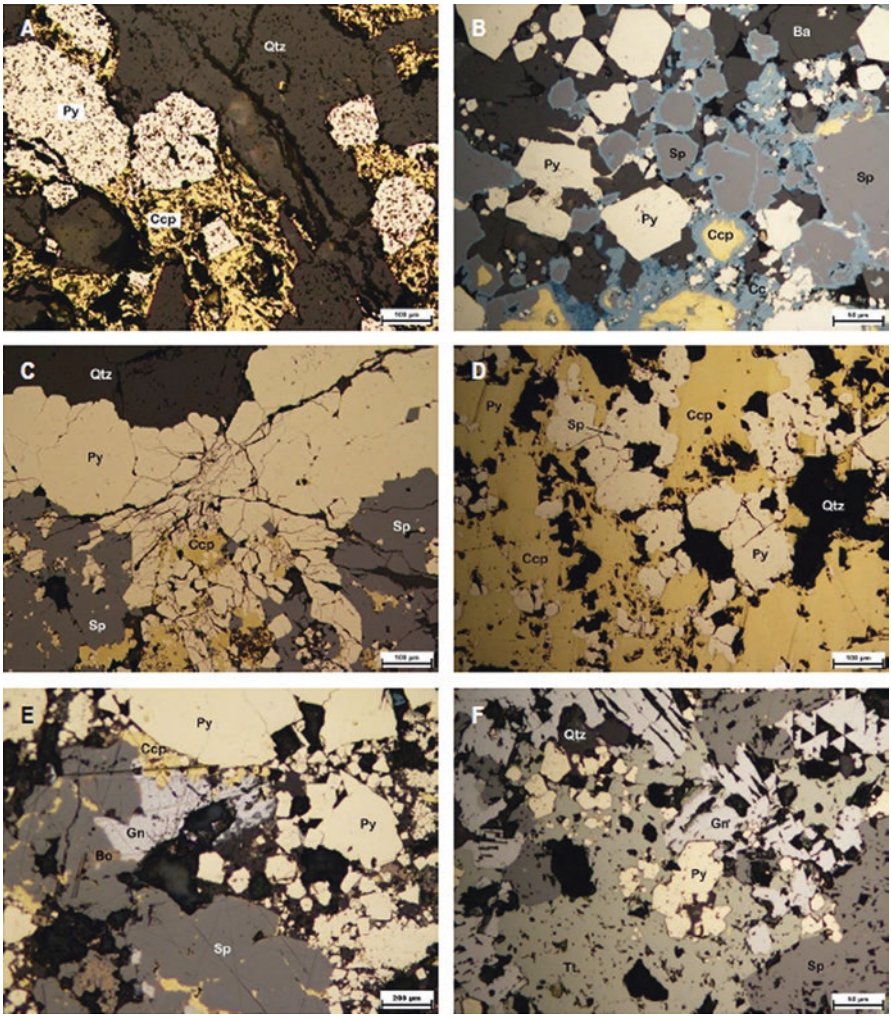

Fig. 9.11 Common micro-ore textures from (**a**) Murgul Damar stockwork ore, (**b**) Cerattepe massive ore, (**c**) Çayeli clastic ore, (**d**) Kutlular massive yellow ore, (**e**) Lahanos semi-black ore, and (**f**) Köprübaşı black ore (*Qtz* quartz, *Ccp* chalcopyrite, *Py* pyrite, *Cc* chalcocite, *Sp* sphalerite, *Gn* galena, *Tt* tetrahedrite, *Bo* bornite)

for the deposits. Post-depositional alteration or mild metamorphism resulting from younger volcanic activity during Eocene that cut through the orebodies may be responsible from the presence of CO_2 in some of the fluid inclusions reported from individual deposits (e.g. Murgul deposits) (Ciftci 2000; Gökçe 2001; Zerener 2005; Demir et al. 2013).

The Kuroko-type deposits of Turkey have more isotope data reported to date compared with the other VMS deposits occurring in the country including S, O, H, Cu and Pb.

Table 9.4 Reserves, grades and commodity-based types of major Kuroko-type deposits of the region

Deposit	Avg. metal content (%)			ppm		Reserve (Mt)	Type
	Cu	Zn	Pb	Au	Ag		
Kutlular[a, b, c]	2.49	0.46	0.04	Nr	Nr	1.22	Pyritic Cu
Çayeli[c]	2.88	4.34	0.11	1	68	30.0	Cu-Zn
Kotarakdere[k]	1.43	Nr	Nr	Nr	Nr	0.94	Pyritic Cu
Lahanos[d]	4.23	3.31	0.01–3.6	Nr	Nr	2.4	Cu-Zn
Kızılkaya[e]	3.5	2.5	0.7	Nr	Nr	5.0	Cu-Zn
Killik[d]	2.5	5.0	0.7	Nr	Nr	0.17	Cu-Zn
Harkköy[k]	0.96	0.94	0.27	Nr	Nr	6.22	Cu-Zn-Pb
Murgul Damar[g]	1.10	0.1	0.05	Nr	Nr	20	Cu
Murgul Çakmakkaya[g]	0.99	0.1	<0.01	Nr	Nr	1.0	Cu
Murgul Çarkbaşı[g, j]	0.85	0.1	<0.01	Nr	Nr	1.3	Cu
Cerattepe[g]	5.2	2.0	0.5	1.2–4	25–140	3.9	Cu-Au
Ağalık[h]	0.6	2.0	0.02	Nr	Nr	1.4	Cu-Zn
Karılar[i]	0.5–1.1	0.7–2.5	1.0	Nr	Nr	0.10	Cu-Zn
Karaerik[j]	0.03	0.01	<0.01	Nr	Nr	Nr	Cu-Zn
Köprübaşı[f]	0.83	6.56	4.68	Nr	221	10.0	Zn-Pb
İsraildere[j, k]	1.53	0.1	0.01	Nr	Nr	0.20	Cu
Kanköy[g]	1.9	0.7	0.05	Nr	Nr	0.9	Cu-Zn
İrsahan[k]	0.5–1.0	Nr	Nr	Nr	Nr	1.0	Pyritic Cu
Kuvarshan[k]	2.16	Nr	Nr	Nr	Nr	0.75	Cu
Sinkot[k]	0.40	Nr	Nr	Nr	Nr	5.0	Pyritic Cu
Murgul Başköy[k]	3.18	1.24	Nr	Nr	Nr	0.1	Cu-Zn
Seyitler[k]	1.68	2.51	Nr	0.35	37	2.8	Cu-Zn
Peronit[k]	0.89	2–12	Nr	Nr	Nr	0.25	Zn-Cu
Melo[k]	1.5–3	3–10	Nr	Nr	Nr	0.35	Zn-Cu
Kutonit[k]	Nr	Nr	Nr	Nr	Nr	0.30	Zn-Cu
Murgul Kızılkaya[k, l]	1.09	Nr	Nr	Nr	Nr	1.9	Cu
Akarşen[k, l]	2.30	1.1	0.05	1.5	28	0.8	Cu-Zn
Hod[l]	2.3	0.2	Nr	12.2	Nr	7.13	Cu-Au

[a]Turhan and Avenk (1976)
[b]Yıldız (1988)
[c]Çağatay and Eastoe (1995)
[d]Çiftçi and Hagni (2005)
[e]Eyuboğlu et al. (2014)
[f]Ersecen (1989)
[g]DPT (2001)
[h]Çağatay (1993)
[i]JICA (1998)
[j]Pejatovic (1979)
[K]MTA (2009)
[l]Personal communication

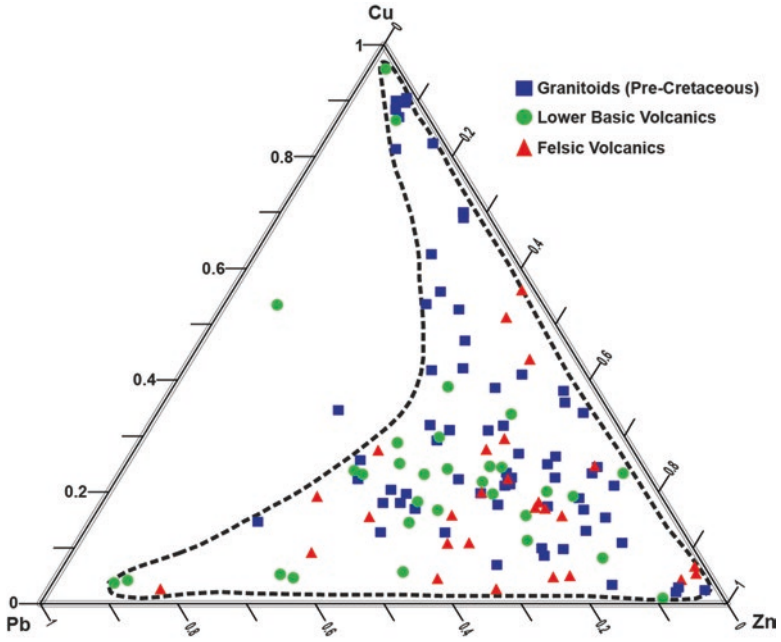

Fig. 9.12 Ternary plot for Cu, Zn, and Pb contents of felsic hostrocks and underlying lithologies including lower mafic volcanics (LBC), and pre-Late Cretaceous granitoids

The $\delta^{34}S$ data for pyrite, chalcopyrite, galena, bornite, sphalerite all vary within a fairly narrow range between −4 ‰ to +6 ‰ (concentrating between −0.5 ‰ and + 4 ‰), indicative of a fairly specific origin. Although "deep-seated" sulfur may be a potential source in the Pontide district, a significant contribution of seawater sulfate cannot be ruled out since the most important source of sulfur in Phanerozoic deposits is seawater sulfate that was inorganically reduced (Çağatay and Eastoe 1995; Huston 1999; Gökçe and Spiro 2000; Ciftci 2000; Revan et al. 2014). Negative values may be due to biogenic reduction of seawater sulfate. However, this mechanism should be subtle and locally effective (e.g. vent chimneys). Otherwise there would be broader overall $\delta^{34}S$ ranges, which is not the case (Ohmoto and Rye 1979). $\delta^{34}S$ values from the sulfates, ranging from 17.7 ‰ to 21.5 ‰ (mainly from gypsum and barite), a few per mil higher than the $\delta^{34}S$ value of contemporaneous seawater sulfate. Figure 9.14 shows comparative sulfur isotope data for all VMS deposits occurring in Turkey.

Figure 9.15 shows the bulk Cu/Zn ratio vs. the mean sulfur isotope ratio of the massive ores from a variety of VMS deposits for comparison. The Cu-Zn type VMS deposits have narrow distributions for the $\delta^{34}S$ indicating a homogenous source, whereas Zn-Pb-Cu VMS deposits have wider distributions of $\delta^{34}S$. It also shows that the deposits from the same mining district tend to plot along a trend with a positive slope, suggesting that as a general rule the higher the Cu/Zn ratio, the heavier the

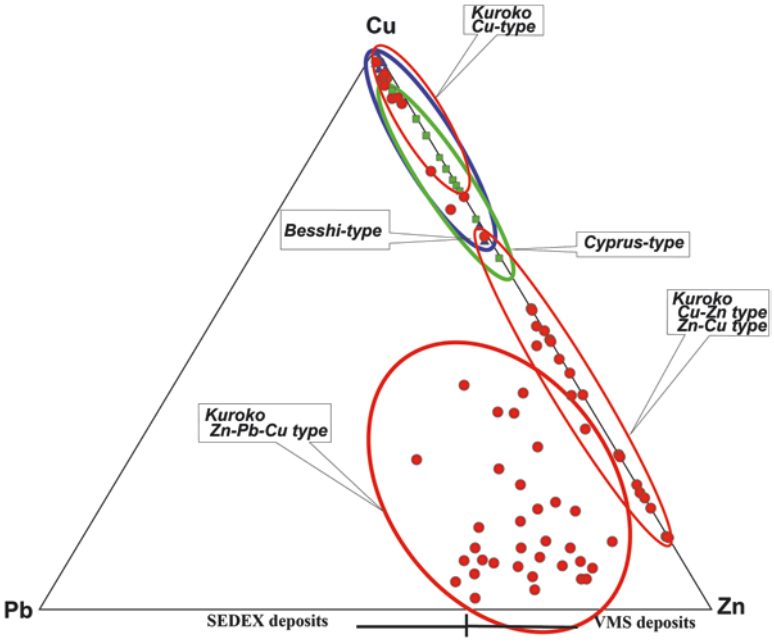

Fig. 9.13 Ternary plot for Cu, Zn, and Pb contents of the Kuroko-type VMS deposits of Turkey along with the other VMS deposits in Turkey. The VMS/SEDEX boundary is after. Franklin et al. (1981)

sulfur isotopic composition of the deposit. Large variations in $\delta^{34}S$ indicate possible multiple sources for the sulfur or changes in the depositional temperatures. In addition to the large variations in the $\delta^{34}S$ values, the ubiquitous presence of sulfates in Zn-Pb-Cu type VMS deposits suggests a large sulfur contribution from seawater.

The $\delta^{34}S$ values for most igneous rocks center around 0% ± 5% (Ohmoto and Rye 1979). However, there are regional deviations from this range due mainly to alteration of the original composition. Apparent similarity between the $\delta^{34}S$ values of igneous rocks and those of the ore deposits suggests that considerable portions of the sulfur came from the igneous rocks. Although such composition of the $\delta^{34}S$ could be produced by mixing between the seawater and the pristine ore fluids or the inorganic reduction of seawater sulfate, or equilibrium reactions between the circulating seawater and the basement rocks, due to close stratigraphic association of the deposits with the magmatic rocks in the region, the results from this study indicate that the sulfur is predominantly magmatic in origin.

$\delta^{65}Cu$ of chalcopyrite from these deposits range between +0.34 ‰ and −0.62 ‰ in comparison with various VMS deposits worldwide (Fig. 9.16). Chalcopyrite from the VMS deposits of the eastern Pontides have a mean $\delta^{65}Cu = -0.13$ ‰. $\delta^{65}Cu$ of chalcopyrite is generally heavier than that of corresponding bornite. The range of $\delta^{65}Cu$ for chalcopyrite from VMS deposits in the eastern Pontides is larger than that observed from Alexandrina, a Devonian VMS deposit in the southern Urals, but is

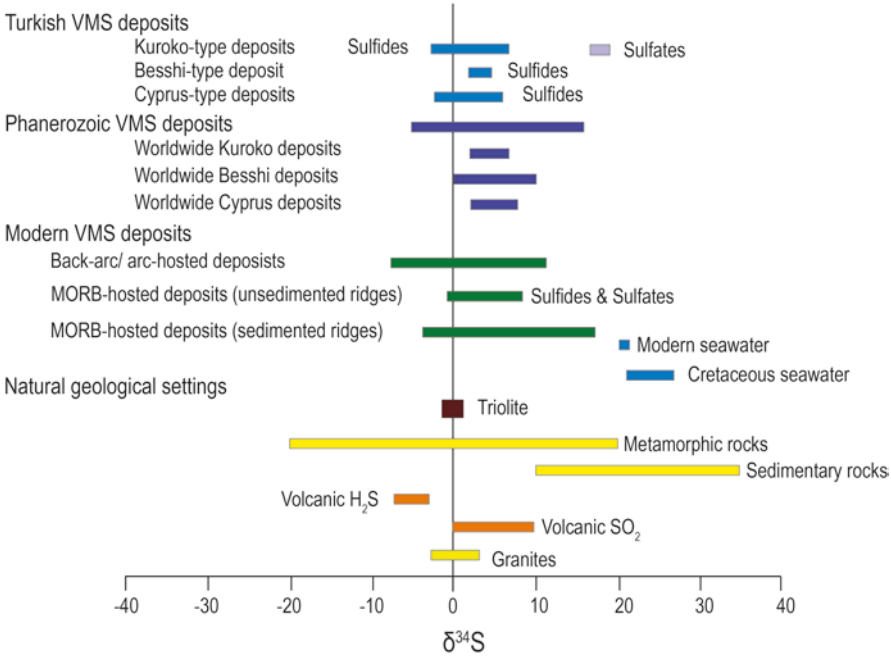

Fig. 9.14 The ranges of $\delta^{34}S$ values of sulfides and sulfates associated with the Kuroko-type VMS deposits and other VMS deposits of Turkey as compared with other deposit and natural sulfur reservoirs. (Data from Ohmoto and Rye 1979; Arnold and Sheppard 1981; Kerridge et al. 1983; Zierenberg et al. 1984; Shank and Seyfried 1987; Woodruff and Shanks 1988; Çağatay and Eastoe 1995; Huston 1999; Gökçe and Spiro 2000; Revan et al. 2014; Ciftci 2000)

significantly smaller than the up to 3 ‰ variations observed from individual modern sea-floor hydrothermal fields along modern mid-ocean ridges. The range of Cu isotope variation in VMS deposits from the eastern Pontides is interpreted to result from processes related to both oxidation and leaching of previously deposited copper, within the various rocks constituting the basement rocks of the region by seawater and to its subsequent deposition elsewhere in the hydrothermal system (Housh and Çiftçi 2008).

The $\delta^{18}O$ values for quartz from the Turkish VMS deposits range between +7.5 and 12.5, essentially indicating that the ore-forming fluids could have been circulating seawater with −0.6 to +2.9 for $\delta^{18}O$ values or a mixture of seawater and magmatic waters (Ciftci 2000). Gökçe (2001) interpreted O-H isotope data acquired from fluid inclusions studies for the Murgul deposits such that the most of the water in ore-forming hydrothermal solutions are meteoric in origin; however, there seem to be a small amount of seawater mixing and/or interaction. $\delta^{18}O$ of ocean water is buffered near −1 to 0. Uniformity of $\delta^{18}O$ in seawater as far back as the Early Paleozoic has been indicated by a number of investigators (Knauth and Roberts 1991; Kolodny and Luz 1991).

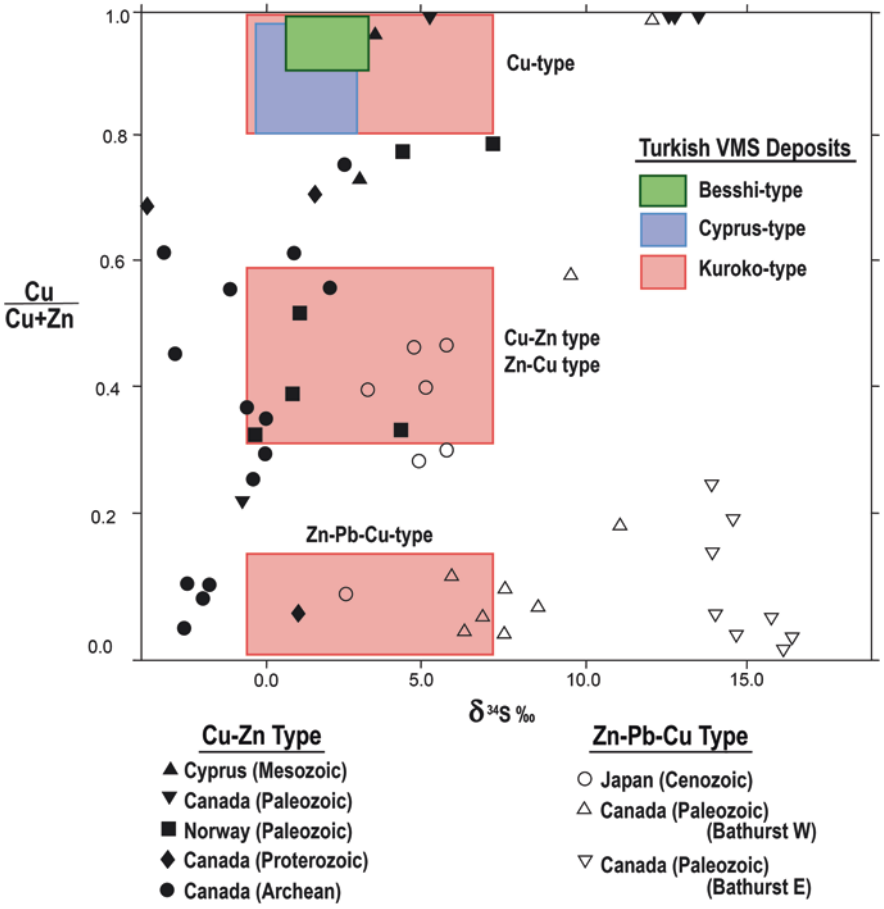

Fig. 9.15 Average sulfur isotope ratios versus the bulk Cu/(Cu+Zn) ratio of the sulfide minerals from the VMS deposits occurring worldwide and in Turkey. (Modified from Lydon 1988)

Lead isotope results (Table 9.5) acquired mainly from galena for the major ore deposits of the region are very similar with respect to their narrow compositional range and being less radiogenic. The data show a narrow range within the region indicating that the metal-transporting hydrothermal fluids were very homogeneous with respect to their lead isotope contents. Thus, it is probable that these deposits are genetically related with respect to lead metal source.

From the above geochemical data, we suggest a large portion of the lead in the VMS ore deposits of the eastern Pontides was sourced from the igneous activity in a magmatic arc setting.

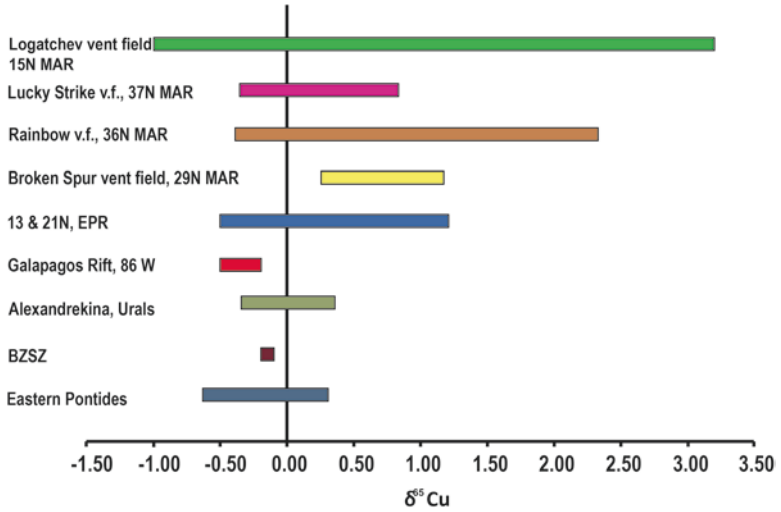

Fig. 9.16 Copper isotope compositions of chalcopyrite from the volcanogenic massive sulfide deposits of the eastern Pontides as well as data from one deposit (Maden-Elazığ) in the BZSZ, the Devonian Alexandrinka VMS deposits in the southern Urals (Rouxel et al. 2004) and for black smoker deposits from hydrothermal vent fields along mid-ocean ridges (*MAR* Mid Atlantic Ridge, *EPR* East-Pacific Rise). (Zhu et al. 2000, 2002)

Table 9.5 $^{206}Pb/^{204}Pb$, $^{207}Pb/^{204}Pb$ and $^{208}Pb/^{204}Pb$ ratios of sulfide ores from the Kuroko-type deposits of Turkey

Deposit	$^{206}Pb/^{204}Pb$ (±2σ)	$^{207}Pb/^{204}Pb$ (±2σ)	$^{208}Pb/^{204}Pb$ (±2σ)
Kutlular	18.506 ± 0.023	15.626 ± 0.023	38.616 ± 0.068
Cayeli Black Ore	18.445 ± 0.266	15.714 ± 0.161	38.714 ± 0.812
Seyitler	18.559 ± 0.022	15.670 ± 0.022	38.730 ± 0.064
Akarşen	18.468 ± 0.030	15.566 ± 0.044	38.604 ± 0.130
Tunca	18.860 ± 0.012	15.787 ± 0.014	39.387 ± 0.039
İrsahan	18.522 ± 0.030	15.610 ± 0.030	38.594 ± 0.123
Kızılkaya	18.553 ± 0.009	15.607 ± 0.008	38.591 ± 0.018
Tunca (sphalerite)	18.719 ± 0.017	15.667 ± 0.015	38.812 ± 0.040
Kanköy	18.497 ± 0.004	15.658 ± 0.004	38.662 ± 0.011
Murgul Çakmakkaya (pyrite)	18.676 ± 0.010	15.748 ± 0.010	38.967 ± 0.027
Murgul Damar	18.528 ± 0.006	15.596 ± 0.011	38.570 ± 0.019
Kutonit	18.571 ± 0.006	15.668 ± 0.007	38.762 ± 0.023
Cerattepe	18.578 ± 0.033	15.645 ± 0.035	38.883 ± 0.202
Harkköy	18.535 ± 0.017	15.652 ± 0.022	38.686 ± 0.049
Killik	18.543 ± 0.025	15.625 ± 0.097	38.588 ± 0.289
Kuvarshan	18.593 ± 0.037	15.652 ± 0.038	38.832 ± 0.095
Kotarak Dere	18.291 ± 0.144	15.635 ± 0.168	38.457 ± 0.540
Akköy	18.448 ± 0.013	15.604 ± 0.014	38.563 ± 0.049

9.4.5 Age of the Deposits

The VMS deposits of the eastern Pontides occur in two stratigraphic horizons. Felsic rocks of first horizon (the Kızılkaya Formation) were formed before and/or during the accumulation of the Santonian-Campanian (?) red limestone level, which is one of the key horizons for the eastern Pontides orogenic belt. Fossil record indicates that the Kızılkaya Formation deposited during Turonian (?)- Santonian (Güven 1993; Eyüboğlu 2000). However, there is no fossil record for the felsic rocks of the second horizon – the Çayırbağ Formation. This horizon is covered by the Bakırköy Formation of Maastrichtian - Paleocene age, which consists mainly of calciturbidites. These stratigraphic relations indicate a Santonian-Maastrichtian age range for the felsic rocks of the second horizon in Tirebolu area (Eyüboğlu et al. 2014)

Beside stratigraphic relations and the fossil records, two methods were used to date the eastern Pontide VMS deposits: (I) the Pb-Pb method on galena, one of the principal ore minerals and (II) the U-Pb method on zircon contained by the felsic volcanic host-rocks.

Lead isotope ratios measured on galena for three major VMS deposits of the region – the Murgul main ore body (Artvin), Lahanos (Espiye-Giresun), and Köprübaşı (Tirebolu-Giresun) were used to date the deposits. The two-stage model of Stacey and Kramers was assumed and the calculated age is 89 my (Coniacian) (Ciftci 2000).

These deposits occur in two different stratigraphic horizons within the late Cretaceous sequence. SHRIMP zircon U–Pb analyses from ore-bearing dacites yield weighted mean $^{206}Pb/^{238}U$ ages ranging from 91.1 ± 1.3 (Coniacian – Turonian) for the Kızılkaya Formation to 82.6 ± 1 Ma (Campanian) for the Çayırbağ Formation (Eyüboğlu et al. 2014).

9.4.6 Exploration Guides

9.4.6.1 Alteration Characteristics

Typical alteration zoning in the footwall rocks of a massive Kuroko ore body, from the central to the outer zone, consists of sericite/chlorite-, montmorillonite-, zeolite-II- and zeolite-I zones. The sericite/chlorite zone coincides fairly closely with the stockwork ore zone; the montmorillonite zone extends about 500 m outward from the stockwork zone; the zeolite-I zone represents the background alteration of submarine volcanics. The hydrothermal alteration (i.e., sericite/chlorite- and montmorillonite zones) commonly extends into the hanging-wall rocks of VMSs, indicating that hydrothermal activity continued after the formation of sulfide ores.

Epigenetic mineralization (stockworks and some of the disseminated mineralization) within the host rock generally shows a number of associated alteration zones. A very generalized configuration is as follows: (I) the stockwork ore zone is surrounded by an innermost zone of chloritization that forms the core of the

alteration zones, (II) a sericitized zone surrounds the core zone and (III) a strong silicic alteration zone may accompany these zones particularly in the upper part of the alteration pipe, immediately beneath the massive orebody in some of the Kuroko-type deposits of Japan. Formation of large quantities of zeolite and the absence of epidote and kaolinite are very unique but present in the Kuroko deposits. This is attributed to environmental conditions in which the deposition takes place, and the physicochemical characteristics of the hydrothermal fluids.

In general, Late Cretaceous volcanic host rocks were subjected to intense potassic, phyllic (sericitic), argillic (kaolinitic and smectitic), silicic, propylitic and hematitic alteration processes during fluid–rock interaction related to VMS mineralization (Karakaya et al. 2012). Thus, hydrothermal alteration zones are well developed around both massive and stockwork zones extending from 250 m to 3 km in dimension in many of them, thereby forming quite extensive exploration targets. In the study areas, alteration index (AI) values increase towards the ore horizon that is consistent with mineralogical observations. High AI values may be due to the breakdown of plagioclase, volcanic glass and their replacement by illite. In particular, illite-mica+quartz assemblage associated with the ore mineralization in the footwall rocks appears to be significant (Çağatay and Boyle 1977). This is a consistent occurrence on the regional scale. These alteration zones are represented by silicification-pyrite-illite, illite-silicification, illite/smectite-silicification and smectite zones accompanying kaolinite and halloysite in the dacitic pyroclastics. Alteration zones developed in the Kutlular footwall and hanging wall rocks reveal several geochemical characteristics that could be indicative of systematic changes with increasing proximity to the orebody, such as Na depletion, elevated AI and chlorite-carbonate-pyrite index (CCPI) (Abdioğlu and Arslan 2009). In the Murgul deposits, an early phyllic and argillic alteration zones developed in the center close to the orebody then surrounded by a later silicic alteration zone (Özgür 1985; Schneider et al. 1988).

Well-developed alteration zones facilitate the effectiveness of soil geochemistry for the discovery of concealed VMS deposits in the region. Pb-As and Cu-Zn pairs were succesfully used as pathfinder elements to locate target areas in the region (Çiftçi et al. 2005; Köprübaşı et al. 2014).

9.4.6.2 Structural Geology

The extrusion and intrusion of magmas and localization of VMS mineralization were controlled mainly by the NE–SW trending block-fault systems, where the dacitic rocks were intensely fractured and brecciated during pre-mineralization Alpine orogenic events. These fault zones provide permeable pathways for the flow of magma as well as hydrothermal fluids.

Rhyolites/dacites generally occur as domes and are spatially and genetically related with the VMS occurrences throughout the region (Fig. 9.17). Successful recognition of such structures will greatly contribute to the targeting of buried deposits.

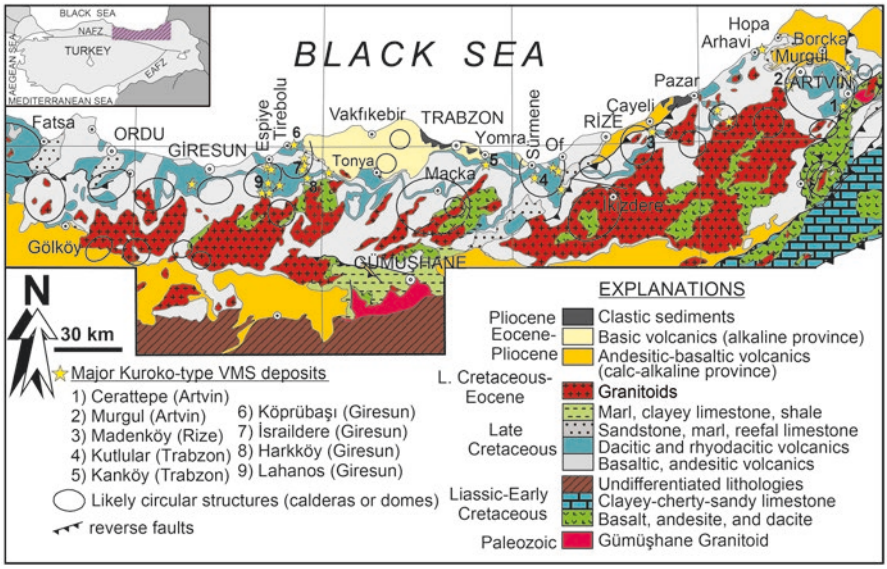

Fig. 9.17 Distribution of circular structures (domes, collapsed domes, and calderas) within the EPTB in association with host lithologies and the VMS deposits. (Eyüboğlu et al. 2014 and references therein)

9.4.6.3 Lithological Association

Since the felsic volcanics of Late Cretaceous age are the main host of the massive sulfide deposits, these deposits are considered to be strata-bound. Thus detailed geological mapping can be used to find target areas.

Another lithological association that can be used as marker bed in exploration for these deposits is late Cretaceous "red pelagic limestones" occurring throughout the region (Fig. 9.18). They typically contain *globotruncana* and have a characteristic red wine color, which is overlain by red marls and turbidites. Color and clay content change towards top, becoming lighter and more purplish due to the changes in its lithology and richer in clay content grading into marl. It is consistently thinly bedded and can be split. This marker bed outcrop in many ore fields in the region.

9.4.6.4 Geophysics

Although there is no successful application leading to an ore deposit discovery using both ground and air geophysical methods in the region, ore deposit model-based techniques, alone or in combination can be successful for exploration purposes. The mineralogy of the ore deposits, structural and lithological controls on the ore-forming systems, should also be prioritized. Since the area is heavily vegetated and has extremely rugged topography, airborne geophysical surveying is not a

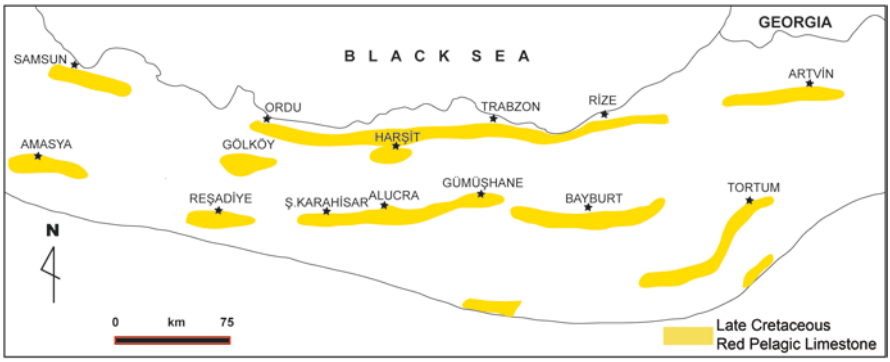

Fig. 9.18 Areal distributions of the red pelagic limestones throughout the EPTB that are marker beds for the Late Cretaceous VMS occurrences. (Compiled from Pelin et al. 1982; Güven 1993)

preferred exploration method in the area. However, airborne surveying employing helicopter rather than an aero plane to maintain constant flight altitude and speed that will enable to make better topography and terrain corrections could be used to generate useful geophysical data rather than ground methods.

Presence of mafic volcanics in the region and the rough topography (resulting in no terrain correction) hinders ground gravity surveying.

Radiometric surveys (both air and ground) may be useful where intense potassic alteration is present, although its effectiveness downward is limited to about a meter, and could be effected by granitic intrusions, which is the case in the region. Caution should be taken since the felsic volcanics are spatially related to the shallowgranitic intrusions.

IP (ground induced polarization) could be successfully applied; however, caution should be taken since the presence of pervasive pyrite will suppress chargeability of other sulfides, particularly chalcopyrite. Another complication is the presence of groundwater and soil humidity. Due to the nature of the felsic volcanics, such water is generally SO_4-saturated, which results in false chargeability anomalies, particularly along drainage channels, such as creeks. In order to avoid such erroneous conclusions, ground only CSAMT (Controlled Source Audio Magnetotelluric), an EM method, can be employed to measure electric and magnetic field components since it is effective down to a few hundred meters and not affected by rugged topography to test the depths continuation of resistivity values generated by the IP method. In this combined method, low resistivity values can be used to delineate the mineralized zones and/or changes in lithologies.

TEM (Transient Electromagnetic Method), an EM method, measures secondary EM generated by the conductive structures as a result of induction using strong currents from a loop. Its applicability is limited in rugged terrains, however airborne TEM can be used to survey large areas to measure electrical conductivities within the areas. This is very rapid, practical yet effective method for terrains like the eastern Pontides.

Recent developments in airborne geophysical methods will enable the acquisition of magnetic and gamma ray data or TEM and gravity, which can be corrected against topography, terrain, direction, IGRF (the International Geomagnetic Reference Field), hardware and peripheral-sourced radiation, radiation in air, extra-terrestrial radiation, cosmic rays, and radon gas effect to get more defined and representative data (Aydin 2004).

In conclusion, alteration, mineralogical, lithological and structural data along with geophysical data need to be cautiously evaluated for successful target selection.

9.4.7 Ore Genesis

Genesis and formation of the Kuroko-type VMS deposits in the EPTB can only be understood thorough understanding of it tectonic evolution. The EPTB evolved during the subduction of the Afro-Arabian plate beneath the Euro-Asian plate and the resulting closure of the northern branch of Tethys Ocean (Robinson et al. 1995; Okay and Şahintürk 1997) and lies within a tectonic corridor stretching from southern Georgia and northern Armenia to Bulgaria and Romania, where a large number of similar deposits occur.

The basement of the region consists of a mafic volcanic complex, "Lower Basic Complex", which is intruded by a number of igneous bodies that have varying ages from the early Cretaceous to Eocene. Except for a few outcrops in the northern zone of the region, they are mostly exposed in the southern zone. These rocks would have served as source rock, particularly for copper through the hydrothermal circulation. This is the main reason for the formation of Cu-rich Kuroko-type deposits in the region.

The late Cretaceous volcanic rocks overlying the Lower Basic Complex are highly variable in composition from rhyolite to basalt. The VMS ore deposits are hosted by the felsic volcanic rocks as explained earlier in this chapter. The age of igneous rocks in the region range from Paleozoic to Eocene. The igneous rocks of Paleozoic age can be considered as part of the basement rock complex and have no genetic association with the VMS deposits. The emplacement of the intrusive bodies between early Cretaceous and late Cretaceous is particularly significant with respect to the VMS deposits of late Cretaceous due to (1) time-space relationship with the felsic rocks, (2) hydrodynamic and heat source requirements for the formation of such massive orebodies, and (3) forming a potential metal source.

Emplacement of the early Cretaceous granitoids has two fundamental effects in the region with respect to the genesis of ore deposits: (1) they provided a large heat source that gave rise to the formation of localized to district scale hydrothermal convection cells, which circulated through the Lower Basic Complex and the overlying felsic volcanic complex, and (2) the granitoids were the roots for the felsic volcanism that was active throughout the late Cretaceous as suggested by the spatial distribution of the felsic volcanic rocks being closely associated with the granitoids

(Fig. 9.9). The felsic volcanism also formed rhyolite domes that have been thought to be the heat source for the hydrothermal activities. However, the size of the domes or rhyolite plugs are too small to create and feed such a large scale hydrothermal systems and for a significantly long period of time to be able to extract sufficient metals from the host and underlying rocks. The fact that the felsic volcanic rocks have similar geochemical characteristics to the granitoids supports a genetic relationship between those two rock types. Figure 9.19 illustrates genetic model of Kuroko-type VMS deposits with varying grade and sizes.

9.5 Cyprus: Type Deposits

9.5.1 Introduction

Cyprus-type VMS deposits, also known as Ophiolite-hosted VHMS (volcanic-hosted massive sulfide) deposits, are seen in 1/8 of more than 200 known ophiolite belts throughout the world. Although this deposit type occurs in the Troodos ophiolite in Cyprus, its modern analogues occur in the Mid-ocean ridges. However, the term "Cyprus-type" specifically means a type locality and should be used cautiously since the host-rocks of the type deposits are not typical of Mid-ocean ridge ophiolitic rocks but rather mafic volcanics (Galley and Koski 1999) of ophiolites associated with supra-subduction zones. Thus, Cyprus-type – as a subgroup – should be used for the deposits hosted by the volcanics with ophiolite affinity occurring in comparable settings such as the suture zones formed in Anatolia formed by the closure of Tethyan ocean or other similar settings occurring elsewhere all around world. The other subdivision, "VMS's associated with mid oceanic ridges" covers all the modern massive sulfides related to the Mid-ocean ridges.

Apart from the difference in their tectonic environments, they both are a significant source of base metals, particularly for Cu and to a lesser extent, for Zn, since these are comparatively more Cu-rich within the VMS clan (Figs. 9.5 and 9.13). These deposits may reach up to 45 Mt in size, averaging 5 Mt worldwide and gold and silver rarely reach to mineable grades (Table 9.6).

The ophiolite-hosted deposits occurring in the mid-ocean ridge settings are formed as a consequence of hydrothermal circulation driven by heat source generated by the layered ultramafic-mafic plutonic magma chambers found below the sea-floor spreading axes. The massive sulfides are formed from metal-bearing exhalative fluids, typically from black smokers. Therefore, these VMS deposits are considered to be "syngenetic" in character. The size of the VMS is governed by the spreading rates. Larger deposits are associated with the slower spreading centers such as Josephine ophiolite, Oregon. Sedimentary intercalations within the volcanic section are an indication of slow spreading. However, in the supra-subduction ophiolites (Cyprus-type sensu stricto), the ore-forming system responsible from the sulfide accumulation is more complicated because the heat source driving the hydrothermal systems is not clearly defined.

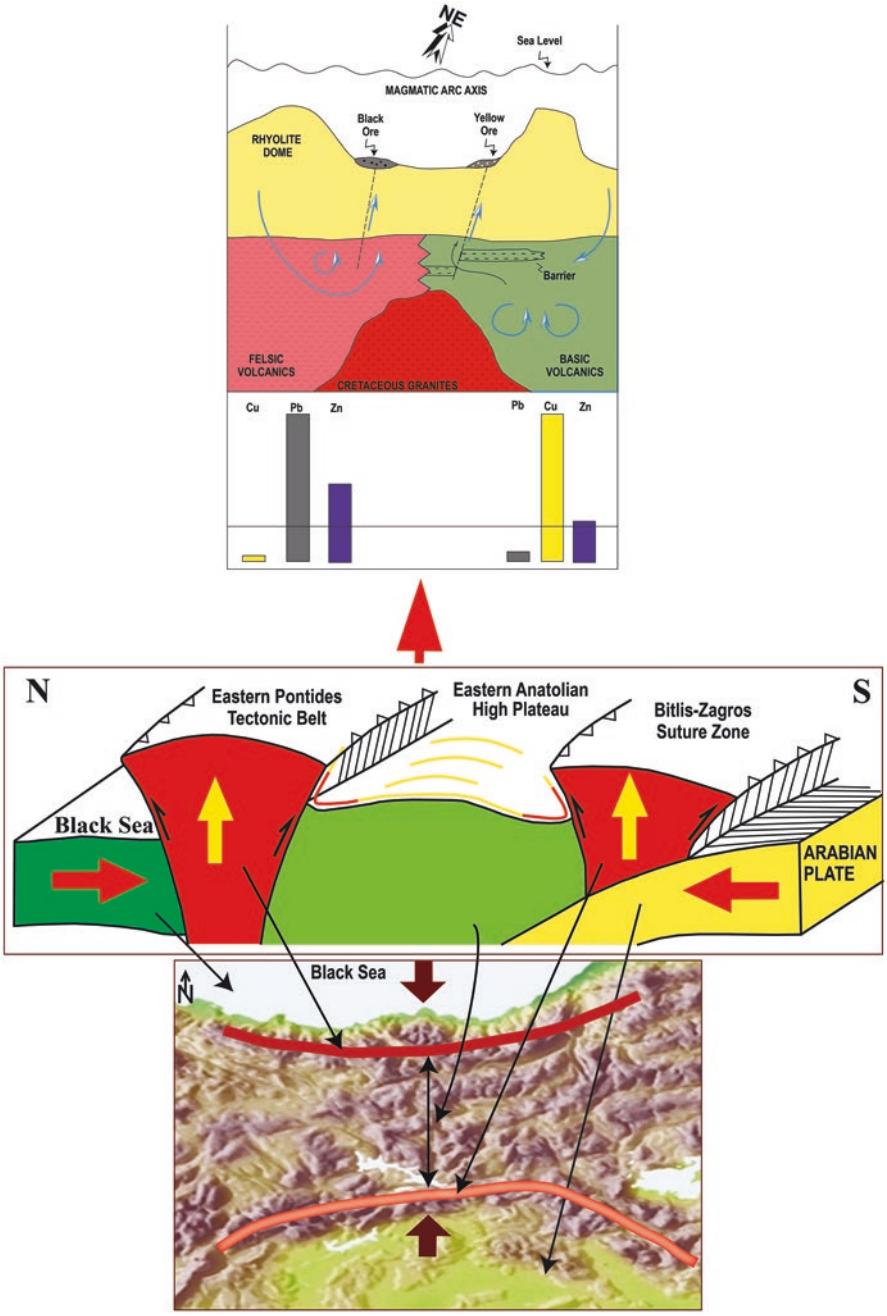

Fig. 9.19 A proposed genetic model for the VMS mineralization with varying size and base metal contents. (Adapted from Eyüboğlu et al. 2014 and references therein)

Table 9.6 Comparative average grade and tonnage data for the Turkish Cyprus-type deposits with some of the counterparts worldwide

Deposit	Country	Cu (%)	Zn (%)	Ag (ppm)	Au (ppm)	Reserve (Mt)
Limni	South Cyprus	1.0	0.2	Nr	Nr	16
Mavrovouni	South Cyprus	4.5	0.5	Nr	Nr	15
Skouriotissa	South Cyprus	2.5	1.0	Nr	Nr	6
Ice	Canada	1.48	~1	Nr	Nr	4.6
Madenköy	Siirt-Turkey	2.02	<0.5	Nr	Nr	41.5
Maden	Elazığ-Turkey	0.2–10.8	<05	Nr	Nr	3.5
Ormanbaşı Hill	Adıyaman-Turkey	0.9–3.9	0.02–2.8	0.05–0.45	1.9–11	0.67
İncekoz	Adıyaman-Turkey	0.2	Nr	Nr	Nr	4.2
Derdere	Diyarbakır-Turkey	0.7–5.6	0.2–19.2	<0.3	Nr	Nr
Koçali	Adıyaman-Turkey	>0.5	<0.2	Nr	Nr	3.23
Ortaklar	Gaziantep-Turkey	3.5	1.15	1.3	6.3	12.0
Mağaradoruk	Kastamonu-Turkey	3.24	<0.5	1.5	5–20	25.0
Aşıköy	Kastamonu-Turkey	1.56	<0.5	2.48	10	11.23
Toykondu	Kastamonu-Turkey	4	<0.5	Nr	Nr	0.38
Kızılsu	Kastamonu-Turkey	2–4	<0.5	Nr	Nr	0.74
World Avg.		2.78				5.0

The ophiolite-hosted VMS deposits often occur as clusters and can occur at any stratigraphic level within the ophiolitic sequence from the top of the magma chamber to the overlying sedimentary cover sequences (Harper 1999). However, massive sulfides are generally found within the volcanic portion of the sequence and/or between the overlying sediments and the mafic volcanics. In the Deposits generally consist of a stratiform massive sulfide body and an underlying stockwork zone that may extend vertically as deep as 3 km and laterally as wide as 500 m (e.g. the Aarja deposit, Oman). These two may co-occur or one may be missing or displaced due to the post depositional events (Galley and Koski 1999). In Turkish examples, the majority of the sulfide deposition is hosted by the pillow lavas and/or basaltic/diabasic volcanics.

Cyprus-type VMS deposits have similar ore mineral assemblages. They are all pyrite-rich (the earliest phase), with major chalcopyrite and minor to trace sphalerite. Gold and cobalt-bearing minerals may reach significant levels. Sandy texture, a variety of replacement textures, and brecciation are common in the massive zones, while disseminations, veins and veinlets are prevalent in the stockwork zones where pyrite and quartz dominate with minor amounts of chalcopyrite. Trace amounts of native copper, secondary bornite, as well as marcasite, galena, pyrrhotite, cubanite, stannite-besterite and hematite have also been reported (Richards et al. 1989). Some of the Turkish examples contain abnormally high magnetite (Yıldırım et al. 2016) and cobalt in the form of linnaeite (Altun et al. 2015).

Turkish Cyrus-type VMS deposits occur in two tectonic regions: in the Central Pontides (I) and along the aproximately 500 km-long Bitlis-Zagros Suture Zone (BZSZ) in southeastern Turkey (II). Some of them, both in the Maden and Küre

areas, have been mined by ancient civilizations as old as the period of the Assyrian Empire and even before.

The Cyprus-type VMS deposits of the Central Pontides cluster in the Küre area. They are located west of the town of Küre (Kastamonu), and they roughly align from north to south in the order of Toykondu, AŞıköy, Kızılsu, and Mağaradoruk (formerly Bakibaba) and they all can be considered as multiple lenses of one giant ore-forming hydrothermal system. They are interpreted to be originally concordant and have been both deformed and changed their attitude due to the post tectonic activities.

Mining activities in the region date back to the Greek and Roman times and have continued during the Seljuk, Republic of Genoa, and the Ottoman times. Ottoman time mining activities in the area were mainly in the Bakibaba deposit until 1845 (Bakibaba is the oldest among the others as evidenced by artifacts and slags indicated).

Following the foundation of the General Directorate of Mineral Research and Exploration (MTA), the area was subject to exploration programs starting in 1935 and continuing today. The Aşıköy was explored in 1944, while the Bakibaba area exploration started in 1963 and ended with the discovery of two new ore bodies named the north and south sections (Sarıcan 1968). The northern section was operated by government-owned Karadeniz Bakır (K.B.İ.) since 1968 and abandoned in1990 due to a pyrite fire in the galleries (Ildız and Dağcı 1990).

The Küre area deposits were later acquired by Cengiz Holding in 2004 and have been mined in an open pit until 2009 (Altun et al. 2009). The AŞıköy deposit was subject to new exploration and reserve enlargement between 2005 and 2008. The deposit is still actively mined by open pit methods (Altun et al. 2015). The Mağaradoruk deposit was also subject to new explorations starting in 2008 and ending with the discovery of a 25 Mt reserve ore body grading up to 3.24% Cu.

The Bitlis-Zagros Suture Zone (BZSZ) represents one of the remnants of Paleotethyan and Neotethyan oceanic crust, between the approximately E-W-trending Pontides, Anatolides, Taurides, and Border orogenic belts. The Neotethyan oceanic basins and continental margins were uplifted during a Permian collisional events between Laurasia and Gondwana (Ketin 1983; Şengör and Yılmaz 1981; Robertson et al. 2004; Okay 2008). As a result, ore-forming systems were formed and kept active for long enough to form a significant number of ore bodies of variable size and grades. This zone has a roughly arcuate shape and extends from Hakkari at the easternmost tip to Gaziantep at the westernmost end through Siirt, Diyarbakır, Elazığ, and Adıyaman cities (Figs. 9.1 and 9.20). The Cyprus-type VMS deposits and prospects are extensive along this zone and occur in association either with the Middle Eocene Maden complex in Siirt area and with the Late Triassic-Late Cretaceous Koçali complex in Adıyaman-Gaziantep area (Şaşmaz et al. 1999; Akıncı 2009; Yıldırım et al. 2010, 2012a, b, 2016; Yıldırım 2013; İlhan 2013; Akyıldız et al. 2015).

They align from northeast to southwest in the order of Madenköy (Şirvan-Siirt), Yazıcık (Mutki-Bitlis), Andılar (Palu-Elazığ), Maden (aka Ergani) (Maden-Elazığ), Derdere (Çüngüş-Diyarbakır), Ormanbaşı Hill (Sincik-Adıyaman), Koçalı

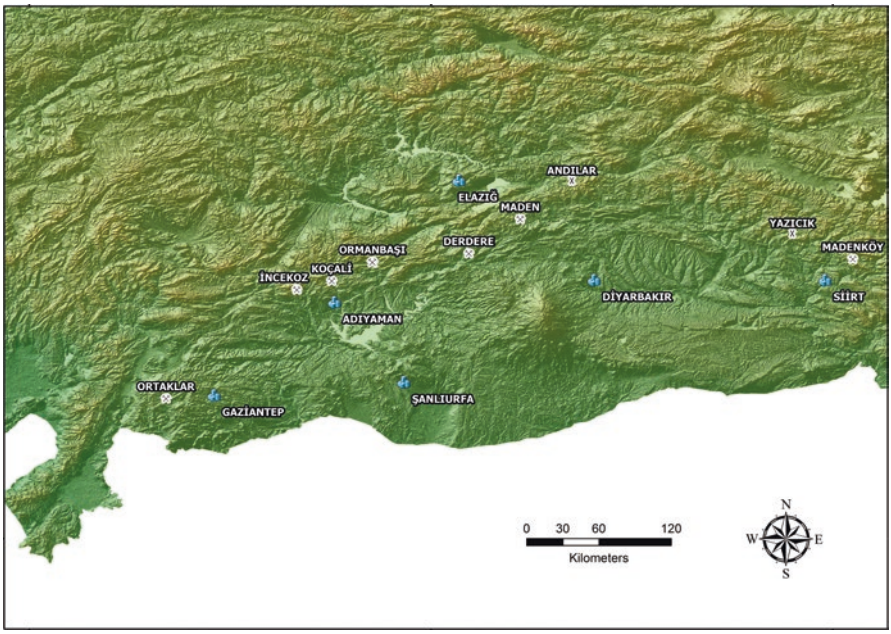

Fig. 9.20 Locations of the Cyprus type deposits along the BZSZ

(Adıyaman), İncekoz (Tut-Adıyaman), and Ortaklar (Gaziantep) ore bodies (Fig. 9.20). They are also considered to be originally concordant and later deformed.

The Maden area (Elazığ) deposits among the others are the oldest known deposits in Turkey. Mining activities date back to 2000 BC first by Assyrians, then Romans, Arabians, and Ottomans. It is called the "Arghana Mine" in the old literature. Many works have been published on this mine and mining activities since 1889. Maden comprises a main ore body and 5 satellite bodies that include Mihrap Dağı and Weiss to west, Kısabekir to east, Putyan to north, and Hacan to south. Only the main orebody was mined historically. After the Ottomans, the mine has been operated since 1924 by Ergani Bakır, a government-owned company. Later in 1945, it was handed over by Etibank, another government company, and following privatization in 1995 by Ber-Öner in 1995 for 10 years, and it was finally acquired by Eti Gümüş in 2007. Since then, it is under development to expand the reserves with sporadic productions.

Madenköy (Şirvan-Siirt) was also mined since prehistoric times. First exploration results were reported from 1947, 1958, to 1962. Extensive drilling and detailed explorations was initiated later in 1970. A feasibility project was completed jointly by MTA and Outokumpu in 1981. As a result, 24 Mt of reserve at 2.03% Cu was reported. Prospect was handed over to Etibank in 1985 and an international consortium was constituted to exploit the mine ending in 1989. The prospect was put up for sale and acquired by Park Elektrik Madencilik Sanayi ve Ticaret Ltd. in 2004. All the other deposits and prospects are discoveries since 2000s.

9.5.2 Geological Framework

9.5.2.1 Central Pontides

The Central Pontides comprise a part of the western Pontides tectonic belt of Turkey where the oldest lithologic units are Paleozoic metamorphic rocks including gneiss, schist and quartzite, and Pre-Liassic ophiolitic rocks, such as serpentinite, diabase and basalts (Pehlivanoğlu 1985). Metamorphic massifs in "Western Pontides" belongs to "Rhodope-Pontide" continent. The "Paleoethys" oceanic crust to the north in Permo-Triassic had become an active continental margin by southward subduction (Şengör and Yılmaz 1983; Yılmaz 1980). These authors also stated that thick flyschoidal deposit had been sedimented on the "Paleotethys" oceanic crust in Early Jurassic, and that the Küre ophiolite, representing a "Paleotethys" oceanic crust, had been placed on the "Rhodope-Pontide" continental margin due to the closure of "Paleotethys" in Dogger time. The Küre basin could be formed in association with the beginning of detachment of Eastern and Western Pontides in Early Mesozoic, rather than being a European marginal basin (Şengün 2006). Fossiliferous Late Paleozoic rocks are encountered in most of the region and represented by Carboniferous coals. It has large and small outcrops of allochthonous thrust slices on Cretaceous flysch. Permian is represented by clastic rocks, such as conglomerate, sandstone and sandy shales in places where they overlie coaly units, and by greywacke and limestone in other places.

In this belt, Triassic rocks are present only as massive limestones to the east of Küre below Liassic flysch between Devrekani and Abana. Liassic sequences, which contain black shale, siltstone, sandstone and greywacke, unconformably overlie the pillow lavas of the ophiolitic sequence (Bailey et al. 1966; Güner 1980; Pehlivanoğlu 1985). The rock units in the Kastamonu area can be regarded as basement and cover rocks. Basement rocks that host the VMS deposits include (I) the pre-Liassic Küre ophiolite, characterized by dismembered ophiolitic rocks (serpentinites, peridotites, diabases and mid ocean ridge basalts), (II) the Liassic epi-ophiolitic Akgöl Formation, comprising black shale and subgreywacke (Ketin and Gümüş 1963), and (III) Dogger plutonic and volcanic rocks (granodioritic intrusions and dacitic dikes) (Yılmaz 1980). All these have been intruded by late dacitic and granodioritic rocks during the Dogger (Çakır 1995).

The VMS deposits of Küre area are associated with basement rocks and hosted by extensively altered basaltic rocks with typical pillow structures and the black shales, which have widespread occurrence in the area (Bailey et al. 1966; Güner 1980; Pehlivanoğlu 1985). The host rocks were isoclinally folded and thrust over the black shales and subgreywackes together with the ore body. Therefore, the ore body has a prograde metamorphic history involving burial, heating, and associated deformation (Fig. 9.20).

9.5.2.2 Bitlis-Zagros Suture Zone (BZSZ)

Southeast Anatolia orogenic belt was formed during a continent-continent collision involving closure of the Tethyan Ocean from the Cretaceous to Miocene (Şengör and Yılmaz 1981). The evolution of the orogenic belt is characterized by the transport of nappes to the south, thrusted onto the Arabian Plate (Yıldırım and Yılmaz 1991; Yılmaz 1993; Yılmaz et al. 1993). This region is also known as "*Border Folds Belt*" (Ketin 1983; Herece 2008). Yılmaz (1990, 1993) and Yılmaz et al. (1993) suggested that the orogenic belt consists of three different tectonic units, from north to south, the Nappe zone, Imbrication zone and Arabian Platform. The tectonic units are also E-W trending and separated from each other by North dipping thrust planes. Sediments of the Mesozoic platform cover the Precambrian-Paleozoic basement as concordant bodies or tectonic slices. These nappes occur in the region from Adıyaman-Gölbaşı, Kılıçdağ-South of Hatay and west of Kilis regions. The Koçali-Karadut Nappe, including the Koçali Complex as well as the Karadut Complex, is one of the nappes in the tectonic slices. The Maden Complex on the other hand crops out widely along the southern margin of the Bitlis Massif, as tectonic slivers, either directly under the Bitlis metamorphic rocks or through an intervening thrust sheet of the ophiolitic mélange. The Maden Complex consists of Eocene sandstone, conglomerate, red pelagic limestone, basaltic lava, and tuff. In a few localities the Maden Complex is reported as lying unconformably over the Bitlis metamorphic rocks, however, in most places it is positioned between the Tertiary formations of the Arabian Platform and the Bitlis Massif. The Maden Complex can be regarded as products of a short-lived Mid-Eocene back arc basin, above the northward dipping subduction zone between the Arabian Platform and the Anatolide-Taurides (Yiğitbaş and Yılmaz 1996).

9.5.3 Ore Geology

All of the Cyprus type VMS deposits of Turkey occur in association with supra-subduction ophiolites along the suture zones. They have been displaced during the closure of both the Neotethys and the Paleotethys.

In the Küre area, ultrabasic rocks composed of serpentinized peridotite, dunite and pyroxinites at the bottom, the overlying Küre formation, which consists of basaltic rocks and black shales, and cross cutting gabbro-diorite and dacites are located around the Küre VMS deposits. Ultrabasic rocks are found in NW of Küre, Elmakütüğü hill, around Ömer Yılmaz locality and in east of Karacakaya hill. The lower boundary of ophiolites in Küre region is not observed and boundaries with other units are faulted (Altun et al. 2015).

The Küre formation, which has widespread occurrence in the Küre area, is mainly composed of basaltic rocks and black shales. Basaltic rocks are commonly observed in the form of pillow lavas. The unit was defined by Kovenko (1944) and Ketin (1962) as diabase, by Bailey et al. (1967) as mafic volcanic rocks (pillow lava,

breccia, tuff), by Güner (1980) as a basaltic sequence, by Çağatay and Arda (1984) as spilite, by Pehlivanoğlu (1985) as mafic volcanic sequence and by MMAJ (1995) as Küre volcanics. Basaltic volcanic rocks include basalts, hyaloclastic and pillow lavas and may reach up to 2000 m in thickness. Massive basalt lavas in lower layers grade into pillow lavas (pillows range between 25 and 200 cm in diameter) and breccias towards the upper layers (Güner 1980; Çağatay and Arda 1984; Pehlivanoğlu 1985). Basalts are tholeiitic in character and are the product of oceanic ridge volcanism (Güner 1980).

Black shales overlie the basaltic volcanics of Küre ophiolite (Pehlivanoğlu 1985) and reach up to 150–200 m in thickness. However, several black shales were observed within basalts around the Küre VMS deposits. Some of them are closely associated with mineralization, but others are observed between basalts and/or as lenses in basalts. Black shales are cut by Dogger aged granitic intrusions, dacite dyke and sills. Although these shales are considered to be cap rocks for the massive sulfides, they are located both as footwall and hangingwall rocks of in the Mağaradoruk deposit.

Intrusions of gabbros and diorites of varying sizes are observed around Küre in lower parts of the basaltic sequence (Pehlivanoğlu 1985). Younger dacites occur as dykes and sills in the area. However, they both have no relationship with the mineralizing system.

The Küre mineralizations are closely associated with basalt-black shale units. Concordant to semi-concordant lenticular bodies occur both within and on the basalts, along the contacts between basaltic volcanics and shales. Shales mostly serve as blanket layer suggesting that they could actually be responsible for trapping the ore-forming fluids. Although thin ore bands in the form of well-sorted pyrite and chalcopyrite in places, where the mineralization thins out, were observed within the shales, they mostly have fairly sharp contacts with the massive ore zones (Fig. 9.21).

In the Bitlis-Zagros Suture Zone, two complexes, the Koçali and the Maden, host significant number of ore deposits and prospects. In additions to the known deposits, new discoveries in the region made the area one of the favorable targets in the country.

The Koçali Complex has two distinct lithologic units: the Koçali Ophiolite (ophiolite nappe) and the volcano-sedimentary Koçali Mélange, which consists of a folded, thrust-imbricated succession of basaltic lavas, volcaniclastics, pelagic carbonates, and radiolarites. The Koçali Mélange is a tectonic slice, thrusted by the Koçali Ophiolite on a regional scale and, unconformably overlain by Arabian Platform sediments (Yıldırım et al. 2016). The succession tectonically overlies the Karadut Complex. The Koçalı Ophiolite and the mélange were tectonically intercalated during obduction onto the Arabian Plate (Yıldırım et al. 2012a, b; Robertson et al. 2016). Interbedded cherts within the mélange contain radiolarians of Late Triassic to Late Jurassic age. The lower part of the succession of Mid-Late Triassic age (Tarasa Formation) is dominated by enriched mid-ocean ridge basalt (E-MORB). The overlying Late Triassic to Mid-Jurassic interval (Konak Formation) is characterized by ocean island basalt (OIB) and E-MORB (Uzunçimen et al. 2011; Varol et al. 2011; Robertson et al. 2016). Figure 9.22 shows regionwide outcrops of

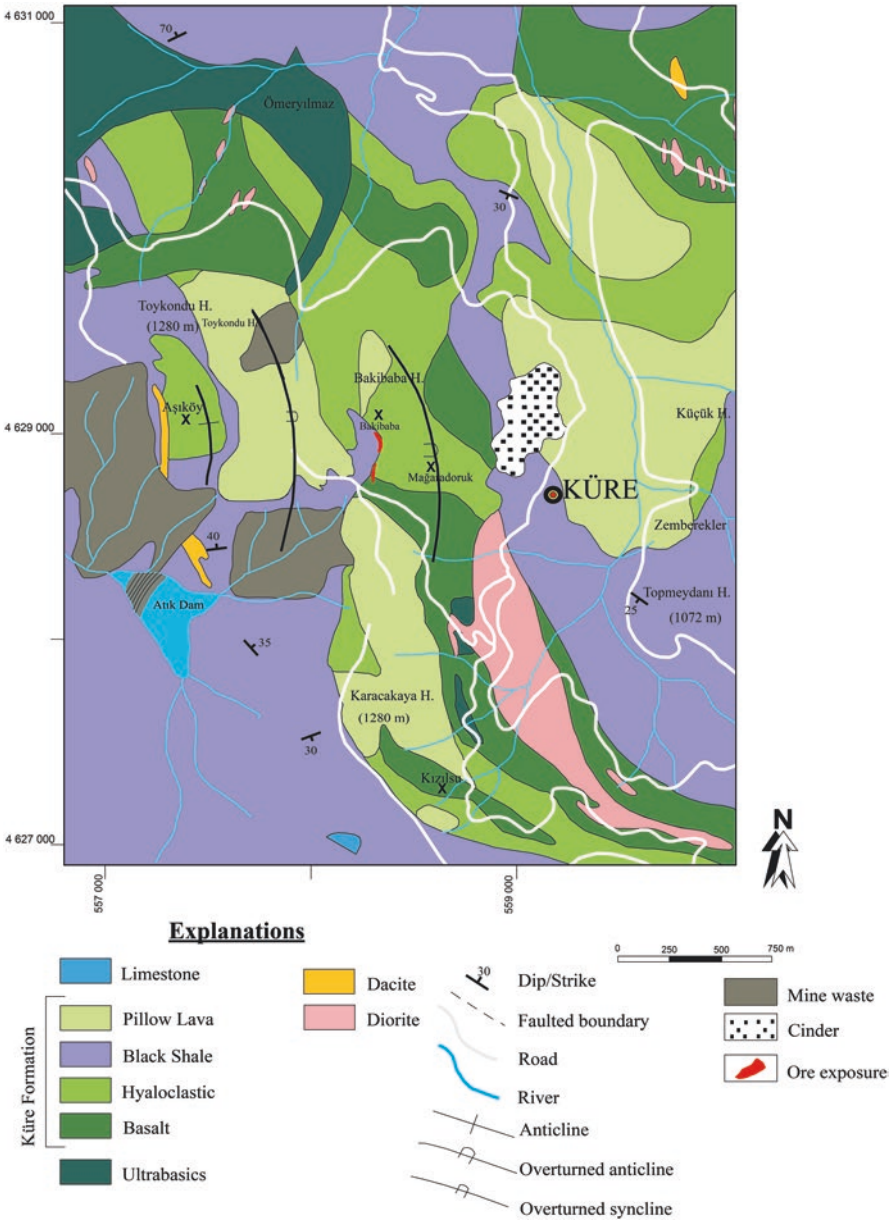

Fig. 9.21 Geological map of the Küre area deposits and their spatial relationship (adapted from Altun et al. 2015)

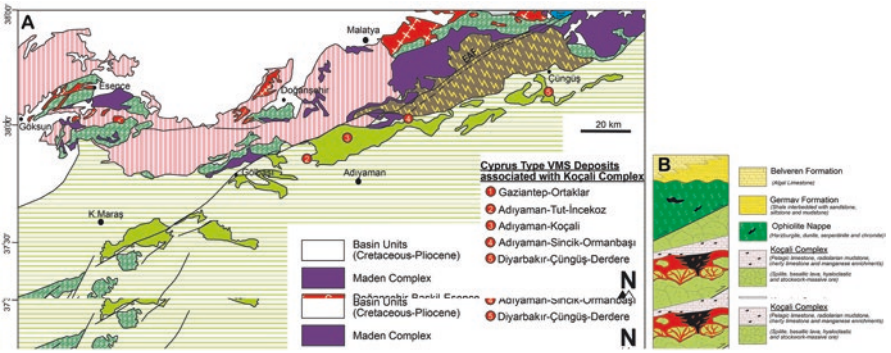

Fig. 9.22 (**a**) Geological map of the Koçali Complex and associated Cyprus-type deposits and (**b**) lithostratigraphic column for the Koçali deposit. (Adapted from Yıldırım et al. 2016 and references therein)

the complex with a type section showing common features shared by most of the deposits hosted by the Koçali Complex.

The Maden Complex is composed of basalt, basaltic andesites, diabase, pillow lavas, sandstone-shale intercalations, red-gray mudstones, calcareous shale and limestone blocks (olistoliths) of varying sizes. The thickness of the complex varies from 100 to 750 m (Açıkbaş and Baştuğ 1975). The complex unconformably overlies the Guleman ophiolites around the town of Maden (Elazığ), the Hazar unit east of Hazar Lake, and the Pütürge metamorphics around the town of Pütürge (Malatya). Volcano-sedimentary units of the complex have been divided into four formations (Açıkbaş and Baştuğ 1975): the Ceffan formation (basal conglomerate, sandstone, sandy limestone), the Arbo formation (sandy–clayey limestone–tuffite–neritic limestone), the Melafan formation (pelagic limestone, mudstone, spilitic lavas, radiolarite, chert), and the Karadere formation (altered basalt and andesite). Paleontological evidences indicate that the complex is of Middle Eocene age (Perinçek 1979) and dated as 48 Ma using the K–Ar geochronology (Yazgan 1984). The Madenköy (Şirvan-Siirt), Yazıcık (Mutki-Bitlis), Andılar (Palu-Elazığ) and Maden (Maden-Elazığ) occur in the Middle Eocene Maden Complex, Derdere (Çüngüş-Diyarbakır), Ormanbaşı Hill (Sincik-Adıyaman), Koçalı (Adıyaman), İncekoz (Tut-Adıyaman), and Ortaklar (Gaziantep) deposits are hosted by the Late Triassic-Late Cretaceous Koçali Complex (Saşmaz et al. 1999; Akıncı 2009; Yıldırım et al. 2016). Figure 9.23 shows outcrops of the Maden Complex and associated ore deposits within a typical sequence representing the main lithologies of the complex.

The Maden deposits (Elazığ) one of the two long-time known major occurrences in the BZSZ are represented by the Anayatak (main orebody), which is located in Maden town, 50 km SE of Elazığ. The mine is the only economic deposit along a 20-km-long narrow belt parallel to the thrust faults within the BZS zone. Other smaller bodies, such as Kısabekir, Mergen Tepe and Mızır Tepe have been mined out several decades ago, but a smaller reserve still exist NW of Anayatak in the Weiss pit to be minable by underground methods.

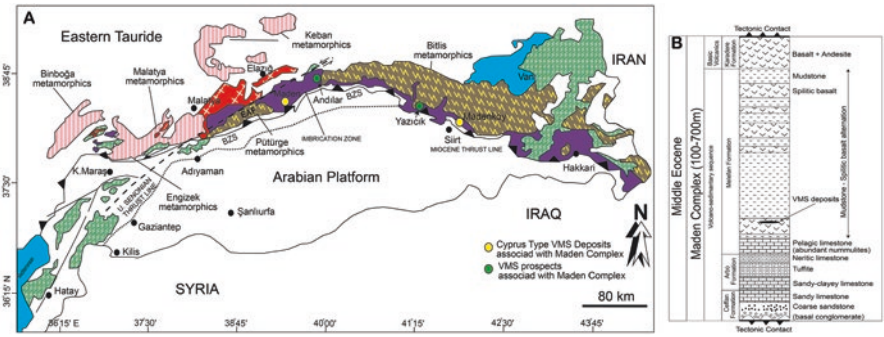

Fig. 9.23 (**a**) Geological map of the Maden Complex and associated Cyprus-type deposits and (**b**) a representative lithostratigraphic column for the Maden deposit. (Adapted from Yıldırım et al. 2016 and references therein; Şaşmaz et al. 2014)

The Maden (Elazığ) deposits are hosted between Eocene mudstones and chloritized basalts, and within sheeted diabase dykes (Bamba 1976; Wijkerslooth 1944). The Madenköy (Siirt) deposit, on the other hand, occurs in porphyritic spilites (Çalgın 1978; Yıldırım and Alyamaç 1976; Ulutürk 1999). The İncekoz mineralization (Tut-Adıyaman) occurs as fracture fillings in sheeted-dike complexes. The Koçali (Adıyaman) mineralization occurs as stockwork and disseminations in spilitized pillow basalts, Ormanbaşı Hill (Sincik-Adıyaman) deposits occur as lenticular and strata-bound massive ore within highly altered, spilitized mafic volcanics corresponding to upper layers of the Koçali complex (Tarasa formation of Sungurlu 1973). The mineralizations is characterized by reworked lenticular and stratiform shapes within mudstone, diabase, spilitic basalts and claystone-shales (Yıldırım et al. 2012a, b).

Derdere (Çüngüş-Diyarbakır) mineralization occurs in highly altered, partially spilitized mafic volcanics. These are submarine volcanics corresponding to the uppermost portion of the Koçali complex. The mineralized zone is overlain by sandstones and pelagic sedimentary rocks. Host-rocks of the Koçali complex, the mafic volcanics and peridotites, are intensively altered in that the peridotites are completely serpentinized and the mafic volcanics are carbonated, chloritized and locally silicified, where close the ore mineralization.

Ortaklar (Gaziantep) deposit is hosted within pelagic limestone, siliceous limestone, radiolarian mudstone and basaltic pillow lavas, alternating with lenses of radiolarites, hyaloclastites and spilitized basalts. These units are imbricated with each other along the thrust belt and extensively deformed. Primary spatial relationships of the lithological units are no longer original due to the imbrication. Footwall rocks are represented by highly altered basaltic volcanics, which contain stockwork and disseminated ore below the massive ore body. Footwall rock alteration exhibits a mineral assemblage of quartz+albite+chlorite+ epidote+carbonate, which indicates greenschist facies ocean floor metamorphism. In addition, hematitization and sericitization to a lesser extent are also observed in the footwall rocks (Yıldırım et al. 2016 and references therein).

9.5.4 Mineralogy and Geochemistry

The main ore minerals in typical Cyprus-type deposits are pyrite and chalcopyrite, sphalerite, pyrrhotite and magnetite (Constantinou and Govett 1972). These are accompanied by minor to trace linnaeite and valleriite (Table 9.7).

The Küre area deposits are mainly in the form of massive, stockwork and disseminated sulfides composed mainly of pyrite and chalcopyrite.

Some of the ore bodies hosted within basalts, some are in black shales or on basalts, overlain by black shales. The black shale overlying the massive sulfide ore consists of ore bands, which are mainly composed of sometimes well sorted pyrite and chalcopyrite in places where the mineralization pinches out. Both black and gray shales consist of illite, quartz, chlorite, siderite and muscovite, and subordinate coal-like material, graphite, pyrite, chalcopyrite, chrome spinel, ilmenite, and hematite (Güner 1980; Çağatay and Arda 1984).

Table 9.7 Common minerals reported from the main examples of the Cyprus-type deposits worldwide, including the Turkish deposits

Ore minerals	Gangue minerals
Pyrite	Quartz
Pyrrhotite	Calcite
Chalcopyrite	Barite
Sphalerite	Siderite
Magnetite	Epidote
Linnaeite	Talc
Galena	Sericite
Bornite	Chlorite
Fahlerz	Rutile
Ilmenite	Ilvaite
Bravoite	Cr-spinel
Chalcocite	Plagioclase
Marcasite	Amphibole
Hematite	Pyroxene
Covellite	Olivine
Goethite	Anatase
Native Gold	Gypsum
Native Silver	Chalcedony
Native copper	
Mushketovite	
Chromite	
Molybdenite	
Valleriite	
Limonite	
Cuprite	
Malachite	
Azurite	
Neodigenite	

Both ore and gangue minerals in all Küre area deposits are highly comparable. However, their relative abundances may vary. A significant difference is in cobalt content, which may reach up to a few percent in linnaeite (e.g. Mağaradoruk deposit).

One of the largest Küre area deposits, the Mağaradoruk deposit, consists mainly of pyrite, chalcopyrite, subordinate marcasite, sphalerite, covellite, neodigenite, malachite, azurite, sulfosalts, trace bravoiite, linnaeite, carrollite, limonite, hematite, magnetite and minor to trace chalcocite, cuprite, tenorite, pyrrhotite, valleriite, bornite, galena, native copper, native gold, chromite, rutile, and anatase. Main gangue minerals include quartz, siderite-ankerite, calcite, dolomite and chlorite (Altun et al. 2015 and references therein).

The Madenköy (Siirt) deposit, hosted by pillow lavas, comprises, from top to bottom, pyrite, pyrite + chalcopyrite, pyrite + chalcopyrite + sphalerite, pyrite + chalcopyrite + magnetite or only magnetite with pervasive chloritization and ends with occasional fracture-filling ores including chalcopyrite, pyrite, and magnetite. Minor to trace marcasite, galena, pyrrhotite, bornite, covellite, chalcocite, valleriite, bravoiite, linnaeite, fahlerz, gold, and silver also occur in the main zone while the main gangue minerals are quartz, chlorite, barite, siderite and carbonates, mostly calcite.

In the Derdere mineralization, major ore minerals include pyrite, sphalerite, and chalcopyrite with secondary chalcocite, covellite, and limonite. Major chlorite and barite with minor quartz and calcite account for the gangue minerals. Dominant ore structures are massive and locally stockwork and disseminations.

In Maden (Elazig) deposits, major ore styles are massive (Kısabekir, Anayatak (main ore body), Mihrap Dağı, and Weiss), dissemi-nations, stockworks and locally concordant layering (Putyan and Hacan). Major ore minerals are pyrite, chalcopyrite, sphalerite, magnetite, native copper with exogenic bornite.

The Ortaklar deposit, one of the most recent discoveries, consists of a gossan zone at the top, followed by a thick, massive ore zone and a poorly developed stockwork zone. Primary mineralization is characterized by distinctive styles including brecciated sulfides, graded beds, stockworks and chimney fragments. Two distinct ores, massive magnetite and massive sulfide co-occur in the Ortaklar deposit. Their co-occurrence is still disputed, but some textural evidence and their spatial relationships with the host rocks may indicate that magnetite and sulfide minerals were generated in different stages (Yıldırım et al. 2016). Each of the zones has its own mineral assemblages. In the oxidation zone, hematite, limonite, goethite, azurite, malachite, gypsum, chalcedony and pyrite-silica veins are observed. In the massive zone, ore minerals in decreasing order include pyrite, magnetite, chalcopyrite, and sphalerite with trace hematite, native copper, and sulfosalts. In the stockwork ore zone, which is the least common, pyrite, chalcopyrite, magnetite, and sphalerite occur as veinlets with widespread quartz. Euhedral to subhedral pyrites show cataclastic texture throughout the sulfide zone, which indicates the deposit was subjected to intense deformation.

The İncekoz deposit, another recent discovery, is composed primarily of major pyrite, minor chalcopyrite, and trace fahlerz, and secondary bornite, chalcocite,

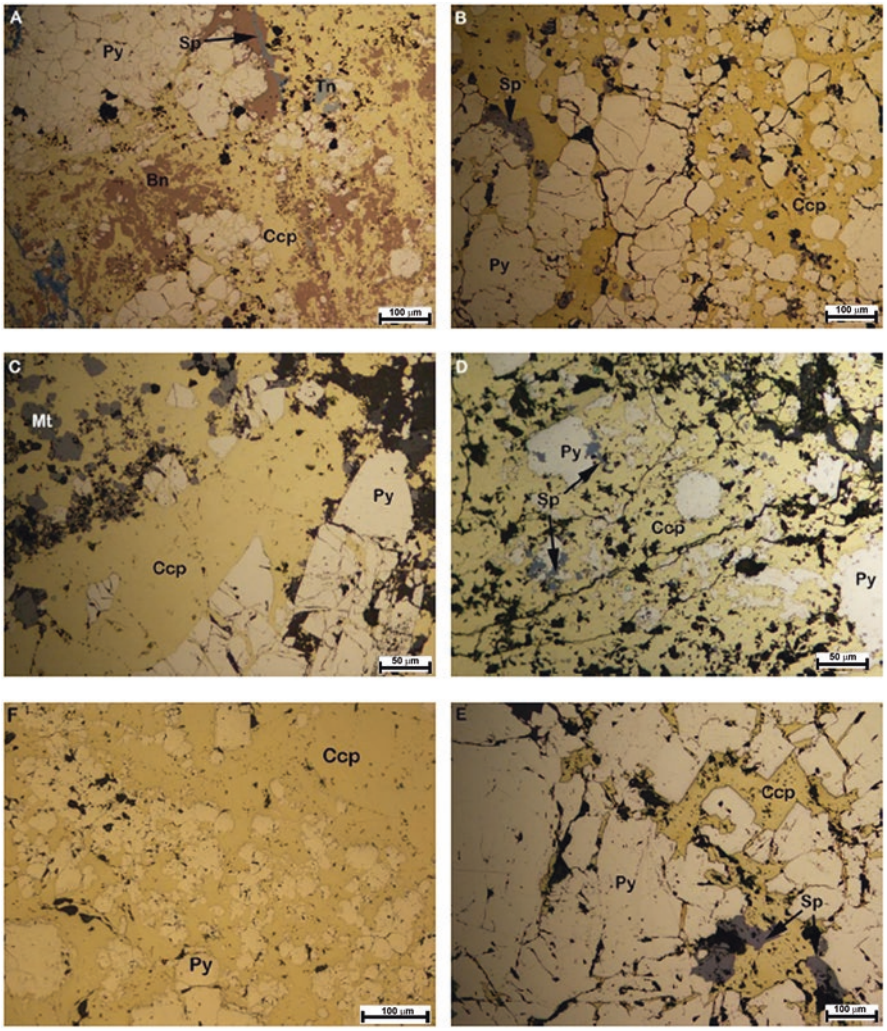

Fig. 9.24 Common micro-ore textures representing (**a**) Maden, (**b**) Madenköy, (**c**) Ortaklar, (**d**) Koçali, (**e**) Mağaradoruk, and (**f**) Aşıköy (*Qtz* quartz, *Ccp* chalcopyrite, *Py* pyrite, *Sp* sphalerite, *Gn* galena)

covellite, and hematite. In the oxidation zone, malachite, azurite, hematite, and limonite are widespread. Ore mineralization is mainly in the form of fracture filling stockworks. Massive formations are either absent or subtle. Figure 9.24 reveals typical ore minerals and common micro-ore textures in the main Cyprus-type deposits occurring both in the Küre area and along the BZSZ. A paragenetic sequence for the major ore minerals is shown in Fig. 9.25.

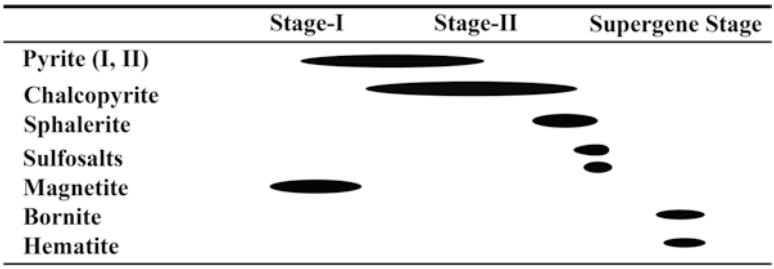

Fig. 9.25 Simplified paragenetic sequence for the principle ore minerals occurring in the Cyprus-type deposits of Turkey

Geochemical data acquired from most of the major Cyprus-type deposits of Turkey indicate that copper, zinc, iron (mostly magnetite), and cobalt reach mineable grades. Among them, copper may reach up to 12 wt. % in massive ore (e.g. Maden-Elazığ). However, in most of the deposits it ranges typically from about 1.5 to 4 wt. %. Although zinc always occurs in significant quantities (up to 2 wt. %), none of the past or current producers did produce zinc. Some of the examples (e.g. Mağaradoruk deposit) are reported to have high cobalt (in the form of linnaeite) up to 3.5 wt. %. Lead is extremely low in all the known deposits, although it is reported to exist in trace quantities as galena. Most of the deposits of this type have a well-developed gossan zone (e.g. Ortaklar deposit), where wide range of oxide minerals predominate, which is also very important particularly for gold and silver. Gold and silver may reach up to 2 ppm and 10 ppm, respectively. Their plots on the Cu-Zn-Pb ternary diagram overlap with some of the Kuroko and Besshi-type deposits (Fig. 9.13). In the copper grade vs tonnage diagram are comparable with some of the world examples (Fig. 9.5).

$\delta^{34}S$ values of sulfides (mainly pyrites) from VMS deposits occurring in the Troodos ophiolites vary between −1.1 ‰ and 7.5 ‰, concentrating within +4 ‰ to +7 ‰ interval (Clark 1971; Hutchinson and Searle 1970; Jamieson and Lydon 1987). As sulfur isotope variations can be observed in the same deposit, it can also be observed between similar deposits of the same type. But it is clear that sulfur was mainly derived from associated magmatic rocks. Sulfur isotope data of pyrite and chalcopyrite representing the Cyprus-type VMS deposits are comparable with the Cyprus-type deposits occurring worldwide. The $\delta^{34}S$ values for pyrite and chalcopyrite range from 2 ‰ to 8 ‰, indicating that the ore forming hydrothermal fluids were associated with sub-seafloor igneous activity, which is typical for the Cyprus-type VMS deposits. Thus sulfur isotope data show a fairly narrow distribution indicating homogeneous source with prevalent magmatic signature (Fig. 9.14). The $\delta^{34}S$ vs metal ratios diagram shows a distinct field for this type, some overlap with the copper rich-Kuroko and the Besshi-type deposits of Turkey (Fig. 9.15).

Limited lead isotope data representing sulfide ore, mainly pyrite/chalcopyrite, show remarkable similarity with those of the other Turkish VMS deposits, both the Kuroko-type and Besshi-type, in that all are less radiogenic and sourced by lower

crust and upper mantle. Copper isotope data from Maden (Elazığ) fall in the same range with those belong to the Kuroko-type deposits of Turkey (Fig. 9.16). These values are interpreted as a result of oxidation and leaching from the various rocks within the underlying rock section by the seawater (Housh and Çiftçi 2008).

9.5.5 Age of the Deposits

The Küre area deposits should have formed either concurrently with the host basalts during Liassic-pre Liassic submarine volcanism or as a result of hydrothermal processes, which occurred following the volcanism. The Küre deposits occur within these basalts, along the contacts between the basalts and shales, and within the shales. The Late Triassic (Norian) bivalve *Monotis salinaria* in the shales (Okay et al. 2015) agrees with recent data acquired through the $^{187}Os/^{188}Os$ dating on the main stage pyrites, yielding an age of 180 Ma (Toarcian) (Akbulut et al. 2016). However additional geochronological data are required to constrain ore mineralization event within the framework of the geologic and tectonic evolution of the Küre area.

SE Anatolian Orogenic belt deposits occurring along the Bitlis-Zagros Suture Zone (BZS), the boundary between Anatolian and Arabian plates in SE Turkey, as a result of the closure of southern branch of Neotethys during Late Cretaceous – Miocene, are associated with Cretaceous intra-oceanic supra-subduction zone ophiolitic slabs, which tectonically overlie the Mesozoic platform carbonates and Paleozoic sediments of the Arabian plate (Yıldırım and Yılmaz 1991; Yılmaz 1993; Yılmaz et al. 1993).

These deposits are hosted either by mafic volcanics of the Koçali Complex of Late Triassic-Early Cretaceous age based on the fossil evidences (mainly radiolaria) and stratigraphic correlations (Sungurlu 1973; Perinçek 1979; Uzunçimen et al. 2011) or mafic volcanics of the Maden Complex, which is of Middle Eocene age based on the fossil evidences (Perinçek 1979) and is 48 Ma (Ypresian) through the K–Ar geochronology (Yazgan 1984).

9.5.6 Exploration Guides

In exploring for Cyprus-type VMS deposits, alteration mineralogy, lithogeochemistry and geophysical methods are employed alone or in combination. There are successful examples resulting in new discoveries.

9.5.6.1 Alteration Characteristics

Historically the principal guide for the presence of sulfide mineralization was provided by surface indications in the form of oxidation and alteration. In typical Cyprus-type deposits, wall-rock alteration generally develops around epigenetic

stockwork zones. Smectite and chlorite-smectite are the major alteration minerals. Alteration zones developed around the stockworks can be divided into three different types including P-, K- and M-type alteration pipes, so called due to the pipe-like nature of the stockwork mineralization (Gillis and Robinson 1990). P-type pipes, named after the Pitharokhoma deposit, have chlorite-illite, smectite and chlorite-smectite mixed layer alteration associated with the sulfide mineralization. K-type pipes, named after the Kokkinopezoula mine, have smectitic and chlorite-smectite mixed layer alteration, as seen in P-type alteration. But, no chlorite-albite alteration is present, and a continuous alteration sequence from smectitic through chlorite-smectite to chlorite-rectorite facies is present. M-type pipes, named after the Mathiati mine, have entirely different alteration mineralogy. Host rocks occurring in the central stockwork zone are altered to a chlorite-quartz-pyrite-anatase assemblage, which is not seen in other types of pipe-like alterations. Chlorites of this type have comparatively distinct Fe-rich composition (Richards et al. 1989).

Most of the deposits in Turkey exhibit surface alteration halos to varying extents that could be a useful tool in explorations where preserved. Gossans may develop on top of some orebodies, which is also a very useful field guide in locating promising sites. Table 9.8 summarizes typical alteration characteristics associated with the major Turkish VMS occurrences.

Alteration in the enclosing basaltic rocks mainly consists of chloritic, propylitic (epidote–chlorite–albite) and lesser sericitic, silicic types. Calcite veins generally develop within host mafic rocks as a result of the destruction of both Ca-rich plagioclases and calcic pyroxenes and amphiboles. Table 9.8 summarizes alteration mineralogy and relevant characteristics.

Table 9.8 Hostrocks and alteration mineralogy associated with the major Cyprus-type deposits of Turkey

Deposit	Hostrock	Alteration	Gossan
Küre	Basalts (lava and pillow)-black shale	Silicification, sericitization, carbonatization, chloritization, albitization, epidotization	Moderate
Ortaklar	Pillow basalts-spilitic basalts-hyaloclastite breccia	Silicification, carbonatization, argillization, hematitization, chloritization, albitization, epidotization	Extensive
Ormanbaşı	Mudstone-diabase-spilitic basalts-shale	Chloritization, albitization, silicification, hematitization, kaolinitization	Moderate
Derdere	Spilitic basalts	Chloritization, albitization, carbonatization, epidotization	Weak
Madenköy	Porphyritic basalts	Chloritization	Moderate
Maden	Diabase-basic volcanics-mudstone-serpentinites	Chloritization, kaolinization, silicification	Weak
Koçali	Pillow basalts	Chloritization	Weak
İncekoz	Sheeted basic dykes	Chloritization, carbonatization, silicification, hematitization, epidotization, limonitization	Weak

Some of these zones may overprint each other. While some can be considered as proximal, others are distal. In the Kure deposits, sericitization, carbonation and silicification are widespread around the mineralized zones. Sericitization is overprinted by chloritization (Fe-rich chlorite). Thus the host-rocks are mostly chloritized and carbonatized away from the ore bodies. Epidotization has widespread occurrences in upper parts of ore bodies. Strong enrichment in Fe and Mg, and depletion in Ca, Na, and K appear to be useful guides for exploration. As such Fe2O3 total Fe + MgO/CaO+Na2O may prove to be an effective indicator of footwall alteration pipes associated with VMS orebodies (Çağatay 1993).

In the Maden area deposits, silicification, kaolinization and chloritization are widespread in diabasic host rocks. In the İncekoz mineralization, alteration zones also contain weak ores represented by 1–2 m to 100–120 m long and 1–2 cm to 4–5 m thick zones. In enclosing volcanics, intense chloritization, lesser carbonatization (in the form of veins and veinlets), silicification, limonitization, hematitization, and epidotization are developed. In the Derdere mineralization, host spilitized basaltic volcanics are are intensly chloritized, carbonatized, and epidotized in places. Pyroclastics occurring within the spilitic basalts contain abondant zeolites (Şaşmaz et al. 1999).

In the Ortaklar deposit, hydrothermal alteration, which is limited both horizontally and vertically, is observed in the form of silicification, argillization, and hematitization near the ore body and along its contacts with the hanging wall rocks. Host basaltic volcanics are intensely altered. The alteration is represented by a mineral assemblage of quartz + albite + chlorite + epidote + carbonate, which can be interpreted as products first of spilitization and then chloritzation and/or propylitic alteration. In addition, hematitization and sericitization are also observed in the footwall rocks. The alteration observed in footwall rocks indicates that hydrothermal activity occurred after footwall rocks formed and before sedimentation of hanging wall rocks (Doyle and Allen 2003). A weak alteration in hanging wall rocks can also be interpreted as an indication of decreasing hydrothermal activity (Iijima 1974). Argillic alteration and silicification, which are observed around the ore body locally, may be the products of supergene alteration (Yıldırım et al. 2016).

9.5.6.2 Structural Geology

Most of the Cyprus-type occurrences in Turkey are localized by a combination of structural and lithologic controls. Some of the structures are of regional scale such as the Bitlis-Zagros suture zone, some are local-scale faults and folds that likely played critical role in generating favorable sites for ore deposition. A thorough understanding of structural geology – ore deposition relation is a main key for exploration programs. Some important examples are summarized below.

In the Küre area, a series of thrust faults and plunging anticlines/synclines between the Küre ophiolite and the Akgöl Formation are the major structures of the area. Liassic volcanic rocks and black shales around Küre have been well-folded, and their fold axes trend approximately in a N-S direction. The dome with its long

axis is in N-S direction in Aşıköy, has a high inter-limb angle (Bailey et al. 1967; Pehlivanoğlu 1985). Basalts between Aşıköy and Mağaradoruk, which overlie black shales east of this anticline, are mostly pillow lavas. There is also a N-S extending overturned anticline between Aşıköy and Bakibaba (now Mağaradoruk) and a nearly N-S trending overturned anticline east of Bakibaba-Mağaradoruk deposits. This overturned anticline also plunges towards the south in the Mağaradoruk deposit (Altun et al. 2015).

In the Küre area, host basalts in Mağaradoruk and Bakibaba were most probably in the same basalts at the bottom of Aşıköy, and they form an overturned anticline pushed westward, whose long axis is N-S trending. Massive ore bodies are sited both within these basalts and along the contacts with black shales, and within black shales. Ore bodies in Mağaradoruk deposit are overturned due to post depositional deformation. The large orebody in Mağaradoruk is located in non-overturned lower part of the western flank of the overturned anticline (Altun et al. 2015).

The Toykonduk orebody (a past producer) is sharply bounded by the intersection of two faults, trending, respectively, N63°E and N15°W. Bailey et al. (1966) suggested that these were pre-existing fractures (prior to mineralization) and controlled the initial position of ore rather than displacing it. There is no apparent brecciation or dragging of ore along the faults. Veins and veinlets of chalcopyrite and pyrite occur along the axial planes of isoclinal folds around Toykunduk Hill (Çakır 1995).

Ore-bodies form highly tilted lenses (60–85°) in most parts of Aşıköy, Bakibaba and Mağaradoruk deposits. However, these attitudes were acquired at a later stage following the formation of ore deposit (Altun et al. 2015).

In the Maden area, the host volcanics to the main orebody has an elliptic outline extending NW-SE with approximate size of 700 × 300 m. Orebodies are not deformed or tilted like the Küre area deposits.

In the İncekoz deposit, ore is controlled by fractures and small scale syngenetic faults occurring in association with the sheeted dykes. These acted as pathways for the ore-forming fluids. Mineralization occupies fracture and occurs as subordinate disseminations.

9.5.6.3 Lithogeochemistry

Past and recent discoveries strongly indicate that the Cyprus-type deposits of Turkey are strata-bound since all of them are associated with the mafic volcanics of ophiolites along the suture zones. Consequently, such lithological association is very useful in exploring favorable sites for these deposits. Contacts between black shale and basaltic volcanics are regarded as the primary target zones for exploration programs.

Co/Ni ratio of both mafic volcanics and soils developed on these volcanics can be very useful. Zaccarini and Garuti (2008) emphasize that Co/Ni ratio in massive sulfide deposits, of which their main host rock is serpentinite varies between 0.29 and 1.97. However; the ratio of massive sulfide varies between 1.09 and 8.

9.5.6.4 Geophysics

Although historically the main tracers for the presence of sulfide mineralizations were surface oxidation- and alteration-related, modern exploration programs require more information beneath the surface cover. Surface indications are still extensively used to plan ground-based geophysical techniques. Considering mineralogy of the ore deposits, their architectures, structure-lithologic controls on ore-forming systems – since faults and fracture zones forming the focus of hydrothermal activity and their identification is the first step in the selection of likely targets for sulfide accumulation (Lydon 1988). A number of techniques are used alone or in combination. One of the most useful techniques for such investigations is aeromagnetic surveys (Rona 1978, 2005).

IP (induced polarization; ground-based) has been successfully applied in Cyprus (Maliotis and Khan 1977) and is successfully applied in exploration, particularly in terrain of exposed pillow lavas or limited sedimentary cover. Recent developments of this technique, enables the modelling of the various geophysical parameters leading to more accurate selection of drilling targets.

Gravity/microgravity is also effectively used. In the presence of dense lithologies within the rock section, the combination of gravity and magnetic methods may be used to avoid unsuccessful target generations.

Magnetic (including aeromagnetic) methods may also be effective where presence of magnetite in ore mineral paragenesis is significant. EM (electromagnetic; both ground and aero) methods are also employed and becoming more preferred.

The application of Geographic Information Systems (GIS) technology, which can enable the simultaneous overlap of several datasets could also be very effective in finding target areas.

In conclusion, all available geological (alteration, lithogeochemical and structural) and geophysical indicators need to be taken into consideration in the selection of a target area most likely to host the VMS deposits.

9.6 Besshi: Type Deposits

9.6.1 Introduction

Besshi-type deposits generally have large reserves (from under a million tonnes to 300) but contain lower base metal concentrations comparing with the other VMS systems and are considered to be low-grade copper deposits, typically ranging from about 0.3% up to 4%. Zinc may reach mineable grades (sometimes up to 6%). Besshi-type deposits often also contain cobalt, which is not common to the other VMS's. Average abundance of gold and silver is low. Some of the Besshi-type deposits are mined for sulfur due to insignificant metal grades (e.g. Gossan Lead, Virginia-USA).

Unlike the other VMS, these deposits reveal much more diverse mineralogy. The Besshi-type mineralization typically occurs as concordant masses of laterally extensive thin, stratiform and tabular layers within thick sequences of marine sedimentary rocks including black shale, arkose, greywacke that may be intercalated with volcanic tuffs and lavas of mafic composition. Although the mineralized zones may be thin (with some exceptions that may reach up to a few meters), they are laterally very extensive (up to several kilometers). Common ore styles include disseminations, veins, and massive layers. Most of the Besshi-type deposits are either deformed and/or metamorphosed. As a result, some of the primary features may be obscured such as the feeders that are revealed as the stockwork zones in most of the VMS deposits. Sedimentary host-rocks are later metamorphosed to schists, quartzites, metacherts, and metapelites, and the basalts to amphibolites.

These deposits appear to have formed in a variety of tectonic environments ranging from oceanic extensional environments, such as back-arc basins, oceanic ridges close to continental margins, to early-forming rift basins in the continental plates. The host-rocks are thick, terrigenous clastic sedimentary sequences interlayered with calc-alkaline basaltic to andesitic tuffs and flows, products of tholeiitic mafic magmatism (with pyroxenes and olivine, which have a high iron content relative to their sodium and potassium content and with plagioclase feldspar). The clastic host-rocks are generally thinly laminated sedimentary rocks resembling turbidites. The clastic sedimentary rocks are sometimes graphitic in the Canadian examples of this type. It has been suggested that the size of the sulfide deposits reflects the volume of mafic volcanic rocks in the ore-forming system; the more mafic volcanic rocks present in the basinal stratigraphy, the more copper there may be in the exhalative sulfide body. The felsic volcanic rocks are generally absent within the sequence. Although not emphasized, a chloritic alteration halo may develop around the ore bodies within the host-rocks due mainly to the water-rock interactions during the hydrothermal activities.

Occurrences of known Besshi-type VMS deposits in Turkey are restricted to the Central Pontides where they occur in a fairly narrow zone within the Çangaldağ complex (Fig. 9.26) (Dönmez et al. 2013; Günay et al. 2015, 2018). All of the known occurrences are associated with the Akgöl Formation in the area, which itself consists of volcanic, subvolcanic and sedimentary lithologies, all metamorphosed at the greenschist facies. In this respect, all the known occurrences are of strata-bound character. Among those only the Cozoğlu deposit was operated from 2010 to 2014, and but it is now closed. It produced about 0.65 Mt of ore with grades of 1.92% Cu and <0.5% Zn (no Au and Ag were reported). Two recent discoveries – Hanönü area deposits (two nearby deposits Gökırmak (Dönmez et al. 2013) and Hanönü), which are underway for mining and Zeybek prospect, which is still under exploration, made the area one of the targets in the country. The Hanönü-Taşköprü district is comparable with the other districts hosting similar deposits in the world at both district scale and individual deposits scale (Table 9.9). Major features of Turkish occurrences are listed in Table 9.2.

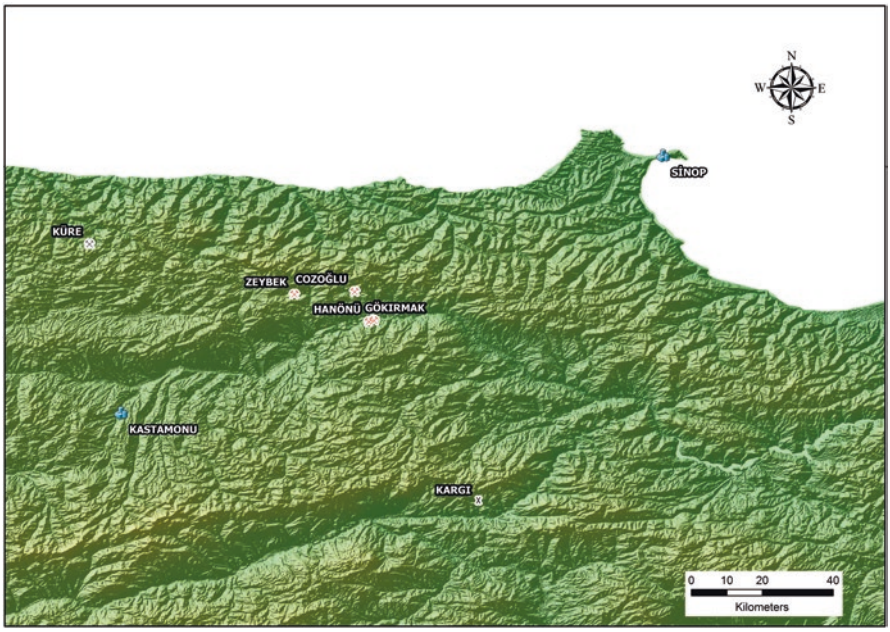

Fig. 9.26 Location map of the Besshi-type deposits (in red) occurring in the Central Pontides with nearby Küre deposit and Kargı prospect

9.6.2 Geological Framework

The area is geologically and tectonically associated with the Alpine–Himalayan Orogeny, which was a result of the collisions between the Laurasian, Gondwanan and Indian continents, and the smaller Anatolide, Tauride and Arabian terranes during the Tertiary (Dercourt et al. 1986; Şengör 1987; Şengör and Yılmaz 1981). Permo-Triassic Elekdağ and Küre ophiolites crop out in nearby areas and are considered to be Paleotethys-ophiolites, products of this collision and closure of the Paleo-Tethys. Middle Jurassic Çangaldağ Complex is 45 km in length and 10 km in width, extending in a NE-SW direction. It consists a thick 10 km tectonic stack of volcanic, volcaniclastic and fine-grained clastic rocks, metamorphosed in low-greenschist facies during the Early Cretaceous (Yılmaz 1988; Ustaömer and Robertson 1993; Okay et al. 2014). The complex is interpreted either as a pre-Jurassic ophiolite (Yılmaz 1988; Tüysüz 1990) or as a pre-Jurassic ensimatic volcanic arc (Ustaömer and Robertson 1993, 1994). The geochemistry of the volcanic rocks suggests the latter (Ustaömer and Robertson 1999). Thus, the complex consists of ensimatic island arc volcanics and fore-arc basin sediments, remnants of oceanic crust, and volcano-clastic deposits. Oceanic crust fragments are comprised of pillow lavas, sheeted dykes, isotropic gabbros and radiolarites. Island arc

Table 9.9 Average grade and tonnage for the Turkish Besshi-type deposits compared with some of the Besshi-type deposits worldwide (Lydon 1988; Lobanov et al. 2014)

Deposit	Country	Cu (%)	Zn (%)	Ag (ppm)	Au (ppm)	Reserve (Mt)
Besshi	Japan	2.5	0.3	6.6	0.2	30
Hitachi	Japan	1.3	0.3	4	0.2	29
Yanahara	Japan	1.2	Nr	58	0.6	25
Shimokawa	Japan	2.3	1.3	10	0.9	8
Shirataki	Japan	1.3	0.3	4	0.1	5
Sazare	Japan	1.7	0.4	7	0.1	4.2
Goldstream	Canada	4.5	3.1	20	Nr	3.22
Granduc	Canada	1.7	Nr	7	0.1	39
Windy Craggy	Canada	1.4	0.3	4	0.2	297
Ice	Canada	1.48	Nr	Nr	Nr	4.6
Fyre	Canada	2.1	Nr	Nr	0.73	15.4
Hart River	Canada	1.45	3.65	50	1.37	0.52
Ducktown	USA	1	0.9	3	0.3	163
Gossan Lead	USA	0.5	1.5	8	<0.1	40
KhokAdar	Mongolia	Nr	Nr	Nr	Nr	Nr
Bayan Airag	Mongolia	Nr	Nr	Nr	1	10
Kyzyl-dere	Georgia	2	Nr	Nr	Nr	40
Karchiga	Kazakhstan	1.73	0.4	7.2	0.16	10.8
Vavilonskoye	Kazakhstan	1.47	0.3	Nr	Nr	9
Dal'neye	Russia	0.5	10	Nr	Nr	1.5
Kyzyl-tash	Russia	0.7–1.3	1–3.8	Up to 100	0.1–0.9	Nr
Edegeikoye	Russia	Nr	Nr	Nr	Nr	Nr
Poselshchik	Russia	0.52	Nr	7.2	0.2	96
Mainskoye	Russia	2.09	0.62	Nr	Nr	0.8
Gökırmak	1.64	0.4	72	0.1	5	24.45
Hanönü	0.78	<1	21–337	<0.1	1.1–18.1	4.5
Cozoğlu	1.1	<0.5	20–300	<0.1	1–20	0.6
Zeybek	0.47	0.15	18–370	<0.1	1.2–15.3	10
World Avg.		1.3	0.4	5.7	0.2	18.9

volcanics include a series of basaltic andesite, dacite and rhyolite. Volcanoclastic deposits are composed of schists intercalated with rhyolitic tuffs. The Çangaldağ Complex is part of the Karakaya Complex on the regional scale. Within this complex, the Cretaceous Domuzdağı Mélange, an ophiolitic mélange, occurs in the area (Fig. 9.27). These two are interpreted as products of a marginal basin along the southern edge of Eurasia before the Late Jurassic (Robertson 2002; Ustaömer and Robertson 1999). Figure 9.27 shows a simplified geological map of the area for the major lithologies and structural elements.

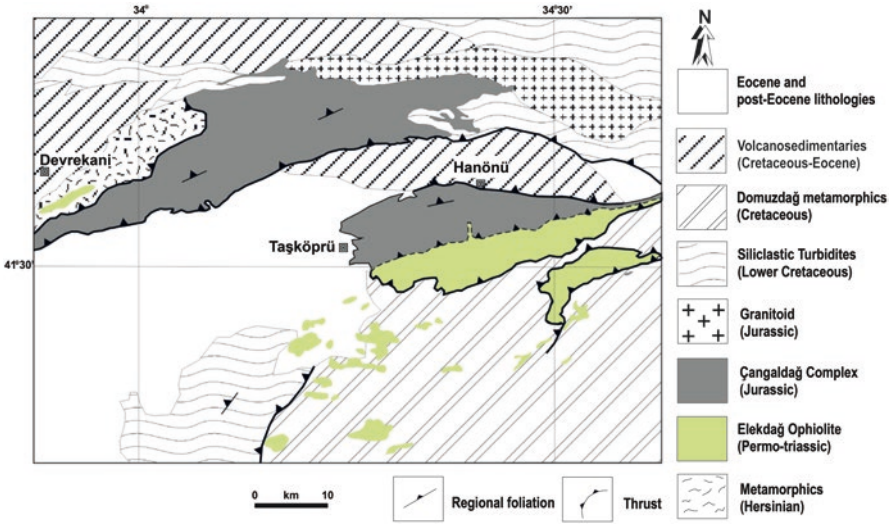

Fig. 9.27 Geological map of the Hanönü-Taşköprü area with a representative lithostratigraophy. (Adapted from Dönmez et al. 2014)

9.6.3 Ore Geology

The Besshi-type deposits are intermediate between the Cyprus and/or Cu-Zn type VMS and the SEDEX-type deposits with regards to their host-rock associations, geological/tectonic settings, ore and gangue mineralogy, and other geochemical characteristics.

Although these deposits are considered VMS-type, there is still some debate on the mechanism of sulfide deposition. In typical VMS, the massive sulfides result from the exhalation of hydrothermal fluids through focused discharges onto the seafloor forming sulfide chimneys (e.g. black smokers). However, in the Besshi model, hydrothermal brine pools form on the seafloor after exhalation and replacement of clastic sedimentary rocks by sulfur-bearing hydrothermal fluids flowing upward in a convection cell system but did not actually exhale onto the seafloor. Because most of the examples of this type are metamorphosed or deformed, it is difficult to recognize the ore controls. Most of the examples lack feeder zones. However, syn-depositional faults and mafic volcanic centers play important role in the genesis of the Besshi-type deposition. Although the hydrothermal system is contemporaneous with the volcanism, and this type of sulfide deposition is also considered to be "syngenetic", most of the sulfide mineralization takes place through epigenetic replacement of host-rocks, which is another typical characteristic of this type mineralization.

In the larger picture, the Küre district contains long-known, significant copper mineralizations associated with the ophiolites occurring in the area. However, cop-

per mineralizations occurring in the area in the Taşköprü-Hanönü area have different characteristics, although they too are related to the same geological/tectonic evolution of the area at the regional scale. Hydrothermal systems in such supra-subduction settings should be powered by basic volcanic centers fed by partial melting and dehydration of subducting oceanic plate. One of the challenges in understanding the genesis of these deposits is that their host rocks are metamorphosed and therefor all the primary structures are overprinted. In addditon, no clear connection with the volcanic centers is observed or reported to date. Field studies of discovered deposits and their core logs show laminated sulfide mineralizations concordant with schistosity within metamorphosed clastic volcanics and sediments. Micro-ore textures from all four deposits are fairly similar. Presence of disseminated early pyrite and late stage chalcopyrite filling intergranular spaces and progressively replacing other sulfides (such as sphalerite and trace galena and sulfosalts if present) indicate continuous discharge of Cu-rich fluids into the system.

9.6.4 Mineralogy and Geochemistry

Although the world examples reveal diverse mineralogy, the Turkish counterparts occurring in the Hanönü-Taşköprü district have relatively simple mineralogy and micro-ore textures. Ore and gangue minerals that are common both in the other Besshi-type VMS's and in the Turkish examples are listed in Table 9.10. Ore minerals are fine to medium grained; rarely exceed 200 μ in diameter. Pyrite, the most common sulfide, occurs as euhedral to subhedral disseminations and represents the

Table 9.10 Common minerals reported from the major examples of the Besshi-type deposits worldwide (minerals in bold are from Turkish examples)

Ore minerals	Gangue minerals[a]
Pyrite	**Quartz**
Pyrrhotite	**Calcite**
Chalcopyrite	Ankerite
Sphalerite	Siderite
Magnetite	**Graphite**
Arsenopyrite	Albite
Galena	**Sericite**
Bornite	**Chlorite**
Tetrahedrite-Tennantite	**Amphiboles**
Cobaltite	Tourmaline
Stannite	**Biotite**
Molybdenite	**Actinolite**
Marcasite	**Talc**
Cubanite	**Graphite**
Valleriite	**Feldspars**

[a]Barite is characteristically no present in the Besshi-type deposits

earliest phase in the paragenetic sequence. Pyrite may occur as multiple generations (at least two generations were observed). This second common phase, anhedral chalcopyrite and minor to trace anhedral sphalerite infill intergranular spaces and vugs of early pyrite and the gangue grains. Traces of sulfosalts, galena, magnetite, supergene bornite are also present in the mineral paragenesis (Figs. 9.28a–d and 9.29). These mineralizations may also exhibit recrystallization and replacement textures in addition to cataclastic textures (particularly by pyrite) and micro-folds, which were developed in brittle and ductile deformation conditions.

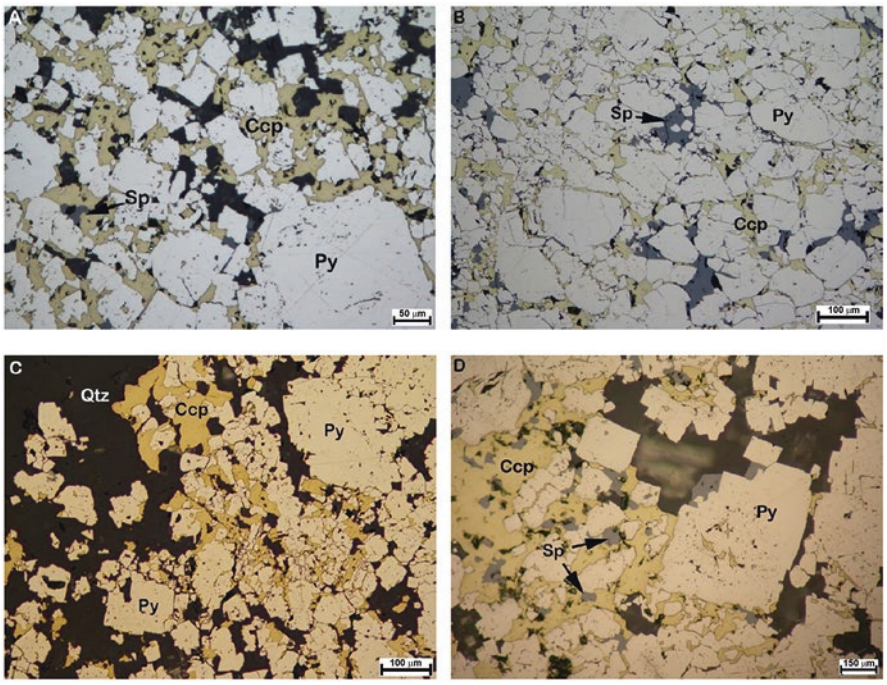

Fig. 9.28 Typical ore minerals and ore textures observed in (**a**) Gökırmak, (**b**) Cozoğlu, (**c**) Zeybek, and (**d**) Hanönü deposits (*Qtz* quartz, *Ccp* chalcopyrite, *Py* pyrite, *Sp* sphalerite)

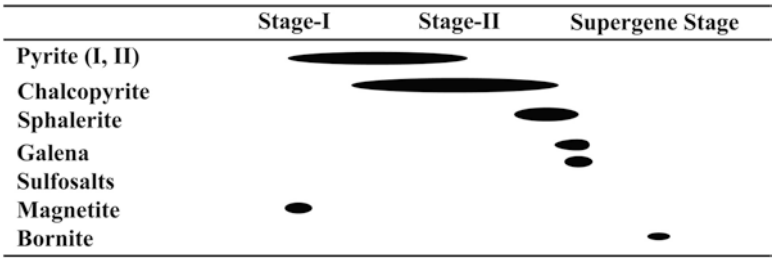

Fig. 9.29 Generalized paragenetic sequence for the main ore minerals occurring in the Besshi-type deposits of Turkey

Geochemical analyses of average bulk ores representing the Besshi-type deposits of Turkey reveal that only copper and zinc may reach mineable grades. Lead always occurs at ppm levels. Gold and silver are characteristically low as compared with the Kuroko and Cyprus type occurrences. Silver rarely reaches mineable grades. The Cu-Zn-Pb ternary diagram overlaps with some of the Kuroko and Cyprus – type deposits (Fig. 9.13). The copper grade vs tonnage diagram is also comparable with some of the world examples of Besshi deposits (Fig. 9.5).

Sulfur isotope data of pyrite and chalcopyrite are similar to other massive sulfide deposits of Turkey and the Besshi-type deposits occurring worldwide. Limited data, however, show a very narrow distribution with prevalent magmatic signature (Fig. 9.14). Another comparative plot of the VMS deposits of Turkey with the other world renowned VMS deposits is the $\delta^{34}S$ vs metal ratios diagram that shows distinct field for each, some overlap with copper rich-Kuroko and Cyprus-type deposits (Fig. 9.15).

Galena and pyrite/chalcopyrite lead isotope data of all major Turkish VMS deposits (including Besshi deposits) show remarkable similarity in that all are less radiogenic and indicative of sources from lower crust and mantle.

9.6.5 Age of the Deposits

The Hanönü-Taşköprü area deposits are concordant with the general schistosity suggesting that ore mineralization took place concurrently with sedimentation during and shortly after the Çangaldağ ensimatic arc formation. Thus the age of the arc can be considered as the minimum age for the ore deposition. Although there are no geochronological data for the complex, which is considered to be Paleozoic-Triassic age from the general geodynamic models (Ustaömer and Robertson 1994), recent data acquired from zircon using the U-Pb dating for the felsic components of the arc volcanics gave 168 and 169 Ma (Middle Jurassic) (Okay et al. 2014). The rocks of the complex were later metamorphosed to low-greenschist facies during the Early Cretaceous (Yılmaz 1988; Ustaömer and Robertson 1993; Okay et al. 2014). Since the felsic rocks are part of the arc formation, these can be taken as minimum age for the complex, and consequently for the syngenetically formed ore deposits.

9.6.6 Exploration

9.6.6.1 Alteration Characteristics

In the typical Besshi model, a chloritic alteration halo develops in the country rock surrounding the sulfide horizons, which may be a relic of pre-deformational alteration. Other alteration minerals that may show up in the host rocks of the Besshi deposits are quartz, carbonate, pyrite, sericite, and graphite. However, in the Turkish examples, phyllic alteration, represented by quartz + sericite accompanied by pyrite

± chalcopyrite ± sphalerite is commonly observed. Phyllic alteration zones may locally reach up to 300 m in lateral extent. However, none of the Besshi-type occurrences exhibited marked alteration zones at the surface. Because the Besshi-type deposits do not commonly exhibit extensive feeder alteration systems in the footwall rocks below the massive sulfide bodies, footwall alteration may not be a useful tool in exploration compared with the intense silicic and argillic alterations common around the other VMS deposits.

However, geochemical characterization of host-rocks would be a useful method of regional exploration since the Besshi-type deposits are all strata-bound. Lithogeochemical surveys of cobalt versus nickel distributions might also be useful, given that the Besshi sulfides have a distinctive cobalt-nickel ratio greater than one.

9.7 Conclusions

Favorable tectonic settings for ore deposits were developed in Turkey as a result of the Alpine orogeny extending from the European Alps to the Himalayan ranges of northern India and southern China. Such sites were part of the geological structures that have been formed by fairly complex geological events including long-lived subductions, accretions and collisions associated with the closure of the Tethyan Ocean. Therefore, Anatolia has great potential for the formation of volcanogenic massive sulfide deposits (VMS) of various types. Some were mined by ancient civilizations in the prehistoric times, some have been mined since the last century, some are recent discoveries and, some are yet to be discovered.

From the scientific point of view, VMS deposits are special among the ore deposits in that they have a distinctive mineralogy, architecture, and origin. VMS deposits are hydrothermal, strata-bound, and partly or wholly syngenetic mineralizations. Viewed from economic perspective, VMS deposits are significant source for the base metals (a major source of copper, to a lesser extent of zinc and lead) and a number of precious and semiprecious metals. In general, they have relatively modest reserves (<50 Mt), high grades and diverse metal contents.

The VMS deposits of Turkey can be viewed in three different styles: Kuroko-, Cyprus-, and Besshi-type. They occur in three distinct tectonic environments: (I) Eastern Pontides, (II) Central Pontides and (III) Bitlis-Zagros Suture Zone. Kuroko-type VMS deposits occur only in the Eastern Pontides in association with the felsic volcanics of the late Cretaceous age (82.6–91.1 Ma) without exception and are formed within the axial zone of a magmatic arc setting. Whereas Cyprus type VMS deposits occur in the Central Pontides around the Küre area in association with the Küre Formation of Norian-Toarcian age (237–180 Ma), which is consisted of mafic volcanics intercalated with black shales and along the Bitlis-Zagros Suture Zone formed as a result of the closure of southern branch of Neotethys during Late Cretaceous – Miocene, are associated with either by mafic volcanics of the Koçali Complex of Late Triassic-Early Cretaceous age or mafic volcanics of the Maden Complex, which is of Middle Eocene (Ypresian) (48 Ma), both can be considered

as supra-subduction setting. Besshi-type deposits, on the other hand, occur strictly in the Central Pontides, in Hanönü-Taşköprü area in association with the Akgöl Formation consisting of low-grade metamorphic siliciclastic sedimentary rocks within the Middle Jurassic (168–169 Ma) Çangaldağ Complex that is itself consisted of ensimatic island arc volcanics and front-arc basin sediments, remnants of oceanic crust, and volcano-clastics.

In addition to the known VMS districts and individual VMS deposits in these districts, new discoveries, both VMS deposits and districts, are anticipated in the years to come through better understanding of the geological evolution of Turkey.

Acknowledgements Author would like to express his gratitude and appreciation to Prof. Dr. Yücel Yılmaz, Prof. Dr. Aral Okay, and Prof. Dr. Gültekin Topuz (Istanbul Technical University), Dr. Efem Altınok (Kocaeli University), Prof. Dr. Yener Eyüboğlu (Karadeniz Technical University), Dr. Gonca Dardeniz Arıkan (Koç University), Cahit Dönmez, Nail Yıldırım, Mustafa Küçük, Kürşad Bekar, and Dr. Kurtuluş Günay (General Directorate of Mineral Research and Exploration), Hüseyin Yılmaz, Dr. Yılmaz Altun, Onur Aydın, and Ercan Direkli (Cengiz Holding), Deniz Aslan (Acacia Mining), Tuğrul Tokgöz (Zeta Proje Müh. Ltd. Şti.) for scientific discussions and both data and sample acquirements. Dr. Cafer Özkul and Recep Uğuraçar (Dumlupınar University), İbrahim Akpınar (Gümüşhane University), Hüseyin Kocatürk, Ali Tuğcan Ünlüer, Dr. Serkan Angı, Halil Aydın, Ömer Taş, and N. Merve Sütçü (Istanbul Technical University) are all acknowledged and gratefully thanked for their help both in formatting of the text and technical drawings of the figures used in this chapter. Prof. Dr. Franco Pirajno (University of Western Australia) and Dr. Martin Yates (University of Maine) are thanked for their through reading for language and scientific soundness.

References

Abdioğlu E, Arslan M (2009) Alteration mineralogy and geochemistry of the hydrothermally altered rocks of the Kutlular (Sürmene) massive sulfide deposit, NE Turkey. Turk J Earth Sci 18:139–162

Açıkbaş D, Baştuğ C (1975) V. Bölge Cacaz-Hani Yöresi Kuzey sahalarının jeoloji raporu ve petrol olanakları [Geology survey report and petroleum potentials of V. Region Cacaz-Hani area northern territories]. TPAO Raport No: 917 (in Turkish, unpublished)

Adamia SA, Lordkipanidze M, Zakariadze G (1977) Evolution of an active continental margin as exemplified by the Alpine history of the Caucasus. Tectonophysics 40(3–4):183–199

Adamia SA, Chkhotua M, Kekelia M, Lordkipanidze M, Shavishvili I, Zachariadze G (1981) Tectonics of the Caucasus and adjoining regions—implications for the evolution of the Tethys Ocean. J Struct Geol 3(4):437–447

Akbulut M, Oyman T, Çiçek M, Selby D, Özgenç İ, Tokçaer M (2016) Petrography, mineral chemistry, fluid inclusion microthermometry and Re–Os geochronology of the Küre volcanogenic massive sulfide deposit (Central Pontides, Northern Turkey). Ore Geol Rev 76:1–18

Akıncı ÖT (1984) The Eastern Pontide volcano-sedimentary belt and associated massive sulphide deposits. Geol Soc London Spec Public 17(1):415–428

Akıncı ÖT (2009) Ophiolite-hosted copper and gold deposits of southeastern Turkey: formation and relationship with seafloor hydrothermal processes. Turk J Earth Sci 18(4):475–509

Akyıldız M, Yıldırım N, Gören B, Yıldırım E, Ilhan S (2015) The origin of vein-type copper-lead-zinc deposits Host in Palaeozoic metamorphic rocks at the Southeast Anatolian Orogenic Belt (Küplüce-Adıyaman, Southeastern Turkey). J Afr Earth Sci 102:191–202

Alpan T (1971) Trabzon-Of Arasının Jeolojik Etüt Raporu [Geological survey report for Trabzon-Of]. General Directorate of Mineral Research and Exploration report no. 1177 (in Turkish, unpublished)

Altherr R, Topuz G, Siebel W, Şen C, Meyer H-P, Satır M, Lahaye Y (2008) Geochemical and Sr–Nd–Pb isotopic characteristics of Paleocene plagioleucitites from the eastern Pontides (NE Turkey). Lithos 105(1):149–161

Altun Y, Yılmaz H, Hatko C, Yılmaz B (2009) Kastamonu- Küre Bakır yatakları ve bu yataklarda 2005–2008 yılları arasında yapılan arama çalışmaları ile elde edilen sonuçlar [Kastamonu-Küre copper deposits and results of explorations conducted during 2005–2008]. Eti Bakır A.Ş. General Directorate, Kastamonu (in Turkish, unpublished)

Altun Y, Yilmaz H, Şiner İ, Yazar F (2015) The secrets of massive sulfide deposits on mid-ocean ridges and Küre-Mağaradoruk copper deposit. Bull Min Res Exp 150:51–64

Arnold M, Sheppard SM (1981) East Pacific Rise at latitude 21 N: isotopic composition and origin of the hydrothermal sulphur. Earth Planet Sci Lett 56:148–156

Arslan M, Aslan Z (2006) Mineralogy, petrography and whole-rock geochemistry of the Tertiary Granitic Intrusions in the Eastern Pontides, Turkey. Asian J Earth Sci 27(2):177–193

Arslan M, Tüysüz N, Korkmaz S, Kurt H (1997) Geochemistry and petrogenesis of the eastern Pontide volcanic rocks, Northeast Turkey. Chem Erde 57:157–188

Arslan M, Boztuğ D, Temizel İ, Kolayli H, Şen C, Abdioğlu E, Ruffet G, Harlavan Y (2007) $^{40}Ar/^{39}Ar$ geochronology and Sr-Pb isotopic evidence of post-collisional extensional volcanism of the eastern Pontide paleo-arc, NE Turkey. Special Supplement. Geochim Cosmochim Acta 71(15S):A38

Aslaner M (1977) Turkiye Cu-Pb-Zn yataklarınn jeolojik ve bölgesel sınıflamasıyla plaka tektoniği yönünden incelemesi [Investigation of Cu-Zn-Pb deposits of Turkey with regards to geological and regional classification within the framework of plate tectonics]. Karadeniz Technical University publication no. 85, Trabzon (in Turkish)

Aslaner M, Gedikoğlu A (1984) Harşit (Tirebolu-Giresun) metallik cevherleşme tipleri [Metallic mineralization types of Harşit (Tirebolu-Giresun) Area]. Karadeniz Tech Univ Geol J 3:1–15

Aslaner M, Van A, Yalçınalp B (1995) General features of the Pontide metallogenic belt. Geology of the Black Sea Region General Directorate of Mineral Research and Exploration and Chamber of Geological Engineers, Ankara, pp 209–213

Aydın İ (2004) Jeofizikte Radyometrik Yöntem ve Gamma Işın Spektrometrisi [Radiometric method and Gamma ray spectrometry in Geophysics]. SDÜ publication no.49, Isparta, Turkey (in Turkish)

Bailey E, Barnes J, Kupfer D (1966) Geology and ore deposits of the Küre district, Kastamonu province, Turkey. CENTO Summer Training Program in Geological Mapping Techniques, pp 17–73

Bailey H, Barnes J, Kupfer D (1967) Türkiye Kastamonu ile Küre Bölgesi cevher yatakları ve jeolojisi [Ore deposits of Turkey Kastamonu and Küre area and their geology]. General Directorate of Etibank report (in Turkish, unpublished)

Bamba T (1976) Ophiolite and related copper deposits of the Ergani mining district, Southeastern Turkey. Bull Min Res Exp 86:36–50

Barrie CT, Hannington MD (1999) Classification of volcanic-associated massive sulfide deposits based on host-rock composition. Rev Econ Geol 8:1–11

Bektaş O, Şen C, Atıcı Y, Köprübaşı N (1999) Migration of the Early Cretaceous subduction-related volcanism toward the back-arc basin of the eastern Pontide magmatic arc (NE Turkey). Geol J 34:95–106

Bossert H (1954) Untersuchungen hieroglyphen-hethitischer Wörter. 1. das Wort 'gut' in den kleinasiatischen Sprachen. MIO

Boztuğ D, Harlavan Y (2008) K–Ar ages of granitoids unravel the stages of Neo-Tethyan convergence in the eastern Pontides and central Anatolia, Turkey. Int J Earth Sci 97(3):585–599

Boztuğ D, Jonckheere R, Wagner G, Yeğingil Z (2004) Slow Senonian and fast Palaeocene–Early Eocene uplift of the granitoids in the Central Eastern Pontides, Turkey: apatite fission-track results. Tectonophysics 382(3):213–228

Boztuğ D, Erçin Aİ, Kuruçelik MK, Göç D, Kömür İ, İskenderoğlu A (2006) Geochemical characteristics of the composite Kaçkar batholith generated in a Neo-Tethyan convergence system, Eastern Pontides, Turkey. J Afr Earth Sci 27(3):286–302

Buser S (1970) Murgul bakır ocağı çevresinin jeolojisi [Geology of Murgul copper mine and its surrounding]. General Directorate of Mineral Research and Exploration report no. 5073 (in Turkish, unpublished)

Ciftci E (2000) Mineralogy, paragenetic sequence, geochemistry and genesis of the gold and silver bearing Upper Cretaceous mineral deposits, northeastern Turkey. PhD dissertation, University of Missouri-Rolla, USA (unpublished)

Çağatay MN (1993) Hydrothermal alteration associated with volcanogenic massive sulfide deposits; examples from Turkey. Econ Geol 88(3):606–621

Çağatay A, Arda O (1984) Küre Bölgesindeki kayaçların mineralojik incelenmesi [Mineralogic investigation of rocks in the Küre area]. Kastamonu (in Turkish, unpublished)

Çağatay MN, Boyle DR (1977) Geochemical prospecting for volcanogenic sulfide deposits, eastern Black Sea region, Turkey. J Geochem Explor 6:35–56

Çagatay M, Eastoe C (1995) A sulfur isotope study of volcanogenic massive sulfide deposits of the Eastern Black Sea province, Turkey. Mineral Deposita 30(1):55–66

Çakır Ü (1995) Geological characteristics of the Aşıköy-Toykondu (Küre-Kastamonu) Massive Sulfide Deposits. Bull Min Res Exp 117:29–40

Çalgın R (1978) Siirt-Madenköy bakır yatağının jeolojisi ve mineralizasyonu [Geology and mineralogy of Siirt-Madenköy copper deposit]. Maden Tetkik ve Arama Genel Müdürlüğü Rapor: 5651 (in Turkish, unpublished)

Çamur MZ, Güven İH, Murat E (1996) Geochemical characteristics of the Eastern Pontide volcanics, Turkey: an example of multiple volcanic cycles in the arc evolution. Turk J Earth Sci 5(2):123–144

Çapkinoğlu Ş (2003) First records of conodonts from. Turk J Earth Sci 12(2):199–207

Çiftçi E (1993) Killik-Espiye-Giresun polimetalik cevherleşmesi üzerindeki topraklarda Pb-As jeokimyasi ile hedef saptanmasının uygulanması [Application of soil geochemistry in target delineation using As-Pb geochemistry in soils developed on the Killik (Espiye-Giresun) polymetallic mineralization]. MSc thesis, Institute of Natural Sciences, Karadeniz Technical Universty, Trabzon, 93p (in Turkish with English abstract, unpublished)

Çiftçi E, Hagni RD (2005) Mineralogy of the Lahanos deposit a Kuroko-type volcanogenic massive sulfide deposit from the eastern Pontides (Giresun, NE Turkey). Geol Bull Turkey 48(1):55–64

Çiftçi E, Kolayli H, Tokel S (2005) Lead-arsenic soil geochemical study as an exploration guide over the Killik volcanogenic massive sulfide deposit, Northeastern Turkey. J Geochem Explor 86(1):49–59

Çiftehan H, O'Brien NP (1998) The Cerattepe Cu–Au–Ag deposit. Abstract 3rd symposium geology of Turkey 153

Clark AL (1971) Strata-bound copper sulfides in the Precambrian Belt Supergroup, northern Idaho and northwestern Montana. In: Proceedings of the third quadrennial IAGOD symposium, Soc. Mining Geologists Japan Spec 3, Tokyo-Kyoto, Japan, pp 261–267

Constantinou G, Govett GJS (1972) Genesis of sulfide deposits, ochre and umber of Cyprus. Inst Min Met 8(b):33–46

Demir Y, Uysal İ, Sadıklar MB (2013) Mineral chemical investigation on sulfide mineralization of the İstala deposit, Gümüşhane, NE-Turkey. Ore Geol Rev 53:306–317

Dercourt J, Zonenshain L, Ricou L-E, Kazmin V, Le Pichon X, Knipper A, Grandjacquet C, Sbortshikov I, Geyssant J, Lepvrier C (1986) Geological evolution of the Tethys belt from the Atlantic to the Pamirs since the Lias. Tectonophysics 123(1–4):241–315

Dewey JF, Pitman WC, Ryan WBF et al (1973) Plate tectonics and evolution of the Alpine system. Geol Soc Am Bull 84:3137–3180

Dilek Y, Imamverdiyev N, Altunkaynak Ş (2010) Geochemistry and tectonics of Cenozoic volcanism in the Lesser Caucasus (Azerbaijan) and the peri-Arabian region: collision-induced mantle dynamics and its magmatic fingerprint. Int Geol Rev 52(4–6):536–578

Dönmez C, Günay K, Yıldız H, Şahin Ş (2013) Gökırmak ve Devrettepe- Hanönü (Kastamonu) Cu cevherleşmesi. [Gökırmak and Devrettepe- Hanönü (Kastamonu) Cu mineralization]. Gen Direct Miner Res Explor Nat Resour Econ Bull 16:127–135

Dönmez C, Günay K, Tablacı A, Özkümüş S, Yıldız H, Şahin Ş, Mengeloğlu MK, Akduman L, Keskin S, Tiryaki O, Çiftçi Y, Yıldırım N (2014) Silisiklastik-Mafik Volkanitlerle İlişkili VMS Cevherleşmelerine Türkiye'den İlk Örnek: Hanönü-Kastamonu [First example of VMS mineralizations related to siliciclastic-mafic volcanics in Turkey: Hanönü-Kastamonu]. 67th Geological Congress of Turkey Abstracts, Ankara

Doyle MG, Allen RL (2003) Subsea-floor replacement in volcanic-hosted massive sulfide deposits. Ore Geol Rev 23(3):183–222

DPT (Devlet Planlama Teşkilatı) (2001) Sekizinci Beş Yıllık Kalkınma Planı Madencilik Özel İhtisas Komisyonu Bakır-Pirit Çalışma Grubu Raporu, Ankara [Ministry of Development 8th 5-year Plan by Specialized Mining Commission]

Egeran N (1946) Türkiye'de maden yataklariyle tektonik birlikler arasındaki münasebetler [Relations between the ore deposits and the tectonic units in Turkey]. Bull Min Res Exp 35:44–49 Ankara

Eğin D, Hirst D, Phillips R (1979) The petrology and geochemistry of volcanic rocks from the northern Harşit river area, Pontid Volcanic Province, Northeast Turkey. J Volcanol Geotherm Res 6(1–2):105–123

Ersecen N (1989) Known ore and mineral resources of Turkey. Directorate of Mineral Research and Exploration publication no. 185, 108p

Esin U, Harmankaya S (1999) Aşikli. In: Özdoğan M, Başgelen N (eds) Neolithic Turkey, the cradle of civilization: new discoveries. Arkeoloji ve Sanat Yayınları, İstanbul, pp 226–132

Eyüboğlu Y (2000) Geology and geochemical characteristics of the area between Tirebolu-Doğankent (Giresun), NE Turkey. MSc thesis, Institute of Natural Sciences, Karadeniz Technical University, Trabzon, 195p (in Turkish with English abstract, unpublished)

Eyüboğlu Y (2010) Late cretaceous high-K volcanism in the eastern Pontides orogenic belt, and its implications for the geodynamic evolution of NE Turkey. Int Geol Rev 52(2–3):142–186

Eyüboğlu Y, Bektaş O, Pul D (2007) Mid-cretaceous olistostromal ophiolitic melange developped in the back-arc basin of the eastern Pontide magmatic arc (NE Turkey). Int Geol Rev 49(12):1103–1126

Eyüboğlu Y, Santosh M, Yi K, Bektaş O, Kwon S (2012) Discovery of Miocene adakitic dacite from the eastern Pontides Belt (NE Turkey) and a revised geodynamic model for the late Cenozoic evolution of the eastern Mediterranean region. Lithos 146:218–232

Eyüboğlu Y, Santosh M, Yi K, Tuysuz N, Korkmaz S, Akaryali E, Dudas FO, Bektas O (2014) The eastern Black Sea-type volcanogenic massive sulfide deposits: geochemistry, zircon U–Pb geochronology and an overview of the geodynamics of ore genesis. Ore Geol Rev 59:29–54

Franklin JM, Lydon J, Sangster DF (1981) Volcanic-associated massive sulfide deposits. Econ Geol 75:485–627

Franklin JM, Gibson H, Jonasson I, Galley A (2005) Volcanogenic massive sulfide deposits. Econ Geol 100th anniversary vol. 98, pp 523–560

Galley AG, Koski R (1999) Setting and characteristics of ophiolite-hosted volcanogenic massive sulfide deposits. Rev Econ Geol 8:221–246

Gedikoğlu, A. (1978) Harşit Granit Karmaşığı ve Çevre Kayaçları [Harşit Granite complex and its country rocks (Giresun- Doğankent)]. Assoc. Prof. Dissertation, Institute of Natural Sciences, Karadeniz Technical University, Trabzon, 161p (in Turkish with English abstract, unpublished)

Gillis KM, Robinson PT (1990) Patterns and processes of alteration in the lavas and dykes of the Troodos ophiolite, Cyprus. J Geophys Res 95(B13):21523–21548

Gökce A (2001) Fluid inclusion, oxygen and hydrogen isotope studies of the Çakmakkaya and Damarköy (Murgul – Artvin) copper deposits and their significances on the genesis of these deposits. Geol Bull Turkey 44(2):23–37

Gökce A, Spiro B (2000) Sulfur-isotope characteristics of the volcanogenic Cu-Zn-Pb deposits of the Eastern Pontide Region, Northeastern Turkey. Int Geol Rev 42(6):565–576

Gorshkov GS (1969) Geophysics and geochemistry of andesite volcanism of the Circum Pacific belt. Proc Andesite Conf Sci Rep 16:91–98

Günay K, Dönmez C, Baran C, Tiryaki O, Yıldız H, Sözcü A, Miski H, Şahin Ş, Çiftçi E, Tablacı A, Özkümüş S, Yıldırım N (2015) Zeybek Bakır Cevherleşmesinin Jeolojisi ve Mineralojisi (Taşköprü-Kastamonu) [Geology and mineralogy of the Zeybek copper mineralization]. 68th Geological Congress of Turkey Abstracts, Ankara

Günay K, Dönmez C, Oyan V, Yıldırım N, Çiftçi E, Yıldız H, Özkümüş S (2018) Geology and geochemistry of sediment-hosted Hanönü massive sulfide deposit (Kastamonu – Turkey). Ore Geol Rev 101:652–674

Güner M (1980) Geology and massive sulfide ores of the Küre area, the pontic ranges, Northern Turkey. Miner Res Explor Bull 93(94):19–64

Güven IH (1993) Geological and metallogenic map of the Eastern Black Sea Region; 1: 250000 Map. Directorate of Mineral Research and Exploration, Trabzon

Harper G (1999) Structural styles of hydrothermal discharge in ophiolite/sea-floor systems. Rev Econ Geol 8:53–73

Hawkins JD (1969) A hieroglyphic hittite inscription from Porsuk. Anatol Stud 19:99–109

Herece E (2008) Doğu Anadolu Fayı (DAF) Atlası [Atlas of East Anatolian fault (EAF)]. General Directorate of Mineral Research and Exploration, Special publication series 13, 359p (in Turkish)

Housh T, Çiftçi E (2008) Cu isotope geochemistry of volcanogenic massive sulphide deposits of the eastern Pontides, Turkey. IOP Conf Ser Earth Environ Sci 2(1):1–6

Huston DL (1999) Stable isotopes and their significance for understanding the genesis of volcanic-hosted massive sulfide deposits: a review. Rev Econ Geol 8:157–179

Hutchinson WR, Hodder WR (1972) Possible tectonic and metallogenic relationships between porphyry copper and massive sulfide deposits. CIM Trans 75:16–22

Hutchinson RW, Searle DL (1970) Strata-bound pyrite deposits in Cyprus and relations to other sulfide ores. Soc Mineral Geol Jpn Spec Issue 3:198–205

Iijima A (1974) Clay and zeolitic alteration zones surrounding Kuroko deposits in the Hokuroku district, northern Akita, as submarine hydrothermal-diagenetic alteration products. Min Geol 6:267–289

Ildız T, Dağcı Z (1990) Bakibaba rezerv hesapları raporu [Reserve assessments report for Bakibaba deposit]. Karadeniz Bakır İşletmesi Genel Müdürlüğü, Ankara (unpublished)

İlhan S (2013) The origin of massive sulfide deposits within the Kocali Complex (Adıyaman). PhD thesis, Institute of Natural and Applied Sciences, Çukurova University, Adana, 247p (in Turkish with English Abstract, unpublished)

Jamieson HE, Lydon J (1987) Geochemistry of a fossil ore-solution aquifer: chemical exchange between rock and hydrothermal fluid recorded in the lower portion of research drill hole CY-2a, Agrokipia, Cyprus. Cyprus Crustal Study Project, Initial Report, Holes CY-2 and CY-2a Geol Surv Can Spec Pap 85–29

JICA (1998) Report on the mineral exploration in the Espiye area, the Republic of Turkey: summary by Metal Mining Agency of Japan (MMAJ), 119 p

Kandemir R, Yılmaz C (2009) Lithostratigraphy, facies, and deposition environment of the lower Jurassic Ammonitico Rosso type sediments (ARTS) in the Gümüşhane area, NE Turkey: implications for the opening of the northern branch of the Neo-Tethys Ocean. J Asian Earth Sci 34(4):586–598

Kaptan E (1982) New discoveries in the mining history of Turkey in the neighborhood of Gümüşköy, Kütahya. Bull Min Res Exp 97–98:59–67

Karakaya MÇ, Karakaya N, Küpeli Ş, Yavuz F (2012) Mineralogy and geochemical behavior of trace elements of hydrothermal alteration types in the volcanogenic massive sulfide deposits, NE Turkey. Ore Geol Rev 48:197–224

Karslı O, Chen B, Aydin F, Şen C (2007) Geochemical and Sr–Nd–Pb isotopic compositions of the Eocene Dölek and Sariçiçek plutons, eastern Turkey: implications for magma interaction in the genesis of high-K calc-alkaline granitoids in a postcollision extensional setting. Lithos 98:67–96

Kaygusuz A, Aydınçakır E (2009) Mineralogy, whole-rock and Sr–Nd isotope geochemistry of mafic microgranular enclaves in Cretaceous Dagbasi granitoids, Eastern Pontides, NE Turkey: evidence of magma mixing, mingling and chemical equilibration. Chem Erde 69(3):247–277

Kaygusuz A, Siebel W, Sen C, Satir M (2008) Petrochemistry and petrology of I-type granitoids in an arc setting: the composite Torul pluton, eastern Pontides, NE Turkey. Int J Earth Sci 97:739–764

Kerridge JF, Haymon RM, Kastner M (1983) Sulfur isotope systematics at the 21 N site, East Pacific Rise. Earth Planet Sci Lett 66:91–100

Ketin İ (1962) Explanatory text of the geological map of Turkey at 1/500 000 scale, Sinop sheet. General Directorate of Mineral Research and Exploration, Ankara, 111p (in Turkish, Unpublished)

Ketin İ (1966) Tectonic units of Anatolia (Asia Minor). Bull Min Res Exp 66:23–34

Ketin İ (1983) An overview of the geology of Turkey. Istanbul Technical University Library Publication 1259, 595p

Ketin İ, Gümüş Ö (1963) Sinop-Ayancık arasında III. bölgeye dahil sahaların jeolojisi [Geological survey for Region III between Sinop-Ayancık]. TPAO report no. 288, Ankara (unpublished)

Knauth LP, Roberts SK (1991) The hydrogen and oxygen isotope history of the Silurian-Permian hydrosphere as determined by direct measurement of fossil water. In: Stable isotope geochemistry: a tribute to Samuel Epstein, Geochemical Society, Sp Publ 3, pp 91–104

Kolaylı H (1989) Alterasyondaki kimyasal değişimlerin incelenmesiyle Kutlular (Sürmene) tipi sülfit yataklarında merceğin saptanması [Delineation of Orebody in Kutlular (Sürmene) – type Massive Sulfide Deposits through the study of geochemical variations in alteration]. MSc thesis, Institute of Natural Sciences, Karadeniz Technical University (in Turkish with English abstract, unpublished)

Kolodny Y, Luz B (1991) Oxygen isotopes in phosphates of fossil fish—Devonian to recent. Stable isotope geochemistry: a tribute to Samuel Epstein, Geochem Soc Spec Publ 3, 1057119

Köprübaşı N, Ciftci E, Cordan S, Köprübaşı N, Özkul C, Tükel FŞ (2014) Comparative geochemical study of soils developed on characteristic black and yellow polymetallic massive sulfide deposits in Eastern Pontides (NE Turkey). Turk J Earth Sci 23(2):129–146

Korkmaz S, Tüysüz N, Er M, Musaoğlu A, Keskin İ (1995) Stratigraphy of the eastern Pontides, NE-Turkey. In: Erler A, Ercan T, Bingöl E, Örçen S (eds) Geology of the Black Sea region. MTA, Ankara, pp 59–68

Kovenko V (1944) Küre'deki eski bakır yatağı ile yeni keşfedilen Aşıköy yatağının ve Karadeniz orta ve doğu kesimleri sahil bölgesinin metallojenisi [Metallogeny of old copper deposit and the newly discovered Aşiköy deposit in Küre area and central and eastern parts coastal lines of Black Sea]. Bull Min Res Exp 32:180–211

Kraeff A (1963) Geology and mineral deposits of the Hopa-Murgul region (Western Part of the province of Artvin, Turkey). Bull Min Res Exp 60:45–60

Large RR (1992) Australian volcanic-hosted massive sulfide deposits; features, styles, and genetic models. Econ Geol 87(3):471–510

Lobanov K, Yakubchuk A, Creaser RA (2014) Besshi-Type VMS Deposits of the Rudny Altai (Central Asia). Econ Geol 109(5):1403–1430

Lydon JW (1988) Ore deposit models# 14. Volcanogenic massive sulfide deposits part 2: genetic models. Geosci Can 15(1):43

Maddin JD, Muhly T, Stech R (1999) Early Metalworking at Çayönü. In: Hauptmann A et al (eds) The Beginnings of Metallurgy. Der Anschnitt, Beiheft 9. Deutsches Bergbau-Museum, Bochum, pp 37–44

Maliotis G, Khan M (1977) Comparison of IP transient shapes over disseminated and massive sulfide sheets in lower pillow lavas of Cyprus. In: Geophysical Journal of the Royal Astronomical Society, vol 1. Blackwell Science Ltd Osney Mead, Oxford, Ox2 0el, pp 266–267

Manetti P, Peccerillo A, Poli G, Corsini F (1983) Petrochemical constraints on the models of Cretaceous-Eocene tectonic evolution of the Eastern Pontic chain (Turkey). Cretac Res 4(2):159–172

MMAJ (Metal Mining Agency of Japan) (1995) The Republic of Turkey report on the mineral exploration of Küre Area (unpublished)
MTA (2009) Türkiye Yer Altı kaynakları (illere göre) [Subsurface resources of Turkey (city-based)]. Earth Sciences and Culture Series 5. ISBN: 975-605-4075-32-4
Ohmoto H, Rye R (1979) Isotopes of sulfur and carbon. In: Barnes HL (ed) Geochemistry of hydrothermal ore deposits. Wiley, New York, pp 509–567
Okay AI (1996) Granulite facies gneisses from the Pulur region, eastern Pontides. Turk J Earth Sci 5:55–61
Okay AI (2008) Geology of Turkey: a synopsis. Anschnitt 21:19–42
Okay AI, Leven EJa (1996) Stratigraphy and paleontology of the upper Paleozoic sequence in the Pulur (Bayburt) region, eastern Pontides. Turk J Earth Sci 5:145–155
Okay AI, Göncüoğlu MC (2004) The Karakaya complex: a review of data and concepts. Turk J Earth Sci 13(2):75–95
Okay AI, Şahintürk O (1997) Geology of the Eastern Pontides. In: Robinson AG (ed) Regional and petroleum geology of the Black Sea and Surrounding Region, Am Assoc Petr Geol Memoir 68, pp 291–311
Okay AI, Tüysüz O (1999) Tethyan sutures of northern Turkey. Geol Soc London Sp Publ 156(1):475–515
Okay AI, Sunal G, Tüysüz O, Sherlock S, Keskin M, Kylander-Clark ARC (2014) Low-pressure–high-temperature metamorphism during extension in a Jurassic magmatic arc, Central Pontides, Turkey. J Metamorph Geol 32(1):49–69
Okay AI, Altiner D, Kilic AM (2015) Triassic limestone, turbidites and serpentinite–the Cimmeride orogeny in the Central Pontides. Geol Mag 152(03):460–479
Ovalıoğlu R (1969) Türkiye Cu-Zn-Pb madenleri ve bunları arama değerlendirme problemleri [Cu-Zn-Pb deposits of Turkey and exploration and evaluation problems]. I.Turkiye Madencilik Bilimsel ve Teknik Kongresi, Ankara (in Turkish, unpublished)
Özgür N (1985) Zur Geochemie und Genese der Kupferlagerstätte Murgul, E-Pontiden/Türkei [On the geochemistry and genesis of the Murgul copper deposit, E-Pontide/Turkey]. PhD thesis, Freie Universitat berlin, 139p (in German, Unpublished)
Özgür N (1993) Volcanogenic massive sulphide deposits in the east Pontic metallotect, NE Turkey. Resour Geol 17:180–185
Pearce JA, Harris NBW, Tindle AJ (1984) Trace element discrimination diagrams for the tectonic interpretation of granitic rocks. J Petrol 25:956–983
Pehlivanoğlu H (1985) Kastamonu-Küre piritli bakır yatakları (Bakibaba, Aşıköy) ve çevresinin jeoloji raporu [Geological survey report for Kastamonu-Küre pyritic copper deposits and their vicinity]. General Directorate of Mineral Research and Exploration report no. 1744 (in Turkish, unpublished)
Pejatovic S (1979) Metallogeny of the Pontide-type massive sulfide deposits. General Directorate of Mineral Research and Exploration publication no. 177, 98p
Pelin S, Özsayar T, Gedikoğlu A, Tülümen E (1982) Doğu Pontidlerde Ust Kretase yaşlı biomikritlerin oluşumu [Formation of upper Cretaceous biomicrites in the Eastern Pontides]. Karadeniz Tech Univ Geol J 2:69–81 (in Turkish)
Perinçek D (1979) Geological investigation of the Çelikhan-Sincik-Koçali area (Adıyaman province). Revue Fac Sci de l'Université d'İstanbul B 44:127–147
Petrascheck WE (1954/1955) Anadolu ve Güneydoğu Avrupası metal provensler arasındaki münasebetler [Relations between the Anatolian and Southeastern European Metal Province]. General Directorate of Mineral Research and Exploration report no. 46/47 (In Turkish, unpublished)
Poulsen H, Hannington M (1995) Auriferous volcanogenic sulfide deposits. In: Eckstrand, OR, Sinclair, WD, and Thorpe RI (eds) Geology of Canadian mineral deposit types, Geology of Canada, no. 8, Decade of North American Geology (DNAG): Geological Society of America, Part 1, pp 183–196
Revan MK, Genç MVV, Ünlü T, Delibaş O, Hamzaçebi S (2013) Original findings on the ore-bearing facies of volcanogenic massive sulphide deposits in the Eastern Black Sea region (NE Turkey). Bull Min Res Exp 147:73–89

Revan MK, Genç Y, Maslennikov VV, Maslennikova SP, Large RR, Danyushevsky LV (2014) Mineralogy and trace-element geochemistry of sulfide minerals in hydrothermal chimneys from the Upper-Cretaceous VMS deposits of the eastern Pontide orogenic belt (NE Turkey). Ore Geol Rev 63:129–149

Rice SP, Robertson AHF, Ustaomer T, Inan N, Tasli K (2009) Late cretaceous–early Eocene tectonic development of the Tethyan suture zone in the Erzincan area, eastern Pontides, Turkey. Geol Mag 146(04):567–590

Richards H, Cann J, Jensenius J (1989) Mineralogical zonation and metasomatism of the alteration pipes of Cyprus sulfide deposits. Econ Geol 84(1):91–115

Robertson AHF (2002) Overview of the genesis and emplacement of Mesozoic ophiolites in the Eastern Mediterranean Tethyan region. Lithos 65(1):1–67

Robertson AHF, Ustaömer T, Pickett EA, Collins AS, Andrew T, Dixon JE (2004) Testing models of Late Palaeozoic–Early Mesozoic orogeny in Western Turkey: support for an evolving Open-Tethys model. J Geol Soc 161(3):501–511

Robertson AHF, Parlak O, Yıldırım N, Dumitrica P, Taslı K (2016) Late Triassic rifting and Jurassic–Cretaceous passive margin development of the Southern Neotethys: evidence from the Adıyaman area, SE Turkey. Int J Earth Sci 105(1):167–201

Robinson A, Banks C, Rutherford M, Hirst J (1995) Stratigraphic and structural development of the Eastern Pontides, Turkey. J Geol Soc 152(5):861–872

Rona PA (1978) Criteria for recognition of hydrothermal mineral deposits in oceanic crust. Econ Geol 73(2):135–160

Rona PA (2005) TAG hydrothermal field: a key to modern and ancient seafloor hydrothermal VMS ore-forming systems. In: Mineral deposit research: meeting the global challenge, Springer, pp 687–690

Rose AW, Hawkens HE, Webb JS (1979) Geochemistry in mineral exploration, 2nd edn. Academic Press, London, p 657

Rouxel O, Fouquet Y, Ludden JN (2004) Copper isotope systematics of the Lucky Strike, Rainbow, and Logatchev sea-floor hydrothermal fields on the Mid-Atlantic Ridge. Econ Geol 99(3):585–600

Sarıcan K (1968) Bakibaba cevher yatağı arama ve değerlendirme çalışmaları raporu [Exploration and evaluation survey report for Bakibaka ore deposit]. Küre Etibank, Karadeniz Bakır İşletmeleri Raporu (in Turkish, unpublished)

Şaşmaz A, Gümüş G, Sağıroğlu A (1999) A typical example of allochtonous Cyprus type copper mineralizations: Derdere mineralizations. Geol Bull Turkey 42(1):105–117 (in Turkish with English abstract)

Şaşmaz A, Türkyilmaz B, Öztürk N, Yavuz F, Kumral M (2014) Geology and geochemistry of middle Eocene Maden complex ferromanganese deposits from the Elazığ–Malatya region, eastern Turkey. Ore Geol Rev 56:352–372

Schneider H, Özgür N, Palacios C (1988) Relationship between alteration, rare earth element distribution, and mineralization of the Murgul copper deposit, northeastern Turkey. Econ Geol 83(6):1238–1246

Schneiderhöhn H (1955) Die Kupferlagerstätte Murgul im Schwarz-meer-Küstengebiet, Provinz Çoruh, Nordost-Türkei [The Murgul copper deposit in the Black Sea coastal area, Çoruh province, North-east Turkey]. Erzmetall 8:468–478

Schoop U-D (1995) Die Geburt des Hephaistos: Technologie und Kulturgeschichte neolithischer Metallverwendung im Vorderen Orient

Şen C (2007) Jurassic volcanism in the Eastern Pontides: is it rift related or subduction related? Turk J Earth Sci 16(4):523–539

Şengör AMC (1987) Tectonics of the Tethysides: orogenic collage development in a collisional setting. Annu Rev Earth Planet Sci 15(1):213–244

Şengör AMC, Yılmaz Y (1981) Tethyan evolution of Turkey: a plate tectonic approach. Tectonophysics 75(3–4):181–241

Şengör AMC, Yılmaz Y (1983) Türkiye'de Tetis' in evrimi: Levha tektoniği açısından bir yaklaşım [Evolution of Tethys in Turkey: a plate tectonics approach]. TJK Yerbilimleri Özel Dizisi 1, 75 pp (in Turkish)

Şengün M (2006) A critical review of the Anatolian geology: a dialectic to sutures and evolution of the Anatolian Tethys and Neotethys. Bull Min Res Exp 133:1–29

Shanks WC, Seyfried WE (1987) Stable isotope studies of vent fluids and chimney minerals, southern Juan de Fuca Ridge: sodium metasomatism and seawater sulfate reduction. J Geophys Res Solid Earth 92(B11):11387–11399

Sungurlu O (1973) VI. Bölge Gölbasi-Gerger arasindaki sahanin jeolojisi [Geological survey for the area between VI. Region Gölbaşı-Gerger]. Turkish Petroleum Corporation (TPAO) report no. 80 (in Turkish, unpublished)

Tokel S (1972) Stratigraphical and volcanic history of the Gümüşhane Region, NE Turkey. PhD thesis, University College London, UK (unpublished)

Topuz G (2002) Retrograde P–T path of anatectic migmatites from the Pulur Massif, Eastern Pontides, NE Turkey: petrological and microtextural constraints. In: Abstracts first International symposium of the Faculty of Mines (İTÜ) on Earth Sciences and Engineering İstanbul, Turkey, p 110

Topuz G, Altherr R (2004) Pervasive rehydration of granulites during exhumation? an example from the Pulur complex, Eastern Pontides, Turkey. Mineral Petrol 81(1–2):165–185

Topuz G, Altherr R, Satır M, Schwarz WH (2001) Age and metamorphic conditions of low-grade metamorphism in the Pulur massif, NE Turkey. In: Fourth international Turkish geology symposium abstracts, Adana, Turkey, p 215

Topuz G, Altherr R, Kalt A, Satır M, Werner O, Schwarz WH (2004) Aluminous granulites from the Pulur complex, NE Turkey: a case of partial melting, efficient melt extraction and crystallisation. Lithos 72(3):183–207

Topuz G, Altherr R, Schwarz WH, Dokuz A, Meyer H-P (2007) Variscan amphibolite-facies rocks from the Kurtoğlu metamorphic complex (Gümüşhane area, Eastern Pontides, Turkey). Int J Earth Sci 96(5):861

Topuz G, Altherr R, Siebel W, Schwarz WH, Zack T, Hasözbek A, Barth M, Satır M, Şen C (2010) Carboniferous high-potassium I-type granitoid magmatism in the Eastern Pontides: the Gümüşhane pluton (NE Turkey). Lithos 116(1):92–110

Turhan K, Avenk T (1976) Trabzon-Sürmene Kutlular yatağı rezerv hesabı [Trabzon-Sürmene Kutlular deposit reserve assesment]. General Directorate of Mineral Research and Exploration report no. 1417 (in Turkish, unpublished)

Tüysüz O (1990) Tectonic evolution of a part of the Tethyside orogenic collage: the Kargi massif, northern Turkey. Tectonics 9(1):141–160

Tüysüz N (1995) Lahanos (Espiye-Giresun) masif sülfit yatağına ait cevher mineralleri ve dokularının cevher oluşumu açısından incelenmesi [Study of ore minerals and textures for understanding of ore formation in Lahanos (Espiye-Giresun) massive sulfide deposit]. Geosound 26:79–92

Ulutürk Y (1999) Siirt Madenköy bakır yatağı [Siirt Madenköy copper deposit]. General Directorate of Mineral Research and Exploration report no. 7562 (in Turkish, unpublished)

Ustaömer T, Robertson AHF (1993) A late Paleozoic-Early Mesozoic marginal basin along the active southern continental margin of Eurasia: evidence from the Central Pontides (Turkey) and adjacent regions. Geol J 28:219–238

Ustaömer T, Robertson AHF (1994) Late Palaeozoic marginal basin and subduction-accretion: the Palaeotethyan Küre complex, central Pontides, northern Turkey. J Geol Soc 151(2):291–305

Ustaömer T, Robertson AHF (1996) A paleotethyan tectonic evolution of the North Tethyan margin in the central Pontides, N Turkey. In: Proceedings of International symposium on the Geology of the Black Sea Region, I, pp 24–33

Ustaömer T, Robertson AHF (1999) Geochemical evidence used to test alternative plate tectonic models for the pre-Upper Jurassic (Palaeotethyan) units in the Central Pontides, N Turkey. Geol J 34:25–53

Uzunçimen S, Tekin UK, Bedi Y, Perincek D, Varol E, Soycan H (2011) Discovery of the Late Triassic (Middle Carnian–Rhaetian) radiolarians in the volcano-sedimentary sequences of the Kocali Complex, SE Turkey: correlation with the other Tauride units. J Asian Earth Sci 40(1):180–200

Van A (1990) Pontid Kuşağında Artvin Bölgesinin Jeokimyasi, Petrojenezi ve Masif Sülfit Mineralizasyonları [Geochemistry, petrogenesis and massive sulfide mineralization in the Artvin area in the Pontide Belt]. PhD thesis, Institute of Natural Sciences, Karadeniz Technical University, Trabzon, 117p (in Turkish with English abstract, unpublished)

Varol E, Bedi Y, Tekin UK, Uzuncimen S (2011) Geochemical and petrological characteristics of Late Triassic basic volcanic rocks from the Kocali complex, SE Turkey: implications for the Triassic evolution of southern Tethys. Ofioliti 36(1):101–115

Vıcıl M (1975) Artvin-İrsahan madeni Cu-Pb-Zn yatağının 1:2000 lik jeoloji raporu [1:2000 scale geological survey report for Artvin-İrsahan Cu-Zn-Pb deposit]. General Directorate of the Mineral Research and Exploration r eport no. 1296 (in Turkish, unpublished)

Wijkerslooth P (1944) Elazığ ili (Ergani-Maden) bakır yatakları hakkındaki bilgiye yeni bir ilave [New contribution to the understanding of Elazığ (Ergani-Maden) copper deposits]. Bull Min Res Exp 33:76–104

Woodruff LG, Shanks WC (1988) Sulfur isotope study of chimney minerals and vent fluids from 21 N, East Pacific Rise: hydrothermal sulfur sources and disequilibrium sulfate reduction. J Geophys Res 93(B5):4562–4572

Yalçın Ü (2000) Anfänge der Metallverwendung in Anatolien [Beginnings of metal use in Anatolia]. Anatolian Metal I. der Anschnitt. Die Zeitschrift für Kunst und Kultur im Bergbau, Beiheft Bochum. Deutches Bergbau-Museum 13:17–30

Yalçın Ü, İpek Ö (2016) Datierung des Bergbaus. In: Yalçın Ü, İpek Ö (eds) “Prähistorische Kupfergweinnung in Derekutuğun, Anatolien” [Prehistoric copper foundry in Derekutuğun, Anatolia]. Band I: Montanarchäologische Forschungen in den Jahren 2009–2011. Ein Vorbericht. Der Anschnitt Beiheft 30. Deutsches Bergbau-Museum, Bochum

Yazgan E (1984) Geodynamic evolution of the Eastern Taurus region. In: Geology of the Taurus Belt. Proceedings of International symposium. Mineral Research and Exploration Institute of Turkey, pp 199–208

Yener KA (2000) The domestication of metals: the rise of complex metal industries in Anatolia. Brill, Leiden

Yiğit O (2009) Mineral deposits of Turkey in relation to Tethyan metallogeny: implications for future mineral exploration. Econ Geol 104(1):19–51

Yiğitbaş E, Yilmaz Y (1996) New evidence and solution to the Maden complex controversy of the Southeast Anatolian orogenic belt (Turkey). Geol Rundsch 85(2):250–263

Yıldırım N (2013) Havza-Kuşak Madenciliği Kapsaminda Keşfedilen “GD Anadolu Kıbrıs Tipi VMS Metalojenik Kuşağı”: Koçali Karmaşığı, Adiyaman Bölgesi, Türkiye [SE Anatolia Cyprus-type VMS Metallogenic Belt – discovered within the scope of Basin-Range mining, Koçali Melange, Adiyaman region, Turkey]. General Directorate of Mineral Research and Exploration Natural Resources and Economy Bulletin 14, pp 47–55

Yıldırım R, Alyamaç F (1976) Siirt ili Madenköy-Hürmüz yöresi jeoloji etüdü [Geological survey of Siirt-Madenköy-Hürmüz area]. General Directorate of Mineral Research and Exploration report no. 5851 (in Turkish, Unpublished)

Yıldırım M, Yılmaz Y (1991) Güneydoğu Anadolu orojenik kuşağının ekaylı zonu [Imbricated zone of the Southeast Anatolian Orogenic Belt]. Turkish Assoc Pet Geol Bull (TAPG) 3:57–73

Yıldırım N, İlhan S, Akyıldız M, Yıldırım E, Dönmez C (2010) The importance of the ophiolites of the southern branch of the Neotethys (Koçali ophiolitic complex), in terms of the Cyprus Type VMS Deposits. In: 7th International symposium on Eastern Mediterranean Geology. Turkey, Adana

Yıldırım N, İlhan S, Yıldırım E, Dönmez C (2012a) The geology, geochemistry and genetical features of the Ormanbaşi Hill (Sincik, Adiyaman) copper mineralization. Bull Min Res Exp 144:75–104

Yıldırım N, Parlak O, Robertson (2012b) A Geochemistry and tectonic significance of the Koçali ophiolite and the related Koçali melange, Adiyaman region, SE Turkey. In: EGU General Assembly conference abstracts 1253

Yıldırım N, Dönmez C, Kang J, Lee I, Pirajno F, Yıldırım E, Günay K, Seo JH, Farquhar J, Chang SW (2016) A magnetite-rich Cyprus-type VMS deposit in Ortaklar: a unique VMS style in the Tethyan metallogenic belt, Gaziantep, Turkey. Ore Geol Rev 79:425–442

Yılmaz Y (1972) Petrology and structure of the Gümüşhane granite and surrounding rocks, North-Eastern Anatolia. PhD thesis, University of London (unpublished)

Yılmaz O (1980) Daday-Devrekani masifi kuzeydoğu kesimi litostratigrafi birimleri ve tektoniği [Lithostratigraphic units and their tectonic settings in NE of the Daday-Devrekani massif]. Yerbilimleri Derg 5(5/6):101–131

Yılmaz O (1988) L'ensemble ophiolitique de Çangal (Turquie du Nord): Mise en évidence d'un métamorphisme occéanique et d'un rétrométamorphisme cataclastique tardif [The ophiolitic ensemble of Çangal (Northern Turkey): demonstration of an oceanic metamorphism and a late retroacetic retrometamorphism]. Geol Alp 64:113–132

Yılmaz Y (1990) Comparison of young volcanic associations of western and eastern Anatolia formed under a compressional regime: a review. J Volcanol Geotherm Res 44(1–2):69–87

Yılmaz Y (1993) New evidence and model on the evolution of the southeast Anatolian orogen. GSA Bull 105:251–271

Yılmaz Y (1997) Geology of Western Anatolia. Active tectonics of NW Anatolia the Marmara poly project, eds Schindler and Pfister VDF, ETH Zurich, pp 31–54

Yılmaz Y, Yigitbaş E, Genç S (1993) Ophiolitic and metamorphic assemblages of southeast Anatolia and their significance in the geological evolution of the orogenic belt. Tectonics 12:1280–1297

Zaccarini F, Garuti G (2008) Mineralogy and chemical composition of VMS deposits of northern Apennine ophiolites, Italy: evidence for the influence of country rock type on ore composition. Mineral Petrol 94(1–2):61

Zerener M (2005) Doğu Karadeniz Bölgesi metalojenik kuşağında bulunan murgul masif sülfid yatağının hidrotermal çözeltileri ve gelişimi [Hydrothermal fluids and their evolution resulting in the formation of Murgul massive sulfide deposit occurring in the Eastern Black Sea metallogenic belt]. Institute of Applied Sciences, Süleyman Demirel Üniversitesi, 43p (in Turkish with English abstract, unpublished)

Zhu X, O'nions R, Guo Y, Belshaw N, Rickard D (2000) Determination of natural Cu-isotope variation by plasma-source mass spectrometry: implications for use as geochemical tracers. Chem Geol 163(1):139–149

Zhu X, Guo Y, Williams R, O'nions R, Matthews A, Belshaw N, Canters G, De Waal E, Weser U, Burgess B (2002) Mass fractionation processes of transition metal isotopes. Earth Planet Sci Lett 200(1):47–62

Zierenberg RA, Shanks WC, Bischoff JL (1984) Massive sulfide deposits at 21 N, East Pacific Rise: chemical composition, stable isotopes, and phase equilibria. Geol Soc Am Bull 95(8):922–929

Zimmer E (1938) Murgul bakır madeni [Murgul copper mine]. Bull Min Res Exp 2:13–21 (in Turkish)

Chapter 10
Carbonate-Hosted Pb-Zn Deposits of Turkey

Nurullah Hanilçi, Hüseyin Öztürk, and Cem Kasapçı

Abstract The carbonate-hosted Pb-Zn deposits in Turkey are located in the Tauride belt, which is a part of Alpine-Himalayan orogenic systems. Most of the carbonate-hosted Pb-Zn deposits that occur in the Tauride passive margin carbonate sequence have been identified as MVT because of the geological environment, ore characteristics, formation temperature and isotope geochemistry (e.g., the Hadim-Bozkır region, Aladağ-Zamantı region). The style of mineralization and geochemical data of Zn-Pb deposits in the Hakkari region is resembles to the SEDEX type deposits in terms of slightly higher homogenization temperature and lower salinity than MVT, stratiform ore zones parallel to each other, and high contents of As, Mo, Sb, Tl and Hg. Apart from the MVT and SEDEX Pb-Zn deposits, there is a carbonate-hosted Pb-Zn deposit in the Horzum (Adana-Turkey) province, which has been identified as a carbonate-replacement Pb-Zn deposit (CRD Pb-Zn) due to its higher formation temperature (average 235 °C) and higher temperature mineral paragenesis (e.g. bornite, arsenopyrite and argentite) than the MVT.

The mining history of the carbonate-hosted Pb-Zn deposits in Turkey goes back to Roman times. At present, approximately 0.2 Mt of Pb-Zn carbonate-oxide ore with average grades of 20% Zn and 8% Pb are produced annually from the carbonate-hosted deposits in the Tauride belt in Turkey. Currently, mining takes place at shallow depths (0–50 m), and drilling programs are limited so that in the generally carbonate sequences of the Tauride belt, especially in the Hakkari Province, there is a significant potential for finding new and possibly" world-class" carbonate-hosted Pb-Zn deposits.

N. Hanilçi (✉) · H. Öztürk · C. Kasapçı
Department of Geological Engineering, Avcilar Campus, İstanbul University-Cerrahpaşa, İstanbul, Turkey
e-mail: nurullah@istanbul.edu.tr

F. Pirajno et al. (eds.), *Mineral Resources of Turkey*, Modern Approaches in Solid Earth Sciences 16, https://doi.org/10.1007/978-3-030-02950-0_10

10.1 Introduction

It is known that the sediment-hosted Pb-Zn deposits have been classified in two main classes by Leach et al. (2010). The first class is "clastic-dominated Pb-Zn (CD Pb-Zn) deposits" (traditionally called sedimentary exhalative-SEDEX) that occur within the shale, sandstone, siltstone and/or carbonates belonging to clastic sedimentary sequences. The tectonic settings of the CD Pb-Zn deposits are passive margins, back-arc, continental rifts and sag basins (Leach et al. 2010). The second class are the Mississippi Valley-type (MVT) Pb-Zn deposits which occur in platform carbonates of passive margin tectonic environments. The main characteristics of the MVT deposits are: (i) epigenetic, (ii) strata-bound, (iii) occur in platform carbonates (limestone and dolostone), (iv) have no relationship with magmatic activity and (v) formed mostly at low temperatures (ranging from 75 to 175 °C) by saline (20 ± 5 wt% NaCl eq.) basinal brines that may have had inputs from evaporite dissolution (e.g., Leach and Sangster 1993; Leach et al. 2005; Pirajno 2009; Wilkinson 2014; Bodnar et al. 2014). Apart from these two main classes, there are also carbonate-hosted Pb-Zn deposits called "Carbonate Replacement Deposits" (CRD; also known as Leadville-type mineralization as described by e.g. Megaw et al. 1988; Thompson and Beaty 1990; Kamona 2011). They occur via magmatic-hydrothermal processes at a high temperature (>200 °C) produced by felsic to intermediate magmatism and are clearly different from MVT and SEDEX types, because of their temporal and spatial relationship to the magmatic intrusions.

The aim of this chapter is to review the geological environments, general characteristics and the understanding of the genesis of the carbonate-hosted Pb-Zn deposits in Turkey (Fig. 10.1). The CRD Pb-Zn deposits (Horzum and Pınargözü), the MVT Pb-Zn±Ba±F deposits (Hadim-Bozkır, Göktepe, Gazipaşa, Ortakonuş,

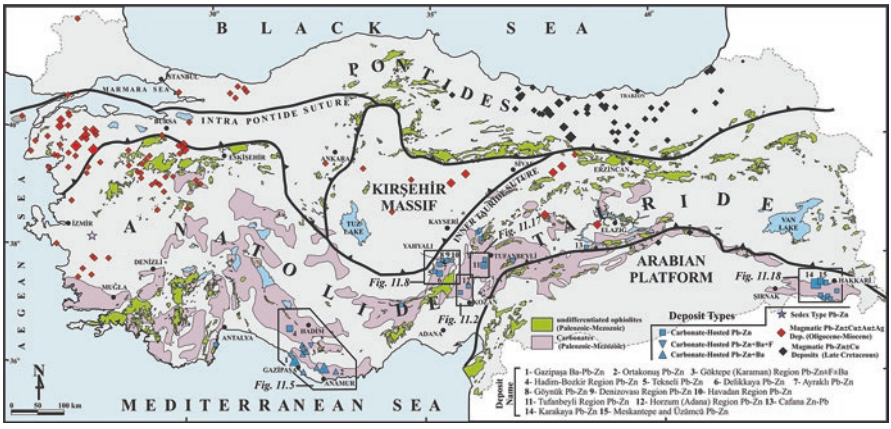

Fig. 10.1 Distribution of Pb-Zn deposits and occurrences in Turkey (Tectonic elements modified from Okay and Tüysüz (1999) and Robertson and Ustaömer (2009))

Aladağ-Zamantı and Tufanbeyli Province) and SEDEX type Pb-Zn deposits (Hakkari Province) are the focus of this chapter.

10.2 Carbonate-Replacement Type (CRD) Pb-Zn Deposits

10.2.1 Horzum and Pınargözü (Adana) Pb-Zn Deposits

The Horzum and the Pınargözü Pb-Zn deposits located about 97 km north of Adana city, are approximately 1.5 km and 7 km north of the Horzum Yaylası settlement, respectively (Fig. 10.2, Table 10.1). Between 1965 and 1997, approximately 0.5 Mt with 30% Zn grade oxide-carbonate ore and 0.4 Mt with 7–14% Zn grade sulphidic ore were mined from the deposits. The proven reserves of the deposits are approximately 500,000 tonnes of oxide-carbonate ore (Akmetal 2015).

The geology of the area consists of Palaeozoic clastics and carbonate rocks that belong to the Geyik Dağı Unit (Fig. 10.2). The Pb-Zn mineralizations are hosted by thickly bedded, massive, dark-grey dolomitic limestone and grey limestone of Middle-Upper Cambrian and are fracture-filling and strata-bound (Figs. 10.2 and 10.3).

The Pb-Zn ores are hosted in limestone and dolomitic limestone as open-space filling or replacement-type through the E-W and NW-SE trending faults cut by the N-S oriented regional scale structural elements. Although the open-space filling ore shows a vein and funnel-shaped geometry, the strata-bound type ore shows a stratiform geometry. The dimensions of the funnel-shaped ore body vary from 40 to 50-m width, 20 to 25-m thickness, and 80 to 100-m length (Temur 1986). The ore zones are oxidized and changed to oxide-carbonate ore at the surface, passing to primary sulphidic ore at depth. The oxidic ore contains smithsonite, (hydro)zincite, cerussite, Fe-(hydr)oxide and rare galena. The primary sulphidic ore lenses (Fig. 10.4a) include sphalerite, pyrite and galena (Fig. 10.4b) and are preserved within the oxidic ore zone.

The primary ore contains sphalerite, pyrite, galena, chalcopyrite, arsenopyrite, marcasite, bornite, chalcocite, freibergite, native Au, electrum, argentite and tetrahedrite-tennantite (Temur 1986). Barite, quartz, calcite and dolomite are the gangue minerals.

The average homogenization temperature (Th) of the fluid inclusions obtained from sphalerite is 235 °C (170–287 °C, $n = 11$) for the Pb-Zn deposits in the Horzum region. Although the deposits are stratabound and carbonate-hosted similar to MVT deposits, the Th data are significantly higher than the typical Th of the MVT deposits (ranging from 75 to 175 °C). In addition, the mineral assemblage in the Horzum region deposits contains high-temperature minerals such as bornite, arsenopyrite, chalcopyrite and enargite, which indicates that the Pb-Zn deposits, which are not known to be related to a magmatic intrusions, and as such can be classified as CRD Pb-Zn deposits.

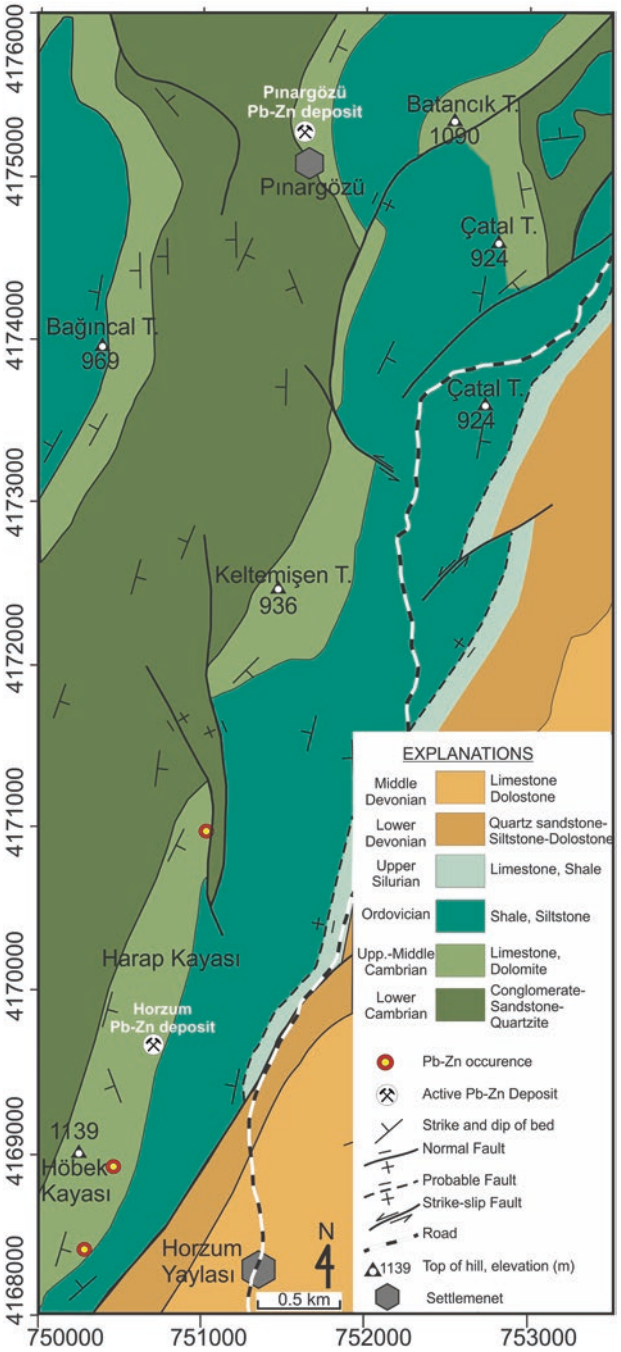

Fig. 10.2 Geological map of the Horzum region (simplified after the MTA 1/25000 geological map) and the location of the Pb-Zn deposits in the region

Table 10.1 General features of the carbonate-hosted Pb-Zn deposits of Turkey

Province name	Deposit and occurrence name	Coordinate (ED50 UTM)		Mineralization style	Host rock	Age of host rock	Ore geometry	Ore paragenesis	Mined ore grade (%)	Mined reserve (Mt)	Ore reserve (Mt)	References
		Y (to RIGHT)	X (to UP)									
Horzum	Horzum	50712	4169650	Vein, strata-bound	Dlm, Lm	L.-M. Cambrian	Vein, funnel-shaped	sp, py, gn, ccp,asy, mrc, cc, fb,arg, Au, Au-Ag, brt, qtz, cal,	30% Zn (oxide-carbonite)	1	0.05	Akmetal (2015) and Temur (1986)
	Pınargözü	51621	4175230	Vein, strata-bound	Dlm, Lm	L.-M. Cambrian	Vein		7–14% Zn (sulphidic ore)		n.d.	
Hadim-Bozkır	Kızılgeriş	433925	4092060	Strata-bound, karstic-fill	Lm	L. Permian	Starata, pocket	sm, cer, hz, lim, sp., gn, py, brt, dol, cal	35% Zn+Pb (Zn>25%)	0.1	n.d.	Alp (1976) and Demir (1998)
	Katranbaşı	432980	4092575									
	Küçüksu	425980	4096810									
	Asartepe	427900	4096800									
	Hanifeyurdu	427650	4097540									
Aladağ-Zamantı	Ayraklı	699750	4218950	Strata-bound, vein, Karstik	Dol, Lm	Devonian	Pocket, Veins	sm, cer, hz,	10–13% Pb	0.8	0.1	Demir (1998)and OREKS (2015)
									12–35% Zn			
	Denizovası	721300	4227300	Strata-bound, karstik, vein	Lm	U.Permian, Jurassic	Veins, pocket,	sm, hz, sz, gn, sp., lim,	%18–34 Zn	1	n.d.	Hanilçi and Öztürk (2011) and Koptagel et al. (2005)
									%2–10 Pb			
	Göynük	712350	4225400	Strata-bound, vein-fill, karstic-fill	Lm	U. Permian, L.-M.Triassic	Strata, vein, pocket	sm, cer, ang, gn, goe, lpd, sp., py	20% Zn	0.3	n.d.	
									10% Pb			
	Delikkaya	699250	4101200	Vein-fill, karstic-fill	Lm, Dlm	Middle Jurassic	Vein, pocket, lens	sp, gn, py, ccp, apy,mrc, ang, cer, beu, sm, hz, zc, sd, hem, lim, qtz, cal, dol	40% Zn+Pb (Zn>25%)	2.7	n.d.	Demir (1998) and Hanilçi and Öztürk (2011)

(continued)

Table 10.1 (continued)

Province name	Deposit and occurrence name		Coordinate (ED50 UTM) Y (to RIGHT)	X (to UP)	Mineralization style	Host rock	Age of host rock	Ore geometry	Ore paragenesis	Mined ore grade (%)	Mined reserve (Mt)	Ore reserve (Mt)	References
	Tekneli		693200	4102150	Vein-fill, karst-fill	Lm	U.Permian	Vein, pocket	sp, py, mrc, gn, ccp, apy, fb, sm, hz, hmp, cer, lim	21% Zn 4% Pb	0.4	n.d.	Çopuroğlu (1996) and Demir (1998)
	Suçatı		606922	4106265	Vein-fill, karst-fill	Lm, Dlm	Middle Jurassic	Vein, pipe-shaped	py, mrc, gn, sp., ang, cer, sm, hz, zc, hem, lim, cal, dol, brt	25% < Zn	0.1	n.d.	Demir (1998), Hanilçi and Öztürk (2011)
	Havadan	Çakılpınar	726100	4226200	Strata-bound, vein-fill, karstic-fill	Lm	Jurassic	Strata, vein, pocket	sm, cer, ang, goe, lpd, gn, sp., py	23% Zn 10% Pb	0.41		Demir (1998) and Koptagel et al. (1998)
		Köprüüstü	725700	4225050									
		Tekke	727564	4225200									
		Karnıyarık	728395	4225302									
		Köyüstü (Aksu)	728800	4225150									
Tufanbeyli	Akçal[a]		265900	4230200	Strata-bound, vein-fill, karst-fill	Dol	M. Devonian	Pocket, vein	sm, hz, cer, gn, lim, dol, sp., pr, mrc, cal, brt, hem	21% Zn 2% Pb	0.1	n.d.	Demir (1998)and Mengeloğlu (1996)
	Belbaşı[a]		267300	4232500									
	Kodamandere[a]		265500	4221000		Lm, Dlm	Jurassic-Cretaceouse			21% Zn 3% Pb	0.013		
	Beşiktaş[a]		269500	4225800		Lm, Dlm	Jurassic-Cretaceouse			21% Zn 5% Pb	0.025		

Göktepe	Pınarüstü (PU)	450100	4057380	Strata-bound, vein-fill,	Lm	U.Permian	Strata, vein	sp, gn, py, sm, cer, ang, lim, fl, brt, cal, dol	n.d.	n.m.		Kuşçu (1985) and Demir (1998)
	Sarıpınar (SP)	448440	4059110									
	Tufandağ (TD)	448620	4057700	Strata-bound, vein-fill,	Lm, Oslm	U. Permian, L.-M.Triassic			n.d.	n.m.		
	Üçtepeler (ÜZ)	450570	4059210									
	Düden (DZ)	455080	4056010									
	Haydar (HY)	451190	4057850	Strata-bound, vein-fill,	Oslm	L.-M.Triassic			n.d.	n.m.		
	Makam (MK)	457500	4055000									
	Kuzubögedi(KB)	458890	4055010									
	Muzvadi (MZ)	461210	4043210	Vein-fill	Dlm	Jurassic	Vein	sp, gn, py, sm, cer, ang, brt, dol	n.d.	n.m.		
	Berem (BZ)	450850	4041790	Strata-bound, vein-fill, breccia-fill	Dlm, Oslm	Jurassic, L.-M.Triassic	Strata, vein		n.d.	n.m.		
Gazipaşa	Karalar	439301	4021625	Vein and fracture-fill, breccia-fill	Lm	Permian	Vein	brt, gn, sp., py, ccp, lim, qtz, cal	n.d.	Mined for barite		Gökçe and Bozkaya (2003), Çopuroğlu (1994)
	Burhan Mahallesi			Vein-fill	Dlm	Permian	Vein, lensoidal	brt, gn, td, tn, cer, cv, id	n.d.	n.m.		Ayhan (1982) and Sadıklar and Amstutz (1981)
	Aydap Yuları			Strata-bound, fracture-fill, karstic-fill	Lm	Permian	Strata, vein	brt, gn, sp., py, tn, td, ccp, cv, cc, sm, cer, ang, lim, ma, az, lim	n.d.	n.m.		
Anamur	Ortakonuş	491800	3908400	Strata-bound, vein-fill	Limestone	U.Triassic	Lensoidal, vein	gn, sp., py, pj, mrc, hem, ang, sm, brt, dol, cal	29% Zn 6%Pb	0.11	n.d	Blümel (1964), Gümüş (1989), and Demir (1998)

(continued)

Table 10.1 (continued)

Province name	Deposit and occurrence name	Coordinate (ED50 UTM)		Mineralization style	Host rock	Age of host rock	Ore geometry	Ore paragenesis	Mined ore grade (%)	Mined reserve (Mt)	Ore reserve (Mt)	References
		Y (to RIGHT)	X (to UP)									
Hakkari	Karakaya	364750	4150750	Strata-bound, stratiform	Lm	Late Triassic	Strata, vein, pocket	sm, hmp, hz, zc, cer, ang, goe, sid, cal, dol, brt, gn, sp., py	21% Zn 5% Pb	0.2	4	Hanilçi and Öztürk (2008), Santoro et al. (2013), and Karakaya Co (2015)
	Meskantepe	368150	4150700	Strata-bound, stratiform	Lm	Late Triassic	Strata, vein, pocket	sm, hz, zc, cer, ang, hmp, goe, sp., gn, py, brt, cal, dol, sid, qtz	24% Zn 6% Pb	0.7	A few	
	Üzümcü	372510	4150250	Strata-bound, stratiform	Lm	Late Triassic	Strata, pocket	sm, hz, zc, hmp, cer, ang, sp., gn, py, br, cal, dol	027% Zn 5% Pb	0.1	n.d	
	Kurşuntepe	382900	4123900	Strata-bound, vein-fill	Lm	U. Permian.-Early Triassic	Strata, vein	sp, gn, py, brt, dol, cal, qtz	27% Zn 8% Pb	0.07	n.d	
	Armutlu	362750	4150450	Strata-bound, karst-fill	Lm	Late Triassic	Strata, pocket	sm, hmp, hz, zc, cer, ang, goe, sid, cal, dol, brt, gn, sp., py	21% Zn 5% Pb	0.09	8	
	Oğul	389417	4145910	Strata-bound	Lm	Late Triassic	Strata	gn, sp., py, sm, cer,ang, lim, goe, brt	n.p.	n.m.	n.d.	
	Akkaya	364300	4133750	Vein-fill	Dlm, Dol	Jurassic	Vein	sm, cer, geo, lim, gn, brt	15% Zn 6–12% Pb	0.07	n.d.	
	Deştan	368750	4124000	Karst-fill, vein-fill	Lm	Permian	Pocket, vein	sm, cer, gn	n.p.	n.m.	n.d.	

ang anglesite, *apy* arsenopyrite, *arg* argentite, *az* azurite, *beu* beudantite, *bn* bornite, *brt* barite, *cal* calcite, *cc* chalcocite, *ccp* chalcopyrite, *cer*cerussite, *cv* covellite, *Dlm* dolomitic limestone, *dol* dolomite, *fb* freibergite, *fl* fluorite; *gn* galena, *goe* goethite, *hem* hematite, *hmp* hemimorphite, *hz* hydrozincite, *id* idaite, *lim* limonite, *Lm* limestone, *lpd* lepidocrocite, *ma* malachite, *mrc* marcasite, *n.d.* no data, *n.m.* no mining, *Oslm* Oolitic-stromatolitic limestone limestone, *pj* plumbpjarosite, *py* pyrite, *qtz* quartz, *sd* siderite, *sm* smithsonite, *sp* sphalerite, *td* tetrahedrite, *tn* tennantite, *zc* zincite

[a]The location of the mineralization is within the 500 m diameter area of this coordinate

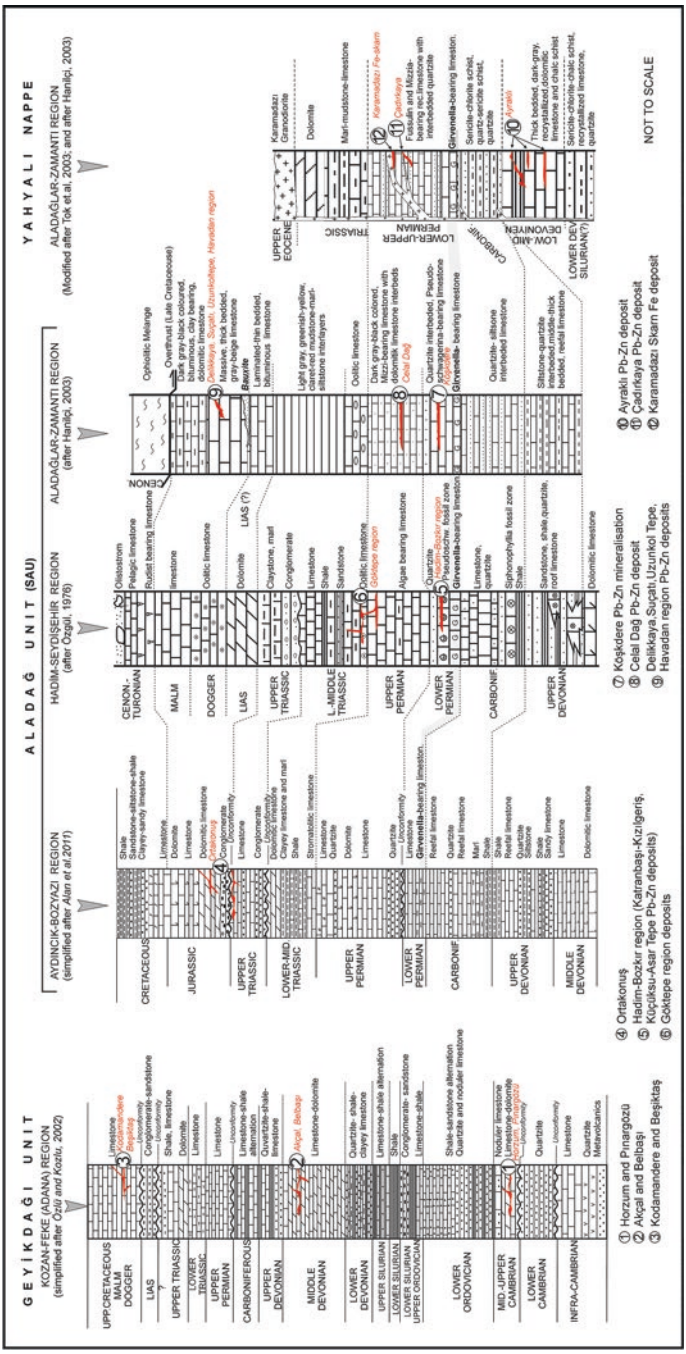

Fig. 10.3 Lithostratigraphic columns of the carbonate-hosted Pb-Zn deposits in the Geyikdağı, Aladağ and Yahyalı Units in the Tauride, Turkey

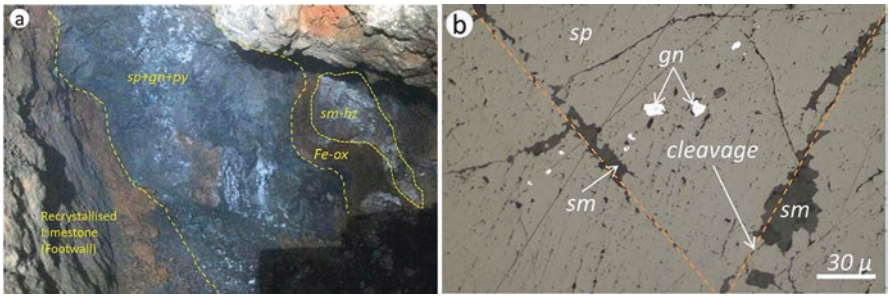

Fig. 10.4 (**a**) Sphalerite-rich primary sulphide ore lens that includes sphalerite (sp), galena (gn) and pyrite (py) and (**b**) the development of smithsonite (sm) through cleavages and cracks of sphalerite (sp)

10.3 Mississippi Valley Type (MVT) Pb-Zn Deposits

10.3.1 Hadim-Bozkır (Konya) Region Pb-Zn Province

The carbonate-hosted Pb-Zn deposits in the Hadim-Bozkır (Konya) province are located 20 km west of the Hadim settlement (Fig. 10.5). The ores are concentrated in the Kızılgeriş-Katranbaşı and Küçüksu localities (Table 10.1) in that province. Between 1965 and 1990, approximately 0.1 Mt with an average of 35% Zn+Pb (Zn>%25) grade oxide-carbonate ore were mined. There are no current reserve data for these deposits.

The Pb-Zn deposits in the province that occur in the *Pseudoschwagerina*-bearing Lower Permian limestones (Fig. 10.6a), which overlie the *Girvanella*-bearing limestones and belong to the Siyah Aladağ Unit, are the host units of the deposits (Fig. 11.3). The Katranbaşı–Kızılgeriş deposit strikes N40°-50°W and dips 40–45°NE; the Küçüksu deposit strikes N30°–40°W and dips 30–35°SE.

The ore bodies are of the strata-bound type and generally occur as concordant lenses to the strike of the host carbonates (Fig. 10.6b). The ore thicknesses vary from 0.5 to 3 m, and the ore zone extends at least 600 m in length in the Kızılgeriş-Katranbaşı, and 200 m in length in the Küçüksu (Fig. 10.7).

The ores are highly porous, soft, and brownish due to the surface oxidation of the iron sulphides. The ore bodies were oxidized into carbonate Pb–Zn minerals, mainly smithsonite and cerussite, but some sulphidic ore minerals, such as galena and sphalerite, were also preserved at several localities. N–S trending faults cut the Katranbaşı ore body, and the N35°E trending fractures are filled with the carbonate ore. Dolomitization is a widespread alteration type in the limestones, and such zones contain disseminated sulphides such as pyrite, sphalerite, and galena (Hanilçi and Öztürk 2011).

Chemical analyses undertaken in the region (Alp 1976) indicate that the Pb-values (2.75%) of the Katranbaşı deposit are higher than those of the other deposits in the region (average 0.3%, $n = 3$). Although the Zn-content of the Kücüksu deposit is

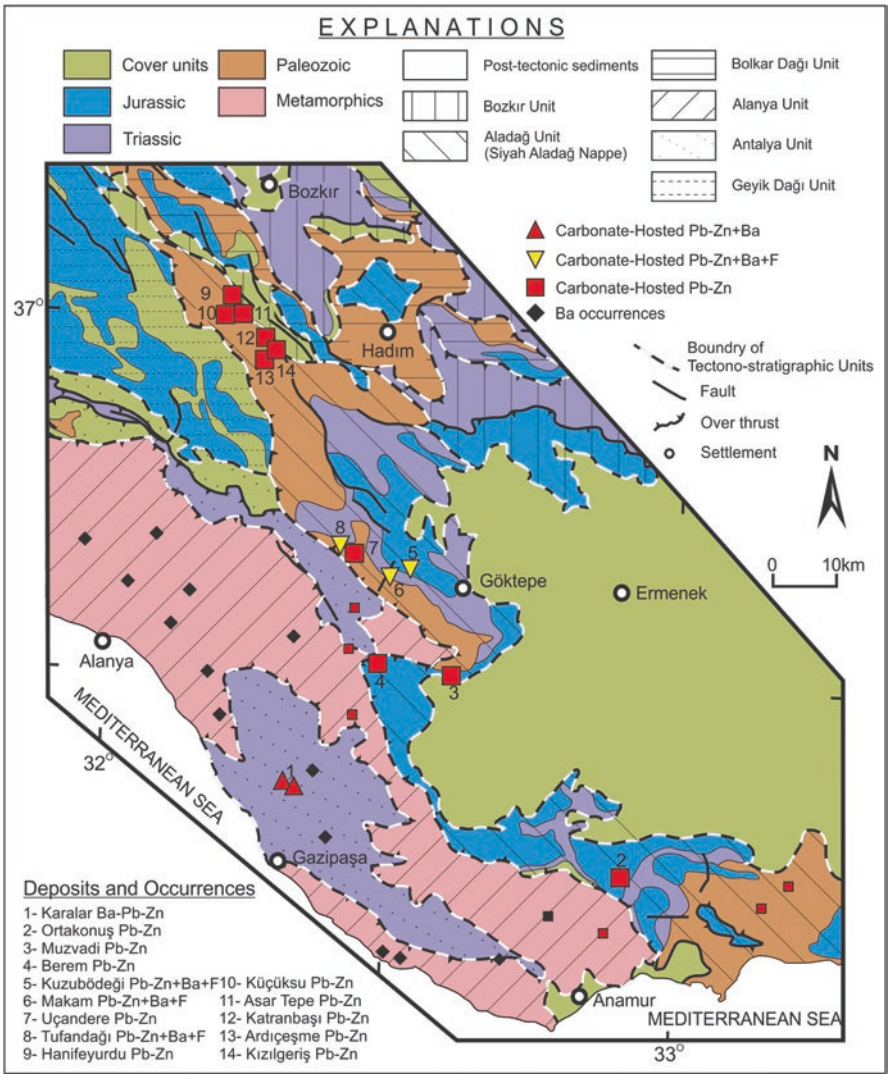

Fig. 10.5 Map showing the geology and locations of the carbonate-hosted Pb-Zn±Ba±F deposits and occurrences in the Hadim-Bozkır, Göktepe, Gazipaşa and Anamur areas (The geology is simplified from the MTA 1/100000 map, the tectono-stratigraphic boundary is after from Özlü 1976, and the locations of the Göktepe region Pb-Zn mineralizations are after from Kuşçu (1985))

36%, the other deposits have 27% on average ($n = 13$). Furthermore, Ag and Cu are scarce in the Kızılgeriş and Küçüksu–Asar Tepe deposits (average 0.002%). Additionally, the deposits in the region have similar Cd values (average 0.14%, $n = 18$), according to available data (Alp 1976). The $\delta^{34}S_{CDT}$ values of the Hadim-Bozkır deposits vary from 3.43‰ to 13.70‰ for galena with an average of 8.97‰,

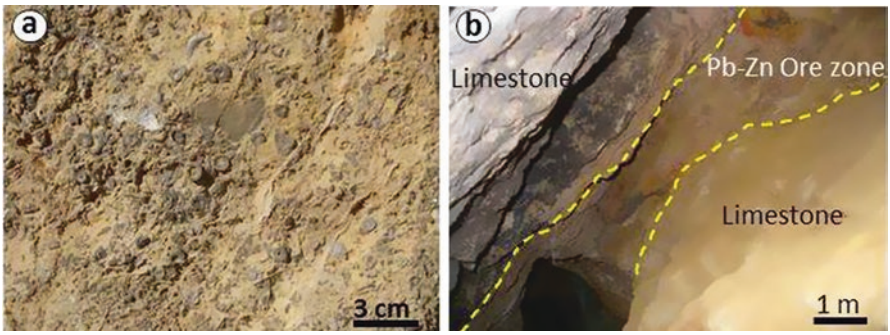

Fig. 10.6 (**a**) The *Pseudoschwagerina*-rich Lower Permian limestone that is the host-rock of the strata-bound type Pb-Zn mineralization in the Hadim-Bozkur region, and (**b**) the strata-bound type ore zone in the Katranbaşı deposit

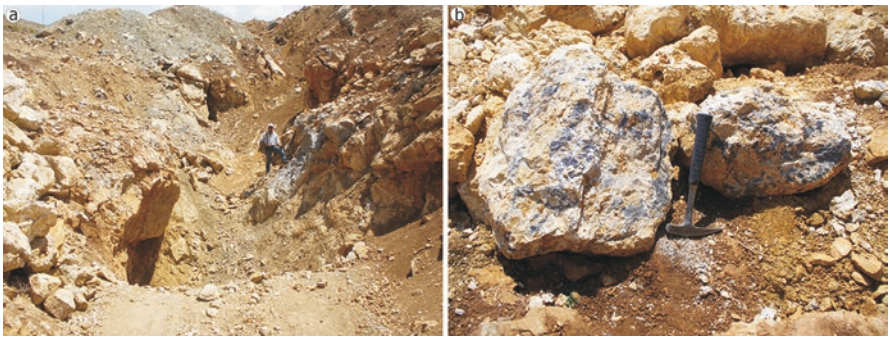

Fig. 10.7 (**a**) Makam (MK) Pb-Zn-F occurence associated with the N60E trending fault zone within the Lower-Middle Triassic oolitic-stromatolitic limestones in southern part of Saçak Tepe (Göktepe), (**b**) galena (dark grey)-rich Pb-Zn-F ore

which indicates a crustal source of the sulphur. Hanilçi and Öztürk (2011) suggested that the Pb-Zn deposits in the Hadim-Bozkır region formed as MVT Pb-Zn mineralization due to the strata-bound character of the ore, simple ore paragenesis, stable sulphur isotope composition, and alteration character.

10.3.2 Göktepe (Karaman) Pb-Zn±F±Ba Mineralizations

The carbonate-hosted Pb-Zn±F±Ba occurrences in the Göktepe (formerly known as Fariske) province is located approximately 10 km **(i)** northeast and **(ii)** west of the Göktepe settlement (Fig. 10.5). The Pb-Zn±F±Ba occurrences in northeast Göktepe are located along a NE-SW trend as the Kuzubögedi (KB), Makam (MK), Düden (DD), Üçtepeler (UT), Pınarüstü (PU), Sarıpınar (SP), Haydar (HY), Uçandere

(UD) and Tufandağ (TD) mineralizations (Fig. 11.5, Kuşçu 1985). The Sarıpınar (SP) mineralization has been mined in the past, but presently there are no data on the grade and amount of production.

The Göktepe province deposits occur in the *Mizzia*-bearing Upper Permian limestone (the PU and SP deposits), *Mizzia*-bearing Upper Permian limestone and Lower-Middle Triassic oolitic- stromatolitic limestone (the TD, UT and DD deposits) in the Lower-Middle Triassic oolitic- stromatolitic limestone (the UD, HY, MK and KB deposits) of the Siyah Aladağ Unit (Fig. 11.3, Kuşçu 1985). The mineralizations are strata-bound and vein-type (Fig. 11.7), and are 10 to 300-m in length with 0.3 to 1-m thickness. The ore zone extends from 2 to 25 m and is clearly identified by alteration represented by silicification and dolomitization. The ore assemblage includes galena, sphalerite, fluorite, calcite, and rare barite. Smithsonite, cerussite and Fe-(hydr)oxide are also present.

The Pb-Zn±F±Ba occurrences in the western part of the Göktepe are Muzvadi (MZ) and Berem (BZ), which are located 3 km southeast and 9 km southwest of Muzvadi village, respectively (Fig. 11.5). Both the Muzvadi and the Berem Pb-Zn occurrences are observed along a NE-SW trend.

The Muzvadi mineralization occurs within the Jurassic dolomitic limestones as veins of 1–20 cm thickness and breccias due to tectonism (Kuşçu 1985). The Berem mineralization occurs both within the Jurassic dolomitic limestones as vein-fill, breccia-fill, and as stratabound transitional between the Jurassic dolomitic limestone and the Lower-Middle Triassic oolitic-stromatolitic limestone (Kuşçu 1985). The Muzvadi and Berem ores include sphalerite, galena, barite and dolomite. Neither mineralizations does include fluorite in northeast of the Göktepe (Kuşçu 1985).

The Göktepe Pb-Zn±F±Ba deposits are hosted in carbonate rocks of the Siyah Aladağ Nappe Unit. The mineralization is strata-bound, epigenetic, with veins and breccias, with ore and gangue minerals that include sphalerite, galena, pyrite, marcasite, fluorite, dolomite, calcite, quartz and rare barite. The wall-rocks show dolomitic alteration. No magmatic rocks are present in and around the mineralization area. All of these features are similar to those of the MVT deposits, and indicate that the Göktepe province carbonate-hosted Pb-Zn±F±Ba mineralization was generated via basinal water (Kuşçu 1985).

10.3.3 Gazipaşa (Antalya) Ba-Pb-Zn Province

Widespread Ba-Pb-Zn mineralizations in Gazipaşa province occurred within the Permian limestones (Bıçkıcı Formation), which show advanced diagenetic features belonging to the Antalya Unit (Bozkaya and Yalçın 2005). The important mineralization areas are Karalar, Burhan Mahallesi, Aydap and Yuları (e.g., Petrascheck 1967; Sadıklar 1978; Sadıklar and Amstutz 1981; Ayhan 1982; Gökçe and Bozkaya 2003).

The Karalar Ba-Pb-Zn deposits (Boyalık, Büyük Ocak and Sulu Ocak) occur as veins within cracks and fractures of Permian limestones (Gökçe and Bozkaya 2003).

The strikes of the veins changes between N70W and N85W, dipping from 35 to 89° to the SE and NE. The thicknesses of the veins are between 0.3 and 6 m. In places, the mineralizations in the Karalar have developed along the thrust contact between Permian limestone and Triassic rocks as breccia-fill and stockwork veins (Gökçe and Bozkaya 2003). This feature indicates that the mineralization should have developed syn- or post-tectonically. The ore is barite-rich and includes 15% galena in addition to sphalerite, pyrite, rare chalcopyrite, limonite, quartz and calcite in the association (Gökçe and Bozkaya 2003). The alteration developed in the ore zone consists of silicification and ankeritization (Petrascheck 1967).

A sedimentary syngenetic (Sadıklar and Amstutz 1981; Ayhan 1982) and one epigenetic (Gökçe and Bozkaya 2003) formation model has been proposed for the Karalar Ba-Pb-Zn deposits.

The Burhan Mahallesi Ba-Pb-Zn deposits occur along the NW-SE trending zone with a length of 1 km as intermittent lenses. The mineralization is developed within the Permian recrystallized dolomitic limestone and locally in calcschists as veins whose thicknesses change from 0.3 to 2.5 m (Ayhan 1982). Barite and galena are the dominant minerals, and are accompanied by tennantite, tetrahedrite, pyrite, cerussite, covelline and idaite (Ayhan 1982).

The Aydap and Yuları Pb-Zn deposits were mined occasionally after the *First World War* but there are no data regarding the mining and grades of the ore (Ayhan 1981). The mineralization is hosted in recrystallized limestone as strata-bound, fracture-fill, karst-infill and breccias (Ayhan 1981). The ore style is dominantly vein-type along NW-SE trending fractures. The ore minerals include galena, sphalerite, tennantite, tetrahedrite, pyrite and chalcopyrite as primary minerals and covellite, chalcocite, smithsonite, cerussite, anglesite, limonite, malachite-azurite and Fe-hydr(oxide) as secondary minerals (Ayhan 1981).

The different genetic models suggested for the Gazipaşa province carbonate-hosted Ba-Pb-Zn deposits; are epigenetic (Petrascheck 1967), syn-sedimentary (Striebel 1965; Sadıklar and Amstutz 1981), epigenetic via remobilization from the primary sedimentary deposits (Ayhan 1982), and vein-type formation (Gökçe and Bozkaya 2003). The ore styles include strata-bound type, vein and karst-infill type clearly confirming the epigenetic character. The formation temperature of the barite, quartz and sphalerite range from 70 to 160 °C for the Karalar deposits (Gökçe and Bozkaya 2003, 2008). These show that the characteristics of the fluids in Karalar deposits were; (i) they contained NaCl, $CaCl_2$, and $MgCl_2$, (ii) the salinity was 13.5 wt% NaCl eq. for barite and 7 wt% NaCl eq. for quartz and sphalerites and (iii) $\delta^{18}O$ and δD isotopes support a meteoric origin of the fluids. The above authors suggested that the deposits formed by circulation of deep meteoric water that dissolved the Pb and Zn metals from the basement rocks, and Ba from the marine sediments. The isotope data indicate that the Pb in galena was derived from an upper crustal source, and sulphur from the crustal source for galena and barite from the Late Triassic to Recent sulphate-rich (evaporitic) reservoir (Gökçe and Bozkaya 2007).

10.3.4 Ortakonuş (Anamur) Pb-Zn Deposit

The deposit is located 18 km northeast of the Anamur settlement (Fig. 10.5, Table 10.1). From the mid-1800s to *World War II* approximately 100,000 tonnes of ore have been mined and exported (Demir 1998). The deposit reopened for mining between 1985 and 1989, and approximately 10,000 tonnes of ore with 29% Zn and 6% Pb grade ore have been produced.

The Ortakonuş Pb-Zn deposit occurs within the Upper Triassic limestone of the Aladağ Unit as strata-bound lenses and small veins (Gümüş 1989). The ore zone intermittently continues as lenses in an ENE-WSW direction for approximately 1.5 km and is parallel to the fold axes in the region (Gümüş 1989). The ore contains sulphide minerals including galena, sphalerite, pyrite and marcasite, and hematite, anglesite, smithsonite, plumbojarosite as secondary minerals. Gangue minerals are barite, dolomite and calcite (Gümüş 1989). It has been suggested that the ore was generated under the low temperature conditions as suggested by the presence of framboidal pyrite and alternating bands of fine-grained sphalerite and wurtzite (Blümel 1964).

10.3.5 Aladağlar-Zamantı Pb-Zn Province

The Aladağlar-Zamantı Pb-Zn province is located in the Eastern Tauride Mountains on the border of Kayseri and Niğde city (Figs. 10.1 and 10.8). Economically, the most important carbonate-hosted Pb-Zn deposits in Turkey are concentrated in the Aladağlar Mountains and on the eastern and western sides of the Zamantı River (Fig. 10.8) hence the name of "Aladağlar-Zamantı Province" (e.g., Metag and Stolberg 1971; Ayhan et al. 1984; Çevrim 1984; Hanilçi and Öztürk 2011). Mining activities extend back to the Bronze Age by the Hittites (e.g., Ayhan et al. 1984; Yıldırım 2008) followed by the Roman Empire, Seljuks, and Ottomans (e.g., Imreh 1965; Ayhan and Lengeranlı 1986; Yıldırım 2008; Bahar and Koçak 2010). There are more than 50 known Pb-Zn occurrences in the province, but among these only 37 were occasionally mined until 1998 (Demir 1998). At present, the Delikkaya, Suçatı, Göynük and Ayvan deposits and a few deposits in the Havadan region are in operation. It is estimated that the total production of carbonate zinc ore was approximately 5.7 Mt in Aladağ-Zamantı province until 2015 (Table 10.1).

The carbonate-hosted Pb-Zn deposits in the Aladağ-Zamantı province are located in both the Yahyalı Nappe and the Aladağ (referred to as the Siyah Aladağ Nappe in the Yahyalı region) Units (e.g., Hanilçi and Öztürk 2003, 2005, 2011, Figs. 10.8 and 10.3). Both tectono-stratigraphic units have similar lithological features (Fig. 10.3). The Yahyalı Nappe has undergone low-grade greenschist facies metamorphism, which is the equivalent of the unmetamorphosed Siyah Aladağ Nappe (Tok et al. 2004). Both units include *Girvanella*-bearing limestone as a marker horizon that represents the Carboniferous-Lower Permian transition in the Taurides (e.g., Özgül 1976; Okuyucu 2002; Tok et al. 2004, Fig. 10.3).

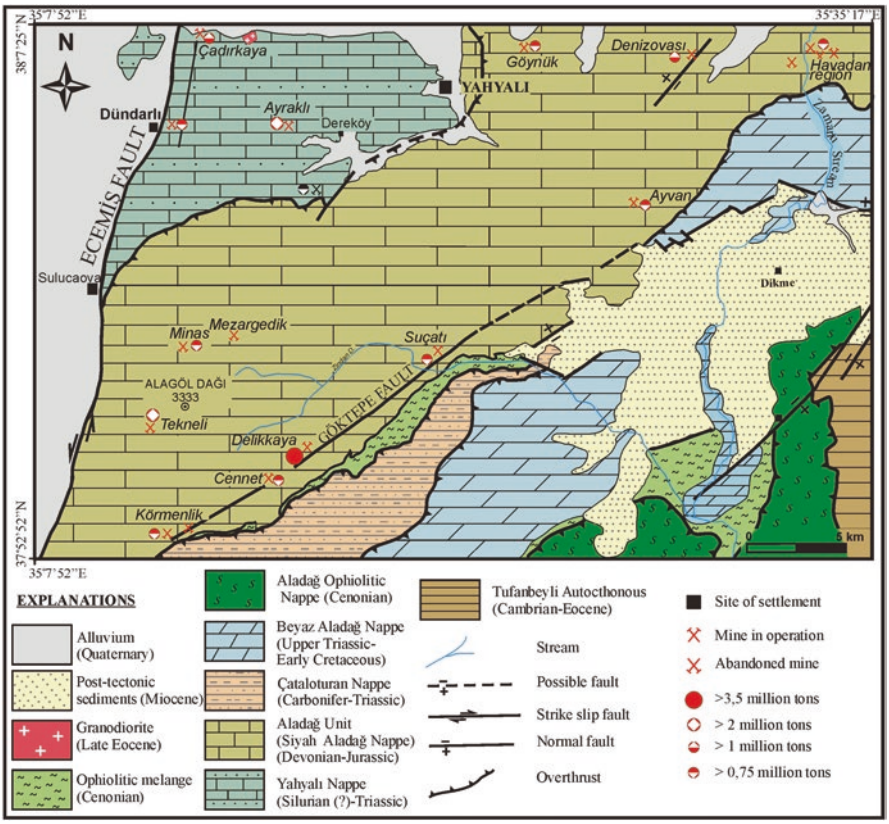

Fig. 10.8 Tectono-stratigraphic units of the Aladağlar-Zamantı region (simplified after Tekeli et al. (1983)) and the locations of the carbonate-hosted Pb-Zn deposits (Modified after Hanilçi and Öztürk 2011)

10.3.5.1 The Delikkaya Pb-Zn Deposit

The Delikkaya Pb-Zn deposit is located 36 km SW of Yahyalı (Fig. 10.8, Table 10.1). The deposit is the largest in the Aladağlar-Zamantı province, and mining was carried out since Roman times (e.g., Ayhan et al. 1984; Hanilçi 2003; Yıldırım 2008). It is estimated that approximately 2.7 Mt of ore with an average of 40% Zn+Pb (Zn>25%) grade has been mined up to 2015 in that deposit.

The deposit is hosted the thick bedded, massive Middle Jurassic limestone and dolomitic limestone of the Siyah Aladağ Nappe Unit as vein and karst-infill types controlled by a N55-65E striking, SE dipping fault zone. The known dimensions of the deposit are approximately 500 m long and 130 m deep. Mining began as an open pit on the surface (Fig. 10.9a) and then continued as underground mining to avoid a costly increase in the stripping ratio. The ore body has a vein geometry and is dis-

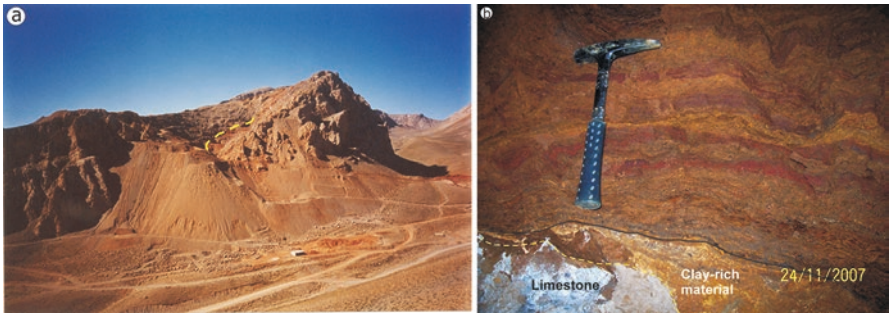

Fig. 10.9 General view of (**a**) a vein type ore at an open-pit and (**b**) a pocket type ore occurring as karst-fill, which shows the intra-karstic sedimentation of an Fe-Pb-Zn-oxide-carbonate in the Delikkaya Pb-Zn deposit

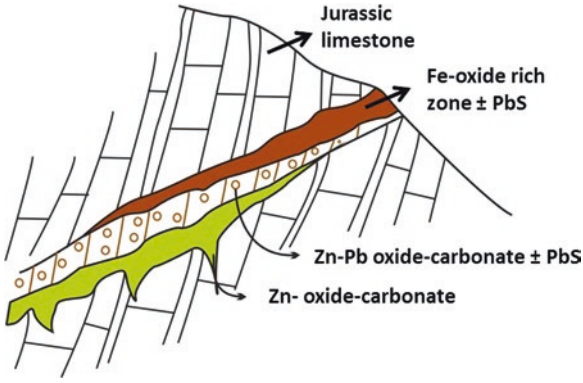

Fig. 10.10 Schematic section showing ore zonation related to supergene oxidation at the Delikkaya deposit

cordant to the country rocks. However, there are some karstic cavity-filling deposits, which show lenticular shapes with dimensions of approximately 30 × 50 × 5 m (Fig. 10.9b). Dolomitization is the widespread alteration; dolomite has been replaced by sphalerite and this can be observed where the primary ore is preserved.

The Delikkaya deposit represents a typical example of supergene enrichment and karstification processes including well-developed intra-karstic sedimentation (Fig. 10.9b). The ore body shows a zoned nature with iron oxides at the top, Zn-Pb-oxide-carbonate and lead sulphides in the middle, and zinc oxide-carbonates at the bottom (Fig. 10.10).

The mineralogical association in the Delikkaya deposit consists of sphalerite, galena, pyrite, marcasite and rare chalcopyrite as primary sulphides; anglesite, cerussite, beudantite, smithsonite, hydrozincite, zincite, siderite, hematite, and limonite as secondary. Quartz, calcite and dolomite are the gangue minerals (Hanilçi and Öztürk 2011).

10.3.5.2 The Tekneli Pb-Zn Deposit

The deposit is located 15 km south of the Dündarlı (Niğde) settlement and 6 km northwest of the Delikkaya deposit (Fig. 10.8, Table 10.1). Mining for lead began during Roman times (Demir 1998), and continued during the Ottoman period until the end of the 1990s. Approximately 0.4 Mt of ore with 21% Zn and 4% Pb was mined between 1973 and 1998 (Demir 1998).

The deposit occurs within the thick bedded *Mizzia*-bearing limestone of Permian age, which belongs to the to Sihay Aladağ Nappe Unit (Fig. 10.3). There are three parallel veins (I, II and III) oriented along a north-south trending anticline axis (Eren et al. 1993; Demir 1998). Those veins are located in both limbs of the anticline. The longest vein (Vein-I) is 2.2 km in length, from 1 to 8 m thick, striking between N20W and N20E and dipping 60–80°NE and SE (Demir 1998). Vein-II is located to the west of the Vein-I, is 240 m in length and varies from 4 to 15 m in thickness. The strike and dip of this vein are N10-30W, and 70–90°NE, respectively (Demir 1998). Vein-III continues intermittently for 450 m in a N-S direction. The ore zone is 6 m in thickness and dips toward the west at a 20–30° angle (Demir 1998).

The ore veins were mostly oxidised in-situ and changed to zinc-lead oxide-carbonate minerals. Karst-infill type ore is a limited development in this deposit due to the weak porosity of the host limestones (Demir 1998). The primary ore consists of sphalerite, pyrite/marcasite, galena, very rare arsenopyrite, chalcopyrite and freibergite as and of smithsonite, hydrozincite, hemimorphite, cerussite and limonite as supergene minerals (Çopuroğlu 1996; Demir 1998).

10.3.5.3 The Suçatı Pb-Zn Deposit

The Suçatı deposit is located 23 km SW of Yahyalı (Fig. 10.8, Table 10.1). Mining operations began in 1957 and have intermittently continued up to the present day; approximately 0.1 Mt of ore have been mined.

The deposit occurs within the thick-bedded and fractured, massive Middle Jurassic limestone of the Siyah Aladağ Nappe Unit (Figs. 10.8 and 10.3). The ore mainly occurs within two faults striking: N15–20°E and dipping 80°SE. Karstic cavities and associated fractures are N15–30°W oriented, dipping 50–70°SW. The cross-cutting main tectonic features caused the karstic cavities to develop horizontally; thus, the ore bodies are pipe-shaped with an average width of 5 m and depth of 25 m. There are also some vein type ore bodies (Fig. 10.11a), which vary in widths from centimetres to metres, average 40 m in length and are related to the fractures. In places the primary sulphide ore consisting of sphalerite and galena has been preserved from oxidation.

The Suçatı deposit displays similarities with the Ayraklı and Delikkaya deposits in terms of their intra-karstic features (Fig 10.11b), but there is an obvious difference: it contains well-rounded quartz–barite-bearing galena pebbles up to 10 cm in diameter (Fig. 10.11c). The pebbles are exogenic to the system because quartz and barite do not occur in the ore body. Therefore, the pebbles were probably trans-

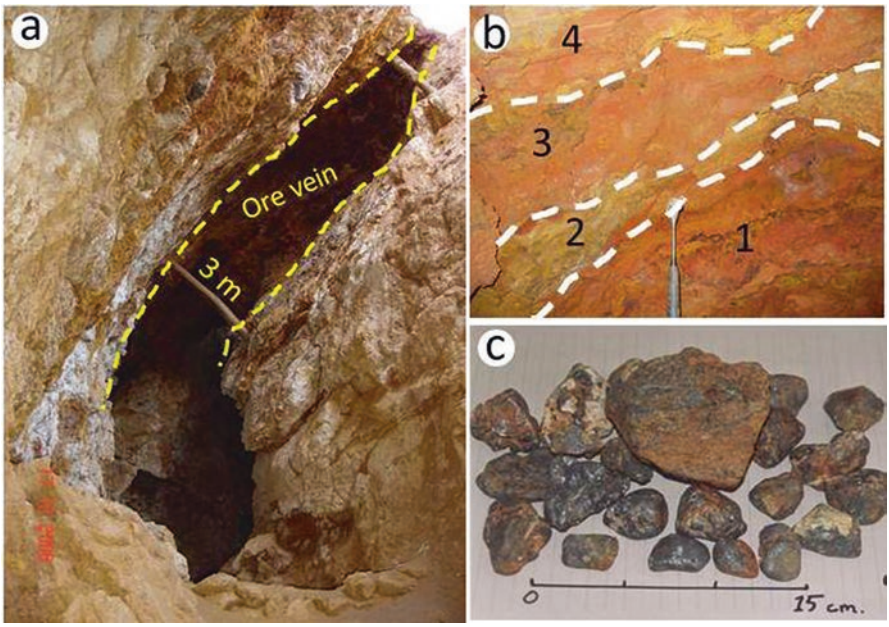

Fig. 10.11 (**a**) Outcrop of the vein-type ore zone that has a thickness of 2 m and is totally oxidised in the Suçatı deposit, (**b**) Intra-karstic sedimentation feature showing zonation from the bottom to top; (1) limonite-clay, (2) cerussite, galena-limonite-zinc oxide, (3) clay-limonite-galena and (4) cerussite-galena-limonite-zinc oxide. (**c**) Well-rounded galena pebbles with barite (white) within the karst-fill ore pockets

ported into the karstic holes as a clastic material and rounded by transportation and/or water energy.

10.3.5.4 The Ayraklı Pb-Zn Deposit

The Ayraklı Pb-Zn deposit is located 17 km southwest of the Yahyalı settlement (Fig. 10.8). From 1962 to 2015, approximately 0.8 Mt of carbonate ore with 12–35% Zn and 10–13% Pb was mined. At present, the annual production is approximately 25,000 tonnes of carbonate ore with an average of 12% Zn and 13% Pb.

The Ayraklı Pb–Zn deposit occurs in the recrystallized Devonian limestone of the Yahyalı Nappe Unit as stratabound and karstic-type (Figs. 10.3 and 10.8). The ore formed both in Devonian thickly bedded, crystalline carbonates and at the contact between crystalline carbonates with the calcschists. Two types of ores have been described in the deposit: the strata-bound and the karstic. The strata-bound ore occurs at two different levels in the Middle Devonian sequence. The first level represents the primary ore of the deposit. This level is lens-shaped and mainly includes sphalerite, galena and framboidal pyrite/marcasite within the calcschists and at the calcschists –bituminous schist black crystalline limestone contacts

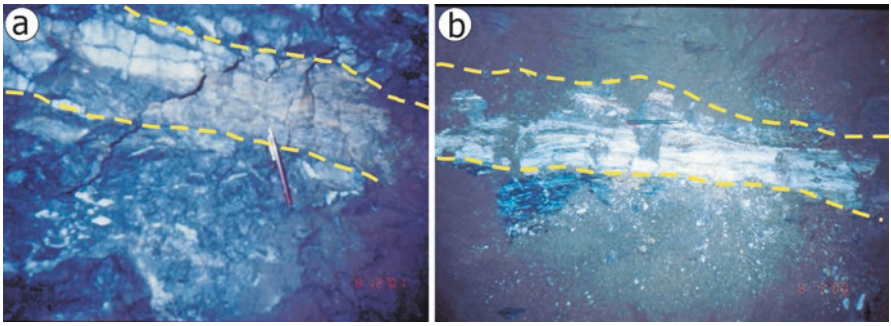

Fig. 10.12 (**a**) Strata-bound type, primary ore level with sphalerite, galena and framboidal pyrite and (**b**) an in-situ oxidized strata-bound ore level with white hydrozincite and smithsonite in the Ayraklı deposit

(Fig. 10.12a). The second level comprises a white, dense, 25 to 60-cm in thick, in-situ oxidized-carbonatized (mainly smithsonite and hydrozincite) ore lenses that are concordant to the bedding of the recrystallized carbonates (Fig. 10.12b).

Mining is carried out in karstic-type ore zones. The karst-infill and replacement type secondary ores formed from the primary sulphidic ore reveal lense and vein shapes. The ore thickness changes from 1–5 to 10 m for the vein and lense, respectively. Intra-karstic sedimentation features are well developed in the lense-shaped ores. This type of ore shows very good alternations of fine grained galena coated by cerrusite (grey levels), with limonite and clays (Fig. 10.13a). The vein type replacement ore is characterized by high grade smithsonite with skeletal-porous (Fig. 10.13b) and botryoidal (Fig. 10.13c) textures that formed through to the replacement processes.

10.3.5.5 The Göynük Pb-Zn Deposit

The Göynük deposit is located 7 km NE of Yahyalı (Fig. 10.8, Table 10.1). Mining dates back to Roman times (Imreh 1965), and, according to the limited data, approximately 0.3 Mt with an average of 20% Zn and 10% Pb grade oxide-carbonite ore had been mined up to 2014.

The deposit occurs between and within the Late Permian *Mizzia*-bearing limestone and Early-Middle Triassic limestone that belong to the Sihay Aladağ Nappe Unit (Fig. 10.3). The ore is trough-shaped, in a fault zone, which is nearly parallel to the bedding planes as vein-type. The direction of the trough-shaped ore zone is N60°E dipping 15°–35°NW. The primary ore was completely oxidised and changed to Zn-Pb oxide-carbonates *in-situ* and/or re-accumulated into karstic cavities. The length of the ore zone is approximately 150 m, and the thickness ranges from 1 to 5 m. The bottom of the vein-type ore zone is sharp, and both the vein and karst-infill type ores begin with clay-rich materials at the bottom. The karst-infill type ore mostly shows intra-karstic sedimentation features with zonation and lamination of the zinc and lead-rich levels (Fig. 10.14).

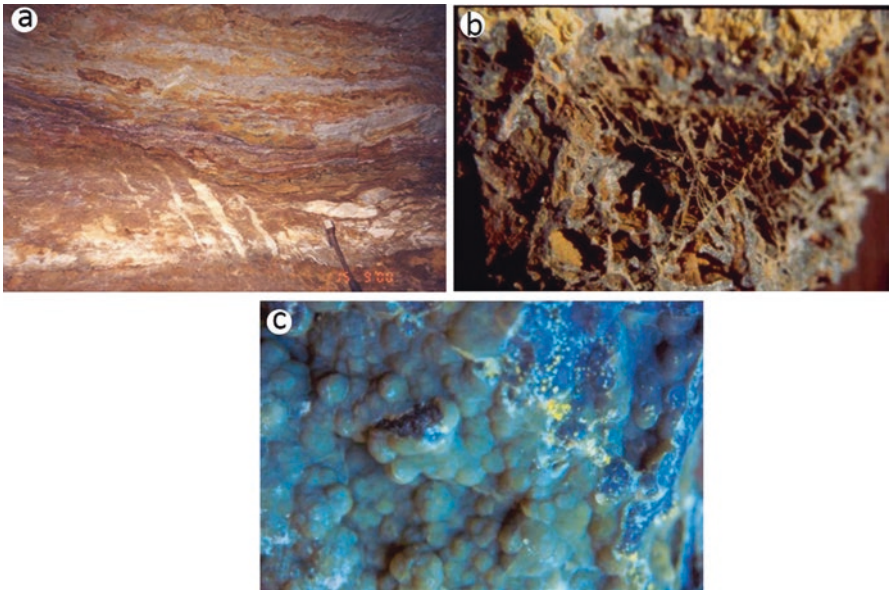

Fig. 10.13 Ore textures in karstic-type ores in the Ayraklı Pb-Zn deposit; (**a**) Laminated-banded ore texture developed by the intra-karstic sedimentation of fine-grained galena, limonite and clays, (**b**) skeletal-porous, and (**c**) botryoidal textured ore developed by replacement processes

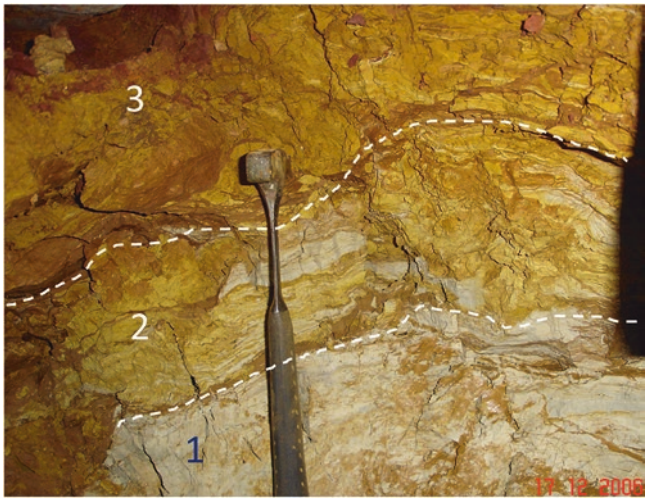

Fig. 10.14 An intra-karstic sedimentation feature is well developed in the karst-fill type ore pockets in the Göynük deposit. The bottom of the karst-fill ore begins with clay-rich mud and then, toward the top, (1) fine-grained lead-oxide (white-grey), mostly cerussite, (2) lamination of cerussite-zinc oxide zone and (3) a limonite-cerussite-zinc oxide zone

The ore minerals are mainly smithsonite, cerussite, anglesite, galena, goethite, lepidocrocite. Preserved sphalerite and pyrite (Koptagel et al. 1998) have been found within the oxidized ore zone. Koptagel et al. (2005) suggested that the ore was syngenetic and was deposited by chemical precipitation from seawater saturated in metal ions during the Maestrichtian. However, the ore zone is strata-bound, parallel to the host limestone beds, but in some places also cuts the bedding planes, which reflects an epigenetic origin.

10.3.5.6 The Denizovası Pb-Zn Deposits

The carbonate-hosted Pb-Zn deposits in the Denizovası lie 20 km east of the Yahyalı (Kayseri) settlement (Fig. 10.8, Table 10.1). The deposits occur in two different locations, Uzunkol Tepe and Celal Dağ (Table 10.1) within the Siyah Aladağ Nappe Unit (Fig. 10.3). To the present, approximately 1 Mt of Pb-Zn ore has been mined from these deposits. Several artefacts such as ancient galleries, wooden shovels and slags indicate that mining goes back possibly to Roman times (Hanilçi and Öztürk 2011).

The Uzunkol Tepe deposit occurs within the dolomitized Jurassic limestones, which are light grey thick-bedded, and highly fractured (Fig. 10.3). The ore is controlled by a N45–60E striking 75°NW dipping fault zone for 750 m. Post-mineralization faults cross-cut and offset the ore body (Hanilçi 2003). The ore body is mainly of vein type; however, karstic cavities associated with fault zones are generally of lense-shaped. The thicknesses of the ore veins vary from 1 to 5 m and are on average 2 m.

The Celal Dağ deposit occurs within the *Mizzia*-bearing limestone of the Upper Permian (Fig. 10.3). The ore is mainly strata-bound and is parallel to the N45E and 45°NW striking host limestones (Fig. 10.15a), and also occurs along fault zones as veins (Fig. 10.15b). The strata-bound ore zone is oxidized in-situ and is completely changed to a non-sulphide zinc ore with a high iron-oxide content. The thicknesses of the in-situ oxidised strata-bound and vein-type ore zones range from 0.3 to 3 m and 1.5 and 5 m, respectively.

The Celal Dağ deposit also includes a preserved primary ore zone located approximately 700 m NW of the oxidised ore zone. The primary ore occurs within the *Mizzia*-bearing limestones as a strata-bound lens that is 15–30 cm thick, 1.5 to 2 m-long and strikes N25–30E. The ore zone includes primary galena and sphalerite (Hanilçi and Öztürk 2011).

10.3.5.7 The Havadan Pb-Zn Deposits

The Havadan region Pb-Zn deposits are located approximately 15 km east of Yahyalı and are near the Zamantı River (Fig. 10.8). There are many Pb-Zn deposit and showings in the Havadan region and the history of mining reaches back to Roman times. The most important deposits are the Çakılpınar, Süleyman Fakılı, Köprüsütü,

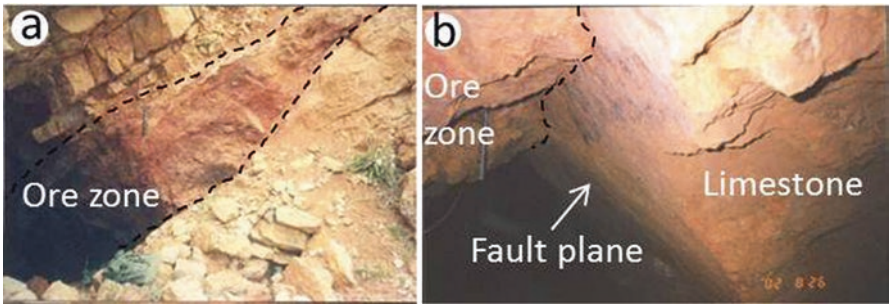

Fig. 10.15 The Celal Dağ deposit occurs within the Mizzia-bearing Upper Permian limestone as: (**a**) a strata-bound type oxidized in-situ and changed to iron-rich zinc-oxide-carbonate, and (**b**) a vein-type ore controlled by faults (Hanilçi 2003)

Tekke, Karnıyarık, Kantarbeli, Köyüstü (Aksu), Ufuk and Demircidere (Table 10.1). According to Demir (1998) approximately 0.23 Mt of oxide-carbonate ore with average grades of 22% Zn and 4% Pb were mined from the Havadan deposits between 1973 and 1998. After that, between 2006 and 2015, 0.18 Mt of ore with average grades of 24% Zn and 17% Pb have been mined.

The Havadan deposits occur within the thick bedded, massive Jurassic limestone of the Siyah Aladağ Nappe Unit (Aladağ Unit), at a similar stratigraphic level as those of the Suçatı, Delikkaya and Uzunkol Tepe ores (Fig. 10.3). The deposits in this region occur in fault zones as vein-types (Fig. 10.16a) and as a karst-infill types developed within the karstic holes near the veins. Most of the vein-type deposits are oriented along N50-80E (e.g., Köyüstü (Aksu), Kantarbeli, Çakılpınar, Köprüüstü and Tekke deposits), but some of the veins are oriented along N40-55W (Türbeüstü and Karnıyarık deposits). The lengths and thicknesses of the ore veins range from 50 to 300 m and from 1 to 5 m, respectively. In the vein-type and karst-infill type deposits, the basal parts of the ore consist clay-rich materials (Fig. 10.16b).

The ore is totally oxidized to zinc and lead oxide-carbonate minerals. The ore minerals mainly include smithsonite, cerussite-anglesite, goethite, lepidocrocite and rare galena coated by cerussite-angesite and sphalerite (Koptagel et al. 1998).

10.3.5.8 The Genetic Models for Aladağlar-Zamantı Pb-Zn Province

There are different genetic models for the carbonate-hosted Pb-Zn deposits in the Aladağlar-Zamantı province that include (i) hydrothermal vein fill associated with magmatic intrusion (Imreh 1965; Petrascheck 1967; Metag and Stolberg 1971; Ayhan 1984; Ayhan and Lengeranlı 1986; Kusçu and Cengiz 2001), (ii) leaching of the metals from the ophiolitic rocks and primary ore-bearing Permian limestones and precipitation in karstic systems (Çevrim 1984) and (iii) a syn-sedimentary origin of the mineralizations associated with rifting in an early stage of the opening of the Neo-Tethyan Ocean (Koptagel et al. 2001). The carbonate-hosted Pb-Zn deposits of

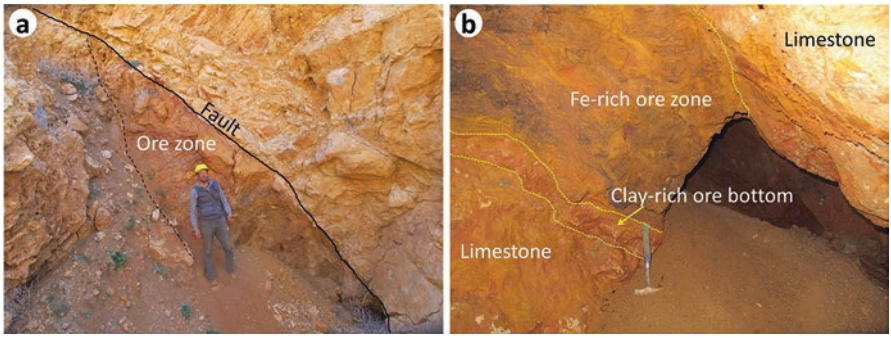

Fig. 10.16 (**a**) The ore zone controlled by the N40W, 50°SW fault zone in the Demircidere mineralization and (**b**) vein-type ore zone beginning with clay-rich materials at the bottom

the Eastern and the Central Taurides (Hanilçi 2003; Hanilçi and Öztürk 2003, 2005, 2008, 2011) reveal similarities to the Mississippi Valley-type (MVT) Pb-Zn deposits, particularly in terms of the host rocks, geological setting and nature of ores. Both the Central and Eastern Taurides consist of the same tectono-stratigraphic units (Siyah Aladağ Nappe Unit) and both have undergone rapid uplifting and karstification processes that destroyed the primary sulphide ores. Fluid inclusions (13–26 wt% NaCl eq. salinity, homogenization temperatures of 112 °C, 174.5 °C and 211 °C for the Celal Dag, Delikkaya and Ayraklı deposits) sulphur isotopes ($\delta^{34}S$ values between −5.4‰ and +13.70‰), radiogenic lead isotope data ($^{206}Pb/^{204}Pb$ between 19.058 and 18.622; $^{207}Pb/^{204}Pb$ between 16.058 and 15.568; and $^{208}Pb/^{204}Pb$ between 39.869 and 38.748, typical of the upper continental crust and orogenic belts) indicate that the carbonate-hosted Pb-Zn deposits in the Aladağlar-Zamantı and Hadim-Bozkır region are similar to MVT Pb–Zn deposits described elsewhere. The primary MVT deposits are associated with the Late Cretaceous–Palaeocene closure of the Tethyan Ocean and formed during the transition from an extensional to a compressional regime. Palaeogene nappes that typically limit the exposure of ore bodies indicate a pre-Palaeocene age of ore formation (Hanilçi and Öztürk 2011).

10.3.5.9 The Tufanbeyli Pb-Zn Province

The geological framework of the Tufanbeyli province is characterised by Palaeozoic and Mesozoic carbonates of the Geyikdağ Unit (Özgül 1976, Figs. 10.3 and 10.17). The carbonate-hosted Pb-Zn deposits and occurrences in the region are hosted in the Middle Devonain dolostone and dolomitic limestones (Figs. 10.3 and 10.17). Although there are no data regarding the mining history, it is estimated that the mining history could reach back to Roman times, like the other deposits in the Taurides, due to the underground galleries and widespread slags. Recently, approximately 0.13 Mt of oxide carbonate ore have been mined in the Akçal-Belbaşı deposits

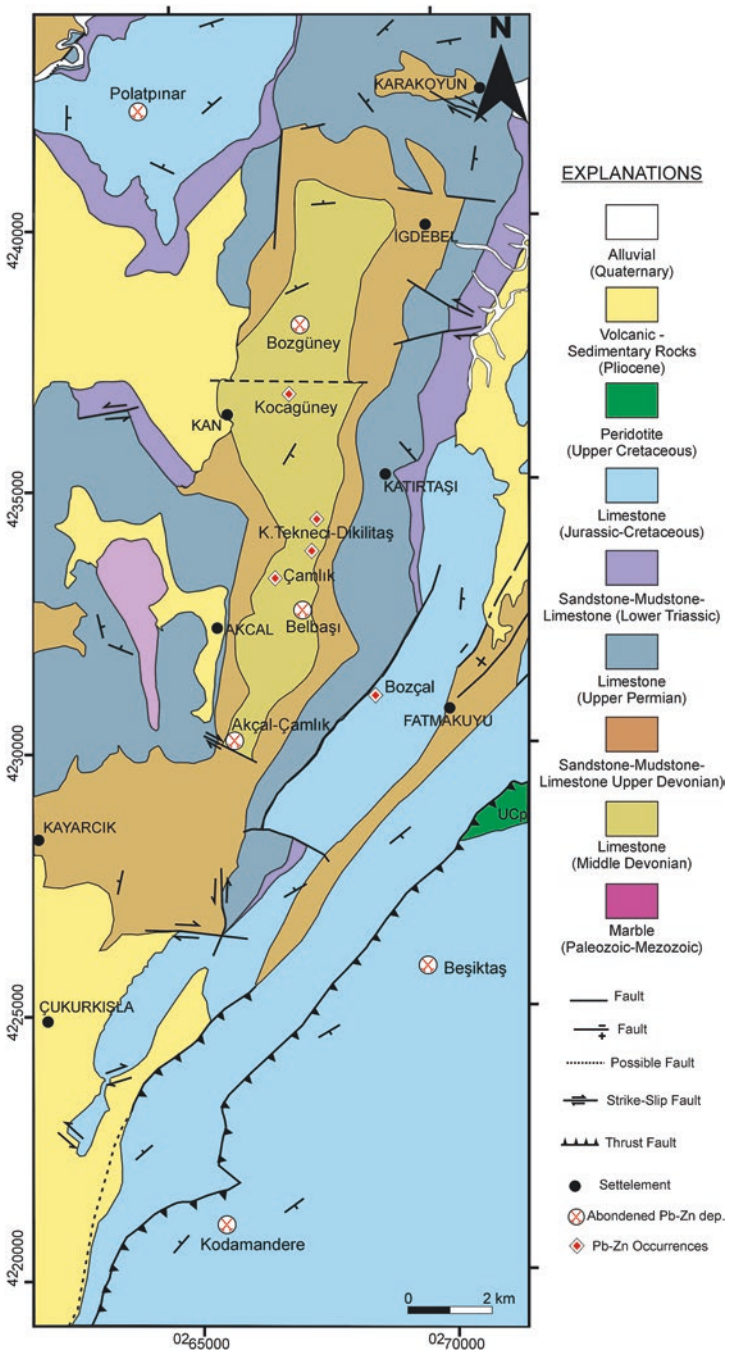

Fig. 10.17 A geological map (simplified after MTA 2014) of the Tufanbeyli region and the locations of the carbonate-hosted Pb-Zn deposits

(0.1 Mt), Kodamandere (19,000 tonnes) and the Beşiktaş deposit (13,000 tonnes) for ÇİNKUR until 1995 (Demir 1998; Mengeloğlu 1996). Apart from the deposits briefly described below, the Tufanbeyli region also includes carbonate-hosted Pb-Zn mineralizations such as the Çamlık, Küçük Teknecik, Dikilitaş, Kocagüneytepe, Bozçaldağı, Bozgüney and Polatpınar Ba-Pb-Zn deposit (Fig. 10.17).

The Akçal and Belbaşı deposits hosted in Middle Devonian dolomites are stratabound type (MTA 1993). The ore thicknesses vary from 0.3 and 2 m. The ore attitude changes due to post-mineralization local faults (Mollamustafaoğlu 1975a). Approximately 0.1 Mt of ore with average grades of 21% Zn and 2% Pb has been produced (Demir 1998). The mineralization is oxidized to oxide- carbonate zinc ore containing mainly smithsonite, hydrozincite, cerussite and Fe(hydr)oxides. There are rare preserved primary ore lenses that include sphalerite, galena and pyrite/marcasite in the oxidized ore body. Barite and calcite are the gangue minerals of the mineralization (Mollamustafaoğlu 1975a).

The Kodamandere deposit occurs in Jurassic-Cretaceous limestone and dolomitic limestones of the Geyikdağı Unit. The ore zone is completely oxidized to smithsonite, cerussite and Fe-(hydr)oxide. Approximately 13,000 tonnes of oxide-carbonate Zn-rich ore with average grades of 21% Zn and 3%Pb had been mined for ÇİNKUR until 1995 (Mollamustafaoğlu 1975a).

The Beşiktaş deposit is within the Jurassic- Cretaceous limestone along a NE-SW directed strike-slip fault zone and in karstic cavities developed along that fault (Mollamustafaoğlu 1975b). The oxidized ore includes smithsonite, zincite, cerussite, hematite and limonite. Approximately 25,000 tonnes of oxide-carbonate Zn-rich ore with 21% Zn and 5%Pb average grades, has been mined for ÇİNKUR until 1995 (Demir 1998).

10.4 Hakkari Pb-Zn Province

The carbonate-hosted Pb-Zn deposits of the Hakkari Province occur on the Hakkari mountains that are located in the south-eastern corner of Turkey on the Arabian Platform (Figs. 10.1 and 10.18). The Cominco Mining Co conducted mineral exploration in this province from 2001 to 2003, but despite some minor findings, the company withdrew in 2008.

Although there is limited documentation regarding the mining history of the province, the presence of ancient galleries and a wooden shovel (like in the Aladağ-Zamantı region) in the ore zone suggests that the mining dates back to Roman times. Recent documentation (Dalyan 2011) indicates that the Nestorian people extracted lead from the surface ore veins in the Hakkari region in the nineteenth century, during the Ottoman period. Recently, mining began in 2004 at the Üzümcü and Meskantepe deposits, in 2007 at the Kurşuntepe deposit, in 2009 at the Karakaya deposit, in 2012 at the Akkaya deposit and in 2014 at the Armutlu deposit. From

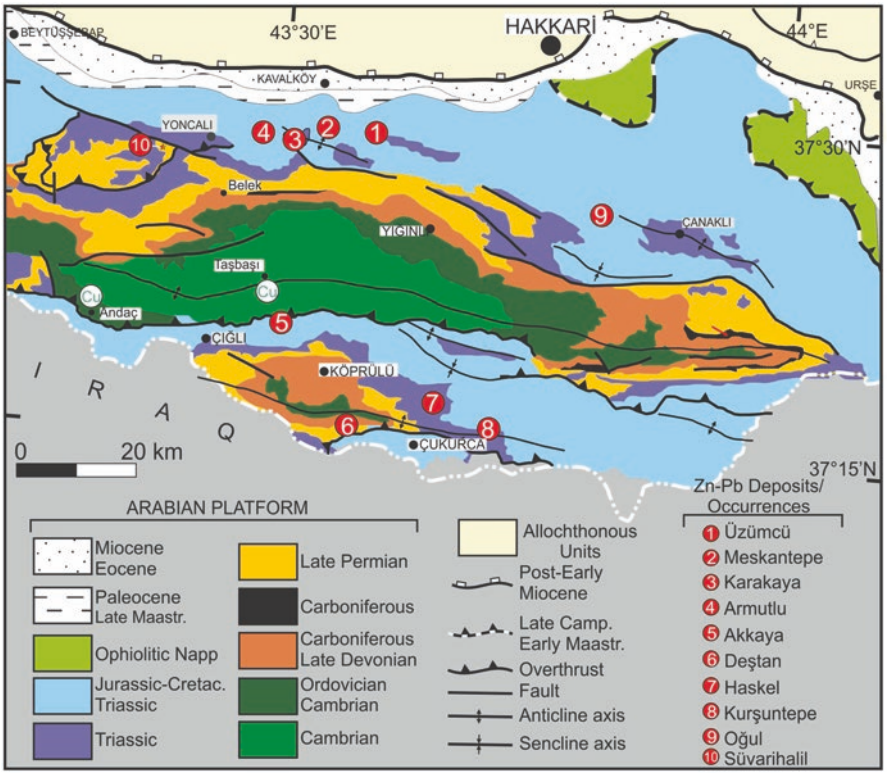

Fig. 10.18 A geological map of the Hakkari region (the Arabian platform simplified from Perinçek 1990, allocthounes units are taken from Elmas and Yılmaz 2003) and the locations of the carbonate-hosted Pb-Zn deposits (Modified after Hanilçi and Öztürk 2008)

2005 to 2016, approximately 1 Mt of ore with averaging of 22% Zn and 5% Pb were mined.

Although there has been limited drilling in the Armutlu and Meskantepe deposits, no reserve data are available for these deposits. However, according to data obtained from the surface geology, it is assumed that the region may have a few tens of millions of tonnes of ore potential.

10.4.1 Geological Setting

The Hakkari province Pb-Zn deposits occur in carbonate-host rocks of Permian to Jurassic age that forms the middle section of a thick passive margin sediments belonging to Arabian Platform (Figs. 10.1 and 10.18).

The geological framework of the province consists of Cambrian to Ordovician quartzites, Devonian clastics and carbonates, Carboniferous black shales, Permian

thick bedded black limestones, Triassic shales and limestones and Jurassic and Cretaceous carbonates (Perinçek 1990). Except for the Ordovician and Devonian boundary, the formations are concordant and typically represent a passive margin sequence. Cretaceous autocthonous carbonates are tectonically overlain by a ophiolitic melange from the north (Fig. 10.18). This melange is known as the Yüksekova complex and represents deformed deep sea sediments of the Neothethyan Ocean.

The region reveals an E-W trending folding axis associated with the N–S compressional regime. The Alpine orogenesis was the latest mountain bulding event from the Late Cretaceous to Miocene and resulted in folding of the sedimentary sequences on the passive margin and in the closure of the Tethyan Ocean and its remnant basins.

10.4.2 The Karakaya Pb-Zn Deposit

The Karakaya deposit is located approximately 43 km southwest of the Hakkari settlement (Fig. 10.18, Table 10.1). Approximately 0.2 Mt averaging 21%Zn and 5%Pb has been mined between 2009 and 2016.

The Karakaya deposit is located in the southern and northern limbs of a west plunging anticline. The deposit occurs within the Late Triassic - Jurassic (?) carbonates and includes centimetre to meter scale ore levels that are parallel to one another (Fig. 10.19a). The ore zones continue intermittently for approximately 3.5 km, striking from N35W to N70W and with dips from 65 to 85°NE. There are three main ore zones (Ore Zone I, II and III) that are *strata-bound*-stratiform with average thicknesses of 2.5 m, 3 m and 6 m, respectively (Fig. 10.19a). In some locations, the thickness of ore zone reaches up to 13 m, as in the Karakaya Main Deposit (Fig. 10.19b). The Ore Zone III also includes more than 13 parallel ore leyers that have different thicknesses from 5 to 70 cm. The ore zones are oxidised mostly in-situ as a direct replacement of primary ore to oxide/carbonate minerals. The oxidised ores include smithsonite, hemimorphite, hydrozincite, cerussite, anglesite, goethite, siderite, calcite, and dolomite. Rare barite, galena, sphalerite and pyrite are among the remnants of the primary ore.

10.4.3 The Meskantepe Pb-Zn Deposit

The Meskantepe deposit is located approximately 35 km southwest of Hakkari (Fig. 10.18, Table 10.1). Approximately 0.7 Mt averaging of 24% Zn and 6% Pb have been mined from 2004 to 2016.

The Meskantepe deposit is located in the same ore zones of the Karakaya deposit. The ore zones are located on the western and eastern sides of the Meskan Tepe (2087 m a.s.l) and continue intermittently for 1.9 km on the western side and for approximately 2 km on the eastern side. The Meskantepe deposit is a *strata-*

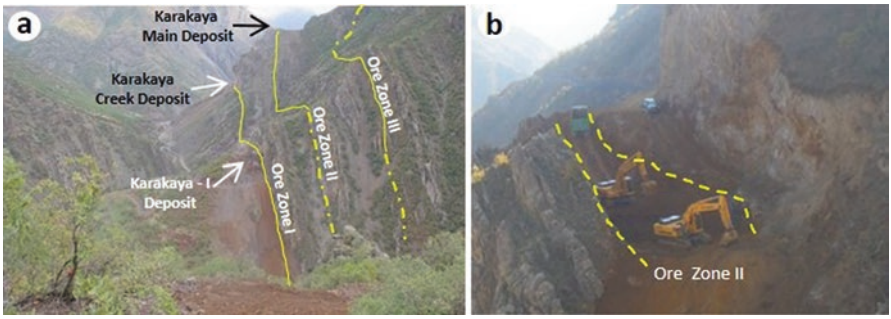

Fig. 10.19 (**a**) Main non-sulphide ore zones of the Karakaya Pb-Zn deposits. The average thicknesses of the ore zones (Ore Zone I, II and III) are 2.5 m, 3 m and 6 m, respectively. (**b**) The thickness of Ore Zone II in the Karakaya Main Deposit can reach up to 13 m

bound-stratiform type sited between thin bedded limestones interbedded with clastics to middle and thick bedded bituminous carbonates (dolomite) of the Late Triassic – Jurassic (?). The thicknesses of the main ore zones range from 1 to 3 m, in some locations exceeding 6 m due to wall-rock replacement. The strikes and dips of the ore zones are E-W and 10–60° N, respectively. The ore is oxidised to oxide/carbonate Zn-Pb at the surface (Fig. 10.20a). Non-sulphide ore zone contain relics of primary sulphide ore lenses. The primary sulphide ore shows banded features consisting of pyrite/marcasite and sphalerite, with rare galena alternations (Fig. 10.20b).

10.4.4 The Üzümcü Pb-Zn Deposit

The Üzümcü deposit is located approximately 23 km southwest of the Hakkari (Fig. 10.18, Table 10.1). Approximately 0.1 Mt with an average of 27% Zn and 5% Pb has been mined from 2005 to 2016.

The Üzümcü deposit is located in the same ore zones of the Meskantepe deposit. The ore occurs within the Late Triassic –Jurassic (?) limestone as mainly *strata-bound*-stratiform type (Fig. 10.21a, b) and vein types. The strike and dip of the ore zone are N15-40°W and 30–55°SW, respectively. The Üzümcü ore zone is the eastward continuity of the Meskantepe deposit and continues intermittently for approximately 1.5 km. The deposit primarily includes four ore zones that have thicknesses from 1 to 5 m and are parallel to one another.

The ore is an oxide/carbonate Pb-Zn. The Üzümcü deposit also includes some relics of primary sulphide lenses (Fig. 10.21c) in the non-sulphide ore zone. The primary ore lenses include mainly banded pyrite, sphalerite and galena. The oxidized ore consists of smithsonite, hydrozincite, hemimorphite, goethite-limonite, cerussite, relics of galena, barite, calcite and dolomite.

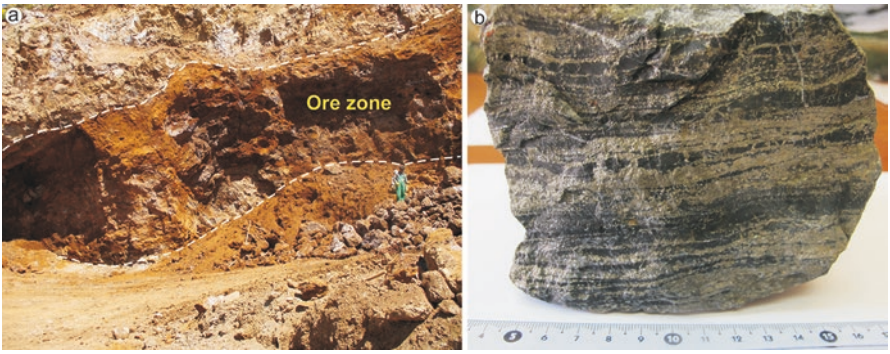

Fig. 10.20 (**a**) Non-sulphide ore zone on the western side of Meskan Tepe and (**b**) the preserved primary sulphide ore that contains sphalerite (dark levels) and pyrite/marcasite alternations within the non-sulphide ore zone

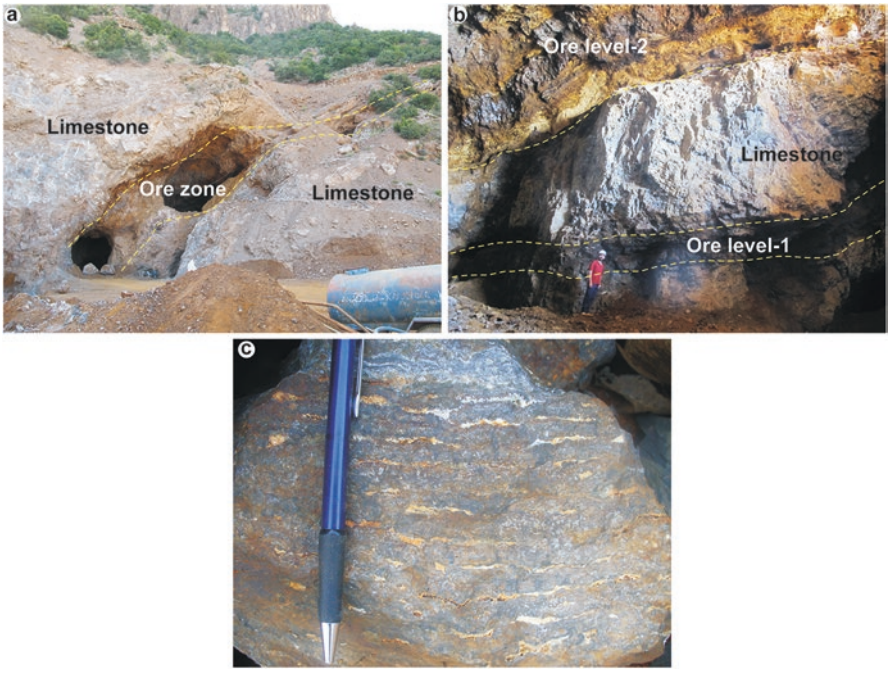

Fig. 10.21 The Üzümcü deposit occurs as (**a**) a *strata-bound* - stratiform type and (**b**) includes different ore levels that are parallel to one another. (**c**) Üzümcü non-sulphide ore zone contains preserved primary sulphidic ore lenses that contain pyrite, galena and sphalerite banding

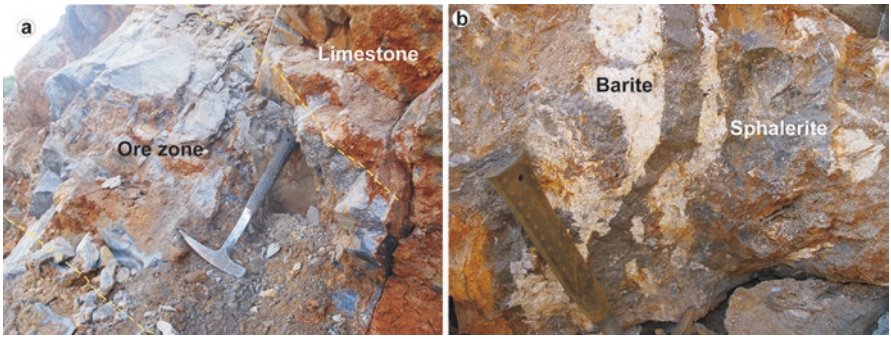

Fig. 10.22 (**a**) Strata-bound type ore zone mainly includes sphalerite, and (**b**) the vein-type ore zone includes sfalerite and a significant amount of barite in the Kurşuntepe Pb-Zn deposit

10.4.5 The Kurşuntepe Pb-Zn Deposit

The deposit is located approximately 7 km northeast of the Çukurca settlement (Fig. 10.18, Table 10.1). About 7000 tonnes of ore with an average grade of 27% Zn and 8% Pb were mined in 2007.

The Kurşuntepe deposit is an example of the primary sulphide ores in the region. The deposit includes two ore zones. The first zone is strata-bound and occurs along the contact between the Late Permian (Midian-Dorashamian) and Early Triassic (Indian) micritic limestones (Fig 10.22a). The second ore zone is a vein-type and occurs throughout an E-W trending fault zone between the Late Permian (Late Culfian-Dorashamian) and Early Triassic limestones (Hanilçi and Öztürk 2008).

The strike and dip of the strata-bound and vein-type ore zones are N40W, 45°SW and E-W, 80–87°S, respectively. The lengths and thicknesses of the strata-bound and vein-type ore zones are 70 m and 80 m, and 1–3 m and 3 m, respectively. While the strata-bound type ore zone consists of mainly sphalerite with rare galena, the vein-type ore zone includes sphalerite, galena and significant barite (Fig. 10.22b).

10.4.6 The Oğul, the Akkaya and the Deştan Pb-Zn Mineral Deposits

The Oğul, Akkaya and Deştan Pb-Zn mineral deposits are located approximately 22, 48 and 69 km south of Hakkari, respectively (Fig. 10.18, Table 10.1).

The Oğul mineralisation is strata-bound within the Middle-Late Triassic (?) carbonates (Fig. 10.18). The mineralization includes a few ore levels that are parallel to one another. The ore zone has N70 W strike and 43°NE deep (Fig. 10.23a). The length of the Fe-rich ore outcrop is approximately 130 m and the ore thickness varies between 0.3 m and 7 m.

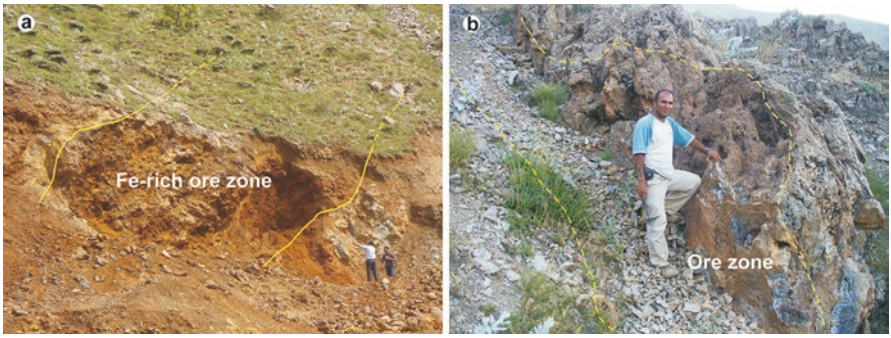

Fig. 10.23 (**a**) Strata-bound type ore zone in the Oğul mineralization that is oxidized and changed to Fe-(hydr)oxide rich non-sulphide ore at the surface, and (**b**) the vein-type ore zone in Akkaya mineralization that includes intermixed oxide-sulphide ores containing smithsonite, hemimorphite, cerussite, sphalerite, galena and barite

The Akkaya mineral deposit occurs as a vein-type throughout the N40 W trending fault zone cutting thick-bedded Jurassic dolomitic limestones and dolomites. The length of the ore outcrop is 100 m, and its thickness is approximately 2.5 m (Fig. 10.23b). The ore zone includes a mixture of oxide-sulphide ore consisting smithsonite, cerussite, Fe-(hydr)oxide, sphalerite, galena and rare barite. The ore zone passes downward to primary sulphide ore that includes sphalerite, pyrite and galena. Approximately 7000 tonnes of ore with averages of 15% Zn and 6–12% Pb in the bulk ore (oxide-sulphide intermixed ore) were produced during exploration work.

The Deştan mineralisation occurs in Permian limestone as veins and cavity fills. There are ancient small underground tunnels and slag residues around it. The ore is concentrated in fractures trending N20–60°E, 70–85°SE. The ore is composed of smithsonite and galena coated by cerussite.

In summary, the carbonate-hosted Pb-Zn deposits in the Hakkari region include (i) primary sulphide zones of vein type ± strata-bound types in the Permian and Triassic limestone-dolomitic limestones (Kurşuntepe deposit), and intermixed oxide-sulphide ore veins in the Jurassic carbonates (Akkaya deposit), and (ii) non-sulphide ore zones showing *strata-bound*-stratiform character hosted in the Late Triassic-Jurassic (?) carbonates (i.e.Karakaya, Meskantepe, Üzümcü, Armutlu, Oğul deposits). In some deposits (Meskantepe, Üzümcü and Karakaya), non-sulphide ore zones include relics of primary sulphide ore lenses. The mineral primary sulphide zones preserved in non-sulphide ore zones consists of sphalerite, galena, marcasite/pyrite, quartz and barite.

In the Hakkari region non-sulphide deposits (i.e. Karakaya, Meskantepe, Üzümcü and Armutlu deposit) were formed by in-situ oxidation or direct-replacement of *strata-bound*-stratiform primary sulphidic ores. Besides, Zn was remobilised in to karstic cavities and redeposited as high grade wall-rock-replacement and karst-infill (Hanilçi and Öztürk 2008; Santoro et al. 2013). This type of ore is characterised by high grade Zn and trace amounts of Pb.

The style of mineralization and geochemical data of the Hakkari region Zn-Pb deposits bears comparison with MVT style mineralization in terms of its strata-bound character, radiogenic lead ($^{206}Pb/^{204}Pb$ between 18.325 and 18.756; $^{207}Pb/^{204}Pb$ between 15.579 and 15.700; and $^{208}Pb/^{204}Pb$ between 38.421 and 39.034), its simple mineralogy and lack of igneous activity. It also resembles SEDEX type deposits in terms of slightly higher homogenization temperature (between 170 and 200 °C in quartz, and average 211 °C for sphalerite) and lower salinity (between 3.5% and 18% NaCl equiv.) than MVT, its parallel ore zones, and high contents of As (0.2%; up to %1.2), Mo (302 ppm), Sb (251 ppm; up to 926 ppm), Tl (109 ppm; up to 1143 ppm) and Hg (35 ppm) in the non-sulphide ore zones (Hanilçi et al. 2016, 2017a, b; Santoro et al. 2013).

The ore mineralogy, ore texture and wall-rock features indicate a primary sulphide Zn-Pb mineralisation in the Hakkari region that probably resembles a SEDEX type rather than Mississippi Valley-type (MVT). The Pb-Zn mineralizations could have been formed during the rifting and spreading of the Neo-tethyan Ocean (Late Triassic-Jurassic(?)) as *strata-bound*-stratiform type by deep circulation of fluids. The primary sulphide ore could have been oxidised and changed to direct-replacement and wall-rock replacement type non-sulphides during the Upper Tertiary (Santoro et al. 2013). The Hakkari region has good potential for the discovery of new Pb-Zn deposits.

10.5 Conclusions

The carbonate-hosted Pb-Zn deposits of Turkey occur in the Tauride carbonate platform. These deposits can be divided into eight provinces. These include from west to east; (1) Hadim-Bozkır, (2) Göktepe, (3) Gazipaşa, (4) Anamur, (5) Horzum and Pınargözü, (6) Aladağlar-Zamantı, (7) Tufanbeyli and (8) Hakkari province. These deposits display formation characteristics of MVT (Hadim-Bozkır, Göktepe, Gazipaşa, Anamur, Aladağlar-Zamantı), CRD (Horzum and Pınargözü) and SEDEX (Hakkari). The mining history of those provinces goes back to Roman period. The most important Pb-Zn Provinces where active mining continues are the Aladağlar, Hakkari and Horzum.

All deposits have oxidized to a large extent and transformed into non-sulphide zinc deposits. While the deposits in Hakkari Province are oxidized mainly as in-situ, the deposits in the other provinces effected from multi karstification processes and deposited as direct replacement and in karstic-infill type high grade zinc deposits. In some deposits (i.e. Horzum and Hakkari Province), non-sulphide ore zone has produced and passed to primary sulphide ore zone thought the depth.

Mining activities carried out at shallow depths in all provinces mentioned above. Therefore, there is still significant potential for discovering big deposits in around the existing deposits. The newly discovered Hakkari Pb-Zn Province are the most important province as potential among the eight provinces. Despite very limited exploration work, the Hakkari Province includes a few tens of million tonnes of ore resources.

Acknowledgements The authors thank Cemil Alp (Geological Eng.) and Abdullah Malkoçoğlu (Mining Eng.) for the Havadan region deposit data, Çavuş Altunbulak (Geological Eng.) and Ali Elmaağaç (Mining Eng.) for the Ayraklı deposit data, Mustafa Koyuncu (Koyuncu Maden Company) for the Göynük deposit data, and Akmetal Mining for the Horzum deposit data. Thanks to Dr. David A. Banks (University of Leeds) for his critical contribution on geochemical interpretation. We thank Prof. Franco Pirajno, Dr. Bahadır Şahin and Cahit Dönmez for their helpful editorial advice. This chapter was supported by İÜ-BAP (YADOP-37096) and by the TUBITAK (project ÇAYDAG-114Y554).

References

Akmetal M (2015) Horzum kurşun/çinko sahası [Horzum lead/zinc licenced mine area]. http://www.akmetalmadencilik.com/horzum-kursuncinko-sahasi. Accessed 19 June 2017

Alp C (1976) Hadim Yöresinin Maden Jeolojisi ve Pb–Zn Etütleri Ön Raporu [Mine geology of Hadim region and preliminary prospecting report on Pb-Zn]. General directorate of mineral research and exploration report no. 574, p 38 (in Turkish, unpublished)

Ayhan A (1981) Die Genese Der Blei-Zink-Lagerstaetten Von Aydap Und Yulari Bei Gazipaşa (Antalya) Und Ihre Remobilizations Probleme. Bull Min Res Exp 95–96:57–68

Ayhan A (1982) Galena-bearing barite occurrences between Burhan Mahallesi–Yuları Köyü (Gazipaşla–Antalya, Turkey). Geol Bull Turkey 25:105–117 (in Turkish with English abstract)

Ayhan A (1984) Genetic comparison of lead–zinc deposits of Central Taurus. In: Tekeli O, Göncüoglu MC (eds) International symposium on the Geology of the Taurus Belt, September 1983, General Directorate of Mineral Research and Exploration Ankara, Ankara-Turkey, pp 335–342

Ayhan A, Lengeranlı Y (1986) Yahyalı-Demirkazık (Aladağlar Yöresi) Arasının Tektonostratigrafik Özellikleri [Tectonostratigraphic Properties of Yahyalı-Demirkazık (Aladağlar Region)]. Geol Eng 27:31–45 (in Turkish)

Ayhan A, Lengeranlı Y, Çeltek N, Aksoy E (1984) Aladağlar (Batı Zamantı) Yöresi (Yahyalı-Çamardı) Jeolojisi ve Kursun-Çinko Etüdleri [Aladaglar (Batı Zamanti) region (Yahyalı-Çamardı) geology and lead-zinc prospects]. General directorate of mineral research and exploration report no. 1483, p 112 (in Turkish, unpublished)

Bahar H, Koçak K (2010) Pb, Zn ±Ag±Cu±Sn mining at Taurus mountains in Antique period. J Fac Eng Arch Selçuk Univ 25:3 (in Turkish with English abstract)

Blümel GJ (1964) Ortakonuş-Anamur Pb-Zn Ocağı Sahasında Yapılan Saha Çalışmaları Hakkında Kısa Rapor [Brief report on the fieldwork studies made on the Ortakonuş-Anamur Pb-Zn deposit]. General directorate of mineral research and exploration report no. 3581 (in Turkish, unpublished)

Bodnar RJ, Lecumberri-Sanchez P, Moncada D, Steele-MacInnis M (2014) Fluid inclusions in hydrothermal ore deposits. In: Holland HD, Turekian KK (eds) Treatise on geochemistry, vol 13, 2nd edn. Elsevier, Oxford, pp 119–142

Bozkaya Ö, Yalçın H (2005) Diagenesis and very low-grade metamorphism of the Antalya Unit: mineralogical evidence of Triassic rifting, Alanya-Gazipaşa, Central Taurus Belt, Turkey. J Asian Earth Sci 25:109–119

Çevrim M (1984) Die Zink-Blei-vererzungen des Aladag-Giebietes/TÜRKEI mit betrachtungen zur palaokastentwicklung PhD thesis Aachen, Rheinisch-Westfälischen Technischen Hochschule, p 184 (unpublished)

Çopuroğlu İ (1994) Karalar-Gazipaşa (Antalya) Galenit-Barit Yatağının Mineralojik-Petrografik ve Jenetik İncelenmesi [Mineralogical-petrographic and genetic investigation of Karalar-Gazipaşa (Antalya) Galena-Barite deposit]. Bull Min Res Exp 116:29–36 (in Turkish with English abstract)

Çopuroğlu İ (1996) Yahyalı (Kayseri) Demirkazık (Niğde-Çamardı) Yöresi Çinko-Kurşun Yataklarının Mineralojisi ve Jenezi [Mineralogy and genesis of Yahyalı (Kayseri) and Demirkazık (Niğde-Çamardı) region zinc-lead deposit]. Bull Min Res Exp 118:35–46 (in Turkish)

Dalyan MG (2011) Robbery, blood feud, and gunpowder in Nestorian community. Asian Soc Sci 7(8):81–87

Demir N (1998) Niğde-Çamardı-Tekneli yöresindeki çinko-kurşun maden yataklarının bölgesel jeolojik evrimi ile ilişkileri [Relations with regional geological evolution of zinc-lead deposits in Niğde-Çamardı-Tekne region]. PhD thesis Çukurova University, p 159 (in Turkish, unpublished)

Elmas A, Yılmaz Y (2003) Development of an oblique subduction zone-tectonic evolution of the Tethys Suture zone in Southeast Turkey. Int Geol Rev 5:827–840

Eren RH, Uz B, Özpeker I (1993) Tectonics and Pb-Zn mineralizations of Tekneli area in Taurides. Geosound 22:45–60

Gökce A, Bozkaya G (2003) Karalar geology and fluid inclusion characteristics of the Karalar (Gazipaşa-Antalya) Barite – Galena deposits. Geol Bull Turk 46:1–16 (in Turkish with English abstract)

Gökce A, Bozkaya G (2007) Lead and sulfur isotopic studies of the barite–galena deposits in the Karalar area (Gazipaoa–Antalya), Southern Turkey. J Asian Earth Sci 30:53–62

Gökçe A, Bozkaya G (2008) Fluid inclusion and stable isotope characteristics of the Karalar (Gazipaşa, Antalya) Barite–Galena deposits, Southern Turkey. Geol Ore Deposits 50(2):145–154

Gümüş A (1989) Metalik Maden yatakları [Metallic ore deposits]. Bilim Ofset, İzmir, p 528 (in Turkish)

Hanilçi N, Öztürk H (2003) Stable isotope and microthermometric studies in carbonate-hosted Pb-Zn deposits in Aladağlar, Eastern Taurus, Turkey. Abstract Books 56th Geological Congress of Turkey, pp 112–114

Hanilçi N (2003) Formation of the carbonate-hosted Pb–Zn deposits in Central and Eastern Taurus [unpublished Ph. D. thesis]. Natural Science Institute, Istanbul University, Istanbul, p 166

Hanilçi N, Öztürk H (2005) Mississippi valley type Zn-Pb deposits in the Aladağlar-Zamantı (Eastern Taurus) region: Ayraklı and Denizovası Zn-Pb deposits, Turkey. İstanbul Earth Sci Rev 18(2):23–43 (in Turkish with English abstract)

Hanilçi N, Öztürk H (2008) Hakkari region Zn-Pb deposits: preliminary evidence for their geological features and formation. In: Öztürk H, Hanilçi N, Kahriman A, Özkan ŞG (eds) Proceedings symposium on geology and mining of Pb-Zn deposits of Turkey. İstanbul University, Istanbul, pp 244–264 (in Turkish with English abstract)

Hanilçi N, Öztürk H (2011) Geochemical/isotopic evolution of Pb-Zn deposits in the Central and Eastern Taurides, Turkey. Int Geol Rev 53(13):1478–1507

Hanilçi N, Öztürk H, Banks DA, Koral H (2016) Carbonate-Hosted Zn-Pb deposits in the Hakkari-Şırnak region: a newly discovered Tethyan Metallogenic province in Turkey. SEG 2016 conference, Tethyan Tectonics and Metallogeny, Çeşme, Turkey (Abstract), September 2016, pp 25–28

Hanilçi N, Öztürk H, Banks DA (2017a) Geochemical stratigraphy of the Karakaya non-sulphide Zn-Pb deposit, Hakkari, SE Turkey. Proceedings of the 14th SGA Biennial Meeting, 20–23 August 2017, Québec City 2, pp 669–671

Hanilçi N, Öztürk H, Banks DA (2017b) Trace element and stable sulpur isotope geochemistry of the Hakkari region Zn-Pb deposits. 8th Geochemistry symposium, 2–6 May 2018, Antalya, Abstract Book, pp 194–195

Imreh L (1965) Zamanti metal cevherleşmesi bölgesinin kurşun-çinko mineralizasyonları [Lead-zinc mineralizations of the Zamanti metallogenic province]. Bull Min Res Exp 65:85–108 (in Turkish)

Kamona F (2011) Carbonate-hosted base metal deposits. In: Dar IA (ed) Earth and environmental sciences. ISBN: 978-953-307-468-9. In Tech. https://doi.org/10.5772/25885. http://www.intechopen.com/books/earth-and-environmental-sciences/carbonate-hosted-base-metal-deposits

Karakaya Co. (2015) The ore zones of Karakaya Pb-Zn deposits and Ore Potential. p 25. August 2015 (unpublished)

Koptagel O, Efe A, Ceyhan F (1998) Genesis of the Göynük Pb-Zn Mineralization (Yahyalı-Kayseri). Geol Bull Turk 41(2):53–62 (in Turkish with English Abstract)

Koptagel O, Efe A, Ceyhan F, Erik D (2001) General features of Pb-Zn mineralization, Denizovası-Havadan region (Eastern Yahyalı-Kayseri): an approach to its genesis. Geol Bull of Turk 44(3) Ayhan Erler Special Issue: 15–55 (in Turkish with English Abstract)

Koptagel O, Ulusoy U, Efe A (2005) A study of sulfur isotopes in determining the genesis of Göynük and Celaldağı Desandre Pb-Zn deposits, Eastern Yahyalı, Kayseri, Central Turkey. J Asian Earth Sci 25:279–289

Kuşçu M (1985) Pb-Zn occurrences of the Göktepe (Ermenek-Konya) district. Bull Geol Soc Turk 28:35–46 (in Turkish with English Abstract)

Kuşçu M, Cengiz O (2001) Genesis of the middle Taurus carbonate-hosted Zn-Pb deposits by stable isotope ($S^{34/32}$) ratios. Geol Bull Turk 44(3) Ayhan Erler Special Issue: 59–73 (in Turkish with English Abstract)

Leach DL, Sangster DF (1993) Mississippi Valley-type lead-zinc deposits. Geol Assoc Can Spec Pap 40:289–314

Leach DL, Sangster, DF, Kelley KD, Large RR, Garven G, Allen CR, Gutzmer J, Walters S (2005) Sediment-hosted lead-zinc deposits: a global perspective. Econ Geol 100th Anniversary Vol 561–608

Leach DL, Bradley DC, Huston D, Pisarevsky SA, Taylor RD, Gardoll SJ (2010) Sediment-hosted lead-zinc deposits in earth history. Econ Geol 105:593–625

Megaw PKM, Ruiz J, Titley SR (1988) High-temperature, carbonate-hosted Ag-Pb-Zn (Cu) deposits of Northern Mexico. Econ Geol 83(8):1856–1885

Mengeloğlu MK (1996) Doğu Akdeniz bölgesi Kurşun-Çinko Envanteri [Lead-zinc inventory of Eastern Mediterranean Region]. MTA Eastern Mediterranean regional directorate, report no. 11950 (in Turkish, unpublished)

Metag and Stolberg (1971) Zamantı Kursun-Çinko Projesi Nihai Raporu, Maden Sahalarının Jeolojisi ve Paleontoloji [Final report of the Zamantı lead-zinc project, geology and paleontology of the mining licenced areas]. DPT Undersecretariat report, vol. IV, p 191 (in Turkish Unpublished)

Mollamustafaoğlu İ (1975a) Belbaşı Çinko Madeni Arama Çahşmaları Nihai Raporu [Final exploration report of the Belbaşı zinc deposit]. ÇİNKUR-Kayseri (in Turkish, unpublished)

Mollamustafaoğlu İ (1975b) Tufanbeyli-Kireç-Beşiktaş Pb-Zn Madeni (İR:613) Arama Çalışmaları Nihai Raporu [Final exploration report of the Tufanbeyli-Kireç-Beşiktaş Pb-Zn deposit (İR:613)]. ÇİNKUR, Kayseri (in Turkish, unpublished)

MTA (1993) Türkiye Kurşun-Çinko Envanteri [Lead-zinc inventory of Turkey]. Publication of general directorate of mineral research and exploration, Publication no. 199. p 94 (in Turkish)

Okay A, Tüysüz O (1999) Tethyan sutures of northern Turkey. Geol Soc London Spec Publ 156:475–515

Okuyucu C (2002) Toroslarda Anadolu Platformu Karbonifer – Permiyen geçisinin mikropaleontolojik incelemesi [Micropaleontological investigation of Carboniferous – Permian transition of the Anatolian platform in the Taurus]. PhD thesis, Hacettepe University Ankara, p 207 (in Turkish, unpublished)

OREKS (2015) Oreks Company, Annual production report of Ayraklı Zn-Pb deposit, 15 p. (unpublished company report)

Özgül N (1976) Some geological aspects of the Taurus orogenic belt (Turkey). Bull Geol Soc Turk 19:65–78 (in Turkish with English abstract)

Perinçek D (1990) Stratigraphy of the Hakkkari region, Sourteastern Anatolia. Bull Turk Pet Geol Assoc 2:21–68

Petrascheck WE (1967) Batı Toros kalkerlerindeki kurşun çinko yatakları [Lead zinc deposits in carbonates of West Tauride]. Maden Tetkik Arama Enst 68:38–48 (in Turkish with English Abstract)

Pirajno F (2009) Hydrothermal processes and mineral systems. Springer, Berlin, p 1250
Robertson AHF, Ustaömer T (2009) Upper palaeozoic subduction/accretion processes in the closure of palaeotethys: evidence from the Chios Melange (E Greece), The Karaburun Melange (W Turkey) and the Teke Dere Unit (Sw Turkey). Sediment Geol 201:29–59
Sadıklar MB (1978) Schwerspat-und Bleiglanz-Vorkommen und ihre geologisch-petrogr. Lage im Gebiet der Dörfer Kıcık, E. Güney und Seyfe (Zeytinada) bei Gazipaşa-Antalya (Turkei). Dipl. Arb. Univ, Heidelberg, p 111
Sadıklar MB, Amstutz GC (1981) Kıcık, Endişegüney ve Seyfe (Gazipaşa/Antalya-Türkiye) yöresindeki tabakaya bağlı barit-galen zuhurları [Stratabound galena-barite occurrences in Kıcık, Endişegüney and Seyfe (Gazipaşa/Antalya-Turkey) region]. Bull Min Res Exp 95–96:113–123 (in Turkish)
Santoro L, Boni M, Herrington R, Cleeg A (2013) The Hakkari nonsulfide Zn–Pb deposit in the context of other nonsulfide Zn–Pb deposits in the Tethyan Metallogenic Belt of Turkey. Ore Geol Rev 53:244–260
Striebel H (1965) Die Bleierz-Baryt-Lagerstaette von Karalar-Gazipaşa/Turkkei und ihr geologischer Rahmen. PhD thesis (unpublished). Naturwiss Fak University of München, p 48
Tekeli O, Aksay A, Ürgün BM, Işık A (1983) Geology of Aladağ Mountains. In: Tekeli O, Göncüoglu, MC (eds) International symposium on the Geology of the Taurus Belt, September 1983, General Directorate of Mineral Research and Exploration Ankara, Ankara-Turkey, pp 143–158
Temur S (1986) Genetic study of pyrite-bearing zinc-lead deposits in the Horzum (Kozan-Adana) district. Bull Earth Sci 13:31–48
Thompson TM, Beaty DW (1990) Geology and the origin of ore deposits in the Leadville District, Colorado: part II. Oxygen, hydrogen, carbon, sulfur, and lead isotope data and development of a genetic model. Econ Geol Monogr 7:156–179
Tok T, Şenel M, Alan İ, Keskin H, Taptık A, Kop A (2004) The stratigraphy and structural characteristics of Yahyalı Nappe and its correlation with similar units in Tauride Belt. 57th Geological Congress of Turkey, Abstracts Book, pp 267–268
Wilkinson JJ (2014) Sediment-hosted zinc–lead mineralization: processes and perspectives. In: Holland HD, Turekian KK (eds) Treatise on geochemistry, vol 13, 2nd edn. Elsevier, Oxford, pp 219–249
Yıldırım S (2008) History of lead-zinc mining in the Anatolia. In: Öztürk H, Hanilçi N, Kahriman A, Özkan S (eds) The geology, mining, and existing problems of Turkish Pb-Zn deposits. Istanbul University, Istanbul, pp 5–32 (in Turkish with English abstract)

Chapter 11
Turkish Borate Deposits: Geological Setting, Genesis and Overview of the Deposits

Cahit Helvacı

Abstract Boron is widely distributed in the earth's crust and the element boron does not exist freely by itself in nature, rather it occurs in combination with oxygen and other elements in salts, commonly known as borates. Boron is a rare element in the Earth's crust, but extraordinary concentrations can be found in places. Four main continental borate provinces are recognized at a global scale. They are located in Anatolia (Turkey), California (USA), Central Andes (South America) and Tibet (Central Asia). The origin of borate deposits is related to Cenozoic volcanism, thermal spring activity, closed basins and arid climate. Borax is the major commercial source of boron, with major supplies coming from Turkey. Colemanite is the main calcium borate and large scale production is restricted to Turkey. Main borax (tincal) deposits are present in Anatolia (Kırka), California (Boron), and two in the Andes (Tincalayu and Loma Blanca). Colemanite deposits with/without probertite and hydroboracite are present in west Anatolia, Death Valley, California, and Sijes (Argentina). Quaternary borates are present in salars (Andes) and playa-lakes and salt pans (USA and Tibet). The Karapınar playa-lake is located in central Turkey. The formation of borate deposits consisting of a sodium– and calcium–borate hydrates group associated with playa-lake sediments and explosive volcanic activity. Some conditions are essential for the formation of economically viable borate deposits, playa-lake volcano-sedimentary sequences: formation of playa-lake environment; concentration of boron in the playa lake, sourced from andesitic to rhyolitic volcanics, direct ash fall into the basin, or hydrothermal solutions along faults; thermal springs near areas of volcanic activity; arid to semi-arid climatic conditions; and lake water with a pH of between 8.5 and 11. A large number of minerals contain boric oxide, but the three that are most important from a worldwide commercial standpoint are borax, ulexite, and colemanite, which are produced in a limited number of countries. Turkey has the largest borax, ulexite and colemanite reserves in the world and all the world's countries are dependent upon the colemanite and ulexite reserves of Turkey. The main borate districts are located in Bigadiç, Kestelek, Sultançayır, Emet, Kırka and Göcenoluk areas. Most of the world's commercial

C. Helvacı (✉)
Faculty of Engineering Geology Department, Dokuz Eylul University, Izmir, Turkey
e-mail: cahit.helvaci@deu.edu.tr

F. Pirajno et al. (eds.), *Mineral Resources of Turkey*, Modern Approaches in Solid Earth Sciences 16, https://doi.org/10.1007/978-3-030-02950-0_11

borate deposits are mined by open pit methods. Boric acid is one of the final products produced from most of the processes. Further research on the mineralogy and chemistry of borate minerals and associated minerals will the production and utilization of borate end-products. Many modern industries need industrial borate minerals, and many individuals use their products. Therefore, borates and associated products are critical for the sustainable development of the world.

11.1 Introduction

Borate was first used in Babylon more than 4000 years ago. Its name originated from the Persian burah (boorak), borax was already known to the Babylonians who brought it from the Himalayas some 4000 years ago for use in the manufacture of rings, amulets, and bracelets. The Egyptians used borax in mummifying, and around 300 AD the Chinese were familiar with borax glazes, as were the Arabs three centuries later. Borax was first brought to Europe in the thirteenth century, presumably by Marco Polo, and since that time by traders from Tibet and Kashmir.

Boron is the fifth element of the periodic table and is the only electron-deficient non-metallic element. Thus, boron has a high affinity for oxygen, forming strong covalent boron-oxygen bonds in compounds known as borates. Because it is strongly fractionated into melts and aqueous fluids, processes that led to formation of continental crust such as partial melting and emission of volatiles, also concentrated boron, resulting in enrichment by four to eight orders of magnitude from <0.1 ppm in primitive mantle to 17 ppm in average continental crust, and to several wt% in pegmatites and evaporites. Boron is extremely dispersed in nature, averaging 0.1 ppm in land-surface water, 3 ppm in the Earth's crust, and 4.6 ppm in seawater. By at least 3.8 Ga, boron had been concentrated sufficiently to form its own minerals, which are thought to have stabilized ribose, an essential component of ribonucleic acid and a precursor to life. Boron has two isotopes, ^{10}B and ^{11}B; the former has a large capture cross-section that makes it an excellent neutron absorber. These two stable isotopes differ significantly in atomic weight so that boron isotopic compositions of minerals and rocks retain signatures from their precursors and the processes by which they formed. Boron compounds comprise a great diversity of crystal structures.

Borates are among the most interesting of the world's industrial minerals, first for precious metal working and later in ceramics. They form an unusually large grouping of minerals, but the number of commercially important borates is limited, and their chemistry and crystal structure are both unusual and complex (Kistler and Helvacı 1994; Helvacı 2005). Over 250 boron-bearing minerals have been identified, the most common being sodium, calcium and magnesium salts. By the 1770s, the French had developed a source of tincal, the old name for crude borax, in Purbet Province, India, and at about the same time natural boric acid (sassolite) was discovered in the hot springs in the Maremma region of Tuscany, Italy. The middle of the nineteenth century was a particularly active time for the discovery and commercial

development of borate deposits. In particular, Chile started to mine the borate resources of the salar de Ascotan in 1852 and within a few years their output accounted for a quarter of the world's annual supply of 16.000 tons. In 1856 John Veatch discovered borax in Clear Lake, Lake County, California, which led eventually to the start up of the California Borax Company in 1864 and to the beginning of that State dominance of the borate industry. Demand encouraged exploitation of large-scale deposits in Turkey and the United States.

Boron chemistry and reactivity are also fascinating because they form a wide variety of oxygen compounds that occur in an essentially unending variety of simple to exceedingly complex molecules. Determining their crystal structures has given rise to a separate subfield of crystallography. The boron isotopes ^{10}B and ^{11}B, varying widely in nature and their different reactivity during both physical and chemical changes means that they are an important tool in predicting many geologic and other events, again forming a specialized field in geology. Borates are defined by industry as any compound that contains or supplies boric oxide (B_2O_3). A large number of minerals contain boric oxide, but the three that are most commercially important worldwide are: borax, ulexite and colemanite. These are produced in a limited number of countries dominated by the United States and Turkey, which together furnish about 90% of the world's borate supplies. Production in the United States originated in the Mojave Desert of California; borax and kernite are mined from a large deposit at Boron. Borate containing brines are pumped from Searles Lake, and a limited amount of colemanite is mined from Death Valley. There are over 40 borate deposits located along an 885 km trend in the high Andes near the common borders of Argentina, Bolivia, Chile, and Peru, some of which are currently in production. Turkish production is controlled by Eti Maden/Etibor, the National Mining Enterprise, which supplies most of the commercially traded ulexite and colemanite from mines in the Bigadiç and Emet districts, plus borax from the huge deposit at Kırka (Kistler and Helvacı 1994; Helvacı and Alonso 2000; Helvacı 2005, 2015).

The borate deposits of Turkey occur in western Anatolia, south of the Marmara Sea within an area roughly 300 km east-west by 150 km north-south. The main borate districts are Bigadiç, Kestelek, Sultançayır, Emet and Kırka (Fig. 11.1). The early history of borate mining in Turkey goes back to Roman times. Substantial amounts of borates have been produced in Turkey since the end of the 1800s. In 1885, a French company was operating the Sultançayırı mine in Balıkesir province. There is a record of production since 1887, which indicates that production has been continuous to the present day except for war times. Until 1954 all recorded production came from Sultançayır, but since 1950 extensive exploration has resulted in the discovery of several important new Turkish deposits. Bigadiç deposit; Balıkesir province, has operated since 1950, and major production in the M. Kemalpaşa deposit (Kestelek), Bursa province, began in about 1952. In 1956 the Emet borate deposits, Kütahya province, were discovered by Dr. Gawlik whilst carrying out a survey of lignite deposits for MTA. After the discovery, the Emet deposits became the main source of colemanite in the western world. Finally, the most outstanding discovery was the Kırka borate deposit which is a massive borax body, with estimated reserves several times greater than those of Boron, California (İnan 1972;

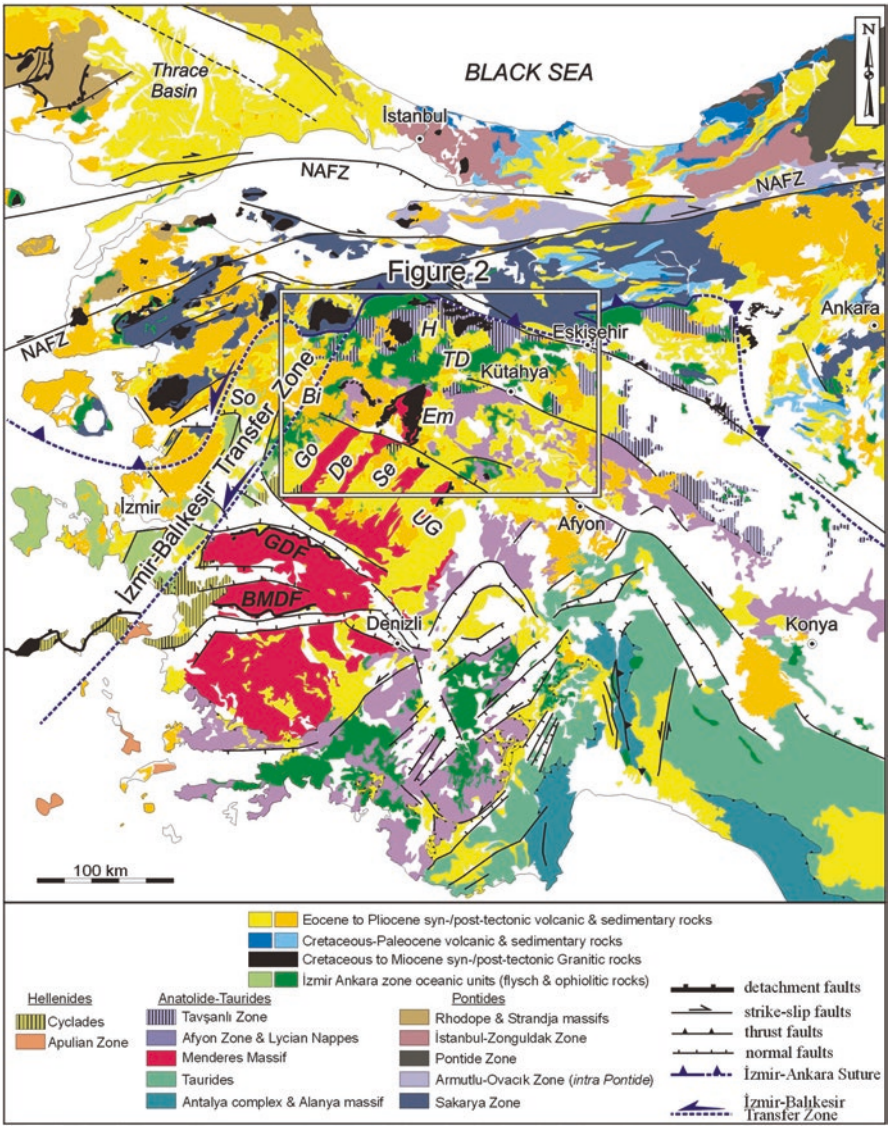

Fig. 11.1 Simplified geological map of western Anatolia showing the main tectonostratigraphic units and major tectonic elements in the region (Compiled from 1/500.000 scaled geological maps of Turkey (MTA 2002). NAFZ: North Anatolian Fault Zone)

Baysal 1972; Arda 1969; Travis and Cocks 1984; Dunn 1986; Kistler and Helvacı 1994; Helvacı 2005). Today, however, borate mining is confined to four distinct areas in Turkey: Emet, Kırka, Bigadiç and Kestelek.

Modern borate mining in Turkey began in 1865 when the Compagnie Industrialle des Mazures mined borates from the Aziziye Mine near Susurluk and shipped the

ore back to France for processing (Travis and Cocks 1984). The most important worldwide borate deposits occur in western Anatolia and have been the topic of several papers which dealt with their genesis and ore formation (İnan 1972; Baysal 1972; Helvacı 1983, 1984, 1986, 1995, 2005, 2015; Kistler and Helvacı 1994; Palmer and Helvacı 1995, 1997; Helvacı et al. 1993; Helvacı and Orti 1998, 2004; Helvacı and Alonso 2000). They originated in continental Tertiary lacustrine basins during a period characterized by intense magmatic activity affecting western Anatolia. These borate deposits are interbedded with volcanosedimentary rocks, and the borate deposits and associated sedimentary rocks are deposited within playa lake environments (Floyd et al. 1998; Helvacı and Alonso 2000).

Turkey is currently the largest producer of borate minerals and has the world's largest reserves. Production more than doubled in 1980 to over one million tonnes (approximately 1.500.000 tonnes) and further increases, particularly of borax from Kırka, are likely to lead to Turkey dominating the world markets. Turkey is already the major world producer of colemanite, much of which comes from the Emet valley (e.g. 2500 mt in 2011). The Eti Maden planned to expand its share in the world boron market from 36% to 39% by 2013, increasing sales to $1 billion by expanding its production facilities and product range.

In this paper, stratigraphic, volcanic and tectonic observations from these basins will be presented in order to outline the main features of the borate bearing basins and the tectono-stratigraphic model for borate formation in western Anatolia.

11.2 Geology

The western Anatolia region is composed of several continental blocks that were originally separated by the northern branch of the Neo-Tethys marked today by the Vardar-İzmir-Ankara Suture (Fig. 11.1; Şengör and Yılmaz 1981). The Vardar-İzmir-Ankara Suture separated the Sakarya continent to the north and the Anatolide–Tauride block to the south and was formed by late Mesozoic northward subduction and accretion (Fig. 11.1, Şengör and Yılmaz 1981). The southernmost part of the region is marked by the south Aegean volcanic arc, which is formed from subduction of the African plate along the Hellenic trench (Pe-Piper and Piper 2007).

The geology of western Anatolia is characterized by Tertiary volcano-sedimentary deposits covering a basement that includes several continental fragments and suture zones. Western Anatolia has a complex history of Late Cenozoic tectonic and magmatic activity. The basement units comprise; (1) the Menderes and Cycladic massifs, (2) the İzmir-Ankara Zone (comprising; (a) the Bornova flysch zone, (b) the Afyon zone, and (c) the Tavşanlı zone), (3) the rocks of the Sakarya Continent to the north, and (4) the Lycian Nappes to the south (Şengör and Yılmaz 1981; Fig. 11.1). The İzmir-Ankara zone comprises the Bornova Flysch zone, the Afyon zone and the Tavşanlı Zone. The Bornova Flysch Zone comprises chaotically deformed Upper Maastrichtian – Palaeocene greywacke and shale with Mesozoic neritic limestone blocks of several kilometers in diameters (Okay et al. 1996). The Tavşanlı Zone

forms a blueschist belt, representing the northward subducted passive continental margin of the Anatolide-Tauride platform (Okay et al. 1996). The Afyon zone comprises shelf-type Devonian to Palaeocene sedimentary sequence metamorphosed to greenschist facies (Okay et al. 1996)

The geometry, stratigraphy, tectonics and volcanic components of the borate bearing Neogene basins in western Anatolia offer important insights into on the relationship between basin evolution, borate formation and mode of extension in western Anatolia. Some of the borate deposits in NE-SW trending basins developed along the İzmir-Balıkesir Transfer Zone (İBTZ) (e.g. Bigadiç, Sultançayır and Kestelek basins), and other deposits in the NE-SW trending basins which occur on the northern side of the Menderes Core Complex (MCC) are the Selendi and Emet basins. The Kırka borate deposit occurs further to the east and is located in a completely different geological setting (Figs. 11.1, 11.2, and 11.3). The region has experienced several tectonic events including subduction, obduction, continental collision and subsequent crustal thickening, extension and crustal thinning that occurred between several continental blocks and suture zones (Fig. 11.1). These were finally shaped by the Alpine orogeny related to Neo-Tethyan events (Şengör and Yılmaz 1981). The main continental blocks are, from north to the south, the Sakarya zone of the Rhodope-Pontide Fragment and the Menderes Massif of the

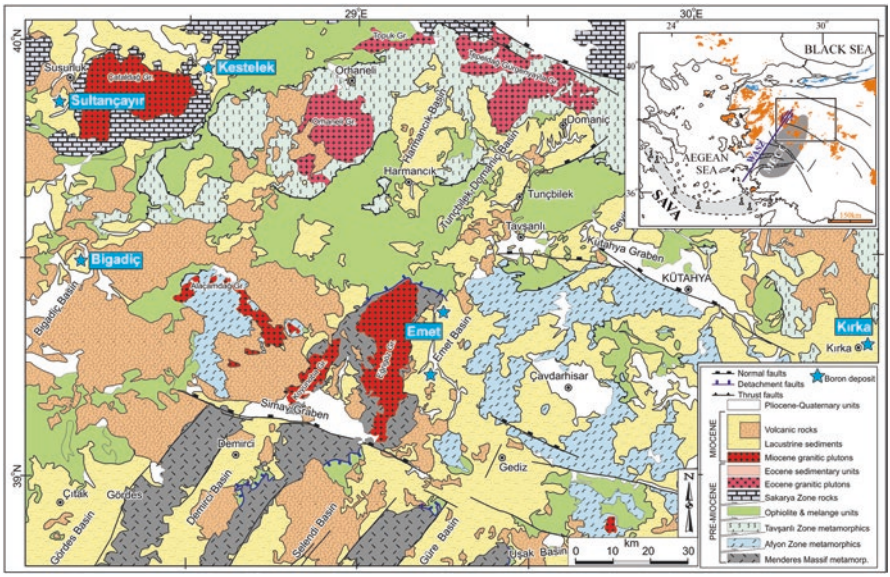

Fig. 11.2 Simplified geological map of the Neogene located NE of the Menderes Massif. The numbers in squares indicate published age data of the Miocene volcanic rocks with the references in parenthesis: (1) Seyitoğlu (1997a, b); (2) Ersoy et al. (2012a, b); (3) Çoban et al. (2012); (4) Ersoy et al. (2010); (5) Karaoğlu et al. (2010); (6) Ercan et al. (1997); (7) Prelevic et al. (2012); (8) Innocenti et al. (2005); (9) Ocakoğlu (2007); (10) Bellon et al. (1979). The age data for the granitic plutons are from Ring and Collins (2005); Hasözbek et al. (2011); Altunkaynak et al. (2012) and references therein

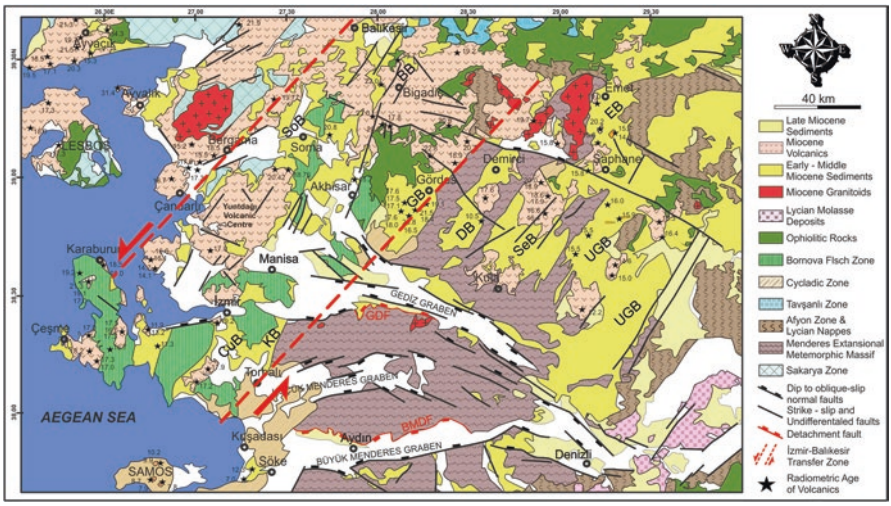

Fig. 11.3 Geological map of western Anatolia showing the distribution of the Neogene basins, radiometric ages of the volcanic intercalations in the Neogene sediments and major structures (Modified from 1/500,000 scaled geological map of Turkey (MTA); and studies cited in the text). Abbreviations for granitoids: *EyG* Eybek, *KzG* Kozak, *AG* Alaçamdağ, *Kog*, Koyunoba, *EG* Eğrigöz, *BG* Baklan, *TG* Turgutlu and *SG* Salihli granitoids. Abbreviations for basins: *KB* Kocaçay Basin, *BB* Bigadiç Basin, *CuB* Cumaovası Basin, *SoB* Soma Basin, *GB* Gördes Basin, *DB* Demirci Basin, *SeB* Selendi Basin, *UGB* Uşak–Güre Basin, *EB* Emet Basin. Abbreviations for detachments: *GDF* Gediz (Alaşehir) Detachment Fault, *SDF* Simav Detachment Fault, *BMDF* Büyük Menderes Detachment Fault. (After Ersoy et al. 2014)

Anatolides. These two blocks are separated by the İzmir-Ankara zone that is represents closure of a northward subducted Neo-Tethyan oceanic realm. The Menderes Massif is also overlain by the Lycian Nappes to the south. The İzmir-Ankara zone was formed by late Paleocene to early Eocene closure of the northern branch of the Neo-Tethys Ocean between the Sakarya continent and the Anatolide block, with the latter including the Menderes Massif and the Lycian Nappes (Şengör 1984; Şengör and Yılmaz 1981; Okay et al. 1996). The Menderes Massif is tectonically overlain by several nappes of the İzmir-Ankara Zone to the west and north, and by the Lycian nappes mainly to the south and east. In the west, the nappes are generally composed of graywackes and limestones with ophiolitic rocks of the Bornova flysch zone, while to the northeast, they are metaclastics, metabasites, and recrystallized limestones of the Afyon zone (Fig. 11.1).

Western Turkey is one of the most famous regions in the world that have been studied in respect of scientific, economic and historical aspects (Helvacı and Yağmurlu 1995; Helvacı and Alonso 2000; Ersoy et al. 2014). The geological history of western Anatolia is related to Alpine-contractional and subsequent-extensional tectonic activities. The region also contains several industrial raw-material deposits (borates, zeolites, clays, coal etc.) and metallic ore deposits (Au, Ag, Pb, Zn etc.) (Helvacı and Yağmurlu 1995). These commercial deposits are

mainly related to Alpine extensional tectonics that occurred after Oligocene time. This time interval is marked by intense crustal deformation, plutonic-volcanic activity and terrestrial sedimentation; accompanied by formation of metallic deposits and industrial minerals such as gold, silver and borates (Helvacı and Alonso 2000; Yiğit 2009). The areas located in a region that hosts both gold and borate deposits in the Neogene volcano-sedimentary rock units, and the borate deposits are the subject of this paper.

11.2.1 General Outlines of the Neogene Basins Hosting Borate Deposits in Western Anatolia

Western Anatolia has been the focus of many geological studies of the extensional tectonics in this region. The NE–SW-trending Neogene volcano-sedimentary basins that characterize western Anatolia, are mainly located on the northern part of the Menderes Massif – a progressively exhumed mid-crustal metamorphic unit that has undergone Neogene extensional tectonics in the area (Yılmaz et al. 2000; Helvacı et al. 2006; Ersoy et al. 2014). The NE–SW-trending basins are Bigadiç, Gördes, Demirci, Selendi, Emet, Güre and Uşak basins. Many studies have been carried out in these basins and different evolutionary models have been proposed by various authors for the stratigraphic and tectonic evolution of these NE–SW-trending volcanosedimentary basins. The NE–SW-trending basins were deformed by NE–SW and NW–SE-trending faults during the late Miocene, and by E–W-trending normal faults in the Pliocene–Quaternary. The region has been extended in an N–S-direction since at least the early Miocene, and that this extension occurred episodically in several phases (Helvacı et al. 2006; Ersoy et al. 2014).

The stratigraphy, tectonics and volcanic components of the Neogene basins in western Anatolia offer some key insights into the relationship between the basin evolution and mode of extension in this intensely and chaotically deformed and extended area. With the present-day configurations, two main types of Neogene basins are recognized in the western Anatolia: (a) NE–SW and (b) ~E–W trending basins. Stratigraphy and tectonic features of the NE-SW trending basins reveal that their evolution was more complex. The E–W-trending basins are typical grabens which are still being deformed under ~N–S-extension (Ersoy et al. 2014).

The NE–SW-trending basins which occur on the northern side of the Menderes Core Complex (MCC), are the Demirci, Selendi, Uşak-Güre and Emet basins. The basins, formed on the MCC were evolved as successive supra-detachment basins and include two main sedimentary sequences: the early Miocene Hacıbekir Group and the early-middle Miocene İnay Group (Bozkurt 2003; Helvacı et al. 2006; Ersoy et al. 2011). There are also NE–SW-trending basins developed along the İzmir-Balıkesir Transfer Zone (İBTZ) (e.g., Kestelek, Sultançayır, Bigadiç and Gördes basins) (Helvacı et al. 2006; Ersoy et al. 2012a, b).

11.2.2 Volcanism of Neogene Basins in Western Anatolia

Exhumation of the Menderes Massif resulted in the formation of several NE–SW-trending basins on its northern flank (the Demirci, Selendi, Güre and Emet basins), and related basin formation along the İzmir-Balıkesir Transfer Zone in the west of Gördes basin (Bozkurt 2003; Helvacı et al. 2006; Ersoy et al. 2011). The Miocene volcanic rocks occur in NE–SW-trending supra-detachment basins developed on the metamorphic rocks of the Menderes Massif (Yılmaz 1990; Yılmaz et al. 2000; Helvacı et al. 2009; Karaoğlu et al. 2010; Ersoy et al. 2010, 2011, 2012a, b).

The geological evolution of western Anatolia during Neogene time is characterized by basin formation and contemporaneous wide-spread volcanic activity. The basins in the region were developed mainly in two directions: NE- and E–W-trends (Fig. 11.3). The main NE-trending basins are Bigadiç, Gördes, Demirci, Selendi and Uşak-Güre basins, while the E–W-trending basins are characterized by actively deforming grabens such as the Simav, Gediz, Büyük Menderes and Küçük Menderes grabens. The E–W-trending basins are younger in age and cut the NE-trending basins (Fig. 11.3). The NE-SW trending basins host the world class huge borate deposits, which are the main subject of this paper. The western Anatolian extensional basins are also rich in terms of geothermal energy resources due to their extensional tectonic setting and high heat flow (Çemen et al. 2014).

In western Anatolia, volcanic rocks from the latest Oligocene to Quaternary can be divided into two groups based on their chemical composition with temporal and spatial distribution (Yılmaz 1990; Güleç 1991; Seyitoğlu and Scott 1992; Ercan et al. 1997; Seyitoğlu 1997a, b; Yılmaz et al. 2000; Aldanmaz et al. 2000; Helvacı et al. 2009). The magmatic rocks of the Late Oligocene – Early Miocene time are mainly rhyolite to basaltic andesite in composition and exhibit calc-alkaline and shoshonitic affinity. These rocks are enriched in HREE with respect to LILE and LREE, and have higher $^{87}Sr/^{86}Sr$ and lower $^{143}Nd/^{144}Nd$ isotopic composition (e.g., Bingöl et al. 1982; Güleç 1991; Aldanmaz et al. 2000). There is a time break in volcanic activity from the end of the Middle Miocene to beginning of the Late Miocene in western Anatolia (Yılmaz 1990). The volcanic rocks of mainly Late Miocene – Early Pliocene and are more basic in composition and exhibit an alkaline character. These rocks are depleted in HREE and enriched in LILE, HFSE, MREE and LREE. The volcanic rocks of the Late Miocene – Early Pliocene exhibit lower $^{87}Sr/^{86}Sr$ and higher $^{143}Nd/^{144}Nd$ isotopic ratios (Güleç 1991; Aldanmaz et. 2000). In addition, the alkaline basaltic volcanism in the Miocene-Pliocene changed from a potassic to a sodic character (Kula volcanics: Güleç 1991; Alıcı et al. 2002).

The geologic evidence indicates that the evolution of the magmatic activity in the region was related to post-collisional extensional tectonics and that the Miocene volcanic rocks in the NE–SW trending basins were emplaced during early-middle Miocene episodic exhumation of the Menderes Massif as a core complex. The Menderes Massif was asymmetrically uplifted and collapsed, starting from the north and continuing to the south during the early to middle Miocene. The high-K calc-alkaline, shoshonitic, and ultrapotassic volcanic rock groups were produced

during this interval in the region. Geochemical data show that the origin of the high-K calc-alkaline volcanics include crustal contributions to the mantle-derived magmas. While rhyolites dominated during the early Miocene, andesites are seen during the middle Miocene. At the same time, rapid increase in the amount of the ultrapotassic and shoshonitic volcanic rocks is compatible with lithospheric thinning (Ersoy et al. 2012a, b).

In the NE-trending basins, the late Cenozoic volcanic activity is represented mainly by Early-Middle Miocene calc-alkaline moderate to felsic volcanic rocks and Plio-Quaternary alkaline volcanism. In addition to these, in the Bigadiç Basin, Early Miocene alkali basaltic volcanism has been documented (Helvacı and Erkül 2002; Helvacı et al. 2003; Erkül et al. 2005b). To the east, the data show that the alkaline volcanism had already begun in the Early Miocene in the NE-trending basins, and alkaline lamproitic volcanic rocks were also introduced (Ersoy and Helvacı 2007). Volcanic intercalations in the NE–SW-trending Neogene volcano-sedimentary basins can be grouped as: early Miocene high-K calc-alkaline andesite, dacite and rhyolite; early-Miocene mafic volcanics; middle Miocene high-K calcalkaline andesite and dacite; middle Miocene mafic volcanics; Late Miocene mafic lavas; and Quaternary alkali basaltic volcanism.

Early-Miocene mafic volcanic units in Bigadiç basin comprise the Gölcük basalt (calc-alkaline shoshonite), which differs from the other early-Miocene mafic samples of the Selendi and Emet basins that have higher K contents (shoshonitic to ultrapotassic Kuzayır lamproite and Kestel volcanics). The early Miocene volcanism in all the NE–SW-trending basins is characterized by a bimodal volcanic association, dominated by calc-alkaline dacitic–rhyolitic members. During the early Miocene, wide-spread dacitic-rhyolitic volcanism occurred in the region (Helvacı and Erkül 2002; Erkül et al. 2005b; Ersoy and Helvacı 2007). The middle Miocene volcanism in the region is characterized by a second-stage bimodal volcanic association, including a group of high-K calc-alkaline to andesites and dacites, and a group of shoshonitic to ultrapotassic mafic products such as lamproites, ultrapotassic shoshonites and ultrapotassic latites. These volcanic rocks interfinger with the Middle Miocene İnay Group in the Demirci, Selendi, Güre and Emet basins (Ersoy and Helvacı 2007).

During the late Miocene a series of volcanic rocks (comprising mildly alkaline basalts, K-trachybasalt and shoshonites) were produced which are characterized by the absence of the felsic magmas, and occur only in the Demirci and Selendi basin. Finally, the Quaternary is represented by the strongly alkaline basaltic (tephrite, basanite, phonotephrite) volcanic activity emplaced on the northern flank of the Gediz graben (Kula volcanics).

The Neogene volcanic activity in western Anatolia was developed contemporaneously with development of NE-trending basins, giving rise to formation of thick volcano-sedimentary successions and several mineral deposits. In this respect, tectonic evolution of the Neogene basins, especially of the NE-trending ones, is a fundamental theme in studying the Neogene volcanic evolution as well as the related mineral deposits of the region. Therefore, it is clear that tectonic shaping of the

basins played a key role in the volcanic evolution and deposition of the borate and other related mineral deposits of the region (Table 11.1).

The Miocene borate deposits of western Turkey are associated with extensive medium- to high-K calc-alkaline ignimbritic volcanism and a differentiated comagmatic alkaline trachybasalt–trachydacite lava suite. Ignimbritic air-fall and reworked pumiceous clastic materials are intimately associated with the lake sediments that host the borate deposits. Local ignimbritic volcanism is considered to be the primary source of the B for the Kırka and other borate deposits. The geochemical composition of the ignimbrites associated with the borates exhibit a number of features that might prove useful in the exploration for borates in similar volcanic domains. In particular, 'fertile' ignimbrites generally belong to a high-K calc-alkali suite, are well-evolved and fractionated (Kr/Rb is low) with a high-silica rhyolitic bulk composition, exhibit a combined high content of B, As, F, Li and Pb, with high Br/La and Br/K ratios, and a mildly fractionated REE pattern and large positive Eu anomaly (Floyd et al. 1998). Other apparent discriminants involving both compatible and incompatible elements are largely a function of different degrees of partial melting and fractionation. It is suggested that the initial source of the B and other associated elements was from LIL-rich fluids released by the progressive dehydration of altered oceanic crust and pelagic sediments in a subduction zone. The absence or presence of sediments in a segmented subduction zone may influence the variable lateral distribution of borates in active margins on a global scale. Once the crust has become enriched in B via previous or contemporary subduction-related calc-alkali magmatism, the effects of tectonic environment, climate and hydrothermal activity influence the local development of the borate deposits (Floyd et al. 1998).

11.3 Correlations of Borate-Bearing Neogene Basins

The Neogene volcano-sedimentary succession in Bigadiç basin contains the Kocaiskan volcanics (23.6 ± 0.6–23.0 ± 2.8 Ma, Table 11.1) that are composed of andesitic volcanics and the unconformably overlying Bigadiç volcano-sedimentary succession (Fig. 11.4). The latter consists of borate-bearing lacustrine sediments and coeval felsic (Kayırlar, Sındırgı and Şahinkaya volcanics; 20.8 ± 0.7–17.8 ± 0.4 Ma K–Ar and Ar/Ar ages) and mafic (Gölcük basalt, 19.7 ± 0.4 Ma K–Ar and 20.5 ± 0.1 Ma Ar/Ar ages) volcanic rocks (Helvacı 1995; Helvacı and Alonso 2000; Helvacı and Erkül 2002; Helvacı et al. 2003; Erkül et al. 2005a, b). These rock units are unconformably overlain by late Miocene–Pliocene continental sediments consisting of detritus and alluvium. The radiometric ages and the stratigraphic relationships clearly indicate that the borate-bearing succession was deposited during the early Miocene.

The NE–SW-trending Gördes basin contains a similar volcanosedimentary sequence to that of Bigadiç basin. These two basins contain an early Miocene volcano-sedimentary sequence. The Bigadiç and Gördes basins are characterized by

Table 11.1 Radiometric age data from the volcanic rocks associated with the borate bearing Neogene basins in western Anatolia

Basin and unit	Sample	Rock type	Radiometric age (Ma), material	References
Kestelek basin				
	KE-1	Trachandesitic tuff	17.4 ± 0.3 (hornblende, K/Ar)	Helvacı and Alonso (2000)
Sultançayır basin				
	S-1	Rhyolitic tuff	20.0 ± 0.5 (feldspar, K/Ar)	
Bigadiç basin				
Kocaiskan volcanics	F-110	Andesite	23.00 ± 2.80 (biotite, K–Ar)	Helvacı and Erkül (2002), Helvacı et al. (2003), and Erkül et al. (2005a, b)
Gölcük basalt	F-199	Shoshonite	19.70 ± 0.40 (groundmass, Ar–Ar)	
	F-199	Shoshonite	20.50 ± 0.10 (groundmass, Ar–Ar)	
Sındırgı volcanics	F-194	Rhyolite	20.20 ± 0.50 (biotite, Ar–Ar)	
	F-197	Dacite	20.30 ± 0.30 (biotite, Ar–Ar)	
Şahinkaya volcanics	F-195	B. andesite	17.80 ± 0.40 (hornblende, K–Ar)	
Kayırlar volcanics	F-214	Latite	20.60 ± 0.70 (biotite, K–Ar)	
Çamköy basalt	B-6	Basalt	18.30 ± 0.20 (feldspar, K–Ar)	Helvacı (1995)
Selendi basin				
Eğreltidağ volcanics	SE-1	Rhyolite	18.90 ± 0.60 (biotite, K–Ar)	Seyitoğlu (1997a, b)
	521	Dacite	18.90 ± 0.10 (plagioclase, Ar/Ar)	Helvacı and Ersoy (2006), Helvacı et al. (2012), and Ersoy et al. (2008)
	521	Acidic tuff	20.00 ± 0.20 (amphibole, Ar/Ar)	
Kuzayır lamproite	518	Lamproite	17.90 ± 0.20 (groundmass, Ar/Ar)	
	518	Lamproite	18.60 ± 0.20 (phlogopite, Ar/Ar)	
Yağcıdağ volcanics	SE-3	Trachydacite	14.90 ± 0.60 (biotite, K–Ar)	Seyitoğlu (1997a, b)
	S1/3	Acidic tuff	16.42 ± 0.99 (feldspar, Ar/Ar)	Purvis and Robertson (2005)
	YF-2	Dacite	16.43 ± 0.32 (plagioclase, Ar/Ar age)	Helvacı and Ersoy (2006), Helvacı et al. (2006), and Ersoy et al. (2012a, b)

(continued)

Table 11.1 (continued)

Basin and unit	Sample	Rock type	Radiometric age (Ma), material	References
Emet basin and Gediz–Şaphane region				
Akdağ volcanics	E6	Rhyolite	20.20 ± 0.40 (biotite, K/Ar)	Seyitoğlu (1997a, b)
	E-3	Rhyolite	19.00 ± 0.20 (biotite, K/Ar)	Helvacı and Alonso (2000)
Köprücek volcanics	E-1	Pyroclastic	16.80 ± 0.20 (biotite, K/Ar)	
Dereköy basalt	E9	UK latite	15.40 ± 0.20 ± (feldspar, K/Ar)	
	E3	UK latite	14.90 ± 0.60 (whole rock, K–Ar)	Seyitoğlu (1997a, b)
	So7-15	UK latite	15.70 ± 0.50 (whole rock, K–Ar)	Çoban et al. 2012
Kestel volcanics	821	UK latite	15.91 ± 0.07 (biotite, Ar/Ar)	Helvacı and Ersoy (2006), Helvacı et al. (2006), and Ersoy et al. (2012a, b)
	821	UK latite	15.73 ± 0.11 (biotite, Ar/Ar)	
Kırka basin				
	K-2(1)	Rhyolite	18.5 ± 0.2 (biotite, K/Ar)	Helvacı and Alonso (2000)
	K-2	Rhyolitic ignimbrites	19.0 ± 0.2 (biotite, K/Ar)	
	2a-1 (K1-955.8 m)	Basalt	18.63 ± 0.2 (New Ar/Ar data)	Helvacı and Yücel-Öztürk (2013) and Seghedi and Helvacı (2014)
	2a-2 (K6-1063 m)	Trachyte	18.69 ± 0.04 (New Ar/Ar data)	
	2c	Lamproite lavas	16.91 ± 0.05 (New Ar/Ar data)	
	2d(K-1)	Trachyte	16.1 ± 0.2 (feldspar, K/Ar)	

early Miocene volcano-sedimentary successions which were deposited along early Miocene strike-slip and related normal faults (Ersoy et al. 2012a, b). The Demirci, Selendi, Emet and Güre basins have similar stratigraphic, geochemical and tectonic characteristics. The basin-fill of these Neogene basins are; (a) Lower Miocene Hacıbekir Group, (b) Middle Miocene İnay Group, (c) locally developed late Miocene sedimentary and basaltic volcanic rocks and (d) Quaternary sediments and basaltic volcanics, which are separated by regional-scale major unconformities (Fig. 11.4; Ercan et al. 1978, 1983; İnci 1984; Seyitoğlu 1997a, b; Yılmaz et al. 2000; Ersoy and Helvacı 2007; Ersoy et al. 2010).

The NE–SW-trending Selendi, Emet and Güre basins, which developed on the Menderes Core Complex, have similar lithostratigraphies that comprise two main volcano- sedimentary successions: the Lower Miocene Hacıbekir Group, and the

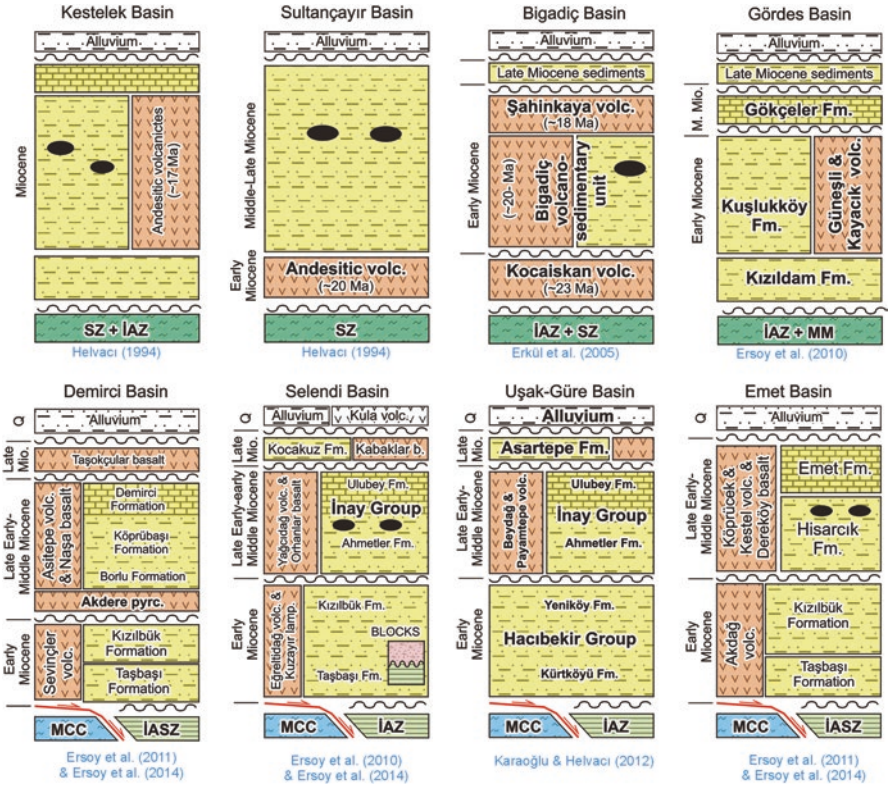

Fig. 11.4 Stratigraphic columns of the borate bearing basins in Western Anatolia. *MM* metamorphic rocks of the Menderes Massif, *İAZ* İzmir-Ankara zone rocks, *SZ* metamorphic rocks of the Sakarya zone, *MCC* Metamorphic Core Complex. (Modified after Ersoy et al. 2014)

unconformably overlying Middle Miocene İnay Group. These two groups are locally overlain by late Miocene volcanic and sedimentary units and recent sediments. The Lower Miocene Hacıbekir Group in the Demirci, Selendi, Emet and Güre basins was deposited in a supra-detachment basin formed on the Simav detachment fault (SDF). The Hacıbekir Group consists of conglomerates of the Kürtköyü Formation and sandstone–mudstone alternations of the Yeniköy Formation in the Demirci, Selendi and Güre basins and Taşbaşı and Kızılbuk formations in the Emet basin. The İnay Group is intercalated with several syn-sedimentary andesitic to rhyolitic lava flows, dykes and associated pyroclastics in the Selendi, Emet and Gördes basins.

In the Emet basin, the Köprücek volcanics (16.8 ± 0.2 Ma K–Ar age; Helvacı and Alonso 2000) crop out to the northern part of the Emet basin. The unit is composed of andesitic to rhyolitic lava flows, dykes and associated pyroclastics which interfinger with the Hisarcık Formation. The Köprücek volcanics are overlain by the limestones of the Emet Formation. The thickness of the pyroclastic intercalations in the Hisarcık Formation increases towards the north of the basin (Helvacı

and Ersoy 2006; Helvacı et al. 2006; Ersoy et al. 2012a, b; Figs. 11.3 and 11.4). In the southern part of the basin, the Hisarcık Formation is also conformably overlain by basaltic lava flows of the Dereköy basalt. Along the basal contact of the Dereköy basalt several pepperitic textures are developed, indicating a syn-sedimentary emplacement of the lavas. The Dereköy basalt has been dated as 15.4 ± 0.2 and 14.9 ± 0.3 Ma (K–Ar ages, Seyitoğlu 1997a, b; Helvacı and Alonso 2000; Table 11.1). The Kırka borate deposit occurs further to the east and is located in completely different geological setting and volcanostratigraphic succession.

As far as the economic potential of Neogene basins is concerned, a limited number of basins in western Turkey contain world class borate reserves, with mineralization present as stratabound deposits in Neogene volcano-sedimentary successions. These sediments, as well as being enriched in B, are also variably enriched in Li, S, Sr and As. Potential sources for these elements include lacustrine sediments, local basement rocks and volcanics with hot spring activity. Volcanism occured throughout the sedimentary infilling of these basins, as shown by the presence of tuffaceous sediments, volcanic clasts in conglomerates, interbedded and cross cutting lavas and travertines from hot spring activity. Data from Bigadiç, Emet and Kırka basins show that early volcanism is felsic and largely calc alkaline, although sometimes alkaline, whereas later volcanism is intermediate and exclusively alkaline. K-Ar dating of volcanic samples from the borate basins indicate that the first phase of volcanism occurred in the Early Miocene with the second phase in the Middle Miocene. Field evidence from the basins indicates that the felsic volcanism occurred prior to and during borate mineralisation whilst the intermediate alkaline volcanism occurred later. Correlation of the geochemical characteristics of the volcanic units will help us to understand the interrelationships between the formation of the borate deposit and volcanic evolution of the region.

In order to establish the role of local volcanism as a source of boron, the relationship between volcanism and associated sediments in the Emet (colemanite and probertite deposit), Bigadiç (colemanite and ulexite) and Kırka (borax deposit) basins were studied together with a study volcanic rocks associated with the borate deposits of Kırka, Emet, Bigadiç, Kestelek and Sultançayır districts have been performed. The geochemical work focussed on boron and trace elements distribution on volcanics belonging to two main stages of magmatic activity. High boron contents have been found in volcanics surrounding the borate deposits. The volcanics of Lower-Middle Miocene age are mainly andesites to rhyolites of calk-alkaline affinity and show a range in B from 25 to 270 ppm. Consistently lower values (19–67 ppm) are shown by volcanites of Upper Miocene age (Helvacı 1977; Fytikas et al. 1984; Floyd et al. 1998; Helvacı and Alonso 2000) having shoshonitic and potassic affinities. In the light of the present data the high B contents in these rocks can be explained by interaction between the volcanics and circulating boron-rich hot water. Presence of widespread secondary minerals (e.g. zeolites, calcites) supports the hypothesis of interaction with circulating shallow level water. Magmatic activity may have been responsible for generating a high thermal gradient in the study area which provided the energy to drive thermal circulating water that was

able to mobilize boron from sedimentary and volcanic sequences. An alternative hypothesis for generating such borate deposits is suggested by the presence in several deposits of volcanic rocks interfingered with sediments forming peperitic textures. This indicates there may have been direct contributions of volcanics and magmatic volatiles to the lacustrine basins.

11.3.1 Bigadiç, Susurluk and Kestelek Basins

The basin-fill that lies unconformably above the basement rocks, includes Upper Cretaceous–Palaeocene Bornova Flysch Zone, Lower–Middle Eocene Başlamış Formation and Oligocene detrital rocks (Erdoğan 1990; Okay and Siyako 1991) and is represented by two distinct volcano-sedimentary associations separated by a basin-wide angular unconformity. Volcanism in the Bigadiç area is characterized by two different rock units that are separated by an angular unconformity. These units are: (1) the Kocaiskan volcanics that gives K/Ar ages of 23.0 ± 2.8 Ma, and (2) the Bigadiç volcano-sedimentary succession within the borate deposits that yields ages of 20.6–17.8 Ma (Fig. 11.4). Both units are Early Miocene in age and are unconformably overlain by Upper Miocene-Pliocene continental deposits (Helvacı 1983, 1995; Erkül et al. 2005b).

The Kocaiskan volcanics, which are andesitic in composition, are related to the first episode of volcanic activity and comprise thick volcanogenic sedimentary rocks derived from subaerial andesitic intrusions, domes, lava flows and pyroclastic-rocks. The unit comprises andesitic intrusions, lavas, pyroclastic rocks and associated volcanogenic sedimentary rocks, which are unconformably overlain by the Lower Miocene Bigadiç volcano-sedimentary succession (Helvacı and Erkül 2002; Helvacı et al. 2003; Erkül et al. 2005b). The Bigadiç volcano-sedimentary succession, is a Miocene sequence comprising volcanic (e.g. Sındırgı volcanics, Gölcük basalt, Kayırlar volcanics and Şahinkaya volcanics) and lacustrine rocks (e.g. lower limestone unit, lower tuff unit, lower borate unit, upper tuff unit and upper borate unit) (Helvacı 1995; Erkül et al. 2005b) (Fig. 11.4).

The second episode of volcanic activity is represented by basaltic to rhyolitic lavas and pyroclastic rocks, accompanied by lacustrine–evaporitic sedimentation. Dacitic to rhyolitic volcanic rocks, called the Sındırgı volcanites, comprise NE-trending intrusions producing lava flows, ignimbrites, and ash-fall deposits and associated volcanogenic sedimentary rocks. Other NE-trending olivine basaltic (Gölcük basalt – Early Miocene alkali basalt) and trachyandesitic (Kayırlar volcanites) intrusions and lava flows were synchronously emplaced into the lacustrine sediments. The intrusions typically display peperitic rocks along their contacts with the sedimentary rocks (Helvacı 1995; Helvacı and Erkül 2002; Helvacı et al. 2003; Erkül et al. 2005b, 2006; Fig. 11.5). The radiometric age data reveal that the formation of the Bigadiç volcano-sedimentary succession is restricted to a period between 20.6 ± 0.7 and 17.8 ± 0.4 Ma. K/Ar dating of the Sındırgı volcanics yield an age of 20.2 ± 0.5 and 19.0 ± 0.4 Ma from rhyolites and dacites, respectively (Table 11.1).

Fig. 11.5 Peperitic textures related to plagioclase-phyric trachyandesites of the Kayırlar volcanic unit, Bigadiç deposit, Turkey

The total age corresponds to a K/Ar age of an olivine-basalt sample, namely 20.5 ± 0.1 Ma, and an Ar/Ar age of 19.7 ± 0.4 Ma. The K/Ar date of the NE-trending dyke of the Kayırlar volcanites is 20.6 ± 0.7 Ma. The K/Ar dating of lavas of the Şahinkaya volcanics gave 17.8 ± 0.4 Ma. (Helvacı and Erkül 2002; Helvacı et al. 2003; Erkül et al. 2005b) (Fig. 11.6).

Geochemical data from the Bigadiç area are also related to the extensional regime, which was characterized by bimodal volcanism linked to extrusion of coeval alkaline and calc-alkaline volcanic rocks during the second volcanic episode. The formation of alkaline volcanic rocks dated as 19.70.4 Ma can be related directly to the onset of the N–S extensional regime in western Turkey. In the Bigadiç basin widespread high-K calcalkaline andesitic to rhyolitic lava flows, domes and pyroclastic rocks are interlayered with borate-bearing lacustrine deposits (Helvacı 1995; Helvacı and Alonso 2000; Erkül et al. 2005b). The ages of the intermediate to felsic volcanism lie between 23.0 and 17.8 Ma, and interlayered high-K calcalkaline shoshonites within the basin have ages of 20.5–19.7 Ma (Helvacı 1995; Erkül et al. 2005b). The volcanic unit cutting the upper borate zone in the Bigadiç Basin is assigned a late Miocene in age on the basis of its geochemical features. The geochemistry of the shoshonitic rocks in the area is similar to those of other late Miocene mafic rocks in the İzmir-Balıkesir Transfer Zone (İBTZ) (Ersoy et al. 2012a, b; Seghedi et al. 2015).

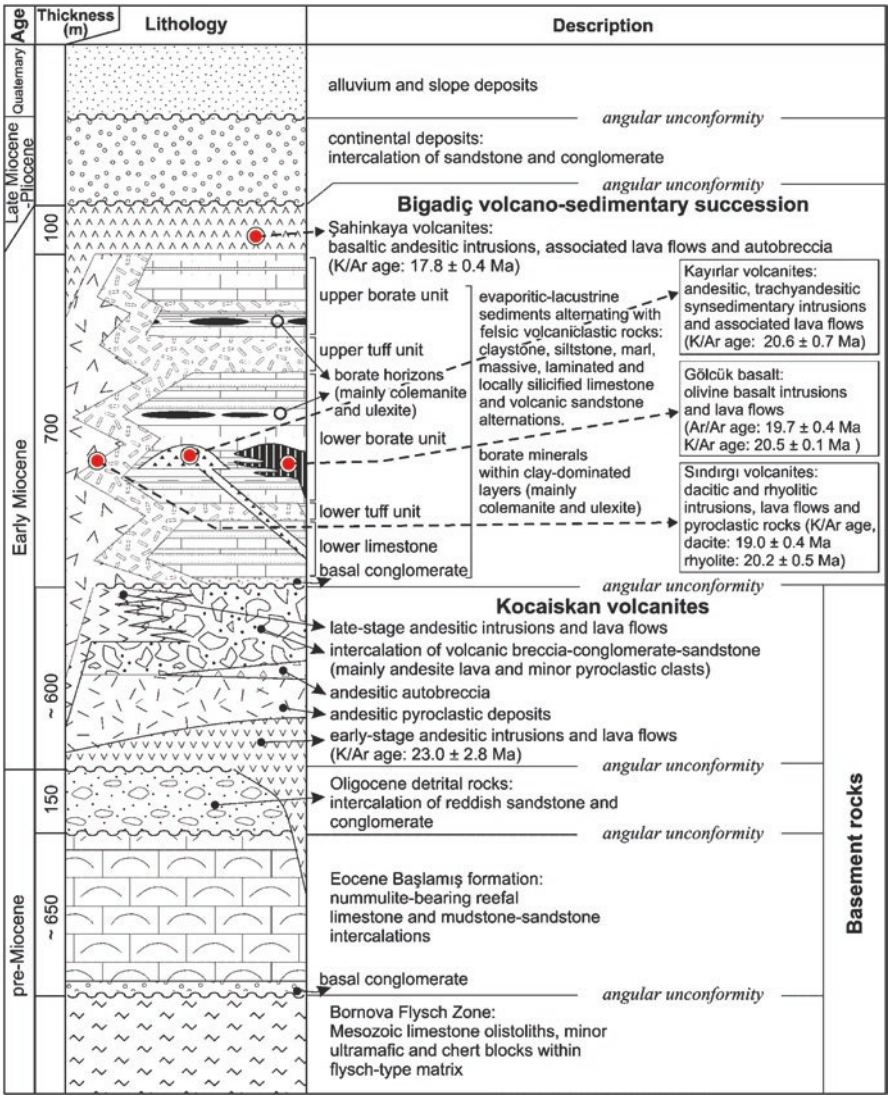

Fig. 11.6 Simplified stratigraphic column of the Bigadiç borate basin. Red dot illustrates K–Ar ages of a rock in millions of years. Numbers in parentheses indicate age data sources: Erkül et al. (2005 a,b), (2) Gündoğdu et al. (1989), (3) Krushensky (1976), (4) Helvacı (1995) and (5) Benda et al. (1974)

This early-middle Miocene volcanism continues further NE (towards Susurluk-Çaltıbük; Helvacı 1994; Helvacı and Alonso 2000; Fig. 11.1) with widespread andesitic to rhyolitic lava flows and associated pyroclastic rocks interlayered with lacustrine sediments in Sultançayır and Kestelek basins. The Miocene sequence in

the Sultançayır basin consists of the following in ascending order: andesite and agglomerate; tuff; sandy conglomerate; limestone; sandy claystone containing boratiferous gypsum, bedded gypsum and tuff; and clayey limestone (Helvacı 1994). K/Ar age dating of one tuff sample taken from the tuff unit yields an age of 20.01 Ma (Helvacı 1994; Helvacı and Alonso 2000).

The Miocene sequence in the Kestelek basin contains basement conglomerate and sandstones; claystone with lignite seams, marl, limestone, and tuff; agglomerates and volcanic rocks; the borate zone comprises clay, marl, limestone, tuff and borates; and limestones with thin clay and chert bands. The volcanic activity gradually increased and produced tuff, tuffite and agglomerate, and andesitic, trachytic and rhyolitic volcanic rocks that are interbedded with sediments. K/Ar age dating of one tuff sample taken from the borate zone yields an age of 17.4 Ma (Helvacı 1994; Helvacı and Alonso 2000) (Table 11.1, Figs. 11.3 and 11.4).

11.3.2 Selendi Basin

The Neogene stratigraphy of the Selendi Basin rests on a basement consisting of both Menderes Massif and İzmir-Ankara zone rocks (Ercan et al. 1978; Seyitoğlu 1997a, b; Ersoy and Helvacı 2007). Three volcano-sedimentary units constitute the Neogene stratigraphy and each one was accompanied by different volcanic activities (Ersoy and Helvacı 2007). At the base, the Lower Miocene Hacıbekir Group tectonically overlies the Menderes Massif and unconformably overlies the İzmir-Ankara zone rocks (Figs. 11.3 and 11.4). Two contrasting volcanic associations accompanied deposition of the Hacıbekir Group during the Early Miocene: the Eğreltidağ volcanic unit and the Kuzayır lamproite (Ersoy and Helvacı 2007). The Middle Miocene İnay Group, unconformably overlying the Hacıbekir Group consists of conglomerates, widely exposed claystone-sandstone-marl alternation and limestones. The claystone-sandstone-mudstone horizons include several borate occurrences such as howlite and colemanite (Helvacı and Alonso 2000). The İnay Group is also interfingered by two contrasting volcanic associations: the Yağcıdağ volcanic unit and the Orhanlar Basalt. These units are unconformably overlain by the Upper Miocene Kocakuz Formation and the Kabaklar Basalt. Finally, the Plio-Quaternary sediments and volcanic units unconformably overlie the older units. The final volcanic activity is represented by the Kula volcanics (Fig. 11.7). The stratigraphy of the basin is very similar to the Emet Basin. In particular, the İnay Group can be correlated with the borate-bearing units in the Emet Basin. The Yağcıdağ volcanic unit can also be correlated with the Beydağ volcanics in the Uşak-Güre Basin that include gold mineralization (Kışladağ gold deposit) (Helvacı and Ersoy 2006; Helvacı et al. 2006; Ersoy and Helvacı 2007; Ersoy et al. 2008; Helvacı 2012).

Fig. 11.7 The vent area of a lava flow, Kula volcanics, Turkey (Location: 38.6 North, 28.7650 East Altitude:551 m above sea)

11.3.3 Emet Basin

The Emet basin (Akdeniz and Konak 1979; Helvacı 1984, 1986; Fig. 11.4), is located between the Eğrigöz granitoid intruded into the Menderes Massif metamorphic rocks to the west, and the Afyon zone metamorphic rocks to the east (Figs. 11.1 and 11.2). The stratigraphy of Emet basin comprises two Neogene volcanosedimentary units separated by a regional unconformity (Fig. 11.4). These units can be correlated with similar rocks from other basins on the basis of their age, lithology and deformational features, and they are named as the Hacıbekir and İnay groups. In this basin, the İnay Group hosts the world's biggest colemanite and probertite borate deposits (Gawlik 1956; Helvacı 1984, 1986; Helvacı and Orti 1998; Helvacı and Alonso 2000; Garcia et al. 2010).

The Hacıbekir Group consists of the Taşbaşı and Kızılbük formations and the Akdağ and Kestel volcanics (Fig. 11.4). The Taşbaşı Formation crops out to the western and southwestern parts of the Emet basin, and is made up of reddish-brown colored conglomerates with grayish sandstone intercalations deposited in alluvial fan facies (Fig. 11.4). The Taşbaşı Formation is locally interfingered with rhyolitic pyroclastic rocks of the Akdağ volcanics, and is conformably overlain by the Kızılbük formation. The Akdağ volcanics have yielded 20.3 ± 0.6 (Seyitoğlu 1997a,

b) and 19.0 ± 0.2 Ma (Helvacı and Alonso 2000) K–Ar ages (Table 11.1). The Kızılbük formation crops out in a large area to the western and southwestern parts of the Emet basin, and is composed of coal-bearing yellowish sandstone–siltstone–mudstone alternations and laminated limestone of fluvio-lacustrine origin. The Kızılbük formation is interfingered with pyroclastic rocks of the Akdağ volcanics, which are composed of rhyolitic lava flows, domes, pyroclastics and epiclastics. The Kestel volcanics emplaced in a NE–SW-direction to the southwest of the basin, and are composed of syn-sedimentary mafic lava flows. These volumetrically small volcanic rocks conformably overlie the Kızılbük formation and the age of the Kestel volcanics is stratigraphically accepted to be early Miocene (Fig. 11.8).

The İnay Group in Emet basin is made up of the Hisarcık and Emet formations that interfinger with the Köprücek volcanics and the Dereköy basalt (Figs. 11.4 and 11.8). The Hisarcık formation (Akdeniz and Konak 1979) crops out in a large area in the Emet basin and is composed of conglomerates, pebblestones and sandstone intercalations. The age of the Hisarcık Formation is accepted to be middle Miocene on the basis of volcanic intercalations in the İnay Group. Towards the center of the basin, the Hisarcık Formation passes laterally into the Emet Formation that is composed of sandstone – claystone – mudstone alternations of fluvio-lacustrine origin. The fine-grained parts of the unit, especially the mudstone –claystone levels contain large borate deposits which are mined for colemanite and probably probertite in the future (Helvacı and Alonso 2000; Helvacı and Ersoy 2006; Helvacı et al. 2006; Ersoy et al. 2012a, b; Garcia-Veigas et al. 2011).

The Köprücek volcanics crop out in the northern part of Emet basin. The unit is composed of andesitic to rhyolitic lava flows, dykes and associated pyroclastics

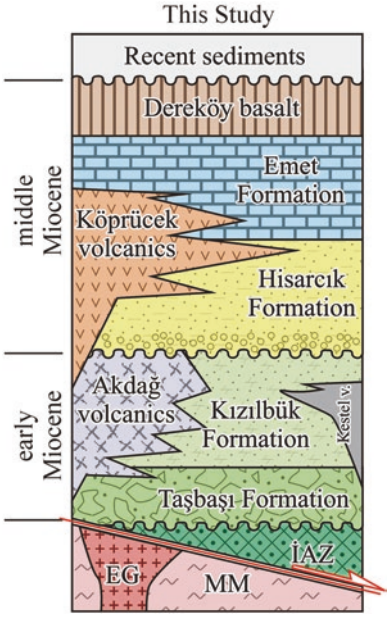

Fig. 11.8 Generalized stratigraphic section of the Emet basin (not on scale). *MM* Paleozoic Menderes Metamorphic basement, *EG* Eğrigöz Granitoid, *IAZ* carbonates and ophiolitic rocks of Izmir-Ankara Zone; Taşbaşi Formation: conglomerates; Kızılbük Formation: clastic unit containing coal; Akdag, Kestel, Köprücek and Dereköy: volcanic units; Hisarcık Formation: carbonates with clastic, and tuff deposits, containing borates; Emet Formation: upper limestone unit. (Modified after Helvacı 1984)

which interfinger with the Hisarcık Formation. The Köprücek volcanics are overlain by the limestones of the Emet formation. The pyroclastic intercalations yield 16.8 ± 0.2 Ma K–Ar age (Helvacı and Alonso 2000; Table 11.1). In the southern part of the basin, the Hisarcık Formation is also conformably overlain by basaltic lava flows of the Dereköy basalt. Along the basal contact of the Dereköy basalt several peperitic textures are developed, indicating a syn-sedimentary emplacement of the lavas. The Dereköy basalt has been dated as 15.4 ± 0.2 and 14.9 ± 0.3 Ma (K–Ar ages; Seyitoğlu 1997a, b; Helvacı and Alonso 2000) (Table 11.1 and Fig. 11.8).

The Emet borate deposits were formed in two separate basins, possibly as parts of an interconnected lacustrine playa lake, in areas of volcanic activity, fed partly by thermal springs and partly by surface streams (Helvacı and Alonso 2000). All the lavas at Emet are enriched in B (≤68 ppm), Li (≤55 ppm) and As (≤205 ppm), slightly enriched in Sr (≤580 ppm), but have relatively low levels of S (≤80 ppm). The older felsic lavas contain higher B levels than the more recent intermediate alkaline lavas. The Early Miocene felsic volcanism at Emet basin has high levels of elements associated with mineralization, as well as having a close spatial and temporal relationship with the borates and it is therefore considered a likely source. Possible mechanisms by which volcanism might supply B, S, Sr, As and Li to the basin sediments include the leaching of volcanic rocks by hot meteoric waters, the direct deposition of ash into the lake sediments, or the degassing of magmas. Thermal springs associated with local volcanic activity are thought to be the possible source of the borates (Helvacı 1977, 1984; Helvacı and Alonso 2000).

The geological data show that the Emet basin can be correlated with the Selendi and Uşak-Güre basins. In the Uşak-Güre basins, the Lower Miocene Hacıbekir Group is unconformably overlain by the Middle Miocene İnay Group that contain the Middle Miocene latitic volcanics (Beydağ volcanics). The Beydağ volcanics hosted to the biggest porphyry gold deposits (Kışladağ gold deposits) in western Turkey (Ercan et al. 1978; Seyitoğlu 1997a, b; Ersoy and Helvacı 2007; Helvacı et al. 2009; Karaoğlu et al. 2010; Helvacı 2012).

11.3.4 Kırka and Göcenoluk Basin

The Miocene sequence of the Kırka Basin, rests unconformably on a basement including Paleozoic metamorphics, Mesozoic mélange units and Eocene sediments and consists of volcanic rocks and tuffs, lower limestone with marl and tuff interbeds, borate zone, upper claystone; upper limestone containing tuff and marl with chert bands; and basalt (Arda 1969; İnan et al. 1973; Helvacı 1977; Gök et al. 1980; Sunder 1980; Palmer and Helvacı 1995) (Fig. 11.9). The stratigraphy and mineralogy of the Kırka borate deposit was revealed by (İnan et al. 1973; Helvacı 1977; Palmer and Helvacı 1995; Floyd et al. 1998; Helvacı and Alonso 2000; Helvacı and Orti 2004; Garcia-Veigas et al. 2011).

The Kırka area, a newly discovered caldera area which was not recognized before (Seghedi and Helvacı 2014), is situated in the northernmost part of the

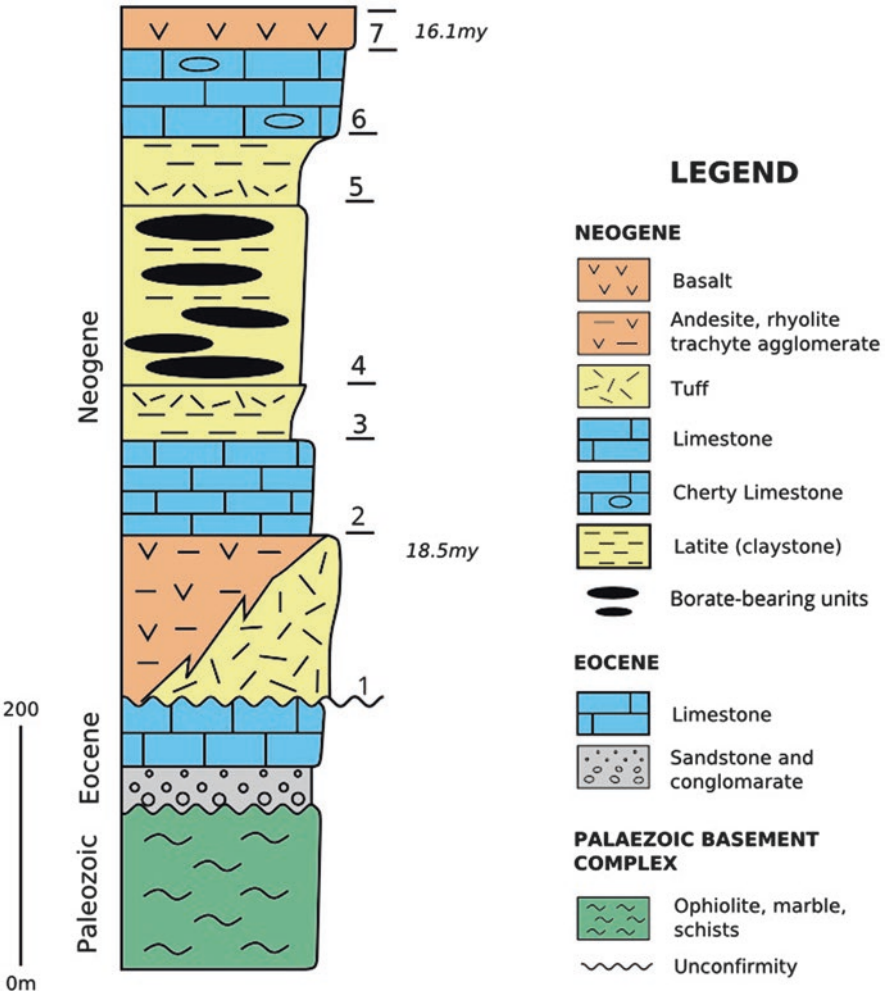

Fig. 11.9 Stratigraphic column of the Kırka borate deposit. Neogene rock units: (1) Tuffs, (2) Lower limestone, (3) Lower clay, marl and tuff, (4) Borate unit, (5) Upper clay, tuff, marl and coal bands, (6) Upper cherty limestone, (7) Basalt. (After Inan et al. 1973; Helvacı 1977; Sunder 1980)

Miocene Eskişehir–Afyon volcanic area (EAV). It is well known and the largest in the world for its borate deposits (e.g., İnan et al. 1973; Helvacı 1977, 2005; Kistler and Helvacı 1994; Helvacı and Alonso 2000; Helvacı et al. 2012; García-Veigas and Helvacı 2013). The caldera, which is roughly oval (24 × 15 km) in shape, is one of the largest in Turkey and is thought to have been formed in a single stage collapse event, at ~19 Ma that generated huge volume extracaldera outflow ignimbrites (Floyd et al. 1998; Seghedi and Helvacı 2014). It was recognized that the borates formed in closed system environments and were connected with thick calc-alkaline volcano-sedimentary successions associated with marls, mudstones, limestones and

sandstones. Recent exploratory drilling in the Göcenoluk area intersected a thick succession of dolostones, tuffs and three borate-bearing units (Lower, Intermediate and Upper Borate Units) (Fig. 11.10).

The most extensive volcanic deposits related to caldera formations are represented by ignimbrites distributed all around the caldera (Floyd et al. 1998) (Figs. 11.11 and 11.12). However, the most well-preserved outflow pyroclastics are dominantly distributed toward the south of caldera (Floyd et al. 1998). The base of the volcanic sequence seems to be exposed at the structural margin of the caldera and sometimes associated with lag breccias. Field observations allowed an estimate of the exposed thickness of 160–200 m that includes the caldera-forming ignimbrites (Floyd et al. 1998). The slightly to moderately welded ignimbrite facies is less well-represented toward east, north and west outside of caldera and always associated with thick fall-out deposits. The ignimbrites are also associated with fall-out deposits. The trachyte domes largely developed as two main structures elongated N-S at the northern margin of caldera (10–15/7 km) and cover the caldera-related ignimbrites and associated deposits, the rhyolite domes, as well the basement deposits. The northern slopes of both the trachytic tuff deposits and lamproitic lava flows are covered by Late Miocene limestones. The reconstruction of intra-caldera deposits are based on the outcrop exposures and drillings (Seghedi and Helvacı 2014).

Large rhyolitic ignimbrite occurrences are closely connected to the Early Miocene initiation of extensional processes in central-west Anatolia along the Tavşanlı-Afyon zones (Floyd et al. 1998) (Figs. 11.1 and 11.9). Field correlations, petrographical, geochemical and geochronological data lead to a substantial reinterpretation of the ignimbrites surrounding Kırka area, known for its world-class borate deposits, as representing the climatic event of a caldera collapse, unknown up to now and newly named the "Kırka-Phrigian caldera". Intracaldera post-collapse sedimentation and volcanism (at ~18 Ma) was controlled through subsidence-related faults with generation of a series of volcanic structures (mainly domes) showing a large compositional range from saturated silicic rhyolites and crystal-rich trachytes to undersaturated lamproites (Fig. 11.9, Table 11.1). The volcanic rock succession provides a direct picture of the state of the magmatic system at the time of eruptions that generated caldera and post-caldera structures and offer an excellent example of silicic magma generation and associated potassic and ultrapotassic intermediate-mafic rocks in a post-collisional extensional setting (Seghedi and Helvacı 2014).

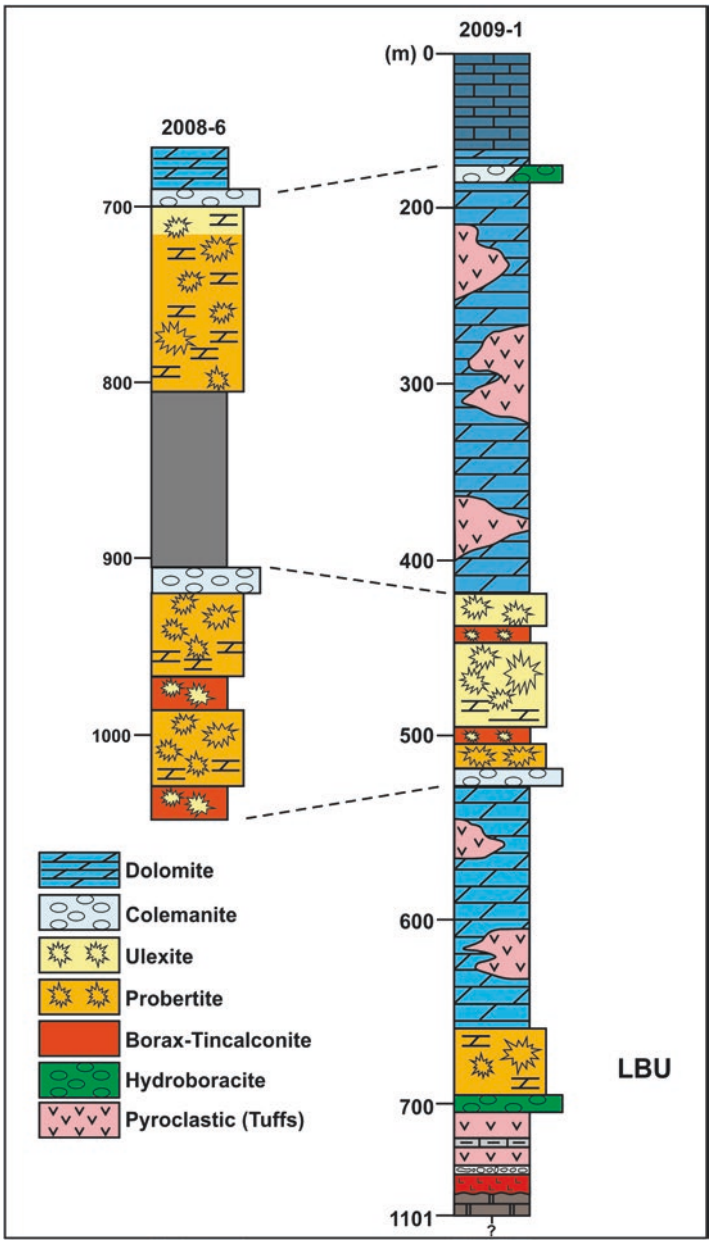

Fig. 11.10 Lithological borehole log correlation of Göcenoluk 2008–6 and Göcenoluk 2009–1 boreholes based on mineral associations. *UBU* Upper Borate Unit, *IBU* Intermediate Borate Unit, *LBU* Lower Borate Unit

Fig. 11.11 Extensive and spectacular ignimbrites outcrops nearby the Kırka borate deposit

Fig. 11.12 Close view of typical ignimbritic rocks near the Kırka area

11.4 Depositional Model and Mineralogy of Borate Deposits

11.4.1 Depositional Model of Borate Deposits

The most important economic deposits are closely related to Tertiary volcanic activity in orogenic belts. They are situated close to converging plate margins; characterized by andesitic-rhyolitic magmas; arid or semi-arid climates; and non-marine evaporite environments. Turkish, United States, South American and many other commercial borate deposits are non-marine evaporites associated with volcanic activity. Major borate deposits are found in tectonically active extensional regions associated with collisional plate boundaries (Ozol 1977; Jackson and McKenzie 1984; Floyd et al. 1998; Helvacı 2005, 2015) (Fig. 11.13). Commercial borate deposits in the USA, South America, and Turkey are thought to be associated with Neogene continental sediments and volcanism.

The formation of borate deposits can be tentatively summarized into three main types as follows (Fig. 11.14): (1) a skarn type associated with intrusives and consisting of silicates and iron oxides; (2) a magnesium oxide type hosted by marine evaporitic sediments; and (3) a sodium and calcium borate hydrates type associated with lacustrine (playa lake) sediments (non-marine basins) and explosive volcanic activity.

The borate minerals in the non-marine lacustrine basins were generated in saline lakes emplaced in volcanogenic (mainly pyroclastic) terrains with intense hydrothermal influence, under arid to semi-arid conditions, and in some cases at low temperatures. The following conditions are essential for the formation of economically viable borate deposits in playa lake volcanosedimentary sediments (Fig. 11.15): (a) formation of playa lake environment; (b) boron concentration in playa lake sourced from from andesitic to rhyolitic volcanics, direct ashfall into the basin or hydrothermal solutions along graben faults; (c) thermal springs nearby volcanism; (d) arid to semi-arid climatic conditions; and (d) pH of lake water between 8,5 and 11.

The formation of large economic borate deposits requires a boron-rich source and a means of transporting and concentrating the boron in a restiricted environment. An arid to semiarid climate also seems to be essential during the deposition and concentration of economic amounts of soluble borates in the basin in which they can collect. These soluble borates can, in the long run, be preserved only by burial; however, the lack of deposits of soluble borates older than mid-Tertiary may indicate that even burial is not able to protect borates over long periods of geological time. Where a degree of concentration does occur, it is usually a result of local volcanic activity (as a source of boron), a body of water such as a lake (to dissolve boron compounds), evaporative conditions (to concentrate the solution to the point of precipitation), and the deposition of a protective layer of sediment (to preserve the highly soluble borate minerals).These conditions are present in collisional tectonic settings, for which western Anatolia is a prime example in collision-related tectonic events in ancient mobile belts (Figs. 11.13 and 11.15).

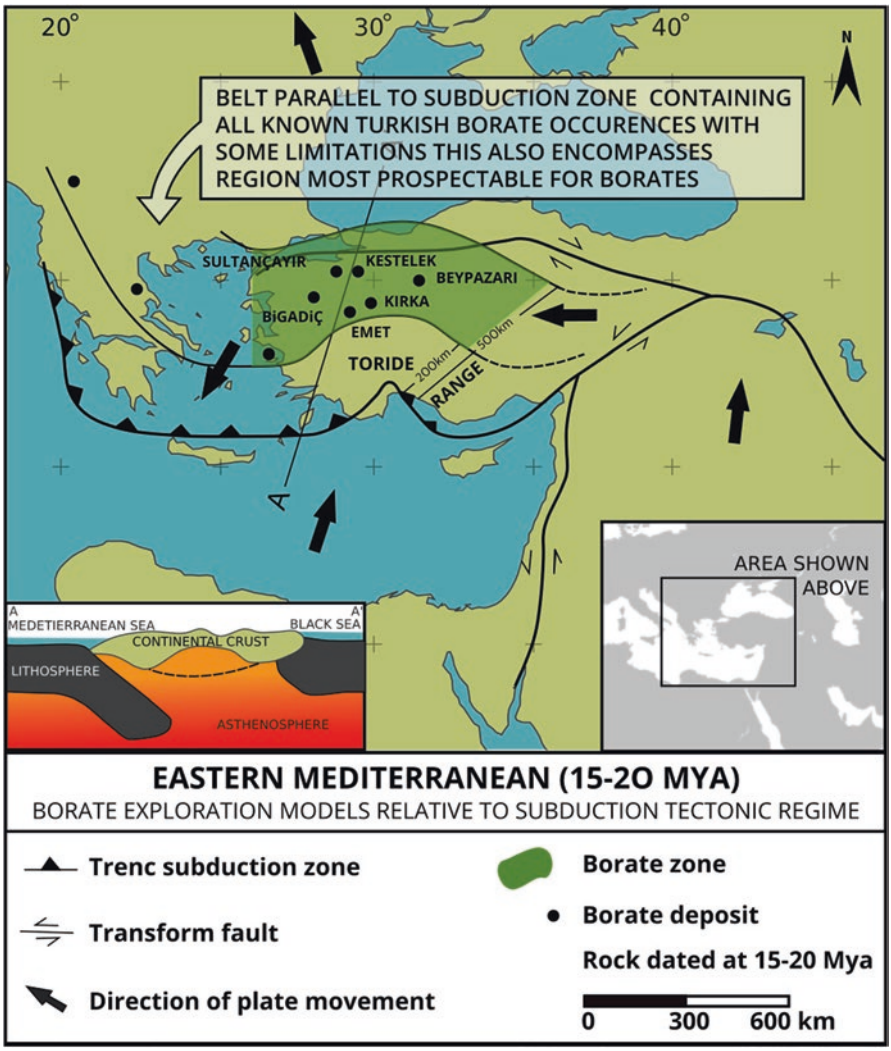

Fig. 11.13 Known deposits and borate exploration model according to the subduction tectonic model for Eastern Mediterranean (15–20 My)

The largest borate deposits that originated as chemical precipitates are found interbedded with clays, mudstones, tuffs, limestones, and similar lacustrine sediments. There is a strong evidence that most of these deposits were closely related in time to active volcanism. Thermal springs and hydrothermal solutions associated with volcanic activity are regarded as the most likely source of the boron (Fig. 11.15). The Konya-Karapınar basin (Turkey) is surrounded by volcanes which have been active from the Late Miocene to recent. Active volcanism is evidenced by the discharge of thermal and mineral waters and magmatic gases. Na, B, Cl, SO_4

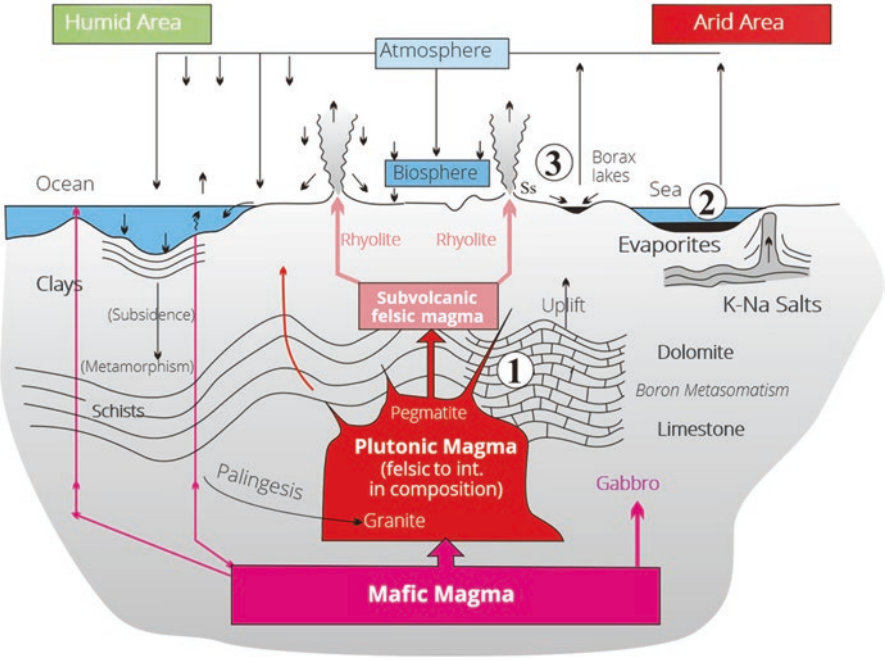

Fig. 11.14 Scheme for the cycle of boron. (1) Skarn deposits; (2) Marine deposites; (3) Playa-lake deposits. (Modified after Watanebe 1964)

and CO_2 are carried into the basin by thermal and mineral waters related to this volcanism. Potentially economic deposits of borate, chlorite, sulfate and carbonate salts related to this volcanic activity are presently forming within the basin (Helvacı and Ercan 1993).

11.4.2 Mineralogy

Borax, kernite, colemanite, and ulexite are the main boron minerals, which provide the source for most of the world's production from Turkey, South America, and the United States (Palache et al. 1951; Muessig 1959; Watanebe 1964; Aristarain and Hurlbut 1972; Helvacı 1978, 2005, 2015; Kistler and Helvacı 1994; Grew and Anovita 1996; Garrett 1998).

Borate minerals are formed in various geological environments, over 250 minerals are known to contain boron, and they are found in various geological environments, as skarn minerals related to intrusives, mainly silicates and iron oxides; magnesium oxides related to marine sediment; and hydrated sodium and calcium borates related to continental sediments and volcanic activity (Table 11.2). Borax, ulexite, colemanite and datolite are commercially significant today. Borax or tincal,

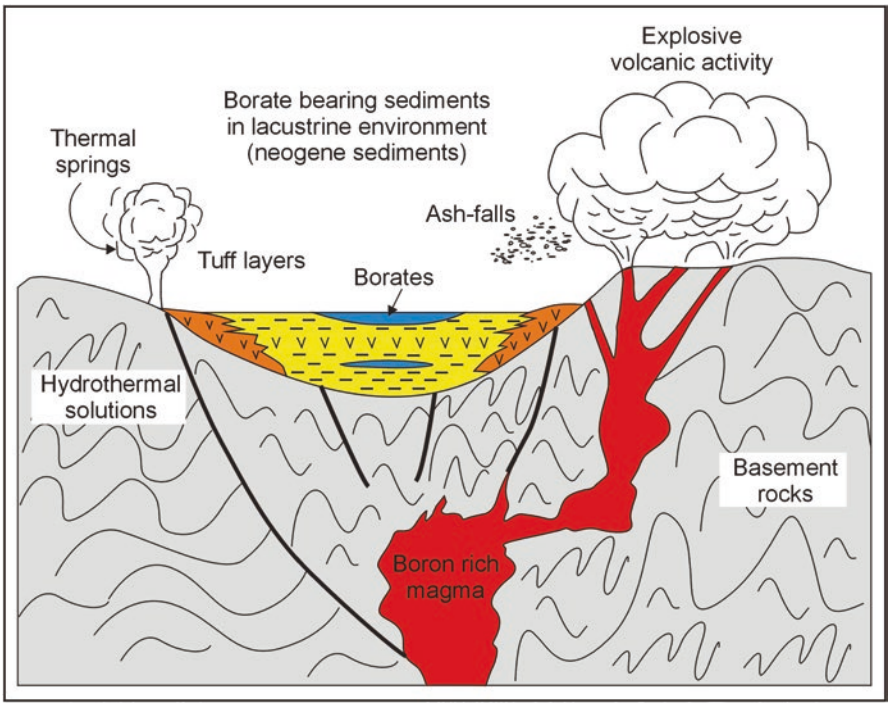

Fig. 11.15 Generalized playa lake depositional model showing the formation of borate deposits in Neogene basins of western Anatolia, Turkey. (After Helvacı 2005)

a natural sodium borate decahydrate, may be regarded as the major commercial source of boron with supplies coming from the United States, Argentina, and Turkey. The principal commerical mixed sodium-calcium borate, ulexite, is produced in Turkey and several countries in South America, whereas large-scale production of the main calcium borate, colemanite, is restricted to Turkey (Table 11.2).

Borax is by far the most important mineral for the borate industry. Colemanite is the preferred calcium-bearing borate used by the non-sodium fiberglass industry. It has low solubility in water, although it dissolves readily in acid. Turkey is the world's major source of high grade colemanite. Colemanite is not known to occur in major deposits outside Turkey and North America, although the higher hydrate, inyoite, is mined on a limited scale in Argentina. Ulexite is the usual borate found on or near the surface, in playa-type lakes and marshes of Recent to Quaternary age throughout the world, where it occurs as soft, often damp, masses of fibrous crystals. These "cotton balls" or "papas" are collected in major amounts in South America and China. The Salar deposits of South America consist of beds and nodules of ulexite, with some borax or inyoite, associated with Holocene playa sediments, consisting primarily mud, silt, halite, and gypsum.

Table 11.2 Borate minerals, formulas and chemical composition

	Structural formula	Empirical formula	Oxid like formula
Ca-borates			
Priceite	$Ca_2(B_5O_7(OH)_5).H_2O$	$Ca_4B_{10}O_{19}.7H_2O$	4CaO 5B2O3 7H2O
Colemanite	$Ca(B_3O_4(OH)_3).H_20$	$Ca_2B_6O_{11}.5H_2O$	2CaO 3B2O3 5H2O
Meyerhofferite	$Ca(B_3O_3(OH)_5).H_20$	$Ca_2B_6O_{11}.7H2O$	2CaO $3B_2O_3$ $7H_2O$
Inyoite	$Ca(B_3O_3(OH)_5).4H_20$	$Ca_2B_6O_{11}.13H2O$	2CaO $3B_2O_3$ $13H_2O$
Ca-Na-borates			
Probertite	$NaCa(B_5O_7(OH)_4).3H_2O$	$NaCaB_5O_9.5H_2O$	Na_2O 2CaO $5B_2O_3$ $10H_2O$
Ulexite	$NaCa(B_5O_6(OH)_6).5H_2O$	$NaCaB_5O_9.8H_2O$	Na_2O 2CaO $5B_2O_3$ $16H_2O$
Na-borates			
Kernite	$Na_2(B_4O_6(OH)_2).3H_2O$	$Na_2B_4O_7.4H_2O$	Na_2O $2B_2O_3$ $4H_2O$
Tincalconite	$Na_2(B_4O_5(OH)_4).3H_20$	$Na_2B_4O_7.5H_2O$	Na_2O $2B_2O_3$ $5H_2O$
Borax	$Na_2(B_4O_5(OH)_4).8H_20$	$Na_2B_4O_7.10H_2O$	Na_2O $2B_2O_3$ $10H_2O$
Mg-borates			
Szaibelyite	$Mg(BO_2(OH))$	$Mg_2B_2O_5.2H_2O$	2MgO B_2O_3 $2H_2O$
Pinnoite	$Mg(B_2O(OH)_6)$	$MgB_2O_4.3H_2O$	MgO B_2O_3 $3H_2O$
Mcasllisterite	$Mg(B_6O_7(OH)_6)_2.9H_2O$	$Mg_2B_{12}O_{20}.15H_2O$	2MgO $6B_2O_3$ 15H2O
Hungchaoite	$Mg(B_4O_5(OH)_4).7H2O$	$MgB_4O_7.9H_2O$	MgO $2B_2O_3$ 9 H_2O
Kurnakovite	$Mg(B_3O_3(OH)_5).5H_2O$	$Mg_2B_6O_{11}.15H_2O$	2MgO $3B_2O_3$ $15H_2O$
Inderite	$Mg(B_3O_3(OH)_5).5H_2O$	$Mg_2B_6O_{11}.15H_2O$	2MgO $3B_2O_3$ $15H_2O$
Mg-Na-borates			
Aristarainite	$Na_2Mg(B_6O_8(OH)_4)_2.4H_2O$	$Na_2MgB_{12}O_{20}.8H_2O$	Na_2O MgO $6B_2O_3$ $8H_2O$
Rivadavite	$Na_6Mg(B_6O_7(OH)_6)_4.10H_2O$	$Na_6MgB_{24}O_{40}.22H_2O$	3Na_2O MgO $12B_2O_3$ $22H_2O$
Mg-Ca-borates			
Hydroboracite	$CaMg(B_6O_8(OH)_6).3H_2O$	$CaMgB_6O_{11}.6H_2O$	CaO MgO $3B_2O_3$ $3H_2O$
Inderborite	$CaMg(B_3O_3(OH)_5)_2.6H_2O$	$CaMgB_6O_{11}.11H_2O$	CaO MgO $3B_2O_3$ $11H_2O$
Mg-K-borates			
Kaliborite	$KHMg_2(B_{12}O_{16}(OH)_{10}).4H_2O$	$K_2Mg_4B_{24}O_{41}.19H_2O$	K_2O 4MgO $12B_2O_3$ $19H_2O$
Sr-borates			
Veatchite	$Sr_2(B_{11}O_{16}(OH)_5).H_2O$	$Sr_4B_{22}O_{37}.7H_2O$	4SrO $11B_2O_3$ $7H_2O$
Tunellite	$Sr(B_6O_9(OH)_2).3H2O$	$SrB_6O_{10}.4.H_2O$	SrO $3B_2O_3$ $4H_2O$
Borosilicates			
Bakerite	$Ca_4B_4(BO_4)(SiO_4)_3(OH)_3.H_2O$	$Ca_8B_{10}Si_6O_{35}.5H_2O$	8CaO $5B_2O_3$ $6SiO_2$ $5H_2O$
Howlite	$Ca_2B_5SiO_9(OH)_5$	$Ca_2SiHB_5O_{12}.2H_2O$	4CaO $5B_2O_3$ $2SiO_2$ $5H_2O$

(continued)

Table 11.2 (continued)

	Structural formula	Empirical formula	Oxid like formula
Searlesite	$NaBSi_2O_5(OH)_2$	$NaBSi_2O_6.H_2O$	$Na_2O\ B_2O_3\ 4SiO_2\ 2H_2O$
Boroarseniates			
Cahnite	$Ca_2B(AsO_4)(OH)_4$	$Ca_2AsBO_6.2H_2O$	$4CaO\ B_2O_3\ As_2O_5\ 4H_2O$
Teruggite	$Ca_4MgAs_2B_{12}O_{22}(OH)_{12}.12H_2O$	$Ca_4MgAs_2B_{12}O_{28}.18H_2O$	$4CaO\ MgO\ 6B_2O_3\ As_2O_5\ 18H_2O$
Borophosphates			
Luneburgite	$Mg_3B_2(PO_4)_2(OH)_6.5H_2O$	$Mg_3P_2B_2O_{11}.8H_2O$	$3MgO\ P_2O_5\ B_2O_3\ 8H_2O$
Borosulfates			
Fontarnauite	$Na_2Sr(SO_4)(B_4O_6(OH)_2).3H_2O$	$Na_2SrSB_4O_{11}.4H_2O$	$Na_2O\ SrO\ SO_3\ 2B_2O_3\ 4H_2O$

11.5 Borate Deposits of Turkey

Turkish borate deposits were formed in the Tertiary lacustrine sediments during periods of volcanic activity, forming in separate or possibly interconnected lake basins under arid or semi-arid climatic conditions (Meixner 1965; Özpeker 1969; İnan et al. 1973; Helvacı and Firman 1976; Helvacı 1986, 1989, 1995, 2005, 2012, 2015; Kistler and Helvacı 1994; Palmer and Helvacı 1995, 1997; Helvacı and Orti 1998, 2004; Helvacı and Alonso 2000). Sediments in the borate lakes often show clear evidence of cyclicity, and much of the sediments in the borate basins seem to have been derived from volcanic terrains (Figs. 11.16 and 11.17). Volcanic rocks in the vicinity of the borate basins in which the borate deposits were formed are extensive and are represented by a calc-alkaline series ranging from felsic to mafic and by pyroclastic rocks which are interbedded with the sediments. Pyroclastic and volcanic rocks of rhyolitic, dacitic, trachytic, andesitic and basaltic composition are interfingered with these lacustrine sediments (Fig. 11.4). The existence of volcanic rocks in every borate district suggests that volcanic activity may have been necessary for the formation of borates. Thermal springs, which at present precipitates travertine, are widespread in the deposits.

Sedimentary-thickness varies from one deposit to another, probably because of deposition in a chain of interconnected lakes. The volcanosedimentary sequences exceed over 1000 m in the deposits. The extreme thickness of the borate zones at Emet, Bigadiç and Kırka indicates that there were somewhat different conditions existing at the time of the formation of these deposits. The borate deposits have the following features in common: They are restricted to non-marine lacustrine sediments in sedimentary closed basins where fresh water limestone deposition was quite common both before and after borate formation, and are deposited under arid or semi-arid climatic conditions. The palaeogeographic scenario seems to have consisted of shallow lakes fed partly by hot springs and partly by streams which carried sediments from the surrounding volcanic, limestone and basement terrain (Fig. 11.15).

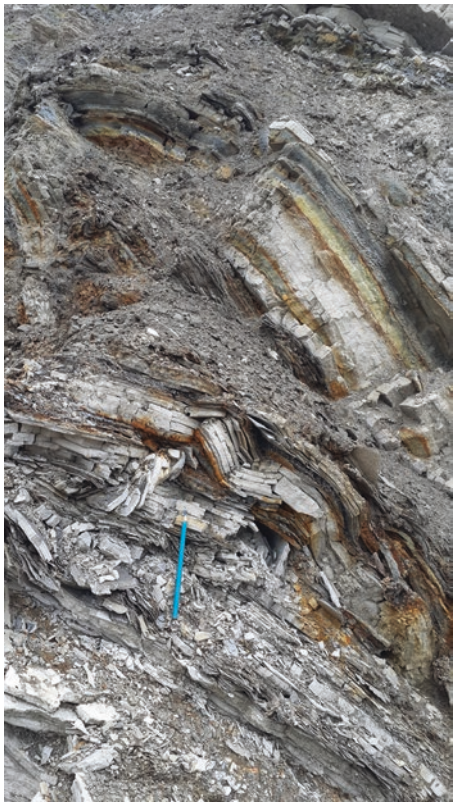

Fig. 11.16 Playa lake volcanosedimentary rocks deformation in the Bigadiç borate deposits, Simav opencast mine, Neogene basins of western Anatolia, Turkey. Neogene basins of western Anatolia, Turkey

Fig. 11.17 Sediments in the borate lake showing clear evidence of cyclicity in the volcaniclastic lacustrine evaporitic sequences associated with borate deposits, Bigadic borate deposit, Turkey

Western Anatolia consists of the largest borate reserves in the world and all the deposits formed during Miocene time in closed basins with abnormally high salinity and alkalinity. Neogene basins consisting of borate deposits were developed during an extensional tectonic regime in NW Turkey which was marked by NNE trending faults. All these basins were partially filled with a series of tuffaceous rocks and lavas. Boron-rich fluids are presumed to have also circulated along faults into these basins (Fig. 11.15). The sediments deposited in the borate lakes are generally represented by tuffaceous rocks, claystones, limestones and Ca-, Na-, Mg-, Sr- borates (Table 11.2). The borates are enveloped between clay-rich horizons and limestones respectively (Figs. 11.4 and 11.18).

The mineralogy of the Turkish borate deposits varies considerably and borate minerals recorded from the Turkish deposits are mainly Ca; Ca-Mg; Na and Mg borates. A rare Sr-bearing borate has been found at Kırka (Baysal 1972; Helvacı 1977) and Ca-As- and Sr-bearing borates have been reported from the Emet district (Helvacı and Firman 1976 and Helvacı 1977). The Kırka borate deposit is the only Turkish deposit is known to contain any of the minerals borax, tincalconite, kernite, inderite, inderborite and kurnakovite. Borate minerals are associated with calcite, dolomite, gypsum, celestite, realgar, orpiment and sulphur (Helvacı et al. 2012; Table 11.2).

Fig. 11.18 Section of borate zone interbedded with clay and tuff, and limestone overburden, in the opencast mine of the Espey deposit, Emet, Turkey

The known borate deposits of Turkey formed in the Neogene basins, and occur in five distinct areas (Figs. 11.2 and 11.13). These are: Bigadiç colemanite and ulexite deposits (Ca and Ca-Na Borate); Sultançayır pandermite deposits (Ca-type); Kestelek colemanite deposits (Ca-type); Emet colemanite deposits (Ca-type); and Kırka and Göcenoluk borax deposits (Na-type).

11.5.1 Bigadiç Deposit

Bigadiç deposit contains the largest colemanite and ulexite deposits known in the world. The borate minerals occur in two distinct zones, lower and upper, seperated by thick tuff beds changed during diagenetic processes to montmorillonite, chlorite and to zeolites (Fig. 11.19). Borate minerals formed in two zones separated by thick tuff beds that have been altered to montmorillonite, chlorite, and zeolites (mainly heulandite) during diagenesis. Colemanite and ulexite predominate in both borate zones (Figs. 11.4, 11.20, and 11.21), but other borates, including howlite, probertite, and hydroboracite are present in the lower borate zone; whereas inyoite, meyerhofferite, pandermite, tertschite, hydroboracite, howlite, tunellite, and rivadavite are found in the upper borate zone. Calcite, anhydrite, gypsum, celestite, K feldspar, analcime, heulandite, clinoptilolite, quartz, opal-CT, montmorillonite, chlorite, and illite are also found in the deposit (Özpeker 1969; Helvacı et al. 1993; Helvacı 1995; Helvacı and Orti 1998; Yücel-Öztürk et al. 2014) (Table 11.2).

The Bigadiç deposits formed within Neogene perennial saline lakes sediments located in a northeast-southwest-trending basin (Fig. 11.19) and were fed by thermal springs associated with local volcanic activity under arid climatic conditions. The volcano-sedimentary sequence in the deposits consists of (from bottom to top) basement volcanics, lower limestone, lower tuff, lower borate zone, upper tuff, upper borate zone, and olivine basalt. The borate deposits formed under arid conditions in perennial saline lakes fed by hydrothermal springs associated with local volcanic activity. The deposits are interbedded with tuffs, clays, and limestones (Figs. 11.19 and 11.22).

Colemanite nodules in both borate zones formed directly from solution, within unconsolidated sediments just below the sediment-water interface, and continued to grow as the sediments were compacted (Fig. 11.23). It is unlikely that the colemanite formed by dehydration of inyoite and/or by replacement of ulexite after burial. Later generations of colemanite and ulexite are found in vugs and veins and as fibrous margins of early formed nodules (Fig. 11.24). Other diagenetic changes include the partial replacement of colemanite by howlite and hydroboracite and ulexite by tunellite. Nodular-shaped colemanite ancl ulexite minerals predominate in both borate zones. Colemanite and Ulexite show alternating horizons, and the transformation of one mineral to another has not heen observed and the boundary between them is always sharp. Because these minerals are readily dissolved, secondary pure and transparent colemanite and ulexite are often encountered in cavities

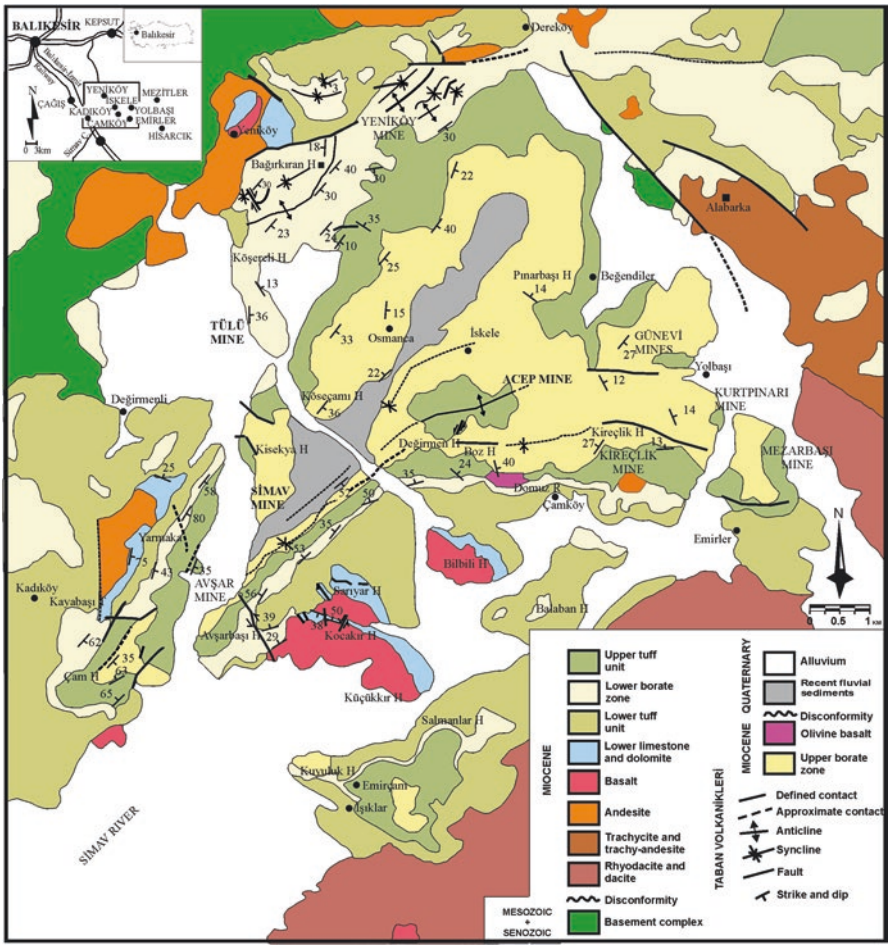

Fig. 11.19 Locality and geological map of the Bigadiç borate district

of nodules and cracks (Fig. 11.24). Some colemanite and ulexite is weathered and completely replaced by calcite.

Probertite bands are found in some ulexite horizons, especially in the lower borate zone. It forms in the same chemical environment as ulexite and indicates a period of more extreme desiccation and possibly subaerial exposure within the lakes. Euhedral tunellite formed during dissolution and recrystallization of some Sr-rich ulexite horizons. In the Bigadic deposits, hydroboracite formed by replacement of colemanite, with Mg^{2+} ions supplied from adjacent tuffs and clays by ion exchange. Howlite grew in clays alternating with thin colemanite bands and coincided with periods of relatively high Si concentrations. Diagenetic processes also produced small howlite nodules embedded in unconsolidated colemanite nodules. The initial solutions that formed the alkaline perennial saline lake(s) were low in

Fig. 11.20 Colemanite nodules in varying sizes intercalated with associated sediments, Tülü open pit mine deposit, Bigadiç, Turkey. (After Helvacı 2015)

Cl^- and SO_4^{-2} and high in boron and Ca^{2+}, with subordinate Na+. The Bigadiç borates are the largest colemanite and ulesite deposits in the world and the high-grade colemanite and ulexite ores (30% and 29% B203 respectively) should supply a substantial proportion of the world's needs for many years (Fig. 11.25).

11.5.2 Sultanyaçır Deposit

In this deposit borates are interbedded with gypsum, claystone, limestone, and tuff. Pandermite (priceite) is abundant, but other borates include colemanite and howlite (Figs. 11.26 and 11.27; Table 11.2). Gypsum exists abundantly and calcite, zeolite, smectite, illite, and chlorite are the other associated minerals in this deposit (Orti et al. 1998; Gündoğan and Helvacı 1993; Helvacı 1994; Helvacı and Alonso 2000).

Calcium-borates, mainly pandermite (priceite) and howlite, but also bakerite and colemanite, are intercalated within the Sultançayır Gypsum in the Miocene Sultançayır Basin (Fig. 11.28). This lacustrine unit, represented by secondary gypsum in outcrop, is characterized by: (1) a clear facies distribution of depocentral laminated lithofacies and debris-flow deposits, a wide marginal zone of sabkha deposits, and at least one selenitic shoal located toward the basin margin;

Fig. 11.21 Ulexite ore lenses intercalated with associated sediments, Kurtpınarı deposit, Bigadiç, Turkey. (After Helvacı 2015)

Fig. 11.22 Depositional cycle in the Tülü deposit (Bigadiç). Facies: tuff layer at the base; (1) alternations of carbonate varves and laminated dark claystones; (2) laminated carbonate; (3) nodular Colemanite, Bigadiç, Turkey. Hammer for scale

Fig. 11.23 Nodular colemanite with radiating structures, Simav open cast, mine, Bigadiç, Turkey

Fig. 11.24 Small white colemanite nodules with radiating structures growing in the cracks during diagenesis, Tülü mine, Bigadiç, Turkey

(2) evaporitic cycles displaying a shallowing-upward trend; and (3) a diagenetic evolution of primary gypsum to (burial) anhydrite followed by its final re-hydration. The calcium borates precipitated only in the depocentre of the lake and were partly affected by synsedimentary reworking, indicating that they formed during very early diagenesis. The lithofacies, which are made up of a host gypsum and borates, indicate that the borates grew interstitially because of the inflow and mixing of borate-rich solutions with basinal brines. Borate growth displaced and replaced primary gypsum beneath a relatively deep depositional floor. Howlite, which has apparently grown in the clays alternates with thin pandermite and colemanite bands. As a result of diagenetic processes, some small howlite nodules are also embedded in the pandermite and colemanite noludes. The anhydritization of primary gypsum took place during early to late diagenesis. This process also resulted in partial replacement of pandermite and accompanying borates (bakerite and howlite) as well as other early diagenetic minerals (celestite) by anhydrite. Final exhumation

Fig. 11.25 Tülü opencast mine, Bigadiç area, Turkey

Fig. 11.26 Pandermite (priceite) nodules within the gypsum beds of the sandy claystone unit, Sultançayırı deposit, Turkey

resulted in the replacement of anhydrite by secondary gypsum, and in the partial transformation of pandermite and howlite into secondary calcite.

11.5.3 Kestelek Deposit

At Kestelek the borate zone consists of clay, marl, limestone, tuffaceous limestone, tuff, and borate. The volcanic activity produced tuff, and agglomerate, and andesitic and rhyolitic lavas that are associated with the sediments (Helvacı 1994; Helvacı Alonso 2000). This sequence is capped by a unit consisting of loosely cemented

Fig. 11.27 Banded lithofacies of priceite (white material) intercalated between laminated secondary gypsum (grey material). The priceite mass displaces the laminae of secondary gypsum, Sultançayır deposit, Turkey

conglomerate, sandstone, and limestone. The borate minerals occur interbedded with clay as nodules or masses and as thin layers of fibrous and euhedral crystals. Colemanite, ulexite, and probertite predominate, with hydroboracite occuring rarely. Secondary colemanite occurs as transparent and euhedral crystals in the cavities of nodules, in cracks and in vugs (Fig. 11.29, Table 11.2).

Colemanite, ulexite, and probertite predominate, with hydroboracite occuring rarely. Calcite, quartz, zeolite, smectite, illite, and chlorite are the associated minerals. Secondary colemanite occurs as transparent and euhedral crystals in the cavities of nodules, in cracks and in vugs (Fig. 11.30). Probertite, which forms in the same chemical environment with ulexite in the Kestelek deposit, indicates a period of higher temperature within the playa lake. The initial solutions crystallizing the borates in the Kestelek deposit are deduced to have had a very low concentration of chloride, low concentrations of sulphate and high concentrations of boron and calcium with some sodium.

11.5.4 Emet Deposit

At Emet the borate-bearing Neogene sequence rests unconformably on Paleozoic metamorphic rocks that consist of marble, mica-schist, calc schist, and chlorite schist, and the sediments contains the borate deposits are interclated with clay, tuff, and marl containing the lensoidal borate formations (Figs. 11.4, 11.8, and 11.31); The unit consisting of clay, tuff and marl containing the borate deposits has

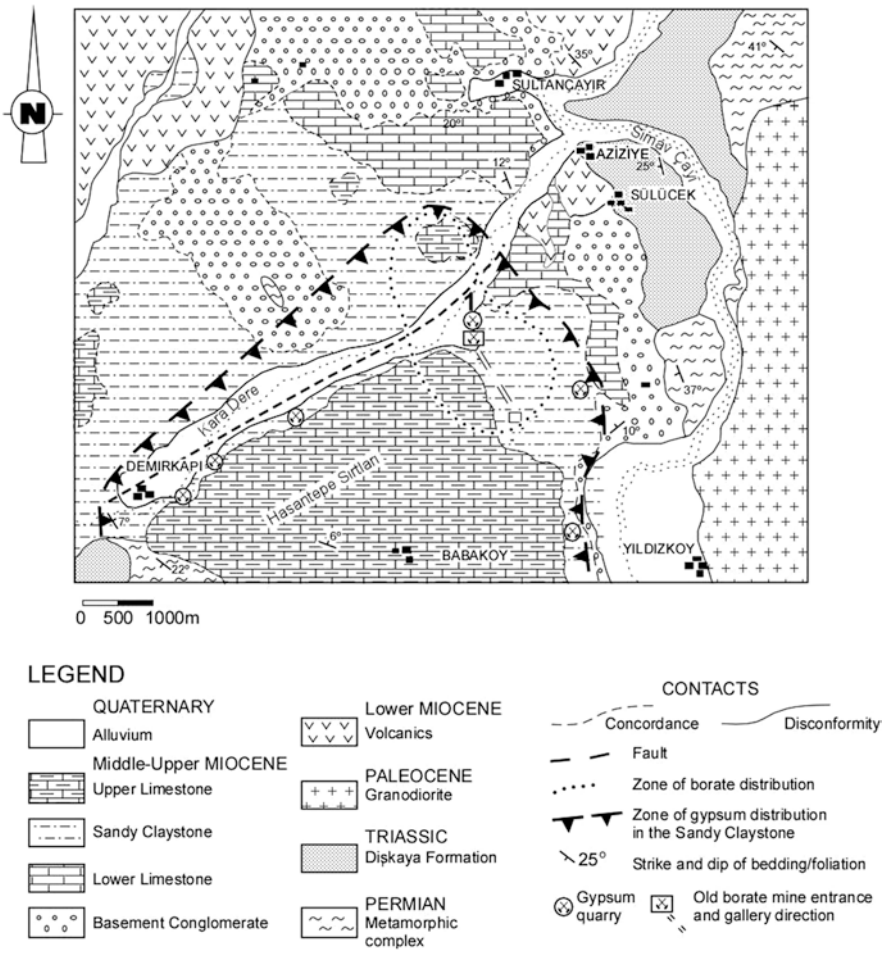

Fig. 11.28 Geological map of the Sultançayır boratiferous gypsum basin

abundant realgar and orpiment at some horizons indicating that arsenic and boron have a genetic relationship and volcanic origin at Emet (Table 11.2).

The Emet borate basin is one of the basins in western Turkey containing significant amounts of borate minerals, mainly colemanite (Fig. 11.32) and probertite with minor ulexite, hydroboracite, and meyerhofferite. The borates are interlayered with tuff, clay, and marl with limestone occuring above and below the borate lenses (Fig. 11.33). The Emet borate deposits contain many of the rare borate minerals such as veatchite-A, tunellite, teruggite, and cahnite (Helvacı and Firman 1976; Helvacı 1977, 1984, 1986; Helvacı and Orti 1998; Garcia-Veigas et al. 2011).

The petrologic study of core samples from two exploratory wells in the Doğanlar sector (Fig. 11.34) using conventional optic and electron microscopy, reveals a complex mineral association in which probertite, glauberite, and halite constitute the

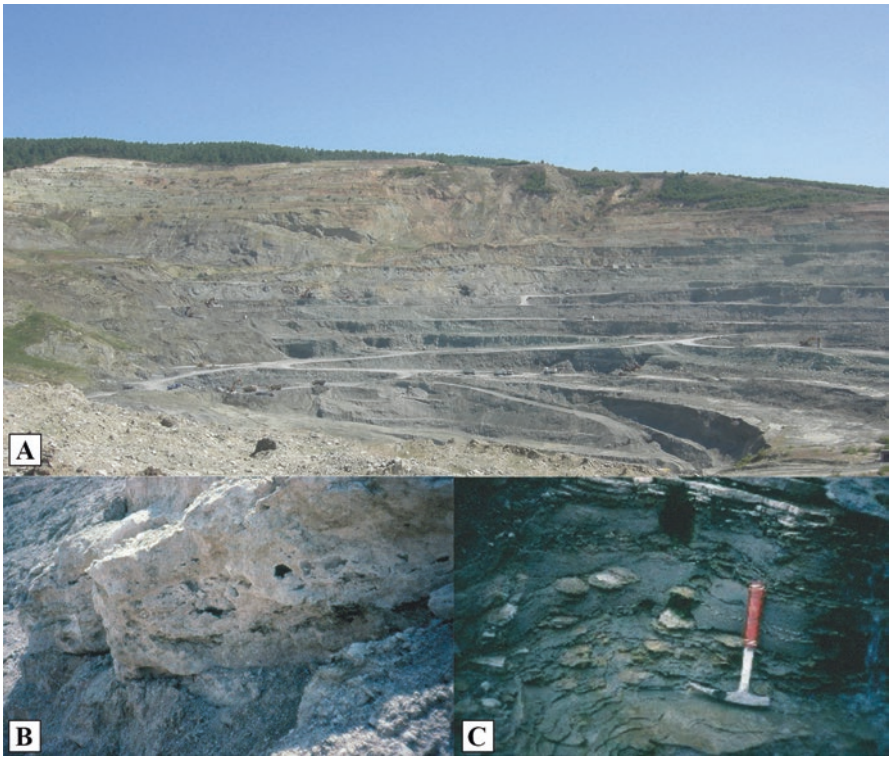

Fig. 11.29 (**a**) Open cast mine in the Kestelek area. (**b**) Euhedral colemanite crystals of massive colemanite zone, growing in cracks and vughs, (**c**) Discoidal Colemanite nodules growing in claystones in the marginal part of the deposit, Kestelek opencast mine

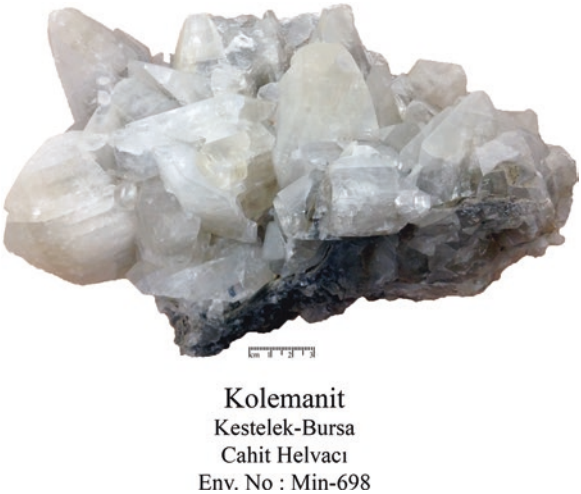

Fig. 11.30 Euhedral colemanite crystals, Kestelek opencast mine, Turkey

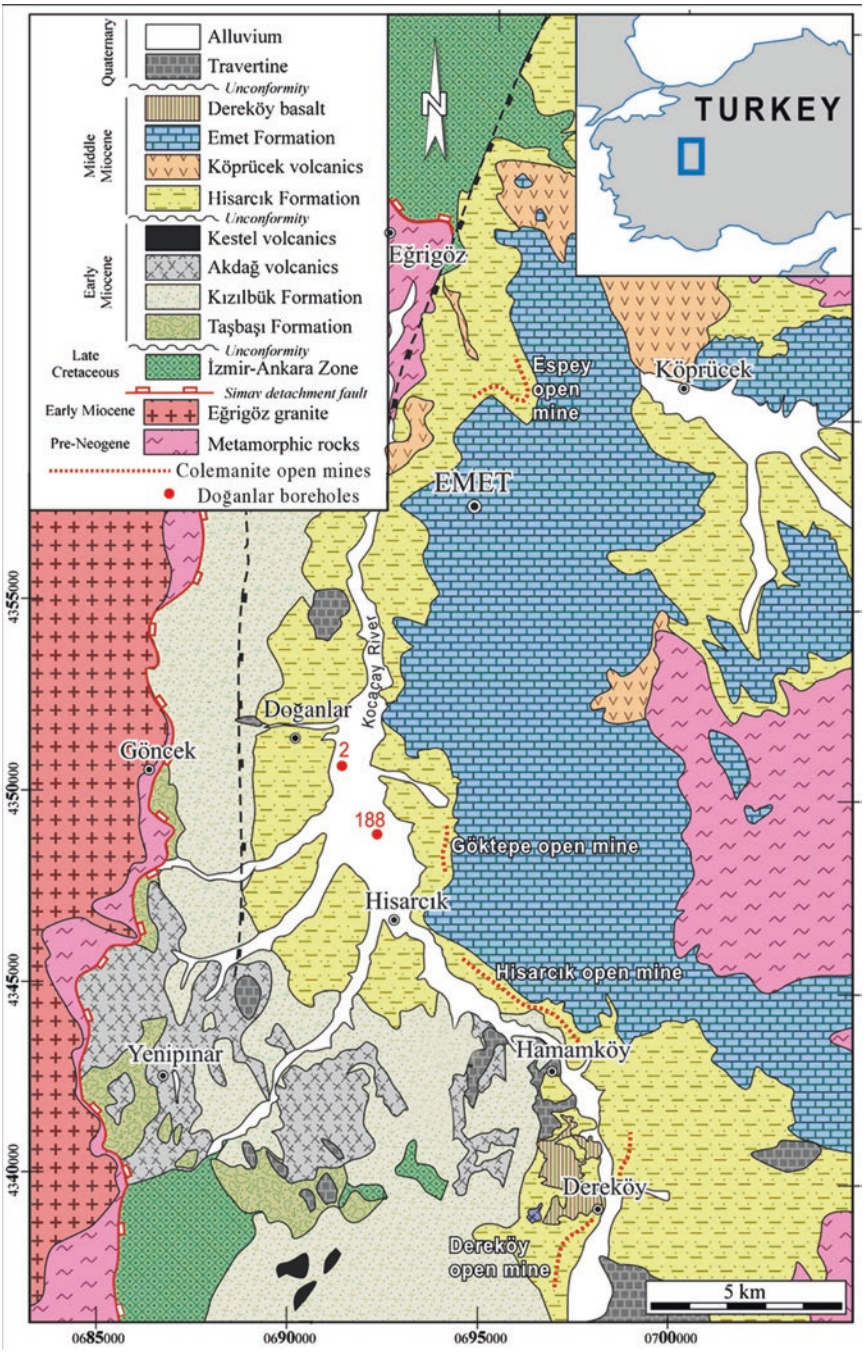

Fig. 11.31 Geological map of the Emet borate district showing the location of the colemanite open pit mines. (Modified after Helvacı 1984)

Fig. 11.32 Colemanite is the principal borate mineral and is interclated with green clay as nodular and elliptical lenses, Hisarcık open pit mine, Emet, Turkey

major primary phases (without mineral precursors) precipitated in a saline lake placed in a volcano-sedimentary context. Other sulfates (anhydrite, gypsum, thenardite, celestite and kalistrontite), borates (colemanite, ulexite, hydroboracite, tunellite, kaliborite and aristarainite), and sulfides (arsenopyrite, realgar and orpiment) are attributed to early diagenesis. The Doğanlar deposit is the most important deposit of probertite known up to now (Garcia-Veigas et al. 2011). A new sulfate-borate minetal (fontarnauite) was found in the deposit and reported in the Canadian Mineralogist (Cooper et al. 2016). Montmorillonite, illite, and chlorite are the clay minerals that have been identified. Zeolites are abundant along the tuff horizons. Native sulfur, realgar, orpiment, gypsum and celestite (Fig. 11.35) occur in the borate zone throughout the area. The Doğanlar deposit is the most important deposit of probertite known up to now. Chemical changes in the groundwater inflow led to the precipitation of Ca-bearing borates (colemanite) in the tuff-flat environment surrounding the lake, while Na–Ca sulfates and borates (glauberite and probertite) precipitated in the center of the lake. Fluid inclusion compositions in halite indicate that the advanced brines correspond to the Na-K-Cl-SO4 type. During restricted stages of the saline lake, the residual brines seeped through the tuff-flat sediments, leading to transformations of previous precipitates that resulted in the formation of K-bearing minerals (Garcia-Veigas et al. 2011).

11.5.5 Kırka and Göcenoluk Deposits

The Neogene volcano-sedimentary sequence rests unconformably partly on Paleozoic metamorphics, Mesozoic ophiolite complex, and Eocene fossiliferous limestone. The Neogene sequence consists of from bottom to top of: volcanic rocks and tuffs; lower limestone with marl and tuff interbeds; borate zone; upper claystone; upper limestone containing tuff and marl with chert bands; and basalt. The Miocene Kırka boratiferous district is the most important Na-borate (borax) resource

Fig. 11.33 Hisarcık open cast mine showing borate zone and limestone overburden, Emet area, Turkey

in the world. Two separate deposits in the Kırka district are located near the villages of Sarıkaya and Göcenoluk (Eskişehir Province) (Figs. 11.9 and 11.10).

Borax is intensively exploited in open-pit mines in the Sarıkaya deposit while only small quarries of colemanite are known in the Göcenoluk deposit (Figs. 11.36, 11.37, and 11.38). The ore body has thickness of up to 145 m, averaging 20–25% B_2O_3. The principal mineral in the Kırka borate deposit is borax with lesser amounts of colemanite and ulexite. In addition, inyoite, meyerhofferite, tincalconite, kernite, hydroboracite, inderborite, inderite, kurnakovite, and tunnelite are found (Baysal

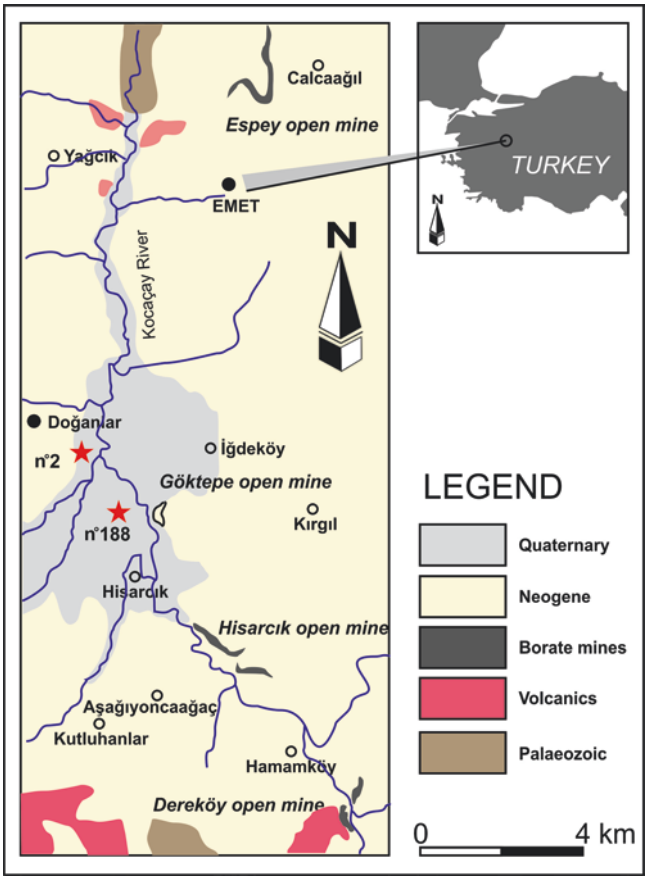

Fig. 11.34 Location of Doğanlar boreholes and geological map of the Emet borate district showing the location of open pit mines and boreholes in western Turkey. (After Helvacı 1986)

1972; İnan et al. 1973; Helvacı 1977; Sunder 1980; Palmer and Helvacı 1995; Floyd et al. 1998; Helvacı and Orti 2004; Seghedi and Helvacı 2014; Table 11.2). This is the only deposit in Turkey that contains sodium borates (borax, tincalconite, and kernite), together with inderborite, inderite, and kurnakovite (Figs. 11.39, 11.40, and 11.41). The borax body is enveloped by a thin ulexite facies, followed outward by a colemanite facies. The whole is enclosed by limestone (Fig. 11.42).

The mineral sequence in the Kırka deposit is Ca/Ca – Na/Na/Ca – Na/Ca (colemanite and/or inyoite/ulexite/borax/ulexite/colemanite and/or inyoite) (Fig. 11.42). The borate layers contain minor amounts of celestite, calcite, and dolomite, and the clay partings contain some tuff layers, quartz, biotite, and feldspar. The clay is made up of smectite-group minerals and less frequently, illite and chlorite minerals. Zeolites occur within the tuff horizons. This deposit is distinct from similar borax deposits at Boron and Tincalayu in having very little intercrystalline (or intracrystal-

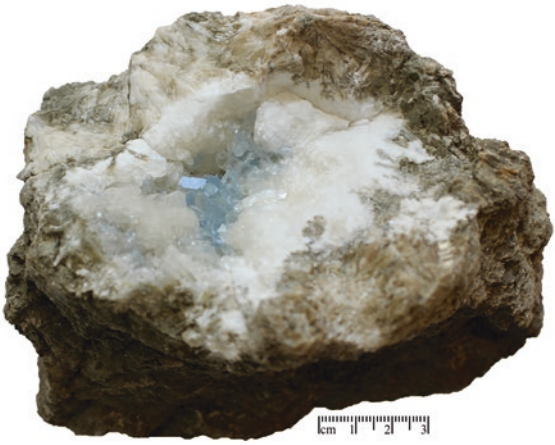

Fig. 11.35 Colemanite nodule with hollow center and cracks filled with secondary generation colemanite and celestine crystals, Hamaköy deposit, Emet area

Fig. 11.36 Kırka opencast borax mine, Kırka deposit, Eskişehir

line) clay; the clay at Kırka is very pale green to white and is high in dolomitic carbonate. The borax crystals are fine, 10–20 mm, and quite uniform in size (Fig. 11.40).

Recent exploratory drilling in the Göcenoluk area intersected a thick succession of dolostones, tuffs and three borate-bearing units (Lower, Intermediate and Upper

Fig. 11.37 Kırka opencast borax mine and mineral processing plant in the background, Kırka deposit, Eskişehir

Fig. 11.38 Overview of the Kırka opencast mine, looking down into the mine area, Kırka deposit, Eskişehir

Borate Units). Here, the most abundant borate mineral is ulexite (Ca-Na-borate) passing at depth to probertite. Borax (Na-borate) is only present in the Intermediate Borate Unit (Fig. 11.10). Minor amounts of colemanite (Ca-borate) and hydroboracite (Ca-Mg-borate) occur at the base, and/or top, of each mineralized unit. Pyroclastic layers within the borate units show intense alteration by alkaline, boron-bearing waters and formation of diagenetic clay minerals (smectites), zeolites (analcime) and borosilicates (searlesite). The Göcenoluk succession is interpreted as a shallow, ephemeral, alkaline lake deposit in which carbonates formed as stromatolites and travertines. Borate precipitation in the Göcenoluk area took place interstitially within muddy and carbonate sediments in a lateral progression from marginal Ca-borates towards Na-Ca-borates and rarely to Na-borates in the center of the lake. Authigenic silicate mineral distribution shows parallel changes toward the center of the lake that reflect increasing pH gradient (Garcia-Veigas and Helvacı 2013).

Fig. 11.39 Laminated lithofacies of borax (brown material) alternating with dolomitic, marly laminae (white laminae). Laminated borax lithofacies with palisade fabric in borax laminae. Clear material corresponds to lutitic matrix and laminae (dolomitic claystone). Dark material corresponds to fresh, crystalline borax

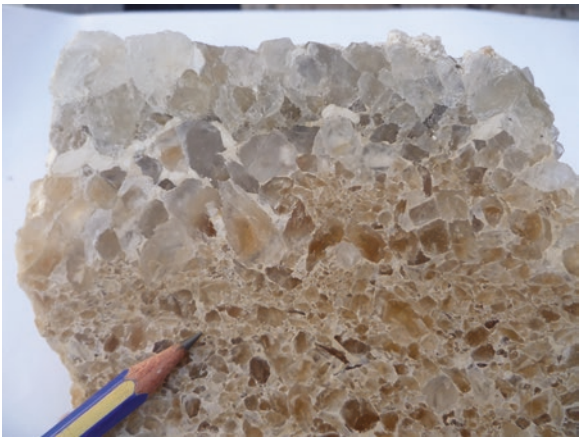

Fig. 11.40 Massive crystalline borax lithofacies. The borax crystals show zoned growth (matrix inclusions) at the top. Borax crystals are transparent and rectangular to equant. These crystals have variable size and are surrounded by an lutitic matrix

Petrologic studies of samples coming from two deep boreholes (1100 m depth) drilled in a marginal part of the basin, near the Göcenoluk village, 5 km west of Kırka, have recorded a thick borate succession. The borate succession in the 2008–6 borehole is mainly formed by an upper probertite unit (~300 m thick) which overlies a lower borax unit (~100 m thick) (Fig. 11.10). Abundant small tunellite crystals are scattered throughout the sequence. Ulexite is a very minor phase. The upper probertite unit consists of nodular probertite interbeded with lavas, tuffs and thin dolomite

Fig. 11.41 View of ulexite layers alternating with nodular and massive lithofacies of colemanite. Crystalline masses, vugh porosity, geodic areas and cemented fractures can be observed, upper section of the Kırka opencast deposit

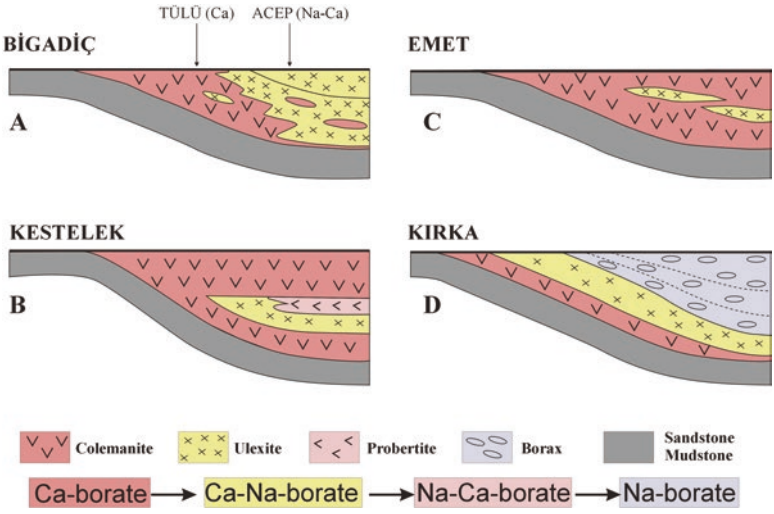

Fig. 11.42 Sequence of boron mineral formations in Turkish borate deposits

layers. Only two colemanite intervals, less than 3 m thick, have been identified. Backscattered electron images and X-ray mapping of both probertite and colemanite exhibit an internal zonation pattern as a result of high and variable strontium contents. The basal borax unit consists of massive beds formed by anhedral cm-size crystals also interbeded with tuffs and dolomites. In both units, borates show evidence of interstitial growth breaking and deforming peloidal dolomite and stromatolitic layers.

Unlike other contemporaneous borate deposits in the Anatolian region, neither metal sulfides nor arseno-sulfides are present at Kırka. Intense water-rock interaction with volcano-sedimentary layers induces the dissolution of feldspars and plagioclases which are usually replaced by probertite. Abundant authigenic zeolites

(mainly analcime) and boron-silicates (searlesite) are formed as a consequence of the silica leached from the weathering of silicates. According to petrographic observations and the internal strontium zonation pattern in both probertite and colemanite crystals are considered to form as primary precipitates which grew interstitially in volcaniclastic sediments and soft dolomitic muds deposited on the bottom of the lake. The absence of well laminated borax in this marginal position suggests that was also formed below the water-sediment interface.

11.5.6 Holocene Borates in the Karapınar-Konya Basin

The basin located around the Karapınar town (Konya) is surrounded by volcanos which have been active various phase from the Late Miocene to present. Currently active volcanism is evidenced by the discharge of thermal and mineral waters and magmatic gases. Potentially economic deposits of borate, chlorite, sulfate and carbonate salts related to this volcanic activity are forming within the basin.

Andesitic lavas of Late Miocene volcanism form Üzecik Mountain, located in the western part of the basin. Karacadağ, which is located in the eastern part of the basin, has a complex domal structure and completed its evolution in a few phases during the entire Pliocene. The lavas which form Karacadağ rise to an elevation of 1995 m and are prdominatly andesite, but locally trachyandesite, basaltic andesite and dasite are present and show a highly viscous flow character.

The southern part of the Karapınar basin is delimineted by lava flows, small volcanic cone and maar proclastics that formed as a result of several volcanic phases which began in the early Quaternary and continued up until a few thousand years ago. Trachyandesitic and andesitic lava flows were formed during the first stage of volcanism in the Quaternary. Radiometric age determinations done whith the K/Ar method gives ages between 1.1 and 1.2 my for these flows. Later, basaltic lavas, scoria and ash formed small volcanic cones and lava flows. Basaltic volcanic cones reach hegihts of 250 m. K/Ar radiometric age determinations give ages between 363.000 and 161.000 year for this stage of volcanism (Helvacı and Ercan 1993).

Later, maars (volcanic craters resulted by explosive eruptions) formed within the basin. Maar pyroclastics, formed successively as products of several different eruptions, are present as consentric rings around the maars. The maars of Meke Obruğu and Yılan Obruğu are in small size. As for the Mekegöl and Acıgöl maars, they are larger explosion crates measuring opproximately 1,5 km in diatemer. Later the maars were filled by waters forming maar lakes. A few thousand years ago, a scoria cone formed within the Meke maar lake during the last phase of basaltic volcanism.

There is evidence of active volcanic activity in the Karapınar basin, such as the thermal, mineral waters and gases still emanating from the maars and along the major fault line in the eastern part of the basin. The gases contain predominantly CO_2 and have almost mantle-origin characteristics, based upon helium-and carbon-isotope ratios (3 He/4 He = 159.10^{-6}; 13c/12c = %0–1.5) (Helvacı and Ercan 1993).

Borate, chlorite, sulfate and minor amounts of carbonate salts are actively forming in the basin. While NaCl is precipitating in the center of the basin, carbonate and CO_2 bearing waters are being discharged and carbonates (probably trona) and Na sulfates precipitated along the fault at the eastern edge of the basin. Ulexite, which is one of the common borate salts, seem to have formed earlier than the other salts and occur as coulifflower or potato-shaped masses within unconsilidated sediment at the depth of ≤1 m. Thenardite and glouberite are forming within the Acıgöl and Meke maar lakes.

The formation of borate and other salts in the Karapınar basin is genetically related to the subalkaline volcanic rocks of this region. Na, B, Cl, SO_4 and CO_2 are carried into the basin by thermal and mineral waters related to this volcanism. Through detailed field, geochemical and drilling studies, it is probable that economically important salt deposits will be discovered in the area (Helvacı and Ercan 1993).

11.6 Mining, Uses and Future Forecasts

Commercial borate deposits in the world are mined by open pit methods (Figs. 11.18, 11.33, 11.36, 11.37, and 11.38). The Kırka mine of Eti Maden in Turkey are huge open pit mines utilizing large trucks and shovels and front end loader methods for ore mining and overburden removal similarly to the world's major borate operations. Ores and overburden are drilled and blasted for easier handling. The boron operation uses a belt conveyor to move ore from the in-pit crusher to a coarse ore stockpile form which it is reclaimed by a bucketwheel that blends the ore before it is fed to the refinery. Kırka utilizes trucks which haul to a crusher near the refenery which is about 0.5 km from the current ore faces.

Mineral processing techniques are related to both the scale of the operation and the ore type, with either the upgraded or refined mineral (borax, colemanite, and ulexite) or boric acid as the final product for most operations. Borax-kernite ores in Kırka are crushed to 2.5 cm and then dissolved in hot water/recycled borate liquor. The resultant strong liquor is clarified and concentrated in large counter-current thickeners, filtered, fed to vacuum crystallizers, centrifuged, and then dried. The final product is refined borax decahydrate or pentahydrate or fused anhydrous borax, or is used as feed for boric acid production. Colemanite concentrates are used directly in specific glass melts or used as a feed for boric acid plants Boric acid is one of the final products produced from most of the processes. The world's largest boric acid facility is located adjacent to the Boron pit and the Emet and Kırka opencast mines.

Evaporites constitute the richest concentrations of boron on Earth, and thus are the main source of boron for its many applications in medicine, electronics and the nuclear industry. Borate was traded at relatively high prices for highly specialized applications into the late years of the nineteenth century. At that time they were being used for medicines, food preservatives, ceramic glazes, and in expanded

applications as metal fluxes. Borate are often defined and sold by their boric oxide or B_2O_3 content, and most statistical data are listed in tons of B_2O_3. Borax pentahydrate and boric acid are the most commonly traded commodities. Boric acid plants are operated by all of the major borate producers. Glass fiber insulation is the major end use in the United States followed by textile glass fiber and borosilicate glass, detergents, and ceramics. Detergent usage continues to be a major end use in Europe (Fig. 11.43).

Boron minerals and their products are indispensable industrial raw materials of today. The principal uses of borates have not changed much in the past decade and major markets include fiberglass, insulation, textile or continuous-filament glass fibers, glass, detergents and bleaches, enamels and frits, fertilizers, and fire retardants (Fig. 11.43). Bleaches and detergents are also the major end use; however, sales for glass and glass fibers including fiberglass, are increasing. Boron fiber-reinforced plastics continue to be utilized in quantity for aerospace frame sheathing where they combine flexibility and light weight with strength and ease of fabrication. Relatively minor uses that are expected to increase in the near future include those in fertilizers, wood preservatives, alloys and amorphous metals, fire and flame retardants, and insecticides. However, the promising field of boron-iron-silicon electrical transformers has not developed as rapidly as predicted due to various cost factors.

Borates have become a relatively modestly priced industrial mineral commodity in recent years following the development of the large deposits at Boron, and more

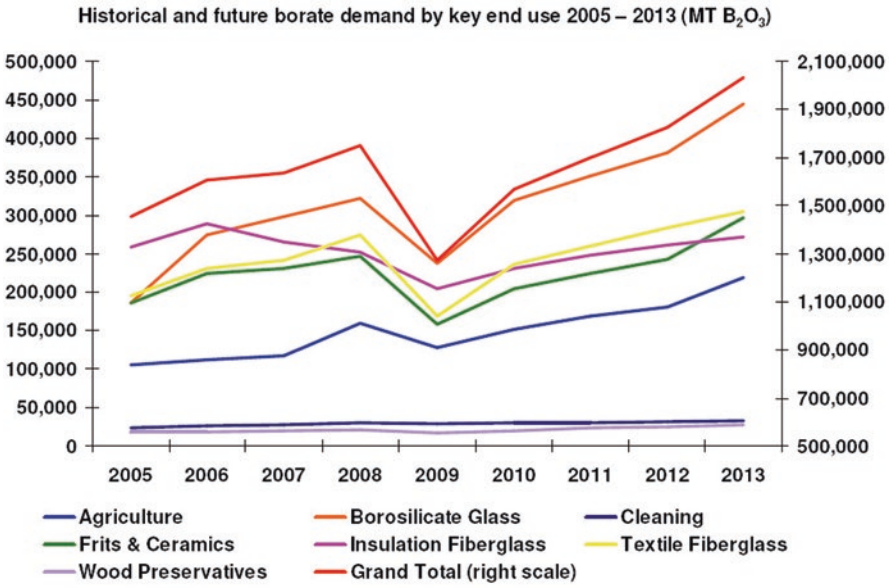

Fig. 11.43 Present and future borate demand by major end use 2005–2013 (MTB2O3). (Source: Rio Tinto)

recently, Kırka. Prices are directly related to the cost of production, of which the major cost is fuel for drying, dehydrating, and melting the refined ore into the products desired by industry. Borates are a lightweight commodity and are generally sold in bulk by rail carload lots, and overseas shipments are made mostly in bulk from special terminals from Bandırma on the Marmara Sea in Turkey, to similar terminals in the Netherlands, Belgium, and the United Kingdom, from where it is moved by barge, as well as rail and truck. Other imports to Europe arrive in Italy and Spain. Imports to the Far East are generally sold in small bag lots. Bulk imports to the United States (mainly colemanite) usually land in Charleston, South Carolina, where there are griding facilities; this colemanite is then shipped to Easter fiberglass manufacturers (Kistler and Helvacı 1994; Helvacı 2005).

Known reserves of borate minerals of Turkey are large, particularly in Turkey and production from Turkey will continue to dominate the world market (Table 11.3). Approximately 75–80% of the world's boron reserves are located in Turkey (Engineering and Mining Journal 2012) (Table 11.3). Turkey's borate deposits are the largest and highest grade (respectively 30%, 29% and 25% B_2O_3) of colemanite, ulexite and borax (tincal) deposits in the world and have sufficient potential to meet the demand for many years (Table 11.3). The borate producing areas of Turkey, controlled by the state-owned mining company Eti Maden AS, are Bigadiç (colemanite and ulexite), Emet (colemanite), Kestelek (colemanite, probertite, and ulexite), and Kırka (borax-tincal). Eti Maden planned to expand its share in the world boron market from 36% to 47% by 2014, increasing sales to $1 billion by expanding its production facilities and product range. In 2009, Turkey exported 4 Mt of borates valued at $104 million (Uyanik 2010). Consumption of borates is expected to increase, spurred by strong demand in the Asian and South American agriculture, ceramic, and glass markets. Consumption of borates by the ceramics industry was expected to shift away from Europe to Asia, which accounted for 60% of world demand in 2011. World consumption of borates was projected to reach 2.0 Mt B_2O_3 by 2014, compared with 1.5 Mt B_2O_3 in 2010 (Rio Tinto Inc. 2011; Roskill

Table 11.3 Reserves and life estimates of the world's borate deposits (Helvacı 2005)

	Known economic reserve (million tonnes of B_2O_3)	Total reserve (million tonnes of B_2O_3)	Estimated life of known reserve (year)	Estimated life of total reserve (year)
Turkey	224.000	563.000	155	389
USA	40.000	80.000	28	55
Russia	40.000	60.000	28	69
China	27.000	36.000	19	25
Chile	8.000	41.000	6	28
Bolivia	4.000	19.000	3	13
Peru	4.000	22.000	3	15
Argentina	2.000	9.000	1	6
Kazakstan	14.000	15.000	10	10
Total	363.000	885.000	253	610

Information Services Ltd. 2010, p. 167; O'Driscoll 2011). Consumption of boron nitride is expected to increase owing to the development of high-volume production techniques coupled with the creation of new technologies.

Boron consumption is directly related to the usage of glass, glass fibers, and ceramics. These materials, along with certain plastics that contain borate products, are seen as having a steady consumer demand in the construction and housewares markets well into the next century. Borates use in nuclear reactor shielding and control is well documented. Other major uses, detergents, plant foods, wood preservation etc. are expected to show a slowly rising demand. Total world borate demand is expected to grow at about 3% per year in the near future, based on industry forecasts (Table 11.3, Fig. 11.43). Based upon recent history, the major world consumers of borates will continue to be the developed countries of North America, Europe, and Japan.

Turkey has an important share in the world markets with borax (tincal) production in Kırka; colemanite and ulexite production in Emet, Bigadiç and Kestelek regions. Between 1980 and 2008, Turkey became the biggest colemanite producer in the world. Turkey's visible and potential reserves are greater than its current production. Even the most pessimistic observers are unanimous on the opinion that these borate reserves should be able to meet demands for a couple of hundred years (Table 11.3). The world is dependant on Turkey with its supplies of widely used colemanite and ulexite. All countries in the world extensively using this mineral are dependant on Turkey's boron supplies.

As far as the National Boron Policy is concerned, after the Nationalization Act in 1979, the intensive work has been done on different borate deposits to show the value of boron mineral potential in Turkey. These natural resources, are superior to their equivalents in the world in every respect, are able to bring the country to an unrivalled position in the boron salts sector. Eti Maden Inc. and the private sector should cooperate in producing end products from boron minerals by following marketing and industry oriented research policies. In terms of mining, operation of our boron mines are at an advantage with respect to geography, transportation, energy, etc. compared to other countries (especially Latin America, USA and China) and suitable for marketing. For example, the boron deposits in South America are at an altitude of 4000 m and those in North America are located in the middle of the desert, hence making it very difficult and problematic to operate them.

It is essential for Turkey to form a new national boron policy, so that it can appraise this natural resource with the highest return. The only way to achieve this goal is by operating boron mines towards the best interest of the country and sustaining the advantages it has. The country's resources need to be evaluated in a planned and programmed manner. Production policy should be grounded on detailed and thorough market research. These important raw-material resources must be restructured and organized to ensure maximum return for the country's economy. Production and marketing of boron minerals should be directed towards end products with a high added-value, instead of raw or semi-finished products, and related investments have to be realized as soon as possible (Table 11.3).

Boron products have a high added-value and they have a strategic role in the area they are used. Recently, boron products have been utilized in different fields of industry and shown an increase parallel to technological innovations. Rising standards of living, advancement of scientific and technological discoveries will eventually result in the demand and necessity for advanced boron compounds. Today, as economic competition is becoming more intense and many studies are being made on natural resources; the existence of a massive boron reserve potential is a great opportunity for Turkey.

11.7 Conclusions

Known reserves of borate minerals are large, particularly in Turkey, South America, and the USA, and production from Turkey and the USA will continue to dominate the world market. However, borates from other areas will probably take up an increasing share of the world market. This trend is already evident, with boric acid from Chile reaching the Far East and Europe, and both Russia and China beginning to export.

There are few substitutes for borates. In most applications, they provide unique chemical properties at a reasonable price; this is particularly true for glass fibres and in the field of heat- and impact-resistant glass. Borates are an essential part of certain plant foods. Their use in nuclear-reactor shielding and control is well documented. Future markets are difficult to predict. Based upon recent history, the major world consumers of borates will continue to be the developed countries of North America, Europe, and Japan.

Today, as economic competition is becoming more intense and many studies are being made on natural resources; the existence of a massive boron resource potential is a great opportunity for Turkey. Production and marketing of boron minerals should be directed towards end products with a high added value, instead of raw or semi-finished products, and related investments have to be realized as soon as possible.

Acknowledgments I am especially grateful to Eti Maden and their mine managers for their generosity during fieldwork in Turkey. This study has been encouraged by several research projects supported by the Dokuz Eylül University (Project Numbers: 2005.KB. FEN.053; 2006. KB. FEN.001; 2009.KB. FEN.026; 2010.KB. FEN.009; and 0922.20.01.36) and the Scientific and Technical Research Council of Turkey (TÜBİTAK, Project No: YDAB. AG-100Y044 and ÇAYDAĞ-103Y124). Review comments by Franco Pirajno considerably improved the manuscript. Mustafa Helvacı is gratefully acknowledged for his typing and drafting assistances of the manuscript.

References

Akdeniz N, Konak N (1979) Simav–Emet–Dursunbey–Demirci yörelerinin jeolojisi [Geology of the Simav–Emet–Dursunbey–Demirci areas]. General Directorate of Mineral Research and Exploration report no. 6547 (In Turkish, unpublished)

Aldanmaz E, Pearce JA, Thirwall MF, Mitchell JG (2000) Petrogenetic evolution of late Cenozoic, post-collision volcanism in western Anatolia, Turkey. J Volcanol Geoth Res 102:67–95

Altunkaynak Ş, Dilek Y, Genç ŞC, Sunal G, Gertisser R, Furnes H, Foland KA, Yang J (2012) Spatial, temporal and geochemical evolution of Oligo-Miocene granitoid magmatism in western Anatolia, Turkey. Gondwana Res 21:961–986

Alıcı P, Temel A, Gourgaud A (2002) Pb-Nd-Sr isotope and trace element geochemistry of Quaternary extension-related alkaline volcanism: a case study of Kula region (western Anatolia, Turkey). J Volcanol Geoth Res 115:487–510

Arda T (1969) Kırka boraks yatağı [Kırka borax deposit]. General Directorate of Mineral Research and Exploration Report no. 436 (In Turkish, unpublished)

Aristarain LF, Hurlbut CS Jr (1972) Boron minarals and deposits. Mineral Rec 3(165–172):213–220

Baysal O (1972) Mineralogic and genetic studies of the Sarıkaya (Kırka) Borate deposits. PhD thesis, Hacettepe University, Turkey (in Turkish, unpublished)

Bellon H, Jarrige JJ, Sorel D (1979) Les activités magmatiques égéennes de l'Oligocène a nos jours, et leurs cadres géodynamiques, données nouvelles et synthèse. Rev Géogr Phys Géol Dyn 21:41–55

Bingöl E, Delaloye M, Ataman G (1982) Granitic intrusions in western Anatolia: a contribution to the geodynamic study of this area. Eclogae Geol Helv 75:437–446

Bozkurt E (2003) Origin of NE-trending basins in western Turkey. Geodin Acta 16:61–81

Çemen İ, Ersoy EY, Helvacı C, Sert S, Alemdar S, Billor Z (2014) AAPG datapages/search and discovery article #90194 2014 International conference and exhibition, Istanbul, Turkey, September 14–17, 2014

Çoban H, Karacık Z, Ece ÖI (2012) Source contamination and tectonomagmatic signals of overlapping Early to Middle Miocene orogenic magmas associated with shallow continental subduction and asthenospheric mantle flows in Western Anatolia: a record from Simav (Kütahya) region. Lithos 140–141:119–141

Cooper MA, Hawthorne FC, Garcia-Veigas J, Alcobé X, Helvacı C, Grew ES, Ball NA (2016) Fontarnauite, $(Na, K)_2$ (Sr,Ca) (SO_4) $[B_5O_8 (OH)]$ $(H_2O)_2$, a new sulfate-borate from Doğanlar (Emet), Kütahya Province, Western Anatolia, Turkey. Can Mineral 53:1–20

Dunn JF (1986) The structural geology of the northeastern Whipple Mountains detachment fault terrane, San Bernardino County, California. MSc thesis (unpublished) Los Angeles, California, University of Southern California, p 172

Engineering and Mining Journal (2012) Industrial minerals-The boron country. Eng Min J 213, 1, January, p 61

Ercan E, Dinçel A, Metin S, Türkecan A, Günay A (1978) Uşak yöresindeki Neojen havzalarının jeolojisi [Geology of the Neogene basins in Uşak region]. Bull Geol Soc Turk 21:97–106 (In Turkish)

Ercan E, Türkecan A, Dinçel A, Günay A (1983) Kula-Selendi (Manisa) dolaylarının jeolojisi [Geology of Kula-Selendi (Manisa) area]. Geol Eng 17:3–28 (in Turkish)

Ercan E, Satır M, Sevin D, Türkecan A (1997) BatıAnadolu'dakiTersiyer ve Kuvaterner yaşlı volkanik kayaçlarda yeni yapılan radyometrik yaşölçümlerinin yorumu [Some new radiometric ages tertiary and quaternary volcanic rocks from West Anatolia]. Bull Min Res Explor 119:103–112 (in Turkish)

Erdoğan B (1990) Tectonic relations between İzmir–Ankara Zone and Karaburun Belt. Bull Min Res Explor 110:1–15

Erkül F, Helvacı C, Sözbilir H (2005a) Stratigraphy and geochronology of the early Miocene volcanic units in the Bigadiç borate basin, Western Turkey. Turk J Earth Sci 14:227–253
Erkül F, Helvacı C, Sözbilir H (2005b) Evidence for two episodes of volcanism in the Bigadic borate basin and tectonic implications for Western Turkey. Geol J 40:545–570
Erkül F, Helvacı C, Sözbilir H (2006) Olivine basalt and trachyandesitepeperites formed at the subsurface/surface interface of a semi-arid lake: an example from the Early Miocene Bigadiç basin, western Turkey. J Volcanol Geotherm Res 149:240–262
Ersoy Y, Helvacı C (2007) Stratigraphy and geochemical features of the Early Miocene bimodal (ultrapotassic and calc-alkaline) volcanic activity within the NE-trending Selendi basin, western Anatolia, Turkey. Turk J Earth Sci 16:117–139
Ersoy EY, Helvacı C, Sözbilir H, Erkül F, Bozkurt E (2008) A geochemical approach to Neogene–Quaternary volcanic activity of the western Anatolia: an example of episodic bimodal volcanism within the Selendi Basin. Chem Geol 255(1–2):265–282
Ersoy EY, Helvacı C, Sözbilir H (2010) Tectonic evolution of the NE-trending superimposed Selendi Basin, Western Anatolia, Turkey. Tectonophysics 488(1–4):210–232
Ersoy EY, Helvacı C, Palmer MR (2011) Stratigraphic, structural and geochemical features of the NE–SW-trending Neogene volcano-sedimentary basins in western Anatolia: implications for associations of supradetachment and transtensional strike-slip basin formation in extensional tectonic setting. J Asian Earth Sci 41:159–183
Ersoy EY, Helvacı C, Palmer MR (2012a) Petrogenesis of the Neogene volcanic units in the NE–SW-trending basins in western Anatolia, Turkey. Contrib Mineral Petrol 163:379–401
Ersoy YE, Helvacı C, Uysal İ, Palmer MR, Karaoğlu Ö (2012b) Petrogenesis of the Miocene volcanism along the İzmir-Balıkesir transfer zone in western Anatolia, Turkey: implications for origin and evolution of potassic volcanism in post-collisional areas. J Volcanol Geotherm Res 241–242:21–38
Ersoy EY, Çemen İ, Helvacı C, Billor Z (2014) Tectono-stratigraphy of the Neogene basins in Western Turkey: implications for tectonic evolution of the Aegean extended region. Tectonophysics 635:33–58
Floyd PA, Helvacı C, Mittwede SK (1998) Geochemical discrimination of volcanic rocks, associated with borate deposits: an exproation tool. J Geochem Explor 60:185–205
Fytikas M, Innocenti F, Manetti P, Mazzuoli R, Peccerillo A, Villari L (1984) Tertiary to quaternary evolution of volcanism in the Aegean region. In: Dixon JE, Robertson AHF (eds) The Geological evolution of the eastern Mediterranean. Geol Soc Lond Spec Publ 17, pp 687–699
García-Veigas J, Helvacı C (2013) Mineralogy and sedimentology of the Miocene Göcenoluk borate deposit, Kırka district, western Anatolia, Turkey. Sediment Geol 290:85–96
García-Veigas J, Ortí F, Rosell L, Gündoğan I, Helvacı C (2010) Occurrence of a new sulphate mineral Ca7Na3K(SO4)9 in the Emet borate deposits, western Anatolia (Turkey). Geol Q 54:431–438
García-Veigas J, Rosell L, Ortí F, Gündoğan İ, Helvacı C (2011) Mineralogy, diagenesis and hydrochemical evolution in a probertite–glauberite–halite saline lake (Miocene, Emet Basin, Turkey). Chem Geol 280:352–364
Garrett DE (1998) Borates. In: Handbook of deposits, processing, properties, and use. Academic Press, London, p 483
Gawlik J (1956) Borate deposits of the Emet Neogene basin. General Directorate of Mineral research and Exploration report no. 2479, Ankara (in Turkish and German, unpublished)
Gök S, Çakır A, Dündar A (1980) Stratigraphy, petrography and tectonics of the borate-bearing Neogene in the vicinity of Kırka. Bull Geol Congr Turk 2:53–62
Grew ES, Anovita LM (1996) Boron. Mineralogy, petrology and geochemistry. Reviews in mineralogy. Miner Soc Am vol 33 Washington, DC, 862p

Güleç N (1991) Crust-mantle interaction in western Turkey: implications from Sr and Nd isotope geochemistry of tertiary and quaternary volcanics. Geol Mag 23:417–435
Gündoğan İ, Helvacı C (1993) Geology, mineralogy and economic potential of Sultançayır (Susurluk-Balıkesir) boratiferous gypsum basin. Bull Geol Soc Turk 36:159–172 (in Turkish with English abstract)
Gündoğdu MN, Bonnot-Courtois C, Clauer N (1989) Isotopic and chemical signatures of sedimentary smectite and diagenetic clinoptilolite of a lacustrine Neogene basin near Bigadiç, western Turkey. Appl Geochem 4:635–644
Hasözbek A, Satir M, Erdoğan B, Akay E, Siebel W (2011) Early Miocene post-collisional magmatism in NW Turkey: geochemical and geochronological constraints. Int Geol Rev 53:1098–1119
Helvacı C (1977) Geology, mineralogy and geochemistry of the borate deposits and associated rocks and the Emet Valley, Turkey. PhD thesis University of Nottingham, England (unpublished)
Helvacı C (1978) A review of the mineralogy of the Turkish borate deposits. Mercian Geol 6:257–270
Helvacı C (1983) Mineralogy of the Turkish borate deposits. Geol Eng 17:37–54
Helvacı C (1984) Occurence of rare borate-minerals: veatchite-A, tunellite, teruggite and cahnite in the Emet borate deposits, Turkey. Miner Deposita 19:217–226
Helvacı C (1986) Geochemistry and origin of the Emet borate deposits, western Turkey. Faculty of Engineering Bulletin, Cumhuriyet University, Series A. Earth Sciences 3, pp 49–73
Helvacı C (1989) A mineralogical approach to the mining, storing and marketing problems of the Turkish borate production. Geol Eng 34–35:5–17
Helvacı C (1994) Mineral assemblages and formation of the Kestelek and Sultançıyır borate deposits. Proceedings of 29th International Geological Congress, Kyoto Part A, pp 245–264
Helvacı C (1995) Stratigraphy, mineralogy, and genesis of the Bigadiç borate deposits, western Turkey. Econ Geol 90:1237–1260
Helvacı C (2005) Borates. In: Selley RC, Cocks LRM, Plimer IR (eds) Encyclopedia of geology, vol 3. Elsevier, Amsterdam, pp 510–522
Helvacı C (2012) Trip to Kışladağ (Uşak) Gold Mine, Kırka and Emet borates deposits. Post colloquium field trip guide book. International Earth Sciences Colloquium on the Agean Region, IESCA 2012, İzmir, Turkey, 41p
Helvacı C (2015) Geological features of Neogene basins hosting borate deposits: an overview of deposits and future forecast, Turkey. Bull Min Res Explor 151:169–215
Helvacı C, Alonso RN (2000) Borate deposits of Turkey and Argentina: a summary and geological comparison. Turk J Earth Sci 24:1–27
Helvacı C, Ercan T (1993) Recent borate salts and associated volcanism in the Karapınar Basin (Konya), Turkey 46th Geological Congress of Turkish Abstracts, pp 102–103
Helvacı C, Erkül F (2002) Soma ve Bigadiçarasındaki (BatıAnadolu) volkanik fasiyeslerin sedimentolojik, petrografik ve jeokimyasal veriler ışığında kökensel yorumu [Interpretation of volcanic facies origin of Soma and Bigadiç area (west Anatolia)]. Dokuz Eylül University AFS Project No: 0922.20.01.36, 82 p. (in Turkish, unpublished)
Helvacı C, Ersoy EY (2006) The facies characteristics and geochemical featuresof the volcanic rocks of the Selendi and Simav area, and their relations with the basin sedimentary rocks, western Anatolia. DEÜ Scientific Research Project no. 03.KB. FEN.058. January 2006, İzmir, 116 p. (in Turkish, unpublished)
Helvacı C, Firman RJ (1976) Geological setting and mineralogy of Emet borate deposit, Turkey. Trans Sect B Inst Min Met 85:142–152
Helvacı C, Orti F (1998) Sedimentology and diagenesis of Miocene colemanite-ulexite deposits (western Anatolia, Turkey). J Sediment Res 68:1021–1033
Helvacı C, Ortí F (2004) Zoning in the Kırka borate deposit, western Turkey: primary evaporitic fractionation or diagenetic modifications? Can Miner 42:1179–1204
Helvacı C, Yağmurlu F (1995) Geological setting and economic potential of the lignite and evaporite-bearing Neogene basins of Western Anatolia, Turkey. Isr J Earth Sci 44:91–105

Helvacı C, Yücel-Öztürk Y (2013) Bor minerallerinin fluorescent yöntemiyle çalışılması [Study of borate minerals with fluorescent method]. DEU 2010 KB FEN 9, 25.03.2013. (In Turkish, unpublished)

Helvacı C, Stamatakis MG, Zagouroglou C, Kanaris J (1993) Borate minerals and related authigenicsilicates in northeastern Mediterraean Late Miocene continental basins. Explor Min Geol 2:171–178

Helvacı C, Sözbilir H, Erkül F (2003) Soma ve Bigadiç arasındaki (BatıAnadolu) volkanik fasiyeslerin sedimentlojik, petrografik ve jeokimyasal veriler ışığında kökensel yorumu [Interpretation of volcanic facies origin of Soma and Bigadiç area (west Anatolia)]. Turkish National Research Council Project No: YDABCAG/100Y044, İzmir, 155 p. (in Turkish, unpublished)

Helvacı C, Ersoy Y, Erkül F, Sözbilir H, Bozkurt E (2006) Selendi Havzasının stratigrafik, petrografik, jeokimyasal ve tektonik veriler ışığında volkono-sedimanter evrimi ve ekonomik potansiyeli [Volcanosedimentary evaluation and economic potential of the Selendi basin with regard to stratigraphy, petrpgraphy, geochemical and tectonic data]. Turkish National Research Council Project no: ÇAYDAĞ/103Y124, Aralık 2006, 134 p. (in Turkish, unpublished)

Helvacı C, Karaoğlu Ö, Ersoy Y, Erkül F, Bozkurt E (2009) Volcano-Tectonic evolution of the Uşak-Eşme-Banaz basin: an approach to stratigraphic, sedimentologic and geochemical view. Dokuz Eylül University Scientific Research Project No: 2005.KB. FEN.053, September 2009, İzmir, 75 p. (in Turkish, unpublished)

Helvacı C, Orti F, Garcia-Veigas J., Rosell L, Gündoğan İ, Yücel-Öztürk Y (2012) Neogene borate deposits: mineralogy, petrology and sedimentology; a workshop with special emphasis on the Anatolian deposits. International Earth Sciences Colloquium on the Agean Region, IESCA 2012, İzmir, Turkey, 64p

Helvacı and Ersoy K (1972) New borate district, Eskişehir-Kırka province, Turkey. Inst Min Met 8l:B163–Bl65

İnan K (1972) New borate district, Eskişehir-Kırka province, Turkey. Inst Min Met 8l: B163–Bl65

İnan K, Dunham AC, Esson J (1973) Mineralogy, chemistry and origin of Kırka borate deposit, Eskişehir Province, Turkey. Trans Sect B Inst Min Met 82:114–123

İnci U (1984) Neogene oil shale deposits of Demirci and Burhaniye regions. 27th International Geological Congress, Abs vol. VII, 13–16 (57)

Innocenti F, Agostini S, Di Vincenzo G, Doglioni C, Manetti P, Savaflç›n MY, Tonarini S (2005) Neogene and quaternary volcanism in Western Anatolia: magma sources and geodynamic evolution. Mar Geol 221:397–421

Jackson J, McKenzie D (1984) Active tectonics of the Alpine-Himalayan Belt between western Turkey and Pakistan. Geophys J R Astron Soc 77:185–264

Karaoğlu Ö, Helvacı C, Ersoy EY (2010) Petrogenesis and 40 Ar/39 Ar geochronology of the volcanic rocks of the Uşak–Güre basin, western Türkiye. Lithos 119:193–210

Kistler RB, Helvacı C (1994) Boron and borates. In: Carr DD (ed) Industrial minearls and rocks, 6th edn. Society for Mining, Metallurgy and Exploration, Littleton, pp 171–186

Krushensky RD (1976) Neogene calc-alkaline extrusive and intrusive rocks of the Karalar Yeşiller area, Northwest Anatolia, vol 40. Bulletin volcanologique, Turkey, pp 336–360

Meixner H (1965) Borate deposits of Turkey. Bull Min Res Explor 125:1–2

MTA (2002) 1/500,000 Scaled Geology Map, General Directorate of Mineral Research and Exploration, Ankara

Muessig S (1959) Primary borates in playa deposits: minerals of high hydration. Econ Geol 54:495–501

O'Driscoll M (2011) Rio Tinto minerals declares force majeure on sodium borates: industrial minerals. January 31. Accessed 1 Oct 2012, at http://www.indmin.com/

Ocakoğlu F (2007) A re-evaluation of the Eskişehir fault zone as a recent extensional structure in NW Turkey. J Asian Earth Sci 31:91–103

Okay Aİ, Satır M, Maluski H, Siyako M, Monie P, Metzger R, Akyüz S (1996) Paleo- and Neo-Tethyan events in northwestern Turkey: geologic and geochronologic contraints. In: Yin A, Harrison M (eds) The tectonic evolution of Asia. Cambridge University Press, Cambridge, UK, pp 420–441

Orti F, Helvacı C, Rosell L, Gündoğan İ (1998) Sulphate-borate relations in an evaporitic lacustrine environmet: the Sultançayır Gypsum (Miocene, Western Anatolia). Sedimentology 45:697–710

Okay AI, Siyako M (1991) The New Position of the İzmir-Ankara Neo-Tethyan Suture between İzmir and Balıkesir. In: Proceedings of the Ozan Sungurlu Symp., pp. 333–355

Ozol AA (1977) Plate Tectonics and the process of volcanogenic-sedimentary formation of Boron. Int Geol Rev 20:692–698

Özpeker İ (1969) Western Anatolian borate deposits and their genetic studies. PhD dissertation, İstanbul Technical University (in Turkish with English abstract, unpublished)

Palache C, Berman H, Frondel C (1951) The system of mineralogy, vol 2, 7th edn. John Wiley & Sons, New York, p 1124

Palmer MR, Helvacı C (1995) The boron geochemistiry of the Kırka borate deposit, western Turkey. Geochim Cosmochim Acta 59:3599–3605

Palmer MR, Helvacı C (1997) The boron istope geochemistry of the Neogene borate deposits of western Turkey. Geochim Cosmochim Acta 61:3161–3169

Pe-Piper G, Piper DJW (2007) Late Miocene igneous rocks of Samos: the role of tectonism in petrogenesis in the southeastern Aegean. Geol Soc Lond, Spec Publ 291:75–97

Preleviç D, Akal C, Foley F, Romer RL, Stracke A, van den Bogaard P (2012) Ultrapotassic mafic rocks as geochemical proxies for postcollisional dynamics of orogenic lithospheric mantle: the case of southwestern Anatolia, Turkey. J Petrol 53:1019–1055

Purvis M, Robertson AHF (2005) Miocene sedimentary evolution of the NE-SW-trending Selendi and Gördes Basins, Western Turkey: implications for extensional processes. Sediment Geol 174:31–62

Rio Tinto plc (2011) Form 20–F – annual report for the fiscal year ended December 31, 2010: Washington, DC, Securities and Exchange Commission, March 15. Accessed 27 Sept 2012, at http://www.secinfo.com/

Ring U, Collins AS (2005) U-Pb SIMS dating of synkinematic granites: timing of core-complex formation in the northern Anatolide belt of western Turkey. J Geol Soc 162(2):289–298

Roskill Information Services Ltd. (2010) Boron – Global industry markets and outlook. Roskill Information Services, London, 243 p

Seghedi I, Helvacı C (2014) Early Miocene Kırka-Phrigian caldera, western Anatolia – an example of large volume silicic magma generation in extensional setting. Geophysical Research Abstracts Vol. 16, EGU2014-5789, 2014 EGU General Assembly, Vienna, 2014

Seghedi I, Helvacı C, Pécskayc Z (2015) Composite volcanoes in the south-eastern part of İzmir–Balıkesir Transfer Zone, Western Anatolia, Turkey. J Volcanol Geotherm Res 291:72–85

Şengör AMC (1984) The cimmeride orogenic system and the tectonics of Eurasia. Geol Soc Am Spec Paper 195 p

Şengör AMC, Yılmaz Y (1981) Tethyan Evolution of Turkey: a plate tectonic approach. Tectonophysics 75:181–241

Seyitoğlu G (1997a) Late Cenozoic tectono-sedimentary development of the Selendi and Uşak–Güre basins: a contribution to the discussion on the development of east–west and north trending basins in Western Turkey. Geol Mag 134:163–175

Seyitoğlu G (1997b) The Simavgraben: an example of young E–W trending structures in the late Cenozoic extensional system of Western Turkey. Turk J Earth Sci 6:135–141

Seyitoğlu G, Scott BC (1992) Late Cenozoic volcanic evolution of the NE Aegean region. J Volcanol Geotherm Res 54:157–176

Sunder MS (1980) Geochemistry of the Sarıkaya borate deposits (Kırka-Eskişehir). Bull Geol Soc Turk 2:19–34

Travis NJ, Cocks EJ (1984) The Tincal trail. A history of borax. Harrap, London, p 311

Uyanik T (2010) Mining: Ankara, Turkey, export promotion center of Turkey. August, 7 p. Accessed 1 Oct 2012, at http://www.tcp.gov.tr/Assets/sip/san/Mining.pdf

Watanebe T (1964) Geochemical cycle and concentration of boron in the earth's crust. V.I. Verdenskii Inst. Geochim Analit Chem USSR 2:167–177

Yiğit O (2009) Mineral deposits of Turkey in relation to Tethyan metallogeny: implications for future mineral exploration. Econ Geol 104:19–51

Yılmaz Y (1990) Comparison of young volcanic associations of western and eastern Anatolia formed under a compressional regime: a review. J Volcanol Geotherm Res 44:1–19

Yılmaz Y, Genç SC, Gürer OF, Bozcu M, Yılmaz K, Karacık Z, Altunkaynak Ş, Elmas A (2000) When did the western Anatolian grabens begin to develop? In: Bozkurt E, Winchester JA, Piper JDA (eds) Tectonics and magmatism in Turkey and the surrounding area. Geol Soc London, Spec Publ 173, pp 353–384

Yücel-Öztürk Y, Ay S, Helvacı C (2014) Bor Minerallerinin Duraylı İzotop Jeokimyası: Bigadiç (Balıkesir) Borat Yatağından Bir Örnek [Stable isotope geochemistry of the Boron minerals: an example from Bigadiç (Balıkesir) borate deposits]. Yerbilimleri 35(1):37–54 (in Turkish with English abstract)

Chapter 12
Turkish Trona Deposits: Geological Setting, Genesis and Overview of the Deposits

Cahit Helvacı

Abstract Trona deposits have limited distribution in the Earth's crust, but extraordinary concentrations can be found in some places, commonly in combination with borate and other salt deposits. Four main continental trona provinces are recognized at a global scale. They are located in Anatolia (Turkey), Wyoming (USA), Whuceng (China) and Botswana (Southern Africa). The origin of trona deposits is related to alkaline volcanism, thermal spring activity, closed basins and arid climate. Quaternary sodium carbonate minerals (trona minerals) are present in salars (Andes), playa lakes (Lake Van, Turkey and Botswana) and salt pans (USA and Tibet).

Some conditions are essential for the formation of economically viable trona deposits: formation of shallow lake environments; source derived explosive andesitic to rhyolitic volcano-sedimentary sequences; concentration of sodium and bicarbonate in the lake, related to direct ash fall into the basin, or hydrothermal solutions along faults; thermal springs near areas of volcanic activity; arid to semi-arid climatic conditions; alkaline lake water.

Many minerals contain Na carbonate, but the three that are most important from a worldwide commercial standpoint are trona, nahcolite, and pirssonite, which are produced in a limited number of countries, along with subordinate bradleyite, shortite and thenardite. Pirssonite occurs in organic-rich muds (oil shales). Trona and nahcolite are precipitated subaqueously (in lake waters) and as an interstitial phase in playa muds. Evaporite minerals are closely related to pyrite in oil shales and are also associated with diagenetic silicates (Mg-rich smectites, zeolites, K-feldspar, searlesite, and idiomorphic quartz) and dolomite formed by reaction of alkaline brines with pyroclastic deposits.

Natural sodium carbonate minerals (soda minerals) are exploited commercially either from buried fossil trona deposits formed in Tertiary playa-lake sediments or by extraction from the brines of recent alkaline lakes and playas. Most of the world's commercial trona deposits are mined by underground and solution mining methods. Many modern industries use industrial trona minerals.

C. Helvacı (✉)
Faculty of Engineering Geology Department, Dokuz Eylul University, Izmir, Turkey
e-mail: cahit.helvaci@deu.edu.tr

F. Pirajno et al. (eds.), *Mineral Resources of Turkey*, Modern Approaches in Solid Earth Sciences 16, https://doi.org/10.1007/978-3-030-02950-0_12

12.1 Introduction

Sedimentary Na-carbonates are an evaporite mineral group formed in alkaline lakes (also known as soda lakes) with pH typically between 9 and 12. In these settings, lake waters are characterized by relative enrichment in $HCO_3^- + CO_3^{2-}$ with respect to $Mg^{2+} + Ca^{2+}$. During evaporation, after Mg^{2+} and Ca^{2+} are almost exhausted during calcite, magnesite, and dolomite precipitation, eventually Na-carbonate rich waters form. In addition, non-evaporite minerals, including authigenic silicates, also form in alkaline lakes in volcaniclastic terrains. More than twenty Na-bearing evaporite minerals are known including carbonates, chlorides, sulphates, borates and borosilicates (Smith and Haines 1964; Eugster and Smith 1965).

In general, fossil soda deposits and recent soda playa-lakes were formed or are presently forming by evaporation within intercontinental basins, in arid or semi-arid areas, fed partly by surface streams and partly by thermal springs, and surrounded by abundant Na-rich volcanic and magmatic rocks. Trona beds are deposited in playa-lake environment in basins, which are restricted by mud flats and fed by Na-rich solutions and springs. Bituminous shales, which are accumulated during the extensional periods of the playa lakes, alternate with trona beds.

The known trona fossil deposits of the world are located within the Green River Formation, Wyoming (U.S.A), Hırka Formation, Beypazarı (Turkey) and Wulidui Formation, Wucheng (China).

The Eocene Green River Formation (Wyoming, USA) is the largest and best-preserved Na-carbonate deposit. This giant lacustrine formation occurs in several sedimentary basins with large volumes of oil shales and economically important Na-carbonate deposits (Bradley 1964; Bradley and Eugster 1969; Eugster and Surdam 1973; Dyni 1996; Smith et al. 2008). Nahcolite, not trona, is stable at high values of dissolved CO_2 (Eugster and Smith 1965). Based on primary nahcolite textures in the Piceance Creek Basin (Colorado) of the Green River Formation, and assuming CO_2 equilibrium between brine and atmosphere, an elevated carbon dioxide level for the early Eocene atmosphere was estimated by Lowenstein and Demicco (2006).

Natural sodium carbonate-bearing minerals occur widely in China. Approximately thirty alkaline lakes and natural soda mines have been exploited. Some of the larger natural soda deposits are concentrated in the Nanyang basin (Henan Province) and in the Inner Mongolia plateau. Proven total sodium carbonate reserves are 154 Mt. About 83.5% of these reserves is contained in Henan Province, and 15.5% of the reserves is contained in the Inner Mongolia Autonomous Region. The Wucheng trona deposit was discovered in 1971 during petroleum exploration. It is located in southem Henan Province, 18 km west of Tongbai County at latitude 32.4°N, longitude 113.5°E. The deposit occurs in the central part of the Paleogene Wucheng basin and was formed in the Eocene Epoch. The trona beds occupy an area of 4.66 km^2 at depths of 643–974 m. Resources of the Wucheng trona deposit total 36.8 Mt sodium carbonate and 17.8 Mt sodium chloride. The sodium carbonate-bearing minerals

include mainly trona and nahcolite associated with shortite, northupite, and NaCl. $Na_2CO_3(MgFe)CO_3$ (Kostick 1994; Helvacı 1998, 2001).

Soda-rich recent alkaline lakes, and playas are: Searles Lake (U.S.A), Lake Magadi (Kenya), San Critobal Ecalepec Playa (Mexico), Sowa Pan Playa (Botswana) and Van Lake (Turkey).

Although modern alkaline lakes exist in arid zones throughout the world, the major Na-carbonate lakes occur along the East African Rift System. Tectonic and climatic controls on rift escarpments and bedrock geology dominated by Na-rich trachyte lavas supplied by recent volcanism led to the establishment of a large number of highly alkaline lakes with variable salinity, depth and chemical composition, ranging from perennial, meromictic lakes (e.g., Lake Bogoria, Kenya; Renaut and Tiercelin 1994) to more concentrated, ephemeral lakes (e.g., Lake Magadi and Lake Natron, Kenya; Eugster 1980). Geysers and perennial hot springs in these alkaline lake systems are fed by deep groundwaters coming from marginal streams that disappear in alluvial fans before they reach valley centers and are more likely derived from deep seated hydrothermal systems (Renaut et al. 2013). Hydrothermal activity and springs play an important role in early maturation of microbial organic matter and also in the formation of evaporite minerals (Renaut and Tiercelin 1994; Earman et al. 2005).

Trona, sodium sesquicarbonate ($Na_2C0_3.NaHC0_3.2H_2O$), called "magadi" in East Africa, is the main Na-carbonate mineral precipitated in some of these modern soda lakes. Na-rich minerals (halite, trona, hanksite and borax) are dominantly found in saline units whereas Na–Ca-rich minerals (gaylussite and pirssonite) predominate in muddy intervals. The ephemeral Lake Magadi (Kenya) has become the type example for alkaline lakes (Jones et al. 1977; Eugster 1980). At present, trona is the main Na carbonate in Lake Magadi, while nahcolite precipitates in Malha crater lake (Sudan), probably as a result of high biogenic CO_2 (Mees et al. 1991). Another well-known Na-carbonate deposit is in Pleistocene Searles Lake (California).

Soda and soda ash are used as a source of Na_2O in glass manufacturing, in the production of various sodium chemicals, in water treatment, paper production, iron desulfurization, and many other uses. Natural sodium carbonate minerals (soda minerals) are exploited commercially either by mining beds of buried fossil trona deposits formed in Tertiary playa-lake sediments or by extraction from the brines of recent alkaline lakes. Soda extraction from the deeper lakes, such as Van Lake, is not presently economical, as soda concentration has not yet reached a sufficient level (Helvacı 2001, 2003). Production from brines and fossil trona deposits is becoming increasingly important, although the bulk of the world's soda ash is produced synthetically by some 60 solvay facilities (production synthetically), in more than 40 countries. Soda production from natural deposits are mainly limited to USA, Mexico and Kenya. Major soda production by solvay factories are mainly located in the Russia, UK, West Germany, France, China, Bulgaria, and Japan. Annual soda production of the world is approximately 30 Mt, whereas Mersin Soda industry in Turkey produces, annually, approximately 300,000 t of soda ash by solvay works. Contributions to Turkey's annual soda ash capacity are

from the Beypazarı natural soda and in addition production from Kazan deposit in the nearest future.

The trona deposits of the Green River Basin in southwestern Wyoming (U.S.A) are the world's largest resource of natural soda ash. Wyoming is often referred to as the "Soda Ash Capital of the World" because of the enormous world-class trona reserves of the Green River Basin. Trona, was precipitated in a lacustrine environment during the contractional stages of the Wilkins Peak Member of the Eocene Green River Formation in southwestern Wyoming. Because it is composed of 70% sodium carbonate, trona is commonly referred to as natural soda ash. Over 90% of the United States soda ash is produced by five Wyoming trona companies. This equates to over 30% of the world's soda ash production. The total resource of the Wyoming trona deposits (22 persistent trona beds) is estimated at 122 billion tonnes (Bt), or 122 gigatonnes (Gt). Of this, 36 Gt of economic trona reserves are mineable by current technology, including conventional "hard rock" methods, mechanized extraction (drum-miner and boring machines), and hydraulically supported longwall shearing (Eugster and Surdam 1973; Kostick 1994; Onargan and Helvacı 2001; Helvacı 1998).

In Turkey, the main trona fossil deposits and occurrences are the Beypazarı, Kazan, Gürün and in the alkaline Lake Van, which is a potential Na-carbonate-rich lake in Turkey (Helvacı 2003). Turkey, Western and Eastern Europe, and the Middle East are the main markets for Beypazarı trona ore. The soda ash demand of the region was approximately 12 million tons in 1996, and the demand, with an increase at a rate of 2.8% per year, is estimated to reach 13 million tons in 2000. Soda extraction from the deeper lakes, such as Van Lake, is not presently economical, as soda concentration has not yet reached sufficient levels (Helvacı 2003).

Resource evaluation studies suggest that Beypazarı Trona Deposit contains 235 Mt of economic trona body grading 56% and above; the declared resource is 607 Mt of economic ore body grading an average of 31% trona in the Kazan Trona Deposit. Known trona resources of Turkey are totally 842 Mt. Solution technology is the preferred exploitation methodology in both deposits. Eti Soda in Ciner Group is the owner of the Beypazarı Trona and Kazan Soda Electricity in Ciner Group is the owner of the Kazan Trona recently. The target of the production capacity of the Beypazarı Processing Plant aims to a production of about 1,600,000 tonnes per year of soda ash, and the production capacity of the Kazan Process Plant is about 2,700,000 tonnes/year (Ciner Group 2009). Productions are 1 Mt of soda ash and additionally 100,000 tonnes of sodium bicarbonate for the food sector per year. Glass and chemical industries are main sectors that use heavy soda ash (Helvacı 1998, 2001; Onargan and Helvacı 2001; Demirci 2000; Ciner Group 2009). Marketing difficulties will not exist after operation of Beypazarı trona deposit begins, and 1 million tonnes of ore per year can be sold in the regions mentioned above. Consequently, the marketing of the Beypazarı trona ore can provide more than 170–180 million US dollars.

12.2 Geology and Mineralogy of Trona Deposits

12.2.1 Geological Setting of the Beypazarı Deposit

The Neogene Beypazari Basin (Fig. 12.1) is located approximately 100 km northwest of Ankara in the Pontides region of central Anatolia and is limited to the north by the western Pontide mountain belt. It is one of the most important basins in Turkey, containing lignite, bituminous shale and trona deposits. The Neogene Beypazarı basin is filled mainly by fluvial, lacustrine, and volcano-sedimentary rocks. Trona, lignite, and bituminous shale occur in the lower part, and Na-sulphate and gypsum occur in the upper part of the sedimentary sequence in the Miocene Beypazarı basin. Paleogene assemblages consist of terrigenous clastics and tuffaceous deposits.

The rock units of the study area are divided into two main groups: pre-Neogene basement rocks and Neogene rock units (Figs. 12.1 and 12.2). The pre-Neogene basement in the basin ranges in age from Paleozoic to Eocene and comprises metamorphic, granitic, ultrabasic, carbonaceous and clastic rocks in the southern part of the basin, and carbonate and flysch assemblages in the northern part (Kalafatçıoğlu and Uysallı 1964; Ketin 1966; Saner 1979; Varol and Kazancı 1981). The Soğukcam

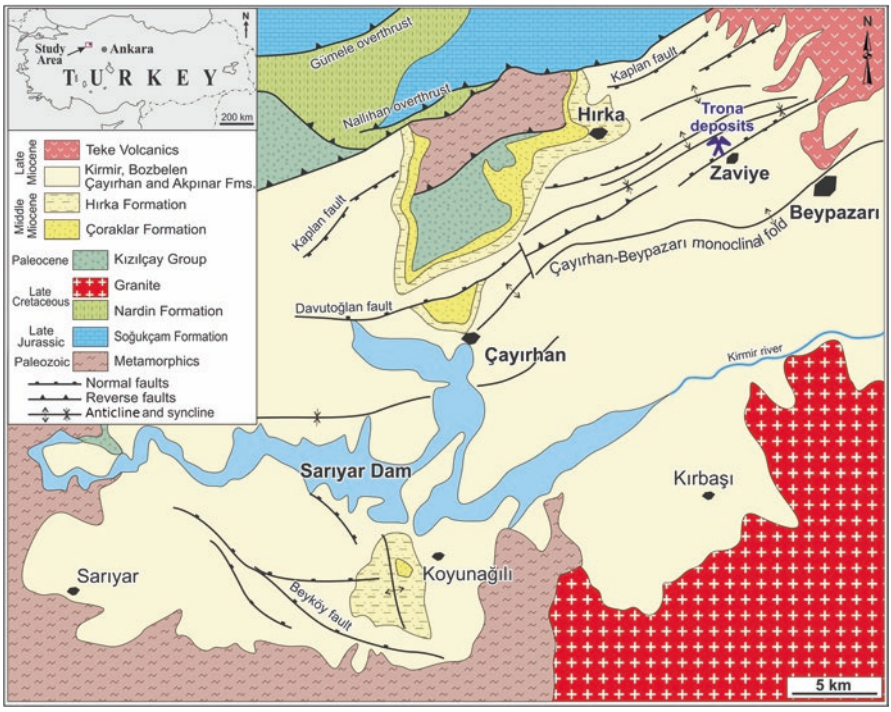

Fig. 12.1 Geological and structural map of the Beypazarı basin. (After Helvacı 2010)

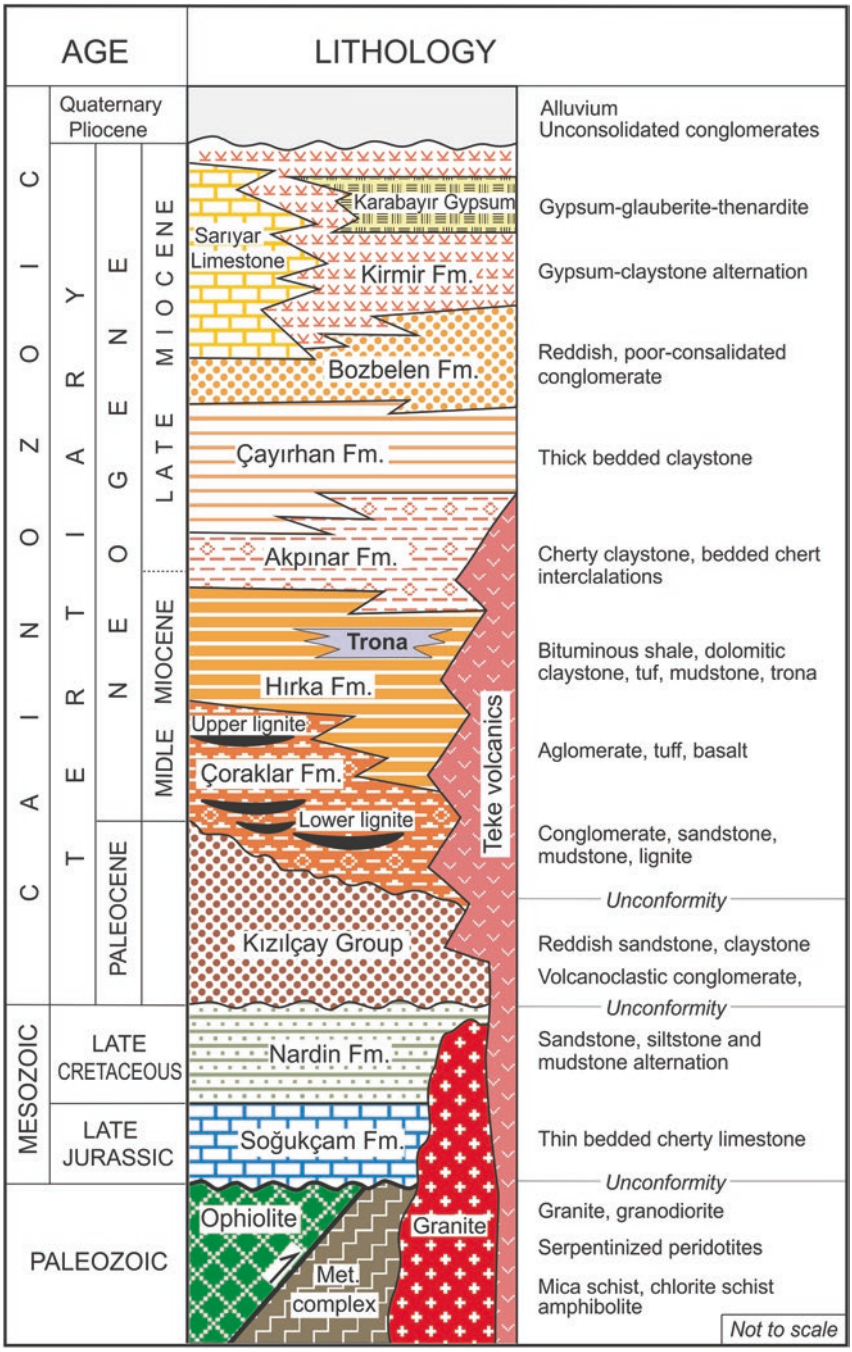

Fig. 12.2 Stratigraphic column of the Beypazarı trona basin. (After Helvacı 2010)

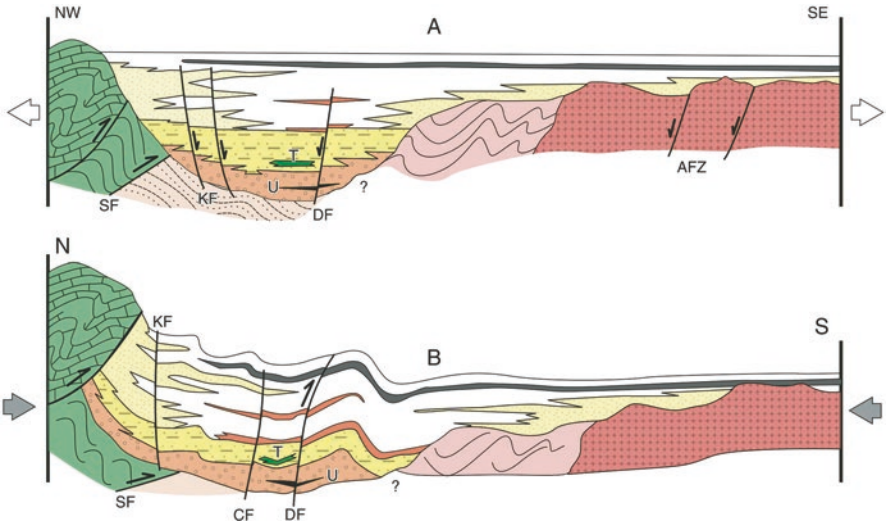

Fig. 12.3 Tectosedimentary evolution of the Beypazarı Miocene basin: (**a**) Miocene extension phase. (**b**) Post-Miocene compressive phase. Big circle—lower alluvial facies; dots—upper alluvial facies; dashed lines—lithofacies of the Hırka Formation; *U* upper lignite, *T* trona; diagonal strips—carbonate rock; white tone—green claystone lithofacies; dark line—evaporite lithofacies (sulphates); *KF* Kaplan fault, *DF* Davutoğlan, *SF* Sekli fault, *AFZ* Ayaş fault zone, *CF* Çömlektepe fault. (After Helvacı 2010)

Limestone, Nardin Formation, and the Kızılcay Group range in age from pre-Permian to middle Eocene (Figs. 12.2 and 12.3). The oldest rocks observed in the study area are Paleozoic metamorphic rocks, which consist of mica schist, chlorite schist, amphibolite, quartzite and marble. The Middle Sakarya Massif consists mainly of metamorphic, acidic-plutonic and ultrabasic rocks and occurs to the South of the Beypazarı basin (Saner 1979; Helvacı et al. 2014).

The inferred age of the metamorphic rocks is pre-Permian along the Middle Sakaya River (Altınlı 1976, 1977). These rocks were intruded by granite. The granites intruded into the metamorphic rocks during post-Permian time. The Beypazarı granitoid is a good example of Late Cretaceous subduction-related magmatism in the Sakarya zone (Helvacı et al. 2014). Aplite and pegmatite veins occur in the granites, strike NE-SW and NW-SE, and dip to the south in Neogene rock units the south (Helvacı and Bozkurt 1994).

The ultramafics rocks are mainly composed of serpentinite, metabasite, red chert, and gabbroic components and were emplaced on the metamorphic rocks along a tectonic (fault) contact during Late Cretaceous time (Çoğulu 1967). Jurassic rocks are represented by thin-bedded, micritic, sparitic, and ammonite-bearing fossiliferous limestones alternating with sandstone, shale, and chert layers, and are named the "Bilecik Limestone" by Altınlı (1978). The Bilecik Limestone grades into a Lower Cretaceous limestone named the "Soğukcam Limestone" by earlier workers in the area under investigation and in the area west of Nallıhan. In the

region, the Upper Cretaceous sequence is represented by turbiditic clastic rocks of the Nardin Formation and rests concordantly on Lower Cretaceous limestones (Önal and others 1988). The Paleocene sequence consists mainly of reddish and grayish conglomerate, sandstone, siltstone, mudstone, thin-bedded limestone, and greenish to brownish volcaniclastic rock units and are named "Kızılçay Group" by Altınlı (1978) and Saner (1979). The Kızılcay Group was deposited in fluvial and lacustrine environments and its total thickness exceeds 2000 m (Önal et al. 1988). Eocene rocks in the area are mostly limestones and sandstones with a total thickness of approximately 250 m.

The Beypazarı Neogene basin and its economic resources were investigated by previous workers over a long period of time. Kayakıran et al. (1986) and Helvacı et al. (1989) investigated some features of the trona deposits of the Beypazarı region. One of the more detailed reports was prepared by Siyako (1984) and described the geological features of the Beypazarı, Çayırhan and Koyunağılı lignite deposits and their reserves.

A Neogene basin extending along an east-west direction from Beypazarı to Nallıhan contains a sedimentary sequence of up to 1200 m total thickness. The pre-Neogene basement rock assemblages of the west Pontides limit the basin to the north. The middle Sakarya massif consisting mainly of ultramafic, granitic and metamorphic rocks which border the basin to the south. The Neogene sedimentary sequence is composed mostly of lacustrine and alluvial sediments which were deposited under the control of a tectonic regime. Synthetic faults are occurred pene-contemporaneously with the growth faults result in a stepwise normal fault system along the basin margins. Intermediate and felsic volcanics, which are dominant in the eastern part of the basin, show lateral interfingering with Miocene sediments. A sedimentary sequence ~1200 m thick, ranging in age from Middle to Late Miocene, crops out in the Beypazarı-Çayırhan district. This basin is mainly filled by fluvial, lacustrine and volcano-sedimentary rocks. The Miocene sequence rests on basement rocks along an angular unconformity; the basement rocks comprise metamorphic, ophiolitic, carbonate and clastic rocks ranging in age from Paleozoic to Eocene. The pre-Neogene sedimentary rocks limit the Neogene basin from the west and vary from Palaeocene to Eocene in age.

The Beypazarı Neogene basin is filled mainly by fluvial, lacustrine, and volcano-sedimentary rocks, including middle to upper Miocene clastics, carbonates, evaporites and volcanogenic units. The Neogene sedimentary sequence filling the Beypazari Basin incorporates middle to upper Miocene clastics, carbonates, evaporites and volcanogenic units, with a thickness of 1200 m. he youngest of these units, the Kirmir Formation, reaches a thickness of 250 m in the central part of the basin (Yağmurlu and Helvacı 1994). Three major facies have been defined in the Beypazarı basin. These are: (1) lower alluvial facies, (2) upper alluvial facies and (3) lacustrine facies. Outlines of the facies relationships and distributions of the lithofacies components of the three facies assemblages are shown in Fig. 12.4 (Helvacı and İnci 1989). The Neogene sedimentary sequence is divided into seven formations (Figs. 12.1 and 12.2), which were deposited in alluvial, fluvial and

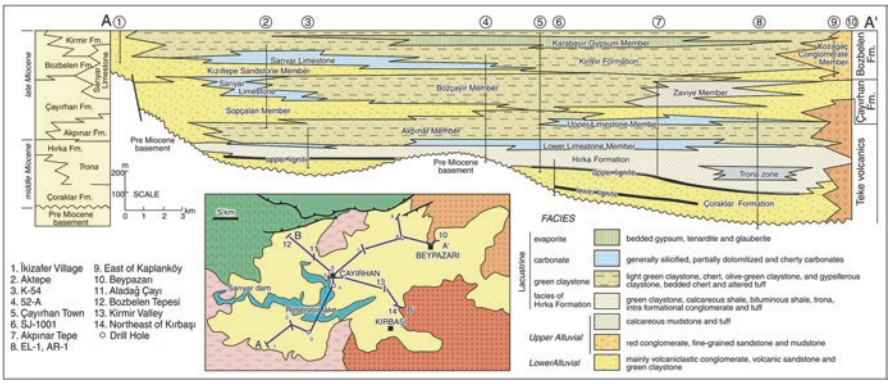

Fig. 12.4 Stratigraphic section showing the distribution of major facies and associated rock assemblages in the Beypazarı trona basin. (After Helvacı 2010)

lacustrine environments (İnci et al. 1988); in ascending order, these are: the Çoraklar, Hırka, Akpınar, Çayırhan, Bozbelen, and Kirmir formations, plus the Sarıyar Limestone and the Teke volcanics (İnci et al. 1988; Helvacı and İnci 1989). The Tertiary volcanic rocks are distributed in the northeastern part of the basin between the Beypazarı and Kızılcahamam areas (Öngür 1977) (Fig. 12.1). The pre-Neogene sedimentary rocks limit the Neogene basin from the west and vary from Paleocene to Eocene in age.

From the early Miocene, the Beypazarı basin was affected by an extensional tectonic regime and gravity tectonics, characterized by growth faults, which continued during the Middle-Late Miocene period. NE-SW–trending normal faults developed, and sedimentation in the basin was controlled by the faults throughout the Miocene Epoch. The stratigraphic and sedimentological features of the sequence and the position of the faults indicate a half graben type of depressional basin. This extensional regime replaced by a single-directional compressional regime during the Late Miocene–Early Pliocene. During this new tectonic phase, reverse faults, imbricate structures, thrust faults and overturned folds were formed within the pre Neogene rock units of the west Pontides, due to NW-SE directed compressional stress. E-W trending reverse faults, asymmetric folds (dipping to the south), monoclinal folds and conjugate faults, trending mainly NW and NE were generated within the Neogene units due to the compressional tectonic forces directed from NW to SE, and the rocks of the northern margin of the basin were thrust over basement rocks (Fig. 12.3). Thus, growth faults which limited the Neogene basin to the north were renewed during this neotectonic phase and resulting in northward-dipping reverse faults throughout the region. In contrast, the growth faults bounding the southern margin were not strongly affected by the neotectonic phase.

12.3 Depositional Setting and Mineralogy of Trona Deposit

The Miocene Beypazarı trona deposits in Central Anatolia, studied by Helvacı (1998, 2010); they have estimated reserves of 250 Mt of soda ash (sodium carbonate) and the second largest Na-carbonate deposit in the world after the Green River deposit, Wyoming, USA. In addition, there are ~400 Mt of lignite, 340 Mt of bituminous shale, and 1 Mt of Na-sulfate in the Beypazarı basin.

The trona deposit, located north of Zaviye village, is associated with shale in lower part of the Hırka Formation and alternates with bituminous shale and claystones. The trona deposit, located 250–300 m below the surface, and was discovered accidentally in the summer of 1982 by the Mineral Research and Exploration (MTA) while carrying out a drilling project on lignite deposits. An extensive exploratory drilling program was undertaken by MTA during the period 1983–1985 on behalf of the Etibank Company. Based on borehole data, it is estimated that the areal extent of the upper trona is ~8 km^2, whereas the areal extent of the lower trona horizon is ~5.5 km^2 to the north of Zaviye village (Figs. 12.1 and 12.5). The trona beds were deposited as two lensoidal bodies within a 70–100 m thick zone in the lower part of the shale unit. A total of 33 trona beds are known: 16 in the lower trona lens and 17 in the upper lens. The total thickness of the lower trona horizon ranges from 40 to 60 m, and the total thickness of the upper trona horizon is ~40 m. The interval between the lower and the upper trona horizons varies from 30 to 35 m. The total thickness of the trona beds in both lenses varies between 21 and 34 m in the central parts, and 2.5 and 12 m in the marginal parts of the ore bodies. The thickness of the individual trona beds in both trona horizons ranges from 0.4 to 2 m. The isopach contours of both trona horizons are restricted by the Zaviye fault. The central part of the trona deposit is generally thicker than the marginal parts. The trona beds grade laterally into dolomitic mudstones and claystones toward the edges of the basin (Fig. 12.4) (Helvacı 1998).

Minerals from the Beypazarı trona deposit were identified by direct-recording X-ray diffractometric analysis using standard-powder and oriented-sample techniques. The predominant mineral of the saline beds is trona; minor amounts of nahcolite are found in the marginal and upper parts of the deposit (Fig. 12.6). Trace pirssonite and thermonatrite occur locally within the deposit (Table 12.1). Trona and dolomite are associated with one another throughout the trona zone. Calcite, zeolites, feldspar and clays are the most common minerals within the associated rocks of the trona deposit. Trona crystals, generally white and occasionally grayish due to the presence of impurities, formed massively and as disseminated crystals in the claystone and shales. The products of zeolitization, dolomitization, and chloritization are rather widespread within the associated rock units. Carbonates and other mineras in the Beypazarı Trona Deposit of the Hırka Formation can be seen in Table 12.1.

Acicular-like trona consists of vertically oriented crystals arranged in fan aggregates (Fig. 12.7a). Rarely, upward- and downward-oriented fans were developed

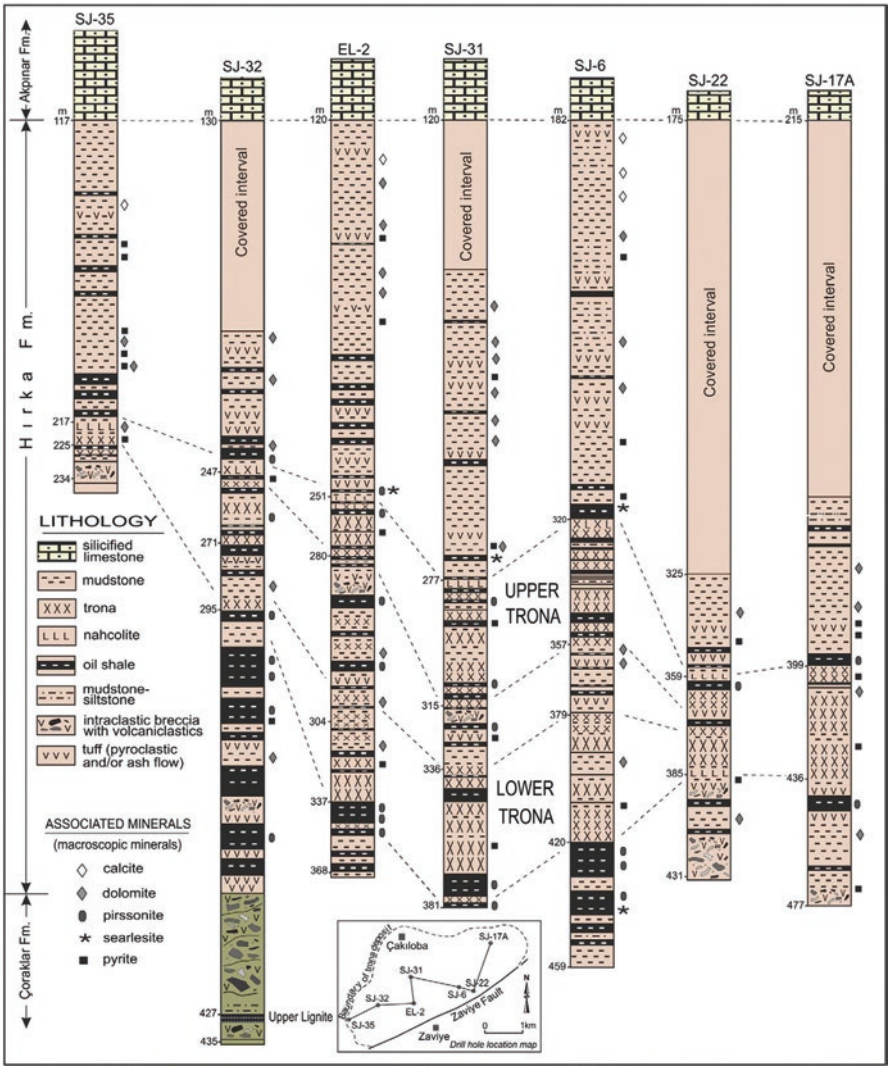

Fig. 12.5 Lithological correlation from boreholes based on distribution of Na-carbonate minerals in the center of the Beypazarı Basin. (After Helvacı 2010)

although those oriented upwards are more common and longer. Massive trona consists of submillimetric, unoriented crystals with scarce matrix (Fig. 12.7b). Radiating-prismatic trona consists of millimeter to centimeter-sized aggregates of bladed crystals organized in nodules grown in unconsolidated mud (Fig. 12.7c). Unoriented crystalline trona consists of millimeter- to centimeter-sized crystals scattered in mud and arranged in bundles (Fig. 12.7d).

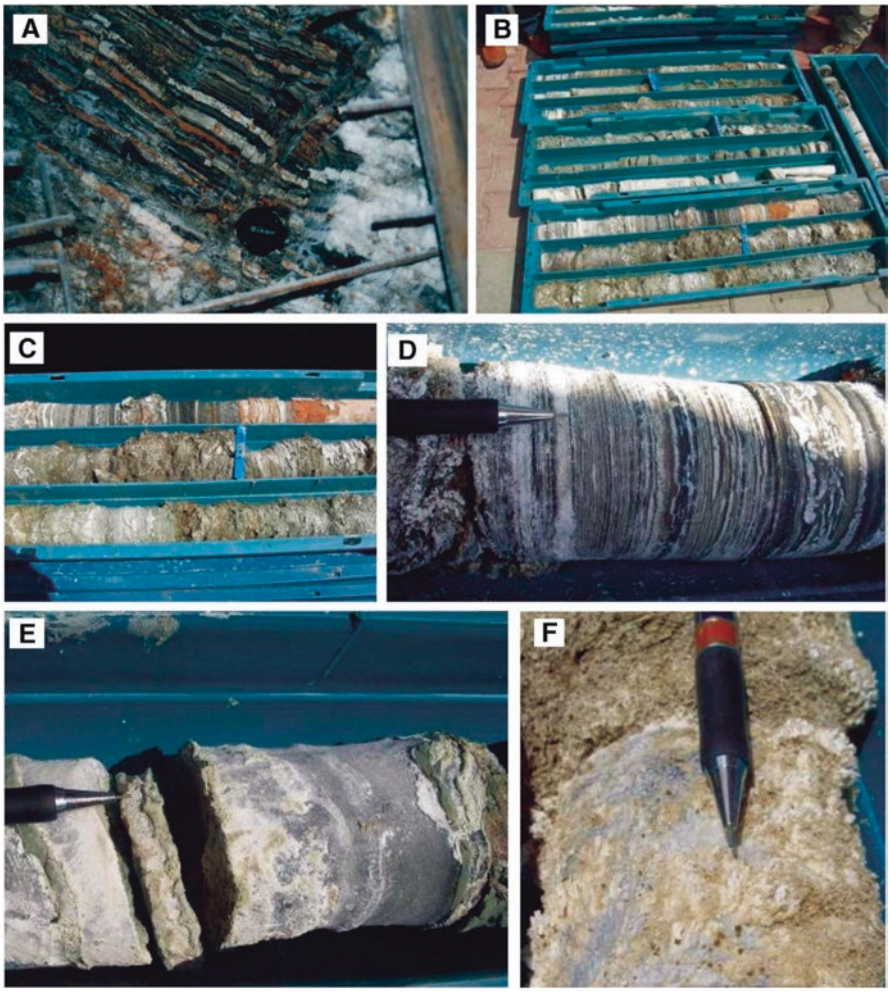

Fig. 12.6 (**a**) Interbedding of trona and bituminous shale beds in the main shaft of the trona mines. (**b–d**)Interbedding of trona and bituminous shale beds from drill holes (**e–f**) Massive trona samples from drill holes. (After Helvacı 2010)

12.4 Chemistry of the Beypazarı Trona Deposit

The Beypazarı Miocene sequence comprises coarse to fine-grained sedimentary rocks with trona, lignite and bituminous shale deposits, carbonates and volcanic rocks. Based upon the lithological features of these rock units, it is concluded that the rocks were deposited within fluvial, lacustrine, and playa lake environments. Laterally, the lacustrine and playa-lake environment sediments intertongue with fluvial sediments, and the Beypazarı basin represents a restricted, evaporite-rich cycle of deposition (Fig. 12.8).

Table 12.1 Carbonates and other minerals in the Beypazarı trona deposit of the Hırka Formation

Sulfides	
Pyrite	FeS_2
Oxides	
Quartz	SiO_2
α – **Quartz**	SiO_2
Opal-C.T.	
Hematite	Fe_2O_3
Carbonates	
Nahcolite	$NaHCO_3$
Trona	$Na_2CO_3.NaHCO_3$
Termonatrite	$Na_2CO_3.2H_2O$
Pirssonite	$Na_2CO_3.CaCO_3.2H_2O$
Brugnatelite	$Mg_6FeCO_3(OH)_{13}.4\ H_2O$
Calcite	$CaCO_3$
Dolomite	$CaCO_3.MgCO_3$
Magnesite	$MgCO_3$
Natron	$Na_2CO_3.10\ H_2O$
Gaylusite	$Na_2CO_3.CaCO_3.5H_2O$
Sulfates	
Gypsum	$CaSO_4.2H_2O$
Hexahidrite	$MgSO_4.6H_2O$
Epsomite	$MgSO_4.7H_2O$
Bloedite	$MgSO_4.\ Na_2SO_4.4H_2O$
Silicates	
Clay minerals	Smectite (Saponite)
	Illite
	Chlorite
	Montmorillonite
Loughlinite	$Na_2Mg_3Si_6O_{16}.8H_2O$
Searlesite	$NaBSi_2O_6.H_2O$
Hornblende	NaKCaMgFeAl, SiAlO(OH)
Tourmaline	$NaMg_3A_{16}B_3Si_6O_{27}(OH)_4$
Epidote	$Ca_2(Al,Fe)_3Si_3O_{12}(OH)$
Biotite	$K(Fe,Mg)_3AlSi_3O_{10}(OH)_2$
Muscovite	$KAl_2Si_3AlO_{10}(OH)_2$
Lepidolite	$K(Li,Al)_3(Al,Si)_4O_{10}(OH,F)_2$
Phlogopite	$KMg_3(Si_3AlO_{10})F_2$
Orthoclase	$KAlSi_3O_8$
Microcline	$KAlSi_3O_8$
High-sanidine	$KAlSi_3O_8$
Albite	$NaAlSi_3O_8$
Analsime	$NaAl(SiO_3)2H_2O$
Natrolite	$Na_2Al_2Si_3O_{10}.2H_2O$
Heaulandite	$CaAl_2Si_7O_{18}.\ 6H_2O$
Clinoptiolite	$NaCaKMgAlOSi.7H_2O$

(continued)

Table 12.1 (continued)

Sanidine	$KAlSi_3O_8$
Chabazite	$CaAl_2Si_4O_{12}$
Mordenite	$(Ca, Na_2, K_2)\ Al_2Si_{10}O_{24}.\ 5H_2O$
Ferrierite	$(Na, K)_2Mg\ (Si, Al)_{18}O_{24}.\ 7H_2O$
Heulandite	$CaAl_2Si_7O_{18}.6H_2O$
Phosphates	
Apatite	$Ca_5(PO_4)_3\ (OH,F,Cl)$
Collaphone	$Ca_5(PO_4)_3CO_3.\ H_2O$

After Helvacı (2010) (Note: The predominant minerals are in boldfont)

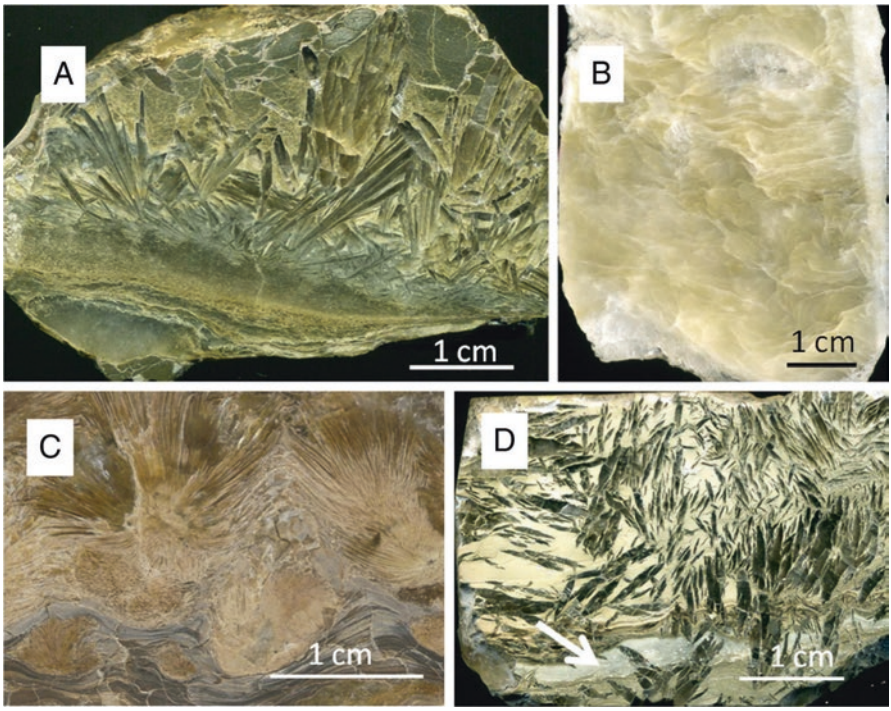

Fig. 12.7 Trona lithofacies: (**a**) acicular trona lithofacies (Upper Trona Unit, hand sample U3A, Beypazarı trona mine); (**b**) massive trona lithofacies (Upper Trona Unit, core sample EL-2-24 at 256.9 m in depth); (**c**) radiating-prismatic texture of the interstitial trona lithofacies (Upper Trona Unit, hand sample U6, Beypazarı trona mine); (**d**) unoriented texture of the interstitial trona lithofacies. White arrow indicates a layer of authigenic K-feldspars (Upper Trona Unit, hand sample D11B, Beypazarı trona mine). (García-Veigas et al. 2013)

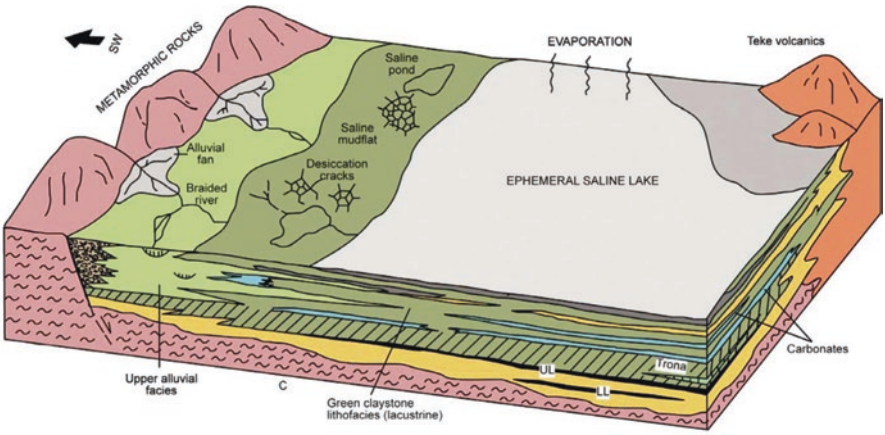

Fig. 12.8 Basinal facies setting and distribution of Na-carbonate minerals in the center of the Beypazarı Basin. (After Helvacı 2010)

The Beypazarı deposit has abundant trona and dolomite, minor amounts of nahcolite, and trace amounts of S, Cl, Sr, As, and B. Variations in the chemistry of trona and nahcolite from Beypazarı are interpreted to reflect the different phases of concentration that occurred in the perennial saline lakes. The Beypazarı deposit contains high-grade trona and nahcolite ores; their chemical compositions are given in Table 12.2. In the deposit, the Na_2O content of the trona ranges between 37% and 41%, and that of the nahcolite between 29% and 36%. The soda minerals in the Beypazarı deposit have minor amounts of impurities and trace elements and are high-grade ores, reaching up to 99% in some beds.

Mg and Si are present in the evaporitic and diagenetic minerals (e.g., Mg in dolomites) and in the claystone, mudstone, bituminous shale and tuff fractions, but mainly in the latter. Al and Fe oxides are only present in the clays, bituminous shales, and tuffs (e.g., Fe in pyrites). During diagenesis, chemical exchange between evaporites, clays, tuffs, and bituminous shales occurred and led to the formation of diagenetic and authigenic minerals such as pyrite, dolomite, K-feldspar, and analcite.

The Na-carbonate minerals were chemically precipitated from brines; these brines may have been partly derived from thermal springs and partly from surface streams and underground waters. Major-element compositions of the nearby volcanic rocks and granites are all enriched in Na relative to the average values for these rock types. Some clay minerals in the trona deposit have been derived from weathering of the tuff. Surface streams and underground waters may have carried dissolved Na, Mg, HCO_3, and CO_3 into the basins from weathering of rocks exposed in the catchment area, but the major source of dissolved ions in the perennial saline lake is thought to have been from leaching of the Neogene volcanic rocks- interfingering with the sediments in the northeastern part of the basin- by thermal springs associated with volcanic activity in the area and by surface streams and underground waters (Helvacı 1998, 2010; Garcia-Veigas et al. 2013).

Table 12.2 Chemical analyses (in wt%) of 16 trona and 3 nahcolite samples collected from drill holes in the Beypazarı trona deposit (After Helvacı 2010)

Trona samples																
Oxide (%)	SJ6-13	SJ6-16	SJ6-18	SJ6-23	SJ6-26	SJ6-28	SJ6-35	SJ6-40	SJ17A-6	SJ17A-8	SJ17A-9	SJ31-5	SJ31-16	SJ32-8	SJ9-14	SJ9-17
SiO_2	0.11	0.43	0.66	0.26	0.53	1.65	1.92	1.04	2.43	1.64	0.7	1.25	1.49	0.39	0.79	1.3
Al_2O_3	0.09	0	0.06	0	0.02	0.4	1.13	0.06	0.28	0.09	0.09	0.06	0.73	0.04	0.13	0.17
$*Fe_2O_3^t$	0.01	0	0.02	0.04	0.2	0.23	0.07	0.23	0.28	0.09	0.04	0.01	0.12	0.02	0.02	0.08
MgO	0.35	0.46	0.54	0.57	0.41	2.08	1.15	1.08	1.7	1	0.73	0.37	1.29	0.32	0.76	0.9
CaO	0	0.15	0.04	0.11	0.08	1.21	0.29	0.6	0.7	0.36	0.36	0.01	0.17	0	0.24	0.38
Na_2O	40.51	41.78	40.08	40.24	39.74	37.21	39.51	39.54	38.37	39.32	39.03	39.83	39.15	40.03	39.57	39.64
K_2O	0.01	0.01	0.02	0.03	0.04	0.12	0.06	0.06	0.17	0.06	0.02	0.03	0.43	0.01	0.04	0.06
SO_3	0.42	0.15	0.61	0.3	0.24	0.57	0.57	0.32	0.08	0.13	0.35	0.52	0.52	0.79	0.12	0.21
CO_2	28.39	29.67	28.46	29.28	28.22	29.63	28.05	28.07	27.25	27.92	29.01	28.28	29.26	28.25	28.98	29.01
H_2O	29.62	27.5	29.11	29.04	29.37	26.87	28.34	28.54	28.04	28.78	28.8	29.06	27.51	29.3	28.88	28.48
Total	99.51	100.51	99.6	99.87	98.85	100.07	99.54	99.54	99.3	99.39	99.13	99.42	100.67	99.15	99.53	100.23

Nahcolite samples			
Oxide (%)	S22-14	S35-13	S35-15
SiO_2	3.91	5.53	2.08
Al_2O_3	0.77	0.61	0.03
$*Fe_2O_3^t$	0.32	0.32	0.12
MgO	2.85	2.48	1.18
CaO	1.55	3.96	0.2
Na_2O	33.18	29.73	35.76
K_2O	0.16	0.33	0.08
SO_3	0.3	0.08	0.19
CO_2	24.01	27	25.53
H_2O	32.23	29.83	35.07
Total	99.28	99.87	100.24

In the system Na_2O-H_2O-CO_2, the main composition of some saline lakes, the activity of water was the most important factor affecting the stability limits of the mineral phases. The partial pressure of CO_2 (PCO_2) is also one of the descriptive variables of the system. In ancient and present-day lakes, nahcolite, trona, natron, thermonatrite, wegscheiderite ($Na_2CO_3.7H_2O$) and $Na_2CO_3.10H_2O$, may be present as mineral phases; the Na + activity, pH and PCO_2 of the deposits are useful in determining the chemical conditions of some ancient lakes. The middle Miocene atmosphere had a higher partial pressure of CO_2 than the present-day atmosphere (e.g., Warren 2010; Garcia-Veigas et al. 2013). During deposition of the upper trona horizon, however, the partial pressure of CO_2 had decreased (relative to that of the lower trona horizon) in so far as nahcolite is not present in the lower trona beds.

12.5 Gürün Deposit

The Gürün basin, which is located in the interior of the Eastern Taurus Region, is bounded between the Suçatı Fault in the east and Şuğul Fault in the north (Fig. 12.9), and approximately covers an area of 100 km^2. Pre-Neogene sedimentary rocks in this part of the Taurus consist of limestone and flysch like sediments, which are Triassic-Jurassic-Cretaceous and middle-upper Eocene in age (Özgül et al. 1973; Aziz and Erakman 1980; Özgül 1981). In terms of stratigraphic, sedimentologic and tectonic features of the trona occurences and bituminous shale contents, the Gürün basin is similar to the Beypazan Neogene basin; it has been studied by İnci et al. (1988), Yağmurlu et al. (1988), Helvacı and İnci (1989), İnci (1991), Yağmurlu and Helvacı (1994) and Helvacı (1998).

The Gürün (Sivas) basin, extending along an east-west, contains a volcano-sedimentary sequence up to 1222 m thick. The middle Miocene sedimentary sequence rests with angular unconformity on the basement rocks, which consist of limestone and flysch sediments ranging in Triassic-Jurassic-Cretaceous and middle-upper Eocene. The sequence has been subdivided into the Gürün Formation and the Karadag volcanics. The Gürün Formation consists of four members in ascending order: Kavak, Gökpınar, Çayboyu and Terzioğlu members. Çayboyu member is composed mainly of sandstone, siltstone, tuff, gypsum, lignite and bituminous shale interbedded with mudstone. Trona occurrences are placed within the Terzioglu member, alternating with bituminous shale, mudstones and tuffs; whereas the lignite deposits occur in the Çayboyu member of the Gürün Formation. The Miocene sedimentary rock units are laterally and vertically gradational with each other. The Karadag volcanics, located in the eastern and northern parts of the basin, interfinger with the upper parts of the Terzioglu member, and also cut the whole rock sequence. The thickness of the sequence increases towards the northern and eastern sides of the basin where it has been faulted. According to spora and pollen fossils, the sedimentary rock units are middle Miocene in age. They were deposited in alluvial, fluvial, lacustrine and playa-lake environments (Önal et al. 2004).

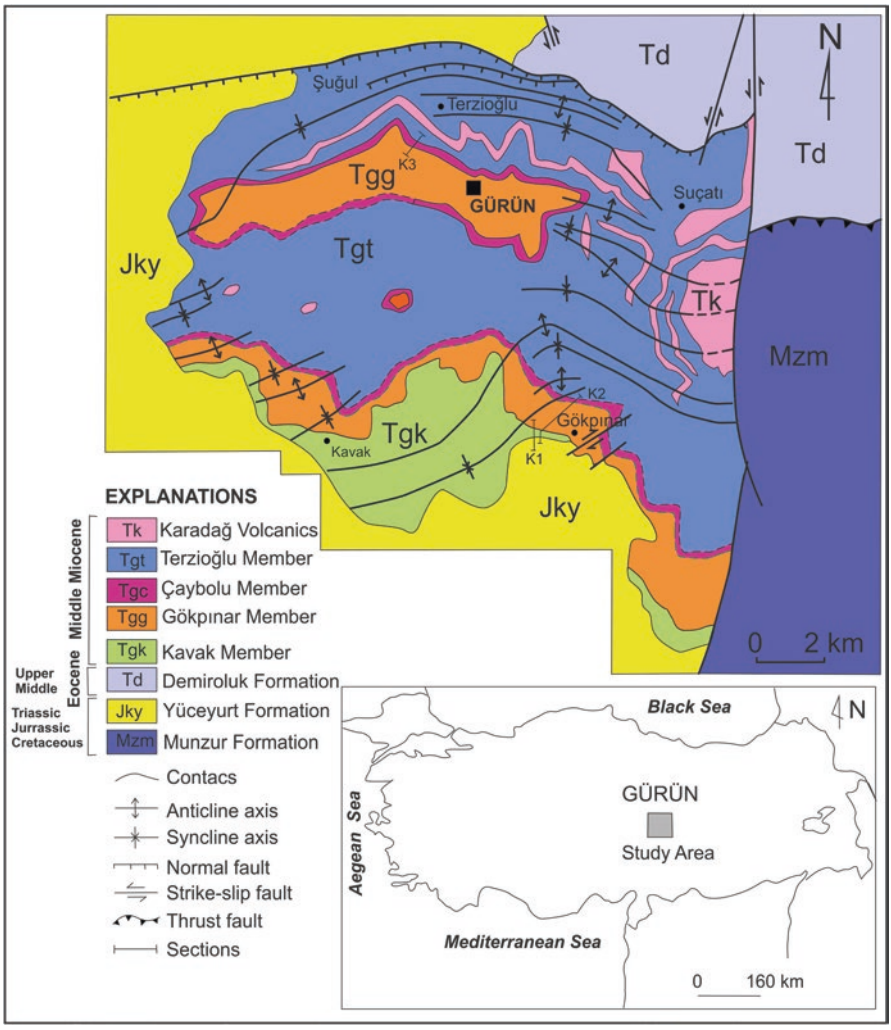

Fig. 12.9 Generalized geological map of the Gürün basin. (After Önal et al. 2004)

12.5.1 Geology and Stratigraphy of the Gürün Deposit

The lithofacies of the Gürün Formation are interpreted to have been deposited in a playa-lake type environment similar to that of the basin described by Eugster and Surdam (1973). The Gürün basin is one of the economically important basins in Turkey, containing occurrences of lignite, bituminous shale and trona. This basin is filled by fluvial, alluvial and lacustrine sediments and volcano-sedimentary rocks. The middle Miocene sedimentary sequence of the basin was divided into two formations and four members (Önal et al. 2001).

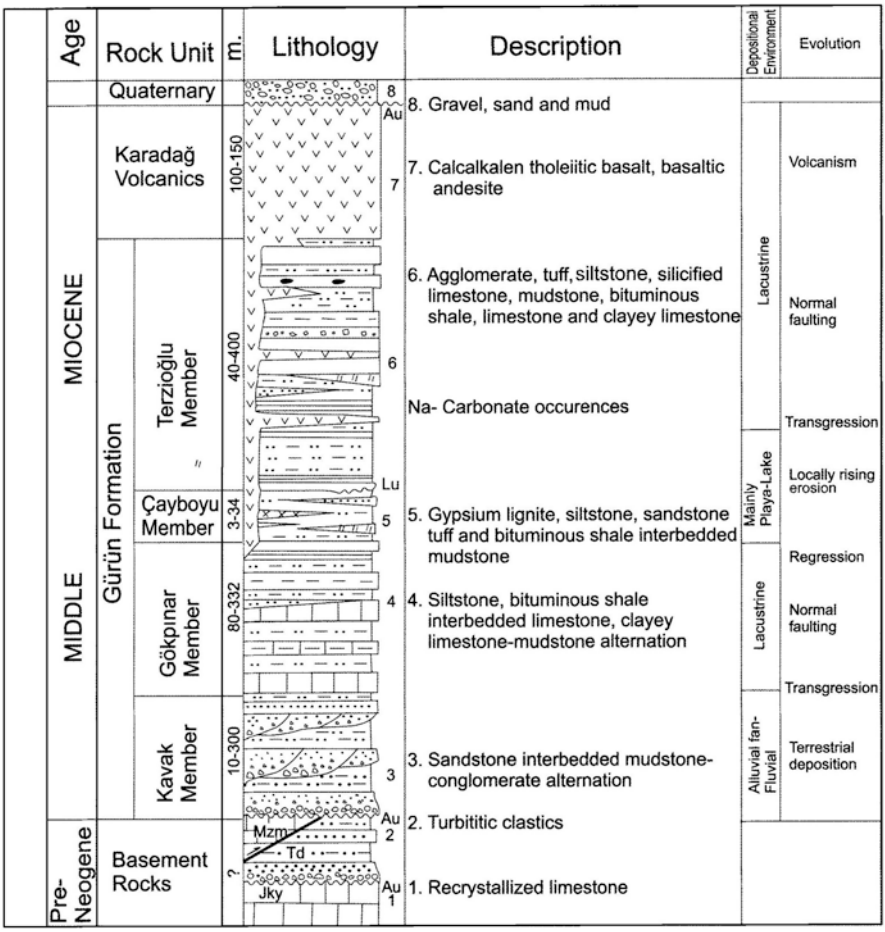

Fig. 12.10 Generalized stratigraphic sequence of the study area (*Jky* Yüceyurt Fm., *Td* Demiroluk Fm., *Mzm* Munzur Lim., *Au* Angular unconformity, *Lu* Local unconformity). (After Önal et al. 2004)

The rock units in the area are divided into two main groups: pre-Miocene basement rocks and middle Miocene rock units (Figs. 12.9 and 12.10). The pre-Miocene basement rocks are Triassic-Jurassic-Cretaceous and middle-upper Eocene in age and consist of limestone and flysch-like sediments. The middle Miocene sedimentary and volcanic units consist of clastic, calcareous, bituminous, evaporitic sediments and volcanic rocks.

The Gürün basin is a half graben filled by alluvial, fluvial and playa-lake deposits of the Gürün Formation. The middle Miocene sedimentary sequence, was deposited in a tectonic regime involving gravity-led tectonics, which began to develop in middle Miocene. The growth faults, which were developed at the northern margin of the basin, controlled the deposition during the middle Miocene. The extensional tectonic

regime, which later changed to a compressional regime during the late Miocene. During this new tectonic phase, NE, SW compression occurring in the region very likely originated from movement on the East Anatolian Fault (Önal et al. 2001).

12.5.1.1 Pre-miocene Rock Units

The pre-Miocene basement consists of Munzur Limestone, Yüceyurt and Demiroluk Formations which are Triassic-Jurassic-Cretaceous and middle-upper Eocene in age (Figs. 12.9 and 12.10). In the region, Triassic-Jurassic-Cretaceous sequence is represented by rudist-bearing fossiliferous and silicified limestones, and were named "Munzur Limestone" by Özgül (1981). Munzur Limestone was emplaced on the Yüceyurt and Demiroluk Formations with a tectonic contact during pre-Neogene time. Middle Jurassic rocks in the area consist of karstic and dolomitic limestone, and are named as "Yüceyurt Formation" by Atabey et al. (1994). The Yüceyurt Formation covers a wide area in the north, west and South of the Gürün area (Fig. 12.9). The unit rests with an angular unconformity on the basement rocks, but it has a faulted contact with the basement rock in the northern and western sides of the Gürün basin.

12.5.1.2 Middle Miocene Rock Units

The middle Miocene sequence is divided into two formations (Figs. 12.9 and 12.10). These are, in ascending stratigraphic order, Gürün Formation; Karadag volcanics (Önal et al. 2001; Ceyhan et al. 2001). The Gürün basin is a half graben filled by alluvial, fluvial and playa-lake deposits of the Gürün Formation and was accumulated under the N-S direction extensional tectonic regime and volcanic rocks. Gürün Fomation is divided into seven members such as the Kavak, Gökpınar, Çayboyu and Terzioğlu members, and the Çayboyu Member has two different evaporitic occurrences.

Gürün Formation Sedimentary rocks at the Gürün Formation consist of conglomerate, sandstone, siltstone, limestone, bituminous shale, gypsum, lignite and tuff, and the formation was originally named by Kurtman (1978). The Gürün Formation was deposited in fluvial, alluvial, lacustrine and playa-lake environments, and its total thickness exceeds 1222 m. Na-carbonate occurrences are seen in the upper parts of the unit. The Gürün Formation is divided into four members (Figs. 12.9 and 12.10). These are in ascending stratigraphic order, the Kavak, Gökpınar, Çayboyu and Terzioğlu members. The unit rests with angular unconformity on the basement rocks, but it has a faulted contact with the basement rocks in the northern and westhern parts of the Gürün basin. The age of the Gürün Formation, according to spora and pollen fossils found within the lignites of the Çayboyu member of the Gürün Formation, is middle Miocene (Önal et al. 2001).

Terzioglu Member This member is made up of micritic lacustrine limestone and locally clayey limestone, silicified limestone, bituminous shale, aglomerate, tuff, intraformational conglomerate and siltstone interbeds, and includes Na-carbonate minerals (such as trona) occurrences. Limestones are gray-white, middle to thick-bedded (30–90 cm), micritic and partially clayey, and include locally gastropod fossils in the upper parts of the unit. Clayey limestones in the lower parts of the unit include ostracod fossils and drying cracks. Silicified limestones are placed in the upper parts of the unit. Mudstones are greenish, moderately consolidated, thin to thick-bedded (2–90 cm), tabular laminated and locally carbonated. Bituminous shales are grayish, thin bedded, moderately consolidated and tabular laminated, are placed as interbeds (10–300 cm) in the lower and middle parts of the unit (Fig. 12.10). The bituminous shale was deposited in a shallow, brackish-water lake environment which expanded by seasonal flooding. Agglomerates occur locally and are interfingered with the upper parts of the unit. The agglomerate clasts are of basalt, andesite and sedimentary rock fragments. Tuffs are generally yellowish-greenish, very thick-bedded (5–6 cm), locally fragmented, moderately consolidated, tabular laminated and fining upward. Siltstones are lenticular and occur very locally. The intraformational conglomerate interbeds indicate synsedimentary deformation and transformation period during the deposition of the Terzioğlu member. This deformation was caused by the east-west-trending Şuğul Fault.

Na-carbonate (trona) is rather common within the lower and middle parts of the Terzioğlu member (Fig. 12.10). The unit includes a transgressive and regressive sequence, and is gradational with the underlying Çayboyu member in the deep parts of the basin, but is also local unconformity with the same member in the shallow parts of the basin. At the type section, The Terzioğlu member is 152 m thick (Fig. 12.10). Lithologic features and fossils indicate that it was deposited in a playa-lake and lacustrine environments (Önal et al. 2001).

Karadag Volcanics these Mid-Miocene volcanics consist of alternating pyroclastic breccia, tuff, calc-alkaline tholeiitic basalt and basaltic andesite lavas, and agglomerate, (Fig. 12.9). The volcanic rocks compositions are generally composed of plagioclase, olivine and clinopyroxene phenocrysts and locally quartz xenocrysts. Karadag volcanics were named as "Karadag member" by Atabey et al. (1994). These volcanics, located in the eastern and northern parts of the Gürün basin, interfinger with the upper parts of the Terzioğlu member, and also locally cut the rock units (Fig. 12.10). Na-carbonate are often leached in the interfingering transition zone. The thickness of volcanics increases towards the eastern faulted parts of the basin. Volcanics generally follow the Suçatı (strike-slip fault) and Şuğul (normal fault) faults (Fig. 12.9). The total thickness of the lava flows exceeds 150 m. Tuff is composed of greenish, thick to massive alternating beds of crystal, lithic and reworked tuff, and volcaniclastic conglomerate. Agglomerates are present below the tuffs and lava flows in some localities.

The Mid-Miocene Gürün basin trends approximately east-west, and is bounded by growth faults to the north and strike-slip fault to the east (Fig. 12.10). The growth fault at the northern part of the basin have high displacements resulting from step-wise structural features, which occur at the contact between Miocene rocks and the basement rocks. Fluvial, alluvial and lacustrine middle Miocene sediments were deposited in asymmetric depressions controlled by the growth faults at the northern margin of the basin (Fig. 12.9).

12.5.2 Mineralogy of the Gürün Deposit

Carbonates and other minerals occurring in the Gürün Formation are given in Table 12.3. In the Gökpınar member, generally calcite is common whereas the Çayboyu member consists mainly of calcite, dolomite, gypsum and aragonite. The Terzioğlu member is composed of dolomite, calcite, aragonite and clay minerals. The bituminous shales of the Terzioğlu member contain starkeite, hegzahydrite, dolomite and calcite (Table 12.3). Na-carbonate mineral are common within the lower and middle parts of the Terzioğlu member (Fig. 12.10). Sodium carbonate minerals in the basin are trona, nahcolite, pirssonite, gaylusite and shortite. The rocks consisting of the Na-carbonate minerals grade into mudstone and clayey limestone towards the edges of the basin.

Table 12.3 Carbonates and other minerals in the Gürün Formation

Oxides	
Zeolite species	$Na_2OAl_2O_3\ SiO_2.H_2O$
Carbonates	
Pirssonite	$NaCO_3.CaCO_3.2HO$
Gaylusite	$Na_2CO_3.CaCO_3.2H_2O$
Shortite	$Na_2CO_3.CaCO_3.2H_2O$
Nahcolite	$NaHCO_3$
Calcite	$CaCO_3$
Dolomite	$CaCO_3.MgCO_3$
Aragonite	$CaCO_3$
Sulfates	
Gypsum	$CaSO_4.2H_2O$
Starkeite	$MgSO_4.4H_2O$
Hexahidrite	$MgSO_4.6H_2O$
Aptitalite	$(K,Na)_3\ Na(SO_4)_2$
Silicates	
Clay minerals	Simectite
	Ilite
	Chlorite

The Gürün middle Miocene basin is mainly filled by clastics and products of adjacent volcanic activity which was centered at the east and north of basin. The most likely sources of sodium for the formation of Na-carbonate (trona) accurences are thermal springs, tuff interbedded with the sediments, and extensive the middle Miocene volcanic rocks interfingering with the sedimentary rocks in the eastern and northern parts of the basin.

During the first phase of evaporite deposition, selenitic gypsum crystals were laid down in 5–15 cm thick layers within the dolomitic mudstones. The second evaporitic phase consists of four different levels of cavity filling within the sandstones and shale alternation at the upper part of sequence originated as 5–10 cm sized satin-spar gypsum crystals with white coloured, partly orientated, fibrous-radial shaped crystal aggregates. XRF major-, minor- and trace- element analyses (La, Ce, Ta, W and U) and low $^{87}Sr/^{86Sr}$ and $\delta^{34}S$ (CDT) values lower than those of marine evaporites indicate that meteoric and volcanic fluids occasionally mixed with the lake water (Önal et al. 2004; Gündoğan et al. 2005). In addition, low $\delta^{18}O$ (SMOW) values in the continental evaporite could be interpreted as mixing of river water with the playa lake environment (Palmer et al. 2004). Selenitic gypsum in the Çayboyu member of the Gürün Formation was precipitated from ground-water during periodic desiccations of the shore-lake plain (Önal et al. 2004).

The Mid- Miocene sequence in the Gürün basin is composed of coarse- to fine-grained sedimentary rocks with Na-carbonate occurrences, lignite and bituminous shale, carbonates and volcanic rocks. The rocks were deposited within alluvial, fluvial, lacustrine and playa-lake environments. The Gürün basin represents a restricted, bituminous shale-rich cycle of deposition. Na-carbonates are rather common within the upper parts of the sequence in the basin. Sodium carbonate minerals in the basin are nahcolite, pirsonite, gaylusite and shortite. Trona is found within the bitiminous shales.

12.6 Kazan Deposit

12.6.1 Geology (Stratigraphy) of the Kazan Basin

Basins such as the Beypazarı, Çankırı-Çorum and Polatlı-Haymana basins, and the more southern Tuzgölü and Sivrihisar-Beylikova basins are the remnants of large marine foreland basins, which were formed in late Cretaceous-Paleogene time along the southern margin of the Pontide collisional zone located south of the North Anatolian Fault (NAF) and the Kizilcahamam Volcanic Province (KVP) (Görür et al. 1998; Dirik and Erol 2000; Karadenizli et al. 2003) (Fig. 12.11).

Miocene sedimentary units in the Central Anatolian basins are mainly lacustrine and floodplain deposits, whereas the Pliocene units are of alluvial and fluvial origin. Neogene deposits in the Kazan region are different in their architecture from those of the neighbouring basins. The most important difference is the scarcity of

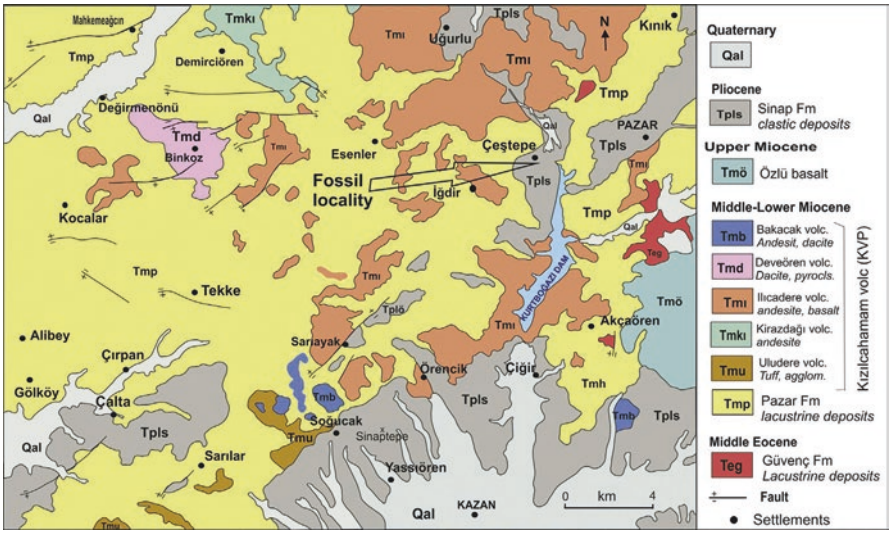

Fig. 12.11 Geological map of the region of Kazan area. (After Şen et al. 2017)

evaporitic deposits in the Kazan Basin, while form thick sedimentary units in other basins (Çayırhan Fm and Kirmir Fm in the Beypazarı Basin, Bayındır Fm and Bozkır Fm in the Çankırı-Çorum Basin (İnci et al. 1988; Karadenizli et al. 2003; Kaymakçı 2000; Varol and Kazancı 1981; Helvacı ve diğer1989). The Kazan Basin has relatively thick Pliocene deposits developed in alluvial-fan and meandering-river depositional environments. The northern part of this basin is filled with the Kızılcahamam volcanics (Öngür 1977). It is delimited to the east and west by the basement rocks (Permo-Triassic, Cretaceous and early Paleogene metamorphic and sedimentary units) (Figs. 12.11 and 12.12) (Şen et al. 2017).

Trona was deposited in the Miocene period in the Beypazari Basin, and in the Eocene period in the Kazan sequence. The Kazan Trona Deposit is located in Kazan Basin in the Central Anatolia, 35 km northwest of Ankara (Fig. 12.11) (Rio Tinto 2002). Four main rock sequences were defined by Toprak and Rojay (2000, 2001) and Rojay et al. (2002). From bottom to top, these are Paleozoic metamorphics, Eocene sequences (Mülk Formation and Akpınar Limestone), Neogene and Plio-Quaternary units. The Eocene units are a transgressive sequence overlying the basement rocks were devolved from a lacustrine to a shallow-marine depositional setting (Arslan et al. 2013) (Fig. 12.12).

The Mülk Formation, as a member of Eocene sequence, is a host unit of the Kazan Trona Deposit. The Formation was divided into four members by Toprak and Rojay (2001), which from bottom to top, include the Taban member, İncirlik member, Asmalıdere member and Fethiye member. The lower sequence of the Mülk Formation, consisting of lacustrine limestone-claystone horizons, hosts the trona

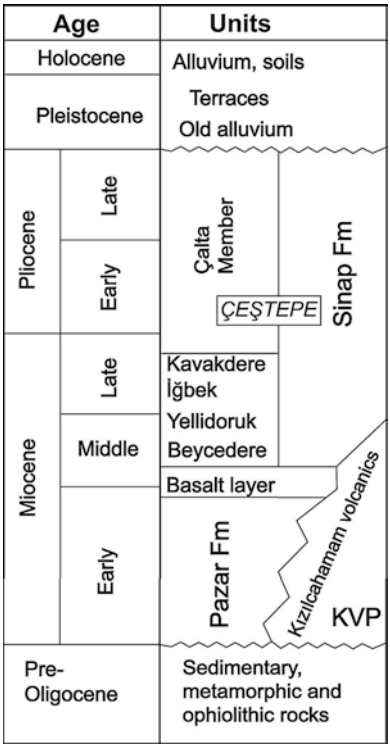

Fig. 12.12 Stratigraphy of Neogene units in the Kazan area. (After Şen et al. 2017)

deposits (Arslan et al. 2013) (Fig. 12.12). On the other hand, this formation also includes limestone with clay, bituminous shale, marl, limestone and sandstone. Göncüoğlu et al. (1996) identified this unit as the Kabalar Member (Şen et al. 2017).

Playa lake systems in Kazan (45 Ma) and Beypazarı (21.5 Ma) trona deposits are characterized by very extensive mud flats around the lake and contemporaneous volcanism. Extraordinary shallow water levels in the basin result in the feeds of the saline crystals to the playa centre during the wet season (Demirci 2000). Boreholes data indicate that the trona zone depth changes from 420 to >850 m and the deposit extends over an area of 20 km^2 in the basin. The thickness of trona beds reaches a maximum 109 m, with an average of 54 m. The study by Kellie et al. (2005) suggest that deposition took place in Eocene time, as revealed by K-Ar age dates from ash fall tuffs in the basin which yielded ages of 45 and 46 Ma. The trona-hosting Mülk Formation reaches a thickness of approximately 700 m (Kellie et al. 2005). The Mülk Formation has been subdivided into three units, which consist of an upper marlstone, a middle mudstone and a lower oil shale. Kellie et al. (2005) showed that the lower shale hosts the trona mineralization.

12.6.1.1 Age of Mineralization

The İncirlik member comprises black to brown, thin and evenly laminated oil shale locally intercalated with dolomitic mudstone, pale-green marlstone and light to dark brown-colored bedded trona. The thickness of the unit is about 385 m. The unit has a gradual lower boundary, but the contact with the overlying Asmalıdere member is rather sharp. An absolute age of 46 ± 1.9 Ma is assigned to the unit based on the K-Ar dating of a tuff specimen. The Fethiye member is composed of green colored, massive marlstone, and locally the member contains pseudomorphs after sodium carbonate minerals. The localized presence of ostracod and pelecypod fossils within the member indicates an overall return to fresher water conditions. The maximum drilled thickness of the unit is 195 m. K-Ar dating of biotite from a core sample collected from the unit gave an age of 45 ± 1.2 Ma (Demirci 2000; Kellie et al. 2005).

12.6.1.2 Kızılcahamam Volcanics

In the study area, Neogene volcanic rocks laterally interfinger with the Pazar Formation. They represent a small part of the southern section of the Kizilcahamam Volcanic Province (KVP). The main part of this province is situated further north and spread across an area of 12,500 km^2. It culminates at Köroğlu Tepe with an altitude of 2400 m (Fig. 12.12). This volcanic province is also known in the literature as the Köroğlu volcanics, Galatia Massif and GalatiaVolcanics (Türkecan et al. 1991). Its main rock types are andesitic, trachytic and basaltic lavas, rhyolitic tuffs andpyroclastics. According to radiometric data, these are the product of three phases of explosive volcanic events between 23 and 11 Myrs (Türkecan et al. 1991; Tankut et al. 1998). During the calm periods, lakes occupied large areas, and terrestrial sedimentary deposits, which also locally include coal formations, were formed. These deposits also include several fossiliferous localities, the best known of which are Güvem-Keseköy with leaves, vertebrate fossils and the Bayındır Pelitçik silicified wood (localities 4 and 5 on Fig. 12.12) (Şen et al. 2017).

12.6.2 Mineralogy of the Kazan Basin

The Kazan trona deposit is a fossil sodium carbonate discovered by a trona exploration technology. In 1998, Rio Tinto Industrial Minerals Exploration intersected trona in the Kazan Basin, 35 km northwest of Ankara covering approximately 20 km^2. The trona resource is in excess of 700 Mt, lying at an average depth of 550 m. The Kazan trona deposit is located in a sedimentary basin and the resource consists of several trona beds which vary widely in their areal extent, thickness and grade. The lenticular trona beds are separated, and overlain by dolomitic shale sediments. These are insoluble, and the grades of the beds are largely determined by the proportion of bands of similar insoluble sediment, known as “oil shale” with a low organic content.

The interburden between the beds ranges from 3 to 10 m and are typically 5 m thick (Fig. 12.7). Bed 3 covers the largest area and is by far the thickest (generally greater than 10 m and often exceeding 20 m) but has only a modest grade of 36% trona. Bed 5 covers a wide area, generally exceeds 2 m in thickness and has the highest grade, averaging 64% trona. Beds 6, 7, 8 and 9 decrease in area, thickness and grade and, therefore, also in economic interest. Dolomitic shale or oil shale sediments separate the trona beds. The predominant soluble mineral is trona ($Na_2CO_3.NaHCO_3.2H_2O$). Nahcolite ($NaHCO_3$) and natrite (Na_2CO_3) also contribute economic value and occur in localized concentrations. Halite (NaCl) occurs in an area of Bed 3 in sufficient concentration to diminish perhaps up to 10% of the potential resource. Additionally, northupite ($Na_2CO_3.NaCl.MgCO_3$) is present within the oil shales.

Gypsum crystals appear to replace microcrystalline anhydrite and gypsum concentrations are seen also as thin lenses parallel to bedding plane. Within gypsum-dominant areas there are occasional calcite pseudomorphs, replacing rare individual euhedral gypsum crystals. Thin, irregular laminae in this rock show structures indicating algal mats, as would be observed in sabhka environments. There are concentrations of organic matter along stylolithic zones, suggesting that some solution process took place after lithification.

The İncirlik member is composed of gypsum and aphanitic anhydrite and/or dolomite, with thin limonite streaks separating them. Some of the gypsum may have developed during late diagenesis, disrupting existing laminations through its growth and expansion. Some gypsum layers appear to have slumped just after deposition. This evaporite deposit, which probably formed in the "mudflat" part of a playa lake or lagoon, must have been affected by development of gas bubbles (CO_2 and/or H_2S), possibly derived from organic remains trapped below.

Nahcolite appears to occur particularly near bed margins. Usually, natrite and nahcolite do not occur together. Chlorides, principally halite (NaCl), is at low levels throughout the deposit, and at higher concentrations in one locality in Bed 3. Shortite ($Na_2Ca_2(CO_3)_2$) is especially associated with northupite and searlesite ($NaBSi_2O_5(OH)_2$) follows in lateral extensions at the margins of the trona seams.

Pirssonite ($Na_2Ca(CO_3)_2.2H_2O$), wegscheiderite and analcime ($Na(Si_2Al)O_6.H_2O$) occur in trace quantities. Insoluble minerals in both the beds and the interburdens include clays and dolomite ($CaMg(CO_3)_2$). The interburdens consist mainly of relatively competent impure fine-grained dolomites, shales and marls, with a low organic content. A feature of the interburdens is the occasional or frequent presence of the mineral northupite.

Trona The most common occurrence of trona is as an amorphous orangey-yellow to brown color referred to as '*maple syrup'* retaining bed-parallel banding reflecting differing amounts of insoluble material. Thin bands of shale often appear within the beds. Less common is trona as rosette or coarser sparry crystals developed along the base of a trona bed. The rosettes are usually seen as growths up from a dolomite substrate and in cases have been broken and reset in a clay/dolomite/trona matrix (Fig. 12.8). The trona is generally white and translucent, and must reflect a redistribution of the mineral from high- to low-pressure zones during a deformation event.

Halite Most of the halite is in Bed 3 with particularly high values, up to 12% average in Bed 3a from drillhole- K11. Halite is one of the most significant minerals and its spatial distribution is largely centred on one area in the NW of the deposit.

Northupite Northupite is a distinctive mineral in Kazan deposit and is prevalent in the interburden. It is present as finely disseminated crystals but also as rounded euhedral macrocrysts in two zones. These northupite horizons are extensive and exist beyond the limits of the bedded trona, providing a good marker horizon across the deposit.

Nahcolite Nahcolite may be locally significant but it is not widespread in the deposit. It is one of the only saline minerals apart from trona to be present as a bedded deposit.

Searlesite This mineral is generally formed as a secondary mineral from an alteration reaction involving zeolite, free silica and borate rich waters which results in secondary K-rich feldspar. Searlesite forms either fine fibrous spherulites within the clay rich zones or as laths within the trona zones and texturally it appears to replace clay minerals (Fig. 12.8). Searlesite, K-feldspar, quartz and Na clay minerals are commonly associated.

Pirssonite Pirssonite occurs as elongate crystals associated with the clay host rock and has a slight Ca excess with respect to the ideal composition.

Shortite Shortite occurs as lath- or wedge-like crystals associated with the clay host mineralogy and they also have a slight Ca excess. Pseudomorphs of shortite persist through much of the overlying stratigraphic column. Shortite is also found between the trona beds in small bed-parallel fractures where it is closely associated with Na mica clays and secondary dolomite.

12.6.3 Depositional Model of the Kazan Deposit

The İncirlik member of the Mülk Formation is the host of the trona deposit. A distinctive ash fall tuff unit is a marker horizon, which can be stratigraphically and geophysically identified in the field.

The Kazan playa/lake depositional area was a sub-basin on the edge of the great Kazan basin lake, separated by a barrier from the fresher, oxygenated waters of the main lake. This allowed periodic recharge by fresh waters of the isolated lake either through changing water levels over time or through storm events. NaCl was deposited in the deeper part of the later (at the depocenter) when the lake reached Na+ saturation. A shallow saline lake surrounded by extensive playa mudflats can become chemically stratified if there is an increase in freshwater inflow, forming a

freshwater cap over saline bottom waters (ectogenic meromictic lake) (Eugster and Hardie 1975).

The transition most likely reflects the fact that the peripheral foreland basin system originated as oceanic trench and later became a shallow marine to subaerial (playa setting) as continental crust entered the subduction zone. A playa model is proposed for the trona precipitation in the Kazan Deposit with the basin controlled by faults and some hot spring activity. The depositional area was a closed shallow lake and surrounded by very extensive mud flats. The size of the closed basin where trona accumulated was around >50 km^2. The upper part of the İncirlik member is characterized by mudflat deposits laid down near the edge of an evaporating lake or lagoon. The rocks essentially consist of microcrystalline anhydrite mud. Under the microscope, darker discontinuous thin lenses of laminae are made of algal filaments, which have trapped some dark coloured clay minerals.

Kellie et al. (2005) indicated that proven trona reserves are >600 Mt of ore grading 31% and a total of 43,600 m drillcore holes have delineated a zone of 15 individual trona beds. The geologically estimated resource is 1.65 Bt of ore grading 30% raw trona ($Na_2CO_3.NaHCO_3.2H_2O$) (Kazan Soda Electricity 2013). The Kazan Process Plant uses the monohydrate process and has a production capacity of heavy soda ash of 2.5 Mt/year and for sodium bicarbonate of 200,000 tonnes/year. The exploitation method is a solution technology which is an environmentally friendly and safe technology.

12.7 Na Carbonate Formation in Lake Van, East Turkey

Eastern Anatolia is a high region with more than half of the area lying at an elevation of about 1.5 km. The region as a whole has belong to the Turkish-Iranian high plateau (Fig. 12.1). Following the collision along the Bitlis-Zagros suture, a north-south convergence between the Arabian Platform and Laurasia has continued uninterrupted until the present. As a result, the continental crust has been shortened, thickened and consequently uplifted to form the Turkish-Iranian high plateau. On the high plateau, volcanic activity began during the Neogene, intensified during the late Miocene-Pliocene and continued until historical times. Large volcanic centres have developed during the Quaternary, which form significant peaks in the Turkish-Iranian high plateau. Among the Quaternary volcanoes, the major volcanic centres are Ararat, Tendürek, Suphan and Nemrut. Nemrut is the largest of a group of volcanoes, that trend north-south. It is a stratovolcano, having a well-defined collapse caldera and a caldera lake. Various volcanic ejecta have been extruded from these volcanic centres over the last 1–2 million years. The Quaternary volcanic centres, although temporally and spatially closely associated, display a wide range of lavas from basalt to rhyolite.

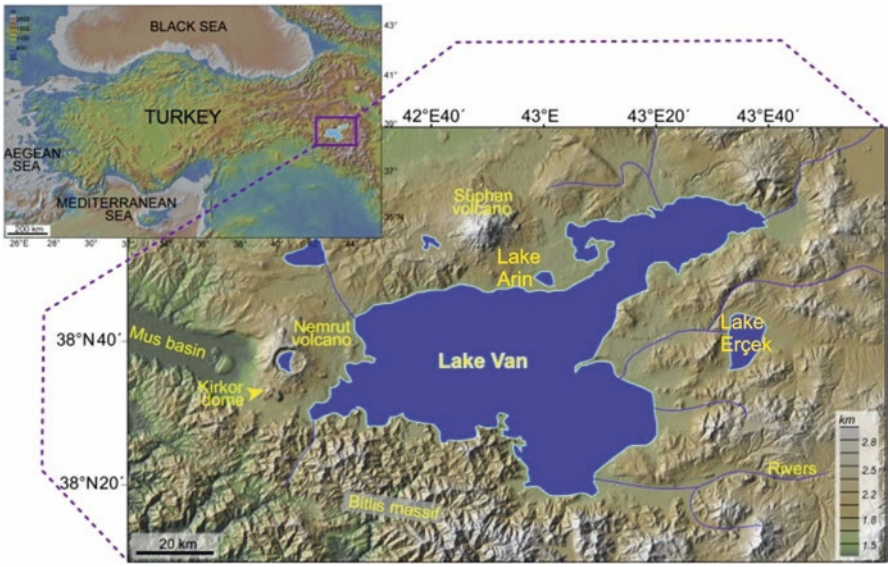

Fig. 12.13 Locality of the Van Lake and adjacent areas. (After Çukur et al. 2013)

Nemrut is one of the most spectacular volcanoes of eastern Anatolia, which exhibits a large collapsed caldera and a caldera lake. Mount Nemrut is the largest within a group of partly coeval volcanoes, situated to the east of Lake Van. Among these, Nemrut, Kirkor and Mazik are the major volcanoes. They extend approximately 50 km in a north-south direction. This group of volcanoes forms a barrier in front of an east-west trending river valley, and has apparently played an important role in the development of Lake Van. The Nemrut volcanic center is located close to the western part of Lake Van and it is only 10 km away from the Tatvan town.

The Eastern Anatolia Region is delimited by the Bitlis-Zagrous Sutur Zone in the south, North Anatolian Fault and East Anatolian Fault in the West, and contains Eocene to Early Miocene shallow marine sediments. Marine environments turned into continental conditions from the beginning of Middle-Late Miocene in the region, due to the north-south compressional tectonic regime starting Early Miocene took place in the region. This region is also represented by continental lacustrine and fluvial facies from Late Miocene up to recent time. This volcanic activity has reached its peak position during the Quaternary period, and it lasted until the historical time in the region.

In these continental lacustrine basins (e.g. Lake Van, Lake Arin, Lake Erçek), evaporite minerals, including trona and carbonate minerals, started to precipate in these lakes. These are mainly closed basin and received the effects of volcanic activity and related hydrothermal systems, resulting in the many evaporitic minerals in these basins. In fact, recently trona and termonatrite minerals were recorded from Van and Arin lakes (Helvacı 2003) (Figs. 12.13 and 12.14).

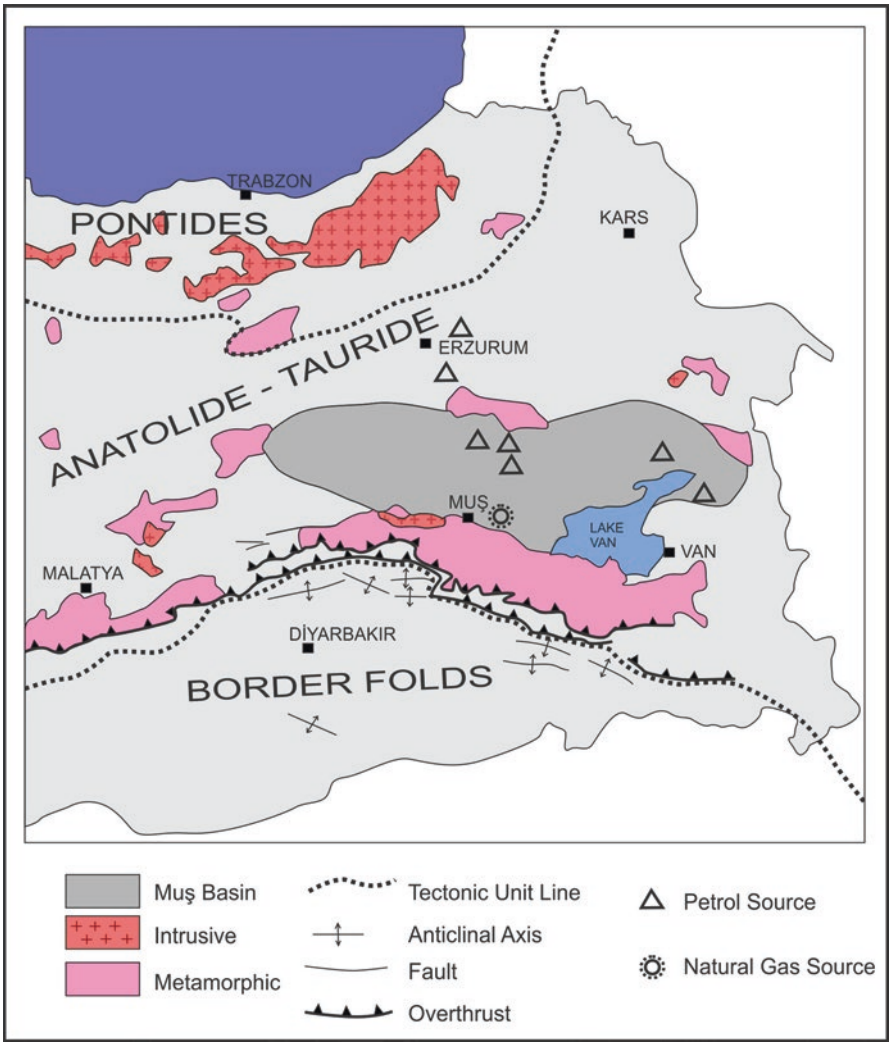

Fig. 12.14 Geological setting of the Van Lake and adjacent areas. (After Şaraoğlu ve Yılmaz 1987)

12.8 Conclusions

Natural sodium carbonate minerals (soda minerals) are exploited commercially either by mining beds of buried fossil trona deposits formed in Tertiary playa-lake sediments or by extraction from the brines of recent alkaline lakes and playas. The known fossil deposits of the world are located within Green River Formation, Wyoming (U.S.A), Miocene Hırka Formation, Beypazarı (Turkey), Eocene Mülk

Formation, Kazan (Turkey) and Wulidui Formation, Wucheng (China). Soda-rich recent alkaline lakes, and playas are as follows: Searles Lake (U.S.A), Lake Magadi (Kenya), San Critobal Ecalepec Playa (Mexico), Sowa Pan Playa (Botswana) and as future potential, Van Lake (Turkey).

Soda and soda ash are used as a source of Na_20 in glass manufacturing, in the production of various sodium chemicals, in water treatment, paper production, iron desulfurization, and many other uses. Although, production from brines and fossil trona deposits is becoming increasingly important, the bulk of the world's soda ash is produced synthetically by some 60 solvay plants, in more than 40 countries. Soda production from natural deposits are mainly limited to U.S.A., Turkey, Mexico and Kenya. Major soda producers by solvay plants are mainly U.S.S.R., U.K., West Germany, France, China, Bulgaria, and Japan. Annual soda production of the world is approximately 30–40 million tonnes.

Acknowledgments The study has been encouraged by several research programs supported by Projects TBAG-685 and Project No: YDABGAG-565 of TÜBİTAK (The Scientific and Technological Research Council of Turkey) and 03.KB. FEN.015 of the Dokuz Eylül University (İzmir, Turkey). Borehole logs were studied by the permission of Eti Maden Inc. and MTA (General Directorate of Mineral Research and Exploration). The author wishes to thank the management and technical staff for their assistance. Review comments by W.L. Griffin and Franco Pirajno considerably improved the manuscript. Mustafa Helvacı and Yasin Aydın are gratefully acknowledged for their typing and drafting assistance with the manuscript.

References

Altınlı İE (1976) Geology of the northern portion of the middle Sakarya River: Istanbul University, fen. Fak Mec: Section 41(1–4):35–36

Altınlı İE (1977) Geology of the eastern territory of Nallıhan (Ankara province): İstanbul university. Fen Fak Mec: Seri B 42(1–2):29–44

Altınlı İE (1978) Geology of the eastern territory of Nallıhan. İstanbul Üniv Fak Mecmuası 42:29–44

Arslan Ş, Yazıcıgil H, Stute M, Schlosser P (2013) Environmental isotopes and noble gases in the deep aquifer system of Kazan Trona Ore Field, Ankara, central Turkey and links to paleoclimate. Quat Res 79(2):292–303

Atabey E, Bağırsak IS, Canpolat M, Gökkaya KY, Günal LS, Kılınç N, (1994) Gürün, Kanga1 (Sivas) – Darende – Hekimhan (Ma1atya) Arasının Jeo1ojisi. [Geology of Gürün, Kangal (Sivas)-Darende-Hekiman (Malatya) areas]. General Directorate of Mineral Research and Exploration Report No: 9760, p 312. (in Turkish, Unpublished)

Aziz A, Erakman B (1980) Tufanbeyli (Adana) – Sarız (Kayseri) – Gürün (Sivas) ilçeleri arasında kalan alanın jeo1ojisi ve hidrokarbon olanakları. [Geology and hydrocarbon potential of Tufanbeyli (Adana)-Sarız (Kayseri)-Gürün (Sivas) areas]. TPAO Report no:1526, p 100 (in Turkish, unpublished)

Bradley WH (1964) The geology of the Green River formation and associated Eocene rocks in southwestern Wyoming and adjacent parts of Colorado and Utah

Bradley WH, Eugster HP (1969) Geochemistry and paleolimnology of the trona deposits and associated authigenic minerals of the Green River formation of Wyoming. U.S. Geological Survey Professional Paper 496-B, p 71

Ceyhan F, Helvacı C, Önal M (2001) Gürün (Sivas) volkanitlerinin petrografi, jeokimya ve petrojenez özellikleri [Petrography, geochemistry and petrogenetic features of Gürün (Sivas) volcanics]. Geosound 39:1–12 (in Turkish)

Ciner Group (2009) Eti Soda, http://www.cinergroup.com.tr/companies/eti-soda/en

Çoğulu E (1967) Etude petrographique de la region the Mihaliççik (Turque). BSMP 47:683–803

Çukur D, Krastel S, Tomonaga Y, Çağatay MN, Meydan AF (2013) The Paleo Van Science Team seismic evidence of shallow gas from Lake Van, eastern Turkey. Mar Pet Geol 48:341–353

Demirci CY (2000) Structural analysis in Beypazarı-Ayaş-Kazan-Peçenek area, NW of Ankara (Turkey). PhD Thesis, Middle East Technical University, Ankara (unpublished)

Dirik K, Erol O, (2000) Tuzgölü ve civarının tektonomorfolojik evrimi Orta Anadolu, Türkiye. Haymana-Tuzgölü-Ulukışla Basenleri Uygulamalı Çalışma (Workshop), TPJD Bülteni, Özel sayı 5

Dyni JR, (1996) Sodium carbonate resources of the Green River formation in Utah, Colorado, and Wyoming. U.S. Geological Survey Open-File Report 96–729 (pp 39)

Earman S, Phillips FM, McPherson BJOL (2005) The role of "excess" CO_2 in the formation of trona deposits. Appl Geochem 20:2217–2232

Eugster HP (1980) Lake Magadi, Kenya, and its precursors. In: Nissenbaum A (ed) Hypersaline brines and evaporitic environments. Elsevier, Amsterdam, pp 195–232

Eugster HP, Hardie LA (1975) Sedimentation in an ancient playa-lake complex: the Wilkins Peak Member of the Green River Formation of Wyoming. GSA Bull 86(3):319–334

Eugster HP, Smith GI (1965) Mineral equilibria in the Searles Lake evaporites, California. J Petrol 6(3):473–522

Eugster HP, Surdam RC (1973) Depositional environment of the Green River Formation of Wyoming: a preliminary report. Geol Soc Am Bull 84:115–120

Göncüoğlu MC, Turhan N, Şentürk K, Uysal Ş, Özcan A, Işık A (1996) Orta Sakarya'da Nallıhan-Sarıcakaya arasındaki yapısal birliklerin jeolojik özellikleri [Geologic features of structural units between Nallıhan-Sarıcakaya in the Middle Sakarya area]. General Directorate of Mineral Research and Exploration Report No: 10094 (in Turkish, unpublished)

Görür N, Tüysüz O, Şengör AMC (1998) Tectonic evolution of the central Anatolian basins. Int Geol Rev 40:831–850

Gündoğan İ, Helvacı C (2005) Mineralogy, petrography and diagenetic aspects of the Beypazarıtrona deposit, Middle Miocene, Turkey. Abstracts book IESCA-2005, İzmir (Turkey), pp 44–45

Helvacı C (1998) The Beypazari trona deposit, Ankara Province, Turkey. Proceedings of the first International Soda Ash Conference, Wyoming State Geol. Survey Public Information Circular, 40(2):67–103

Helvacı C (2001) Natural soda deposits and their economic importance. Geol Bull of Turkey Ayhan Erler Spec Issue 44(3):49–58 (In Turkish with English abstract)

Helvacı C (2003) Doğu Anadolu'nun bor potansiyeli ve Van Gölü soda oluşumları. [Borate potential of Eastern Anatolia and soda formation in Van Lake] Eastern Anatolia Industrial Raw Materials Workshop. 27–30 Agust 2003, Van, Abstract Book, p 46–47

Helvacı C (2010) Geology of the Beypazarı trona field, Ankara, Turkey. Mid-congress field excursion guide book, tectonic crossroads: evolving orogens of Eurasia-Africa-Arabia 4–8 October 2010, Ankara, Turkey

Helvacı C, Bozkurt S (1994) Geology, mineralogy and petrogenesis of Beypazarı (Ankara) granite. Bull Geol Soc Turk 37(2):31–42

Helvacı C, İnci U (1989) Beypazarı trona yatağının jeolojisi, mineralojisi, jeokimyası ve yörenin trona potansiyeli. [Geology, mineralogy, geochemistry of Beypazarı trona deposit and trona potential of the area]. The Scientific and Technological Research Council of Turkey Project No: TBAG-685, 159 p. (In Turkish)

Helvacı C, İnci U, Yılmaz H, Yağmurlu F (1989) Geology and Neogene trona deposit of the Beypazarı region, Turkey. Turk J Eng Environ Sci 13(2):245–256

Helvacı C, Öztürk YY, Satır M, Shang CK (2014) U-Pb zircon and K-Ar geochronology reveal the emplacement and cooling history of the Late Cretaceous Beypazarı granitoid, central Anatolia, Turkey. Int Geol Rev 56(9):1138–1155

İnci U (1991) Miocene alluvial fan-alkaline playa lignite and trona bearing deposits from an inverted basin in Anatolia: sedimentology and tectonics controls on deposition. Sediment Geol 71:73–97

İnci U, Helvacı C, Yağmurlu F (1988) Stratigraphy of Beypazan Neogene Basin, Central Anatolia, Turkey. Newsl Stratigr 18(3):165–182

Jones BF, Eugster HP, Rettig SL (1977) Hydrochemistry of the Lake Magadi Basin, Kenya. Geochim Cosmochim Acta 41:53–72

Kalafatçıoğlu A, Uysallı H (1964) Geology of the Beypazarı-Nallıhan-Seben area. Bull Miner Res Exp 62:1–12

Karadenizli L, Seyitoğlu G, Saraç G, Kazancı N, Şen Ş, Hakyemez Y, Savaşçı D (2003) Early Middle Miocene palaeogeographic evolution of the western margin of Çankırı-Çorum Basin, Central Anatolia, Turkey. Bull Miner Res Exp 126:69–86

Kayakıran S, Çelik E (1986) Beypazarı Trona (Doğal Soda) Yatağı Maden Jeolojisi Raporu. [Mining Geology Report of Beypazarı Trona (Natural Soda) Deposit]. General Directorate of Mineral Research and Exploration Report No: 8079. 122 p. (in Turkish, unpublished)

Kaymakçı N (2000) Tectono-stratigraphical evolution of the Çankırı Basin (Central Anatolia, Turkey). Geol Ultraiect 190:1–247

Kazan Soda Electricity (2013) Kazan Proses Tesisi [Kazan Process Plant]. http://www.kazansoda.com.tr/kazan-proses-tesisi

Kellie RJ, Demirci CY, Mert E (2005) Geology and development of the Kazan trona deposit, central Anatolia, Turkey. Abstracts with Programs – Geol Soc Am 37 (7):466–467

Ketin I (1966) Tectonic units of Anatolia (Asia Minor). Bull Miner Res Exp 66:23–34

Kostick DS (1994) Soda ash. In: Carr DD (ed) Industrial minerals and rocks, 6th edn. SME, Littleton, pp 929–958

Kurtman F (1978) Gürün bölgesinin jeolojisi ve tektonik özellikleri. [Geology and tectonic features of Gürün Region]. Bull Miner Res Exp 91:1–12 (in Turkish)

Lowenstein TK, Demicco RV (2006) Elevated Eocene atmospheric CO_2 and its subsequent declining. Science 313:1928

Mees F, Verschuren D, Nijs R, Dumont H (1991) Holocene evolution of the Crater Lake at Malha, Northwest Sudan. J Paleolimnol 5:227–253

MTA (2002) 1/500.000 scale geological map of Turkey

Önal M, Helvacı C, Inci U, Yağmurlu F, Meriç E, İzver T (1988) Stratigraphy, age, facies and depositional environments of the Soğukcam Limestone, Nardin Formation and Kızılcay Group in north of Çayırhan, northwest of Ankara. TAPG Bull 1(2):152–163

Önal M, Helvacı C, Ceyhan F (2001) Gürün (Sivas) Orta Miyosen Havzasının Jeolojisi. [Geology of Gürün (Sivas) Middle Miocene Basin]. TAPG Bull 13(l):19–134 (in Turkish)

Önal M, Helvacı C, Ceyhan F (2004) Geology and trona potential of the Middle Miocene Gürün (Sivas) basin, Central Anatolia, Turkey. Carbonates Evaporites 19(2):118–132

Onargan T, ve Helvacı C, (2001) Ankara-Beypazarı doğal soda (trona) sahasının önemi ve işletme parametrelerinin irdelenmesi, 4: Endüstriyel Hammaddeler Sempozyumu, 18–19 Ekim 2001, İzmir, s. 155–162

Öngür T (1977) Kızılcahamam GB'sinin volkanolojisi ve petrografi incelemesi. [Volcanology and petrographic investigation of SW of Kızılcahamam area]. Geol Bull Turkey 20:1–12 (in Turkish)

Özgül N (1981) Munzur Dağlarının Jeolojisi. [Geology of Munzur Mountains]. General Directorate of Mineral Research and Exploration Report No: 6995, p 200 (in Turkish, unpublished)

Özgül N, Metin S, Göğer E, Bilgöl I, Baydar O, Erdoğan B (1973) Cambrian and Tertiary rocks around Tufanbeyli area. Geol Bull Turkey l6(1):82–100 (in Turkish with English abstract)

Palmer MR, Helvacı C, Fallick AE (2004) Sulphur, sulphate, oxygen and strontium isotope composition of Cenozoic Turkish evaporites. Chem Geol 209:341–356

Renaut RW, Tiercelin JJ (1994) Lake Bogoria, Kenya Rift Valley, a sedimentological overview. In: Renaut RW, Last WM (eds) Sedimentology and geochemistry of modern and ancient saline lakes, vol 50. Society for Sedimentary Geology (SEPM) Sp Publ, Tulsa, pp 101–124

Renaut RW, Owen RB, Jones B, Tiercelin JJ, Tarits C, Ego JK, Konhauser KO (2013) Impact of lake-level changes on the formation of thermogene travertine incontinental rifts: evidence from Lake Bogoria, Kenya Rift Valley. Sedimentology 60:428–468

Rio Tinto (2002) Kazan project social and environmental report. 25 p. (Annual Report)

Rojay B, Toprak V, Bozkurt E (2002) Core sample analysis in Kazan Soda Project area. Middle East Technical University, Ankara (unpublished)

Saner S (1979) Explanation of the development of the Western Pontid Mountain and adjacent basins, based on plate tectonic theory, northwestern Turkey. Bull Miner Res Exp 93:1–20

Şaraoğlu F, Yılmaz Y (1987) Geological evolution and basin models during Neotectonic episode in the Eastern Anatolia. Bull Miner Res Exp 107:61–83

Sen S, Delfino M, Kazancı N (2017) Çestepe, a new early Pliocene vertebrate locality in Central Anatolia and its stratigraphic context. Ann Paléontologie 103(2):149–163

Şener F (1981) Ankara Beypazarı Soda Aramaları Ön Raporu. [Prliminary report of Ankara Beypazarı Soda Exploration]. General Directorate of Mineral Research and Exploration Report No: 6926. 29 p.(in Turkish, unpublished)

Siyako F (1984) Beypazari (Ankara) kömürlü Neojen havzası ve çevresinin jeolojisi. [Geology of coal-bearing Beypazarı (Ankara) Neogene basin and surroundings area]. MTA. Spec. Rept. 44 p. (in Turkish)

Smith GI, Haines DV (1964) Character and distribution of nonclastic minerals in the Searles Lake evaporite deposit, California. Contributions to general geology. USGS Bull 1181-P:60

Smith ME, Carroll AR, Singer BS (2008) Synoptic reconstruction of a major ancient lake system: Eocene Green River Formation, western United States. GSA Bull 120:54–84

Tankut A, Wilson M, Yihunie T (1998) Geochemistry and tectonic setting of tertiary volcanism in the Güvem area, Anatolia, Turkey. J Volcanol Geotherm Res 85:285–301

Toprak V, Rojay B (2000) Geology baseline study for the Kazan Soda project area. Middle East Technical University, Ankara (unpublished)

Toprak V, Rojay B (2001) Geological investigation in Kazan Soda project area. Middle East Technical University, Ankara (unpublished)

Türkecan A, Dinçel A, Hepşen N, Papak İ, Akbaş B, Sevin M, Özgür İB, Bedi Y, Mutlu G, Sevin D, Ünay E, Saraç G, Karataş S (1991) Stratigraphy and petrology of the Neogene volcanics between Bolu and Çankırı (Köroğlu Mountains). Bull Geol Congr Turkey 6:85–103 (in Turkish with English abstract)

Varol B, Kazancı N (1981) The litho-and biofacies properties of the upper Jurassic-lower Cretaceous carbonate sequence, in Nallıhan-Seben (Bolu) region. Bull Geol Soc Turk 24:31–38

Veigas-Garcia JG, Gündoğan İ, Helvacı C, Prats E (2013) A genetic model for Na-carbonate mineral precipitation in the Miocene Beypazarı trona deposit, Ankara province, Turkey. Sediment Geol 294:315–327

Warren JK (2010) Evaporites through time: tectonic, climatic and eustatic controls in marine and nonmarine deposits. Earth Sci Rev 98(3–4):217–268

Yağmurlu F, Helvacı C (1994) Sedimentological characteristics and facies of the evaporite-bearing Kirmir Formation (Neogene), Beypazan Basin, Central Anatolia, Turkey. Sedimentology 41:847–860

Yağmurlu F, Helvacı C, İnci U, Önal M (1988) Tectonic characteristics and structural evolution of the Beypazan- Nalhhan Neogene Basin, Central Anatolia. J Pure Appl Sci Ser A “GeoSciences” I:127–143

Chapter 13
Geology and Economic Potential of Ni Deposits

Ömer Elitok and Metin Tavlan

Abstract Magmatic sulphide and laterite deposits are the two major sources of the nickel metal in the world. Although the sulphide deposits have been operated since historic times, recently discovered laterite deposits are taking over the majority of the world's nickel production.

Nickel laterites are the supergene weathering products of ultramafic rocks under tropical climatic conditions. Apart from the modern laterites still forming along the equatorial zones, there are fossil laterites in the world, which formed when climate was favourable. Turkey has now a mild temperate climate but the Tethyan ophiolites in Turkey have been weathered to form at least ten lateritic nickel occurrences from Cretaceous to Miocene.

Nickel laterite occurrences in Turkey have a Fe-oxide dominated mineralogy and average 1–1.5% nickel grade. Although none of them is a world-class deposit there are still large-scale investments in deposits containing 20–30 million tonnes of nickel ore. On the other hand, smaller deposits showing favourable grades have been operated for the direct ore shipment purposes to feed Fe-Ni smelters in China and Eastern Europe. Run-of-mine nickel production of Turkey between 2005 and 2014 is nearly 1.5 million tonnes according to General Directorate of Mining Affairs.

13.1 Introduction

Nickel is a chemical element with symbol Ni and atomic number 28. Its melting point 1455 °C and the boiling point is 2913 °C. Nickel was discovered by the Swedish chemist Axel Fredrik Cronstedt in the mineral niccolite (NiAs) in 1751. Nickel (Ni) is a silvery-white lustrous, hard and corrosion resistant metal with major uses in steinless steel, nickel based alloys, aero-space alloys, electroplating, rechargeable batteries, etc.

Ö. Elitok (✉)
Department of Geological Engineering, Süleyman Demirel University, Isparta, Turkey
e-mail: omerelitok@sdu.edu.tr

M. Tavlan
Lyons Cement Plant, CEMEX Construction Materials, Denver, CO, USA

F. Pirajno et al. (eds.), *Mineral Resources of Turkey*, Modern Approaches in Solid Earth Sciences 16, https://doi.org/10.1007/978-3-030-02950-0_13

Generally, there are two types of occurences of nickel ore namely: magmatic sulphides and laterites. Historically, the first modern nickel production in the world was reported to have begun in 1848 from Ni sulphides in Norvay and in 1875 from nickeliferous laterites in New Caledonia (Mudd and Jowitt 2014). Global Ni production has grown steadily throughout the twentieth century. Some of the factors which underpin growing Ni resources include technological innovation, growing demand, and declining mining costs, all of which lead to lowering cut-off grades and declining ore grades (Mudd and Jowitt 2014). Although nickel laterites constitute more than 60% of the world's nickel resources, nearly 40% of global nickel production is from laterites, and the remainder being from sulphide ores (Kuck 2009 referenced in Thorne et al. 2012; Butt and Cluzel 2013; Yıldırım et al. 2013; Mudd and Jowitt 2014 and references therein). In other words, globally, the majority of nickel is produced from sulphide sources, but this is changing to lateritic nickel deposits which are becoming more important Ni sources. Butt and Cluzel (2013) reported that in response to greater demand, new processing technology, and reducing availability of sulphide ores, total Ni production from laterite ores exceeded 50% in 2010 and expected to reach 60% in 2014. The minimum amount of Ni reported globally as mineral resources is 296.2 million tonnes (Mt) Ni, split over a total of 253 sulphide projects containing 118.0 Mt Ni and 224 laterite projects containing 178.2 Mt Ni, for the year 2011 (Mudd and Jowitt 2014).

Economic nickel is mined especially from laterites and sulphides, but a small amount of hydrothermal Ni may become more important in time (Mudd 2010; González-Álvarez et al. 2013; Mudd and Jowitt 2014). Magmatic Ni sulphide deposits form by the segregation of immiscible sulphide liquids from mafic or ultramafic silicate magmas and can be found in different tectonic settings: (1) rifted continental margins; (2) cratonic–intracontinental environments; (3) active orogenic belts; and (4) synvolcanic greenstone belts (Naldrett 1989, 1997). Therefore, they are found in most continents, namely Asia, Australia, North America, and southern Africa (Fig. 13.1). Nickel sulphide deposits are associated mainly with Archean komatiites, Precambrian, Paleozoic and Mesozoic tholeiitic mafic–ultramafic intrusions, and layered intrusions (generally in Large Igneous Provinces, LIPs, see Prajno 2000; Ernst 2014) and hydrothermal-remobilized occurrences with no apparent age or tectonic constraints in Australia (Hoatson et al. 2006).

Nickel laterites are supergene enrichment of Ni formed by prolonged, intense chemical weathering of nickel bearing silicates in ultramafic rocks (e.g. harzburgite and/or dunite of ophiolitic complexes having average % 0.2–0.4 Ni), favoured by warm conditions with abundant rainfall. They occur in tropical to subtropical environments relatively close to the equator, or were close to the equator when the deposits formed (Thorne et al. 2012). Major lateritic Ni deposits in the world occur in New Caledonia, Indonesia, Cuba, Brazil and Australia (Fig. 13.1). The primary forsteritic olivine and orthopyroxene minerals that form the ophiolitic ultramafic rocks and layered mafic intrusions are the source of the Ni. Bedrock lithology, relief, drainage, tectonism, structure, age of weathering, and climate are major factors on the formation of nickel laterites. Elevated climatic temperatures and rainfall are necessary for intense weathering of ultramafic rocks to produce lateritic

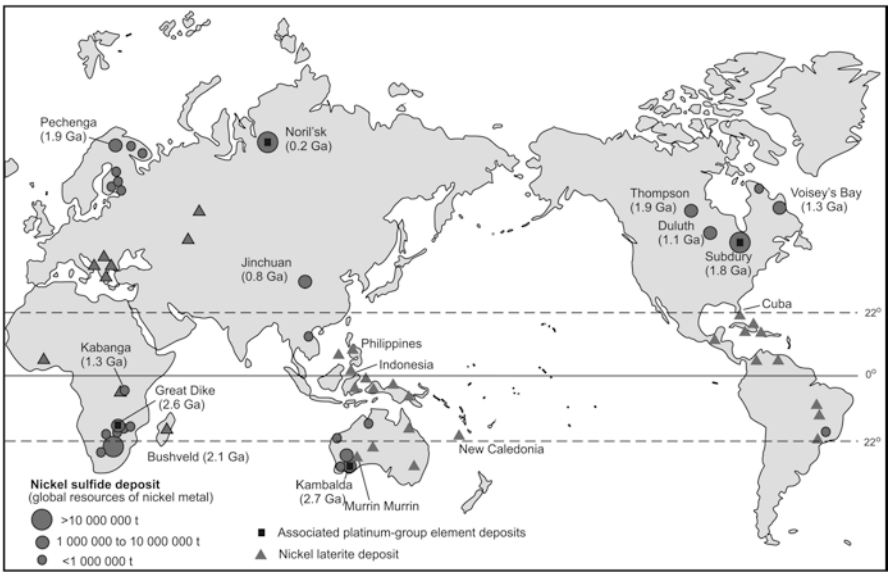

Fig. 13.1 Global distribution of sulfide and laterite Ni deposits. (Elias 2002 referenced in Hoatson et al. 2006)

nickel deposits (Freyssinet et al. 2005). In this case, the rate of chemical weathering should exceed the rate of physical erosion. Tectonic activity must be moderate, permitting progressive formation of a peneplain. When the uplift is not intense enough, the leaching and succeeding remobilization of Ni are reduced and the Ni content remains low. When the tectonic activity is too intense, the relief undergoes a strong dissection and the nickeliferous concentrations are rapidly eroded (Lelong et al. 1976). Based on their mineralogical compositions, Ni laterites are classified as Type A (talc, chlorite, sepiolite, serpentine), Type B (nontronite and saponite formed under semi-arid conditions), and Type C (Fe-(oxyhydr)oxide phases, such as goethite and lepidocrocite) (Alcock 1988; Brand et al. 1998; Gleeson et al. 2003; Wells et al. 2009). Also, similar classifications can be seen in the literature that (1) oxide laterites containing nickel that has either substituted into or is adsorbed onto goethite; (2) hydrous Mg silicate laterites that contain Ni-enriched hydrous Mg silicates, such as serpentine, talc, chlorite, sepiolite and garnierite; and (3) clay silicate laterites that are dominated by Ni-rich nontronite and saponite smectites (Mudd and Jowitt 2014 and references therein). Garnierite is a green colored material with high nickel grade is interpreted in a general sense covering the mixture of hydrous Ni-Mg sheet silicate. The thickest laterite and the richest garnierite formations occur around the closely spaced fractured areas where maximum groundwater circulation and fluid-rock interaction take place (Robb 2005).

A critical sector of the Alpine-Himalayan orogenic belt is characterized by Neotethyan and Paleotethyan ophiolite outcrops in Turkey. Although the climate is mild temperate recently, ultramafic rocks in these tectonic belts were exposed to

supergene weathering under tropical to subtropical climate from Cretaceous to Miocene forming the nickel-bearing lateritic deposits. The ophiolitic associations in Turkey generally have an E-W trending distribution (Fig. 13.2) and these ophiolitic outcrops have been classified by various authors under different names: (i) the Northern Ophiolitic Belt, the Tauride Ophiolitic Belt, and the Peri-Arabic Belt by Juteau (1980), (ii) Group-1 including Pre-Alpine ophiolites and melanges (Pre-Jurassic age) located on the southern edge of the Istanbul Zone, Group-2 including the Northern-Northeastern extending from İzmir to eastward and the Southern sub belt beginning from Marmaris area that continues to eastward to the Hadım, Aladağlar, Tecer-Divriği, Erzurum, Kağızman areas, Group-3 including the Southern and Southeastern Anatolian Ophiolitic Belt (Yılmaz and Yılmaz 2013), (iii) ophiolites along the Inner Pontide Suture Zone, the İzmir-Ankara-Erzincan Suture Zone, the Inner Tauride Suture Zone, the Bitlis-Zagros Suture Zone (Sarıfakıoğlu et al. 2017). Along the North Anatolian Suture Zone, Paleozoic and Mesozoic ophiolites were interpreted to be MORB-type, Late Cretaceous ophiolites of Turkey are suprasubduction zone ophiolites (Yılmaz and Yılmaz 2013). Although ophiolitic outcrops are widespread in Turkey, few lateritic ore deposits have been discovered. Important Ni-laterite deposits are Çaldağ (Turgutlu-Manisa), Gördes (Manisa), Muratdağı (Uşak), Mihalıççık- Sivrihisar (Eskişehir), Sarıçimen (Çaldıran-Van). On the other hand, nickel sulphide deposits were reported from Bitlis-Pancarlı, Bursa-Orhaneli-Yapköydere, Sivas-Divriği-Güneş, Bolu-Mudurnu-Akçaalan and Hatay-Payas-Dörtyol (TMMOB 2012).

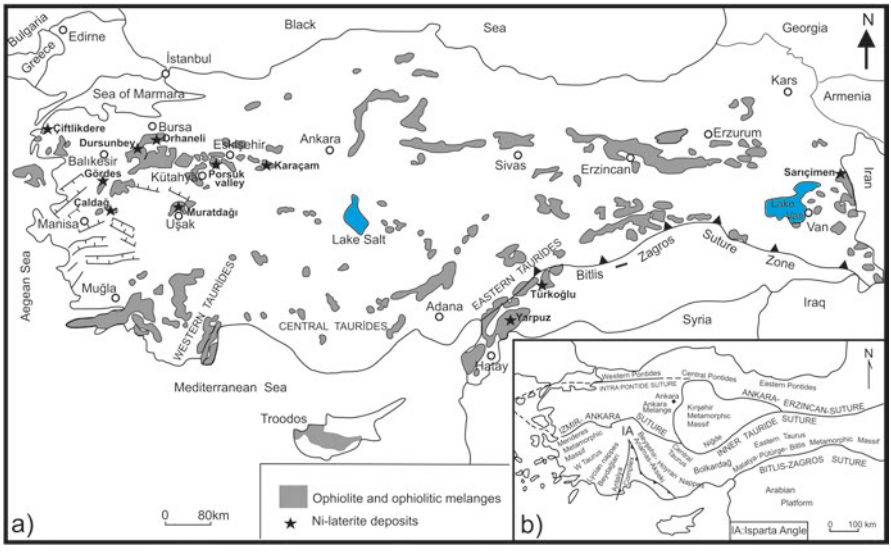

Fig. 13.2 (**a**) Distribution of the ophiolites and location of lateritic nickel deposits in Turkey. (Modified from Juteau 1980), (**b**) Schematic tectonic map showing the main sutures in Turkey. (Modified from Robertson 2002)

13.2 Geology and Economic Potential of the Lateritic Nickel Deposits in Turkey

13.2.1 Çiftlikdere (Çanakkale) Fe-Ni Deposit

The Çiftlikdere deposit is located in the northern margin of the Denizgören Ophiolite that trends NNE along a narrow zone between Ezine Zone and Çamlıca Metamorphics in the Çanakkale area. Approximately 10 m thick oolitic/reworked Fe-Ni laterite overlies the serpentinite protolith in the locality. All occurrences are overlain by schists of Çamlıca Metamorphics along a structurally controlled boundary (Fig. 13.3).

The ore body is composed of greenish (low hematite) and reddish (high hematite) sections. The mineralogy of both sections are clinochlore, illite, magnetite and hematite (XRD analyses); containing 1–1.8% Ni and 25–40% Fe (XRF analyses). Nickel is thought to be included in the clinochlore mineral. Some traces of metamorphism and overgrowth magnetites are observed in thin sections. The deposit has been mined for direct shipping of iron ore to cement factories. The extent and the nickel content of the deposit is not explored in detail.

13.2.2 Çaldağ (Turgutlu-Manisa) Ni Laterite Deposit

The Çaldağ nickel laterite deposit is located in the eastern part of the Bornova Complex (the Bornova Flysch Zone), some 25 km north of Turgutlu (Manisa) in western Anatolia. Serpentinized ultramafic rocks from the ophiolitic Bornova Complex, intermittently exposed to weathering under favourable paleogeographical and paleoclimatic conditions during Tertiary formed the Çaldağ Laterite. The nickel laterite deposits occur at three localities; Doktor pit, North pit, and South pit in Helvacı et al. (2013); and Hematite pit, North pit, South pit in Thorne et al. (2009). Lateritic profile at Çaldağ comprises partly serpentinized peridotites in harzburgite and minor dunite, weathered serpentinite, limonite and silica zones (Fig. 13.4), from bottom to top respectively. The main Ni-bearing mineral is goethite while asbolane, takovite, pecoarite, serpentine, limonite, nontronite and montmorillonite

Fig. 13.3 Çiftlikdere lateritic Fe-Ni deposit preserved between serpentinite protolith and metamorphic cover, Çiftlikdere-Çanakkale

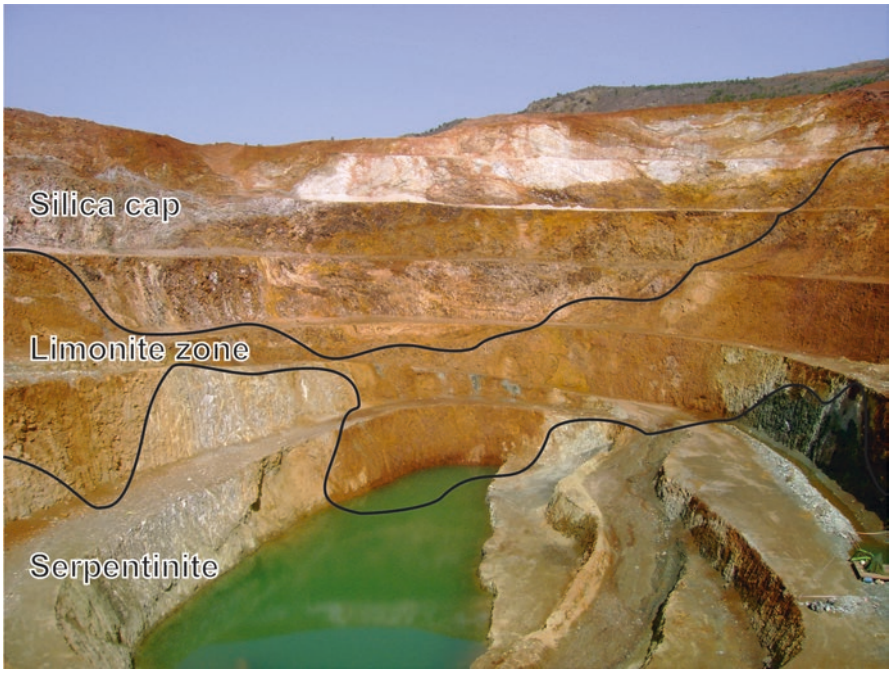

Fig. 13.4 Weathering profile of the Çaldağ laterite, an overview from Hematite (Doktor) pit, Turgutlu-Manisa

contain elevated Ni and Co grades. Quartz, chalcedony, chromite and hematite also found within non-nickeliferous zones (Tavlan 2012; Helvacı et al. 2013).

Some investigations have been carried out related to the mineralogical, textural, geological features, and evolution of the Çaldağ Ni-Co deposit (Çağatay et al. 1981; Thorne et al. 2009; Tavlan et al. 2011; Tavlan 2012; Helvacı et al. 2013), pointing out that Çaldağ has a lateritic profile with 90% oxide and 10% secondary nickel enrichment zones. Covering an area of approximately 6 km^2, the Çaldağ deposit has a Joint Ore Reserves Committee Code (JORC) proven reserve of 33.3 Mt at 1.13% Ni. Helvacı et al. (2013) suggested that lateritic formation formed in two different stages: (i) the first lateritization occured during the Upper Paleocene-Middle Eocene, resulting in colloform goethite, hematite, limonite, Ni-asbolane, Mn-oxides. Lateritic deposits were transported to the north, to its present location by thrust faults, (ii) second lateritization occured during the Oligocene time. However, some researchers suggested that the lateritization period of the Çaldağ is prior Oligocene time: (i) between the Upper Cretaceous and Eocene period (Çağatay et al. 1981), (ii) Middle to Late Eocene (Tavlan et al. 2011).

13.2.3 Gördes (Manisa) Ni Laterite Deposit

The protolith of the Gördes Ni-laterite profile is the Cretaceous ultramafic rocks of the Bornova Flysch Zone (Fig. 13.5). Nickel deposits occur between Akhisar and Gördes counties and around Fundacık, Kalemoğlu, Kabakoz and Çiçekli villages (Ağaçayak 2008). Nickel grade of the laterite deposits between Akhisar and Gördes is less than 1%. However, below silica caps and in deeper parts of the laterite deposits in this area, nickel grade reaches up to 10.24% (TMMOB 2012). Covering an area of over 5 km^2, total bulk mineral resourse of Gördes deposit is 31.3 Mt at 1.28% Ni and 0.03% Co according to environmental impact assessment (EIA) report published in 2009. Investment for the high pressure acid leaching (HPAL) process is completed in Gördes mine and the first trial products were exploited in 2015.

13.2.4 Bursa-Balıkesir Ni Laterite Occurrences

Regional exploration studies confirmed the lateritic weathering of the ophiolites around Bursa-Balıkesir with relatively thin lateritic cover (Dursunbey), local elevated nickel values (Karıncalı-Orhaneli, Çakallar-Mustafakemalpaşa), and

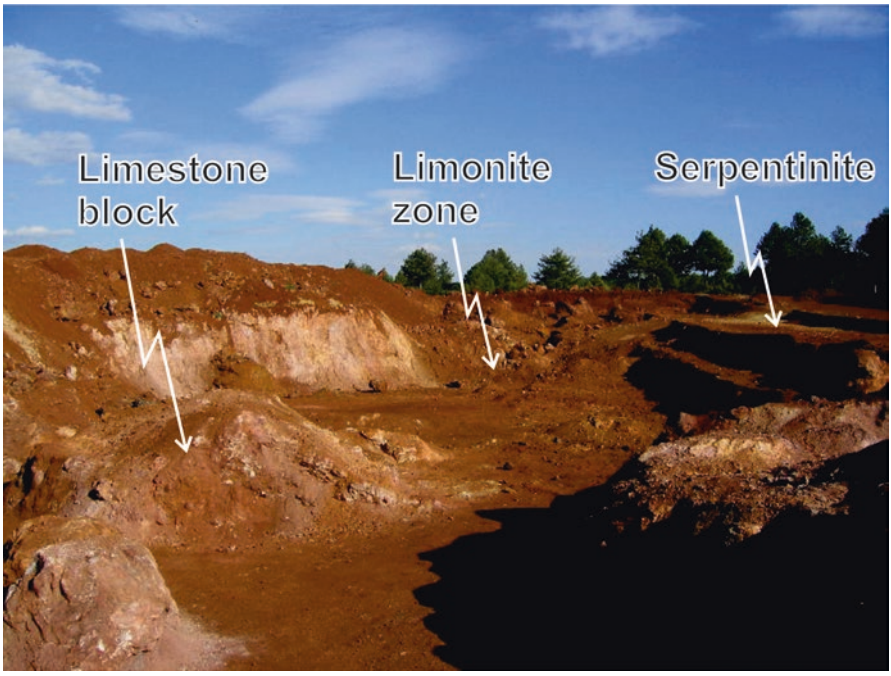

Fig. 13.5 General overview from Gördes Ni-laterite deposit, Gördes-Manisa

evidences of supergene secondary nickel enrichment (Yapköydere-Orhaneli) (Fig. 13.6).

Secondary nickel enrichments are seen as hydrous Mg-silicate, clay and chlorite in vein type structures whereas the limonitic covers are mainly goethite and hematite. Further exploration in the area might help to uncover the buried potential Ni-bearing Fe-oxide deposits or wide and deep supergene Ni-rich vein systems.

13.2.5 Muratdağı (Uşak) Ni Laterite Deposits

The Muratdağı ophiolite crops out in the northeast of Uşak and display nearly east-west trending topographic elongation. The ophiolitic unit include ophiolitc melange and massive harzburgitic peridotites with minor dunite. Nickel laterites occur in places over the massive peridotites, especially in the southern part of the Muratdağı. A TUBITAK Project has been carried out under the Project leadership of M. Selman Aydoğan between 2010 and 2013 related to geology, geochemistry and economic potential of the lateritic nickel deposits around the Muratdağı. The results of the project were published by Kadir et al. (2015). Nickel laterites occur mainly around

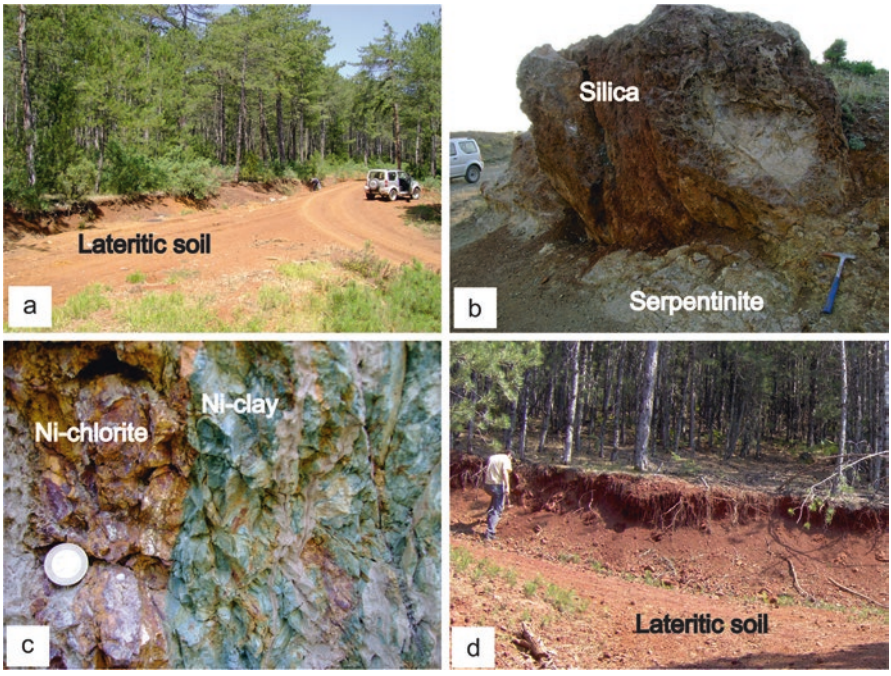

Fig. 13.6 Views from Ni-rich lateritic occurrences from Bursa – Balıkesir region (**a**) lateritic soil from Karıncalı, (**b**) silicified serpentinite with boxwork structures from Çakallar (**c**) high-grade Ni-clays and Ni-chlorite from Yapköydere, (**d**) lateritic soil from Dursunbey

Kapıdağ, Çiçeklikaya Tepe, Güreçikayası Tepe, İpburun Tepe, Kazıkbatmaz Tepe, and Tahtayol Tepe areas (Kadir et al. 2015). Although dominant mineral phases change from place to place, lateritic zones can be separated as (1) harzburgitic bedrock; (2) serpentinized zone; (3) decomposed and ferruginous saprolite; and (4) Fe-S-bearing silica zone (Kadir et al. 2015). The Kapıdağı area is characterized by active sulfur degassing controlled by fault zones resulting in native sulfur and sulfate mineral deposits (Fig. 13.7a). The lateritic zone includes a zone of Ni-Cr-bearing claystone with silicified blocky serpentinites, a ferruginous saprolitic zone, and a zone of Fe-S-bearing silica phases. Green garnierite and sulfate minerals are associated with Fe-(oxyhydr)oxide (Fig. 13.7b). The İpburun Tepe and Güreçikayası Tepe area include ferruginous saprolite zone dominated by Fe-(oxyhydr)oxide phases along with nodular and vein-type garnierite-bearing siliceous blocks (Fig. 13.7c–e) and silcrete cover. The lateritic zone around Çiçeklikaya Tepe include yellow, brownish yellow Ni-Cr-bearing claystone (Fig. 13.7f), blocky silicified serpentinites; and blue-green garnierite bearing saprolite. The Kazıkbatmaz Tepe and Tahtayol Tepe area are characterized by garnierite-bearing ferruginous saprolite, and Fe-S-bearing silica phases (Kadir et al. 2015). However, the nickel content of the deposit is not explored in detail.

13.2.6 Porsuk Valley (Eskişehir) Ni Laterite Occurrences

Porsuk valley Ni-laterite occurrences are found on an 200 m of roadcut near Porsuk dam midway between Kütahya and Eskişehir cities near Kümbet and Sobran villages. Limonitic laterite exposed on the profile (Fig. 13.8) includes up to 1.2% Ni, whilst green secondary nickel rich minerals show up to 16% Ni indicating a well developed Ni-laterite profile. A silica cap covering the limonitic profile extends about 750 m towards to east of the highway which also covered by Neogene-Quaternary sediments towards to north and west.

Further east from the roadcut is a valley with massive nickel-barren silicified serpentinite bluffs overlaying the fresh serpentinite with magnesite veining (Fig. 13.9). Although the nickel is not enriched in this part of the valley, evidence of the regional weathering encourages further exploration in this region.

13.2.7 Karaçam (Mihalıççık-Yunusemre Eskişehir) Ni Laterite Deposits

Karaçam Ni-laterite occurs on the Dağküplü ophiolite located in the İzmir-Ankara-Erzincan Suture Zone (Sarıfakıoğlu et al. 2017). Peridotites within the ophiolitic melange consist of serpentinized harzburgites, dunite, wehrlite with minor pyroxenite, and cumulate mafic-ultramafic rocks and outcrop in the north of Eskişehir

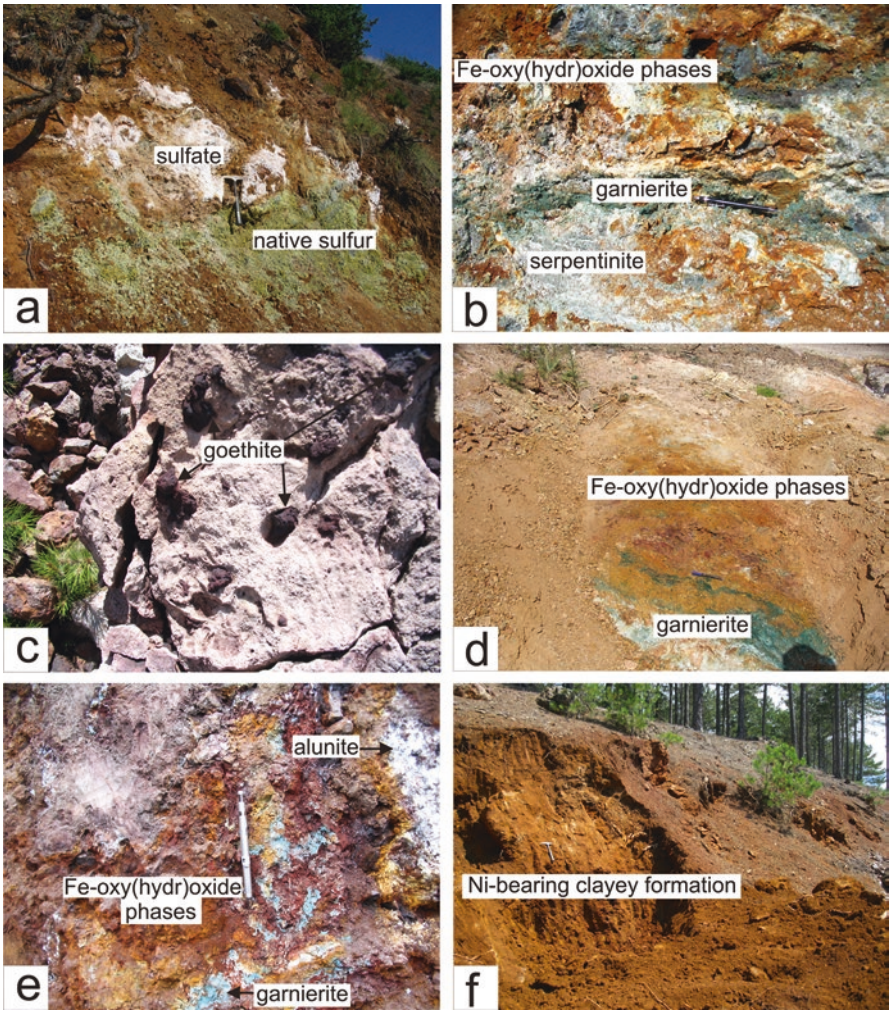

Fig. 13.7 Native sulfur and sulfate deposits (**a**) and Fe-oxy(hydr)oxide phases at the Kapıdağı locality (**b**), goethite occurences derived from ultramafics (**c**), Fe-oxy(hydr)oxide, garnierite phases (**d**), Fe-oxy(hydr)oxide, garnierite and alunite occurences within the blocky saprolite formation at the İpburun Tepe-Güreçikayası locality (**e**), Ni-bearing clayey formation at the Çiçeklikaya locality (**f**), Uşak

Fig. 13.8 Porsuk valley Ni-laterite profile exposed on the Kütahya – Eskişehir road

Fig. 13.9 Non-nickeliferous lateritic silica developed over serpentinite in Porsuk valley

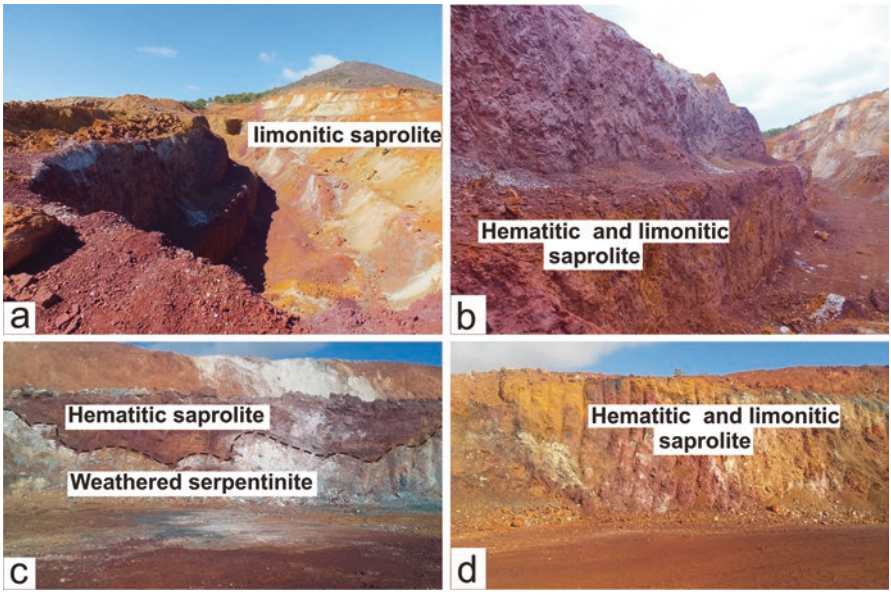

Fig. 13.10 Ni-bearing limonitic and hematitic zones in the east of Karasivri Hill of Karaçam deposit, Mihallıçık-Eskişehir

including the Mihallıçık area (Okay 1981; Asutay et al. 1989; Uslu 2007; Kahya and Kuşcu 2014). Nickel ore is currently mined by the open pit method at the Karaçam area (Fig. 13.10a–d) and over 1 Mt of ore has been shipped to overseas since 2008 (www.fenimining.com). Similar to Çaldağ deposit, goethite is the main Ni-bearing Fe-oxide mineral while secondary high grade Ni-enrichment is found at the lowermost part of the profile within the saprolitic ore. Ni-barren hematitic layers and silica zones form the cap of the lateritic profile. Nickel grade is about 1–4% in the Karaçam-Yunusemre area (TMMOB 2012).

13.2.8 Sarıçimen (Çaldıran-Van) Ni Laterite Deposits

The Sarıçimen Fe-Ni laterite deposit is located 15 km northeast of Çaldıran county in the eastern Anatolian region. Geochemical and mineralogical characteristics of the lateritic deposit in this area were studied in detail by Çolakoğlu (2009). This author interpreted that the Sarıçimen area consist mainly of ophiolitic melange including serpentinite, peridotite, claystone-marl-clayey limestone, chert, conglomeratic limestone, fossiliferous limestone, conglomeratic chert, Fe-Ni laterite, mafic and intermediate igneous rocks. The Fe-Ni laterite deposit in the Sarıçimen area is a transported ferricrete zone, including a conglomerate of ophiolitic fragments, radiolarian cherts, ferricrete and silcrete clastic materials. Average nickel content in the laterite deposit is 0.79 wt%. The transported lateritic zone (Fig. 13.11) has been formed in several stages of geodynamic evolution of the Eastern Anatolian which shows one of the best examples of the continent-continent collision zone in the world and is named as The Eastern Anatolian Contractional Province (EACP) (Bozkurt 2001).

13.2.9 Yarpuz (Osmaniye) Ni Laterite Occurrences

Yarpuz town is located some 10 km east uphill from Osmaniye city. A number of pits developed in the region during the last few decades supply Fe-oxide ore to local cement and steel factories. Lateritic nickel enrichment in some of those localities (Kızılyüce, Ağaoluk, Yuntmağara, Çömüoğlu, Oruçgazi) captured attention of the region since 2000s. Further exploration might add to the regional potential of nickel,

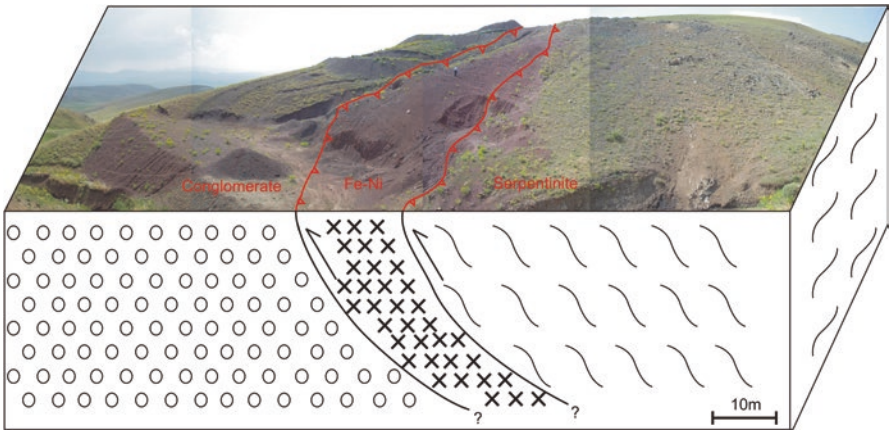

Fig. 13.11 Sarıçimen Fe-Ni laterite bounded by two reverse faults between serpentinite and conglomerate, Çaldıran-Van

some of the Ni-laterite occurrences had already been mined for the direct ore shipping (DOS) purposes though.

13.2.9.1 Kızılyüce Deposit

Kızılyüce is an oxide dominated lateritic deposit developed on top of the weathered serpentinite and capped by silica (Fig. 13.12). Nickel is mainly associated with goethite mineral with an average of 1.4% concentration with an inferred resource of over 1 Mt. Nearly 200 kt Ni-laterite ore is mined and shipped to smelters from Kızılyüce deposit in 2010 to 2011.

13.2.9.2 Ağaoluk Deposit

Both in situ and transported laterites are found in Ağaoluk deposit. Overlaying a serpentinite protolith, the in situ laterite is mainly goethitic and hematitic. The transported laterite is located on a brecciated limestone and is not thicker than a few meters at the outcrops. The evidence of the secondary migration of nickel is the greenish blue minerals cementing the limestone breccia (Fig. 13.13). Up to 10% Ni results are found in the ore by XRD measurement of those minerals, however the limestone/carbonate content limits the exploration of such an ore by hydrometallurgical processes.

Fig. 13.12 General overview from DOS operation at Kızılyüce mine, Yarpuz-Osmaniye

Fig. 13.13 General overview from Ağaoluk Ni-laterite and brecciated carbonate hosted secondary Ni enrichment, Yarpuz-Osmaniye

13.2.10 Türkoğlu (Kahramanmaraş) Fe-Ni Deposit

The Türkoğlu deposit is located on a small hill 25 km south-southeast of Kahramanmaraş. The profile is composed of limonite dominated laterite including clay and silica blocks (Fig. 13.14). The basement is a Cretaceous ophiolitic melange comprising peridotite, diabase, fresh serpentinite, mudstone and radiolarite. The weathered serpentinite is either absent or very thin between the laterite and the basement, therefore the oxide dominated ore is likely transported by the post lateritization tectono-sedimentary processes. Abundant laterite and silica blocks are found in the surrounding Quaternary soil.

Approximately 1–2 Mt of bulk ore occur in the deposit containing nearly 50% Fe 0.7% Ni, being shipped to local cement factories. Although the Ni values are significantly low in 75% of the deposit (below 0.5%), up to 3% Ni bearing clays, Ni-Mn oxide minerals and a few cm thick weathered serpentinites are present.

Further exploration in the area might help to uncover the buried potential Ni laterite deposits.

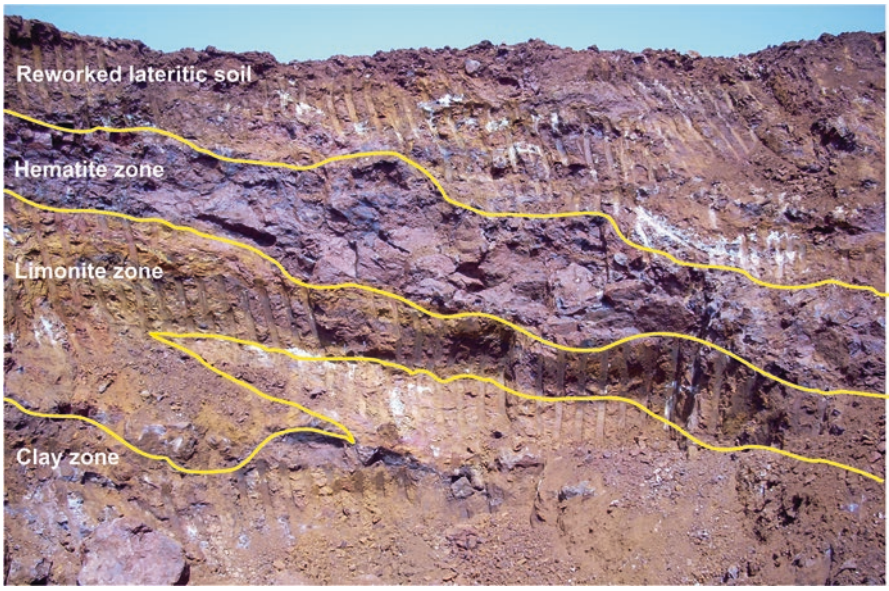

Fig. 13.14 General overview of the limonitic laterite profile from Türkoğlu Fe-Ni deposit, Türkoğlu-Kahramanmaraş

13.3 Ni Production in Turkey

Although mining in Anatolia dates back to thousands years ago, there is no notable information related to nickel research and mining up to the twentieth century. Research related to Ni deposits in Turkey was first reported in 1937 around Çıban village (Kastamonu) by General Directorate of Mineral Research and Exploration (TMMOB 2012). The complex geological and tectonic structures of Turkey allow a variety of mineral deposits as well as nickel ore. However, in terms of mineral resources of Turkey, nickel is classified in "normal-poor" group (TMMOB 2012). Considering the mineral deposit type and geological conditions, Turkey is very favorable to the occurrence of nickel. Due to small reserves, low grade, inadequate research, insufficient development of branches of industry using nickel ore and low commodity prices the mining sector and nickel production in Turkey has not grown to desired levels for a long time. However, Ni ore production has been recorded by General Directorate of Mining Affairs of Turkey. Ni production of Turkey between 2005 and 2017 is given in Table 13.1 and a general production trend is shown in Fig. 13.15. In general, nickel production has increased since 2005 in Turkey. Considering the geological environment and deposit types, Turkey is a favourable country for the discovery of new nickel deposits. However, taking into consideration the world's nickel production, Turkey is not well endowed in Ni reserves.

Table 13.1 Annual run-of-mine nickel production of Turkey between the years 2005 and 2017

Ni production (tons)												
2005	2006	2007	2008	2009	2010	2011	2012	2013	2014	2015	2016	2017
52988	20000	107000	51250	106127	224662	75018	337530	95187	268545	764346	826285	1306800

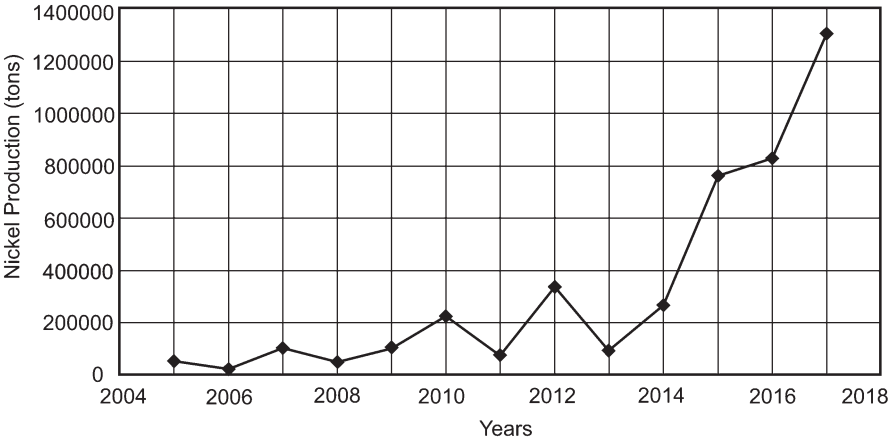

Fig. 13.15 Diagram showing general trend of annual run-of-mine nickel production of Turkey between the years 2005 and 2017

13.4 Conclusions

Magmatic sulphide and laterite deposits are the two major sources of the nickel metal, but a small amount of hydrothermal Ni may become more important in time. Although nickel laterites constitute more than 60% of the world's nickel resources, globally, the majority of nickel (nearly 60%) is produced from sulphide sources. But this is changing to lateritic nickel deposits which are becoming more important Ni sources. Laterites are fundamentally the supergene weathering products of the ultramafic rocks, which occur under favorable climatic conditions. Improvements in hydrometallurgical processing methods during the past two decades and easy/cost effective mining nature of the superficial deposits, directed laterites to took over the majority of the nickel production across the world. Majority of the large Ni-laterite deposits are in the recent tropical-subtropical climate belt; however, there are considerable amount of fossil Ni-laterite occurrences in the world, which formed in the past when climate was favorable but moved along with plate tectonics or stayed out of the current favorable zone as the climate changes.

Turkey, with current mild temperate climate, hosts some large sections of the Tethyan Ophiolites (mainly suprasubduction zone type (SSZ-type) ophiolites) weathered to form more than a dozen Ni-laterite occurrences from Cretaceous to Eocene (and possibly till the Miocene). Yet, only few of them are found economi-

cally feasible to operate (i.e. Çaldağ, Gördes, Karaçam, Kızılyüce). Controlled by the several ambient conditions while weathering, laterites may be classified within a few different mineralogical groups; some well accepted groups are hydrous Mg-silicates, clays and oxides. Although each deposit shows different mineralogical characteristics and might include varying combinations of these groups, the majority of the Ni-laterites in Turkey are oxide dominated. Nickel concentrated in oxide-hydroxide laterites is either found substituted into or adsorbed onto goethite. Thus, Ni-laterite deposits include considerable amount of Fe-oxide ore as well as cobalt and rarely scandium. Discovery of the Turkish Ni-laterite deposits by MTA goes back to the 1930s, however they had to wait till the processing methods became feasible to draw interest. Among these, Çaldağ deposit in Turgutlu-Manisa has JORC proven reserve of 33.3 Mt at 1.13% Ni 0.07% Co and is the largest Ni-laterite deposit in Turkey. It used to be operated for iron ore in the past but being explored in detail and operated for nickel and cobalt only since early 2000s. Since then, mined lateritic ore was either shipped to smelters to generate cash for project development or used in pilot processing plants located downhill. The second largest Ni-laterite deposit, Gördes (Manisa) has a resource of 31.3 Mt at 1.28% Ni, 0.03% Co according to EIA report. With the established HPAL plant, Gördes is the only fully-operated Ni-laterite deposit in Turkey by 2018. The third and fourth deposits in the order are Karaçam (Yunusemre-Eskişehir) and Kızılyüce (Yarpuz-Osmaniye) deposits, where the nickel ore has been directly shipped (DSO) to overseas to be processed in smelters. The other occurrences are either underexplored or very small to operate or contain low nickel grades.

Although, Turkey is a favourable country for the discovery of new nickel deposits, taking into consideration the world's nickel production, Turkey is not well endowed in Ni reserves. In addition to the known occurrences herein discussed, there could still be ophiolites weathered in the geologic past to form ore deposits but buried, under the sediments or overthrusts during a neotectonic period. The possibility of buried deposits might bring a new perspective to the future exploration programs for Ni-laterites in Turkey.

References

Ağaçayak T (2008) Karaçam (Eskişehir) lateritik nikel cevherinin fiziksel ve kimyasal yöntemlerle zenginleştirilmesi [Physical and chemical enrichment of Karaçam (Eskişehir) lateritic nickel ore]. PhD thesis, Selçuk University, Institute of Natural and Applied Sciences, Konya, Turkey, 211p

Alcock RA (1988) The character and resources available to the nickel industry. In: Tyroler CP, Landolt CA (eds) Extractive metallurgy of nickel and cobalt, the metallurgical society. 117th TMS Annual meeting proceedings, Phoenix, Arizona, pp 67–89

Asutay HJ, Küçükayman A, Gözler MZ (1989) Dağküplü (Eskişehir Kuzeyi) ofiyolit karmaşığının stratigrafisi, yapısal konumu ve kümülatların petrografisi [The structural and stratigraphic positiıon of Dağküplü (north of Eeskişehir) ophiolithic complex and petrography of cumulates]. Bull Miner Res Explor 109:1–8 (In Turkish with English abstract)

Bozkurt E (2001) Neotectonics of Turkey—a synthesis. Geodin Acta 14:3–30
Brand NW, Butt CRM, Elias M (1998) Nickel laterites: classification and features. AGSO J Aust Geol Geophys 17–4:81–88
Butt CRM, Cluzel D (2013) Nickel laterite ore deposits: weathered serpentinites. Elemets 9:123–128
Çağatay A, Altun Y, Arman B (1981) The mineralogy of Çaldağ (Manisa-Turgutlu) lateritic iron, nickel-cobalt deposit. Bull Miner Res Explor 95–96:82–96
Çolakoğlu AR (2009) Geochemical and mineralogical characteristics of Fe-Ni laterite ore of Sarıçimen (Çaldıran-Van) area in Eastern Anatolia, Turkey. Turk J Earth Sci 18:449–464
Elias M (2002) Nickel laterite deposits—geological overview, resources and exploitation In: Cooke D, Pongratz J (eds) Giant ore deposits: characteristics, genesis, and exploration. Centre for Ore Deposit Research, University of Tasmania, CODES Special Publication 4, Hobart, Tasmania, pp 205–220
Ernst RE (2014) Large igneous provinces. Cambridge University Press, Cambridge, UK, 653p
Freyssinet P, Butt CRM, Morris RC, Piantone P (2005) Ore forming processes related to lateritic weathering. Economic Geology, 100th Anniversary Volume, pp 681–722
Gleeson SA, Butt CRM, Elias M (2003) Nickel laterites: a review. Soc Econ Geol Newsl 54:10–16
González-Álvarez I, Pirajno F, Kerrich R (2013) Hydrothermal nickel deposits: secular variation and diversity. Ore Geol Rev 52:1–3
Helvacı C, Gündoğan İ, Oyman T, Sözbilir H, Parlak O (2013) Geology, mineralogy and geochemical properties of the Çaldağ Ni-Co laterite deposits. Bull Earth Sci 34–2:101–132 (In Turkish with English abstract)
Hoatson DM, Jaireth S, Jaques AL (2006) Nickel sulfide deposits in Australia: characteristics, resources, and potential. Ore Geol Rev 29:177–241
Juteau T (1980) Ophiolites of Turkey. Ofioliti 2:199–237
Kadir S, Aydoğan MS, Elitok Ö, Helvacı C (2015) Composition and genesis of the nickel-chrome-bearing nontronite and montmorillonite in lateritized ultramafic rocks in the Muratdağı region (Uşak, western Anatolia), Turkey. Clay Clay Miner 63–3:163–184
Kahya A, Kuşcu M (2014) Source of the mineralizing fluids in ultramafic related magnesite in the Eskişehir area, northwest Turkey, along the İzmir-Ankara Suture: a stable isotope study. Turk J Earth Sci 23:1–15
Kuck PH (2009) Nickel: U.S. geological survey mineral commodity summaries. https://minerals.usgs.gov/minerals/pubs/mcs/2009/mcs2009.pdf
Lelong F, Tardy Y, Grandin G, Trescase JJ, Boulange B (1976) Pedogenesis, chemical weathering and processes of formation of some supergene ore deposits. In: Wolf KH (ed) Handbook of strata-bound and stratiform ore deposits. Elsevier, Amsterdam, pp 92–173
Mudd GM (2010) Global trends and environmental issues in nickel mining: sulfides versus laterites. Ore Geol Rev 38:9–26
Mudd GM, Jowitt SM (2014) A detailed assessment of global nickel resource trends and endowments. Econ Geol 109:1813–1841
Naldrett AJ, (1989) Magmatic sulfide deposits. Clarendon Press, New York, 177p
Naldrett AJ (1997) Key factors in the genesis of Norilsk, Sudbury, Jinchuan, Voisey's Bay and other world-class Ni–Cu–PGE deposits: implications for exploration. Aust J Earth Sci 44:283–315
Okay A (1981) The geology and blueschist metamorphism of the ophiolites in northwest Turkey (Tavşanlı – Kütahya). Bull Geol Soc Turk 24:85–95 (In Turkish with English abstract)
Pirajno F, (2000) Ore deposits and mantle plumes. Kluwer Academic Publishers, Dordrecht, 556p
Robb L, (2005) Introduction to ore-forming processes. Blackwell, Oxford, 373p
Robertson AHF (2002) Overview of the genesis and emplacement of Mesozoic ophiolites in the Eastern Mediterranean Tethyan region. Lithos 65:1–67
Sarıfakıoğlu E, Sevin M, Dilek Y (2017) Türkiye ofiyolitleri [Turkey ophiolites]. General Directorate of Mineral Research and Exploration, Special Publication 35, Ankara, Turkey, 100p
Tavlan M (2012) Tectono-stratigraphic evolution of Çaldağ Laterite. Dokuz Eylül University, The Graduate School of Natural and Applied Science, MSc thesis, İzmir, Turkey, 43p (unpublished)

Tavlan M, Thorne R, Herrington RJ (2011) Uplift and lateritization history of the Çaldağ ophiolite in the context of Neo-Tethyan ophiolite obduction and uplift: implications for the Cenozoic weathering history of western Anatolia. J Geol Soc Lond 168:927–940

Thorne R, Herrington R, Roberts S (2009) Composition and origin of the Çaldağ oxide nickel laterite, W. Turkey. Miner Deposita 44:581–595

Thorne RL, Roberts S, Herrington R (2012) Climate change and the formation of nickel laterite deposits. Geology 40–44:331–334

TMMOB (Union of Chambers of Turkish Engineers and Architecs) Türkiye Maden Mühendisleri Odası (Chamber of Mining Engineers) (2012) Nikel Raporu [Nickel report], Ankara, Turkey, 52p (In Turkish)

Uslu İ (2007) Mihalıççık (Eskişehir) çevresindeki kromit ve manyezit yataklarının LANDSAT 7 ETM+ ve ASTER uydu verileri ile incelenmesi [Investigation of chromite and magnesite deposits around Mihalıççık (Eskişehir) using LANDSAT 7 ETM+ and ASTER remote sensing data]. MSc thesis, Ankara University, The Graduate School of Natural and Applied Science Geological Engineering Department, 118p (unpublished)

Wells MA, Ramanaidou ER, Verrall M, Tessarolo C (2009) Mineralogy and chemistry of "garnierites" in the Goro lateritic nickel deposit, New Caledonia. Eur J Mineral 21–22:467–483

Yıldırım H, Morcali H, Turan A, Yücel O (2013) Nickel pig iron production from lateritic ores. The 13th International Ferroalloys Congress, Efficient technologies in ferroalloy industry, June 9–13, Almaty, Kazakhstan. pp 237–244

Yılmaz A, Yılmaz H (2013) Ophiolites and ophiolitic melanges of Turkey: a review. Geol Bull Turk 56–2:61–114

Chapter 14
Uranium, Thorium and Rare Earth Element Deposits of Turkey

Elif Akıska, Zehra Karakaş, and Ceyda Öztürk

Abstract This chapter is about the deposits and the mineral occurrences containing uranium, thorium and rare earth elements in Turkey. The data include exploration studies and the formation/origin and characteristics of these deposits.

Uranium deposits in Turkey are mostly in western Anatolia. Among them, the Köprübaşı (Manisa), Fakılı (Uşak), Küçükçavdar (Aydın) and Sorgun (Yozgat) deposits are of a sedimentary type, while only the Demirtepe (Aydın) deposit is a vein-type uranium deposit. The Sorgun deposit occurs in Eocene sediment while others are from the Neogene age. In the Demirtepe deposit, the ore is found in fault zones within Paleozoic schists. Indications of uranium concentrations are also found in Southern Marmara and Eastern Black Sea, Dadağ, Şebinkarakisar, Ayvacık and Mazıdağ regions.

A complex ore deposit consisting of thorium, rare earth elements, barite and fluorite occurs in the Kızılcaören (Eskişehir) region. The ore occurs as large veins and cement of tectonic breccias. In addition, indications of thorium concentrations are also found in the Malatya–Kuluncak, Kayseri–Felahiye, Sivas and Diyarbakır regions. Beside the Kızılcaören REE mineralisation, Çanaklı (Isparta), Mortaş-Doğankuzu (Konya) and Sofular (Malatya) are important REE mineralisations in Turkey.

14.1 Introduction

Uranium (U) is a radioactive chemical element within the actinide series of IIIB group of the periodic table. It was discovered in 1789 by M. H. Klaproth. Its atomic number is 92 and atomic weight is 238.03 g/mol. Its melting point is 1132.2 °C, boiling temperature is 4131 °C and specific weight is 19.1 g/cm^3. Uranium is the main nuclear fuel raw material and has three radioactive isotopes: U-238, U-235

E. Akıska · Z. Karakaş (✉) · C. Öztürk
Faculty of Engineering, Department of Geological Engineering, Ankara University, Ankara, Turkey
e-mail: karakas@ankara.edu.tr

F. Pirajno et al. (eds.), *Mineral Resources of Turkey*, Modern Approaches in Solid Earth Sciences 16, https://doi.org/10.1007/978-3-030-02950-0_14

and U-234. Uranium never occurs in native form but is combined with various other elements forming uranium-bearing minerals. There are hundreds of uranium-bearing minerals in the earth's crust, however, most of them do not contain uranium of economic proportion. Some of these minerals forming economic deposits are autunite, uraninite, coffinite and torbernite (Marbleport 2014). Uranium occurs in the oxidation states of +6 and +4. Uranium minerals with oxidation states of +4 are primary minerals (uraninite, coffinite, branerite and davidite), however under suitable conditions, they can change into secondary minerals such as carnotite, autunite and torbernite.

Thorium (Th) was discovered in 1828 by Swedish chemist J. J. Berzelius. It is a member of the actinide series. Thorium is a radioactive element and is silver grey metal in its pure form. Its atomic weight is 90 and atomic mass unit is 232.0377. Melting point is 1750 °C, boiling temperature is 4785 °C and specific weight is 11.72 g/cm^3. Thorium has 13 radioactive isotopes from Th-223 to Th-235. Th-232 is the only natural isotope of thorium. Although it is not formed in elemental form, thorium is found in the structure of about 60 minerals. Among these, only monazite {(Ce, La, Y, Th) PO_4} and thorite ($ThSiO_4$) are used for thorium production. These minerals are generally associated with rare earth elements. In comparison to uranium, thorium is more abundant and long-lived, less toxic, leaving less waste product, and the half-lives of its wastes are shorter than those of uranium (TAEK 2015). But it cannot be used as a nuclear fuel.

The rare earth elements (REEs), which include the 15 lanthanide elements (Z = 57 through 71) plus scandium (Z = 21) and yttrium (Z = 39), are so-called because most of them were originally isolated in the eighteenth and nineteenth centuries as oxides from rare minerals. Scandium and yttrium are considered rare earth elements since they tend to occur in the same ore deposits as the lanthanides and exhibit similar chemical properties. Furthermore, efficient separation processes were not developed until the twentieth century because of REEs' chemical similarity. All of the REEs were finally identified in the twentieth century. Promethium, the rarest, was not identified until 1945, and pure lutetium metal was not refined until 1953 (Emsley 2001).

14.2 Uranium

Uranium resources in the world are classified on the basis of their extraction costs. OECD/NEA (Nuclear Energy Agency) and IAEA (International Atomic Energy Agency) categorize the costs as 80 US$ per kg and 80–130 US$ per kg. Based on 1997 data, there is a total of 2.60 Mt of proven reserves in the world at 80 US$ per kg (OECD 1997). Turkey does not have a uranium reserve of this size. The total uranium world-wide reserve with 80–130 US$ per kg is 756,490 tonnes. In this class, Turkey holds 9129 tonnes of uranium reserves. These reserves are generally in western Anatolia, among them the Manisa–Salihli–Köprübaşı, which has a grade of 0.05% U_3O_8 that has special importance (Şaşmaz 2008) (Fig. 14.1). This

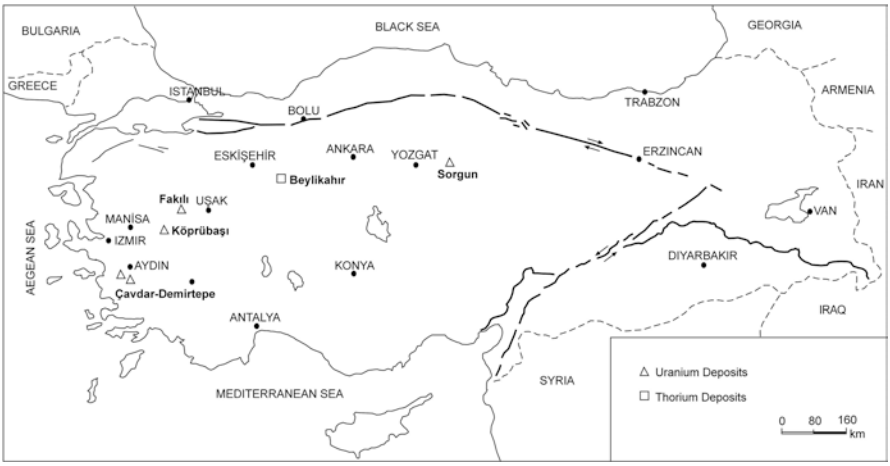

Fig. 14.1 Uranium and thorium deposits of Turkey. (MTA 2010a)

Table 14.1 Uranium grades and reserves in Turkey (DPT 2001; OECD 2014)

Field	Grade (U_3O_8wt. %)	Reserve (U_3O_8 – tonnes)	Host rock
Salihli-Köprübaşı	0.05	2852	Neogene sediments
Eşme-Fakılı	0.05	490	Neogene sediments
Söke-Küçükçavdar	0.04	208	Neogene sediments
Söke-Demirtepe	0.08	1729	Fault zones in Paleozoic schists
Sorgun-Temrezli	0.1	3850	Eocene sediments
Total	0.04–0.1	9129	

occurrence is the first sandstone-type ore deposit that contains uraninite preserved below the water table (Kaplan 1978). The Yozgat–Sorgun deposit with a grade of 0.1% U_3O_8 is the most U-rich in Turkey (Table 14.1).

IAEA classifies the uranium deposits into 14 groups based on age, tectonic setting, source rock and location (Anonymous 2009). They are; "*unconformity-related deposits*", "*sandstone deposits*", "*hematite breccia complex deposits*", "*quartz-pebble conglomerate deposits*", "*vein deposits*", "*intrusive deposits*, "*caldera related volcanic deposits*", "*metasomatite deposits*", "*surficial deposits*", "*collapse breccia pipe deposits*", "*phosphorite deposits*", "*black shale deposits*", "*metamorphic deposits*" and "*other types of deposits*". Most of the uranium deposits in Turkey are of a sedimentary type; only the Demirtepe (Söke-Aydın) deposit is a vein-type uranium deposit (TÜSİAD 1998) (Table 14.1). The Sorgun deposit occurs in Eocene sediment while others are of the Neogene age. In the Demirtepe deposit, the ore is found in fault zones within Paleozoic schists.

14.2.1 Uranium Mineral Exploration

Uranium exploration studies in Turkey were started in 1953 by MTA as short-term prospection works. By 1956 systematic studies were initiated and lasted until 1991 (DPT 2001). However, these works had to be stopped due to limited budget. Studies conducted by MTA in 2004 are continuing (Yörükoğlu 2014). Explorations in the 1st years were carried out on vein-type deposits in the Menderes, Istranca and Bitlis metamorphic massif and in granites in Kırşehir and Şebinkarahisar regions. As a result of these works, although a number of radioactive anomalies were recorded, no uranium deposits were discovered. These anomalies are mostly on small fissures and schistosity surfaces within alteration zones, which contain secondary uranium minerals such as autunite and torbernite. Exploration was then extended to sedimentary uranium deposits in Neogene sediments. As a result of the assessment of surface radioactive anomalies, a total of 9129 tonnes of uranium reserves was discovered in five fields in western Anatolia (TÜSİAD 1998; Table 14.1). However, it is thought that this tonnage does not reflect the real uranium resources of Turkey (TÜSİAD 1998). Recent exploration in the Nevşehir–Dadağ deposit found a uranium reserve of 210.10 tonnes with a grade of 0.015% U_3O_8 (Aksoy et al. 2013). Furthermore, new mineral explorations to be conducted particularly in Southern Marmara and Eastern Black Sea regions may discover new uranium deposits. Uranium concentrations of 3–6 ppm were detected in young sediments at the bottom of the Black Sea and 0.1–0.5 ppm at the bottom of Lake Van. Uranium occurrences in the Çukurovası and Eskine Yaylası fields in the Şebinkarahisar region of the Giresun city contain secondary uranium minerals (Çağatay 1981). The mineralisation in Çukurovası occurs in nummulites-bearing Eocene clastic deposits, whereas the one in Eskine is formed along fractures of an older andesite (Örgün 1972). In the Çukurovası field, 300 tonnes of secondary uranium occurrence (meta-autunite, meta-torbernite etc.) (Çağatay 1981) with a grade of 0.04% U_3O_8 were confirmed (MTA 2010b).

In the Ayvacık–Küçükkuyu field near Çanakkale city, ore with a grade of 0.08% U_3O_8 contains 250 tonnes in Miocene carbonate rocks (MTA 2010c). It is also known that Mazıdağ phosphate deposits contain uranium in concentrations of 20–100 ppm U_3O_8 (Önal 1975; Doyranlı 1978). Uranium concentration is about 100 ppm in some coal deposits (e.g. Elbistan, Beypazarı, Orhaneli and Çan) and 200 ppm in Şırnak asphaltites (TÜSİAD 1998). Pliocene formations in Bulgaria where uranium is produced extend towards Turkey, and these units are still untouched (TÜSİAD 1998).

14.2.2 Main Uranium Deposits in Turkey

14.2.2.1 Köprübaşı (Salihli- Manisa) Uranium Field

14.2.2.1.1 Regional Geology

The area is located about 120-km east of Manisa city (Fig. 14.2). The basement is comprised of Precambrian metamorphic series of the Menderes massif represented by gneiss and pegmatite and quartz veins. Basement rocks are unconformably overlain by Neogene fluvial and lacustrine deposits. Fluvial sediments are composed of coarse-grained deposits at the bottom and fine-grained deposits at the top. Lower coarse-grained deposits (lower unit) are made up chiefly by clay and schist, gneiss block and pebbles with sand cement. Upper fine-grained deposits (upper unit) are composed of "sandstone and conglomerate alternations" that are interbedded with siltstone and mudstone. There is a conglomerate level at the base of the upper fine-grained deposits, and this is followed by middle and upper conglomerate levels (Yılmaz 1982). In some areas, tuffs and silicified layers are interbedded with fluvial sediments. Lacustrine units are at the top and start with mudstones and continue to the top with white-green clay layers. They end up with cherty limestones in the uppermost part (Fig. 14.2).

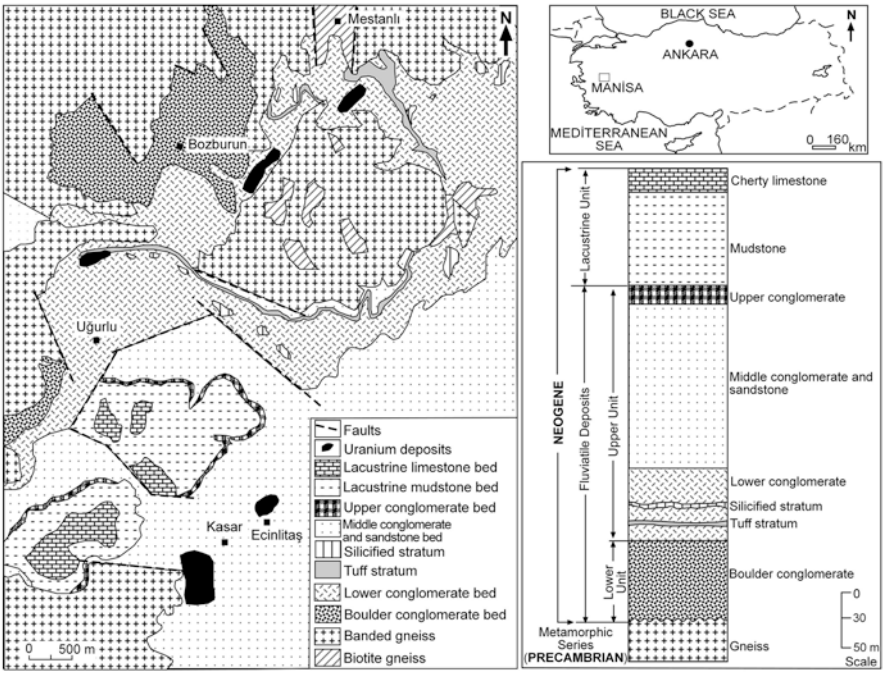

Fig. 14.2 Geological map and the columnar section of the Köprübaşı (Salihli) area. (Simplified from Yılmaz 1982)

14.2.2.1.2 Mineralisation

Studies on uranium deposits in the region were started in 1961 by MTA and continued until 1974. Air-borne surveying, general-detailed systematic prospection, trench, gallery, shaft and drilling operations were conducted. As a result, Kasar, Taşharman, Kocadüz, Yardere, Kocaboğaz, Ecinlitaş, Çetinbaş, Topallı, Uğurlu (Tomaşa) and Kayran uranium deposits were discovered (Şaşmaz 2008). Mineralisation is mostly found in sandstones and conglomerates. Average grades and reserves of deposits are shown in Table 14.2. Mineralisation in the Kasar and Ecinlitaş sectors occurs in middle conglomerate and sandstone levels of the series called the upper unit. Mineralisation in the Topallı, Kayran, Çetinbaş and Uğurlu sectors is in the lower conglomerate level, called the lower unit (Kaçmaz 2007). In other words, all uranium mineralisations in sedimentary rocks are in pore cements of upper-fluvial sediments (Şaşmaz 2008). They are found as disseminations in iron- and manganese-rich levels and as coatings on some pebbles (Kaçmaz 2007). Uranium minerals such as torbernite, meta-torbernite and meta-autunite and alteration minerals such as jarosite and chlorite were detected. The uranium grade in these deposits is in the range 0.01–0.40% U_3O_8. The grade in Fe-rich sediments is up to 1.06% since iron oxides greatly contribute to deposition of secondary uranium phosphates (Kaçmaz 2007).

Pyrite that occurs during or after diagenesis of ore-bearing coarse clastic rocks is very important for uranium deposition. Uranium mineralisation is controlled by pyrite-rich lenses (Yılmaz 1982). Pyrite is oxidized by uranium-rich groundwater which results in oxygen depletion in groundwater in pyrite-rich zones. As a result, SO_3 forms, and then it decomposes to the anions HS and SO_4. US ions formed this way are thought to be the main reducing agent in the formation of Köprübaşı's uranium deposits (Yılmaz 1982).

It is believed that the gneisses of the Menderes and Demirci–Gördes massifs surrounding the basin and Miocene tuffs interbedded with sediments are the source rocks of the sedimentary uranium deposit (Yılmaz 1982; Kaçmaz 2007). The high uranium content of tuffs is related to their rhyolitic composition and glassy character (Kaçmaz 2007).

Table 14.2 Uranium grades and reserves in Köprübaşı (MTA 1976)

Field	Average grade (U_3O_8 wt. %)	Reserve (U_3O_8 tonnes)
Kasar	0.034	548
Ecinlitaş	0.05	300
Çetinbaş	0.0267	247.5
Topallı	0.0385	229.5
Uğurlu	0.03	18.5
Kayran	0.0323	79.5

14.2.2.2 Küçükçavdar–Demirtepe (Söke–Aydın) Uranium Field

14.2.2.2.1 Regional Geology

The study area is located 50-km west of Aydın city (Fig. 14.3). The basement of the region is composed of the Menderes massif, which is represented by three rock groups with discordant contacts (Çine, Kavaklıdere and Marçal Groups). Küçükçavdar-Demirtepe area comprises the rocks units of the Çine massif (Öztunalı 1965). The Çine Group is composed of Precambrian gneiss, metavolcanics and schists. The Neogene units directly overlie the crystalline series on the southern and northern flanks of Menderes Graben. It is composed of conglomerates of various sand and pebble size, clay, marl and limestone interlayers. The Neogene units in the region represent a lacustrine environment. Pebble, sand and silt sediments that were deposited in small Neogene basins formed by faulting are significantly important since they may contain uranium deposition. The Quaternary units are represented by widespread alluvium areas and a debris cone (Fig. 14.3).

14.2.2.2.2 Mineralisation

Uranium mineral systems have been discovered in the Küçükçavdar, Demirtepe, Kisir-Osmankuyu and Arapsu deposits.

14.2.2.2.3 Küçükçavdar Deposit

The Küçükçavdar deposit is hosted in Neogene block, pebble, sand, silt and clay lithologies sets above gneiss and schists of the Menderes massif. It is a sedimentary-type deposit with an epigenetic character. The mineralisation is lenticular or partly layered. Autunite is the main uranium mineral.

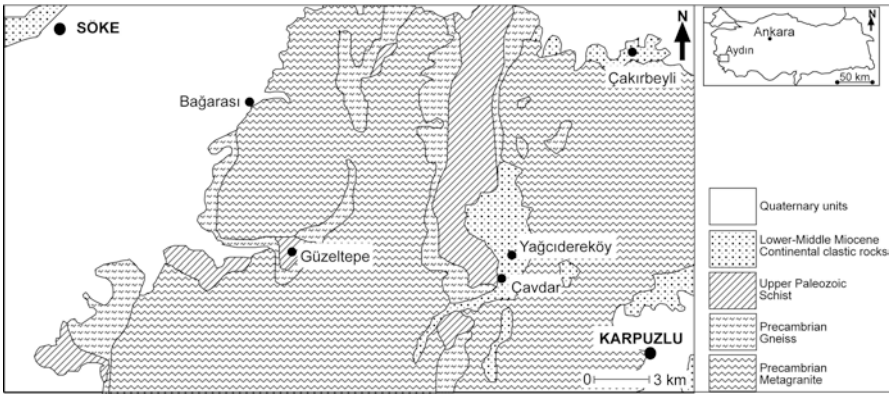

Fig. 14.3 Geological map of the Küçükçavdar-Demirtepe area. (Simplified from MTA 2001)

In the deposit, a total of 208.94 tonnes of proven reserve was found of which 70.39 tonnes with a grade of 0.02–0.03% U_3O_8 and 138.55 tonnes with a grade of >0.03% U_3O_8 (MTA 2010d).

14.2.2.2.4 Demirtepe Deposit

In this deposit which is located in central part of the Çine crystalline massif, gneiss, mica-schist complex and meta-quartzites are widely exposed. The mica-schist complex is an N–S extending, west-dipping asymmetrical overturned fold (Öztunalı 1965; Mataracıoğlu and Aşçı 2008). The uranium mineralisation occurs in fault zones within the mica-schist fold. The mineralisation is a stockwork type deposit with autunite, bassetite, saleeiite and uranopilite as the main ore minerals (Öztunalı 1965).

In this deposit, a total of 1728.21 tonnes of proven and/or possible reserves have been estimated, of which 263.34 tonnes have a grade of 0.0234–0.0956% U_3O_8 and 1456.69 tonnes have a grade of 0.0956% U_3O_8 (MTA 2010d).

14.2.2.2.5 Kisir–Osmankuyu Deposit

In this deposit located in the western part of the Çine massif, four units outcrop exist, which are from bottom to top fine-grained gneiss, coarse-grained gneiss, micaschists and metaquartzites. Mineralisation occurs as thin levels in limonitized weak zones in the vicinity of unconformity between fine-grained gneisses and spotted gneisses (Öztunalı 1965). Gummite, uranotile, torbernite, autunite, meta-autunite, meta-torbernite and phosfuranilite are the main uranium minerals.

In this deposit, a total of 45.90 tonnes of probable reserves have been determined, of which 11.53 tonnes have a grade of 0.02–0.03% U_3O_8 and 34.37 tonnes have a grade of >0.03% U_3O_8 (MTA 2010d).

14.2.2.2.6 Arapsu Deposit

In the Arapsu deposit, autunite and torbernite are the main ore minerals (Arslan and Şenol 2012).

In this deposit, a total of 30.29 tonnes of probable reserves are present, of which 10.78 tonnes are graded 0.02–0.03% U_3O_8 and 19.51 tonnes graded >0.03% U_3O_8 (MTA 2010d).

14.2.2.3 Temrezli (Sorgun–Yozgat) Uranium Deposit

14.2.2.3.1 Regional Geology

The Temrezli deposit is located 30-km east of Yozgat city (Fig. 14.4). Upper Cretaceous granite, granodiorite, monzonite and diorite of the Kırşehir massif are the oldest units in the area forming the basement of the basin. These basement units are overlain by Paleocene intercalations of conglomerate–sandstone–mudstone. They are unconformably covered by Eocene coarse-fine grained sandstone, siltstone and claystone. The Eocene units ending up with andesite and basalt volcanics are unconformably overlain by Pliocene fluvial and lacustrine deposits. Quaternary alluviums are the youngest units in the area (Yalçın et al. 1997; Dümenci et al. 2004; Akçay and Beyazpirinç 2017) (Fig. 14.4).

14.2.2.3.2 Mineralisation

The Temrezli uranium deposit was discovered by the General Directorate of Mineral Research and Exploration (MTA) with more than 500 drill holes drilled between 1958 and 1985, followed by detailed investigations. A result of these activities was

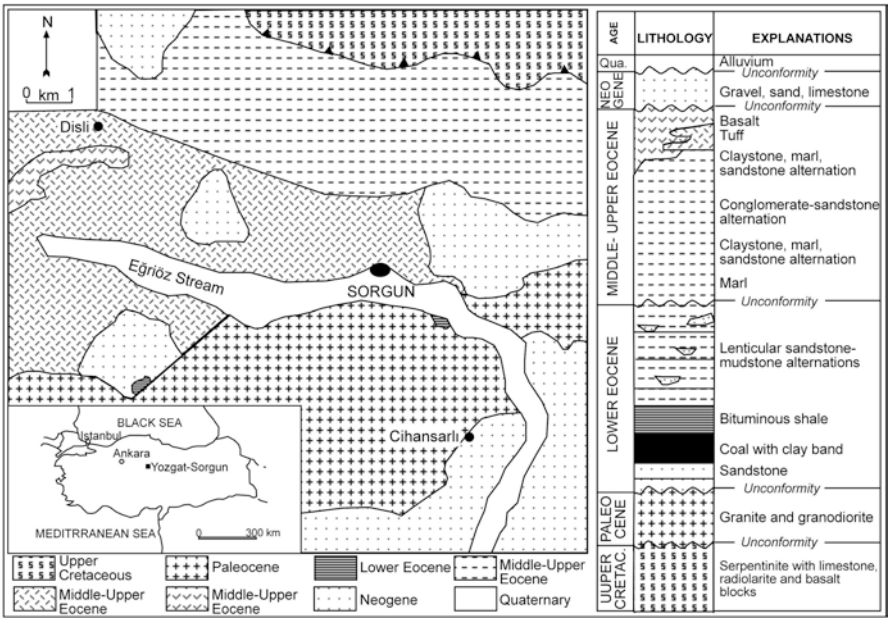

Fig. 14.4 Geological map and the stratigraphic column of the Sorgun area. (Simplified from Karayiğit et al. 1996)

3852 tonnes of probable reserves with a grade of 0.1% U_3O_8 (OECD 2005). Other uranium occurrences occur in the Babalı and İşleyen areas (MTA 2010e).

The Temrezli mineralisation is the highest-grade uranium deposit in Turkey. It is a sandstone-type deposit characterized by epigenetic uranium minerals (generally uraninite or coffinite) within fine-coarse grained sediments deposited in fluvial, alluvial, lacustrine or seashore environments (CSA Global 2014). Uranium mineralisation (overlying the Cretaceous granitic batholith) in the southwestern part of Temrezli basin occurs as stratiform accumulation within silty levels between lower Eocene deltaic-lagoon deposits and within Lutetian aged littoral (shore) zone marine, channel-type conglomerates and silty sandstones in the northeastern part of the basin (Dahlkamp 2009). Under oxidizing and slightly acidic conditions, uranium leaches and is transported by groundwater moving through the sediments. It is then deposited in a reducing environment along the boundary between sand and sand-interlayered clay levels (CSA Global 2014).

Uranium mineralisation in the area occurs as lenses. The depth of these lenses is in the range 25–215 m (Adur Madencilik 2015). The morphology (palaeovalley) of the deposit is controlled by facies changes and structural factors (faults etc.) (Dahlkamp 2009). Most of the uranium discovered is in Ca-bearing secondary minerals such as uranophane, becquerelite and haiweeite. Uraninite and coffinite are also observed in small amounts. In addition, a Ti-bearing brannerite mineral occurs in small amounts (CSA Global 2014).

14.2.2.4 Fakılı (Eşme-Uşak) Uranium Deposit

The sandstone-type Fakılı uranium deposit is located 70-km east of Köprübaşı (Manisa), in western Anatolia (Fig. 14.5).

14.2.2.4.1 Regional Geology

The metamorphic rocks of the Menderes massif and Neogene sediments are exposed around the deposit (Fig. 14.5). The metamorphic rock at the base of the Neogene sedimentary basin is represented chiefly by spotted gneisses. Neogene sediments are divided into three groups, namely: clastic unit at the bottom, overlying marl units and lacustrine limestones at the top (Kaplan et al. 1974). The clastic unit is composed of clay, sand, pebble and conglomerate. The lower part of this unit has a fluvial character and changes upwards into horizontally-bedded lacustrine sediments with increasing lateral continuity. The marl unit consists of clay and tuffite levels and silt, sandstone and marl alternation. The Fakılı uranium deposit is hosted in this unit. The deposit is of a sandstone type and occurs in a lens of 9-m thickness within lacustrine sediments at the base of the Neogene series (Kaplan et al. 1974). The lacustrine limestones are the early sediments of a Neogene lake (Fig. 14.5).

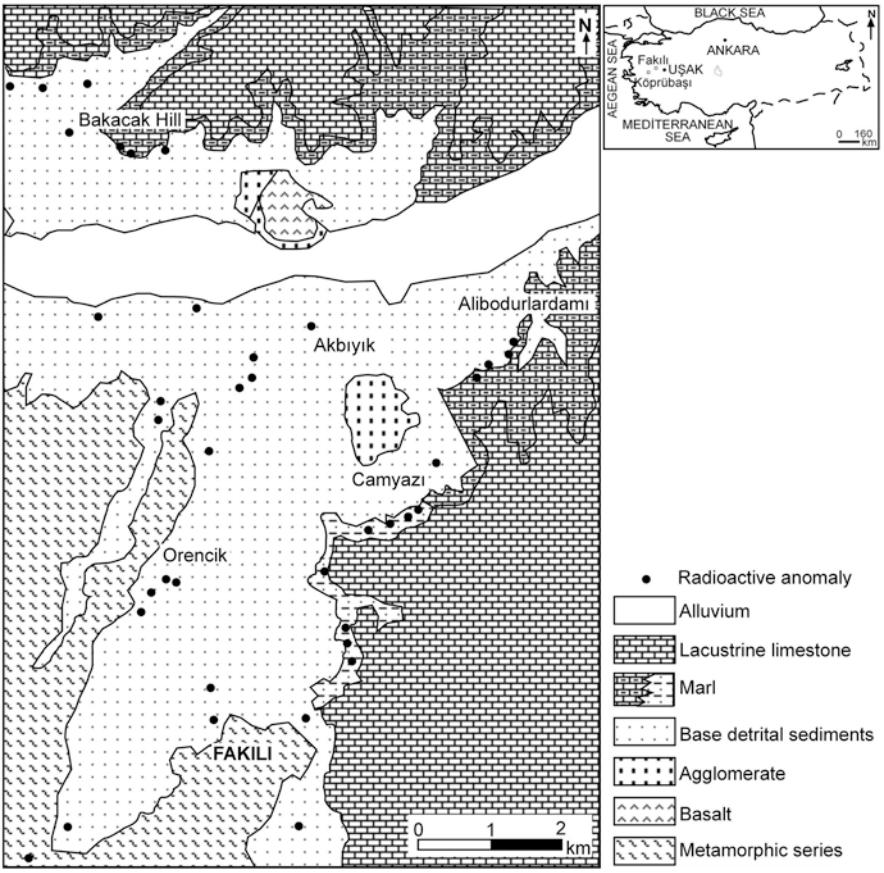

Fig. 14.5 Geological map of the Fakılı area. (Simplified from Kaplan et al. 1974)

14.2.2.4.2 Mineralisation

The Fakılı uranium deposit is composed of two stages: syngenetic and epigenetic. During the sedimentation of the marl unit, lake water was enriched by dissolved uranium. The Neogene clastic unit was in equilibrium with a sulphate component. The sulphate concentration reached a maxima at the top of contact with the marl unit but decreased towards the top. High sulphate concentrations are the result of evaporation in this part of the lake. Evaporation gave rise to an increase in uranium concentration. Lake water that had an acidic character at the beginning became neutral in character depending on a decrease in sulphate concentration and partly on an increase in $CaCO_3$ content. Uranium that was unstable as a neutral solution, started to precipitate intensively following the precipitation of anhydrite. This process is a syngenetic precipitation of uranium as a primary phase. At the end of the Neogene, lake water retreated and Neogene sediments became weathered due to

alteration and atmospheric effects. During the infiltration of water in the vadose zone, uranium reentered the solution and precipitated as sulphate components in heterogeneous zones above the contact at the base of the marl unit. This process of epigenetic concentration explains the lenticular appearance of the Fakılı uranium deposit (Kaplan et al. 1974).

Kaplan et al. (1974) reported that the Fakılı uranium deposit contains 500 tonnes with a grade of 0.045% U_3O_8.

14.2.2.5 Dadağ (Gülşehir-Nevşehir) Uranium Deposit

The area is located south of Dadağ village and 40 km from Nevşehir city (Aksoy et al. 2013; Ünal 2015) (Fig. 14.6).

14.2.2.5.1 Regional Geology

The Ortaköy granitoid of pre-upper Cretaceous age and the metamorphic rocks of the Kırşehir Massif form the basement units in the area (Atabey 1989; Ünal 2015). Fluvial deposits consisting of red wine-coloured conglomerates, fine-grained grey-beige sandstone and sandy marl units of Eocene age overlie the basement (Fig. 14.6). These units are covered with lacustrine sediments that start with limestones and continue with bituminous shales. The Dadağ uranium mineralisation occurs in limestone layers (Ünal 2015). This is overlain by fluvial deposits consisting of conglomerate, sandstone and siltstones. These fluvial deposits are overlain by clayey limestone, limestone, sandy marl and laminated shales, together with sandstone and marl units of a flysch character. Lower Eocene-lower Miocene units are composed of braided river and alluvial fan deposits consisting of conglomerate, sandstone, ligniferous marl, claystone, siltstone and mudstone. Lignites were formed in swamp deposits on the flood plain. Upper Miocene conglomerates, cross-bedded sandstone and claystone units belong to the fluvial and lacustrine deposits. They are overlain by volcano-sedimentary units of ignimbrite character (Yıldız et al. 2016). Quaternary alluviums are the youngest units in the region.

14.2.2.5.2 Mineralisation

Uçakçıoğlu (1987), Aydın (1990), and Çetintürk (1992) produced radiometric anomaly maps in the Nevşehir–Gülşehir, Kırşehir, Kayseri and Niğde regions. The Dadağ uranium mineralisation was discovered by MTA on the basis of field and laboratory data from the Dadağ Radioactive Raw Materials Exploration project conducted in the years of 2012–2014 (Aksoy et al. 2013; Ünal 2014, 2015). Low cps (count per second) values measured in the Eocene conglomerates and sandstones showed no indication of mineralisation. However, some radiometric anomalies were

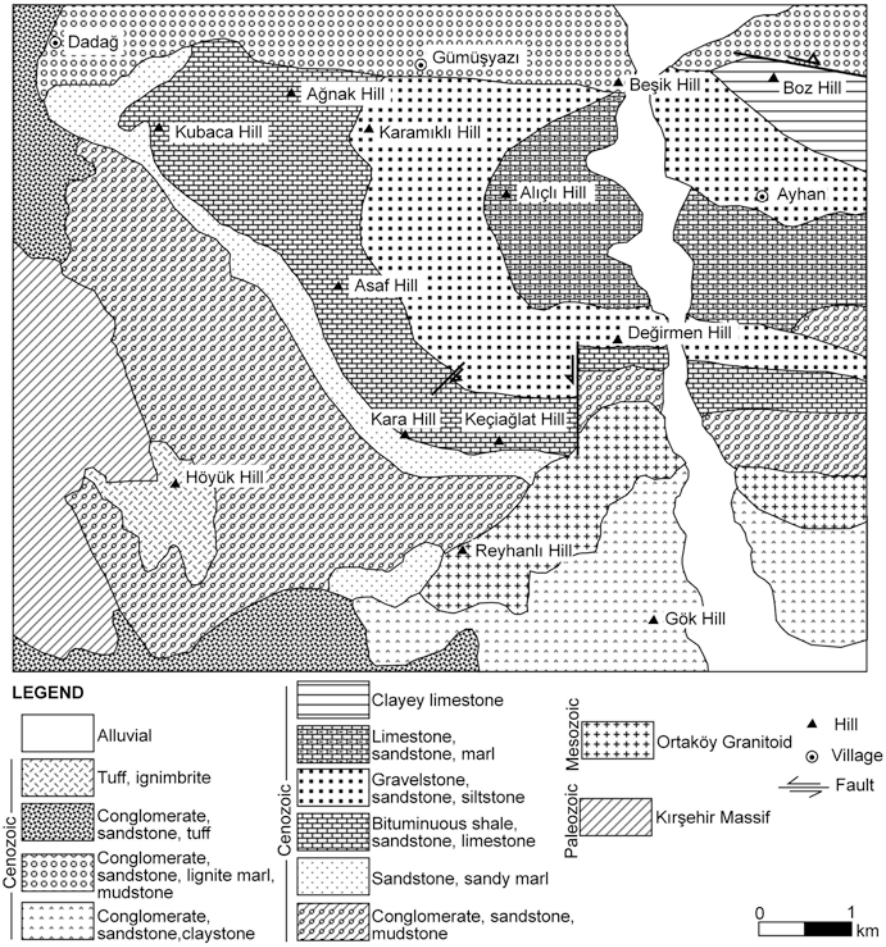

Fig. 14.6 Geological map of the Dadağ uranium deposit. (Simplified from Atabey 1989; Ünal 2015)

recorded in the limestones (Ünal 2015). Aksoy et al. (2013) estimated the reserves of Dadağ mineralisation as 210.10 tonnes with a grade of >0.015% U_3O_8.

The Nevşehir-Dadağ uranium mineralisation occurs within carbonate units and therefore it is carbonate-type deposit (Ünal 2015). Uraninite and kasolite are the main uranium minerals. It is thought that uranium mineralisation is an epigenetic deposit that was formed by uranil-rich hydrothermal fluids circulating through the faults.

14.3 Thorium

Known global thorium reserves are 6.3 Mt (OECD 2014), and selected countries with significant thorium resources are listed in Table 14.3. A complex ore deposit consisting of rare earth elements, barite, fluorite and thorium was discovered in the Kızılcaören region northwest of Sivrihisar town of Eskişehir city, central Turkey (Kaplan 1977). In this area, 380,000 tonnes of proven ThO_2 reserves are recorded. In addition, indications of thorium were also found in the Malatya–Darende–Kuluncak, Kayseri–Felahiye, Sivas and Diyarbakır regions (DPT 1996; Akkoyunlu 2006). Thorium occurrences in these regions may contribute to more substantial Turkish thorium resources once the necessary investigations are conducted (DPT 1996). Considering the general global resources, thorium in Turkey could make a very important contribution in the energy sector in the near future. If thorium could be used as a nuclear raw material, the demand will also define the economic value of various deposits. Therefore, today, all thorium concentrations are a potential source.

Table 14.3 Global thorium reserves (OECD 2014)

Country	Tonnes
India	846,000
Brazil	632,000
Australia	595,000
USA	595,000
Egypt	380,000
Turkey	380,000
Venezuela	300,000
Canada	172,000
Russia	155,000
South Africa	148,000
China	100,000
Norway	87,000
Denmark	86,000
Finland	60,000
Sweden	50,000
Kazakhstan	50,000
Other	1,725,000
Total	6,361,000

14.3.1 Exploration Works

Following the end of World War II in 1945 and the use of the first atomic bomb, several countries started to investigate the role of atomic energy and related raw materials. Accordingly, in 1959 uranium exploration studies were initiated in Turkey (Contencin 1960; Uçmak 1969; Kaplan 2011). Because uranium is a radioactive element, the first study was made by air-borne surveying. As a result of these works, the first discovery was made in the Kızılcaören field (Eskişehir). Four drill holes with total length of 113 m were drilled, and it was found that this area is promising not only for uranium but also for thorium (Kupfahl 1954; Contencin 1960). Extensive field work on this occurrence was done by Kaplan (1977), and the areas were found to contain ore veins and ore-bearing tectonic breccia zones in four sectors—Koca Devebağırtan, Küçük Höyüklü, Yaylabaşı and Kocayayla. In these areas, a total of 72 boreholes were drilled with total length of 12,912 m. The proven reserves of Koca Devebağırtan and Küçük Höyüklü sectors is 380,000 tonnes of thorium oxide (ThO_2) with an average grade of 0.21% ThO_2 (Kaplan 1977). Although the thorium grade reaches up to 3% in selected samples, the average grade is 0.21%. The approximate ThO_2 reserve distribution in Devebağırtan and Küçük Höyüklü sectors is given in Table 14.4. Since sufficient number of boreholes could not be drilled in the Yaylabaşı and Kocayayla sectors, reliable estimates of reserves in these areas are not available.

As a result of these studies, it was found that Kızılcaören contains not only thorium but also fluorite, barite and rare earth elements. Therefore, this deposit was named the "complex ore" (Günalay 1970; Demiröz 1976; Kaplan 1977). In this deposit, explorations for fluorite, barite and bastnasite were implemented at a depth down to 50 m, while explorations for thorium were carried out to a depth of 400 m. All these studies showed that the thorium content of the ore depends on bastnasite and brockite minerals (Kaplan 1977).

14.3.2 Regional Geology

Kızılcaören complex ore is located within the Sakarya Zone which is one of the NE–SW extending tectonic zones of the Pontides. The study area, which is known to host the main thorium deposit in Turkey, comprises an area of 15 km^2 in between Kızılcaören–Karkın and Okçu (Sivrihisar–Eskişehir) (Gültekin and Örgün 2000).

Table 14.4 Approximate distribution of thorium reserves in Kızılcaören (Yüce 1988)

	Reserve (ThO_2 tonnes)	Average grade (ThO_2 wt. %)
Küçük Höyüklü sector	97,560	0.196
Koca Devebağırtan sector	286,424	0.217
Total	383,984	0.212

Ophiolites mostly consisting of serpentinites are the oldest rocks in the Kızılcaören field. The age is late Paleozoic-early Triassic (Bingöl 1976; Şengör and Yılmaz 1981; Üşümezsoy 1987). An E–W large fault zone in the south of field is the contact between ophiolites and Triassic rocks (Özgenç 1993) (Fig. 14.7). According to Gültekin and Örgün (2000), basement rocks and Triassic rocks are the wall rock of ore-bearing veins. As a result of Oligocene and lower-Miocene volcanic activities, silicified trachytic tuff, alkaline trachyte and phonolite formed ore-bearing breccia zones and ore veins (Delaloye and Özgenç 1983; Gültekin and Örgün 2000). Alkaline trachyte and phonolites are a part of post-Oligocene western Anatolian volcanism. Trachyte and phonolites in the area cut the ophiolites along an E–W trending fault to the south (Fig. 14.7). The mineralisation is vertically orientated to two normal faults in the eastern and western parts of the area and the E–W trending fault to the south (Fig. 14.7). The structural elements in the region indicate the presence of large breccia pipes and fracture systems due to an extensional regime in the mineralized area. The large fault to the south and two perpendicular normal faults border the mineralised area. Mineralisation is found only in this area (Özgenç 1993). The mineralisation processes were developed in two main stages: before and after brecciation (Özgenç 1993). Alluviums comprising the youngest units of the area are of Quaternary age.

14.3.3 Ore Genesis

The Kızılcaören thorium and rare earth complex mineralisation was formed in association with Tertiary trachytic and phonolitic alkaline igneous activity, which are emplaced within Paleozoic argillic-sericite schist, phyllite, sandstone and volcanic rocks (Kaplan 1977). The mineralisation is in the form of vein and vein clusters which follow the tectonic breccia zones. The mineralised veins contain calcite,

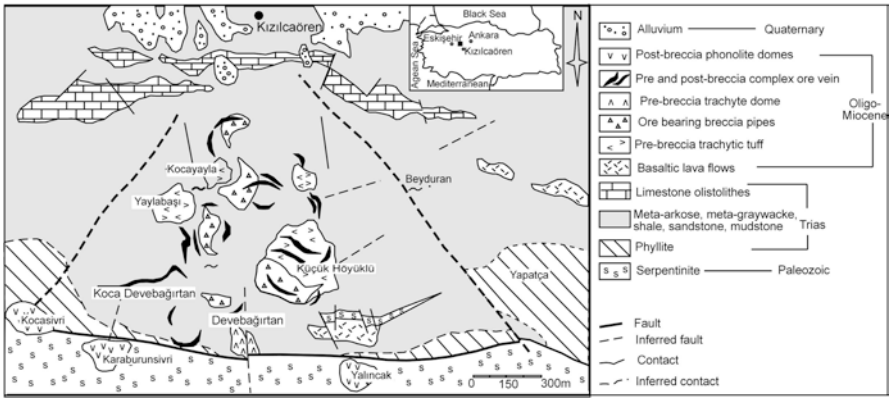

Fig. 14.7 Geological map of the Kızılcaören area. (Simplified from Özgenç 1993)

fluorite, barite and bastnasite accompanied by psilomelane, limonite and dolomite and lesser amounts of apatite and phlogopite. The Kızılcaören bastnasites that are more enriched in thorium than normal bastnasite (Kaplan 2011) were formed at the end of multi-stage mineralisation processes (Çağatay 1981). According to Çağatay (1981), mineralisation occurs within carbonate units in association with manganese and iron oxides that are the cement material of brecciated rocks. Kaplan (1977) suggested that mineralisation formed as a result of hydrothermal activity. The hydrothermal solutions in the first stage were enriched by barium, and the ensuing solutions were in equilibrium with fluorite and iron minerals, whereas the solutions in the final stage were manganese-rich and formed the cement material of the earlier stages. Thorium- and REE-bearing bastnasite were deposited by manganese-rich solutions, and calcite, quartz and chalcedony crystals were formed as late products. According to Çağatay (1981), the mineralisation processes and the mineral paragenesis were as follows: (a) silicification of wall rocks; (b) brecciation; (c) barite and fluorite mineralisation; (d) brecciation; (e) iron (pyrite and limonite forming from pyrite) mineralisation; (f) manganese and carbonate and (g) thorium-REE minerals.

14.4 Rare Earth Elements

The concentration of REEs in the Earth's crust is estimated to be between 150 and 220 ppm, which is higher than the concentration of other metals mined for industrial use, such as Cu or Zn. The concentration of cerium, the most abundant rare earth, is approximately the same as that of copper, although the other REEs are much rarer. However, REEs are not usually concentrated in ore deposits in amounts that can be easily or economically mined (Long et al. 2010)

Specifically, REEs include light REEs (LREEs) such as lanthanum, cerium, praseodymium, neodymium, samarium, europium, and heavy REEs (HREEs) gadolinium, terbium, dysprosium, holmium, erbium, thulium, ytterbium, lutetium, scandium and yttrium. The physical similarities of the atomic radius and charge between REEs led to their separation as distinguishable elements.

Rare earth minerals occur in the form of bastnasite, monazite, xenotime and some other minerals. As shown in the U.S. Geological Survey, Mineral Commodity Summaries, REE reserves worldwide total 140 Mt. They are distributed in China (55 Mt), the United States (13 Mt), India (3.1 Mt), Australia (2.1 Mt), Brazil (2.2 Mt), Malaysia (30,000 tonnes), Russia, Egypt, Canada, South Africa and other countries.

In general, REE-bearing minerals are found in the following primary and secondary geological settings: carbonatites (almost exclusively LREE), pegmatites, hydrothermal veins (enriched in HREE), weathered deposits/laterites (ion adsorption clay) and placers (mostly sands of marine origin).

14.4.1 Main Rare Earth Elements Deposits in Turkey

14.4.1.1 Kızılcaören (Sivrihisar- Eskişehir) Deposit

The Kızılcaören area is the only commercial source of REE in Turkey. The Kızılcaören fluorite-barite-rare earth deposits are situated approximately 15-km southeast of the town of Beylikkahır, Eskişehir province, in northwestern Anatolia (Fig. 14.7) (Gültekin et al. 2003). According to Gültekin et al. (2003), the reserves of this deposit are 4 Mt graded at 0.3% Ce+La+Y.

The Devebağırtan Tepe deposit covering an area of 0.8 km^2 is the largest occurrence in the area (Fig. 14.7). Other economically significant deposits are Koca Devebağırtan Tepe, Yaylabaşı and Küçükhöyüklü, and there are also several smaller occurrences (Stumpfl and Kırıkoğlu 1986).

The mineralisation occurs as large veins and as cements of clasts in tectonic breccia (Kaplan 1977; Nikiforov et al. 2014). In this deposit, three main economic ore types were identified: fluorite ore, massive barite ore and bastnasite+fluorite+barite ore (Gültekin 2005). The mineral assemblage includes fluorite, barite, quartz, calcite, bastnasite, phlogopite, pyrolusite and hematite, as well as minor amounts of plagioclase feldspar, pyrite, psilomelane, braunite, monazite, fluocerite, brockite, goethite and rutile (Gültekin 2005).

The Kızılcaören fluorite-barite-rare earth element (REE) deposit occurs as epithermal veins and breccia fillings in altered Triassic metasandstones and Oligocene-Miocene pyroclastics adjacent to alkaline porphyritic trachyte and phonolite (Gültekin et al. 2003).

14.4.1.2 Çanaklı (Isparta) Deposit

The Quaternary alkaline volcanism of Gölcük, close to Isparta in southwestern Turkey, shows enrichment in the REE (Platevoet et al. 2014; Goodenough et al. 2016) and has been proposed as a possible source for heavy minerals in the nearby Çanaklı placer (AMR 2011). This resource prospect is estimated at 494 Mt at 0.07–0.08 wt.% TREO (Cox et al. 2013). The Çanaklı deposit, part of the Aksu Diamas project in Turkey and owned by AMR Mineral Metal Inc., is a potentially important European source of rare earth elements (REE) (Deady et al. 2016).

Four main geological units are present in the Çanaklı, Isparta area:

- *Allochthonous Mesozoic clastic-dominated sedimentary rocks*: These include the Kızılcadağ melange and olistostrome (mixed lithologies), limestone and clastic sediments
- *Mesozoic carbonate units:* These include massive carbonate rocks which have been overthrust by the allochthonous Mesozoic clastic-dominated sedimentary rocks
- *Late Miocene sedimentary units:* These tertiary clastic sediments thicken to the east and south in the Aksu Basin.

- *Quaternary and recent sediments*: Unconsolidated weathered tuffs, alluvial and eluvial deposits, which are present in most of the topographic depressions in the area. These units host the mineralisation of interest at the prospective sites that are currently being investigated at Çanaklı, Kuyubaşı, Çobanisa, Kuzca and Kurucaova (AMR 2011).

The deposit hosted in Quaternary sediments is situated in a topographic low in Mesozoic limestones. The heavy minerals occur in lenses and are disseminated within channelised debris flows. The mineral assemblage includes allanite, chevkinite and titanite as well as by-products of magnetite, zircon, scadinium, niobium and thorium. They are thought to have originated from repeated phreatoplininan eruptions of the Plio-Quaternary age, related to the alkaline Gölcük volcano, located approximately 20-km northwest of the deposit. It is notable that any future extraction of REE from Çanaklı would be as a by-product of magnetite production (Deady et al. 2016).

Platevoet et al. (2014) describes the Gölcük magma as having a possible carbonatitic component and a strong REE enrichment (Deady et al. 2016). This supports the possibility that Gölcük may have been a potential source of the heavy minerals found at Çanaklı.

14.4.1.3 Mortaş-Doğankuzu (Seydişehir-Konya) Deposit

The Taurides region of Turkey is host to a number of important bauxite deposits (Öztürk et al. 2002). Elevated REE mineralisation in karst bauxite deposits has been identified in multiple deposits, and it is thought that the Mortaş and the Doğankuzu bauxites in the Seydişehir region (Konya) could be potential bearers of REE.

The Mortaş bauxite deposit is one of the largest exposed in the Central Taurus (Karadağ et al. 2006). The deposit is located 25-km south of Seydişehir, Konya, in southern Turkey. The Mortaş and the Doğankuzu deposits are located along the disconformity surface between the Upper Cretaceous shallow-marine neritic limestones (Öztürk et al. 2002; Karadağ et al. 2009). A massive bauxite horizon is enriched in Al and REE. The REE are in the breccia-bearing bauxite horizons but depleted in the earthy bauxite layers (Karadağ et al. 2009).

Total mineable reserves occur in the Mortaş, Doğankuzu, Morçukur, Değirmenlik and Çatmakaya deposits, including a 32-Mt REE potential of 37,528 tonnes and an economic value of about 46.8 billion USD and a deposit in the Seydişehir-Akseki region of 85 Mt of bauxites. These deposits contain 100,000 tonnes of REE, and their economic value is about 125 billion USD (Karadağ et al. 2006).

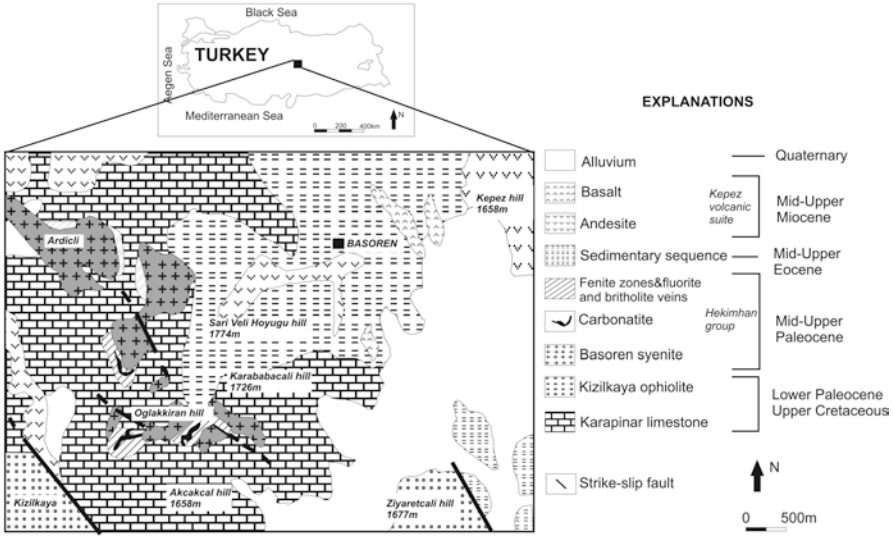

Fig. 14.8 Simplified geological map of the Basören region. (Özgenç 1999)

14.4.1.4 Sofular (Malatya) Deposit

The Sofular Th-REE deposit is located approximately midway between the provincial town of Sivas and Malatya in eastern Turkey. The collision-related Late Cretaceous alkaline igneous rocks occur in the Hasançelebi and Başören regions (Malatya) (Özgenç and İlbeyli 2009). Carbonatitic rocks found within the syenites in the Başören area (Fig. 14.8) (Özgenç and İlbeyli 2009).

In the Başören region, carbonatite-hosted fluorite deposits have been identified by Özgenç and Kibici (1994) and Özgenç (1999). According to Özgenç (1999), carbonatite represents the last stage of intrusions that were responsible for the fenitization of the syenites and deposition of small quantities of fluorite and britholite.

Th and REE minerals are thorite, britholite and bastnasite with high concentrations of Th and REE (up to 70% Th and 70% REE).

14.5 Conclusions

According to DPT (2001) and OECD (2014), it has been determined that the uranium reserves in Turkey are 9129 tonnes (U_3O_8). Uranium deposits are located in Salihli–Köprübaşı (Manisa), Fakılı–Eşme (Uşak), Küçükçavdar and Demirtepe-Söke (Aydın) and Temrezli–Sorgun (Yozgat) areas. Except for Demirtepe (Aydın) vein-type mineralisation, the other uranium deposits are sedimentary rock-hosted. A complex ore deposit consisting of REE, barite, fluorite and thorium occurs in the

Kızılcaören region, northwest of Sivrihisar (Eskişehir). The known ThO_2 reserves are 380,000 tonnes in Turkey (OECD 2014). The ore occurs as large veins and cements of tectonic breccias. Beside the Kızılcaören deposit, Çanaklı (Isparta), Mortaş-Doğankuzu (Konya) and Sofular (Malatya) are the important REE occurrences in Turkey.

References

Adur Madencilik (2015) Adur Madencilik-Temrezli Projesi websitesi [Adur mining company-Temrezli project website]. http://www.adurmadencilik.com/. Accessed 25 Nov 2015

Akçay AE, Beyazpirinç M (2017) The geological evolution of Sorgun (Yozgat)-Yıldızeli (Sivas) foreland basin, petrographic, geochemical aspects and geochronology of volcanism affecting the basin. Bull Miner Res Exp 155:1–31

Akkoyunlu A (2006) Türkiye'de Enerji Kaynakları ve Çevreye Etkileri [Energy sources and their environmental effects in Turkey]. Turkish Asian Center for Strategic Studies

Aksoy M, Alçiçek ÖN, Abiz İO, Ünal İH, Sezen E, Dümenci S, Küçük M (2013) Nevşehir-Avanos Ar-201100174, no'lu ruhsata ait 2012–2013 yılı jeoloji-jeofizik ve sondaj çalışmaları [Geology-geophysics and drilling studies for 2012–2013 on Nevşehir-Avanos Ar-201100174 License]. General Directorate of Mineral Research and Exploration Report no: 7262 (in Turkish, unpublished)

AMR Mineral Metal Inc. (2011) Technical report on the Aksu Diamas Rare Earth Element Project, Isparta district, Turkey. NI 43-101 Technical Report, pp 7–41

Anonymous (2009) World distribution of uranium deposit (UDEPO) with uranium deposit classification. IAEA, TECDOC-1629

Arslan MA, Şenol M (2012) Aydın İli Çevre Durum Raporu [Environmental report of Aydın]. T.C. Environment and Urban Ministry, Directorate of Environment and Urban Planning of Aydın Governorship, Aydın (in Turkish, unpublished)

Atabey E (1989) MTA Genel Müdürlüğü-1/100.000 ölçekli açınsama nitelikli Türkiye jeoloji haritaları serisi, Kayseri-H 19 paftası [General Directorate of Mineral Research and Exploration-1/100.000 scaled geological map of Turkey-Kayseri-H 19 sheet] (in Turkish)

Aydın İ (1990) Orta Anadolu uranyum aramaları havadan gamma ray spektrometri etüd raporu [A report of uranium gamma ray spectrometry survey of Central Anatolia]. General Directorate of Mineral Research and Exploration Report no 9146 (in Turkish, unpublished)

Bingöl E (1976) Batı Anadolu'nun jeotektonik evrimi [Geotechnical evolution of western Anatolia]. Bull Miner Res Exp 86:14–34 (in Turkish and French)

Çağatay N (1981) Türkiye'deki bazı radyoaktif mineralizasyonlar üzerinde mineralojik incelemeler [Mineralogical studies on some radioactive mineralizations in Turkey]. Bull Geol Soc Turk 24:59–65 (in Turkish with English abstract, unpublished)

Çetintürk İ (1992) Kırşehir-Kayseri-Nevşehir-Niğde Çevresi Uranyum Prospeksiyonu [Uranium prospection around Kırşehir-Kayseri-Niğde]. General Directorate of Mineral Research and Exploration Report no 9306 (in Turkish, unpublished)

Contencin G (1960) Sivrihisar Beylikahır Radyoaktif Emaresi [Radioactive signs of Sivrihisar Beylikahır]. General Directorate of Mineral Research and Exploration Report no 3167 (in Turkish, unpublished)

Cox JJ, Masun KM, Fayram T (2013) Technical report on the Aksu Diamas rare earth element and minor metals, Isparta District, Southwest Turkey, NI- 43-101 Report. RPA, Toronto

CSA Global Pty Ltd (2014) Temrezli uranium project, mineral resource estimate and QA/QC analysis report. Report No R175

Dahlkamp FJ (2009) Uranium deposits of the world: Asia. Springer, Berlin, p 478

Deady E, Goodenough K, Lacinska A, Hardy L, Shaw R (2016) REE placer deposits and alkaline volcanic: a case study from Aksu Diamas, Çanakli, Turkey. Mineral Deposits Studies Group Abstract Book, p 30

Delaloye M, Özgenç İ (1983) Petrography and age determinations of the alkaline volcanic rocks and carbonatites of Kızılcaören district; Beylikahır–Eskişehir, Turkey. Schweiz Min Petr Mitt 63:289–294

Demiröz T (1976) Eskişehir-Sivrihisar-Kızılcaören Köyü güneyi nadir toprak elementleri-Th kompleks cevher yatağının Kocadevebağırtan kesimindeki Th rezerv durumu [The Th reserve in the Kocadevebağırtan district from the complex ore beds of Th and rare earth elements of Eskişehir-Sivrihisar-Kızılcaören village]. General Directorate of Mineral Research and Exploration Report no 5566 (in Turkish, unpublished)

Doyranlı B (1978) Dünyada ve Ülkemizde Uranyum ve Toryum Rezervleri ve Nükleer Reaktör Endüstrisi [Uranium and thorium reserves and nuclear reactor industry in our country and in the World]. Eng Mach Uctea Chamb Mech Eng 22(260):5–19 (in Turkish)

DPT (1996) Nükleer Enerji Hammaddeleri-Uranyum-Toryum [Nuclear energy raw materials–uranium–thorium]. Turkish republic prime ministry state planning organization undersecretariat, Mining specialization commission-sub-commission on energy raw materials, Geothermal energy working group report DPT 2429 (in Turkish, unpublished)

DPT (2001) Nükleer Enerji Hammaddeleri Uranyum-Toryum [Nuclear energy raw materials-uranium-thorium]. Turkish republic prime ministry state planning organization under secretariat, Mining specialization commission-sub-commission on energy raw materials]. Geothermal energy working group report DPT 2587 (in Turkish, unpublished)

Dümenci S, Taka M, Karaca M (2004) Yozgat-Sorgun-Temrezli AR: 80310 ve Yozgat Şefaatli-Rızvan AR:80311 no'lu linyit sahalarının jeoloji ve sondaj raporu [Geological and drilling report of Yozgat-Sorgun-Temrezli AR: 80310 and Yozgat Şefaatli-Rızvan AR: 80311 lignite fields]. General Directorate of Mineral Research and Exploration Report no 10670 (in Turkish, unpublished)

Emsley J (2001) Nature's building blocks: an A–Z guide to the elements. Oxford University Press, Oxford

Goodenough KM, Schilling J, Jonsson E, Kalvig P, Charles N, Tuduri J, Deady EA, Sadeghi M, Schiellerup H, Müller A, Bertrand G, Arvanitidis N, Eliopoulos DG, Shaw RA, Thrane K, Keulen N (2016) Europe's rare earth element resource potential: an overview of REE metallogenetic provinces and their geodynamic setting. Ore Geol Rev 72:838–858

Gültekin AH (2005) Epithermal Kizilcaören fluorite-barite REE deposit, Eskisehir, Turkey: preliminary results. Geol Soc India 66:105–116

Gültekin AH, Örgün Y (2000) Kızılcaören (Sivrihisar-Eskişehir) yöresi Tersiyer alkali volkanitlerle ilişkili nadir toprak elementli fluorit-barit yatakları [Fluorite-barite deposits with rare earth elements associated with Tertiary alkaline volcanis in the Kızılcaören (Sivrihisar-Eskişehir) region]. Anadolu Un J Sci Technol 1(1):85–94 (in Turkish with English abstract)

Gültekin AH, Örgün Y, Suner F (2003) Geology, mineralogy and fluid inclusion data of the Kizilcaören fluorite–barite–REE deposit, Eskisehir, Turkey. Asian J Earth Sci 21:365–376

Günalay ME (1970) Eskisehir ili-Sivrihisar ilçesi-Beylikahir bucağı toryum cevheri işletme projesi [Thorium ore management project in Beylikahir village-Sivrihisar-Eskişehir]. General Directorate of Mineral Research and Exploration Report no 4179 (in Turkish, unpublished)

Kaçmaz H (2007) Manisa Salihli-Köprübaşı Uranyum zuhurunun incelenmesi [Investigation of uranium occurrences of Manisa-Salihli-Köprübaşı]. PhD thesis, DEU The Graduate School of Natural and Applied Sciences, 99 p (in Turkish, unpublished)

Kaplan H (1977) Eskisehir-Sivrihisar-Kızılcaören köyü yakın güneyi nadir toprak elementleri ve toryum kompleks cevher yatağı nihai etüdü [Final report of the rare earth elements and thorium ore complex in Eskişehir-Sivrihisar-Kızılcaören village]. General Directorate of Mineral Research and Exploration Report no 8672 (in Turkish, unpublished)

Kaplan H (1978) Nükleer Enerji Hammaddelerinin Aranması ve Arama Yöntemleri [Searching methods of nuclear energy raw materials]. J Geol Eng 6:11–26 (in Turkish with English abstract)

Kaplan H (2011) Kızılcaören Toryum/NTE yatağının keşfi üzerine, Kişisel söyleşi [On the discovery of the Kızılcaören Thorium/REE beds, personal interview]. Min Earth Sci Mag 13:52–62

Kaplan H, Uz S, Çetintürk İ (1974) Le gited'uranium de Fakili (Turquie) et saformation [The Fakili uranium deposits and its formation]. In: Formation of uranium ore deposits. International Atomic Energy Agency, Vienna, pp 453–465

Karadağ MM, Arık F, Ayhan A, Döyen A, Küpeli Ş, Zedef V (2006) Rare earth element (REE) potential of the Mortaş (Seydişehir-Konya) Bauxite deposit. 59th Geological Congress of Turkey, pp 154–156

Karadağ MM, Küpeli Ş, Arık F, Ayhan A, Zedef V, Döyen A (2009) Rare earth element (REE) geochemistry and genetic implications of the Mortaş bauxite deposit (Seydişehir/Konya – Southern Turkey). Chem Erde 69:143–159

Karayiğit Aİ, Eris E, Cicioğlu E (1996) Coal geology, chemical and petrographical characteristics, and implications for coalbed methane development of subbituminous coals from the Sorgun and Suluova Eocene basins, Turkey. In: Gayer R, Harris I (eds) Coalbed methane and coal geology, Geological Society special publication, vol 109. Geol Society, London, pp 324–338

Kupfahl HG (1954) Geological report of the Eskisehir and Sivrihisar districts. General Directorate of Mineral Research and Exploration Report no 2247 (in Turkish, unpublished)

Long KR, Van Gosen BS, Foley NK, Cordier D (2010) The principal rare earth element deposits of the United States – A summary of domestic deposits and a global perspective: U.S. Geological Survey Scientific Investigations Report 2010–5220, p 96

Marbleport (2014) Websitesi [Marbleport website]. http://www.marbleport.com/dogal-kaynaklar/81/nukleer-kaynaklar-toryum-ve-uranyum. Accessed 7 Oct 2015

Mataracıoğlu MO, Aşçı M (2008) Maden aramalarında gravite ve manyetik çözümlerin incelenmesi [Investigation of gravite and magnetic solutions in mineral explorations]. Bull App Geoss 1:46–59 (in Turkish)

MTA (1976) Köprübaşı uranyum pilot tesis çalışmaları hakkında ön rapor [Preliminary report about the Köprübaşı uranium pilot plant studies]. General Directorate of Mineral Research and Exploration Report no 5545 (in Turkish, unpublished)

MTA (2001) Geological map of Turkey: Denizli sheet, scale1:500000. MTA Publication, Ankara

MTA (2010a) Maden Tetkik ve Arama Genel Müdürlüğü websitesi [General Directorate of Mineral Research and Explorations website]. http://www.mta.gov.tr/v2.0/daire-baskanliklari/enerji/images/siteharitalar/8big.jpg. Accessed 22 Oct 2015

MTA (2010b) Maden Tetkik ve Arama Genel Müdürlüğü websitesi [General Directorate of Mineral Research and Explorations website]. http://www.mta.gov.tr/v2.0/turkiye_maden/maden_potansiyel_2010/Giresun_Madenler.pdf. Accessed 22 Oct 2015

MTA (2010c) Maden Tetkik ve Arama Genel Müdürlüğü websitesi [General Directorate of Mineral Research and Explorations website]. http://www.mta.gov.tr/v2.0/turkiye_maden/maden_potansiyel_2010/Canakkale_Madenler.pdf. Accessed 22 Oct 2015

MTA (2010d) Maden Tetkik ve Arama Genel Müdürlüğü websitesi [General Directorate of Mineral Research and Explorations website]. http://www.mta.gov.tr/v2.0/turkiye_maden/maden_potansiyel_2010/Aydin_Madenler.pdf. Accessed 22 Oct 2015

MTA (2010e) Maden Tetkik ve Arama Genel Müdürlüğü websitesi. [General Directorate of Mineral Research and Explorations website]. http://www.mta.gov.tr/v2.0/turkiye_maden/maden_potansiyel_2010/Yozgat_Madenler.pdf. Accessed 22 Oct 2015

Nikiforov AV, Öztürk H, Altuncu S, Lebedev VA (2014) Kızılcaören ore-bearing complex with carbonatites (Northwestern Anatolia, Turkey): formation time and mineralogy of rocks. Geol Ore Depos 56:35–60

OECD (1997) Uranium, resources, production and demand, A joint report by the OECD Nuclear Energy Agency and the International Atomic Energy Agency, OECD Publishing, Paris, p 397

OECD (2005) Uranium 2005: resources, production and demand. A joint report by the OECD Nuclear Energy Agency and the International Atomic Energy Agency, OECD Publishing NEA No. 6098, Paris, p 390

OECD (2014) Uranium 2014: resources, production and demand. A joint Report by the OECD Nuclear Energy Agency and the International Atomic Energy Agency, OECD Publishing NEA No. 7209, p 504

Önal G (1975) Mazıdağı fosfat cevherlerindeki uranyumdan yararlanma olanakları [Uranium utilization facilities in the Mazıdağı phosphate ores]. IV. Turkey Scientific and Technical Mining Congress, pp 517–530 (in Turkish)

Örgün N (1972) Giresun – Şebinkarahisar civarının 1971 yılı detay prospeksiyon çalışmaları ve sondajlı uranyum aramaları [Detailed prospecting studies of Giresun- Şebinkarahisar area in 1971 and investigations of the drilling uranium explorations]. General Directorate of Mineral Research and Exploration Report no 437 (in Turkish, unpublished)

Özgenç İ (1993) Kızılcaören (Sivrihisar – Eskişehir) karbotermal bastneazit-florit-barit yatağının jeolojisi ve nadir toprak element jeokimyası [Geology and REE geochemistry of carbothermal bastnaesite –fluorite – barite deposit of Kızılcaören (Sivrihisar – Eskişehir)]. Geol Bull Turk 36:1–11 (in Turkish with English abstract)

Özgenç İ (1999) Carbonatite-hosted fluorite and britholite mineralisation at Sofular area, Malatya, Turkey. In: Stanley CJ et al (eds) Mineral deposits: processes to processing. In: Proceedings of the fifth biennial SGA meeting and the tenth quadrennial IAGOD symposium, pp 663–666

Özgenç İ, İlbeyli N (2009) Geochemical constraints on petrogenesis of Late Cretaceous alkaline magmatism in East-Central Anatolia (Hasancelebi-Basören, Malatya), Turkey. Mineral Petrol 95:71–85

Özgenç İ, Kibici Y (1994) The geology and chemical–mineralogical properties of britholite veins of Basören village (Kuluncak, Malatya). Geol Bull Turk 37:77–85

Öztunalı Ö (1965) Demirtepe-Çavdar, Osmankuyu-Kisir (Çine Masifi) uranyum zuhurlarının petrografileri ve oluşumları [Petrography and formations of Demirtepe-Çavdar, Osmankuyu-Kisir (Çine Massive) uranium occurrences]. Bull Miner Res Exp 65:109–121 (In Turkish and German)

Öztürk H, Hein RJ, Hanilçi N (2002) Genesis of the Doğankuzu and Mortaş Bauxite deposits, Taurides, Turkey: separation of Al, Fe, and Mn and implications for passive margin metallogeny. Econ Geol 97:1053–1077

Platevoet B, Elitok Ö, Guillou H, Bardintzeff JM, Yagmurlu F, Nomade S, Poisson A, Deniel C, Özgür N (2014) Petrology of quaternary volcanic rocks and related plutonic xenoliths from Gölcük volcano, Isparta angle, Turkey: origin and evolution of the high-K alkaline series. Asian J Earth Sci 92:53–76

Şaşmaz A (2008) Köprübaşı (Manisa) uranyum yatağı çevresinde toprak, su ve bitki örneklerinden uranyum düzeyleri ve olası çevresel etkilerinin belirlenmesi [Determination of uranium occurrences from soil, water and plant samples and possible environmental effects around Köprübaşı (Manisa) uranium bed]. Scientific and Technical Research Council of Turkey Project no 107Y226, 82 p (in Turkish, unpublished)

Şengör AMC, Yılmaz Y (1981) Tethyan evolution of Turkey: a plate tectonic approach. Tectonophysics 75:181–241

Stumpfl EF, Kırıkoğlu MS (1986) Fluorite-barite-rare earth deposit at Kızılcaören, Turkey. Mitt Osterr Ges 78:193–200

TAEK (2015) Toryum yakıt çevrimi [Thorium fuel cycle]. Turkey Atomic Energy Agency Information Document. 80 p. (in Turkish, unpublished)

TÜSİAD (1998) 21. Yüzyıla girerken Türkiye'nin enerji stratejisinin değerlendirilmesi [Evaluation of Turkey's energy strategy while entering the 21st century]. Paper No Tüsiad T/98-12/239, 316 p (in Turkish, unpublished)

Uçakçıoğlu S (1987). Nevşehir-Gülşehir ve civarı uranyum aramaları raporu [Uranium explorations report of Nevşehir-Gülşehir]. General Directorate of Mineral Research and Exploration Report no 8453 (in Turkish, unpublished)

Uçmak F (1969) Eskişehir–Sivrihisar–Beylikahır Bölgesi toryum cevheri nihai raporu [Final report of thorium ores in Eskişehir–Sivrihisar–Beylikahır]. General Directorate of Mineral Research and Exploration Report no 343 (in Turkish, unpublished)

Ünal İH (2014) Dadag uranium deposit in Central Anatolia. International Atomic Energy Agency (IAEA), Vienna

Ünal İH (2015) Ayhan Formasyonu Kubaca Üyesi gölsel çökellerde radyoaktif element içeren birimlerin mineralojik, petrografik ve jeokimyasal incelenmesi, Dadağ Köyü Güneyi, KB Nevşehir [Mineralogical, petrographical and geochemical investigations of units containing radioactive elements in lacustrine deposits of Kubaca member of Ayhan formation]. MSc thesis, Ankara University Graduate School of Natural and Applied Sciences]. 100p (in Turkish, unpublished)

Üşümezsoy Ş (1987) The NW Anatolian Aceretionary oregeny; Western termination of Paleo Tethyan suture belt. Geol Bull Turk 30(2):53–63 (in Turkish with English abstract)

Yalçın H, Karayiğit Aİ, Cicioğlu E, Gümüşer G (1997) Sorgun (Yozgat) Eosen Kömür Baseninin, Orta Anadolu-Türkiye, tüm kayaç jeokimyası ve kil mineralojisi arasındaki ilişkiler [Relationships between clay mineralogy and whole-rock geochemistry of Sorgun (Yozgat) Eocene Coal Basin, Central Anatolia, Turkey]. VIII. National Clay Symposium. Dumlupınar University, 15–24 pp (in Turkish)

Yıldız A, Gürel A, Dursun YG (2016) Physicochemical properties and uses of Karacaören area (Nevşehir) diatomite. Bull Miner Res Exp 152:165–180

Yılmaz H (1982) Menderes Metamorfik Masifi (Türkiye), Neojen sedimanter kayaçlarındaki uranium yataklarının kökeni [Genesis of uranium deposits in Neogene sedimentary rocks, Menderes metamorphic massif; Turkey]. J Geol Eng 5:3–19 (in Turkish with English abstract)

Yörükoğlu K (2014) Hammadde olarak uranyum ve Türkiye uranyum potansiyeli [Uranium and uranium potential of Turkey as a raw material]. Arch Eng Gr Mag 75:40–42 (in Turkish)

Yüce AE (1988) Eskişehir–Beylikahır Okçu NTE'li baritli florit cevher yatağının barit ve florit yönünden değerlendirilmesi [Evaluation of the barite-fluorite-REE ore beds in Eskişehir-Beylikahır Okçu in terms of barite and fluorite]. PhD Thesis, ITU Faculty of Mining (in Turkish, unpublished)

Chapter 15
Bauxite Deposits of Turkey

Nurullah Hanilçi

Abstract The bauxite deposits of Turkey are mainly concentrated in eight provinces, six of which are located in the Anatolide–Tauride, one in the Arabian Platform and one in the Pontides. The eight regions are as follows: The diasporitic bauxite deposits of the (i) Milas–Yatağan (Muğla) region are beneath the base of the Jurassic successions and are located in a high-grade metamorphosed geological setting; (ii) The Yalvaç–Şarkikaraağaç province mainly includes boehmite occurring beneath the base of the Upper Jurassic–Cretaceous units; (iii) The non-metamorphosed Seydişehir–Akseki bauxites mainly consist of boehmite, occurring below the Santonian units; (iv) The Alanya Province bauxites mainly consist of diasporite and rare boehmite in three levels along the unconformable contact between Permian and Lower Triassic, Lower Triassic and Middle(?)–Upper Triassic, and Upper Triassic and Jurassic, respectively; (v) The Bolkardağı (Karaman) bauxites are metamorphosed and mainly consist of diasporite and rare boehmite occurring beneath the base of the Middle Jurassic units; (vi) The Tufanbeyli–Saimbeyli–Kadirli bauxites mainly include diasporite and boehmite lying below the pre-Early Permian and between the Upper Triassic to Early Jurassic units; (vii) The iron-rich bauxites in the Payas–Isahiye Province include hematite, maghemite, berthierine and diasporite between Turonian and Cenonian units; and finally, (viii) The Kokaksu (Zonguldak) province bauxites include diasporite, boehmite between the Lower Carboniferous and Lower Cretaceous units.

15.1 Introduction

Bauxite deposits can be classified genetically into three main groups: lateritic, tikhvin and karstic types (Bárdossy 1982; Bárdossy and Aleva 1990). Lateritic-type bauxites are residual deposits that are derived from underlying aluminosilicate

N. Hanilçi (✉)
Department of Geological Engineering, Avcilar Campus, İstanbul University-Cerrahpaşa, İstanbul, Turkey
e-mail: nurullah@istanbul.edu.tr

F. Pirajno et al. (eds.), *Mineral Resources of Turkey*, Modern Approaches in Solid Earth Sciences 16, https://doi.org/10.1007/978-3-030-02950-0_15

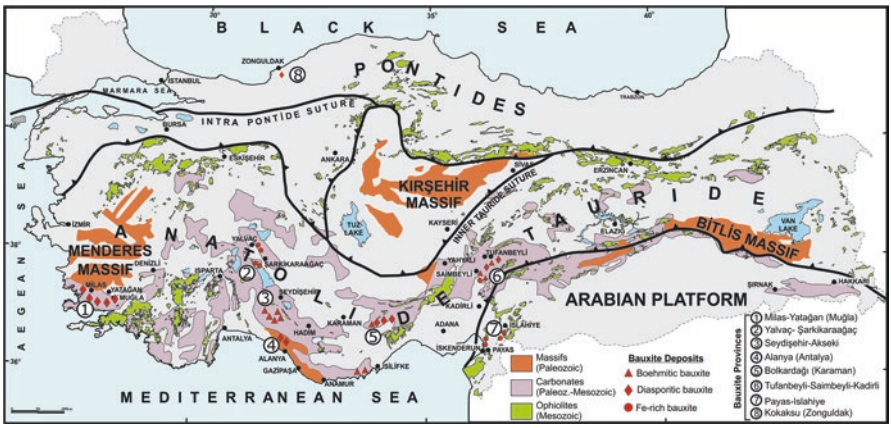

Fig. 15.1 Bauxite provinces of Turkey. (Tectonic elements modified from Okay and Tüysüz 1999; Robertson and Ustaömer 2009)

rocks and can be directly related to the underlying source rocks by their preserved textures and compositions. Tikhvin-type bauxites are detrital bauxite deposits that overlie the eroded surface of aluminosilicate rocks, and karstic-type deposits overlie karstified surfaces of carbonate rocks (Bárdossy and Aleva 1990). Karstic-type bauxites have been divided into autochthonous, para-autochthonous, allochthonous and para-allochthonous subtypes (e.g. Bárdossy 1982; Combes 1990; Combes et al. 1993; Laville 1981). In Turkey, there are mostly karstic-type and less laterite-type bauxite deposits among the main three deposit types.

The aim of this chapter is to introduce the geology, mineralogy and geochemical characteristic of Turkey's bauxite deposits situated in eight provinces. These provinces are (1) Milas–Yatağan (Muğla); (2) Yalvaç-Şarkikaraağaç; (3) Seydişehir–Akseki; (4) Alanya; (5) Bolkardağı (Karaman); (6) Tufanbeyli–Saimbeyli–Kadirli; (7) Payas–Islahiye and (8) the Kokaksu (Zonguldak) Province (Fig. 15.1).

15.2 Milas-Yatağan Province

The Milas-Yatağan bauxite province is located between the Bafa settlement (northwest of Milas) and the Muğla (Fig. 15.1). The deposits in this province occur within a marble and schist series that has undergone greenschist facies metamorphism and covers the high-grade metamorphic core complex (orthogneiss, paragneiss, schist) of the Menderes Massif (Fig. 15.2a, b). Based on the metamorphic grade and mineral paragenesis, the bauxite deposits in this province were divided by Yalçın (1987) into diasporitic bauxite (low-grade metamorphic cover units) and corundum-rich bauxite (high-grade metamorphic inner zone) (Fig. 15.2a). The age of the bauxites in this province is under debate and has been suggested as Jurassic (Yalçın 1987),

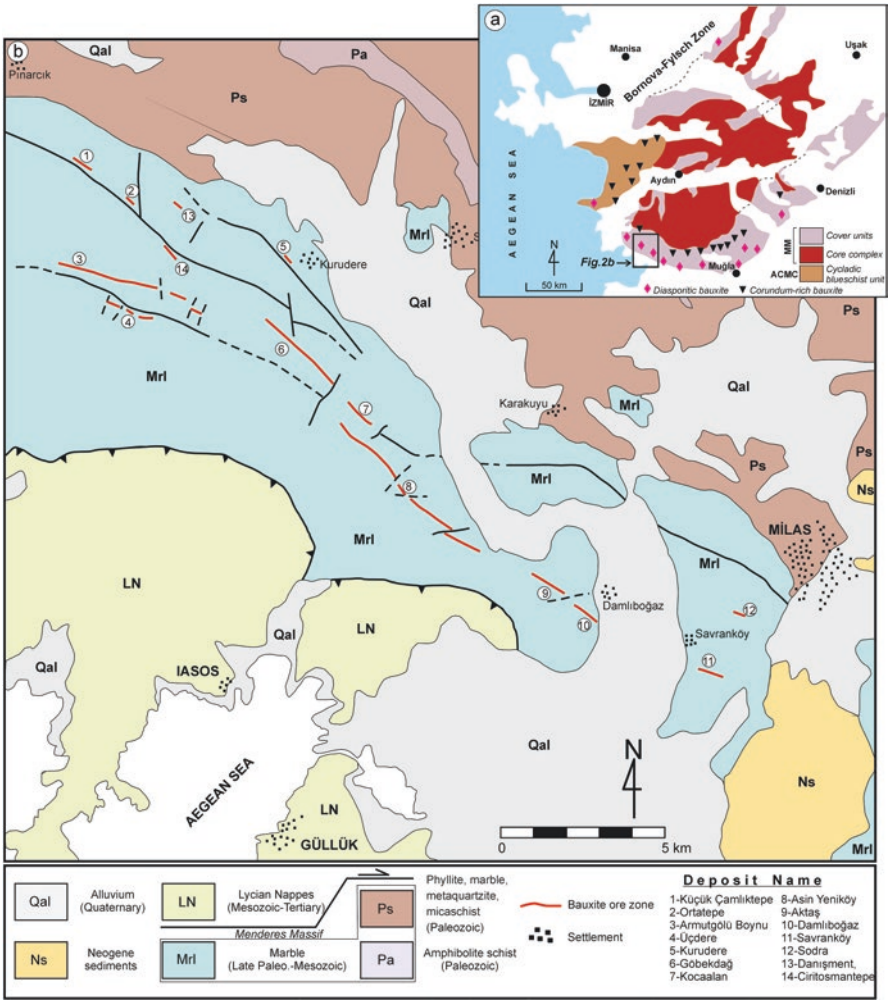

Fig. 15.2 (**a**) Geological map of the cover units and core complex of the Menderes Massif (MM), the Attic-Cycladic Metamorphic Complex (ACMC) and the locations of diasporitic and corundum-rich bauxites. (Simplified after Aydoğan and Moazzen 2012). (**b**) Geological map of the Milas region and the diasporitic bauxite zone within the cover units of the MM. (After Etibank 1975)

Upper Cretaceous (Aydoğan and Moazzen 2012; Garcia-Garmilla et al. 2004) and Upper Cretaceous-Early Paleogene (Hatipoğlu 2011).

Approximately 2 Mt of diasporitic bauxite was extracted between 1972 and 1982 by Etibank from the deposits in the Milas region from open-pit and underground mines (Hatipoğlu 2011). The mining started again in 2005, and approximately 0.5 Mt of ore has been mined through 2016.

Most of the deposits in the Milas-Yatağan province are located between Milas and Bafa Lake. The bauxite zone extends intermittently for 30 km in a N45°W direction from southeast of Milas to Bafa Lake (Fig. 15.2b). The ore zones are separated bodies or sectors due to NE–SW-oriented fault systems. The bauxite zone occurs along the unconformable contact between the white marble (footwall) and grey marble or schist (hanging wall). The bottom contact of the bauxite contains undulations, whereas the top contact is generally regular (Fig. 15.3). The ore thickness varies from place to place but is not less than 1.5 m and can reach up to 12 m. Massive, pisolitic, oolitic and leopard-type textures are common within the bauxite ore. The bauxite zone is generally oriented NW–SE and dips 45–71° to the southwest. This zone contains 14 bauxite deposits, including the Küçükçamlık Tepe, Ortatepe, Armutgölü Boynu, Üçdere, Kurudere, Göbekdağ, Kocaalan, Asin Yeniköy, Aktaş, Damlıboğaz, Savranköy, Sodra, Danişment and Ciritosmantepe (Fig. 15.2b).

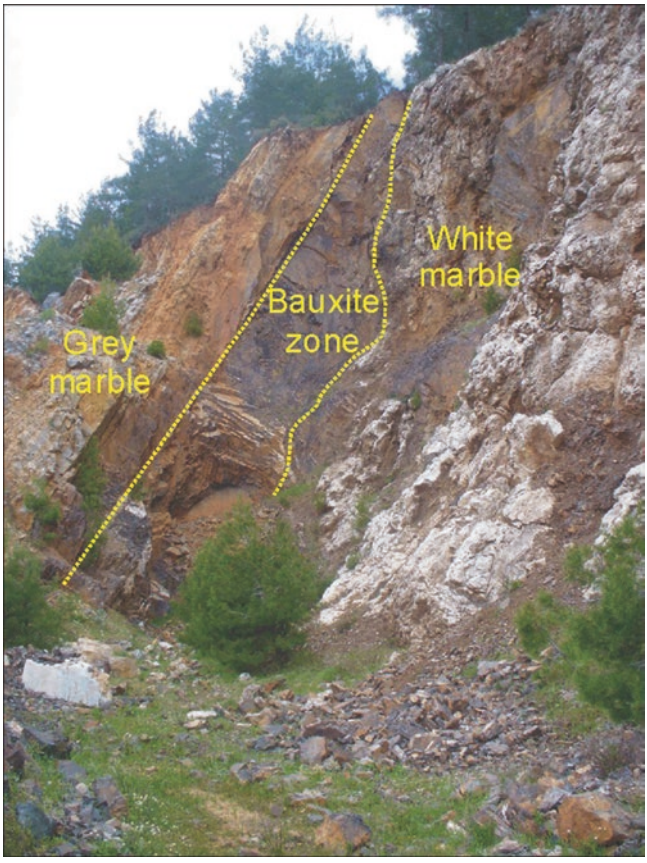

Fig. 15.3 Regular contact of the bauxite zone with the hanging wall and undulatory contact with the footwall marble (Göbekdağ deposit)

Etibank (1975, 1992) estimated the reserves and ore grade of these deposits, and some have been mined in the past (Table 15.1).

The Küçükçamlık Tepe bauxite deposit is located 67 km from the Gulluk port and approximately 3.5 km southeast of Pınarcık village (Fig. 15.2 and Table 15.1). The deposit has been mined with both open-pit and underground methods by Etibank. Currently, underground mining is being performed, especially for gem-quality diaspore (trademarked zultanite) production.

The deposit occurs within the crystallised limestone-marbles of the Menderes Massif. The hanging wall of the ore is marble, but the footwall is composed of both marbles and schists. The deposit is oriented N60–70°W and dips 69–75° SW. The ore body is approximately 350-m long and an average of 4-m thick (between 3 and 5 m). The main ore textures of the deposit are massive, pisolitic-oolitic and leopard. Etibank (1975) estimated the ore reserves at 0.73 Mt with average contents of 57% Al_2O_3, 3.6% SiO_2 and 2.7 TiO_2 (Table 15.1). Approximately 0.3 Mt of ore with an average content of 57% Al_2O_3 and 2–4% SiO_2 was mined between 2005 and 2016. Details of the ore geochemistry of this deposit are given in Table 15.1.

The Danişment bauxite deposit is located approximately 3-km southeast of the Küçükçamlık Tepe deposit (Fig. 15.2 and Table 15.1). The deposit is located 52 km from the Gulluk port. The deposit has been investigated by Etibank with trenches but has not been mined.

The ore zone is approximately 150-m long at the surface and has an average thickness of 6 m. The ore zone is oriented N55–65W and dips to the southwest at 50–65°. Etibank (1975) estimated the ore reserves at 0.56 Mt with average contents of 57% Al_2O_3, 4% SiO_2 and 2.8% TiO_2 (Table 15.1).

The Armutgölü Boynu bauxite deposit is located south of the Küçükçamlık Tepe deposit (Fig. 15.2 and Table 15.1) and is 68 km from the Gulluk port. Parts of the deposit were mined by Etibank between 1972 and 1982 in both underground and open- pit mines. The main part of the ore zone, which is 150-m long and 4-m thick, was mined with open-pit methods. The southern extension of this ore zone is approximately 100-m long and has not been mined because it is relatively thin. Etibank (1975) estimated the ore reserves at 1.45 Mt with average contents of 53% Al_2O_3, 8.7% SiO_2 and 2.7% TiO_2 (Table 15.1). Details of the ore geochemistry of this deposit are given in Table 15.2.

The Sodra bauxite deposit is the located very close to the Milas settlement (Fig. 15.2) and 23 km from the Güllük port. ETIBANK has mined approximately 4000 tonnes of ore from this deposit. The ore zone is located within the marble of the Menderes Massif. The bauxite zone is oriented E–W to N80°W and dips 40°NE. The bauxite zone is 150-m long and approximately 5.5 m thick. Etibank (1975) estimated the ore reserves at 0.23 Mt with average contents of 56% Al_2O_3, 5% SiO_2 and 2.8% TiO_2 (Table 15.1). Details of the ore geochemistry of this deposit are given in Table 15.2.

The Göbekdağ bauxite deposit is located south of the Kurudere settlement (Fig. 15.2 and Table 15.1). The bauxite zone is located along an unconformity between the white marble and grey marble (Fig. 15.4). The Göbekdağ deposit contains two different ore zones, which are located on the northeastern and south-western slopes of the Göbekdağ Hill.

Table 15.1 General features of some of the bauxite deposits in the Milas–Yatağan Province, the Bolkardağı (Karaman) Province and the Seydişehir–Akseki Province

Province name	Deposit and occurrence name	Coordinate (ED50 UTM)		Deposit type	Host rock	Age of host rock	Ore geometry	Ore mineralogy	Average ore grade (%)	Ore reserves (Mt)	Mined reserves (Mt)	References
		X	Y									
Milas-Yatağan	Küçükçamlık Tepe-Orta Tepe	547032	4141650	Karstic	RLm.,Mr.	Jurassic (?) U.Cretaceous (?)	Strata, Lensoidal, Karstic pocket	Dsp, Hem, Mnt-Cld, Qtz, Cal, Rt, Ilm, Crn, Per	57% Al_2O_3 3.6% SiO_2	0.73	0.47	Etibank (1975,1992) and Çağatay and Arman (1982); This study
	Danişment	549136	4141317	Karstic	RLm.,Mr.	Jurassic (?) U.Cretaceous (?)	Strata, Lensoidal, Karstic pocket	Dsp, Hem, Mnt-Cld, Qtz, Cal, Rt, Ilm, Crn, Per	57% Al_2O_3	0.56 4% SiO_2	n.d.	
	Armutgölü Boynu	547787	4138539	Karstic	RLm.,Mr.	Jurassic (?) U.Cretaceous (?)	Strata, Lensoidal, Karstic pocket	Dsp, Hem, Mnt-Cld, Qtz, Cal, Rt, Ilm, Crn, Per	53% Al_2O_3 8.7% SiO_2	1.45	0.13	
	Göbekdağ	553654	4135574	Karstic	RLm.,Mr.	Jurassic (?) U.Cretaceous (?)	Strata, Lensoidal, Karstic pocket	Dsp, Hem, Mnt-Cld, Qtz,Cal, Rt, Ilm, Crn, Per	50% Al_2O_3 14.8% SiO_2	2.59	0.4	
	Aktaş	561040	4129519	Karstic	RLm, Cshs	Jurassic (?) U.Cretaceous (?)	Strata, Lensoidal, Karstic pocket	Dsp, Hem, Mnt-Cld, Qtz, Cal, Rt, Ilm, Crn, Per	54% Al_2O_3 8.6% SiO_2	3.46	n.p.	
	Damlıboğaz	562908	4128368	Karstic	RLm.,Mr.	Jurassic (?) U.Cretaceous (?)	Strata, Lensoidal, Karstic pocket	Dsp, Hem, Mnt-Cld, Qtz, Cal, Rt, Ilm, Crn, Per	51% Al_2O_3 10.4% SiO_2	1.03	0.18	

	Kurudere	553011	4139283	Karstic	RLm.,Mr.	Jurassic (?) U.Cretaceous (?)	Strata, Lensoidal, Karstic pocket	Dsp, Hem, Mnt-Cld, Qtz, Cal, Rt, Ilm, Crn, Per	54% Al_2O_3 7.9% SiO_2	0.13	np.	
	Kocaalan	555972	4133936	Karstic	RLm.,Mr.	Jurassic (?) U.Cretaceous (?)	Strata, Lensoidal, Karstic pocket	Dsp, Hem, Mnt-Cld, Qtz, Cal, Rt, Ilm, Crn, Per	54% Al_2O_3 7% SiO_2	0.79	0.036	
	Üçdere	548245	4137450	Karstic	RLm.,Mr.	Jurassic (?) U.Cretaceous (?)	Strata, Lensoidal, Karstic pocket	Dsp, Hem, Mnt-Cld, Qtz, Cal, Rt, Ilm, Crn, Per	51% Al_2O_3 11.5% SiO_2	0.06	n.p.	
	Cirit Osmantepe	549502	4139393	Karstic	RLm.,Mr.	Jurassic (?) U.Cretaceous (?)	Strata, Lensoidal, Karstic pocket	Dsp, Hem, Mnt-Cld, Qtz, Cal, Rt, Ilm, Crn, Per	57% Al_2O_3 4% SiO_2	0.22	n.p.	
	Asinyeniköy	559035	4130126	Karstic	RLm.,Mr.	Jurassic (?) U.Cretaceous (?)	Strata, Lensoidal, Karstic pocket	Dsp, Hem, Mnt-Cld, Qtz, Cal, Rt, Ilm, Crn, Per	50% Al_2O_3 10.5% SiO_2	3.61	n.d.	
	Sodra	567101	4128384	Karstic	RLm.,Mr.	Jurassic (?) U.Cretaceous (?)	Strata, Lensoidal, Karstic pocket	Dsp, Hem, Mnt-Cld, Qtz, Cal, Rt, Ilm, Crn, Per	56% Al_2O_3 5% SiO_2	0.23	n.p.	
	Savran	565758	4126765	Karstic	RLm.,Mr.	Jurassic (?) U.Cretaceous (?)	Strata, Lensoidal, Karstic pocket	Dsp, Hem, Mnt-Cld, Qtz, Cal, Rt, Ilm, Crn, Per	54% Al_2O_3 6.2% SiO_2	0.40	0.37	

(continued)

Table 15.1 (continued)

Province name	Deposit and occurrence name	Coordinate (ED50 UTM)		Deposit type	Host rock	Age of host rock	Ore geometry	Ore mineralogy	Average ore grade (%)	Ore reserves (Mt)	Mined reserves (Mt)	References
		X	Y									
Bolkardağı (Karaman)	Camızalanı Karakuyu	592000	4117000	Karstic, Lateritic	RLm, Cshs	Triassic	Strata, Karstic pocket	Dsp, Hem, Chl, Mca, Goe, Kln, Dol, Cal, Ant, Qzt, Py	43% Al_2O_3 21% SiO_2	n.d	n.p.	Hanilçi (2013), This study
	Bolkardede Tepe	592935	4114503	Karstic	RDol, RLm	Triassic	Karstic pocket	Dsp, Hem, Goe, Mca, Py, Ant, Pyr, Tlc, Chl	56% Al_2O_3 5% SiO_2	–	0.03	
	Karataş	594035	4112420	Karstic, Lateritic	RLm	Triassic	Karstic pocket, Strata	Dsp, Hem, Ant	56% Al_2O_3 1–5% SiO_2	2	0.5	
	Arpaçukuru	607797	4113520	Karstic	RLm	M. Triassic	Karstic pocket	Dsp, Hem, Goe, Prl, Mca, Ant, Kln	5% Al_2O_3 7.5% SiO_2	1	0.8	
	Kızıldağ Zone	614712	4111745	Lateritic	Slate	L. Triassic	Lateritic			–	–	
	Baharpınarı	588000	4112000	Karstic	Recrystallized dolomitic-limestone	U. Triassic	Karstic pocket	Dsp, Hem, Kln, Chl, Goe, Mca, Bhm, Ant	56% Al_2O_3 2–6% SiO_2	–	0.5	
	Göztaşı	579802	4104624	Karstic	RLm-RDol	M. Triassic	Karstic pocket	Dsp, Hem, Ant, Chl, Mca	58% Al_2O_3 3% SiO_2	0.02	0.12	
	Kavaközü	579615	4102848	Karstic	RLm-RDol	M. Triassic	Karstic pocket	Dsp, Hem, Goe, Ant, Chl, Mca, Qzt	56% Al_2O_3 1–3% SiO_2	0.09	0.010	

	Devebağırtan	580500	4105300	Karstic	RLm-RDol	M. Triassic	Karstic pocket	Dsp, Hem, Ant, Chl, Mca	55–58% Al_2O_3 3–5% SiO_2		–	
	Kemikli Tepe	588220	4109990	Karstic, Lateritic	Phillite, Meta-shale, RLm	U. Triassic	Strata, Karstic pocket	Dsp, Hem, Py, Ab	58% Al_2O_3 3.5% SiO_2	n.d.	n.d.	
	Sarıtay	571868	4096550	Karstic	Limestone	Triassic	Lensoidal	Dsp, Bhm, Hem, Ant, Goe, Chl, Mca, Kln, Qzt	25–56% Al_2O_3 2–30% SiO_2	0.12	n.p.	
	Öşün	620660	4109184	Karstic	Limestone	Permian	Karstic pocket	Bhm, Dsp, Hem, Kln, Chl, Goe, Ant, Qzt, Mca	53% Al_2O_3 7% SiO_2	0.5	0.03	
Seydişehir-Akseki	Mortaş	401000	4127700	Karstic	Limestone	U. Cretaceous	Karstic pocket	Bhm>>Dsp, Hem, Ant, Py, Kln	57% Al_2O_3, 9.2% SiO_2	10.9	9.1	Eti Alüminyum A.Ş. (personal communucation in 2016), This study
	Doğankuzu	401250	4126250	Karstic	Limestone	U. Cretaceous	Karstic pocket, Lensoidal	Bhm>>Dsp, Hem, Ant, Py, Kln	58% Al_2O_3 7% SiO_2	14.9	9.1	Eti Alüminyum A.Ş. (personal communucation in 2016), This study
	Değirmenlik	389560	4124649	Karstic	Limestone	U. Cretaceous	Karstic pocket	Bhm>>Dsp, Hem, Ant, Py, Mrc, Kln	57% Al_2O_3 6.6% SiO_2	11.7	n.p.	Eti Alüminyum A.Ş. (personal communucation in 2016), This study

(continued)

Table 15.1 (continued)

Province name	Deposit and occurrence name	Coordinate (ED50 UTM)		Deposit type	Host rock	Age of host rock	Ore geometry	Ore mineralogy	Average ore grade (%)	Ore reserves (Mt)	Mined reserves (Mt)	References
		X	Y									
	Arvana	410650	4123580	Karstic	Limestone, Fylish-limestone	Mesozoic, Senozoic	Lensoidal	Dsp>>Gbs, Ant, Py	58% Al_2O_3 5.4% SiO_2	0.63[a]	n.d.	Eti Alüminyum A.Ş. (personal communucation in 2016)
	Morçukur	396100	4135250	Karstic	Limestone	U. Cretaceous	Karstic pocket	Bhm>>Dsp, Hem, Goe, Ant, Py, Kln, Qzt, Crs	53% Al_2O_3 11.3% SiO_2 1.8% CaO	6.18[a]	n.d.	Eti Alüminyum A.Ş. (personal communucation in 2016)

Ab Albite, *Ant* Anatas, *Bhm* Boehmite, *Cal* Calcite, *Chl* Chlorite, *Cld* Chloritoid, *Crn* Corundum, *Crs* Cristobalite, *Cshs* Chalk-schist, *Dsp* Diaspore, *Goe* Goethite, *Hem* Hematite, *Ilm* Ilmenite, *Kln* Kaolinite, *Mag* Magnetitie, *Mca* Mica, *Mr* Marble, *Mrc* Marcasite, *n.d.* No data, *n.p.* No production, *Per* Periclase, *Prl* Pyrophillite, *Py* Pyrite, *Qtz* Quartz, *RDol* Recrystallised dolomite, *RLm* Recrystallized limestone, *Rt* Rutile, *Tlc* Talc

[a]The amount of reserves remaining after production

Table 15.2 The mean values of major, trace, and rare earth elements (REEs) of some bauxite deposits of Turkey

Province		**Milas–Yatağan**								**Seydişehir–Akseki**			**Sarkikaraağaç**	
TSU		**MM**								**GYD**				
Deposits		**GB**	**SD**	**SV**	**AK**	**AR**	**KC**	**DM**	**AS**	**MR**	**DK**	**DG**	**KR**	**YS**
		(n = 1)	*(n = 1)*	*(n = 1)*	*(n = 1)*	*(n = 1)*	*(n = 1)*	*(n = 1)*	*(n = 1)*	*(n = 1)*	*(n = 1)*	*(n = 1)*	*(n = 2)*	*(n = 2)*
Major oxides (%)	SiO_2	18.08	8.47	3.4	7.45	1.28	2.47	10.99	3.81	8.91	5.1	3.57	12.185	11.265
	Al_2O_3	40.05	54.29	59.93	53.06	57.79	61.04	51.16	57.72	56.89	59.33	60.33	34.77	12.9
	Fe_2O_3	28.69	22.98	18.08	24.79	25.19	20.43	22.16	24.11	17.31	19.29	19.83	36.71	55.735
	MgO	0.79	0.55	0.18	0.23	0.1	0.14	0.32	0.12	0.15	0.16	0.32	0.185	0.97
	CaO	0.24	0.13	2.85	0.07	0.54	0.45	0.59	0.03	0.13	0.1	0.12	0.19	0.305
	Na_2O	0.11	0.09	0.02	0.06	<0.01	0.02	0.09	0.01	0.03	0.02	0.02	0.035	0.03
	K_2O	2.36	0.53	0.08	1.25	0.01	0.06	1.73	0.1	0.22	0.2	0.02	0.06	0.19
	TiO_2	1.87	2.52	2.31	2.61	2.52	2.82	2.53	2.72	2.52	2.54	2.48	5.075	0.53
	MnO	0.07	0.11	0.13	0.04	0.2	0.06	0.06	0.07	<0.01	<0.01	<0.01	0.38	12.485
	P_2O_5	0.06	0.11	0.03	0.04	0.11	0.11	0.09	0.05	<0.01	<0.01	<0.01	0.12	0.03
	LOI	7.1	9.7	12.6	10	11.8	11.8	9.9	10.9	13.6	13	13	9.95	5.3
	Total	**99.42**	**99.48**	**99.61**	**99.6**	**99.54**	**99.4**	**99.62**	**99.64**	**99.76**	**99.74**	**99.69**	**99.66**	**99.74**
Trace elements (ppm)	Ba	279	95	27	149	7	15	237	28	36	36	44	64.5	313
	Rb	99.8	30.6	3.8	59.3	1	2.9	84	4.9	11.8	6.9	1.2	1	4.55
	Sr	30.6	78.5	51.8	54.6	79.6	42	82.6	61	13.4	17.6	15.7	264.15	104.95
	Th	48.8	44.4	44.3	44.3	51	52.6	45	49	47.8	51.1	53.6	5.35	8.9
	U	6.9	6.1	6.7	7.7	7.5	8.1	6.6	7.8	6	7.2	6.6	1.85	4.25
	V	428	286	403	342	303	336	246	315	241	277	344	665	77
	Zr	348	457.8	453.4	477.7	503.2	545.6	465.5	525.8	464.1	500.6	500.9	319.8	114.6
	Y	190.1	273.4	77	182.8	145.6	355.4	160.1	110.2	49.7	32.2	101.2	13.7	30.2
	Nb	33.1	43.8	40.7	45.7	46.3	53.9	44.4	49.7	43.2	46.1	45.4	35.6	10.35
	Ga	47.1	56.8	64.6	55.7	61.2	67.9	53.6	62.1	50.9	51.4	51.1	46.7	28

(continued)

Table 15.2 (continued)

Province		**Milas–Yatağan**								**Seydişehir–Akseki**			**Sarkikaraağaç**	
TSU		**MM**								**GYD**				
Deposits		**GB**	**SD**	**SV**	**AK**	**AR**	**KC**	**DM**	**AS**	**MR**	**DK**	**DG**	**KR**	**YS**
		(n = 1)	*(n = 1)*	*(n = 1)*	*(n = 1)*	*(n = 1)*	*(n = 1)*	*(n = 1)*	*(n = 1)*	*(n = 1)*	*(n = 1)*	*(n = 1)*	*(n = 2)*	*(n = 2)*
	Hf	9.9	12.7	13.1	13.5	14.5	15.1	13.8	14.9	13.6	14	14.4	8.45	3.05
	Ta	2.3	3.3	3.1	3.5	3.3	3.8	3.3	3.5	3.5	3.3	3.4	2.35	0.75
	Mo	0.3	0.2	2.1	0.5	0.4	0.2	0.4	0.5	7.7	17.1	3.9	1.35	3.2
	Cu	13.1	10.7	75	6.6	36.5	39.1	5.5	41.6	3.3	4.6	3.4	267.85	35.25
	Pb	20.7	27.8	20.1	37	104.4	28.1	13.6	23.4	57.5	46.4	55.1	10.75	197.7
	Zn	76	41	51	27	23	15	33	35	7	7	11	77	328.5
	Ni	33.2	93.8	42.3	46.5	60.9	38.1	43.4	47.4	66.2	58.4	112.7	38.8	78.85
	Cr	650	266	424	417	314	554	212	225	287	342	520	506	51
Rare earth elements (REE. ppm)	La	180.8	321.1	102.4	144.7	699.5	530.3	238.6	146.4	39.5	15.5	75.9	11.75	39.15
	Ce	360.4	291	278	242	388	393.8	280.9	323	191.6	188.1	244	18.4	83.5
	Pr	41.74	68.35	19.31	27.95	69.49	75.53	47.49	27.28	10.56	3.6	18.24	2.375	10.4
	Nd	175.2	283.4	69.8	107.1	194.6	291.6	169.6	97.7	38	12.5	71.1	8.55	39.8
	Sm	38.26	46.23	11.81	22.44	28.43	50.75	26.45	17.58	8.69	3.07	15.85	1.62	9.11
	Eu	7.38	8.66	2.22	4.76	5.91	10.61	5.69	3.42	1.83	0.7	3.59	0.555	2.865
	Gd	32.16	40.79	9.68	22.26	24.95	49.16	24.31	15.73	7.8	3.7	18.34	2.02	8.13
	Tb	4.01	6.56	1.5	3.45	4.07	7.08	3.91	2.56	1.54	0.73	3.06	0.405	1.245
	Dy	22.04	40.33	10.13	21.39	24.18	42.99	23.72	16.09	10.68	5.27	19.55	2.66	7.045
	Ho	4.56	8.43	2.29	4.54	5	9.43	4.86	3.56	2.17	1.2	4.09	0.535	1.32
	Er	13.54	25.56	7.83	13.45	14.46	27.5	14.7	10.81	6.95	3.77	11.46	1.55	3.47
	Tm	1.91	3.85	1.27	1.98	2.34	3.98	2.15	1.72	1.16	0.59	1.72	0.22	0.515
	Yb	12.28	23.55	8.74	12.8	16.38	24.35	13.54	11.19	8.07	4.13	10.68	1.34	3.245
	Lu	1.87	3.68	1.41	1.9	2.56	3.81	2.08	1.81	1.26	0.68	1.55	0.21	0.465
	ΣREE	**896.15**	**1171.49**	**526.39**	**630.72**	**1479.87**	**1520.89**	**858**	**678.85**	**329.81**	**243.54**	**499.13**	**52.19**	**210.26**

Province		Kokaksu	Bolkardağı bauxite									Payas		
TSU		**IZ**	**BU**			**NTU**			**AU**			**AA**		
Deposits		**KO**	**CA**	**KT**	**KK**	**BA**	**KD**	**BP**	**KM**	**AC**	**OS**	**PY-I**	**PY-II**	**PSY**
		(n = 1)	*(n = 5)*	*(n = 1)*	*(n = 1)*	*(n = 2)*	*(n = 3)*	*(n = 5)*	*(n = 2)*	*(n = 4)*	*(n = 4)*	*(n = 2)*	*(n = 2)*	*(n = 1)*
Major oxides (%)	SiO_2	5.64	21.2	1.2	0.9	3.1	9.6	15.7	3.5	11.1	12.6	32.06	30.405	15.94
	Al_2O_3	52.19	43	58.8	76.2	55.2	49.7	50.8	57.9	55.1	60.1	28.05	28.05	14.32
	Fe_2O_3	26.59	21.6	25.1	0.8	27.1	26.5	16.7	22.9	17.9	10	23.99	23.665	60.02
	MgO	0.26	0.5	0.1	0.1	0.2	0.4	0.5	0.1	0.2	0.1	0.235	0.175	0.2
	CaO	0.05	0.1	0	0.7	0.1	0.1	0.1	0.1	0.1	0.1	0.35	0.395	0.23
	Na_2O	0.02	1.2	0	0	0	0.1	0.4	0.1	0.3	0.5	1.07	0.21	0.17
	K_2O	0.2	0.8	0	0	0.1	0.2	1.7	0	0.4	0.1	1.215	0.385	0.13
	TiO_2	2.91	2.1	3	4.1	2.9	2.6	2.3	2.9	2.8	2.9	3.805	4.27	2.03
	MnO	0.01	0	0.1	0	0	0.1	0	0.1	0	0	0.07	0.025	0.07
	P_2O_5	0.01	0	0	0.1	0	0.1	0	0	0	0.1	0.165	0.53	0.27
	LOI	11.7	9.1	11.3	16.6	10.7	8.1	11.3	11.7	11.2	13.1	8.7	11.3	6.2
	Total	**99.58**	**99.6**	**99.6**	**99.5**	**99.6**	**97.6**	**99.6**	**99.4**	**99**	**99.7**	**99.71**	**99.41**	**99.58**
Trace elements (ppm)	Ba	71	55.2	15	16	23	55	81.4	24	50.3	25.8	46.5	55.5	32
	Rb	12.1	27.6	0.5	1.2	5.6	7.9	55.7	1.1	11.8	3.9	22.6	8.8	3.6
	Sr	74.7	53.1	30.7	52.5	30.4	40.3	65.8	56.2	75.9	60.6	187.15	2708.55	157.7
	Th	59.5	38.3	47.5	34.3	53.1	45.6	37.8	47.7	57.8	56.9	6.35	5.7	4.3
	U	17.9	11.4	9.9	36.3	10.4	20.6	8.4	15.6	8	11.1	3.4	2.05	6.7
	V	519	748.2	435	961	380.5	579	379.8	501	252.5	184.8	263.5	345	133
	Zr	897.4	412.4	611.7	752.4	651.6	619.6	525.9	612.1	700.8	591.1	243.05	278.3	130.4
	Y	61.2	75	78.2	72.8	123.2	87.4	126.2	191.5	56.7	68.8	37.2	30.35	206.2
	Nb	88.2	45.8	71.5	89.6	65.7	74.6	56.5	71	61.1	67.5	28.35	40.75	17.5
	Ga	73.8	55.9	70.4	96.3	63.9	61.8	58.9	71.1	59.3	80.9	29.8	42.75	11.4
	Hf	24.3	12	18.1	23.5	18.6	17.5	15.1	16.9	20.6	17.4	6.75	7.7	3.7
	Ta	5.7	3.2	5	6	4.5	5	4.2	5	4.8	4.5	1.7	2.65	1

(continued)

Table 15.2 (continued)

Province		**Kokaksu**	**Bolkardağı bauxite**								**Payas**		
TSU		**IZ**	**BU**			**NTU**			**AU**			**AA**		
Deposits		**KO**	**CA**	**KT**	**KK**	**BA**	**KD**	**BP**	**KM**	**AC**	**OS**	**PY-I**	**PY-II**	**PSY**
		(n = 1)	*(n = 5)*	*(n = 1)*	*(n = 1)*	*(n = 2)*	*(n = 3)*	*(n = 5)*	*(n = 2)*	*(n = 4)*	*(n = 4)*	*(n = 2)*	*(n = 2)*	*(n = 1)*
	Mo	4.5	1.5	1.1	0.2	0.7	1.1	2.1	0.9	2.4	1	2.2	1.15	2.4
	Cu	29	61.6	26.9	8.5	8.8	18.2	48.2	13.1	158.8	63.5	76.3	12.45	21.7
	Pb	84.6	42.2	53.9	7.8	72.7	17.2	39.5	61.3	17.8	42.9	5.45	2.55	7.9
	Zn	57	21.6	34	6	28	50.3	102.6	97	60	12.8	68.5	90	314
	Ni	56.7	154.6	31.9	6.2	74.1	73.6	108.7	83.9	44.2	62.9	214.8	155.45	439
	Cr	403	346	250	520	570	490	304	285	227.5	728	311	290	260
Rare earth elements (REE. ppm)	La	30.4	88.1	90.3	460.7	66.5	146	107.6	337.1	75.8	35.8	34.7	34.2	56.3
	Ce	154.2	191.5	310.2	248.3	265.1	265.6	233.5	635.7	240.5	159	50.95	77.4	56.5
	Pr	5.89	21.1	20.5	80.5	16.1	34.7	24.7	91.8	15.5	7.1	7.53	10.69	10.15
	Nd	20.1	78.1	72.5	288.7	56.7	126.2	88.1	376.1	59.8	26	30.25	50.25	48.5
	Sm	4.42	16.3	14.7	44.1	12.4	22.8	17.2	71.9	10.5	5.2	7.415	11.76	16.24
	Eu	1.03	3.6	3.1	8.9	2.7	4.6	3.8	14.8	1.7	1.2	2.36	4.11	6.1
	Gd	5.85	15.8	14.3	36.4	13.7	21.2	17.9	65.2	8.3	6.4	7.61	16.27	25.63
	Tb	1.3	2.6	2.5	4.7	2.8	3.4	3.2	8	1.4	1.4	1.21	2.68	4.19
	Dy	9.44	15	15.7	24.1	20.1	17.9	19.6	42.2	9	9.6	7.025	12.305	26.27
	Ho	2.13	3	3.1	4.8	4.6	3.6	4.2	7.2	2.1	2.3	1.41	1.665	5.72
	Er	6.41	8.6	10	14.2	14.3	10	12.5	19.2	6.6	7.6	3.865	3.35	15.77
	Tm	0.98	1.4	1.6	2.5	2.3	1.6	2	2.9	1.1	1.3	0.565	0.43	2.1
	Yb	6.04	8.5	11	17.5	14.4	9.8	12.2	18.3	7.7	8.6	3.55	2.635	12.21
	Lu	0.91	1.3	1.6	2.8	2.2	1.5	1.9	2.7	1.3	1.3	0.535	0.36	1.85
	ΣREE	**249.1**	**454.8**	**570.7**	**1238.1**	**493.9**	**668.9**	**548.3**	**1693.1**	**441.2**	**273**	**158.975**	**228.105**	**287.53**

TSU Tectono-stratigraphic Unit, *MM* Menderes Massif, *GYD* Geyikdağı Unit, *IZ* Istanbl Zone, *BU* Bolkardağı Unit, *NTU* Namrun Tectonic Unit, *AU* Aladağ Unit, *AA* Arabian Autochthon, *CA* Camızalanı bauxite zone, *KT* Karataş, *KD* Kızıldağ bauxite zone, *KM* Kemikli Tepe, *KK* Karakuyu bauxite zone, *BA* Boluardıç, *BP* Baharpınarı, *AC* Arpaçukururu, *OS* Öşün, *GB* Göbekdağ, *SD* Sodra, *SV* Savran, *AK* Aktaş, *AR* Armtgölü Boynu, *KC* Küçükçamlık, *DM* Damlıboğaz, *AS* Asinyeniköy, *MR* Mortaş, *DK* Doğankuzu, *DG* Değirmenlik, *KR* Kireli, *YS* Yassıbel, *KO* Kokaksu, *PY-I* Pancarlık Yayla-I, *PY-II* Pancarlık Yayla-II, *PSY* Paşanınereği Yayla

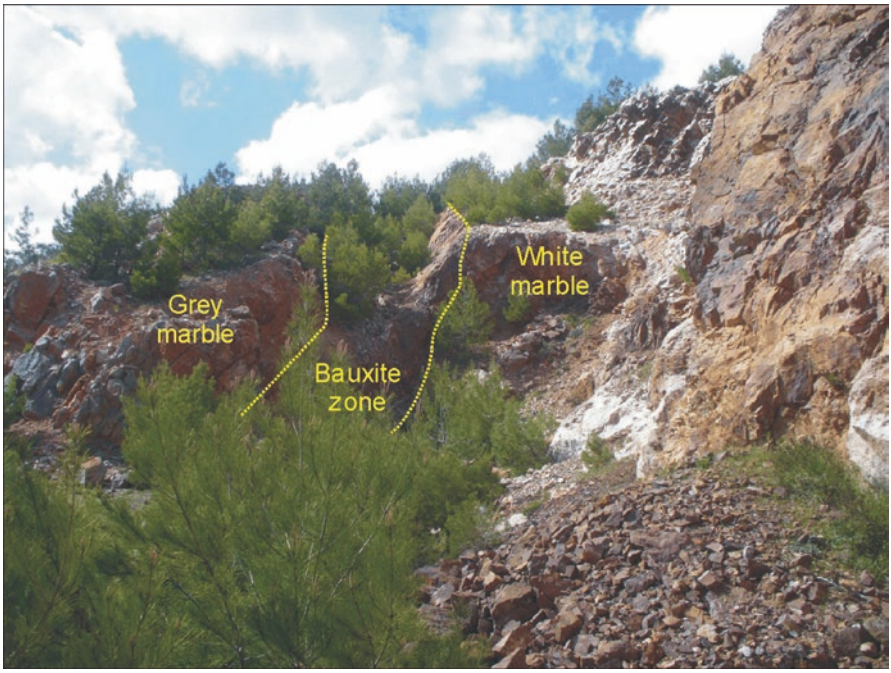

Fig. 15.4 The ore zone in Göbekdağ along the contact between white marble (footwall) and grey marble (hanging wall)

The southwestern ore zone was mined by Etibank as an open-pit mine in the 1970s. This ore zone is oriented N50–60°W and dips 45–71°SW. The ore zone intermittently continues for 3 km (Fig. 15.2), and the thickness varies between 1 and 4 m. The ore reserves of the Göbekdağ SW ore zone were estimated at 2.59 Mt with average contents of 50% Al_2O_3, 14.8% SiO_2 and 2.8% TiO_2 (Table 15.1) by Etibank (1975). Details of the ore geochemistry of this deposit are given in Table 15.2.

The northeastern ore zone is oriented N55–60°W with a dip of 40–60°SW. The ore zone is approximately 650-m long and between 1- and 3-m thick. This ore zone has not been mined yet. The ore reserves of the northeast zone were estimated at 1.5 Mt with average contents of 55% Al_2O_3, 9.6% SiO_2 and 2.9% TiO_2 by *Demireller Mining Co.* (2008).

The Kocaalan bauxite deposit is located 5-km west of the Karakuyu settlement (Fig. 15.2, Table 15.1). The ore zone is covered by olive trees and farmland, so the boundary between the bauxite and wall rock is not clearly exposed (Fig. 15.5). The bauxite zone extends for approximately 1600 m with an orientation of N45–60°E and a dip of 50–70°NE. The ore thickness varies between 1 and 6 m. Etibank (1975) estimated the ore reserves at 0.79 Mt with average contents of 54% Al_2O_3 and 7% SiO_2 (Table 15.1).

The Aktaş bauxite deposit is located 8-km west of Milas (Fig. 15.2 and Table 15.1). The bauxite is located along an unconformity between the white marble

Fig. 15.5 The Kocaalan bauxite ore zone, which is covered by olive trees and farmland

(footwall) and grey marble (hanging wall). The bauxite zone is brownish and greenish-black in colour. The ore zone extends for approximately 1.2 km, is oriented N73–78°W and dips 45–48°SW. The ore thickness varies between 0.5 and 9.5 m (Etibank 1992). Etibank (1992) estimated the ore reserves at 3.46 Mt with average contents of 54% Al_2O_3, 8.6% SiO_2 and 2.4% TiO_2 (Table 15.1). Details of the ore geochemistry of this deposit are given in Table 15.2.

15.3 Yalvaç-Şarkikaraağaç Province

The Yalvaç–Şarkıkaraağaç bauxite province is located between Kireli village (Hüyük–Konya) and Hacıalabaz Dağı (Yalvaç) and extends NW for approximately 60 km (Fig. 15.1). MTA (2009) estimated proven plus indicated ore reserves at 195 Mt for this province. The province is divided into southeastern (Fig. 15.6) and northwestern (Fig. 15.7) parts.

The southeastern part of this province extends approximately 17-km north from Boztepe Hill, which is east of Beyşehir Lake, to the Çaltı settlement (Fig. 15.6). The northwestern part extends approximately 25 km from Çarıksaraylar to Yalvaç (Fig. 15.7). The important bauxite zones in the northwestern part are the Kaletepe, Gucurtaşıtepe, Taşlıtepe, Düzkaya, Hatıbınağılıtepe, Ortataştepe, İslikayatepe (Öncel 1995) and Çarıksaraylar zones (Bozkır 2007; Fig. 15.7).

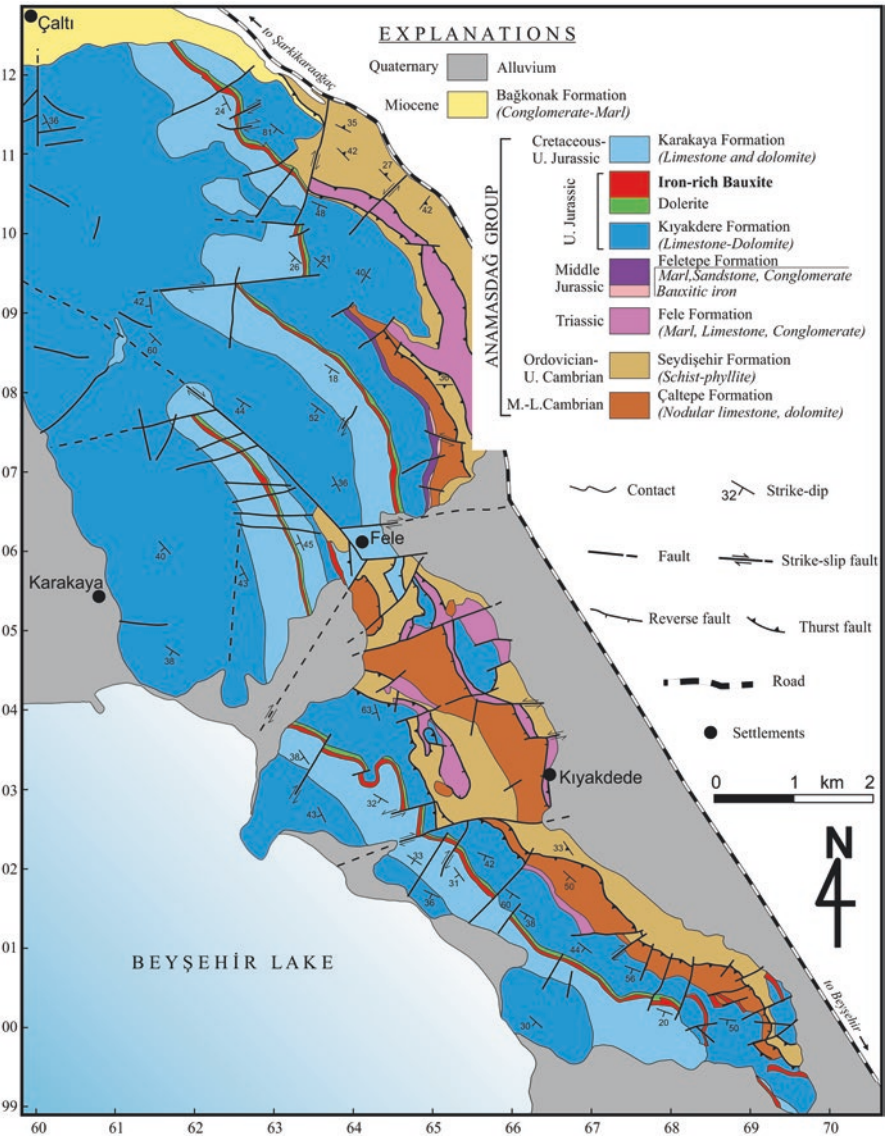

Fig. 15.6 Geological map of the southeastern part of the Yalvaç–Şarkikaraağaç bauxite province. (Simplified after Ayhan and Karadağ 1985)

The Yalvaç-Şarkikaraağaç bauxites formed on mafic lateritised Jurassic volcanic rocks (dolerite-basalt) (Ayhan and Karadağ 1985; Öncel 1995; Bozkır 2007). The dolerite-basalt overlies Middle Jurassic limestone and dolomites of the Kıyakdede Fm and is overlain by limestone and dolomites of the Karayaka Fm (Ayhan and Karadağ 1985). The thickness of the dolerite-basalt varies between 10 and 150 m.

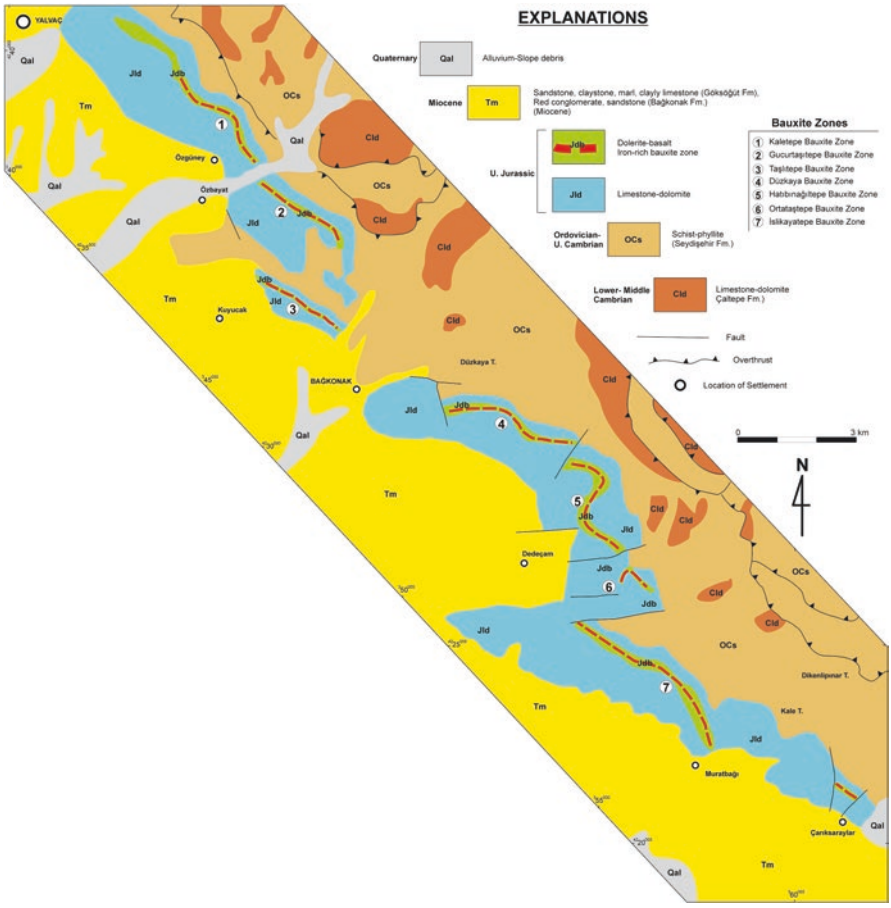

Fig. 15.7 Geological map of the area between Yalvaç and Çarıksaraylar. (Simplified after Umut 2009) and the lateritic bauxite zone that developed on the dolerite-basalt. (Bauxite zone is simplified after Öncel 1995; Bozkır 2007)

The bauxite zone in the Yalvaç-Şarkikaraağaç province varies in thickness from 1 to 10 m. While the bottom of the ore is irregular due to the varying depths of the lateritisation, the top contact is concordant with the hanging wall dolerite-basalt or limestone (Fig. 15.8). The ore displays massive, oolitic and pisolitic textures. The bauxite zone in some locations of the southeastern part includes well-rounded pebbles of dolerite and bauxite, which indicate transportation during the bauxitisation processes (Ayhan and Karadağ 1985).

The major components of the Yalvaç-Şarkikaraağaç province are boehmite and hematite. Diasporite, magnetite, gibbsite, kaolinite, anatase, rutile and goethite are moderate components, and montmorillonite, halloysite, barite, malachite and azurite are minor components (Bulur 1979; Ayhan and Karadağ 1985; Öncel 1995; Özen et al. 2010).

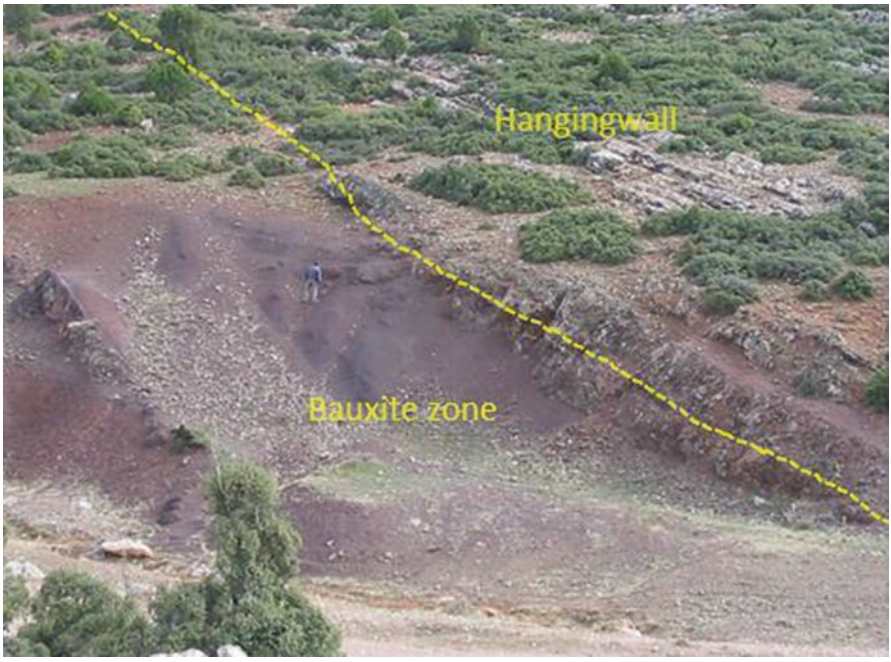

Fig. 15.8 The lateritic bauxite zone southwest of Kireli village, which formed on dolerite-basalt and is overlain by Jurassic carbonates

The chemical composition of the bauxite in this province varies according to the grade of bauxitisation. Öncel (1995) reported that the average composition of the bauxites in the northwestern part of the province is 33.3% Al_2O_3 (17–42%), 38.48% Fe_2O_3 (28–51.7%), 17.8% SiO_2 (9–22%) and 4.21% TiO_2 (2.41–6.07%). Ayhan and Karadağ (1985) reported that the average composition of the bauxites in the southeastern part of the province is 34.21% Al_2O_3 (5.79–58.8%), 28.71% Fe_2O_3 (4.3–75.37%), 19.3% SiO_2 (2.9–35%) and 4.3% TiO_2 (0.34–7%).

The Yalvaç-Şarkikaraağaç bauxite province includes good examples of vertical and horizontal transitions from the bauxite to the protolith (dolerite-basalt) in the field. The less weathered dolerite-basalts are greyish-dark green (Fig. 15.9) and are composed of plagioclase (35–42%) clinopyroxene (22–30%), amphibole (10–14%), orthopyroxene (8–12%), olivine (1–3%) (Bozkır 2007) and opaque minerals (magnetite, hematite, goethite, ilmenite, chromite) (Ayhan and Karadağ 1985; Öncel 1995). The dolerite-basalt rocks have been described as within-plate basalts and calc-alkaline basalts (Öncel 1995). The saprolite zone is brownish-green to reddish-green and preserves the primary rock texture (Fig. 15.10a), but the bauxite forms patches within the saprolite zone (Fig. 15.10b).

The bauxite formed at various levels in the dolerite-basalt rocks. In some places, three bauxite levels developed (Bulur 1979; Ayhan and Karadağ 1985; Öncel 1995). The developments of the levels of bauxite on the dolerite-basalt indicate that both periodic volcanic activity and bauxitisation processes occurred in Malm (Ayhan and Karadağ 1985; Öncel and Söğüt 2008).

Fig. 15.9 Outcrop of the dolerite-basalt which is the parent rock of the Yalvaç–Şarkikaraağaç bauxite province (Y:364629; X:4203030, ED50)

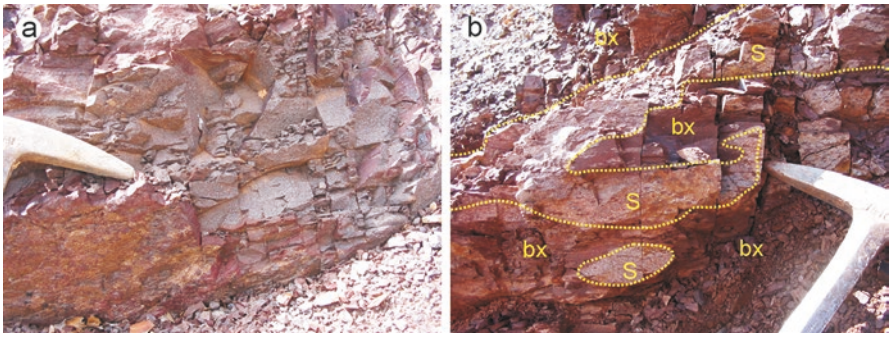

Fig. 15.10 (**a**, **b**) Brownish-green and reddish-green saprolites that developed via weathering of the dolerite-basalt during bauxitisation (Y:364629, X:4203030, ED50)

15.4 Seydişehir-Akseki Province

The Seydişehir-Akseki province is located south of Seydişehir in the Central Tauride carbonate platform (Fig. 15.1). This province is the most economically important bauxite province in Turkey (e.g. Blumental and Göksu 1949; Göksu 1953; Wippern 1962; Özlü 1978, 1979; Patterson et al. 1986; Karadağ 1987; Öztürk et al. 1998; Karadağ et al. 2009). The Mortaş, Doğankuzu, Değirmenlik, Morçukur and Arvana deposits are the most important deposits in the province (Fig. 15.11). These deposits

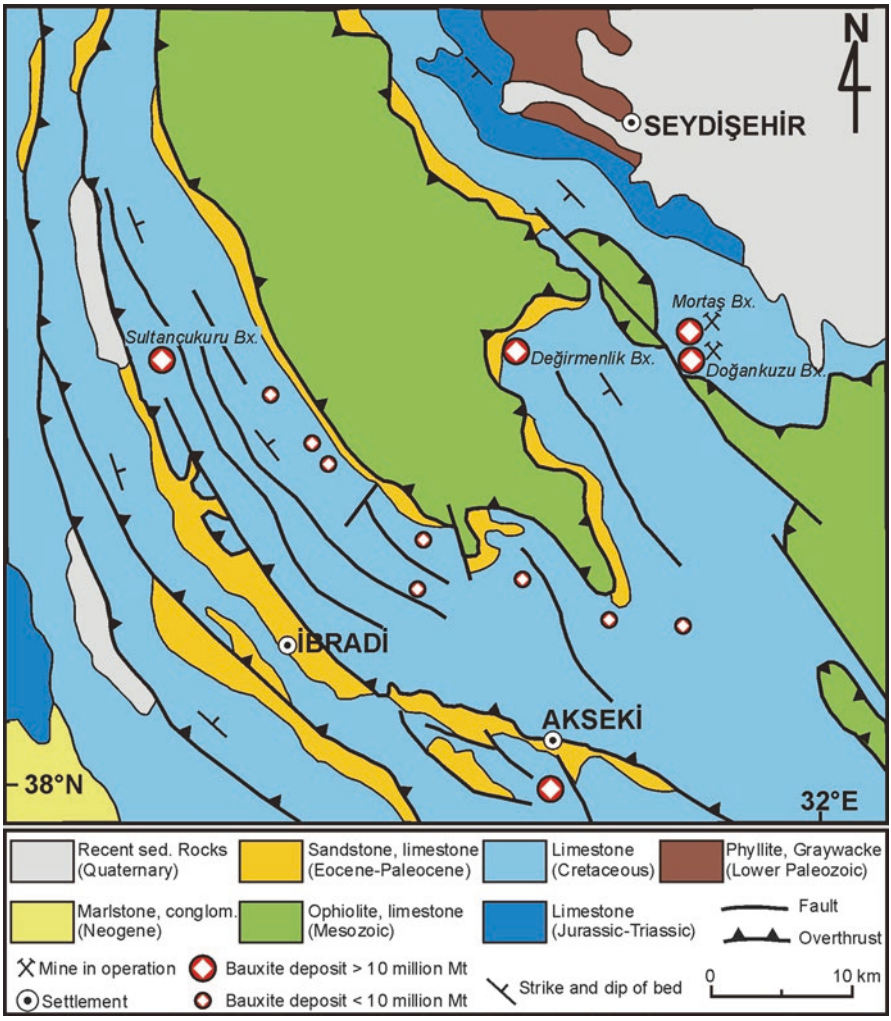

Fig 15.11 Geological map of the Seydişehir-Akseki bauxite province. (After Özlü 1978)

are karstic-type bauxites, and the Doğankuzu, Mortaş, Arvana and Morçukur deposits are mined by the Eti Alüminyum Company (Fig. 15.12).

The Mortaş and the Doğankuzu deposits are located approximately 20-km south of Seydişehir (Fig. 15.11, Table 15.1) with the bauxite formed along the unconformity between Turonian and Santonian limestones (Öztürk et al. 2002). The bauxite developed in karstic depressions and sinkholes in the footwall limestones, resulting in the bottom contact of the bauxite being wavy. The upper contact of the

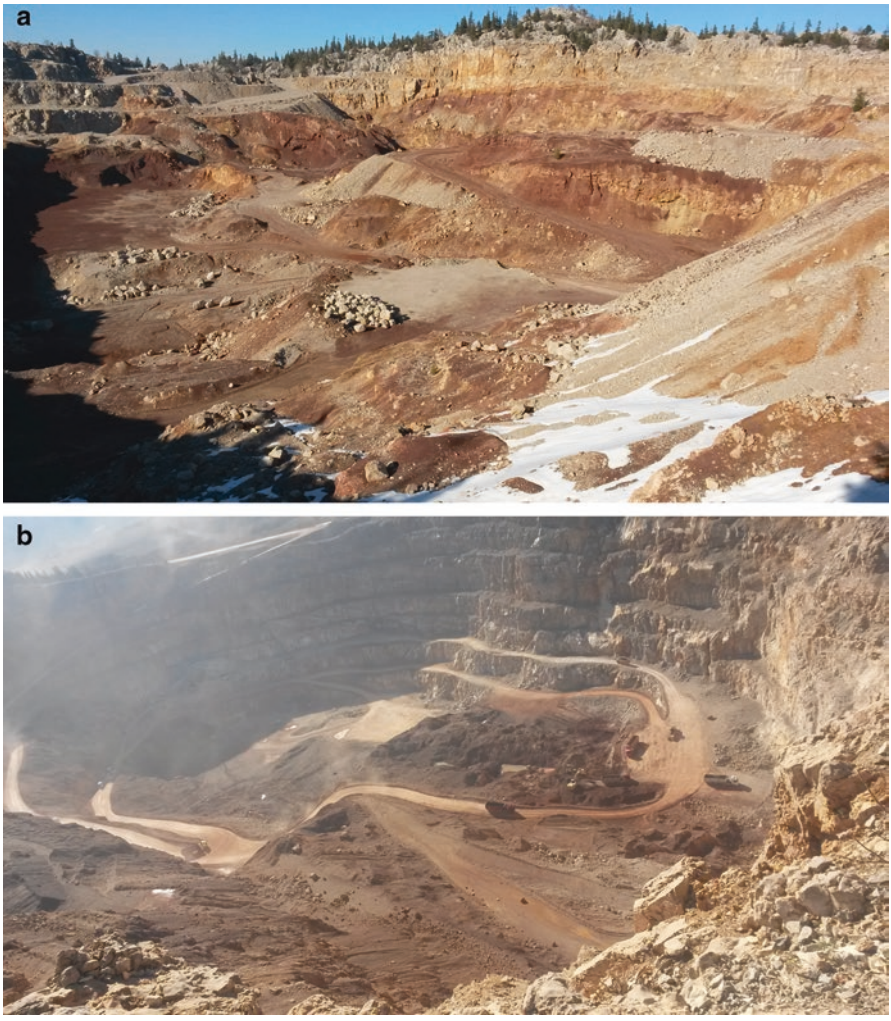

Fig 15.12 General views of the (**a**) Mortaş and (**b**) Doğankuzu bauxite deposits

bauxite is overlain concordantly by the Santonian limestones. Detailed exploration of the Mortaş and Doğankuzu bauxite deposit from 1970 to 1980 determined that the Mortaş deposit contains 10.9 Mt of ore with an average grade of 57% Al_2O_3 and that the Doğankuzu deposit contains 14.9 Mt of ore with an average grade of 58% Al_2O_3 (Pelen 1977; Pelen and Vuran 1978).

The Mortaş deposit is approximately 400-m long and an average of 10-m thick (up to 40 m). The strike and dip of the deposit are NW–SE and 25–30°SW, respectively. The base of the ore zone contains pyrite/marcasite-rich, greyish-green, low-grade ore that transitions laterally into a pinkish-brown bauxite body (Öztürk et al. 2002). In

Fig. 15.13 The bauxite ore zone of the Değirmenlik deposit

places, collapse breccia that is cemented by Al-hydroxides is present at the base of the ore. The main ore body has a massive, oolitic-pisolitic texture. The main ore is composed of boehmite, hematite, and goethite with minor anatase and diaspore.

The Doğankuzu deposit has an ellipsoidal geometry, is approximately 500-m long and varies in thickness between 1 and 40 m. The strike and dip of the deposit are NW–SE and 30°SW, respectively. As in the Mortaş deposit, the base of the bauxite zone contains pyrite/marcasite-rich low-grade ore that transitions into massive pisolitic ore. The mineralogy of the ore is the same as that of the Mortaş deposit. The main massive ore is overlain by 5 to 10-m-thick, yellowish pale-brown, very fine-grained pyrite-bearing limestones that are Turonian in age (Öztürk et al. 2002).

The Değirmenlik (Akseki-Antalya) deposit is located approximately 20-km southwest of Seydişehir (Fig. 15.11). It formed in karstic depressions and sinkholes that developed in Upper Cretaceous limestones (Fig. 15.13). The strike and dip of the deposit are N40°W and 25°SW, respectively. The ore zone is approximately 700-m long and an average of 9 m thick (up to 20 m). The ore has various colours, such as deep brownish red, yellowish-red and greenish-brown. The ore texture is massive and oolitic-pisolitic. The bauxite zone is overlain by thin layered Upper Cretaceous limestone. The Değirmenlik deposit includes boehmite and hematite with minor anatase, diaspore, pyrite/marcasite and kaolinite and contains 11.7 Mt of ore with average contents of 57% Al_2O_3 and 6.6% SiO_2 (Baysal and Engin 1976). Details of the ore geochemistry of the Mortaş, Değirmenlik and the Doğankuzu deposits are given in Table 15.2.

15.5 Alanya Province

The Alanya bauxite province is located in the Alanya metamorphic rocks north of Alanya settlement in southern Turkey (Fig. 15.1). The limited data that are available about the bauxite deposits and occurrences in this province are provided by MTA (1965, 1980), Peyronnet (1971), Wippern (1962), Temur and Kansun (2006), and Öztürk et al. (1995).

The Alanya metamorphics include three bauxite levels that developed on unconformities in Lower Triassic, Middle-Upper Triassic and Jurassic units (Öztürk et al. 1995; Bedi and Öztürk 2001). The first bauxite level occurred along the unconformable contact between Permian marble and Lower Triassic schist and phyllites. The second level occurred along the unconformity between Lower Triassic and Middle (?)-Upper Triassic marble and metadolomites. The third bauxite level developed along the unconformity between Upper Triassic and Jurassic marbles (Bedi and Öztürk 2001). Most of the bauxite occurrences in the Alanya province are represented by the first and the second levels.

The important bauxite deposits and occurrences in the Alanya province are Maşatdağ (Fig. 15.14a), Çatak, Belenbaşı, Höyüklü-Göçebe, Belitliyatak, Çamçukuru (Fig. 15.14b), Asmaca, Derincedere Kayrangöyük, Kaşbeleni and Yazandere (Peyronnet 1971; MTA 1965, 1980). The bauxite includes diasporite and hematite as the main minerals and varying proportions of boehmite, gibbsite, corundum, goethite, magnetite, chamosite, pyrite, marcasite, psilomelane, rutile, kaolinite, chlorite, illite, muscovite, chloritoid, rutile and rectorite (Temur and Kansun 2006). The Alanya bauxite province contains approximately 7.5 Mt of ore with contents of 27–67% Al_2O_3, 4–26% SiO_2, 16–44% Fe_2O_3 and 2–7% TiO_2 (MTA 1965, 1980).

15.6 Bolkardağı (Karaman) Province

The Bolkardağı province is located in southern Turkey (Fig. 15.1). There are three main tectono-stratigraphic units in the Bolkardağı region (Fig. 15.15). From bottom to top, the units are the Bolkardağı Unit (BU), the Namrun Tectonic Unit (NTU) and the Aladağ Unit (AU), and they are in tectonic contact. The Bolkardağı bauxite province (Karaman) includes high-quality diasporitic bauxite deposits of various sizes, which are located within these three tectono-stratigraphic units (Hanilçi et al. 2006). Apaydın and Erseçen (1981) reported ore reserves of approximately 10 Mt in the region. The main bauxite zones are the Camızalanı–Karakuyu, Karataş, Bolkardede and Boluardıç deposits in the BU, the Gerdekes, Kavaközü–Göztaşı–Devebağırtan, Baharpınarı–Kemikli Tepe, Arpaçukuru and Kızıldağ deposits in the NTU, and the Öşün deposit in the AU (Fig. 15.15; Hanilçi 2013). Approximately 2 Mt. of bauxite ore with average contents of 55% Al_2O_3, 25% Fe_2O_3, 3.5% TiO_2 and 1–10% SiO_2 were produced from this region between 2003 and 2016 (personal

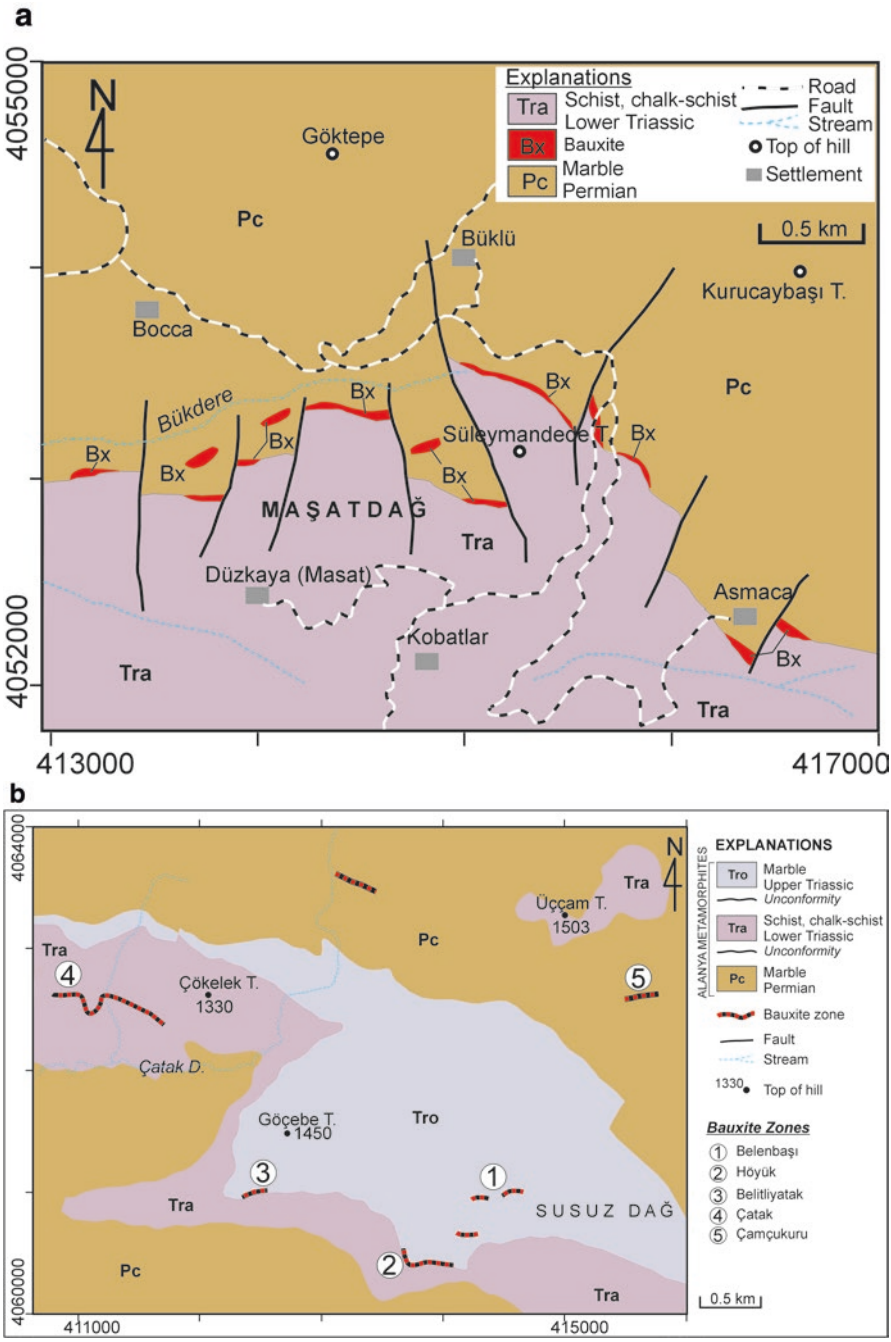

Fig. 15.14 Geological map of (**a**) the Maşatdağ bauxite deposits. (Simplified after Temur and Kansun 2006); (**b**) the Susuzdağ region bauxite zones. (The geological map was simplified from Bedi and Öztürk 2001, and bauxite zones are taken from Peyronnet 1971)

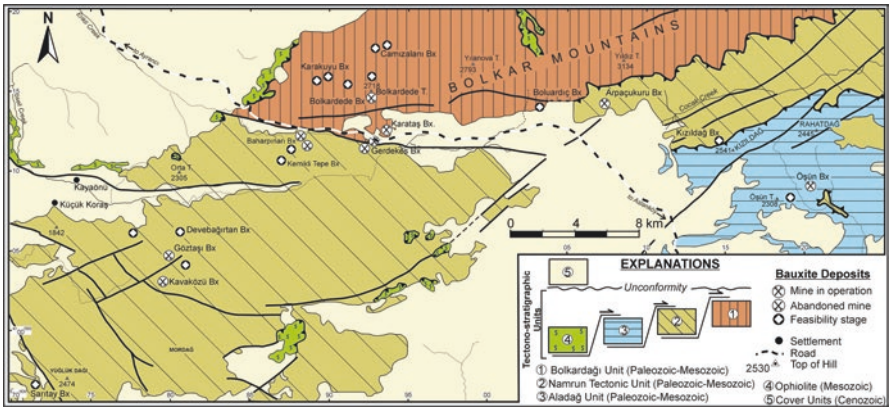

Fig. 15.15 Tectono-stratigraphic units of the Bolkardağı bauxite province. (After Hanilçi 2013)

communucation with Halil Demirel owner of Demireller Minng Co.). ΣREE contents of bauxite deposits in that province show variations (Öztürk et al. 2018).

The Bolkardağı province includes both lateritic-type and karstic-type deposits. The lateritic-type deposits, which gradually transition from the protolith to the bauxite, were investigated in detail by Hanilçi (2013). The deposits in the BU and NTU are metamorphosed, and the primary boehmite changed to diasporite due to this metamorphism. The diasporite ratio of the unmetamorphosed Öşün deposit is less than the other deposits in the region, and this deposit contains approximately 30% boehmite (Al 2015).

15.6.1 Bauxite Deposits in the Bolkardağı Unit (BU)

The Bolkardağı Unit (BU) comprises Carboniferous to Maastrichtian rocks in the region. From older to younger, the BU includes: (i) Carboniferous recrystallised limestone, chalc-schists and rare schists; (ii) Early Permian recrystallised limestone and chalc-schists; (iii) Upper Permian Mizzia-bearing recrystallized limestone and dolomite; (iv) Early–Middle–Late Triassic schist, calc-schist and recrystallized limestone, recrystallised dolomitic limestone, dolomite, schist, calc-schist, and chert-bearing recrystallised limestone interlayered with volcanic rocks; and (v) Jurassic–Cretaceous recrystallised limestone, dolomite, schist, calc-schist, and lenses of recrystallised limestone and various rock blocks (Alan et al. 2007).

The Camızalanı-Karakuyu bauxite zone, the Bolkardede Tepe deposit and Karataş deposit are the largest deposits within the BU (Fig. 15.15, Table 15.1).

The Camızalanı-Karakuyu Bauxite zone is located along the unconformity between Aalenian (Jurassic) thick-bedded recrystallised limestone and Triassic chalk-schists and dolomites. The bauxite zone extends E–W and NE–SW intermittently for approximately 4 km (Fig. 15.16) and dips 20–90° SE (Hanilçi 2013). The

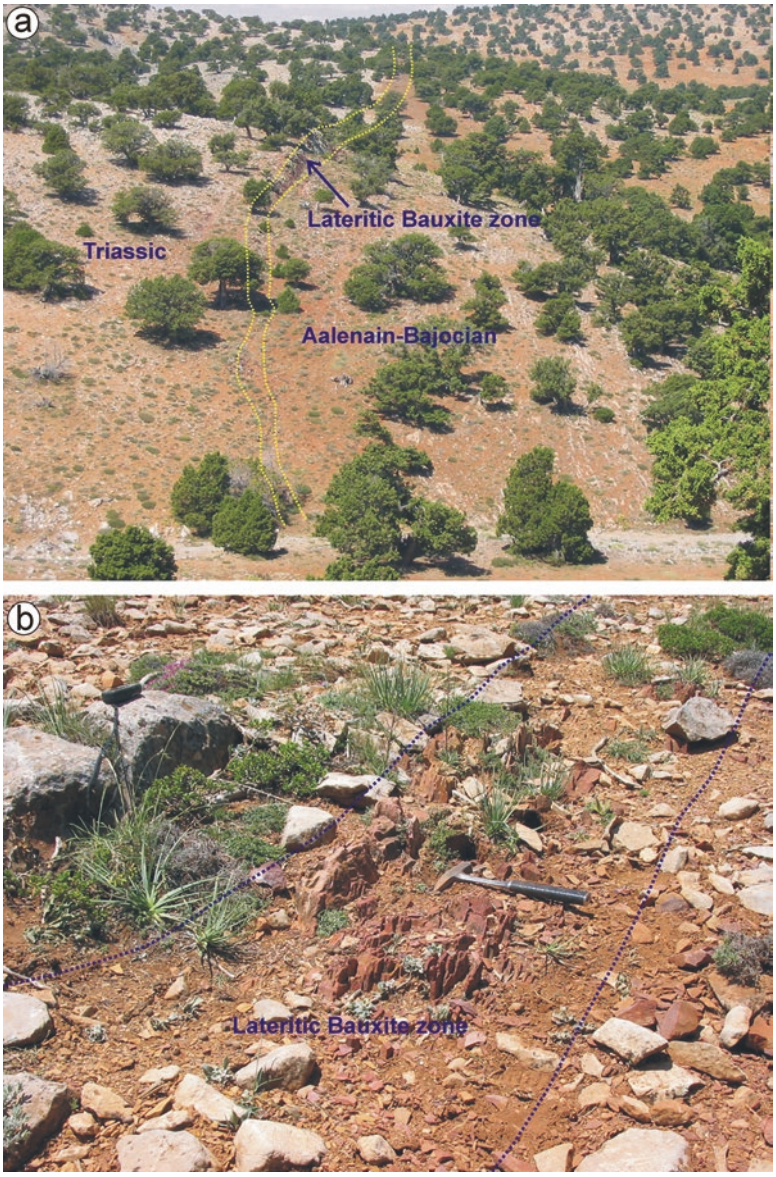

Fig. 15.16 (**a**) The Camızalanı–Karakuyu lateritic bauxite zone along the unconformity between the Triassic and Aalenian-Bajocian units, which extends for approximately 4 km; (**b**) The thickness of the zone (saprolite and bauxite) varies from 1 to 7 m. (After Hanilçi 2013)

bauxite zone has various colours, such as brownish-red, greenish, dark red, greenish-cream and grey. The Camızalanı-Karakuyu bauxite zone is not economically mineable due to its high silica content (average 21% SiO_2; Table 15.2).

The Camızalanı-Karakuyu bauxite zone mostly includes lateritic-type deposits, but some karstic-type bauxites developed in the Triassic and Permian recrystallized limestones. The saprolite zone is composed of chlorite, amphibole, feldspar, quartz, pyrophyllite, mica, calcite, diasporite, goethite and hematite. The well-developed bauxite zone includes anatase, diasporite, goethite and hematite. There are no data about the reserves of the Camızalanı–Karakuyu bauxite zone.

The Bolkardede Tepe bauxite deposit is located at high elevations (2558 m) in the Bolkar Mountains within the BU (Fig. 15.15, Table 15.1). Approximately 0.03 Mt of ore with an average grade of 55% Al_2O_3, 26% Fe_2O_3, 4% SiO_2 and 3% TiO_2 was mined from this deposit between 2003 and 2005 (Demireller Mining Co. 2008). The karstic-type bauxite developed along the unconformity between Triassic recrystallized dolomite, limestone and chalk-schists and Aalenian recrystallised limestone (Fig. 15.17a, b).

The bauxite ore contains massive and oolitic-pisolitic textures. The bottom zone of the bauxite is covered by thin layers (a few cm thick) of pyrite/marcasite-bearing clayey material and is a greenish-earthy colour. The bauxite deposit is mainly composed of diasporite, hematite and anatase with rare secondary goethite, pyrite, pyrophyllite, mica, chlorite, quartz and kaolinite along the fault zones (Table 15.1).

The Karataş bauxite deposit is the largest known deposit within the BU and contains more than 2.5 Mt of proven reserves (Fig. 15.15). The deposit consists of three main bauxite zones within a 2 km^2 area (Fig. 15.18). Approximately 0.5 Mt of ore with an average grade of 56% Al_2O_3, 1–5% SiO_2 and 3% TiO_2 was mined between 2011 and 2015. Details of the ore geochemistry of this deposit are given in Table 15.2.

The deposit developed mostly as karstic-type bauxite in the Triassic recrystallised limestones and as lateritic-type bauxite in some places in the Triassic phyllite-schists (Hanilçi 2013). Three bauxite ore zones in the Karataş deposit are covered unconformably by both Aalenina-Bajocian recrystallised limestone and Miocene limestones. The ore zones are oriented E–W and NE–SW and reach lengths of up to 800 m. The thickness varies from 1 to 15 m. The bottom of the karstic-type bauxite is undulating, and the lower section of the ore begins with yellowish-green to reddish, low-grade, earthy bauxite (Fig. 15.19). The ore contains massive and mostly oolitic and pisolitic textures. Although uncommon, the ore transitions to the protolith in the locations where the lateritic-type bauxite formed on the phyllite-schists. The lateritic-type bauxite has a low ore grade (SiO_2 >10%, Al_2O_3 <45), and the texture is massive and earthy (Hanilçi 2013).

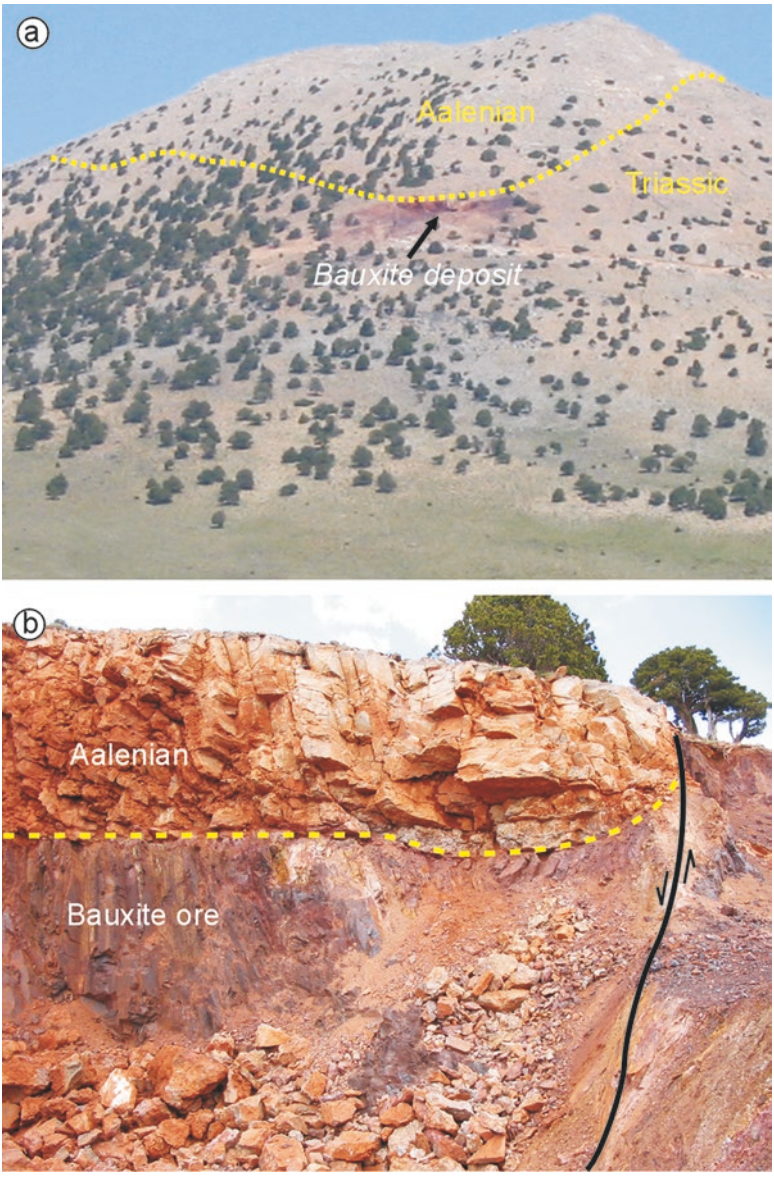

Fig. 15.17 (**a**) The Bolkardede Tepe bauxite deposit formed along the unconformity between the Aalenian and Triassic units as a (**b**) karstic-type deposit

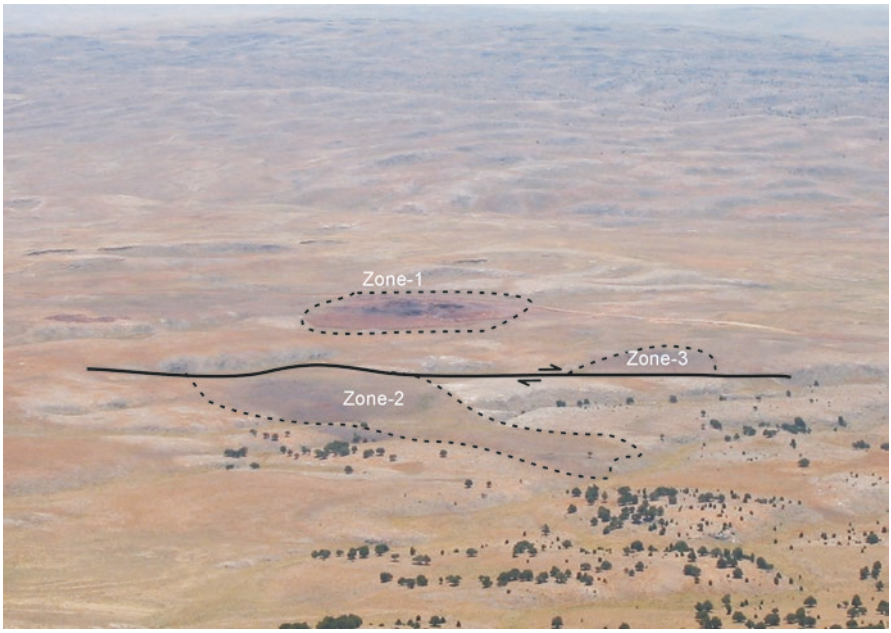

Fig. 15.18 The Karataş bauxite deposit consists of three separate bauxite zone. Zone 1 is the main zone and has been mined in the past.

15.6.2 Bauxite Deposits in the Namrun Tectonic Unit (NTU)

The NTU tectonically overlies the Bolkardağı Unit (Fig. 15.15) and from old to young consists of: (i) Carboniferous recrystallised limestone, phyllites, calc-schist and quartzite; (ii) Permian Girvanella-bearing recrystallized limestone, calc-schist, and quartzite and Mizzia-bearing recrystallised limestone and dolomite; (iii) Triassic slate, recrystallised limestone (Early–Middle Triassic) recrystallised dolomitic limestone, dolomite (Middle–Late Triassic), phyllites, chert-bearing recrystallised limestone and interlayers of volcanic rock (?) (Late Triassic); and (iv) Jurassic-Cretaceous recrystallised limestone and dolomite (Alan et al. 2007).

The Kızıldağ bauxite zone, the Arpaçukuru deposit, the Kavaközü deposit, the Göztaşı Tepe deposit, the Devebağırtan deposit, the Kemikli Tepe-Baharpınarı deposits and Sarıtay deposits are the important deposits occurring within the NTU (Fig. 15.15).

The Kızıldağ bauxite zone is located south of the Bolkar Mountains in the NTU (Fig. 15.5, Table 15.1). This zone is not economical for mining due to its limited thickness (average 3 m) and ore quality (Table 15.2), but it shows excellent transitional features from the protolith to the bauxite zone (Hanilçi 2013). The bauxite

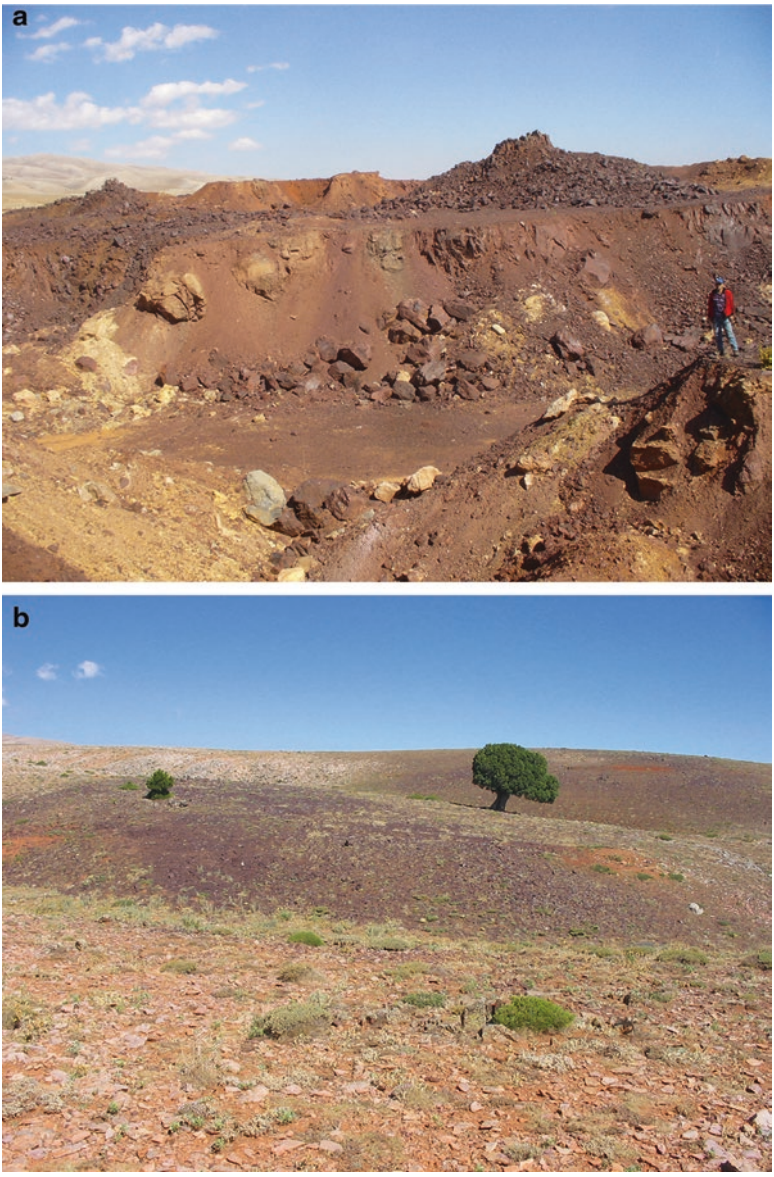

Fig. 15.19 (**a**) The karstic-type ore zone with undulatory karst bottom in Karataş Zone-1 and (**b**) wide outcrops of the Karataş Zone-2 close to the Bolkardede Tepe

zone (Fig. 15.20) developed in the Lower Triassic shale (which was later transformed to slate) and transitions vertically and horizontally into the shale (Fig. 15.21).

The Kızıldağ bauxite zone extends N70°E for approximately 400 m and varies in thickness (from 1 to 3 m). The protolith (shale that was later metamorphosed to slate)

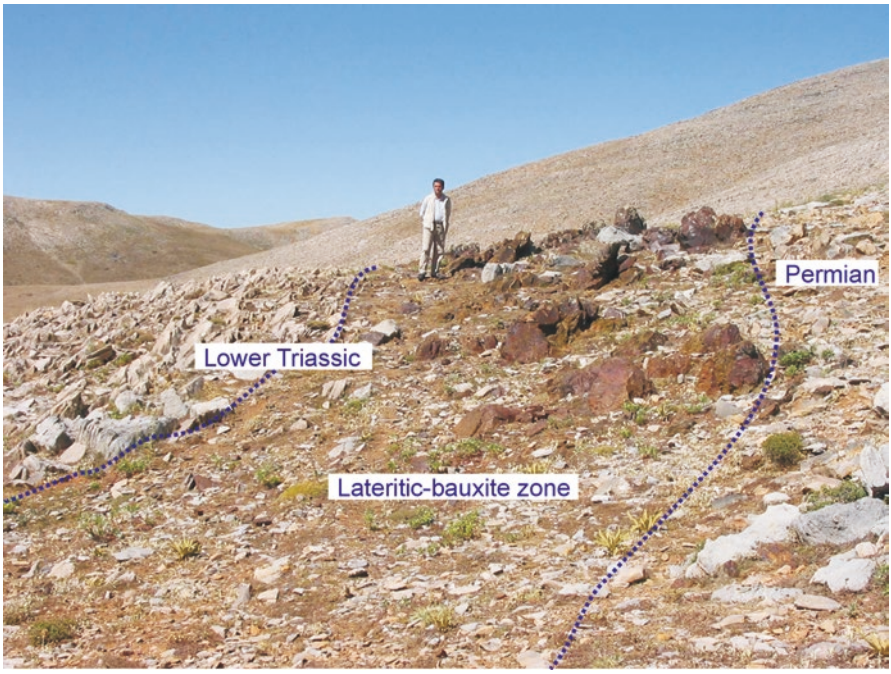

Fig. 15.20 Lateritic bauxite in the Lower Triassic shales (later transformed to slate) of the NTU in the Kızıldağ bauxite zone

is greenish-yellow and is mainly composed of chlorite, mica, feldspar and quartz (Fig. 15.20a). The saprolite zone is greyish-green and is composed of chamosite (iron-chlorite), diasporite, kaolinite, quartz and limonite. The structure of the protolith has been destroyed, and the rock has a massive structure in the saprolite zone (Fig. 15.20b). The bauxitic zone is reddish-brown and is mainly composed of diasporite and haematite with minor boehmite and kaolinite (Fig. 15.20c). The vertical and horizontal transitions of the protolith to the bauxite indicate that the bauxitisation processes postdated the deposition of the Triassic strata (Hanilçi 2013).

The Arpaçukuru bauxite deposit is located in the NTU and is the second largest known deposit in the region with 1.8 Mt of proven ore reserves (Al 2015) (Fig. 15.5, Table 15.2). This deposit is a karstic-type deposit, and approximately 0.8 Mt of ore with an average grade of 52% Al_2O_3 and 7.5% SiO_2 grade were produced between 2006 and 2013 (Al 2015). Detailed ore geochemistry of this deposit is given in Table 15.2.

The Arpaçukuru deposit consists of four ore zones with lengths between 50 and 200 m. The directions of the ore zones vary from NE–SW to NW–SE. Of the ore zones, the southern zone is currently economically mineable due to its silica content (SiO_2 <10%). The Arpaçukuru deposit is 40-m thick and dips toward the northwest at 35°. The bottom surface of the bauxite zone is wavy, and the karstic-type bauxite fills the depressions and sinkholes of the footwall recrystallised limestones. The hanging

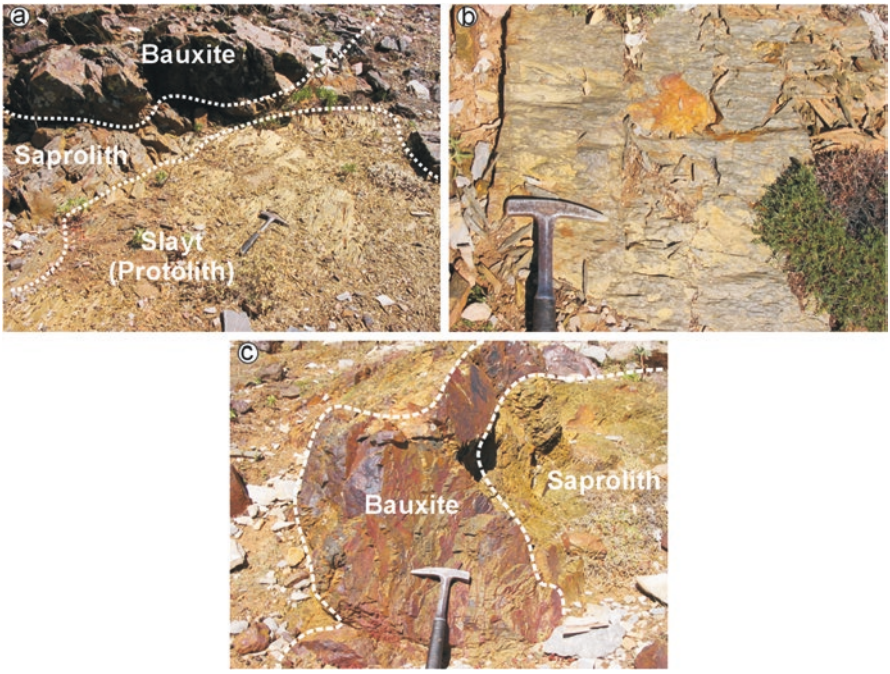

Fig. 15.21 (**a**) The parent rock of the bauxite (protolith); (**b**) the saprolite; (**c**) the relationship between the saprolite and bauxite in the Kızıldağ bauxite zone

wall of the deposit is Aalenian recrystallised limestone and, in some locations, Upper Triassic recrystallised limestones and phyllites-schist due to overturned folds. The bottom of the bauxite zone is represented by kaolinite-rich clayey bauxite that transitions to massive and oolitic–pisolitic bauxite zones towards the top. The bauxite zone is reddish-brown in colour (Fig. 15.22a), but the ore is yellowish-white in some locations due to leaching of the iron via organic acid-rich surface waters (Fig. 15.22b).

The Arpaçukuru deposit is mainly composed of diasporite, hematite and minor anatase, pyrophyllite, goethite, chlorite, mica and boehmite (Table 15.1).

The Kavaközü bauxite deposit is located approximately 8-km southeast of Küçük Koraş village and is in the NTU (Fig. 15.5, Table 15.1). Approximately 0.01 Mt of ore with an average grade of 56% Al_2O_3, 1–3% SiO_2 and 3.5% TiO_2 was mined in 2008.

The karstic-type bauxite deposit formed in Middle Triassic recrystallized dolomite-limestone and is unconformably overlain by Jurassic recrystallised dolomites (Fig. 15.23). The strike and dip of the deposit are N45–50°E and 10–15°SE, respectively, and the length and thickness are 75 m and 2–8 m, respectively.

The Göztaşı bauxite deposit is located approximately 7.5-km southeast of Küçük Koraş village and is in the NTU (Fig. 15.15, Table 15.1). Approximately 0.12 Mt of ore with an average grade of 58% Al_2O_3, 3% SiO_2 and 3% TiO_2 was mined in 2008–2009.

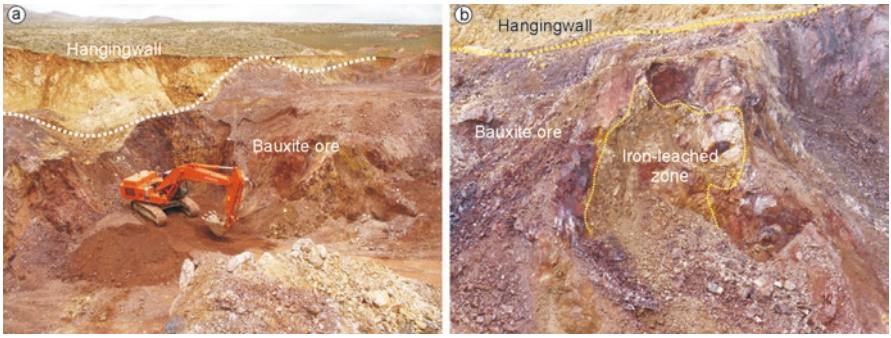

Fig. 15.22 (**a**) Reddish-brown massive bauxite ore body in the Arpaçukuru deposit; (**b**) yellowish-white ore zone, where iron has leached from the ore body

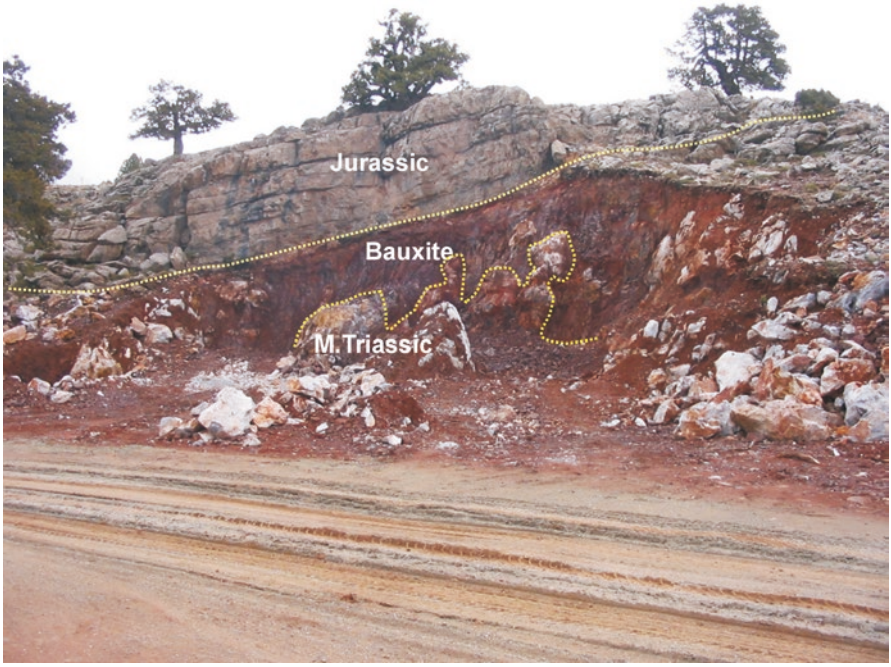

Fig. 15.23 The Kavaközü deposit developed as a karstic-type deposit in the Middle Triassic recrystallized limestones of the NTU. The bottom contact of the ore is undulatory

The deposit is a karstic-type bauxite that formed along the unconformity between Triassic recrystallised dolomite-limestone and Jurassic recrystallised dolomites (Fig. 15.24). The ore is reddish-brown and has massive and oolitic-pisolitic textures. The bauxite developed within a sinkhole and karstic depression that is oriented N60°W. While the upper contact of the ore zone is very regular and sharp, the bottom contact is wavy. The dimensions of the deposit at the surface are 45 m by

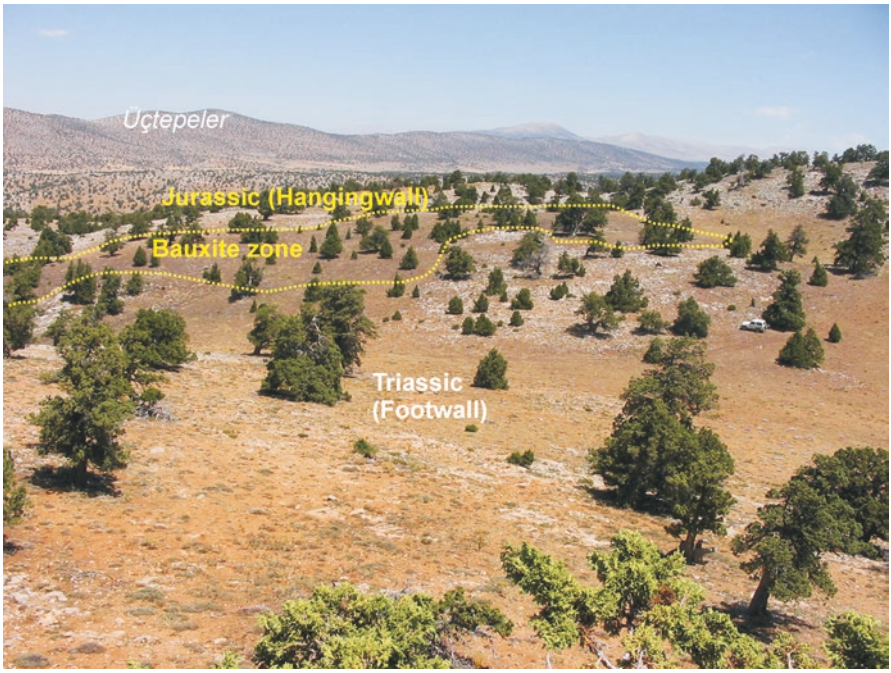

Fig. 15.24 The Göztaşı bauxite deposit formed as a karstic-type deposit in Triassic recrystallised limestone of the TDU

170 m, and it is 15-m thick. The ore mainly consists of diasporite and hematite with minor anatase, boehmite, goethite and kaolinite.

The Kemikli Tepe and Baharpınarı bauxite deposits are located southwest of the Bolkardede Tepe and are within the NTU (Fig. 15.15). Although the deposits are close to each other, the Kemikli Tepe deposit is a lateritic-type deposit, whereas the Baharpınarı deposit is a karstic-type deposit.

Outcrops of the Kemikli Tepe deposit are located on the southern and northern parts of Kemikli Hill. The northern part strikes WNW–ESE and dips to the SSW at 32°. The ore zone extends intermittently for approximately 100 m and is 5 to 10-m thick. The footwall of the ore zone is composed of Upper Triassic phyllites and meta-shales that transition gradually into the saprolite zone and then into the bauxite. The bauxite ore has a massive and homogeneous oolitic and pisolitic texture. It is overlain by Aalenian–Bajocian (Middle Jurassic) recrystallised limestone (Hanilçi 2013). The southern part of the Kemikli Tepe deposit extends discontinuously NE–SW for approximately 200 m and dips toward the NW. The footwall of the bauxite is composed of Upper Triassic recrystallised dolomitic limestone, and the hanging wall is Aalenina–Bajocian (Middle Jurassic) recrystallised limestone. The ore in the northern part accumulated in karstic depressions.

The Baharpınarı deposit is a karstic-type deposit and is located 5-km southwest of Bolkardede Hill (Fig. 15.15). Approximately 0.5 Mt of ore with an average grade

Fig. 15.25 (**a**) The Baharpınarı deposit developed as a karstic-type deposit and is unconformably overlain by Aalenian recrystallized limestone; (**b**) The ore is massive and has an oolitic-pisolitic texture

of 56% Al_2O_3, 2–6% SiO_2 and 3.4% TiO_2 was mined in 2008. The ore zones are oriented N–S and extend discontinuously for approximately 150 m with an average thickness of 20 m. The footwall of the ore is Upper Triassic recrystallised dolomitic limestone, and the ore zone is overlain unconformably by Aalenian–Bajocian (Middle Jurassic) recrystallised limestone (Fig. 15.25a; Hanilçi 2013). The ore is earth red in colour with dark brown pisolites which are composed of hematite (Fig. 15.25b).

15.6.3 Bauxite Deposit in the Aladağ Unit (AU)

The Aladağ Unit (AU) tectonically overlies the NTU and contains: (i) Late Devonian siltstone, shale, limestone, sandy limestone and quartzite; (ii) Carboniferous shale, marl, mudstone, quartzite and limestone; (iii) Early Permian Girvanella-bearing clayey limestone, limestone, Late Permian quartzite, Mizzia-bearing limestone and dolomitic limestone; (iv) Triassic mottled marl, shale, stromatolitic limestone (Early–Middle Triassic), conglomerate, siltstone, clayey limestone and limestone (Late Triassic); (v) Jurassic-Cretaceous limestone, dolomite, Late Cretaceous limestone, sandstone, siltstone, shale, micritic limestone and (vi) various rock blocks that contain flysch (Alan et al. 2007, 2011a, b). This unit is not metamorphosed and contains the karstic-type Öşün bauxite.

The Öşün bauxite deposit formed as karstic-type deposits in sinkholes and karstic depressions that developed on the Permian limestones of the AU (Fig. 15.15). The deposit contains approximately 0.5 Mt of ore with an average grade of 53% Al_2O_3, 7% SiO_2 and 3% TiO_2. Approximately 0.03 Mt of ore was mined in 2015 (Al 2015). Details of the ore geochemistry of this deposit are given in Table 15.2.

The deposit includes three bauxite zones. The footwall of all of the bauxite zones is Permian limestone, and the zones are overlain by Aalenina–Bajocian (Middle Jurassic) limestones (Fig. 15.26).

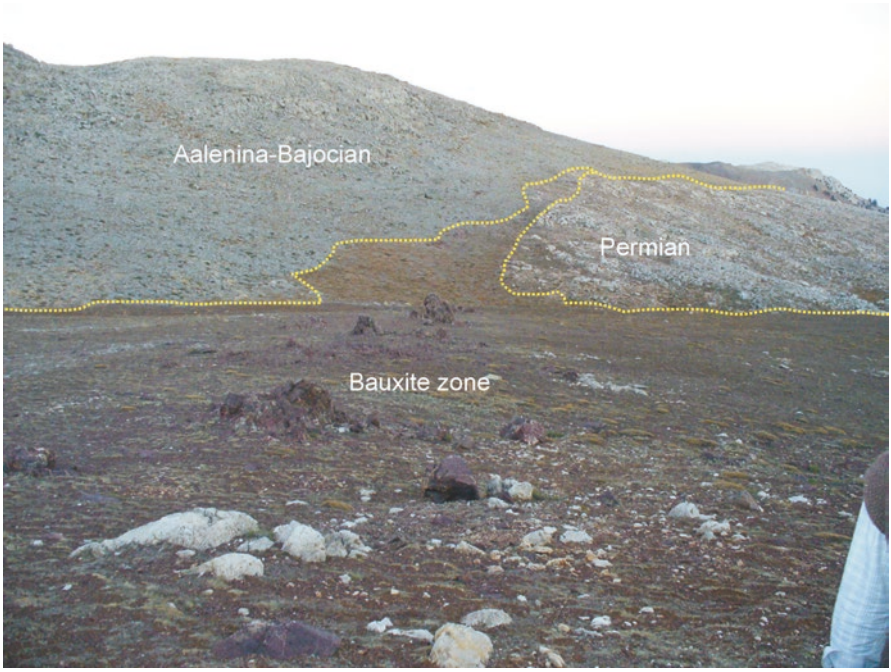

Fig. 15.26 The main ore zone in the Öşün bauxite deposit, which is located in karstic depressions of Permian limestone and is unconformably overlain by Aalenian–Bajocian limestone

Fig. 15.27 The Öşün bauxite ore has pisolitic-oolitic textures with different colours, such as (**a**) reddish-brown and (**b**) white matrix with dark pisolites

The bottom contacts of the bauxites are wavy, and the bauxite accumulated within karstic depressions. The three bauxite zones have dimensions of 230 m by 70 m, 125 m by 50 m and 150 m by 60 m. According to boreholes that were drilled by Demireller Mining Co., the bauxite zones have an average thickness of 15 m. The bauxite ore is reddish, grey, white and greenish-red and contains pisolitic and oolitic structures (Fig. 15.27a, b). Most of the pisolites are composed of iron oxide-

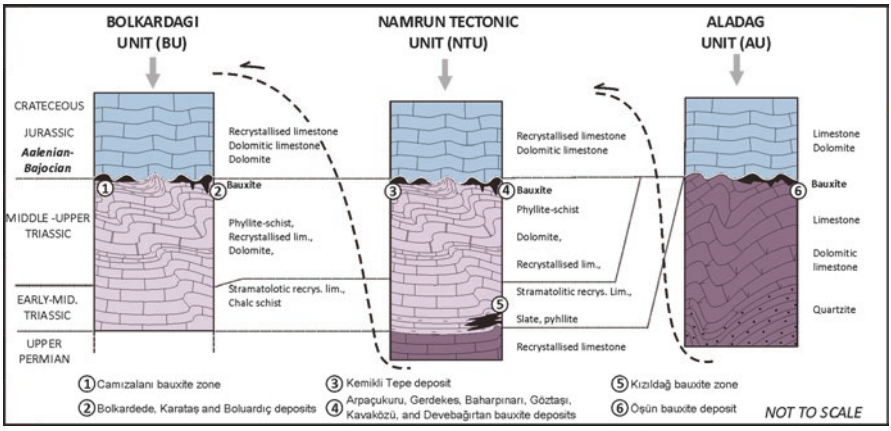

Fig. 15.28 Stratigraphic positions of the bauxite deposits and the correlation of the bauxite-bearing tectono-stratigraphic units in the Bolkardağı province. (After Hanilçi 2013)

hydroxides. Because of leaching of the iron by acidic solutions, the ore is patchy with iron-leached and iron-rich zones. Broken and reworked millimetre-sized pisolites indicate clastic accumulation of the bauxite at the site.

In summary, the bauxite deposits in the Bolkardağı province are located within three tectono-stratigraphic units (Fig. 15.28) (BU, NTU and AU) and are mainly karstic-type deposits, though lateritic-type are present in some places. While the BU and NTU contain both types, the AU contains only karstic-type deposits.

Based on field evidence and geochemical data, Hanilçi (2013) showed that Lower and the Upper Triassic pelitic rocks and shales are the source rocks of the bauxite. The bauxitisation processes began during the post-Upper Triassic and pre-Aalenian by the formation of kaolinite-rich lateritic soil. The kaolinite-rich lateritic soil was transformed to boehmite during low-water activity under hot and humid climatic conditions. The bauxitic materials were transported short distances from the laterite to the karstic depressions, and the karstic-type deposits formed mostly as clastic accumulations. Units of the Aalenian-Bajocian transgression covered the bauxite formations and caused their diagenesis. The Aalenian-Bajocian units overlie the bauxites in the BU, the NTU and the AU, which indicates that these tectonic units were part of the same terrain during bauxitisation. Ophiolite emplacement during the Upper Cretaceous caused the formation and imbrication of these tectono-stratigraphic units. The collisional tectonic regime caused deep burial of the bauxite-bearing tectono-stratigraphic units and subsequent very low-grade metamorphism. The various burial depths of these units explain the mineralogical differences in the deposits. Boehmite is the primary bauxite mineral in the deposits of the uppermost tectonic unit (the AU), whereas diasporite is the primary bauxite mineral in the underlying tectonic units (the BU and the NTU).

15.7 Tufanbeyli-Saimbeyli-Kadirli (TSK) Province

The TSK province is located north of the Tufanbeyli settlement and is SE oriented (Fig. 15.1). The bauxite deposits in this province formed on two unconformities in the Geyikdağı Unit. The first bauxite zone is located along the unconformity between the Upper Carboniferous and Upper Permian units (e.g. the Kızılçaltepe deposit; Özgül 1976), and the second bauxite is located along the unconformity between the Triassic units and the Jurassic carbonates (e.g. the Gümülek Tepe and Küçükçal Tepe deposits; Yılmaz 2004).

The data about the Tufanbeyli-Saimbeyli part of this province are from the 1980s and were obtained by MTA (1980). The important deposits are the Gümülek Tepe, Kızılçal Tepe and Küçükçal Tepe deposits. In addition, the Elpen, Maltaş and Kötümbel bauxite zones contain significant reserves but have high silica contents (36–50% SiO_2; MTA 1980).

The Gümülek Tepe bauxite deposit is located approximately 14-km east of the Tufanbeyli settlement on the southern slope of the Gümülek Tepe (Fig. 15.29). The bauxite zone formed on an unconformity between the Triassic and Jurassic recrystallised limestone and is oriented NW–SE. The ore zone continues for approximately

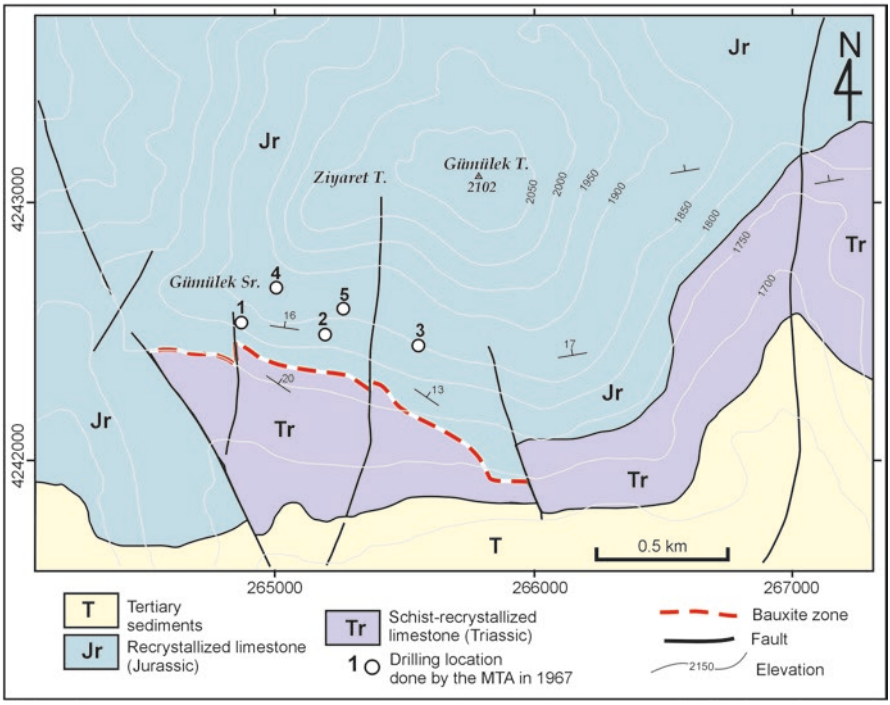

Fig. 15.29 Geological map of the Gümülek Tepe bauxite deposits. (Modified after Kaptanoğlu 1965)

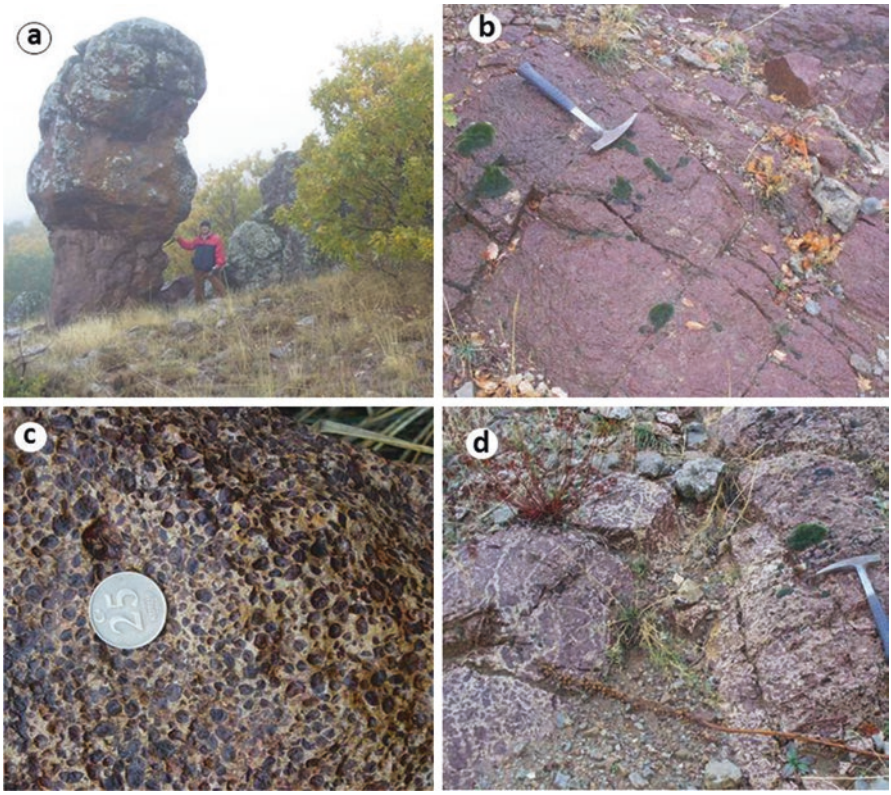

Fig. 15.30 (**a**) The average thickness of the ore is 5 m; (**b**) The ore is generally reddish-brown and has (**c**) pisolitic and (**d**) patchy textures.

1.5 km and is an average 5-m thick (Fig. 15.30a). The ore has various colours, such as reddish-brown, dark-brown and greyish-white, and various textures, such as oolitic-pisolitic, massive, leopard and patchy (Fig. 15.30b–d).

The bauxite zone is mainly composed of diasporite and hematite with moderate amounts of boehmite and minor anatase and kaolinite. The deposit contains approximately 5 Mt. of ore (proven and indicated reserves) with an average grade of 52% Al_2O_3, 25% Fe_2O_3, 7% SiO_2 and 2.9% TiO_2 (MTA 1980).

The Küçükçal Tepe bauxite deposit is located on the western and northern slopes of Küçükçal Hill (Fig. 15.31). The bauxite zone strikes NE–SW and crops out in two locations. The area between these outcrops was investigated by trenches, which revealed the continuity of the ore zone under the Pliocene sediments (Kaptanoğlu 1965). The ore zone formed on an unconformity between the Triassic units and the Jurassic recrystallised limestone that is covered by Pliocene rocks. The ore zone is approximately 1.2-km long and an average of 4-m thick. The deposit contains 1.5 Mt of proven plus indicated ore reserves with an average grade of 52% Al_2O_3, 29% Fe_2O_3, 11%SiO_2 and 2.7% TiO_2 (MTA 1980).

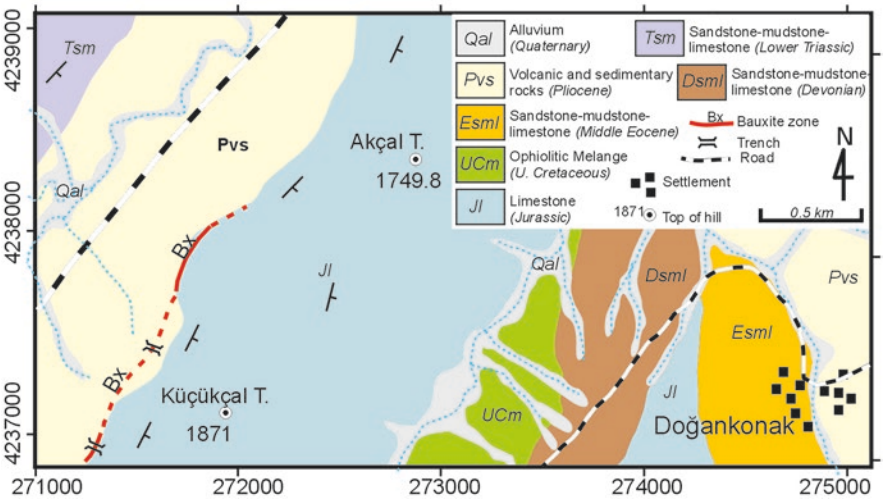

Fig. 15.31 Geological map of the Küçükçal Tepe bauxite deposit. (Map is simplified after MTA 2002 and the bauxite zone is taken from Kaptanoğlu 1965)

The Kızılçal Tepe bauxite deposit is located approximately 2-km southwest of the Kan settlement on the southern slope of Kızılçal Hill (Fig. 15.32). While the Küçükçal Tepe and the Gümülek Tepe bauxite zones are located along the unconformity between the Triassic and Jurassic units, the Kızılçal Tepe deposit formed along the unconformity between the Carboniferous and Upper Permian units. The ore has limited outcrops because it is covered by Pliocene volcanic and sedimentary rocks (Fig. 15.32). Therefore, the ore zone was investigated by trenches, which revealed the continuity of the ore zone under the Pliocene sediments (Fig. 15.32; Kaptanoğlu 1965). The ore zone is approximately 2-km long and an average of average 7.6-m thick. The deposit contains 5.5 Mt of proven ore reserves with an average grade of 50% Al_2O_3, 28% Fe_2O_3, 11% SiO_2 and 3% TiO_2 (MTA 1980).

Except for the Gümülek Tepe, Küçükçal Tepe and Kızılçal Tepe deposits, data are not available for the bauxite occurrences in the Tufanbeyli-Saimbeyli-Kadirli province. These bauxite occurrences include the Naltaş, Elpen, Kötünbel, Belmece Tepe, Himmetli, Bakırdağı, Yalakköy and Alaylıdağ deposits, Tufanbeyli and Saimbeyli and the Kuyuluk (Y:249494, X:4159897, ED50), Karaoğlan (Y:249380, X:4160462, ED50), Uzunkaya, Kaskit (Y:251990, X:4162429, ED50), Kirazlıkoyak, Musluk, Kuşkayası (Y:254964, X:4163118, ED50), Höçkeren Yurt Yeri and Doncu (Y:250978, X:4161687, ED50) deposits in Kadirli.

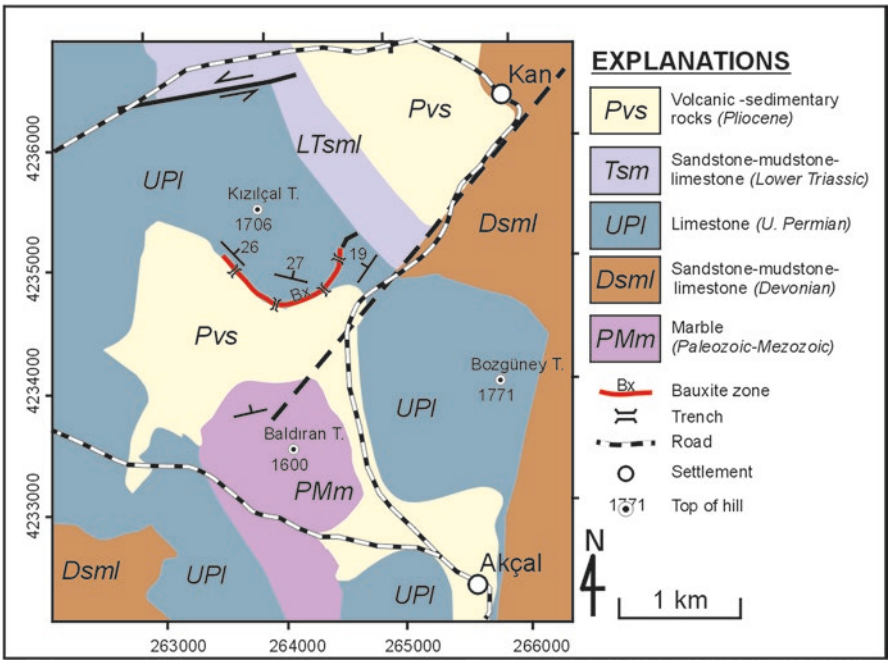

Fig. 15.32 Geological map of the Kızılçal Tepe bauxite deposit. (Map is simplified after MTA 2002, and the bauxite zone is taken from Kaptanoğlu 1965)

15.8 Islahiye-Payas Province

The Islahiye-Payas iron-rich bauxite province is located on the Arabian Platform in southern Turkey (Fig. 15.1). The deposits are concentrated northeast of the Payas and between the Islahiye and Hassa settlements (Fig. 15.33). The iron-rich bauxites formed along the unconformity between the Turonian and Cenonian units as karstic-type deposits.

Data about the iron-rich bauxite deposits in this province were obtained from Koç and Değer (1991) and Çağatay and Arman (1982) for the Payas region and from Göksu (1953) and MTA (1980, 2009) for the Islahiye–Hassa region.

The Payas region deposits are located along the unconformity between the Karadağ limestone (L. Cretaceous) and the Amanas olistostrome (U. Cretaceous) as intermittent lens-shaped deposits and within the Karadağ limestone (Fig. 15.34) as karstic-type deposits (Koç and Değer 1991). The important iron-rich bauxite zones in the Payas region are Fındık Yaylası (II and II), Paşanıneğrisi Yayla, Sarıyokuş Mağarabaşı, Pınarcık Yayla (I and II) and Kozlu Dere (Fig. 15.34). The bottom contact of the iron-rich bauxite is undulating, and the top contact is regular and is overlain by Cenonian limestone (Fig. 15.35a, b). The ore varies in thickness between 1 and 20 m. The ore has various colours, such as greenish-brown, reddish-brown

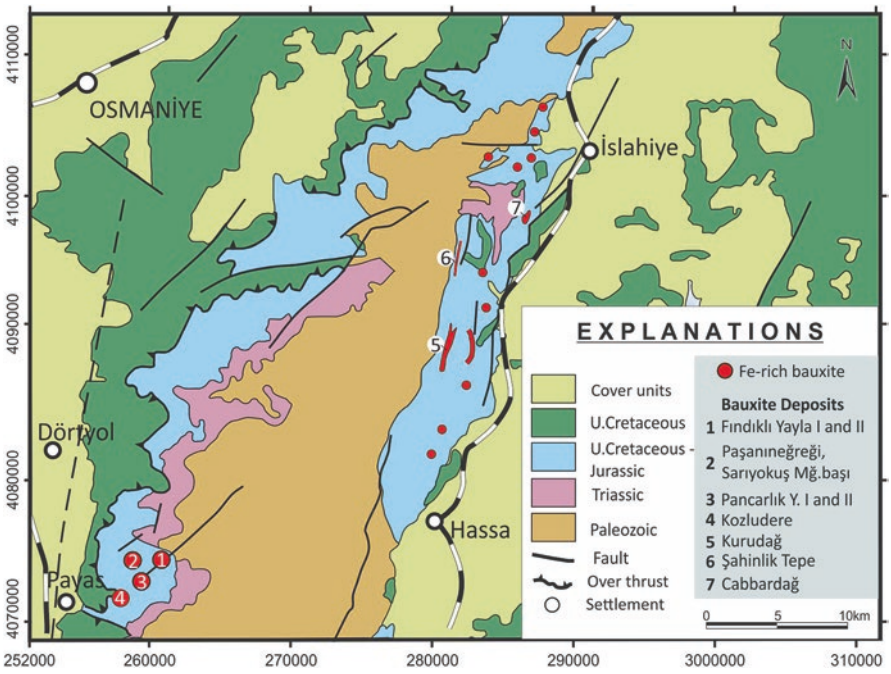

Fig. 15.33 Geological map of the Islahiye-Payas bauxite province. (The geology is simplified from MTA 2002, and the ore locations are taken from Koç and Değer 1991 for Payas and from Göksu 1958 for İslahiye)

and dark brown, and various textures, such as massive, colloidal and oolitic-pisolitic (Koç and Değer 1991).

The bauxite deposits in the Payas region mainly include maghemite and hematite with moderate diasporite and boehmite and minor anatase, rutile, pyrite and kaolinite (Koç and Değer 1991; Çağatay and Arman 1982). The iron-rich bauxite deposits contain approximately 70 Mt of ore (proven and indicated reserve) (MTA 1980) with an average grade of 25% Al_2O_3, 30% Fe, 18.3% SiO_2 and 4% TiO_2 (Koç and Değer 1991). Details of the ore geochemistry of Pancarlık Yayla-I and II, Paşanıneğreği Yayla deposits are given in Table 15.2.

The Islahiye–Hassa region deposits are located between the Islahiye and Hassa settlements and are oriented NE–SW (Fig. 15.33). The deposits formed along the unconformity between Turonian and Cenonian limestones as karstic-type deposits. The bauxite zones in this region are the Cabbardağ, Kurudağ, Şahinlik Tepe, Kaplanbanısı, Hopuzdağ, Tepedağ, Şıhlımanastır, Hassa and Kızılkaya deposits, and the most important deposits are the Kurudağ and Cabbardağ deposits (Fig. 15.33).

The Kurudağ deposit is located approximately 14-km southwest of the Islahiye settlement (Fig. 15.33). The Kurudağ deposit is approximately 3-km long and 0.3-km wide. The ore varies in thickness between 2 and 60 m. The ore body strikes N–S and

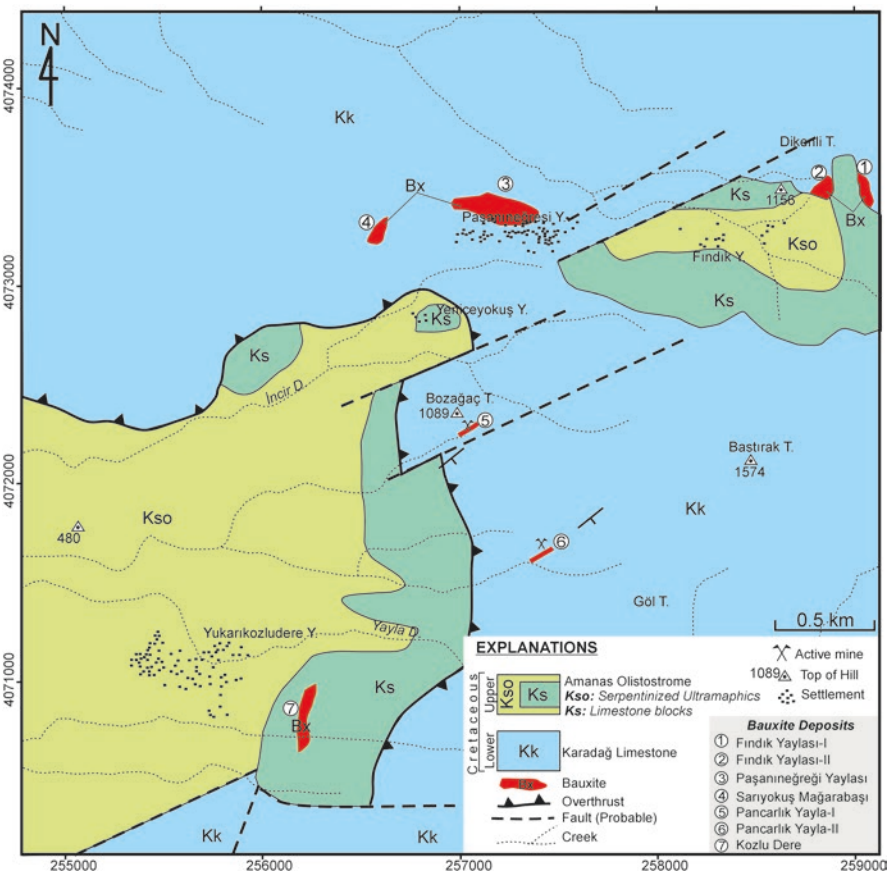

Fig. 15.34 Geological map and location of the iron-rich bauxite deposits in the Payas region. (Modified after Koç and Değer 1991)

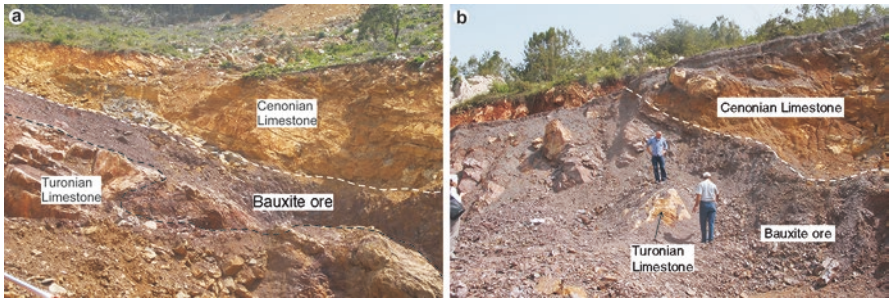

Fig. 15.35 The sharp and regular contact between the hanging wall limestone and iron-rich bauxite zone in the (**a**) Pancarlık Yayla-I and (**b**) Pancarlık Yayla-II deposits

dips 30–40°E. The Kurudağ bauxite deposit is composed of approximately 30% kaolinite, 27% hematite, 21% boehmite, 14% diaspore and 6% anatase and contains 28–68% Al_2O_3, 11–55% Fe_2O_3, 1–25% SiO_2 and 2–9% TiO_2 (Park Elektrik AŞ 2006).

The Cabbardağ bauxite deposit is located approximately 5-km southwest of the Islahiye settlement (Fig. 15.33). The deposit has dimensions of 300 m by 200 m and is up to 40-m thick (MTA 1980; Guleman 1946). The bauxite zone strikes N–S and dips towards the west at 25–30° (Göksu 1953).

The bauxite deposits (Cabbardağ, Kurudağ, Şahinliktepe, Kaplanbanısı, Hopuzdağ and Tepedağ) between Islahiye and Hassa contain approximately 95.8 Mt of ore resources (MTA 2009) with an average composition of 38% Al_2O_3, 33% Fe_2O_3, 17% SiO_2 and 5.7% TiO_2 (Çağatay and Arman 1982).

In summary, in contrast to the other bauxite provinces in Turkey, the Islahiye-Payas iron-rich bauxite province is located on the Arabian Platform. The bauxite formed along unconformities between the Turonian and Cenonian limestones as karstic-type deposits. The mineral paragenesis includes hematite, magnetite, diaspore, boehmite, kaolinite, maghemite, berthierine, anatase, rutile, quartz and pyrite in various proportions. While the deposits of the Payas region are rich in Fe, those in the Islahiye–Hassa region are rich in Al. Because of the hematite, magnetite and very rare chromite in the paragenesis (Çağatay and Arman 1982) suggested that these deposits developed via weathering of the especially Al-rich parts of ophiolitic rocks. The bauxitisation processes occurred on a gentle topography because of long-term atmospheric effects on the Al-silicate-rich rocks and then filled the karstic cavities with transported material (Koç and Değer 1991).

15.9 Kokaksu Province

The Kokaksu bauxite deposit is located in the city of Zonguldak in northern Turkey, which is in the Pontide zone (Fig. 15.1), and is approximately 3 km from the Zonguldak port. The deposit was discovered in 1939 by MTA and was studied in detail by Arni (1938), Göksu (1958), and Yomralıoğlu (1981).

The Kokaksu bauxite deposit is located on the unconformity between Lower Carboniferous (Dinantian) chert-bearing limestone and the Lower Cretaceous (Aptian) sandstone that is known as the Velibey Sandstone (Fig. 15.36) (Göksu 1958). The bauxite crops out in Kokaksu, Sapanlıdere, Aydındere, Erikli, Rüzgarlıçeşme and Güdüllü and contains intermittent lens-shaped karstic-type deposits (Yomralıoğlu 1981). While the bottom contact of the bauxite with the footwall limestone is undulating, the top contact with the hanging wall sandstone is regular. The most extensive outcrops of the bauxite zone are located in the vicinity of Hayat Tepe hill and form 1-km lens-shaped deposits (Fig. 15.36). The thickness of the ore varies between 2.5 and 10 m.

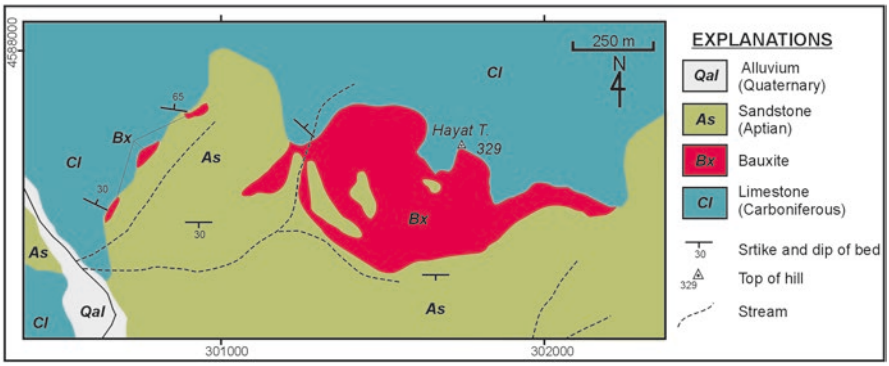

Fig. 15.36 Geological map of the Kokaksu bauxite deposit. (After Göksu 1958)

The ore has various colours, such as reddish-brown, grey, greyish-green and greenish-yellow. The deposit is composed of hard and soft earthy bauxite zones which are intertwined (Göksu 1958), and the hard bauxite is dominant. The hard bauxite has a massive and pisolitic texture. Göksu (1958) suggested that the earthy soft bauxite ore that includes liberated pisolite grains formed secondarily via in-situ weathering of the hard bauxite ore.

The Kokaksu bauxite includes diasporite, boehmite and limonite as major minerals, limonite and kaolinite as moderate minerals and anatase and rutile as rare minerals (Çağatay and Arman 1982). The hard pisolitic bauxite ore has an average grade of 52% Al_2O_3, 5.6% SiO_2, 26.6% Fe_2O_3 and 2.9%TiO_2 (Table 15.2). The deposit was mined occasionally between 1980 and 1982 and contains approximately 7.2 Mt of ore resource.

15.10 Conclusions

The bauxite deposits in the Anatolide–Tauride Platform; are located below the unconformity contacts of Lower Triassic units (Alanya Province), of Jurassic units (Milas–Yatağan, Bolkardağı, Alanya, Tufanbeyli–Saimbeyli–Kadirli and Yalvaç–Sarkikaraagaç Provinces) and of Upper Cretaceous units (Seydişehir–Akseki Province). The Payas–Islahiye bauxites in the Arabian Platform are located below the unconformity contact of the Upper Cretaceous sequence (Turonian–Senonian), while the bauxites of the Pontides occur below the Lower Cretaceous unconformity contact.

The majority of economically mineable bauxite deposits in Turkey are the karstic-type, but lateritic-type deposits (e.g. Yalva–Sarkikaragaç) can be partially economical. While boehmite is the principal ore mineral in the Akseki–Seydişehir and the Yalvaç–Şarkikaraağaç Provinces, diasporite is a dominant ore mineral in the rest of the bauxite provinces in Turkey. Average Al_2O_3 content of economically

mineable deposits are 54% for the Milas–Yatağan, 59% for the Seydişehir–Akseki and 56% for the Bolkardağı Province. ΣREE contents of bauxite deposits in each province show variations. Average ΣREE contents are 131, 225, 249, 358, 709 and 970 ppm for the Yalvaç–Şarkikaraağaç, the Payas, the Kokaksu, the Seydişehir–Akseki, the Bolkardağı and the Milas–Yatağan provinces, respectively.

Acknowledgements The author is grateful to Dr. Cem Kasapçı (PhD) and Fatih Özbaş (MSc) at Istanbul University-Cerrahpaşa for helping to draw the figures. The logistical support of the MTA (General Directorate of Mineral Research and Exploration) during the field studies is appreciated. The author is grateful to the MTA geologists İsmet Alan and Yavuz Bedi for valuable contributions to the Bolkardağ and Alanya province bauxites, respectively. Special thanks to Halil Demirel (MSc., Demireller Mining Co.) and Olgay Al (Mining Eng.) for sharing their company reports, and to Mustafa Adır (MSc. Geologist, Eti Aluminyum A.Ş.) for sharing data about the Seydişehir province bauxite deposits.

This work was partly supported by the Research Fund of Istanbul University, Project No. YADOP-15161.

References

Al O (2015) Production and feasibility report of the bauxite deposits of Demireller Mining Company. p 15. Mersin (unpublished)

Al O (2016) Kocaalan ve Göbekdağ (Milas–Muğla) Boksit Yataklarına ait Jeolojik Rapor [Geological report of Kocaalan and Göbekdağ (Milas-Muğla) bauxite deposits]. p 3. (unpublished)

Alan İ, Şahin Ş, Keskin H, Altun İ, Bakırhan B, Balcı V, Böke N, Saçlı L, Pehlivan Ş, Kop A, Hanilçi N, Çelik ÖF (2007) Orta Toroslar'ın Jeodinamik Evrimi Ereğli (Konya) – Ulukışla (Niğde)-Karsantı (Adana)- Namrun (İçel) Yöresi [Geodynamic Evolution of Central Taurus, Ereğli (Konya) – Ulukışla (Niğde)- Karsantı (Adana)- Namrun (İçel) regions]. General Directorate of Mineral Research and Exploration Report no 11006. Ankara (in Turkish, unpublished)

Alan İ, Şahin Ş, Elibol H, Keskin H, Altun İ, Bakırhan B, Balcı V, Böke N, Kop, A, Esirtgen T, Hanilçi N (2011a) Orta Torosların Jeodinamik Evrimi Bozyazı-Aydıncık-Gülnar-Silifke (İçel) Yöresi [Geodynamic Evolution of Central Taurus, Bozyazı- Aydıncık-Gülnar-Silifke (İçel) regions]. General Directorate of Mineral Research and Exploration Report no 11462. Ankara (in Turkish, unpublished)

Alan İ, Şahin Ş, Kop A, Bakırhan B, Böke N (2011b) The tectonostratigraphic features of the Belemedik tectonic window and its surroundings. Bull Min Res Exp 143:13–35

Apaydın N, Erseçen N (1981) Known ore and mineral resources of Turkey. Publication of Mineral Reseacrh and Exploration Institute, No: 185, p 67. Ankara

Arni P (1938) Kurzer Vorbericht über Ainige Ausbisse eines oxydischen Eisen Alluminium-Erzes, südlich bei Zonguldak [Short preliminary report on some outcrops of an oxide iron ore, south near Zonguldak]. General Directorate of Mineral Research and Exploration Report no 888 (unpublished)

Aydoğan M, Moazzen M (2012) Origin and metamorphism of corundum-rich metabauxites at Mt. Ismail in the Southern Menderes Massif. SW Turk Resour Geol 62(3):243–262

Ayhan A, Karadağ MM (1985) Şarkikaraağaç (Isparta) güneyinde bulunan boksitli demir ve demirli boksit yataklarının jeolojisi ve oluşumu [Geology and origin of bauxitic iron and ferruginous bauxite deposits in the South of Şarkikaraağaç (Isparta)]. Bull Geol Soc Turk 28:137–146 (in Turkish with English abstract)

Bárdossy G (1982) Karst bauxites. Bauxite deposits on carbonate rocks. Elsevier Sci. Publ, Amsterdam, p 441

Bárdossy G, Aleva GJJ (1990) Lateritic bauxites. Developments in economic geology, vol 27. Elsevier Sci. Publ, Amsterdam, p 624

Baysal O, Engin NA (1976) Değirmenlik–Kızıltaş Boksit Yatağı [Değirmenlik-Kızıltaş Bauxtie deposit]. J Earth Sci App Res Centre Hacet Univ 2:140–160 (in Turkish with English abstract)

Bedi Y, Öztürk EM (2001) Alanya–Köprülü (Antalya) Dolayının Jeolojisi (Alanya 028 c1, d1, d2 ve d3 paftaları) [Geology of the Alanya-Köprülü (Antalya) Region (Alanya 028 c1, d1, d2 ve d3 scale map sheets]. General Directorate of Mineral Research and Exploration Report no 10488. (in Turkish, unpublished)

Blumental M, Göksu E (1949) The geology and genesis of the bauxite occurrences of the Akseki region. J Mineral Res Explor Inst Turk 14:1–58

Bozkır Y (2007) REE and formation conditions of bauxites between Çarıksaraylar and Kozluçay (Sarkikaraağaç–Isparta). MSc thesis Selçuk University Graduate School of Naturel Applied Sciences. p 105. (unpublished)

Bulur K (1979) Şarkikaraağaç Isparta-Beyşehir Konya arasındaki boksit sahasının jeolojisi. [Geology of the bauxite deposit between Şarkikaraağaç (Isparta) and Beyşehir (Konya)]. MSc Thesis İstanbul University. p 33. (unpublished)

Combes PJ (1990) Typologie, cadre géodynamique et genèse des bauxites françaises. Geodin Acta 4:91–109

Combes PJ, Oggiano G, Temussi I (1993) Geodynamique des bauxites sardes, typologie, génese et controle paleotectonique. Comptes Rendus de I'Académie des Sciences Sèrie II 316, 403–409

Çağatay A, Arman B (1982) Boksit ve Türkiye'deki Boksit Yatakları [Bauxite and bauxite deposits of Turkey]. Geol Eng Turk 14:28–33

Demireller Mining Co. (2008) Kocaalan ve Göbekdağ (Milas–Muğla) Boksit Yataklarına ait Jeolojik Rapor [Geological report of Kocaalan and Göbekdağ (Milas-Muğla) bauxite deposits]. p 3. (unpublished)

Etibank (1975) Bafa–Milas, Milas–Yatağan–Muğla ve Söke Diyasporit-Zımpara sahaları arama programı [Exploration programme of Bafa-Milas, Milas–Yatağan–Muğla and Söke diaspore–emery deposits]. Etibank Milas Directorate, Report no: 883. p 16. (unpublished)

Etibank (1992) Aktaş (Milas–Muğla) Yatağının Arama Raporu [Exploration report of Aktaş (Milas-Muğla) deposit]. Etibank Department of Mineral Exploration, Ankara. p 22. (unpublished)

Garcia-Garmilla F, Özer S, Sarı B (2004) Cathodoluminescence and metamorphism in rudist shells from the upper cretaceous marbles of Menderes massif (western Turkey). Geogaceta 36:167–170

Göksu E (1953) Akseki (Antalya) Boksit yataklarının Jeoloji, Jenez ve Maden bakımından etüdü ve diğer Türkiye ve Avrupa Boksitleriyle mukayesesi [Geology, genesis and ore prospecting of Akseki (Antalya) bauxite deposits and comparison with Turkey and Europe bauxite deposits]. Geol Bull Turk 04(2):79–136 (in Turkish)

Göksu E (1958) Zonguldak–Kokaksu Boksitleri [Bauxite deposit of Zonguldak-Kokaksu]. Bull Min Res Exp 50:81–93 (in Turkish)

Guleman HA (1946) Türkiye Boksitleri [Bauxites of Turkey]. General Directorate of Mineral Research and Exploration Report no E 1667. (unpublished)

Hanilçi N (2013) Geological and geochemical evolution of the Bolkardaği bauxite deposits, Karaman, Turkey: transformation from shale to bauxite. J Geochem Explor 133:118–137

Hanilçi N, Alan İ, Keskin H, Sahin Ş, Saçlı L (2006) Bolkardağı Bölgesi (Ayrancı–Karaman) Boksit Yatakları: Jeolojisi ve Oluşumuna Ait İlk Bulgular [Bolkardağı Province (Ayrancı–Karaman) bauxite deposits: preliminary evidence for their geology and formation]. Abstract Book 59th Turkey Geology Congress. pp 157–159

Hatipoğlu M (2011) Al (Fe,Ti,Si)-mobility and secondary mineralization implications: a case study of the karst unconformity diasporite-type bauxite horizons in Milas (Muğla), Turkey. J Afr Earth Sci 60:175–195

Kaptanoğlu H (1965) Mağara-Kan Köy Diasporit Zuhurları ve Sondaj Neticeleri [Diasporite outcrops and drilling results of Mağara-Kan Köy]. General Directorate of Mineral Research and Exploration Report non 3829. (İn Turkish, unpublished)
Karadağ M (1987) The geological and petrographic and genetical investigation of the Seydişehir region bauxites: unpublished Ph.D. dissertation, Selçuk, Selçuk University, p 265
Karadağ MM, Küpeli S, Arık F, Ayhan A, Zedef V, Döyen A (2009) Rare earth element (REE) geochemistry and genetic implications of the Mortaş bauxite deposit (Seydişehir/Konya — southern Turkey). Chem Erde-Geochem 69(2):143–159
Koç Ş, Değer MA (1991) Genesis of bauxite bearing iron ore deposits from Payas (Hatay) district. Bul Min Res Exp 113:113–126
Laville P (1981) La formation bauxitique provençale (France). Séquence des facies chimiques et paléomorphologie crétaceè. Chronique de la Recherche Miniére 461:51–68
MTA (1965) Türkiye Zımpara, Diasporit ve Boksit Yatakları [Emery, diaspore and bauxite deposits of Turkey]. Publication of Mineral Research and Exploration, Publication no 122. Ankara, p 18
MTA (1980) Türkiye Aluminyum Envanteri [Aluminum inventory of Turkey]. Publication of Mineral Research and Exploration, Publication no 181. Ankara, p 95
MTA (2002) 1/500 000 scaled geological map of Turkey. MTA
MTA (2009) Türkiye Yeraltı Kaynakları (İllere gore) [Mineral resources of Turkey (According to Province)]. Publication of Mineral Research and Exploration, Earth Science and Culture Series-5. Ankara, p 602. ISBN 978–605-4075-32-4, MTA
Okay A, Tüysüz O (1999) Tethyan sutures of northern Turkey. Geol Soc Lond Sp Publ 156:475–515
Öncel MS (1995) Şarkikaraağaç–Yalvaç (Isparta) arasının jeolojisi ve boksit zuhurlarının mineralojik, petrografik, jeokimyasal incelemesi [Geology of Şarkikaraağaç-Yalvaç (Isparta) and mineralogical, petrographical, geochemical investigation of bauxite occurrences]. PhD thesis Selçuk University. p 147. (in Turkish, unpublished)
Öncel MS, Söğüt AR (2008) Kaletepe Lateritik Boksit Zuhurunun Mineralojik ve Jeokimyasal İncelemesi [Mineralogical and geochemical investigation of lateritic bauxite occurrence in Kaletepe]. SÜ Müh Mim Fak Derg 23(4):73–82 (in Turkish with English abstracts)
Özen Bozkır Y, Arık F, Ayhan A, Öztürk A (2010) Geochemical comparison between the lateritic bauxites Hosted by the Basic Volcanics of Cariksaraylar and Kozlucay Occurrences (Isparta, Turkey). AUI-G, 2010, Sp Issue GEO IASI. pp 80–81
Özgül N (1976) Torosların bazı temel jeolojik Özellikleri [Some basic geological features of the Taurides]. Bull Geol Soc Turk 19:65–78 (in Turkish with English abstract)
Özlü N (1978) Etude géologique minéralogue et géochmıque des bauxites de la région D'Akseki-Seydis¸ehir Taurus occidental-Turquie. PhD dissertation, Pierre Marie Curie University, Paris. p 455. (unpublished)
Özlü N (1979) New facts on the genesis of the Akseki-Seydişehir bauxite deposits. Bull Geol Soc Turk 22:215–226
Öztürk H, Hanilçi N, Işık A (1998) The geology and sulfide zones of the Doğankuzu and Mortaş bauxite deposits, Seydis¸ ehir, Turkey [abs.]: Geological Congress of Turkey, 52nd, Abstracts, p. 6
Öztürk EM, Akdeniz N, Bedi Y, Sönmez İ, Usta D, Kuru K, Erbay G (1995) A different approach to the stratigraphy of the Akanya Nappe. Bull Geol Cong Tur 10:2–10 (Turkish with English Abstract)
Öztürk H, Hein JR, Hanilçi N (2002) Genesis of the Doğankuzu and Mortaş bauxite depoists, Taurides, Turkey separation of Al, Fe and Mn and implications for passive margin metallogeny. Econ Geol 97:1063–1077
Öztürk H, Hanilçi N, Altuncu S, Kasapçı C (2018) Rare Earth Element (REE) resources of Turkey: an overview of their formation types. Bull Min Res Exp. 159, doi: https://doi.org/10.19111/bulletinofmre.471205 (Accepted, In Press)
Park Elektrik AŞ (2006) Islahiye, Kurudağ Boksitleri Sondaj ve Kimyasal Analiz Raporu [Drilling and chemical analysis report of Islahiye, Kurudağ bauxites]. (Unpublished company report)

Patterson SH, Kurtz HF, Olson JC, Neely CL (1986) World bauxite resources: U.S. geological survey professional paper 1076-B, p 151

Pelen A (1977) Doğankuzu (Güney Bloku) boksit yatağı arama raporu [Exploration report of Doğankuzu (South Block) bauxite deposit]. Etibank, ATGB, Bauxite Exploration and Prospect Directorate, Seydişehir. p 21. (unpublished)

Pelen A, Vuran A (1978) Mortaş boksit yatağı arama raporu [Exploration report of Mortaş bauxite deposit]. Etibank, ATGB, Bauxite Exploration and Prospect Directorate, Seydişehir, p 18 (unpublished, in Turkish)

Peyronnet P (1971) Alanya Bölgesinin (Güney Toroslar) Jeolojisi, Metamorfik Boksitin Kökeni [Geology of Alanya District (South Taurus), genesis of metamorphic bauxite]. Bull Min Res Exp 76:154–160 (in Turkish)

Robertson AHF, Ustaömer T (2009) Upper Palaeozoic subduction/accretion processes in the closure of Palaeotethys: evidence from the Chios Melange (E Greece), the Karaburun Melange (W Turkey) and the Teke Dere Unit (Sw Turkey). Sediment Geol 201:29–59

Temur S, Kansun G (2006) Geology and petrography of the Masatdagi diasporic bauxites, Alanya, Antalya, Turkey. J Asian Earth Sci 27:512–522

Umut M (2009) 1:100000 ölçekli Türkiye Jeoloji Haritaları, No: 119, AFYON-L26 PAFTASI. [1:100000 scale geological maps of Turkey, No: 119, AFYON-L26 map scale sheet]. MTA, Ankara, p 22

Wippern J (1962) The bauxites of the Taurides region and their tectonic setting. Bull Min Res Exp 58:47–70

Yalçın Ü (1987) Pertologie und geochemie der Metabauxite SW-Anatoliens. PhD Thesis Bochum Ruhr-Univ. p 136. (Unpublished)

Yılmaz İ (2004) Doğu Toroslarda Mansurlu-Saimbeyli (Adana) alanının Jeolojisi ve tektonik özellikleri [Geology and tectonic features of the Mansurlu-Saimbeyli (Adana) area in the Eastern Taurus]. PhD Thesis İstanbul University. pp 1–194. (in Turkish with English abstract, unpublished)

Yomralıoğlu T (1981) Zonguldak Kokaksu–Aydındere–Erikli Boksitleri Jeoloji İncelemesi [Geological survey of Zonguldak Kokaksu–Aydındere–Erikli bauxites]. General Directorate of Mineral Research and Exploration Report no 3502. (unpublished)

Chapter 16
Magnesite and Olivine Deposits of Turkey

Haşim Ağrılı

Abstract Two types of magnesite occurrences have been identified in Turkey based on their origin of formation. The first is of sedimentary type magnesite occurrences. This type of magnesite is found in Denizli–Çardak and Erzincan–Çayırlı. The second cryptocrystalline type of magnesite constitutes the remainder of the entire resources of Turkey (İrkeç T, Kapkaç F. Türkiye'de Bilinen Manyezit Yatak ve Zuhurlarının Değerlendirilmesi ile Aramalara Yönelik Öneriler [Evaluation of known magnesite deposits and occurrences of Turkey with suggestion for exploration]. General Directorate of the Mineral Research and Exploration Report no 8863, Ankara (in Turkish, unpublished, 1989). There are three main magnesite provinces in Turkey, namely the Kütahya–Eskişehir–Bursa province, the Konya Province and the Çankırı–Erzincan–Erzurum–Sivas Province (Fig. 16.1). Kütahya–Eskişehir–Çankırı and Konya Provinces have the largest magnesite reserves in Turkey. Magnesite reserves of Turkey as of 2016 vary considerably with respect to sources. According to the MTA data, Turkey has about 111 million tonnes of magnesite (41–48% MgO) (www.mta.gov.tr, 2015). Ophiolites in Turkey are quite widespread as a result of the geological evolution of the country. Ophiolitic units have economic potential in terms of hosting industrial raw-materials and metallic-mineral systems. One of the important industrial raw material in ophiolitic units is olivine. The ophiolites expose in Bursa, Muğla, Konya, Isparta, Hatay and Erzincan provinces in Turkey have important olivine occurrences. The Bursa and Erzincan occurrences are situated in the İzmir–Ankara–Erzincan suture zone, whereas the olivine occurrences in Hatay exposed in the northernmost part of the Dead Sea Fault Zone. Olivine occurrences in Muğla are in the westernmost edge of the Taurus Mountains, and lastly, the olivine occurrences in Konya and Isparta are situated in Central Anatolia.

H. Ağrılı (✉)
MTA Central Anatolian 2nd. Regional Directorate,
Selçuklu–Sancak Mh, Konya, Turkey
e-mail: hasim.agrili@mta.gov.tr

F. Pirajno et al. (eds.), *Mineral Resources of Turkey*, Modern Approaches
in Solid Earth Sciences 16, https://doi.org/10.1007/978-3-030-02950-0_16

16.1 Introduction

Ophiolitic rocks in Turkey are widespread as a result of country's geotectonic settings and position. Various mineralization types can be observed in these ophiolitic rocks. One of the most important mineralisations is magnesite. Another important raw material occurring in the ophiolitic rocks is olivine.

The İzmir–Ankara–Erzincan Suture zone, in the Bursa–Kütahya–Eskişehir region, Çankırı–Sivas–Erzincan–Erzurum region and Konya–Isparta region in central Anatolia are important locations in terms of magnesite occurrences, whereas Bursa, Konya–Isparta, Muğla, Erzincan and Hatay regions have significant resources of olivine. Both magnesite and olivine are currently produced in the mentioned regions.

16.2 Magnesite Deposits of Turkey

16.2.1 Cryptocrystalline (Gel) Magnesite Deposits

16.2.1.1 Eskişehir–Kütahya–Bursa Province

Numerous magnesite deposits of various sizes are observed in a 200-km long zone extending from Bursa–Harmancık to Tavşanlı–İnönü–Eskişehir–Mihallıççık eastward. More precisely, we describe individual deposits in Eskişehir–central, Türkmentokat, Mihallıççık, Beylikova, Alpu and İnönü, Kütahya-central, Tavşanlı, Domaniç ve Seyitömer and Bursa–Harmancık (Figs. 16.1 and 16.2).

Magnesite deposits in this province are hosted either by ophiolite suite itself or serpentinites of the tectonic mélange in the İzmir–Ankara suture (Sarıfakıoğlu

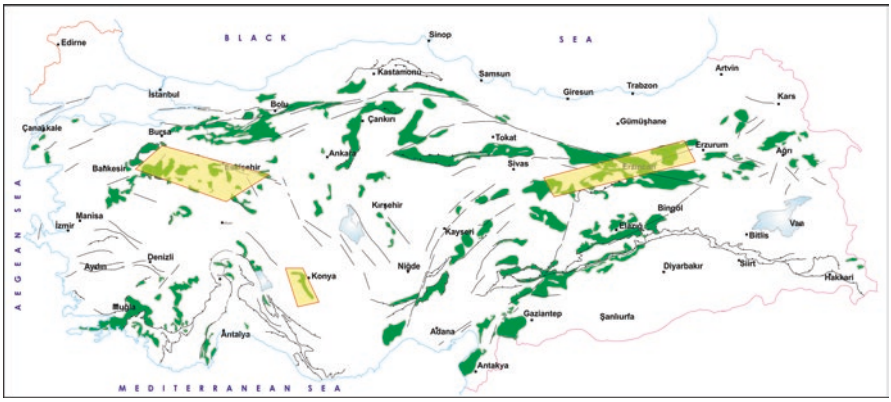

Fig. 16.1 Distribution of ophiolitic rocks and main magnesite areas in the red rectangles. (Simplified from MTA 1:500.000 Geological Map)

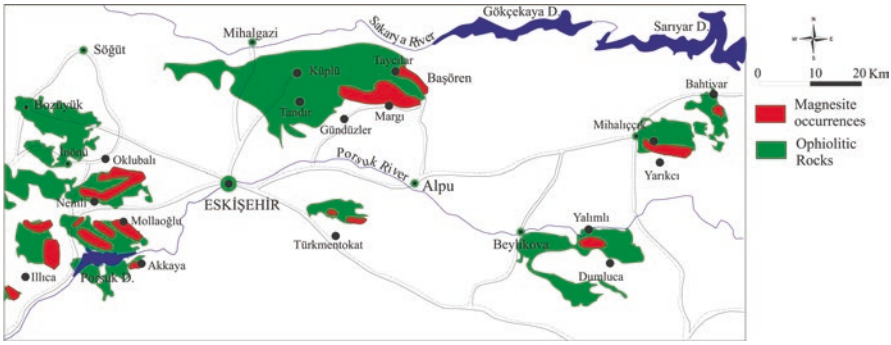

Fig. 16.2 Distribution of magnesite occurrences in the Eskişehir-Kütahya area. (Modified after Çubuk et al. 2011)

2011). Here, the ophiolite suite comprises mostly harzburgites and a lesser amount of dunite, cumulates of gabbros and dolerites. Tectonic mélange on the other hand is composed of serpentine blocks, spilitic basalt, gabbro, diabase, radiolarite and limestone, always with in fault contacts with each other.

CO_2-rich waters play a significant role in the formation of magnesites. Various views are presented regarding the origin of CO_2. These may be of volcanic origin, decarbonatisation of dolomites, meteoric and an origin involving degradation of organic material in soils and decarbonisation of sediments. A mixed origin comprising several of the above mechanisms is also probable (Yılmaz and Kuşcu 2012).

Magnesite deposits are observed in altered peridotites and serpentinites as stockworks, veins, lenticular or nodular bodies developed within joints and fractures of tectonic origin (İrkeç and Kapkaç 1989; Sarıiz 1990; Yersel and Ayday 1992; Çubuk et al. 2011) (Fig. 16.3).

Sarıiz (1990) suggested that magnesites in Türkmentokat area (Eskişehir) are of infiltration type (gel-type) and hydrothermal, with the latter formed under the pressure of 2 kbar and a temperature of 150 °C and with various mole fractions of CO_2. For infiltration type, it is suggested shallow depth (~1 to 2 m). The mineralisation age is proposed as pre-Pliocene, probably Miocene, since magnesite gravels and blocks are observed in the basement gravels of Upper Neogene in the eastern Eskişehir. Mineralisation contains on average magnesite 91.74%, quartz 0.074%, dolomite 2.47%, calcite 1.17% and serpentine 1.72%.

According to Öncel and Denizci (1982), the CO_2 gas from nearby volcanism interacted with groundwater and produced carbonic acid. At a later stage, these CO_2-saturated water infiltrated through the ophiolitic rocks causing serpentinisation and resulting in the formation of magnesites. Subsequent tectonic events further complicated the geometry of deposits.

Magnesites in Mihalıççık area occur as veins and stockworks. Veins are localised either in serpentines or through the boundary with the Middle-Late Miocene siliciclastics. Stockwork magnesites are mostly seen in serpentines underlying the listvenites. The average content of the individual magnesite veins are 43.73%

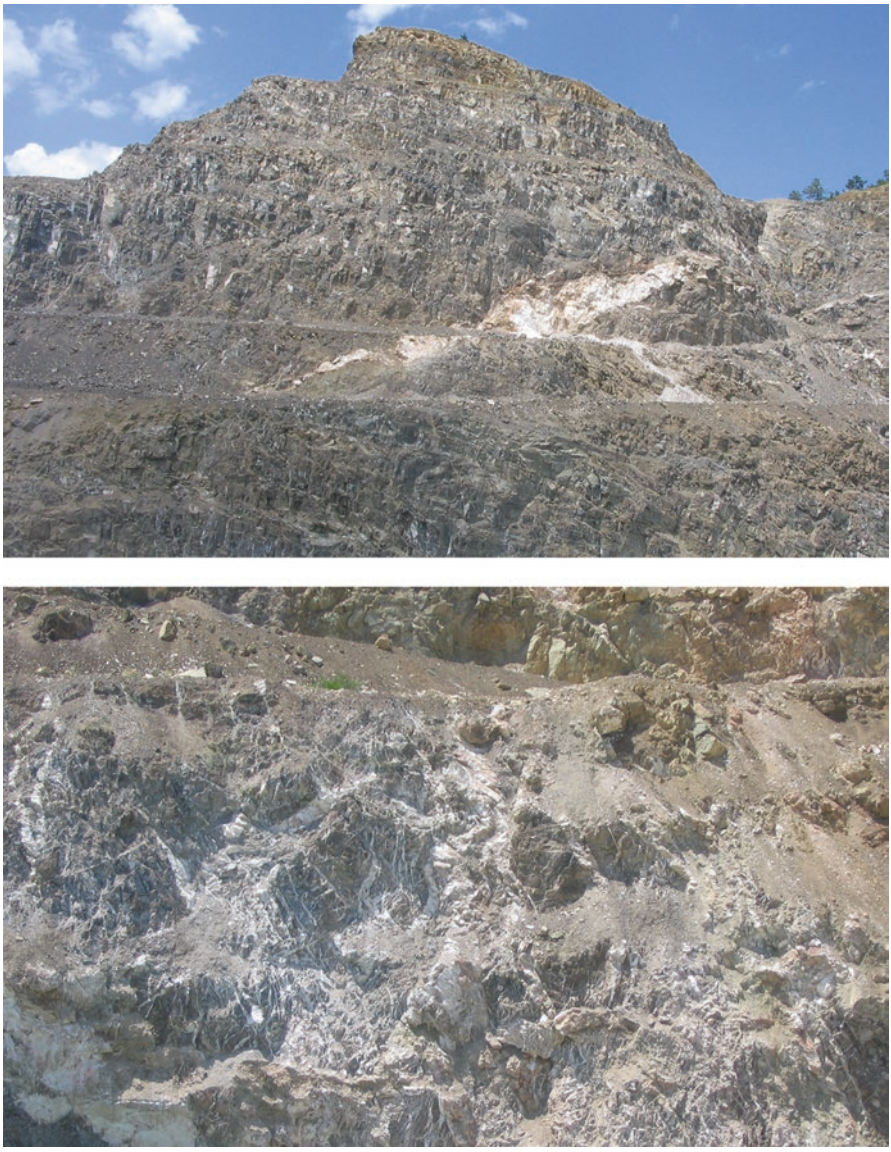

Fig. 16.3 Vein and stockworks of magnesite occurrences in the Eskişehir-Kütahya area

MgO, 2.95% SiO_2, 0.75% Fe_2O_3 and 3.73% CaO while stockwork is 47.04% MgO, 0.39% SiO_2, 0.55% Fe_2O_3 and 1.15% CaO (Yılmaz and Kuşcu 2007).

Isotopic studies by Yılmaz and Kuşcu (2008) indicated two end processes, such as the atmospheric CO_2 and decarbonisation of organic-rich sediments. They suggested that an origin involving a mixture of the above end members and even

volcanic CO_2 is also probable. They proposed that the magnesite deposition occurred after the serpentinisation in low temperatures close to surface.

The Bursa region is located in the westernmost part of the province. Ophiolitic rocks in the region comprises dunite, harzburgite, serpentinised ultramafics and a lesser amount of gabbro. Magnesites are related to serpentinites and occur as nodular and stockwork bodies (Çubuk et al. 2011).

This province is one of the most important province of Turkey economically in terms of hosting significant magnesite deposits that have been mining for many years.

16.2.1.2 Konya Province

Magnesite deposits occurring in Meram, Yunak, Ereğli and Karaman were developed specifically within serpentinites in the altered ultramafic rocks in the Konya Province (İrkeç and Kapkaç 1989; Çubuk et al. 2011) (Fig. 16.4). Some parts of the mineralisation occurs as stockworks and bands in serpentinites and are probably related to the folding, fracturing and overthrusting processes during the obduction of ophiolites (Şimşek 1975). The remaining mineralisation occurs as irregular blocks and lenses of massive nodules (Yeniyol and Önder 1978).

The Çayırbağ magnesite mineralisation is of cryptocrystalline texture developed in the late Cretaceous altered serpentinites. Here, one can distinguish the secondary magnesites that cut across the primary ones. The primary magnesites are more compact and display concoidal fracturing due to higher silica content while the secondary type is softer. Another type of mineralisation in the same area is formed in Miocene sediments in relation to surficial conditions (Tuncay 2000).

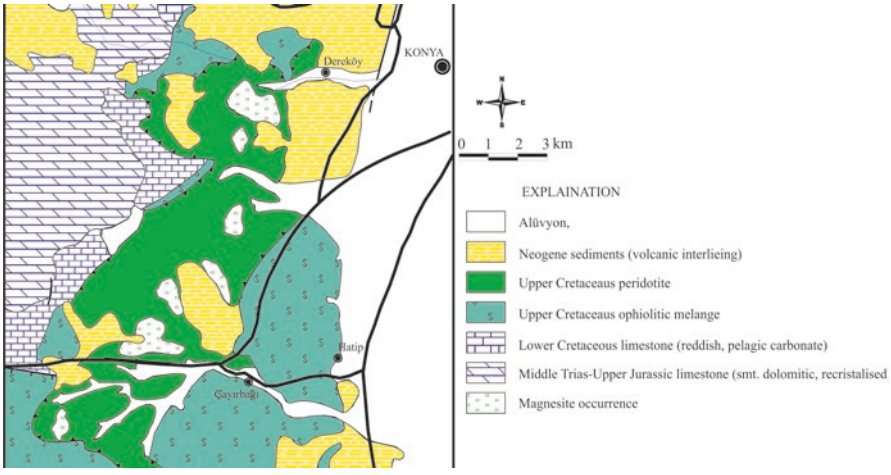

Fig. 16.4 Geological map of the Konya area. (Modified after Çubuk et al. 2011; Şimşek 1975; Kıyıcı and Baybörü 1978)

Yılmaz and Kuşçu (2007) reported that, according to Zedef et al. (2000), the origin of the CO_2 that resulted in the magnesite mineralisation in this province is organically rich sedimentary rocks that are underlain by ophiolites and the mineralisation temperature was in the range 80–100 °C.

According to Önal (2007), the origin of the water that gave rise to the formation of magnesite mineralisation is meteoric or vadose. In Önal opinion, magmatic water was not primarily effective, but they cannot be totally ignored in the formation of secondary magnesites related to the fault zones. According to some diagrams, the mineralisation temperature is lower than 300 °C and CO_2 containing fluid is less than 4%.

Average chemical composition of the province is as follows: 2–6% SiO_2, 0.3–1.2% CaO and 44.3–47.79% MgO (İrkeç and Kapkaç 1989).

16.2.2 Sedimentary Magnesite Mineralisation

16.2.2.1 Denizli Province

The Çardak–Çameli Neogene basin where the sedimentary magnesites are hosted is a depression surrounded by Mesozoic-aged ultramafics and limestones and the Paleocene-aged siliciclastics and carbonates. Neogene sediments are of Late Miocene (?) to Lower Pliocene, and are composed of a lower alternating conglomerate-sandstone-mudstone, a middle limestone–marl–clayey limestone and an upper dominantly limestone subunit (Fig. 16.5). The Lower subunit is formed in alluvial fan environment. The middle subunit is attributed to a lake coastal plain and the limestones at the top were formed in the lake environment. Magnesites accompanied by huntite and sepiolites are observed in ancient coastal plains and lake environments (Akbulut 2003).

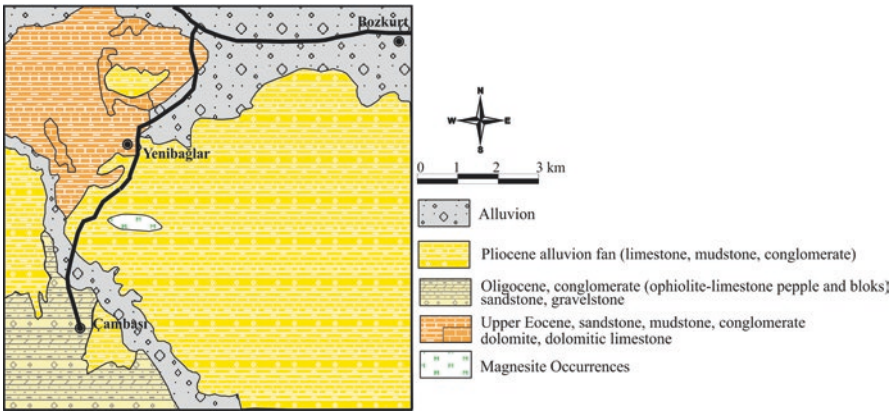

Fig. 16.5 Geological map of the Denizli area. (Modified after Çubuk et al. 2011; Şenel 1997)

Mineralisation is surrounded by the Pliocene sediments and sandwiched between dolomites. The transition between the units is sharp. Transition between sepiolite and magnesite is rather gradual and generally lower part is sepiolitic. Mineralisation here comprises dolomite, hydrated silicates and magnesite (Brennich 1958, 1959).

According to İrkeç and Kapkaç (1989), the average chemical composition is 43.8% MgO, 1.6–3.6% SiO_2 and 2.20–3% CaO, and the proven reserve is 450,000 tonnes.

16.2.2.2 Erzincan Province

In the Çayırlı area where magnesites occurrences are observed, the oldest rocks units are Palaeozoic metamorphic rocks and Anatolian ophiolitic melange. These basement rocks are unconformably overlain by Lower-Middle Miocene detrital and marl units, which are thought to be deposited in marine, lagoonal to lake environments. Magnesites are observed within the lacustrine intervals of marl, mudstone and gravelly mudstone (Arslan 1987; Çubuk et al. 2011).

Individual magnesite levels display bedding. Each magnesite level is high-quality in its medial part and is increasingly siliceous towards the upper and lower contacts. Lower and upper siliceous magnesites would be 15–20 cm thick (İrkeç and Kapkaç 1989; Kocaefe 1982; Çubuk et al. 2011).

The mineralisation has the following composition: 2% SiO_2, 1% CaO, 44–46% MgO and 50–52% LOI (Çubuk et al. 2011; İrkeç and Kapkaç 1989).

16.2.2.3 Isparta Province

Magnesite occurrences in the Isparta province are of sedimentary type. The excess Mg for the formation of magnesite was derived from the alteration of ultramafic rocks and transported by surface and groundwater to the site of deposition. The origin of the CO_2 is supposed to be atmospheric or derived from anaerobic reactions in lignites in deeper levels. Formation temperature of magnesite ranges from 13 to 42 °C. Mineral paragenesis is calcite, dolomite, Mg-calcite, huntite and magnesite ($MgCO_3$). This formation that occurs in freshwater lacustrine is a sedimentary, massive magnesite occurrence (Topak 2006).

16.2.3 Other Mineralisation Sites

16.2.3.1 Erzurum–Erzincan Province

In this province, magnesite mineralisation occurs in three areas, namely Erzurum-Centre, Oltu and Aşkale. Ophiolitic rocks in the area comprise gabbro, microgabbro, diabase and peridotite, while meta-ophiolites are derived from pyroxenite,

olivine-gabbro and sheeted dykes. It is suggested that hot fluids entrained through tectonic fractures gave rise to the formation of listvenite, magnesite, opal and serpentinites (Çubuk et al. 2011).

Magnesites are formed in fault zones juxtaposing various lithologies or in serpentinised dunite and harzburgite bodies (Kocaefe 1982).

Major oxide chemistry of the magnesites of this area is as follow: 42–47% MgO, 0.04–7.10% CaO and 0.05–3.05% SiO_2 (Çubuk et al. 2011).

In the Refahiye district of the Erzincan province, one of the secondary splays of the North Anatolian Fault Zone display magnesites mineralisation within the carbonated and silicified ultramafic rocks. More specifically, the mineralisation has various shapes including lodes, lenses, nodules and blocks at the contacts between silicified and unaltered serpentinites (Çubuk et al. 2011; Kocaefe 1982).

Downward in the mineralisation, SiO_2 decreases to 0.03–13%, while other major oxides are as follow: 41.05–47.75% MgO, 0.11–0.57% CaO and 48.9–51.9% LOI (Kocaefe 1982).

16.2.3.2 Çankırı Province

In the vicinity of Eskipazar, Şabanözü, Kurşunlu and Ilgaz, vein and stockwork mineralisation occurs in ophiolites along the North Anatolian Fault Zone (İrkeç and Kapkaç 1989). The highly fractured nature of rocks along the North Anatolian Fault Zone provided favourable environment for magnesite occurrence (Çubuk et al. 2011).

Ertuğrul (1978) stated that the magnesites in Çankırı city centre are of massive or cauliflower-type and have developed along the fractures (Çubuk et al. 2011).

Average composition of magnesites in the Kurşunlu–Ilgaz area are: 8.26% SiO_2, 1.76% CaO and 42.58% MgO. In other fields nearby, the composition changes significantly: 0.24% SiO_2, 0.9% CaO and 47.37% MgO.

Apart from the above provinces, there are peridotite-hosted veins and stockworks in the Mersin, Balıkesir, Burdur and Kars provinces, and sedimentary magnesites in the Isparta province (İrkeç and Kapkaç 1989).

Magnesites in Mersin province are found in Tarsus. The stratigraphy of this area comprises upper Cretaceous igneous rocks and an ophiolitic suite, Oligocene to Middle Miocene-aged clastic sediments and Quaternary alluvial deposits (Önal 2007). Magnesites occur as dyke-like and small veins of various sizes along the fractures in ultramafic rocks. Tectonic movements following the mineralisation caused local brecciation along the contacts with host rocks (Önal 2007).

16.3 Olivine Deposits of Turkey

16.3.1 Bursa Province

Emre (1986) described the ophiolitic rocks of the Bursa–Orhaneli area (Fig. 16.6) as than "incomplete ophiolitic suite". According to this author, the primary positions of the ophiolitic sub-units are not preserved, cumulates are observed at the base and the tectonites are at the top. Emre (1986) reported that the dunitic host rocks of olivine occur as lenses in the cumulate sub-unit of the ophiolitic suite. The modal mineralogical composition of dunites comprises 93–94% forsterite with an average value of 91%.

Ophiolites in this province exhibit alternations of dunite, wherlite and clinopyroxenite. The trend is N–S with a steep dip (Fig. 16.7). Dunites are mainly composed of olivine and euhedral/semi euhedral chromite. Olivine crystals display deformation twins. Based on these features, they are attributed to the base of the cumulate suite where plastic deformation may have occurred (Ağrılı et al. 2001).

The chemical composition of the dunites with economic olivine occurrences is as follow: 40–50% MgO, 7.2–13.87% total iron oxide, 37.6–41% SiO_2 and 0.33–3.99% Loss on Ignition (LOI) (Ağrılı et al. 2001).

The dunites were derived from a mantle source, while harzburgites have hybrid origins including both the mantle and subducting plates (Çevik 2006). As a result, the chemical composition of dunites is somewhat different: 40.99–50.2% MgO, 34.67–40.6% SiO_2, 6.8–13.7% Fe_2O_3 and 0.1–0.83% Al_2O_3.

16.3.2 Konya-Antalya-Isparta-Burdur Province

Ophiolites in this province are common in the Akseki, Beyşehir, Eğirdir, Yeşilova–Tefenni and Yalvaç areas. Ophiolitic rocks in the Akseki–Beyşehir area are considered part of the Bozkır Unit by Özgül (1976), while Koçyiğit (1983) considered

Fig. 16.6 Geological map of the Bursa-Orhaneli area. (Compiled from Ağrılı et al. 2001)

Fig. 16.7 A view of Bursa–Orhaneli dunites

them as part of the Inner Tauride Ophiolitic Complex. Ophiolitic rocks crop out in Kızıldağ, which is situated in northwestern of Akseki–Antalya and continue through Beyşehir–Konya to the northwest (Fig. 16.8). They thrust over the sedimentary units comprising upper Cretaceous limestone, nummulite-bearing limestone and flysch (Döyen and Zedef 2002).

Olivine minerals are dominant (90–95%) in dunites of the Akseki–Beyşehir area (Fig. 16.9). It is accompanied by 2–3% dark-coloured minerals (possibly chromite) and 1–2% serpentinite (or talc?) developed mostly in fracture zones and a lesser amount of asbestos minerals. The average chemical composition of dunites in the area is as follows: 50.25% MgO, 37.5% SiO_2 and 8.3% Fe_2O_3 (Zedef and Döyen 2001).

Ophiolites in the south of Beyşehir consist of the tectonites (harzburgite, dunite, gabbro, pyroxenite, pegmatoid gabbro) and amphibolite. Dunites occur as irregular bands and lenses in harzburgites, where the thicknesses vary from 1 to 15 m. The unit is typical with its dominant porphyroclastic texture. Dunites consist chiefly of olivine with small amount of orthopyroxene-chromite (Arat et al. 2012).

Ophiolitic rocks in the Yeşilova area belong to the Lycian Nappes of the Alpine zone in the Western Taurides. They are believed to have formed in relation to the northern branch of the Neotethys Ocean. Ophiolites in the area have harzburgite and dunite at the base with lesser chromite patches. They grade upward into dunite, wherlite, clinopyroxenite, banded or massive gabbro and plagiogranite. The ophiolite units are cut by isolated gabbro and diabase dykes (Döyen et al. 2014).

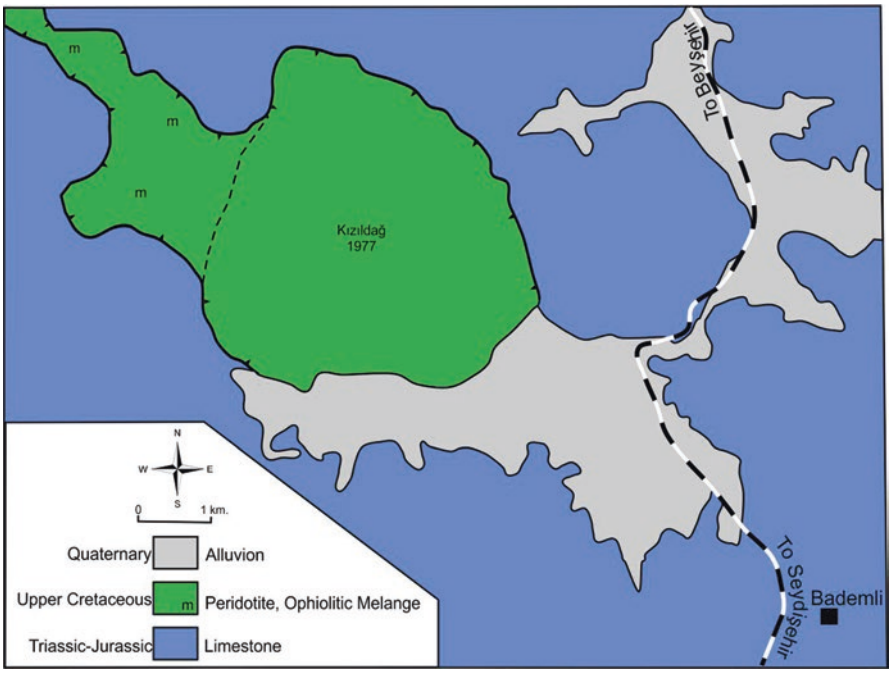

Fig. 16.8 Geological map of Kızıldağ (Beyşehir–Akseki area). (Compiled from Döyen and Zedef 2002)

Fig. 16.9 A view of the Akseki-Beyşehir dunites

Similarly, ophiolites of the Şarkikaraağaç (Isparta) comprise dunite and harzburgite. Dunite and harzburgite mostly display porphyroclastic textures indicating the effects of plastic deformation of these ultramafic tectonites in the upper mantle. Giant crystalline pyroxenites composed of orthopyroxenite and websterite are observed as small dykes and veinlets in the ultramafic tectonites (Elitok 2000).

16.3.3 Muğla Province

Ophiolites of this area are represented by clinopyroxene-rich harzburgite, depleted harzburgite and dunite (Uysal et al. 2009, 2012). They were derived from a depleted mantle source via variable degrees of melting.

Mineral chemistry, whole-rock trace elements analyses and PGE data indicate that the genesis of the Muğla peridotites can be explained by two-stages of melting and re-fertilization processes (Uysal et al. 2009, 2012). The clinopyroxene–harzburgites are the products of first-stage melting and low degrees of melt–rock interaction, formed in a mid-ocean-ridge (MOR) environment. However, the depleted harzburgites and dunites are the products of second-stage melting and related re-fertilization that took place in a supra-subduction zone (SSZ) environment (Uysal et al. 2009, 2012).

Ophiolites in the north of Köyceğiz locally display low LOI values (1%). Chemical compositions of locally 2-m thick dunites that alternate with harzburgites are as follows: 45.50–49.60% MgO and 37.50–40% SiO_2 (Ovayurt et al. 2007).

16.3.4 Hatay Province

Ophiolitic rocks in this province crop out across the Amanos Mountains and display a complete ophiolitic suite (Fig. 16.10). These rocks, from bottom to top, include:

- tectonite peridotites that comprise mainly harzburgites and lesser dunites
- banded gabbro alternating with wherlite and gabbro
- isotropic gabbro that formed from non-cumulus clinopyroxene and gabbro
- mafic-dyke complex
- volcanic rocks comprising pillowed or massive basaltic lava flows (Tekeli and Erendil 1986).

Peridotites comprise two main rock types. Harzburgites (70%) and dunites (30%). Harzburgite contains olivine, orthopyroxene and spinel. Dunites in harzburgites are found as irregular masses reaching kilometre size at some localities. These dunite bodies randomly cut the harzburgite foliations (Tekeli and Erendil 1986).

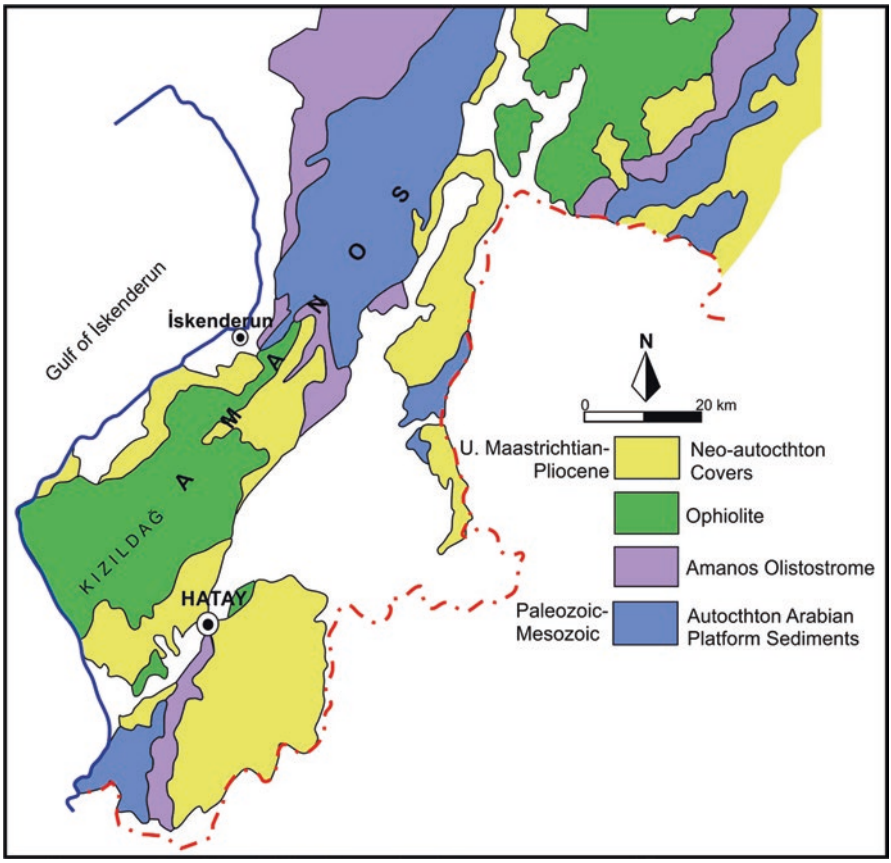

Fig. 16.10 Simplified geological map of Amanos Mountain. (After Tekeli and Erendil 1986)

16.4 Conclusions

Turkey, China and Russia are the leading countries for magnesite reserves and production (USGS Mineral Yearbook 2015). Turkey is favourable in terms of olivine reserves and quality, and its importance is increasing substantially. In terms of genesis, two types of magnesite formations are observed in Turkey. The first of these is the sedimentary magnesite formations located in Denizli–Çardak and Erzincan–Çayırlı. The other one is cryptocrystalline (gel) magnesite, and in fact all the remaining deposits are of these types (İrkeç and Kapkaç 1989).

Olivine can be observed as layers of igneous banding and also as lenses in peridotites associated with unaltered dunites. These raw materials can be of good quality and supplied to both foreign and domestic markets. Due to the commonality of the ophiolitic rocks in Turkey, exploration for the targeting of economic magnesite and olivine occurrences is encouraged.

Acknowledgments I would like to express my gratitude to Prof. Dr. Faruk Ocakoğlu for the translation of this chapter. I am grateful to editors (Franco Pirajno, Cahit Dönmez, Bahadir Şahin) and Assoc. Prof. Dr. Pınar Şen for their valuable and constructive comments that greatly improved the chapter.

References

Ağrılı H, Kayan T, Öztürk OÇ, Ovayurt M, Özkan YZ (2001) Türkiye olivin aramaları projesi Orhaneli-Bursa, Tavşanlı-Kütahya Yöresi, prospeksiyon raporu [Turkey olivine exploration project Orhaneli–Bursa, Tavşanlı-Kütahya regions prospecting report]. General Directorate of the Mineral Research and Exploration Report no 10493 (in Turkish, unpublished)

Akbulut A (2003) Çardak–Çameli Neojen havzası Sepiyolit, Huntit aramaları projesi prospeksiyon raporu [Prospecting report of Çardak-Çameli Neogene Basin sephiolite, huntite exploration project]. General Directorate of the Mineral Research and Exploration Report no 10731, Ankara (in Turkish, unpublished)

Arat İ, Üner T, Çakır Ü (2012) Beyşehir–Hoyran (Konya) ofiyolitindeki tektonitin dokusal özellikleri: Beyşehir (Konya) güneyinden bir örnek [Textural properties of tectonite in the Beyşehir Hoyran ophiolite: an example of southern of Beyşehir (Konya)]. Proceeding Book 65th Geological Congress of Turkey, pp 392–393

Arslan İ (1987) Erzincan–Çayırlı (Aravans) manyezit sahası maden jeolojisi raporu [Mining geology report on Erzincan-Çayırlı (Aravans) magnesite field]. General Directorate of the Mineral Research and Exploration Report no: 8342 (in Turkish, unpublished)

Brennich G (1958) Türkiye'deki manyezitlere dair rapor [Report on magnesites in Turkey]. General Directorate of the Mineral Research and Exploration Report no: 2567 (in Turkish, unpublished)

Brennich G (1959) Hırsızdere (Çambaşı-Denizli) manyezit zuhuru [Hırsızdere (Çambaşı-Denizli) magnesite occurrence]. General Directorate of the Mineral Research and Exploration Report no 2698 (in Turkish, unpublished)

Çevik E (2006). Topuk Köyü ve civarındaki (Orhaneli, Bursa) dünitlerin mineralojik ve jeokimyasal özellikleri ve olivin açısından endüstriyel kullanımının değerlendirilmesi [The mineralogical and geochemical characteristics of the dunites from Topuk village and its vicinity (Orhaneli, Bursa) and evaluation of their industrial usage in terms of olivine]. Msc Thesis, Istanbul University, (in Turkish with English abstract, unpublished)

Çubuk Y, Ağrılı H, Cihnioğlu M, Kıral N, Ölmez M, Selvi Y, Üstün H (2011) Türkiye manyezit envanteri [Magnesite inventory of Turkey]. General Directorate of Mineral Research and Exploration Inventory Series-203, Ankara (in Turkish)

Döyen A, Zedef V (2002) Kızıldağ (Akseki-Antalya) kromit oluşumlarının jeolojik ve jeokimyasal özellikleri [Geological and geochemical features of the Kızıldağ (Akseki- Antalya) chromite occurrences]. Pamukkale Univ J Eng Sci 1:97–108 (in Turkish with English abstract)

Döyen A, Cömlekçiler F, Kocak K (2014) Stratigraphic Features of the Yeşilova Ophiolite, Burdur, South-Western Turkey. STRATI 2013 Part of the Springer Geology book series, pp 493–498

Elitok Ö (2000) Kızıldağ ofiyolitlerinin (Şarkikaraağaç) Jeolojisi ve Petrografisi [Geology and petrography of Kızıldağ ophiolites (Şarkikaraağaç)]. Proceedings 53th Geological Congress of Turkey

Emre H (1986) Orhaneli Ofiyolitinin Jeolojisi ve Petrolojisi [Geology and petrology of Orhaneli ophiolite]. PhD Thesis, İstanbul University, 165 p (in Turkish with English abstract, unpublished)

Ertuğrul H (1978) Çankırı İli (Şabanözü-Eldivan-Merkez) Manyezit Madeni Nihai Raporu (Magnesite Mine Result Report of Çankırı Province Şabanözü-Eldivan-Centre) General Directorate of Mineral Research and Exploration, Report no 6595 (in Turkish, unpublished)

İrkeç T, Kapkaç F (1989) Türkiye'de Bilinen Manyezit Yatak ve Zuhurlarının Değerlendirilmesi ile Aramalara Yönelik Öneriler [Evaluation of known magnesite deposits and occurrences of Turkey with suggestion for exploration]. General Directorate of the Mineral Research and Exploration Report no 8863, Ankara (in Turkish, unpublished)

Kıyıcı B, Baybörü R (1978) Konya İli Çayırbağı Köyü Keklik Pınarı Mevkii Manyezit Yatağı Etüt Raporu (Study Report of Konya Province Çayırbağı Village Keklik Pınarı Site Magnesite Deposite) General Directorate of Mineral Research and Exploration, Report no 6330 (in Turkish, unpublished)

Kocaefe M (1982) Türkiye Manyezit Envanteri [Magnesite inventory of Turkey]. General Directorate of Mineral Research and Exploration Publications no 186 (in Turkish)

Koçyiğit A (1983) Hoyran Gölü Dolayının (Isparta Büklümü) Tektono-Stratigrafik Özelliği [Tectono-stratigraphic characteristic of the vicinity of Hoyran Lake (Isparta Bend)]. In: Tekeli O, Göncüoğlu MC (eds) Geology of the Taurus Belt proceedings international symposium on the geology of the Taurus Belt, 26–29 September 1983. MTA, Ankara, pp 28–29

Önal G (2007) Meram-Çayırbağı (Konya) ve Sarıkavak (Mersin) manyezit Yataklarının Jeokimyasal İncelenmesi [Geochemical investigation of the magnesite deposits of Meram-Çayırbağı (Konya) and Sarıkavak (Mersin)]. MSc Thesis Çukurova University, Adana, 93 p (in Turkish with English abstract, unpublished)

Öncel Z, Denizci F (1982) Eskişehir bölgesi lületaşı ve manyezit etütleri raporu [Report of meerschaum and magnesite surveys in the Eskisehir region]. General Directorate of the Mineral Research and Exploration Report no 7181, 243 p (in Turkish, unpublished)

Ovayurt M, Öztürk OÇ, Kayan T, Ağrılı H (2007) Türkiye Olivin Aramaları Projesi Marmaris (Muğla)-Antalya-Yeşilova (Burdur)- Isparta-Karaman-Pozantı (Adana)-Mersin Ofiyolitleri Olivin Prospeksiyon Raporu [Turkey Olivine exploration project, Marmaris (Muğla)- Antalya-Yeşilova (Burdur)-Isparta-Karaman-Pozantı (Adana)-Mersin ophiolites olivine prospection report]. General Directorate of the Mineral Research and Exploration Report no 11015 Ankara, 29 p (unpublished)

Özgül N (1976) Torosların Bazı Temel Jeoloji Özellikleri [Some geological aspects of the Tauridsus orogenic belt (Turkey)]. Bull Geol Soc Turkey 19:65–78 (in Turkish with English Abstract)

Sarıfakıoğlu E (2011) MTA 1:100.000 Ölçekli Türkiye Jeoloji Haritaları (Kütahya İ23 Paftası) [MTA 1:100 000 scaled geological maps (Sheet Kütahya İ23)]. General Directorate of Mineral Research and Exploration 1:100 000 scaled geological map series No: 157, Ankara

Sarıız K (1990) Formation of Türkmentokat-Karatepe (Eskişehir) magnesite ore beds. Bull Min Res Exp 110:77–96

Şenel M (1997) MTA 1:100.000 Ölçekli Türkiye Jeoloji Haritaları (Denizli J9 (M23) Paftası). [MTA 1:100 000 scaled geological maps, Sheet Denizli J9 (M23)]. General Directorate of Mineral Research and Exploration 1:100 000 scaled geological map series no:16, Ankara

Şimşek M (1975) Konya-Meram Magnezit Sahası Jeoloji Raporu [The geological report of Konya-Meram magnesite field]. General Directorate of the Mineral Research and Exploration Report no 1013 (unpublished)

Tekeli O, Erendil M (1986) Geology and petrology of the Kızıldağ ophiolite (Hatay). Bull Min Res Exp 107:21–37

Topak Y (2006) Yukarıtırtar-Aşağıtırtar Köyleri (Isparta Kuzeydoğusu) Arasında Gözlenen Manyezit Yatağının Oluşumu ve Kökeni [Formation and origin of magnesite ore between Yukarıtırtar-Aşağıtırtar villages (Northeast of Isparta)]. PhD Thesis, Çukurova University, 155p (Unpublished)

Tuncay A (2000) Çayırbağı–Meram (Konya) manyezit yatağının kökeniz üzerine [On the origin of the Çayırbağı-Meram (Konya) magnesite deposits]. Geol Bull Turk 43(2):21–31 (In Turkish with English abstract)

USGS Mineral Yearbook (2015) https://minerals.usgs.gov/minerals/pubs/commodity/magnesium/myb1-2015-mgcom.pdf

Uysal İ, Tarkian M, Sadiklar MB, Zaccarini F, Meisel T, Garuti G, Heidrich S (2009) Petrology of Al- and Cr-rich ophiolitic chromitites from the Muğla, SW Turkey: implications from composi-

tion of chromite, solid inclusions of platinum-group mineral, silicate, and base-metal mineral, and Os-isotope geochemistry. Contrib Mineral Petrol 158:659–674

Uysal İ, Ersoy EY, Karslı O, Dilek Y, Sadıklar MB, Ottley CJ, Tiepolo M, Meisel T (2012) Coexistence of abyssal and ultra-depleted SSZ type mantle peridotites in a Neo-Tethyan Ophiolite in SW Turkey: constraints from mineral composition, whole-rock geochemistry (major–trace–REE–PGE), and Re–Os isotope systematics. Lithos 132–133:50–69

Yeniyol M, Önder V (1978) Yunak ilçesi dolayının jeolojisi ve manyezit yatakları [Geology and magnesite deposits of the vicinity of Yunak District]. General Directorate of the Mineral Research and Exploration, Report no 6485 (in Turkish, unpublished)

Yılmaz A, Kuşcu M (2007) Süleymaniye (Mihalıççık-Eskişehir) manyezitlerinin jeolojisi ve jeokimyası [Geology and geochemistry of Süleymaniye (Mihalıççık-Eskişehir) Area Magnesite]. Geol Bull Turk 50(2):95–107 (in Turkish with English abstract)

Yılmaz A, Kuşcu M (2008) Süleymaniye, Mihalıççık, Eskişehir, Türkiye manyezit oluşumlarının kökeni [Origin of magnesite occurences in Süleymaniye, Mihalıççık, Eskişehir, Turkiye]. Bull Mineral Res Exp 136:19–29 (in Turkish with English abstract)

Yılmaz A, Kuşcu M (2012) Manyezit yataklarının oluşumu, sınıflandırılması, kullanım alanları ve kalite sınıflandırılması [Formation, classification, usage areas and quality classification of magnesite deposits]. Erciyes Univ J Ins Sci Tech 28(1):65–72 (in Turkish with English abstract)

Yersel G, Ayday C (1992) Kütahya Turanocağı ve Ortaocak Manyezit Bölgeleri Sondaj Verilerinin Jeoistatiksel Yöntemlerle Değerlendirilmesi (Evaluation of Drill-Log Data from Kütahya Turanocağı and Ortaocak Magnesite Regions by Geostatistical methods). Geol Bull Turk 35:25–33 (in Turkish with English abstract)

Zedef V, Döyen A (2001) Olivin: Türkiye'de tanınmayan çok amaçlı kullanımı olan bir hammadde ve ülkemiz olivin potansiyeline bir örnek-Kızıldağ (Akseki-Antalya) Olivin Yatağı [Olivine: a raw material with multipurpose use, unrecognized in Turkey and an example to Turkey's olivine potential: Kızıldağ (Akseki-Antalya) olivine deposit]. Proceeding book 4th Industrial Raw Material Symposium 18–19 October 2001, İzmir, pp 299–303

Zedef V, Anthony MJ, Russell EF (2000) Genesis of vein stockwork and sedimentary magnesite and hydromagnesite deposits in the ultramafic terranes of southwestern Turkey: a stable isotope study. Econ Geol 95(2):429–445

Epilogue

The geological make-up of Turkey (mainland Turkey: Anatolia) is characterised by several continental terranes, most of which have a Palaeozoic – Mesozoic history. They were amalgamated during the Early Tertiary by the closure of the Neotethyan branches that generated the Alpine-Himalayan Orogeny. Therefore, Turkey is situated between colliding continents, and currently sits on the Tethyan – Eurasian Orogenic/Metallogenic Belt, one of the world's most important belts, both from the viewpoints of geotectonics and mineral systems. The Variscan, Cimmerian and Alpine orogenies formed by the closure of the Proto-, Paleo- and Neotethyan oceans in the area where Turkish terranes were located have created a very complex overall geological structure. However, Turkey's geological make-up is quite fertile and productive, in terms of forming of mineral deposits, thereby providing excellent target for mineral resources likely to be discovered in the future, as well as a better understanding of the ones currently present.

Turkey is a host of mineral resources of almost every kind, from magmatic, magmatic-hydrothermal, to metamorphic and sedimentary-hosted mineral systems. The tectono-thermal processes that create these types of mineral systems, many with economical potential or economically viable ones. These mineral systems, their geological positions, generic features and economic aspects are covered in the chapters of the book titled 'Mineral Resources of Turkey'. The book covers mineral deposits, as important factors in the economy, and it also tells the reader about the geological context in which they have been discovered. As the currently known mineral resources are important indicators in the search for new ones, it is quite useful to learn about their geological environments.

Within this context, it is important to understand the geodynamic evolution of the various terranes hosting the mineral deposits formation process.

In this framework, ophiolites, the fragments of ancient oceanic crust that overthrust continental crust; host chromium, Cyprus-type VMS deposits (particularly Cu-Zn), iron ore, manganese, magnesite and olivine, and are also an important source of information in understanding the tectonic evolution of Anatolia. Volcanic,

F. Pirajno et al. (eds.), *Mineral Resources of Turkey*, Modern Approaches in Solid Earth Sciences 16, https://doi.org/10.1007/978-3-030-02950-0

plutonic and volcano-plutonic complexes formed as the result of subduction, collision and post-collision events that occurred during the closing process of Neotethys Ocean between the Late Cretaceous and the Late Miocene host porphyry-type ore deposits. The subduction, continental collision, and post-collisional episodes, which occurred as a result of the convergence that took place during the late Cretaceous-Oligo-Miocene period between Eurasia and Afro-Arabia, also enhanced the process of forming skarn type ore deposits. In addition to Cyprus-type VMS deposits and occurrences observed as a part of the ophiolitic settings, the Eastern Pontides contains Kuruko-type VMS related to the felsic volcanism, developed on arc magmatism, and also Besshi-type VMS belt, related to the low grade metamorphic siliciclastic sedimentary rocks, located in the Central Pontides that was discovered in recent years.

The Carbonate-hosted Pb-Zn deposits in Turkey are located on the Tauride Belt, a part of North Gondwanan platform. The iron ore deposits in Turkey are also in the Tauride Belt, usually occurring along contact areas of granitic rocks, and in ophiolites

Turkey's manganese deposits branch out to four categories based on their main rock type, geological-tectonic position, and formation process. These are: (a) Black-shale hosted deposits, (b) Radiolarian chert-hosted deposits, (c) Oligocene-hosted deposits, (d) Volcanic arc-hosted and/or vein-type hosted deposits. Economically significant manganese ores are usually associated with black shales, which are part of the Oligocene sedimentary sequences within the Trace Basin. The presence of black shales is particularly valuable, not only for Mn, but also for the possibility of hosting U, V, Ni, Mo, PGE, REE, as observed and locally mined in the Cambrian-aged black shales in South China and Canada.

The extensional processes that affected West Anatolia had an important role in the geological evolution of Anatolia, which is the mainland of Turkey. These processes have played an effective role in the development of the Neogene lacustrine basins that host borates and contain approximately two-thirds of world's borate reserves. West Anatolia has a geological history of subduction, obduction, continental collision and, subsequently, crustal thickening, extension and crustal thinning. Evaporation processes also have a major role in the economically important borat precipitation. Similarly, trona is the largest mineral resource of the Neogene basins in the Central Anatolia. Trona beds have generically evolved from explosive andesitic rhyolitic volcano-sedimentary series, in shallow lake environments. In addition to the geological processes, arid and semi-arid climate conditions also played a role in the formation of industrial minerals such as borates and trona.

Another economic mineral system highly affected by climate conditions is nickel. As a part of the Alpine – Himalayan Belt in Turkey, ultramafic rocks of the Neotethys ophiolites were exposed to the tropical-subtropical climate conditions, which resulted in the supergene alteration responsible for the formation of lateritic nickel deposits.

Bauxite deposits in Turkey are located principally in eight provinces, of which a significant part of them is in the Anatolide-Taurides, and another in the Arabian Plate, while the remaining deposits are located in the Pontides. Radioactive minerals and rare earth elements are also be found in Turkey's complex geological structure.

The above-mentioned mineral resources, as well as those presented in this book 'Mineral Resources of Turkey' have a significant role in mining activities of Turkey and provide raw material supplies for the national industry sectors. These mineral systems are the subject of scientific research, and provide role models for potential future mines and act as an important guide for exploration strategies and targeting. When we consider the Tethys Metallogeny Belt as a whole, it must be noted that although mineral deposits and occurrences within Turkey's border are quite rich, it is evident that the country still has not reached its full mining potential. Therefore, exploration work that may lead to future discoveries are "a must" in Turkey.